Progress in Marine Science and Technology 1

Proceedings of the 20th International Ship and Offshore Structures Congress

Technical Committee Reports

Edited by
Mirek Kaminski and Philippe Rigo

IOS Press

PROCEEDINGS OF THE 20TH INTERNATIONAL SHIP AND OFFSHORE STRUCTURES CONGRESS (ISSC 2018) VOLUME 1

Progress in Marine Science and Technology

Progress in Marine Science and Technology (PMST) is a peer-reviewed book series concerned with the field of marine science and technology. It includes edited volumes, proceedings and monographs dealing with research in pure or applied science and work of a high international standard on subjects such as: conceptual design; structural design; hydromechanics and dynamics; maritime engineering; production of all types of ships; production of all other objects intended for marine use; shipping science and all directly related subjects; offshore engineering as related to the marine environment; oceanographic engineering subjects related to the marine environment.

Volume 1

ISSN 2543-0955 (print)
ISSN 2543-0963 (online)

Proceedings of the 20th International Ship and Offshore Structures Congress (ISSC 2018)
Volume 1

Technical Committee Reports

Edited by

Mirek L. Kaminski

Delft University of Technology, The Netherlands

and

Philippe Rigo

University of Liege, Belgium

IOS Press

Amsterdam • Berlin • Washington, DC

ISBN 978-1-61499-861-7 (print)
ISBN 978-1-61499-862-4 (online)
Library of Congress Control Number: 2018945814

Publisher
IOS Press BV
Nieuwe Hemweg 6B
1013 BG Amsterdam
Netherlands
fax: +31 20 687 0019
e-mail: order@iospress.nl

For book sales in the USA and Canada:
IOS Press, Inc.
6751 Tepper Drive
Clifton, VA 20124
USA
Tel.: +1 703 830 6300
Fax: +1 703 830 2300
sales@iospress.com

Preface

The first volume contains the eight Technical Committee reports presented and discussed at the 20th International Ship and Offshore Structures Congress (ISSC 2018) in Liege (Belgium) and Amsterdam (The Netherlands), 9–14 September 2018, and the second volume contains the reports of the eight Specialist Committees. The Official discusser's reports, all floor discussions together with the replies by the committees, will be published after the Congress in electronic form.

The Standing Committee of the 20th International Ship and Offshore Structures Congress comprises:

Chairman:	Mirek Kaminski	The Netherlands
Co-chairman:	Philippe Rigo	Belgium
	Segen Estefen	Brazil
	Neil Pegg	Canada
	Yingqiu Chen	China
	Jean-Yves Pradillon	France
	Patrick Kaeding	Germany
	Manolis Samuelides	Greece
	Stefano Ferraris	Italy
	Masahiko Fujikubo	Japan
	Rune Torhaug	Norway
	Carlos Guedes Soares	Portugal
	Yoo Sang Choo	Singapore
	Jeom Kee Paik	South Korea
	Ajit Shenoi	UK
	Xiaozhi Wang	USA

On behalf of the Standing Committee, we would like to thank the sponsors of ISSC 2018.

Mirek Kaminski
Chairman

Philippe Rigo
Co-chairman

Delft, 1st May 2018

This page intentionally left blank

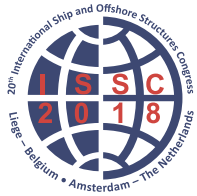

THANKS TO OUR SPONSORS FOR
THEIR FINANCIAL CONTRIBUTION

Move Forward with Confidence


MARIN


DN&T
Design Naval & Transports


SECO


Flanders
Hydraulics Research
Flanders
State of the Art

Contents

Preface v
Mirek Kaminski and Philippe Rigo

Committee No I.1: Environment 1
Thomas Fu, Alexander Babanin, Abderrahim Bentamy, Ricardo Campos, Sheng Dong, Odin Gramstad, Geert Kapsenberg, Wengang Mao, Ryuji Miyake, Alan John Murphy, Fredhi Prasetyo, Wei Qiu and Luis Sagrillo

Committee I.2: Loads 101
Yoshitaka Ogawa, Wei Bai, Guillaume de Hauteclocque, Sharad Dhavalikar, Chih-Chung Fang, Nuno Fonseca, Satu Hänninen, Thomas B. Johannessen, Van Lien, Celso Morooka, Holger Mumm, Jasna Prpic-Orsic, Kang Hyun Song, Chao Tian, Bahadır Uğurlu and Sue Wang

Committee II-1: Quasi-Static Response 171
J.W. Ringsberg, J. Andrić, S.E. Heggelund, N. Homma, Y.T. Huang, B.S. Jang, J. Jelovica, Y. Kawamura, P. Lara, M. Sidari, J.M. Underwood, J. Wang and D. Yang

Committee II.2: Dynamic Response 255
A. Ergin, E. Alley, A. Brandt, I. Drummen, O. Hermundstad, Y.C. Huh, A. Ivaldi, J.H. Liu, S. Malenica, O. el Moctar, R.J. Shyu, G. Storhaug, N. Vladimir, Y. Yamada, D. Zhan and G. Zhang

Committee III.1: Ultimate Strength 335
J. Czujko, A. Bayatfar, M. Smith, M.C. Xu, D. Wang, M. Lützen, S. Saad-Eldeen, D. Yanagihara, G. Notaro, X. Qian, J.S. Park, J. Broekhuijsen, S. Benson, S.J. Pahos and J. Boulares

Committee III.2: Fatigue and Fracture 441
Y. Garbatov, S.K. Ås, K. Branner, B.K. Choi, J.H. Den Besten, P. Dong, I. Lillemäe, P. Lindstrom, M. Lourenço de Souza, G. Parmentier, Y. Quéméner, C.M. Rizzo, J. Rörup, S. Vhanmane, R. Villavicencio, F. Wang and J. Yue

Committee IV.1: Design Principles and Criteria 549
Matthew Collette, Zhihu Zhan, Ling Zhu, Vedran Zanic, Tetsuo Okada, Toshiro Arima, Rolf Skjong, Han Koo Jeong and Gennadiy Egorov

Committee IV.2: Design Methods 609
I. Lazakis, R. Bronsart, J.-D. Caprace, Y. Chen, P. Georgiev, I. Ilnitskiy, L. Moro, P. Prebeg, J. Mendonça Santos, Z. Sekulski, M. Sicchiero, R. Sielski, W. Tang, M. Toyoda and J. Varela

Subject Index 709

Author Index 711

This page intentionally left blank

Proceedings of the 20th International Ship and Offshore Structures Congress (ISSC 2018) Volume I – M.L. Kaminski and P. Rigo (Eds.)

doi:10.3233/978-1-61499-862-4-1

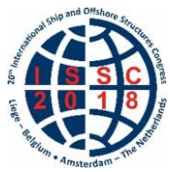

COMMITTEE No I.1

ENVIRONMENT

COMMITTEE MANDATE

Concern for descriptions of the ocean environment, especially with respect to wave, current and wind, in deep and shallow waters, and ice, as a basis for the determination of environmental loads for structural design. Attention shall be given to statistical description of these and other related phenomena relevant to the safe design and operation of ships and offshore structures. The committee is encouraged to cooperate with the corresponding ITTC committee.

AUTHORS/COMMITTEE MEMBERS

Chairman: Thomas Fu, *USA*
Alexander Babanin, *Australia*
Abderrahim Bentamy, *France*
Ricardo Campos, *Portugal*
Sheng Dong, *China*
Odin Gramstad, *Norway*
Geert Kapsenberg, *The Netherlands*
Wengang Mao, *Sweden*
Ryuji Miyake, *Japan*
Alan John Murphy, *UK*
Fredhi Prasetyo, *Indonesia*
Wei Qiu, *Canada*
Luis Sagrillo, *Brazil*

KEYWORDS

Environment, ocean, wind, wave, current, sea level, ice, deep water, shallow water, data source, modelling, rogue waves, climate change, design condition, operational condition, uncertainty.

CONTENTS

1. INTRODUCTION 4
1.1 Applications 4
1.1.1 Design 4
1.1.2 Operation 7
1.2 Waves 13
1.3 Wind 14
1.4 Climate 15
1.4.1 Increasing uncertainty and risk due to climate change. 15
1.4.2 Sea Level Rise 15

2. LONG TERM STATISTICS AND EXTREME VALUE ANALYSIS 16
2.1 Long Term Measurements and Data 18
2.2 Wave Climatology 20
2.3 Climate Trends and Uncertainty 21
2.4 More measurement in extreme conditions 22

3. WAVES & SWELL 24
3.1 Measurements / Data 24
3.1.1 Deterministic wave generation in the laboratory 24
3.1.2 Measurement and analysis 26
3.1.3 Particle Image Velocimetry 28
3.2 Rogue Waves 29
3.3 Analytical & Numerical Models 32
3.3.1 Spectral 33
3.3.2 Phase Resolved 36
3.3.3 Short Term Stochastic / Probabilistic / Machine Learning 39
3.4 Tropical & Extratropical Cyclones 42

4. CURRENTS 43
4.1 Measurements / Data 45
4.1.1 In-situ current measurements 45
4.1.2 Remotely sensed current measurements 46
4.2 Analytical & Numerical Models 46

5. WIND 47
5.1 Current State of the Art 48
5.2 Accuracy Issues 52
5.3 Measurements / Data 52
5.4 Analytical & Numerical Methods 53

6. ICE /ICEBERGS 54
6.1 Measurements / Data 54
6.1.1 Space-borne Measurements 54
6.1.2 Airborne Measurements 55
6.1.3 Ice Management Trials 55
6.1.4 Subsea Measurements 56
6.1.5 Icebergs 56
6.1.6 Thermodynamics 57
6.2 ICE-STRUCTURE INTERACTION 58
6.2.1 Sea Ice 58
6.2.2 Laboratory Testing 59

6.2.3 Iceberg Loading 59
6.2.4 Ice Hydrodynamics 59
6.2.5 Ice Accretion 60
6.3 Analytical & Numerical Models 60

7. COUPLED PHENOMENA 62
7.1 Wave Breaking 62
7.2 Wave-current interactions 63
7.3 Wave-ice interactions 65
7.4 Atmospheric wave boundary layer 66
7.5 Wave influences in the upper ocean 68
7.6 Waves in large-scale air-system – climate 70

8. UNCERTAINTY 71
8.1 Uncertainty in prediction models 71
8.2 Uncertainty in measurements 72
8.3 Challenges in uncertainty quantification 73

9. SPECIAL TOPICS 73
9.1 Future Trends 73
9.1.1 Big Data 73

10. CONCLUSIONS 76
10.1 Summary 76
10.2 Recommendations 76
10.3 Advances 77

REFERENCES 77

1. INTRODUCTION

This report builds upon the work of the previous Technical Committees in charge of Environment. The goal continues to be to review scientific and technological developments in the field since the last report, and to provide context of the developments, in order to give a balanced, accurate and up to date picture about the natural environment as well as data and models which can be used to accurately model it. The content of this report also reflects the interests and subject areas of the Committee membership. Additionally, in accordance with the ISSC I.1 mandate, this Committee has reported on the resources available for design and the operational environment. The Committee has also continued cooperation with the corresponding ITTC Committees initiated in 2010.

The Committee consisted of members from academia, research organizations, research laboratories and classification societies. The Committee formally met as a group in person two times: in Melbourne, Australia (5-6 December 2016) and in Arlington, Virginia, USA (26-27 September 2017), and held a number of regular teleconferences. Additionally, Committee members also met on an ad hoc basis at different scientific conferences and industrial workshops, including the 35th and 36th International Conference on Ocean, Offshore and Arctic Engineering (OMAE 2016 and 2017). With the wide range of subject areas that this report must cover, and the limited space as well as the boundaries presented by the range of specialties and competencies of the Committee members, this Committee report doe s not purport to be exhaustive. However, the Committee believes that the reader will be presented a fair and balanced view of the subjects covered, and we recommend this report for the consideration of the ISSC 2018 Congress.

1.1 Applications

1.1.1 Design

High steep waves and strong winds can create dangerous metocean conditions for ships and offshore engineering activities. This complex load environment results in various responses, stresses, motions etc. Under limited time and geographical region, the loads are described by power spectral densities. Since the densities are changing in time, long-term variability of the environment are described using some spectral parameters, e.g. significant wave height, zero crossing period, wave steepness or average wind speed. The variability of spectral parameters are described by means of uni- or multi-valued long-term distributions. Reliable estimates of the distributions over the oceans are important for safe shipping and offshore engineering activities. Environmental contours derived from the long-term probability density functions are often used. Furthermore, it is also important to clearly specify which type of distribution is relevant, long-term distribution at fixed positions, variability over a region or sea state parameters encountered by a sailing ship.

The long-term distributions of wind and waves for marine design are often employed to determine necessary resistance of ships (offshore structure details) for various material aging processes, where fatigue and crack growth are the most important. The long-term response analysis may be used when specifying design criteria and performing load and response assessment of marine structures. Alternative to full long-term response analysis, the environmental contours are quite often established independently of any structural problem without reference to specific environment design standard. The contour lines correspond to a set of sea states, which may be used to explore design options. Hence, computational intensive response analyses are only required for a limited set of design sea states for each design proposal.

Drago et al. (2015) presents metocean design criteria for the off-shore hydrocarbon extraction activities in very deep waters up to more than 2000 m. For the development of those subsea systems, the metocean design data and criteria to be developed and the applicable methodologies to derive them should be well established, since the system components, e.g., risers,

moorings, etc. can suffer from severe damages due to the occurrence of critical combinations of different variables during a single sea storm due to the surface developments and the connections through the water column. Therefore, this paper considers the joint occurrence of different forcing conditions, and it provides a simplified methodology to perform a sensible multivariate analysis of the contemporary data such as wind, waves and current. Three different cases, i.e., the correlation of extremes of different variables (wind, wave and current), the extreme profiles of current, and the current profile climate, are investigated in the paper. It is concluded that for the wind, wave and current directional extremes correlation, it should be sufficiently enough to provide only the cases which could have relevance in the design analyses, rather than providing the directional correlated extreme of the marginal variable from many different cases.

Bitner-Gregersen (2015) presented a very complex probability density function of the long-term distribution of sea state parameters; mean wind speed; wind direction; main wave direction (sea and swell); current speed; current direction; significant wave height (sea and swell); spectral peak period (sea and swell); sea water level astronomical tides and meteorologically induced surges. The model has been fitted to hind cast data from four locations: Southern North Sea, West Shetland, and Northwest Shelf of Australia and off coast of Nigeria. Presence of wind-sea and swell will affect design and operability of fixed and floating off-shore structures as well as LNG terminals. The presented a joint met-ocean model can be applied for design and operations of marine structures, including LNG platforms. Uncertainties of the proposed fits are examined focusing on location specific features of the wave climate.

The environmental contour concept, commonly applied in marine structural design, allows for the consideration of extreme environmental conditions independently of a particular structure. The idea is to define contours in environmental parameters space (e.g., significant wave height and zero crossing wave period) along which extreme loads and responses with a given return period should lie. In this way, design sea states may be identified along the contour and time consuming long-term load determination and response calculations are only needed for a limited set of design sea states. Alternatively, joint environmental models need to be utilized in full long-term response analysis of marine structures. Vanem and Bitner-Gregersen (2015) compared the recently proposed new approach to estimate environmental contours in the original physical space by direct Monte Carlo simulations with the traditional method employing Rosenblatt transformation. The methods lead to different results, which are compared in a number of case studies. The different results given by these two methods are the practical consequences of the choice of approach. Attention is given to mixed sea systems; in these situations, the two approaches to environmental contours may be very different. Montes-Iturrizaga and Heredia-Zavoni (2016) studied the influence of statistical correlation between significant wave height and peak period on the reliability assessment of mooring lines. This paper proposed to use copulas models to define the joint probability distribution of a set of random variables. It is used to describe the correlation structure of metocean parameters for the reliability analysis of mooring line of a Floating Production, Storage and Offloading vessels (FPSO). The copula models include such as Frank, Gumbel and Gaussian distributions that can be fitted from the hindcast metocean data, in particular significant wave height and peak period. It shows that such correlation structure has big impact on the estimation of the reliability index, while using Gaussian copula will lead to significantly large reliability index in comparison with other copulas models.

Reliability of offshore structures is also dependent on its response to the extreme wave climate. Therefore, an adequate knowledge of the wave climate at a location is a prerequisite. Typically, one is interested in estimates frequency of ultimate failures. Orimolade et al. (2016) investigated the extreme wave climate in the Norwegian Sector of the Barents Sea. Three commonly used methods for the estimation of extreme wave heights, i.e., the initial distribution method, the peak over threshold method, and the annual maxima method, are

used. The estimated 100-year significant wave heights obtained from the three methods differ. While it is difficult to single out the best method among the three, the estimated values give knowledge of the possible range of the extreme significant wave heights at the locations. Generally, the datasets considered in this study suggest that the wave climate is less harsh further north compared to the southern region of the Barents Sea. The datasets do not suggest any temporal trends in the historical significant wave heights at any of the locations.

Most often the sea states are described using long-term distributions of spectral parameters. However in the design responses resulting from interactions of waves (sea elevations) and wind gusts with an offshore structure is needed. Often a linear filtering approach can be applied. However in extreme seas the responses can be hard to determine because of the non-linearity of the interactions. The distributions of responses can be obtained using in situ measurements, model tests or by simulations using dedicated numerical software. In Guo et al. (2016), the various numerically derived extreme responses, e.g. 3 hours extremes, has been compared with results obtained in test tank on ships models. In particular, the influence of forward speed on ship responses in extreme sea is studied.

The long-term distribution changes with geographical location, particularly when one compares open sea and coastal areas. In Bitner-Gregersen (2017), differences between open sea and coastal water wind and wave climate, using hindcast data in the analysis, were investigated. Wind and wave climate is much region and location dependent, affected by local properties of ocean environment. Wind and waves have large impacts on ship design, marine operations and they challenge ability of ships to maintain manoeuvrability in sea states. Recently, it has attracted attention due to the issue of the 2013 Interim Guidelines by IMO, where adverse weather conditions to be used in assessment of ship manoeuvrability have been proposed. Correlations between wind speed and significant wave height as well as significant wave height and spectral peak period are established and compared with the ones suggested by the 2013 Interim.

In Bitner-Gregersen et al. (2016), definition of the severity or adversity of met-ocean conditions under which ships need to maintain manoeuvrability were discussed. Specification of such adverse weather conditions was one of the objectives of the SHOPERA (Energy Efficient Safe SHip OPERAtion) (2013–2016) project, funded by the European Commission in the frame of FP7. Three distinct situations requiring different adverse weather criteria are considered in the project: manoeuvring in the open sea, manoeuvring in coastal waters and low-speed manoeuvring in restricted areas. The purpose of the present study is twofold, first to investigate metocean climate associated with the three selected scenarios and specifying its main properties, second identifying critical metocean characteristics requiring sensitivity studies in numerical simulations and model tests. Both measured and hindcast data are used in the analysis. The North Atlantic deep water metocean environment and three coastal locations are considered. The definitions are basis for formulating power and steering requirements for ships.

From 2015-2017, some research was dedicated to study whether the design criterion should include a possible climate change where the time horizon is the end of 21th century. That is whether the long-term distributions or maximum responses distributions, used in design, may considerably change in future. Weisse et al. (2015) presented the so-called “climate services” for the decision making processes of particular interest in the maritime applications in Europe. A series of examples ranging from naval architecture, offshore wind and more generally renewable energies, shipping emissions, tidal basin water exchange and eutrophication levels, etc., are described covering the generation, transformation and the use of climate information in decision making processes. This paper also investigated the effects of climate change on coastal flood damages and the need for coastal protection is considered. It is concluded that reliable climate information in data sparse regions is urgently needed. For many applications, historical climate information may be as or even more important as future long-term projec-

tions. Aarnes et al. (2017), Bitner-Gregersen and Toffoli (2015), and Vanem (2016) present detailed investigations of possible changes in future distributions of significant wave height, periods and steepness. The fits to historical data are compared with estimates of future wave climates based on several emission scenarios. The results are very uncertain and not yet influencing the present design procedures. In Aarnes et al. (2017), wave model simulations covering the northeast Atlantic have been conducted using 3-hourly near-surface winds obtained from six CMIP5 models. It is found that a decrease in significant wave height in the northeast Atlantic by the end of the 21st century. The study indicates the largest changes in significant wave height near the mean, while the tendency is weaker going into the upper tail of the distribution. Locally, these extremes are approximately one standard deviation higher in the future climate. A similar, but weaker increase is found in the southern coastal areas of Norway.

Wave steepness is an important parameter not only for design and operations of marine structures but also for statistics of surface elevation as well as occurrence of rogue waves. Bitner-Gregersen and Toffoli (2015) investigates potential changes of wave steepness in the future wave climate in the North Atlantic. The Fifth Assessment Report of the Intergovernmental Panel on Climate Change (IPCC) uses four scenarios for future greenhouse gas concentrations in the atmosphere called Representative Concentration Pathways (RCP). Two of these scenarios with radiative forcing of 4.5 and 8.5 W/m2 by the end of the 21st century have been selected to project wave conditions in the North Atlantic. The analysis includes total sea, windsea, and swell. Changes of wave steepness for these wave systems are shown and compared with wave steepness derived from historical data. Long-term probability description of wave steepness variations is proposed. Consequences of changes in wave steepness for statistics of surface elevation and generation of rogue waves are demonstrated. Uncertainties associated with wave steepness projections are discussed.

In many marine and coastal engineering applications, the simultaneous distribution of several metocean variables is required for risk assessment and load and response calculations. For example, a joint probabilistic description is needed to construct environmental contours for probabilistic structural reliability analyses. Typically, the joint distribution of significant wave height and wave period is needed as a minimum, but other environmental parameters such as wind, current, surges and tides might also be relevant. Vanem (2016) presents a study on various joint models for the simultaneous distribution of significant wave height and zero-crossing wave period. The alternative models that have been investigated are a conditional model, a bivariate parametric model and several models based on parametric families of copulas. Each of the models is fitted to data generated from a numerical wave model for the current climate and for two future climates consistent with alternative climate scenarios. Additionally, the potential effect of climate change on the simultaneous distribution will be investigated. Initial investigation reveals that straightforward application of some of the most commonly used copulas will not give reasonable joint models. The reason for this is that they are symmetric, whereas the empirical copulas display asymmetric behaviour. However, asymmetric copulas can be constructed based on these families of copula, and this significantly improves the fit. Analyses of the extremal dependence in the data indicate that the variables are asymptotically independent. Furthermore, the results suggest that extreme significant wave height and zero-crossing wave period tend to be more correlated in a future climate compared to the current climate.

1.1.2 Operation

The reduction of emissions of greenhouse gas (GHG) has become an urgent global task for the prevention of global warming. In order to reduce the GHG emissions from the international maritime sector ahead of the other sectors, amendments to MARPOL ANNEX VI making "Energy Efficiency Design Index (EEDI)" and "Ship Efficiency Management Plan (SEEMP)" mandatory were adopted at the 62nd session of Marine Environment Protection Committee

(MEPC 62) held in July 2011, and have entered into force on 1 January 2013. This was the first legally binding climate change treaty to be adopted since the Kyoto Protocol.

Furthermore, at MEPC 70 held in October 2016, amendments to MARPOL Annex VI to make mandatory the data collection system (DCS) for fuel consumption of ships and amendments to the SEEMP guidelines were adopted. Under the amendments to MARPOL Annex VI, on or before 31 December 2018, in the case of a ship of 5,000 gross tonnage and above, the SEEMP shall include a description of the methodology that will be used to collect the data and the processes that will be used to report the data to the ship's flag State.

On the other hand, in June 2013, the European Commission proposed a strategy for progressively integrating maritime emissions into the EU's policy for reducing its domestic GHG emissions. After a two-year legislative process, involving all EU institutions, this strategy was adopted by the European Parliament in April 2015. The Regulation 2015/757 ('Shipping MRV Regulation') came into force on 1 July 2015. The strategy consists of three consecutive steps:

- Monitoring, reporting and verification of carbon emissions from ships
- GHG reduction targets for the maritime transport sector
- Further measures, including Market-Based Measures (MBM)

The first step of the strategy is the design of a robust Monitoring, Reporting and Verification (MRV) system of carbon emissions for ships exceeding 5,000 gross tonnage (GT) on all voyages to, from and between EU ports applicable from 2018.

At the early stage of deliberations on EEDI regulation, since the EEDI regulation requires to reduce EEDI value by 30 % in phase 3, there was concern that ships with excessively small propulsion power would be constructed just for the purpose of improving the EEDI value. Therefore, discussions on minimum propulsion power in adverse weather condition were started. Consequently, it was required that the installed propulsion power shall not be less than the propulsion power needed to maintain the manoeuvrability of the ship in adverse conditions in accordance with "2013 Interim guidelines for determining minimum propulsion power to maintain the manoeuvrability in adverse conditions" (Resolution MEPC.232(65), 2013). The purpose of the interim Guidelines is to verify that ships, complying with the EEDI requirements, have sufficient installed power to maintain the maneuverability in adverse conditions. The interim minimum propulsion power Guidelines are applicable only to bulk carriers, tankers and combination carriers of 20,000DWT or above to which compliance with required EEDI is required during phase 0 (from 2013 to 2014) and phase 1 (from 2015 to 2019) of the EEDI implementation.

In 2014, in order to revise the interim minimum propulsion power Guidelines, a Japan's research project was launched by Japanese maritime societies. For the same purposes at almost the same time, the EU PF7 project "Energy Efficient Safe Ship Operation (SHOPERA)" was also launched by European maritime societies. In 2015, in order to address the challenges of this issue by more in depth research, SHOPERA and the Japan's research project (these projects hereinafter being collectively referred as "the Projects") have worked together through technical and practical considerations and evaluation. At MEPC 71 held in July 2017, in order to revise the interim Guidelines, draft revised Guidelines reflecting the results of the Projects were introduced (MEPC 71/5/13 and MEPC 71/INF.28, 2017).

The Projects developed three realistic scenarios for evaluating ship's handling in adverse conditions (MEPC 71/INF.29, 2017). The specification of the scenarios was based on a series of interviews with ship owners, ship masters and chief engineers, accidents and weather statistics, as well as the analysis of the seakeeping performance of ships in waves.

Based on the evaluation of results of conducted studies for a series of existing eco-ships, the Projects have reached a conclusion that the following scenario "Weather-vaning in coastal

areas under strong gale condition" is always more demanding, in comparison with other scenarios, with respect to the required installed propulsion power for tankers, bulk carriers and combination carriers. Therefore, this scenario is proposed to be considered as the only required scenario for the evaluation of the sufficiency of ship's propulsion power to maintain the manoeuvrability in adverse conditions for bulk carriers, tankers and combination carriers.

Scenario "Weather-vaning in coastal areas under strong gale condition"

Area	Coastal areas
Weather conditions	BF8 (gale) for L_{pp}<200 m to BF9 (strong gale) for L_{pp}>250 m, linear over L_{pp} between 200 m and 250 m
Encountered wave and wind angle	Head seas to 30 degrees off-bow for a situation of weather-vaning
Propulsion ability	Speed through water at least 2 knots
Steering ability	Ability to keep heading into head seas to 30 degrees off-bow

Based on the assessment of results of the seakeeping performance in waves of a series of existing ships, the interviews held with ship owners, ship masters and chief engineers, shipping log data provided by ship operating companies, metocean statistical data, as well as statistics of accidents and corresponding weather conditions (Beaufort strength), the Projects have developed the adverse weather conditions that should be applied in the assessment.

Because of the diversity of the weather and sea conditions, in view of the many parameters affecting them, the Projects share the view that the adverse weather conditions applied in the assessment should be verified based on the results of the assessment of the operability of a big number of existing ships in specified weather conditions (benchmark). Based on these studies and the validation results for a series of representative existing bulk carriers and tankers, the Projects have reached a conclusion that the following conditions are suitable for the specification of the adverse weather conditions of the scenario:

> BF8 for $L_{pp} < 200$ m, BF9 for $L_{pp} > 250$ m; and linearly interpolated over L_{pp} between 200 m and 250 m.

Based on the results of measurements in coastal areas within 20 nautical miles from the Pacific Coast of Japan and at 20-30 nautical miles from the North Sea coastline of Great Britain regarding the relation between Beaufort number (wind speed) and significant wave height, the Projects determined the significant wave height corresponding to Beaufort number in coastal areas, which should be applied in the assessment of the scenario (coastal areas), considering an additional safety margin.

As a result of the discussion at MEPC 71 held in July 2017, it was agreed to continue discussion at MEPC 72 (will be held in April 2018) due to the fact that different opinions were expressed on the adverse weather condition etc. Furthermore, for the current guidelines, it was agreed to extend the application period towards phase 2 (from 2020 to 2024) of the EEDI implementation.

Present day marine operations use advisory systems that combine weather information, vessel characteristics and criteria to minimize fuel cost, emissions and risk (Simonsen et al., 2012). Optimization of operations requires algorithms to generate and evaluate alternatives and object functions that are used to quantify the result of the operation. Usually constraints are included, such as the ship route should not cross land or shallow water.

Examples of marine operations are ship planning, studies on fatigue damage and the development of warning systems for high sea states and extreme waves. These operations require a more detailed description of sea state variability than the long-term sea-state distributions

used for design purposes. These applications use correlations between sea-state parameters at different locations and moments in time. Such information is often a part of spatio-temporal models of sea state variability. The delimitation treaty between Norway and the Russian Federation, signed in September 2010, has opened new opportunities for the shipping and offshore industry in the Barents Sea and brought the need for further research of metocean and ice conditions in the Arctic regions.

Planning

The shipping industry makes frequent use of planning systems that combine the concepts of weather routing and voyage optimization. The primary objective of planning is to increase ship safety, gain more economic benefit and reduce emissions. Conventional weather routing will determine the minimum distance, duration and fuel consumption of the voyage, but other performance characteristics can be used to optimize the route. For example, Kim et al. (2017) developed a weather routing method to optimize the transport of an offshore structure. The duration of weather systems appeared to be a crucial aspect in the feasibility of the operation. In his study, Kim used the WaveWatch III database. Also minimizing the accumulation of fatigue damage can be used as an object function for planning; Mao et al. (2010a) developed such a model for a small size container ship to be used in a planning system.

Park et al. (2015) proposed a method to use a two-phase approach to weather routing. The first phase optimizes the heading of the ship at each time instant while keeping the speed constant. IMO safety regulations are applied as constraints. The second phase optimizes the speed. They claim that an almost optimal solution is found in a more efficient way than competing methods. Existing density maps of historical ship routes can also be used to plan short to mid-range ship routes, as explained by Azariadis (2017).

De Garcia et al (2016) developed the fatigue damage assessment metodology based on weather routing system by analysing the minimum time route and (MTR) and Great circle route (GCR) of US/Japan route in order to emulate the as real wave load sequences. He used the weather routing planning by several objective, there are maximise safety and crew comfort, minimum fuel consumption and minimum time underway.

Lee et al (2015) proposed a planning path by considering the effects in path planning, a energy efficiency due to maneuverable path. In detail, the plath planner will be analysis based on a realistic energy cost that it determines from loads of vehicle due to tidal current and water depth.

Algorithms

Traditional algorithms used in weather routing simply looked for the shortest route, examples of this are isochrones and isopone methods. More advanced algorithms try to optimize an object function that normally combines several aspects that are combined using weighing factors. Examples of such algorithms are 2D dynamic programming, 3D dynamic programming and Dijkstra's algorithm (Wang et al. 2017). Larsson et al. (2015) presented a Dividing Rectangles (DIRECT) algorithm and also further divide constraints into fuel constraints, generic constraints, and ship-specific constraints.

Grin et al. (2016) used the voyage simulation tool SafeTrans to determine the performance of ferries with respect to comfort, fuel efficiency and schedule. This tool uses Dijskstra's algorithm for weather routing and Monte Carlo simulations for voyage optimization. Different bow flares and routes were compared and optimized to minimize the wave conditions encountered, vibration dose and voyage duration.

Tamaru (2016) proposed an optimization of ship routing plan based on the analyzing isochrones by taking into account ship speed loss, significant wave height and relative heading angle of ship include with spatio temporal seastate information. The optimization solution is

generic algorithm which can decide the minimum time route of spatiotemporal distribution of significant wave height and wave direction.

More detailed and complicated algorithms can be used due to increased computing power. A rational and robust optimization procedure is the key to make the complicated algorithm more trustworty in order to reduce the uncertainties (Vettor and Soares (2016)). However, further improvements are more limited by the quality and time span of weather forecasts than by the complexity of the vessel hydrodynamic models and constraints.

Forecast Data

Commercially available forecast data is typically used in weather routing, but some public sources are documented in literature. Some sources include pilot charts (US National Geospatial-Intelligence Agency), ocean drifter data (US Coast Guard Mariano Global Surface Velocity Analysis, MGSVA), or satellite data (Ocean Surface Current Analyses Real-time, OSCAR). The quality of the database depends on the resolution and number of years available. Lu et al. (2017) conducted benchmarking of the WAVEWATCH III model for the Southern hemisphere by varying spatial and temporal resolution, and validating the results with measured onboard ship motion data. The EC SAFE OFFLOAD project has proposed a procedure utilizing information about wind-sea and swell in the specification of a risk-based approach for the safety of offloading operations from the LNG terminals to shuttle gas tankers. Chang et al. (2015) present a 3D geographic information system (GIS) for the initial planning of routes between Asia and Europe via the Arctic Northeast Passages, including data such as sea ice distribution, shore topology, and water depths. Skoglund et al (2015) conducted the investigation of the use of ensemble weather forecasts. The investigation is conducted because the question of the availibility of forecast data due to re-routing simulation.

Furthermore, if the commercial data forecast is not available, the weather routing systems, could use the numerical prediction based on the location of voyage. For example, Mao and Rychlik proposed the statistic distribution for wind speeds along North Atlantic route.

Constraints

Constraints in weather routing should not only include land avoidance, but also hazards such as ice, and seasonal weather effects. McGonigal et al. (2011) show results of an investigation in the presence of EIFs (Extreme Ice Features) in the area between Ellesmere Island and Prince Patrick Island. The data was collected in August 2008 from satellite images. Roughly 200 EIFs were identified, including 40 ice islands, 93 ice island fragments and 67 multi-year hummock fields. Ice island fragments were defined as less than 1 km in the longer dimension, ice islands had a diameter between 1.6 and 5.2 km, and multi-year hummock fields a diameter between 1.7 and 13.8 km. Mudge et al. (2011) analysed Canadian Ice Service (CIS) records from 1982 to 2010 and studied two passages of Viscount Melville Sound (VMS) by CCGS Amundsen in order to assess feasibility of navigation in the Canadian Arctic region. The authors observed a high degree of spatial and temporal variability in ice conditions in the area of the Northwest Passage with large seasonal variations. The study indicated the importance of timely and accurate ice information in making the Northwest Passage feasible for trade as numerical models are not inaccurate. Erceg et al. (2013) tested the economic feasibility of higher polar classes for LNG transit operations on the route from Rotterdam to Yamal. Reimer et al. (2013) simulate the impact of a Northern Sea route on exhaust gas emission, as well as travelling time. Way et al. (2015) examined the use of speed optimization to determine whether it is potentially more profitable for a container shipping company to ship from Rotterdam to Yokohama through the Suez Canal year round, or to ship through the Northern Sea route during the months it was passable. Monte Carlo simulations were used to calculate the average profit per trip, with the main parameters being the fuel consumption and speed of an ice-class and non-ice-class vessel. The speed in ice-covered water was considered independent of the ice. It was indicated that the variability in schedule might be more suited to bulk shipping than containerized shipping.

Warning and Decision Support Systems

Several authors have studied relations between spectral parameters and occurrence of extreme or rogue waves and the topic is also investigated in the EC EXTREME SEAS project. Clauss et al. (2009) used a short-crested, multi-directional forecast to predict encountering wave trains for alternative cruising velocities and courses. Mori et al. (2011) used Monte Carlo simulations on the Nonlinear Schrodinger equation in two horizontal dimensions and found that increasing directional spread decreases kurtosis, a parameter accepted to be related to higher probability of rogue wave occurrences. On the other hand Tofioli et al. (2011b) found higher kurtosis values when analysing waves in bimodal sea states, with higher occurrences when directional differences were between 20 and 40 degrees.

The distribution of encountered wave slope was used to predict risks for capsizing of vessels, see Leadbetter et al. (2011) and Aberg et al. (2008) for the theoretical background of the method. The development of decision support systems remains in focus. As proposed by Nielsen et al. (2011) and Nielsen and Jensen (2011), they require the collection of relevant data e.g. metocean, ship response, on board. These types of data can also be used for self-learning (see the EC project NavTronic for example). Utne et al. (2017) gave a list of risk-influencing factors for autonomous marine systems, based on the operation and environment parameters, and how those factors can be used proactively (planning) or reactively (decision support). Alford et al. (2016) describe a real-time multi-ship environmental and ship motion forecasting system, using off-the shelf marine radar to give 30s predicted ship motions and identify relevant warning criteria. Reite et al. (2017) present a generic framework that combines onshore analysis of historical data and a tool for real-time decision support onboard to optimize hybrid propulsion of a fishing vessel. This allows for decision support based on measurements rather than mathematical models

Search and Rescue operations require specific decision support systems. Their planning relies on accurate forecasting of the drift of objects under search. The most widely used approach for drift assessment is based on the Leeway method in which Leeway coefficients taking into account combined action of wind and waves are experimentally identified for various classes of objects allowing assessment of drift velocity and direction as a function of wind speed. Breivik et al. (2011) propose a standardised method for assessment of Leeway coefficients from field experiments. Uncertainties in forcing fields (wind and currents) as well as other information such as initial date and location of the drift are accounted for when introducing a stochastic approach based on a Monte Carlo technique for the computation of an ensemble of equally probable perturbed trajectories (Breivik et al., 2008).

Accuracy of drift prediction is highly dependent on the quality of the forecasting of environmental data. It was pointed out during the 4th Int. Workshop on Technologies for Search And Rescue and other Emergency Marine Operations (2011) that the use of HF-radar and Lagrangian oats (SLDMBs) data for assimilation or correction of current can provide efficient improvement of the accuracy of the drift prediction. Iyerusalimskiy et al. (2011) present a state-of-the-art ice load monitoring and alarm system that was installed on a large icebreaking tanker operating between the Barents Sea and Murmansk. The system is designed to measure and record in real time the ice pressure and loads and calculates structural responses in selected locations on the hull.

The scale of the environmental forecast can have an effect on the quality of the warning system. Sasa (2017) describes the optimal routing of short-distance ferries from the evaluation of mooring criteria. For short-distance ferries, ocean wave monitoring systems cause difficulty and confusion because they represent typhoons and depressions that are several hundred kilometers away. Therefore, a different system is devised based on the motions of the ships moored in the harbour, which is more relevant to short-distance ferry services.

Dong et al (2016) proposed the decision support system for a mission by multi performance criteria on ship routing. The criteria aspects considered consist of the expected repair cost, fatigue damage, travel time, and CO2 emission. Furthermore, the risk is also taken into account from the decision maker aspect by integration into the presented approach of utility theory.

Since the encountered metocean conditions will have direct impact on the ship/offshore structural safety, energy efficiency, and emissions during their operation stages, most of ocean-crossing vessels are instrumented with voyage planning or weather routing systems. Such systems can be used to assist ship operation in a more optimal way based on weather forecast information. Furthermore, due to the strict regulation on energy efficiency and air emissions from shipping industry, a large amount of research and innovation within the maritime community have been devoted to develop wind propulsion technologies which utilize wind power to provide auxiliary propulsion forces to ships. Loyd's report (Loyd 2015) and Dagmar et al. (2016) have carried out in-depth analysis on the commercial and technical opportunities and challenges to use wind propulsion technologies in shipping industry. The actual benefits of such technologies pretty much depends on the possible encountered wind and wave conditions a ship may encounter during her service life, as well as the ship's performance in the complex metocean conditions. In Mao and Rychlik (2017), a spatio-temporal wind model is developed based on the transformed Gaussian process using 30 years of environment data from European Centre for Medium-Range Weather Forecasts (ECMWF) and measurements in ships. This model can be used to simulate the wind conditions encountered by a vessel to study the potential wind propulsion energy after the installation of such technologies. Furthermore, similar as the ordinary ship operation in the open sea, to get the best benefit from the wind propulsion technologies will rely even more on the voyage optimization, which helps to choose the best optimal wind conditions for ship navigation (Lu et al.2017). In a preliminary study by Mao et al. (2012), a simple configuration of route planning through change of possible departure time leads to encounter better metocean conditions during a ship's sailing. It is illustrated that using voyage planning has the potential to reduce at least 50% of the fatigue damage accumulation in ship structures when crossing North Atlantic Ocean. In Simonsen et al. (2015), different algorithms used in today's weather routing market have been reviewed. Their cons and pros with respect to optimization capabilities and objectives to enhance ship safety, energy efficiency, and expected time of arrival are also discussed in the paper. In the more recent paper by Wang et al.(2017), a further benchmark study regarding most of the available optimization algorithms in the maritime community has been carried out with its focus on their capability of voyage planning with minimum fuel cost through optimal choice of optimal encountered metocean (wind, wave and current) conditions during sailing. A similar system is also studied by Vettor and Guedes Soares (2016) with a bit focus on the ship's performance when operating at sea and wave spreading.

1.2 Waves

There has been significant progress in both phase-resolved wave modelling and observations of the sea surface over a spatial domain. Again, this is distinct from the more traditional statistical processing of time series collected at a single point in space. Much of the effort in phase-resolved wave measurements has centered on marine RADAR, which can be noncoherent radar (e.g., Qi et al, 2016), or can use coherent Doppler processing (Connell et al. 2015). Other remote sensing approaches include airborne scanning LIDAR (e.g., Reineman et al, 2009), shipboard stereo video (e.g., Schwendeman & Thomson, 2017), and satellite images of sun glitter (Kudryavtsev et al, 2017). Recently, there has also been progress in using arrays of buoys or other point measurements to reconstruct a phase-resolved sea surface (e.g., Takagi et al, 2017).

1.3 Wind

As indicated above, surface wind vectors are vital for operational and scientific issues. For instance, they are routinely used as primary forcing function component for ocean circulation, wave, and current models at global and/or local scales. They have great impact on coastal upwelling, cross shelf transport, deep water formation, and ice transport and variability. They are essential for reliable estimation of momentum (wind stress vector), heat fluxes (latent and sensible), mass flux (e.g. CO_2 and H_2O). They are used to investigate the climate change as well as the storm surge and wave forecasts.

The knowledge of surface wind vectors are requested with various characteristics depending upon the atmospheric, oceanic, and climate application. However, better global spatial and temporal resolutions as well as accuracy are highly needed.

The surface wind vectors are routinely derived from in-situ (mooring buoys, ships) and satellite radar and radiometers measurements, and from numerical weather prediction (NWP) models.

Surface wind speed and/or directions and the related parameters (wind stress, wind divergence, wind curl, and turbulent heat fluxes) are derived from remotely sensed observations. The latter are retrieved from onboard satellite radars and radiometer such as scatterometers, altimeters, radiometers, and SAR. Scatterometer provide, over free land and ice global oceans, both wind speed and direction over a wind vector cell (WVC) of 25km×25km and/or 12.5km×12.5km cross swaths varying between 500km and 1800km width. Altimeters and radiometer provide only wind speed estimates over free and ice global oceans. SAR measurements enable the estimation of wind speed and direction with very high spatial resolution (lower than 1km) at some selected oceanic areas.

The satellite wind products are available with various levels. L2b, L3, and L4 levels are associated with wind retrievals over instrument swath or along track, spatial gridded swath data, and space and time gridded wind fields, respectively. The processing, archiving, and dissemination of satellite products are handled by several space agencies and/or research organizations. Following are some useful links (not exhaustive):

http://cersat.ifremer.fr/

https://podaac.jpl.nasa.gov/OceanWind

http://www.remss.com/

https://sentinels.copernicus.eu/

http://marine.copernicus.eu/

http://www.osi-saf.org/

http://projects.knmi.nl/scatterometer/

In near future, three satellites will be launched in 2018 with onboard scatterometers, radiometers, and/or altimeters. The Chinese-French Ocean Satellite CFOSAT (CNES, NSOAS and CNSA). Two payloads are on-board: the French SWIM (Surface Waves Investigation and Monitoring), a real-aperture radar with a low-incidence conical-scanning beam for directional wave spectra and wind, and a Chinese wind scatterometer with a rotating fan-beam antenna. The EUMETSAT satellite METOP-C will carry on ASCAT-C scatterometer as a part of payload including Advanced Microwave Sounding Unit - A (AMSU-A), Advanced Very High Resolution Radiometer / 3 (AVHRR-3), Global Ozone Monitoring Experiment – 2 (GOME-2), and infrared Atmospheric Sounding Interferometer (IASI), and Microwave Humidity Sounding (MHS). The third program is OceanSat-3 satellite operated by the Indian Space Research Organisation (ISRO). OceanSat-3 payload includes ku-band pencil beam scatterometer, 13-band Ocean Colour Monitor (OCM), and 2-band Long Wave InfraRed (LWIR).

Several satellite projects aiming at the observation of surface wind speed and direction over the global oceans are planned. The Post EUMETSAT Polar System (Pot-EPS named) with second generation scatterometer (SCA) is expected for 2022. The China National Space Administration (CNSA) will operate the program HY-3C expected for 2020. The Russian research organisation Research Center for Earth Operative Monitoring will be in charge of operating METEOR-M N3 satellite, expected for 2020. The Japan Aerospace Exploration Agency's (JAXA's) will maintain the satellite series contributing to climate change research and monitoring through the Global Change Observation Mission (GCOM) satellites. GCOM-W2 and GCOM-3 are planned for 2019 and 2022, respectively.

1.4 Climate

1.4.1 Increasing uncertainty and risk due to climate change.

Several studies on the environmental global climate have emerged recently, with a great concern about future climate changes, risks and impacts. The problems regarding the climate changes are much more associated with local impacts of extreme events than the global average, which tends to be smoothed out. Changes in extreme weather and climate events have been observed since 1950. Some of these changes have been linked to human influences, including a decrease in cold temperature extremes, an increase in warm temperature extremes, an increase in extreme high sea levels and an increase in the number of heavy precipitation events in a number of regions. IPCC-AR5(2014) describe that continued emission of greenhouse gases will cause further warming and long-lasting changes in all components of the climate system, increasing the likelihood of severe, pervasive and irreversible impacts for people and ecosystems. The observed changes in the climate were found to be very heterogeneous; therefore, risks are unevenly distributed and are generally greater for disadvantaged people and communities in countries at all levels of development (IPCC-AR5, 2014).

Bitner-Gregersen (2017) corroborates the local dependences of wind and wave climates, affected by local properties of ocean environment, which impact ship design and marine operations, and they challenge ability of ships to maintain manoeuvrability in sea states. Bitner-Gregersen (2017) present differences between open sea and coastal water wind and wave climate using hindcast data. The study discussed the challenges in providing metocean description for assessment of ship manoeuvrability and uncertainties related to it. The risk of climate-related impacts results from the interaction of climate-related hazards with the vulnerability and exposure of human and natural systems, including their ability to adapt (IPCC-AR5, 2014). Rising rates and magnitudes of warming and other changes in the climate system, accompanied by ocean acidification, increase the risk of severe, pervasive and in some cases irreversible detrimental impacts.

1.4.2 Sea Level Rise

Coastal communities throughout the world are exposed to numerous and increasing threats, such as coastal flooding and erosion, saltwater intrusion and wetland degradation (Rueda et al., 2017). Flooding is one of the most dangerous consequences related to climate changes. Rueda et al. (2017) present the first global-scale analysis of the main drivers of coastal flooding due to large-scale oceanographic factors, which is a multidimensional problem (e.g. spatiotemporal variability in flood magnitude and the relative influence of waves, tides and surge levels). Rueda et al. (2017) show that 75% of coastal regions around the globe have the potential for very large flooding events with low probabilities, 82% are tide-dominated, and almost 49% are highly susceptible to increases in flooding frequency due to sea-level rise. Over the period 1901–2010, global mean sea level rose by 0.19 [0.17 to 0.21] m and the rate of sea level rise since the mid-19th century has been larger than the mean rate during the previous two millennia, according to IPCC-AR5 (2014). This report, based on tide gauge and satellite altimeter, shows that is very likely that the mean rate of global averaged sea level rise was 3.2 [2.8 to 3.6] mm/yr between 1993 and 2010. Under all Representative Concentration Pathways

(RCP) scenarios from IPCC-AR5 (2014), the rate of sea level rise will very likely exceed the observed rate of 2.0 [1.7–2.3] mm/yr during 1971–2010, with the rate of rise for RCP8.5 during 2081–2100 of 8 to 16 mm/yr.

2. LONG TERM STATISTICS AND EXTREME VALUE ANALYSIS

Long-term distributions and Extreme Value Analysis play an important role on marine projects, metocean design criteria and coastal management. The process of estimating extreme quantiles associated with return periods of interest involves large uncertainties and long processes vulnerable to error propagation; as for example from input data with intrinsic biases, storm selection, idealized requirements of distribution functions and extrapolation. Widely-used methods, as Peaks Over Thresholds (POT), assume that events are identically distributed, the process is stationary and events are independent – which is nearly impossible to find in environmental time-series as winds, waves and currents. Thus, several studies have emerged investigating the possible trends in the frequency of events, duration of the storms, statistical models to better extrapolate the quantile functions and spatial techniques.

Godoi et al. (2017) studied extreme events of waves in New Zealand using 44 years of hindcast data. They found the interannual variability is largest along the north coast of the country and on the east coast of the South Island, suggesting relationships with La Niña-like effects and the Southern Annular Mode. They argue the known trend for a more positive Southern Annular Mode may explain the increasing number of extreme events shown in their study. Sartini et al. (2015), at the Italian coast, calculated return levels by the Goda method, the Generalized Extreme Value (GEV) and the Generalized Pareto Distribution–Poisson point process models and the Equivalent Triangular Storm (ETS) algorithm. All models follow the Peak-Over-Threshold (POT) approach which require an optimal threshold implementation, save for the GEV analysis, which is applied to model significant wave height maxima pertaining to time-blocks. Sartini et al. (2015) argues in favor of the versatility of the GPD–Poisson model, while the GEV and ETS models exhibit limitations in assessment of a variety of wave fields, greatly diversified in semi-closed basins. Sulis et al. (2017) compared the results of the most commonly used extreme wave analysis methods applied to a 20 year wave hindcast in the Gulf of Cagliari (South Sardinia, Italy). While conventional distributions recommended by Goda (e.g. the Gumbel and Weibull distribution) represent the most common methods in engineering applications, accurate results in the paper indicate that the community should consider the Generalized Pareto Distribution (GPD) as one of the most performing credible candidates. Sulis et al. (2017) corroborates with several previous studies, including Campos et al. (2016) who achieved the best results using Pareto, Pearson Type-3 and Weibull distributions.

Laface et al. (2016) propose a new solution, in the context of equivalent storm models, for long-term statistics of ocean storms. The paper has proposed a new model for an improvement of the class of equivalent storm models that are widely used in maritime engineering for investigating the long term statistics, coastal processes as well as for the evaluation of progressive damage of coastal structures. Laface et al. (2016) explain that the main concept consists of replacing the actual storm with an equivalent one, from a specific perspective, depending on the scope of the analysis to perform. Finally, in comparison with previous methods, their solution provides a better representation of actual storm duration.

In the structures design, short and long term statistical distributions of wave height, crest height and wave periods, as well as joint distributions, are important for structural integrity assessment. Hagen et al. (2017) combined the short-term statistics with the long-term scatter diagram for an offshore location at the Norwegian and long term scatter diagrams generated. Based on these scatter diagrams, extreme value estimates are calculated for wave height and crest height, and corresponding wave periods determined. They found that wave periods generated are somewhat shorter than prescribed in design recipes. Authors also investigated the

statistical uncertainty of extreme value estimates as function of number of simulations. Muraleedharan et al. (2015) deeply studied the distribution of significant wave height and associated peak periods using 21 years of wave hindcast in the North Atlantic. The joint distribution of wave heights and periods are extremely important for offshore structures and ship motions. Moving to a multivariate study, Zhou et al. (2017) investigated the extreme water level, current velocity and wave height in Laizhou Bay, China using simulation results from MIKE21 and Gumbel distribution.

Considering that wave spectra often exhibit multiple peaks due to the coexistence of wind waves and swells, Laface et al. (2017) described the waves by partitioned sea states that can be interpreted physically as representing independent wave systems. The sensitivity of return values of significant wave height to swell contribution was investigated via an application of the Equivalent Triangular Storm Model (ETS). The results of Laface et al. (2017) show that the contribution of swell is more significant for storms of small and medium intensity and decreases for increasing storm intensities. Further return values variability neglecting swell is less than 7% at any point for return periods up to 100 years.

As an alternative to extreme value analyses based on hindcast data, Wimmer et al. (2016) estimated return values of significant wave height directly from measurements by satellite altimeters over the North Atlantic. Return values were calculated by fitting a Generalized Pareto Distribution to all values above a threshold, which was allowed to vary spatially. The novel method of Wimmer et al. (2016) gave return values that were up to 37% smaller than those estimated by fitting a Fisher-Tippet distribution to all the data.

The spatial and regional distributions of extreme quantiles have been further explored during the last few years. Sartini et al. (2017) studied the spatial and temporal modelling of extreme wave heights in the Mediterranean Sea based on a 37-year wind and wave hindcast database at 10-km resolution. A point-wise Generalized Extreme Values model was employed to generate the assessments results. Overall, the spatial model proved capable of providing an accurate description of extreme return levels of significant wave heights and their spatial variability, especially on a basin-wide scale and with greatest precision on the mesoscale. However, Sartini et al. (2017) argues that return level estimates are found less reliable in certain coastal areas because the traditional point-wise approach is not refined enough to address the entire wave spectrum of an area as complex as the Mediterranean Sea. Sartini et al. (2017) incorporated the Mean Sea Level Pressure fields as covariates to improve localized assessment. These covariates represent meteorological forcing and allow analysis of the role of different cyclonic regimes in defining wave features and their spatial variability.

A number of studies recently applied the method developed by Hosking and Wallis (1997): Regional Frequency Analysis (RFA) based on L-moments. Although it was initially developed for flood events, it was adapted to extreme winds and waves. The RFA consists of using data from different sites with related statistics to better estimate the quantile function, which can be used for regional or site-specific analyses. The concept comes from the fact that if event frequencies are similar for different observed quantities, more robust conclusions can be reached by analyzing all of the data samples together than by using only a single sample. As most extreme analyses are based on hindcast data with regular grid resolutions, RFA suggests that the inclusion of neighboring grid-points improves the estimate of the quantile functions (Campos and Guedes Soares, 2016). Additionally, RFA is especially suitable for long return values extrapolations and short time-series lengths; because it trades space for time, reducing the confidence interval amplitude even in very long return periods. Campos and Guedes Soares (2016) applied the RFA based on L-moments to calculate spatial extreme return values of significant wave height in the South Atlantic Ocean. They obtained reliable extreme return values at each grid point with very low variance of the distribution parameters estimators and narrow confidence intervals. Considering the return period of 100 years, the significant wave heights vary from 5.5 to 11.2 meters within the considered domain in southern and southeast-

ern Brazil. In the North Atlantic Ocean, Lucas et al. (2017) applied the RFA for several locations at the coast of Portugal using data from HIPOCAS (Hindcast of Dynamic Processes of the Ocean and Coastal Areas of Europe).

The regionalization and exclusion of sites with discordant statistics are essential steps of the RFA, as well as the goodness-of-fit tests applied to the regional quantile functions. Hosking and Wallis (1997) defined a heterogeneity test for selected regions and a goodness-of-fit test based on the kurtosis of the empirical and modeled distributions. Vanem (2017) applied RFA on extreme significant wave heights in the North Atlantic Ocean for historical and projected ocean wave climates. A set of homogeneous regions were identified as ocean regions with similar characteristics, and the effect of climate change on the ocean wave climate could be studied, both with regards to changes in extreme quantiles at certain location and to overall spatial changes. Results from Vanem (2017) confirm that RFA can be useful in the analysis of extreme ocean waves. In particular, regional frequency analysis yields narrower uncertainty bounds and hence more robust estimation of extreme quantiles, corresponding to long return periods.

2.1 Long Term Measurements and Data

Long and reliable environment data is the first step for any climate characterization, extreme value analysis, ship design and coastal management. As it is the primary information in projects at sea, the reliability and accuracy of such data is crucial. Buoy and satellite measurements are preferred sources of data when compared to hindcasts but it must be properly quality controlled, organized and sufficiently long. The Centre ERS d'Archivage et de Traitement (CERSAT) of the French Research Institute for Exploitation of the Sea (IFREMER) is a center that continuously organizes, evaluates, quality controls and calibrates all the altimeter data public available, providing reliable netcdf output files easy to handle, which facilitates the use. They provided a public database with easy access at:

ftp://ftp.ifremer.fr/ifremer/cersat/products/swath/altimeters/waves/data

Queffeulou and Croizé-Fillon (2017) describe in detail the data and the methodology applied in the CERSAT/IFREMER satellite wave data processing and quality control. Regarding heave-pitch-roll buoys, CERSAT/IFREMER has also systematically organized and quality controlled the data joining a vast amount of buoys, which can be downloaded at:

ftp://eftp.ifremer.fr/globwave/insitu_final_format/oceansites/wave_sensor/

ftp://eftp.ifremer.fr/globwave/insitu_final_format/coriolis/wave_sensor/

The National Data Buoy Center has also provided quality controlled buoy data, public available and organized at the following site:

http://www.ndbc.noaa.gov/historical_data.shtml

The crossing information of in-situ buoy data with satellite tracks allows the cross-validation and calibration of datasets. Joining many sources of measurements, Young et al. (2017) performed a calibration and cross validation of global wind and wave database of altimeter, radiometer, and scatterometer measurements. A combined satellite dataset consisting of nine altimeter, 12 radiometer, and two scatterometer missions of wind speed and wave height is calibrated in a consistent manner against NDBC data and independently validated against a separate buoy dataset. Young et al. (2017) investigated the performance of each of the instruments at extreme values using quantile–quantile comparisons with buoy data. The various instruments were cross validated at matchup locations where satellite ground tracks cross. The resulting calibrated and cross-validated dataset from Young et al. (2017) is believed to represent the largest global oceanographic dataset of its type, which includes multiple instrument types calibrated in a similar fashion.

When measurements are not found or insufficiently long, the use of numerical modeling simulated for preterit conditions become important. Numerical hindcasting from surface winds provides essential space-time information to complement buoy and satellite observations for studies of the marine environment. Several reanalyses have been developed and evaluated, becoming nowadays a reasonably trustful source of information, especially in deep waters and open areas. The European Centre for Medium-Range Weather Forecasts (ECMWF) and the National Centers for Environmental Prediction (NCEP) are the main centers continuously generating reanalysis data. In terms of recent developments, ERA-20C is ECMWF's first atmospheric reanalysis of the 20th century, from 1900-2010. It assimilates observations of surface pressure and surface marine winds only, being an outcome of the ERA-CLIM project. Different from the previous reanalysis, ERA-20C is an extremely long source of data which allows deeper investigations on climate changes, projections of long-term events and site characterizations. Poli et al. (2016) describe the reanalysis which can be found at:

https://www.ecmwf.int/en/research/climate-reanalysis/era-20c

The main limitations of the reanalysis products are the simulations under extreme conditions and coastal areas, due to the resolution of the grids. Perez et al. (2017) recently developed a global wave hindcast for coastal applications, GOW2. This information is extremely useful for coastal studies and can be used both directly or as boundary conditions for regional and local downscalings. For developing the GOW2 hindcast, WAVEWATCH III wave model is used in a multigrid two-way nesting configuration from 1979 onwards. The multigrid includes a global grid of half degree spatial resolution, specific grids configured for the Arctic and the Antarctic polar areas, and a grid of higher resolution (about 25 km) for all the coastal locations at a depth shallower than 200 m. Available outputs include hourly sea state parameters (e.g. significant wave height, peak period, mean wave direction) and series of 3-h spectra at more than 40000 locations in coastal areas. Comparisons with instrumental data from Perez et al. (2017) show a clear improvement with respect to existing global hindcasts, especially in semi-enclosed basins and areas with a complex bathymetry. The effect of tropical cyclones is also well-captured thanks to the high resolution of the forcings and the wave model setup. Li et al. (2016) used WAVEWATCH III and SWAN models in a nested grid system to model basin-wide processes as well as high-resolution wave conditions around the Hawaiian Islands from 1979 to 2013. The wind forcing included the Climate Forecast System Reanalysis (CFSR) for the globe and down-scaled regional winds from the Weather Research and Forecasting (WRF) model. The hindcast of Li et al. (2016) captures heightened seas in interisland channels and around prominent headlands, but tends to overestimate the heights of approaching northwest swells and give lower estimates in sheltered areas. With the rapid increase of computational power, the reanalysis and hindcasts in the future tend to have higher resolution, more robust data assimilation, and better physics, which significantly improve the quality of data at coastal regions and under extreme conditions.

Using the wave model WAVEWATCH III, Beya et al. (2017) developed a calibrated hindcast for the coast of Chile. A correction method was applied to the statistical parameters in order to reduce systematic errors of the model. Beya et al. (2017) constructed an Atlas that showed better performance when compared to existing databases under normal wave conditions. They reported deficiencies in estimating of extreme values, which has important consequences in the design of coastal structures.

As an alternative to the use of traditional hindcasts based on numerical models, Jane et al. (2016) investigated the spatial dependence of the wave height at nearby locations applying a new copula-based approach for predicting the wave height at a given location. By working directly with wave heights, it provides an alternative method to hindcasting from observed or predicted wind fields when limited information on the wave climate at a particular location is

available. It is shown to provide predictions of a comparable accuracy to those given by existing numerical models.

Finally, the local knowledge at the coast can be additional important information to evaluate the sea level and wave climate, as discussed by Reineman et al. (2017). By examining the local knowledge of more than one thousand California surfers collected through an online survey, Reineman et al. (2017) extrapolates their evaluations to estimate the susceptibility of California surf-spots to sea level rise based on the principle of tidal extrapolation. Vulnerability classifications are derived from the relationship between wave quality, tide effects, and sea floor conditions.

2.2 Wave Climatology

A number of studies over the last decade have shown that over the last 30 years the ocean surface wind and wave climate has changed on global and regional scales. Although these reports are based on a number of different observational techniques, including ship observations and satellite data, all show a consistent positive trend over the last decades, with extreme values growing faster than the mean. Magnitude of the reported trends can be different, depending on the instrumentation used for observations (for example, global wind trends based on SSM/I radiometers are only half of those reported by altimeter measurements (Young et al., 2011a, b)).

Model hindcasts (reanalyses) did not show such consistency. There are two main third-generation wave models used for global applications, WAVEWATCH-III (American) and WAM (European). Long-term forecasts are available for both of them. Here, we will refer to Durant et al. (2014), which is a 30-year hindcast with WW3 (1979-2009), and Aarnes et al. (2015) reanalysis of the ERA-Interim hindcast with WAM for the period of 1979-2012. The latter was done for two stand-alone ECMWF (European Centre for Medium-range Weather Forecast) operational wave model (EC-WAM) runs with and without wave altimeter assimilation.

Durant et al. (2014) focusses on the Central and South Pacific, which is the main area of controversy with respect to the model hindcasts. Here, it can be noted that trends in the Southern Ocean throughout the full period are not reliable and, contrary to the observations, can be even negative. These are due to discontinuities in the CFSR wind data set used to force the wave model. The discontinuity is apparent around 1993/1994.

Trends in the ERA-Interim wind and wave data were investigated by Aarnes et al (2015). They found that in general the trends in this data set are affected by the introduction of assimilation of the altimeter wave height data in 1991. The authors note that the 48 hour forecast values (t=48), rather than the current analysis at t=0, may be more suitable for calculating the trends. This is because while the data assimilation generally has a large effect at t=0, this effect is somewhat reduced after a few days of model integration. The authors also note that their calculated wind and wave trends are somewhat different to those of Young et al (2011); in general they are smaller and do not show significant positive trends at high latitudes.

Thus, regardless of many details not mentioned here, we can point out two major problems with using the model reanalysis data for investigating weak long-term metocean trends. First, since the wave models are forced by outputs of the wind models, change of practice or tuning the winds may affect the predicted wave trends significantly or even adversely. Second, the introduction of assimilation of in situ and, particularly, satellite remote sensing data makes the model performance inconsistent throughout, particularly as the influence of data assimilation on the model outputs is ever-growing.

Therefore, the satellite observations, which are available for almost the same period as the longest modelling hindcasts, and provide global coverage (although not with the same spatial and temporal resolution), exceedingly become the main benchmark for metocean climate and

its trends. Young et al. (2017) proposed an extended work on the earlier altimeter analysis of wind-wave trends, by combining data of other satellite metocean platforms and by trying to reconcile the earlier discrepancies with radiometers.

The combined satellite dataset consists of nine altimeter, 12 radiometer, and two scatterometer missions of wind speed and wave height and is calibrated in a consistent manner against NDBC data and independently validated against a separate (ECMWF) buoy dataset. The various instruments are cross validated at matchup locations where satellite ground tracks cross. The resulting calibrated and cross-validated dataset is believed to represent the largest global oceanographic dataset of its type, which includes multiple instrument types calibrated in a similar fashion. This work provides satellite calibrations against buoys for all the missions mentioned. Careful analysis of the methods for recovering the wind speed allowed bringing altimeter and radiometer/scatterometer wind trends much closer to each other. It worth noticing here that both systems have a fair weather bias at wind speeds exceeding 20 m/s and hence the extreme wind speeds may be underestimated.

In 2011, Chinese altimeter mission Hai-Yung-2 was launched. Liu et al. (2016) found wave-height trends similar to the other altimeter missions, but wind-speed measurements are not calibrated at this stage.

2.3 Climate Trends and Uncertainty

Ocean waves and surface winds significantly affect coastal structures and offshore activities and impact many vulnerable populations of low-lying islands. Therefore, better understanding of their variability plays an important role in potentially reducing risk in such regions. With the increase of in-situ and remotely-sensed data, as well as reanalysis products, the study of climate trends and intrinsic uncertainties has improved in the recent years. Ulbrich et al. (2009) performed a fundamental study on extra-tropical cyclones in the present and future climate. Based on the availability of hemispheric gridded data sets from observations, analysis and global climate models, objective cyclone identification methods were developed and applied. Thus, Ulbrich et al. (2009) give a comprehensive review of the actual knowledge on climatologies of mid-latitude cyclones for the Northern and Southern Hemisphere for the present climate and for its possible changes under anthropogenic climate conditions. In the Northern Hemisphere, Ulbrich et al. (2009) describe that under anthropogenic climate change (ACC) conditions, the number of all cyclones will be reduced in winter, but in specific regions (over the Northeast Atlantic and British Isles, and in the North Pacific) the number of intense cyclones increases in most models. For the average over the hemisphere, an increase in the number of extreme cyclones is found only when "extreme" is defined in terms of core pressure, while there is a decrease in several models when defining "extreme" from the Laplacian of surface pressure or vorticity around the core. In the Southern Hemisphere, Ulbrich et al. (2009) describe that under ACC conditions a southward shift of this band is identified, more or less meridional equally distributed. This will lead to less cyclonic activity around 50°S and increased activity around 60°S. Results of Ulbrich et al. (2009) are in agreement with IPCC AR4 report stating that "*the most consistent results from the majority of the current generation of models show, for a future warmer climate, a poleward shift of storm tracks in both hemispheres that is particularly evident in the SH, with greater storm activity at higher latitudes.*"

Kumar et al. (2016) investigated the influence of climate variability on extreme ocean surface wave heights using ECMWF reanalysis. In this study, global impacts of natural climate variability such as El Niño–Southern Oscillation (ENSO), North Atlantic Oscillation (NAO), and Pacific decadal oscillation (PDO) on extreme significant wave height (SWH) were analyzed using ERA-Interim (1980–2014) and ECMWF twentieth-century reanalysis (ERA-20C; 1952–2010) datasets. The major ENSO influence on Hmax is found over the northeastern North Pacific (NP), with increases during El Niño and decreases during La Niña, and its coun-

ter responses are observed in coastal regions of the western NP. Composite analysis of different ENSO and PDO phase combinations reveals stronger (weaker) influences when both variability modes are of the same (opposite) phase. Overall, Kumar et al. (2016) found that the response of extreme significant wave heights to natural climate variability modes is consistent with seasonal mean responses.

Focused on coastal areas, Barnard et al. (2015) synthesized multi-decadal, co-located data assimilated between 1979 and 2012 that describe wave climate, local water levels and coastal change for 48 beaches throughout the Pacific Ocean basin. They found that observed coastal erosion across the Pacific varies most closely with El Niño/Southern Oscillation, with a smaller influence from the Southern Annular Mode and the Pacific North American pattern. Barnard et al. (2015) concluded that, if projections for an increasing frequency of extreme El Niño and La Niña events over the twenty-first century are confirmed, then populated regions on opposite sides of the Pacific Ocean basin could be alternately exposed to extreme coastal erosion and flooding, independent of sea-level rise.

Important studies were published concerning the prediction of possible climate trends. Martínez-Asensio et al. (2016) studied the ability of statistical wind-wave models to capture the variability and long-term trends of the North Atlantic winter wave climate. Stefanakos and Vanem (2017) obtained very good results of climatic forecasting of wind and waves using fuzzy inference systems. Stefanakos and Vanem (2017) models are coupled with a nonstationary time series modelling, which decomposes the initial time series into a seasonal mean value and a residual part multiplied by a seasonal standard deviation. Two long-term datasets for an area in the North Atlantic Ocean were used, namely NORA10 (57 years) and ExWaCli (30 years in the present and 30 years in the future). Muraleedharan et al. (2016) investigated regression quantile models for estimating trends in extreme significant wave heights in two Portuguese locations, using 44 years hindcast produced in the HIPOCAS project. The regression quantile models of Muraleedharan et al. (2016) showed the ability to model the historical trends that may subsist in long term data sets, a feature that the traditional fitting of extreme distributions does not account for. Hithin et al. (2015) studied trends of wave height and period in the Central Arabian Sea using satellite altimeter data from 1996 to 2012. Hithin et al. (2015) showed a positive trend of 0.63 cm/yr in the annual mean significant wave height. In contrast, a negative trend of 2.66 cm/yr is found for the annual maximum significant wave height due to the decreasing trend of extreme tropical cyclone events. The annual mean and maximum wave period show a decrease of 0.005 s/yr and 0.011 s/yr, respectively.

2.4 More measurement in extreme conditions

Extreme meteorological and oceanographic (metocean) conditions are essentially air-wave-sea interaction phenomena. To describe, simulate and predict the extreme storms, both tropical and extra-tropical, often extrapolations from moderate conditions are used, but physics of air-sea interactions, wave dynamics, atmospheric boundary layer (BL), upper ocean currents and mixing, are very different in extreme weather conditions (see e.g. Babanin (2011) for a review).

In the atmosphere, the effect of sea-drag saturation was confirmed in field and laboratory observations where the critical wind speed at 10 m reference height U10 was found as

$$U_{10} = 32\text{-}33 \text{ ms}^{-1} \quad (1)$$

Physics of the drag saturation, i.e. of change of the dynamic regime of the atmospheric boundary layer, is complex and at this stage not clear. The ocean surface at hurricane winds, even visually, enters a different dynamic regime, with sporadic whitecaps replaced by surface where the foam extends from crest to crest and interface becomes hazy. Wave asymmetry saturates at wind speeds of

$$U_{10} \approx 34 \text{ ms}^{-1} \quad (2)$$

which signifies change of the mechanism for wave breaking: from the breaking being driven by nonlinear evolution of steep water waves to the breaking being caused by the direct wind action. Subtle by comparison are changes of the dynamic regime in the upper ocean at extreme conditions and of the air-sea gas exchanges, but they do occur and occur at approximately the same threshold wind speeds: the fluxes still grow rapidly, but in relative terms at a much lower rate by comparison with the moderately strong winds. Furthermore, bubble injection becomes the dominant mode of gas transfer. Change of regime of the air-sea gas transfer is observed at

$$U_{10} > 35 \text{ ms}^{-1} \quad (3)$$

Thus, the general consensus in the community is that wind speeds in the range of 30-40 ms^{-1} signify a regime change. This means that extrapolations of measurements, dependences and mechanisms obtained in benign and moderately strong conditions should be re-validated and used with extreme caution when applied to tropical cyclones and perhaps extreme extratropical storms too. It is likely that these mechanisms, and therefore the respective dependences, are different, and are yet to be explicitly obtained, described and parameterized.

Progress of in situ observations is vital for extreme-weather science, because of uncertainty of some estimates, for example, source functions for spray production, can be many orders of magnitude. On the atmospheric side, structure and composition of the boundary layer close to the surface needs to be understood. This requires measurements of wind profiles in the constant-flux layer (up to 100-200 m above the surface) and preferably within the wave boundary layer (10-20 m), which is the sublayer with its specific dynamics due to spray and wave-coherent pressure/velocity oscillations (Babanin and McConochie, 2013).

Most of the fluxes are created, moderated or facilitated by the waves on the ocean interface. Therefore, accurate measurements of waves, including their full frequency-wavenumber directional spectra are necessary. Among the wave measurements, significance of wave breaking in formation of the fluxes is hard to overstate. Near-surface turbulence, both on the oceanic and atmospheric sides, radiation stresses, injections of air bubbles into the water, which facilitate gas exchanges, and emission of spray into the air, which accelerates evaporation, disruption of the skin layer and hence intensification of the heat transport - these and other dynamic and thermodynamic features and small-scale processes between the atmosphere and the ocean owe their rates and very existence to the wave breaking. Stereo-imaging, particularly high-speed and high-resolution video recording can provide detailed information of the three-dimensional surface behaviors of this kind (Fedele et al., 2013).

Measurements below the ocean surface may hold the key to the coupled physics of tropical cyclones. Traditionally hurricanes are treated as a meteorological phenomenon, and because of formidable logistical difficulties, ocean response to the hurricane forcing is very rarely measured. To stress that these are not ordinary oceanographic deployments, it has to be understood that significant wave heights in the hurricanes can be in excess of 10 m, and hence, such measurements have to be effectively done within the wave crests, by devices which either tolerate or avoid crossing the air-sea interface. Use of surface following platforms, such as wave gliders, shows a promise in this regard, even in tropical-cyclone conditions (Lenain and Melville, 2014).

3. WAVES & SWELL

3.1 Measurements / Data

3.1.1 Deterministic wave generation in the laboratory

There has been a considerable interest in the precise generation of waves in the laboratory. This concerned mainly very large steep waves that have been used for extreme load cases. Rather than generating very long wave trains and considering the extremes for analysis, a special short wave train with one or a small number of interesting extreme waves is generated on a specified position in the basin. There are several types of these so-called deterministic waves:

- Focusing waves and single wave events: A focusing wave is defined as a superposition of two-dimensional waves consisting of subsequent wave frequencies with increasing propagation speeds, in such a way that all components meet in time and space at the "focusing point".
- Deterministic wave sequences in a sea state: For a given design spectrum of a unidirectional wave train, the phase spectrum contributes to all local characteristics. The most unfavourable event under storm conditions is the in-phase superposition of component waves in the seaway. Randomly, the time series may contain a dangerous wave sequence, a coincidence which would require a much extended test duration. Applying the transient wave technique, a single wave event can be integrated in a random sea deterministically.
- Wave tank realization of observed wave records: Some interesting wave events are reported and registered from field measurements. Depending on water depth and ability of the wave maker, it is possible to generate them in a model basin.

The state of the art methods to generate and calibrate deterministic wave sequences has been described by Schmittner et al. (2014). The most used way to generate an extreme wave is by superposing different frequency components at a specified focal location as introduced by Rapp and Melville, (1990); Clauss, (2002) and Ma et al., (2010). The motions of the wave maker are determined by transforming the desired wave from the focal point backwards to the position of the wave maker. In most cases linear theory is used which often leads to a non-focused wave mainly due to nonlinear effects (Liu et al., 2016). The phase of each wave component should be corrected depending on its steepness (Fernández et al., 2014). Alternatively, non-linear wave models can be used (Duz et al., 2016), but this usually calls for an iterative solution since calculations backwards in time are normally impossible.

A special type of "rogue" or "freak" wave is the so-called breather-solution of the non-linear Schrödinger equations. This wave evolves from a modulation instability known as Benjamin-Freir or Bespalov-Talanov instability. Although it initially appeared to be just a theoretical possibility, these types of freak wave are successfully generated in the wave basin (Chabchoub et al., 2011, 2013, 2016). In the experiment, the localization of the wave energy in both space and time was confirmed. The measured surface elevation agreed quite well with the theoretical solution, the maximum amplification of the carrier wave was close to 3, which is the theoretical value predicted by the NLS equation . This type of wave has recently attracted much attention (Osborne and Ponce de León, 2017); it has been proposed as a prototype of ocean rogue waves due to its intense localization and because it seems to appear from nowhere and disappear without a trace. This latter characteristic has been reported for many known rogue wave events. Shemer and Alperovich (2013) also conducted an experiment to investigate the evolution of the Peregrine breather. The experimental results were compared to the numerical simulations based on the NLS and the Dysthe equations. The comparison indicated that the Dysthe equation can predict the evolution of the Peregrine breather better than

NLS. It was found that, with identical initial conditions, the Dysthe equation yields a lower increase rate of the envelope than predicted by NLS, resulting in a maximum amplification is lower than 3 and a location of the extreme wave crest far away from the one predicted by the NLS equation.

Onorato et al. (2013) conducted experiments to study the interaction between extreme waves, which were generated by a Peregrine breather solution. The devastating effect of such an extreme wave on a model of a 90 m chemical tanker was discussed. Unlike previous experiments conducted in deep water, these extreme waves were generated in a finite water depth to reproduce extreme conditions in the North Sea, such as the Draupner wave.

Deng et al. (2015) conducted an experiment on the evolution of the Peregrine breather in a wave flume with water depth kh = 5.65. They produced a maximum wave crest 2.86 times the initial wave height at a distance of 7 wave lengths from the wave generator. The surface elevation of the extreme did not exactly follow the theoretical shape; this was attributed to imperfections of the wave generation by a flap. The extreme wave was used to study the force on a vertical circular cylinder; the measured force appeared to correlate to the numerical predictions.

The important role played by rogue waves on structural loading of ships and offshore structures is discussed in the DNV-GL position paper (Bitner-Gregersen and Gramstad, 2015). This document reviews several research activities of DNV-GL and discusses generation mechanisms of rogue waves, their probability of occurrence, warning criteria and possible consequences.

Ken Takagi et al. (2017) derived a formulation for wave prediction using multipoint measured data for short crested waves. The formulation can be applied for both stationary process and non-stationary process. Based on this formulation, a convolution integral formula which represents the relation of free surface elevation between multipoint measurement and target point prediction is obtained. Through validation, the method is applicable to the wave warning system in short crested waves.

P.R. Shanas et al. (2017) measured waves in the Red Sea from a buoy located in the central Red Sea in order to show the presence of multi-directional waves. Superimposition occurs that leads to an increase in significant wave height and decrease in mean wave period on a diurnal cycle. Monthly features of superimposed waves have been analysed based on a correlation analysis. The analysis has been further extended to the entire Red Sea by implementing a third generation spectral wave model, WAVEWATCH III. Monthly and spatial variability of the superimposed and non-superimposed have been discussed. The waves at 58% area of the Red Sea are dominated by unidirectional waves, while the 28% area is dominated by superimposed waves and 14% area has nearly the same contribution of two wave systems.

Nagi Abdussamie et al. (2017) conducted model tests to investigate the global responses of a conventional tension leg platform (TLP) due to wave-in-deck loads associated with extreme wave events in irregular long-crested waves of a cyclonic sea state. The obtained results demonstrated the variability of all the measurements and provided insights into the effect of wave-in-deck loads on the platform behavior, tendon tensions and slamming pressures and showed qualitative correlations between these parameters.

Victor A. Godoi et al. (2017) presented a detailed climatology of extreme wave events for New Zealand waters, in addition to estimates of significant wave height (Hs) for up to a 100-year-return period. Extreme events were explored using 44 years (1958-2001) of wave hindcast data. Results indicate some similarities to patterns previously shown in the mean wave climate, with the largest waves found in southern New Zealand, and the smallest ones observed in areas sheltered from southwesterly swells.

Michael Banks et al. (2017) report this paper on results of an experimental investigation into the interaction between unidirectional waves and a horizontally moored semisubmersible model. The magnitudes of heave and pitch motions of the model were found to increase as the wave steepness increased.

3.1.2 Measurement and analysis

Stansberg et al. (2009), give an overview of different methods to measure waves in the laboratory. Different systems for point measurements were compared in a side-by-side experiment in a wave basin; the systems consisted of intrusive (the capacitive and resistive wave probes) and non-intrusive (the servo and acoustic wave probes) sensors. The results indicate the following uncertainties (u95) for the different sensors:

- Capacitive probes: 1.8 mm
- Resistive probes: 1.5 mm
- Servo probe: 2.0 mm
- Acoustic probes: 1.0 mm

Stansberg et al. recognize that the challenge is in spatial/temporal measurements. It is practically impossible to put many sensors in a small area; apart from physical aspects there is also the danger of electronic interference. An array of separate sensors at a distance of typically half the wave length of interest is being used to measure 3D wave spectra. Naaijen et al., (2009) used an array of 10*10 sensors; Hennig et al., (2015) used a relatively small device having 6 sensors arranged on a circle and a 7^{th} sensor in the center for short-crested waves.

Stansberg et al. (2009) also describe optical systems using stereo cameras above the wave surface. These systems have been successfully used in outdoor conditions, but suffer from reflection and lighting problems in laboratory conditions. Another option is to generate a laser sheet that illuminates a line on the water surface over a distance of 2 – 2.5 m. This line is then recorded by a single camera.

Stansberg et al. present an update of their 2009 investigation in 2011 (Stansberg et al. 2011). The focus is on the measurement of a 3D wave surface. Essentially the same sensors and the analysis of the signals are being reviewed. All sensors are in use in at least one of the major European towing tanks, but it is apparent that there is not a clear optimum solution for a given problem. Much depends on local conditions like water depth and lighting, if stationary measurements or measurements at speed are required and if long-crested waves from one direction are to be measured or short-crested waves from a range of directions.

Richon et al. (2009) presented the development of system using a laser pointing vertically downwards to the water surface and a camera to record the intersection point. The accuracy of this system was claimed to be better than ± 1 mm. Day et al. (2011) used a similar system, but used low cost components. He published results of wave measurements using a traditional wave probe, an acoustical probe and the laser system. The first two appeared to give very similar readings while the laser system showed mainly higher wave crests and deeper wave troughs to a lesser extent, Figure 1

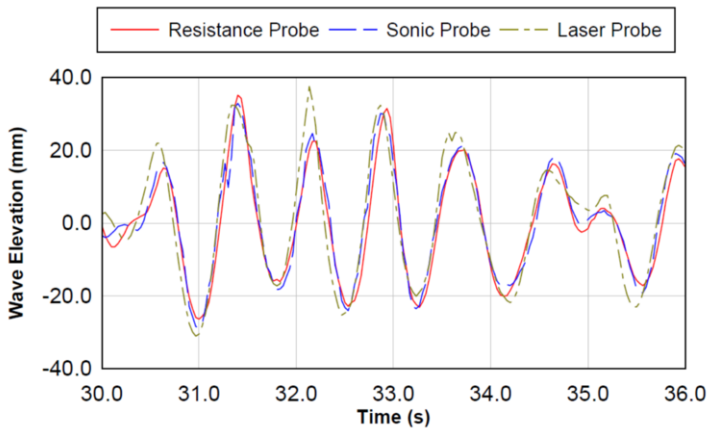

Figure 1: Wave measurement by 3 different sensors: classical resistance probe, acoustical (sonic) probe and a laser point measurement (from Day et al. 2011).

Gomit et al., (2013) describe two systems, the first consisting of stereo cameras measuring the free surface and the second of a combined laser system and one camera below and two other cameras above the wave surface. The first system uses floating particles on the free surface to correlate the images from the two cameras. Since the particles are moved sideways by the passing model, it is not useful to measure the wave pattern in the wake of the model. The second system uses particles floating in the fluid. These particles are illuminated by a laser sheet parallel to the free surface. The position of the particles is then recorded by one camera on the bottom of the basin and two cameras above the water surface. The wave elevation is determined by comparing the undistorted image from below to the distorted (due to refraction) image from above. Since this measurement is done on a fixed position in the basin, it can only be used to measure a stationary wave field.

When a model of a ship at speed is tested in waves, it is of interest to measure the wave just in front of the model. The classical wave probe has some problems due to run-up at the front and ventilation at the back of the wires. Although the errors are not very large, there is a drive to use non-intrusive sensors. An acoustical sensor is one option; the development of a practical system is published by Bouvy et al. (2009). For the problem of a measurement at speed a system above water is required; this system suffers from spikes and/or gaps in the signal when the reflected pulse is not received by the sensor. This problem is solved by reconstructing the signal in the sensor so that a smooth output is achieved. Alternative methods are being discussed by Perelman et al. (2011). They compare results from a single ultrasonic probe to results from the measurement of a line on the wave surface illuminated by a laser sheet from the bottom of the basin and results from a stereo imaging technique. In general, the two measurements agree very well, see Figure 2. For some conditions there is a problem with the signal from because the signal of the ultra-sonic probe is quite noisy, while there is a drop-out in the measurement of the deepest wave trough. The laser sheet measurement suffers from reflection problems although the measurement for the most important area is fine. There is some difference in the measurement of the wave crests in that the wave crest can be quite undefined when it is just overturning and when there are air inclusions. The laser sheet gives a very bright reflection from an air inclusion, so in this case it tends to measure the lower side of the air inclusion while the ultra-sonic probe, measuring from above, tends to measure the upper surface.

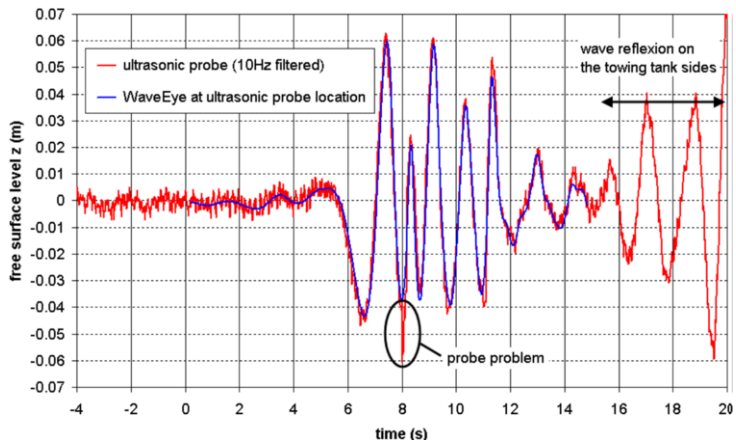

Figure 2: Measurement of a stationary wave field by a single ultra-sonic probe and by a system of 5 video cameras measuring a line on the surface that is illuminated by a laser sheet generated on the bottom of the basin (from Perelman et al. 2011).

3.1.3 Particle Image Velocimetry

Minnick et al. (2010) carried out the experiment employed Particle Image Velocimetry (PIV) techniques to obtain a data set of the vector field below the free surface for regular waves of varying steepness and realizations of irregular seaways both with and without embedded wave groups of large amplitude. In addition to the crest elevation the associated water particle velocities determine the magnitude of the impact load to a large extent. Especially in breaking waves the horizontal particle velocities can become extremely high and difficult to predict by commonly used methods for estimating wave kinematics. Lindeboom and Scharnke (2016) present Particle Image Velocimetry (PIV) measurements to capture the kinematics of different types of near breaking and breaking waves. A difficult problem appeared to be to have sufficient particles in the crest of the wave. A point of consideration is that many repeat tests and repeat measurements are necessary for a reliable (low uncertainty) measurement. Lindeboom and Scharnke used 20 repeat tests, but they concluded that this was insufficient. Nevertheless, their results correlate very well to results from CFD calculations as shown by Duz et al. (2016), Figure 3.

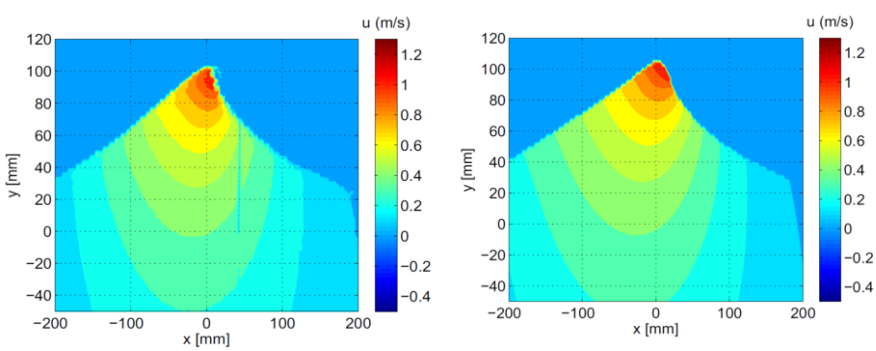

Figure 3: Horizontal velocity in a wave crest. Left: measured velocity using PIV techniques; Right: Velocity as calculated by CFD.(from Duz et al. 2016).

3.2 Rogue Waves

Rogue waves, commonly also referred to as freak waves, are waves that are much larger than what is expected for a given sea state, based on averaged properties of this sea state - typically the significant wave height Hs. A recent review on rogue waves and different mechanisms that are suspected to generate such waves can be found in Adcock and Taylor (2014). Another recent review with focus on rogue waves and their impact on ships and offshore structures is given in Bitner-Gregersen and Gramstad (2015).

There is still no consensus on a single unique definition of a rogue wave, but the most common approach is to define a rogue wave as a wave whose wave height or crest height exceeds some thresholds related to Hs. Various criteria exist, but a common definition is

$$\frac{H}{H_s} < 2 \text{ and/or } \frac{C}{H_s} < 1.25,$$

where H and C are the (zero-crossing) wave height and crest height of an individual wave, as illustrated in Figure 4. The significant wave height Hs is typically measured from a 20-minute time series in which the wave was recorded.

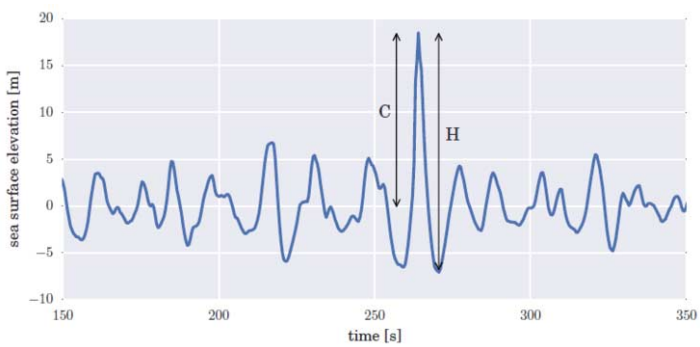

Figure 4: Illustration of wave height and crest height as used in the common definition of a freak wave. From Bitner-Gregersen and Gramstad (2015).

Given such a definition one can quite easily estimate the probability of such waves occurring, for example according to linear or second-order theory, see e.g. Bitner-Gregersen and Gramstad (2015).

Of course, also other properties of large waves may be of interest, for example the typical shape of a rogue wave or the characteristics of the wave group in which a rogue wave is observed. Gemmrich and Thomson (2017) studied surface elevation records from two locations in the northeast Pacific and investigated the properties of the recorded rogue-waves with respect to the characteristics of the wave groups. They also looked at the unexpectedness of the waves defining a rogue and unexpected wave as a wave that in addition to satisfying the criteria above, also is much larger (e.g. more than two times larger) than a given number of surrounding waves, and therefore in a sense is unexpected for a casual observer. This criterion was also studied theoretically by Fedele (2016), deriving some expressions for the probability of occurrence of unexpected waves. Naturally, waves that are both rogue and unexpected have a lower occurrence frequency than just being rogue.

Traditionally, a topic that has received much focus in the context of rogue waves is the effect of modulational instability. Modulational instability is a well-known nonlinear process that is present in water waves, as well as in other many other systems of nonlinear and dispersive waves. Modulational instability has the effect that different wave components in a spectrum can exchange energy through so-called nonlinear near-resonant four-wave interactions. Naturally, this effect is not described by the standard linear or second-order wave models, and there has therefore been some focus on nonlinear wave models in this respect, see also Section 3.3.2, and Onorato and Suret (2016) for a recent review. Typically, the modulational instability is studied through the framework of the Nonlinear Schrödinger (NLS) equation. An approach based on the NLS framework is the so-called nonlinear Fourier-transform (Osborne, 2010) that gives some insight into to effect of modulational instability. It has been suggested that this methodology can be applied to ocean engineering applications (Jeans et al., 2017, Osborne and Leon, 2017, Yim et al., 2017). Using a phase averaged framework - the Alber equation - the modulational instability in real ocean conditions was studied by Gramstad (2017), who showed that the spectral width at the base of the spectrum is more relevant than the width of the peak when it comes to predicting the importance of modulational instability in a sea state. It should also be mentioned that there has been a lot of interest lately on the presence of rogue waves also in other fields of physics, and on the fact that that this phenomenon is really multidisciplinary (Residori et al., 2017).

As discussed in Section 3.3.2, the effect of modulational instability is described by the Nonlinear Schrödinger-type equations for water waves, in terms of its so-called breather solutions. In recent years, there has been an increasing interest in these analytical solutions both from a theoretical point of view and from a more practical point of view as a prototype for oceanic rogue waves and with ocean engineering applications in mind (Onorato et al., 2013). It has been shown in several experimental studies that these solutions can quite well be reproduced in experimental wave-tank facilities by carefully controlling the condition at the wave-maker (e.g. Chabchoub et al., 2011). Also various properties of these solutions in experimental conditions have been investigated. Peric et al. (2014) studied the breaking dynamics of a breather-type rogue wave experimentally and numerically. Chabchoub (2016) showed that the evolution of a Peregrine breather survived and could be tracked also when superposed on top of a random JONSWAP background spectrum. It has been suggested that such breather solutions (e.g. the Peregrine breather) could be used as a "design wave" for studying the effect of large waves on ships and other marine structures, e.g. in sea-keeping tests (Onorato et al., 2013, Klein et al., 2016). This approach of using the breather solutions to study wave-structure interactions was for example recently used to study slamming for a chemical tanker advancing in extreme waves (Wang et al., 2016) and the structural response of deck structures from events caused by rogue waves (Qin et al., 2017a, Qin et al., 2017b).

Although there during the last two decades has been much focus on the effects related to modulational instability in the context of rogue waves, there has also been an increasing concern whether such dynamics are relevant for realistic ocean conditions. It is very well documented that modulational instability effects are relevant also for irregular random waves if the sea state is sufficiently narrow banded and sufficiently long-crested (e.g. Gramstad and Trulsen, 2007, Onorato et al., 2009). However, one may argue that very few realistic ocean spectra are sufficiently narrow and unidirectional for modulational instability to be an important effect. Based on this some authors have the view that the most important generation mechanism for the generation of oceanic rogue waves is simply spatio-temporal focusing due to the dispersive nature of water waves, enhanced by second-order non-resonant nonlinearities - also referred to as constructive interference or linear focusing (e.g. Fedele, 2015, Fedele et al., 2016). This view is also supported by some recent studies (Christou and Ewans, 2014, Fedele et al., 2016, Benetazzo et al., 2017) that through analysis of field data show that the occurrence of rogue waves in their data does not exceed linear wave theory enhanced with second-order nonlinear corrections - i.e. second-order wave theory. On the other hand, other

studies have shown that enhanced rogue wave occurrence in the ocean is observed more often in sea states with narrow directional wave spectra (Waseda et al., 2011), consistent with the physical mechanism of modulational instability.

In another recent paper, Donelan and Magnusson (2017) carried out directional analyses on the well-known rogue wave Andrea, recorded at the Ekofisk platform in the North-Sea. They argued that the generation of this wave could be explained simply by constructive interference. Based on their analysis Donelan and Magnusson (2017) also suggested that the breaking-limited maximum crest height of a rogue waves is C/Hs=1.7, where C denote the crest height.

Another recent focus in the research on rogue waves is the importance of considering rogue waves as space-time maxima of the sea-surface. Naturally, most recordings of the sea surface, for example from wave buoys, wave probes, etc. measure the surface in a single point. However, such measurements may greatly underestimate (especially in short-crested seas) the actual maximum wave displacements that can occur on sea surface areas even smaller than the wave characteristics dimensions, namely, the wavelength and the crest length (Benetazzo et al., 2015). Hence, the probability that a marine structure (which always has a footprint larger than zero) encountering a rogue wave is significantly larger than the probability of observing a rogue wave in a time series recorded in a single point. This is illustrated in Figure 5 which shows the theoretical probability density function of spatial-temporal (ST) extreme second-order nonlinear crest heights in five different ST regions considered by Benetazzo et al. (2017) using stereo wave imaging systems that measure the sea surface over a large spatial region.

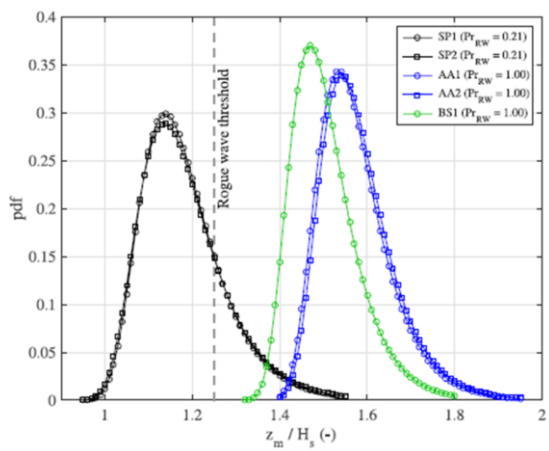

Figure 5: Theoretical probability density function (pdf) of spatial-temporal (ST) extreme second-order nonlinear crest heights in five different ST regions. In the legend, PrRW = Pr(max[z(x, y, t)] > 1.25Hs | (x, y) ∈ Ω, t ∈ D) is the probability that the maxim

Another situation that has been suggested to be associated with higher occurrence probability of rogue waves is crossing sea states. Theoretically, this is based on properties of the coupled Nonlinear Schrödinger equations that predict some amplification of the modulational instability for two Stokes waves propagating with an oblique angle of about 50 degrees (Onorato et al., 2006). An increase in occurrence probability of rogue waves in crossing sea states has also been shown in numerical simulations using HOSM (Toffoli et al., 2011), although for quite special type of crossing seas, namely two directionally narrow identical wave spectra with the same energy and same peak frequency. Trulsen et al. (2015) investigated the crossing sea

state associated with the sinking of the oil-tanker Prestige in 2002, and found no evidence for increased occurrence of rogue waves. In this case, however, the two wave systems had a crossing angle of about 90 degrees, a situation where the NLS theory does not predict any enhancement of the modulational instability. Fedele et al. (2016) also discussed the possible effect of crossing sea in the case of the Draupner wave and carried out HOSM simulations for different crossing angles, concluding that in any case the second-order effects were dominant and third-order contributions on skewness and kurtosis were negligible.

Based on some recent results it has also been suggested that rogue waves may occur as a result of a wave field being brought out of equilibrium, for example by changing bottom bathymetry or currents (Onorato and Suret, 2016, Trulsen, 2017). Thus, this is suggested to be an effect of nonlinear dynamics, but not directly attributed to the effect of modulational instability. Such effects was recently studied numerically by Ducrozet and Gouin (2017), who studied waves propagating over variable bathymetry. Consistent with previous numerical and experimental results they found increased occurrence of rogue waves on the shallower side of a slope when the waves were propagating from deeper to shallower depths. They found, however, that this effect was weakened when considering directionally spread wave fields.

Murray Rudman et al. (2016) applied Smoothed Particle Hydrodynamics to model rouge wave impact on a semi-submersible platform with a focus on the effect that different mooring systems have on platform motion and mooring tension. The results show that a hybrid of the Tension Leg Platform and Taut Spread Mooring systems could have advantages over non-hybrid systems.

Zhe Hu et al. (2015) proposed a combined wave-dam-breaking (CWDB) model in this paper. This model is deduced from the Ritter's solution, by including the influence of the rogue wave propagation as well as the delayed effect of the dam-breaking problem. The CWDB model is validated by making comparisons with both numerical results and existing experimental measurements.

Zhe Hu et al. (2017) simulated the nonlinear rogue-wave overtopping phenomenon in a numerical wave tank in this paper. The simulation results are compared against the theoretical solution predicted by the dam-breaking model. Hydroelastic effects are considered by applying a fully-coupled fluid-structure interaction model.

3.3 Analytical & Numerical Models

Struthi et al. (2017) used an improvised methodology to estimate impact forces on a jacket structure and proposed a slamming coefficient for the structure. The slamming coefficient estimated in this study was in agreement with the theoretical formulas and existing literature. The result shows that the slamming coefficient should be found exclusively for structure configurations rather than using slamming coefficient used for a single cylinder.

Hao Qin et al. (2017) used a 2-D numerical wave flume to generate freak wave. A simplified method is proposed to approximate the deck-house wall as an Euler beam with intermediate elastic bearings. The fluid-structure interaction is considered by applying an implicit iterative algorithm. By comparing the crest shapes and the impact forces of the nonlinear freak wave and a regular wave with the same wave length and height, it is seen that the impact caused by the nonlinear freak wave is more severe.

Chengdi Wang et al. (2017) develop a new significant wave height (Hs) and dominant wave period (Tp) scheme (termed as WHP) for open oceans, using15 years of hourly observational wind-wave data from eight buoys off the northwest coast of the United States (US). Comparison results show that the WHP scheme gives an almost best performance in predicting Hs and Tp for the open oceans across different regions.

'Jorge Perez et al. (2017) presented the GOW2 database, along-term wave hindcast covering the world coastline with improved resolution in coastal areas and along ocean islands. For developing the GOW2 hindcast, WAVEWATCH III wave model is used in a multigrid two-way nesting configuration from 1979 onwards. Comparisons with instrumental data show an improvement with respect to existing global hindcasts, especially in semi-enclosed basins and areas with a complex bathymetry.

3.3.1 Spectral

Wave modelling efforts and applications can be broadly classified into two large groups: phase resolving (or direct) models (see Section below) and phase average (usually spectral) models – subject of this Section. Direct models can explicitly simulate basic equations of fluid mechanics, but at oceanic scales such models are not practical or even feasible, and therefore spectral models are employed for wind-wave forecast. These are based on parametric, often speculative approaches, but their physics has been advancing lately (see e.g. Rogers et al., 2012, Zieger et al., 2015, Stopa et al., 2016, Babanin et al., 2017).

Evolution of wind-generated waves can be described by the wave action $N=F/\omega$ balance equation

$$\frac{\partial N}{\partial t} + \nabla \cdot [(\mathbf{c}_g + \mathbf{U})N] + \nabla_{\mathbf{k}} \cdot [\mathbf{c}_{\mathbf{k}} N] = \frac{I + L + D + B}{\omega} \tag{4}$$

where $F(\omega,\mathbf{k})$ is wave energy density spectrum, ω is intrinsic (from the frame of reference relative to any local current) radian frequency, $\mathbf{k}$ is wavenumber (bold symbols signify vector properties). In linear case, temporal and spatial scales of the waves are linked through the dispersion relationship

$$\omega^2 = gk \cdot \tanh(kd) \tag{5}$$

where g is the gravitational constant, d is water depth. The left-hand side of (4) represents time/space evolution of the wave action density as a result of the energy source terms on the right. Here, $\mathbf{c}_g$ is group velocity, $\mathbf{c}_{\mathbf{k}}$ means the spectral advection velocity, $\mathbf{U}$ is the current speed. ∇ here is the horizontal divergence operator, and $\nabla_{\mathbf{k}}$ is such operator in spectral space.

On the right, source terms are phenomenologically represented by atmospheric energy input from the wind, I; nonlinear interactions of various orders within the wave spectrum, L, whose role is to redistribute the energy within the spectrum; dissipation energy sinks, D; wave-bottom interaction processes, B; and more sources are possible in specific circumstances. Note that all the source terms, as well as the group and advection velocities and the advection current are spectra themselves. L is a conservative term, i.e. its integral is zero, but the other integrals define energy fluxes in and out the wave system (see Babanin et al. (2017) for more details).

Ideas of predicting the wave spectrum can be traced back to the 50s, and but only since the 90s the technical developments of computing facilities made the modern third-generation models practical in the context of the global wave forecast and hindcast. Global applications, however, come at a cost, and not only computational. In finite-depth and shallow environments, waves essentially become a different physical object. Dispersion is reduced or even ceases, nonlinearity grows, but active nonlinear mechanisms change, balance between energy input and dissipation is no longer maintained, and a variety of new physical processes come into existence because of various wave-bottom interactions and sediment response. Respective wave models are notable for a lesser degree of physics and larger degree of parametric and ad hoc tuning.

In this regard, resent NOPP effort (Tolman et al., 2013) produced a most essential update of the deep-water physics of spectral models since inception of the third-generation models. It resulted in new packages of such physics, ST4 and ST6, developed, tested and implemented in WAVEWATCH-III – the American national global wave-forecast model (WAVEWATCH III Development Group, 2016).

ST6 (Rogers et al., 2012, Zieger et al., 2015, Aijaz et al., 2016) signify the observation–based physics. New wind-input and and a number of dissipation functions for the phase-average spectral models were introduced. The input, whitecapping (breaking) dissipation and negative input (wave attenuation due to adverse winds) were obtained in field in situ observations in Lake George (Australia), at moderate-to-strong wind-wave conditions. The respective parameterisations are built on quantitative measurements and incorporate new observed physical features, which until very recently were not known and hence missing. Two novel features of the wind-input source function are those that account for the effects of full airflow separation (and therefore relative reduction of the input at strong wind forcing) and for nonlinear behavior of this term. The breaking term also incorporates two new features evident from observational studies. First, the dissipation consists of two parts—a strictly local (in wavenumber space) dissipation term and a cumulative term which includes integral of the spectrum. Second, there is a threshold for wave breaking, below which no breaking occurs. Such threshold means zero whitecapping dissipation, and therefore, for wave spectra below the threshold (full development, decaying seas, swell) a new dissipation function due to wave/water-turbulence interactions was developed and implemented. It was proposed theoretically (Babanin, 2012, 2017) and is consistent with the observed decay rate of ocean swell (Young et al., 2013). Further development of ST6 saw a new nonlinear interaction term, which accommodates both resonant and quasi-resonant interactions (Gramstad and Babanin, 2016). ST6 version of SWAN (the coastal engineering spectral wave model), in addition to the above, also accommodates observation-based terms for coupled for wave-bottom interactions including ripple formation/dissolution (Smith et al., 2011), for infragravity waves (Nose et al., 2016), for nonlinear wave-current interactions (Rapizo et al., 2017).

ST4 is a physics package with new dissipation functions (WAVEWATCH III Development Group, 2016). Like in the Lake George physics, whitecapping dissipation has a threshold and cumulative term, and because of the breaking threshold the swell dissipation is described by a separate term whose formulation appeals to the swell/air-turbulence interactions, but functionally is similar to ST6. Stopa et al. (2016) conducted a detailed comparison of performance of ST4 and ST6, which highlighted a need for spectral metrics in addition to the traditional integral properties (wave height, mean wave period, direction).

While parameterizations of whitecapping dissipation and wind input, and therefore spectral wave modelling in typical storms have progressed essentially over the last years, large uncertainties remain in the prediction of swell, extreme metocean circumstances, wave-current and wave-ice interactions. Most of these conditions are rare, but have high impact.

Swell, however, is not rare and is present in more than 80% of ocean spectra. It is not extreme, but provides significant adverse impacts on maritime operations such as shipping, loading, dredging. Yet, its prediction by wave-forecast models is poor, both in terms of wave amplitude and, particularly, arrival time. The very definition of ocean swell is ambiguous: while it is usually perceived as former wind-generated waves, in fact it may reconnect with the local wind through nonlinear interactions. Jiang et al. (2016) developed a method for identifying swell events and verifying swell arrival time in the models by means of buoy data. The results indicated that the model (WAVEWATCH-III) usually predicts an early arrival of swell, about 4 h on average. Furthermore, histogram of the arrival time shows that swells can be as early as 20 hours and as late as 20 hours. Since the model/observation error is not consistent even in its sign, it cannot be tune-fixed, and understanding the physics of swell propagation is necessary. As discussed in the paper, many mechanisms can contribute both to acceleration and

deceleration of swell on its way across the oceans. Those need to be separated, understood, parameterized and then reunited in the models, in order to improve the forecast. Observations and experiments of such mechanisms are extremely difficult. Changes to the swell forced by these processes are slow, respective time and length scales are of the order of thousands of wave periods and lengths. Wave flumes are not large enough for simulating these phenomena, and observation of the propagating and dispersing swell packages over global oceans is only possible with satellites, whose capability in this regard still appears marginal.

At the other extreme of metocean conditions, Liu et al. (2017) evaluated the current state of wave modelling in tropical cyclones, and the potential for improvements. Using the well-observed hurricane case of Ivan (2004) as an example, they investigated and inter-compared the performance of two wave models under hurricane conditions: WAVEWATCH-III and the University of Miami Wave Model (UMWM). Within WW3, all the four different source term packages (ST2/3/4/6), old and new, were employed for comparison purposes. Based on the comparisons between model results and measurements from various platforms, it was concluded that UMWM shows less accuracy than WW3 in integral wave parameters. Among the four WW3 source term packages, the older parameterization ST2 systematically underestimates high waves. The remaining three packages (ST3/4/6) perform reasonably well, but tend to overestimate energy of waves traveling in oblique and opposing winds which is typical occurrence in the hurricanes. It was shown that enhancing the strength of negative wind input can somewhat improve model skills in such situations, but uncertainty of the DIA parameterization of the nonlinear interactions remains the dominant source of errors, not possible to fix at this stage as the computational cost prevents the use of exact nonlinear integral.

As far as ocean currents are concerned, these are common conditions both in the open ocean and coastal areas. Major currents such as Gulfstream, Kuroshio or Agulhas are well known for harsh seas and high likelihood of abnormal (rogue) waves. Tidal inlets with waves on strong and variable currents are a typical feature of shipping routes in coastal areas. While linear effects of currents on waves, such as refraction, Doppler shift or relative speed with respect to the wind are assumed to be implicitly or explicitly included in wave-forecast models (often unverified and not validated), nonlinear effects are usually left out or even unknown. These include changes to nonlinear interactions in presence of currents with horizontal or vertical velocity gradients, wave/current energy and momentum exchanges, nonlinear modifications of the wave spectrum. Babanin et al. (2017) review the state of the art of this problem. Linear and nonlinear dynamics of waves on currents are discussed, depth-integrated and depth-varying approaches are described and examples of numerical model performance for waves on currents in realistic oceanic scenarios are presented.

Wave-ice interactions have been an exotic field of research for a long time, but with the Arctic opening from ice in summer months, the wave-ice modelling acquires important practical meaning. Among various theories for the wave-ice interactions some are different qualitatively, i.e. wave scattering (without dissipation) and dissipation (with or without scattering), others differ quantitatively, to the extent that some theories predict wavelength to increase in presence of ice, whereas others to decrease. In the field, all the mechanisms are acting together, depending on their relative magnitude, and practical guidance of the existing theoretical knowledge in forecasting waves in marginal ice zones is limited. Additional complications in this regards are due to necessity of also knowing initial conditions for the ice coverage and properties, and to be able to predict effects of waves on ice – this makes wave-ice interaction an essentially coupled problem. Developments of this aspect of wave modelling are very rapid: from no wave-ice modules some five years ago, to 5 new modules in WAVEWATCH-III alone presently. We refer the reader to Rogers et al. (2016) for the most recent update.

3.3.2 Phase Resolved

Spectral (phase averaged) models, as described in section 3.3.1, provide sea state description in terms of the wave spectrum and parameters that can be derived from the wave spectrum, such as the significant wave height, period, wave direction, and so on. Naturally, phase-averaged models do not provide any information about the instantaneous sea surface and e.g. associated water particle kinematics. To obtain such information wave models that also describe the wave phases, so-called phase-resolving models, are needed. Essentially, such models are based on the basic hydrodynamic equations (Navier-Stokes equation or Euler equations for potential flow), but numerous models exist that provide simplifications and special cases under various conditions and assumptions.

Most such simplified models assume that waves are weakly nonlinear. This is an assumption that usually can be justified for the evolution of realistic ocean waves. Of course, some processes, for example the breaking and overturning of waves or waves hitting a structure, are generally strongly nonlinear in their local dynamics. However, the general dynamics of propagating sea waves is generally weakly nonlinear. Based on this, one may distinguish between three classes of wave models: (i) linear wave model, (iii) second-order wave model, and (iii) higher order (nonlinear) wave models.

The linear wave model provides the linear approximation to the basic equations for waves, and for a given wave spectrum it assumes that the sea surface is a superposition of independent wave components. That is, the wave phases are assumed independent. This assumption provides a particularly simple description that is both efficient to simulate numerically, easy to analyze analytically and can be used to derive various properties such as statistical distributions (e.g. Gaussian distributed sea surface and Rayleigh distributed wave crests and wave height) or information about water particle kinematics, for example. For waves on deep or intermediate constant water depth, the natural extension of the linear wave model is the second-order wave model, in which the second order bound waves components are also taken in to account. Hence, the second-order wave model can in a sense be viewed as a generalization of the Second-order Stokes wave for random waves. Yet, the second-order model still assumes that the wave field consists of independent free wave components and consequently ignore more complicated nonlinear effects such as energy exchange between wave components. Second-order remains an important tool in many engineering applications and is currently the main model used to provide short-time wave information in the offshore industry. For example, many of the widely used statistical distributions for wave-heights and crest-heights are based on second-order theory.

For more accurate phase-resolving description of ocean waves higher-order models must be applied. Different from the linear and second-order theory, typically there are no analytical solutions in higher-order models, and applications of higher-order models normally involve numerical simulations of partial differential equations describing the evolution of the waves. Although there is a rapid increase in the use of Computational Fluid Dynamics (CFD) tools that simulate the full Navier-Stokes equation, also in applications to water waves and wave-structure interaction, such tools are generally still too computationally demanding to be used for large-scale problems that require wave information over a large spatial area over a long period. This is particularly the case for full 3D modelling of short-crested waves. Nevertheless, in the future CFD is expected to become an increasingly important tool also for wave simulations, and several commercial and open-source CFD simulations tools have modules for simulations of waves.

Simplified models based on potential flow theory combined with additional simplifications of the full equations remain very important for the modelling of waves in engineering applications. Typically, approximate/simplified models rely on some simplifications based on assumptions for which some parameters are assumed small. As already described, weak nonlin-

earity is one such assumption where the wave amplitude is assumed small compared to the wave length and/or water depth. Others common simplifications rely on small wave-length compared to water depth (deep water), small depth compared to wave-length (shallow water), or weakly varying depth or wave modulations (e.g. narrow-band assumption or assumption of weakly varying bathymetry).

Models that assume shallow water include models such as the Korteweg-de Vries (KdV) equation, the Kadomtsev-Petviashvili (KP) equation and Boussinesq-type equations. In their classical forms these models assumes shallow water depth and weak nonlinearity. During the last decades, there has been a development of improved Boussinesq-type models that are valid also for quite deep water conditions (improved dispersion properties) including also highly and fully nonlinear formulations (e.g. Memos et al., 2016); see also Kirby (2016) for a recent review. There are also continuous efforts to include other physical effects into such models (Kirby, 2016) such as wave breaking (e.g. Kim et al., 2017) and wind growth (e.g. Liu et al., 2016).

Another important class of simplified nonlinear models is those that in addition to weak nonlinearity also assume that the wave-field is represented by a narrow wave spectrum so that modulations of the wave field takes place on longer temporal and spatial scales than the dominant wave period and wavelength of the wave train. The most basic of these models is the so-called cubic Nonlinear Schrödinger equation (NLS) for water waves (Zakharov, 1968). Numerous extension and modifications of the basic cubic NLS equation have been presented, including NLS-type equations valid to higher order of nonlinearity and/or bandwidth, for finite and variable water depth, for interaction with currents, for two crossing wave systems, to mention some.

Traditionally, due to their relative simplicity, and most importantly, the existence of exact analytical solutions, NLS-type equation has played an important role in the understanding of the nonlinear dynamics of water waves. The so-called breather solutions of NLS-type equations represents the effect of modulational instability and are often linked to the generation of rogue waves in the ocean, see more detailed discussion in section 3.3. In recent years, there has been an increasing interest in these analytical solutions in the context of rogue waves. However, most of the work on this topic is quite theoretical and the direct relevance for real-world engineering applications is sometimes difficult to see. The strict mathematical validity of the NLS equation was recently studied by Düll et al. (2016). Another recent focus within the topic of NLS equations has been the analogy to other fields of physics where nonlinear dispersive waves are present and where NLS-like equations also can be applied and where rogue wave solutions are observed (Chabchoub et al., 2015, Residori et al., 2017).

An important strength of the NLS-type equations is that they are very efficient to simulate numerically. Traditionally they have therefore been applied in many studies where large scale numerical wave simulations are desired, such as investigation of statistical properties of waves. In more recent years, with the increase in available computational power, there has been a shift towards more accurate and more computationally demanding models such as other models discussed in this section, such as HOSM, Boussinesq-models or even CFD and fully nonlinear potential flow codes. It should be mentioned that one advantage of NLS-type equations compared to many other models is that they can be formulated as space-evolution equations as well as time-evolution equations. The space-evolution form is particularly suitable for direct comparison with wave-tank experiments (i.e. waves propagating in space from a wave-paddle). The relation between the temporal and spatial forms of the NLS equation is recently discussed in Chabchoub and Grimshaw (2016).

An illustration of the applicability of various phase-resolving models, including the cubic NLS equation and the higher order NLS equation (Dysthe), for deep and intermediate water-depth with respect to nonlinearity and spectral bandwidth is shown in Figure 6.

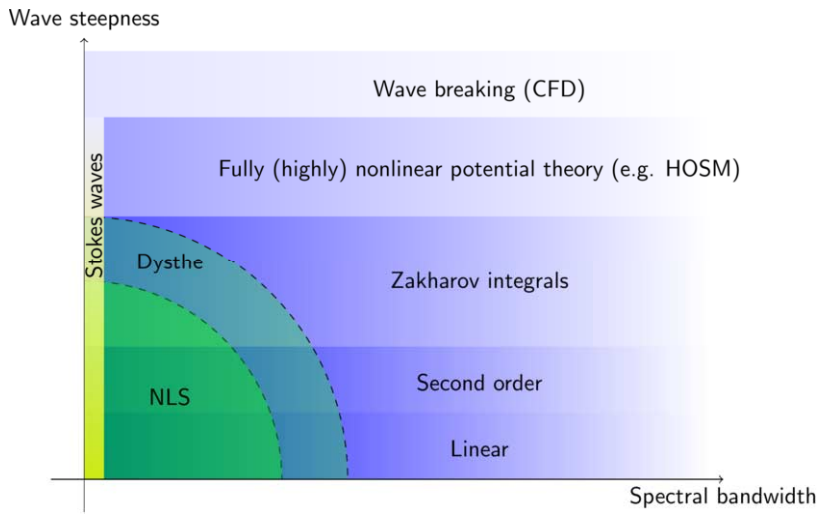

Figure 6: Illustration of the range of validity for various wave descriptions for deep and intermediate depth water waves. From Bitner-Gregersen and Gramstad (2015).

Because of the continuous increase available computational power there has been an increase in applications of more accurate models based on the fully nonlinear potential flow equations. Some overview of this topic can be found in the recent book Chalikov (2016). Common approaches for such models include Boundary Element Methods (BEM) for which the equations are solved via Greens functions and integral equations at the boundaries, and volume methods for which the solution is found numerically by discretizing the fluid domain and solving the equations by finite difference of finite element methods. In general, both such models may be quite flexible in the sense that they can handle complex computational domains or wave-structure interactions. On the other hand, such models are typically quite computationally heavy.

Another model that has seen many applications to phase-resolved modelling of waves is the so-called Higher Order Spectral Model, often abbreviated HOS or HOSM. The original HOSM formulation is due to Dommermuth and Yue (1987) and West et al. (1987), and it has later been shown that other models derived independently using other approaches (e.g. Craig and Sulem, 1993) are numerically equivalent to the original HOSM formulation. Currently, there is an available open-source HOSM code named HOS-ocean (Ducrozet et al., 2016). The same group has also released a HOSM code (HOS-NWT) that can be used as a numerical wave tank, including features of an ocean wave basin: directional wavemaker, reflective walls and absorbing beach (Ducrozet et al., 2012).

HOSM is based on an expansion of the fully nonlinear free surface boundary conditions under the assumption that the wave steepness (ratio of amplitude to wave-length) is relatively small. Since this expansion in principle can be taken to very high order by adjusting the nonlinear order (often denoted M) in the code, HOSM is sometimes referred to as a fully-nonlinear model. However, in practice HOSM is normally used with some relatively low order truncation of nonlinearity (M=3 or 5 for example), although higher order may be applied, so "highly-nonlinear" is probably a more appropriate term. HOSM has the advantage that it discretizes the horizontal plane only and applies a pseudo-spectral approach where highly efficient FFT routines are used. This makes HOSM very numerically efficient, and it is a particularly useful tool for large-scale problems for which more advanced methods are too computationally demanding. HOSM can also quite efficiently provide the water particle kinematics in the fluid

domain (Bateman et al., 2003). On the other hand, HOSM is less flexible with respect to its computational domain, where it is typically restricted to a periodic square domain over a flat bottom. There are however modifications to the HOSM formulation that allow variable bathymetry (Gouin et al., 2016, 2017).

HOSM also has the limitation that the expansions do not converge if waves become very steep and close to the breaking limit, and naturally it cannot describe breaking waves without further modifications. Traditionally, dissipation due to breaking have been modelled in HOSM in a very simple manner based on smoothing (Fourier-filtering) of the solution (see e.g. Xiao et al., 2013). Recently, there has been some effort to introduce more realistic breaking models into HOSM, as well as into other nonlinear wave models. Seiffert and Ducrozet (2016) implemented a criterion for the onset of breaking into HOSM based on the works of Barthelemy et al. (2015) and Saket et al. (2016). In the work of Seiffert and Ducrozet (2017) two different breaking models were added to a HOSM model and validated against wave tank experiments.

3.3.3 Short Term Stochastic / Probabilistic / Machine Learning

The short-term wave characteristics are required for design and operation of offshore structures and industrial facilities within the coastal areas. These extreme single waves, for example, cause the highest loads and wave overtopping volumes on structures and thereby represent the design conditions important to be accurately defined. Under-prediction of the design maximum wave height causes unsafe designs, while over-prediction causes too conservative and thus expensive designs. Nayak and Panchang (2015) analyzed short-term wave height distributions in intermediate water depths using spectral wave data from two gauges and NDBC buoy 42035 during Hurricane Ike. They compared frequently used distributions such as the Rayleigh, the scaled Rayleigh and the 2-parameter Weibull distributions. Their analysis of wave heights suggests a good fit to the scaled Rayleigh distribution, which over-predicts by 1% to 9% for the data examined, and the average of the highest ten percent the waves, H1/10 was also over-predicted by similar magnitude (< 10%). However, Nayak and Panchang (2015) found that the over-prediction was more pronounced for the maximum wave height by as much as 40% in some cases. The two-parameter Weibull distribution was observed to provide a good fit, but the parameters of the distribution were not consistent with those developed by Forristal. Nayak and Panchang (2015) which concluded that the analysis using the scaled Rayleigh distribution (which utilizes the spectral width) showed a better prediction than the original Rayleigh distribution, but with a high variability.

Amrutha and Kumar (2015) analyzed the water surface displacement measured using waverider buoy moored at 13 m water depth in the west coast of India to study the short-term statistics of waves covering full one year period. The study indicates that the values of the observed maximum wave height as a function of duration are not consistent with the theoretical expected value, with a significant variation (1.29–2.19) in the ratio between highest 1% wave and significant wave height compared to the theoretical value of 1.67. Unlike Nayak and Panchang (2015), Amrutha and Kumar (2015) found the significant wave height ∼8% lower than that predicted by the conventional Rayleigh distribution periods for the study area. Nørgaard and Andersen (2016) examined if Rayleigh distribution can be used to determine extreme wave heights in non-breaking swell conditions in deep waters. Nørgaard and Andersen (2016) concluded that the Rayleigh-distribution is under-predicting the low-exceedance wave heights in irregular swell waves. This is expected to be caused by wave non-linearity and thus a new modified wave height distribution is suggested, where the shape parameter in the distribution is dependent on the wave non-linearity, represented by the Ursell-number. The new proposed wave height distribution for non-linear and non-breaking waves is highly applicable for practical engineering design of both near-shore and offshore structures under influence of swell-waves.

In terms of predictions of individual waves especially important for warning systems, Zhu et al. (2016) proposed a novel feature extraction approach for identifying ocean wave characteristics in real time. The algorithm was developed through the integration of the fuzzy C-means clustering algorithm, statistics formulation, short-time Fourier transforms, high frequency radar data processing and window function analysis. In order to demonstrate the proposed algorithm developed by Zhu et al. (2016), two Wellen radar systems were installed in South Korea. The testing results demonstrated that the proposed algorithm is effective in extracting characteristic features from a variety of ocean waves. It is expected that system will accurately predict natural hazards and provide adequate warning time for people to evacuate from threatened coastal areas. Takagi et al. (2017) derived a formulation for the prediction of individual wave using multi-point measurements, which can be applied not only for the stationary process but also the non-stationary process. Examples based on numerical experiments of long crested waves show that prediction error is small when the prediction time is short and the measurement point is sufficiently far from target. Takagi et al. (2017) concluded that the method is applicable to the wave warning system in short crested waves.

Moving to the frequency domain, Giske et al. (2017) presented a new method for efficient calculation of auto- and cross-spectral densities in the stochastic modelling of ocean waves and wave loads, which may contribute to more efficient long-term response prediction. The cross-spectral densities of the first order wave excitation forces are considered, but the method is straightforwardly generalized to other cross-spectral densities, e.g. for wave elevation, wave kinematics or second order loads.

New researches on spatial-temporal characteristics of ocean waves have been produced recently. Alvise et al. (2017) presented the analysis of the temporal profile and height of space-time (ST) extreme wind waves to verify, to what extent, one can estimate the shape and the crest-to-trough height of near-focusing large 3D wave groups. Wave data were gathered from an observational ST sample of sea surface and they were examined to detect the highest waves (exceeding the rogue wave threshold) of specific 3D wave groups close to the apex of their development. First Alvise et al. (2017) examined the local maximum elevations of the groups within the framework of statistical models for ST extreme waves, and compared with observations and predictions of maxima derived by one-point time series of sea surface elevations. Then they analyzed the temporal profile near the maximum wave crests and compared with the expectations of the linear and second-order nonlinear extension of the Quasi-Determinism (QD) theory. Alvise et al. (2017) showed that the elevations close to the crest apex are narrowly distributed around a mean profile, whilst a larger dispersion is observed away from the maximum elevation. The developments Alvise et al. (2017) are currently in process of being implemented in a numerical spectral model for wave extreme prediction. Podgorski and Rychlik (2016) proposed measures of three-dimensional spatial wave size, expressed in terms of properly defined characteristics: the crest-height, the length, and the wave front location. Their statistical distributions are presented in explicit integral forms for the deep water seas modeled as Gaussian fields. The approach of Podgorski and Rychlik (2016) allows for investigation of the effect that shape and directionality of the sea spectrum have on the joint distributions of the size characteristics.

In terms of new developments on probabilistic distributions, Antão and Guedes Soares (2016) studied a bivariate gamma distribution fitted to an empirical joint probability density of wave steepness and height for deep water waves. A transformation of this distribution was also fitted to waves from a wave tank experiment in order to observe how the skewness of the bivariate gamma distribution changes. Antão and Guedes Soares (2016) concluded that the quality of the obtained fits compared with fits of a Gumbel copula for the same data. Seyffert et al. (2016) contributed to the theoretical basis for the occurrence of rare wave groups. The theory is compared with numerical Monte Carlo simulations in addition to physical oceanographic data. Seyffert et al. (2016) argued that the wave groups, in run length, shape, and amplitude,

are shown to be dependent on the wave spectrum and its spectral moments, a prescribed exposure time, and a pre-selected mean wavegroup period.

Error/Bias correction applied to numerical models

Wind and wave forecasting represent a useful tool for safety assessment of maritime works and activities. Metocean forecasting uncertainty is usually corrected by using either the mean calibration factor or the time series method, and has been widely used. However, within the frame of maritime work management it is necessary to forecast, with an acceptable probability of error, whether or not the wind speed and wave height at a given location will exceed prefixed thresholds within a specified temporal window. Models that seek to predict environmental variables invariably demonstrate bias when compared to observations. Although the numerical models have shown a significant improvement over the last decades, bias correction (BC) algorithms are still necessary and important, both for forecast and hindcast simulations. Wang et al. (2017) constructed a new non-parametric correction model to improve wave model accuracy through modifying a previous approach. The new correction model introduces a kernel algorithm to learn error information from both value magnitude and series trend through training datasets, and utilizes the information to correct potential errors in hindcast outputs. Wang et al. (2017) argued that the two-dimensional learning method is more effective than the previous one-dimensional which only learns error information from the value magnitude.

Parker and Hill (2017) introduced and compared a subset of BC methods with the goal of clarifying a "best practice" methodology for application of BC in studies of wave-related processes. Specific focus was paid to comparing parametric vs. empirical methods as well as univariate vs. bivariate methods. The techniques were tested on global WAVEWATCH III datasets compared to buoy observations at multiple locations, for both wave heights and periods. Results from Parker and Hill (2017) showed that all methods performed uniformly in terms of correcting statistical moments for individual variables with the exception of a copula based method underperforming for wave period. When comparing parametric and empirical methods, no difference was found. Between bivariate and univariate methods, Parker and Hill (2017) showed that bivariate methods greatly improve inter-variable correlations, emphasizing that is essential to employ methods that consider dependence between variables. Girolamo et al. (2017) illustrated a general criterion useful to correct wave forecast, providing an engineering tool able to assess the safety of the temporal window needed to complete a specified maritime work. The paper provided a detailed description of the method, together with the application to a real case.

Ensembles and Probabilistic Forecasts

Although the atmospheric ensemble forecasting is utilized since the 90s, the wave ensemble forecasts have become more popular during the last few years. The use of probabilistic forecasts based on ensembles has the benefit of calculating the uncertainties associated with the numerical prediction as well as improving the skill of the model especially after the fifth day of forecast. It is known that accurate wave forecasts during typhoon events are extremely important in aiding the mitigation and minimization of their potential damage to the coastal infrastructure, and the protection of coastal communities. Therefore, it is expected the development and use of wave forecasts will increase significantly in the next years. Pan et al. (2016) presented a practical approach to optimizing model-ensemble wave heights in an attempt to improve the accuracy of real-time typhoon wave forecasting. A locally weighted learning algorithm was used to obtain the weights for the wave heights computed by the WAVEWATCH III wave model driven by winds from four different weather models (model-ensembles). The optimized weights are subsequently used to calculate the resulting wave heights from the model-ensembles. Results of Pan et al. (2016) showed that the optimization is capable of capturing the different behavioral effects of the different weather models on

wave generation. Comparison with the measurements at the selected wave buoy locations shows that the optimized weights, obtained through a training process, can significantly improve the accuracy of the forecasted wave heights over the standard mean values, particularly for typhoon-induced peak waves. Pan et al. (2016) indicated that the algorithm is easy to implement and practical for real-time wave forecasting. Pezzutto et al. (2016) compared the performance of two wind and wave short range ensemble forecast systems for the Mediterranean Sea, based on the respective systems: the Met Office Global-Regional Ensemble Prediction System and the Nettuno Ensemble Prediction System. Attention is focused on the differences between the two implementations (e.g. grid resolution and initial ensemble members sampling) and their effects on the prediction skill. Pezzutto et al. (2016) state that assessment of the added value of the ensemble techniques at short range in comparison with the deterministic forecast from Nettuno reveals that adopting the ensemble approach has small, but substantive, advantages.

The statistical characteristic of ocean wave could consist of two parts that are used for long-term prediction and short-term prediction. In general, the different method/approximations are used for both of long-term and short-term prediction.

Duan et al (2016) proposed a hybrid EMD-SVR model in order to predict the short term of significant wave height. With this method, the limitation from conventional statistical model in the forecasting of nonlinear and non-stationary waves could be improved. The validation of the method is compared with that of AR, EMD-AR, SVR and EMD-SVR models by using the same data from NDBC buoys.

Minoura, M (2016) also proposed stochastic sea state models by employing Fourier series expansions. All components of sea state, significant wave height, mean wave period, wave direction, mean wind speed, and wind direction are found in good correlation with that of the hindcasting seastate data. Several aspects are used in order to clarify the accuracy of the proposed model. These are probability density function, mean value, variance value, cross relation function and persistence duration of sea-state.

3.4 Tropical & Extratropical Cyclones

Tropical cyclones can develop a heavy force circular wind that is characterized from a low pressure in the center and a closed low-level atmosphere circulation. Since a heavy wind force is developed, the extreme wave or freak wave might be generated simultaneously. It is commonly known that the direction of circulation depends on the location, counterclockwise wind blowing in the northern hemisphere and clockwise blowing in the southern hemisphere. The different names for a tropical cyclone are typhoon, hurricane, tropical storm, etc.

The tropical cyclone, i.e. hurricane wave, might become a catastrophic disaster that causes heavy damage on the land or infrastructure on the coast or port, i.e. coastal bridge (Guo, et all (2015). The failure of the coastal bridge could impact the transportation and cause economic losses. In order to predict sufficient clearance on the coastal bridge from hurricane wave force, Gao develop an analytical solution by using Eigen function matching method so that the boundary value problem of the submerged coastal bridge deck is derived.

Since a tropical cyclone can also generate an extreme wave or freak wave, it is very important to know the characteristics of the newly generated wave swell source. Sandhya et al (2016) conducted study of the Indian coast in order to describe the in situ field data during extreme cyclone conditions. Then, he investigated the all components of wave energy spectra by using linear wave theory (ridge analysis).

The freak wave or rogue wave is the other extreme wave condition, with very steep, and a much larger wave. The condition of very steep, much larger than the common sea state is a given that the maritime community to handle and work with these conditions (Bitner-Gregersen E, 2017).

The freak wave could categorized based on nonlinearity and irregularity of nearshore waves, such as power spectral, occurrence frequency of freak waves, skewness kurtosis, wave grouping and its distribution (Zhuo, Z and Sato S). It is concluded that the occurrence of freak waves is dependent on the kurtosis and the groupiness factor based on the two typhoon observation on the Suruga coast Shizoka Prefecture of Japan in 2013.

Deng et al (2016) conducted an experimental investigation on deterministic freak waves. The experimental condition is setup so that four freak waves were generated with different steepness values. A phase amplitude iteration scheme was applied in order to optimize the deterministic wave sequences by taking into account the different wave steepness values. The third order stokes wave theory was used to predict wave speed by adopting local trough to trough periods and freak wave height.

Kai Yin et al. (2017) used the coupled ADCIRC+SWAN models to investigate the effects of potential sea level rise (SLR) and typhoon intensification (TI) on storm surges and waves in Pearl River Estuary, China. The results demonstrated that TI has a greater impact on storm surge, whereas SLR has a greater impact on wave heights in the estuary.

Zhilin Sun et al. (2015) carried out a numerical study based on the ECOMSED model to investigate the storm surge induced by super typhoon 5612 (WANDA) along Zhengjiang coast, China. The results presented good agreement with the observed data. Overtopping probabilities of seawalls corresponding to each track designed based on WANDA were achieved.

P.L.N. Murty et al. (2014) implemented a coupled wave + surge hydrodynamic modeling system (ADCIRC+SWAN) to simulate storm surge, still water level landfall in the Odisha State, east coast of India, during October, 2013. This coupled model provides a realistic description on the dynamic interaction of tides, wind, waves and currents.

Zhantao Zhuo and Shiji Sato (2015) investigated typhoon wave characteristics with an objective to extract essential wave parameters influential to stability of coastal structures. The relationships among various parameters were examined regarding the nonlinearity and the irregularity of nearshore waves, such as power spectrum, occurrence of freak waves, skewness and kurtosis, wave grouping and distribution of wave height.

H.Q. Zhang and B.C. Nie (2016) analysed typical wave parameters caused by typhoon near Donghai Bridge, a demonstration area of offshore wind farm. Anisotropic energy dissipation in the wave propagation direction is considered and further applied in this model. This new model is used to simulate and forecast wave evolution caused by Chan-Hom (201509).

Jin-hai Zheng et al. (2017) investigated the central pressure and the maximum wind speed of three categories, which are typhoons making straight landfall, typhoons active in offshore areas and typhoons moving northward after landfall, on basis of a 65-year dataset (1949-2013). Statistical analysis suggested that the minimum central pressure increased northward and shoreward gradually. The relationship between the maximum wind speed and the minimum central pressure was established through second-order polynomial fitting.

Shun-qi Pan et al. (2016) presented a practical approach to optimizing model-ensemble wave height in an attempt to improve the accuracy of real-time typhoon wave forecasting. A locally weighted learning algorithm is used to obtain the weights for the wave heights computed by the WAVEWATCH III wave model driven by winds from four different weather models (model-ensembles). The optimized weights are subsequently used to calculate the resulting wave heights from the model-ensembles.

4. CURRENTS

Fossen and Lekkas (2017) presented a globally κ-exponentially stable adaptive disturbance observer intended for an indirect adaptive control approach and a globally convergent direct adaptive control law for estimation and compensation of ocean currents, which could be ap-

plied to the horizontal-plane motion of surface vessels and autonomous underwater vehicles. These two nonlinear adaptive path-following algorithms were based on a classical LOS guidance principle for marine craft, and integral action is obtained by parameter adaptation.

Hu et al. (2016) designed a three-dimensional current sensor which could measure the horizontal velocity and small upwelling. The horizontal flow velocity was measured by the ball and the vertical flow velocity was measured by the thin disc through the results of horizontal flow velocity measurement. The device could be used to measure the velocity in the range of 0mm/s~400mm/s and the minimum flow velocity which could be accurately measured is about 8 mm/s.

Mayerle et al. (2015) constructed a three-dimensional process-based model for sediment transport coupled with wave-current models based on the Delft3D modelling system in conjunction with the field measurements for the sediment motion and presented transport of a mixture of cohesive sediments and sands in the Paranagua Estuarine Complex in the south of Brazil.

Zhang et al. (2017) established a set of three-dimensional numerical models to investigate the mechanisms of local scour around three adjacent piles with different arrangements under steady currents. The results revealed that the dimensionless pile spacing had a significant effect on the flow field and local scour around the three adjacent piles.

Almar et al. (2016) presented a method based on the application of the Radon transform on longshore spatio-temporal images and the results showed an overall good agreement with the synthetic field in-situ currents. This remote sensing method allowed a long term monitoring of the longshore current and its cross-shore structure.

Xu and Lin (2017) proposed a new two-step projection method in connection with an ISPH model that used both current time step and future time step, which achieved much better energy conservation than the traditional ISPH model, even with the use of a much larger time step.

Scott et al. (2016) demonstrated that strong boundary-controlled rip flows existed in association with groynes, and that the development of these currents in a fetch-limited environment is principally related to the deflection of the alongshore current by the coastal structure through field measurements from Boscombe beach. A calibrated and validated numerical model (XBeach) was used to explore the key environmental controls on rip behaviour across a range of groyne configurations and wave conditions not observed in the field.

Choi et al. (2015) used the Boussinesq model FUNWAVE to perform a numerical simulation of the SandyDuck field experiment for 2 October 1997 in order to investigate surf zone hydrodynamics in a directional random wave environment with the observed directional offshore spectrum and field topography, including the scoured depression below the FRF pier structure. The simulation results agreed well with the experimental data to reveal a wave height distribution of the random waves as well as the well-developed longshore current and its energetic fluctuation.

Yang et al. (2015) carried out a numerical model investigation with COULWAVE to study the wave-induced flow in wetland mound–channel systems at different water levels, vegetated conditions, and mound configurations. Numerical results showed that rip current strength and primary circulation size depend on mound spacing, water depth, wave height, and vegetation cover.

Chen and Christensen (2017) developed a numerical model for fluid-structure interaction analysis of flow through and around an aquaculture net cage, which was based on the coupling between the porous media model and the lumped mass structural model. Since the interaction effects between the net cage and the flow were considered and the time stepping procedure was introduced, the solver could be applied in both steady and unsteady conditions.

Liu et al. (2017) established the ocean-current-induced electric field model for current movement and obtained the measurement principle of an expendable current profiler (XCP) through model analysis. Based on this analysis, a method was proposed for the measurement of the nanovolt-scale ocean-current-induced electric field.

Xiao et al. (2017) described a novel non-intrusive reduction model which was based on the Smolyak sparse grid method and implemented under the framework of advanced 3D unstructured mesh finite element ocean model (Fluidity) for three-dimensional (3D) free surface flows. It was shown that the accuracy of solutions from free surface flow NIROM, which showed a good agreement with the high fidelity full ocean model, was maintained while the CPU cost was reduced by several orders of magnitude.

Yang et al. (2016) investigated the two-dimensional flow over two inclined flat plates with the same length and thickness in a staggered arrangement at low Reynolds numbers by numerical simulation and recommend the IBM method to handle the location and boundary condition for the plates.

Chen et al. (2015) conducted several groups of numerical simulations of ship navigation based on the Princeton Ocean Model (POM) in the North Pacific Ocean and focuses on the ocean surface current in the East China Sea (ECS) to investigate the effect of the Kuroshio Current on ship navigation quantitatively as well as the next step of making a weather routing system and found that the POM model could generate a high-quality Kuroshio Current distribution that could be applied to conduct numerical simulations of ship navigation.

Wang and Zou (2015) established a comprehensive set of data, consisting of current velocity measurements on barred beaches with slopes of 1:100 and 1:40, as well as wave transformation and setup data in order to examine the bimodal longshore current velocity profile for purely wave-driven currents, with emphasis on the second peak and ratio of two peaks. The 2-D model based on vertically integrated equations (external mode) of Nearshore POM was performed to compute the measured velocity profile.

Klebert et al. (2015) presented the full-scale measurements of the deformation and current reduction of a large-scale fish sea cage submitted to high currents and applied a simulation model based on super-elements describing the cage shape whose results showed good agreement with the cage deformations.

4.1 Measurements / Data

Ocean currents have received tremendous attention for decades on the basis of its important role in marine engineering. The parameters of velocity and direction are the main concerns of measurement of ocean currents in the field of ocean engineering.

4.1.1 In-situ current measurements

Field measurement is extremely essential for researchers to study the ocean currents. Scott et al. (2016) used fixed instruments and GPS-drifters to conduct a 10-day field experiment at Boscombe and found that there was a close correspondence between the existence of strong boundary-controlled rip flows and groynes.

There are a variety of flow velocity measuring instruments and the Acoustic Doppler Current Profiler is the most widely used equipment in the modern testing field. In order to study the interaction between the sea cage and the bathymetry chart, Klebert et al. (2015) conducted a field experiment to measure the deformation and current reduction using an Acoustic Doppler Current Profiler and Acoustic Doppler Velocimeter. However, the Acoustic Doppler Current Profiler can hardly be used to measure the vertical velocity owing to its lower accuracy. To compensate for this shortcoming, Hu et al. (2016) designed a three-dimensional current sensor which could measure the horizontal velocity and small upwelling. Because of the powerful

facility to measure the horizontal and vertical flow velocity separately, the device can fit the needs of small, three-dimensional, transient and deep sea.

Some new detection methods are proposed recent years. Fossen and Lekkas (2017) presented two nonlinear adaptive path-following algorithms which can be used for estimation and compensation of ocean currents. Liu et al. (2017) established the ocean-current-induced electric field model for current movement and obtained the measurement principle of an expendable current profiler by model analysis. On this basis, they gave a new way of measurement of the nanovolt-scale ocean-current-induced electric field.

Ocean current observations can be found at a number of web-sites. NOAA's National Oceanographic Data Center (NODC), http://www.nodc.noaa.gov/, provides current data from a number of sources as does the Bundesamt für Seeschifffahrt und Hydrographie (Federal Maritime and Hydrographic Agency), http://www.bsh.de/en/index.jsp, of the German Federal Ministry of Transport, Building and Urban Development. The Southern Oscillation Index/El Nino web site, http://www.pmel.noaa.gov/tao/elnino/nino-home.html provides access to a number of links to a number of data products including surface currents.

4.1.2 Remotely sensed current measurements

Due to the advantages of low cost and intuitive use, video remote sensing has become more and more common as an efficient tool to monitor the offshore environment. Uiboupin and Laanemets (2015) used the bias-corrected SST imagery to estimate the mean upwelling characteristics in the Gulf of Finland (Baltic Sea). In this method, the information of the upwelling is extracted from sea surface temperature obtained from satellite remote sensing technology. Almar et al. (2016) presented a method to estimate the longshore current from video based on the Radon transform and the results showed an overall good agreement with the synthetic fields and in-situ currents. Wijaya (2017) proposed an alternative method to determine the surface current from radar images based on Dynamic Averaging and Evolution Scenario method.

Near-realtime global ocean surface currents derived from satellite altimeter and scatterometer data can be found at NOAA's Ocean Surface Current Analyses – Real Time (OSCAR) web site (http://www.oscar.noaa.gov/index.html). The data is validated against moored and floating buoy data, and the method to derive surface currents with satellite altimeter and scatterometer data is the outcome of several years NASA sponsored research.

4.2 Analytical & Numerical Models

Some ocean current models are applied to solve the practical engineering problems and promote further development. Sediment transport, which proves to be closely related to harbors and navigation channels, has received much attention in recent years. Mayerle et al. (2015) constructed a three-dimensional process-based model coupled with wave-current models to investigate the sediment transport in the Paranagua Estuary Complex in Brazil. The ocean model clearly illustrates the sediment transport and morphological changes in estuaries. Wang et al. (2016) applied the Aqua-FE^{TM} model to simulate the effects of wave and current on gravity cage with two different meshes. Lamas et al. (2017) analyzed the response on yaw motions of a Tension Leg Wellhead Platform on flow-induced motions with CFD dynamic analysis. Zhang et al. (2017) conducted a systematic analysis on the mechanisms of local scour around three adjacent piles by establishing a set of numerical models, which successfully described the impact of the pile spacing on the flow field, bed elevation contours and scour depth.

Ocean model outputs have been employed to describe the interaction of currents and structure, which has been becoming the focus of research and the hotspot. Chen et al. (2015) used the POM ocean model to study the impact of the Kuroshio Current on ship navigation. It is found that the POM model performs well in generating a high-quality Kuroshio Current dis-

tribution. Pan et al. (2016) applied WADAM, MULDIF and WASIM to investigate the impact of a current on the relative motions and wave drift forces for two offshore floaters and gave the comparison analyses on these three models. Chen and Christensen (2017) developed a numerical model based on the coupling between the porous media model and the lumped mass structural model to analyze the interaction of flow and an aquaculture net cage.

Some new algorithms and new numerical models have been put forward in recent years. Xu and Lin (2017) proposed a new two-step projection method in connection with an ISPH model that used both current time step pressure and future time step pressure, which was able to get better energy conservation than the traditional ISPH model, even if a much larger time step was used. Xiao et al. (2017) described a novel non-intrusive reduction model which was based on the Smolyak sparse grid method and implemented under the framework of advanced 3D unstructured mesh finite element ocean model for three-dimensional free surface flows. It was shown that the accuracy of solutions from free surface flow NIROM, which was well fitted with the high fidelity full ocean model, was maintained while the CPU cost was much lower.

5. WIND

Umesh et al. (2017) summarized the results of validation performed with wave spectra using SWAN model off coastal Puducherry, located in the east coast of India and studied the impact of wind forcing from ECMWF ERA Interim winds and QuikSCAT-NCEP blended winds on resultant wave spectra. They found that wave model output was critically sensitive to the choice of the wind field product and blended winds generated more realistic wave fields in coastal location and could reproduce the growth and decay of waves in the real-time based on model simulations.

Chen et al. (2017) numerically investigated the energy harvesting performance of a fully-activated flapping foil under wind gust conditions and the effects of the gust frequency, the oscillation amplitude of gust, and the phase difference between the gust and the pitch were systematically examined. By comparing with the results from the uniform flow, they found that the energy harvesting efficiency under wind gust conditions can be changed greatly.

Campos and Soares (2016) performed two pairs of comparisons between HIPOCAS and ERA reanalysis by considering the wind speed and significant wave height and found that ERA-Interim presented the best results against measurements but suggests some underestimation under extreme events at mid-high latitudes, while HIPOCAS tended to overestimate the measurements and over-predict both ERA reanalyses in the range of extreme values.

Cambazoglu et al. (2016) evaluated the impact of resolution on wind predictions within regions of Turkish Straits System and Chesapeake Bay using a quadruple nest of COAMPS® (27 km to 1 km) to find an optimal configuration of spatial and temporal resolution and suggested the use of hourly atmospheric products at 3-km resolution for oceanic forcing purposes.

Stefanakos (2016) obtained the wind and wave parameters by coupling the well-known Fuzzy Inference Systems (FIS) in combination with Adaptive Network-based Fuzzy Inference Systems (ANFIS) with a nonstationary time series and found that the forecasts based on the proposed methodology outperform the ones using only FIS/ANFIS models through the comparison of the error measures from the two approaches.

Tagliaferri et al. (2015) proposed two methods for short term forecasting of wind direction with the aim to provide input for tactic decisions during yacht races based on artificial neural networks (ANN) and support vector machines (SVM), respectively. They found that although the ANN forecast based on the ensemble average of ten networks showed a larger mean absolute error and a similar mean effectiveness index than the SVM forecast, its accuracy increased significantly with the size of the ensemble.

Chen et al. (2015) proposed a new algorithm to retrieve wind speed and wind direction from marine X-band radar image sequence, which related wind vector not only to the gray level intensities of radar images, but also to the sea states explicitly. The method of preprocessing radar image was proved to be effective implemented and was suitable for identifying barriers from the sea clutter.

Bennett and Mulligan (2017) investigated three different spatially-varying surface wind which included two 2D parametric wind models and a 3D atmospheric model with data assimilation, and atmospheric pressure fields used for forecasting or hindcasting hurricane waves on the continental shelf. They suggested that the results of this study were relevant for other tropical cyclones that undergo extratropical transition or were influenced by other atmospheric disturbances at mid-latitudes, resulting in storms with large spatial size and high asymmetry.

Caires et al. (2016) proposed a semi-parametric method based on the theory of max-stable processes that could be used to determine the time- and space-evolving wind fields associated with a given return value of wind speed at a specified reference location. The main recommendation of this study is that the proposed method be considered further for the determination of temporally and spatially evolving hydraulic conditions.

Pillai et al. (2017) explored the application of a wind farm layout evaluation function and layout optimization framework to Middelgrunden wind farm in Denmark, which has been built considering the interests of wind farm developers in order to aid in the planning of future offshore wind farms using the UK Round 3 wind farms as a point of reference to calibrate the model. The results showed that both optimization algorithms were capable of identifying layouts with reduced levelized cost of energy compared to the existing layout while still considering the specific conditions and constraints at this site and those typical of future projects.

Castro-Santos and Diaz-Casas (2015) determined the influence that location had in the lifecycle of a floating offshore wind farm and applied the methodology to a floating offshore wind farm with semisubmersible platforms and located in the Galicia area (North-West of Spain), which could clarify the importance of the economic and strategic location settings when a floating offshore wind farm was constructed in any region.

Lakshmi et al. (2017) performed a comprehensive analysis on storm surge computation utilizing WRF-ARW winds run with three different grid resolutions for the recent very severe cyclonic storms Phailin and Hudhud that had landfall along the east coast of India by considering two different sets of WRF-ARW winds constructed using GFS and FNL initial conditions under three varied horizontal grid resolutions.

Emanuel (2017) presented a fast, physically motivated intensity algorithm consisting of two coupled ordinary differential equations predicting the evolution of a wind speed and an inner core moisture variable, which included the effects of ocean coupling and environmental wind shear but does not explicitly simulate spatial structure and produced a smaller increase in global tropical cyclone frequency in response to global warming, but a comparable increase in power dissipation compared to the existing method.

Wang et al. (2017) proposed a new gradient wind field model for translating TCs, based on the vector summation of the rotational wind speed and the translation speed, which could better describe the realistic wind field than the existing Georgiou's model incorporating Blaton's adjusted curvature.

5.1 Current State of the Art

The assessment of the environment impact over global ocean as well as over regional basins requires the knowledge of high accurate wind speed and direction with high space and time resolutions. The wind variables would be derived from the operational numerical weather prediction models (NWP) such as European Center for Medium Weather Forecasts (ECMWF)

analyses and from ECMWF re-analyses ERA Interim. Indeed NWP provide estimates of winds and of additional parameters such as sea state, air temperature and humidity, sea surface temperature (SST) on a regular grid with a high temporal resolution generally between 3:00 and 6:00. However, their spatial resolution is relatively low, especially for the needs of local and coastal environmental studies. For example, in these areas the coastal topography has a significant impact on the spatio-temporal changes of marine meteorology which in turn produce fine scale variability of surface parameters. A feature of the coastal dynamics atmospheric production of expansion vessels supercritical downstream structures marked mountain. This acceleration of the winds causes significant spatial variations of surface wind not included in the analyses and the impact weather and ocean level is poorly determined. Another feature of the coastal winds is the sea breeze. It is produced by strong contrasts of temperature and can reach 10 m/s and assign a coastal strip of tens of kilometers. Accurate prediction of sea breeze is necessary for operational wind farms to assess energy intake to the power grid.

For further improvement of the surface wind space and time characteristics relied on the main weather conditions occurring over global and/or regional oceanic scales. The scientific community makes use of remotely sensed data and of the associated surface wind analyses. Radars and radiometers onboard polar satellites provide valuable information on surface winds, with high spatial resolution, and global coverage. Satellite observations allow access to synoptic and global estimates of geophysical parameters with high spatial resolution ranging between 1km and 50km with an accuracy equivalent to that estimated from the buoy measurements. The characteristics of the satellite surface wind speeds and directions useful for environmental impact achievements are summarized in Table 1. It provides satellite mission, onboard instrument of interest for surface wind observation, period of data availability, repeat orbit (i.e. requiring time between two successive observations at same location) for polar sun-synchronous satellites, space grid resolution (i.e. also called Wind Vector Cell (WVC)), and the centers producing and distributing data. Most of these data are also archived by IFREMER for scientific use. Table 1: Characteristics of sources providing satellite surface winds required for environmental impact shows about 30 independent wind sources, including 12 scatterometers, 2 SAR, 10 radiometers, and 8 altimeters. For instance, the European Space Agency (ESA) operated two scatterometers onboard the European Remote Sensing Satellites ERS-1 (1991 – 1996) and ERS-2 (1995 – 2011). Three scatterometers have been operated by the National Aeronautic Space Administration (NASA): NASA scatterometer (NSCAT) (1996 – 1997) onboard the Japanese Advanced Earth Observing Satellite (ADEOS-1), SeaWinds onboard QuikSCAT satellite (1999 - 2009), and SeaWinds onboard (ADEOS-2/Midori) (2002 – 2003). The latest European scatterometers are the Advanced SCATterometer ASCAT-A (2006 – present) and ASCAT-B (2013 – present) onboard METOP-A and –B satellites, Ocean SCATterometer (OSCAT) onboard OCEANSAT2 satellite (2009 – present), and HY-2A scatterometer (2011 – present). ASCAT-A/B, OSCAT, and HY-2A are operated by European Meteorological Satellite organization (EUMETSAT), and the Indian Space Research Organization (ISRO), respectively.

Higher wind speed and direction retrievals will be derived from two SAR onboard ENVISAT and SENTINEL 1A ESA satellites, respectively.

To enhance surface wind sampling in space and time over oceanic areas, winds from radiometers such as the Special Sensor Microwave Imager (SSM/I) on board Defense Meteorological Satellite Program (DMSP) F10, F11, F13, F14, and F15, F16, F17, and F18 satellites, the polarimetric radiometer WindSat onboard CORIOLIS satellite, and the altimeters onboard ERS-1, ERS-2, Topex/Poseidon, ENVISAT, JASON1, and JASON2 satellites.

All wind speeds and directions available for the project are related to level 2 product (data over instrument swath or along tracks) associated with each satellite mission and provided by the producer agencies (CNES, ESA, EUMETSAT OSI SAF, IFREMER, ISRO, KNMI, NASA, RSS)

Scatterometers, SAR, and WindSat provide valuable information on both wind speed and direction, whereas passive microwave imagers (e.g. SSM/I) and altimeters provide information on wind speed (only). Radars and radiometers provide accurate retrievals in almost all atmospheric and oceanic conditions. In general, they are available with a spatial resolution lower than 1km for SAR, 7km along altimeter tracks, and varying between 25 and 12.5 km² for scatterometers and radiometers. Figure 7 shows examples of sampling length distributions of remotely sensed wind derived from ASCAT-A/B and SSM/I-F16/F17 over the European of interest, available for one day (***left panel***) and one month (right panel). Areas located 12km to 25km off coasts exhibit significant sampling that would meet the requirements dealing with the potential assessment of wind renewable marine energy. To overcome near coast winds not available from scatterometers and radiometers, the project will use SAR data. Figure 8 shows an example of sampling length of SENTINEL 1A SAR observations occurring during the period January – April 2016.

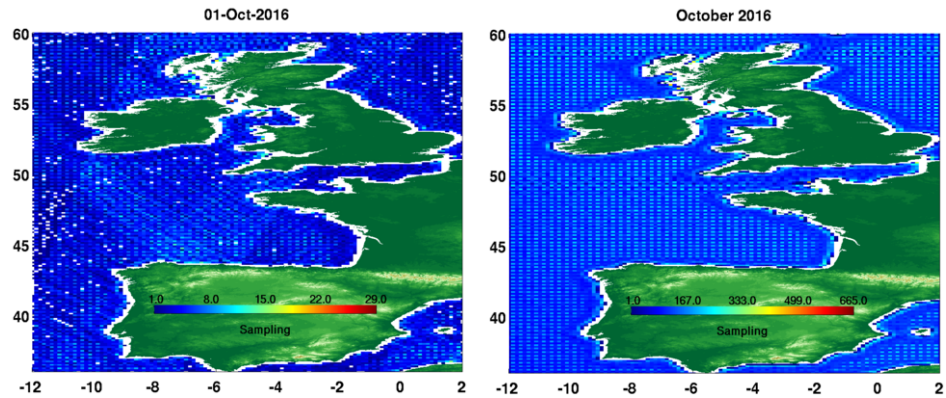

Figure 7: Spatial distributions of remotely sensed winds derived from ASCAT-A/B and SSM/I-F16/F17 over ARCWIND oceanic zone calculated for October, 1st 2016 (left panel) and for full October 2016 (right).

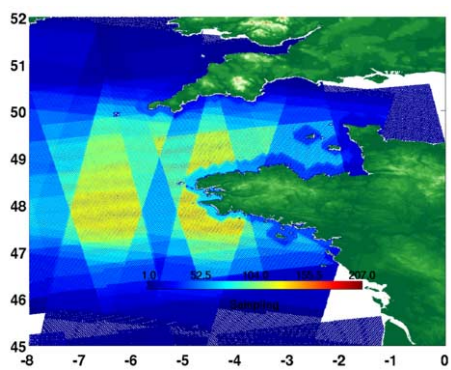

Figure 8: Spatial distributions of remotely sensed winds over a North West Atlantic oceanic area calculated from SENTINEL 1A SAR data occurring during the period Jan. – April 2016

Table 1: Characteristics of sources providing satellite surface winds required for environmental impact

Satellite	Instruments	Period	Orbit (days)	Spatial grid	Sources
ERS-1	Scatterometer altimeter	1992 - 1996	3	50/25km² 7km	ESA/IFREMER
ERS-2	Scatterometer altimeter	1996 - 2011	35	50/25km² 7km	ESA/IFREMER
ADEOS-1	Scatterometer (NSCAT)	1996 - 1997	4	25km²	NASA/JPL
QuikSCAT	Scatterometer (SeaWinds)	1999 - 2009	4	12.5km²	NASA/JPL
ADEOS-2	Scatterometer (SeaWinds)	2002 - 2003	4	25km²	NASA/JPL
OceanSat2	Scatterometer (OSCAT2)	2009 - 2013	2	25km²	ISRO/KNMI
Metop-A	Scatterometer (ASCAT-A)	2007 - Present	29	25/12.5km²	OSI SAF
Metop-B	Scatterometer (ASCAT-B)	2012 - Present	29	12.5km²	OSI SAF
HY-2A	Scatterometer	2012 - Present	14	25km²	NSOAS/KNMI
ISS	Scatterometer (RapidScat)	2014 - Present		12.5km²	NASA/JPL
ENVISAT	SAR altimeter	2002 - 2011	35	1km²	ESA
SENTINEL 1A	SAR	2015 - Present		1km²	ESA
SENTINEL 3	Altimeter	2015 - Present	27	300m	ESA
Topex/ Poseidon	altimeter	1992 - 2005	10	7km	CNES
Jason1	altimeter	2001 - 2013	10	7km	CNES/NASA
Jason2	altimeter	2008 - Present	10	7km	CNES/NASA
Jason3	altimeter	2006 - Present	10	7km	CNES/NASA
DMSP F10-F18	Radiometers(SSM/I)	1992 - Present		25km²	RSS
CORIOLIS	Radiometer(WindSat)	2003 - Present	8	25km²	RSS
SMAP	Radiometer	2015 – Present	8	25km²	NASA/JPL
SCATSAT-1	Scatterometer	2016- Present	2	25km²	ISRO
CFOSAT	Scatterometer	2018 -	13	50km² / 25km²	CNSA/CNES

5.2 Accuracy Issues

The remotely sensed wind accuracy is mainly determined through comprehensive comparisons with mooring wind data. The comparison issues require proper spatial and temporal procedures aiming at generating satellite and in-situ collocated data (matchup data). The agreement between the two sources is good. The root mean square difference is about 1.10m/s and 18°, for wind speed and direction, respectively. To assess the consistency between retrievals from various satellite instruments, inter-comparisons are performed between space and time collocated data derived from two satellite sensors. For instance, Figure 9 shows an example of comparisons between wind speed (left panel) and direction (right panel) matchups from ASCAT and Sentinel 1A SAR.

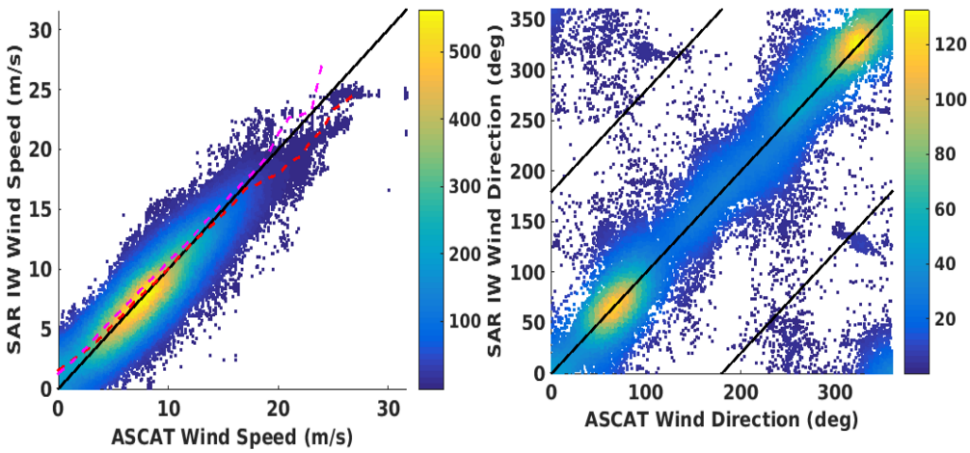

Figure 9: Sentinel SAR IW wind speed (left panel) and direction (right panel) versus ASCAT retrievals. Results are shown for all scatterometer and SAR matchups occurring over the North West Atlantic oceanic area.

5.3 Measurements / Data

Wind measurements are perhaps one of the most ambiguous metocean properties. The standard wind speed at 10 m height is almost never measured directly. Even if an anemometer mast has a sensor at 10 m above the mean water surface, it is always located in finite depth where the level of this surface varies in response to tides, seiches and other forcings. Measurements at deep-water offshore rigs are placed at elevations much higher than 10 m, and measurements from offshore discus buoys are typically below 10 m height and are also subject to buoys' heave and tilt. Therefore, any of the in situ measurements require interpolation to the standard 10 m level before being used.

Such extrapolations are not unambiguous. They usually invoke the assumption of the wall boundary layer and logarithmic profile associated with it. Both are problematic if applied in a broad range conditions. For light winds (less than 5 m/s), the 10 m height can be outside the constant-flux layer , and for extreme conditions wave crests can be higher than 10 m, and certainly the buoy masts will be below crests over a wave period.

Babanin and McConochie (2013) conducted comparisons of mean wind speeds and wind-momentum fluxes, based on measurements throughout the wave boundary layer, including wave-follower measurements very near the surface. Significant deviations from the constant-

flux expectations are found, even if corrected for the Monin-Obukhov stratification effects. The turbulent stress towards the surface is reduced dramatically, some 7 times in their measurements, whereas the mean wind speed is increased by some 5% compared to predictions based on the logarithmic profile. Practical significance of such observations is large, for example, for measurements conducted within the Wave Boundary Layer by buoys. If such buoy wind speeds extrapolated away from the surface by means of logarithmic profiles, to the 10 m standard height or above, the actual values of wind speeds may be overestimated. If the buoys are used to directly measure turbulent stresses, then, depending on the height of the anemometer mast on the buoy, such stresses can be very essentially underestimated. In the meteorological context, implications of these results are not very clear. On one hand, the concept of the constant flux layer needs serious modifications. On the other hand, the observed reduction of the turbulent stresses can be expected, since near the wavy surface part of the momentum flux is supported by wave-induced pressure/velocity fluctuations (e.g. Hara and Sullivan, 2015). Relative change of the total vertical flux of horizontal momentum, if any, needs to be determined by means of detailed modelling of the boundary layer with account on wave-induced effects.

Measurements of winds in extreme tropical cyclones have been, and remain subject to controversy for the last decade due to a number of dynamics and thermodynamics involved due to presence of spray in the air, extended whitecapping on the surface, changes to the surface roughness and aerodynamics at extreme winds – all of which influence the wind profile in the boundary layer. Smith and Montgomery (2014) provide theoretical reasoning supported by observational evidence as to why significant departures from the normally assumed logarithmic layer might be expected, questioning its use in the inference of the drag coefficient at high wind speeds. They also draw attention to a study examining a range of boundary-layer schemes demonstrating that a recently articulated boundary-layer spin-up mechanism transcends the presence of a log layer.

Apart from in situ measurements, satellite remote sensing has become a broadly employed technology for metocean observations including estimates of the winds. Young et al. (2017) evaluated the performance of the satellite systems across the full magnitude of the measured values of U10. Their analysis shows that across the range 0–15 m/s, altimeter, radiometer, and scatterometer instruments provide values of U10 that are consistent with buoy data and between the various instrument systems. For wind speeds above 15m/s, the altimeter appears to underestimate U10, whereas the radiometer/scatterometer data appear in reasonable agreement with the limited fixed-platform anemometer data. The radiometer and scatterometer cannot accurately measure wind speed in heavy rain. The exclusion of these cases, which often are associated with high winds, produces a fair weather bias. The distance between altimeter tracks is often many hundreds of kilometers and the repeat time for a given track up to 10 days. This relatively course spatial coverage means that the altimeter potentially undersampled storm events and may miss wind speed extremes. Cross validation between the instruments confirms that the altimeter underestimates extreme wind speeds. As reliable ground truth calibration data at high wind speeds are very limited, all systems (altimeter, radiometer, scatterometer) should be used with caution for wind speeds greater than 20m/s.

The final calibrated combined satellite database provides a valuable resource for the study of a wide range of metocean properties including the wind speeds. The datasets are available in the public domain (altimeter—Globwave, http://globwave.ifremer.fr/; radiometer/scatterometer—Remote Sensing Systems (REMSS), http://www.remss.com/).

5.4 Analytical & Numerical Methods

In Mao and Rychlik (2016), and Rychlik (2015), the spatio-temporal random model for variability of mean wind speed in Northern Atlantic was proposed. The model can be used to derive long-term wind speed distributions at fixed location and encountered by a vessel. Means

to evaluate parameters of the Weibull distribution for encountered wind speeds are given. The model can also be used to find the distribution of yearly maximums at fixed location and maximum wind speed along a rout. The model can also be used to simulate time series of mean wind speeds.

6. ICE /ICEBERGS

6.1 Measurements / Data

With the Arctic Ocean becoming open of ice in summer, shipping and offshore industry are advancing into Arctic and other freezing seas. Moreover, because of the summer melt, multi-year ice is being replaced by the first-year ice in the Arctic which makes navigation potentially possible round the year. As a result, there is a surge of efforts on modelling the waves in ice in order to enable metocean forecast for the Arctic. Such forecast requires knowledge of the ice cover, its thickness and other properties such as floe size distribution in the Marginal Ice Zones (MIZ) in real time. Therefore, Arctic expeditions which include ice measurements are on the rise. In 2012-2017, U.S. Office of Naval Research funded two five-year campaigns through the MIZ and Sea State Departmental Research Initiatives (DRI) broadly dedicated to different aspects of wave-ice interactions, with significant ice component in both of them. The latter DRI focused on Arctic conditions during the late summer and early autumn, especially the freeze-up of the Beaufort and Chukchi seas, to capture the strongest storms and maximum open water. This focus complemented the MIZ DRI that was studying the summer breakup and ice retreat. In situ observations were collected primarily during respective two cruises in spring and autumn of 2015, supplemented by long-term moorings, autonomous platforms and satellite remote sensing (Thomson et al., 2013). A special issue of the Journal of Geophysical Research, dedicated to these filed campaigns, is in progress at the time of writing, where state-of-the-art methods of in situ ice measurements, as well as outcomes of the field campaigns will be described in detail.

Satellite measurements of ice, both in the Arctic and Antarctica, are largely limited to the percentage of water surface covered by ice (ice cover). Radiometers conduct and provide the ice cover routinely, but do not measure waves, and hence there was a need to distinguish water surface from icescape (i.e. to measure ice cover) by altimeters which also take direct measurements of wave height and estimate the surface winds over the open water as described above. Such method was developed in Liu et al. (2016). Because of the heterogeneous nature of sea ice (e.g. leads, cracks, and ripples), individual altimeter waveforms exhibit a greater variability than those from the open water. A threshold value for the standard deviation of Ku-band backscatter was used to detect waveforms over sea ice, with 0.2 dB being found to provide optimal results in comparison to the three-parameter classifier proposed earlier for the microwave radiometer. Thus, the one-parameter classifier was obtained and tested and the 0.2 dB threshold can be applied to all altimeter missions to measure ice cover.

New satellite technologies are able, in addition to the ice cover, to measure ice thickness and ice-floe distribution necessary for the operational wave forecast, are rapidly emerging. NASA's Ice, Cloud, and land Elevation Satellite (ICESat) ran a series of campaigns over Antarctica from 2003 to 2008 that were used by Kurtz and Markus (2012) to calculate ice thickness. The ICESat data produced ice thickness averages at a 25 km resolution with an uncertainty of 23 cm. High-resolution ice-floe imaging of MIZ is possible by means of TerraSAR-X or in optical diapason, but such data are not routinely acquired and computer requirements for storage and processing of such images in large quantities are still prohibitive.

6.1.1 Space-borne Measurements

According to Cooley et al. (2016), remote sensing techniques must have the appropriate balance of spatial and temporal resolution to effectively examine river break up processes. In their study, they apply an automated ice detection algorithm using MODerate-Resolution Im-

aging Spectroradiometer (MODIS) satellite imagery data to identify ice breakup patterns. MODIS reflectance is used to classify each pixel of an area as snow/ice, mixed ice/water or open water. The algorithm is used to examine the Mackenzie, Lena, Ob' and Yenisey rivers from 2000–2014. Results from the analysis identify many possible drivers for the breakup progression however they are dependent on the river system.

The Cloud-Aerosol Lidar with Orthogonal Polarization (CALIOP) is a satellite that has been making continuous global snow and ice measurements since 2006. The polar-orbiting CALIOP obtains data between 82°S to 82°N which provides insight into the Arctic ice cover. CALIOP has an advantage over the MODerate-Resolution Imaging Spectroradiometer (MODIS) passive remote sensor because it can make reliable measurements during both the daytime and night-time seasons. Lu et al. (2017) have developed a new retrieval method for surface type identification which they apply to the past 10 years of available data. Their results are validated against data taken from the MODIS/Aqua, NASA team and AMSR-E which indicate good agreement. Overall, CALIOP provides the ability to study ice cover year-round at higher temporal and spatial resolution compared to previous passive sensors.

The Finnish Meteorological Institute (FMI) has developed a new approach for generating real-time automated ice thickness charts. Karvonen et al. (2016) present the methodology and compare their results against reference data sets from the Russian Caspian ice charts provided by the Scientific Research Center Planeta. The ice thickness is estimated by combining a thermodynamic snow/ice model with Synthetic Aperture Radar (SAR) data that has been segmented using a series of algorithms. Karvonen et al. (2016) conclude that this method can estimate ice thickness with a relative error less than 30%.

A regional coupled model system, HAMMER, was developed as part of the IRO-2 project to provide sea ice forecasting. In March 2014, Dobrynin et al. (2015) completed a field campaign in the Barents Sea to test the HAMMER system. HAMMER is made up of an atmospheric model, a sea ice model, and an ocean circulation model. The ice concentration and ice thickness are initialized using remote sensing data. The system incorporates global weather and ice forecasting data from the European Centre for Medium Range Weather Forecasts (ECMWF) and the Arctic wide ice-ocean forecast (ICEDAS). The system updates the model initialization parameters daily based on new forecast and measurement data. Furthermore, this system has the capability to feed forecast data directly into a route optimization system. Overall, the researchers found that the HAMMER results were within reasonable agreement with the ship-borne observations.

6.1.2 Airborne Measurements

Airborne Electromagnetic (AEM) induction is a method of measuring sea ice thickness via an electromagnetic (EM) induction device suspended from helicopter or plane. With an EM induction device, it is possible to identify the water-ice interface from their contrasting electrical conductivity. With the addition of a laser altimeter, which ranges the air-ice interface, the thickness of the ice can be found. Hendricks et al. (2014) employed this measurement technique near Barrow, Alaska on their field campaign in April 2013 as a proof-of-concept. They found that one of the most significant advantages of this technique is that it can be used for surveys of shallow regions with grounded sea ice that would otherwise be inaccessible by boat. Further validation work including systematic surveys paired with satellite data will be needed to refine this technique.

6.1.3 Ice Management Trials

On the Offshore Newfoundland Research Expedition in April 2015, Neville et al. (2016) participated in a series of ice management trials near the south-east coast of Labrador. These trials were completed to gather data to support numerical models used to simulate ice management operations. Collected data was used to quantify the rate of ice management in terms of

the incoming and outgoing ice conditions. Methods used to collect field data involved aerial footage taken from a helicopter, ice drift beacons, and footage taken from the ship.

Oden Arctic Technology Research Cruise 2015 (OATRC 2015)

In autumn 2015, the Norwegian University of Science and Technology and the Swedish Polar Research Secretariat (SPRS) conducted a research cruise named the "Oden Arctic Technology Research Cruise 2015" (OATRC 2015) which was supported by the ExxonMobil Upstream Research Company. The research cruise involved two icebreakers, Oden and Frej, who sailed north of Svalbard to conduct full scale trials of new technologies relating to ice management (Lubbad et al. (2016)).

One of the technologies tested on OATRC 2015 was a shipborne sea ice thickness and concentration measurement system. Lu et al. (2016) installed a series of shipboard Ice Concentration and Ice Thickness Cameras which worked with their corresponding image detection algorithms to provide a real-time quantification of the surrounding ice. The Ice Concentration Cameras were set up on the bridge facing obliquely towards the transiting direction. This provided a 180° view of the ice conditions towards the horizon. The Ice Thickness Camera was installed off the port side of the bridge looking vertically downward. This was done in order to obtain images of ice tilted up which exposed their thickness. The results of their trials indicated good agreement between the measured concentration and the ice observer's documentation. Measurements from the Ice Thickness Camera were compared against the measurements of an Electromagnetic (EM) inductive device which was mounted on the bow of the ship. The Ice Thickness Camera illustrated good agreement with the EM inductive device measurements.

Using the data collected from OATRC 2015, Holub et al. (2017) describe a system which can provide real-time ice drift measurements by applying photogrammetric feature detection and matching algorithms to marine radar or synthetic aperture radar (SAR) satellite data. The ship's radar data is evaluated and compared against GPS drift beacons deployed during the research cruise. The initial results showed that radar and SAR can successfully be used to measure ice drift.

6.1.4 Subsea Measurements

Upward Looking Sonar (ULS) instruments can be used to examine the underwater profile of ice with a temporal resolution of about 1 second, and horizontal and vertical spatial resolutions of about 1 m and 0.05m respectively. Fissel et al. (2015) applied methods of geometrical characterization to seven-years of ULS data to identify large ice keels, hummocky ice features, and massive ice features. Continuous year-long ULS data was obtained from the Chukchi Sea, Beaufort Sea and off the coast of North East Greenland. The results of the analysis allowed the researchers to identify geographical variability of massive ice features (MIF) between NE Greenland and the Canadian Beaufort Sea. The number of MIF detected in NE Greenland was found to be 5.5 times greater than the number of MIF in the Beaufort Sea location.

6.1.5 Icebergs

Detection

Iceberg detection is most commonly performed by visual inspection, sometimes with the aid of satellite imagery or marine radar. However, these methods tend to lose their effectiveness in low visibility, poor weather conditions and high sea states. Abdel-Moati et al. (2017) propose the application of infrared based optical imaging technology in automated iceberg detection. The primary advantages of infrared sensors are their higher immunity to fog and ability to work in the dark. Abdel-Moati et al. completed a series of laboratory experiments investi-

gating three infrared regions while varying the polarization. They found that none of the combinations of imagers and polarization filters worked in all scenarios and instead suggested that a multi-spectral camera could be used instead.

Drift Forecasting

An operational iceberg drift forecast model was developed by Turnbull et al. (2015) in support of a scientific coring campaign off Northwest Greenland. The coring operations took place from August-October 2012 in Melville Bay where there was a high concentration of icebergs. The model was designed to incorporate near real-time input including, in-situ metocean parameters, observed iceberg drift and size, tidal currents, and weather forecasts. Hindcast simulations were used, applying observed iceberg trajectories to tune the air and water drag coefficients of a given iceberg. During the campaign, researchers found that the model performed well in locations with strong and persistent non-tidal currents. The model did not perform as well in locations where ocean currents were dominated by tidal and inertial forcings.

Profiling

Due to the considerable threat of icebergs to offshore facilities and operations, iceberg modelling has been an important area of research for the design of offshore structures, drift forecasting and iceberg management systems. In recent years, photogrammetric methods have been used to obtain accurate 3D profiles of numerous icebergs.

In the summer of 2014, a group from Memorial University of Newfoundland completed a series of autonomous iceberg mapping missions by using an Autonomous Surface Craft (ASC) (Wang et al. (2015)) and a Slocum underwater glider (Zhou et al. (2014)). For the above-water surveys, the ASC collected iceberg images, GPS positions, laser range information and vehicle orientation information. Wang et al. (2015) applied methods of volume intersection and occluding contour finding to generate 3D models of the icebergs. Underwater mapping of an iceberg was performed by Zhou et al. (2014) using a mechanical scanning sonar. Insufficient data was collected to form a closed surface; however these trials confirmed the potential of this system.

In June of 2012, Younan et al. (2016) conducted a field program offshore Newfoundland and Labrador collecting 3D profiles of grounded and floating icebergs. The above-water profile of the iceberg was obtained by circumnavigating an iceberg while collecting: photographs from 3 ship-mounted cameras, position and heading data, and laser range data. Photogrammetric methods were then used to generate a 3D model. The underwater iceberg mapping was completed using a remotely operated vehicle (ROV) outfitted with a multibeam sonar. During this program 35 high definition iceberg models were successfully logged and generated.

6.1.6 Thermodynamics

According to Turnbull et al. (2016), thermodynamic models of sea ice can be used in predicting seasonal patterns in ice concentration, thickness, and flexural strength. In February 2016, Turnbull et al. deployed six Temperature Acquisition Cables (TACs), along with two anemometers on snow-free, land-fast sea ice in Pistolet Bay, Newfoundland. Combining these measurements with the available meteorological data, an alternative method for solving the sea ice surface temperature was developed. This method consists of a linear function which depends on the surface meteorological parameters. With further development of this model, Turnbull et al. suggests that it could be used for remote estimation of ice compressive and flexural strength.

6.2 ICE-STRUCTURE INTERACTION

6.2.1 Sea Ice

When a ship is transiting in sea ice, its hull is subjected to a variety of ice impact pressures. Since the 1980's, computerized measurement techniques have been used to collect time-series impact loads on various vessels. This has allowed for the development of structural design criteria based on the pressure versus contact area relationship obtained from full scale data. Most recently, a large shuttle tanker, the M/T Timofey Guzhenko was outfitted with state-of-the-art sensors capable recording continuous long-term ice pressures and structural responses. Between 2009 and 2013, the system recorded close to 30,000 bow impact events. From this dataset, Kim et al. (2016) investigate three impact events representing peak force and peak local pressure events. Using finite element (FE) analysis, the measured ice pressure data was applied to an FE model of the ship's grillage. The results of this analysis were used as a verification check for the ice load monitoring system which confirmed the structure did not experience yielding.

Development of a numerical ice simulator was undertaken as part of DYPIC (Dynamic Positioning in ICE), an international research project focused on developing Dynamic Positioning technology in ice (Kerkeni et al, 2014). The Norwegian University of Science and Technology started developing the model in 2010 using a physics engine to model rigid body motions and evaluate contact forces of a DP vessel operating in floe ice. Some of the latest model developments are presented in Scibilia et al. (2014) with the incorporation of an ice splitting model along with an ice fracture solver which simulates local ice compaction around an icebreaker. Scibilia et al. use data obtained on the OATRC 2012/2013 trials to make qualitative comparisons of observed physical processes with the results of the numerical model. Based on their simulations, they found that the results exhibited the same visual behaviour as observed in the field.

The GEM simulation tool (Daley et al. (2014)) was initially developed as part of the STePS2 project at Memorial University of Newfoundland as a tool used to estimate local ice loads on a vessel operating in pack ice. In this simulation, every ship-ice and ice-ice collision is modelled. One of the key features of GEM is that simulations can be run much faster than real-time. This is partly attributed to underlying assumptions of the collision model which reduces 2D collisions into equivalent 1D collisions. In Daley et al. (2014) a sample simulation is provided along with the resulting impact load statistics. These results are then compared against the available data concerning ice impact loads in sea ice.

Through incorporating a 2D discrete element method, Zhou and Peng (2014) propose a numerical method for simulating the performance of a dynamically controlled vessel in level ice. The waterline of the hull and ice edge are modelled using a series of nodes. In the case of the hull waterline, a closed polygon is formed; whereas the nodes of the ice edge will form a broken line. Ship-ice interaction is detected using a polygon-based detection technique. Three separate contact scenarios are used in solving for the ice induced forces. The results of the model were validated against sea trials of a full-scale R-class icebreaker. A dynamic positioning model was implemented using a line of sight guidance scheme and a PID algorithm.

A similar 2D discrete element method is used by Dai (2016), however instead of modelling level ice, pack ice was modelled using circular floes. In addition to ship-ice collisions, ice-ice collisions were also considered.

Hisette et al. (2017) created a simulation using the discrete element method to model a ship breaking through an ice ridge. Artificial ice ridges are generated in the simulation using buoyancy, where a series of submerged ice blocks are released below the surface and float up to form an ice ridge. The simulation results are compared against model tests which include a

qualitative comparison of underwater videos of the ridge and a quantitative comparison of time-series data.

6.2.2 Laboratory Testing

A series of dynamic positioning (DP) model scale tests were complete by Wang et al. (2016) in the ice tank facility at OCRE-NRC in 2015. The trials consisted of 372 runs using 17 different ice sheets. The test variables included floe size, floe thickness, concentration, inclusion of brash ice, ice drift speed, and heading direction. The ice loads were not directly measured during the tests, but instead estimated from the thruster response. An NRC developed DP algorithm was used in the model and provided satisfactory behavior in most cases. Manual control of the model was required during some of the more severe ice conditions tested.

Bergsma et al. (2014) examine the use of artificial ice as an alternative to refrigerated ice for testing the ice submersion resistance of a ship at model scale. A series of towing tank tests were completed at the Maritime Research Institute Netherlands (MARIN) using pre-sawn polypropylene for artificial ice. The results of the tests with artificial ice were validated against the Lindqvist formula. It was found that the submersion resistance of the artificial ice was higher than the Lindqvist prediction at low ship speeds. Bergsma et al. assume that this is due to the friction of the material at low velocities. Good agreement with the Lindqvist prediction was achieved at higher ship velocities.

6.2.3 Iceberg Loading

In cases where icebergs pose a risk to offshore gravity based structures (GBS), special consideration must be given to ensure that the risk of a topsides impact is reduced to an acceptable level Stuckey et al. (2016). This is typically done by altering the geometry of the structure, either by elevating the topsides, or enlarging the footprint. To optimize the geometry of a GBS, Stuckey et al. (2016) developed a numerical model to estimate the frequency of icebergs that impact the topsides using 3D models of a given platform and iceberg models of various shapes and sizes. Iceberg models were generated from a database of iceberg profile measurements and set adrift next to the platform. The simulation was completed multiple times to gain a statistical understanding of the initial point of contact and crushing behaviour of the various iceberg shapes that might be encountered.

6.2.4 Ice Hydrodynamics

A review of the hydrodynamics of icebergs was undertaken in Sayeed et al. (2017). This review examines the current literature on iceberg and bergy bit motion during interaction and impact with an offshore structure. This topic is broken down into four main parts: the far field wave induced motions; the near field interaction effects; collision modeling; and a summary of past full-scale trials. It is brought to light that with the current state of research is lacking in many aspects of understanding the near field hydrodynamic effects of icebergs. It is argued that the inability to properly model these effects often lead to overestimations in impact velocity and therefore impact energy. Better understanding of hydrodynamic interaction could lead to improved load predictions allowing for more efficient design of offshore structures.

Sayeed et al. (2015) conducted model tests investigating the hydrodynamic interaction between ice masses and offshore structures. The variables tested included the size and shape of the ice masses as well as the wave particulars. Three spheres of different diameter along with an irregular shaped ice block were used as model icebergs. Their work showed that hydrodynamic proximity and wave reflection had a considerable effect on small ice masses near larger structures. A reduction in impact velocity is observed which indicates that the hydrodynamic effects cause a reduction in the impact load.

Experiments were performed by Chander et al. (2015) to investigate the forces involved in submerged ice collisions. This was done in Memorial University's Fluids lab using a high-speed camera to film the trajectory and impact of a spherical ice model (10cm polypropylene) with a model ship hull. A waterproof load cell was used to record the impact forces. Added mass was calculated using the velocity and acceleration data obtained from image analysis performed using MatLab. In their experiments, the added mass coefficients were found to be close to 0.5 for lower values of Reynolds number but increased suddenly as the ice model approached the plate. For all tests, the added mass coefficient was at a maximum at the point of impact.

6.2.5 Ice Accretion

Ice accretion can pose a significant hazard to vessels and offshore structures in cold regions. Not only does ice accretion lead to unsafe working conditions for crew on deck, but can also threaten the stability of the vessel which may cause the vessel to capsize. Mintu et al. (2016) provide a review of existing literature related to ice accretion covering: field measurements, experimental studies and numerical models. A critique of the current international standards is also provided.

In their review, Mintu et al. (2016) emphasize the complexity of ice accretion where the amount of icing will depend on several parameters including the meteorological conditions, the wave heights, vessel speed and direction relative to the waves. Experience also shows that the amount of icing is also dependant on the location of the structure/vessel relative to the location of the spray and waterline.

Examining the state-of-the-art research on ice accretion, Mintu et al. (2016) found that many research approaches tend to focus on just one aspect of ice accretion due to high level of complexity. On the other hand, they have found that classification societies and regulatory authorities have oversimplified the problem, providing generalized equations for determining icing allowances. Furthermore, they have found a lack of consistency between the standards, indicating further research on ice accretion is needed to develop a more consistent design standard.

Through analysis of infrared and visual images, Fazelpour et al. (2016) proposes a method for measuring the ice thickness on a cylindrical component. Laboratory experiments were conducted in a cold room using two cylindrical components: one covered by saline ice, and one covered by fresh ice. The experimental results indicate that the method is reliable in determining the thickness of ice.

6.3 Analytical & Numerical Models

Shu et al. (2015) make an assessment of sea ice simulations in the Coupled Model Intercomparison Project Phase 5 (CMIP5) during 1979 to 2005. Forty-nine models, almost all of the CMIP5 climate models and earth system models with historical simulation, are used. For the Antarctic, multi-model ensemble mean results can give good climatology of sea ice extent (SIE), but the linear trend is incorrect. For the Arctic, both climatology and linear trend are better reproduced. Sea ice volume is first evaluated but with too small results as a result of sea ice thickness simulated in CMIP5 is too thin.

Croxall et al. (2015) present the new 3.6 version of the Louvain-la-Neuve sea ice model (LIM), which will be used for the next Climate Model Inter-comparison Project (CMIP6). In the new model, the robustness, versatility and sophistication of the code are focused on and improved. The model simulated sea distributions at a global scale with nominal 2-degree resolution and at a regional scale with 2 km resolution around the Svalbard Archipelago. The results are consistent with the observed data.

Rae et al. (2015) adopt the new sea ice configuration GSI6.0 to simulate the sea ice extent, thickness and volume compared with the previous configuration and with observationally-based datasets. In the Arctic, the sea ice is thicker in all seasons than in the previous configuration, and there is now better agreement of the modelled concentration and extent with the HadISST dataset. In the Antarctic, a warm bias in the ocean model has been exacerbated at the higher resolution of GC2.0, leading to a large reduction in ice extent and volume.

Stroeve and Notz (2015) present the insights on past and future sea-ice evolution from combining observations and models. It is concluded that models and observations agree well on the sensitivity of Arctic sea ice to global warming. In contrast, a robust reduction of the uncertainty range of future sea-ice evolution remains difficult, in particular since the observational record is often too short to robustly examine the impact of internal variability on model biases. Process based model evaluation and model evaluation based on seasonal-prediction systems provide promising ways to overcome these limitations.

Interaction of ice and structures

Yu et al. (2015) simulate the wind turbine dynamic response under surface ice loads using FAST. For conditions in which the ice forcing is essentially decoupled from the structural response, ice forces are established from existing models for brittle and ductile ice failure. For conditions in which the ice failure and the structural response are coupled, a rate-dependent ice model is described. Analytical ice mechanics models are presented that incorporate ice floe forcing, deformation, and failure. For lower speeds, forces slowly build until the ice strength is reached and ice fails resulting in a quasi-static condition. For intermediate speeds, the ice failure can be coupled with the structural response and resulting in coinciding periods of the ice failure and the structural response. A third regime occurs at high speeds of encounter in which brittle fracturing of the ice feature occurs in a random pattern, which results in a random vibration excitation of the structure.

Shu et al. (2017) study on small wind turbine icing and its performance. Results show that ice rapidly reduces the rotation speed and load power of the wind turbine. The ice growth rate rises initially and then declines with time. Ice linearly increases from the root to the tip and mainly accumulates at the leading edge. As the rotation speed slows down, the ice-covered area moves to the pressure side. Higher wind velocity and lower temperature lead to more severe ice, but they do not change the ice shape.

Metrikin et al. (2015) investigates dynamic positioning (DP) in level ice conditions using experimental and numerical approaches. A novel numerical model for simulating DP operations in level ice is presented. The fracture of level ice is calculated on-the-fly based on numerical solution of the ice material failure equations, i.e., the breaking patterns of the ice are not pre-calculated. Several ice basin experiments are reproduced in the numerical simulator, and the results of the physical and numerical tests are consistent.

Bae et al. (2016) present the numerical simulation for the collision between side structure and level ice in event of side impact scenario. Different models of indenter were taken into account in order to observe structural responses and influences of external parameters, namely ice topology, while the described location parameters were taken as the ship's internal parameters. Impact force was presented with total energy, as well as the ratio between kinetic and internal energy. The deformation pattern was used as a verification of the collision process and its subsequent results.

Song et al. (2015) present the fluid-structure-interaction analysis of an ice block-structure collision. Numerical simulations of a collision between an ice block and a floating structure have been carried out using the FSI analysis technique of the LS-DYNA code for a more realistic and accurate prediction of the impact loadings. The simulation results were compared with laboratory experiments where a floating structure was impacted with an approximately

one ton ice block at a speed of 2 m/s. The results of the numerical simulations compared favorably with actual experiments using freshwater ice blocks.

Mierke et al. (2015) study the applicability of the Lattice Boltzmann based free surface flow solver elbe to the simulation of complex ship-ice interactions in marine engineering. Basic methodology and initial validation of the fluid-structure coupling of elbe and ODE is presented. As elbe uses graphics processing units (GPUs) to accelerate the numerical calculations, the coupled numerical tool allows for investigations of ship-ice interactions in very competitive computational time and on off-the-shelf desktop hardware.

Hu and Zhou (2015) make an experimental and numerical study on ice resistance for icebreaking vessels. Different numerical methods are presented to calculate ice resistance, including semi-analytical method and empirical methods. A model test of an icebreaking vessel that was done in an ice basin has been introduced for going straight ahead in level ice at low speed, with a good comparison between model test results and numerical results.

Huisman et al. (2016) present a numerical model to predict the interaction between floating objects and the surrounding level ice, especially breaking of level ice due to bending. This method assumes the formation of circumferential cracks as a result of the bending moment in order to achieve a more realistic breaking pattern. The ice-breaking model is validated for a two-dimensional elastic beam.

7. COUPLED PHENOMENA

Wave-induced effects in the lower atmosphere and the upper ocean have been a major research topic over the last decade (see e.g. Babanin et al. (2012) for introduction). It is rapidly becoming clear that many large-scale geophysical processes are essentially coupled with the surface waves, and those include weather, tropical cyclones, storm surges, climate and other phenomena in the atmosphere, at air/sea and sea/land interface, and many issues of the upper-ocean mixing and ocean currents below the surface. Besides, the wind-wave climate itself experiences large-scale trends and fluctuations (Young et al., 2011), and is subject to changes in the weather climate.

Before that, coupling of the wave-related air-sea interactions into weather and climate research had not been conducted due to two main reasons. In terms of geophysics, the reason is the traditional perception that processes of such distant scales can be studied and modeled separately, and exchange between the scales can be parameterized as some larger-scale average (mean fluxes of energy and momentum in this case). In technical terms, the computational costs of such coupling have been prohibitive until recently. Things, however, are changing.

7.1 Wave Breaking

Wave breaking, if it did not exist, would have to be invented. Its role in the coupled air-surface-ocean systems is hard to overestimate. On the surface, it limits the wave growth and hence prevents occurrence of very high waves, and serves as a major dissipation mechanism in wave models. Above the surface, it facilitates the fluxes of momentum and energy, heat and moisture. Breaking produces spray and spume, which links waves to the aerosol production and thus all the way to inland corrosion, cloud physics, climate. Below the surface, breaking is a major source of turbulence and the main source of bubbles. The former is relevant for ocean mixing, sediment sediment suspension and transport, the latter to gas exchange, aeration and thus to biology, underwater acoustics. Wave momentum lost due to the breaking goes to surface currents and contributes to scattering of surface debris and pollutants.

Wave breaking is closely related to the problem of rogue waves. Those are waves of maximal possible height, and this height is controlled by the breaking. Babanin and Rogers (2014) argued that the enhancement above the mean wave height can be due to quasi-linear superposition of waves and/or because of nonlinear effects such as instabilities of wave trains. Both

appear to be important and possible. Individual waves can be focused into a superposition due to either dispersive or directional features of wave fields. While probability of the former in oceanic conditions is very low, the directional focusing appears to be rare, but regular events. Nonlinear wave fields should be separated into stable and unstable conditions, with different probability distributions for wave heights/crests and therefore wave breaking. In stable conditions, wave statistics are determined by the quasi-linear focusing, whereas in unstable wave trains high transient wave events can occur. Their maximal height/steepness is determined by combined dynamics of the instability growth and the limiting wave breaking. Research argument about relative importance of linear superposition and nonlinear dynamics, leading to wave breaking, is continuing (e.g. Chalikov and Bulgakov, 2017).

With the growing interest to the wave-coupled phenomena, wave-breaking effects in the coupled systems have been actively studied. Brumer et al. (2017) considered concurrent wave-field and turbulent flux measurements acquired during the Southern Ocean (SO) Gas Exchange (GasEx) and the High Wind Speed Gas Exchange Study (HiWinGS) projects. These permitted evaluation of the dependence of the whitecap coverage on wind speed, wave age, wave steepness, mean square slope, and wind-wave and breaking Reynolds numbers. Xie (2016) considered effects of winds on breaking in surf zone, using a two-phase flow model. Both spilling and plunging breakers over a steep (1:35) sloping beach have been studied under the influence of wind, with a focus during wave breaking. Detailed information of the distribution of wave amplitudes and mean water level, wave-height-to-water-depth ratio, the water surface profiles, velocity, vorticity, and turbulence fields have been presented and discussed. The inclusion of wind alters the air flow structure above water waves, increases the generation of vorticity, and affects the wave shoaling, breaking, overturning, and splash-up processes.

The important role of wave breaking in dissipation and models for wave forecast remain in focus of research. Zieger et al. (2015) discussed a new whitecapping dissipation function in WAVEWATCH-III. The new dissipation term features the inherent breaking term and a cumulative dissipation term, which is due to breaking of short waves caused by longer waves in the spectrum. Salmon et al. (2015) considered scaling of depth-induced breaking in spectral models. A joint scaling dependent on both local bottom slope and normalized wavenumber is presented. In order to account for the inherent differences between uni-directional (1D) and directionally spread (2D) wave conditions, an extension of the wave breaking dissipation models is proposed. By including the effects of wave directionality, rms errors for the significant wave height are reduced for the best performing parameterizations in conditions with strong directional spreading. Linking wave models with the coupling problem, Scanlon et al. (2016) estimated whitecap coverage from such models. High-resolution measurements of actively breaking whitecap fraction and total whitecap fraction from the Knorr11 field experiment in the Atlantic Ocean are compared with estimates of whitecap fraction modeled from the dissipation source term of the ECMWF wave model. The results reveal a strong linear relationship between model results and observed measurements, thus indicating that the wave model dissipation is an accurate estimate of total whitecap fraction.

7.2 Wave-current interactions

The surface waves are wind-generated, but the respective fluid motion is mostly part of the water side of interface and is strongly linked to the upper-ocean dynamics including the ocean currents. Wave-current interactions are common conditions both in the open ocean and in coastal areas. Major currents such as the Gulfstream, Kuroshio, or Agulhas are well known for harsh seas and high likelihood of abnormal (rogue) waves. Tidal inlets with waves on strong and variable currents are a typical feature of shipping routes in coastal areas. While linear effects of currents on waves, such as refraction, Doppler shift, or relative speed with respect to the wind are assumed to be implicitly or explicitly included in wave-forecast models (often unverified and not validated), nonlinear effects are usually left out or, at this stage, even unknown. These include changes to nonlinear interactions in the presence of currents

with horizontal or vertical velocity gradients, wave–current energy and momentum exchanges, nonlinear modifications of the wave spectrum.

The review paper by Babanin et al. (2017) outlines principles of phase-resolving and phase-average wave models, with emphasis on the state of the art of wave-current interaction physics. They argue that these interactions are the least well-developed part of such models. Linear and nonlinear dynamics of waves on currents are discussed; depth-integrated and depth-varying approaches are described; examples of numerical model performance for waves on currents in realistic oceanic scenarios are presented.

Waves, in turn, can substantially influence the surface currents through their Stokes drift, and even more so through radiation stress due to the momentum lost in wave breaking (even in deep water). These influences are largely missing in modelling the ocean circulation of open oceans, and they certainly need to be reinstated because of their importance, for example, in search and rescue missions. In principle, this can be done by coupling the wave models with the circulation models, but this should be done with caution. The present-day wave forecast models were not designed to produce correct fluxes for input and dissipation of energy, but rather to provide an approximate balance of those in order to predict the resulting wave growth and wave height reasonably well.

Most essential is the role of waves in influencing and even producing currents in finite depths. Here wave breaking is extensive, and this role is known and well accounted for in coastal circulation and coastal engineering models. Apart from direct wave-current applications, a more complex suit of wave current-turbulence interactions, both on the atmospheric and ocean sides, is gaining attention over the recent years. While energies involved are small in the context of changes to the waves or currents, they may play an additional and missing feedback in the atmospheric boundary layer, where airflow then generates both surface waves and currents, and in the upper ocean mixing.

A number of laboratory and field experiments have been conducted to pin down elements of the missing wave-current physics recently. In laboratory, Rapizo et al. (2016) investigated the effects of a co-flowing current field on the spectral shape of water waves. The results indicate that refraction is the main factor in modulating wave height and overall wave energy. The structure of the current field varies considerably, some current-induced patterns in the wave spectrum were observed. At high frequencies, the energy cascading generated by nonlinear interactions is suppressed, and the development of a spectral tail is disturbed, as a consequence of the detuning of the four-wave resonance conditions. Furthermore, the presence of currents slows the downshifting of the spectral peak. The suppression of the high-frequency energy under the influence of currents is more prominent as the spectral steepness increases. The energy suppression is also more accentuated and long-standing along the fetch when the directional spreading of waves is sufficiently broad. Additionally, the directional analysis shows that the highly variable currents broaden the directional spreading of waves. The broadening is suggested to be related to random refraction and scattering of wave rays. Thus, the variable currents have significant implications both on spectral and phase-revolving (i.e. rogue waves) evolution of wave fields.

Laboratory study by Toffoli et al. (2015) investigated specifically rogue waves in opposing currents. Interaction with an opposing current amplifies wave modulation and accelerates nonlinear wave focusing in regular wavepackets. This results in rogue waves, even if the wave conditions are less prone to extremes. Laboratory experiments in three independent facilities were presented to assess the role of opposing currents in changing the statistical properties of unidirectional and directional mechanically generated random wavefields. The results demonstrate in a consistent and robust manner that opposing currents induce a sharp and rapid transition from weakly to strongly non-Gaussian properties. This is associated with a substantial increase in the probability of occurrence of rogue waves for unidirectional and directional

sea states, for which the occurrence of extreme and rogue waves is normally the least expected.

The stronger nonlinearity in adverse currents signifies higher wave steepness, which must affect the rate of energy dissipation. Rapizo et al. (2017) studied the current-induced dissipation through a data set in the tidal inlet of Port Phillip Heads, Australia. The wave parameters analysed were significantly modulated by the tidal currents. Wave height in conditions of opposing currents (ebb tide) can reach twice the offshore value, whereas during co-flowing currents (flood), it can be reduced to half. The wind-wave model SWAN is able to reproduce the tide-induced modulation of waves and the results show that the variation of currents is the dominant factor in modifying the wave field. In stationary simulations, the model provides an accurate representation of wave height for slack and flood tides. During ebb tides, wave energy is highly overestimated over the opposing current jet. A modification to enhance dissipation as a function of the local currents was proposed. It consists of the addition of a factor that represents current-induced wave steepening and it is scaled by the ratio of spectral energy to the threshold breaking level. The new term asymptotes to the original form (Zieger et al., 2015) as the current in the wave direction tends to zero. The proposed modification considerably improves wave height and mean period in conditions of adverse currents, whereas the good model performance in co-flowing currents is unaltered.

Overall, wave-current interactions are the last loose element of physics of wave forecast models, and, to an extent, of ocean circulation modeling. A rich variety of dynamics are involved, some of which are not well understood, and complicated mathematics to describe such dynamics, make it an exciting research field at the boarder of wave, ocean and meteorological applications.

7.3 Wave-ice interactions

Wave-ice interactions have long been an exotic field of research, but with the Arctic opening from ice in summer months, epy wave-ice modeling acquires important practical meaning. Among the various theories to explain wave-ice interactions, some differ qualitatively, i.e. wave scattering (without dissipation) and dissipation (with or without scattering); others differ quantitatively to the extent that some theories predict wavelength to increase in presence of ice, whereas others predict wavelength to decrease. In the field, all the mechanisms are acting together, depending on their relative magnitude, and practical guidance of the existing theoretical knowledge in forecasting waves in marginal ice zones is limited. Additional complications in this regard are due to necessity of also knowing initial conditions for the ice coverage and properties, and to be able to predict effects of waves on ice—this makes wave-ice interaction an essentially coupled problem.

The wave-ice problem can be roughly subdivided into three large groups of interactions. First is the interaction of waves with solid or uniform ice. Note that solid and uniform is not the same. Solid ice can consist, for example, of pancake ice floes frozen together, whose structure is then not uniform. At the other end of extremes, the frazil ice is uniform, but not solid. Visco-elastic properties of ice in such conditions cause dissipation and change of rate of propagation of wave energy. Below the ice, additional turbulent dissipation occurs in the ice-water boundary layer, and scattering of wave energy by ice ridges further contributes to wave-energy attenuation in the main wave propagation direction (without dissipating he energy).

Once the ice is broken, which is the definition of the Marginal Ice Zone (MIZ), the dissipation mechanism is different. It is due to various interactions of ice floes with each other, such as collisions, rafting etc. – all of which take energy from the mean wave motion.

For wave models to be able to predict waves in ice automatically, they should be able to identify the moment of ice breakage by waves. Dimensionless criteria of such breakage in the

broad range of ice conditions remain an open research issue, particularly as the ice conditions are also not usually known in the operational regime.

A few field experiments have demonstrated the fracture and break up of ice pack and therefore the retreat of ice edge induced by strong wave events in both the Arctic and Antarctic MIZs (e.g. Collins et al., 2015, Kohout et al., 2016). A potential and more effective mechanism that accelerates ice retreat may be the positive wave-ice feedback discussed by Thomson and Rogers (2014): due to the fetch effect, the gradual reduction of ice cover provides more opportunities for the emerging of energetic waves, and subsequently such waves can propagate much farther into ice and cause much more ice break-up. The influences of turbulent characteristics of under-ice currents and ice drift on the energy dissipation rates of waves propagating below continuous ice cover were investigated in situ by Marchenko et al. (2016).

Remote sensing methods, like in the other branches of Metocean applications, are increasingly becoming an essential method of field research of wave-ice interactions in their own right. Given the novelty of the problem, some of the emerging methods are highly innovative. Cambell et al. (2014) conducted observation of waves interacting with ice by using stereo imaging. This was applied to three distinct ice types: brash, frazil, and pancake. Ardhuin et al. (2017) offered a new method of measuring waves in ice by using SAR imagery. The iterative nonlinear algorithm estimates phase-resolved deterministic maps of wave-induced orbital velocities, from which elevation spectra can be derived.

Analytical research was the strong part of the wave-ice discipline even before the present boom, and with the new motivation it continued to offer new theories and advances to existing theoretical mechanisms. Mosig et al. (2015) conducted comparison of visco-elastic models for wave attenuation. Montiel et al. (2016) proposed a new method to solve the traditional time-harmonic multiple scattering problem under a multidirectional incident wave forcing with random phases. Zhao and Shen (2016) suggested a continuum approach by means of diffusion approximation to the ocean wave scattering by ice floes. A problem of wave-ice speed, connected with the dissipation and yet separate, was comprehensively addressed by Collins et al. (2016) whose investigation considers theoretical models and empirical studies related to the dispersion of ocean surface gravity waves propagating in ice covered seas.

Field and analytical research is usually underpinned by laboratory experiments which allow us to look in details on physical mechanisms involved. Bennets et al. (2015) offered an experimental model of transmission of ocean waves by an ice floe. Thin plastic plates with different material properties and thicknesses were used to model the floe. Toffoli et al. (2015) used the model to validate in laboratory conditions the canonical, solitary floe version of contemporary theoretical models of wave attenuation. Amplitudes of waves transmitted by the floe were presented as functions of incident wave steepness for different incident wavelengths.

Thus, the rich and complex nature of wave-ice interactions caused a surge of dedicated research in recent years. This combined the relative novelty of the topic with the sudden demand on the practical outcomes for wave forecast in the freezing seas and specifically in MIZ. The research topic however remains fragmented at this stage and is in still need of some common thread to be established.

7.4 Atmospheric wave boundary layer

Connection of the surface waves with the wind is most intimate and makes the Wave Boundary Layer different to any other boundary layer in fluid mechanics or geophysics. The wind generates the waves, but the waves then change the very wind which produced them. The waves do not provide a constant roughness because they grow, they move and they break. In the classical wall-layer sense, the waves are not roughness at all, as the roughness scale of the logarithmic profiles in the constant-flux layer is orders of magnitude smaller than the wave height. The logarithmic profile is characteristic of the constant turbulent flux, and in WBL

this is not the case. The total flux in WBL is indeed constant, but apart from the turbulent flux, it is also supported by form drag which goes into wave growth and tangential drag which passes momentum to the surface currents. As a result, the actual turbulent flux in the constant-flux layer is reduced towards the surface and the wind profile in WBL deviates from the logarithmic profile (see Babanin and McConochie, 2013, Hara and Sallivan, 2014). We refer to the new book of Chalikov (2016) which has chapters on wind-wave interactions and Wave Boundary Layer written by one of the leading experts in this field.

Since the concept of constant-flux layer and the role of the surface waves in modifying the balance of turbulent stresses very near the surface have already been discussed in Section 5A, here we will concentrate on the atmospheric wave boundary layer in other less common conditions. There are also specific changes to the atmospheric boundary layer at very light winds and very strong winds. In the latter case, the air is full of water droplets due to continuous wave breaking, and with water being 1000 times heavier than air, the spray can impact on the boundary layer substantially. This topic has been a subject of extensive research over the last decade.

Starting the review from extreme wind conditions, Smith et al. (2014) challenged the very concept of the logarithmic boundary layer in the inner core of the hurricanes. While their argument is meteorological, it refers to near surface peculiarities of the wind stress vector. This stress must be connected with the complex nature of wave spectrum in the hurricanes, i.e. the waves are always at angle to the wind in the tropical cyclones, up to 180 degrees in some quadrants (Liu et al., 2017).

Troitskaya et al. (2016) continued research of the boundary-layer spray in extreme-wind conditions by means of a theoretical model. Air-sea momentum exchange was investigated during the entire life cycle of a droplet, torn off the crest of a steep surface wave, and its fall down to the water, - in the framework of a model covering the following aspects of the phenomenon: (1) motion of a heavy particle in the air flow (equations of motion); (2) structure of the wind field (wind velocity, wave-induced disturbances, turbulent fluctuations); (3) generation of the sea spray; and (4) statistics of droplets (size distribution, wind speed dependence). Contrary to some other models of the sea spray, it is demonstrated that the spray in strong winds leads to an increase in the surface drag up to 40% on the assumption that the velocity profile is neutral.

In precision laboratory tests, Troitskaya et al. (2017) investigated the physical mechanism behind the sea-spray production in hurricanes experimentally. By means of high-speed video, they identified it as the bag-breakup mode of fragmentation of liquid in gaseous flows. This regime is characterized by inflating and consequent bursting of the short-lived objects, ‘bags’, comprising sail-like water films surrounded by massive liquid rims then fragmented to giant droplets with sizes exceeding 500 micrometers. From first principles of statistical physics, they develop a statistical description of these phenomena and showed that at extreme winds the bag-breakup is the dominant spray-production mechanism.

Cox et al. (2017) revisited another extreme-wind problem, the remarkable 1883 sea rescue where oil was used to reduce large breakers during a storm. Modeling of the oil film’s extent and waves under the film suggests that large breakers were suppressed by a reduction of wind energy input. Modification of surface roughness by the film is hypothesized to alter the wind profile above the sea and the energy flow.

Behaviour of the atmospheric boundary layer at the other extreme, light wind, is probably understood even less than the hurricane conditions. In the meantime, it has practical significance in a broad range of applications, for example, water evaporation in ponds. Wen and Mobbs (2014, 2015) simulated laminar air–water flow of a non-linear progressive wave at low to moderate wind speeds. While in the water differences between the solutions of potential and viscous flows are very small, in the air they are substantial (Wen and Mobbs, 2014).

The velocity distribution in the airflow in the wave boundary layer is strongly influenced by the background wind speed and it is found that three wind speeds, U = 0, U = umax (the maximum orbital velocity of a water wave), and U = c (the wave phase speed), are important in distinguishing different features of the flow patterns. In the opposing wind from zero to 1.5 times the wave phase speed, it is revealed that at any speed of the opposing wind there exist two rotating airflows, one anti-clockwise above the wave peak and one clockwise above the wave trough. These rotating airflows form a buffer layer between the main stream of the opposing wind and the wave surface. The thickness of the buffer layer decreases and the strength of rotation increases as the wind speed increases. The profile of the average x-component of velocity reveals that the water wave behaves as a solid surface producing larger wind stress compared to the following-wind case.

Thus, in spite of being one of the oldest topics in the context of wave interactions with marine environments, the atmospheric boundary layer and wave influences there remain the active area of research. New features are being revealed not only at extreme ends of wind-wave interactions, i.e. light winds and hurricane, but also in benign and moderate wind conditions.

7.5 Wave influences in the upper ocean

Dynamic wave influences in the upper ocean can be subdivided into two parts: momentum which the waves pass to the surface currents and the energy which is passed to the upper layer of the ocean. The latter, apart from the currents, goes to the turbulence and mixes the ocean. If the mixing is limited to the ocean's mixed layer, then its effect is limited to sediment suspension and transport of other admixtures. If, however, the mixing through the picnocline occurs because it is close enough to the surface (which is usually the case in spring-summer period), then such mixing can affect thermohaline circulation, cool the surface – with important consequences for large-scale processes discussed in Section 7.6 below. Note that we do not include wave breaking influences here, which were the topic of Section 7.1 they are powerful bursts of momentum and energy transfer, but are different: random, sporadic and concentrated very near the surface, at the scale of wave height.

Wave momentum is present in the ocean as Stokes drift and is ultimately passed to the ocean through wave breaking (although some amount of it goes back to the air (Iafrati et al., 2014)). The Stokes drift is easily derived for monochromatic waves, but not so directly for spectral waves which the real ocean seas always are. Breivik et al. (2016) explored a new approximation to the Stokes drift velocity profile based on the exact solution for the Phillips spectrum. The profile is compared with the monochromatic profile and the recently proposed exponential integral profile. ERA-Interim spectra and spectra from a wave buoy in the central North Sea are used to investigate the behavior of the profile. It is found that the new profile has a much stronger gradient near the surface and lower normalised deviation from the profile computed from the spectra. Based on estimates from two open-ocean locations, an average value was estimated for a key parameter of the profile. Given this parameter, the profile can be computed from the same two parameters as the monochromatic profile, namely the transport and the surface Stokes drift velocity.

Another attempt on Stokes forces in phase-average equations was done by Suzuki and Fox-Kemper (2016). This interesting paper describes Craik-Leibovich equations of the dynamics of upper ocean flow interacting with nonbreaking, not steep, surface gravity waves. It formulates the wave effects in these equations in terms of three contributions to momentum: Stokes advection, Stokes Coriolis force, and Stokes shear force. Each contribution scales with a distinctive parameter. Moreover, these contributions affect the turbulence energetics differently from each other such that the classification of instabilities is possible accordingly. Stokes advection transfers energy between turbulence and Eulerian mean-flow kinetic energy, and its form also parallels the advection of tracers such as salinity, buoyancy, and potential vorticity. Stokes shear force transfers energy between turbulence and surface waves. The Stokes Corio-

lis force can also transfer energy between turbulence and waves, but this occurs only if the Stokes drift fluctuates. Furthermore, this formulation elucidates the unique nature of Stokes shear force and also allows direct comparison of Stokes shear force with buoyancy. As a result, the classic Langmuir instabilities of Craik and Leibovich, wave-balanced fronts and filaments, Stokes perturbations of symmetric and geostrophic instabilities, the wavy Ekman layer, and the wavy hydrostatic balance are framed in terms of intuitive physical balances.

In terms of the wave-induced turbulence, unrelated to the breaking, there are three different mechanisms proposed for generation of such turbulence over the years. None of them cancels the other two - all are feasible, so the upper-ocean dynamics is a matter of their relative significance. Historically the first one was due to viscous solutions of wave equations being able to produce vorticity which, stretched by random waves, becomes turbulence. The second mechanism (see Benilov (2012) for a recent update), is turbulence generated by potential (non-viscous) waves, hence the turbulence must be pre-existing, which is always the case in the ocean. The Benilov theory is a linear instability theory of 3D turbulence to 2D wave orbital motion, hence it is a mechanism different to Langmuir turbulence which requires Stokes drift and therefore nonlinear waves, and three-dimensional ocean. Therefore, Langmuir turbulence is a yet different mechanism. This is a phase-average theory where the Stokes drift shear plays a role of mean flow shear.

Over the reported period, all the three mechanisms were further explored by researchers. Filatov et al. (2016) considered nonlinear generation of vorticity by surface waves in water with non-zero viscosity, hence the first mechanism. They demonstrated that waves excited on a fluid surface produce local surface rotation owing to hydrodynamic nonlinearity. The effect was examined theoretically and an explicit formula for the vertical vorticity in terms of the surface elevation was obtained. The theoretical predictions were confirmed by measurements of surface motion in a cell with water where surface waves are excited by vertical and harmonic shaking of the cell. The experimental data are in good agreement with the theoretical predictions.

Tsai et al. (2015) worked with the second mechanism of wave-induced turbulence. Numerical simulation of monochromatic surface waves propagating over a turbulent field was conducted to understand the turbulence production by nonbreaking waves. The numerical model solves the primitive equations subject to the fully nonlinear boundary conditions on the exact water surface. The result predicts growth rates of turbulent kinetic energy consistent with previous measurements and modelling. It also validates the observed horizontal anisotropy of the near-surface turbulence that the spanwise turbulent intensity exceeds the streamwise component. Such a flow structure is found to be attributed to the formation of streamwise vortices near the water surface, which also induces elongated surface streaks. It could be mentioned that such behaviour is consistent with expectations of the Benilov theory, where the 3D vortexes are unstable to the wave orbits in planes perpendicular to the orbits. The averaged spacing between the streaks and the depth of the vortical cells approximates that of Langmuir turbulence. The strength of the vortices arising from the wave–turbulence interaction, however, is one order of magnitude less than that of Langmuir cells, which arises from the interaction between the surface waves and the turbulent shear flow. In contrast to Langmuir turbulence, production from the Stokes shear does not dominate the energetics budget in wave-induced turbulence. The dominant production is the advection of turbulence by the velocity straining of waves.

D'Asaro et al. (2014) works in the more traditional Langmuir-turbulence paradigm. They tested the wave-turbulence assumptions using parallel experiments in a lake with small waves and in the open ocean with much bigger waves. Under the same wind stress and adjusting for buoyancy flux, they find the mixed layer average turbulent vertical kinetic energy in the open ocean typically twice that in the lake. The increase is consistent with models of Langmuir turbulence, in which the wave Stokes drift, and not wave breaking, is the dominant mecha-

nism by which waves energize turbulence in the mixed layer. Applying these same theories globally, they found enhanced mixing and deeper mixed layers resulting from the inclusion of Langmuir turbulence in the boundary layer parameterization, especially in the Southern Ocean. It should be pointed out, however, that the enhancement of turbulence once the wind/waves increase, and this is observed, is not a direct verification of the Langmuir turbulence as all the above mechanisms also predict such enhancement if waves grow.

Therefore, with wave-induced turbulence and mixing being a relatively new topic, research in this field concentrates on clarifying and validating physical concepts responsible for such turbulence. While qualitatively three different mechanisms possible, and all of them appear to be relevant, their quantitative significance is subject to active research.

7.6 Waves in large-scale air-system – climate

The wave-coupled effects in large-scale air-sea systems were singled out the previous Section because they bring the wave modelling into uncharted waters of large-scale and long-term simulations of weather, climate and general oceanic circulation. Here, 'large-scale' means large by comparison with the scale of wind-generated waves. Weather and climate are phenomena of very different scales (days and years or even longer in time, hundreds of kilometers and global in space). Both scales, however, are much larger with respect to the scale of ocean surface waves (seconds in time and hundreds of meters in space).

Zambon et al. (2014), Reichl et al. (2016), Yablonsky et al. (2015), Aijaz et al. (2017), Stoney et al. (2017) all investigated impact of wave-induced mixing on Tropical Cyclones (TC). TCs, or hurricanes as they are called in the Americas and typhoons in Asia, feed on the energy of the warm ocean, and therefore the Sea Surface Temperature (SST) feedback can have in impact on their intensity. Prediction of Cyclone intensity has resisted improvements over decades, and waves is one of physical phenomena which is missing in the hurricane models.

Zambon et al. (2014) applied coupled ocean-atmosphere-wave-sediment transport (COAWST) model to Hurricane Ivan and highlighted the significance of the wind-wave-current interactions during tropical cyclones. The wind-generated currents and waves produce a vertical shear leading to turbulence, which then mixes the upper ocean layer by entraining cooler water from the thermocline up into the well-mixed ocean surface (Yablonsky et al., 2015, Reichl et al., 2016)] ultimately cooling the SST. Aijaz et al. (2017) describe an implementation of a new wave model that simulates the turbulence generated by nonbreaking waves in a coupled ocean-wave-hurricane modelling system. The Princeton Ocean Model (POM) with hurricane forcing was coupled with the WAVEWATCH-III surface wave model. The SST response from the modelling experiments indicates that the nonbreaking wave-induced mixing leads to significant cooling of the SST and deepening of the mixed layer. In a similar study, Stoney et al. (2017) implemented a wave-mixing parameterisation as a modification to the k-ε turbulence scheme, used within MOM5 ocean model. The inclusion of surface wave mixing led to surface temperature differences of around 0.6C near the storm track, typically with warm anomalies on the side with the strongest winds and cool anomalies in other regions. This pattern was explained by an initial wave-induced deepening of the mixed layer, which can modify the subsequent shear-induced entrainment and upwelling.

Staneva et al. (2016) investigated the effect of wind waves on water level and currents during two storms in the North Sea by using a high-resolution Nucleus for European Modelling of the Ocean (NEMO) model forced with fluxes and fields from a high-resolution wave model. The additional terms accounting for wave-current interaction in this study were the Stokes-Coriolis force, the sea-state-dependent energy and momentum fluxes. The individual and collective role of these processes was quantified and the results were compared with a control run without wave effects as well as against current and water-level measurements from coastal stations. A better agreement with observations was found when the circulation model is forced by sea-state-dependent fluxes, especially in extreme events. Moreover, the modelled

vertical velocity profile fits the observations very well when the wave forcing is accounted for. The contribution of wave-induced forcing was quantified indicating that this represents an important mechanism for improving water-level and current predictions.

Walsh et al. (2017) tested a new parameterization of mixing processes in the upper ocean in a ¼ degree resolution global ocean-climate model MOM5. The parameterization represents the effect of turbulent mixing by unbroken waves as an additional turbulent shear production term in the k-ε mixing scheme. The results show that the inclusion of this parameterization has a noticeable effect on ocean climate, particularly in regions of high wave activity such as the Southern Ocean. Inclusion of this process also leads to some reduction in the biases of the simulated climate, including mixed layer depth, compared with available observations.

A large review of wave-induced mixing on ocean and climate modelling was offered by Qiao et al. (2016). Heated from above, the oceans are stably stratified. Therefore, the performance of general ocean circulation models and climate studies through coupled atmosphere–ocean models depends critically on vertical mixing of energy and momentum in the water column. Many of the traditional general circulation models are based on total kinetic energy (TKE), in which the roles of waves are averaged out. Although theoretical calculations suggest that waves could greatly enhance coexisting turbulence, no field measurements on turbulence have ever validated this mechanism directly. To address this problem, a specially designed field experiment was conducted. The experimental results indicate that the wave–turbulence interaction-induced enhancement of the background turbulence is indeed the predominant mechanism for turbulence generation and enhancement. Based on this understanding, the authors propose a new parametrization for vertical mixing as an additive part to the traditional TKE approach. This new result reconfirmed the past theoretical model that had been tested and validated in numerical model experiments and field observations. It establishes the critical role of wave–turbulence interaction effects in both general ocean circulation models and atmosphere–ocean coupled models, which could greatly improve the understanding of the sea surface temperature and water column properties distributions, and hence model-based climate forecasting capability.

In Summary, Section 7 outlines multiple effects and feedbacks which surface ocean waves have in the lower atmosphere and upper ocean. These include wave breaking, wave-current and wave-ice interactions, Wave Boundary Layer in the wind flow, wave-induced currents and mixing in the upper ocean. Taken beyond the problem of wave dynamics and wave forecast, these effects can have impact on large-scale processes such as weather, including tropical cyclones, ocean circulation and climate.

8. UNCERTAINTY

Many parameters cause uncertainties in environmental modeling and measurements. Data analysis also contributes to uncertainties in measurements and numerical predictions, such as the applied mathematical model, filters and choice of data samples. This section summarizes the uncertainties in prediction models, full-scale measurements and model-scale measurements as well as the challenges in quantifying the uncertainties.

8.1 Uncertainty in prediction models

In general, uncertainties in prediction models depend on the choice of method, equations to describe the real physics, level of approximation, introduction of empirical parameters, rounding errors, grid generation and understanding of the physical model by practicians.

Wave-forecast models, apart from uncertainties due to limitations of their physics, whose many aspects have been discussed above, critically depend on uncertainties of their forcing fields: winds, currents, ice, and bottom topography. As a rule of thumb, for example, 10% of wind-speed error translates into 20% error in wave height.

Errors in wind speed have many sources, one of the main of which is uncertainties of the physics of meteorological models. This is particularly noticeable for extreme winds, where, for instance, high-resolution hurricane-wind model tuned for one region (e.g. Gulf of Mexico) do not perform well in another region such as South-Eastern Asia (Liu et a., 2017). Assimilation of in situ data has its own problems because of extrapolation of measurements to the standard 10 m height (e.g. Babanin and McConochie, 2013), which is especially difficult for high seas. Satellite wind measurement, assimilated broadly nowadays, differ depending on the platform (i.e. altimeters or radiometers), and again with particular biases towards high end of wind speeds (Young et al., 2017). We refer to Section 5.1 on the wind measurements issues, and here will comment that the common practice to overcome the wind-forcing problem these days, is the use of ensemble of the winds produced by different models, in order to provide a likely wave-forecast outcome.

Surface currents are less common forcing fields for wave forecast, often not even taken into account, but their impact on uncertainties in wave prediction is not limited to local areas of strong currents. Ardhuin et al. (2016) demonstrate that small-scale variability of currents in the open ocean has large impact on wave heights in the North Atlantic. Such impact should be even bigger in the Southern Ocean where strong currents, and their eddies, are common features of oceanographic environment, superposed under powerful storms which radiate swells all over the globe round the year. Improving this uncertainty is feasible as high resolution currents are becoming increasingly available through satellite observations and oceanographic forecast, but this would require dedicated efforts on advancing of the physics of wave models (see Section 7.2).

Uncertainties due to ice-field inputs into wave-forecast models are only essential in certain geographic regions and seasons, but these uncertainties are big. At operational scale, it is only relative percentage of the ice cover with respect to the open water that is usually available, whereas wave-ice interactions critically depend on more detailed knowledge of ice properties (e.g. Rogers et al., 2016). Here, however, even if the full information on ice were available, quality of the physics of wave modelling in Marginal Ice Zone is still marginal.

8.2 Uncertainty in measurements

There are many sources of uncertainties in measurements, such as instruments used for full-scale and model-scale measurements, remote sensing technique and associated software, location of measurement and reference point, and calibration of instrument.

Uncertainty in measurements of winds and ice were partially addressed in Section 8.1 above. With respect to the winds, we would also reiterate the discussion of Section 5.1, and in particular the fact that the standard wind input in modelling is the wind speed at 10 m height which is almost never measured directly, but is inferred on the basis of extrapolations which are approximate and do not cover the full range of metocean conditions.

The wave-measurement uncertainties are of different nature. A variety of reliable in situ methods and instrumentations are available these days, and the satellites provide the global coverage. Satellites, however, require in situ calibrations, and there are very few in the Southern Hemisphere. Thus, the remote sensing of waves in the Northern Hemisphere is available and well calibrated, but south of equator they are known for their biases.

In the model-scale tests, parameters, such as physical property of water, initial conditions, wavemaker control, wave reflection from beaches and model, interaction between wind and wave, refraction due to uneven seabed on shallow water, wave-current interaction and test duration, cause uncertainties in measurements. With respect to instrumentation, errors in wave probes, current meters and power supply contribute to the measurement uncertainties. Examples of quantifying the uncertainties in model tests are presented in the work of Qiu et al. (2017) and Kim and Hermansky (2014).

8.3 Challenges in uncertainty quantification

Quantification of uncertainties and associated methodology in the aspects discussed above remain as challenges. It should be pointed out that human factors are an important factor contributing to uncertainties in measurements and predictions. It is a real challenge to quantify the uncertainties caused by human factors.

According to the ISO-GUM methodology (ISO, 2008), uncertainties in measurements are quantified by using Type A and Type B categories. An example of applying this methodology is presented in the work of Qiu et al. (2014). While it has been widely used by the ITTC, its applications by the ISSC community for environmental modeling and measurement are limited. Progress is being made by the joint ITTC-ISSC Committee to identify the gaps in quantifying uncertainties with the objective to develop a unified methodology.

9. SPECIAL TOPICS

9.1 Future Trends

9.1.1 Big Data

Big Data and Machine Learning have rapidly grown over the last years in different areas and applications, including the environmental sciences. Alternative methods using data mining and neural networks, for example, have shown great improvement compared to traditional approaches – suggesting that its applications tend to significantly expand in the next years. As an introductive data mining relevant for future studies, Hashim et al. (2016) focused on finding the sequence of the most influential parameters among the factors that affect the offshore wave height. A dataset comprising of four climatic input parameters: sea surface wind speed, wind direction, air temperature, and sea surface temperature; as well as one output parameter (significant wave height) was generated. As a result, the following sequence of parameters has the most to least influence on the predictions of Hs: wind speed, air temperature, sea surface temperature and wind direction. In addition, Hashim et al. (2016) found that combination of three variables, namely wind speed, air temperature, and wind direction, forms the most influential set of input parameters with RMSEs of 0.82, 0.44 and 0.62, respectively for the predicted Hs. Hashim et al. (2016) suggest that the accuracy of wave height prediction may improve when air temperature and sea surface temperature are included as inputs along with wind speed and direction. Ghorbani et al. (2017) investigated the potential of the Chaos theory integrated with multiple linear regression (Chaos-MLR) in prediction of wave heights and wave periods, collected at four moorings in the coastal environment of Tasmania. The intercomparisons demonstrated that the Chaos-MLR and pure MLR models yield almost the same accuracy in predicting the significant wave heights and the zero-up-crossing wave periods. Whereas, the augmented Chaos-MLR model is performed better results in term of the prediction accuracy compared to previous prediction applications of the same case study.

Statistical models have advantages in short-term wave prediction as complex phenomena are substantially simplified; however, conventional statistical models have limitations in forecasting nonlinear and non-stationary waves. Duan et al. (2016) developed a hybrid empirical model decomposition (EMD) support vector regression (SVR) model designated as EMD-SVR for nonlinear and non-stationary wave prediction. Auto-regressive (AR) model, single SVR model and EMD-AR model were studied to validate the performance of the proposed model. Considerable improvements were found in the comparisons among the EMD-SVR and other models. The coefficient of efficient values indicate the EMD-SVR model shows good model performances and provides an effective way for the short-term prediction of nonlinear and non-stationary waves. Ibarra-Berastegi et al. (2015) analyzed the performance of three types of statistical models and a well-known physics-based model for forecasting the wave energy flux. Three techniques are used: analogues, random forests (a machine learning algorithm) and a combination of the two. The numerical model applied is the Wave Model

(WAM). Ibarra-Berastegi et al. (2015) found that over horizons between 3 and 16–19 h at locations near the coast, the random forests models outperform the others, including WAM. These models exploit the inherent predictability associated with the strong autocorrelation present in ocean energy values.

In recent years, Bayesian optimization (BO) has emerged as a practical tool for high-quality parameter selection in prediction systems. Cornejo-Bueno et al. (2017) showed that BO can be used to obtain the optimal parameters of a prediction system for problems related to ocean wave features prediction. They proposed the Bayesian optimization of a hybrid Grouping Genetic Algorithm for attribute selection combined with an Extreme Learning Machine (GGA-ELM) approach for prediction. The system used data from neighbor stations in order to predict the significant wave height and the wave energy flux at a goal marine structure facility, which was tested in a real problem involving buoys data in the Western coast of the USA, improving the performance of the GGA-ELM without a BO approach. Harpham et al. (2011) outlined an application of the Bayesian statistical methodology which combines ensemble of multiple predictions and new sources of observational data such as GNSS reflectometry and FerryBoxes. The method of Harpham et al. (2011) modifies the probabilities of ensemble wave forecasts based on recent past performance of individual members against a set of observations from various data source types. Each data source is harvested and mapped against a set of spatio-temporal feature types and then used to post-process ensemble model output.

Precise prediction of wave heights is still an evading problem whether it is done using physics based modeling or by extensively used data driven technique of Artificial Neural Network (ANN). A numerous of recent papers have presented encouraging results using ANN, especially when combined with traditional numerical wave models. Campos and Guedes Soares (2016) developed and evaluated hybrid models using statistical tools to reduce the bias of significant wave heights. The “hybrid model” consists of two models working together: (1) numerical wave model (in this case, WAM) and (2) Artificial Neural Network and linear regression. The numerical model predicts the wave heights while the target of the statistical model was used to predict the residue (difference of measurement minus model); finally combined to provide a final accurate estimation at the Brazilian coast. The model using linear regression proved to be efficient in reducing bias, but not the scatter index (SI) or the root mean square error (RMSE). The neural network model presented the best results, especially with 16 to 32 neurons at the intermediate layer. The final bias was reduced from 0.13 to 0.06 meters and SI from 0.12 to 0.03.

In recent years, machine learning approaches are being widely used for the prediction of wave heights. However, these approaches involve batch learning algorithms that are not well-equipped to address the demands of continuously changing data stream. Kumar et al. (2017) conducted a study to predict the daily wave heights in different geographical regions using sequential learning algorithms, namely the Minimal Resource Allocation Network (MRAN) and the Growing and Pruning Radial Basis Function (GAP-RBF) network. They compared the performance of MRAN and GAP-RBF with Support Vector Regression (SVR) and Extreme Learning Machine (ELM). Results of Kumar et al. (2017) showed that the MRAN and GAP-RBF outperform the SVR and ELM with minimal network resources, in the daily wave height prediction, and also predict the significant wave heights accurately. Kumar et al. (2017) concluded that MRAN outperforms GAP-RBF with minimal architecture.

Berbić et al. (2017) applied neural networks and support vector machine for significant wave height prediction for the following 0.5—5.5 hours, using information from 3 or more time points. In the first stage, predictions were made by varying the quantity of significant wave heights from previous time points and various ways of using data are discussed. Afterwards, the influence of wind was taken into account. Predictions of were made using two machine learning methods — artificial neural networks (ANN) and support vector machine (SVM). Sánchez et al. (2017) presented a mathematical model that uses artificial neural networks for

the assessment of the wave energy potential of sites, based on data recorded by wave monitoring instrumentation. The performance of the neural network model was compared to that of the Nearshore Wave Prediction System (NWPS), which combines SWAN, WAVEWATCH III and other numerical models. The performance of the neural network trained with the 23 years' hindcast was satisfactory; better than the NWPS in terms of relative bias but worse in terms of scatter index. Therefore, Sánchez et al. (2017) concluded that neural networks can make an optimal use of the data produced by wave monitoring instrumentation and are useful to characterize the wave energy resource of a coastal site. In Dixit and Londhe (2016), Neuro Wavelet Technique (NWT) was used specifically to explore the possibility of prediction of extreme events for five major hurricanes Katrina 2005, Dean 2007, Gustav 2008, Ike 2008, Irene 2011 at four locations (NDBC wave buoys stations) in the Gulf of Mexico. Neuro Wavelet Technique was employed by combining Discrete Wavelet Transform and Artificial Neural Networks. To develop these Neuro wavelet models to forecast the waves with lead times of 12 hr to 36 hr in advance, previously measured significant wave heights at same locations were used. From the results Dixit and Londhe (2016) concluded that the Neuro Wavelet Technique can be employed to solve the ever eluding problem of accurate forecasting of the extreme events.

Lo et al. (2015) developed artificial neural network (ANN)-based models for forecasting precipitation, in which the training parameters were adjusted using a parameter automatic calibration (PAC) approach. A classical ANN-based model, the multilayer perceptron (MLP) neural network, was used to verify the utility of the proposed ANN–PAC approach. The traditional multiple linear regression model was selected as the benchmark for comparing the accuracy of the ANN–PAC model. In addition, two MLP ANN models based on a trial-and-error calibration method were constructed by manually tuning the parameters. Lo et al. (2015) found that the results yielded by the ANN–PAC model were more reliable than those yielded by the manually tuning and traditional regression models. In addition, the computing efficiency of the ANN–PAC model decreased with an increase in the number of increments within the parameter ranges because of the considerably increased computational time, whereas the prediction errors decreased because of the model's increased capability of identifying optimal solutions. Kumar et al. (2017) proposed the use of an ensemble of Extreme Learning Machine (Ens-ELM) to predict the daily wave height, exploring the randomness of initialization in ELM to obtain better generalization performance. For each sample in the data set, the output of the ELM with the least mean square for each sample in the data set is reported as its output. The Ens-ELM network is trained using the past wave data and the measured atmospheric conditions obtained in these stations between Jan 1, 2011 and Dec 31, 2014 and is tested with data in these stations between Jan 1, 2015 and Aug 30, 2015. In this study, the performance of Ens-ELM is evaluated in comparison with ELM, Online Sequential ELM (OS-ELM), and Support Vector Regression (SVR). From this study, Kumar et al. (2017) infer that the Ens-ELM outperforms ELM, OS-ELM and SVR in the daily wave height prediction.

Durán-Rosal et al. (2017) presented a methodology for the detection and prediction of Segments containing very high significant wave height (SSWH) values in oceans. A genetic algorithm (GA) combined with a likelihood-based local search is proposed for the first stage (detection), and the second stage (prediction) is tackled by an Artificial Neural Network (ANN) trained with a Multiobjective Evolutionary Algorithm (MOEA). Given the unbalanced nature of the dataset, the MOEA is specifically designed to obtain a balance between global accuracy and individual sensitivities for both classes. The results of Durán-Rosal et al. (2017) showed that the GA is able to group segments of significant wave heights in a specific cluster of segments and that the MOEA obtains ANN models able to perform an acceptable prediction of these SSWH.

Various methods are typically used to estimate the characteristics of nearshore wave breaking, mostly based on empirical, analytical and numerical techniques. Kouvaras and Dhanak (2017)

extended the approach of Deo et al. (2001) approach, using neural networks, to predict other characteristics of wave breaking, including the type of wave breaking, and the position of breaking over a fringing reef, as well as the associated wave setup, and the rate of dissipation of wave energy. The corresponding neural network models for wave setup within the surf zone and the difference in energy flux between the incident and broken wave have success rates of approximately 89% and 94% respectively. Kouvaras and Dhanak (2017) argue that the method may be extended to provide predictive models for consideration of a range of natural coastal conditions, random waves, and various bottom profiles and complex geometry, based on training and testing of the models using representative field and laboratory observational data, in support of accurate prediction of near-shore wave phenomena.

Krasnopolsky et al. (2016) introduced a neural network (NN) technique to fill gaps in satellite data, linking satellite-derived fields of interest with other satellites and in situ physical observations. They proved that NN technique provides an accurate and computationally cheap method for filling in gaps in satellite ocean color observation fields and time series.

10. CONCLUSIONS

10.1 Summary

To take-away from this report is that while much progress is being made, the committee has several concerns:

- Operating in polar and other regions due to lack of knowledge / data and large uncertainty / increased risk.
- The effect of climate change on waves and met-ocean phenomenon, including ice, and associated effect on structures.
- The uncertainty in climate change models and the uncertainty in environmental prediction models. This uncertainty stems from the lack of uncertainty quantification.

10.2 Recommendations

The committee would like to make the following recommendations:

- For continued advancement all environmental time series data should be saved in its unfiltered form for others to use – develop standard big data format and meta data requirement.
- There is a need for improved uncertainty quantification methods, and these methods should be utilized by the community.
- With the increased use of data analytics and higher fidelity numerical tools there is a need for more computing resources to be available to the community.
- ISSC should include computer science/numerical methods experts on this committee.
- Other ISSC committees should start to consider the effect of climate change on their areas. The Environment committee should increase its interaction with other committees with respect to climate change.
- With the increasing activity in Polar Regions, there is a need for a polar sea state definition for design. Data to generate the definitions is needed.
- The ISSC should continue to encourage sharing of environmental information to improve forecasts as public service
- Identify fixed test sites in the ocean for developing benchmark data sets.
- Continue working with the ITTC to develop uncertainty quantification procedures and encourage them to include longer term environmental uncertainty quantification.

- There is a need for in situ measurements in extreme conditions, particularly coupled air/waves/ocean interactions and fluxes

10.3 Advances

The committee was encouraged by the progress and activity in the field, including new facilities, new techniques, and new models. These include:

- University of Miami Surge-Structure-Atmosphere-Interaction Tank (SUSTAIN).
- The utilization of big data analytics / machine intelligence.
- The use of existing fixed test sites (wave energy test sites and wind farms etc.) in the ocean for developing benchmark data sets.
- The advent and increased use of undersea gliders, wave gliders, wave riders, small buoys, UAVs and UUVs in gathering oceanographic data which could lead to more data becoming available.
- Comprehensive inter-calibrated and validated satellite metocean database for the full period of satellite observations (University of Melbourne)

REFERENCES

Aarnes, O. J., Abdalla, S., Bidlot, J. R., & Breivik, Ø. (2015). Marine wind and wave height trends at different ERA-Interim forecast ranges. Journal of Climate, 28(2), 819-837.

Aarnes, O. J., M. Reistad, O. Breivik, E. Bitner-Gregersen, L. Ingolf Eide, O. Gramstad, A. K. Magnusson, B. Natvig, and E. Vanem (2017). Projected changes in significant wave height toward the end of the 21st century: Northeast Atlantic, J. Geophys. Res. Oceans, 122, 3394–3403, doi:10.1002/2016JC012521.

Abdel-Moati, H. et al. (2017). Near field ice detection using infrared based optical imaging technology. Opt. and Laser Technol.

Aberg, S. Rychlik, I. Leadbetter, R. (2008). Palm distributions of wave characteristics in encountered seas, Annals of Appl. Prob., Vol 18 (3), pp. 1059-1084.

Adcock, T. A. A. & Taylor, P. H. (2014). The Physics of Anomalous ('Rogue') Ocean Waves. Reports on Progress in Physics, 77, 105901-105901.

Aijaz, S., Ghantous, M., Babanin, A.V., I. Thomas, Ginis, B., and Wake, G. (2017). Non-breaking wave-induced mixing in upper-ocean during tropical cyclones using coupled hurricane-ocean-wave modelling. Journal of Geophysical Research Oceans, 122, 3939–3963, doi:10.1002/2016JC012219

Aijaz, S., Rogers, W.E., and Babanin, A.V. (2016). Wave spectral response to sudden changes in wind direction in finite-depth waters. Ocean Modelling, 103, 98-117

Akpınar, A., Bingölbali, B., Van Vledder, G.Ph., (2016). Wind and wave characteristics in the Black Sea based on the SWAN wave model forced with the CFSR winds. Ocean Engineering 126, 276–298.

Alford, L., Lyzenga, D., Nwogu, O., Beck, R., Johnson, J., Zundel, A., Andrews, M., Coller, J., Katz, E., McKelvey, C., O'Brien, A., Smith, G., and Wijesundara, S., (2016). Performance Evaluation of a Multi-Ship System for Environmental and Ship Motion Forecasting, Proc. 31st Symp. on Naval Hydrodynamics, 11-16 Sep, Monterey, CA.

Almar, R., Larnier, S., Castelle, B., Scott, T. & Floc'h, F. (2016). On the use of the Radon transform to estimate longshore currents from video imagery. Coastal Engineering, 2016, 114: 301-308.

Alpers W., A. Mouche, J. Horstmann, A. Y. Ivanov., V. S. Barabanov (2015). Application of a new algorithm using Doppler information to retrieve complex wind fields over the Black Sea from ENVISAT SAR images. Int. Journal of Remote Sensing, 36(3), 863-881.

Alvise, B., Francesco, B., Filippo, B., Sandro, C., Mauro, S., (2017). Space-time extreme wind waves: Analysis and prediction of shape and height. Ocean Modelling 113, 201–216.

Amrutha, M.M., Kumar, V.S., (2015). Short-term statistics of waves measured off Ratnagiri, eastern Arabian Sea. Applied Ocean Research 53, 218–227.

Amrutha, M.M., Kumar, V.S., Sandhya, K.G., Nair, T.M.B., Rathod, J.L., (2016). Wave hindcast studies using SWAN nested in WAVEWATCH III - comparison with measured nearshore buoy data off Karwar, eastern Arabian Sea. Ocean Engineering 119, 114–124.

Antão, E.M., Guedes Soares, C., (2016). Approximation of the joint probability density of wave steepness and height with a bivariate gamma distribution. Ocean Eng. 126, 402–410.

Appendini, C.M., Camacho-Magaña, V., Breña-Naranjo, J.A., (2016). ALTWAVE: Toolbox for use of satellite L2P altimeter data for wave model validation. Advances in Space Research 57, 1426–1439.

Ardhuin F, Gille ST, Menemenlis D, Rocha CB, Rascle N, Chapron B, Gula J, Molemaker J (2016). Small-scale open ocean currents have large effects on wind wave heights. J Geophys Res 122, DOI 10.1002/2016JC012413

Ardhuin, F. J. Stopa, B. Chapron, F. Collard, M. Smith, J. Thomson, M. Doble, B. Blomquist, Collins III, C.O., and Wadhams, P. (2017). Measuring ocean waves in sea ice using SAR imagery: A quasi-deterministic approach evaluated with Sentinel-1 and in situ data. Remote Sensing of Environment, 189, 211–222

Ashton, I.G.C., Johanning, L. (2015). On errors in low frequency wave measurements from wave buoys. Ocean Engineering 95 11–22.

Azariadis, P., (2017). On Using Density Maps for the Calculation of Ship Routes, Evolving Systems : An Interdisciplinary J. for Adv. Sc. and Techn., 8(2), pp. 135–145. doi: 10.1007/s12530-016-9155-7.

Babanin, A.V. (2012). Swell attenuation due to wave-induced turbulence. Proceedings of the ASME 2012 31st International Conference on Ocean, Offshore and Arctic Engineering OMAE2012, July 1-6, 2012, Rio de Janeiro, Brazil, ISBN 978-0-7918-4489-2, 5p

Babanin, A.V. (2017). Similarity theory for turbulence, induced by orbital motion of surface water waves. Procedia IUTAM, 20, 99-102

Babanin, A.V., (2011). Breaking and Dissipation of Ocean Surface Waves. Book, Cambridge University Press, 480p

Babanin, A.V., and McConochie, J. (2013) Wind measurements near the surface of waves. Proceedings of the ASME 2013 32nd International Conference on Ocean, Offshore and Arctic Engineering OMAE2013, June 9-14, 2013, Nantes, France, 6p

Babanin, A.V., Onorato, M., and Qiao, F. (2012). Surface waves and wave-coupled effects in lower atmosphere and upper ocean. Journal of Geophysical Research, 117, doi:10.1029/2012JC007932, 10p.

Babanin, A.V., van der Westhuysen, A., Chalikov, D., and Rogers, W.E. (2017). Advanced wave modelling including wave-current interaction. In “The Sea: The Science of Ocean Prediction, Eds. Nadia Pinardi, Pierre F.J. Lermusiaux, Kenneth H. Brink and Ruth Preller”, Journal of Marine Research, 75, 239–262

Bae D M, Prabowo A R, Cao B, et al. (2016). Numerical simulation for the collision between side structure and level ice in event of side impact scenario[J]. Latin American Journal of Solids and Structures, 2016, 13(16): 2991-3004.

Barnard, P.L., Short, A.D., Harley, M.D., Splinter, K.D., Vitousek, S., Turner, I.L., Allan, J., Banno, M., Bryan, K.R., Doria, A., Hansen, J.E., Kato, S., Kuriyama, Y., Randall-Goodwin, E., Ruggiero, P., Walker, I.J., Heathfield, D.K., (2015). Coastal vulnerability across the Pacific dominated by El Niño/Southern Oscillation. Nature Geoscience, v.8, pp. 801-807.

Barthelemy, X., Banner, M., Peirson, W., Fedele, F., Allis, M. & Dias, F. (2015). On the Local Properties of Highly Nonlinear Unsteady Gravity Water Waves. Part 2. Dynamics and onset of Breaking. arXiv Preprint arXiv:1508.06002.

Bateman, W. J. D., Swan, C. & Taylor, P. H. (2003). On the Calculation of the Water Particle Kinematics Arising in a Directionally Spread Wavefield. J. Comput. Phys., 186, 70-92.

Benetazzo, A., Ardhuin, F., Bergamasco, F., Cavaleri, L., Guimarães, P. V., Schwendeman, M., Sclavo, M., Thomson, J. & Torsello, A. (2017). On the Shape and Likelihood of Oceanic Rogue Waves. Scientific Reports, 7, 8276.

Benetazzo, A., Barbariol, F., Bergamasco, F., Torsello, A., Carniel, S. & Sclavo, M. (2015). Observation of Extreme Sea Waves in a Space–Time Ensemble. Journal of Physical Oceanography, 45, 2261-2275.

Benilov, A. Y., (2012). On the turbulence generated by the potential surface waves. J. Geophys. Res. (Oceans), 117, doi:10.1029/2012JC007948

Bennett, V. C. & Mulligan, R. P. (2017). Evaluation of surface wind fields for prediction of directional ocean wave spectra during Hurricane Sandy. Coastal Eng., 2017, 125: 1-15.

Bennetts, L.G., Alberello, A., Meylan, M.H., Cavaliere, C., Babanin, A.V., and Toffoli, A. (2015) An idealised experimental model of ocean surface wave transmission by an ice floe. Ocean Modelling, 96, 85-92, http://dx.doi.org/10.1016/j.ocemod.2015.03.001

Bentamy A., Grodsky, S. A., Elyouncha, A., Chapron, B., Desbiolle, F. (2016). Homogenization of Scatterometer Wind Retrievals, Int. J. Climatol. doi:10.1002/joc.

Bento, A.R., Gonçalves, M., Campos, R.M., Guedes Soares, C., (2016). Comparison Between Two Forecast Systems Implemented with WAM and WAVEWATCH 3 for the North Atlantic. Proceedings of the 35th International Conference on Ocean, Offshore and Arctic Engineering - OMAE2016. June 19-24, 2016, Busan, South Korea.

Berbić, J., Ocvirk, E., Carević, D., Lončar, G., (2017). Application of neural networks and support vector machine for significant wave height prediction. Oceanologia 59, 331-349.

Bergsma, J. et al. (2014). On the Measurement of Submersion Ice Resistance of Ships, Using Artificial Ice. In: International Ocean and Polar Engineering Conference. Busan, Korea: International Society of Offshore and Polar Engineers, pp. 1125-1131.

Bernier, N.B., Alves, J.-H.G.M., Tolman, H., Chawla, A., Peel, S., Pouliot, B., Bélanger, J.-M., Pellerin, P., Lépine, M., Roch, M., (2015). Operational Wave Prediction System at Environment Canada: Going Global to Improve Regional Forecast Skill. Wea. Forecasting.

Beyá, J., Álvarez, M., Gallardo, A., Hidalgo, H., Winckler, P., (2017). Generation and validation of the Chilean Wave Atlas database. Ocean Modelling 116, 16–32.

Bitner-Gregersen E. (2015). Joint met-ocean description for design and operations of marine structures, Applied Ocean Research, Vol.51, pp.279-292.

Bitner-Gregersen, E (2017). Rethinking rogue waves, DnVGL Feature, DNVGL.

Bitner-Gregersen, E. and Gramstad, O., (2015). Rogue Waves: impact on ships and offshore structures, DNV-GL Strategic Research and Innovation, Position Paper 05-2015.

Bitner-Gregersen, E.M., (2017). Wind and Wave Climate in Open Sea and Coastal Waters. Proceedings of the ASME 2017 36th International Conference on Ocean, Offshore and Arctic Engineering OMAE2017.

Bitner-Gregersen, E.M., and Toffoli, A. (2015). Wave steepness and rogue waves in the changing climate in the North Atlantic, Proceeding of the ASME 2015 34th International Conference on Ocean, Offshore and Arctic Engineering, St. John's, Newfoundland, Canada.

Bitner-Gregersen, E.M., Guedes Soares, C., and Vantorre, M. (2016). Adverse weather conditions for ship maneuverability, Transport. Research Procedia, Vol.14, pp.1631-1640.

Bouvy A., Henn, R. and Hensse, J. (2009). Acoustic wave height measurements in a towing facility, Proc. 1st Int. Conf. on Adv. Model Meas. Techn. for the EU Maritime Ind. (AMT ’09), 1 - 2 Sep, Nantes, France.

Breivik, O. , Bidlot, J.-R., and Janssen, P.A.E.M. (2016). A Stokes drift approximation based on the Phillips spectrum. Ocean Modelling, 100, 49–56

Breivik, Ø., Allen, A. A. (2008). An operational search and rescue model for the Norwegian Sea and the North Sea, Journal of Marine Systems, Vol 69(1-2), pp. 99-113.

Breivik, Ø., Allen, A. A., Maisondieu, C., Roth, J-C., (2011). Wind-induced drift of objects at sea: The Leeway field method. Applied Ocean Research, Vol 33, pp. 100-109.

Brumer, S.E., Zappa, C.J., Brooks, I.M., Tamura, H., Brown, S.M., Blomquist, B.W., Fairall, C.W. And Cifuentes –Lorenzen, A. (2017). Whitecap Coverage Dependence on Wind and Wave Statistics as Observed during SO GasEx and HiWinGS. Journal of Physical Oceanography, 47, 2211-2235

Caires, S., Groeneweg, J., van Nieuwkoop, J. (2016). Lifting of time-and space-evolving winds for the determination of extreme hydraulic conditions. Coastal Engineering, 2016, 116: 152-169.

Calini, A., Schober, C.M., (2017). Characterizing JONSWAP rogue waves and their statistics via inverse spectral data. Wave Motion 71, 15–17.

Cambazoglu, M. K., Blain, C. A., Smith, T. A., Linzell, R. S. (2016). Relationships between wind predictions and model resolution over coastal regions. Ocean Engineering, 2016, 112: 97-116.

Campbell, A. J., Bechle, A. J., and Wu, C. H. (2014). Observations of surface waves interacting with ice using stereo imaging, J. Geophys. Res. Oceans, 119, 3266–3284, doi:10.1002/2014JC009894.

Campos, R.M., Guedes Soares, C., (2016). An hybrid model to forecast significant wave heights. In: Guedes Soares, C., Garbatov, Y., Sutulo, S., Santos, T.A. (Eds.), Maritime Technology and Engineering. Taylor and Francis Group, CRC Press, London, pp. 473–479, ISBN 978-1-138-03000-8, DOI: 10.1201/b21890-138.

Campos, R.M., Guedes Soares, C., (2016). Assessment of three wind reanalyses in the North Atlantic Ocean. Journal of Operational Oceanography, v. 10, 30–44.

Campos, R.M., Guedes Soares, C., (2016). Comparison and assessment of three wave hindcasts in the North Atlantic Ocean. Journal of Operational Oceanography, v. 9, 26-44.

Campos, R.M., Guedes Soares, C., (2016). Comparisons of HIPOCAS and ERA Wind and Wave Reanalyses in the North Atlantic Ocean. Ocean Engineering, v. 112, 320–334.

Campos, R.M., Guedes Soares, C., (2016). Estimating Extreme Waves in Brazil Using Regional Frequency Analysis. Proceedings of the 35th International Conference on Ocean, Offshore and Arctic Engineering - OMAE2016. June 19-24, 2016, Busan, South Korea.

Candella, R.N., (2015). Rogue waves off the south/southeastern Brazilian coast. Nat Hazards.

Castro-Santos, L. & Diaz-Casas, V. (2015). Economic influence of location in floating offshore wind farms. Ocean Engineering, 2015, 107: 13-22.

Chabchoub, A. & Grimshaw, R. (2016). the Hydrodynamic Nonlinear Schrödinger Equation: Space and Time. Fluids, 1, 23.

Chabchoub, A. (2016). Tracking Breather Dynamics in Irregular Sea State Conditions. Physical Review Letters, 117, 144103.

Chabchoub, A., Hoffmann, N. P. and Akhmediev, N., (2011). Rogue wave observation in a water wave tank, Physical Review Letter, Vol. 106, 204502.

Chabchoub, A., Hoffmann, N., Branger, H., Kharif, C., & Akhmediev N., (2013). Experiments on wind-perturbed rogue wave hydrodynamics using the Peregrine breather model, Physics of Fluids, Vol 25, 101704 (2013); doi: http://dx.doi.org/10.1063/1.4824706.

Chabchoub, A., Kibler, B., Finot, C., Millot, G., Onorato, M., Dudley, J. M. & Babanin, A. V. (2015). The Nonlinear Schrödinger Equation and the Propagation of Weakly Nonlinear Waves in Optical Fibers and on the Water Surface. Annals of Physics, 361, 490-500.

Chalikov, D. V. (2016). Numerical Modeling of Sea Waves, Springer international Publishing.

Chalikov, D., & Bulgakov, K. (2017). Estimation of wave height probability based on the statistics of significant wave height. J. Ocean Eng. Mar. Energy, DOI 10.1007/s40722-017-0093-7, 7p.

Chander, S. et al. (2015). Hydrodynamic Study of Submerged Ice Collisions. In: Int. Conf. on Offshore Mechanics and Arctic Engineering. St. John's, Newfoundland: ASME.

Chang K.Y., He S.S., Chou C.C., Kao S.L. and Chiou A.S., (2015). Route Planning and Cost Analysis for Travelling through the Arctic Northeast Passage Using Public 3d Gis, Int. J. of Geographical Inform. Sc., 29(8), pp. 1375–1393.

Chen, C., Shiotani, S. & Sasa, K. (2015). Effect of ocean currents on ship navigation in the east China sea. Ocean Engineering, 2015, 104: 283-293.

Chen, H. & Christensen, E.D. (2017). Development of a numerical model for fluid-structure interaction analysis of flow through and around an aquaculture net cage. Ocean Engineering, 2017, 142: 597-615.

Chen, S.S., Curcic, M., (2016). Ocean surface waves in Hurricane Ike (2008) & Superstorm Sandy (2012): Coupled model predictions & observations. Ocean Modelling 103, 161–176.

Chen, Y. L., Zhan, J. P., Wu, J., Wu, J. (2017). A fully-activated flapping foil in wind gust: Energy harvesting performance investigation. Ocean Engineering, 2017, 138: 112-122.

Chen, Z. B., He, Y. J., Zhang, B., Qiu, Z. F. (2015). Determination of nearshore sea surface wind vector from marine X-band radar images. Ocean Engineering, 2015, 96: 79-85.

Chendi Wang, Jianfang Fei, Juli Ding, Ruiqing Hu, Xiaogang Huang, Xiaoping Cheng. (2017). Development of a new significant wave height and dominant wave period parameterization scheme. Ocean Engineering, volume 135, 2017, pages 170-182.

Choi, J., Kirby, J. T., Yoon, S. B. (2015). Boussinesq modeling of longshore currents in the SandyDuck experiment under directional random wave conditions. Coastal Engineering, 2015, 101: 17-34.

Christou, M. & Ewans, K. (2014). Field Measurements of Rogue Water Waves. J. Phys. Oceanogr., 44, 2317-2335.

Clauss, G., Kosleck, S., and Testa, D., (2009). Critical Situations of Vessel Operations in Short Crested Seas – Forecast and Decision Support System, Int. Conf. on Offshore Mech. and Arctic Eng. (OMAE), May 31-Jun 5, Honolulu, Hawaii, USA.

Clauss, G.F., (2002). Dramas of the sea: episodic waves and their impact on offshore structures, Applied Ocean Research, Vol. 24, pp. 147–161.

Collins, C. O., Rogers, W. E., Marchenko, A., and Babanin, A. V. (2015). In situ measurements of an energetic wave event in the Arctic marginal ice zone, Geophys. Res. Lett. pp. 1–8.

Collins, O. C. I., Rogers, W. E. and Lund, B. (2016). An investigation into the dispersion of ocean surface waves in sea ice, Ocean Dynamics , doi:10.1007/ s10236-016-1021-4.

Cooley, S. and Pavelsky, T. (2016). Spatial and temporal patterns in Arctic river ice breakup revealed by automated ice detection from MODIS imagery. Remote Sensing of Environment, 175, pp. 310-322.

Cornejo-Bueno,L., Garrido-Merchán, E.C., Hernández-Lobato, D., Salcedo-Sanz, S., (2017). Bayesian Optimization of a Hybrid System for Robust Ocean Wave Features Prediction. Neurocomputing (2017), doi: 10.1016/j.neucom.2017.09.025.

Cox, C. S., Zhang, X. and Duda, T. F. (2017). Suppressing breakers with polar oil films: Using an epic sea rescue to model wave energy budgets. Geophys. Res. Lett., 44, 1414–1421, doi:10.1002/2016GL071505.

Craig, W. & Sulem, C. (1993). Numerical Simulation of Gravity Waves. J. Comput. Phys., 108, 73-83.

D'Asaro, E.A., Thomson, J,. Shcherbina, A.Y., Harcourt, R.R., Cronin, M.F., Hemer, M.A., and Fox-Kemper, B. (2014). Quantifying upper ocean turbulence driven by surface waves. GEOPHYSICAL RESEARCH LETTERS, 41, 102–107, doi:10.1002/2013GL058193

Dabbi, E.P., Haigh, I.D., Lambkin, D., Hernon, J., Williams, J.J., Nicholls, R.J., (2015). Beyond significant wave height: A new approach for validating spectral wave models. Coastal Engineering 100, 11–25.

Dai, J. (2016). Numerical simulation for dynamic positioning in pack ice. MEng. Memorial University of Newfoundland.

Daley, C. et al. (2014). GPU-Event-Mechanics Evaluation of Ice Impact Load Statistics. In: Arctic Technology Conference. Houston, Texas: Offshore Technology Conference.

Day, S., Clelland, D. and Valentine, G. (2011). Development of a low-cost laser wave measurement system, Proc. 2nd Int. Conf. on Advanced Model Measurement Techn. for the Maritime Ind, (AMT'11), 4 – 6 Apr, Newcastle upon Tyne, UK.

De Garcia, L., Osawa, N., Tamaru, H., Fukasawa, T., (2016). A study on the influence of ship weather routing in Fatigue Life prediction of ship structure, JASNAOE Annual Autum Meeting, 2016, JASNAOE

Deng Y., Yang, J., Tian, X., Li, X., Xiao, L., (2016). An experimental study on deterministic freak waves: generation, propagation and local energy, Ocean Engineering 118 (2016) 83-92.

Deng Y., Yang, J., Zhao, W., Li, X., Xiao, L., (2016). Freak wave forces on a vertical cylider, Coastal Engineering 114 (2016) 9-18

Deng, Y., Yang, J., Tian, X. and Li, X., (2015). Experimental investigation on rogue waves and their impacts on a vertical cylinder using the Peregrine Breather model, Ships and Offshore Structures, Vol. 11, pp. 757-765.

Deo, M. C., Jha, A., Chaphekar, A. S., Ravikant, K., (2001). Neural networks for wave forecasting. Ocean Engineering, vol. 28, no. 7, p. 889–898

Desbiolles Fabien, Bentamy Abderrahim, Blanke Bruno, Roy Claude, Mestas-Nunez Alberto M., Grodsky Semyon A., Herbette Steven, Cambon Gildas, Maes Christophe (2017). Two Decades [1992-2012] of Surface Wind Analyses based on Satellite Scatterometer Observations. Journal Of Marine Systems , 168, 38-56 .

Dixit, P., Londhe, S., (2016). Prediction of extreme wave heights using neuro wavelet technique. Applied Ocean Research 58, 241–252.

Dobrynin, M. et al. (2015). Prediction of Arctic Sea Ice for Ship Routing: Forecast Experiment and Ship Cruise. In: Arctic Technology Conference. Copenhagen, Denmark: Offshore Technology Conference.

Dommermuth, D. G. & Yue, D. K. P. (1987). A High-Order Spectral Method For the Study of Nonlinear Gravity Waves. J. Fluid Mech., 184, 267-288.

Donelan, M. A. & Magnusson, A.-K. (2017). The Making of the Andrea Wave and Other Rogues. Scientific Reports, 7, 44124.

Dong, Y., Frangopol, D.M., Sabatino, S., (2016), A decision support system for mission based ship routing considering multiple performance criteria, Reliability engineering and system safety 150 (2016) 190-201.

Drago, M., Mattioli, M., and Quondamatteo, F. (2015). MetOcean design criteria for deep water offshore systems. Proceedings of the ASME 2015 34th International Conference on Ocean, Offshore and Arctic Engineering, May 31-June 5, 2015, St. John's, Newfoundland, Canada.

Drost, E.J.F., Lowe, R.J., Ivey, G.N., Jones, N.L., Péquignet, C.A., (2017). The effects of tropical cyclone characteristics on the surface wave fields in Australia's North West region. Continental Shelf Research 139, 35–53.

Duan, W Y., Han, Y., Huang, L.M., Zhao, B.B., Wang, M.H., (2016). A hybrid EMD-SVR model for the short term prediction of significant wave height, Ocean Engineering 124 (2016) 54-73.

Ducrozet, G. & Gouin, M. (2017). Influence of Varying Bathymetry in Rogue Wave Occurrence Within Unidirectional and Directional Sea-States. Journal of Ocean Engineering and Marine Energy.

Ducrozet, G., Bonnefoy, F., Le Touzé, D. & Ferrant, P. (2012). A Modified High-Order Spectral Method for Wavemaker Modeling in a Numerical Wave Tank. European Journal of Mechanics - B/Fluids, 34, 19-34.

Ducrozet, G., Bonnefoy, F., Le Touzé, D. & Ferrant, P. (2016). Hos-Ocean: Open-Source Solver for Nonlinear Waves in Open Ocean Based on High-Order Spectral Method. Computer Physics Communications, 203, 245-254.

Düll, W.-P., Schneider, G. & Wayne, C. E. (2016). Justification of the Nonlinear Schrödinger Equation for the Evolution of Gravity Driven 2d Surface Water Waves in a Canal of Finite Depth. Archive for Rational Mechanics and Analysis, 220, 543-602.

Durán-Rosal, A.M., Fernández, J.C., Gutiérrez, P.A., Hervás-Martínez, C., (2017). Detection and prediction of segments containing extreme significant wave heights. Ocean Engineering 142, 268–279.

Durrant, T., Greenslade, D., Hemer, M., & Trenham, C. (2014). A global wave hindcast focussed on the Central and South Pacific (Vol. 40, No. 9, pp. 1917-1941).

Duz, B., Bunnik, T., Kapsenberg, G. & Vaz, G., (2016). Numerical simulation of nonlinear free surface water waves - coupling of a potential flow solver to a URANS/VoF code, Proc. 35th Int. Conf. on Ocean, Offshore and Arctic Eng, OMAE2016, Jun 19-24, Busan, Korea

Duz, B., Lindeboom, R., Scharnke, J., Helder, J. and Bandringa H. (2016). Comparison of Breaking Wave Kinematics from Numerical Simulations with PIV Measurements, 36th Int. Conf. on Ocean, Offshore & Arctic Eng. OMAE2017, Jun 25-30, Trondheim, Norway.

Emanuel, K. (2017). A fast intensity simulator for tropical cyclone risk analysis. Natural Hazards, 2017, 88(2): 779-796.

Erceg, S., Ehlers, S., Ellingsen, I., Slagstad, D., von Bock und Polach, R., and Erikstad, S.O., (2013). Ship Performance Assessment for Arctic Transport Routes, Int. Conf. on Offshore Mech. and Arctic Eng. (OMAE), June 9-14, Nantes, France.

Fan, Y., Rogers, W.E., (2016). Drag coefficient comparisons between observed and model simulated directional wave spectra under hurricane conditions. Ocean Modelling 102, 1–13.

Fazelpour, A. et al. (2016). Infrared Image Analysis for Estimation of Ice Load on Structures. In: Arctic Technology Conference. St. John's, Newfoundland: Offshore Technology Conference.

Fedele, F. (2015). On the Kurtosis of Deep-Water Gravity Waves. Journal of Fluid Mechanics, 782, 25-36.

Fedele, F. (2016). Are Rogue Waves Really Unexpected? Journal of Physical Oceanography, 46, 1495-1508.

Fedele, F., Benetazzo A., Gallego G., Shih P.C., Yezzi A., Barbariol F. and Ardhuin F. (2013). Space–time measurements of oceanic sea states. Ocean Modelling, 70, p.103-115

Fedele, F., Brennan, J., Ponce De León, S., Dudley, J. & Dias, F. (2016). Real World Ocean Rogue Waves Explained Without the Modulational Instability. Scientific Reports, 6, 27715.

Fenoglio-Marc, L., Dinardo, S., Scharroo, R., Roland, A., Sikiric, M.D., Lucas, B., Becker, M., Benveniste, J., Weiss, R., (2015). The German Bight: A validation of CryoSat-2 altimeter data in SAR mode. Advances in Space Research 55, 2641–2656.

Fernández, H., Sriram, V., Schimmels, S. and Oumeraci, H., (2014). Extreme wave generation using self-correcting method-Revisited, Coastal Engineering, Vol. 93, pp. 15-31.

Filatov, S.V., Parfenyev, V.M., Vergeles, S.S., Brazhnikov, M.Yu., Levchenko, A.A. and Lebedev, V. V. (2016). Nonlinear Generation of Vorticity by Surface Waves. Phys. Rev. Lett., 115, 054501, 5p

Fissel, D. B. et al. (2015). The Distribution of Massive Ice Features by Ice Types from Multi-Year Upward Looking Sonar Ice Draft Measurements. In: Arctic Technology Conference. Copenhagen, Denmark: Offshore Technology Conference.

Fore, A. G., Stiles, B. W., Chau, A. H., Williams, B., Dunbar, R. S., & Rodriguez, E. (2014). Point-wise wind retrieval and ambiguity removal improvements for the QuikSCAT

climatological data set. Geoscience and Remote Sensing, IEEE Transactions on, 52(1), 51-59.

Fossen, T. I. & Lekkas, A. M. (2017). Direct and indirect adaptive integral line of sight path following controllers for marine craft exposed to ocean currents. International Journal of Adaptive Control and Signal Processing, 2017, 31(4): 445-463.

ftp://ftp.ifremer.fr/ifremer/cersat/products/swath/altimeters/waves/documentation/publications/Sepulveda_etal_2015.pdf

Gemmrich, J. & Thomson, J. (2017). Observations of the Shape and Group Dynamics of Rogue Waves. Geophysical Research Letters, 44, 1823-1830.

Ghorbani, M.A., Asadi, H., Makarynskyy, O., Makarynska, D., Yaseen, Z.M., (2017). Augmented chaos-multiple linear regression approach for prediction of wave parameters. Engineering Science and Technology, an International Journal 20, 1180–1191.

Girolamo, P.D., Di Risio, M., Beltrami, G.M., Bellotti, G., Pasquali, D., (2017). The use of wave forecasts for maritime activities safety assessment. Applied Ocean Research 62, 18–26

Giske, F.-I.G., Leira, B.J., Øiseth, O., (2017). Efficient computation of cross-spectral densities in the stochastic modelling of waves and wave loads. Applied Ocean Research 62, 70–88.

Godoi, V.A., Bryan, K.R., Stephens, S.A., Gorman, R.M., (2017). Extreme waves in New Zealand waters. Ocean Modelling 117, 97–110.

Gomit, G., Calluaud, D., Chatellier, L., David, L. & Fréchou, D. (2013). Optical measurements of free surface for the analysis of ship waves in towing tank, Proc. 3rd Int. Conf. on Advanced Model Meas. Techn. for the Maritime Ind, (AMT'13), Sep, Gdansk, Poland.

Gouin, M., Ducrozet, G. & Ferrant, P. (2016). Development and Validation of a Non-Linear Spectral Model for Water Waves over Variable Depth. European Journal of Mechanics - B/Fluids, 57, 115-128.

Gouin, M., Ducrozet, G. & Ferrant, P. (2017). Propagation of 3d Nonlinear Waves over an Elliptical Mound with a High-Order Spectral Method. European Journal of Mechanics - B/Fluids, 63, 9-24.

Gramstad, O. & Trulsen, K. (2007). Influence of Crest and Group Length on the Occurrence of Freak Waves. J. Fluid Mech., 582, 463-472.

Gramstad, O. (2017). Modulational Instability in Jonswap Sea States Using the Alber Equation. ASME 2017 36th International Conference on Ocean, Offshore and Arctic Engineering. Trondheim, Norway.

Gramstad, O., and Babanin, A.V. (2016). The generalized kinetic equation as a model for the nonlinear transfer in third generation wave models. Ocean Dynamics, 66, 509-526, doi:10.1007/s10236-016-0940-4

Gramstad, O., Bitner-Gregersen, E. and Vanem E. (2017). Projected changes in the occurrence of extreme and rogue waves in future climate in the North Atlantic , Proc. 36th Int. Conf. on Ocean, Offshore and Arctic Eng., OMAE2017, June 25-30, Trondheim, Norway.

Grin, R., Dallinga, R., and Boelen, P., (2016). Voyage Simulations Techniques as Design Tool for Ferries, Proc. RINA Conf. Design & Operations of Ferries & Ro-Pax Vessels, May 25-26, London, UK.

Guo, A, Fang, Q., Li, H., (2015). Analitical solution of hurricane wave force acting on submerged bridge decks, Ocean Engineering 108 (2015) 519-528.

Guo, B., Bitner-Gregersen, E.M., Sun, H., and Helmers, J.B. (2016). Statistics analysis of ship response in extreme seas, Ocean engineering, Vol. (119), pp.154-164.

Hagen, Ø., Grue, I.H., Birknes-Berg, J., Lian, G., Bruserud, K., (2017). Analysis of Short-Term and Long-Term wave statistics by time domain simulations statistics. Proceedings of the ASME 2017 36th Int. Conference on Ocean, Offshore & Arctic Engineering OMAE2017.

Hao Qin, Wenyonng Tang, Hongxiang Xue, Zhe Hu, JIngting Guo. (2017). Numerical study of wave impact on the deck-house caused by freak waves. Ocean Engineering, volume 133, 2017, pages 151-169.

Hara, T., and Sullivan, P.P. (2015). Wave boundary layer turbulence over surface waves in a strongly forced condition, J. Phys. Oceanogr., 45, 868–883

Harpham, Q., Tozer, N., Cleverley, P., Wyncoll, D., Cresswell, D., (2016). A Bayesian method for improving probabilistic wave forecasts by weighting ensemble members. Environmental Modelling & Software 84, 482-493.

Hashim, R., Roy, C., Motamedi, S., Shamshirband, S., Petković, D., (2016). Selection of climatic parameters affecting wave height prediction using an enhanced Takagi-Sugeno-based fuzzy methodology. Renewable and Sustainable Energy Reviews 60, 246–257.

Hendricks, S. et al. (2014). Sea Ice Thickness Surveying with Airborne Electromagnetics - Grounded Ridges and Ice Shear Zones near Barrow, Alaska. In: Arctic Technology Conference. Houston, Texas: Offshore Technology Conference.

Hennig, J., Scharnke, J., Schmittner, C.E. and Berg J. van den (2015). ShorT-CresT: Directional wave measurements at MARIN, Proc. 34th Int. Conf. on Ocean, Offshore and Arctic Eng., OMAE2015, May 31-June 5, St. John's, Newfoundland, Canada.

Hennig, J., Scharnke, J., Swan, C., Hagen, O., Ewans, K., Tromans, P. and Forristall, G., (2015). Effect of short-crestedness on extreme wave impacts – A summary of findings from the Joint Industry Project 'ShorTCresT', Proc. 34th Int. Conf. on Ocean, Offshore and Arctic Eng. (OMAE). ASME Paper OMAE2015-41167.

Hisette, Q. et al. (2017). Discrete Element Simulation of Ship Breaking Through Ice Ridges. In: International Ocean and Polar Engineering Conference. San Francisco, California: International Society of Offshore and Polar Engineers, pp. 1401-1409.

Hithin, N.K., Kumar, V.S., Shanas, P.R., (2015). Trends of wave height and period in the Central Arabian Sea from 1996 to 2012: A study based on satellite altimeter data. Ocean Engineering 108, 416–425.

Holub, C. et al. (2017). Ice Drift Tracking Using Photogrammetric Methods on Radar Data. In: International Ocean and Polar Engineering Conference. San Francisco, California: International Society of Offshore and Polar Engineers, pp. 1338-1342.

Hoque, Md.A., Perrie,W., Solomon, S.M., (2017). Evaluation of two spectral wave models for wave hindcasting in the Mackenzie Delta. Applied Ocean Research 62, 169–180.

Hosking, J.R.M., Wallis, J. R. (1997). Regional Frequency Analysis – An Approach Based on L-Moments. Cambridge University Press, Cambridge, UK.

Hu J, Zhou L. (2015). Experimental and numerical study on ice resistance for icebreaking vessels[J]. International Journal of Naval Architecture and Ocean Engineering, 2015, 7(3): 626-639.

Hu S. S., Wang Y., Liu Z. S., Wang H. Y. (2016). Exploration of measurement principle of a three-dimensional current sensor for measuring the upwelling. Ocean Engineering, 2016,127: 48-57.

Huisman M, Janßen C F, Rung T, et al. (2016). Numerical Simulation of Ship-Ice Interactions with Physics Engines under Consideration of Ice Breaking[C]//The 26th International Ocean and Polar Engineering Conference. International Society of Offshore and Polar Engineers, 2016.

Iafrati, A., Babanin, A.V. and Onorato, M. (2014). Modelling of ocean-atmosphere interaction phenomena during the breaking of modulated wave trains. Journal of Computational Physics, 271, 151-171

Ibarra-Berastegi, G., Saénz, J., Esnaola, G., Ezcurra, A., Ulazia, A., (2015). Short-term forecasting of the wave energy flux: Analogues, random forests, and physics-based models. Ocean Engineering 104, 530–539.

IPCC, (2014): Climate Change 2014: Synthesis Report. Contribution of Working Groups I, II and III to the Fifth Assessment Report of the Intergovernmental Panel on Climate Change [Core Writing Team, R.K. Pachauri and L.A. Meyer (eds.)]. IPCC, Geneva, Switzerland, 151 pp.

ISO (2008). Guidance for Uncertainties in Measurement (GUM), JCGM100.

Iyerusalimskiy, A., Choi J., Park G., Kim Y., Yu, H. (2011). The interim results of the long-term ice loads monitoring on the large Arctic tanker, Proc. of the Int. Conf. on Port and Ocean Eng. under Arctic Conditions (POAC11), Montreal, Canada.

Jane, R., Valle, L.D., Simmonds, D., Raby, A., (2016). A copula-based approach for the estimation of wave height records through spatial correlation. Coastal Eng. 117, 1–18.

Jeans, G., Xiao, W., Osborne, A. R., Jackson, C. R. & Mitchell, D. A. (2017). The Application of Nonlinear Fourier Analysis to Soliton Quantification for Offshore Engineering. 36th Int. Conference on Ocean, Offshore & Arctic Engineering (OMAE). Trondheim, Norway.

Jiang, H., Babanin, A.V., and Chen, G. (2016). Event-based validation of swell arrival time. Journal of Physical Oceanography, 46, 3563-3569

Jiang, H., Babanin, A.V., Liu, Q., Stopa, J.E., Chapron, B., Chen, G., (2017). Can contemporary satellites estimate swell dissipation rate? Remote Sensing of Environment 201, 24–33.

Karvonen, J. et al. (2016). Improving Sea Ice Information and Weather Forecasting for Operational Purposes. In: International Ocean and Polar Engineering Conference. Rhodes, Greece: International Society of Offshore and Polar Engineers, pp. 1163-1166.

Kerkeni, S. et al. (2014). DYPIC Project: Technological and Scientific Progress Opening New Perspectives. In: Arctic Technology Conference. Houston, Texas: Offshore Technology Conference.

Kim, B. and Kim, T. (2017). Monte Carlo Simulation for Offshore Transportation, Ocean Eng., Vol 129, pp. 177–190. doi: 10.1016/j.oceaneng.2016.11.007.

Kim, B. and Kim, T-W., (2017). Weather routing for offshore transportation using genetic algorithm, Appl Ocean Res., Vol 63, Pp. 262 – 275.

Kim, H. et al. (2016). Characterization of Full Scale Operational Ice Pressures and Hull Response on a Large Arctic Tanker. In: Arctic Technology Conference. St. John's, Newfoundland: Offshore Technology Conference.

Kim, J., Pedersen, G. K., Løvholt, F. & Leveque, R. J. (2017). A Boussinesq Type Extension of the Geoclaw Model - A Study of Wave Breaking Phenomena Applying Dispersive Long Wave Models. Coastal Engineering, 122, 75-86.

Kim, Y. and Hermansky, G., (2014). Uncertainties in seakeeping analysis and related loads and response procedures, Ocean Engineering 86 68–81.

Kirby, J. T. (2016). Boussinesq Models and their Application to Coastal Processes across a Wide Range of Scales. J. of Waterway, Port, Coastal, & Ocean Eng., 142, 03116005.

Klebert, P., Patursson, Ø., Endresen, P. C., Rundtop, P., Birkevold, J., Rasmussen, H. W. (2015). Three-dimensional deformation of a large circular flexible sea cage in high currents: Field experiment and modeling. Ocean Engineering, 2015, 104: 511-520.

Klein, M., Clauss, G. F., Rajendran, S., Guedes Soares, C. & Onorato, M. (2016). Peregrine Breathers as Design Waves for Wave-Structure Interaction. Ocean Eng., 128, 199-212.

Kohout, A. L., Williams, M. J. M., Toyota, T., Lieser, J. and Hutchings, J. (2016). In situ observations of wave-induced sea ice breakup, Deep-Sea Research Part II: Topical Studies in Oceanography , 131 , 22–27, doi:10.1016/ j.dsr2.2015.06.010.

Kouvaras, N., Dhanak, M.R., (2017). Prediction of characteristics of wave breaking in shallow water using neural network techniques. Proceedings of the ASME 2017 36th International Conference on Ocean, Offshore and Arctic Engineering OMAE2017.

Krasnopolsky, V., Nadiga, S., Mehra, A., Bayler, E., Behringer, D., (2016). Neural Networks Technique for Filling Gaps in Satellite Measurements: Application to Ocean Color Observations. Computational Intelligence & Neuroscience, Vol. 2016, Article ID 6156513, 9 pages.

Kumar, N.K., Savitha, R., Al Mamun, A., (2017). Ocean wave height prediction using ensemble of Extreme Learning Machine. Neurocomputing 0 0 0, 1–9.

Kumar, N.K., Savitha, R., Al Mamun, A., (2017). Regional ocean wave height prediction using sequential learning neural networks. Ocean Engineering 129, 605–612.

Kumar, P., Min, S.-K. , Weller, E., Lee, H., Wang, X.L., (2016). Influence of Climate Variability on Extreme Ocean Surface Wave Heights Assessed from ERA-Interim and ERA-20C. Journal of Climate, v.29, 00. 4031-4046.

Kumar, U.M., Swain, D., Sasamal, S.K., Reddy, N.N., Ramanjappa, T., (2015). Validation of SARAL/AltiKa significant wave height and wind speed observations over the North Indian Ocean. Journal of Atmospheric and Solar-Terrestrial Physics 135, 174–180.

Kurtz, N. T. and Markus, T. (2012). Satellite observations of Antarctic sea ice thickness and volume. J. Geophys. Res., 117, 2012. doi: 10.1029/2012JC008141

Laface, V., Arena, F., (2016). A new equivalent exponential storm model for long-term statistics of ocean waves. Coastal Engineering 116, 133–151.

Laface, V., Arena, F., Kougioumtzoglou, I.A., Santos, K.R.M., (2017). Joint Time-Frequency analysis of small scale ocean storms via the harmonic wavelet transform. Proceedings of the ASME 2017 36th Int. Conf. on Ocean, Offshore and Arctic Engineering OMAE2017.

Laface, V., Arena, F., Maisondieu, C., Romolo, A., (2017). On Long Term statistics of ocean storms starting from partitioned sea states. Proceedings of the ASME 2017 36th International Conference on Ocean, Offshore and Arctic Engineering OMAE2017.

Lakshmi, D. D., Murty, P. L. N., Bhaskaran, P. K., Sahoo, B., Kumar, T. S., Shenoi, S. S. C., Srikanth, A. S. (2017). Performance of WRF-ARW winds on computed storm surge using hydodynamic model for Phailin and Hudhud cyclones. Ocean Eng., 2017, 131: 135-148.

Lamas, F., Ramirez, M. A. & Fernandes, A. C. (2017). Yaw galloping of a TLWP Platform under high speed currents by analytical methods and its comparison with experimental results. Proc. of the OMEA 2017 Conference, 25-30 June 2017 Trondheim, Norway.

Larson, E., Simonsen, M., and Mao, W. (2015). DIRECT Optimization Algorithm in Weather Routing of Ships, Proc. 25th Int. Offshore and Polar Eng. Conf. (ISOPE), June 21-26, Kona, Hawaii, USA.

Lavidas, G., Venugopal, V., Friedrich, D., (2017). Sensitivity of a numerical wave model on wind re-analysis datasets. Dynamics of Atmospheres and Oceans 77, 1–16.

Leadbetter, M.R., Rychlik, I., Stambaugh, K., (2011). Estimating Dynamic Stability Event Probabilities from Simulation and Wave Modeling Methods, 12th Int. Ship Stability Workshop, Washington DC, USA.

Lee, H.S., (2015). Evaluation of WAVEWATCH III performance with wind input and dissipation source terms using wave buoy measurements for October 2006 along the east Korean coast in the East Sea. Ocean Engineering 100, 67–82.

Lee, T., Kim, H. Chung, H., Bang, Y., Myung, H., (2015). Energy efficient path planning for a marine surface vehicle considering heading angle, Ocean Engineering 107 (2015) 118-131

Lenain, L. & Melville W.K. (2014). Autonomous surface vehicle measurements of the ocean's response to Tropical Cyclone Freda. J. Atmos. Oceanic Technol., 31, p.2169–2190

Li, J.-G., Saulter,A. (2012). Assessment of the updated Envisat ASAR ocean surface wave spectra with buoy and altimeter data. Remote Sensing of Environment 126, 72–83.

Li, N., Cheung, K.F., Stopa, J.E., Hsiao, F., Chen, Y.-L., Vega, L., Cross, P., (2016). Thirty-four years of Hawaii wave hindcast from downscaling of climate forecast system reanalysis. Ocean Modelling 100, 78–95.

Lin, Y-H., Fang, M-C. and Yeung, R.W., (2013). The optimization of ship weather-routing algorithm based on the composite influence of multi-dynamic elements, Appl. Ocean Res, Vol 43, pp. 184 – 194.

Lindeboom, R.C.J. and Scharnke, J., (2016). Determination of wave kinematics in breaking waves making use of Particle Image Velocimetry, NATO Specialists Meeting "Progress and Challenges in Validation Testing for Comp. Fluid Dyn.", 26 - 28 Sep, Avila, Spain.

Liu, D.Y. Ma, Y.X., Dong, G.H. and Perlin, M., (2016). Detuning and wave breaking during nonlinear surface wave focusing, Ocean Engineering, Vol. 113, pp. 215-223.

Liu, K., Chen, Q. & Kaihatu, J. M. (2016). Modeling Wind Effects on Shallow Water Waves. Journal of Waterway, Port, Coastal, and Ocean Engineering, 142, 04015012.

Liu, Q., Babanin, A., Fan, Y., Zieger, S., Guan, C., Moon, I.-J., (2017). Numerical simulations of ocean surface waves under hurricane conditions: Assessment of existing model performance. Ocean Modelling 118, 73–93.

Liu, Q., Babanin, A.V., Zieger, S., Young, I.R., and Guan, C. (2016). Wind and wave climate in the Arctic Ocean as observed by altimeters. Journal of Climate, 29, 7957-7975

Liu, Q., Lewis, T., Zhang, Y., Sheng, W., (2015). Performance assessment of wave measurements of wave buoys. International Journal of Marine Energy 12, 63–76.

Liu, S. H., Zhang, Q. S., Zhao, X., Zhang, X. Y., Li, S. H., Jing, J. E. (2017). Study of an expendable current profiler detection method. Ocean Engineering, 2017, 132: 40-44.

Lo, D.-C., Wei, C.-C., Tsai, E.-P., (2015). Parameter Automatic Calibration Approach for Neural-Network-Based Cyclonic Precipitation Forecast Models. Water 2015, 7, 3963-3977.

Loyd's Register Marine, (2015). Wind-powered shipping: A review of the commercial, regulatory and technical factors affecting uptake of wind-assisted propulsion, Southampton: Lloyd's Register Group Limited.

Lu, L-F., Sasa, K., Sasaki, W., Terada, D., Kano, T. and Mizojiri, T., (2017). Rough wave simulation and validation using onboard ship motion data in the Southern Hemisphere to enhance ship weather routing, Ocean Engineering, Vol 144, pp. 61 – 77

Lu, R. ; Ringsberg, J. ; Mao, W. (2017). Wind-assisted propulsion for shipping: status and perspectives, Proceedings of the International Conference on Ships and Offshore Structures (ICSOS 2017) in Shenzhen, China, September 11-13, 2017. p. 561-571.

Lu, W. et al. (2016). A Shipborne Measurement System to Acquire Sea Ice Thickness and Concentration at Engineering Scale. In: Arctic Technology Conference. St. John's, Newfoundland: Offshore Technology Conference.

Lu, X. et al. (2017). Observations of Arctic snow and sea ice cover from CALIOP lidar measurements. Remote Sensing of Environment, 194, pp. 248-263.

Lubbad, R. et al. (2016). Oden Arctic Technology Research Cruise 2015. In: Arctic Technology Conference. St. John's, Newfoundland: Offshore Technology Conference.

Lucas, C., Guedes Soares, C., (2015). On the modelling of swell spectra. Ocean Engineering 108, 749–759. Ocean Engineering 108, 749–759.

Lucas, C., Muraleedharan, G., Guedes Soares, C., (2017). Regional frequency analysis of extreme waves in a coastal area. Coastal Engineering 126, 81–95.

Ma, Y., Dong, G., Perlin, M., Liu, S., Zang, J. and Sun, Y., (2009). Higher-harmonic 29 focused-wave forces on a vertical cylinder, Ocean Engineering, Vol. 36, pp. 595-604.

Mao, W. ; Rychlik, I. (2017). Estimation of Weibull distribution for wind speeds along ship routes. Journal of Engineering for the Maritime Environment. 231 (2) p. 464-480.

Mao, W. and Rychlik, I. (2016). Estimation of Weibull distribution for wind speeds along ship routes, Proceedings of the Institution of Mechanical Engineers, Part M: Journal of Engineering for the Maritime Environment, DOI: 1475090216653495.

Mao, W., Li, Z., Ringsberg, J.W., and Rychlik, I. (2012). Application of a ship-routing fatigue model to case studies of 2800 TEU and 4400 TEU container vessels. Journal of Engineering for the Maritime Environment. Vol.226(3), pp.222–234.

Mao, W., Ringsberg, J., and Rychlik, I. (2010b). Development of a fatigue model useful in ship routing design, J. of Ship Research, Vol 54(4), pp. 281-293

Mao, W., Rychlik, I., and Storhaug, G. (2010a). Safety index of fatigue failure for ship structure details, J. of Ship Research, Vol 54(3), pp. 197-208

Marchenko, A.V., Gorbatsky, V.V. and Turnbull, I.D. (2015). Characteristics of under-ice ocean currents measured during wave propagation events in the Barents Sea. Proc. of the 23nd International Conference on Port and Ocean Engineering under Arctic Conditions June 14-18, 2015 Trondheim, Norway, 11p

Martínez-Asensio, A., Marcos, M., Tsimplis, M.N., Jordà, G., Feng, X., Gomis, D., (2016). On the ability of statistical wind-wave models to capture the variability and long-term trends of the North Atlantic winter wave climate. Ocean Modelling 103, 177–189.

Mayerle, R., Narayanan, R., Etri, T., Wahab, A.K.A. (2015). A case study of sediment transport in the Paranagua Estuary Complex in Brazil. Ocean Engineering, 2015, 106: 161-174.

McGonigal, D., Hagen, D. and Guzman, L., (2011). Extreme Ice Features Distribution in the Canadian Arctic, Proc. Int. Conf. on Port and Ocean Eng. under Arctic Conditions (POAC11), Montreal, Canada.

Memos, C. D., Klonaris, G. T. & Chondros, M. K. (2016). On Higher-Order Boussinesq-Type Wave Models. J. of Waterway, Port, Coastal, and Ocean Engineering, 142, 04015011.

MEPC 71/5/13 (2017). Progress and present status of the draft revised Guidelines for determining minimum propulsion power to maintain the manoeuvrability of ships in adverse conditions. Submitted by Denmark, Germany, Japan, Spain and IACS to IMO, 2017.

MEPC 71/INF.28 (2017). Draft revised Guidelines for determining minimum propulsion power to maintain the manoeuvrability of ships in adverse conditions. Submitted by Denmark, Germany, Japan, Spain and IACS to IMO, 2017.

MEPC 71/INF.29 (2017). Supplementary information on the draft revised Guidelines for determining minimum propulsion power to maintain the manoeuvrability of ships in adverse conditions. Submitted by Denmark, Germany, Japan and Spain to IMO, 2017.

Metrikin I, Kerkeni S, Jochmann P, et al. (2015). Experimental and numerical investigation of dynamic positioning in level ice[J]. Journal of Offshore Mechanics and Arctic Engineering, 2015, 137(3): 031501.

Michael Banks, Nagi Abdussanmie, (2017). The response of a semisubmersible model under focused wave groups: Experimental investigation, Journal of Ocean Engineering and Science, 2017.

Mierke D, Janßen C, Rung T. (2015). GPU-accelerated large-eddy simulation of ship-ice interactions[C]//Proc. 6th Int. Conf. on Comp. Methods in Marine Engng. 2015: 229-240.

Minnick, L., Bassler, C., Perceival, S. and Hanyok, L., (2010). Large-scale wave kinematics measurements of regular waves and large-amplitude wave groups, Proc. 29th Int. Conf. on Ocean, Offshore and Arctic Eng. (OMAE). ASME Paper OMAE 2010-20240.

Minoura, M (2016). Stochastic sea state model based on Fourier series expansion, Proceeding of 26th ISOPE, Rhodes, Greece

Mintu, S. et al. (2016). State-of-the-Art Review of Research on Ice Accretion Measurements and Modelling. In: Arctic Technology Conference. St. John's, Newfoundland: Offshore Technology Conference. .

Montes-Iturrizaga, R. and Heredia-Zavoni, E. (2016). Reliability analysis of mooring lines using copulas to model statisticaldependence of environmental variables Applied Ocean Research, Vol.59, pp.564-576.

Montiel, F., Squire, V.A. and Bennetts, L.G. (2016). Attenuation and directional spreading of ocean wave spectra in the marginal ice zone. J. Fluid Mech., 790, 492-522.

Mori, N., Onorato, M., and Janssen, P.A.E.M., (2011). On the Estimation of the Kurtosis in Directional Sea States for Freak Wave Forecasting, J. of Physical Oceanography, Vol 41, pp. 1484-1497.

Mosig, J. E. M., Montiel, F., and Squire, V. A. (2015). Comparison of viscoelastic-type models for ocean wave attenuation in ice-covered seas, Journal of Geophysical Research: Oceans , pp. 1–17, doi:10.1002/ 2015JC010700

Mudge, T.D., Fissel, D.B., de Saavedra Álvarez, M. M. and Marko, J.R. (2011). Investigations of Variability for Ship Navigation through the Northwest Passage, 1982-2010, Proc. Int. Conf. on Port and Ocean Eng. under Arctic Conditions (POAC11), Montreal, Canada.

Muraleedharan, G., Lucas, C., Guedes Soares, C., (2016). Regression quantile models for estimating trends in extreme significant wave heights. Ocean Engineering 118, 204–215.

Muraleedharan, G., Lucas, C., Martins, D., Guedes Soares, C., Kurup, P.G., (2015). On the distribution of significant wave height and associated peak periods. Coastal Engineering 103, 42–51.

Murray Rudman, Paul W. Cleary. (2016). The influence of mooring system in rogue wave impact on an offshore platform. Ocean Engineering, volume 115, 2016, pages 168-181.

Murty, P.L.N., Sandhya, K.G., Bhaskaran, Prasad K., Jose, F., Gayathri, R., Balakrishnan Nair, T.M., Kumar, T.S., Shenoi, S.S.C. (2014). A coupled hydrodynamic modeling system for PHAILIN cyclone in the Bay of Bengal. Coastal Engineering, vol. 93, 2014, pages 71-81.

Naaijen, P., van Dijk, R.R.T., Huijsmans, R.H.M. and El-Mouhandiz, A.A., (2009). Real time estimation of ship motions in short crested seas, Proc. 28th Int. Conf. on Ocean, Offshore and Arctic Engineering (OMAE). ASME Paper OMAE2009-79366.

Nagi Abdussamie, Yuriy Drobyshevski, Roberto Ojeda, Giles Thomas, Walid Amin. (2017). Experimental investigation of wave-in-deck impact events on a TLP model. Ocean Engineering, volume 142, 2017, pages 541-562.

Nam, J.-H., Park, I., Lee, H.J., Kwon, M.O., Choi, K. and Seo, Y.-K. (2013). Simulation of Optimal Arctic Routes Using a Numerical Sea Ice Model Based on an Ice-Coupled Ocean Circulation Method, Int. J. of Naval Arch. and Ocean Eng., Vol 5(2), pp. 210–226. doi: 10.2478/IJNAOE-2013-0128.

Nayak, S., Panchang, V., (2015). A Note on Short-term Wave Height Statistics. Aquatic Procedia 4, 274 – 280. International Conference on Water Resources, Coastal and Ocean Engineering (ICWRCOE 2015).

Nelissen, D. Traut, M., Köhler, J., Mao, W., Faber, J. and Ahdour S. (2016). Study on the analysis of market potentials and market barriers for wind propulsion technologies for ships. European Commission, DG Climate Action, 2016. 128 p.

Neville, M. A. et al. (2016). Physical Ice Management Operations - Field Trials and Numerical Modeling. In: Arctic Technology Conference. St. John's, Newfoundland: Offshore Technology Conference.

Niclasen, B.A., Simonsen, K., (2007). Note on wave parameters from moored wave buoys. Applied Ocean Research 29, 231–238.

Nielsen, U.D. and Jensen, J.J., (2011). A novel approach for navigational guidance of ships using onboard monitoring systems. Ocean Eng., Vol 38, pp. 444 - 455.

Nielsen, U.D., Jensen, J.J., Petersen, P.T. and Ito, Y., (2011), Onboard monitoring of fatigue damage rates in the hull, Marine Structures, Vol 24 (2), pp. 182 - 206.

Nikishova, A., Kalyuzhnaya, A., Boukhanovsky, A., Hoekstra, A., (2017). Uncertainty quantification and sensitivity analysis applied to the wind wave model SWAN. Environmental Modelling & Software 95, 344-357.

Nørgaard, J.Q.H., Andersen, T.L., (2016). Can the Rayleigh distribution be used to determine extreme wave heights in non-breaking swell conditions? Coastal Engineering 111, 50–59.

Nose, T., Babanin, A.V., and Ewans, K. (2016). Directional analysis and potential for spectral modelling of infragravity waves. Proceedings of the ASME 2016 35th International Conference on Ocean, Offshore and Arctic Engineering OMAE2016, June 19-24, 2016, Busan, South Korea, 11p

Noshokaty, S., (2017). Shipping Optimisation Systems (SOS): Tramp Optimisation Perspective, J. of Shipping and Trade, Vol 2(1), pp. 1–36. doi: 10.1186/s41072-017-0021-y.

Ogeman, V., Mao, W. and Ringsbergs, J. W. (2013). Comparison of computational methods for evaluation of wave-load-induced fatigue damage accumulation in ship structure details, Proc. 5th Int. Conf. on Comp. Methods in Marine Eng. (MARINE 2013), May 29-31, Hamburg, Germany.

Onorato, M. & Suret, P. (2016). Twenty Years of Progresses in Oceanic Rogue Waves: the Role Played By Weakly Nonlinear Models. Natural Hazards, 84, 541-548.

Onorato, M., Cavaleri, L., Fouques, S., Gramstad, O., Janssen, P. A. E. M., Monbaliu, J., Osborne, A. R., Pakozdi, C., Serio, M., Stansberg, C. T., Toffoli, A. & Trulsen, K. (2009).

Statistical Properties of Mechanically Generated Surface Gravity Waves: A Laboratory Experiment in a Three-Dimensional Wave Basin. J. Fluid Mech., 627, 235-257.

Onorato, M., Osborne, A. R. & Serio, M. (2006). Modulational Instability in Crossing Sea States: A Possible Mechanism for the formation of Freak Waves. Phys. Rev. Lett., 96, 014503.

Onorato, M., Proment, D., Clauss, G. & Klein, M. (2013). Rogue Waves: From Nonlinear Schrödinger Breather Solutions To Sea-Keeping Test. Plos one, 8, E54629.

Orimolade, A.K., Haver, S., and Gudmestad, O.T. (2016). Estimation of extreme significant wave heights and the associated uncertainties: A case study using NORA10 hindcast data for the Barents Sea, Marine Structures, Vol.49, pp.1-17.

Osborne, A. (2010). Non-Linear Ocean Waves and the Inverse Scattering Transform, Academic Press.

Osborne, A. R. & Leon, S. P. D. (2017). Properties of Rogue Waves and the Shape of the Ocean Wave Power Spectrum. ASME (2017) 36th international Conference on Ocean, offshore and Arctic Engineering (OMAE). Trondheim, Norway.

Pan, S., Fan, Y., Chen, J., Kao, C., (2016). Optimization of multi-model ensemble forecasting of typhoon waves. Water Science and Engineering, 9(1):52-57.

Pan, Z. Y., Vada, T., Finne, S., Nestegård, A., Hoff, J. R., Hermundstad, E. M. & Stansberg, C. T. (2016). Benchmark Study of Numerical Approaches for Wave-Current Interaction Problem of Offshore Floaters. Proceedings of the OMEA 2016 Conference, 19-24 June 2016 Busan, South Korea.

Park, J., and Kim, N. (2015). Two-phase approach to optimal weather routing using geometric programming, J. of Marine Sc. and Techn., 20, pp. 679 - 688.

Parker, K., Hill, D.F., (2017). Evaluation of bias correction methods for wave modeling output. Ocean Modelling 110, 52–65.

Perelman, O., Wu, C.H., Boucheron, R. and Fréchou, D. (2011). 3D wave fields measurements techniques in model basin: Application on ship wave measurement, Proc. 2nd Int. Conf. on Advanced Model Measurement Techn. for the Maritime Ind, (AMT'11), 4 – 6 Apr, Newcastle upon Tyne, UK.

Perez, J., Menendez, M., Losada, I.J. GOW2: (2017). A global wave hindcast for coastal applications. Coastal Engineering, volume 124, 2017, pages 1-11.

Peric, R., Hoffmann, N. & Chabchoub, A. (2014). Initial Wave Breaking Dynamics of Peregrine-Type Rogue Waves: A Numerical and Experimental Study.

Pezzutto,P., Saulter, A., Cavaleri, L., Bunney, C., Marcucci, F., Torrisi, L., Sebastianelli, S., (2016). Performance comparison of meso-scale ensemble wave forecasting systems for Mediterranean sea states. Ocean Modelling 104, 171–186.

Pillai, A. C., Chick, J., Khorasanchi, M., Barbouchi, S., Johanning, L. (2017). Application of an offshore wind farm layout optimization methodology at Middelgrunden wind farm. Ocean Engineering, 2017, 139: 287-297.

Podgorski, K., Rychlik, I., (2016). Spatial size of waves. Marine Structures 50, 55-71.

Poli, P., Hersbach, H., Dee, D.P., Berrisford, P., Simmons, A.J., Vitart, F., Laloyaux, P., Tan, D.G.H., Peubey, C., Thepaut, J.-N., Tr´emolet, Y., Holm, E.V., Bonavita, M., Isaken, L., Fisher, M., (2016), ERA-20C: An Atmospheric Reanalysis of the Twentieth Century. Journal of Climate, 29, 4083-4097.

Portilla, J., Caicedo, A.L., P.adilla-Hernández, R., Cavaleri, L., (2015). Spectral wave conditions in the Colombian Pacific Ocean. Ocean Modelling 92, 149–168.

Portilla-Yandún, J., Cavaleri, L., Van Vledder, G.Ph., (2015). Wave spectra partitioning and long term statistical distribution. Ocean Modelling 96, 148–160.

Qiao, F, Yuan, Y., Deng, J,. Dai, D. and Song, Z. (2016). Wave–turbulence interaction-induced vertical mixing and its effects in ocean and climate models. Phil. Trans. R. Soc. A, 374: 20150201, http://dx.doi.org/10.1098/rsta.2015.0201

Qin, H., Tang, W., Hu, Z. & Guo, J. (2017a). Structural Response of Deck Structures on the Green Water Event Caused By Freak Waves. Journal of Fluids and Structures, 68, 322-338.

Qin, H., Tang, W., Xue, H., Hu, Z. & Guo, J. (2017b). Numerical Study of Wave Impact on the Deck-House Caused By Freak Waves. Ocean Engineering, 133, 151-169.

Qiu, W., Roussset, J.M. & Rodriguez, C., (2017). Benchmark Studies on Two-Body Interactions in Waves: Model Tests & Uncertainty Analysis, Joint ITTC-ISSC Workshop, Wuxi, 2017.

Qiu, W., Sales, J.J., Lee, D., Lie, H., Magarovskii, V., Mikami, T., Rousset, J.M., Sphaier, S., and Wang, X., (2014). Uncertainties related to Predictions of Loads and Responses for Ocean and Offshore Structures, Ocean Engineering, Vol. 86, pp. 58-67.

Queffeulou, P., Croizé-Fillon, D., (2017). Global altimeter SWH data set. Laboratoire d'Océanographie Physique et Spatiale IFREMER. Report available at ftp://ftp.ifremer.fr/ifremer/cersat/products/swath/altimeters/waves/documentation/altimeter_wave_merge__11.4.pdf

Rae J G L, Hewitt H T, Keen A B, et al. (2015). Development of global sea ice 6.0 CICE configuration for the Met Office Global Coupled Model[J]. Geoscientific Model Development Discussions (Online), 2015, 8(3).

Rapizo, H., Babanin, A.V., Provis, D., and Rogers, W.E. (2017). Current-induced dissipation in spectral wave models, Journal of Geophysical Research Oceans. 122, 2205–2225, doi:10.1002/2016JC012367

Rapizo, H., Waseda, T., Babanin, A.V. and Toffoli, A. (2016). Laboratory experiments on the effects of a variable current field on the spectral geometry of water waves. Journal of Physical Oceanography, 46, 2695-2717

Rapp, R.J. and Melville, W.K., (1990). Laboratory measurements of deep-water breaking waves, Phil. Trans. of the Royal Soc., Series A, Vol. 331, pp. 735-800.

Reichl, B. G., Wang, D., Hara, T., Ginis, I. and Kukulka, T. (2016). Langmuir turbulence parameterisation in tropical cyclone conditions. J. Phys. Oceanogr., 46, 863–886, doi:10.1175/JPO-D-15-0106.1.

Reimer, N., and Duong, Q.T (2013). Prediction of Travelling Time and Exhaust Gas Emission of Ships on the Northern Sea Route, Int. Conf. on Offshore Mech. and Arctic Eng. (OMAE), June 9-14, Nantes, France.

Reineman, D.R., Thomas, L.N., Caldwell, M.R., (2017). Using local knowledge to project sea level rise impacts on wave resources in California. Ocean & Coastal Management, 138, 181-191.

Reite, K., Ladstein, J., and Haugen, J. (2017). Data-driven Real-time Decision Support and its Application to Hybrid Propulsion Systems, OMAE2016-61031, Int. Conf. on Offshore Mech. and Arctic Eng. (OMAE), June 25-30, Trondheim, Norway.

Residori, S., onorato, M., Bortolozzo, U. & Arecchi, F. T. (2017). Rogue Waves: A Unique Approach to Multidisciplinary Physics. Contemporary Physics, 58, 53-69.

Resio, D.T., Vincent, L., Ardag, D., (2016). Characteristics of directional wave spectra and implications for detailed-balance wave modeling. Ocean Modelling 103, 38–52.

Resolution MEPC.232(65), (2013). Interim guidelines for determining minimum propulsion power to maintain the manoeuvrability in adverse conditions. IMO, 2013.

Richon, J. B., Reeves, M., Darquier M. and Fréchou D. (2009). Development of a Laser Gauge for Dynamic Wave Height Measurements in the B600 Towing Tank. Proc. 1st Int. Conf. on Advanced Model Measurement Techn. (AMT '09), 1 - 2 Sep, Nantes France.

Robertson, B., Jin, Y., Bailey, H., Buckham, B., (2017). Calibrating wave resource assessments through application of the triple collocation technique. Renewable Energy 114, 166-179.

Rogers, W. E., Thomson, J., Shen, H. H., Doble, M. J., Wadhams, P., and Cheng, S. (2016). Dissipation of wind waves by pancake and frazil ice in the autumn beaufort sea. Journal of Geophysical Research: Oceans, 121 (11), 7991–8007

Rogers, W.E., Babanin, A.V., and Wang, D.W. (2012). Observation-consistent input and whitecapping-dissipation in a model for wind-generated surface waves: Description and simple calculations. Journal of Atmospheric and Oceanic Technology, 29(9), 1329-1346

Rousset C, Vancoppenolle M, Madec G, et al. (2015). The Louvain-La-Neuve sea ice model LIM3. 6: global and regional capabilities[J]. Geoscientific Model Development, 2015, 8(10): 2991-3005.

Rueda, A., Vitousek, S., Camus, P., Tomás, A., Espejo, A., Losada, I.J., Barnard, P.L., Erikson, L.H., Ruggiero, P., Reguero, B.G., Mendez, F.J., (2017). A global classification of coastal flood hazard climates associated with large-scale oceanographic forcing. Scientific Reports | 7: 5038 | DOI:10.1038/s41598-017-05090-w.

Rychlik, I. (2015). Spatio-temporal model for wind speed variability. Annales de l'ISUP, Vol. 59, pp. 25-55.

Saket, A., Peirson, W. L., Banner, M. L., Barthelemy, X. & Allis, M. J. (2016). On the Threshold for Wave Breaking of Two-Dimensional Deep Water Wave Groups in the Absence and Presence of Wind. Journal of Fluid Mechanics, 811, 642-658.

Salmon, J.E., Holthuijsen, L.H., Zijlema, M., van Vledder, G.Ph., and Pietrzak, J.D. (2015). Scaling depth-induced wave-breaking in two-dimensional spectral wave models. Ocean Modelling 87 (2015) 30–47

Samiksha, S.V., Polnikov, V.G., Vethamony, P., Rashmi, R., Pogarsk, F., Sudheesh, K., (2015). Verification of model wave heights with long-term moored buoy data: Application to wave field over the Indian Ocean. Ocean Engineering 104, 469–479.

Sánchez, A.S., Rodrigues, D.A., Fontes, R.M., Martins, M.F., Kalid, R.A., Torres, E.A., (2017). Wave resource characterization through in-situ measurement followed by artificial neural networks' modeling. Renewable Energy, doi: 10.1016/j.renene.2017.09.032 .

Sandhya, K G., Remya, P.G., Balakrishnan Nair, T.M., Arun, N., (2016), On the co-existence of high energy low frequency waves and locally generated cyclone waves off the Indian east coast, Ocean Engineering 111 (2016) 148-154.

Sartini, L., Besio, G., Cassola, F., (2017). Spatio-temporal modelling of extreme wave heights in the Mediterranean Sea. Ocean Modelling 117, 52–69.

Sartini, L., Mentaschi, L., Besio, G., (2015). Comparing different extreme wave analysis models for wave climate assessment along the Italian coast. Coastal Eng., 100, 37–47.

Sasa, K. (2017). Optimal Routing of Short-Distance Ferry from the Evaluation of Mooring Criteria, Int. Conf. on Offshore Mech. & Arctic Eng. (OMAE), June 25-30, Trondheim, Norway.

Sayeed, T. et al. (2017). A review of iceberg and bergy bit hydrodynamic interaction with offshore structures. Cold Regions Science and Technology, 135, pp. 34-50.

Sayeed, T. M. et al. (2015). Experimental Investigation of Ice Mass Hydrodynamic Interaction with Offshore Structure in Close Proximity. In: International Conference on Offshore Mechanics and Arctic Engineering. St. John's, Newfoundland: ASME.

Scanlon, B., O. Breivik, J. –R. Bidlot, P.A. Janssen, E. M., Callaghan, A.H., Ward, B. (2016). Modeling Whitecap Fraction with a Wave Model. Journal of Physical Oceanograpy, 46, 887-894

Schmittner, C., Brouwer, J. and Henning, J., (2014). Application of focusing wave groups in model testing practice, In: Proc. of the 33rd Int. Conf. on Ocean, Offshore and Arctic Eng. (OMAE). ASME Paper OMAE2014-23949.

Scibilia, F. et al. (2014). Full-Scale Trials and Numerical Modeling of Sea Ice Management in the Greenland Sea. In: Arctic Technology Conference. Houston, Texas: Offshore Technology Conference.

Scott, T., Austin, M., Masselink, G. & Russell, P. (2016) Dynamics of rip currents associated with groynes—field measurements, modelling and implications for beach safety. Coastal Engineering, 2016, 107: 53-69.

Seemanth, M., Bhowmick, S.A., Kumar, R., Sharma, R., (2016). Sensitivity analysis of dissipation parameterizations in a third-generation spectral wave model, WAVEWATCH III for Indian Ocean. Ocean Engineering 124, 252–273.

Seiffert, B. & Ducrozet, G. (2016). Deep Water Wave-Breaking in a High-Order Spectral Model. 31th Intl Workshop on Water Waves and Floating Bodies. Plymouth, United States.

Seiffert, B. & Ducrozet, G. (2017). A Comparative Study of Wave Breaking Models in a High-Order Spectral Model. the ASME 2017 36th international Conference on Ocean, offshore and Arctic Engineering (OMAE). Trondheim, Norway.

Sepulveda, H.H., Queffeulou, P., Ardhuin, F., (2015). Assessment of SARAL AltiKa wave height measurements relative to buoy, Jason-2 and Cryosat-2 data. Marine Geodesy, 38 (S1),449-465, doi: 10.1080/01490419.2014.1000470. Report available at

Seyffert, H.C., Kim, D.-H., Troesch, A.W., (2016). Rare wave groups. Ocean Engineering 122, 241–252.

Shanas, P.R., Aboobacker, V.M., Albarakati, A.M.A., Zubier, K.M. (2017). Superimposed wind-waves in the Red Sea. Ocean Engineering, volume 138, 2017, pages 9-22.

Shu L, Liang J, Hu Q, et al. (2017). Study on small wind turbine icing and its performance[J]. Cold Regions Science and Technology, 2017, 134: 11-19.

Shu Q, Song Z, Qiao F. (2015). Assessment of sea ice simulations in the CMIP5 models[J]. The Cryosphere, 2015, 9(1): 399-409.

Shun-qi Pan, Yang-ming Fan, Jia-ming Chen, Chia-chuen Kao (2016). Optimization of multi-model ensemble forecasting of typhoon waves. Water Science and Engineering, volume 9, issue 1, 2016, pages 52-57.

Siadatmousavi, S.M., Jose, F., Silva, G.M., (2016). Sensitivity of a third generation wave model to wind and boundary condition sources and model physics: A case study from the South Atlantic Ocean off Brazil coast. Computers & Geosciences 90, 57–65.

Simonsen, H.M.; Larsson, E. ; Mao, W., and Ringsberg, J.W. (2015). State-of-the-art within ship weather routing, Proceedings of the ASME Thirty-fourth International Conference on Ocean, Offshore and Arctic Engineering (OMAE2015) in St John's, Newfoundland and Labrador, Canada, May 31-June 5, 2015.. p. 11(pp.).

Skoglund, L., Kuttenkeuler, J., Rosen, A., Ovegard, E., (2015). A comparative study of deterministic and esemble weather forecasts for weather routing, Journal of Marine Science Technology (2015) 29:429-441

Smith, G., Babanin, A.V., Riedel, P., Young, I.R., Oliver, S., and Hubbert, G. (2011). Introduction of a new friction routine into the SWAN model that evaluates roughness due to bedform and sediment size changes. Coastal Engineering, 58, 317-326

Smith, R.K., and Montgomery, M.T. (2014). On the existence of the logarithmic surface layer in the inner core of hurricanes. Q. J. R. Meteorol. Soc., 140, 72–81, DOI:10.1002/qj.2121

Song M, Kim E, Amdahl J. (2015). Fluid-structure-interaction analysis of an ice block-structure collision[C]//Proceedings of the International Conference on Port and Ocean Engineering Under Arctic Conditions. 2015.

Staneva, S., Alari, V., Breivik, Ø, Bidlot, J.-R. & Mogensen, K. (2016). Effects of wave-induced forcing on a circulation model of the North Sea. Ocean Dynamics, DOI 10.1007/s10236-016-1009-0

Stansberg, C.T., Frechou, D., Henn, R., Hennig, J., Bouvy, A., Borleteau, J-P., Ollivier M. and Ran, H. (2009). 3D Structures in wave elevation patterns, Proc. 1st Int. Conf. on Adv. Model Meas. Techn. for the EU Maritime Ind. (AMT '09), 1 - 2 Sep, Nantes, France.

Stansberg, C.T., Frechou, D., Henn, R., Hennig, J., Bouvy, A., Borleteau, J-P., Ollivier M. and Ran, H. (2011). Investigation of techniques for 3d wave surface measurements and analysis, Proc. 2nd Int. Conf. on Adv. Model Meas. Techn. for the Maritime Ind., (AMT'11), 4 – 6 Apr, Newcastle upon Tyne, UK.

Stefanakos, C. (2016). Fuzzy time series forecasting of nonstationary wind and wave data. Ocean Engineering, 2016, 121: 1-12.

Stefanakos, C.N., Vanem, E., (2017). Climatic forecasting of wind and waves using fuzzy inference systems. Proceedings of the ASME 2017 36th International Conference on Ocean, Offshore and Arctic Engineering OMAE2017.

Stoney, L., Walsh, K., Babanin, A.V., Ghantous, M., Govekar, P. and Young, I.R. (2017). Simulated ocean response to tropical cyclones: The effect of a novel parameterization of mixing from unbroken surface waves. Journal of Advances in Modeling Earth Systems, 9, doi:10.1002/2016MS000878, 22p

Stopa, J.E., Ardhuin, F., Babanin, A., Ziege, S., (2016). Comparison and validation of physical wave parameterizations in spectral wave models. Ocean Modelling 103, 2–17.

Stroeve J, Notz D. (2015). Insights on past and future sea-ice evolution from combining observations and models[J]. Global and Planetary Change, 2015, 135: 119-132.

Struthi, C., Sriram. V. (2017). Wave impact load on jacket structure in intermediate water depth. Ocean Engineering, volume 140, 2017, pages 183-194.

Stuckey, P. et al. (2016). Modelling Iceberg-Topsides Impacts Using High Resolution Iceberg Profiles. In: Arctic Technology Conference. St. John's, Newfoundland: Offshore Technology Conference.

Sulis, A., Cozza, R., Annis, A., (2017). Extreme wave analysis methods in the gulf of Cagliari (South Sardinia,Italy). Ocean & Coastal Management 140, 79-87.

Suzuki, N., and Fox-Kemper B. (2016). Understanding Stokes forces in the wave-averaged equations, J. Geophys. Res. Oceans, 121, 3579–3596, doi:10.1002/2015JC011566

Tagliaferri, F., Viola, I. M., Flay, R. G. J., (2015). Wind direction forecasting with artificial neural networks and support vector machines. Ocean Engineering, 97, pp.65-73.

Takagi, K., Hamamichi, S., Wada, R., Sakurai, Y., (2017). Prediction of wave time-history using multipoint measurements. Ocean Engineering 140, 412–418.

Tamaru, H. (2016) About the Optimum Route by the Weather Routing, JASNAOE Annual Autum Meeting, 2016, JASNAOE.

Thomson, J., and Rogers, W. E. (2014). Swell and sea in the emerging Arctic Ocean, Geophysical Research Letters , 41 (9), 3136–3140, doi:10.1002/ 2014GL059983

Thomson, J., Squire, V., Ackley, S., Roger,s E., Babanin, A., Guest, P., Maksym, T., Wadhams, P., Stammerjohn, S., Fairall, C., Persson, O., Doble, M., Graber, H., Shen H., Gemmrich, J., Lehner, S., Holt, B., Williams, T., Meylan, M., and Bidlot, J. (2013). Sea State and Boundary Layer Physics of the Emerging Arctic Ocean. Science Plan. Technical Report, APL-UW TR1306, Applied Physical Laboratory, University of Washington, 58p

Toffoli, A., Bennetts, L.G., Meylan, M.H., Cavaliere, C., Alberello, A., Elsnab, J. and Monty, J.P. (2015). Sea ice floes dissipate the energy of steep ocean waves, Geophys. Res. Lett., 42, doi:10.1002/2015GL065937

Toffoli, A., Bitner-Gregersen, E. M., Osborne, A. R., Serio, M., Monbaliu, J. and Onorato, M. (2011). Extreme Waves in Random Crossing Seas: Laboratory Experiments and Numerical Simulations, Geophysical Research Letters, Vol 38, doi: 10.1029/2011.

Tolman H.L., Banner M.L., Kaihatu J.M., (2013). The NOPP operational wave model improvement project. Ocean Modelling, 70, 2–10

Troitskaya, Y., Kandaurov, A., Ermakova, O., Kozlov, D., Sergeev, D. and Zilitinkevich, S. (2017) Bag-breakup fragmentation as the dominant mechanism of sea-spray production in high winds. Nature, 7, 1614, DOI:10.1038/s41598-017-01673-9

Troitskaya, Y., Ezhova, E., Soustova, I. and Zilitinkevich, S. (2016). On the effect of sea spray on the aerodynamic surface drag under severe winds. Ocean Dynamics, 66, 659–669

Trulsen, K. (2017). Rogue Waves in the Ocean, the Role of Modulational Instability, and Abrupt Changes of Environmental Conditions That Can Provoke Non Equilibrium Wave Dynamics. In: Velarde, M. G., Tarakanov, R. Y. & Marchenko, A. V. (Eds.) the Ocean in Motion- Circulation, Waves, Polar Oceanography Springer-Verlag.

Trulsen, K., Nieto Borge, J. C., Gramstad, O., Aouf, L. & Lefèvre, J. M. (2015). Crossing Sea State and Rogue Wave Probability during the Prestige Accident. Journal of Geophysical Research: Oceans, 120, 7113-7136.

Tsai. W.-T., S.-M. Chen, G.-H. Lu, (2015). Numerical Evidence of Turbulence Generated by Nonbreaking Surface Waves. J. Phys. Oceanogr., 45, 174-180

Tsou, M C (2016), Multi target collision avoidance route planning under an ECDIS framework, Ocean engineering 121 (2016) 268-278

Turnbull, I. et al. (2015). Operational iceberg drift forecasting in Northwest Greenland. Cold Regions Science and Technology, 110, pp. 1-18.

Turnbull, I. et al. (2016). Empirical Prediction of Sea Ice Surface Temperature from Surface Meteorological Parameters in Pistolet Bay Northern Newfoundland. In: Arctic Technology Conference. St. John's, Newfoundland: Offshore Technology Conference.

Uiboupin, R. & Laanemets, J. (2015). Upwelling parameters from bias-corrected composite satellite SST maps in the Gulf of Finland (Baltic Sea). IEEE Geoscience & Remote Sensing Letters, 2015, 12(3): 592-596.

Ulbrich, U., Leckebusch, G.C., Pinto, J.G., (2009). Extra-tropical cyclones in the present and future climate: a review. Theor Appl Climatol , 96, 117–131.

Umesh, P. A., Bhaskaran, P. K., Sandhya, K. G., Nair, T. B (2017). An assessment on the impact of wind forcing on simulation and validation of wave spectra at coastal Puducherry, east coast of India. Ocean Engineering, 2017, 139: 14-32.

Utne, I., Sørensen, A., and Schjølberg, I., (2017). Risk Management of Autonomous Marine Systems and Operations, Int. Conf. on Offshore Mech. and Arctic Eng. (OMAE), June 25-30, Trondheim, Norway.

Vanem, E. (2016). Joint statistical models for significant wave height and wave period in a changing climate, Marine Structures, Vol.49, pp.180-205.

Vanem, E., (2017). A regional extreme value analysis of ocean waves in a changing climate. Ocean Engineering 144, 277–295.

Vanem, E., and Bitner-Gregersen, E.M. (2015). Alternative Environmental Contours for Marine Structural Design—A Comparison Study. Journal of Offshore Mechanics and Arctic Engineering, Vol.137, 051601-1.

Varlas, G., Katsafados, P., Papadopoulos, A., Korres, G., (2017). Implementation of a two-way coupled atmosphere-ocean wave modeling system for assessing air-sea interaction over the Mediterranean Sea. Atmospheric Research xxx, xxx–xxx.

Veltcheva, A., Guedes Soares, C., (2016). Analysis of wave groups by wave envelope-phase and the Hilbert Huang transform methods. Applied Ocean Research 60, 176–184.

Veltcheva, A., Guedes Soares, C., (2016). Nonlinearity of abnormal waves by the Hilbert–Huang Transform method. Ocean Engineering 115, 30–38.

Vettor, R and Soares, C G (2016). Development of a ship weather routing system, Ocean Engineering 123 (2016) 1-14

Victor A. Godoi, Karin R. Bryan, Scott A. Stephens, Richard M. Gorman. (2017). Extreme waves in New Zealand waters. Ocean Modelling, 2017.

Walsh, K.J.E., Govekar, P., Babanin, A.V., Ghantous, M., Spence, P., and Scoccimarro, E. (2017). The effect on simulated ocean climate of a parameterization of unbroken wave-induced mixing incorporated into the k-epsilon mixing scheme. Journal of Advances in Modeling Earth Systems, 9, 735-758, doi:10.1002/2016MS000707

Wang, C., Zhang, H., Feng, K. R., Li, Q. W. (2017). A simple gradient wind field model for translating tropical cyclones. Natural Hazards, 2017, 88(1): 651-658.

Wang, H., Mao, W., and Eriksson, L. (2017). Benchmark study of five optimization algorithm for weather routing, Proceedings of the ASME 2017 36th Int. Conference on Ocean, Offshore and Arctic Engineering, OMAE2017, June 25 - 30, 2017, Trondheim, Norway.

Wang, J. et al. (2016). Ice Model Tests for Dynamic Positioning Vessel in Managed Ice. In: Arctic Technology Conf.. St. John's, Newfoundland: Offshore Technology Conference.

Wang, L., Liang, B., Li, H., (2017). A new non-parametric correction model and its applications to hindcasting wave data. Ocean Engineering 132, 11–24.

Wang, S., Zhang, H. D. & Guedes Soares, C. (2016). Slamming Occurrence for A Chemical Tanker Advancing in Extreme Waves Modelled With the Nonlinear Schrödinger Equation. Ocean Engineering, 119, 135-142.

Wang, X. X., Wan, R., Zhao, F. F., Huang, L. Y., Sun, P. & Tang, Y. L. (2016). Comparative study of dynamics of gravity cages with different meshes in waves and current. Proceedings of the OMEA 2016 Conference, 19-24 June 2016 Busan, South Korea.

Wang, Y. & Zou, Z. L. (2015). An experimental and numerical study of bimodal velocity profile of longshore currents over mild-slope barred beaches. Ocean Engineering, 2015, 106: 415-423.

Wang, Y. et al. (2015). A Method of Above-water Iceberg 3D Modelling Using Surface Imaging. In: International Ocean and Polar Engineering Conference. Kona, Big Island, Hawaii: International Society of Offshore and Polar Engineers, pp. 1706-1712.

Waseda, T., Hallerstig, M., Ozaki, K. & Tomita, H. (2011). Enhanced Freak Wave Occurrence With Narrow Directional Spectrum in the North Sea. Geophysical Research Letters, 38, N/A-N/A.

WAVEWATCH III® Development Group, The 2016 User manual and system documentation of WAVEWATCH III® version 5.16. Tech. Note 329, NOAA/NWS/NCEP/MMAB, College Park, MD, USA, 326p

Way, B., Khan, F., and Veitch, B., (2015). The Northern Sea Route vs. the Suez Canal Route – an Economic Analysis Incorporating Probabilistic Simulation Optimization of Vessel Speed, Int. Conf. on Offshore Mech. and Arctic Eng. (OMAE), May 31-June 5, St. John's, Canada.

Weisse R., Bisling P., Gaslikova L., Geyer B., Groll N., Hortamani M., Matthias V., Maneke M., Meinke I., Meyer E.M., Schwichtenberg F., Stempinski F., Wiese F. and Wöckner-Kluwe K. (2015). Climate services for marine applications in Europe, Earth Perspectives Vol.2(3), DOI 10.1186/s40322-015-0029-0.

Wen, X., and Mobbs, S. (2014). Numerical Simulations of Laminar Air–Water Flow of a Non-linear ProgressiveWave at Low Wind Speed. Boundary-Layer Meteorol., 150, 381–398

Wen, X., and Mobbs, S. (2015). Numerical Simulations of Air–Water Flow of a Non-linear Progressive Wave in an Opposing Wind. Boundary-Layer Meteorol., 156, 91–112

West, B. J., Brueckner, K. A., Janda, R. S., Milder, D. M. & Milton, R. L. (1987). A New Numerical Method for Surface Hydrodynamics. J. Geophys. Res., 92, 11803-11824.

Wijaya, A. P. (2017). Dynamic averaging method to detect sea surface current from radar images. Proc. of the OMAE 2017 Conference, 25-30 June 2017 Trondheim, Norway.

Wimmer, W., Challenor, P., Retzler, C., (2016). Extreme wave heights in the North Atlantic from Altimeter Data. Renewable Energy 31, 241–248.

Xiao, D., Fang, F., Pain, C. C. & Navon, I. M. (2017). Towards non-intrusive reduced order 3D free surface flow modelling. Ocean Engineering, 2017, 140: 155-168.

Xiao, W., Liu, Y., Wu, G. & Yue, D. K. P. (2013). Rogue Wave Occurrence and Dynamics By Direct Simulations of Nonlinear Wave-Field Evolution. J. Fluid Mech., 720, 357-392.

Xie, Z., (2016). Numerical modelling of wind effects on breaking waves in the surf zone. Ocean Dynamics, 67, 1251–1261

Xu, H. H. & Lin, P. Z. (2017). A new two-step projection method in an ISPH model for free surface flow computations. Coastal Engineering, 2017, 127: 68-79.

Yaakob, O., Hashim, F.E., Omar, K.M., Md Din, A.H., Koh, K.K., (2016). Satellite-based wave data and wave energy resource assessment for South China Sea. Renewable Energy 88, 359-371.

Yablonsky, R. M., Ginis, I., Thomas, B., Tallapragada, V., Sheinin, D. and Bernardet, L. (2015). Description and analysis of the ocean component of NOAA's operational

hurricane weather research and forecasting (HWRF) model. J. Atmos. Oceanic Technol., 32, 144–163

Yang, C.-S. and Ouchi, K. (2017). Application of Velocity Bunching Model to Estimate Wave Height of Ocean Waves Using Multiple Synthetic Aperture Radar Data, J. of Coastal Res, Vol 79(Sp1), pp. 94–98. doi: 10.2112/SI79-020.1.

Yang, D., Pettersen, B., Xiong, Y. L. (2016). Interactions between two flat plates at different positions in a current. Ocean Engineering, 2016, 119: 75-85.

Yang, L., Zhou, X., Mertikas, S.P., Zhu, L., Yang, L., Lei, N., (2017). First calibration results of Jason-2 and SARAL/AltiKa satellite altimeters from the Qianli Yan permanent Cal/Val facilities, China. Advances in Space Research 59, 2831–2842.

Yang, Y., Irish, J. L., Socolofsky, S. A. (2015). Numerical investigation of wave-induced flow in mound–channel wetland systems. Coastal Engineering, 2015, 102: 1-12.

Yim, S. C., Osborne, A. R. & Mohtat, A. (2017). Nonlinear Ocean Wave Models and Laboratory Simulation of High Seastates and Rogue Waves. ASME 2017 36th Int. Conference on Ocean, offshore and Arctic Engineering. Trondheim, Norway.

Yin, K., Xu, S., Huang, W., Xie, Y. (2017). Effects of sea level rise and typhoon intensity on storm surge and waves in Pearl River Estuary. Ocean Engineering, volume 136, 2017, pages 80-93.

Younan, A. et al. (2016). Overview of the 2012 Iceberg Profiling Program. In: Arctic Technology Conference. St. John's, Newfoundland: Offshore Technology Conference.

Young, I.R., Babanin, A.V., and Zieger, S. (2011a). Response to Comment on "Global trends in wind speed and wave height". Science, 334, 166-167

Young, I.R., Babanin, A.V., and Zieger, S. (2013). The decay rate of ocean swell observed by altimeter. Journal of Physical Oceanography, 43, 2322-2333

Young, I.R., Sanina, E., and Babanin, A.V. (2017). Calibration and cross-validation of a global wind and wave database of Altimeter, Radiometer and Scatterometer measurements. J. of Atmospheric and Oceanic Technology, 34, 1285-1306, doi:10.1175/JTECH-D-16-0145

Young, I.R., Vinoth, J., (2013). An "extended fetch" model for the spatial distribution of tropical cyclone wind–waves as observed by altimeter. Ocean Engineering 70, 14–24.

Young, I.R., Zieger, S., and Babanin, A.V. (2011b). Global trends in wind speed and wave height. Science, 332, 451-455

Yu B, Karr D G, Song H, et al. (2016). A surface ice module for wind turbine dynamic response simulation using FAST[J]. Journal of Offshore Mechanics and Arctic Engineering, 2016, 138(5): 051501.

Zakharov, V. E. (1968). Stability of Periodic Waves of Finite Amplitude on the Surface of a Deep Fluid. Journal of Applied Mechanics and Technical Physics, 9, 190-194.

Zambon, J. B., He, R., and Warner, J. C. (2014). Investigation of hurricane Ivan using the coupled ocean-atmosphere-wave-sediment transport (COAWST) model, Ocean Dyn., 64, 1535–1554, doi:10.1007/s10236-014-0777-7.

Zhang, H.Q., Nie B.C. (2016). Modelling windwave driven by typhoon Chan-Hom (201509) in the East China Sea. Theoretical & Applied Mechanics Letters, volume 6, 2016, pages 297-301.

Zhang, Q., Zhou, X. L. & Wang, J. H. (2017). Numerical investigation of local scour around three adjacent piles with different arrangements under current. Ocean Engineering, 2017, 142: 625-638.

Zhantao Zhuo, Shinji Sato (2015). Characteristics of wave grouping and freak wave observed by two typhoons. Procedia Engineering, volume 116, 2015, pages 277-284.

Zhao, X., and Shen, H. (2016). A diffusion approximation for ocean wave scatterings by randomly distributed ice floes. Ocean Modelling, 107, 21–27

Zhe Hu, Hongxiang Xue, Wenyong Tang, Xiaoying Zhang. (2015). A combined wave-dam-breaking model for rogue wave overtopping. Ocean Engineering, volume 104, 2015, pages 77-88.

Zhe Hu, Wenyong Tang, Hongxinag Xue, Xiaoying Zhang, Kunpeng Wang. (2017). Numerical Study of rogue wave overtopping with a fully-coupled fluid-structure interaction model. Ocean Engineering, volume 137, 2017, pages 48-58.

Zheng, J., Sang S., Wang J., Zhou C., Zhao H. (2017). Numerical simulation of typhoon-induced storm surge along Jiangsu coast, Part I: Analysis of tropical cyclone. Water Science and Engineering, volume 10, issue 1, 2017, pages 2-7.

Zhilin Sun, Senjun Huang, Hui NIe, Jiange Jiao, Saihua Huang, Lili Zhu, Dan Xu. (2015). Risk analysis of seawall overflowed by storm surge during super typhoon. Ocean Engineering, volume 107, 2015, pages 178-185.

Zhou, C., Zheng, J., Zhang, J., Fu, X., (2017). Study on the extreme high water levels and wave heights of different return periods in Laizhou Bay, China. Proceedings of the ASME 2017 36th International Conference on Ocean, Offshore and Arctic Engineering OMAE2017.

Zhou, M. et al. (2014) Working towards seafloor and underwater iceberg mapping with a Slocum glider. In: Autonomous Underwater Vehicles (AUV). Oxford, Mississippi: IEEE.

Zhou, Q. and Peng, H. (2014) Numerical Simulation of a Dynamically Controlled Ship in Level Ice. International Journal of Offshore and Polar Engineering, 24(3), pp. 184-191.

Zhu, N., Kim, Y., Kim, K.-H., Shin, B.-S., (2016). Change detection of ocean wave characteristics. Expert Systems With Applications 51, 245–258.

Zhuo, Z., Sato, S., (2015). Characteristics of Wave Grouping and Freak Wave Observed by Two Typhoons. Procedia Engineering 116, 277 – 284. 8th International Conference on Asian and Pacific Coasts (APAC 2015).

Zieger, S., Babanin, A.V., Rogers, W.E., and Young, I.R. (2015). Observations-based input and dissipation terms for WAVEWATCH III. Ocean Modelling, 96(1), 2-25, http://dx.doi.org/10.1016/j.ocemod.2015.07.014

This page intentionally left blank

Proceedings of the 20th International Ship and Offshore Structures Congress (ISSC 2018) Volume I – M.L. Kaminski and P. Rigo (Eds.)

doi:10.3233/978-1-61499-862-4-101

COMMITTEE I.2

LOADS

COMMITTEE MANDATE

Concern for the environmental and operational loads from waves, wind, current, ice, slamming, sloshing, green water, weight distribution and any other operational factors. Consideration shall be given to deterministic and statistical load predictions based on model experiments, full-scale measurements and theoretical methods. Uncertainties in load estimations shall be highlighted. The committee is encouraged to cooperate with the corresponding ITTC committee.

AUTHORS/COMMITTEE MEMBERS

Chairman: Dr. Yoshitaka Ogawa, *Japan*
Dr. Wei Bai, *UK*
Dr. Guillaume de Hauteclocque, *France*
Dr. Sharad Dhavalikar, *India*
Prof. Chih-Chung Fang, *China (Taiwan)*
Dr. Nuno Fonseca, *Norway*
Dr. Satu Hänninen, *Finland*
Dr. Thomas B. Johannessen, *Norway*
Ms. Van Lien, *USA*
Prof. Celso Morooka, *Brazil*
Dipl.-Ing. Holger Mumm, *Germany*
Prof. Jasna Prpic-Orsic, *Croatia*
Dr. Kang Hyun Song, *Korea*
Dr. Chao Tian, *China*
Prof. Bahadır Uğurlu, *Turkey*
Dr. Sue Wang, *USA*

KEYWORDS

Wave induced loads, Hydroelasticity, Slamming, Whipping, Sloshing, Green water, Loads due to collision and grounding, Vortex induced vibrations, Vortex induced motions, Mooring system, Lifting operation, Floating offshore wind turbines, Probabilistic method, Design waves, Cables/risers, Fatigue, Uncertainty analysis.

CONTENTS

1. INTRODUCTION 103

2. COMPUTATION OF WAVE-INDUCED LOADS 103
   2.1 Zero-Speed Case 104
      2.1.1 Body-wave interactions 104
      2.1.2 Body-wave-current interactions 105
      2.1.3 Multibody interactions 106
   2.2 Forward-Speed Case 108
   2.3 Hydroelasticity Methods 111
      2.3.1 Hydroelasticity methods of ships 111
      2.3.2 Hydroelasticity methods of VLFS 113

3. SHIP STRUCTURES - SPECIALIST TOPICS 113
   3.1 Slamming and Whipping 113
   3.2 Sloshing 116
      3.2.1 Introduction 116
      3.2.2 Experimental Investigations 116
      3.2.3 Numerical Simulation 117
      3.2.4 Sloshing Suppression 118
      3.2.5 Sloshing and Ship Motions 119
   3.3 Green Water 121
   3.4 Experimental and Full Scale Measurements 122
   3.5 Loads due to Damage following Collision / Grounding 124

4. OFFSHORE STRUCTURES - SPECIALIST TOPICS 125
   4.1 Vortex-induced vibrations (VIV) and Vortex-induced motions (VIM) 125
      4.1.1 VIV 125
      4.1.2 VIM 128
   4.2 Mooring Systems 130
   4.3 Lifting operations 133
   4.4 Wave-in-deck loads 135
   4.5 Floating Offshore Wind Turbines 137

5. PROBABILISTIC MODELLING OF LOADS ON SHIPS 139
   5.1 Probabilistic Methods 139
   5.2 Equivalent Design Waves 141
   5.3 Design Load Cases and Ultimate Strength 142

6. FATIGUE LOADS FOR SHIPS 144

7. UNCERTAINTY ANALYSIS 147
   7.1 Load uncertainties 147
   7.2 Uncertainties in Loading conditions 148
   7.3 Uncertainties due to operational factor 149

8. CONCLUSIONS 149

REFERENCES 151

1. INTRODUCTION

The content of this committee's report is composed in accordance with its mandate by the expertise of its membership. Its structure and content follow along similar lines to those adopted in previous ISSC reports, that is ISSC2012, ISSC2015 and so forth. Wave-induced loads on ships are reviewed in two different sections, namely 2 and 3. Section 2 focuses on two-dimensional(2D) and three-dimensional(3D) methods, dealing with linear and nonlinear methods and including applications of the so called CFD (Computational Fluid Dynamics) methods. Section 3 reviews specialist topics such as slamming, whipping, sloshing and green water loads as well as loads due to damage following collision and grounding. Wave-induced loads on offshore structures are reviewed in section 2 and 4, the former dealing with single and multi-body interactions, including a note on the effects of current and bathymetry. On the other hand, section 4 focuses on specialist topics, such as vortex-induced vibrations (VIV), vortex-induced motions (VIM), cables and risers, offshore lifting, offshore installation, submersibles and floating offshore wind turbines. Continuing from previous reports, in section 6 and 7, current state of progress in probabilistic approach of loads on ship including short-term and long-term predictions and fatigue loads is examined focusing on applications to ships and offshore structures. Finally, uncertainties in experimental and full-scale measurements and computational methods are discussed in section 7.

2. COMPUTATION OF WAVE-INDUCED LOADS

In recent years, the trend for further development and enhancement of numerical methods for the computation of wave loads continued, with new technological challenges of the marine industry setting the focus areas. Developments included the computation of wave loads acting on floating structures and vessels advancing in sea way as well as methods to account for hydroelastic phenomena and violent hydrodynamic loads.

For stationary floating bodies, progress was made regarding loads from steep non-linear waves, the impact of wave-current interaction and various multi body interaction problems, as encountered during offloading operations between FPSO and shuttle tanker or crane operations with heavy cargo in seaway, for instance.

Safety concerns regarding manoeuvrability triggered research on the wave loads acting on low powered vessels operating in severe sea states, but also the loads on vessels advancing at design speed through waves remained of great interest in recent years. Several benchmark studies on sea keeping calculation codes have been carried out, illustrating the need to identify the most suitable code for the given ship form and operation speed profile. In this context strip theories have been extended for more accurate predictions of wave sagging moments, including 2D+T approaches for higher ship speeds. The enhancement of 3D potential theory methods continued to be of great interest too, being true for Green function based approaches and Rankine methods.

RANS methods become increasingly popular, however due to excessive computational cost in comparison with strip and panel methods they are still reserved for niche applications, e.g. nonlinear excitation of springing vibration or green water phenomena.

Although not directly related to wave loads, work on added resistance in waves is discussed in this section too, since such work provides improved understanding of involuntary speed reduction and hence, more realistic assumptions regarding ship speeds in adverse weather conditions.

Also the investigation of hydroelastic effects continued to be of great interest in recent years and thus new publications on the hydroelastic response of ships and Very Large Floating Structures (VLFS) in waves are discussed in this section too.

2.1 Zero-Speed Case

2.1.1 Body-wave interactions

A time-domain 3D Rankine panel method based on a simplified variant of the mixed Eulerian–Lagrangian (MEL) scheme is developed by T. Shivaji and D. Sen (2015) for studying steep nonlinear waves interacting with ship shape body and offshore configurations at zero speed. One of the important numerical problems of an MEL-type time-domain solution scheme for the full nonlinear floating body problem is associated with the coupling between hydrodynamic forces and rigid body motions which tend to cause numerical instability inhibiting long-duration time-domain simulation. Improved numerical schemes such as the acceleration potential method of Tanizawa (1995, 1996), the implicit coupled scheme of Dombre et al. (2015) have been devised to handle this coupling. In the work presented by T. Shivaji and D. Sen (2015) a method similar to acceleration potential with the linearization of diffraction and radiation potentials is devised. This makes the implementation different and simpler compared to original method of Tanizawa (1995, 1996). This method enables to produce very long-duration simulation results. In this work (1) a fully linear formulation where all external forces are computed on the mean wetted surface, and (2) an approximate nonlinear computation where the hydrodynamic interaction forces (diffraction and radiation forces) are determined on the mean surface and the forces arising from the incident steep waves and hydrostatic restoring forces are determined based upon the exact wetted surface under the nonlinear incident wave. Numerical computations for three realistic marine structures, the barge, the S175 hull, and the semisubmersible are presented. The linear computations for which very long duration simulations are achievable from the presented method are validated against results from other available methods. It is found that the nonlinearities of the forces and motions are strongly dependent on the above water hull geometry. Compared to a small water-plane area hull (the semisubmersible), or a wall-sided hull (the barge), a flared hull (S175) results in pronounced nonlinear features in the forces and motion time-histories. The method is developed for stationary floating bodies undergoing oscillation about their mean location, thus not suitable for freely drifting body.

When the ship operates in adverse weather conditions, drift forces play major role with respect to the manoeuvrability of the vessel. As such to address the minimum power requirement of IMO, extensive experimental and numerical investigations were carried out in the EU SHOPERA project (Potthoff, R and Moctar, B, 2016). Post Panamax 14000 TEU container ship DTC used for benchmarking of drift forces in SHOPERA was used by Cong Liu et al (2017) for numerical computations of drift loads. These computations are based on volume of fluid (VOF) and overset mesh methods, discretized by finite volume method (FVM). Problem is treated as a zero forward speed case. NAOE-FOAM-SJTU solver, developed under the framework of the open source OpenFOAM was utilized for this study. An open source library waves2Foam is imposed in this solver to handle the wave problem. Seven wave conditions with a wide range of incident angle are considered. The wavelength is in the range of short waves. The prediction of wave drift forces agrees well with the measurements. The maximum value of longitudinal drift forces is captured at the heading angle of 60° in numerical computations which is in-line with the EFD. The peak value of transverse drift computed is for the case of 90° which is also in accordance with the EFD. However, the under prediction of this value is attributed towards the geometry simplification (absence of bilge keel in numerical model) and strong nonlinear effects (wave breaking) when wave crest hits port (or starboard) side. The time history curves of drift forces illustrate that nonlinear behaviour is more notable when the incident wave is from the bow. The FFT results of drift forces explain that the natural frequency of roll plays a significant role in these time history curves. All these curves fluctuating within the frequency of waves and the FFT results show that only the wave frequency dominates these motions. Basic ability to deal with the maneuverability in waves is achieved through this work.

Arbitrary Lagrangian Eulerian (ALE) formulation is used for tracing markers on free surface as well as wave-body intersections. The feature of ALE is that complex mesh is generated only once at the beginning and fluid marker is moved along prescribed path at all other time steps. Since the prescribed path for each marker is equidistantly arranged, at any instant, the relative positions of adjacent markers are well maintained, and thus good mesh quality can be ensured throughout the computation. In order to trace the exact wave-body intersections i.e. waterline, the marker (intersection) is enforced to move along cross section line of body surface, which can take into account complex body geometry above still waterline.

Zhang and Kashiwagi (2017) studied interactions between water waves and non-wall-sided surface using fully nonlinear potential theory based on ALE formulation. In this computation, HOBEM and 4th-order Runge-Kutta method are adopted as initial boundary value problem (IBVP) solver. For improving computational efficiency, the total velocity potential is split into incident wave component and disturbed one. Diffraction of nonlinear waves by non-wall-sided surface is studied and validated with the example of a circular cylinder. Because the prescribed path is well organized in space, good mesh quality is ensured even though the body has complex geometry. To prove capacity of this scheme, nonlinear wave diffraction by ship geometry is also studied and results show good agreement with experimental results.

2.1.2 Body-wave-current interactions

Station keeping analysis is an important activity in the design of any vessel/DP system that eventually determines the machinery and thruster configuration and thruster size selection. In order to obtain reliable results, it is crucial to apply engineering tools that realistically represent the flow physics and resulting hydrodynamic forces. Present computer tools are based on the assumption that wave drift and current forces can be superimposed. However, there are also mutual interaction effects between waves, current and hulls that should be accounted for in the evaluation of the wave drift forces.

In MULDIF, a 3D diffraction/radiation panel code developed by SINTEF Ocean (Sprenger et al 2017) within the framework of a JIP, wave-current-body interaction is taken into consideration by a new potential flow numerical model. A case study with offshore vessels and general cargo ships of different main dimensions has been performed to assess the capabilities of MULDIF for station keeping purposes in wave and current environments. The first-order vessel motions as well as mean second-order drift forces for zero forward speed without current have been calculated. Through an interface to SINTEF Ocean's vessel response code VERES, viscous roll damping due to hull-water friction, flow separation at bilge keels, lift effects as well as normal forces acting on bilge keels and hull pressure created by the presence of bilge keels is included. Thus, realistic roll response is obtained. Roll reduction tank effects are considered through the external damping matrix. Model tests for the selected vessels have been performed in SINTEF's Ocean Basin in a soft-mooring arrangement in different irregular sea states and headings in deep water. The models were equipped with two two-component force transducers, measuring the x- and y- components of the forces. The yaw moments have been calculated from the y-force measurements. In order to measure the vessel motions in six degrees of freedom, an optoelectronic position measuring system has been used.

The verification and validation of the wave-current interaction effects on first order motions and mean second order drift forces using MULDIF has been published earlier by Stansberg et al (2013) and Hermundstad et al (2016) for various types of bodies. Based on the results of the case study performed for the two offshore vessel hulls (Sprenger et al, 2017), it is concluded that it is important to consider the effect of wave-current interaction in the early design phase. First order motions are influenced by the presence of currents, this effect is increasing with increasing current velocity and decreasing vessel size. A stronger impact of wave-current interaction is observed for mean second order wave drift forces and yaw moments. With increasing current velocities, wave-current interaction effects lead to higher loads, especially in

sea states with lower peak periods. For higher current velocities above 1.5 m/s, the loads calculated with interaction effects are dropping again below the values that are calculated without wave-current interaction. The total forces without wave-current interaction are not conservative but lower compared to the results with interaction effects over a wide range of peak periods. Total mean longitudinal forces without wave current interaction are up to 35% lower for some sea states.

More research is necessary in this area to get insight of wave-current interaction. The most relevant task is to extend the validation of the wave-current interaction effects on first order motions and mean second order wave loads on ship type floating bodies. Such an experimental and numerical study should cover a variety of combinations of current angles and wave headings. To establish a more realistic numerical model, the actual current coefficients for the hulls should be determined, e.g. by CFD, and applied in the validation study instead of generic coefficients.

2.1.3 Multibody interactions

Multiple floating structures are widely used in different areas of marine operations. During offshore installation and underway replenishment, two vessels are side by side positioned in close proximity. When two vessels are moored side-by-side with a narrow gap between them, intense free surface motions may be excited in the gap as a result of complex hydrodynamic interactions. These influence motions of the vessels and forces in mooring lines. Higher wave elevations in between two floating vessels stand as a hindrance in operations like offloading. A configuration with minimum wave elevation is recommended for these reasons.

The computational scheme of 3D MEL developed by T. Shivaji and D. Sen (2015) based on a numerical tank approach for interaction of large-amplitude waves with a single floating body is extended to the problem of wave-interaction with multiple floating bodies (Shivaji Ganesan and D. Sen, 2016). The coupled system of two side-by-side fixed and/or floating bodies interacting with a large amplitude nonlinear wave is studied using a direct time domain solution method. The numerical scheme is implemented over a time-invariant boundary surface to solve the boundary value problem for the unknown velocity potentials. A 4th order Adams–Bashforth–Moulton scheme is used for time marching of rigid-body motion histories of the individual bodies and evolution of the free-surface including the gap region in which large resonant fluid motions occur. A systematic study has been carried out to evaluate the performance of the developed time domain method in simulating the forces and motions as well as the fluid motion in the gap region between the two body system in various arrangements and in different wave-headings. At first, the computed numerical results have been validated and verified with computational and experimental results available in literature for standard geometries such as vertical truncated cylinders and rectangular boxes. Secondly, effectiveness of the damping lid model which is introduced to suppress wave resonance in the gap region is investigated including its influence on maximum sway forces on fixed and floating rectangular barges in side-by side configurations. Thirdly, comparative studies on absolute and relative motion response for two cases (two rectangular barges, and a FLNG-FPSO + shuttle tanker) in side-by-side arrangement are detailed to bring out the importance of nonlinearities arising due to steep nonlinear incident waves. Finally, coupled motions of the two-body system of an FPSO and a shuttle tanker floating in side-by-side configuration in a steep nonlinear wave field are studied in which the two bodies are connected through hawsers and the FPSO is moored to the ground. Additionally, there is a fender between the two bodies. Developed numerical scheme is suitable for multiple (more than two) body interaction. The effectiveness of damping lid method is highlighted. Importance of nonlinear FK formulation in such problems is revealed.

Seung-Ho Ham et al (2015) have derived a Discrete Euler–Lagrange (DEL) equation to represent the motion of a multi- body system, in which many bodies are connected physically by

joints or wire ropes. By discretizing and re-formulating the traditional Euler–Lagrange equation, authors obtained a discrete time integrator. The integration scheme mixes the Stömer–Verlet method for dynamic equations with the linearly implicit Euler method for constraint equations. The stability and performance issues are dealt with the new formulation. Equations of motions are automatically derived which was the major constraint of similar previous works. It is achieved by defining the equations of joint constraints and their derivatives. In addition, the stretching of the wire rope is mathematically modelled as constraints for stability. Linearized hydrostatic and hydrodynamic forces are used similar with previous works. Authors applied the DEL equation to a mass–spring system with the large spring coefficient. A spring pendulum modelled by a constraint-based wire rope was tested. Despite the large spring coefficient, the DEL equation with the constraint-based wire rope shows relatively stable motion. The automatic formulation was also tested by three-dimensional multiple pendulums. Finally, a floating crane and a heavy load connected by constraint-based wire rope, based on set of regular waves with different wave heights, directions and periods was simulated.

Hyewon Lee et al (2015) dynamically simulated a wireline riser tensioner (WRT) system to analyze the dynamic response of the riser string in a mobile offshore drilling unit (MODU) such as a drilling rig or a drillship. The main function of the WRT system is to sustain the tension to avoid buckling, regardless of the MODU motion. The WRT system consists of a tensioner ring, a wireline, pneumatic cylinders, and air pressure vessels (APVs). It reduces the vertical (heave) motion of the top of the riser string caused by the MODU motion. In this study, the equations of motion of the drilling rig and the WRT system were formulated based on multibody system dynamics. The discrete Euler–Lagrange equation was used to formulate the equations of motion. For the external forces, both the hydrostatic and hydrodynamic forces were considered. Several simulations were performed with various sea states to analyze the motion of the riser string and the efficiency of the WRT system. Furthermore, the gas volume inside the APVs was changed to investigate its impact on the efficiency and performance of the WRT system.

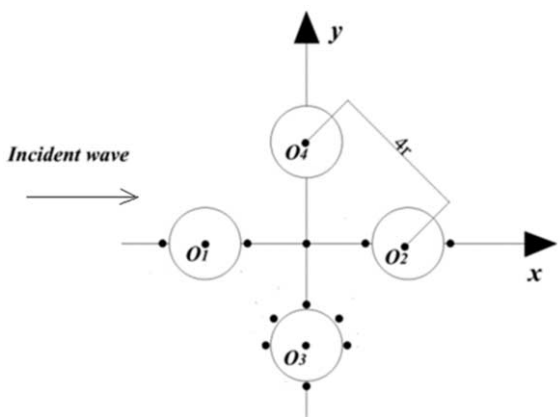

Figure 1: Top view of the arrangement of the four cylinders model, Z. Wang et al (2017).
(This figure is originally reproduced in this report)

Zhengke Wang et al (2017) investigated the problem of hydrodynamic interactions among multiple floating bodies located in proximity in waves with the help of four cylinders as shown in Fig. 1. In this figure, dots represent the locations where free surface elevations are measured. Commercial software FLUENT is used to study the interaction phenomenon of an adjacent four-cylinder body in water waves. A time domain simulation on the problem of a four-cylinder body in regular waves is carried out based on viscous flow theory. The continui-

ty equation and Navier-Stokes equations are taken as the governing equations, and a volume of fluid (VOF) method is used for free-surface capturing. The wave run-ups on the surface of each cylinder are then systematically investigated, and its corresponding wave forces are also discussed and analysed. By comparing with a single cylinder in the same wave condition, the influence mechanism of interaction among multiple floating bodies on wave forces is investigated. Highest wave elevation at the centre of the array is observed. Also, the wave elevations at the inner side of each cylinder are larger than the outside.

Chen and Zhu (2017) employed three-dimensional time domain Rankine source method with HOBEM to solve hydrodynamic interactions of side by side vessels with and without forward speed. Radiation and diffraction problems are solved with linearity theorem. For forward speed problem, both double body (DB) flow and uniform stream (US) linearized computations are carried out. Added mass, damping coefficients, hydrodynamic forces and motions responses of side by side vessels are computed and hydrodynamic interactions are investigated. Zero speed case is investigated with an example of side by side arranged modified Wigley hull and a rectangular barge. Further, numerical investigation is carried out for a Supply ship and a Frigate advancing in waves parallel in close proximity. Ship motions of DB linearization computation are generally better agreement with experiments than of US linearization method. It suggests steady flow has significant effects on side by side ships unsteady motions and a more exact basis flow model would improve computation accuracy. Results of motions response of smaller Frigate in condition of two ships on parallel course are quite different with that of single ship condition due to the existence of bigger Supply ship. In addition, results show two ships with forward speed would be subject to attracting lateral force, which shall increase with speed and the reduction of lateral distance. If the principal dimensions of two close ships have much difference, influences of hydrodynamic interactions on the smaller ship would be greater.

A multi objective optimisation programme (using MATLAB) has been developed by Shashikala and Shankar (2017) for optimising the gap between ship and tugboat for minimum wave elevation. Ship and tug boat are modelled using ANSYS AQWA for different spacing between the two. Response of ship and tug boat along the wave elevation at different points on the floating bodies are calculated under regular and random waves. Optimisation coding simultaneously optimise wave elevation at tug boat, ship and the centre of the gap. The range of optimum spacing has been obtained from the code. Difference in the optimum spacing for different approach headings (900 and 00) is observed. For lower frequencies (less than 1 rad/s) wave elevation in the gap does not change much. Drastic changes in the wave elevation in the gap are noted for higher frequencies.

2.2 Forward-Speed Case

The forward-speed case is both an important and challenging topic in the field of computational hydrodynamics. One recent demonstration of the challenge is the statistical analysis of Kim and Kim (2016) on the performance of 17 seakeeping analysis codes. To study the effect of forward speed, heave, pitch and, vertical bending moment were studied at Froude numbers 0.05 and 0.12. The analysis shows that the numerical results become more scattered at the higher Froude number, which indicates that the increasing forward speed is a difficulty for the computational methods. One well-known issue for the forward-speed case is the balancing between the run time of a solver and the level of detail of modelling flow. Determining e.g. which nonlinear effects should be modelled is not necessarily self-evident. Recently, Hirdaris et al. (2016) studied the influence of nonlinearities on the symmetric hydrodynamic response of a 10,000 TEU containership by comparing the results of four different numerical methods and model experiments. As an example of their findings, the differences between predicted and measured vertical bending moments vary depending on both position and heading and further investigations are recommended especially for locations away from amidships. In a third recent benchmark study on forward-speed case, Gourlay et al. (2015) reports that the

results of four modern commercially available numerical codes on ship motions in shallow water show good agreement with model test results without a special trend of over- or under-prediction. Next, the studies with the main focuses on the application of one or two methods on structural loads and ship motions are described. Finally, some studies addressing mainly added resistance of a ship advancing in waves are mentioned shortly.

Recent studies on strip theories have addressed the prediction of sagging moment. Vásque et al. (2016) address the prediction of sagging moment in extreme waves by comparing numerical and experimental results of vertical bending moments for a bulk carrier and a roll-on/roll-off ship. The results demonstrate that a partially nonlinear time domain strip theory assuming linear radiation and diffraction (Fonseca and Guares Soares 1998a,b) overestimates the sagging bending moment in extreme waves, even though the same method has shown good agreement with model tests data in moderate amplitude waves. Rajendran et al. (2015a, b) offer improvements to the prediction of sagging moments by extending the method. Rajendran et al. (2015a) extend the method by including the surge mode in head seas. The numerical and experimental results for the S175 container ship and a chemical tanker indicate that the surge reduces the vertical bending moment at deck level while its effect on the vertical motion is negligible or small. Rajendran et al. (2015b) extend the method by including the body nonlinear radiation and diffraction forces. The results of the new and the original code are compared with experiments for a modern cruise ship. The effect of body nonlinear hydrodynamic forces on sagging moment is observed through comparisons.

Recent studies on strip theories address also 2D+T methods. Bandyk and Hazen (2015) improve the prediction of forward-speed effect of a body-exact theory based on a time-domain Rankine source method by a 2D+T strip theory variation. Meng and Qiu (2015) present an application of a body exact 2D+T strip theory for the prediction of the motions of a high-speed displacement ship.

In the field of 3D potential theory based methods using a Green function, several recent studies address the development of methods.

Guha and Falzarano (2015a) developed a three-dimensional panel method for the calculation of hydrodynamic force coefficients for ships with moderate forward speed in the frequency domain. The code uses the zero-speed infinite depth Green function and considers the effect of forward speed using encounter frequency. The frequency independent part of the Green function is evaluated analytically. The method is validated for ship motions and forces.

Kalske and Manderbacka (2017) extend a three-dimensional panel method to conduct computationally efficient forward-speed computations in frequency domain. The applied extension uses the zero-speed Green's function with correct frequency of encounter and speed correction terms corresponding to the terms in the Modified Strip Theory. The method is vali-dated for ship motions.

Yao and Dong (2016) study local steady flow effects on hydrodynamic interaction between two parallel ships advancing in waves. They have developed frequency domain methods with and without incorporation of local steady flow through m-terms in the boundary conditions. The numerical results are compared against experiments for wave loads and free motions of two parallel ships with an identical speed in regular head waves. The method predicting the local steady effects gives more accurate results, especially around the resonant frequencies.

Sengupta et al. (2016) present a simplified approach based on the 3D time-domain panel method using a transient free surface Green’s function for the prediction of nonlinear ship loads and motions. A modified form of the body-kinematic condition is proposed to approximately incorporate partial nonlinearities in the diffraction potential. The results on forces, motions and vertical bending moments are presented for a Wigley hull and S175 hull.

Kukkanen and Matusiak (2014) present a nonlinear time domain method that uses the transient tree-dimensional Green function. The program includes both the exact and linear body boundary conditions. The capability of method to predict nonlinearities in the ship motions and hull girder loads is demonstrated by comparing the numerical and original experimental results for a ro-ro passenger ship with a bulbous bow and a flat bottom stern.

Qiu et al. (2017) developed further a panel-free method using the forward-speed Green function by an algorithm to re-arrange the control points for Non-Uniform Rational B-Splines (NURBS) surfaces. Improved ship motions and load predictions are demonstrated thanks to reliable and accurate m-term computations.

Gonzalez et al. (2017) extend an existing time domain panel method for the computation of the non-linear free water surface by implementing the mixed Eulerian-Lagrangian approach. The validation of the code is presented regarding the wave resistance of a submerged spheroid and Wigley hull, and non-linear wave forces on a standing cylinder. Simulation of a catamaran model in head waves is demonstrated.

Chen and Liang (2016) present a new multi-domain method, which uses an analytical control surface surrounding bodies. In the analytical domain external to the control surface, the linear boundary condition on the free surface is satisfied using a Green function method. In the domain internal to the control surface containing the bodies, different methods capable of e.g. modelling viscous effects and non-linearities can be applied.

Mohammadi et al. (2015) applies the panel method MAESTRO-Wave and the strip method VERES to study static still water and dynamic wave-induced loads on a trimaran ship in intact and damage conditions.

Some recent studies have addressed three-dimensional Rankine panel methods.

Riesner et al. (2016) developed a non-linear time-domain boundary element method to predict ship motions and loads in waves. The predictions of radiation forces using either damping or added masses based approach are compared. The damping coefficient based approach performs better at zero speed, while, in some cases, the added masses based approach can give better results with increasing forward speed.

Chen and Zhu (2017c) present a three-dimensional time domain Rankine Source method with high order boundary element method (HOBEM) to solve hydrodynamic interaction of vessels side by side with and without forward speed. The results indicate good accuracy of the method in general and suggest that the accuracy of predicting steady flow has significant effects on the accuracy of predicting unsteady motions of ships side by side.

Von Graefe et al. (2014) compare the three-dimensional Rankine Panel method GL Rankine and a zero-speed free-surface Green function method for the prediction of sectional loads of a 6500 TEU container ship. GL Rankine solves the linear seakeeping problem in the frequency domain and takes directly into account the forward speed effect, while the Green function method uses an encounter-frequency correction for the forward speed effect. GL Rankine gives better results in general and especially at a larger forward speed.

In the field of RANS, recent studies address validation of methods and analysis of flow.

Motions and slamming of high-speed planing hulls is one recent topic. Fu et al. (2014) compares the results of RANS-solvers CFDShip-Iowa and NFA (Numerical Flow Analysis software) against experimental results for USNA planing geometry at Froude number 1.8-2.1. Mousaviraad et al. (2015) focus on the validation and analysis of Fridsma prismatic planing hull at Froude number 1.19 in regular and irregular waves using CFDShip-Iowa V4.5.

Mousaviraad et al. (2016) study the capability of the RANS-solver CFDShip-Iowa V4.5 to predict the ship-ship interactions in calm water and waves. In the case of replenishment condition, the results show average error values comparable to single-ship results and smaller error

than that of previously applied potential flow methods. In the overtaking condition, a close agreement between computed and measured time histories is obtained.

Hänninen et al. (2016) analyse further previously validated RANS results to define flow features that cause the development of vertical second harmonic wave loads, which can excite springing of a large cruise ship in short and steep head waves. The results underline that the careful prediction of three-dimensional and impact-type behaviour of the flow is relevant for the modelling of excitation of second-order resonant springing.

He et al. (2017) present numerical simulations on the green water of a Wigley hull conducted with the CFD software FINE/Marine. The focus is on the analysis of dynamic pressure on deck and superstructure.

Recently, several studies have addressed the computation of added resistance of a ship advancing in waves. Guha and Falzarano (2015b) improve the near field formulation of added resistance by including the effect of hull flare angle at the mean water surface in the context of a 3D Green function frequency domain solver. Hong et al. (2015a) applies three dimensional frequency domain forward-speed Green function and suggest that the prediction of added resistance using Maruo's far-field formulation can be improved by adding an appropriate value of added depth to the actual vertical coordinate in the three-dimensional Kochin functions. In a further study, Hong et al. (2017) improve the stability of results by evaluating the Green function using the adaptive Gauss-Legendre quadrature. Qian et al. (2015) studies the motions and resistance of a small-waterplane-area-twin-hull with inclined struts using a strip theory, RANS and model tests. Kim et al. (2016a) apply URANS for the prediction of added resistance and motions of KCS in regular head waves. Park et al. (2016) compares the capability of a frequency domain strip method and a time domain Rankine panel method to predict ship motions and added resistance at different drafts against experimental results. Kim et al. (2017a) study the added resistance of KVLCC2 in short and long waves and Kim et al. (2017b) for various speeds and wave steepnesses in head waves using the 3-D linear potential method PRECAL and the RANS-method STAR-CCM+. Kim et al. (2017c) study the added resistance of an LNG carrier in waves using the RANS-method Star-CC+, a Rankine panel method WISH and model tests. Lyu and el Moctar (2017) demonstrate that a for-ward speed Rankine source boundary element method and a RANS solver coupled with the nonlinear rigid body equations of motion are reliable methods for the prediction of wave-induced second order hydrodynamic loads of different ships. Seo et al. (2017) study added resistance and vertical motions of a 3600 KRISO containership (KCS) for various head waves using Open FOAM.

2.3 Hydroelasticity Methods

2.3.1 Hydroelasticity methods of ships

In the past few years 2D hydroelasticity method was utilized to resolve specific problems. Bennett et al. (2015a) studied the global wave-induced loads and whipping responses of a ship encountering an abnormal wave sequences. The influence of heading angle on the vertical responses of a 13,000TEU containership was investigated by Zhu & Moan (2015) by using 2D strip method and 2.5D strip theory in time domain. Heo et al. (2016) developed a numerical method to predict ship springing response of a ship based on 2D quadratic strip theory. Using a body nonlinear time domain method based on strip theory, Rajendran et al. (2016a, 2016b) predicted the spring and whipping response of containerships in waves. Lin et al. (2017) analyzed the springing responses of a 350,000DWT VLCC by combining 2-D strip method and 3-D Finite Element Method (FEM) in the frequency domain.

Several 3D linear hydroelasticity methods were proposed and developed both in frequency domain and time domain. Kashiwagi et al. (2015) proposed two practical methods for ship hydroelasticity problems with forward speed, of which one was the 3D time-domain Green-

function method and the other was the frequency domain Rankine panel method. Kara (2015) and Sengupta et al. (2017) developed 3D time domain hydroelasticity methods to predict the hydroelasticity of floating bodies based on the boundary-integral equation method with three-dimensional transient free surface Green function, satisfactory agreement was achieved between their numerical results. Yang et al. (2015a) presented two methods based on the time domain Green's function and the inner and outer regions matching technique respectively to predict hydroelastic responses of ship advancing in waves in time domain. Based on the above method, the time domain hydroelastic responses of CSSRC 20,000 TEU ultra large containership with zero speed was investigated by Wang et al. (2017). Kang & Kim (2017) investigated hydroelastic interactions of a deformable floating body with random waves in time domain. They proposed an efficient way of obtaining distributive loads for the hydrodynamic integral terms including convolution integral by using Fubini theory. Using a simplified coupling model with non-deformable local tank, Malenica et al. (2015) studied the global hydroelastic response of the ships coupling with the sloshing effect.

The three-dimensional nonlinear hydroelasticity methods developed continuously by considering the nonlinear factors such as the instantaneous position variation of body surface, the incident wave force, the restoring force and the slamming force, etc. Kim et al. (2015b) proposed several high-fidelity procedures for numerical analysis of ship hydroelasticity and a fully coupled model was introduced containing the 3D Rankine panel method, the 2D generalized Wagner model, the 1D/3D FEM. Considering the nonlinear restoring force and slamming force, Chen (2015, 2017a) developed a kind of 3D nonlinear time domain hydroelastic method, in which a proportional, integral and derivative (PID) autopilot model is applied to solve the divergence problem of motion equations and load responses of a 13,000TEU container ship in oblique regular waves. Park et el. (2017) used a fully coupled fluid–structure interaction model to compute the mean drift force on a flexible barge. Both the near-field method and the far-field method were employed in the computation of drift force. Ren et al (2016) investigated the longitudinal wave loads of a trimaran by using a 3D time-domain nonlinear hydroelasticity theory considering the influence of nonlinear factors such as slamming. It was found that the computed value under ultimate working conditions was significantly larger than the LR Trimaran rule value.

A Joint Industry Project of Wave-Induced Loads on Ships III (WILS JIP III) was conducted by Korea Research Institute of Ships and Ocean Engineering (KRISO). Drop tests of 2D sections as well as seakeeping tests of a 10,000-TEU containership and many comparisons between numerical method and experiment were carried out in the project. The parametric study of slamming and whipping of the containership was analyzed by Kim & Kim (2015a) based on a fully numerical model consisting of a 3D Rankine panel model, a 3D finite element model and a 2D GWM. Meantime, Kim (2015c) carried out numerical simulation of springing and whipping response of the containership by using 3D nonlinear time-domain method which considers nonlinear hydrostatic restoring and Froude-Krylov forces. Lauzon et al. (2015) focused on the comparison between the experimental results and numerical results computed by the hydro-structure software developed by Bureau Veritas. On the basis of Fluid Structure Interaction (FSI) model, the wave induced global loads and whipping responses of the containership were also investigated by Lee et al. (2015b).

To predict strong nonlinear loads reasonably and consider the viscous effect, CFD tools are utilized to investigate the hydroelastic response of large ships. Lakshmynarayanana et al. (2015) studied the fluid-structure interaction of flexible floating bodies in waves by coupling CFD software (Star-CCM+) and FEA software (Abaqus). The whipping response of a Joint High Speed Sealift model moving in a large seaway was studied in time domain by using open source CFD codes OpenFoam and higher-order boundary element method in Craig et al. (2015)'s study. Robert et al. (2015) proposed a numerical approach which combined a viscous flow solver and a beam model to investigate the hydroelastic response of a flexible barge in

time domain. Computational methods which couples the Reynolds-averaged Navier-Stokes (RANS) equations and nonlinear motion equations was presented by Moctar et el. (2017) to assess slamming-induced hull whipping.

2.3.2 Hydroelasticity methods of VLFS

Very Large Floating Structures (VLFSs) have drawn attention from many researchers worldwide. For the hydroelasticity issue of the VLFSs deployed in open and deep sea are concerned, Mirafzali et el. (2015) employed a meshless numerical method to solve the interaction of fully nonlinear water waves with the floating elastic plate. A semi Lagrangian method and a leap frog time marching scheme were used to calculate the displacement and the velocity potential on the free and plate surfaces. Cheng et al. (2016) investigated the hydroelastic responses of a mat-like, rectangular VLFS edged with dual horizontal/inclined perforated plates using Eigen function expansion-matching method (EEMM), FEM-BEM hybrid method and compared the results with experimental data. Using the Euler-beam model, Wang et el.(2016a) investigated the hydroelastic responses of a horizontal plate impacting with the water at both forward and downward speeds theoretically and numerically.

If a floating body is deployed near seashores in complicated geographical environment, the wave conditions, wave loads and the hydroelastic responses of the floating structure will be quite different from those in open and deep sea. Recently China Ship Scientific Research Center (CSSRC) have proposed several numerical approaches for the analysis of a VLFS near islands and reefs. Yang et al.(2015b) and Li et al. (2016) treated the uneven seabed as a fixed body boundary condition to account for its influence on the diffraction and radiation of floating structures. Ding et al. (2016) and Wu et al. (2016a) analysed the effect of inhomogeneous wave distribution on the VLFS by considering different wave conditions on each sub-module of the VLFS. Bu unifying the Boussinesq equation and the Rankine source method, Wu et al. (2017a, 2017b) and Ding et el. (2017) established a direct coupled method to analyse the hydroelastic response of floating bodies in the inhomogeneous waves induced by the complicated geographic environment when the floating body is deployed near islands and reefs. Considering the constant and variable seabed, Karperaki et el.(2016) analyzed the transient hydroelastic response of floating elastic plates based on the Euler-Bernoulli strip and the linearized shallow water equations. Cheng et al. (2017) employed a 2D fully nonlinear numerical wave tank to investigate the interaction between a monochromatic wave and a floating elastic plate over the variable seabed. By treating the flexible floating structure as “elastic beam connected rigid sub modules”, a practical numerical hydroelastic analysis method has been investigated by Lu et al. (2016). Based on the above method in frequency and time domain, Wei et al. (2017, 2018) and Fu et al. (2017) applied different incident wave condition onto different modules to analyze the effect of inhomogeneous wave distribution on the hydroelastic response of the floating plate and the floating bridge respectively.

3. SHIP STRUCTURES - SPECIALIST TOPICS

3.1 Slamming and Whipping

Sea surface impact on ship hull, known has slamming is a one of the loads the structure has to withstands, especially in rough seas. In top of the local structure load directly induced by slamming events, the consequence vibratory response, called “whipping” is of primary importance. This section focuses on the slamming loads themselves, and much less on the whipping issue. Indeed, strictly speaking, the whipping should not be considered as a load but as a response. Besides, more relevantly, this whipping issue will be thoroughly covered by next section “I.3 Hydro-elastic response”. Here it is just noted that the whipping issue is of high practical relevance, which makes the accurate assessment of the slamming phenomena a crucial step. It is also noted that the practical global response model (that compute the ship motions, including the effect of slamming loads) are, nowadays, generally made of a potential, time-domain code (often weakly non-linear) coupled to 2D potential model for slamming

(most of the time Generalized Wagner Model). These kinds of model are described in (Malenica & Derbanne, 2014) or (Tuitman, 2010). Applications and assessments of these models with regards to model test were conducted in several projects (WILS II and III), and quite a few papers, see for instance (Kim, Kim, Yuck, & Lee, 2015) and (de Lauzon, Benhamou, Malenica, & others, 2015). Full CFD on irregular waves including slamming is not common practice, but can nevertheless be found (Oberhagemann, Shigunov, Radon, Mumm, & Won, 2015) and is very probably something that will develop in the future.

The difficulty to incorporate 3D model into practical, engineering sea-keeping calculation is probably one of the reason why most of the research on slamming loads is quite concentrated on 2D approaches. That said, some of the below described papers do report possible limits of the 2D strip approximation. To begin with, the papers investigating 2D impact are thus reviewed. Some of them improved the numeric of quite widespread model, some others focus on more complex phenomena, that are not, today, included in practical design tools.

To begin with the 1st category, i.e. numerical improvements, (de Lauzon, Grgi, Derbanne, & Malenica, 2015a) present new approach to improve the Generalized Wagner Model is introduced. It uses BEM and Kelvin's Green function. The key new feature is to separate the singular part from the regular one. The singular part is integrated semi-analytically. The model has been successfully validated through comparison with analytical results as well as experiments. Compared to existing, model, the key advantage is the robustness, and the ability to deal with a very wide range of shape and arbitrary velocities.

Another improvement to numerical is also presented in (Wang & Faltinsen, 2017). This work allows solving for the Dobrovol'skaya's boundary integral equations for quite small deadrise angle, down to 1°, while previously used method encounter difficulties below 4°. Results were successfully compared to standard BEM calculation for higher deadrise angle. For small angle, the results are consistent with asymptotical model.

Bao, Wu, & Xu (2017) studied that the free fall of finite wedge is investigated with potential, non-linear model. Compared to classic infinite wedge impact at imposed velocity, two difficulties are to be tackled: the finite width makes important the flow detachment, and the motion equation has to be solved in a coupled fashion. Results are compared to SPH computation and to experimental results, yielding a very decent agreement. It is also shown that, in the simulated case, a flow computed ignoring detachment would lead to slightly different motion. Also, as expected and documented in previous study, the coupling between the body motion and the slamming model yield decreased loads (due to the deceleration when the wedge hits the water).

Alaoui, Nême, & Scolan (2015) focus on an experimental set up capable to accurately measure the slamming and pressure at constant velocity. The accuracy of the constant was checked, and repetition test were made, successfully: the results are repeatable. Also, it has been observed that the pressure and impact were almost not dependent on velocity: Cs and Cp are approximately constant. Furthermore, the values of those coefficients are in accordance with some analytical and numerical analysis.

Sun, Sun, & Wu (2015) focus on two specific features, firstly, the entry is in waves, and not in calm water as most of the academic cases. Several conditions are tested (relative wave length, phasing…). Secondly, the gravity, neglected in most of the simplified model is included. The paper reaches conclusions about the relevance of gravity: negligible when the impact time is much less than the ratio of entry speed to the acceleration due to the gravity, and then it affects significantly the pressure distribution when the impact time progress. The wave characteristics, as well as its phasing with regards to the wedge, have of course significant effects. Those effects are found difficult to sketch. Also, it is noted that the discontinuity at the wedge tip, which would require a proper Kutta condition, is not handled at this moment.

Above described paper are based on potential theory, which is currently the bases for practical, engineering, purpose. However, the approximated description of the physics (no flow detachment, incompressible flow) together with the improving CPU power call for more sophisticated models. Quite some research is currently undertaken on CFD (in a broad sense, including SPH), and part of it is quite relevant to slamming. A lot of effort has been performed to demonstrate the ability of CFD to assess slamming events and to improve the confidence in this tool. The different contributions definitively demonstrate the added value of CFD to slamming assessment. They also point to the increasing relevance of code and hardware related issue. The algorithm and equation are important, but the computational aspects (scalability, CPU/GPU) are crucial to make the method competitive. Then, CFD is now used to investigate some special phenomena that would be quite challenging to tackle with potential flow tools (compressibility is the main example)

As a start on CFD validation, we can cite many studies (Hong, Kim, Hwang, & others (2017), Southall, et al. (2015) and Charles Monroy, et al. (2017)) which undertake a quite comprehensive benchmark of various code to assess slamming loads and pressure. Two geometries are investigated: a wedge, and a ship section. Model tests results were provided by WILS III JIP. While comparison between the various codes and the model tests is decent, some scatter can be observed. Generally; the CFD codes match better with the experiment, especially on the ship section, where the potential theory is not able to deal with the flow separation at the bulb. Of course, CFD calculations times of magnitudes slower: reported calculation times were in seconds for potential codes, hours for CFD). Interestingly, the papers shows that the scatter among CFD codes is wider that among potential codes. With very similar software (if not identical), results are can vary, highlighting mesh sensitivity, but also the additional expertise required to handle CFD codes compared to potential ones.

Wen & Qiu (2015) used a Constraint Interpolation Profile approach (CIP) to solve the Navier-Stokes equation. The calculation is done in multiphase, for 3D geometry. Emphasis is put on the parallelization of the code, which results in more acceptable calculation time. Computation on a falling edge and a ship section is performed and comparison with experiment, BEM and VOF CFD is made, showing a quite good agreement.

Buruchenko & Canelas (2017) validated a SPH code through comparison with experimental results as well as other CFD code (VOF and CIP). The results of SPH-dual-physics are very comparable to other results from VOF and CIP, and agree quite well with the experiment. Unfortunately, the computational cost of the various method used is not reported/compared

Kamath, Bihs, & A. Arnsten (2016) used the open source code REEF3D to compute the free-fall of wedge (incompressible). Reef3D uses finite difference on cartesian grid, and free-surface is here capture with level-set. Computed wedge velocity is compared to experiment, showing a very good agreement.

While a lot of papers are focused on improving the CFD tool and checking its results with model test, CFD is now mature enough to be used as a tool to investigate some phenomena.

In (Elhimer, Jacques, Alaoui, & Gabillet, 2017), the effect of aeration on slamming forces is investigated, both numerically and experimentally. First, impact forces of a cone entering into aerated water are calculated, using the finite elements software ABAQUS. Different aeration rate are tested (from 0% to 10%), for a range of impact velocity. Results show significant effect of aeration on impact forces, which can be reduced up to 70% compared to the pure water/incompressible case. The force (and pressure) decrease is dependent on the velocity. Then experiment is performed, using a hydraulic shock machine, void fraction was measured with optical probes. Numerical results confirm the trends observed numerically (i.e. decrease of the impact force with aeration rate), however, the numerical model seems to significantly overestimate the loads for aerated case (while this overestimation is very slight in case of pure water).

Ma, et al. (2015) studied the compressibility effect on flat plate, where this effect is expected to be very significant. On the numerical side, the model used is a compressible two phases model, on the experimental side, forces and pressure were recorded thanks to an S-type cell and five miniature pressure transducers. The numerical model was able to quite accurately match the experiment, and correctly reproduced the pulsatile slamming loads.

While, that the focus is generally on monohull (containership) bow, slamming can also be a relevant issue on other places. For instance, (Swidan, et al., 2016) experimentally investigate wetdeck slamming loads on a catamaran. Documented drop tests with catamaran hull are quite scarce, especially in 3D, and this work fills this gap. To ensure the accuracy of the tests, uncertainty analysis has been undertaken, and tests have shown a good repeatability. Results showed a classic evolution of the impact loads with V^2. Also, in top of the flow analysis undertaken, the paper provides a good dataset for benchmarking numerical codes.

Stern slamming has been investigated in (Wang & Soares, 2016), on chemical tanker, both numerically and experimentally. The test conditions are irregular head waves. Numerically, the 3D sea-keeping has been performed to compute the ship motion, and slamming forces has been evaluated in second steps, in decoupled way. Two different slamming models has been used MLM (Modified Longvinovich Model), and ALE (LS-dyna implementation). Compared to experiment, both models largely over-predict the slamming forces. The first explanation given is the difference between the calculated motion and the experimental ones. The second is the importance of the 3D effects. The 2D numerical results were reported as highly sensitive to slight motions changes.

While, most of the drop test are performed with 2D section, (Wang, Wu, & Guedes Soares, 2016) investigate the slamming loads on a 3D bow. The geometry investigated is the bow of sea-river link ship, instrumented with pressure sensor. On the numerical side, the impact is model with finite element (3D) with ALE. The numerical impacts were made a constant speed, while the experiments were free fall. Several drop heights and pitching angle have been investigated. Overall, the agreement between model tests and experimental results are decent but not perfect. Compressibility effect in the model tests were reported at 0° pitch angle. Unfortunately, no comparison to the widely used 2D strip approach is made.

3.2 Sloshing

3.2.1 Introduction

Sloshing is the oscillatory motion of the free liquid surface inside partially filled containers that may possess strong nonlinear character depending on the level of excitation. It may result large impact forces on container walls and have significant coupling effects with ship motions, thus has practical importance regarding the performance and safety of marine transportation systems. During the reporting period, main theoretical and experimental interest was on the interaction between sloshing and global ship motions and sloshing suppression using baffles.

3.2.2 Experimental Investigations

In recent years, model testing has been mostly used to observe the physics of the sloshing-coupled ship motion problems, to investigate the efficiency of sloshing suppression, and to obtain validation data for the numerical tools.

Zhao *et al*. (2014) conducted 2-D model tests for a Floating Liquefied Natural Gas (FLNG) section excited in sway, heave, and roll, with the main interest of identifying the mutual effects between the ship motions and internal free surface. They observed strong coupling for sway and roll motions compared to the heave motion, and also concluded that for the same wave excitation, the sloshing oscillations tend to be severer for lower filling ratios. The interaction of sloshing fluid and roll response of LNG carriers was examined by Zhao *et al*.

(2016a) through a barge-like vessel having two spherical tanks. Here, the objective was quantifying the magnitude of the interaction for different sea and loading conditions. Zhao and McPhail (2017) conducted a similar set of experiments with spherical tanks filled with liquid cargo and equivalent frozen-cargo having the same dynamic characteristics, to observe the effect of liquid cargo motions on the global roll response of a barge-like vessel at an intermediate load condition. Xu *et al*. (2017) examined the effect of sloshing on the hydrodynamic responses of an FLNG-LNGC (LNG Carrier) system during side-by-side operation by ballasting the vessels with both solid and liquid cargo. They found that sloshing may have beneficial effect on FLNG motion for certain loading combinations and that the relative motions between the vessels are composed of wave-frequency and low-frequency components.

Nayak and Biswal (2015) investigated the hydrodynamic damping potential of centrally installed objects in three different configurations–bottom mounted vertical baffles, surface-piercing vertical baffle, and bottom mounted submerged block–perpendicular to the lateral excitation in partially filled rectangular tanks. They indicated that the baffles can be effective for sloshing damping near the resonance conditions, yet surface-piercing baffles provide higher damping for similar physical setting. Yu *et al*. (2017) demonstrated both experimentally and numerically (through CFD) the effectiveness of floating plates on sloshing suppression in a membrane-type LNG tank subjected to harmonic rolling excitation. The test results showed that the suppressing device not only reduces the wave run-up along the longitudinal bulkhead, but can also decrease impact loads acting on the bulkhead. Xue *et al*. (2017) performed an extensive set of tests to study the sloshing damping effects associated with vertical baffles of different configurations in a rectangular tank subjected to a horizontal excitation of wide range of frequency. They found that the effectiveness of the baffles in sloshing suppression depends not only on the relations between forcing frequency and natural frequency of sloshing, but also on its configuration and location.

Coupling of the floodwater and rolling motion of a box shaped barge was experimentally studied by Manderbacka *et al*. (2015). They observed that the flooded water can act like a passive anti-rolling tank if the sloshing natural frequency is close to the roll frequency. Similarly, Bennett and Phillips (2017) experimentally investigated the effect of floodwater and transient flooding on the motions and structural response of a ship hull following a grounding. Their results indicated that the second order sloshing effects due to the movement of the floodwater free surface are present at encountered wave frequencies close to the peak response of the ship and they may dominate the severity of the responses around these frequencies.

3.2.3 Numerical Simulation

The numerical methods developed for sloshing simulation can be categorized under two groups: studies based on the potential flow assumption, with or without the inherent nonlinearities, and studies that involves the viscous effects. The fluid-structure interaction was also considered in some numerical models.

Lin et al. (2015) proposed a Scaled Boundary Finite Element Method (SBFEM) to obtain the sloshing frequencies and corresponding mode shapes of liquid storage tanks having arbitrary axisymmetric cross-section. Kolaei et al. (2015a) studied the sloshing problem of horizontal tanks subjected to simultaneous longitudinal and lateral excitations by first reducing the dimension of the computation domain by applying the separation of variables technique and then applying a higher-order Boundary Element Method (BEM) scheme in a multimodal setting. Their comparisons with CFD simulations revealed some of the problem-dependent limitations of the potential flow based solutions. Stephen et al. (2016) used the Finite Element Method (FEM) and mixed Eulerian-Lagrangian formalism within the fully nonlinear potential flow framework to study the sloshing of 2-D rectangular tanks under combined horizontal, vertical and rotational motions. They specially discussed the coupling effects on sloshing os-

cillation. A mesh-free potential flow based numerical model for simulating the free surface waves was developed by Wu et al. (2016b), where a local polynomial collocation method was applied for solving the Laplace equation at each time step. The method is applied to predict the liquid sloshing in rectangular and cylindrical swaying tanks. Chen et al. (2017b) provided a regularized boundary integral equation formulation for the nonlinear sloshing problem that avoids some of the drawbacks–regarding singularity and discretization–of the traditional BEM solutions. The energy dissipation neglected in the potential flow theory was taken into account in this study by assuming a linear damping term proportional to the particle velocity.

By adopting the linear potential theory and FEM, Bochkarev et al. (2016) investigated the interaction of sloshing and hydroelastic behavior of thin-walled cylindrical shells of arbitrary shape under the conditions of non-stationary loading and periodic excitation. Ravnik et al. (2016) studied the dynamics of a shell structure with partially filled compartments through the mode summation approach. The FEM and BEM were used for describing the structural response and linearized liquid sloshing, respectively.

It is well known that the meshless particle methods are better in modelling the merging and splitting in fluid domain and tracking the free surface. Luo et al. (2016) used the Consistent Particle Method (CPM) to study the sloshing problem in tanks under translational and rotational excitations with regular or random nature. Unlike the more traditional particle methods, i.e., Smoothed Particle Hydrodynamics (SPH), the spurious pressure fluctuation, resulting from the applied derivative approximation schemes, can be eliminated with the CPM. The technique was applied for the analysis of an LNG container in a real ship under typical sea conditions. Sufyan et al. (2017) proposed a local dynamic mesh refinement and coarsening technique for unstructured grids, where a level-set function was used as the criterion for the implementation of mesh refinement. The technique was implemented in the FEM solution of the sloshing problem in a rectangular tank. Grotle et al. (2017) studied sloshing at shallow-liquid depths in a rectangular container by using the Reynolds-averaged Navier-Stokes (RANS) equations with an open-source finite difference CFD solver REEF3D. They simulated the forced sloshing within the proximity of the fundamental mode and also provided experimental observations.

3.2.4 Sloshing Suppression

Baffled sloshing suppression is still a very active field that researchers proposed new analysis tools, relying on both potential and viscous flow models, to investigate the special aspects of the problem or to analyze different configurations.

Kolaei et al. (2015b) developed a BEM based multimodal numerical tool for simulating the fluid sloshing in baffled tanks by including the damping, induced by the baffles, from the mean energy dissipation rate. They studied partially filled circular tanks with three different longitudinal baffles (bottom-mounted, top-mounted, and center-mounted) and illustrated the effects of baffle designs on the sloshing modes, hydrodynamic coefficients, and damping ratio. Wang et al. (2016b) studied the transient lateral sloshing in a partially-filled cylindrical tank with multi baffles (as floating circular baffle, wall-mounted ring baffle, floating ring baffle and their combination) using the SBFEM with a multimodal approach. They concluded that the sloshing force monotonically increases with the length of the baffle, and its influence decreases with increasing the interspace between the baffle and the free surface, and also added that the consideration of only the first sloshing mass is adequate to represent the dynamic behavior.

Cho and Kim (2016) investigated the use of vertical porous baffles for the purpose of dissipating more energy. They used the matched eigenfunction expansion method within a potential flow setting, where the porosity is included by inertial and quadratic drag terms. Both numerical and experimental results indicated that the dual vertical porous baffles can significantly

suppress sloshing. The impact of vertical porous baffles was further studied by Cho et al. (2017) using a similar numerical and experimental setting.

The effectiveness of the baffles for the suppression of the sloshing in a rolling 2-D rectangular tank was demonstrated by Tang et al. (2015) by using the Moving Particle Semi-implicit method. Yin et al. (2015) studied the sloshing in rectangular tanks with or without baffle both numerically and experimentally. They adopted the open source viscous flow solver OpenFOAM for numerical analysis and showed the influence of single baffle on reducing the dynamic pressure and sloshing amplitude. Lu et al. (2015) proposed a finite element based viscous numerical model for the sloshing problem in tanks with or without baffle. They investigated the role of sloshing frequency in dissipation, effect of the excitation amplitude on the sloshing response, and estimation of the damping. Their comparisons with respect to the solutions of the potential flow theory for baffled and non-baffled cases offer certain suggestions and limitations on the use of potential flow approximation for sloshing prediction. Hwang et al. (2016) developed a fluid-structure interaction solver based on Moving Particle Simulation to study the sloshing flows in rolling tanks with elastic baffles. They presented sloshing flow comparisons between tanks without baffle and with rigid and elastic baffles of different Young's modulus. Liu et al. (2017) proposed a hybrid RANS/LES (Large Eddy Simulation) model in conjunction with the Volume Of Fluid (VOF) interface capturing technique to improve the predictive accuracy of RANS and the computational efficiency of LES for the numerical prediction of violent liquid sloshing. They employed the model to study a tank with a vertical baffle and a horizontal baffle.

3.2.5 Sloshing and Ship Motions

Regarding the designs of LNGC, FPSO, FLNG, and FSRU, and due to the increasing capacities and changes in operational conditions, the practical demand of sloshing analysis has been rising in recent times. In particular, the mutual interactions between the ship motion and liquid sloshing in tanks have been studied extensively. The numerical investigations for this coupled problem were usually performed by adopting different mathematical models or different types of solvers for individual analyses. This is mostly due to the dissimilar nature of the involved problems, i.e., highly nonlinear and small time scaled sloshing problem vs. the classical seakeeping problem (with or without considering nonlinearities), but partly dictated by achieving practical simulation times. Although the ship motion was assumed linear in most cases, considering the violent sloshing flow and resulting impact, it is not surprising that the majority of the theoretical development were in the form of time-domain approaches.

Wang and Arai (2015) analyzed the coupling problem of ship and sloshing tank for an LNGC in regular and irregular waves using a time domain model and considering four different loading conditions. They applied a 3-D finite difference scheme for the internal liquid movement and the strip method for the seakeeping problem. The predicted ship motion RAOs and sloshing wave amplitudes indicated that the influence of sloshing on ship response is significant for lateral motions and relatively weak for longitudinal motion.

Jia et al. (2015) investigated the dynamic response of liquid containers by applying a di-rect coupling scheme. Here, the CFD and FEM are applied for the sloshing liquid and tank structure, respectively, which were then related through the balances of force, heat flux and temperature and no-slip boundary condition. The presented results addressed three issues that might be critical in the design of FLNG tanks: the strength of the tank structure under the peak impact loads, the resonant vibration when the ship is excited near the natural frequencies of the tank, and fatigue of the tank structure caused by the periodic loads due to sloshing.

Bai *et al*. (2015) developed a numerical model to simulate the sloshing flows due to ship motions in 2-D rectangular tanks by applying the level set method to capture the complicated free surface motion. They studied an LNG tank excited by the realistic ship motions in sea conditions, where the RAOs of the LNG carrier were used directly to excite the sloshing in the

tank. They concluded that the most critical sloshing wave is generated when the sea wave frequency approaches the resonant sloshing frequency and that the free surface elevation excited by each resonant frequency decreases with the increase of the filling depth due to the corresponding smaller RAOs applied.

Gao and Vassalos (2015) studied the coupled dynamics of the floodwater and damaged ship, where the water sloshing inside the compartments may significantly influence the ship motion. An integrated numerical method combining a Navier-Stokes solver and nonlinear 2-D seakeeping theory was used to simulate the behavior of the damaged ship response in waves. The numerical model was applied for a Ro-Ro ferry in regular beam sea state.

Paik *et al*. (2015) developed a probabilistic approach to determine the nominal values for tank sloshing loads in structural design of LNG FPSOs. They selected a limited number of sloshing scenarios according to the operative factors (such as wind speed and direction, wave height and period, etc.) using a probabilistic sampling technique. Vessel motion analysis is conducted for each scenario and the resulting vessel motions are applied to a RANS solver. The nominal values of sloshing loads can be determined based on the acceptance criteria for the exceedance curves that are formed in relation with the sloshing peak pressure, impulse, or rise time.

The coupling effect between the sloshing flow and global ship motions was investigated by Jiang et al. (2015); they adopted the VOF method for the internal flow (through OpenFOAM) and an impulse response function method for the external potential flow. The communication between separate flow problems was established by using the ship response as the moving-wall boundary condition for the internal problem and applying the computed pressure forces in return to the external problem, at proper time steps. The method was applied for the analysis of an LNG-FPSO model with two partially-filled prismatic tanks. They examined the effects of coupling on global response and sloshing impact loading, depending on the incident wave direction, frequency, amplitude, and liquid filling ratio. They found that the coupling effect is relatively small for heave and pitch motions of the ship in head seas, yet dominant at low-filling ratios in beam sea condition. Moreover, for low filling ratios, ship motion response is very sensitive to the incident wave steepness, especially at around the sloshing natural frequency and resonant ship motion frequency values, and also nonlinear effects due to sloshing become important on global response.

Servan-Camas *et al*. (2016) studied the coupled sloshing-seakeeping problem by employing an SPH solver for the sloshing flow in a weakly compressible Lagrangian setting and the FEM for the potential flow associated with the time dependent wave diffraction and radiation around the ship. The coupling between independent solvers was established by exchanging the body movement and force/moment data through adjusted time steps for each part. Cercos-Pita *et al*. (2016) improved the methodology by including empirical damping terms and considering the nonlinearities associated with the ship motions, i.e., calculating the diffraction and restoring forces at the instantaneous wetted surface.

Saripilli and Sen (2017) adopted a similar numerical setting to integrate the external and internal flow problems. They applied the time-domain boundary element method for the ship motion problem and used the OpenFOAM for the Finite Volume Method (FVM) based solution of sloshing fluid. They solved the coupled problem for a modified S175 and concluded that the sloshing-induced pressures on the interior of the tank can be much lower if the coupling effects are considered. Sen and Saripilli (2017) extended the study by focusing on the roll motion and studying the effect of multiple tanks.

Malenica *et al*. (2017) presented an overview of the current approaches and issues for the solution of the coupled ship motion-sloshing problem and assessment of the structural response of liquid tanks. They identified some complications regarding the model experiments for

sloshing-induced impact and modeling of the hydro-structure interactions induced by the sloshing loads in the containment units of the LNG vessels.

If both the ship motion and internal tank sloshing problems are represented using the potential flow theory, more efficient computations can be realized. Particularly, under the assumption of linear motion, frequency-domain solutions for the coupled problem were presented in the past, e.g., Molin *et al*. (2002), Malenica *et al*. (2003), Newman (2005), Gou *et al*. (2011). The frequency-domain approach may function as a practical approximation tool for the coupled problem, yet the nonlinear features of the internal flow cannot be accurately captured and excessive coupling effects, such as singular solutions or abrupt fluctuations at the sloshing resonances, can be predicted. The BEM solution of Zhang (2015) aimed at avoiding the simultaneous occurrence of the sloshing in all the wedge-shaped tanks of a LNG carrier that may endanger ship stability. Special attention was given to identifying the effects of inclined tank walls on dynamic characteristics as well as studying the sloshing wave elevation histories due to sway, roll, surge, and pitch type motions at the fundamental frequencies. Lee *et al*. (2015a) numerically and experimentally investigated the linear hydroelastic analysis of floating structures with liquid tanks subjected to regular water waves. They applied the FEM for the floating structure and internal fluid, and the BEM for the external fluid, and considered the couplings between structural motion, sloshing, and water waves by incorporating al interaction terms. In the analytical investigation of the coupling between the vessel motion and liquid sloshing in multiple tanks, Zhang (2016a) focused on the coupling mechanism rather than targeting the whole problem. The external environment as well as disturbance factors that may alter the dynamic characteristics of the system were omitted and excitation of the ship was initiated by the internal free surface motion. Hu *et al*. (2017) applied a potential flow solver and conducted model tests to investigate the hydrodynamic characteristics of an FLNG under the condition of a sloshing LNG-tank. They indicated that the effect of sloshing on the global motion response in the modes of pitch, heave and yaw are negligible, yet for surge and sway motions, a noticeable peak response appears near the first-order resonant period of the LNG tank. Nonlinear potential flow solver for the sloshing problem is another option, which is more complex than linear solver but still computationally efficient compared to the viscous flow based computations. Su and Liu (2017) analytically solved the 2-D coupled problem for a barge in frequency- and time-domains. They adopted the nonlinear Boussinesq-type equations for simulating the internal flow and used the impulse response function, obtained from the frequency-domain solution, for the ship motion problem.

3.3 Green Water

Youn Kyung Song et al (2015) investigated green water velocities and impact pressures caused by the impact of over topping waves on a fixed deck structure in a large-scale, three-dimensional deep-water wave basin. Using the bubble image velocimetry technique, detailed two-dimensional surface flow pattern on a horizontal plane, including the temporal and spatial distributions of the maximum horizontal velocities are successfully obtained. Pressure measurements are also carried out along four different vertical positions at three different locations on the horizontal plane. Based on the mean velocity distributions on the deck surface, the most significant spatial variability of the propagating green water flow is the protruding wave front near the centre of the deck during the early stages of the wave over topping. The maximum front speed of 1.5C was observed first near the midpoint of the deck along the deck centreline with C being the wave phase speed. The flow velocities decreased to below 1C once the wave front passed the rear edge of the deck. Most of the measured pressures showed impulsive impacts characterized by a sudden rise of the pressure peak. The highest pressure was observed as 1.65ρC2 at a midpoint and at rear edge of the deck with ρ being the water density. Correlations between wave kinetic energy and dynamic pressure are examined to determine the impact coefficients. The phase speed based impact coefficient is found to vary within a narrow range between 0.29 and 1.69 and a practical value of 1.5 is suggested to be used in

applications. It appears that the impact pressure on the structures is strongly affected by the changing front shape of the broken wave and the impulsiveness of the impinging wave that contains a considerable amount of air entrainment.

Daniel F.C. Silva et al (2017) presented the development of a methodology for detailed CFD simulation of green water events. Based on model test data, extreme green water events resulting from beam and quartering waves are selected and the wave vessel interaction is simulated, including the water on deck propagation. The commercial CFD code ANSYS FLUENT® was customized to have boundary conditions to represent specific wave intervals from irregular sea state realizations and vessel movements prescribed based on experiments. By using a VOF-multiphase and SST-turbulent setup, the accuracy of 2D and 3D simulations are evaluated by comparison with experimental data in terms of free surface evolution and loads, with good agreement in most cases. Some deviations on the loads were observed, but they are coherent with the complex local flow conditions of typical impact flows due to effects such as wave breaking and air entrapment. The methodology presented in this paper gives access to high spatial resolution free surface position, water velocities and load distribution, phenomena usually not available from experiments, which leads to new possibilities in the investigation of shadowing effects and dynamic loads during green water and wave impact extreme events.

Shuo Wang et al (2017) presented a numerical approach based on potential theory in frequency domain for FPSO green water assessment, considering nonlinear effects from bilge keels, spread mooring and asymmetrically arranged risers. Commercial radiation diffraction code ANSYS AQWA is used to find relative wave elevations. Damping coefficients are based on experimental decay tests. Comparison with experimental measurement shows that, by properly considering the linear and nonlinear effects due to appendages and attachments using proposed numerical approach, the relative wave elevation response of the FPSO in irregular wave can be predicted accurately and efficiently in frequency domain. The relative wave elevation response in oblique and beam sea wave is found to be affected by additional stiffness, added mass and damping from bilge keel, mooring and risers. Such results also suggest that the green water occurrence at side of FPSO in oblique wave may be reduced by bilge keel, mooring and risers. However, effects from these appendages and attachments are generally not affecting green water prediction at any location of FPSO in head sea/stern sea condition; prediction at centre of bow & stern in oblique wave and beam-sea are not affected either.

Gauanghua He et al (2017) have performed a time-domain simulation of green water on a Wigley hull sailing in regular head waves. To predict the strong non-linear phenomenon of green water, a numerical model is established by utilizing FINE/Marine, a multiphase-flow software based on free-surface capturing method. The problem of green water impacting on deck is systematically investigated by varying the wavelengths and wave amplitudes. Based on viscous flow theory, a solid-liquid-gas three-phase flow coupling model is developed for more realistic simulation by adopting the Blend Reconstruction Interface Capturing Scheme (BRICS) which reduces numerical diffusion near the free surface. This model can well process problems of breaking waves and evolution of complicated free surface. By using this numerical model, impact loads on deck and hull, ship-motion characteristics and hydrodynamic characteristics during the green water process are investigated. The emphasis of this paper locates on the analysis of dynamic pressure on deck and superstructure during the green water process and the influence of main characteristic parameters.

3.4 Experimental and Full Scale Measurements

Note that experiments on sloshing and green water loads are reviewed in Section 3.2 and 3.3.

Research on the measurement of loads on ships again focussed on the magnification of extreme and fatigue loads by wave induced vibration. A complete review of current experimental research in this field is beyond the scope of this Section and partly redundant with Section 3.1. Hence, only a very brief summary of current research is presented here.

Whipping and springing vibrations are randomly excited and thus the challenge is to condense the unknown modal parameters solely from the measured response. Therefore, Dessi and Faiella (2015) and Kim, Ahn and Park (2016) investigated methods to determine the natural vibration modes and damping characteristics for a slender and a blunt hull shape from the forced response measured at backbone models in regular and irregular waves. The authors found that the proper orthogonal decomposition method and the cross random decrement technique can be reliably used to identify the dominating natural vibration modes and the corresponding damping properties at a high confidence level.

Hong, Kim and Kim (2015a) discussed Systematic experiments on the bow flare slamming loads and resulting whipping vibration of a 10kTEU container ship. While, Kim, Ahn and Park, (2015) reported on a model test series regarding second order wave induced vibration of a large blunt vessel. Further, it has been reported on many model tests carried out to validate new numerical methods, covering different focus areas, ship types and vessel sizes: (Kim, Kim and Kim, 2015b), (Zhu and Moan, 2015), (Kim, 2015), (Wu, 2015), (Wang et al., 2016c), (Cai, Jiao and Ren, 2016) and (Zhang et al., 2016b).

In experiments on wave loads it is important that the desired wave parameters can be accurately simulated. Mozumi (2015) proposed a new method to measure the wave surface elevation in a wave basin by means of an array of small floats attached to a flexible net. Compared to conventional wave wire methods, this enables to trace oblique structures in three-dimensional, non-linear wave trains.

Full scale measurements of wave induced vibration give a better picture of the typical wave loads experienced during normal service than model tests since they must not rely on assumptions regarding the operational profile, the encountered wave environments etc.. Andersen and Jensen (2015) discussed that the expected extreme values of the wave bending moment are derived based on the dynamic hull stresses as monitored on three container ships over longer periods. In two cases the measured wave bending moments are shown to exceed the class design values, however, it must be considered that conventional class rules use safety factors on the quasi-static wave bending moment to account for whipping instead of explicitly increasing the rule design wave bending moment.

Storhaug and Kahl (2015) investigated the influence of wave induced torsional hull vibration on the fatigue damage of a 8.4kTEU and a 8.6kTEU vessel. Although similar in size, the ships were found to have strongly different torsional vibration damping, but for both vessels it was confirmed that torsional vibration damping significantly exceeded that of vertical vibration.

Ki, Park and Jang (2015) reported on measurements on a 14kTEU vessel during 1.3 years operation in Europe – Asia trade. Due to the mild encountered wave climate the highest measured wave bending moment was found to be only 70% of the design value. Further it was demonstrated that fatigue damage of the hull due to torsional vibration was insignificant.

Thanks to the advance of performance and condition monitoring systems in recent years, also hull load monitoring systems have become increasingly popular in shipping. As pointed out by Storhaug, Aagaard and Fredriksen (2016) such systems, due to their potential implications on ship safety, must be strictly quality controlled. A calibration procedure is proposed which accounts for the variation of the bending moment by static hull deflection (“hydroelastic effect”) and the axial strains caused by the fluid pressures at the ship ends (“end effects”).

Enhanced shipping activities in polar regions are expected in near future and thus also the monitoring of ice induced loads becomes increasingly important. E.g. (Suominen et al., 2015) reported on the determination of ice-induced loads by shear strain measurements at the main load carrying hull frames. The transfer functions between ice load and measured strains were reliably calculated for known location of the ice load, but if this is not the case the authors report on the risk of severely over- or underestimating the ice load.

Also warning systems on excessive ship motions and/or loads are further developed. Reliable far field wave observations are a prerequisite for a reliable system.

Yoshida, Orihara and Yamasaki (2015) summarise the findings of 5 years wave observations and motion monitoring by an onboard system. Wave height, period and direction measured by the wave radar showed fair agreement with crew observations and seaway forecasts. Also, the pitch motions computed from the measured wave data showed good agreement with the actually measured ones, however, agreement for rolling motions was less satisfactory.

Alford et al. (2015) implemented an environmental and ship motion forecasting system using a marine Doppler radar for far field wave observation, nonlinear wave theory to propagate the wave surface forward in time and seakeeping theory to predict vessel motions. Sea trials confirmed radar observations favourably comparing to in-situ buoy measurements, reasonable agreement of predicted and measured vessel motions and the ability of the forecast system to capture extreme waves during hurricane conditions.

Schwarz-Röhr, Ntambantamba and Härting (2016) addressed the inverse problem, i.e. to conclude from measured ship motions on the prevailing wave spectrum. Trials with a 20m vessel showed promising results but also demonstrated the need to consider the actual loading condition, inertia and speed dependent damping of the vessel in more detail.

3.5 Loads due to Damage following Collision / Grounding

Load implications on the ship after accidental damage remained an area of concern to the design and operation of ships. Accidental damage to ships and, subsequent, flooding can occur in a number of ways, but generally damages due to collision and grounding are most frequently observed and, hence, research focussed on these types of damage scenarios.

The study of Primorac Bužančić et al., (2015) investigated the effect on collision and grounding damage on the still water bending moment of a Suezmax double hull oil tanker. They employed a Monte Carlo simulation to generate possible damage scenarios and established histograms of relative bending moments considering the correlation between damage location and maximum bending load. They found that grounding damages in fully loaded condition can be expected to result in much stronger enhancement of the still water bending moments than collision damages.

Parunov, Corak and Gledic (2015) discuss the effect of collision and grounding damage on the vertical wave bending moment (VWBM) at the example of an Aframax tanker. They compare the widely used added mass method (mass of flooded seawater becomes a part of the ship mass) and the lost buoyancy method (damaged structure and tank contents are removed), the former being applicable for small damages and the latter better suited for large damage extents. The authors showed that RAOs of midship VWBM increase with increasing damage size and that the added mass method systematically provided larger maximum RAOs than the lost buoyancy method. Based on a comparison with model tests of a damaged warship, the authors concluded further that the RAOs of VWBM were overpredicted with the added mass method and slightly underpredicted by the lost buoyancy method.

Bennett and Phillips (2015b) report on an experimental investigation of the effect of damage on the motions and VWBM of a Leander Class frigate comparing the intact condition with one and two compartment damage conditions. Results show that the inclusion of an abnormal mass distribution due to damage has a significant effect on the magnitude of the motion and response RAOs in head and beam seas and that the severity of this effect increases with forward speed. For the two compartments damage case at higher wave frequencies up to 50–100% increases in the VWBM response were observed. Also, the advantages of digital imagery to analyse transient flooding processes is discussed. Numerical investigations for the same vessel and damage scenarios are dealt with in Bennett and Phillips (2015c). The results of the initial development of a two-dimensional hydroelastic model to predict the motions and glob-

al loads of the damaged ship in regular waves using a quasi-static approach are discussed and compared to the experimental data. Promising agreement between numerical method and experiments was found and thus, the ability to carry out systematic studies of the influence of damage location, severity and ship speed on the effect of damage on a vessel was demonstrated, however, presently under neglection of the transient flooding phase and three-dimensional effects. In future the authors aim to include these effects and to combine the method with a statistical analysis of the probability of occurrence of damage locations for collision or grounding. Thus a rational method to assess the consequences of collisions and groundings for the safety of individual ship designs may be developed.

4. OFFSHORE STRUCTURES - SPECIALIST TOPICS

Great advances in research for VIM in column stabilized platforms were observed. Driven by the crescent use those kinds of platform particularly by the petroleum, among other industry sectors, research was intensified, and important contributions are observed in the literature as described in bellow. Effort in development of mathematical models as well as CFD techniques through validations with laboratory experiment results, including real scale measurements were carried out in the last years. Main findings on those studies are evaluated as discussions presented in bellow. VIV is usually associated to underwater offshore structure with slender shapes, and, in its essence, it is the same what happens with the VIM in offshore floating platforms in sea current. Large effort has been made in the past to understand the physical phenomenon of the VIV, and fundamental studies are available obtained through scientific oriented research. Based on those results design oriented computer codes were developed for industry use. In this section, some studies related to mooring lines dynamics and coupled systems with floating structures are introduced.

Modeling of mooring lines dynamics due to direct waves and current, among others, and mainly those incoming from floating structure response to waves has been carefully studied. Investigations of nonlinear response of the mooring line dynamics as well as modeling of synthetic ropes were also observed.

Offshore operation to install equipment on to the seabed, and lifting operations to this purpose and other services in the open sea is always an important issue for the industry. Operational safety concerns and to make faster the operations are always key issues in the lifting operations. Active controlled lifting systems, numerical simulation models and tools and advanced study to develop reliable flexible multibodies system dynamic models were reported in the literature.

Advances were also observed on wave in deck loads issues in fixed platforms. This problem was taken in group research (JIP) projects, and main results have been reported in the literature. Based on those results and others reported in the literature, which including by means of CFD. Results also contributed for the establishment of procedures by the classification societies.

The large increase of interest for energy generated by the wind through national programs in different countries worldwide, many research have been developed. Prototype of floating wind turbines were installed with different type of floaters, and long term operational test in actual sea are being conducted, besides laboratory experiment to observe floating platform behaviour and performance and quality of energy generated by the wind turbines affected by platform motions.

4.1 Vortex-induced vibrations (VIV) and Vortex-induced motions (VIM)

4.1.1 VIV

Slender marine structures subjected to a flow, such as risers, may be subjected to vortex induced vibrations (VIV). This is a result of oscillating lift and drag forces related to shedding

of vortices. Such vibrations may induce dynamic stresses and significantly contribute to fatigue damage. They may also lead to amplified drag loads. Uncertainties on the prediction of VIV are partly related to the very complex nature of the fully coupled hydro-elastic response, mainly in the hydrodynamic modelling. A simple and conservative approach consists of using empirical response based models, which predict the steady state VIV amplitude as a function of hydrodynamic and structural parameters. These are formulated in offshore design codes for most flow regimes. Vedeld et al. (2016) propose a new response model to conservatively calculate the cross-flow VIV at low KC number regime related to wave dominated flow conditions.

Some of the present challenges in terms of VIV prediction by "force based" and "flow based" numerical models consist of: identify the correct variation and interplay of excitation and responses in space and in time; capture the possible stochastic behaviour of the responses; represent the response of higher order modes; calculate the responses in time varying flows. Most of the recent work on calculation methods have been performed on: frequency domain (FD) or time domain (TD) semi-empirical models and computational fluid dynamics (CFD) methods. Semi-empirical methods represent the structural part by analytical models, finite elements (FEM), or finite differences, while the hydrodynamics is based on empirical data from model tests. Recently novle model test study on vessel motion-induced VIVs have been performed by Wang et al. (2015a, 2016e, 2017a) and Cheng, J. et al. (2016), ranging from steel catenary riser (SCR), the water intake riser (WIR), the free-hanging drilling riser (FHR) and the steel lazy wave riser (SLWR). ITTC (2017) presents a comprehensive review of the experimental work in this topic, while the following paragraphs focus more on numerical methods.

A joint industrial and academic effort has been made to provide “Guideline on analysis of vortex-induced vibrations in a riser and an umbilical” which includes best practices on structural modelling, current profile description, heave induced VIV, fatigue calculation and VIV suppression. This study aims to understand and eventually reduce the considerable variation that is often seen today in VIV predictions. Part of these results on the empirical parameters are presented by Voie at al. (2017).

State of the art engineering tools to calculate VIV mostly apply FD semi-empirical methods. The following paragraphs describe some of the latest investigations with FD methods. Accurate VIV predictions require a good structural damping model, which usually is contributed mainly from material damping. For umbilical, different layers of the riser can slip between each other which leads to additional slip damping. Often structural damping data is not available and must be estimated. Passano et al. (2016) generalized a FD semi-empirical code (VIVANA) by considering material and slip damping. The latter is an input dependent on the mean tension and curvature amplitude. A specific finite element software is applied to estimate the slip damping (UFLEX2D) as a function of several parameters. The new procedure was tested in a numerical study with an umbilical in a lazy wave configuration and the results show that VIV is sensitive to the structural damping level. Parts of the umbilical with low tension have significant larger damping due to slip.

Another dominant parameter for VIV prediction is the hydrodynamic coefficient data base, including both excitation/damping force and added mass coefficients. Recently a novel inverse finite element method has been developed by Song et.al 2016. With the application of this method, for the first time, the real hydrodynamic coefficients distribution along a flexible pipe undergoing VIV are presented. The results indicated great differences between the real coefficients on a vibrating 3D flexible pipe and conventional ones got through 2D forced oscillation tests. This new observation demonstrated us the huge differences between the reality and current practices, and it has been one of the significant progresses in the VIV field in last several years. Zhang et.al (2017a) and Fu.et.al (2017a) further discovered great ramps of VIV hydrodynamic coefficients between the bare cylinder and the adjacent buoyancy elements, where the added mass coefficient could reach up to 40, which has been proved to be within

the same level as those observed by forced oscillation tests by Wu et al. (2017c). Furthermore, Zhang et.al (2017a) discovered that the sum of structural mass and added mass will be always continuous along the flexible pipe with staggered buoyancy modules under VIV conditions. This novel finding provides guidelines for the hydrodynamic coefficient model application in VIV predictions for risers with buoyancy elements, like steel laze wave risers.

The FD VIVANA software was applied by Wu et al. (2016b) to predict the VIV of a steel lazy-wave riser with staggered buoyancy elements in current. Due to different diameters, there is a competition between the vortex induced forces on the buoyancy elements and the riser. These effects are not considered by standard FD computer codes. Comparisons with experiments show that the response frequencies are over predicted, indicating that hydrodynamic force coefficients generalized from bare cylinder VIV tests may not be valid for riser segments with staggered buoyancy elements. Wu et al. (2017c) performed forced cross-flow (CF) VIV model tests with a rigid cylinder with staggered buoyancy elements. The forces on one of the buoyancy elements and on the complete test segment were measured and the related hydrodynamic data applied in VIVANA to predict the VIV response and fatigue damage of a flexible cylinder with staggered buoyancy elements previously model tested. Good predictions were achieved.

More recently, a unique modal space direct VIV prediction method has been developed and validated by Lu et.al (2017a). Different from the conventional empirical methods, this new method converted the VIV prediction problem into modal space, and solved the equations by graphically finding their crossing point of two curves of modal response and modal hydrodynamic force without any numerical iterations and calculation of energies. This method achieved 100% matches with those results by empirical method, but with clearer physical meanings and numerical stabilities, which will for sure advance the understandings of VIV prediction theories.

Although more focus has been given to CF vibrations in the past, in-line (IL) vibrations may contribute significantly to the fatigue damage of risers. IL vibrations are coupled to the CF motion and induce higher order harmonic loads in the CF direction. Wu et al. (2017d) present a combined IL and CF load model implemented into a frequency domain tool, together with validation by comparisons with test data with a flexible cylinder. A case study is also presented, consisting of a deepwater top tension riser subjected to sheared currents. The combined IL and CF response analysis gives less conservative estimation of the fatigue damage, as compared to pure CF analysis. Yin et al. (2017) performed model tests with a circular cylinder subjected to forced motions taken from measurements with a flexible pipe under VIV. The identified IL excitation coefficients were applied in VIVANA to predict the combined IL and CF VIV motions and compare with model test data. Application of the updated IL coefficients improves the prediction of the combined IL and CF VIV responses.

Time domain models allow the surrounding flow to be time varying, contrary to FD methods. Thorsen et al. (2016) applied a TD semi-empirical method with an improved hydrodynamic damping formulation and optimized exciting force model based on experiments. The resulting model is applied to simulate the CF oscillations of an elastic cylinder in stationary and oscillatory flows. Comparisons with experiments show good agreement in terms of frequency content, mode and amplitude of vibration. Thorsen and Sævik (2017a) used the same numerical model to investigate the VIV on a riser subjected to waves. The method was generalized in Thorsen et al. (2017b) by representing the structure by a nonlinear FEM and including the mean IL drag forces and related displacements and by Ulveseter et al. (2017a) to predict pure IL VIV. Further developments were presented by Ulveseter et al. (2017b) to investigate the stochastic response of long slender beams under stationary currents. The mean non-dimensional frequency of the synchronization is modelled as a simplified Gaussian process. The new model represents responses with jumps between eigen-frequencies and modes.

Comparisons with experimental data with a long riser in sheared current shows realistic predictions of the chaotic response.

Tsukada and Morooka (2016) present a numerical procedure to estimate VIV forces for a catenary riser, in the time domain, by applying the independence principle. Semi-empirical approach is adopted to estimate VIV forces, and it is proposed to be obtained them from lift coefficients (CL) and phases related to the riser movements determined from an experimental data set. And, Teixeira and Morooka (2017) present a TD semi-empirical method to calculate the CF VIV and IL displacement in uniform and sheared currents. The force model is selected depending whether the riser segment is on "power-in" (lock-in regions), or "power-out". Comparisons with experiments show good agreement in terms of VIV frequency, mode of vibration, envelops of maximum displacement and RMS of curvature. For sheared currents, the strain test data is underestimated, which is attributed to higher harmonic effects not correctly predicted.

Application of CFD is an alternative under development to the use of semi-empirical methods. Qiu et al. (2017a) presented a numerical benchmark study on the drag and lift coefficients of a marine riser with smooth surface. The flow was stationary and the Reynolds number range included the critical range. Eight organizations participated using methods based on Reynolds averaged Navier-Stokes equations (RANS), detached eddy simulation (DES) and large eddy simulation (LES). The dispersion of numerical results is very large. For example, the drag coefficient errors compared, to test data, are distributed from small values up to more than 250 %. Results from LES in general compare better with the experiments. It is possible to conclude that direct simulation of the flow around cylinders is still not mature.

As part of a study started several years ago, Constantinides et al. (2016) modelled a steel lazy wave riser subjected to in-plane current with 3D CFD simulations (AcuSolve). The software is based on a finite element solution of the Navier-Stokes equations. RANS is applied to model the turbulence. The structural problem is represented by linear superposition of natural modes calculated by the FEM code ABAQUS, while an iterative coupling scheme is used to couple with the hydrodynamic loading. Calculated strain standard deviations overpredict model test data, although the tendencies are correctly captured.

Tabib et al. (2017) conducted a fundamental study for the 3D flow past a fixed cylinder subjected to combined uniform and pulsating inflow conditions applying LES (OpenFOAM). Three Reynolds numbers are considered, including the transition regime. The pulsating inflow increases the asymmetry of the vortex shedding, the shedding frequency gets locked to the frequency of the pulsating inflow (for the cases studied) and the pulsating inflow increases the drag coefficient. Interaction between IL and CF VIV was investigated experimentally and with LES numerical simulations by Aronsen et al. (2017). Prescribed motion tests with "figure of eight" oscillations, in two opposite orbital directions, were performed with a rigid cylinder to measure IL and CF forces. The hydrodynamic forces are different for the two orbital directions. The forces present harmonics at multiples of the oscillation frequency, which are related to oscillations in the IL direction. LES predictions agree well in terms of global forces including higher order harmonics, vortex shedding modes and hydrodynamic coefficients.

4.1.2 VIM

Column supported offshore structures such as spars, tension leg platforms (TLPs) or semi-submersibles can experience vortex induced motions (VIM) when exposed to currents. VIM may occur for any oscillatory mode of the structure if the Eigenfrequency is close to the vortex shedding frequency from the structure. In areas such as the Gulf of Mexico where loop currents and associated eddies may occur, VIM may be an important design driver. Recommendations for taking VIM into account in the design of floating structures are given in DNVGL (2015), API (2015) and ISO (2013).

VIM may influence the design of mooring lines and risers of offshore structures in three ways. Firstly, the presence of VIM leads to an increased inline mean drag coefficient on the floater, secondly, the low frequency VIM motions of the floater may be large, and thirdly the VIM motions introduce additional low frequency load cycles in the mooring lines and risers. Susceptibility of a structure to VIM is conveniently expressed by the reduced velocity which is a measure of the ratio of vortex shedding frequency to Eigenfrequency in a relevant degree of freedom. In order to quantify VIM, model testing or, increasingly, Computational Fluid Dynamics (CFD) simulations are necessary since analytical methods are not generally available.

Whereas VIM has been observed in the laboratory for many types of column supported offshore structures, only Spar platforms have been observed to be subject to significant VIM in operational conditions. Generally, field observations show less VIM than prediction based on towing tests. Although this effect is not fully understood, it is clear that the full scale Reynolds Number (Re) is typically two orders of magnitude larger in the field than in the laboratory. Furthermore, the presence of waves and the variation in current in time and depth are typically ignored in model tests. Also, mooring lines, risers and other appurtenances which may not be modelled accurately in the laboratory may introduce significant additional damping in the full scale prototype.

The discrepancy between laboratory and full scale measurements has motivated a considerable research effort on the modelling of VIM by CFD. A project funded by the Research Partnership to Secure Energy for America (RPSEA) entitled 'Vortex Induced Motion Study for Deep Draft Column Stabilized Floater', has addressed the VIM response in detail through the use of both CFD and model scale testing (Antony et al., 2015). The project has produced a number of comprehensive CFD studies investigating the sensitivity of a deep draft semisubmersible to geometric parameters and to investigate the accuracy and modelling requirements of the CFD codes by comparing with model test results. The CFD codes which have been employed have been AcuSolve™ from Altair Engineering, Fluent™ from ANSYS, STAR CCM+™ from CD-Adapco (Antony et al., 2015), and the open source program OpenFOAM™ (Kara et al., 2016a).

An outcome of this work has been the publication of a best practice document for the analysis of VIV and VIM on offshore structures by CFD. Kara et al. (2016b) provide a summary of main techniques together with a discussion of their merits, give recommendations for modelling and quality assurance, and carry out a case study of a deep draft semisubmersible and compare the results with model test results.

In a more comprehensive Joint Industry Project, the VIM JIP managed by MARIN together with the University of Sao Paulo, the objective has been to compare CFD analysis with model test results and prototype data for a range of structures and provide recommendations for VIM quantification. Based on model testing, CFD analysis and full scale measurements on identical hull forms it was concluded that whereas scale effects, the presence of waves and the effect of current unsteadiness is of minor importance, the effect of additional damping from risers, mooring lines and other sources have a significant effect on the VIM amplitudes (Koop et al., 2016a). The accurate quantification of the prototype damping level is highlighted as a remaining challenge. Shear currents were not investigated as part of this JIP although it was suggested that this may not be a main explanation for lower VIM response in full scale, particularly not for relatively shallow multi column structures.

Scale effects were investigated directly by comparing CFD results at model scale and full scale Re (Koop et al., 2016b). It was stressed that the accurate calculation of VIM by CFD requires careful modelling and extensive validation of the results. It was concluded that the VIM amplitudes were quite similar in the two Re regimes but that a shift to lower reduced velocities occurs for the full scale case. It was acknowledged, however, that this observation

is at odds with other published results and that further investigation is necessary (Koop et al., 2016a). Useful literature reviews of the effect of wave, damping and mass ratio on VIM are included as appendices in this paper.

The effect of damping was investigated further experimentally as part of the RPSEA project. Sterenborg et al. (2016) investigated two deep draft semisubmersibles at subcritical Re and at reduced velocities ranging between 3 and 10. An external active damping system was developed which provided linear damping of the motion normal to the flow. The damping system consisted of active linear actuators which provided forces at the fairlead positions so that additional added mass or damping could be introduced while ensuring that the system was non-intrusive when switched off. It was found that external damping greatly affected the VIM amplitudes with reductions of 60% of nominal response for 25% of equivalent critical damping.

The importance of including the significant contributions to damping was highlighted in both the RPSEA project and in the VIM JIP. Jang et al. (2017) investigated a deep draft semisubmersible in a careful CFD analysis fully coupled with the mooring and riser system and compared the VIM results with an uncoupled analysis. The CFD analysis was carried out using Star CCM^{+TM} and it was concluded that the damping introduced by the mooring lines and the risers had the potential to significantly reduce the VIM amplitudes. It was also recommended to account for the asymmetry in the restoring since this could affect the coupling between the horizontal degrees of freedom and thereby affect mooring line and riser fatigue life.

In a similar study, Tang et al. (2017) carried out a coupled analysis of a Spar-type wind turbine combining aerodynamic forces calculated by blade momentum theory, first and second order wave excitation forces calculated by 3D potential theory, and vortex induced loading calculated using CFD with a nonlinear response model including mooring lines and nonlinear restoring of the Spar. It was concluded that the vortex induced motions could be governing for roll and pitch motion and that they could also influence other degrees of freedom due to nonlinear coupling between the modes.

Suppression of VIM by active or passive means has received considerable attention in the last years and considerable work is ongoing both to fully understand the VIM phenomenon and to identify effective suppression devices which do not significantly increase the drag on the floater. An interesting development is studies of suppression of VIM by water jets in the near field. Guan et al. (2017) applied a LES solver to the problem of estimating VIM with a jet flow on the wake side of the columns. The method was applied to a low $Re=2x10^2$ four column configuration in 2D and a higher $Re=2x10^4$ 3D analysis of a deep draft semisubmersible. They concluded that the VIM was significantly suppressed when a jet flow was present but found that the drag coefficient increased in the 3D case. Fu et al. (2016) used the Lattice Boltmann method to investigate 2D flow around a cylinder with a jet flow into the approach flow at $Re=6x10^4$. It was concluded that the jet flow resulted in a substantial reduction in the lift force on the cylinder and that further work is necessary to investigate this phenomenon in more detail.

4.2 Mooring Systems

ISSC (2015) presents a classification of methods available for solving the mooring lines dynamics and of methods for solving the coupled floater and mooring/riser systems dynamics, together with a discussion on the advantages and disadvantages of each approach. This Section starts directly with the latest developments on methods and tools for mooring analysis, namely for deterministic calculation of mooring line loads.

Existing lumped mass methods and finite element methods for cable dynamics provide accurate predictions of static and dynamic line tensions for many of the practical applications with chain and steel wire rope. Some of the present challenges include: modelling of snap loads,

high frequency mooring line dynamics, correct modelling of synthetic ropes dynamic behaviour and accurate estimation of platform low frequency motions in high seastates.

Snap loads on mooring lines may have different origins and they are characterized by a large local increase in tension that propagates along the cable. Palm et al. (2017) present a high-order discontinuous Galerkin (DG) formulation for cable dynamics to capture snap loads in mooring cables with high accuracy. The DG method consists of a finite volume scheme with each cell approximated using finite elements. The problem is formulated in a conservative form. An *hp* adaptive scheme is used to dynamically change the mesh size *h* and the polynomial order *p*, based on the local solution quality. An error indicator and a shock identifier are implemented to capture shocks with slope-limited linear elements, while using high-order Legendre polynomials for smooth solution regions. The authors report very good modelling of idealized shock waves by the method, as well as very good agreement with experimental data with snap load propagation in a mooring chain.

Chen and Basu (2017) investigated the structural shock wave propagation in a mooring cable. The wave is generated by fairlead excitation, propagates to the anchor and reflected back. The equations representing the lines' dynamics are formulated in a Lagrangian frame and solved with a finite-differences method.

Jayasinghe at al. (2017) describe and discuss high frequency mooring line dynamics observed in two FPSO installations. While standard mooring analyses account for low frequency and wave frequency loading of the lines only, this study identified torsional vibrations in deep water wire rope sections and high frequency oscillations of chain links within the chain hawse tubes. The root reasons were pointed as coupled axial-torsion effects for the first and heave induced VIV for the latter. The frequencies are one order of magnitude higher than typical wave frequencies. The authors point out that the related degradation mechanisms cause damage to mooring systems and that the possibility of such vibrations needs to be assessed and evaluated during the design.

Ghoshal et al. (2016) investigate the instability of mooring cables induced by combined hydrodynamic and ice loads. The authors present an analytical method based on model superposition for the cable vibrations. The model considers the geometric nonlinearity (nonlinear strain), while most mooring analysis neglect this effect. This nonlinearity plays a role in the auto parametric excitation of the cable which, combined with out-of-plane pulse loads due to ice, may lead to vibrations and instability.

Design of marine energy converters mooring systems is challenging for several reasons, including the behaviour in relatively small water depth, possible influence on the device efficiency and significant contribution to global costs. Luxmoore et al. (2016) propose a new active mooring system for wave load reduction in marine energy systems. The system is named Intelligent Active Mooring System (IAMS) and it applies a nonlinear load-extension curve that is adjustable to the wave conditions. The IAMS system is represented in numerical simulations by an analytical model validated through comparisons with test data obtained at the Dynamic Marine Component test facility at the University of Exeter. The authors perform dynamic simulations for a moored buoy with the IAMS system incorporated into the mooring lines and compare the results with prototype test data for validation. Further numerical studies with the validated model show the IAMS system can reduce significantly the mooring line tensions.

Existing methods for line dynamics provide accurate predictions for many of the practical cases. Presently, the uncertainty in mooring analysis is mostly related to the fairleads forcing motions prediction, namely of the platform low frequency motions. Standard diffraction analysis under-predicts the low frequency motions of Semi-submersibles in high sea states. The same is observed for FPSOs under certain conditions. The EXWAVE JIP (Joint Industry Project), ran from 2015 to 2017, with the objective of improving methods, procedures and stand-

ard industry practice in design prediction of extreme mooring line loads (Fonseca 2016, 2017). The focus was on the prediction of low frequency wave excitation, including wave-current interaction effects. The project proposes a semi-empirical formula to correct potential flow wave drift forces on Semis by accounting for viscous drift and wave-current interaction effects (Fonseca and Stansberg, 2017). Regarding FPSOs, experimental and numerical evidence shows that Newman's approximation for calculation of wave drift forces may be unconservative, even for deep water conditions and long natural periods of the system (Fonseca and Stansberg, 2017).

One more challenge with mooring analysis is related to large computational effort required for systems with many mooring lines and risers, especially when coupled computations are needed, in combination with a large matrix of environmental conditions. de Pina et al. (2016) propose a method based on artificial neural networks (ANNs) for the analysis of mooring systems of floating production units. The approximation method is suggested for preliminary design of complex systems with many lines and risers, where accurate simulation tools require a very large computational effort. The ANN method mimics the behaviour of the simulation model by identifying the relationship between the given inputs and the outputs. The method is applied to a Semi-submersible spread moored in deep water with four clusters of four lines and comprising 25 flexible and rigid risers. The ANN is trained based on the outputs from a quasi-static mooring analysis code. It is concluded that the ANNs provide fairly accurate values for the mooring line tensions and platform offsets.

Sidarta et al. (2017) propose an ANN based procedure for prediction of mooring line tensions from the platform motions. Good accuracy of predicted tensions is achieved, when compared to numerical simulations for conditions not included in the training data. The authors suggest the procedure may be used to assist the monitoring of moored systems.

Synthetic fibre ropes have advantages for deep water moorings due to almost neutral submerged weight. Compared to chain and wire ropes, they are characterized by much more complex nonlinear dynamic behaviour and correct numerical modelling is still challenging. This is related to the material properties, namely time dependent characteristics, viscoelasticity, viscoplasticity and large stretch, which need to be taken into consideration. Relevant experimental and numerical work has been developed as described below.

The usual approach for mooring system analysis with respect to axial stiffness is to use the upper bound axial stiffness for calculation of extreme tensions and the lower bound stiffness for horizontal offsets. This approach is conservative. More accurate methods may be applied, provided the dynamic stiffness properties are known. The Syrope JIP performed extensive change in length testing and proposes a conceptual model for the behaviour of polyester ropes describing the length of the rope depending on the preceding largest mean tensions (Falkenberg et al. 2017). Guidance for use of the model in mooring analysis is given. The authors give also recommendations for testing of ropes and analysis of test data for identification of model parameters.

The viscoelastic properties of synthetic fiber ropes may result on creep behaviour and creep rupture. Lian et al. (2015) propose a creep–rupture model to represent the creep behaviour of synthetic fiber ropes. The method is based on continuum damage mechanics, consistent with the fundamental laws of thermodynamics. The authors describe the identification method to achieve the model parameters from test data.

Huang et al. (2015) propose a new stress-strain constitutive model which accounts for the loading history and the time-dependent property of synthetic fiber ropes under cyclic loading. The nonlinear constitutive model combines a viscoelastic theory with a viscoplastic spring-dashpot-slider model. An identification method based on the dynamic test data is also proposed to estimate the model parameters. Predictions from the model are compared with test

data in terms of dynamic stiffness and hysteresis loop of aramid and polyester ropes under cyclic loading. The agreement is good.

The effects of aging and repeated load cycles on the rope performance is another research area. Lian et al. (2017) performed fatigue tests on high modulus polyethylene (HMPE) ropes. The analysis of test data shows the dynamic stiffness of HMPE ropes increases with increasing mean load and it decreases with increasing loading amplitude. The authors propose and empirical expression to predict the damage evolution under long term cycling loads. The expression accounts for the mean load and load amplitude. Flory at al. (2017) discuss axial compression fatigue in fibre mooring ropes, bringing analysis from recent failures. Axial compression should be avoided by proper rope design and operation of the lines, however, since the mechanisms leading to compression of fibers or yarns are not well known, problems related to axial compression fatigue are still reported. It is concluded that the rope structure, namely the rope and strand lay length, may cause axial compression fatigue when the subjected to many cycles and when the rope is prone to bend or rotate.

Synthetic ropes present advantages for floating marine renewable energy (MRE) systems, as compared to conventional chain or steel ropes. Since the requirements are different from those of the offshore oil and gas industry, specific studies are needed to assess the applicability of this technology to the MRE sector. Differences related to numerical modelling comprise, at least, highly dynamic loading characteristics, much lower water depths and different ratio horizontal offsets vs water depth. Weller et al. (2015) present a comprehensive review on the topic of synthetic ropes in the context of marine renewable energy systems. Focus in on the performance characteristics, classification, testing and application aspects.

Weller et al. (2014) present results and conclusions on the axial stiffness and damping for nylon 6 parallel stranded rope samples tested in the context of operational mooring loads representative of MRE devices. Harmonic and irregular loading regimes were applied to assess the influence of load history on time averaged and time varying performance. The authors conclude that the bedding-in level has significant influence on the short-term performance of the mooring system. It was also observed that the previous load history influences the instantaneous stiffness, which is in line with other studies, and it influences also the damping of the lines. The authors suggest that the rope performance is very much influenced by the instantaneous strain. A follow up investigation aimed at understanding the influence of aging on the rope performance (Weller et al. 2015). Tension-tension tests were performed on samples of a mooring line which was tested at sea for 18 months. The axial stiffness and line damping qualitative behaviour is qualitatively similar to that observed for the new samples. However, the aged samples show increased compliance, lower load capacity and reduced fatigue performance. Inspection showed fibre-on-fibre abrasion damage, with a contribution from debris found in the rope structure.

4.3 Lifting operations

Offshore lifting operations include air and subsea lifting. Two of its most important aspects are safety and operability. As the industry demands offshore operations with higher lifting capacities in deeper water depths and severe environment conditions, advanced technologies such as motion compensation systems, which are used to reduce the relative vertical motion of the load caused by the vessel-movement, time domain coupled vessel-lifting simulations and testing and verification methods have been developed and employed to support the lifting operations. Besides, regulatory bodies and industry have been updating the standards and guidelines for safer lifting operations.

The Bureau of Safety and Environmental Enforcement (BSEE) has initiated the lifting crane safety assessment study in 2014 and was carried out by ABSG (2015). The study involved analysis of lifting cranes and material handling equipment operating in the United States outer continental shelf (OCS), analysis of lifting incidents, and a review of industry standards and

practices. More than nine hundreds of cranes have been analysed including their crane mount type, boom type, capacity, manufacture/service provider, crane age, and incident information. The study indicated that the most of the incidents occurred during material handling, followed by pipe handling. It also indicates that the failures resulted from human error are more than twice the equipment capacity/functionality deficiency failures. It has been indicated that previous standards and regulations may not sufficiently reflect the modern subsea lifting operations. To facilitate the industry needs, classification societies have been updating their guidelines to address design, operation, inspection, and maintenance requirements for lifting operations. ABS (2016) has made a major update of the ABS Guide for Certification of Lifting Appliances based on industry feedback. Among others, the update includes new sections about subsea lifting requirements, motion compensation and rope tensioning systems for cranes. The DNVGL (2016) has updated the standards for marine operations to reflect current industry practices.

Woodacrea et al. (2015) provided a comprehensive review of vertical heave motion compensation systems used in ocean vessels from the early 1970s to modern systems. The paper examined in details of passive, active and hybrid active-passive heave compensation systems, and compared hydraulic versus electric winch drive systems. The paper indicates that the phase lags between the sensors and the system may have been the main reason for limiting total compensation against heave motions. The paper suggests that the model-predictive control may be able to improve the performance of active heave compensation systems. Richtera et al. (2017) presented an active heave compensation system using motion predictions based on a least squares algorithm. Its overall promising performance is demonstrated using a full-scale test bench.

One of the modern offshore lifting operations is the installation of offshore wind farms, which includes lifting the foundations using floating crane vessels, deploying and retrieving jack-ups' legs, and lifting turbine nacelles and rotors at a large lift height. Numerical simulation of these critical installation scenarios in the planning phase is very important for the safe and effective operations. Although motion simulations of floating vessels in frequency or time domain are standard industrial tasks nowadays, for lifting operations, however, multibody simulations must be performed, because the vessel motions influence the motions of the free hanging crane load and vice versa. Li et al. (2015) presented a numerical modelling and time-domain simulations of the lowering operation of an offshore wind turbine monopole with a diameter of 5.7 m. The study indicates that when using a floating installation vessel, the interactions between the motions of the vessel/crane and the monopole is quite large. Vorhölter et al. (2015) reported a time-domain analysis of typical lifting operations for the offshore wind industry. The study includes the designs of crane vessels in a range from converted conventional heavy-lift carriers over offshore construction class vessels to crane derrick barges with crane capacities up to 3,000 t are compared to each other by simulating typical lifting operations in the offshore wind industry. The lifting operations are simulated with non-linear seakeeping tools and the motion of the free hanging load is computed for operational setups. The results from these analyses can be used for operational limits of existing crane vessels and for design of future crane vessels.

Jeong et al. (2016) presented the simulation of lifting operations in an offshore support vessel. The simulation includes the calculation of dynamic responses of the vessel and the equipment. It also includes analysis of the lifting wire rope tension and the potential collision of the lifting object with surrounding objects for various operating conditions. The dynamic responses of the motions, the wire tension, and the relative position of the lifting object to other structures were calculated based on a multibody system dynamics approach. The simulation includes the lifting in air, going through the splash zone and sinking in deep water. During the lifting in water, the slamming load is calculated including the lowering speed and the geometry of the object. The analysis results show that fast lowering speeds result in a large variation

of wire tension. However, it should be pointed out that slamming load calculation is a complex process and the prediction of the slamming load in this study is quite preliminary and needs to be further improved.

A study of dynamic simulation of subsea equipment installation using an offshore support vessel based on flexible multibody system dynamics was carried out by Hong et al. (2016). In this study, the flexibility of the crane boom is included in the simulation model. The deformation of the crane boom varies during the lifting operation due to the vessel's motion induced by waves and winds. The flexible crane boom modelled using finite element approach is included in the equations of motion of a multibody system. The results indicate that using the flexible crane boom model resulted in higher dynamic amplification factors than using a rigid body model for the crane boom for various conditions analysed.

The offshore lifting operation is a complex process that involves multibody and control system. The consequence of an operation failure could be very costly. Testing and verifying the simulation tools and control systems is very important. However, it is difficult or expensive to establish certain test conditions to simulate real operations. The Hardware-In-the-Loop-Simulation (HILS) can be an effective method for testing the control system. Zhao et al. (2016) presented their study on the use of HILS for a heave compensator which is used to keep the position or the lowering speed of a lifting object. The HILS studied is composed of a control system and a HILS that is a simulation model of the support vessel by a software. The verification of the control system for the crane operation has been carried out with both a software programmable logic controller (software-in-the loop) and a hardware programmable logic controller (hardware-in-the-loop).

The safety of lifting operations and the up-time are very important for the offshore industry. The vessel up-time can be increased with heave compensation, particularly under adverse weather conditions. A robust simulation tool that can simulate the complete sequence of a lifting operation with all required details will increase the safety and efficiency of the real operation. Direct simulations should be performed during the planning of offshore crane operations as far as possible and feasible, especially for the complex lifting operations. Continuous improvement of the simulation tools to include all important parameters, such as the shielding effect from a large lifting object, damping, lifting speed and so on, may need to be included in the simulations.

4.4 Wave-in-deck loads

The problem of estimating the probability and magnitude of wave-in-deck loads on both fixed and floating structures has received considerable attention during the reporting period. The ShorTCresT Joint Industry Project (JIP) which was completed in 2014 concluded that whereas the crest height of the largest waves may not be significantly larger than second order predictions, the largest waves may be prone to wave breaking and thus have significantly larger particle velocities in the crest region (Hennig et al., 2015). This finding has given rise to the concern that the established practice for wave-in-deck loads on jacket structures may be significantly inaccurate. The established design practice involves calculating the crest elevation with the relevant return period for design and representing the associated wave-in-deck load with a regular wave with the same crest elevation and an associated period. If the wave which is governing for design is a breaking wave, the regular wave approach may give too low loads if the water velocity in the crest region is the governing property of load transfer.

Motivated by the concern that wave breaking is not adequately taken into account in structural evaluations of jacket structures, Mærsk Oil carried out the Tyra Field Extreme Wave Study 2013-2015 (Tychsen & Dixon, 2016, Tychsen et al., 2016). The aim of this project was to carry out a full long-term simulation of loading and structural response of the structures on the Tyra field at approximately 45 m water depth in order to verify their structural integrity. The study involved an extensive model test campaign, analysis work and CFD analysis in order to

calibrate the models which were used in the Monte Carlo simulation of the structures. This study concluded that the existing industry practice has non-conservative shortcomings, particularly relating to the assumption of a deterministic link between the crest elevation and wave load, and the presence of wave breaking.

The findings from the ShorTCresT JIP and the Tyra study have motivated several follow up JIPs, notably the BreaKin JIP (www.marin.nl) and the LOADS JIP. The LOADS JIP (Swan et al., 2016) aims to further clarify the role of wave breaking for the structural reliability of jacket structures in deep and intermediate water depths, and to propose an efficient Monte Carlo simulation methodology which will incorporate the effect of nonlinear crest elevations, short-crestedness and the effect of wave breaking in load calculations.

On 30th of December 2015, the semisubmersible drilling rig COSL Innovator was hit by a large wave. The wave impacted against the front of the deck box on the lower deck and the mezzanine deck, broke 17 windows and caused one fatality. The Petroleum Safety Authority of Norway (PSA) has issued an investigative report about the incident (PSA, 2016). As a result of this accident, the air gap and the associated horizontal wave-in-deck impact loads for Mobile Offshore Units (MoUs) have received considerable attention in the reporting period.

DNVGL has issued two Offshore Technical Guidance notes in order to aid the analysis of MoUs. DNVGL-OTG-13 (2017) gives recommendations for air gap calculations whereas DNVGL-OTG-14 (2017) gives recommendations for horizontal wave impact loads, evaluation of global structural integrity and recommendations for model testing of MoUs with negative airgap in front of the deck box. DNVGL-OTG-14 provides generic load curves for horizontal wave impact loads conditional on the airgap exceedance in front of the deck box (Johannessen et al., 2017).

The recommendations in DNVGL-OTG-13 are based on linear radiation-diffraction analysis and gives recommendations for empirical corrections to these results in addition to considering effects due to slowly varying motion and static heel. A review of the methodology recommended in DNVGL-OTG-13 was presented by Pessoa & Moe (2017).

Linear radiation-diffraction methods have significant shortcomings in calculating air gap of semisubmersibles in storm conditions. The shallow pontoons and large column diameter of many modern MoUs, and the presence of currents, make the calculations particularly challenging. There is considerable work currently underway to improve the methodology of analysis and it is expected that several publications will be available in the next reporting period. There is ongoing work on weakly nonlinear time domain simulations for air gap predictions (Kvaleid et al., 2014), on the quantification of the effect of wave-current interaction on air gap (Hermundstad et al., 2017), and on air gap predictions by CFD methods, predominantly Volume of Fluid formulations.

There is also ongoing work on tackling the full problem of wave-in-deck and air gap calculation by CFD where the floater motion, the wave surface elevation and the wave-in-deck loads are solved simultaneously. CFD has been applied successfully (Pakozdi et al., 2015, 2017) to enhance model test results by iteratively matching measured surface elevation to the surface elevation calculated in CFD, thereby obtaining the wave properties and loads over the entire structure for a measured event.

Research about improved analysis techniques mainly focuses on the deterministic problem of air gap and wave impact loading. CFD is computationally intensive and only a relatively small number of wave events can be investigated. For wave-in-deck problems, the statistical problem of estimating the load or response within a prescribed annual probability of occurrence is a significant challenge. The problem of estimating wave impact loads with a prescribed annual probability of occurrence and the relative importance of the long term and short term variation in seastate parameters and individual waves respectively, has been dis-

cussed by Johannessen & Hagen (2016). The statistics of air gap and wave impact over a deck with a finite extent has been discussed by Hagen et al. (2016), whereas the safety of fixed and floating structures subject to wave-in-deck loads have been discussed in the context of uncertainties in metocean conditions by Haver (2017).

4.5 Floating Offshore Wind Turbines

With the first offshore wind farm stated delivering electricity in 2017, it has been predicted that the development of offshore wind farm will continue to grow. James and Costa Ros (2015) provided comprehensive market and technology review of floating offshore wind. It reported that semi-submersible, spar-buoy and tension-leg platform are three dominant floating wind concepts mainly due to their motion performance and relatively mature fabrication and installation technologies. It also reported that, among others, advanced modeling tools, including numerical and model testing, are very important for understanding and optimizing the performance of the offshore floating wind turbines.

A lot of studies on the simulations and model tests have been carried out recently. Caille et al (2017) reported the work on the model test and simulation comparison for a tension leg platform (TLP) floating wind system. The model test was conducted in 2015 at MARINs offshore basin with the model scale of 1/40. The model includes turbine, platform and moor-ing system. The simulation was performed with Ocaflex coupling with recorded aerodynamic forces at tower top and with DeepLinesWind use the aerodynamic loading computed with boundary element method from the measure wind. The paper indicates that for the loads on the platform by using aerodynamic forces inputs and using DeepLinesWind calculation from wind speeds are quite close are comparable with the measurement. to those for ations is very satisfactory for both the FCS and SCS approaches: mean values and RMS are in very good agreement as well as the frequency content of the signals. Oggiano et al. (2015) carried out an experimental investigation on a 1/40 model scale of two different tension-leg-buoy (TLB) platforms, including tower and mooring system, at a wave tank in Deep Wave Basin at IFREMER facilities in Brest, France. The test results are compared with CFD simulations, using Volume of Fluid (VOF) method included in the STAR-CCM+ code from CD-adapco. Good agreement were found for the tower motion and mooring line tension in regular wave by comparisons with heave free decay tests.

Lopez-Pavon and Souto-lglesias (2015) proposed improvement in the hydrodynamic design of semisubmersible concept by investigations of hyrdrodynamic coefficients of a semi-submersible floating offshore wind turbine through experiment and numerical simulations. Forced heave oscillation tests were conducted in a towing tank with a 1/20 model scale for one column of the platform, in order to compare hydrodynamic coefficients of a plain solid heave plate and a flapped reinforced one. Measurements of dynamic pressures on both heave plates, added mass and damping coefficients were also presented. Numerical simulations were conducted with a wide-spread frequency domain panel method (WADAM) and a RANS CFD commercial code (ANSYS CFX).

Allen et al (2017) reported the 6-year effort in research and scale model testing of floating wind turbines as part of the VolturnUS project from the DeepCwind Consortium. The 1/50 scale model tests have been carried out for a generic tension leg platform (TLP), a semi-submersible (semi), and a spar-buoy (spar) floating platform at MARINs test facility. In 2015, the University of Maine has established an advanced Wind/Wave test facility and a 1:52 scale model of the floating wind turbine of the Volturn as a final design was carried out in 2016. A number of model tests have provided the key insights into the behavior of floating offshore wind turbine (FOWT) platforms as well as improving the ability to perform model tests of FOWTs. Data from these tests has been used for numerical simulation validation for engineering software FAST and a number of other analysis tools. Viselli (2014) and Viselli et al (2015) reported the model test of a 1:8 scale floating wind turbine offshore in the Gulf of

Maine. In the summer of 2013, UMaine launched a 1:8-scale model VolturnUS offshore Castine, ME ([32], and [36]). This concrete semi-submersible platform supported a fully operational scaled wind turbine and was the first grid-connected floating offshore turbine deployed in the United States.

Tomasicchio et al (2017) published their work on the dynamic response of a spar buoy wind turbine under different wind and wave conditions. The responses were studied through model tests of 1/40 scale and numerical simulation using program FAST. The model tests were conducted at the Danish Hydraulic Institute (DHI) offshore wave basin. The simulation program FAST was calibrated using the measurement data and the mooring lines were modeled as quasit-static taut or catenary lines in the FAST simulation program to simulate the coupled system of mooring, platform and turbine. The paper indicates that the simulations shown a good agreement with the dynamic responses determined by the observed results in terms of displacements, rotations, forces accelerations. The paper also indicts that mooring line loads are overestimated in the range of higher frequencies.

Bayati et al (2017) provide their work on the use of numerical and experimental method to simulate the surge and pitch motions of a semi-submersible floating offshore wind turbine through the "hardware-in-the-loop (HIL)" approach. It is a hybrid approach that combines the measurements and computations in real time during the tests which allows some parameters obtained through computation for inputs to the testing, while the computation takes in the testing results, or say testing in the simulation loop. The HIP approach provides the possibility of exploring the advantages of each facility and overcoming the scaling issues when testing both wind and waves in a single test facility. The paper presented the validation of the approach using simplified cases of two degree of freedom system (surge and pitch) for free decays, regular and irregular waves. The results show the approach is promising and is possible for the application of 6-DoF system.

Karimirad et al (2017) presented the comparison of real-time hybrid model testing with numerical simulations. The experimental data is from a 1:30 scaled model of a semisubmersible wind turbine. Numerical simulations were performed by using software SIMA by MARINTEK that simulates the coupled aero-hydro-servo-elastic system. The results in terms of dynamic time series, spectra and statistics of the responses are compared between the two methods for different load cases considering irregular waves and turbulent wind. Test results agree with numerical simulations and that either Newman's approximation or the full second order QTF can give good agreement in the low-frequency responses for this platform when combined with the selected hydrodynamic viscous drag coefficients.

It has been indicated that the as wind farms are moving towards deeper water, the floating vertical axis wind turbine (VAWT) seems to be a very promising alternative to the floating horizontal axis wind turbine (HAWT) which has been widely studied. The development of floating VAWTs is still at its early stage. Borg and Collu (2015) presented a comparison between the dynamics of horizontal and vertical axis offshore floating wind turbines. Cheng, Y., Ji, C.Y., Zhai, G.J., et al. (2016) have developed fully coupled method for numerical modeling and dynamic analysis of floating vertical axis wind turbines. The actuator cylinder (AC) flow model for aerodynamics of floating VAWTs is established with the consideration of turbulence effects, dynamic inflow and dynamic stall. The aerodynamic code is then coupled with SIMO-RIFLEX to achieve a fully coupled simulation tool which can account for the aerodynamic, hydrodynamics, structural dynamics and controller dynamics in the system. The simulation tool has been validated with another software using a land based VAWT and a semi VAWT and good comparison was achieved.

Cheng et al (2015) also carried out study on the dynamic responses of three floating wind turbine concepts of VAWT with a two-bladed 5 MW Darrieus rotor. The turbine was mounted on floating support structures of spar buoy, semi-submersible, and tension leg platform (TLP).

Fully coupled nonlinear time domain simulations were conducted. A series of load cases with turbulent wind and irregular waves were carried out to investigate the dynamic responses of these three FVAWT concepts by estimating the generator power production, the platform motions, the tower base bending moments, and the mooring line loads. The findings indicate that the motions of the spar and semi-submersible may be higher, but the mooring line load are relatively low, while these findings are opposite for TLP concept. The paper does not recommend TLP as a good substructure for a vertical axis wind turbine unless the cyclic variation of aerodynamic loads is significantly reduced.

Overall, it has been indicated that there are integrated modeling tools exist and the accuracy of the software currently available are generally good or very good in comparison with model testing. However, industry modeling experts have suggested that some platform designers are not accurately capturing the holistic system response (e.g. coupled analysis of the turbine, platform, moorings, and anchors), and that further work is needed to improve modeling tools James and Costa Ros (2015). Such tools would need to incorporate all aspects of the floating wind system to undertake coupled analysis of the various components. Of particular importance maybe is the need to incorporate feedback from offshore demonstrations to validate the models. This may also need to be closely tied with efforts to develop advanced control systems. The modeling gap around the geotechnical conditions at a site, which greatly impacts the mooring and anchoring system, may need to be developed. Without the ability to model anchor geotechnical dynamics, there is a risk that this will result in conservative and more expensive designs.

Advanced tank testing facilities such as the University of Maine and others can help to de-risk and optimize the design as much as possible before moving to full-scale offshore demonstrations, which can ultimately lead to less conservative and more competitive designs.

5. PROBABILISTIC MODELLING OF LOADS ON SHIPS

The design process of ship structure requires knowledge of extreme lifetime loads, where wave induced loads contribute significantly. These wave loads represent the environmental conditions encountered through the entire life of the ship. The wave loads can be obtained from the processes of combined with the extreme of random process theory and long-term statistics. These techniques enable waves to be defined in a mathematical form that can be used to calculate wave loads on the ship and ultimately the response of the ship to these loads.

5.1 Probabilistic Methods

Because of a consequence of linearization, the linear superposition of hydrodynamic problems is allowed with the aid of perturbation analysis. Superposition plays a great and basic role in efforts towards the solution. The responses of a ship in irregular waves can be considered as the summation of the responses to regular waves of all frequencies. In this principle, obtaining the prediction of statistical characteristics of motions and structural responses of the ship is available in irregular waves.

Soukissian (2014) used two general bivariate probability models (significant wave height–wave direction, wind speed–wind direction and wave direction–wind direction) for the analytic description of the wind and wave climate of an area, taking account of directional characteristics in addition to the usual linear metocean parameters. The probabilistic description of the wind and wave regime is confined to the linear characteristics of sea states and wind conditions, i.e., the significant wave height, wave period and wind speed. Rapidly emerging applications, such as offshore wind and wave energy utilization, are largely dependent on the accurate description of the directional wind and wave characteristics of the areas.

C´orak et al. (2015) presented the article deals with correlation analysis between wave and whipping bending moments and their load combination factors. It is shown that reconstruction of the time signal from the frequency domain is suitable method for the prediction of the most

probable values of bending moments and short-term load combination factors. The significant influence of the random phase angles on the extreme values of bending moments and load combination factors is confirmed. Since some realizations show a significant scatter, large number of time simulations are needed for the prediction of the most probable values. The comparison of a limited number of model test data with the most probable values derived from the numerical simulations has revealed a decreasing trend of the short-term load combination factors with the increasing ratio of the most probable extreme wave and whipping bending moments. It can be concluded that the overall whipping influence and the load combination factors are expectedly higher for the larger ship.

Lucas and Guedes Soares (2015) presented the results of the fit of three bivariate models to twelve years of significant wave height and mean zero-crossing period data of swell, wind sea components, and combined sea states from Australia. The conditional model with a lognormal distribution for the significant wave height and lognormal distributions for the zero-crossing period gave the best fit for the total sea states and for the wind component. In case of the swell component the conditional model with a Weibull distribution to the significant wave height and a lognormal distribution to the mean zero-crossing period gave a relatively close fit to the data.

Bitner-Gregersen et al. (2016) drawn attention on the uncertainties associated with wave description as this is an important input to assessment of loads and motions and fatigue damage of ships and offshore structures as well as to model testing. Several of these uncertainties still require further research and are not fully quantified herein. Effects of some of these uncertainties on assessment of loads and responses is demonstrated putting particular focuses on very steep waves, their impact is significant. The identified uncertainties related to the metocean description apply also to these structures. Awareness of importance of accounting for uncertainties associated with environmental description in risk assessment of ship, offshore and renewable energy structures is continuously increasing with in the marine and renewable energy industry.

Alibrandi and Koh (2017) presents the dynamic analysis of a deepwater floating production systems has many complexities.The sea state is random; hence the need of stochastic dynamic analysis. In the paper, the evaluation of the non-Gaussian distributions of the responses of the systems is developed through the well-known First-Order Reliability Method (FORM) and the recently proposed Secant Hyperplane Method (SHM). They give rise to two stochastic Equivalent Linear Systems (ELS) allowing to determine any quantity of engineering interest: The Tail Equivalent Linear System (TELS) based on FORM and the Tail Probability Equivalent Linear System (TPELS) based on SHM. The TELS is the Equivalent Linear System (ELS) having the same design point of the original nonlinear system. The Tail Probability Equivalent Linear System (TPELS) is the ELS where the difference in terms of tail probability between the TPELS and the original system is minimized. A simplified 2-degrees-offreedom model is used to demonstrate how these methods can be effective for stochastic dynamic analysis of a marine riser.

Silva-González et al. (2017) modelled the probability distribution of extreme values with the peaks over threshold method. It requires an appropriate estimation of the threshold above which exceedances are considered to be a sample from a generalized Pareto distribution. They used the applicability of four methods developed for hydrological, coastal engineering, financial and stock market purposes, to the case of wave heights from extreme sea conditions due to storms, where significantly less amount of data may be available. Based on the results of this assessment, an improved square error method is formulated, which further allows evaluating the uncertainty in threshold estimation, as well as the uncertainty in the estimation of wave heights for the given return periods.

5.2 Equivalent Design Waves

The concept of design waves is used in the direct calculations to reduce the number of load cases to be checked for yielding, buckling, ultimate or fatigue strengths of marine structures. A design wave is an equivalent wave or wave group representing the long-term response of the dominant load parameter under consideration. The equivalent design wave or response conditioned waves are then defined by the following parameters: ship speed, frequency, wave heading, wave amplitude and phase.

Fukasawa and Kadota (2015) presented the research on the method for determining significant short-term sea states for fatigue strength of a ship. In the paper, taking accounts of stress histories which would be effective in the crack initiation and propagation, the significant short-term sea states for fatigue strength of a Post-Panamax container ship was clarified by estimating the occurrence probability of the stress range of the ship in her lifetime. The dominant short-term sea state to each occurrence probability of stress range varies from the sea state of smaller significant wave height to that of larger ones. The mean wave period is not that much different but is slightly increasing with the decrease of probability.

Klein et al. (2016) introduced the Peregrine breather solution of the nonlinear Schrödinger-type equation as an innovative design wave. The major benefits are the potential to generate abnormal waves of certain frequency up to physically possible wave heights, the symmetrical abnormal wave shape and the availability of an analytical solution. To evaluate the applicability of the Peregrine breather solution as design wave, wave-structure investigations with a LNG carrier were performed in a set of Peregrine breathers at certain frequencies. The investigations comprised model tests as well as numerical simulations. Zhang and Guedes Soares (2016) studied the behaviour of an LNG carrier and chemical tanker responses to abnormal waves simulated by the nonlinear Schrödinger equation. Wang et al. (2016b) presented that the wave surfaces of extreme sea states are generated by a nonlinear Schrödinger equation, and the ship motions in thee xtreme waves are calculated numerically by a nonlinear time domain seakeeping code.

Fang and Chan (2016) presented that a three-dimensional linearised potential theory has been used for the investigations of wave load characteristics of the high speed trimaran travelling in short-term waves. The wave loads including the shear forces, bending moments and torsional moments at one transverse section of the trimaran ship hull and longitudinal section of connected deck are predicted at various wave heading and ship speeds. The characteristics of longitudinal and transverse sectional wave load responses of the trimaran ship have been discussed and can be used for the selection of ship speed and heading in design wave conditions.

Fukasawa and Hiranuma (2016) presented that the long-term prediction of vertical wave bending moment is made firstly for various size container ships. The time-domain nonlinear simulations are then conducted in design short-term sea states with the use of design irregular wave method. The vertical wave bending moment required by UR S11A is much larger than that by UR S11 in sagging side. With the increase of the size of container ship, the maximum vertical wave bending moment calculated by using the design irregular wave becomes larger in sagging side than that by IACS requirement S11A. The maximum vertical wave bending moment calculated by using the design irregular wave exceeds that by IACS requirement in hogging side in larger container ships.

Wang and Guedes Soares (2016a) presented calculations of ship motions, slamming occurrence probability and slamming loads on the bow of a ship hull in irregular waves. The results are compared with the experimental data from model tests of a 170m chemical tanker with Fn=0 in head seas. Ship motions are calculated by using a partially nonlinear time domain code based on strip theory. Two estimated significant slamming events are simulated by using the Arbitrary-Lagrangian Eulerian (ALE) algorithm, based on the calculated relative entry velocities in the numerical procedure. Hauteclocque et al. (2017) presented a systematic and

consistent approach to develop new wave loads formulae, based on the direct computation. The rules are based on the equivalent design wave approach that has been shown accurate. The result is the new rule formulae that are implemented in the new BV rules for container ships. Those new load definitions match quite accurately to state-of-the-art calculations and are thus expected to reflect more closely the reality. The uncertainties of the derived formulae (compared to direct calculation) is well characterized, allowing further partial safety factor calibration.

Aggarwal et al. (2017) presented the dynamic characteristics of spar based floating 5 MW offshore wind turbine (OWT) under operational and survival conditions. The OWT is subjected to combined wind and wave loads according to irregular Pierson-Moskowitz spectrum. In this paper, the extreme values are obtained by fitting the peaks in the tail regime using a Weibull-distribution. While one obtains Gaussian responses under the survival loads, the operational conditions have non-Gaussian responses and also larger than survival ones.

Darie and Rörup (2017) presented the paper deals with the current efforts to address the complexity of calculation of extreme loads associated with non-linear finite element structural analysis. A hydrodynamic approach based on 3-D Rankine method is used. The generated loads for critical load case are transferred to a global structural FE model. Finally, using the non-linear finite element method, the hull girder ultimate capacity of container ship is calculated. Investigation on HGULS (Hull Girder Ultimate Strength) margins against the direct calculated load obtained by spectral approach was carried out for three large container ships. The calculated loads (EDW; Equivalent Design Wave) are higher than allowable loads given by UR S11 A, since the IACS routing factor is ignored in this investigation. The FE results, in terms of capacity usage factors, show for these three container ships, that the oblique seas, particularly 60 deg. wave heading can be important for HGULS assessment. The presented effects of oblique sea on HGULS assessment are covered in the existing rules, UR S11 A, by a partial safety factor for the vertical wave bending moment.

5.3 Design Load Cases and Ultimate Strength

Various design loads used in the strength assessment of ship structures have been introduced by classification societies. Most of these design loads have been determined as standard loads. Ultimate strength design assigns each load with a load factor and combines the resulting modified load values in various ways. The hull girder strength is the most critical failure mode for the hull structure and the design load conditions are the key factors for the ship ultimate strength analysis.

Ozdemir et al. (2015) presented the results of new method depends on the estimated buckling strength values. If the estimated buckling strength is closer to the those of FEM calculations, ultimate strength by the new method would be more accurate. However, in case of stiffened panels with many stiffeners and thinner plate, derived formula underestimated the buckling strength as well as ultimate strength. This may be attributed the underestimation of effective breadth of slender plates beyond local plate buckling.

Naruse and Kawamura (2015) presented that the reduction of ultimate strength and reliability index of the two bulk carriers after similar scale collision is computed and compared. Residual rate of ultimate strength, RSI. of the bulk canier after CSR is larger than the bulk carrier before CSR. However, reliability index of the bulk carrier before CSR is larger. Reduction of ultimate strength and reliability index after corrosion is computed and compared. It is found that good effect for corrosion by using double hull structure.

Tunea and Uguflu (2015) conducted a series of nonlinear finite element analyses to determine the effect of system parameters on load-carrying capacity of stiffened plates. Ultimate strength investigation on multi-parameter space is performed by regression analyses provided that the parameters have linear relation. The increase of both plate slenderness and stiffener

slenderness affects the ultimate strength negatively. The ultimate strength is more sensitive to the variation of the stiffener slenderness compared to the plate slenderness. The stiffener-to-plate area ratio and slenderness ratio have similar influences on load-carrying capacity. The ultimate strength decreases with the increasing parameters.

Kotajima et al. (2016) presented that the non-linear FEA is carried out by using a commercial FEM software, LS-Dyna, in order to understand the longitudinal collapse behavior of the amidship section structure of a container ship under the dynamic loading. The half-sinusoidal loads of hogging moment with different period were applied to the ship structure. It is found that the residual deformation after the loading is different if the period or amplitude is different. It is concluded that the effect to the ultimate strength is very small, while there is a possibility of small increase of ultimate strength under the dynamic loading with short period compared with that under the quasi-static load.

Rajendran et al. (2016a) presented a body nonlinear numerical method based on strip theory to analyze the vertical responses of a bulk carrier, container ship and a passenger ship. The numerical ship responses in abnormal waves and extreme sea conditions are also compared with the measurements in a wave tank. The pronounced bow flare induces strong nonlinearities in the vertical responses in rough seas and the linear or evenpartially body nonlinear methods are not enough for accurate calculations in those conditions. Rajendran et al. (2016c) presented the same code was used to calculate the vertical responses of a container ship in extreme sea conditions including abnormal waves. The study emphasized that for ships with large bow flare and in extreme sea conditions, the body nonlinear hydrodynamic forces played a significant role on the load acting on ships.

Peschmann et al. (2016) presented the new developed requirements of the UR S11A on existing containership designs. It is shown that even though the load requirements have changed significantly, the impact on the existing designs is limited and the safety margin of existing ships can be judged as appropriate. It is emphasized that the consequence on actual design scantlings could be limited by considering permissible hull girder values that more closely reflect the actual still water bending moments and shear forces along the hull. The new developed requirements in the UR S11A are more transparent, consistent and ship specific. In addition, it extends and harmonises the application of some key elements of the CSR and applies them to container ships. In connection with the new requirement UR S34, a significant step has been made to align requirements to enhance the safety of new innovative containership designs.

Fischer et al. (2016) developed a simplified procedure for the determination of the ultimate load and associated spindle torque of propeller blades. Various FE analyses were carried out to investigate the elasticplastic load-carrying behavior of propeller blades. The results obtained with the simplified procedure show good agreement with nonlinear FE analyses of a blade candidate where reduced spindle torque is observed due to failing local section. The ultimate blade load associated with the bending moment may be calculated using the shortest distance between failing section and load application point, with an allowance of 5% to avoid nonconservative results in sections with pronounced curvature.

Peschmann and von Selle (2017) considered the experience gained during the implementation phase of the GBS Standards from a Classification Society perspective following the initial verification. The IMO Goal Based Standards for Bulk Carriers and Oil Tankers (GBS) were adopted and implemented in the SOLAS convention. IACS developed the Common Structural Rules for Bulk Carriers and Oil Tankers (CSR), which included GBS considerations. IACS and the individual member Classification Societies submitted the CSR to the IMO for the GBS verification audit and the GBS initial verification audit confirmed that the CSR complies with the GBS. Therefore, the linkage between the CSR and the GBS were confirmed.

Zhang et al. (2017) presented an overview of recent investigations on the ultimate strength of hull girders and the attention has been particularly paid on large container ships hogging bending. Through the limited number of analyses on larger container ships, it is seen that the CSR method gives 10% to 15% higher than FE results and the LR 20202 method for hull girders' ultimate capacity in hogging bending. For hull girder collapse analysis of large container ships in hogging conditions, a double bottom factor of 1.15 is a first good approximation. However, initial analysis using simplified analytical methods show that the double bottom factor is in the range of 1.1 to 1.2 for container ships between 3600 TEU to 22 000 TEU.

Fang et al. (2017) predicted the structural responses of a high-speed monohull with different wave amplitudes. The hydrodynamic loads of a high-speed monohull have been simulated with different wave amplitudes and applied to the FEM model for the structural response calculations in regular design waves. Based on the numerical predictions, the longitudinal stress RAO (Response Amplitude Operators) increase in sagging condition when the wave amplitudes increase. Furthermore, the longitudinal stress RAO decrease in hogging condition when the wave amplitudes increase. The nonlinear effects of structural responses for a high-speed monohull are significant with various wave amplitudes in design wave conditions.

Kim and Paik (2017) presented that the aim of this paper is to develop a fully automated methodology for the optimum design of hull structural scantlings for merchant cargo ships. The ships are modelled by plate-shell finite elements. A full optimization technique with multi-objectives is applied for minimizing structural weight and maximizing structural safety. The developed procedure is applied to the hull structural scantlings of a very large crude oil carrier (VLCC), and this test demonstrates the procedure's capacity to meet the strength requirements of common structural rules. The proposed procedure reduces the number of man-hours required by about 20%, lightens the structural weight by 3% and improves the safety factors for the critical members.

6. FATIGUE LOADS FOR SHIPS

It is understood from previous ISSC Loads Committee Section that fatigue design most often requires the assessment of a lifetime vertical bending moment histogram for a ship. The lifetime bending moment histogram summarizes the ranges of bending moment magnitudes and their corresponding number of cycles expected during the ship's service life. These bending moments include those due to changes in wave height and slam induced whipping. Typically, the longitudinal bending moments and shears are determined from the weight and buoyancy distributions, treating the ship as a free-free beam. In many cases, the effects of lateral bending and/or torsional loadings may not need to be included when computing the lifetime stress histogram for a monohull due to the fact that the most important internal forces and moment on a monohull are the vertical shear and longitudinal bending moment obtained in head and following sea. However, the effects of transverse moments, horizontal bending moment and torsion are significant for vessels with large deck openings, e.g. container ships, or also for multihull designs such as catamarans or trimarans due to the presence of side hulls and the cross structures between the hulls. Multihulls are subject to more primary types of wave loads than monohulls. Since the interaction and phasing of multihull loads cannot be easily described by generalized formula, it is expected that direct hydrodynamic and structural analysis methods will be increasingly used to determine the resulting spectrum of stress cycles at the locations of interest within the hull structure. The complication arises because the various primary loadings are acting at different magnitudes and frequencies that superimpose each other as they combine and interact to produce a certain stress variation at the structural detail of interest. Smaller cycles from the less dominant primary loads are expected to combine with the more dominant primary loads. The slowly varying narrowband response and associated Rayleigh distributed extreme assumptions usually made for monohull responses to an active seaway, would thus be inappropriate for multhulls. As a multihull form encounters and responds to an active seaway at specific speeds and headings, the main structural members of

the ship are loaded in numerous ways. E.g. for a trimaran, the forward monohull portion of the hull is loaded by the familiar longitudinal vertical and longitudinal lateral bending moments produced by vertical and lateral shear forces, as well as torsion about the longitudinal axis. These loadings, of course, continue aft into the trimaran portion but are influenced by the presence of the outer hulls. The outer hulls themselves can respond in a number of ways, whether in-phase or out-of phase with one another and the center hull. In addition, the presence of the center hull obviously shelters one of the outer hulls depending on the heading, so there is likely also a leeward and waveward component to the outer hull loadings. Be that as it may, the loadings associated with the outer hulls are pitch connecting (torsional moment about the transverse axis relative to the center hull), transverse bending (prying and squeezing of the outer hulls about a longitudinal axis), and splaying (torsion of the outer hulls relative to the center hull about a vertical axis). Aside from identifying bending moments associated with each type of outer hull primary loading, it is not known whether these bending moments are the result of vertical forces, lateral forces, or some combination of both. In fatigue loading, for a trimaran there are six dominant types of loadings to consider; three associated with the center hull and three associated with the outer hulls. These six primary bending moments include vertical bending moment, lateral bending moment, torsion, transverse bending moment (prying and squeezing), pitch connecting moment (relative pitch) and splaying moment (relative yaw).

The majority of loads imposed on trimarans are cyclic in nature therefore the possibility of failure by fatigue is possibly higher. Indeed, in general, most structural failures that occur in service life of a ship result from fatigue. While there is a large knowledge on the fatigue performance of conventional designs, there is very little work done and little knowledge in relation to multihull structures.

In the study by Shehzad et al. (2013), an attempt has been made to utilize the linear seakeeping code ANSYS AQWA, 3D, potential flow theory, frequency response functions to compute the ship response to a sinusoidal wave with unit amplitude for different frequencies and wave headings. Then, the stress transfer functions are calculated by global FE analysis of the trimaran. The study also investigates the effect of Wirsching's rain flow cycle correction factor and contribution of fatigue damage caused by individual heading direction towards cumulative fatigue damage of the hot spots. According to the calculation results, it is also concluded that for the given structural design the connection of cross deck and wet deck with the main hull and the connection of the main hull with the wet deck at the transverse bulk head suffers maximum fatigue damage. Moreover, the predicted fatigue life was found to be considerably less than the design life of the vessel, which indicated the need to enhance the structural design at these particular locations. Therefore, the authors recommend that the fatigue strength assessment of trimaran cross structures should be analyzed by direct calculation methods at the initial design stage.

A study by Liao et al. (2015) compared different methods to determine the global loads for fatigue assessment and the resulting predicted fatigue life time. They compared the stillwater and wave loads provided in the IACS harmonized common structural rules (CSR-H) for bulk carriers and tankers with the loads from spectral analysis and an equivalent design wave approach. They observed significant differences in the load spectra derived by the different approaches and, consequently, also large variations regarding the predicted fatigue life time at the analyzed hot spots. The authors conclude that further work is necessary to ensure that similar results are obtained with different methods for load determination and that care must be taken that the differences of the approaches regarding the methodology to determine the overall fatigue life time, must be properly considered.

The study from Thompson (2015) validated the spectral fatigue analysis software, STRUC_R, developed by Cooperative Research Ships (CRS) using a naval vessel sea trial data. The root mean square (RMS) longitudinal stress and zero-crossing frequency calculated using spectral

fatigue analysis software for one dimensional long crested sea and two-dimensional wave spectrum models are compared with measured data to better quantify the uncertainty introduced by one dimensional wave spectra. The comparison results indicated the use of one dimensional long crested wave spectra tended to over predict RMS stress and under predict zero-up-crossing frequency. Although the use of two-dimensional wave spectra reduces the uncertainty in spectral fatigue analysis, similar results are shown using either set of wave spectra.

Different to the work discussed so far the study from Bigot et al. (2016) focusses on local rather than global effects of wave induced loads. The authors discuss the influence of intermittent wetting at side shell stiffeners in vicinity of the waterline and several models which have been developed to account for the resulting nonlinear effect in fatigue strength evaluation procedures, emphasizing also the differences obtained by using regular and irregular seaway.

Also, Wang W. et al. (2016d) investigated local effects of cyclic wave loads. They evaluated the contribution of ship motions to the fatigue life reduction of pre-swirl stator fins (devices arranged upstream of the propeller to enhance propulsion efficiency) using a hybrid approach (potential viscous flow coupled CFD). The study also evaluated a boundary element method (BEM) on predicting the hydrodynamic loads on the fins. The BEM prediction was roughly 20% less than CFD which is considered a reasonable conservative fatigue life estimate given the advantage of much shorter computational time. Further it was shown that the cyclic loads on the fins caused by ship motions were very small, hence, ample safety margin against fatigue damage due to this kind of hydrodynamic load was found.

So far from most research has focused on providing more accurate experimental and/or numerical predictions of ship motions/vibration and thereby more reliable fatigue loading induced by wave loads. However, in recent years also the accompanying linear damage accumulation models have received some attention, discussing the influence of the time sequence of loads and the load history regarding acceleration/retardation of the propagation of wave induced cracks. In this context Oka et al. (2015) pointed out the importance of hull girder vibration on ship fatigue strength. The study examined the fatigue strength using three types of stress wave form, the measured time histories (RAW), the Low Frequency (LR) wave form obtained by removing the high frequency component by low-pass filter, and the envelope wave form of the measured time histories (ENV). The results showed that the fatigue damage) calculated by the RAW waveform was approximately twice the damage calculated with the LR wave form, however the difference between RAW and ENV was not significant. Furthermore, the authors discuss the differences in damage prediction using the conventional Miner approach in comparison with crack propagation analysis taking account of the time sequence of loads. They found significant differences regarding the predicted fatigue life time.

Hodapp et al. (2015) proposed a nonlinear crack growth model based on finite element analysis of plasticity-induced crack closure instead of the classical Miner approach for calculation of structural damage due to seaway loads. The authors claim that simple instances of variable amplitude loading are analogous to typical ship loading sequences through so-called “storm model” loading. In contrast to previous studies, this approach is readily generalized as it relies solely on material constitutive model. The proposed storm load model facilitates ship fatigue life prediction (crack propagation phase) in which both the order of the loading (load sequence effects) and material hysteresis (load interaction effects) are included. By application of the storm model it was shown that load sequence and load interactions effects are first order phenomena and must be considered in fatigue life prediction and that the results may differ considerably from those obtained with classical approaches.

Independently from the determination of wave induced fatigue loads or the different approaches for the estimation of the fatigue life time, in general, fatigue failure is prevented by

controlling the working stress range. Usually the most efficient way to control stress is to either increase local scantlings or modify geometry to reduce stress concentrations and discontinuities. In the overall process of structural design the prevention of fatigue falls mainly within the scope of detail design. But for cyclic stresses that are not locally controllable, such as wave-induced hull girder stresses, care must be taken to ensure that these stresses remain sufficiently small so as not to cause fatigue in the hull girder.

7. UNCERTAINTY ANALYSIS

This section reviews only uncertainties related to wave-induced loads, loading conditions and uncertainties due to operational factor.

7.1 Load uncertainties

To assess the reliability and quantification of risks associated with complex marine structures and systems, it is essential to understand and quantify uncertainty involved (Papanicolaoua et al., 2014). For the design of a safe ship, it is necessary to assess the reliability of seakeeping analysis and wave load estimation as well as operational conditions in which the ship should perform its mission.

Wave loads uncertainty may be classified in two main groups (Guedes Soares, 1996): uncertainty of linear theory based model and uncertainty of non-linear effects. The main source of uncertainty in both linear theory and non-linear effects calculation is uncertainty related to metocean description. It is expected that this uncertainty will represent the largest challenge for the shipping, offshore and renewable energy industry in the future (Bitner-Gregersen at al., 2014). Generally speaking, uncertainties may be classified into two groups: aleatory and epistemic. Related to metocean description (Bitner-Gregersen at al., 2016), aleatory uncertainty (natural and physic) takes into account natural randomness of random variable, such as variability of wave intensity in time. This uncertainty is also known as intrinsic or inherent and cannot be reduced or eliminated. Epistemic (knowledge based) uncertainty can be reduced by collecting more information as well as by improving the applied models. This uncertainty can be: data related, statistic related, model related or due to climatic variability. Data related uncertainties refer to imperfection of measured data or numerically generated data (or combined – the gap between measured data is filled by numerically generated data). Uncertainties due to insufficient number of data and applied technique for obtaining the probability density function parameters are statistic uncertainties, while imperfection, simplification and idealisation made in physical model for an event, choice of probability density function as well as climate variability are model related uncertainties. Bitner-Gregersen at al. (2016) use different wave data and models for specifying design and operational criteria for two types of marine structures and discuss different associated uncertainties.

Lu et al., (2017) and Sasa et al. (2017) have analysed three extreme cases of bulk-carrier sailing during storms at Southern Hemisphere. They reproduced the environment by three different wind inputs with various spatial and temporal resolutions. The simulated waves (wave hindcasts) and ship responses were validated and compared using measured on-board ship motion data. The compared data show significant uncertainty related to weather database, as well as seakeeping theory and speed prediction technique.

It is important to assign an uncertainty measure to the waves and responses that are being estimated as a base for ship motion and loads evaluation. Real time estimation of waves and ship responses using on-board measurements has been under investigation in recent years (Nielsen, 2006; Montazeri et al., 2015; Pascoal et al., 2017). In general, two main concepts have been applied to estimate the on-site directional wave spectrum on the basis of ship response measurements: a parametric method which assumes the wave spectrum to be composed by parameterised wave spectra; or a non-parametric method where the directional wave

spectrum is found directly as the values in a completely discretised frequency-directional domain without a priori assumptions on the spectrum.

A proper prediction of responses due to extreme waves is important for ship safety in extreme sea. Guo et al. (2016) address statistical description of heave and pitch motions and vertical bending moment in extreme sea states by taking an LNG tanker as an example. Wada et al. (2017) proposes a practical approach to extreme value estimation for small samples of observations with truncated values, or high measurement uncertainty, facilitating reasonable estimation of epistemic uncertainty.

Uncertainty in linear theory calculation is closely related to calculation of transfer functions. According to Temarel et al. (2016) primary uncertainties sources in numerical seakeeping analysis are related to different mathematical modelling of (initial) boundary value problem, different numerical modelling of the assumed mathematical model, non-converged or in accurate hull geometry modelling, insufficient or incorrect knowledge regarding mass distribution and human, i.e., user error.

Uncertainty of non-linear effects may be classified in two groups: different sagging and hogging value in bending moment and influence of slamming and whipping on extreme bending model.

Numerical nonlinear time domain simulation methods is developed to assess slamming-induced hull whipping on sectional loads of three containerships in head seas (el Moctar et al., 2017). The effect of the nonlinear vertical wave-induced bending moments on the chemical tanker hull girder reliability are accounted for in the reliability assessment problem through model correction factors, which are estimated using direct calculation methods based on linear and nonlinear strip theory formulations and the most likely response wave method (Gaspar et al., 2016).

As a part of an ISSC–ITTC benchmark study which was intended to analyse the accuracy of the numerical methods and the uncertainty involved with the predictions of the ship responses, Rajendran and Guedes Soares (2016a) analysed the symmetric distortions of a container ship in large amplitude waves which are by means of time domain code coupled with a finite element model. Rajendran et al., (2016b) used linear to fully body nonlinear numerical methods based on strip theory to analyse the vertical responses of a bulk carrier, containership and a passenger ship. The ships are categorized based on their bow flare angles and the effects of the bow flare variation on the vertical responses are investigated numerically. It is proved that pronounced bow flare induces strong nonlinearities in the vertical responses in rough seas and the linear or even partially body nonlinear methods are not enough for accurate calculations in those conditions.

7.2 Uncertainties in Loading conditions

Loading conditions and the corresponding loads are important for the safety of ships. Although uncertainty of loading condition have been identified by industry as a considerable problem, and not only in the context of the recent ship accidents of MOL COMFORT and MSC NAPOLI (Temeral at al. (2016)), these uncertainties are rarely covered by scientific research. The problem is difficult to analyse because of lack of statistical data related to problem. Such data is difficult to collect partly because of the difficulty in fully understanding the loading/unloading operation process and partly because of intrinsic uncertainties in measuring cargo loading conditions data.

The study of Gaggero et al. (2017) reports a analysis on the uncertainties in assessing loading conditions of handy size bulk carriers. The authors analyse the uncertainties in hold/tank filling level and uncertainties in centre of gravity. In an investigation on loading conditions of three handy size bulk carriers, a total number of 209 voyages was considered in a span of 22 months. Statistical analyses were carried out, aimed at providing information on the uncer-

tainties in the calculations of the hull girder still water loads. Probability distribution functions were proposed to statistically describe the uncertainties of ship draft, filling level of cargo holds and tanks, corresponding weights and centre of gravity positions.

7.3 Uncertainties due to operational factor

The long-term prediction of wave induced hull girder loads considering the effect of various operational circumstances should give a relatively more realistic evaluation of the extreme hull girder loads. However, these circumstances are not easy to foresee. Acero et al. (2016) developed the methodology for assessment of the operational limits and the operability of marine operations during the planning phase. Prpić-Oršić et al. (2014) have presented the real life operation of ultra large container ships from the point of view of shipmasters. The paper provides some insight in uncertainty related to master decisions during voyage.

The speed at which ship would sale is important parameter in seakeeping analysis especially whenever the nonlinear effects are taken into consideration (Guedes Soares, 1996). The choice of design speed or speed profile during life time of the ship is important decision which have consequences in long term predictions and it is a key factor for ship route planning (Mao et al., 2016) and ship route optimization (Vettor&Guedes Soares, 2016).

8. CONCLUSIONS

Regarding computation of wave induced loads, the potential flow model remains, in general, one of the dominated efficient solvers for numerical simulation of wave-body interactions at zero speed, including the influence of a range of nonlinearities. Therefore, further development of 3D potential theory method is still valuable. The versatility and increased accuracy of RANS solvers for capturing important characteristics of wave-body interactions has been demonstrated. For further development and enhancement of numerical methods for the computation of wave loads should continue. For the further investigations to establish more reliable numerical tools, experimental and numerical study should cover a variety range of nonlinearities.

Regarding Slamming and Whipping, Studies in this reporting period was focused on improving the Generalized Wagner Model and CFD tool. Furthermore, some studies focused on the application of CFD tool on investigation of slamming and whipping related phenomena. It is expected that further study should be continuously conducted to clarify slamming phenomena itself and the effect of whipping on real ship such as container ships.

Regarding Sloshing, main theoretical and experimental interests were on the interaction between sloshing and global ship motions and sloshing suppression using baffles in this reporting period. Model testing has been mostly used to observe the physics of the sloshing-coupled ship motion problems, to investigate the efficiency of sloshing suppression, and to obtain validation data for the numerical tools.

Not only theoretical and experimental study but also numerical studies for various type of numerical approach were investigated. Numerical methods developed for sloshing simulation can be categorized under two groups: studies based on the potential flow assumption, with or without the inherent nonlinearities, and studies that involves the viscous effects. The fluid-structure interaction was also considered in some numerical models.

In addition to above studies, Baffled sloshing suppression is still a very active field that researchers proposed new analysis tools, relying on both potential and viscous flow models, to investigate the special aspects of the problem or to analyse different configurations.

Regarding Green Water, some numerical studies were conducted in this reporting period. Because green water is very difficult to measure either under laboratory conditions or in the field, and very difficult to simulate numerically, it is expected that continuous studies should be conducted.

Regarding full scale measurement, it is remarkable that most of measurements focused on wave induced vibration. It is preferable that full scale measurement for wave induced vibration gives a better picture of the typical wave loads experienced during normal service than model tests since they must not rely on assumptions regarding the operational profile, the encountered wave environments and so on. It is expected that further investigation should be continued.

Furthermore, further utilization for warning systems on excessive ship motions and/or loads are focused in this reporting period. It is remarkable to clarify the relation between ship response and encounter wave quantitively in some of those studies.

Regarding Loads following damage, load implications on the ship after accidental damage remained an area of concern to the design and operation of ships. Accidental damage to ships and, subsequent, flooding can occur in number of ways, but generally damages due to collision and grounding are most frequently observed. Based on these background, research focused on these types of damage scenarios in this reporting period.

Regarding VIV, many studies are conducted in this reporting period. Most of the recent works on calculation methods, which were focused in this report, have been performed on: frequency domain (FD) or time domain (TD) semi-empirical models and computational fluid dynamics (CFD) methods. At this moment, there is still rooms for the modification of the accuracy of direct simulations due to the very complex nature of the fully coupled hydro-elastic response. On the other hand, a joint industrial and academic effort has focused on providing the guideline on analysis of vortex-induced vibrations in a riser and an umbilical for best practices in terms of structural modelling, current profile description, heave induced VIV, fatigue calculation and VIV suppression.

Regarding VIM, through comparison CFD analysis with model test results and prototype data for a range of structures, it was concluded that whereas scale effects, the presence of waves and the effect of current unsteadiness is of minor importance, the effect of additional damping from risers, mooring lines and other sources have a significant effect on the VIM amplitudes.

Scale effects were investigated directly by comparing CFD results at model scale and full-scale Reynolds number. It was acknowledged, however, that this observation is at odds with other published results and that further investigation is necessary.

The accurate quantification of the prototype damping level has been highlighted as a remaining challenge. Particularly, importance on a deep draft semisubmersible has been highlighted. Through a careful CFD analysis fully coupled with the mooring and riser system and compared the VIM results with an uncoupled analysis, it was concluded that the damping introduced by the mooring lines and the risers had the potential to significantly reduce the VIM amplitudes.

Regarding Mooring Systems, research generally focuses on a range of methods for coupling the dynamics of mooring lines, floaters and risers and assessing the validity of partly, fully coupling methods, as well as frequency, time and hybrid frequency/time domain approaches. In addition to the continuous those studies, challenging studies were conducted for design of marine energy converters mooring systems and effective computation for mooring systems with many mooring lines and risers, especially when coupled computations are needed.

Furthermore, research into different materials, and their properties, used in mooring lines, e.g. Synthetic fibre ropes, high modulus polyethylene (HMPE) ropes and so on, is of great importance in terms of including in the dynamic simulations and assessment of fatigue damage.

Regarding lifting systems, numerical simulation models and tools and advanced study to develop reliable flexible multibodies system dynamic models were reported in this reporting period.

Regarding wave in deck loads in fixed platforms, intensive studies were conducted and in this reporting period by Joint Industry Project (JIP). Remarkable outcomes were obtained both of methodology including by means of CFD and of the establishment of procedures by the classification societies.

Regarding floating wind turbines, prototype of floating wind turbines were installed with different type of floaters, and long term operational tests in actual sea are being conducted in this reporting period. It is necessary to assess the validity of design wave and design loads based on the feedback of full scale measurement of constructed floating wind turbines in near future.

Regarding probabilistic model of loads on ships, the focus of investigations within this reporting period has been on equivalent design waves and evaluation of design loads introduced by classification societies. It is expected that further investigation on probabilistic methods which can assess design waves and design loads more quantitatively in near future.

Regarding fatigue loads for ships, efforts within this reporting period were focused not only on providing more accurate experimental and/or numerical predictions of ship motions/vibration and more reliable fatigue loading induced by wave loads but also on investigating the influence of the time sequence of loads and of the load history relating with the propagation of wave induced cracks. Further investigations are expected to clarify the fatigue strength of a ship by accounting for stress histories which are effective in crack initiation and propagation.

Regarding uncertainties analysis, some analysis related to wave-induced loads, loading conditions and uncertainties due to operational factor were conducted. However, findings are limited in some parts of uncertainties. It is preferable that further study should be conducted particularly, for example, uncertainties in the application of model tests and numerical results in real operation of ship and floating structure.

REFERENCES

ABS (2016) Guide for Certification of Lifting Appliances, 2016

ABSG (2015) Crane Safety Assessment Findings, Results, and Recommendations, Final Report, submitted to BSEE, 2015

Acero, W.G., Li, L., Gao, Z., Moan, T. (2016) Methodology for assessment of the operational limits and operability of marine operations. Ocean Engineering 125, 308-327

Aggarwal, N., Manikandan, R. and Saha, N. (2017) Nonlinear short term extreme response of spar type floating offshore wind turbines, Ocean Engineering,130, 199–209.

Alaoui, A. E., Nême, A., & Scolan, Y. M. (2015). Experimental investigation of hydrodynamic loads and pressure distribution during a pyramid water entry. Journal of Fluids and Structures, 54, 925-935. doi:https://doi.org/10.1016/j.jfluidstructs.2015.01.018

Alibrandi, U. and Koh, C. G. (2017) Stochastic dynamic analysis of floating production systems using the First Order Reliability Method and the Secant Hyperplane Method, Ocean Engineering,137, 68–77.

Alford, L. A., Beck, R. F., Johnson, J. T., Lyznga, D., Nwogu, O. and Zundel, A. (2015) 'A real-time system for forecasting extreme waves and vessel motions', in International Conference on Offshore Mechanics and Arctic Engineering. St. Johns's: ASME, pp. 1–8.

Andersen, I. M. V. and Jensen, J. J. (2015) 'Extreme value prediction of the wave-induced vertical bending moment in large container ships', in 7th International Conference on Hydroelasticity in Marine Technology. Split, pp. 389–402.

Antony, A., Vinayan, V., Holmes, S., Spernjak, D., Kim, S. J., & Halkyard, J. (2015, May). VIM study for deep draft column stabilized floaters. In Offshore Technology Conference. Offshore Technology Conference.

API (2015). Design and Analysis of Stationkeeping Systems for Floating Structures, API RP 2 SK, 3rd Ed. 2005, Reaffirmed 2015. American petroleum Institute.

Aronsen, K.H., Huang, Z.Y., Skaugset, K.B., Larsen, C.M. (2017), Interaction between IL and CF VIV – on the importance of orbital direction. Proceedings of the ASME 2017 36th International Conference on Ocean, Offshore and Arctic Engineering OMAE2017, June 25-30, Trondheim, Norway, paper 62404.

Bai,W., Liu, X., Koh, C.G. (2015), Numerical study of violent LNG sloshing induced by realistic ship motions using level set method, Ocean Engineering, 97, 100-113.

Bandyk, P.J. & Hazen G.S. (2015) A forward-speed body-exact strip theory. Proceedings of the ASME 2015 34th International Conference on Ocean, Offshore and Arctic Engineering, OMAE2015, Mai 31 –June 5, 2015, St. John's, Newfoundland, Canada.

Bao, C. M., Wu, G. X., & Xu, G. (2017). Simulation of freefall water entry of a finite wedge with flow detachment. Applied Ocean Research, 65, 262-278.

Bayati, I. Belloli, M. Facchinetti, A. (2017) Wind Tunnel 2-Dof Hybrid/HIL Tests on the OC5 Floating Offshore Wind Turbine, OMAE2017, June 25-30, 2017, Trondheim, Norway

Bennett, S.S. Hudson, D.A., Temarel, P., (2015a) The effect of abnormal wave sequences on 2D hydroelastic predictions of global loads, Proceedings of 7th International Conference on Hydroelasticity in Marine Technology, September 16-19, 2015, Split, Croatia, 363-374.

Bennett, S. S. and Phillips, A. B. (2015b) 'Experimental investigation of the influence of hull damage on ship responses in waves', in Analysis and Design of Marine Structures. London: Taylor & Francis Group, pp. 3–10.

Bennett, S. S. and Phillips, A. B. (2015c) 'On the hydroelastic modelling of damaged ships', in 7th International Conference on Hydroelasticity in Marine Technology. Split, pp. 507–518.

Bennett, S.S., Phillips, A.B. (2017), Experimental investigation of the influence of floodwater due to ship grounding on motions and global loads, Ocean Engineering, 130, 49-63.

Bigot, F. et al. (2016) Comparison of Different Models for the Fatigue Analysis of Details Subject to Side Shell Intermittent Wetting Effect, Proceeding of PRADS2016, Copenhagen.

Bitner-Gregersen, E.M., Ewans, K.C., Johnson, M.C. (2014) Some uncertainties associated with wind and wave description and their importance for engineering applications. Ocean Engineering 86, 11-25

Bitner-Gregersen E. M., Dong, S., Fu, T., Ma, N., Maisondieu, C., Miyake, R. and Rychlik I. (2016) Sea state conditions for marine structures' analysis and model tests, Ocean Engineering,119, 309–322.

Bochkarev, S.A., Lekomtsev, S.V., Matveenko, V.P. (2016), Dynamic analysis of partially filled non-circular cylindrical shells with liquid sloshing, International Journal of Applied Mechanics, 8.

Borg M, Collu M. (2015) A Comparison Between The Dynamics Of Horizontal And Vertical Axis Offshore Floating Wind Turbines, Philosophical Transactions of the Royal Society of London A: Mathematical, Physical and Engineering Sciences 2015; 373(2035).

Buruchenko, S. K., & Canelas, R. B. (2017). Validation of Open-Source SPH Code DualSPHysics for Numerical Simulations of Water Entry and Exit of a Rigid Body. V002T08A021. doi:10.1115/omae2017-61221

Cai, S., Jiao, J. and Ren, H. (2016) 'Study on the Load Behavior of a Large Ship in Head and Oblique Regular Waves', in International Conference on Ocean, Offshore and Arctic Engineering. Rhodes: ISOPE, pp. 426–433.

Caille F. Bozonnet, P. e Perdrizet, T. Poirette, Y. Melis, C. (2017) Model Test and Simulation Comparison for an Inclined-Leg TLP Dedicated to Floating Wind, OMAE2017, June 25-30, 2017, Trondheim, Norway.

Cercos-Pita, J.L., Bulien, G., Pérez-Rojas, L., Francescutto, A. (2016), Coupled simulation of nonlinear ship motions and a free surface tank, Ocean Engineering, 120, 281-288.

Charles Monroy, C., Sopheak Seng, S., Louis Diebold, L., Alexis Benhamou, A., Sime Malenica, S., & others. (2017). A Comparative Study of the Generalized Wagner Model

and a Free-Surface RANS Solver for Water Entry Problems. International Journal of Offshore and Polar Engineering, 27, 135-143.

Chen, Z.Y., Lu, G.C., He, G.H. (2015) Hydroelastic analysis of effect of various nonlinear factors on load responses, Proceedings of the Twenty-fifth International Ocean and Polar EngineeringConference, Hawaii, USA.

Chen, X. & Liang, H. (2016) Wave properties and analytical modelling of free-surface flows in the development of the multi-domain method. Journal of hydrodynamics 28(6): 971-976.

Chen, L. and Basu, B. (2017) A numerical study on the in-plane wave propagation in mooring cables. Procedia Engineering 173, 934-939.

Chen, Y-.H., Hwang, W.-S., Tsao, W.-H. (2017a), Nonlinear sloshing analysis by regularized boundary integral method, Journal of Engineering Mechanics, 143.

Chen, Z.Y., Jiao, J.L., Li, H. (2017b) Time-domain numerical and segmented ship model experimental analyses of hydroelastic responses of a large container ship in oblique regular waves, Applied Ocean Research, 67: 78-93.

Chen, X. & Zhu, R.-C. (2017c) Time domain analysis of side by side vessel's motion responses during offshore installation and underway replenishment. Proceedings of the Twenty-seventh (2017) International Ocean and Polar Engineering Conference, San Francisco, California, June 25−30, 2017.

Cheng, Z. Wang, K. Gao, Z. Moan, T. (2015) Dynamic Response Analysis Of Three Floating Wind Turbine Concepts With A Two-Bladed Darrieus Rotor, Journal of Ocean and Wind Energy, 2:213-222

Cheng, J., Cao, P., Fu, S., Constantinides, Y., (2016) Experimental and Numerical Study of Steel Lazy Wave Riser Response in Extreme Environment. V005T004A055.

Cheng, Y., Ji, C.Y., Zhai, G.J., et al. (2016) Dual inclined perforated anti-motion plates for mitigating hydroelastic response of a VLFS under wave action, Ocean Engineering, 121: 572-591.

Cheng, Z. Madsen, H. A. Gao, Z. Moan, T. (2016) A Fully Coupled Method for Numerical Modeling and Dynamic Analysis of Floating Vertical Axis Wind Turbines. Renewable Energy, 2016

Cheng, Y., Ji, C.Y., Zhai, G.J., et al. (2017) Fully nonlinear numerical investigation on hydroelastic responses of floating elastic plate over variable depth sea-bottom, Marine Structures, 55: 37-61.

Cho, I.H., Choi, J.-S., Kim, M.H. (2017), Sloshing reduction in a swaying rectangular tank by a horizontal porous baffle, Ocean Engineering, 138, 23-34.

Cho, I.H., Kim, M.H. (2016), Effect of dual vertical porous baffles on sloshing reduction in a swaying rectangular tank, Ocean Engineering, 126, 364-373.

Constantinides, Y., Stover, M., Steele, A., Santala, M. (2016), CFD modelling and validation of steel lazy-wave riser VIV. Proceedings of the ASME 2016 35th International Conference on Ocean, Offshore and Arctic Engineering OMAE2016, June 19-24, Busan, South Korea, paper 54945.

C´orak, M., Parunov, J. and Guedes Soares C. (2015) Probabilistic load combination factors of wave and whipping bending moments, Journal of Ship Research, 59-1, 11–30.

Craig, M., Piro, D., Schambach, L., et al. (2015) A comparison of fully-coupled hydroelastic simulation methods to predict slam-induced whipping, Proceedings of 7th International Conference on Hydroelasticity in Marine Technology, September 16-19, 2015, Split, Croatia, 575-590.

Cusano, G., Ruscelli, D., Sebastiani, L., & Ungaro, A. (2009). How Hydroelastic Considerations May Affect Practical Ship Design. Hydroelasticity 2009. Southampton, UK.

Darie, I. and Rörup, J. (2017) Hull girder ultimate strength of container ships in oblique sea, Proceedings of the 6th International Conference on Marine Structures , 8-10 May, Lisbon, Portugal.

de Lauzon, J., Benhamou, A., Malenica, S., & others. (2015). Numerical Simulations of WILS Experiments. The Twenty-fifth International Ocean and Polar Engineering Conference.

de Lauzon, J., Grgi, M., Derbanne, Q., & Malenica, S. (2015a). Improved generalized wagner model for slamming. PROCEEDINGS of the 7th internalitional conference on hydroelasticity in marine technology.

de Pina, A.A., Monteiro, B.F. Albrecht, C.H., Pires de Lima, B., Jacob, B.P., 2016. Artificial Neural Networks for the analysis of spread-mooring configurations for floating production systems. Applied Ocean Research, 59, 254-264.

Dessi, D. and Faiella, E. (2015) 'Analysis of modal damping in elastic floating structures', in 7th International Conference on Hydroelasticity in Marine Technology. Split, pp. 279–292.

Ding, J., Tian, C., Wu, Y.S., et al. (2016) Hydroelasticity of a VLFS in non-uniform incident waves, The 12th International Conference on Hydrodynamics, September 18-23, Egmondaan Zee, Netherlands, 1-11.

Ding, J., Tian, C., Wu, Y.S., et al. (2017) Hydroelastic analysis and model tests of a single module VLFS deployednear islands and reefs, Ocean Engineering, 144: 224-234.

DNVGL (2015). Position Mooring, DNVGL-OS-E301 Edition July 2015

DNVGL (2016) Marine Operations and Marine Warranty, 2016

DNVGL-OTG-13 (2017) Prediction of air gap for column stabilised units. March 2017.

DNV GL-OTG-14 (2017) Horizontal wave impact loads for column stabilised units', April 2017

Dombre E, et. Al. (2015) Simulation of floating structure dynamics in waves by implicit coupling of a fully non-linear potential flow model and a rigid body motion approach, J Ocean Eng Mar Energy 1:55–76

Elhimer, M., Jacques, N., Alaoui, A. E., & Gabillet, C. (2017). The influence of aeration and compressibility on slamming loads during cone water entry. Journal of Fluids and Structures, 70, 24-46. doi:https://doi.org/10.1016/j.jfluidstructs.2016.12.012

el Moctar, O., Ley, J., Oberhagemann, J., Schellin, T. 2017. Nonlinear computational methods for hydroelastic effects of ships in extreme seas. Ocean Engineering 130, 659-673

Falkenberg, E., Åhjem, V., Yang, L. (2017) Best practice for analysis of Polyester rope mooring systems. Offshore Technology Conference, Houston, Texas, 1-4 May, paper OTC-27761-MS.

Fang, C. C. and Chan, H.S. (2016) Numerical investigation on global wave loads of a high speed trimaran in irregular waves, Proceedings of 7th PAAMES and AMEC, 13-14 October, Hong Kong.

Fang, C. C., Dai, M. J. and Chiu, J. T. (2017) The structural response analyses of high-speed monohull with different wave amplitudes, Proceedings of TEAM, 25-28 September, Osaka, Japan.

Fischer, C., Fricke, W. and Junglewitz, A. (2016) Development of a Simplified Procedure for the Determination of the Ultimate Load and Associated Spindle Torque of Propeller Blades, Journal of Ship Research, 60-3, 171–185.

Flory, J.F., Banfield, S.J., Ridge, I.M.L., Carr, R. (2017) Axial compression fatigue in long-lay-length fiber mooring ropes. Offshore Technology Conference, Houston, Texas, 1-4 May

Fonseca, N. and Stansberg, C.T. (2017a) Wave drift forces and low frequency damping on the Exwave Semi-submersible. Proceedings of the ASME 2017 36th International Conference on Ocean, Offshore and Arctic Engineering, OMAE2017, June 25-30, Trondheim, Norway - paper 62540.

Fonseca, N. and Stansberg, C.T. (2017b) Wave drift forces and low frequency damping on the Exwave FPSO. Proceedings of the ASME 2017 36th International Conference on Ocean, Offshore and Arctic Engineering, OMAE2017, June 25-30, Trondheim, Norway - paper 62540.

Fonseca, N., Ommani, B., Stansberg, C.T., Bøckmann, A., Birknes-Berg, J., Nestegård, A., de Hauteclocque, G., Baarholm, R. (2017) Wave Forces and Low Frequency Drift Motions

in Extreme Seas: Benchmark Studies. Offshore Technology Conference, Houston, Texas, 1-4 May, paper OTC-27803-MS.

Fonseca, N., Stansberg, C.T., Nestegård, Bøckmann, A., Baarholm, R. (2016) The EXWAVE JIP: Improved procedures to calculate slowly varying wave drift forces on floating units in extreme seas. Proceedings of the ASME 2016 35th International Conference on Ocean, Offshore and Arctic Engineering, OMAE2016, June 19-24, Busan, South Korea, - paper 54829.

Fonseca, N., Guares Soares, C. (1998a) Time-domain analysis and wave loads of large-amplitude vertical ship motions. J. Ship Res. 42, 139-153.

Fonseca, N., Guades Soares, C. (1998b) Nonlinear wave induced responses of ships in irregular seas. Proceedings of the 17th International Conference on Offshore Mechanics and Arctic Engineering (OMAE 98). ASME, Lisbon, Portugal.

Fowler, M.J. Goupee, A.J. Allen, C. Viselli, A. Dagher, H. (2017) 1:52 Scale Testing of the First US Commercial Scale Floating Wind Turbine, VolturnUS: Testing Overview and the Evolution of Scale Model Testing Methods, OMAE2017, June 25-30, 2017, Trondheim, Norway.

Fu, T.C., Brucker, K.A., Mousaviraad, S.M., Ikeda, C.M., Lee, E.J., O'Shea, T.T., Wang, Z., Stern, F. & Judge, C.Q. (2014) An assessment of computational fluid dynamics predictions of the hydrodynamics of high-speed planing craft in calm water and waves. 30th Symposium on Naval Hydrodynamics, Hobart, Tasmania, Australia, 2-7

Fu, G., Younis, B. A., Sun, L., & Dai, S. (2016). Vortex Shedding Control Using Jets: A Computational Study With Lattice Boltzmann Method. In ASME 2016 35th International Conference on Ocean, Offshore and Arctic Engineering. American Society of Mechanical Engineers.

Fu, S.X., Wei, W., Ou, S.W., et al. (2017) A time-domain method for hydroelastic analysis of floating bridges in inhomogeneous waves, Proceedings of the ASME 2017 36th International Conference on Ocean, Offshore and Arctic Engineering, June 25-30, 2017, Trondheim,Norway.

Fu, S., Lie, H., Wu, J., Baarholm, R., (2017a) Hydrodynamic Coefficients of a Flexible Pipe With Staggered Buoyancy Elements and Strakes Under VIV Conditions. ASME 2017, International Conference on Ocean, Offshore and Arctic Engineering (pp.V002T08A044).

Fukasawa, T. and Kadota, K. (2015) Research on the method for determining significant short-term sea states for fatigue strength of a ship, Proceedings of TEAM, 12-15 October, Vladivostok, Russia.

Fukasawa, T. and Hiranuma, M. (2016) Considerations on the longitudinal strength of container ship from the viewpoint of extreme vertical wave bending moment, Proceedings of PRADS, 4-8 September, Copenhagen, Denmark.

Gaggero, T., Gaiotti, M., Rizzo, C.M. (2017) Effects of uncertainties in loading conditions of bulk carriers on hull girder still water loads. Marine Structures 55, 214-242

Ganesan T. Shivaji, Sen D. (2015) Time domain simulation of large amplitude wave structure interactions by a 3D numerical tank approach, J. Ocean Eng. Mar energy

Gao, Z.L., Vassalos, D. (2015), The dynamics of the floodwater and the damaged ship in waves, Journal of Hydrodynamics, 27, 689-695.

Gaspar, B., Teixeira, A.P., Guedes Soares, C. (2016) Effect of the nonlinear vertical wave-induced bending moments on the ship hull girder reliability. Ocean Engineering 119, 193-207

Ghoshal, R., Yenduri, A., Ahmed, A., Chen, Z., Wang, W., Hussain, A., Jaiman, R.K., Qian, X., 2016). Instability of mooring cables in presence of ice-load. Proceedings of the ASME 2016 35th International Conference on Ocean, Offshore and Arctic Engineering, OMAE2016, June 19-24, Busan, South Korea, paper 54713.

Gonzalez, D.F., Bechthold, J. & Abdel-Maksoud, M. (2017) Application of a boundary element method for wave-body interaction problems considering the non-linear water surface.

Proceedings of the ASME 2017 36th International Conference on Ocean, Offshore and Arctic Engineering, OMAE2017. June 25-30, 2017, Trondheim, Norway.

Gou, Y., Kim, Y., Kim, T.-Y. (2011), A numerical study on coupling between ship motions and sloshing in frequency and time domains, 21st International Offshore and Polar Engineering Conference, ISOPE 2011, Hawaii, USA.

Gourlay, T., von Graefe, A., Shigunov, V. & Lataire, E. (2015) Comparison of AQWA, GL Rankine, MOSES, OCTOBUS, PDStrip and WAMIT with model test results for cargo ship wave-induced motions in shallow water. OMAE2015.

von Graefe, A., el Moctar, O., Oberhagemann, J. & Shigunov, V. (2014) Linear and nonlinear sectional loads with potential and field methods. Journal of Offshore Mechanics and Arctic Engineering 136.

Grotle, E.L., Bihs, H., Æsoy, V. (2016), Experimental and numerical investigation of sloshing under roll excitation at shallow liquid depths, Ocean Engineering, 138, 73-85.

Guan, M.Z., Narendran, K., Miyanawala, T.P., Ma, P.F. & Jaiman, R.K. (2017). Control of flow-induced motion in multi-colum offshore platform by near-wake jets. In Proceedings 36th International Conference on Ocean, Offshore and Arctic Engineering, Trondheim, Norway, OMAE2017-61605

Guedes Soares, C. (1996) On the definition of rule requirements for wave induced vertical bending moments. Marine Structures 9, 409–425.

Guha, A. & Falzarano, J. (2015a) Estimation of hydrodynamic forces and motion of ships with steady forward speed. International Shipbuilding Progress 62: 113-138.

Guha A and Falzerano J. (2015b) The effect of hull emergence angle on the near field formulation of added resistance. Ocean Engineering 105: 10-24.

Guo, B., Bitner-Gregersen, E.M., Sun, H., Helmers, J.B. (2016) Statistics analysis of ship response in extreme seas. Ocean Engineering 119, 154-164

Hagen, Ø., Johannessen, T.B. & Birknes-Berg, J., (2016), Airgap and wave in deck impact statistics. In Proceedings 35th International Conference on Ocean, Offshore and Arctic Engineering, Busan, Korea, OMAE2016-54927.

Hänninen, S.K., Mikkola, T. & Matusiak, J. (2016) Development of vertical second harmonic wave loads of a large cruise ship in short and steep head waves. Ocean Engineering 118:17-27.

Hauteclocque, G., Monroy, C., Bigot, F. and Derbanne Q. (2017) New rules for container-ships Formulae for wave loads, Proceedings of the 6th International Conference on Marine Structures , 8-10 May, Lisbon, Portugal.

Haver, S., (2016), Airgap and Safety: Metocean Induced Uncertainties Affecting Airgap Assessments. In 3rd Offshore Strurcural Reliability Conference, OSRC2016, Stavanger, Norway

He Guanghua, Zhang Zihao, Tian Naiwen and Wang Zhengke (2017) Nonlinear Analysis of Green Water Impact on Forward-speed Wigley Hull, Proceedings of the 27th International Ocean and Polar Engineering Conference, San Francisco, CA, USA, June 25-30,

Hennig, J., Scharnke, J., Swan, C., Hagen, Ø., Ewans, K., Tromans, P. & Forristall, G. (2015), Effect of short-crestedness on extreme wave impact – A summary of findings from the joint industry project 'ShortCresT'. In Proceedings 34th International Conference on Ocean, Offshore and Arctic Engineering, St. John's, Canada, OMAE2015-41167.

Heo, K., Koo, W., Park, I., et al. (2016) Quadratic strip theory for high-order dynamic behaviour of a large container ship with 3D flow effects, International Journal of Naval Architecture and Ocean Engineering, 8: 127-136.

Hermundstad Elin, et. Al. (2016) Effects of wave-current interaction on floating bodies, Proceedings of the ASME 2016 35th International Conference on Ocean, Offshore and Arctic Engineering,

Hermundstad, E.M., Hoff, J.R., Fonseca, N.& Bjørkli, R., (2017), Wave-current interaction effects on airgap calculations', In Proceedings 36th International Conference on Ocean, Offshore and Arctic Engineering, Trondheim, Norway, OMAE2017-62548.

Hirdaris, S.E., Lee, Y., Mortola, G., Incecik, A., Turan, O., Hong, S.Y., Kim, B.W., Kim, K.H., Bennett, S., Miao, S.H. & Temarel, P. (2016) The influence of nonlinearities on the symmetric hydrodynamic response of a 10,000 TEU Container ship. Ocean Engineering 111:166-178.

Hodapp P. et al. (2015) Nonlinear Fatigue Crack Growth Predictions for Simple Specimens Subject to Time Dependent Ship Structural Loading Sequences, Society of Naval Architects and Marine Engineers, SNAME 2015.

Hong D.C., Kim J.G., Song K.H., Lee H.K. (2015) Numerical study of the added resistance of ship advancing in waves using far-field and near-field methods. Proceedings of the ASME 2015 34th International Conference on Ocean, Offshore and Arctic Engineering, OMAE2015. May 31-June 5, 2015, St. John's, Newfoundland, Canada.

Hong, S. Y., Kim, K. and Kim, B. (2015a) 'An experimental investigation on bow slamming loads on an ultra-large containership', in 7th International Conference on Hydroelasticity in Marine Technology. Split, pp. 229–244.

Hong, J. Roh, M., Ham, S. Ha, S. (2016) Dynamic Simulation Of Subsea Equipment Installation Using An Offshore Support Vessel Based On Flexible Multibody System Dynamics, Journal of Marine Science and Technology, Vol. 24, No. 4 PP. 807-821

Hong, D.C., Ha, T.B. & Song, K.H. (2017) Numerical study of forward-speed ship motion and added resistance. Proceedings of the ASME 2017 36th International Conference on Ocean, Offshore and Arctic Engineering, OMAE2017. June 25-30, 2017, Trondheim, Norway.

Hong, S. Y., Kim, K.-H., Hwang, S. C., & others. (2017). Comparative Study of Water-Impact Problem for Ship Section and Wedge Drops. International Journal of Offshore and Polar Engineering, 27, 123-134.

Hu, Z.-Q., Wang, S.-Y., Chen, G., Chai, S.-H., Jin, Y.-T. (2017), The effects of LNG-tank sloshing on the global motions of FLNG system, International Journal of Naval Architecture and Ocean Engineering, 9, 114-125.

Huang, W., Liu, H., Lian, Y., Li, L., 2015. Modeling nonlinear time-dependent behaviors of sybtehtic fiber ropes under cycling loading. Ocean Engineering, 109, 207-216.

Hwang, S.-C., Park, J.-C., Gotoh, H., Khayyer, A., Kang, K.-J. (2016), Numerical simulations of sloshing flows with elastic baffles by using a particle-based fluid-structure interaction analysis method, Ocean Engineering, 118, 227-241.

Ian Thompson (2015), Influence of Sea State Models on Calculated Naval Vessel Stress Spectra, International Conference on Ships and Shippping Research 2015.

ISO (2013). International Standard 19901-7:2013, Petroleum and natural gas industries.

ITTC (2017), The Ocean Engineering Committee: Final Report and Recommendations to the 28th ITTC. Proceedings of 28th ITTC, Volume I, Wuxi, China, September 17–23.

James, R. and Costa Ros, M. (2015) Floating Offshore Wind: Market and Technology Review, The Carbo Trust, UK, 2015

Jang, H., Kyoung, J., Kim, J.W., Yan, H. & Wu, G. (2017). CFD study of fully coupled mooring and riser effects on vortex induced motion of semi-submrsible. In Proceedings 36th International Conference on Ocean, Offshore and Arctic Engineering, Trondheim, Norway, OMAE2017-62433

Jayasinghe, K., Carra, C., Potts, A.E., Kilner, A.A., 2017. Investigations into observed high frequency mooring line dynamic behaviours. Offshore Technology Conference, Houston, Texas, 1-4 May, paper OTC-27668-MS.

Jeong, D. Roh, M. and Ham, S. (2016) Lifting Simulation Of An Offshore Supply Vessel Considering Various Operating Conditions, Journal of Advances in Mechanical Engineering, 2016, Vol 8 (6), 1-13.

Jia, D., Agrawal, M., Wang, C., Shen, J., Malachowski, J. (2015), Fluid-structure interaction of liquid sloshing induced by vessel motion in floating LNG tank, 34th International Conference on Ocean, Offshore and Arctic Engineering, OMAE 2015, Newfoundland, Canada.

Jiang, S.-C., Teng, B., Bai, W., Gou, Y. (2015), Numerical simulation of coupling effect between ship motion and liquid sloshing under wave action, Ocean Engineering, 108, 140-154.

Johannessen, T.B. & Hagen, Ø., (2016), Characteristic levels of strongly nonlinear wave load effects. In Proceedings 35th International Conference on Ocean, Offshore and Arctic Engineering, Busan, Korea, OMAE2016-54963.

Johannessen, T.B., Hagen, Ø., & Lande, Ø., (2017), On the distribution of wave impact loads on offshore structures. In Proceedings 36th International Conference on Ocean, Offshore and Arctic Engineering, Trondheim, Norway, OMAE2017-62057.

Kalske, S. & Manderbacka, T. (2017) Development of a new practical ship motion calculation method with forward speed. Proceedings of the Twenty-seventh (2017) International Ocean and Polar Engineering Conference, San Francisco, California, June 25−30, 2017.

Kamath, A., Bihs, H., & A. Arnsten, Ã. (2016). Study of Water Impact and Entry of a Free Falling Wedge Using CFD Simulations. V002T08A020.

Kang, H.Y. & Kim, M.H. (2017) Time-domain hydroelastic analysis with efficient load estimation for random waves, International Journal of Naval Architecture and Ocean Engineering, 9: 266-281.

Kara, F. (2015) Time domain prediction of hydroelasticity of floating bodies, Applied Ocean Research, 51: 1-13.

Kara, M. C., Kaufmann, J., Gordon, R., Sharma, P. P., & Lu, J. Y. (2016a). Application of CFD for Computing VIM of Floating Structures. In Offshore Technology Conference. Offshore Technology Conference.

Kara, M. C., Kaufmann, J., Bertram, V., Gordon, R. & Sharma, P. (2016b). Best practices for CFD analysis of VIM and VIV for offshore structures. In Proc. 21st Offshore Symposium, SNAME, Houston, Texas

Karimirad, M. Bachynski, E.E. Berthelsen, P.A. Ormberg, H. (2017) Comparison of Real-Time Hybrid Model Testing of a Braceless Semisubmersible Wind Turbine and Numerical Simulations, OMAE2017, June 25-30, 2017, Trondheim, Norway.

Karperaki, A.E., Belibassakis, K.A., Papathanasiou, T.K. (2016) Time-domain, shallow-water hydroelastic analysis of VLFS elastically connected to the seabed, Marine Structures, 48: 33-51.

Kashiwagi, M., Kuga, S., Chimoto, S. (2015) Time- and frequency-domain calculation methods for ship hydroelasticity with forward speed, Proceedings of 7th International Conference on Hydroelasticity in Marine Technology, September 16-19, 2015, Split, Croatia, 477-492.

Ki, H., Park, S. and Jang, I. (2015) 'Full scale measurement of 14k TEU containership', in 7th International Conference on Hydroelasticity in Marine Technology. Split, pp. 311–328.

Kim, D. H. and Paik, J. K. (2017) Ultimate limit state-based multi-objective optimum design technology for hull structural scantlings of merchant cargo ships, Ocean Engineering,129, 318–334.

Kim, J.-H., Kim, Y., Yuck, R.-H., & Lee, D.-Y. (2015). Comparison of slamming and whipping loads by fully coupled hydroelastic analysis and experimental measurement. Journal of Fluids and Structures, 52, 145-165.

Kim, S. P. (2015) 'Nonlinear time domain simulations of slamming , whipping and springing loads on a containership', in 7th International Conference on Hydroelasticity in Marine Technology. Split, pp. 637–650.

Kim, Y., Ahn, I.-G. and Park, S. G. (2015) 'On the second order effect of the springing response of large blunt ship', in 7th International Conference on Hydroelasticity in Marine Technology. Split, pp. 403–413.

Kim, Y., Ahn, I. and Park, S. (2016) 'On the Modal Parameter Estimation of a Segmented Ship Model with a Hydroelastic Response', in International Conference on Ocean, Offshore and Arctic Engineering. Rhodes: ISOPE, pp. 448–454.

Kim, J.H. & Kim, Y. (2015a) Parametric study of numerical prediction of slamming and whipping and an experimental validation for a 10,000-TEU containership, Proceedings of the Twenty-fifth International Ocean and Polar Engineering Conference, Hawaii, USA, 96-103.

Kim, M., Hizir, O., Turan, O. & Incecik, A. (2017a) Numerical investigation on added resistance with wave steepness for KVLCC2 in short and long waves. Proceedings of the Twenty-seventh (2017) International Ocean and Polar Engineering Conference, San Francisco, California, June 25−30, 2017.

Kim, M., Hizir, O., Turan, O. & Incecik, A. (2017b) Numerical studies on added resistance and motions of KVLCC2 in head seas for various ship speeds. Ocean Engineering 140:466-476

Kim, Y., Kim, J.H., Kim, Y. (2015b) Development of a high-fidelity procedure for the numerical analysis of ship structural hydroelasticity, Proceedings of 7th International Conference on Hydroelasticity in Marine Technology, September 16-19, 2015, Split, Croatia, 457-475.

Kim, Y. & Kim, J.-H. (2016) Benchmark study on motions and loads of a 6750-TEU containership. Ocean Engineering 119:262-273.

Kim Y.-C., Kim K.-S., Kim J., Kim Y. & Kim M.-S. (2016a) CFD application to prediction of ship motions and forces in regular head wave using URANS approach. Proceedings of the Twenty-sixth International Ocean and Polar Engineering Conference, Rhodes, Greece, June 26 – July 1, 2016.

Kim, T., Yoo, S., Oh, S., Kim, H.J., Lee, D. & Kim. B. (2017c) Numerical and experimental study on the estimation of added resistance of an LNG carrier in waves. Proceedings of the Twenty-seventh (2017) International Ocean and Polar Engineering Conference, San Francisco, California, June 25−30, 2017.

Kim, S. (2015c) Nonlinear time domain simulations of slamming, whipping and springing loads on a containership, Proceedings of 7th International Conference on Hydroelasticity in Marine Technology, September 16-19, 2015, Split, Croatia, 637-649.

Klein, M., Clauss, G. F., Rajendran, S., Guedes Soares C. and Onorato, M. (2016) Peregrine breathers as design waves for wave-structure interaction, Ocean Engineering,128, 199–212.

Kolaei, A., Rakheja, S., Richard, M.J. (2015a), Three-dimensional dynamic liquid slosh in partially-filled horizontal tanks subject to simultaneous longitudinal and lateral excitations, European Journal of Mechanics B/Fluids, 53, 251-263.

Kolaei, A., Rakheja, S., Richard, M.J. (2015b), A coupled multimodal and boundary-element method for analysis of anti-slosh effectiveness of partial baffles in a partly-filled container, Computers & Fluids, 107, 43-58.

Koop, A., de Wilde, J., Fujarra, A., Rijken, O., Linder, S., Lennblad, J., ... & Phadke, A. (2016a). Investigation on Reasons foor Possible Difference Between VIM Response in the Field and in Model Tests. In at Proceedings 35th International Conference on Ocean, Offshore and Arctic Engineering, OMAE2016-54746, Busan, Korea.

Koop, A., Rijken, O., Vaz, G., Maximiano, A. & Reseeti, G. (2016b). CFD Investigation on Scale and Damping effects for Vortex Induced Motions of a Semi-Submersible Floater. In Offshore Technology Conference. Houston TX.

Kotajima, S., Kawamura, Y., Wang, D. and Okada, T. (2016) A study on ultimate strength of container-ship hull girder under dynamic loading, Proceedings of TEAM, 10-13 October, Mokpo, Republic of Korea.

Kukkanen, T. & Matusiak, J. (2014) Nonlinear hull girder loads of a RoPax ship. Ocean Engineering 75:1-14.

Kvaleid, J., Oosterlak, V. & Kvillum, T., (2014), Non-linear air gap analysis of a semi-submersible compared with linear analyses and model tests. In Proceedings 33th International Conference on Ocean, Offshore and Arctic Engineering, San Francisco, California, USA, OMAE2014-24044

Lakshmynarayanana, P.A., Temarel, P., Chen, Z. (2015) Coupled fluid-structure interaction to model three-dimensional dynamic behaviour of ship in waves, Proceedings of 7th International Conference on Hydroelasticity in Marine Technology, September 16–19, 2015, Split, Croatia, 623-636.

Lauzon, J.de., Benhamou, A., Malenica, S. (2015) Numerical simulations of WILS experiments, Proceedings of the Twenty-fifth International Ocean and Polar Engineering Conference, Hawaii, USA, 104-113.

Lee Hyewon, Roh Myung-Il, Ham Seung-Ho and Ha Sol (2015) Dynamic simulation of the wireline riser tensioner system for a mobile offshore drilling unit based on multibody system dynamics, Ocean Engineering, 106, 485 – 495

Lee, K.-H., Cho, S., Kim, K.-T, Kim, J.-G., Lee, P.-S. (2015a), Hydroelastic analysis of floating structures with liquid tanks and comparison with experimental tests, Applied Ocean Research, 52, 167-187.

Lee, Y., White, N., Southall, N., et al. (2015b) Impact loads and whipping responses on a large container ship, Proceedings of the Twenty-fifth International Ocean and Polar Engineering Conference, Hawaii, USA, 82-88.

Li, L. Gao, Z. Moan, T. (2015) Response Analysis of a Nonstationary Lowering Operation for an Offshore Wind Turbine Monopile Substructure, Journal of Offshore Mechanics and Arctic Engineering, 2015, Vol. 137

Li, Z.W., Ding, J., Tian, C., et al. (2016) Numerical study on hydroelastic responses of very large floating structures in variable seabed bathymetry, The Second Conference of Global Chinese Scholars on Hydrodynamics, November 11-14, Wuxi, China, 777-785.

Lian, Y., Liu, H., Huang, W., Li, L. (2015) A creep-rupture model of synthetic fiber ropes for deepwater moorings based om thermodynamics. Applied Ocean Research, 52, 234-244.

Lian, Y., Liu, Haixiao, Zhang, Y., Li, Linan, 2017. An experimental investigation on fatigue behaviors of HMPE ropes. Ocean Engineering 139, 237-249.

Liao et al. (2015) Load Uncertainties Effects on the Fatigue Life Evaluation by the Common Structural Rules, International Conference on Ocean, Offshore and Arctic Engineering (pp. 1–10). St. John's: ASM 2015.

Lin, G., Liu, J., Li, J., Hu, Z. (2015), A scaled boundary finite element approach for sloshing analysis of liquid storage tanks, Engineering Analysis with Boundary Elements, 56, 70-80.

Lin, Y., Ma, N., Wang, D.Y., et al. (2017) Hydroelastic analysis and experimental validation of a 350,000 DWT very large crude carrier, Proceedings of the ASME 2017 36th International Conference on Ocean, Offshore and Arctic Engineering, June 25-30, Trondheim, Norway.

Liu, H., Huang, W., Lian, Y., Li, L. (2014) An experimental investigation on nonlinear behaviors of synthetic fiber ropes for deepwater moorings under cycling loading. Applied Ocean Research, 45, 22-32.

Liu, D., Tang, W., Wang, J., Xue, H., Wang, K. (2017), Hybrid RANS/LES simulation of sloshing flow in a rectangular tank with and without baffles, Ships and Offshore Structures, 12, 1005-1015.

Liu Cong, et.al. (2017) Computation of Wave Drift Forces and Motions of DTC Ship in Oblique Waves, Proceedings of the 27th International Ocean and Polar Engineering Conference, San Francisco, CA, USA, June 25-30

Lu, L., Jiang, S.-C., Zhao, M., Tang, G.-Q. (2015), Two-dimensional viscous numerical simulation of liquid sloshing in rectangular tank with/without baffles and comparison with potential flow solutions, Ocean Engineering, 108, 662-677.

Lu, D., Fu, S., Zhang, X., Guo, F., Gao, Y., (2016) A method to estimate the hydroelastic behaviour of VLFS based on multi-rigid-body dynamics and beam bending. Ships and Offshore Structures, 1–9.

Lu, L., Sasa, K., Sasaki, W., Terada, D., Mizojiri, T. (2017) Rough wave simulation and validation using onboard ship motion data in the Southern Hemisphere to enhance ship weather routing. Ocean Engineering 144, 61-77.

Lu, Z., Fu, S., Zhang, M., Ren, H., Song, L., (2017a) A Non-Iterative Method for Vortex Induced Vibration Prediction of Marine Risers. ASME 2017, International Conference on Ocean, Offshore and Arctic Engineering (pp.V002T08A028).

Lucas C. and Guedes Soares C. (2015) Bivariate distributions of significant wave height and mean wave period of combined sea states, Ocean Engineering,106, 341–353.

Luo, M., Koh, C.G., Bai, W. (2016), A three-dimensional particle method for violent sloshing under regular and irregular excitations, Ocean Engineering, 120, 52-63.

Luxmoore, J.F., Grey, S., Newsam, D., Johanning, L. (2016) Analytical performance assessment of a novel active mooring system for load reduction in marine energy converters. Ocean Engineering, 124, 215-225.

Lyu W and el Moctar O (2017) Numerical and experimental investigation of wave-induced second order hydrodynamic loads. Ocean Engineering 131, 197-212

Ma, Z. H., Qian, L., Causon, D. M., Mingham, C. G., Mai, T., Greaves, D., & Raby, A. (2015, #jul#). The Role of Fluid Compressibility in Predicting Slamming Loads During Water Entry of Flat Plates.

Malenica, Š., Zala, M., Chen, X.B. (2003), Dynamic coupling of seakeeping and sloshing, 13rd International Offshore and Polar Engineering Conference, ISOPE 2003, Hawaii, USA.

Malenica, S., & Derbanne, Q. (2014). Hydro-structural issues in the design of ultra large container ships. International Journal of Naval Architecture and Ocean Engineering, 6, 983-999.

Malenica, S., Vladimir, N., Choi, Y.M., et al. (2015) Global hydroelastic model for liquid cargo ships, Proceedings of 7th International Conference on Hydroelasticity in Marine Technology, September 16-19, 2015, Split, Croatia, 493-505.

Malenica, Š., Diebold, L., Kwon, S.H., Cho, D.-S. (2017), Sloshing assessment of the LNG floating units with membrane type containment system where we are? Marine Structures, 56, 99-116.

Manderbacka, T., Ruponen, P., Kulovesi, J., Matusiak, J. (2015), Model experiments of the transient response to flooding of the box shaped barge, Journal of Fluids and Structures, 57, 127-143.

Mao, W., Rychlik, I., Wallin, J., Storhaug, G. (2016) Statistical models for the speed prediction of a container ship. Ocean Engineering 126, 152-162

Meng, W. & Qiu, W. (2015) Nonlinear computation of ship motions in the time-domain using 2D+T theory. Proceedings of the ASME 2015 34th International Conference on Ocean, Offshore and Arctic Engineering, OMAE2015, Mai 31 –June 5, 2015, St. John's, Newfoundland, Canada.

Mirafzali, F., Tavakoli, A., Mollazadeh, M., (2015) Hydroelastic analysis of fully nonlinear water waves with floating elastic plate via multiple knot B-splines, Applied Ocean Research, 51: 171-180.

Moctar, O., Ley, J., Oberhagemann, J., et al. (2017) Nonlinear computational methods for hydroelastic effects of ships in extreme seas, Ocean Engineering, 130: 659-673.

Mohammadi, S.M., Khedmati, M.R. & Vakilabadi, K.A. (2015) Effect of hull damage on global loads acting on a trimaran ship. Ship and Offshore Structures 10(6):635-625

Molin, B., Remy, F., Rigaud, S., de Jouette, C. (2002), LNG-FPSO's: frequency domain, coupled analysis of support and liquid cargo motion, 10th IMAM Conference, IMAM 2002, Rethymnon, Greece.

Montazeri, N., Jensen, J.J., Nielsen, U.D. (2015) Uncertainties in ship-based estimation of waves and responses. In Proceedings of OCEANS '15, Washington, DC, USA

Mousaviraad, S.M., Sadat-Hosseini S.H., Carrica, P.M. & Stern, F. (2016) Ship-ship interaction in calm water and waves. Part 2: URANS validation in replenishment and overtaking conditions. Ocean Engineering 111: 627-638.

Mousaviraad, M., Zhaoyuan, W. & Stern, F. (2015) URANS studies of hydrodynamic performance and slamming loads on high-speed planning hulls in calm water and waves for deep and shallow conditions. Applied Ocean Research 51:222-240.

Mozumi, K. (2015) '3D stereo imaging of abnormal waves in a wave basin', in International Conference on Ocean, Offshore and Arctic Engineering. St. John's: ASME, pp. 1–5.

Naruse, Y. and Kawamura, Y. (2015) A comparison of structural reliability of ultimate strength of bulk carriers before and after the effectuation of CSR, Proceedings of TEAM, 12-15 October, Vladivostok, Russia.

Nayak, S.K., Biswal, K.C. (2015), Fluid damping in rectangular tank fitted with various internal objects – An experimental investigation, Ocean Engineering, 108, 552-562.

Newman, J.N. (2005), Wave effects on vessels with internal tanks, 20th Workshop on Water Waves and Floating Bodies, Spitsbergen, Norway.

Nielsen, U.D. (2006) Estimations of on-site directional wave spectra from measured ship responses. Marine Structures 19, 33-69

Oberhagemann, Shigunov, Radon, Mumm, & Won. (2015). Hydrodynamic load analysis and ultimate strength check of an 18000 TEU containership. PROCEEDINGS of the 7th internalitional conference on hydroelasticity in marine technology.

Oggiano, L., Arens, E., Myhr, A., Nygaard, T.A., Evans, S. (2015). CFD Simulations on a Tension Leg Buoy Platform for Offshore Wind Turbines and Comparison with Experiments, Proceedings of the Twenty-fifth International Ocean and Polar Engineering Conference, Kona, Big Island, Hawaii, USA.

Oka et al. (2015) A Study on the Effect of Hull Girder Vibration on the Fatigue Strength, In G. S. & Shenoi (Ed.), na (pp. 293–300). London: Taylor & Francis Group.

Ozdemir, M., Yao, T., Yanagihara, D. and Ergin, A. (2015) Ultimate strength assessment of ship panels under overall collapse, Proceedings of TEAM, 12-15 October, Vladivostok, Russia.

Paik, J.K., Lee, S.E., Kim, B.J., Seo, J.K., Ha, Y.C., Matsumoto, T., Byeon, S.H. (2015), Toward a probabilistic approach to determine nominal values of tank sloshing loads in structural design of liquefied natural gas FPSOs, Journal of Offshore Mechanics and Arctic Engineering, 137.

Pákozdi, C., Östeman, A., Stansberg, C. T., Peric, M., Lu, H., & Baarholm, R. (2015). Estimation of Wave in Deck Load Using CFD Validated Against Model Test Data. In 25th International Ocean and Polar Engineering Conference. Kona, Hawaii, USA, ISOPE-I-15-586

Pákozdi, C., Östman, A., Abrahamsen, B.C., Økland, O.D., Vestbøstad, T. M., Lian, G. & Stansberg, C. T., (2017), New combined CFD and model testing technique for identification of wave impact loads on a semisubmersible. In Proceedings 36th International Conference on Ocean, Offshore and Arctic Engineering, Trondheim, Norway, OMAE2017-62643.

Palm, J., Eskilsson, C. and Bergdahl, L. (2017) An hp-adaptive discontinuous Galerkin method for modelling snap loads in mooring cables. Ocean Engineering, 144, 266-276.

Papanikolaoua, A., Mohammedb, E.A., Hirdarisc, S.E. (2014) Stochastic uncertainty modelling for ship design loads and operational guidance. Ocean Engineering 86, 47-57

Parunov, J., Corak, M. and Gledic, I. (2015) 'Comparison of two practical methods for seakeeping assessment of damaged ship', in Marstruct 2015. London: Taylor & Francis Group, pp. 37–44.

Park, D.-M., Kim, Y., Seo, M.-G. & Lee, J. (2016) Study on added resistance of a tanker in head waves at different drafts. Ocean Engineering 111: 569.581.

Park, D.M. Kim, J.H., Kim, Y. (2017) Numerical study of mean drift force on stationary flexible barge, Journal of Fluids and Structures, 74: 445-468.

Pavon, C.L., Souto-Iglesias, A. (2015). Hydrodynamic coefficients and pressure loads on heave plates for semi-submersible floating offshore wind turbines: A comparative analysis using large scale models", Renewable Energy.

Pascoal, R., Perera, L.P., Guedes Soares, C. (2017) Estimation of directional sea spectra from ship motions in sea trials. Ocean Engineering 132, 126-137

Passano, E., Abtahi, S., Ottesen, T. (2016), A procedure to include slip damping in a VIV analysis of an umbilical. Proceedings of the ASME 2016 35th International Conference on Ocean, Offshore and Arctic Engineering OMAE2016, June 19-24, Busan, South Korea, paper 54816

Peschmann, J., Storhaug, G., Derbanne, Q., Xie, G., Zheng, G., Ishibashi, K. and Kim, J. (2016) Impact Study on the new IACS Longitudinal Strength Standard for Containerships (UR S11A), Proceedings of PRADS, 4-8 September, Copenhagen, Denmark.

Peschmann, J. and von Selle H. (2017) IACS common structural rules as an element of IMO goal based standards for bulk carriers and oil tankers, Proceedings of the 6th International Conference on Marine Structures , 8-10 May, Lisbon, Portugal.

Pessoa, J. M., & Moe, A. M. (2017). Air Gap on Semisubmersible MODUs Under DNVGL Class - Current & Future Design Practice. In Offshore Technology Conference, Houston, Texas, USA, OTC-27693-MS

Petroleum Safety Authority of Norway (PSA), (2016), Investigation into an accident with fatal consequence on COSL Innovator, 30 December 2015, PSA 06/07/2016

Potthoff, R and Moctar, B (2016) Presentation of Benchmark results: SHOPERA Benchmark Workshop, SHOPERA, London

Primorac Bužančić, B., Slapnicar, V., Munic, I., Grubisic, V., Corak, M. and Parunov, J. (2015) 'Statistics of still water bending moment of damaged ships', in Altosole, M. and Francescutto, A. (eds) 18th International Conference on Ships and Shipping Research. Lecco: NAV 2015, pp. 580–589.

Prpić-Oršić, J., Parunov, J., Šikić, I. (2014) Operation of ULCS - real life. International Journal of Naval Architecture and Ocean Engineering 6, 1014-1023

Qian, P., Yi, H. & Li, Y. (2015) Numerical and experimental studies on hydrodynamic performance of a small-waterplane-area-twin-hull (SWATH) vehicle with inclined struts. Ocean Engineering 96:181-191.

Qiu, W., Peng, H., Wang, J. & Nizam, S. (2017) Improving the panel-free method for the prediction of ship motions and wave induced loads. Proceedings of the ASME 2017 36th International Conference on Ocean, Offshore and Arctic Engineering, OMAE2017. June 25-30, 2017, Trondheim, Norway.

Qiu, W., Lee, D-Y, Lie, H., Rousset, J-M., Mikami, T., Sphaier, S., Tao, L., Wang, X., Magarovskii, V. (2017a) Numerical benchmark studies on drag and lift coefficients of a marine riser at high Reynolds numbers. Applied Ocean Research, Vol.69, 2017, pp.245-251.

Rajendran, S., Fonseca, N. & Soares, C.G. (2015a) Effect of surge motion on the vertical responses of ships in waves. Ocean Engineering, 96:125-138.

Rajendran, S., Fonseca, N. & Soares, C.G. (2015b) Simplified body nonlinear time domain calculation of vertical ship motions and wave loads in large amplitude waves. Ocean Engineering 107:157-177.

Rajendran, S., Guedes Soares, C. (2016a) Numerical investigation of the vertical response of a containership in large amplitude waves. Ocean Engineering 123, 440-451

Rajendran, S., Vasquez, G., Guedes Soares, C. (2016b) Effect of bow flare on the vertical ship responses in abnormal waves and extreme seas. Ocean Engineering 124, 419-436

Richtera, J.K. Schauta, S. Walserb, D. Schneiderb, K. Sawodnya, O. (2017), Experimental validation of an active heave compensation system: Estimation, prediction and control, Control Engineering Practice, Vol 66, Sept 2017, pp 1-12

Riesner, M., von Graefe, A., Shigunov, V. & el Moctar, o. 2016. Prediction of non-linear ship responses in waves considering forward speed effects. Ship Technology Research – Schiffstechnik, 63 (3), 135-144

Saripilli Jai Ram, Sen, D. (2017a), Numerical Studies of Coupling Effect of Sloshing on 3D Ship Motions, International Journal of Offshore and Polar Engineering, 27, 1, 27 - 35

Saripilli Jai Ram, Sen, D. (2017b) Numerical Studies on Sloshing Loads using Sloshing Coupled Ship Motion Algorithm, Proceedings of the 27th International Ocean and Polar Engineering Conference, San Francisco, CA, USA, June 25-30

Sen Debabrata, et. Al. (2017) Numerical studies on slosh-induced loads using coupled algorithm for sloshing and 3D ship motions, Proceedings of the ASME 2017 36th International Conference on Ocean, Offshore and Arctic Engineering, OMAE2017, June 25-30, Trondheim, Norway

Sengupta, D., Datta, R. & Sen, D. 2016. A simplified approach for computation of nonlinear ship loads and motions using a 3D time-domain panel method. Ocean Engineering 17:99-113

Seo, S., Park, S. & Koo, B.Y. (2017) Effect of wave period on added resistance and motions of a ship in head sea simulations. Ocean Engineering 137:309-327.

Seung-Ho Ham, Myung-Il Roh, Hyewon Lee, Sol Ha (2015) Multibody dynamic analysis of a heavy load suspended by a floating crane with constraint-based wire rope, Ocean Engineering, 109, 145 – 160

B. Serván-Camas, J.L. Cercós-Pita, J. Colom-Cobb, J. García-Espinosa, A. Souto-Iglesias (2016) Time domain simulation of coupled sloshing–seakeeping problems by SPH–FEM coupling, Ocean Engineering, 123, 383 – 396

Shashikala A.P, Shankar K Varma, (2017) Optimization of Separation Distance between Two Floating Bodies, Proceedings of the 27th International Ocean and Polar Engineering Conference, San Francisco, CA, USA, June 25-30

Shivaji Ganesan T. , Debabrata Sen (2016) Time domain simulation of side-by-side floating bodies using a 3D numerical wave tank approach, Applied Ocean Research, 58,

Sidarta, D.E., Kyoung, J., O'Sullivan, J., Lambrakos, K.F. (2017) Prediction of offshore platform mooring line tensions using artificial neural network. Proceedings of the ASME 2017 36th International Conference on Ocean, Offshore and Arctic Engineering, OMAE2017, June 25-30, Trondheim, Norway, paper 61942.

Silva Daniel F.C et. Al. (2017) Green water loads on FPSOs exposed to beam and quartering seas, Part II: CFD simulations, Ocean Engineering, 140, 1 August 2017, 434-452

Silva-González, F., Heredia-Zavoni, E. and Inda-Sarmiento, G. (2017) Square Error Method for threshold estimation in extreme value analysis of wave heights, Ocean Engineering,137, 138–150.

Song Youn Kyung, Chang Kuang-An, Ariyarathne Kusalika and Mercier Richard (2015) Surface velocity and impact pressure of green water flow on a fixed model structure in a large wave basin, Ocean Engineering, 104, 40 – 51.

Song, L., Fu, S., Cao, J., Ma, L., Wu, J., (2016) An investigation into the hydrodynamics of a flexible riser undergoing vortex-induced vibration. Journal of Fluids & Structures, 63, 325-350.

Soukissian, T. H. (2014) Probabilistic modelling of directional and linear characteristics of wind and sea states, Ocean Engineering,91, 91–110.

Southall, N., Choi, S., Lee, Y., Hong, C., Hirdaris, S., & White, N. (2015, #jul#). Impact Analysis using CFD, A Comparative Study.

Sprenger Florian et. Al.(2017) Comparative study of motions and drift forces in waves and current, Proceedings of the ASME 2017, 36th International Conference on Ocean, Offshore and Arctic Engineering, OMAE2017, June 25-30, Trondheim, Norway

Stansberg C. T., Hoff, J. R., Hermundstad, E. M., Baarholm, R. J., 2013, Wave drift forces and responses in current" Proceedings of the 32nd International Conference on Ocean, Offshore and Arctic Engineering.

Sun, S. Y., Sun, S. L., & Wu, G. X. (2015). Oblique water entry of a wedge into waves with gravity effect. Journal of Fluids and Structures, 52, 49-64.

Swan, C., Latheef, M. & Ma, L., (2016), The loading and reliability of fixed steel structures in extreme seas: recent advances and required improvements. In 3rd Offshore Strurcural Reliability Conference, OSRC2016, Stavanger, Norway

Swidan, A., Thomas, G., Ranmuthugala, D., Amin, W., Penesis, I., Allen, T., & Battley, M. (2016). Experimental drop test investigation into wetdeck slamming loads on a generic catamaran hullform. Ocean Engineering, 117, 143-153.

Tanizawa K, 1995, A nonlinear simulation method of 3-D body motions in waves, 1st report. J Soc Nav Arch Jpn 178:179–191

Tanizawa K , 1996, Long time fully nonlinear simulation of floating body motions with artificial damping zone, J Soc Naval Archit of Jpn 180:311–319

Temarel, P., Bai, W., Bruns, A., Derbanne, Q., Dessi, D., Dhavalikar, S., Fonseca, N., Fukasawa, T., Gu, X., Nestegård, A., Papanikolaou, A., Parunov, J., Song, K.H. (2015) Loads - Committee I.2 report. Proceedings 19th International Ship and Offshore Structures Congress (ISSC2015), 7-10 September, Cascais, Portugal.

Tuitman, J. T. (2010). Hydro-elastic response of ship structures to slamming induced whipping.

Tunea, E. and Uguflu, B. (2015) Ultimate strength analysis for the assessment of stiffener-plate design configuration, Proceedings of TEAM, 12-15 October, Vladivostok, Russia.

Rajendran, S. Fonseca, N., Guedes Soares, C., (2016a) A numerical investigation of the flexible vertical response of an ultra large containership in high seas compared with experiments, Ocean Engineering, 122: 293-310.

Rajendran, S. Guedes Soares, C., (2016b) Numerical investigation of the vertical response of a containership in large amplitude waves, Ocean Engineering, 123: 440-451.

Ravnik, J., Strelnikova, E., Gnitko, V., Degtyarev K., Ogorodnyk, U. (2016), BEM and FEM analysis of fluid-structure interaction in a double tank, Engineering Analysis with Boundary Elements, 67, 13-25.

Ren, H.L., Chen, L.L., Li, H., et al. (2016) Study of the design wave loads of a trimaran based on 3D time-domain hydroelastic theory (in Chinese), Journal of Harbin Engineering Univesity, 37(1): 19-23.

Robert, M., Monroy, C., Reliquet, G., et al. (2015) Hydroelastic response of a flexible barge investigated with a viscous flow solver, Proceedings of 7th International Conference on Hydroelasticity in Marine Technology, September 16-19, 2015, Split, Croatia, 607-621.

Saripilli, J.R., Sen, D. (2017), Numerical studies of coupling effect of sloshing on 3D ship motions, International Journal of Offshore and Polar Engineering, 27, 27-35.

Sasa, K., Faltinsen, O.M., Lu, L., Sasaki, W., Prpić-Oršić, J., Kashiwagi, M., Ikebuchi, T., (2017) Development and validation of speed loss for a blunt-shaped ship in two rough sea voyages in the Southern Hemisphere. Ocean Engineering 142, 577-596

Schwarz-Röhr, B., Ntambantamba, B. and Härting, A. (2016) 'Estimating Seaway from Ship Motions', in Proceeding of PRADS2016. Copenhagen, pp. 1–7.

Sen, D., Saripilli, J.R. (2017), Numerical studies on slosh-induced loads using coupled algorithm for sloshing and 3D ship motions, 36th International Conference on Ocean, Offshore and Artic Engineering, OMAE 2017, Trondheim, Norway.

Sengupta, D., Kumar Pal, S., Datta, R. (2017) Hydroelasticity of a 3D floating body using a semi analytic approach in time domain, Journal of Fluids and Structures, 71: 96-115.

Serván-Camas, B., Cercós-Pita, J.L., Colom-Cobb, J., García-Espinosa, J., Souto-Iglesias, A. (2016), Time domain simulation of coupled sloshing-seakeeping problems by SPH-FEM coupling, Ocean Engineering, 123, 383-396.

Shehzad K. et al. (2013), Study on Spectral Fatigue Assesment of Trimaran Structure, Research Journal of Applied Sciences, Engineering and Technology 2013.

Stephen, J.J., Sannasiraj, S.A., Sundar, V. (2017), Numerical simulation of sloshing in a rectangular tank under combined horizontal, vertical and rotational oscillations, Journal of Engineering for the Maritime Environment, 230, 95-113.

Sterenborg, J., Koop, A., de Wilde, J., Vinayan, V., Antony, A., & Halkyard, J. (2016). Model Test Investigation of the Influence of Damping on the Vortex Induced Motions of Deep Draft Semisubmersibles using a Novel Active Damping Device. In Proceedings 35th International Conference on Ocean, Offshore and Arctic, Busan, Korea, OMAE2016-54810.

Storhaug, G., Aagaard, O. and Fredriksen, Ø. (2016) 'Calibration of hull monitoring strain sensors in deck including the effect of hydroelasticity', in International Conference on Ocean, Offshore and Arctic Engineering. Rhodes: ISOPE, pp. 487–494.

Storhaug, G. and Kahl, A. (2015) 'Full scale measurements of torsional vibrations on Post-Panamax container ships', in 7th International Conference on Hydroelasticity in Marine Technology. Split, pp. 293–311.

Su, Y., Liu, Z.Y. (2017), Coupling effects of barge motion and sloshing, Ocean Engineering, 140, 352-360.

Sufyan, M., Ngo, L.C., Choi, H.G. (2017), A dynamic adaptation method based on unstructured mesh for solving sloshing problems, Ocean Engineering, 129, 203-216.

Suominen, M., Romanoff, J., Remes, H. and Kujala, P. (2015) 'The determination of ice-induced loads on the ship hull from shear strain measurements', in International Conference on Marine Structures MARSTRUCT. London: Taylor & Francis Group, pp. 375–383.

Tabib, M., Rasheed, A., Fuch, F.G. (2017), Analysis of unsteady hydrodynamics related to vortex induced vibrations on bluff-bodied offshore structure. Proceedings of the ASME 2017 36th International Conference on Ocean, Offshore and Arctic Engineering OMAE2017, June 25-30, Trondheim, Norway, paper 61207

Tang, Z., Zhang, Y., Wan, D. (2015), Numerical study of sloshing in baffled tanks by MPS, 25th International Ocean and Polar Engineering Conference, ISOPE 2015, Hawaii, Unite States.

Tang, Y., Li, Y., Liu, L., Jin, W. & Qu, X. (2017). Study on Influence of Vortex Induced Loads on the Motion of Spar.Type Wind Turbine based on Aero-Hydro-Vortex-mooring Coupled Model. In Proceedings 36th International Conference on Ocean, Offshore and Arctic Engineering, Trondheim, Norway, OMAE2017-62620.

Teixeira, D.C. and Morooka, C.K. (2017) A time domain procedure to predict vortex-induced vibration response of marine risers. Ocean Engineering 142, 419–432

Temarel, P., Bai, W., Bruns, A., Derbanne, Q., Dessi, D., Dhavalikar, S., Fonseca, N., Fukasawa, T., Gu, X., Nestegård, A., Papanikolaou, A., Parunov, J., Song, K.H., Wang, S. (2016) Prediction of wave-induced loads on ships: Progress and challenges. Ocean Engineering 119, 274-308

Thorsen, M., Sævik, S., Larsen, C. (2016) Time domain simulation of vortex-induced vibrations in stationary and oscillating flows. Marine Structures 51.

Thorsen, M., Sævik, S., Larsen, C. (2017a) Non-linear time domain analysis of cross-flow vortex-induced vibrations. Marine Structures 51.

Thorsen, M., Sævik, S. (2017b) Simulating riser VIV in current and waves using an empirical time domain model. Proceedings of the ASME 2017 36th International Conference on Ocean, Offshore and Arctic Engineering OMAE2017, June 25-30, Trondheim, Norway, paper 61217.

Tomasicchio, G.R. Avossa, A.M. Riefolo, L. Ricciardelli, F. Musci, E. D'Alessandro, F. Vicinanza, D. (2017) Dynamic Modelling of a Spar Buoy Wind Turbine, OMAE2017, June 25-30, 2017, Trondheim, Norway.

Tsukada, R.I and Morooka, C.K. (2016) A numerical procedure to calculate the VIV response of a catenary riser . Ocean Engineering 122, 145-161

Tychsen, J. & Dixen, M., (2016), Wave kinematics and hydrodynamic load on intermediate water depth structures inferred from systematic model testing and field observations – Tyra Field Extreme Wave Study 2013-2015. In 3rd Offshore Strurcural Reliability Conference, OSRC2016, Stavanger, Norway

Tychsen, J., Risvig, S., Fabricius Hansen, H., Ottesen Hansen, N. & Stevanato, F., (2016), Summary of the impact on structural reliability of the findings of the Tyra Field Extreme Wave Study 2013-2015. In 3rd Offshore Strurcural Reliability Conference, OSRC2016, Stavanger, Norway

Ulveseter, J.V., M.J., Sævik, S., Larsen, C.M. (2017a) Time domain model for calculation of pure in-line vortex-induced Vibrations, Journal of Fluids and Structures 68, 158–173.

Ulveseter, J.V., Thorsen, M.J., Sævik, S., Larsen, C.M. (2017b) Stochastic modelling of cross-flow vortex-induced vibrations. Marine Structures, 56, 260-280.

University of Maine. (2014). W2 Wind-Wave Basin.

Vásque, G., Fonseca, N. & Soares, C.G. (2016) Experimental and numerical vertical bending moments of a bulk carrier and a roll-on/roll-off ship in extreme waves. Ocean Engineering 124: 404-418.

Vettor, R., Guedes Soares, C. 2016. Development of a ship weather routing system. Ocean Engineering 123, 1-14.

Vedeld, K., Sollund, H., Fryileiv, O., Nestegård, A. (2016) A response model for vortex induced vibrations in low KC number flows. Proceedings of the ASME 2016 35th International Conference on Ocean, Offshore and Arctic Engineering OMAE2016, June 19-24, Busan, South Korea, paper 55000.

Viselli, A. M., (2014), Model Test of a 1:8 Scale Floating Wind Turbine Offshore in the Gulf of Maine, Electronic Theses and Dissertations. Paper 2185.

Viselli, A. M., Goupee, A. J., Dagher, H. J., and Allen, C. K., (2015), VolturnUS 1:8: Conclusion of 18-Months of Operation of the First Grid-Connected Floating Wind Turbine Prototype in the Americas, Proc. Of the ASME 2015 34th International Conference on Ocean, Offshore and Arctic Engineering, St. John's, Newfoundland, Canada.

Voie P, Wu J, Resvanis T.L., Larsen, C.M., Vandiver K., Triantafyllou, M., Baarholm, R. (2017) Consolidation of Empirics for Calculation of VIV Response. Proceedings of the ASME 2017 36th International Conference on Ocean, Offshore and Arctic Engineering OMAE2017, June 25-30, Trondheim, Norway, paper 61362.

Vorhölter, H. Hatecke, H. Feder, D. (2015) Design Study of Floating Crane Vessels for Lifting Operations in the Offshore Wind Industry, 12th International Marine Design Conference · IMDC 2015

Wada, R., Waseda, T., Jonathan, P. 2016. Extreme value estimation using the likelihood-weighted method. Ocean Engineering 124, 241-251

Wang, X., Arai, M. (2015), A numerical study on coupled sloshing and ship motions of a liquefied natural gas carrier in regular and irregular waves, Journal of Engineering for the Maritime Environment, 229, 3-13.

Wang, J., Fu, S., Baarholm, R., Wu, J., Larsen, C.M., (2015a) Out-of-plane vortex-induced vibration of a steel catenary riser caused by vessel motions. Ocean Engineering 109, 389-400.

Wang, S., & Soares, C. G. (2016). Stern slamming of a chemical tanker in irregular head waves. Ocean Engineering, 122, 322-332.

Wang, S. and Guedes Soares C. (2016a) Experimental and numerical study of the slamming load on the bow of a chemical tanker in irregular waves, Ocean Engineering,111, 369–383.

Wang, Y., Wu, W., & Guedes Soares, C. (2016). Slam Induced Loads on a 3D Bow With Various Pitch Angles. V007T06A061.

Wang, S., Karmakar, D., Guedes Soares, C. (2016a) Hydroelastic impact of a horizontal floating plate with forward speed, Journal of Fluids and Structures, 60: 97-113.

Wang, W., Peng, Y., Zhou, Y., Zhang, Q. (2016b), Liquid sloshing in partly-filled laterally-excited cylindrical tanks equipped with multi baffles, Applied Ocean Research, 59, 543-563.

Wang, X., Gu, X., Temarel, P. and Hu, J. (2016c) 'Investigation of springing in ship structures using experimental methods and 3-D hydroelastic theory', J Mar Sci Technol, 21, p. pp 271-281.

Wang, W. et al. (2016d) Ship Motions Contribution to the Fatigue Life of a Pre-swirl Stator, PRADS2016, Copenhagen.

Wang, J., Xiang, S., Fu, S., Cao, P., Yang, J., He, J., (2016e) Experimental investigation on the dynamic responses of a free-hanging water intake riser under vessel motion. Marine Structures 50, 1-19.

Wang, Q.B., Tian, C., Ding, J., et al. (2017) Hydroelastic analysis of CSSRC 20,000 TEU ultra large containership in time domain, The Ninth International Conference of Navy and Shipbuilding Nowadays (NSN), June 29-30, St. Petersburg, Russia, 47-56.

Wang, J., & Faltinsen, O. M. (2017). Improved numerical solution of Dobrovol'skaya's boundary integral equations on similarity flow for uniform symmetrical entry of wedges. Applied Ocean Research, 66, 23-31.

Wang, J., Fu, S., Wang, J., Li, H., Ong, M.C., (2017a). Experimental Investigation on Vortex-Induced Vibration of a Free-Hanging Riser Under Vessel Motion and Uniform Current. Journal of Offshore Mechanics and Arctic Engineering 139, 041703.

Wang Shuo, Wang Xin and Woo Wai Lok (2017) Numerical Green Water Assessment for an FPSO with Consideration of Nonlinear Effects from Bilge Keel, Spread Mooring and Asymmetric Risers, Proceedings of the 27th International Ocean and Polar Engineering Conference, San Francisco, CA, USA, June 25-30

Wang Zhengke, He Guanghua, Zhang Zhigang, Qi Chi (2017) Effect of Wave Interaction among Multiple Floating Bodies on Hydrodynamic Forces, Proceedings of the 27th International Ocean and Polar Engineering Conference, San Francisco, CA, USA, June 25-30

Wei, W., Fu, S.X., Moan, T., et al. (2017) A discrete-modules-based frequency domain hydroelasticity method for floating structures in inhomogeneous sea conditions, Journal of Fluids and Structures, 74:321-339 .

Wei, W., Fu, S., Moan, T., Song, C., Ren, T., (2018) A time-domain method for hydroelasticity of very large floating structures in inhomogeneous sea conditions, Marine Structures, 57, 180–192.

Wen, P., & Qiu, W. (2015). CIP and Parallel Computing Based Numerical Solutions of 3-D Slamming Problems. V011T12A020.

Weller, S.D., Johanning, L., Davies, P., Banfield, S.J., 2015. Synthetic mooring ropes for marine renewable energy applications. Renewable Energy, 83, 1268-1278.

Weller, S.D., Davies, P., Vickers, A.W., Johanning, L., 2014. Synthetic rope responses in the context of load history: Operational performance. Ocean Engineering, 83, 111-124.

Weller, S.D., Davies, P., Vickers, A.W., Johanning, L., 2015. Synthetic rope responses in the context of load history: The influence of aging. Ocean Engineering, 96, 192-204.

Woodacrea, R.J.BaueraR.A.Iraniba (2015), A review of vertical motion heave compensation systems, Ocean Engineering, Vol 104, August 2015, pp 140-154

Wu, M. (2015) 'Fatigue analysis for a high-speed vessel with hydroelastic effects', in 7th International Conference on Hydroelasticity in Marine Technology. Split, pp. 343–362.

Wu, N.-J., Hsiao, S.-C., Wu H.-L. (2016), Mesh-free simulation of liquid sloshing subjected to harmonic excitations, Engineering Analysis with Boundary Elements, 64, 90-100.

Wu, Y.S., Zou, M.S., Tian, C., et al. (2016a) Theory and applications of coupled fluid-structure interactions of ships in waves and ocean acoustic environment, Journal of Hydrodynamics, 28(6):923-936.

Wu, J., Lekkala, M.R., Ong, M.C. (2016b) Prediction of riser VIV with staggered buoyancy elements. Proceedings of the ASME 2016 35th International Conference on Ocean, Offshore and Arctic Engineering OMAE2016, June 19-24, Busan, South Korea, paper 54502.

Wu, Y.S, Ding, J. Li, Z.W., et al.. (2017a) Hydroelastic responses of VLFS deployed near islands and reefs, Proceedings of the ASME 2017 36th International Conference on Ocean, Offshore, and Arctic Engineering, June 25-30, 2017, Trondheim, Norway.

Wu, Y.S., Ding, J., Tian, C., et al. (2017b) Hydroelastic behaviors of VLFS in complicated ocean environment, The 10th International Workshop on Ship and Marine Hydrodynamics (IWSH 2017), November 4-8, 2017, Taiwan.

Wu, J., Lie, H., Fu, S., Baarholm, R., Constantinides, Y. (2017c) VIV responses of riser with buoyancy elements: forced motion test and numerical prediction. Proceedings of the ASME 2017 36th International Conference on Ocean, Offshore and Arctic Engineering OMAE2017, June 25-30, Trondheim, Norway, paper 61768.

Wu, J., Lekkala, M.R., Ong, M.C., Passano, E., Voie, P.E. (2017d) Prediction of combined IL and CF VIV responses of deepwater risers. Proceedings of the ASME 2017 36th International Conference on Ocean, Offshore and Arctic Engineering OMAE2017, June 25-30, Trondheim, Norway, paper 61766.

Xi Chen, Ren-chuan Zhu, 2017, Time Domain Analysis of Side by Side Vessels' Motion Responses During Offshore Installation and Underway Replenishment, Proceedings of the 27th International Ocean and Polar Engineering Conference, San Francisco, CA, USA, June 25-30

Xu, Q., Hu Z., Jiang, Z. (2017), Experimental investigation of sloshing effect on the hydrodynamic responses of an FLNG system during side-by-side operation, Ships and Offshore Structures, 12, 804-817.

Xue M.-A., Zheng, J., Lin, P., Yuan, X. (2017), Experimental study on vertical baffles of different configurations in suppressing sloshing pressure, Ocean Engineering, 136, 178-189.

Yang, P., Gu, X.K., Tian, C., et al. (2015a) 3D hydroelastic response of a large bulk carrier in time domain, Proceedings of 7th International Conference on Hydroelasticity in Marine Technology, September 16-19, 2015, Split, Croatia, 529-540.

Yang, P., Liu, X.L., Ding, J., et al. (2015b) Hydroelastic responses of a VLFS in the waves influenced by complicated geographic environment, Proceedings of 7th International Conference on Hydroelasticity in Marine Technology, September 16-19, 2015, Split, Croatia, 541-559.

Yao, CB & Dong, WC. (2016) Numerical study on local steady flow effects on hydrodynamic interaction between two parallel ships advancing in waves. Engineering Analysis with Boundary Elements 66: 129-144.

Yin, C., Wu, J., Wan, D. (2015), Numerical study on liquid sloshing in three-dimensional rectangular tanks with different filling rates and fixed baffle, 25th International Ocean and Polar Engineering Conference, ISOPE 2015, Hawaii, Unite States.

Yin, D., Passano, E., & Larsen, C. M. (2017) Improved In-line VIV Prediction for Combined In-line and Cross-flow VIV Responses. ASME. J. Offshore Mech. Arct. Eng. 2017; doi:10.1115/1.4038350.

Yoshida, H., Orihara, H. and Yamasaki, K. (2015) 'Long-term wave measurement by an onboard wave radar meter and prediciton of ship motions based on the onboard wave

measurements', in Proceedings of the ASME 34th International Conference on Ocean, Offshore and Arctic Engineering. St. John's, pp. 1–7.

Yu, Y.-M., Ma, N., Fan, S.-M., Gu, X.-C. (2017), Experimental and numerical studies on sloshing in a membrane-type LNG tank with two floating plates, Ocean Engineering, 129, 217-227.

Zhang, C. (2015), Analysis of liquid sloshing in LNG carrier with wedge-shaped tanks, Ocean Engineering, 105, 304-317.

Zhang, C. and Soares, G. (2016) Ship responses to abnormal waves simulated by the nonlinear Schrödinger equation, Ocean Engineering, 119, 143-153.

Zhang, C. (2016a), Analytical study of transient coupling between vessel motion and liquid sloshing in multiple tanks, Journal of Engineering Mechanics, 142.

Zhang, K., Ren, H., Li, H. and Yan, L. (2016b) 'Nonlinear Hydroelasticity of Large Container Ship', in International Conference on Ocean, Offshore and Arctic Engineering. Rhodes: ISOPE, pp. 434–440.

Zhang, S., Villavicencio, R. and White, N. (2017) Ultimate strength of the hull girder of large container ships, Proceedings of the 6th International Conference on Marine Structures , 8-10 May, Lisbon, Portugal.

Zhang Jie and Kashiwagi, M., (2017) Application of ALE to nonlinear wave diffraction by a non-wall-sided structure, Proceedings of the 27th International Ocean and Polar Engineering Conference, San Francisco, CA, USA, June 25-30.

Zhang, M., Fu, S., Song, L., Wu, J., Lie, H., Ren, H., (2017a) Hydrodynamics of Flexible Pipe With Staggered Buoyancy Elements Undergoing Vortex-Induced Vibrations. ASME 2017, International Conference on Ocean, Offshore and Arctic Engineering (pp.V002T08A030).

Zhao, W., Yang, J., Hu, Z., Xiao, L., Tao, L. (2014), Hydrodynamics of a 2D vessel including internal sloshing flows, Ocean Engineering, 84, 45-53.

Zhao, L. Roh, M. Ham, S. (2016) Hardware-In-The-Loop Simulation For A Heave Compensator Of An Offshore Support Vessel, Proceedings of the 35th International Conference on Ocean, Offshore and Arctic Engineering, OMAE 2016, June 19-24, 2016, Busan, South Korea

Zhao, W., McPhail, F., Efthymiou, M. (2016a), Effect of partially filled spherical cargo tanks on the roll response of a barge like vessel, Journal of Offshore Mechanics and Arctic Engineering, 138.

Zhao, W., McPhail, F. (2017), Roll response of an LNG carrier considering the liquid cargo flow, Ocean Engineering, 129, 83-91.

Zhu, S. and Moan, T. (2015) 'Effect of heading angle on wave-induced vibrations and extreme vertical bending moments in a ultra large container ship model', in 7th International Conference on Hydroelasticity in Marine Technology. Split, pp. 375–388.

Zhu, S., Moan, T. (2015) Effect of heading angle on wave-induced vibrations and extreme vertical bending moments in a ultra large container ship model, Proceedings of 7th International Conference on Hydroelasticity in Marine Technology, September 16-19, 2015, Split, Croatia, 375-387.

Proceedings of the 20th International Ship and Offshore Structures Congress (ISSC 2018) Volume I – M.L. Kaminski and P. Rigo (Eds.)

doi:10.3233/978-1-61499-862-4-171

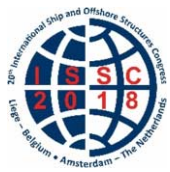

COMMITTEE II-1

QUASI-STATIC RESPONSE

COMMITTEE MANDATE

Concern for the quasi-static response of ships and offshore structures, as required for safety and serviceability assessments. Attention shall be given to uncertainty of calculation models for use in reliability methods, and to consider both exact and approximate methods for the determination of stresses appropriate for different acceptance criteria.

AUTHORS/COMMITTEE MEMBERS

Chairman: J.W. Ringsberg
J. Andrić
S.E. Heggelund
N. Homma
Y.T. Huang
B.S. Jang
J. Jelovica
Y. Kawamura
P. Lara
M. Sidari
J.M. Underwood
J. Wang
D. Yang

KEYWORDS

Benchmark study, class rule-related software, corrosion, direct calculations, experiments and testing, extreme load, fatigue assessment, finite element analysis, IACS Common Structural Rules, IMO Goal-Based Standards, impact loads, load modelling, offshore structures, optimisation, probabilistic approach, quasi-static response, reliability analysis, residual strength, ship structures, strength assessment, stress response calculation, structural integrity, uncertainty analysis.

CONTENTS

1. INTRODUCTION 174
1.1 General introduction to strength assessment approaches 175

2. LOAD MODELLING 176
2.1 Operational/design loads 177
2.1.1 Wave loads and extreme loads 177
2.1.2 Wind loads 177
2.1.3 Ice loads 178
2.1.4 Sloshing and slamming loads 179
2.1.5 Turret loads, mooring loads, and towing loads 179
2.2 Accidental loads 180
2.2.1 Collision and grounding 180
2.2.2 Fire, explosion and associated secondary loads 183
2.3 Load combinations for application 185
2.4 Experiments and monitoring 185
2.5 Concluding remarks 186

3. STRUCTURE MODELLING AND RESPONSE ANALYSIS 186
3.1 Structure modelling and analysis methods 187
3.1.1 Simplified analysis/first principles 187
3.1.2 Direct calculations 187
3.1.3 Reliability analysis 188
3.1.4 Optimisation-based analysis 188
3.2 Failure modes and response analysis 188
3.2.1 Buckling and ultimate strength 189
3.2.2 Fatigue strength 191
3.2.3 Residual strength 192
3.2.4 Whipping 193
3.3 New metallic materials, composite and sandwich structures 194
3.4 Ageing structures 195
3.4.1 Corrosion 195
3.4.2 Fatigue cracks 195
3.4.3 Dents 196
3.5 Concluding remarks 197

4. UNCERTAINTY AND RELIABILITY ANALYSIS 197
4.1 Uncertainties in load modelling 197
4.1.1 Still water and wave loads 197
4.1.2 Wind loads 198
4.1.3 Ice loads 198
4.1.4 Sloshing and slamming loads 198
4.1.5 Impact loads 199
4.1.6 Loads combinations 199
4.2 Uncertainties in structural modelling 200
4.2.1 Corrosion deterioration 200
4.2.2 Fabrication-related imperfections 200
4.2.3 Impact damage 200
4.2.4 Ultimate strength and buckling 201
4.2.5 Fatigue damage 201
4.3 Reliability and uncertainty analysis 202
4.3.1 Reliability analysis 202

4.3.2 Uncertainty analysis by stochastic finite element method 203
4.3.3 Other probabilistic analysis methods 205
4.4 Risk-based inspection, maintenance and repair 205
4.5 Concluding remarks 206

5. DEVELOPMENT OF RULES AND SOFTWARE SYSTEMS 207
5.1 Development of international rules and regulations 207
5.1.1 IMO Goal-Based Standards 207
5.1.2 New DNV GL rules 207
5.1.3 Lloyd's Register rule development 208
5.1.4 Materials and extra high strength steels 208
5.1.5 Rules and standards for strength analysis of container ships 209
5.1.6 Arctic/Ice 209
5.1.7 Other updates of class rules 209
5.2 Development of structural design software systems 210
5.2.1 Class rule-related software 210
5.2.2 Automatic mesh generation 211
5.3 Concluding remarks 213

6. OFFSHORE AND OTHER SPECIFIC MARINE STRUCTURES 214
6.1 Fixed offshore structures 214
6.1.1 Uncertainty, reliability for soil property and wave loads 214
6.1.2 Load, extreme response due to nonlinearity of Morison's force 215
6.1.3 Fatigue 215
6.2 Floating offshore structures 216
6.2.1 Uncertainty and reliability analyses 216
6.2.2 Loads: nonlinear hydrodynamic loads and coupled loads 216
6.2.3 Fatigue and fracture: coupled loads, safety margin 217
6.3 Other specific marine structures 218
6.3.1 RoRo vessels and car carriers 218
6.3.2 Livestock carriers 218
6.4 Concluding remarks 219

7. BENCHMARK STUDIES 219
7.1 Ship structural response from different wave load schematisation 220
7.1.1 Description of the ship structures, models, loads and loading conditions . 220
7.1.2 Results 223
7.1.3 Concluding remarks 225
7.2 FSI analysis of a stiffened plate subjected to slamming loads 226
7.2.1 Model description 226
7.2.2 Description of the simulation software packages and analyses 227
7.2.3 Results 230
7.2.4 Concluding remarks 231

8. CONCLUSIONS AND RECOMMENDATIONS 232

REFERENCES 235

1. INTRODUCTION

Ships and floating offshore installations are large-scale, complex structures that are designed and built to operate for long periods in an ever-changing environment. For safe and sustainable structural design, the design process should follow the limit-state-based design philosophy that encompasses serviceability, ultimate strength, fatigue and accidental limit states. For engineering economy in the early design stage, quasi-static approaches are commonly employed to evaluate loads. It is then important to have good understanding of the difference between quasi-static analysis and dynamic response analysis and available engineering techniques (e.g., empirical approaches, direct analysis methods, and reliability analysis), as well as the associated modelling procedures that can be applied for design assessment. In the development of innovative designs and unique marine structures, useful information can also be obtained from direct load, response, and strength analyses. In these cases, the relationship between limit states and the corresponding loading conditions should be clarified in a precise manner.

A convenient and useful computational tool for structural response analysis is the finite element (FE) method, which can efficiently model the complexity and interaction of components and parts of large structures and the maritime environment if properly employed. The knowledge and treatment of uncertainties that may relate to the modelling of loads and structures and constitutive material modelling can significantly impact the accuracy and reliability of the results. Recent advances in computer and software technology have enabled and almost standardised the analysis of complex ships and offshore structures during the design process under operational conditions using the FE method.

ISSC Technical Committee II.1 has presented thorough reviews of various strength assessment approaches with a focus on topics such as simplified analysis, direct-calculation reliability analyses, optimisation-based analyses (including reliability), composite structures, uncertainties, and design trends, and development and challenges of ship structures (refer to Aksu *et al.* 2006, 2009, 2012). A previous report by ISSC Technical Committee II.1 (Ringsberg *et al.* 2015) presented a comprehensive review of calculation procedures divided into (i) different levels of analysis related to design stages, (ii) recent work on the design of production load modelling with an emphasis on rule- versus rational-based ship design, (iii) structural modelling using the FE method divided into global analysis and detailed analysis, (iv) recommendations for structural response assessment with regard to the fluid-structure-interaction (FSI), buckling and ultimate strength, fatigue strength, and ship dynamics, and (v) validation of the results from numerical calculations in terms of model scale experiments and full-scale monitoring. One of the core chapters of the report addresses the uncertainties associated with reliability-based quasi-static response assessment, including methods and criteria for reliability and risk-based structural assessment in the context of the structural capacity. The report presented a summary and discussion of the developments in international rules and regulations for ship structures and specific ship types, such as service vessels for windmills and offshore platforms, container ships, and LNG/LPG tankers. Various types of floating and fixed offshore structures were addressed by a review of methods for uncertainty, risk, and reliability analysis. The previous committee performed and presented a benchmark study, in which design against impact loads (slamming) was investigated for a free-fall lifeboat case (refer to Ringsberg *et al.* (2017) for the complete benchmark study).

The mandate of this committee encompasses an extensive field of research topics. Following the discussions from the former ISSC congress in 2015, the committee decided that the report should prioritise and emphasise the most relevant issues during the reporting period. The report should highlight and present examples of the most important progress since the former two to three reporting periods. As a result, the committee's work presented in the current report is less detailed in some areas but fulfils the mandate of the committee. This committee

also decided to omit subsea structures, such as pipelines, risers, and wellheads, as these structures were considered to fall outside of the scope of the committee's mandate.

The current committee report is organised as follows: the remaining sections of this chapter provide a general introduction to strength assessment approaches for the quasi-static response of ships and offshore structures. The objective of the chapter is to provide a brief overview of modelling of quasi-static loads and the procedures and available technologies for the evaluation of associated responses within the context of reliability assessment. Chapters 2 to 4 are the core chapters of the report with reference to the committee's mandate. Chapter 2 presents load modelling, including the categorisation of the loads imposed during operation and life. The chapter explores the loads that can be transmitted to structures during operations or accidental situations and outlines the recent research conducted in support of knowledge gain in these areas. Chapter 3 presents a review of structure modelling and response analyses and focuses on the development of structural modelling and response analysis methods that implement or facilitate implementation of a quasi-static approach to structural analysis. The chapter is divided into multiple sections to address structural modelling and response methods, failure modes and response analysis, new materials, ageing structures and experiments, monitoring and validation. In Chapter 4, recent studies and advances in awareness of the risks that relate to uncertainties in loads and structural modelling, which are crucial for safe design, are presented. The importance of uncertainties associated with reliability-based quasi-static response assessment is discussed. Methods and criteria for reliability- and risk-based structural assessment are presented in the context of structural capacity methods. A review of recent studies and methods that consider existing and aged vessels with regard to risk-based inspection, maintenance and repair is presented.

Chapter 5 presents recent developments in international rules and regulations, such as the IMO Goal-Based Standards, the new DNV GL rules, Lloyd's Register rules, materials and extra-high-strength steels, strength analysis of container ships, and the IMO Polar Code. This chapter also includes a review of class rule-related software developed by Classification societies as a support of early concept (first-principle) design to detailed design and manufacturing. One section presents the most recent developments during the reporting period in automatic mesh generation tools. Chapter 6 discusses specific marine structures, such as jacket platforms, FPSOs, very large floating structures, and livestock carriers. The latter are examples of structures that are very complex, require analysis methods that are not always easily identified in guidelines, regulations and rules. The chapter provides some examples from the literature during the reporting period to highlight advances in quasi-static analysis methods and the assessment of these specific marine structures.

All ISSC committees are encouraged to perform benchmark studies. During the reporting period, this committee decided to perform two benchmark studies, which are presented in Chapter 7. The first study explores wave load modelling and structure response analysis in a ship structure, whereas the second study investigates the design against impact loads (slamming) of a floating offshore structure. The conclusions and recommendations for future work and progress of the committee's work are presented in Chapter 8.

1.1 General introduction to strength assessment approaches

An extensive variety of strength assessment approaches can be employed in the design assessment and structural optimisation of ships and offshore structures. In the preliminary stage, simplified solutions, although conservative, are usually applied. For detailed design, more detailed, time-consuming and potentially precise methods are usually applied. Irrespective of their degree of fidelity, the available methods reflect three main aspects, namely, (a) modelling idealisations/assumptions, (b) process of load derivation and application to a model, and (c) uncertainty modelling and quantification. Each of these aspects is introduced in separate sections of this report.

Modelling of loads by quasi-static analysis

Within the reporting period, the trend is similar to the trend described in the previous report by Ringsberg *et al.* (2015). The development of suitable methods for the simulation and evaluation of quasi-static responses that incorporate the influence of nonlinearities by multi-physics methods has proved challenging, particularly within the context of industrial applications. This challenge is primarily attributed to the lack of unified validation studies or verification schemes that can limit the number of uncertainties related to the computation of wave-induced dynamic loads. As techniques become more sophisticated and assumptions become more complex, uncertainties may vary and increase. Equally, validation, computation time and complexity may become an issue when we try to understand, simplify or validate the modelling assumptions. Within the context of quasi-static/dynamic response, the use of weakly nonlinear or fully nonlinear methods is feasible over the medium- to long-term provided that validation efforts are extended and modelling assumptions are well understood; refer to Chapters 2 and 4.

Response calculation

The approaches in which the uncertainty of loads and structural resistance are covered by one or more safety factors are often referred to as the deterministic (or working stress design) approach and the load and resistance factor design (or partial safety factor) approach. These methods are extensively employed in the design of ships and offshore structures. Within these classes of calculations, one can further distinguish between simplified, analytical or semi-analytical analysis and direct calculation methods, referring to either the way the quasi-static loads are derived or the complexity of the structural model. Classification rules provide guidance on modelling and acceptance criteria based on either beam theory or direct calculations using the FE method. FE analysis remains the principal approach for investigating the structural response under accidental loading scenarios that may be associated with grounding, collision, ice structure interaction, or design for crashworthiness; refer to Chapter 3.

Reliability analysis

Reliability can be defined as the ability of a structure to comply with given requirements under the operational conditions that it may experience throughout its service life. Due to their inherent variability, probabilistic analysis methods in principle are capable of idealising the influence of these effects. In this context, reliability analysis may be employed to measure the probability of structural failure by considering both the loads that act on a vessel and the resistance (strength) of the structure.

Strength assessment approaches can be classified into four categories (Ringsberg *et al.* 2015): (0) deterministic approach, (I) partial safety factor approach, (II) approximate reliability analysis, and (III) fully probabilistic approach. The first two approaches (0 and I) have been well implemented in design standards (refer to Chapters 4 to 6). Based on the allowable stress design method (deterministic approach), the maximum acting stresses on a structure should not exceed the critical value of material strength divided by a safety factor. The disadvantage of this method is that it relies on the evaluation of a suitable safety factor that may not necessarily consider load combinations or the use of different materials at the moment. Class II and III approaches have the potential to provide a better indication of the structural reliability at the expense of additional information and computational effort. In reliability-based design, the design value of the target reliability index can be derived by analytical probabilistic processes. The concept of probabilistic analysis can be used to calibrate the values of the partial factors in load and resistance factor design (LRFD) methods.

2. LOAD MODELLING

One critical aspect of the design of ships and offshore structures is the evaluation of the loads imposed during operation and life. These loads can then result in a structural response that can

be assessed via the applicable criteria for the intended platform. This chapter explores the loads that can be imparted to structures during operations or in an accidental situation and outlines the recent research conducted in support of knowledge gain in these areas.

In general, loads applied on ships and offshore structures can be divided into two major categories: operational loads and accidental loads. Operational/design loads are typically loads that are derived from the intended day-to-day operations of a structure, including lifetime considerations for the occurrence of loads based on the expected operational scenario of a structure. Accidental loads are attributed to accidents; collisions and groundings are examples of these types of loads. This chapter also outlines research on items such as load combinations and experiments conducted in these areas.

2.1 Operational/design loads

This section explores the various types of operational/design loads and the research efforts conducted since the committee's last ISSC report in 2015. Operational/design loads can be defined as the loads that a structure is typically expected to encounter during operations and its lifetime, considering the statistical methodologies for factoring the occurrence of extreme loads (i.e., rogue waves) and providing safety mechanisms via probabilities of non-exceedance and appropriate safety factors.

2.1.1 Wave loads and extreme loads

A recent example of the evaluation of wave loads is a study of offshore structures by Elhanafi (2016). This research focused on the prediction of wave loads for a wave energy converter, in which the author explored the loading effects on an oscillating water column (OWC) by utilising two-dimensional (2D) and three-dimensional (3D) computational fluid dynamics (CFD) models that considered a matrix of wave characteristics, such as wave height and period. The author also considered pneumatic damping and obtained an adequate correlation for regular wave interactions. Future research is suggested for extreme environments and further exploration and validation of 3D modelling methods. Other studies of extreme loads have been performed by Vázquez *et al.* (2016), in which the authors conducted experimental and numerical investigations for the vertical moments of bulk carriers and roll-on/roll-off vessels. The authors demonstrate that the vertical bending moment is the basis for the design of mid-ship sections and that vessels can experience abnormal waves, such as the New Year's Eve Wave (NYW) and the Single Abnormal Wave North Alwyn (SWNA). Model testing and numerical methods can be employed to evaluate regular and irregular waves, including abnormal waves. The studies revealed that the bow flare and freeboard characteristics of the two vessel types affected the estimation and comparison of the bending moments, including the linear assumptions of the numerical models that affected the comparisons with experimental data. Exploration of the area of the extreme loads on the dynamic collapse of bulk carriers was also performed (Xu *et al.* 2015b) to address the nonlinear behaviours of structures, in which a one-frame space model was utilised to conduct the analysis. The results indicated that the load-carrying capacity of the hull girder decreases after the ultimate strength is reached and provides data on the effects of the 1/1000 probability of exceedance load effects on the hull girder. Overall, wave loading efforts have focused on utilising CFD techniques to model the loads, evaluating the structural response under extreme loads and gaining a deeper understanding of the behaviours of structures when extreme loads are encountered. These efforts are especially critical when considering that weight and cost have to be assessed when designing a ship according to a desired operational profile.

2.1.2 Wind loads

The wind loads applied to ships and offshore structures represent another ongoing area of research. Wnęk and Guedes Soares (2015) conducted experimental testing in a wind tunnel and compared the results with the results of CFD models. Their study was performed in a

wind tunnel in the Instituto Superior Técnico (IST) in Lisbon (Portugal) and included scaled models of a floating LNG platform and an LNG carrier. The scaled models were set up to measure resultant forces/moments along three Cartesian axes that are derived from wind loads applied at various angles of attack. Numerical simulations that utilise the commercial software ANSYS ICEM CFD were also conducted to perform a comparison with the experimental results, including mesh density studies for the air boundaries. Their results noted mesh density effects and wind angle of incidence effects, which indicate that methods should be addressed to best capture the boundary layer effects along the walls of the model; these results demonstrated reasonable agreement for certain conditions. Other researchers, such as Bentin *et al.* (2016), have focused on the wind impacts with regards to the optimisation tools for routing and evaluating wind-assisted propulsion devices. In this case, experimental data were collected for more than a year to apply towards the development of a model that can save up to 53% of energy when route optimisation is combined with wind propulsion. This process is route-dependent and subject to the prevailing wind directions. Future application of this technology may include dependency on fuel cost and regulations outlined by governing bodies. Although winds affect routing, a different area of interest is the wind loads on moored ships, especially as they exert external pressure loads on the hull, which need to be properly accounted. Redondo *et al.* (2016) evaluated the wind and wave combinations on moored ships by capturing mooring forces on the ships and mooring devices. The authors developed a scaled model that captured the characteristics of the port, including sediment conditions, and evaluated the effects of water and wind parameters, individually and combined. The combination of these forces reveals an increase in ship motion and amplitude. Future studies were suggested in areas where a loaded container ship is subject to these combined effects, including their influence on the safe operation of industrial equipment on the loading and offloading cargo. Wind loads continue to be an area of interest, in which CFD tools, computer models, and model testing are helping to characterise these coupled effects and provide data that can be employed in areas such as weather routing for improved efficiency.

2.1.3 Ice loads

Operational ice loads on the hulls of ships and offshore structures may be categorised as “stationary” or “moving”. Stationary loads act at one point on a hull structure, whereas moving loads exhibit tangential motion along the hull. In Kim and Quinton (2016), the force-displacement curve, variation of contact area and pressure distribution for moving ice loads that act on an elastic plate were determined. The study presents the results of moving ice load experiments on an elastic plate and compares them with previously published results for similar experiments involving stationary ice loads. The experiments and numerical analysis suggest that the difference in the magnitude of an ice load and trend of the pressure distribution between stationary and moving loading conditions is negligible if the structure remains elastic during the ice-structure interaction.

The constant added mass (CAM) method and the FSI method are extensively employed to simulate ship-ship and ship-ice collisions. In the CAM method, the hydrodynamic effect of the surrounding water is treated as a constant added mass, whereas the surrounding fluid flow is explicitly modelled in the FSI method. In Song *et al.* (2016a), the two methods are compared, and the causes of the differences in the results are explained. The comparisons indicated that the FSI method yields better results for the motion of the floater and the CAM method was faster but predicted a higher peak contact force and more dissipated energy in the ice mass than the FSI method.

Park *et al.* (2015) undertook an accidental limit state-based ship collision analysis to identify the operability of aged non-ice classed ships in the Arctic Ocean. Internal collision mechanics analysis of the struck vessel structures was performed at a right angle with an initial velocity. The striking ship and struck ship were the same ship—a 157,500 DWT Suezmax class double hull oil tanker. Various Arctic ambient temperature conditions—room temperature to -80°C—

were applied to the ambient exposed plating of the struck ship. Time-variant corrosion wastage was employed in the case of age-related damage. The FE software LS-Dyna was conducted to apply the nonlinear constitutive curves of the materials from a series of tensile tests at low temperatures. The operability of aged ships in the Arctic condition was estimated based on the results.

The ice interaction of a structure is an ongoing area of research and a subject of in-depth study of other ISSC committees. Numerical approaches are being evaluated to determine the methodology to address ice-related effects, especially for ships that are not initially designed to operate in high-latitude conditions.

2.1.4 Sloshing and slamming loads

Sloshing effects are typically observed across various vessels. Cheon *et al.* (2016) performed a study of an LNG-FPSO, in which the research efforts were devoted to conducting a scaled test to investigate the sloshing effect on tanks. A sloshing scaled tank was placed above a test fixture excited with six degrees-of-freedom (DOF) motion time histories that were derived from numerical simulations and piezoelectric pressure sensors were installed on the wall of the model. The model included several pressure sensor arrays and average methodologies to overcome a travelling pressure wave problem, and a test matrix including various tank filling heights. The test predictions were larger than expected and dependent on the tank-filling conditions. Additional research and full-scale experimental data are needed to provide additional data points and better understand the scaling factors of pressures. In the area of slamming and whipping, numerical and experimental work was conducted by Kim *et al.* (2015a) to assess a fully coupled hydroelastic model. The authors utilised an 18,000 TEU container ship for the investigation, conducted a 1/60 model test in the Samsung Ship Model Basin under head sea conditions, and compared the results with the results of a one-dimensional (1D) beam and 3D FE model with a Generalised Wagner Model coupled with a 3D Rankine panel method. The results indicated that fully coupled 3D models provided the best results for slamming assessments compared with de-coupled analysis, which tends to lean towards conservativism.

Slamming was also explored for the bow sections of a wave-piercing catamaran in a study by Swidan *et al.* (2016). A notional hull form for a wave-piercing catamaran similar to INCAT Tasmania designs was developed and equipped with load cells and pressure transducers to measure the slamming events at maximum impact velocities of 4.45 m/s during a drop test. Several tests were performed to alleviate uncertainties from velocities and randomness. The results indicated that the maximum slam pressure occurred when the interior archway is filled with water, which is affected by the immersion of the demi hulls. This finding suggests to the designer that the air gap can be increased to reduce pressures, and experiments also highlighted a pressure/velocity relationship for these conditions. However, the pressure transducer location is critical; their data suggested that the application of a quasi-2D approach can provide invalid data when investigating the slamming effects of catamarans.

2.1.5 Turret loads, mooring loads, and towing loads

FPSO ships utilise turret mooring systems. Recent studies have emphasised the prediction of the ship heading (e.g., Milne *et al.* 2016), especially wind, waves, and current effects, leveraging full-scale data from the Raroa FSPO, a 3D boundary element code Nemoh, and met-ocean predictions utilising a SWAN model. Reasonable estimates of the heading within 5% of measured values were obtained, which provides supporting data that indicates that Nemoh can be used to develop estimates of the lateral drift force and yaw moments. Towing is typically associated with the movements of other naval structures. A novel approach to towing was investigated by Yulmetov and Løset (2017) to gain knowledge in the area of towing icebergs to clear areas of ocean traffic. The authors proposed a model for towing ice; this research focuses on experimental validation of this model coupled with simulations. The experimental evaluation was performed at the Hamburg Ship Model Basin, and non-smooth discrete ele-

ment method codes were utilised for the numerical efforts. The broken ice concentration on the basin was varied as the iceberg was towed, where the ice concentration influenced the towing force to its greatest extent. The breath of the tow tank was another parameter, as the rigid boundaries created effects that may not be present in open areas where broken ice can be pushed but not crushed out of the way of the towed iceberg. The authors outlined the limitation of the model as a pre-decisional support tool and improvements in towing that was set up to capture more realistic conditions. The wind effects on mooring are another subject of experimentation (e.g., Redondo *et al.* 2016); the authors coupled wind with waves in a controlled experimental study to evaluate their combined effects. The authors utilised a unique system to develop force and moment loads on a scaled vessel using linear springs and actuators. The spectral results of the coupled ship and wind motions indicated that the ship motion across the frequency range is amplified by the inclusion of wind loads and that special considerations are needed when the sail area of a vessel is large, such as in the case of cruise ships and container ships. This spectral characteristic has also been examined by Kumar *et al.* (2016) in Pohang New Harbour. The harbour was designed to protect moored vessels from typhoon-type events; however, small portions of waves continued to radiate through the entrance. The simulations and numerical models are developed to analyse the wave field around each vessel in the harbour, evaluate local resonance, identify the safest location for mooring, consider irregular geometry within the harbour, and develop a computationally effective model to predict moored ship motions.

2.2 Accidental loads

The previous section addressed operational loads, whereas this section explores accidental loads from collisions and groundings, as well as fire/explosive loads. Although explosive loads are adequately addressed in other ISSC committee reports, this content is limited to quasi-static response applications.

2.2.1 Collision and grounding

Collisions and groundings are a fairly severe set of accidental loads that sometimes cause detrimental damage to vessels. The work presented in Marinatos and Samuelides (2015) aimed to define a procedure that outlines the numerical simulations conducted to evaluate the responses of ship structures in accidental loading conditions. Ship structures experience different modes of failure, such as tension, bending, tearing and crushing. In these conditions, the particular effects of material curves, rupture criterion, mesh size, and strain rate have a profound effect on the results. Different material models and simulation techniques were employed for the simulation using the explicit FE software Abaqus, which consists of eighteen indentation tests conducted by different research groups. The tests refer to the quasi-static, dynamic transverse and in-plane loading of various thin-walled structures, which represent parts of a ship structure. Consistency in the numerical results was observed with the use of an equivalent plastic strain criterion, in which a formulation of cut-off values for tri-axialities below 1/3 was included.

The effect of a new highly ductile steel material on the crashworthiness of hull structures in oblique collisions was investigated by Yamada *et al.* (2016), who used nonlinear ship-to-ship collision simulations. A series of nonlinear FE analyses were performed using two Very Large Crude Carriers (VLCCs) with changing striking speed and collision angle. A comparison of absorbed energy and critical striking velocity for both conventional ship and new ship were discussed. Lee *et al.* (2016b) present ship collision analysis results for the world's first FLNG. The purpose of the analysis was to ensure that its hull structure has sufficient strength against collision events. Storheim and Amdahl (2014) present collision scenarios with bow and stern impacts against the column of a floating platform and the jacket legs and braces. The effect of the ship-platform interaction on the distribution of damage was investigated by modelling both structures using nonlinear shell finite elements. The numerical analyses were

utilised to develop a novel pressure-area relation for the deformation of the bulbous bow and stern corners of the supply vessel. Procedures for the strength design of the stiffened panels were discussed; refined methods and criteria were proposed. Travanca and Hao (2015) present a series of FE numerical simulations with the aim of providing a comprehensive understanding of the strain energy dissipation phenomenon, particularly for the ship-structure interaction. Ships of different dimensions and layouts are modelled for impact simulations. From the FE analyses, simplified approaches are derived in terms of the relative stiffness of the two structures for assessing the responses and energy absorptions of the two structures. The conclusions can be applied to a broader range of collision assessment of offshore steel jacket platforms that are subjected to high-energy ship impacts.

The damage caused by accidental frontal collision of a supply vessel with an FPSO unit is examined in dos Santos Rizzo *et al.* (2015). This damage has a negative influence on the ultimate shear strength of the platform and stiffened side panels and should be carefully assessed. Nonlinear quasi-static FE analyses using the software Abaqus are presented. Geometric imperfections are introduced by considering the first buckling mode shape of the panel. A displacement loading control is imposed to the bulb to evaluate the plastic deformation and spring back effect. The ultimate shear strength is assessed considering the geometric imperfection and the residual stresses from the collision. A parametric variation is performed to investigate the influence of bulb displacement, initial imperfection amplitudes and plate thickness.

Liu and Guedes Soares (2015) present a simplified analytical method to examine the crushing resistance of web girders subjected to local static or dynamic in-plane loads. A theoretical model, which was inspired by existing simplified approaches, is developed to describe the progressive plastic deformation behaviours of web girders. The elastic buckling zone, which absorbs almost zero energy, is captured and confirmed by the numerical results. In addition, the analytical method derives expressions to estimate the average strain rates of the web girders during the impact process and evaluate the material strain rate sensitivity with the Cowper-Symonds constitutive model. These adopted formulae, which are validated with an existing drop weight impact test, can adequately capture the dynamic effect of web girders.

Heinvee and Tabri (2015) present a set of analytical expressions for the calculation of damage opening sizes in tanker groundings. The simplified formulae were given for the grounding force, longitudinal structural damage and the opening width in the inner and outer plating of a tanker's double bottom. The simplified formulae are derived based on a set of numerical simulations conducted with tankers of different dimensions, including lengths of 120 m, 190 m and 260 m. Given the formulation for the normalised contact pressure, the actual contact force for a ship is considered to be a product of the average contact pressure and the contact area. To improve the prediction of the onset of the inner bottom failure, a critical relative penetration depth as a function of the ratio of the rock size and the ship breadth was established.

The shape of the sea bottom is an important factor that determines the extent of grounding damage on ships, including the loss of water tightness. Sormunen *et al.* (2016) present a four-step methodology for mathematically analysing sea bottom shapes, where individual peaks are identified and isolated from larger datasets. The objective is to develop mathematical rock models that can be employed in grounding damage analysis. The research by Sormunen *et al.* (2016) was continued by Yu *et al.* (2016b), where a framework for studying, testing and evaluating rock models in terms of resulting grounding damage is presented. The FE method is applied to analyse and compare the grounding damage of rock models of actual rock using otherwise identical grounding scenarios. The results indicate that rock models with a reasonable statistical fit did not always yield similar grounding energy compared with the results using real rock. Differences in energy are especially caused by the rough surface of the real rocks. Knowledge of these relationships can be applied towards estimating grounding damage of ships in future investigations; however, rock surface unevenness should also be evaluated.

Closed-form analytical solutions for the energy released from deforming and crushing structures and the impact impulse during ship collisions were developed and published by Pedersen and Zhang (1998). Zhang *et al.* (2017d) employed these experimental results to analyse the validity and robustness of the closed-form analytical methods and improve the accuracy of some parameters. A total of 60 experimental results have been analysed and compared with the analytical results. This paper presents the outcome and concludes that the results by the analytical methods are consistent with the experimental results. This paper also introduces a simple concept to account for the effective mass of liquids with free surfaces performed onboard a ship and demonstrates how the analytical analysis procedure can be expanded to consider the effect of ship roll on the energy released for crushing.

Faisal *et al.* (2017) presented a rapid method for calculating the hull collapse strength of double hull oil tankers after collisions. The statistical characteristics of hull girder collapse after collision are investigated. Four double hull oil tankers with different sizes are considered: Aframax, Panamax, Suezmax and VLCC. A set of 50 credible collision scenarios was selected by a sampling technique that is associated with collision hazard identification based on a historical ship collision database. Four parameters, namely, vertical collision location, damage penetration, striking ship's bulbous bow height, and striking ship's bulbous bow length, are determined as a consequence of the corresponding collision scenario. An intelligent supersize FE method is utilised to compute the progressive collapse behaviours of hull girder structures with detected collision damages. The residual hull girder strength indices can be determined and formulated with a closed expression that is associated with collision damages and ship length. The developed formulations are useful to quickly calculate the hull collapse strength of double hull oil tankers immediately after collisions.

Corroded tankers may be subjected to significant structural damage if involved in collision accidents. For understanding or preventing collision accidents, various studies are being proposed by researchers to improve the analysis method. In Noh *et al.* (2016), four types of double hull oil tankers (Aframax, Panamax, Suezmax and VLCC) are employed. A probabilistic approach is used to create ship-ship collision scenarios for each target structure and the ultimate longitudinal hull girder strength of the hypothetical oil tanker's hull cross-section. The ALPS/HULL is an intelligent supersize FE method software which is employed for the simulation. A relevant probability density function is introduced using the results from FE simulations of the ship-ship collisions which is commonly used to predict residual strength.

In a study by AbuBakar and Dow (2016), the accidental loads and damage mechanisms incurred on a ship's bow during a ship collision are analysed using nonlinear FE analyses to investigate the capability of the ship's bow to absorb the energy generated during a collision event. The study employed the effect of the rupture due to excessive plasticity of material prior to failure. The study investigates the effect of collision angle and ship speed during an extreme collision event of a ship striking a rigid wall with a full ship model. The correlation between the numerical simulations and available current analytical approaches applied in the EURO-code and other empirical approaches reveal that FE analyses generally produce more conservative results and are capable of capturing the impact force effect due to the ship bow softening effect.

For a design evaluation, a fast, practical and accurate method is needed to determine the absorbed energy and collision damage extent in ship collision analysis. The most well-known simplified empirical approach to collision analysis was created by Minorsky (1959) and its limitation is also well recognised. Zhang and Pedersen (2017) have developed simple expressions for the relation between the absorbed energy and the damaged material volume, which considers the structural arrangements, the material properties and the damage modes. The purpose of the study is to re-examine collision damage analysis in ship design assessments by comprehensive validations with experimental results from the public domain. A total of 20 experimental tests have been selected, analysed and compared with the results calculated us-

ing the proposed method. The findings conclude that the proposed method has reasonable accuracy with a mean value of 0.988 and a standard deviation of 0.042.

2.2.2 Fire, explosion and associated secondary loads

Ships and offshore structures are exposed to fire and explosion loadings. These fire and explosion accidents can have grave consequences not only for the ships and offshore platforms but also the safety of personnel.

Fire loads

Parametric uncertainty in choosing the numerical values for the frequency and consequence analysis during a fire risk analysis is a critical issue for determining the design accidental load (DAL). Chu *et al.* (2017) applied the Latin hypercube sampling technique to investigate different fire exceedance curves, in which DAL fire was demonstrated by selecting different sets of representative values. The distribution and confidence interval of the DAL fires revealed an extensive distribution with varying uncertain and critical parameters. The investigation provided quantitative information about inherent uncertainty; this type of additional information enables better decision-makings. Kang *et al.* (2017a) explored a framework for using computational fire simulations during the early phase of ship design, which focused on how to arrange fire control options with minimal changes in existing design procedures. Jin and Jang (2015) and Jin *et al.* (2015) applied a fully quantitative-probabilistic fire risk analysis procedure to evaluate the design temperature distribution and probable failed area of interested objects for a semi-submersible vessel. The failed area of an object is predicted by introducing two different risk analysis tools, namely, cumulative failure frequency and the temperature exceedance curve. Jin *et al.* (2016) introduced an approximation method to reduce the time cost of analysis, which depends on the number of input scenarios in the same fire risk analysis procedure.

Sun *et al.* (2017) discussed the load characteristics in the process modules of offshore platforms under jet fire. Jet fire represents a major fire risk in the process modules of offshore oil and gas platforms. The heat loads generated by jet fire in these areas may cause significant consequences and warrants further investigation. In this research, a Fire Dynamics Simulation (FDS) code is chosen to model different jet fire scenarios. Valuable suggestions for modelling jet fire scenarios in process modules and load characteristics for the prescribed jet fire scenarios are discussed.

When a steel structure is subjected to fire attack, the thermal material degradation of steel members can induce premature material yielding, and the thermal axial expansion and bowing on a steel structure can change its structural geometry. These thermal effects produce the material and geometric nonlinearities of a structure, which defy the accurate behavioural prediction based on general methods of analysis. Iu (2016) proposed an equivalent thermal load procedure to determine the thermal expansion effect prior to a fire analysis. In this procedure, the thermal expansion effect is incorporated into the higher-order element formulation, and the geometric and material nonlinearities are considered by the higher-order elements. The present nonlinear fire analysis can replicate realistic behaviour, including thermal effects, geometric effects and material nonlinear effects of an entire steel structure that complies with a realistic fire scenario in an effective manner using the least number of elements.

High-strength steels are increasingly common in structural engineering applications due to their favourable strength-to-weight ratio, excellent sustainability credentials and attractive physical and mechanical properties. However, at elevated temperatures, the grades that are underused in structures lack reliable information about their structural performance. Varol and Cashell (2017) reviewed high-strength steels in structural applications, including the key design considerations. Their review is focused on the lateral torsional buckling response of laterally unrestrained beams. In this study, an FE model is developed to investigate torsional

buckling behaviour at ambient and elevated temperature. Similarly, Reis *et al.* (2016) also reviewed the behaviours of steel plate girders that are subjected to shear buckling at both normal temperatures and elevated temperatures. Sensitivity analyses of the influence of initial imperfections were discussed. Different values for the maximum amplitude of geometric imperfections were considered, and residual stresses were also considered. The effect of the end supports and configuration were also investigated to understand the strength enhancement given by the rigid end support at normal temperatures and confirm if the strength enhancement can be maintained in the case of fire.

Hydrocarbon gas explosions loads

Hydrocarbon gas explosion is a critical hazard that causes a significant environmental impact and loss of valuable assets and lives, as observed from the historical disasters in the oil and gas industry. In response to these events, stronger international rules and regulations have been established to ensure the safety of these structures. Considerable effort has been devoted to quantify accidental design loads for flammable gas based on probabilistic approaches, which requires extensive CFD simulations. The demand for 3D nonlinear dynamic FE structural simulations has significantly increased with rapid progress in computer performance.

Heo (2016) discussed uncertainties in explosion hazard analysis, which cause large variations in probabilistic explosion responses, and compared the gaps between provisions for design load estimation based on probabilistic approaches with current structural design and analysis schemes. Sun *et al.* (2016) applied the Failure Modes and Effect Analysis (FMEA) method to determine which equipment has a high Risk Priority Number (RPN) and discovered that the gas washing pry of an FPSO unit in the operation phase has a high RPN. The leak rate of gas with a specified hole diameter is calculated based on an appropriate leak source model according to the actual operating conditions of the gas washing pry. Then, a CFD simulation was performed to analyse the diffusion behaviour to identify the distribution law of gas and the hazardous area of gas in the leakage conditions. One explosion model is selected for the damaging overpressure of the explosion on each equipment surface and the influence scope of the explosion overpressure to evaluate personnel and equipment risk.

Paris and Dubois (2017) reviewed recent research developments to evaluate global explosion loading on complex systems, such as offshore/onshore process. During the engineering phase, a “Design Explosion Loads Specification” is often developed by the safety discipline to provide the necessary explosion response inputs to other engineering disciplines for each individual item of a safety critical system. This step is an efficient method for managing an explosion in the design for each individual item of a safety critical system. When a combination of items needs to be addressed, this approach may yield an overly conservative design. An alternative methodology based on CFD simulation is presented in this paper to obtain more adequate global blast loads for design verification. The new methodology focuses on the development of dedicated blast load cases for the design to address both internal explosion events and external explosion events that are related to complex items, such as entire onshore/offshore modules.

Secondary loads

Kang *et al.* (2016, 2017b) proposed a numerical model that is based on the time-history of a blast load. In this history, considerable negative phase pressures were observed in the gas explosion analysis results. The idealised model was employed to characterise the dynamic response under the explosion loading. The structural responses of various structural models were thoroughly investigated using the FE method.

A blast load was reviewed by Burgan *et al.* (2016) from the perspective of weight saving of topside. They treated the over-conservativeness in blast wall design to enable a realistic assessment. Three analysis techniques were utilised to compare the effect on the response of the

blast wall: (a) Lagrangian, (b) uncoupled Eulerian-Lagrangian (UEL), and (c) coupled Eulerian-Lagrangian (CEL). The paper demonstrates how coupled analysis considers the effect of the interaction between the load and the response of the wall. As the complexity of the analysis increases from Lagrangian to UEL and CEL, the computational demand significantly increases.

Zheng *et al.* (2015) conducted a theoretical analysis to investigate the dynamic response of fully clamped stiffened plates under blast loads. Based on the large deflection theory of plate and the energy conservation theory, an elastic-plastic analytical method for predicting the response of stiffened plates to explosion loading is developed, in which the effect of the elastic deformation of plates is considered. In the paper, dynamic loads of the initial shock wave and quasi-static pressure generated by an inner explosion are substituted by three different types of equivalent loads. The elastic-plastic analytical method and nonlinear FE method are employed to analyse the dynamic responses of six stiffened plates under explosion loading. Compared with the existing experimental data, the results of the elastic-plastic analytical approach proposed in the paper are consistent with the experimental and numerical results.

2.3 Load combinations for application

Load combination is an ongoing area of research, in which the phasing of loads or methodology for combinations can affect the results. A critical aspect is the ability to quantify how loads are combined, specifically utilising measurements to derive the phasing and magnitude. Recent efforts by Schiere *et al.* (2017) have examined the modal response using strain gages but difficulties were encountered when they attempted to identify the magnitude of vertical bending and torsion moments, as the latter has a significantly smaller magnitude. Parunov *et al.* (2017) presented an assessment of the residual ultimate strength of an Aframax-class double hull oil tanker that was damaged in a collision and subjected to combined horizontal and vertical bending moments. Residual strength interaction diagrams are developed with the purpose of rapid residual ultimate longitudinal strength assessment of the damaged oil tanker under combined bending moments. The developed interaction diagrams are compared with previously published research and the Smith-type progressive collapse analysis method for biaxial bending (Dow *et al.* 1981). Although ultimate strength has typically been reliant on the vertical bending moment, Mohammed *et al.* (2016) numerically experimented with the evaluation of this ultimate strength when a torsional moment is coupled. Utilising a progressive collapse approach, the authors numerically evaluated the effects to include torsion and a vertical moment, which were sequentially applied (torsion was applied first in the sequence); the authors outlined the necessity to include this sequencing in future research. These findings align well with those by other researchers, such as research Temarel *et al.* (2016), who determine that a spectral analysis can identify extreme loads for design. However, they note that these various extreme loads do not simultaneously occur. Equivalent design waves have also been employed in direct analysis, in which they are selected based on the dominant load parameters and applied to coupled fluid and structural models. This methodology depends on the process that is utilised to select the dominant load parameters, which highly influences its accuracy. The load combination arena is an ongoing area of research with various methods that are utilised to select the phasing and load combination or to bound the design space.

2.4 Experiments and monitoring

Experiments are critical for providing essential data in a controlled environment and removing some of the stochastic effects of real-life data monitoring. One such investigation is a study of the progressive collapse behaviours and residual strengths of damaged box girders under longitudinal bending moments, as outlined in Cho *et al.* (2016a). The experimental models were box girder structures that consist of stiffened plates. The box girder models and longitudinal bending conditions adopted in this study can represent the situation of a damaged ship hull girder after collisions. Numerical analyses that simulate a bending test were per-

formed through a nonlinear FE analysis solver. For the numerical analyses, the tested box girder models were employed and different levels of damage were induced on the models, with the exception of one model, which remained intact. Numerical modelling and analyses were performed using the Abaqus CAE/FEA software and compared to test data for validation of the FE analyses. The findings indicated that the reduction in ultimate strength is dependent on the extent of damage and its location. The results of this study can serve as a basis for the prediction of the residual strength of an actual ship hull girder that is subjected to accidental collisions. Mooring loads are also an area of experimentation and monitoring. The loadings of quay walls were investigated in Paulauskas (2016), analytical methods were used to investigate mooring loads, coupled with a visual simulator that was calibrated using laser mooring systems, and methods to account for the inertia loads were developed. The author emphasised the effect of passing ships and the wind load on moored vessels and the utility of data that were collected to calibrate the simulators.

2.5 Concluding remarks

The research presented in this chapter outlines some of the current trends in research, from which several conclusions can be formed. Due to the increased availability of numerical methods and their widespread usage across many applications, many researchers have coupled their experimental efforts with numerical methods to correlate their results and develop best practices for utilising numerical codes. This finding is coupled with a trend to develop a comprehensive understanding of loads, in particular, extreme loads such as collisions and groundings, which can cause detrimental damage to structures. This need for a comprehensive understanding and design should be balanced with cost, weight, and operational profiles for vessels. Another area is explosive loads; some authors have focused on quasi-static methods to design a structure to address this topic. Ice loadings and ice operations, in which the operating conditions at high latitudes are changing and vessels that are not initially designed with this purpose are beginning to operate in such environments, comprise another area of research.

3. STRUCTURE MODELLING AND RESPONSE ANALYSIS

Advances in the development of complex mathematical methods for the structural analysis of ships and offshore structures, their implementation within commercially available software and the availability of increased computing performance have enabled the common application of methods, such as FE analysis, in the design process. CFD also follows this development trend, with rules for the implementation of CFD in the detailed design phase for the derivation of loads; these are now available from some Classification societies, such as DNV GL's special hull notation Computational Structural Analysis (CSA) (DNV 2013). Despite of these advances, simple and quick methods are required by designers to undertake iterative structural strength assessments within the time constraints of the design process. In the early stage design process, designs are evolving too quickly or insufficient definitions are available to realise the potential of detailed FE analysis, CFD, or other methods for assessing dynamic response. Therefore, simplifications or alternative methods are required.

Throughout the design process, quasi-static methods are implemented, regardless of whether they relate to the application of load or the structural analysis. For early structural definition, designers may apply rule-based calculation procedures or analytical calculations based on loads that have been dynamically calculated and rationalised to a reduced set of static loads, for example, to account for wave loads or ship motions. In a subsequent design, whole platform stress and fatigue analysis may be undertaken by FE analysis via the application of quasi-static wave loads, which induce a desired peak bending moment and shear force distribution into a structure. For a longitudinal bending strength assessment, a progressive collapse method (e.g., the Smith method) or the Idealised Structural Unit Method (ISUM) may be implemented to assess the ultimate bending strength of a ship's section by iterative incremental

application of a bending moment in a quasi-static manner. Quasi-static analysis remains a key approach to structural analysis.

This chapter focuses on the development of structural modelling and response analysis methods that implement or facilitate the implementation of a quasi-static approach to structural analysis, in which a quasi-static load is often considered as the basis of the analysis. The chapter has been divided into numerous sections to address structural modelling and response methods, failure modes and response analysis, new materials and ageing structures. Throughout the sections, simplified or analytical methods, direct calculation methods, experimental analysis, loads and load combinations are considered.

3.1 Structure modelling and analysis methods

Whilst the majority of loading scenarios are dynamic or transient, the reduction of the loading environment to a quasi-static load or series of loads as an individual loading condition or a combination of conditions can significantly reduce the complexity of the subsequent structural analysis. This section concentrates on the development of methods or the implementation of techniques that facilitate quasi-static analysis.

3.1.1 Simplified analysis/first principles

Simplified analysis by first principles or "hand" calculations are well founded in the design and analysis of ship structures, with textbooks such as "Roark's Formula's for Stress and Strain" (Young and Budynas 2011), "Ultimate Limit State Design of Steel-Plated Structures" (Paik and Thayamballi 2003), or "Ship Structural Analysis and Design" (Hughes and Paik 2010), which are often featured in the armoury of the structural naval architect. These approaches form the basis of many design standards and Classification society rules.

Within the reporting period, numerous papers that develop analytical methods or undertake direct analysis to verify previously proposed methods have been published. Papers by Benson *et al.* (2014), Cui *et al.* (2017b), Dekker and Walters (2017), Glassman and Garlock (2016), Khedmati *et al.* (2016), Kitarović *et al.* (2015) and Zhang (2016) are noted. These papers are subsequently discussed in this chapter in relation to the type of analysis. Developments in the rule applications of these approaches are covered in Chapter 5 of this report.

3.1.2 Direct calculations

Direct calculation via the use of FE analysis and methods that facilitate FSI are increasingly becoming standard practice for ships and offshore structural designs. The application of these techniques for dynamic analysis is addressed by the ISSC Technical Committee II.2 Dynamic Response. The focus of this report is the application of techniques to implement quasi-static loading for different analysis requirements.

The main papers within the reporting period that apply FE analysis to the analysis of ships and ship-like structures are papers by Estefen *et al.* (2016), Gannon *et al.* (2016), Tanaka *et al.* (2015) and Zhang *et al.* (2016). These papers are subsequently discussed in this report in relation to the analysis methods, and therefore, are not discussed here to avoid repetition.

Combined FSI analysis continues to develop with a substantial amount of dynamic analysis rather than quasi-static analysis. However, the fluid loading is often transferred from the fluid analysis, for example, CFD as a quasi-static load to a separate FE solver to understand the structural response. Kumar and Wurm (2015) utilised this method and presented a comparative study of bi-directional FSI for large deformations of layered composite propeller blades. Changes in the pressure distribution, stress distribution, thrust, torque and pitch angle of the blade are presented, with quasi-static loading transferred from CFD analysis to FE analysis and the distorted geometry re-meshed and transferred to the CFD in a two-way loop.

3.1.3 Reliability analysis

Structural reliability analysis provides a crucial method for the design of ships and offshore structures, which enables the quantification of uncertainties when designing a safe structure. This quantification may be achieved in the direct design of a structure or the development of rule-based criteria or allowable stresses that suitably account for uncertainties. Reliability analysis requires the assessment of a structure's capability via appropriate modelling. A reliability analysis may require a model to be run 10^6 times, including different combinations of variables to inform about the sensitivity of the structure and subsequent probability of failure during its life. To successfully perform a reliability analysis, the runtime of models should be minimised by simplifications, such as a quasi-static approach. Reliability analysis is considered to be an important methodology; therefore, it is considered in Chapter 4 of this report.

3.1.4 Optimisation-based analysis

An increasing number of studies that employ different optimisation techniques to rationally improve structural design objectives have been identified. The main design objectives include weight, cost and vertical centre of gravity (VCG). Andrić *et al.* (2017b) extend the "standard" scantling optimisation approach for fixed topology to an approach that investigates the influence of different topology variants on optimal structural scantlings. The methodology combines the fast concept exploration of design variants using generic 3D FE models and a two-step decision support procedure that is based on topology and scantling optimisation. How different topological variants can produce different optimal structural scantlings with respect to chosen design objectives (mass and VCG) has been demonstrated.

Temple and Collette (2015) developed a framework to design optimal ship structures considering production and maintenance costs using a multi-objective genetic algorithm. Fatigue and corrosion were considered as damage processes on a yearly basis to estimate the cost of maintenance. A probabilistic service extension metric was employed to account for the uncertainty in the life span. Kim and Paik (2017) optimised a VLCC considering ultimate strength and structural mass as an objective. The coupling of strength assessment with an optimisation algorithm enables a 20% reduction of man-hours by automated computer-assisted design. Andrade *et al.* (2017) demonstrated that FE analysis combined with design of experiments and a response surface method can be a fast approach to generating competitive structural designs.

Ringsberg (2015) presented a study of the performance of car deck structures made of steel and composite materials for a PCTC vessel. Conceptual designs were optimised and evaluated by an FE analysis with respect to stakeholder defined criteria, e.g., strength and the maximum allowed deflection during loading. A weight and cost estimation performed for four different car deck designs was presented. Stone and McNatt (2017) presented a method for the multi-objective optimisation of a ship structure using an integrated hydrodynamic code, 3D FE structural response, limit state evaluation and structural optimisation with Maestro design system software. An example frigate optimisation case demonstrates that the proposed method is very useful for performing ultimate strength-based structural optimisation with multiple objectives, namely, minimisation of the structural weight and VCG, and maximisation of structural safety.

3.2 Failure modes and response analysis

To understand the ultimate limit state of a structure and quantify the reserve between the structural capability and load over the life of a structure, the observed failure modes must be quantified. From a design perspective, quasi-static methods for failure mode assessment are very important, such that the design can be rapidly progressed without a requirement for more complex and time-consuming analysis. This section reviews advances in quasi-static buckling analysis, ultimate strength assessment, fatigue assessment, residual strength assessment and whipping analysis.

3.2.1 Buckling and ultimate strength

Stiffened panels and plates

Gannon *et al.* (2016) numerically investigated the influence of residual stress and distortion due to welding on the behaviour of tee- and angle-stiffened plates under axial compression. The results indicated that the ultimate strength may be reduced by 12.5% due to the presence of welding-induced residual stress. Kim *et al.* (2017a) developed an empirical formula for the ultimate strength of stiffened panels, which is a function of the plate and stiffener slenderness ratio with two correction coefficients obtained by FE analysis. A review of ultimate strength analysis methods for steel plates and stiffened panels in axial compression has been presented by Zhang (2016). Analysis approaches for ultimate strength and their employment in ship designs are reviewed and discussed. The author presents a developed design formula for the ultimate strength of stiffened panels using a comprehensive nonlinear FE analysis. Considering the ultimate strength of stiffened grillages, Benson *et al.* (2015) provide a development of the orthotropic plate approach, which is related to the development of the Smith progressive collapse method, such that the total and inter-frame collapse can be assessed. Considering the bi-axial buckling strength of stiffened panels, Cui *et al.* (2017b) investigated numerous analytical approaches that are suitable for practical design application compared with FE analysis. Their study indicates that the Vlasov assumption in relation to stiffener rigidity may cause an overestimation of the buckling capability, whereas methods that assume the flexibility of stiffeners yield satisfactory results compared with FE analysis. Khedmati *et al.* (2016) present empirical formulae for assessing the ultimate strength of aluminium stiffened panels under combined transverse and lateral pressure; these formulae were developed by regression analysis from FE analyses that include the effect of the heat affected zone.

The ultimate strength of stiffened panels subject to combined in-plane axial and shear loads are investigated by Takami *et al.* (2015) for steel panels and Syrigou *et al.* (2015) for aluminium alloy plating. Jiang and Zhang (2015) performed numerical investigation of the influence of lateral pressure on the nonlinear behaviours of stiffened panels subjected to in-plane stresses. The results indicated that the effect of pressure on the ultimate strength depends on the ratio of longitudinal and transverse stresses and that the collapse loads are more sensitive to pressure when the external loads are dominated by longitudinal stresses. Gordo and Guedes Soares (2015) demonstrated that the form of assumed initial imperfections has greater importance than its maximum amplitude for the ultimate strength of long steel plates. Glassman and Garlock (2016) developed an analytic model for the ultimate post-buckling shear strength of steel plates that is very accurate for an extensive range of material and geometric parameters. Dekker and Walters (2017) developed an analytic model that can predict wrinkling and folding of thin and moderately thick shells. The model does not require calibration, employs a stress-strain curve, and can predict the onset of material failure. The method is consistent with a highly detailed FE model.

Various feasible approaches to enhancement of the plate elastic shear buckling strength are comprehensively investigated in Kitarović *et al.* (2015). Based on derived theoretical envelopes of the considered approaches, stiffening parallel to the longer plate edges is identified as the most effective approach to the considered problem. A simplified analytical formulation, which is convenient for utilisation in structural design of the plated structures, is proposed. The development of a new proof of plate capacity under combined in-plane loads for ship design and classification has been presented by Hayward and Lehmann (2016, 2017). The new proof is based on an improved understanding of plating collapse obtained from an extensive series of nonlinear FE analyses that encompasses the complete range of structural configurations and load combinations relevant to the shipbuilding industry. Compared with existing proofs, the new proof incorporates a physical-based approach towards the tensile stress effect on plate capacity and captures the influence of both plate slenderness and aspect ratio under compressive bi-axial loads.

Structural problems that arise from a larger bilge radius and associated structural arrangement around the bilge shell, which are not sufficiently identified, have been investigated by Okada *et al.* (2016, 2017). The authors developed theoretical formulae, assuming a curved plating connected to a continuous stiffened flat plating with regular stiffener spacing. In these cases, the stipulation in the CSR-H is not always rational, and the authors propose modified structural design methodologies around the unstiffened bilge shell plating. Previous research on buckling and the ultimate strengths of curved plates by Kim *et al.* (2014) has been fulfilled with an experimental study by Lee *et al.* (2016a). The results from the experimental data were applied for fine-tuning and slight modification of the design formula presented in Kim *et al.* (2014) with new correction factors.

Hull girder ultimate strength

Current research in ultimate hull girder strength calculation has developed to include different effects (such as global horizontal bending and torsion moments, and double bottom pressure) in 3D nonlinear FE analyses and the parallel development of new simplified methods that can simulate these effects with acceptable accuracy.

Pei *et al.* (2015) demonstrated radical computational savings when using the ISUM method for predicting the ultimate strength and post-ultimate behaviour of a bulk carrier. The approach was coupled with FE analyses and a load calculation method for the level of a complete ship structural model. Mohammed *et al.* (2016) presented an ultimate strength analysis of a container ship under combined vertical bending and torsional loading using nonlinear FE analyses. The margin of safety between the ultimate capacity and the maximum expected moment were established, which demonstrates that torsion does not significantly alter the capacity of the structure in the study case. In contrast to this research, Darie and Rörup (2017) revealed the importance of oblique seas for the evaluation of the hull girder ultimate strength of container ships. The analysis was completed by coupling FE analysis with 3D hydrodynamic analysis based on Ranking code. This approach evaluated vertical, horizontal and torsional global loads that appears in different wave headings and calculated the hull girder ultimate strength capability around amidship. Tanaka *et al.* (2015) present a simplified method for analysing the ultimate strength of a hull girder under combined bending and torsional loads. The method reduces the section to a series of thin-walled beams and implements the Smith progressive collapse method (Dow *et al.* 1981) to calculate the ultimate strength by accounting for warping and shear stresses. The results are compared with explicit FE analyses and physical tests, which show agreement when the bending moment is dominant. However, as torsion becomes dominant, correlation deteriorates, which indicates that additional development of the method is required.

Fujikubo and Tatsumi (2017) presented an extended Smith method that considers the effect of double bottom pressure on hull girder ultimate strength, which is especially important for container and bulk carrier ships. In addition to the standard Smith discretisation of a hull girder cross-section, the double bottom is idealised as plane grillage extended over a hold length. The results were compared with nonlinear FE analyses, and acceptable accuracy was achieved with vast savings in CPU time. Gordo (2017) investigated the effect of double bottom pressure under alternate hold loading on the ultimate strength of a bulk carrier and revealed that the effect can significantly reduce the hull girder strength in the hogging condition. Applying a quasi-static approach to the loading of a Suezmax tanker, Estefen *et al.* (2016) employed FE analyses to investigate the influence of geometrical imperfections on the ultimate strength of the double bottom. The study reveals that an imperfection mode consistent with the elastic buckling mode will provide the most conservative assessment of ultimate bending strength. Zhang *et al.* (2016) present a method to assess the bending capability of a ship's hull after shakedown. Shakedown is considered to be the initial cyclic loading of a structure, which can cause a progression away from the assumed elastic condition. The paper suggests that the ultimate bending strength may be reduced after shakedown. Fujikubo *et al.* (2015) investigated

the effect of shear stresses on the hull girder ultimate strength of a container ship based on different definitions of partial FE models.

Kitarović *et al.* (2016) consider the hull girder ultimate strength of a bulk carrier as determined by an IACS incremental-iterative progressive collapse analysis method. In addition to the original IACS prescribed load-end shortening curves, new curves determined by the nonlinear FE analysis have been presented. The results obtained by both sets of curves are compared and discussed on both the local level (structural components load-end shortening curve) and the global (hull girder) level. A similar investigation, which is based on the improved accuracy of load-end shortening curves to be used for hull girder progressive collapse, have been performed by Kvan and Choung (2017). Morshedsoluk and Khedmati (2016) used an extended formulation of the coupled beam theory that considered the effect of a superstructure to calculate the ultimate strength of composite ships.

3.2.2 Fatigue strength

Numerous research studies have been conducted to observe the scenario of fatigue durations. In recent years, designers and Classification societies have worked to prevent another accident, such as MOL Comfort, and ensure the safety for crews and goods. They have improved monitoring systems to promptly obtain information from the hull girder and developed simplified methods for efficiently and accurately predicting fatigue damage.

Since the MOL Comfort accident in 2013, the monitoring of hull displacement has become important in the maritime industry. Storhaug and Aagaard (2016) present the calibration of hull monitoring strain sensors on a deck, which considers both static loadings and dynamic loadings. The calibration provided an accurate calibration procedure and indicated excessive uncertainties in the loading computer, which can be used to reduce the probability of risk, such as in the case of MOL Comfort. Magoga *et al.* (2016) present a comparative study between assumed stress spectra and derived stress spectra from strain measurements, with respect to the fatigue life for three structural details of naval aluminium High-Speed Light Craft (HSLC). The study was performed to obtain the best model of the measured stress range data normalised by the design stress ranges. The results indicated agreement between the linear model and the Weibull model, which estimate the fatigue life based on a Gaussian model correlated with derived spectra and fleet maintenance data.

Due to the recent CSR-H from IACS, the evaluation of fatigue life is greater than 25 years. Liao *et al.* (2015) compared the fatigue life evaluated by the rules with the fatigue life evaluated by advanced hydro-structure coupled analyses and examined the fatigue life of various hot spots located amidship. They demonstrated that the fatigue life predictions obtained by direct spectral analyses significantly deviated from the rules. This finding confirmed that the rules for still water and wave load uncertainties can substantially affect the fatigue prediction.

Micone and Waele (2015) present a comparison of fatigue design codes with a focus on offshore structures. The criteria of fatigue strength for different Classification societies significantly differ, and the fatigue phenomenon is sensitive relative to these codes. The S-N curve for the fatigue design method is simple but may cause conservatism due to the pre-defined load range. The British Standards Institution (BSI) presents the most complete information for applying a fracture mechanics approach, whereas DNV GL offers the most updated and complete information for applying an endurance approach. Current research and rule development activities on the fatigue strength of thick plates are presented by von Selle *et al.* (2016) due to the use of a thicker plate in construction and the trend of optimised structures with higher tensile steel. In the DNV GL fatigue rules, a comparison with former DNV and GL fatigue rules is provided, which confirms the hot-spot area stress and nominal stress concept, especially for the cutting plate edges of thick plates and the welded joint, which are stress concentration points.

Van Lieshout *et al.* (2017) conducted a validation of the corrected Dang Van multi-axial fatigue criterion applied to turret bearings of FPSO offloading buoys. With the three considered cases, they corrected the characteristic parameters (α and β) of the Dang Van curve and confirmed the correction using full-scale and long-duration fatigue tests. The results concluded the application of the Dang Van criterion, which can be efficiently applied to FPSO offloading buoys with a revised locus of hydrostatic stresses.

Horn and Jensen (2016) present a method for reducing the uncertainty of Monte Carlo-estimated fatigue damage using the first-order reliability method (FORM). The objective of the FORM is to minimise the function to determine the design point with a linear approximation. Compared with conventional simulations, the FORM design point should be significantly and properly defined, which will affect the applicability of prediction for fatigue damage. A similar study by Singh and Ahmad (2015) presents a probabilistic analysis and risk assessment of a deep-water composite production riser against the fatigue limit state. The proposed methodology is based on the S-N curve approach and Palmgren-Miner rule with the consideration of 12 sea states and a reliability assessment using a stochastic FE analysis. The FORM and Monte Carlo method are used to calculate the probability of failure; the results confirmed that the FORM is suitable for the reliability assessment of marine structures.

Some study cases represent the trend of the importance of fatigue problems, such as Mao *et al.* (2015), who present a study using a beam theory-based approach for the fatigue assessment of container ship structures. They performed an investigation using experimental records from two container ships and a comparison with the results from direct FE analysis. A new procedure was proposed to obtain relative results from a linear regression analysis with the results from only one sea state FE analysis results considering its efficiency and accuracy. Another example is a case study by Park *et al.* (2017), who performed a fatigue damage evaluation of an LNG tank. This efficient time-domain stress analysis was combined with a modal analysis, which employed quasi-static deformation modes. With the three basic assumptions in this study, the structural response is almost static, and the contact force is independent of friction. An efficient and accurate time-domain fatigue analysis that can be applied to the structural details near the rolling key and chock of an independent type tank is provided.

3.2.3 Residual strength

The global strength assessment of a ship in a seaway is generally undertaken by reducing the problem to a quasi-static scenario of a ship balanced on a wave. In a damage scenario, the same assumption is made. With these assessments, understanding the influence of the damage on the structural response is important. Underwood *et al.* (2015) demonstrated the potential influence of damage on the total failure mode of steel grillages. Subsequently, Underwood *et al.* (2016) demonstrated similar effects within a box girder and proposed that damage analysis should be considered at both the interframe level and compartment level to capture these effects.

Under collision loads, the failure mode of a structure can also change. Considering tubular structures, Bandi *et al.* (2015) introduced a design method for the progressive collapse of thin-walled tubular components under axial and oblique impacts using FE analysis. On a larger scale, Cerik (2015) used FE analyses and experiments to demonstrate how damage can cause sharp catastrophic asymmetric failure of ring-stiffened cylinders, whereas the presence of an additional structure prevents this catastrophic failure but causes failure similar to the undamaged form for orthogonally stiffened cylinders.

Numerous papers investigate the effect of the loss of a column within steel framed structures. Of primary interest to civil structures, the increased open spaces within cruise liners prompt an increased use of pillars. Chen *et al.* (2016a) include a formulation that considers the axial load within a beam as its length increases and structure yields after removal of a central supporting column.

Noting the importance of material data for use in analysis, Calle and Alves (2015) provided a review of material failure modelling in ship collisions. Calle *et al.* (2017), Hosseini *et al.* (2016) and Storheim *et al.* (2015) investigate material failure criteria, fracture estimation and strain-ageing effects of materials, respectively. With a focus on ship-to-ship collisions, Zhang *et al.* (2017d) presented experimental verification of closed-form analytical solutions for the energy released during ship collisions, as previously presented by Pedersen and Zhang (1998). Heinvee and Tabri (2015), Liu and Guedes Soares (2015, 2016), Liu *et al.* (2015) and Sun *et al.* (2015b) present analytical methods in relation to energy absorption in stiffened plates and web girders during collision events. Samuelides (2015) presented procedures that were applied for the assessment of the crashworthiness of marine structures subjected to impact loads and noted the requirement to identify and determine uncertainties. Gao *et al.* (2015) demonstrated an elastic-plastic ice material model for ship-iceberg collision simulations utilising the Tsai-Wu yield surface model and developing new empirical failure criterion. Bin *et al.* (2016) presented an analytical method based on the improved Smith's method to assess the damage and predict the residual strength of a ship in a shoal grounding scenario.

The development of techniques for residual strength assessment continue with a significantly greater focus on dynamic rather than simplified quasi-static approaches. However, evidence exists of some of the advances in dynamic evidence that provide verification and development of closed-form analytical or quasi-static FE approaches.

3.2.4 Whipping

Contributions from impulsive slamming loads and the consequent vibratory response (whipping) to fatigue and extreme loading may be significant for long slender ships with large openings, such as container vessels. Within the reporting period, concern for how it affects the fatigue and ultimate strengths of ships and how it should be included in numerical models and simulations in the design and assessment of a ship's performance continue to be the focus of numerous studies, for example, refer to DNV GL (2015).

An essential input parameter in numerical tools and model tests that affect the vibration level is damping. Storhaug *et al.* (2017) presented a study in which the damping for several container ships and other ship types was determined based on measurement data. Several damping methods were applied to determine the most reliable method. The Random Decrement Technique (RDT) and the spectral method were recommended. The results indicated significant differences in damping among ship types. A target damping of 1.7% for container ships and a target damping of 0.7% for blunt ships were proposed. For container ships, the damping appeared to slightly reduce with vessel size but with moderate confidence. Temarel *et al.* (2016) presented a review study, in which they critically assessed the methods employed for the evaluation of wave-induced loads on ships. Analytical, numerical and experimental approaches were examined. A sensitivity analysis of the response analyses, which is a regular part of a structural reliability study, is performed to identify and estimate uncertainties and reduce these uncertainties to as large an extent as possible.

Storhaug and Andersen (2015) presented a study with the objective of explaining why hogging collapse accidents occurred in moderate to small storms. The method of extrapolation of model test measurements of whipping was used to identify the dimensioning sea states for three container ships. The findings concluded that moderate storms and head or bow quartering seas at realistic speed with voluntary speed reduction are regarded as an acceptable design basis for estimating the total moment, including whipping for container ship design.

During the reporting period, the committee has reviewed numerous papers, which present numerical simulations and analyses that involve whipping. The majority of the studies have been performed using simulation software and methods that fall outside of the mandate of the current committee that refers to quasi-static response analysis. This trend may be attributed to the positive advancement of simulation software and computer capacity, which enables ad-

vanced and detailed simulations with reasonable time effort and computational cost. Fukasawa and Hiranuma (2016) presented time-domain nonlinear simulations of three container ships (1,700 TEU, 6,000 TEU and 20,000 TEU) and compared the calculated vertical wave bending moments with the unified IACS (2015a) requirements. Shin *et al.* (2015) investigated the importance of various hydroelastic modelling approaches for the global symmetric and anti-symmetric response of a 16,000 TEU ULCS design. Two- and three-dimensional linear and weakly nonlinear flexible FSI models that respectively combine the Vlasov beam and 3D FE analysis structural dynamics with a B-spline Rankine panel and Green's function hydrodynamics were assessed and compared. Comparisons between rigid body and hydroelastic predictions demonstrated the importance of considering the effect of hull flexibility on the dynamic response and the suitability of different idealisations in preliminary or detailed design stages.

3.3 New metallic materials, composite and sandwich structures

The development of novel materials and structural topologies for the construction of marine structures continues with an accelerating pace. Castegnaro *et al.* (2017) presented the development of a 4.6 m flax-epoxy and balsa wood racing sailboat, from the materials selection to the manufacturing technique. Tensile tests on the flax-epoxy laminates revealed the typical scatter of natural bio-composites. Godani *et al.* (2015) performed experimental and numerical studies that demonstrated the high sensitivity of inter-laminar shear strength of GFRP composites to air inclusions. Different void shapes were modelled using a range of element formulations. Lee *et al.* (2015a) investigated a glass fibre-reinforced polyurethane foam (as used for LNG tank insulation) in cryogenic and room temperatures under compressive loading. A temperature and strain-rate dependent constitutive material model was proposed and implemented in an FE analysis, which demonstrates agreement with the experimental results. Shahbaztabar and Ranji (2016) developed an analytic model for the free vibration analysis of symmetrical cross-ply laminated plates resting on an elastic foundation subjected to uniform in-plane loads and in contact with water on one side; the results correlated well with experiments. Yu *et al.* (2016a) developed a method for the free vibration and buckling of laminated composite plates based on the first-order shear deformation laminate theory and B-spline interpolation functions. The method enables effective modelling of cut outs with complicated shapes and reasonable accuracy. Kotsidis *et al.* (2015) performed static and fatigue tests of hybrid composite-to-steel butt joints that consist of double lap steel-FRP parts and an FRP sandwich. Damage propagation and response of the joint was described. Rahm *et al.* (2017) experimentally investigated the fire resistance of an FRP sandwich bulkhead with thermal insulation and a multiple core FRP sandwich bulkhead without insulation and was able to demonstrate structural fire integrity beyond 60 minutes whilst reducing the structural weight and thickness compared with a reference panel.

Although the marine industry favours steel as a material, lightweight construction can be achieved by seeking new topologies via sandwich construction. Jelovica and Romanoff (2015) and Jelovica *et al.* (2016) investigated buckling and natural frequencies of laser-welded steel sandwich panels. Secondary bending was demonstrated to postpone local instabilities and increase load-carrying capacity while stiffness of the laser welds, joining the faces and the core, have a significant influence on vibrations. Huang *et al.* (2015) and Yan *et al.* (2016a) investigated lightweight steel-concrete-steel composite shells subjected to patch loading, which simulate applications in offshore platforms in ice-covered waters, compared with experiments and developing analytical formulations.

Several studies focused on exploring the benefits of composite materials in replacing steel structures in ships. Ringsberg (2015) presented a study of the performance of a car deck panel fabricated with steel and composite materials to optimise the strength-weight ratio by FE analyses. Stipčević *et al.* (2015) presented an FE analysis study of the bending response of composite panels in the upper decks of a car carrier considering BV Rule compliance. Tawfik

et al. (2017) presented a study of the use of composite materials for the hatch covers of a bulk carrier; the results conclude that the alternative construction reduces the weight and operating cost of a vessel or provides extra strength of the hatch covers. Developments of novel steels and structural designs for LNG tanks have focused on improved structural performance, reliability and cost-optimisation of joints and insulation systems (Ehlers *et al.* 2017, Lee *et al.* 2015b, Niu *et al.* 2017).

3.4 Ageing structures

Throughout the life of a structure, its ability to continue to resist load will change due to degradation of the structural material, degradation due to the response to cyclic loading, and the impact of accidental loading. This section focuses on quasi-static methods to assess the capability of an aged or ageing structure.

3.4.1 Corrosion

In the design and analysis of ships and offshore structures, allowances are made for corrosion to ensure that the capability of the structure remains sufficient throughout its life. During the term of this committee, numerous papers have been published to investigate the effect of corrosion. Cui *et al.* (2017a) investigated the effect of corrosion on the ultimate bending strength of a ship's hull that was subject to uniform corrosion at varying depths and demonstrated the subsequent degradation in strength. A similar study was presented by Zhang *et al.* (2017f), who represented the corrosion as pitting and developed a strength reduction formulae based on the lost volume. Zhang *et al.* (2017b) presented an experimental study and provided empirical equations to predict the ultimate strengths of corroded stiffened panels. Wang *et al.* (2015c) developed empirical formulations for the ultimate strengths of stiffened steel panels that feature grooving corrosion under axial compression, which revealed correlation with FE analyses at lower column slenderness values. Saad-Eldeen (2015a) presented a study to analyse a severely damaged box girder subjected to the combined action of non-uniform and inter-crystalline corrosion. A series of comparative static nonlinear FE analyses are conducted, and the effect of stiffness reduction on the moment-curvature relationships, failure modes, and ultimate strength, as well as the movement of the neutral axis, were presented and discussed.

3.4.2 Fatigue cracks

Welded structures of all sizes and shapes exhibit fatigue failure primarily in the welded region, rather than in the base material, due to imperfections and flaws that relate to the welding procedure. Therefore, the welded region has received and continues to receive a substantial amount of attention from researchers. Wang *et al.* (2015b) performed a multi-scale investigation of the residual strength of a jacket platform with fatigue crack damage by multi-scale FE analysis. Presently, an efficient method to evaluate the influence of cracks on structural performance is lacking due to the immense scale difference between the meso-scale damage and the macro-scale structure. The results indicate that the proposed multi-scale method can accurately describe fatigue crack damage in a macro-scale structure and be applied to investigate the influence of meso-scale structural damage under extreme loads.

Ao and Wang (2015) investigated the residual ultimate strength characteristics of box girders with variable inclination cracks under torsional loading. A series of FE models are established by changing the crack length and crack angle using FE analyses and verified by comparison with previously developed formulae. Yan *et al.* (2016b) presented a prediction of fatigue crack growth in a ship detail under wave-induced loading. Fatigue life prediction based on fracture mechanics has become the focus of research on the strength of ship structures. However, a general formula for calculating stress intensity factors (SIF) is difficult to summarise, and the application of the fatigue crack propagation theory is limited to simple structures and simple loads. Therefore, the SIF of a crack in a ship detail was calculated by combining FE analysis capabilities, and a method for generating the ship fatigue loading spectrum is demon-

strated based on the design wave approach. Lotsberg *et al.* (2016) used probabilistic methods for planning inspections for fatigue cracks in offshore structures. Due to the nature of the fatigue phenomena, small changes in basic assumptions can have a significant influence on the predicted crack growth. The calculated fatigue life based on the S-N approach is sensitive to the input parameters. Fracture mechanics analysis is required for the prediction of crack sizes during the service life to account for the probability of detection after an inspection event. Analysis based on fracture mechanics needs to be calibrated to the analysis of fatigue test data or S-N data. Calculated probabilities of fatigue failure using probabilistic methods are even more sensitive to the analysis methodology and to input parameters in the analyses. Thus, the use of these methods for planning inspection requires considerable knowledge and engineering skill. Therefore, industry has asked for guidelines that can be used to establish reliable inspection results using these methods. During previous years, DNV GL has performed a joint industry project for establishing probabilistic methods for planning in-service inspection for fatigue cracks in offshore structures. The recommendations from this project are included in recommended practice. The essential features of the probabilistic methods developed for this type of inspection planning are described in this paper.

Yue *et al.* (2017) investigated fatigue crack propagation in bulb stiffeners, which are extensively employed in ship structures. The shape of a 3D surface crack in a full-scale bulb stiffener fatigue test was measured and estimated by the Nominalisation Crack Opening Displacement method. Crack propagation in the bulb stiffener was based on the 2D Paris law and linear FE analyses; the predicted fatigue crack propagation was verified by full-scale fatigue tests.

The hammer peening process is a well-known method for improving the fatigue life of welded joints by generating a compressive residual stress field near the weld toe, which is recognised as the fatigue crack initiation site. Morikage *et al.* (2016) investigated the mechanism of fatigue crack propagation in a compressive residual stress field by comparing the results with the experimental results. The results clarified the fact that the morphology of a surface crack, which propagated in the compressive residual stress field, differed from the morphology of a surface crack in a neutral stress field, especially under a low stress intensity factor condition. Tian *et al.* (2017) introduced a structural intensity approach to study the crack detection for offshore platforms. The Line Spring Model of a surface crack is proposed based on the plate crack structure, and thus, the relationship among the additional angle, displacement and crack relative depth is achieved. The expression of appended structural intensity for crack damage is derived. Using the structural intensity approach, cracks are easily detected on the key point. The K-shape welded pipe point is detected using a structural intensity approach, and the crack can be accurately detected.

3.4.3 Dents

Accidental loading often causes localised deformation or dents in a structure, which are attributed to the support of docking, wave impact, contact by quays or floating objects, and dropped objects. The ability to analyse a structure to confirm its residual strength in its dented state is important when assessing whether a structure can remain in service or whether immediate repair is required. Within the reporting period, Saad-Eldeen *et al.* (2015a, 2015b) presented a series of experimental ultimate bending strength analyses of box girders with dents. The results were compared with FE analyses, in which loading was applied in a quasi-static manner to compare the impact on both ultimate strength and flexural rigidity. Additional studies by Saad-Eldeen *et al.* (2014, 2016a, 2016b) investigated the impact of dents on the ultimate strength of steel plates, with or without openings. The analysis was experimental with comparative assessments undertaken by FE analyses. The post-collapse behaviours are discussed, and the inflection plate slenderness with and without dents is observed, for which the behaviour of the plate changed. A certain dent breadth-to-plate breadth ratio, which reveals

the different plate response, is established. Subsequently, Saad-Eldeen *et al.* (2014) developed a generalised expression of the ultimate strength reduction factor due to dents.

3.5 Concluding remarks

Structural analysis via the application of quasi-static loading remains an important approach in the design and analysis of ships and offshore structures. Whilst significant research continues in the time domain, this research is important to investigate methods that simplify the analysis process whilst providing suitable accuracy to rapidly develop structural designs, that do not constrain the designer to a limited tool set or require complex and time-consuming analysis early in the design process, when data may not be available to implement these techniques in a useful and meaningful manner.

4. UNCERTAINTY AND RELIABILITY ANALYSIS

Recently, reliability analysis has become more important for the design of ships and offshore structures. Proper evaluation of uncertainties in the target structures and estimation of uncertainties in the responses of the structures are necessary for reasonable reliability analysis. Two main categories of uncertainties exist:

- *Aleatory uncertainty*, i.e., physical uncertainty. Aleatory uncertainty consists of physical uncertainty, which is inherent, and intrinsic uncertainty. Aleatory uncertainty is a natural randomness of a quantity, such as the variability in the strength of materials. This physical uncertainty or natural variability is a type of uncertainty that cannot be reduced.
- *Epistemic uncertainty*, i.e., uncertainty related to imperfect knowledge. Epistemic uncertainty consists of statistical uncertainty, model uncertainty and measurement uncertainty, which are classified as a type of uncertainty associated with limited, insufficient or imprecise knowledge.

This chapter focuses on the recent developments in uncertainty modelling of loads and structures, and recent application of reliability analysis to practical problems. Recent developments of uncertainty analysis methods and risk-based maintenance concepts associated with quasi-static response assessment have been reported.

4.1 Uncertainties in load modelling

4.1.1 Still water and wave loads

Based on the probabilistic model of the configuration of damage to ship structures in IMO's Marine Environment Protection Committee (MEPC), some papers begin to study the probability of the still water bending moment, statistical description of wave-induced loads and the effect of statistical uncertainty due to different time spans of simulations of ship responses for damaged ships. Rodrigues *et al.* (2015) performed a probabilistic analysis of the hull girder still water loads on a shuttle tanker for parametrically distributed collision damage spaces. The collision-induced probabilistic distribution of the damaged boxes was also investigated. Bužančić Primorac *et al.* (2015) investigated the statistical properties of the still water bending moment of a double hull oil tanker that was damaged in a collision or grounding accident. Random damage scenarios were generated by Monte Carlo simulation using IMO probability distributions of damage parameters. This probabilistic model can be applied to the structural reliability assessment of damaged ships.

Regarding the uncertainties in the wave-induced bending moment, Temarel *et al.* (2016) presented a review paper on the uncertainties in predicting wave-induced loads and the probabilistic approaches for the evaluation of long-term response. Gaspar *et al.* (2016) evaluated the effect of the nonlinear vertical wave-induced bending moments on the ship hull girder reliability based on the FORM. Note that the probabilistic modelling for the hull girder strength, still water bending moment and vertical wave-induced bending moment is detailed. Guo *et al.*

(2016) presented a statistical analysis method of ship response in extreme seas, which addressed the statistical description of heave and pitch motions and vertical bending moments by taking an LNG tanker as an example. Iijima *et al.* (2017) examined the effect of ship operation on the hydroelastic behaviours of three large container ships (6,000 TEU, 10,000 TEU and 19,000 TEU). The uncertainty of the wave-induced vibration with respect to ship speed is evaluated.

4.1.2 Wind loads

The retrieval of wind profiles considering statistical uncertainties remains the main topic of recent studies. Achtert *et al.* (2015) presented notable research on the estimation of wind loads that employed the combination of a commercial Doppler LIDAR with a custom-made motion-stabilisation platform. The retrieval of wind profiles in the Arctic atmospheric boundary layer during both cruising and ice-breaking with statistical uncertainties is demonstrated and compared with land-based measurements, which enables the retrieval of vertical winds with a random error less than 0.2 m/s. Xie *et al.* (2016) performed a simulation-based study of wind loads on semi-submerged objects in ocean wave fields. The results indicated that waves can cause significant variations in wind loads; these effects were not adequately recognised and have not been quantified in previous studies. Zhang *et al.* (2017c) examined probabilistic modelling of the drifting trajectory of an object under the effect of wind and currents for maritime search and rescue. An optimal estimation algorithm was proposed to obtain random wind and current velocities based on the spatial correlated fields.

4.1.3 Ice loads

The ISO 19906 standard provides guidance for the calculation of design ice loads using both deterministic approaches and probabilistic approaches (ISO 2010). In determining design loads for different environmental factors, both principal actions and companion actions must be considered. The ISO 19906 enables the designer to calculate the companion wave action as a specified fraction (combination factor) of the Extreme Level (EL) design wave load. Alternatively, the designer can explicitly calculate appropriate companion wave loads. Fuglem *et al.* (2015) presented probabilistic methods to estimate iceberg-wave companion loads. A probabilistic methodology was developed to determine the joint probability distribution of iceberg impact and companion wave forces, and the combined EL and Abnormal Level (AL) values were determined. The effective companion wave loads were significantly less than the effective companion wave loads determined based on the ISO 19906 combined load factors. Xu *et al.* (2015a) performed an experimental study of dynamic conical ice force. A comparison of ice forces from small-scale tests with full-scale measured data from a conical structure has been accomplished. Ranta *et al.* (2015) conducted ice load estimation using combined finite-discrete element simulations and aimed to demonstrate the applicability of these simulations in a statistical study on ice loads and the estimates of their errors. Hansen *et al.* (2015) presented new statistical methods for calculating extreme spatial ice distributions that may be applied in the design process. Statistics for global loads and directional dependency of icing and methods for assessing the expected duration of icing events are described. Heinonen and Rissanen (2017) investigated the coupled-crushing analysis of a sea ice-wind turbine interaction and suggested that the magnitude and time variation of sea ice load depends on various factors, such as the thickness and velocity of ice and the size and shape of a structure.

4.1.4 Sloshing and slamming loads

Model tests remain the main approach in the study of sloshing and slamming loads in recent years and provide a significant amount of information about the uncertainties of these loads. Kim *et al.* (2017b) investigated the scale effect on 3D sloshing flows. A series of model tests were conducted for three differently scaled tanks. The key sloshing load parameters, such as the pressure peak and rise time of sampled sloshing pressures, were systematically analysed by a statistical approach. Ryu *et al.* (2016) investigated sloshing design load prediction of a

membrane-type LNG cargo containment system with a two-row tank arrangement in offshore applications. Due to the uncertainties entangled with the scale law that transforms the measured impact pressure to the full-scale impact pressure, a comparative approach was taken to derive the design sloshing load. Swidan *et al.* (2016) presented a series of drop-test experiments to investigate the slamming loads experienced by a generic wave-piercer catamaran hull form during water impacts. The systematic and random uncertainties associated with the drop test results are quantified. Stagonas *et al.* (2016) demonstrated the use of a pressure mapping system for measuring wave impact-induced pressures. The results concluded that the pressure mapping system has the capacity to provide pressure distribution maps with reasonable accuracy by careful calibration and setup.

4.1.5 Impact loads

Impact loads can be considered as transient forces that are generated during accidents and operations and include numerous uncertainties. Jia and Moan (2015) investigated the hydrodynamic effects in ship collision. Their findings reveal that the equivalent added mass for the sway motion depends on not only the duration of collision impact and impact force but also on the collision position, whereas the equivalent added mass for the yaw motion can be assumed to be independent of the collision position. Park *et al.* (2015) presented an accidental limit state-based ship collision analysis approach. Time-variant corrosion wastage was employed in the case of age-related damage. In the case of a collision event, low Arctic temperatures may affect the crashworthiness and delay the ageing effect compared with regular temperatures.

The shape of the sea bottom is an important factor that determines the extent of grounding damage on ships and the loss of water tightness. Sormunen *et al.* (2016) presented a four-step methodology for mathematically estimating sea bottom shapes for grounding damage calculations. A statistical binormal model was suggested to describe the bottom shape, which yielded better goodness-of-fit test results than the results obtained by the cone and polynomial models. Montes-Iturrizaga *et al.* (2016) presented a reliability analysis of mooring lines using copulas to model the statistical dependence of environmental variables. The influence of the statistical dependence between significant wave height and peak period on the reliability assessment of mooring lines is examined. The differences in the estimates of reliability using the Gaussian copula compared with the other copulas can be significantly large. The influence of the uncertainty in significant wave height and the influence of the mean and uncertainty of the breaking strength is also analysed.

4.1.6 Loads combinations

Probabilistic load combination factors of wave and whipping bending moments are investigated by Ćorak *et al.* (2015a, 2015b). The correlation analysis between wave bending moments and whipping bending moments is performed, and a practical method for calculation of the most likely load combination factor among the considered bending moments is presented. By application of the stated method, a significant influence of the random phase angles on the extreme values of the bending moments and load combination factors is confirmed. The von Karman approach with a correction for the pile-up effect is employed for a bow flare slamming load assessment. The procedure is demonstrated using the example of a 9,200 TEU container ship.

Regarding the combination of wave load and wind load, Horn *et al.* (2017) investigated a three-parameter joint probability distribution method. The combined load was a function of not only the environmental parameters, such as the significant wave height, wave peak period and mean wind speed, including their correlation, but also the wave directional offset compared with the mean wind heading (the wind-wave misalignment), as the wind-wave misalignment may excite low-damped vibrational modes and cause changes in the accumulated fatigue damage in the wind turbine foundation compared with collinear wind and waves.

4.2 Uncertainties in structural modelling

4.2.1 Corrosion deterioration

Methods to simulate a random corrosion process have been developed. In the method by Kawamura *et al.* (2015), the corrosion progress from the line coating defect, as observed in the on-board exposure test of the steel plates in a real ship structure, was simulated by generating the corrosion pits on the line defect and expanding the shape of the pits based on some random parameters. Osawa *et al.* (2016b) developed a method to simulate under-film corrosion for epoxy coated steel panels within a ship's water ballast tank environment. The incubation and extension of coating failure is simulated using 2D cellular automaton, and the steel diminution is simulated by IACS CSR-H's three-phase probabilistic model. Analysis parameters are determined using the results of on-board exposure and cyclic corrosion tests. The change in the corroded surface shape is simulated for both conventional steel panels and corrosion resistant steel panels. Osawa *et al.* (2016a) developed a "spattering model" to simulate coating degradation starting from thin film thickness regions (e.g., free edges and weld beads).

Gaspar *et al.* (2015b) evaluated the influence of the aspect ratio of the plate on their ultimate compressive strength reduction due to the effect of the non-uniform corrosion patterns. They considered the random field model to represent the spatial distribution of random corrosion depths (corrosion pattern). The results indicated that the strength reduction due to the effect of the non-uniform corrosion is significant in the longitudinal structures of the ship hull girder. Rahmdel *et al.* (2015) predicted the ultimate strength reduction caused by pitting corrosion of an offshore structure at various ages. The introduced stepwise approach contemplates the nonlinearity of pitting corrosion with time by considering the experimental data. Shi *et al.* (2016) investigated the influence of pitting corrosion on the residual ultimate strength of stiffened panels by a series of nonlinear FE analysis. The results indicate that the pits will induce the buckling failure of a stiffened panel.

4.2.2 Fabrication-related imperfections

Fabrication-related imperfections are important to evaluate the uncertainty of the strength of structures. Gul and Altaf (2015) analysed the effects of fabrication-induced imperfections, non-dimensional geometric parameters and material characteristics on the ultimate strength of stiffened plates in a marine structure. Their findings revealed that imperfections have a significant effect on the ultimate buckling strength of a stiffened plate. As the plate flexural slenderness increases, the imperfection effect becomes more dominant and the post-buckling response also becomes sharply unstable. Ghanbari Ghazijahani *et al.* (2015) provided experimental data on the effect of geometrical imperfections on the buckling capacity of locally dented conical shells under axial compression. The results indicate changes in the buckling mode and the capacity for damaged thin specimens as outlined with an average total capacity reduction of 11%.

4.2.3 Impact damage

Ship residual strength in collisions or grounding scenarios can be assessed in terms of the residual strength factor, which is defined as the ratio of time-variant hull girder capacity in damaged conditions to the time-variant hull girder capacity of an intact gross scantling girder. Campanile *et al.* (2015, 2016) investigated the statistical properties of bulk carriers' residual strength. Three damage scenarios (collision scenario, 1st grounding scenario, and 2nd grounding scenario) were analysed according to the current requirements of CSR-H for bulk carriers and oil tankers, assuming as a reference case the bulk carrier section scheme proposed in the last ISSC Report. A collapse probabilistic assessment method under impact loads was proposed by Youssef *et al.* (2016) to assess the risk of ship hull collapse due to collision. A probabilistic approach is applied to establish the relationship between the exceedance probability of collision and the residual ultimate longitudinal strength index. Kim *et al.* (2015b) investi-

gated environmental consequences associated with collisions that involve a double hull oil tanker. Using probabilistic approaches, credible scenarios of ship-ship collision are selected to create a representative sample of the most possible collisions.

Reed and Earls (2015) presented a study of stochastic identification of the structural damage condition of a ship bow section under model uncertainty. A non-contact approach to identify and characterise imperfections within the submerged bow section of a representative ship hull is proposed. A fluid-structure model that predicts the spatio-temporal pressure field and a Bayesian, reversible jump Markov chain Monte Carlo approach is used to generate the imperfection parameter estimates and quantify the uncertainty in these estimates. Gerlach and Fricke (2016) presented an experimental and numerical investigation of the behaviours of ship windows subjected to quasi-static pressure loads and impact loads. A method to calculate the failure probabilities of glass panels under pressure loads is presented. Failure probabilities for the glass panels in the tests are determined and failure mechanisms are clarified.

The deformation behaviours of ship structural members under load depends on uncertainty modelling using material, geometric, and structural considerations, as captured in an appropriate reliability framework. Obisesan *et al.* (2015) presented a new stochastic framework for modelling the performance of ship structures during collisions by assessing the dependency of the deformation behaviours of ship structural members on the uncertainties from the material and geometric properties. Storheim *et al.* (2017) recommended disregarding the strain-rate hardening in simulations of relatively slow accidental actions, such as ship impacts, unless material tests are available and the rate-hardening models can be properly calibrated for the entire strain range. The conclusion is that material model properties and fracture criterion specified in the new DNV-GL RP-C208 are unnecessarily conservative. Based on the experience from the benchmark study, this study concludes that material properties that give a more generous response may have to be employed for these design purposes.

4.2.4 Ultimate strength and buckling

Recently, reliability related to the ultimate strength of a stiffened panel has been investigated by some researchers. Leheta *et al.* (2017) performed reliability analyses using Monte Carlo simulation to compute and compare the time-invariant reliability indices of stiffened panels with either conventional T-stiffeners or novel Y-stiffeners (hat + tee/angle) profiles in a double hull oil tanker's bottom and deck panels under axial compressive loads. The ultimate strength and the applied axial compressive stress formulations in the limit state functions are obtained based on the IACS CSR for Oil Tankers considering the failure modes: unstiffened plate buckling, stiffener beam-column buckling, and stiffener flexural-torsional buckling (tripping). Chen (2017) presented an assessment method for the panel reliability of a ship-shaped FPSO unit. Beam-column buckling and flexural-torsional buckling are regarded as two primary failure modes of stiffened panels. The variability of corrosion wastage and material properties are considered when modelling the panel's time-dependent ultimate strength. The uncertainty of axial compressive loads induced by hull girder bending is evaluated based on the probabilistic characteristics of the still water bending moment and the vertical wave-induced bending moment. The environmental severity factor and the effect of corrosion wastage on the panel reliability are investigated. Sensitivity measures for random variables are applied.

4.2.5 Fatigue damage

Regarding the uncertainty assessment of fatigue damage, Lim *et al.* (2017) discussed a study of the uncertainty in the accumulated fatigue damage in a top-tensioned riser due to vortex-induced vibration. Fatigue damage is estimated by the rainflow cycle counting method and an interesting approach of fatigue damage estimation based on Polynomial Chaos Expansion (PCE). PCE is used to represent the model parameters (a residual of the cylinder maximum amplitude, the natural frequency, and the current velocity) and accumulated fatigue damage

(response surface). Yeter *et al.* (2015) presented the fatigue reliability assessment, which accounts for an in-service crack growth on a welded tubular joint of an offshore wind turbine (OWT) support structure. The results of this study underpin risk-based inspection planning for OWT support structures. The uncertainties with respect to the crack growth, stress evaluation and failure assessment diagram were included in the reliability estimates.

4.3 Reliability and uncertainty analysis

Reliability analysis methods are extensively applied in rule-making processes and design procedures. In this section, recent applications and developments of reliability analysis for ships and offshore structures are reported. When we consider uncertainties in structural models and loads, the response of a structure has uncertainties that should be evaluated for rational reliability analysis and the corresponding design process of structures. Recent developments in uncertainty analysis methods by stochastic FE analyses are also reported.

4.3.1 Reliability analysis

New rule formulations and methods of reliability assessment for the ultimate strength of ships by applying Structural Reliability Analysis (SRA) have been controversial research areas in recent years. The FORM and the Monte Carlo Importance Sampling (MCIS) method are extensively applied. Benhamou *et al.* (2017) reported three rule formats: Working Stress Design (WSD), Implicit Working Stress Design (IWSD) and Load and Resistance Factor Design (LRFD). The constant Partial Safety Factor (PSF) formulation and the variable PSF formulation were discussed using these three rule formats. Hørte and Sigurdsson (2017) reported the use of SRA as a tool for code calibration with two examples: “development of the hull girder ultimate capacity criterion for tankers” and “calibration of mooring design code”. By applying SRA to wellhead fatigue analysis, the accumulated probability of fatigue failure as a function of time was presented, and possibilities and benefits of applying SRA in structural engineering were demonstrated. Chen (2016) evaluated the uncertainty of the still water bending moment based on the loading conditions from FPSO operational manuals, and a stochastic model of the extreme value of vertical wave-induced bending moment was developed in accordance with extreme value theories. A FORM coupled with a finite difference method was proposed for reliability estimates to address the complicated implicit limit state function for hull girder ultimate strength assessment. Ćorak *et al.* (2017) present a methodology for the assessment of the structural reliability of an oil tanker that was damaged in a hypothetical grounding accident in the Adriatic Sea. The extent of the damage to the ship’s hull after a grounding accident depends on several parameters, such as the ship speed, rock size, penetration depth, and longitudinal and transversal location of stranding along the hull. These parameters are assumed to be random variables described by probability density functions in this study. Based on defined statistical properties, random realisations of grounding parameters are simulated by Monte Carlo simulation. Four design equations are adopted to predict the collapse pressure of pipelines with corrosion defects. Regarding the application of SRA to offshore structures, Zhang *et al.* (2017e) described a structural reliability method to analyse the drilling operability envelope of the offshore drilling riser deployment. The uncertainties are primarily derived from wave and current loadings. The efficient structural reliability method Moment Method Based on Entropy Theories and Genetic Algorithm (MEGA) is adopted to obtain the failure probabilities. The reliability method complements the current deterministic approach for new riser design and untested ultra-deep water. Emami Azadi (2017) investigated the reliability analysis method of a three-leg North Sea jack-up platform for various types of ship impact scenarios. The findings of this study indicated that the type of bow or broadside impact and the spud-can-soil modelling may have a considerable effect on the reliability of the jack-up platform during a ship collision.

In recent studies about life assessment of ship structures, structural reliability analysis has an important role. Ibrahim (2016) presented an overview of structural life assessment with relia-

bility analysis. Despite the structural parameter uncertainties, probabilistic analysis requires the use of reliability methods for assessing fatigue life by considering the crack propagation process and assessing the first passage problem, which measures the probability of the exit time from a safe operating regime. The main results reported in the literature pertain to ship structural damage assessments from slamming loads, liquid sloshing impact loads of liquefied natural gas in ship tankers, ship grounding accidents and collision with solid bodies. Under these extreme loadings, structural reliability is the major issue in the design stage of ocean structures. Gaspar and Guedes Soares (2015) reported a system reliability analysis of a ship deck structure for buckling collapse and corrosion limit states. The generalised corrosion of the deck structure is modelled as a random process of correlated uniform thickness reductions described by a nonlinear time-dependent model. The time-variant system failure probabilities are computed using Monte Carlo simulation. The results indicate that the probability of occurrence of a local failure of the ship deck structural system increases significantly over time. The effect of the correlation length of the random process of corrosion on the system failure probability is significant. Bai *et al.* (2016) investigated a time-dependent reliability assessment method of offshore jacket platforms that considers the resistance degradation. For the resistance probability model of the jacket platform, the corrosion effect was considered for the degradation of the resistance. A proper corrosion model was examined. For the load effect probability model, the typhoon load effect, which contains wind, wave and current loads, was employed. Jensen (2015) presented a combination of Monte Carlo simulation and the FORM in fatigue damage estimation in nonlinear systems.

In recent years, some new techniques of reliability analysis have been developed. Gaspar *et al.* (2015a) presented an adaptive response surface approach in the reliability analysis of plate elements under uniaxial compression. A response surface model based on second-order polynomials is combined with the FORM to compute reliability estimates for moderate computational times. Chojaczyk *et al.* (2015) presented a review of the application of Artificial Neural Network (ANN) models in structural reliability analysis by categorising the analysis into five main topics: (1) types of ANNs, (2) ANN-based methods of failure probability computation, (3) ANN training set improvement techniques, (4) comparison of ANN-based reliability methods, and (5) reliability-based structural design and optimisation using ANNs. The findings concluded that ANN-based reliability methodologies are robust and efficient for the analysis of complex structures.

4.3.2 Uncertainty analysis by stochastic finite element method

As shown in the reviewed papers, the estimation of the uncertainty of structural response has become an important issue in recent years. Figure 1 depicts the general idea of uncertainty analysis, in which the inherent randomness (such as material properties, shape, loads, and corrosion) is treated as the input parameters defined by the probability density function of the random variables (θ_1, θ_2) and the probabilistic characterisation of the response (e.g., stress, displacement, strength) should be evaluated by the uncertainty analysis. The "Analysis Method" in the figure is generally a numerical method based on the analysis model, such as the FE method. Recently, the Stochastic Finite Element Method (SFEM) has been developed for the uncertainty analysis of structures. In this section, the recent development of uncertainty analysis by SFEM is reviewed. Stefanou (2009) detailed the development of SFEM prior to 2009. Arregui-Mena *et al.* (2016) reported the recent development and practical application of SFEM in the fields of materials science, biomechanics, and engineering. In the engineering field, the SFEM is used to estimate the reliability and performance of materials and structures, such as soils, bridge structures, components of machines or other structures, assuming that inherent uncertainty exists in the materials and the size and dimension of structures.

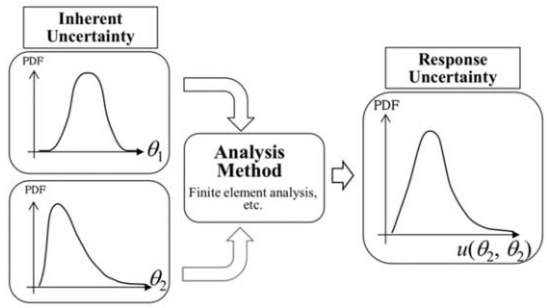

Figure 1: General concept of uncertainty analysis.

Generally, the SFEM can be categorised into two major types: the "non-intrusive method" and the "intrusive method". Representative of the "non-intrusive method", the Monte Carlo simulation method is the most prevalent technique used to evaluate response uncertainty. A large number of simulations of the "Analysis Method" should be performed using numerous different samples of the input parameters (refer to Figure 1). Thus, the required statistics of the response can be estimated from the large number of responses. Due the recent application of a non-intrusive method, Schoefs *et al.* (2016) developed a deterministic analytical formulation of the stress concentration factor from the approximation given by the Regressive eXtended Finite Element Method (RXFEM). In this paper, first, the main computational principle of XFEM is shown for the case of given geometries. Second, the stochastic response is obtained by the XFEM of N realisations of different geometries, and by a post-process, the N stochastic response solutions are used to evaluate N solutions of the stress concentration factor. Last, the approximation of the response surface of the stress concentration factor is derived using the least-squares method.

In the intrusive method, the construction of a stochastic response surface does not require multiple simulations of the "Analysis Method", as the analysis procedure is directly modified to the new analysis procedure for the stochastic analysis. The typical representative methods include the "perturbation methods" and "response surface method with spectral approach".

For the perturbation method, Xu *et al.* (2016) reported a study of the free vibration characteristics of a random functionally graded material (FGM) beam. In this paper, a perturbation method-based stochastic FE method is used to study an FGM beam considering uncertainties in elastic modulus and mass density. Wu *et al.* (2015) reported a modified computational scheme of the Stochastic Perturbation Finite Element Method (SPFEM). Although this modified SPFEM can only handle low-level uncertainties, it can provide second-order estimates of the mean and variance without differentiating the system matrices with respect to the random variables. In this paper, the modified scheme is applied to linear or nonlinear structures with correlated or uncorrelated random variables. A 1D elastic bar with uncertainty in Young's modulus and the eigenvalue problem of a plane steel frame with uncertainty in stiffness are discussed as examples of linear structures. The nonlinear truss with uncertainty in Young's modulus and non-dimensional transient heat conduction with uncertainty in thermal conductivity are reported as nonlinear examples. Da Silva and Cardoso (2017) reported the formulation for stress-based robust topology optimisation of continuum structures considering uncertainties in Young's modulus. In this paper, the first-order perturbation approach is used to quantify the uncertainties. The midpoint method is used to perform random field discretisation. The probability of failure is bounded by the one-sided Chebychev inequality and validated with the use of the Monte Carlo simulation method. The correlation length and the number of standard deviations considered in the formulation have an important role in both the obtained topology and probability of failure. Kamiński and Świta (2015) evaluated the critical pressure of the cylindrical vertical underground steel container with Gaussian uncertainty in

its cross-sectional thickness and Young's modulus using the SPFEM. The fourth-order probabilistic characteristics of the structural response are discussed, and the reliability index is calculated by the FORM for the limit-state function defined as the difference between the critical pressure and the maximum pressure.

Recently, the SFEM using the response surface methodology has been developed as the intrusive method, which may originate from the spectral approach by Ghanem and Spanos (2003). Sepahvanda (2016) reported the theory and application of the spectral Stochastic Finite Element Method (sSFEM) of the nonlinear structural dynamics with parametric uncertainty. In this paper, the uncertainty in the damping coefficient is represented by PCE, and the nonlinear stochastic FE is solved using the collocation method. Do *et al.* (2016) reported the structural analysis method with uncertainty in both the Young's modulus and the body force (self-weight) of structures by sSFEM. In this paper, the Young's modulus and body force (self-weight) of structures are modelled by Karhunen-Loeve (KL) expansion. The displacement response is represented using PCE. Chen *et al.* (2016b) reported the SFEM based on a response surface methodology considering the uncertainty in the shape of structures, in which the Hermite PCE is used to represent the uncertainty of shapes and the response surface. The uncertainty of the response of displacement, strain and stress can be effectively estimated by this method, which solves the main stiffness equation only once.

4.3.3 Other probabilistic analysis methods

Experimental uncertainty analysis is commonly utilised in hydrodynamic testing to establish the uncertainty in a result as a function of the input variables. Woodward *et al.* (2016) investigated the uncertainty analysis procedure for a ship inclining experiment. A methodology for calculating a confidence interval for the location of the centre-of-mass of a ship from an inclining experiment and for any load condition is presented. The uncertainty compared with an assumed metacentric height of 0.15 m is provided for four classes of ships.

A modelling approach that employs Bayesian belief networks to model various influencing variables in a seaport system is proposed by John *et al.* (2016) in risk assessment to improve the resilience of a seaport system. The use of Bayesian belief networks allows the influencing variables to be represented in a hierarchical structure for collaborative design and modelling of the system. Fuzzy analytical hierarchy process is utilised to evaluate the relative influence of each influencing variable.

4.4 Risk-based inspection, maintenance and repair

Ageing marine structures may experience structural deterioration, such as corrosion and fatigue, which may cause a reduction of their resistance and subsequent structural failure. Load effects on ship structures contain high levels of uncertainty and may exceed the associated design loads. Inspection and maintenance of ageing structures are needed to ensure satisfactory structural performance during their life cycles. Ordinary Classification society Rules are based on periodic (fixed interval) dry-docking and surveys. In the oil and gas industry, asset integrity management is often based on risk-based methodologies. For ships and floating offshore installations, this approach can serve as an alternative to the traditional periodical classification survey scheme. The increased attention to high-risk structural areas and components and less-intensive inspection of low-risk areas will simultaneously enhance safety and optimise inspection resources. Realising the operational efficiencies and cost savings that can be achieved, the military and defence industry and cargo shipment sector have already shown interest in this new approach (LR 2016a, LR 2016b). In general, the most significant strength deterioration mechanisms associated with ship structures are coating failure, corrosion and fatigue. Using risk-based approaches, the benefit of better coating standards and better structural details can be exploited. Risk-based approaches will also help optimise inspection regimes and prioritise inspection.

Dong and Frangopol (2015) investigated a probabilistic methodology for optimum inspection and maintenance planning of ship structures to mitigate risk of corrosion and fatigue. For the risk assessment, structural reliability analysis associated with ultimate flexural failure of the hull's mid-ship section was considered with evaluation of the consequences (i.e., direct costs) associated with structural failure. Frangopol and Soliman (2016) proposed a probabilistic optimisation approach, in which uncertainties in the damage assessment associated with corrosion and fatigue were considered. A multi-objective optimisation problem that accounts for structural deterioration scenarios and various uncertainties is formulated for the optimum inspection and repair planning of ship structures. Soliman *et al.* (2016) proposed a probabilistic framework for optimising the inspection, monitoring, and maintenance activities during the service life of fatigue critical structures. A probabilistic fatigue crack growth is considered to evaluate time-based performance and probability of failure. Doshi *et al.* (2017) demonstrated reliability-based inspection planning of structural details using a fracture mechanics-based fatigue evaluation for a VLCC. In this study, life is obtained using the Paris equation, and Bayesian methods are utilised for updating the reliability of the structural detail. Then, the reliability of various cases, such as no detection of cracks, and detection of cracks with and without repair, is evaluated at mid-ship locations of the VLCC. This paper demonstrates that reliability-based inspections are a feasible technique for integrity management of ship structural details. Hifi and Barltrop (2015) presented a methodology for calibrating the prediction models of structural defects and degradations. The methodology involves combining data from experience and prediction models to correct structural reliability models, which helps to produce better inspection and maintenance strategies and improve the durability of new and existing ships. Temple and Collette (2015) presented an optimisation framework (Pareto front) to estimate both production costs and maintenance costs for a naval vessel's internal structure and develop trade-spaces between these two objectives to obtain a design that balances both costs. A nominal naval destroyer-type vessel mid-ship section is used as a case study.

Seo *et al.* (2015) considered a risk assessment and inspection planning procedure for corroded subsea pipelines. In the proposed method, the probability of failure is estimated for corrosion damage (pit depth) using a time-variant model derived from measured data in the subsea industry. For the evaluation of the consequence of failure, the burst pressure is considered. These methods can be used to offer a standardised procedure of design and inspection/maintenance planning of pipeline systems.

Decò and Frangopol (2015) developed a method of real-time optimal short-range routing of ships based on a risk assessment with reliability analysis and structural health monitoring (SHM) information. The SHM data are integrated into a risk assessment of ship hulls by Bayesian updating, in which a novel closed-form solution for short-term statistics based on Rayleigh prior distribution is developed. Optimal short-range routing of ships is accomplished by solving two- and three-objective optimisation problems and is illustrated on a joint high-speed sealift.

Sørensen (2017) described reliability analysis of wind turbines with a special focus on structural components. The target reliability level for wind turbine structural components is considered, and reliability-based calibration of partial safety factors for the extreme state and fatigue limit state is presented. A reliability- and risk-based approach, in which a life-cycle approach that considers the total expected costs during the entire lifetime of a structure, is employed.

4.5 Concluding remarks

In this chapter, recent developments in uncertainty assessment and reliability analysis associated with quasi-static response are reported. In relation to load modelling, many studies of the uncertainties of various loads, such as wave loads, wind loads, ice loads, impact loads and

load combinations, are performed. An uncertainty evaluation of loading with wave-induced elastic vibration, such as uncertainty caused by slamming, is an important research topic. Uncertainty modelling of structural response and uncertainty of age-related deterioration of structures by corrosion and fatigue are important research subjects. Uncertainty evaluation of the residual strength of damaged ships, such as ships during collisions, is an important research subject in recent years.

Many papers related to structural reliability analysis are reviewed in this chapter. Reliability analysis methods have become a practical and very powerful tool for decision-making in ship design, design code calibration for ships and offshore structures, and maintenance planning during ship operation. Recent development of the stochastic FE method for the evaluation of response uncertainty is also reported. The probabilistic and uncertainty evaluation concepts continue to be important research topics for the rational design of ships and offshore structures.

5. DEVELOPMENT OF RULES AND SOFTWARE SYSTEMS

This chapter contains a description of the latest developments in rules and software systems. Section 5.1 contains a review of the development of international rules and regulations, and Section 5.2 discusses the development of structural design software systems. The review is not exhaustive; only selected class rules and software are reviewed. The selection is based on the competence available in the committee.

5.1 Development of international rules and regulations

5.1.1 IMO Goal-Based Standards

The IMO Goal-Based Standards (GBS) for ships were introduced by IMO in 2002. These standards are broad, over-arching safety and environmental standards that are based on high-level goals and associated functional requirements. These standards currently apply to oil tankers and bulk carriers (IMO 2010). The new SOLAS regulation II-1/3-10 renders the GBS applicable to ships with lengths greater than 150 m and ships for which a building contract was placed on or after July 1, 2016. The 12 IACS Classification societies have submitted rules for oil tankers and bulk carriers to IMO for GBS verification. These rules consist of the IACS CSR and specific member requirements. In May 2016, the IMO's Maritime Safety Committee (MSC) accepted that these rules have been aligned to the goals and functional requirements set by the organisation.

5.1.2 New DNV GL rules

Following the merger of DNV and GL in 2013, the new DNV GL rules for Classification of Ships (DNV GL 2016a) entered into force in January 2016. The new hull structure rules are based on more advanced methods for the prediction of loads and responses, with a clear link to direct analysis. The rules provide an increased safety level and accommodates challenges related to the development of novel and unusual designs.

One of the most significant advances in the new rules is the introduction of Equivalent Design Waves (EDWs) to calculate environmental loads; refer to Heggelund *et al.* (2016). This concept has been previously employed by GL in direct calculations and by CSR (oil tankers and bulk carriers) and has been developed to be applicable for more slender ship types. The EDWs enable a more accurate representation of the load components (e.g., hull girder bending, hull girder torsion, sea pressure and tank pressure) and the phase between them. Consequently, a more precise stress description is obtained, which provide a better basis to optimise the structure. Although the loads in the CSR-H are only applicable to bulk carriers and oil tankers (which have similar characteristics), DNV GL has constructed new EDWs that are applicable for all ship types and sizes via numerous direct wave load and regression analyses.

To verify that the new methodology is consistent with operational experience, extensive consequence assessments of existing designs have been performed.

Buckling is the most important failure mode. Several direct calculation methods can be employed according to the new DNV GL rules: Closed Form Methods (CFM) represented by equations, semi-analytical methods (PULS) or nonlinear FE analysis for single panels and hull girder ultimate strength evaluation. A new class guideline—"CG-0128 Buckling" (DNV GL 2016b)—describes these methods. In the new rules, elastic buckling is allowed. The hull girder ultimate capacity shall be assessed by prescriptive methods, as described in CG-0128.

The fatigue assessment is based on the EDW method. The loads are given for the probability of exceedance 10^{-2} as these loads yield the greatest contribution to fatigue damage. Whipping and springing are recognised as contributing to and increasing the loads for all ships. The class notation whipping-induced vibration supports both advanced numerical analyses and simplified methods based on empirical factors. With the empirical factors, the wave bending moment for ultimate strength and fatigue is expected to increase by 10 to 20% depending on ship size.

5.1.3 Lloyd's Register rule development

Since 2014, the following key changes have been made to the Lloyd's Register (LR) Rules and Regulations for the Classification of Ships (LR 2014):

- Class notations have been amended in relation to the development of the LR ShipRight Structural Design Assessment (SDA), Fatigue Design Assessment (FDA) and Whipping Design Assessment (WDA) procedures from July 2014.
- Direct calculation requirements for container ships have been amended, including changes to permissible stresses from 2015.

Since 2014, the following key changes have been made to the Lloyd's Register Rules and Regulations for the Classification of Naval Ships (LR 2017a):

- Amendments to the requirements for rudder design from January 2015.
- Amendments to Local Design Load calculations from January 2015.
- Sections related to design requirements for rudders from January 2016 have been replaced.
- Anchoring and windlass requirements have been updated from January 2016.

During the reporting period, the following SDA procedures have been published by Lloyd's Register:

- Guidance notes for ShipRight SDA buckling assessment. August 2017.
- Fatigue design assessment: application and notations. June 2017.
- Procedure for semi-submersibles. July 2016.
- SDA procedure for the primary structure of passenger ships. April 2017.

Lloyd's Register continues to develop their goal-based submarine rules, with the current focus of bringing the classification process to submarine design, without publishing specific rules and regulations for the design of submarines.

5.1.4 Materials and extra high strength steels

During the reporting period, an increasing acceptance of the use of extra-high-strength steels was observed. In 2016, Bureau Veritas updated their rules; thus, high-strength grades are mentioned as regular types of steel. IACS UR W31 provides requirements for the use of steel plates with a minimum yield strength 460 MPa (IACS 2015d). This material can be applied to longitudinal structural members in the upper deck region of container carriers (such as hatch side coaming, hatch coaming top and the attached longitudinals). This material can be applied as brittle crack arrest steel required by UR S33 (IACS 2015b). The new DNV GL rules con-

tain requirements for extra-high-strength steels and brittle crack arrest steels. Eight strength levels with a specified minimum yield strength from 420 MPa to 960 MPa are defined. The IACS UR S33 describes the requirements for use of extremely thick steel plates (50-100 mm). A brittle crack arrest design is adopted.

5.1.5 Rules and standards for strength analysis of container ships

In 2015, the IACS Committee on Large Container Ship Safety (CLCSS) issued a report that concludes that the MOL Comfort break-up possibly occurred as the sea loads exceeded the hull girder ultimate strength at the time of the casualty.

In 2015, the IACS General Policy Group approved the new UR S11A "Longitudinal Strength Standard of Containerships" (IACS 2015a). The standard contains a completely revised set of requirements using the principles of IACS CSR. Consequently, the following key elements are considered in the new requirements:

- Net scantling approach, including definitions of corrosion additions.
- New formulations for wave-induced vertical bending moment and shear force based on nonlinear load computations for more than 120 ships.
- Yield check based on stress checks for normal and shear stresses compared with the permissible section modulus and plate thickness.
- Buckling check and hull girder ultimate strength check that follows the CSR approach.
- Hull girder strength assessment considers the effect of whipping (per individual classification society procedure).

The research on the MOL Comfort accident prompted the development of IACS UR S34, which addresses the functional requirements for FE analyses of container ships (IACS 2015c). Global (full ship) and cargo hold analyses are described. The loads are based on the North Atlantic wave environment. The load components and loading conditions to be considered are described. For the global strength, hull girder bending and torsion are analysed.

Whipping and springing are highly relevant for ultra-large container ships. The Lloyd's Register 2014 rules include mandatory requirements for the assessment of whipping and springing on the global hull girder loads (LR 2014). ABS (2017) published new guidance for a springing assessment. DNV GL updated the methods for the assessment of whipping and springing in their new rules; refer to DNV GL (2016c) Section 5.1.2. DNV GL has also developed a method for calculation of slamming and whipping, which accounts for all sea states that a vessel may encounter. This method includes not only extreme sea states at slow sailing speeds but also extreme sea states in moderate seas, when strong slamming impacts can be induced due to high ship speeds. By statistically evaluating AIS data in combination with weather hindcast data, DNV GL confirmed that severe storms are typically avoided by shipmasters via re-routing. These statistical observations, combined with the enhanced use of hull monitoring systems, enable more realistic assumptions about the environmental and operational conditions experienced by a vessel during its service life.

5.1.6 Arctic/Ice

The IMO Polar Code (IMO 2015) entered into force in January 2017. The safety part of the code includes design and requirements related to operation in polar regions, including ice. The requirements for the use of steels in cold temperatures have been extended.

5.1.7 Other updates of class rules

Many IACS members and flag states have developed separate sets of rules to address a sophisticated manner with operations related to wind farms and wind energy. Examples are Bureau Veritas' "Guidance note for certification of offshore access systems" (BV 2016) and "Rule note for classification of offshore handling system" (BV 2014). These new rules are

moving towards an offshore approach, in which several types of cases are defined (operational, accidental).

Rules for marine/maritime autonomous vessels have not changed during this period. However, this topic is relevant, and the committee will likely establish new rules for these vessel types during the next period. A review of these rules by the next committee is recommended.

5.2 Development of structural design software systems

5.2.1 Class rule-related software

The trend in hull structure rules is towards more advanced methods for the prediction of loads and structural response. In 2015, the ISSC Technical Committee IV.2 Design Methods (refer to Collette *et al.* 2015) mentioned an increased use of 3D FE analyses, dynamic loading approaches and spectral fatigue analyses. As discussed in the previous sections, this development is incorporated in new class rules. Extensive computational capabilities are required. This recent development has generated updates of existing tools and the development of new tools for structural design based on class rules. The use of simplified methods for load application (such as the methods described in Section 7.1) will be less frequent in the future, whereas methods such as equivalent design waves (EDWs) will become more prevalent.

DNV GL

Both the Poseidon package and Nauticus Hull package have been updated to support the new DNV GL rules for both prescriptive analysis and FE analysis. The updates include better modelling capabilities and automation of calculation tasks, as well as improved result processing and reporting functionalities. The tools for exchanging models with yard design and FE systems have been developed. The toolbox for prescriptive calculations includes rule calculator functionality with an enhanced overview of rule compliance and support for design iterations. The modelling and rule check capability is enhanced with a module for importing 2D drawings. This module contains a rule calculator to enable calculations of plates and stiffeners to be directly provided from the drawing.

The FE analysis module includes improved functionality for the import of FE models from other FE systems (Patran/Nastran, ANSYS) and early design tools (NAPA Steel, AVEVA Marine), as well as the import of hull forms. Hull girder load adjustment is integrated into the module. Screening of the FE model is included to identify critical areas. The module contains improved efficiency for generating local fine mesh FE models of critical details. A new tool for very fine mesh fatigue analysis is integrated into GeniE, and automatic yield, buckling and fatigue check according to the new rules are also included.

Lloyd's Register and ABS

"Common Structural Rules Software LLC" is a joint venture company formed by Lloyd's Register and ABS to provide a suite of software tools for CSR. The new software comprises prescriptive analyses and FE analyses and enables the assessment of entire vessel structures according to the IACS CSR-H for bulk carriers and oil tankers. The software consists of two applications: the CSR Prescriptive Analysis (PA) application, which is used to assess hull girder ultimate strength and hull local scantling, and the CSR FE analysis tool, which uses an FE analysis for strength and fatigue assessment.

ClassNK

ClassNK has released similar software: Primeship-HULL (CSR). The data link with NAPA Steel has been updated to include all structural members in the fore and the aft of bulk carriers and oil tankers. This update facilitates the exchange of an entire ship model from NAPA Steel.

Lloyd's Register

The Lloyd's Register (LR) of Shipping RulesCalc software, updated in 2014, is available for rule compliance purposes against the LR Rules and Regulations for the Classification of Ships (LR 2014). Links to 3rd party design software, such as NAPA and Tribon, as well as LR's own ShipRight SDA software, are provided.

Updated in 2017, the LR ShipRight design assessment tool is available to undertake structural and fatigue assessment that provides "end-to-end" assessment of a structure against Lloyd's Register's "direct calculation procedures", including structural design assessment (SDA) and fatigue design assessment (FDA). The software is designed for the assessment of ships and offshore units, specifically FPSOs, FLNGs, container ships, membrane tank LNG ships and ore carriers. Interface capability with Nastran/Patran is also provided.

Bureau Veritas

In 2016, Bureau Veritas (BV) entered into a strategic partnership with Dassault Systèmes to deliver product life cycle management solutions to ships and offshore platforms. BV is using Dassault's 3D-Experience platform for design reviews. This platform interfaces with BV's calculation tools to reduce the approval time for new ship designs, which reduces the modelling time from weeks to days if the 3D CAD model is available. BV also acquired HydrOcean in 2015 to gain CFD capabilities. BV is also using the 3D-Experience platform to automatically generate FE models of ships, which are assessed using its VeriStar Hull software.

5.2.2 Automatic mesh generation

Automatic generation of global models in an early stage design can be turned around quickly using programs such as Maestro or other tools. However, when more detailed local assessments and detailed verification of the accuracy is needed, the time to develop these models substantially increases. Creating a detailed global FE model of a complex marine structure is typically a very time-consuming task. Therefore, the first FE analysis is typically performed rather late in the design process and serves as a validation of the design. To save time, this analysis is typically performed as few times as possible.

The marine industry has already suggested the significant potential to reduce the modelling time if the FE models can be directly created from 3D CAD models. This potential would enable detailed analyses to be performed early in the design process and reduce the risk of major design modifications in subsequent stages. This approach would also be helpful as a part of an (automatic) optimisation process; refer to Figure 2.

Figure 2: Approaches for the creation of models for FE analysis (Holmberg and Hunter 2011).

The idea of using a single tool for the entire process, starting with the creation of a 3D model at early design stages, has been profusely required in naval shipbuilding. This tool should be capable of generating an adequate and valid calculation mesh (i.e., FE mesh) for submittal to an FE solver based on geometry, scantlings and material properties from the 3D CAD model. The tool should be part of an integrated system that encompasses all stages in the design process (refer to Figure 3).

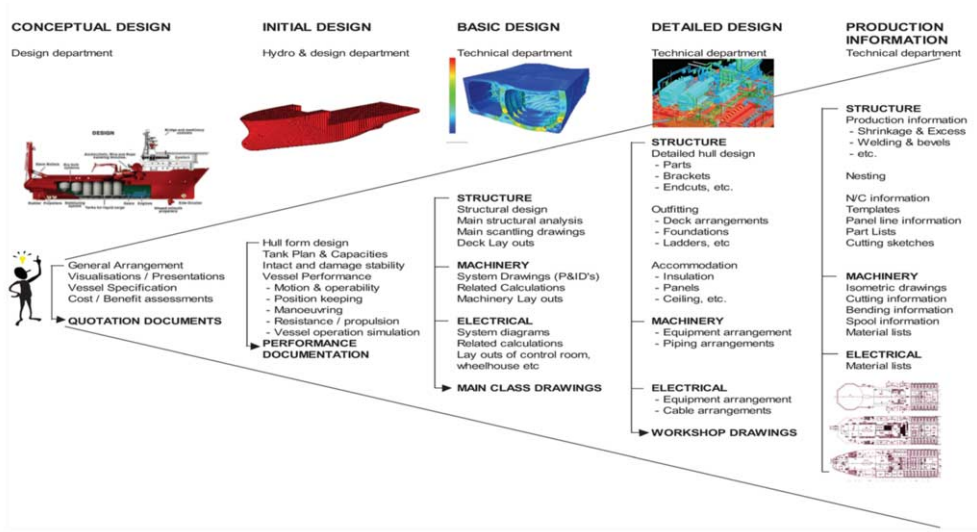

Figure 3: Design stages in the ship design process (Pérez 2015).

Many FE tools include standard formats for direct import of 3D CAD models. Due to the complexity of marine structures, these tools tend to fail. A significant amount of time is frequently used to mitigate the errors produced by the automatic mesh generation process (e.g., eliminating bad nodes, elements, and connections) which are preventing a successful analysis. Another challenge is that a marine structure contains an enormous number of structural details that must be idealised in a proper manner in the model. Therefore, an automatic mesh generator must be guided to ensure that the mesh is based on best-practice modelling techniques. To compensate for this finding, tools especially made for complex marine structures have been constructed.

Many FE tools include standard formats for direct import of 3D CAD models. Due to the complexity of marine structures, these tools tend to fail. A significant amount of time is frequently used to mitigate the errors produced by the automatic mesh generation process (e.g., eliminating bad nodes, elements, and connections) which are preventing a successful analysis. Another challenge is that a marine structure contains an enormous number of structural details that must be idealised in a proper manner in the model. Therefore, an automatic mesh generator must be guided to ensure that the mesh is based on best-practice modelling techniques. To compensate for this finding, tools especially made for complex marine structures have been constructed.

The current development of class rule-related software includes improved functionality for import/generation of FE models from early design tools. Note the following recent studies and attempts in this area:

- NAPA Designer/NAPA Steel includes a new CAD-style 3D modelling tool—NAPA Designer. This tool claims to streamline the shipbuilder's working process with automatically created classification drawings and global FE models from NAPA Steel. The software has direct interfaces to several Classification society software and claims to significantly reduce the modelling time.
- The AVEVA Marine software has the capability of enabling direct export to ANSYS FE software in the form of the ANSYS Parametric Design Language (APDL).
- Zeitz *et al.* (2014) presented a structural optimisation of a container vessel mid-ship section realised by coupling the GL structural design tool POSEIDON with the

CAESES/FRIENDSHIP-Framework as an example of rational structural design in the early design stage.

- Pérez (2015) proposed to use a single tool for the entire design process starting with the creation of a 3D CAD model in the early design stages. The main challenges of this approach are related to the integration at all stages and disciplines into a single CAD tool.
- Acin and Kostson (2015) presented some of the relevant modelling tools available in Strand7 and discussed how routine and repetitive tasks can be automated and customised using the Application Programming Interface (API).
- Son *et al.* (2016) developed interfaces between design software to enhance productiveness in modelling, even in the environment of CSR-H.
- Andrić *et al.* (2016) presented the development of the structural design support system OCTOPUS-CSR for concept and preliminary design phases. This system can contribute to reduced production cost and increased profit and durability of a bulk carrier.

In contrast to the integration of different tools, Stilhammer *et al.* (2015) claim to cover the entire structural design process within the environment HyperWorks. However, a substantial amount of detail, especially with respect to the implementation of loads and evaluation criteria, has to be developed and added before this tool can be efficiently applied in daily practice.

An important aspect of these tools is the creation of an FE mesh on a set of complex surfaces. The ISSC Technical Committee IV.2 Design Methods (refer to Collette *et al.* 2015) commented on continued dissatisfaction with the industry standard NURBS for modelling hull surfaces. This discontent is attributed to complications that range from handling complex geometry to mathematical limitations in the NURBS formulations that hinder automatic data processing. To improve the efficiency of integrated design tools, the algorithms for creating an FE mesh on complex surfaces have been investigated.

Lin *et al.* (2015) described enhanced algorithms for data transfer from 2D AutoCAD drawings to 3D FE models. This study comprised feature recognition rules and algorithms for automatic mesh generation. Wang *et al.* (2015a) explored algorithms for intersections between ship hull surfaces and its frames. Different methods and algorithms were combined to provide higher mesh quality and close approximation to an actual ship hull structure. Petrolo and Carrera (2016) presented a novel structural modelling strategy that claimed to be promising in a CAD/FE method coupling scenario.

5.3 Concluding remarks

The development towards the use of direct calculation methods in ship design continues and is reflected in both the rules and the calculation tools from the Classification societies, including an increased use of 3D FE analyses, dynamic loading approaches and spectral fatigue analyses. A thorough review was performed for the new DNV GL Rules and the latest development of LR Rules based on available competence in the committee. The rules demonstrated progress towards more advanced methods for both wave load and response calculations. After the MOL Comfort accident, new methods for the assessment of whipping and springing have been published by several Classification societies, e.g., ABS, DNV GL and LR. The development of rules for marine/maritime autonomous vessels has not occurred during the reporting period. New rules for these vessel types will likely emerge during the next period. A review of these rules is recommended for the next committee.

Despite efforts to develop structural design software systems, a tool that is widespread in use and significantly reduces the time required to establish the required FE models (from weeks to days) is needed. The efforts mentioned in this study are based on the assumption that a 3D CAD model is available at the time the FE model is needed. This assumption may not be consistent with the work process required by the yard/designer, especially if FE analyses are to be used as a design tool rather than a design verification tool. As noted by Pérez (2015), the chal-

lenge is to integrate all stages and disciplines into a single tool. Although this challenge exists, smaller improvements (such as the use of APIs in Strand7 or NAPA Steel macros) are more efficient and can significantly reduce modelling time (from months to weeks).

6. OFFSHORE AND OTHER SPECIFIC MARINE STRUCTURES

The environmental loads on offshore structures are more specific than the environmental loads for a ship travelling worldwide and depend on the structural type and operation site. Thus, the extent of the dependency on the classification rules in terms of the design load calculations for offshore structures is substantially smaller than that for the design load calculations for a conventional ship. Instead, direct analysis methods based on sophisticated theories and procedures have been developed to reflect the unique characteristics of each structure. This approach differs from the approach for ships, and the review of the trend is helpful to achieve an in-depth understanding of the design load procedures provided by the class rules.

Within the reporting period, research efforts on the prediction of extreme design loads have been continuously driven towards improvements in the analysis accuracy via nonlinear time-domain analysis, sophisticated soil-structure interaction, and coupled hydrodynamics analysis. Fatigue strength in offshore structures is more critical to scantling design than ships, and considerable research has addressed the nonlinearity of environmental loads to overcome the limitation of spectral analysis. Probabilistic and reliability methods are adopted to reasonably treat various uncertain factors, especially factors embedded in soil properties, fire and explosion simulation, and crack propagation. Special purposed marine structures, such as RoRo vessels, car carriers and livestock carriers, warrant investigation of the strength assessment procedure, which has been established considering its particular structural characteristic. The structural aspects of livestock carriers are briefly introduced.

6.1 Fixed offshore structures

6.1.1 Uncertainty, reliability for soil property and wave loads

The reliability of fixed offshore structures and systems depends on many factors, such as the reliability of soil. The types of mechanical damage caused by seabed and soil, which is commonly observed on some members of offshore platforms, include denting, out-of-straightness, corrosion and fatigue cracks. The structural behaviour of an offshore structure or system shall be evaluated by modelling the structure, seabed and relevant artificial supports and performing static and dynamic analyses.

The definitions of the characteristic soil properties in numerical codes require analysis by a geotechnical engineer in defining the design soil profile, i.e., they are qualitative and descriptive. Nadim (2015) presented an overview of the uncertainty and variability of mechanical soil properties in offshore site investigation, and proposed some ideas for utilising the reliability tools in an optimal manner. First, the paper addressed how to extract the maximum amount of information from geotechnical site investigation; second, the paper discussed how to establish characteristic or representative soil properties for design while considering the uncertainties caused by the natural variability of soil properties.

In a marine environment, a series of soil layers deposited beneath the foundations has particular importance in the response of seabed and seabed-structure systems considering the constant effect of incoming cyclic waves. The response variations are presented in terms of pore water pressure and shear stress distributions within the layers. Ülker (2014) modelled a dynamic response of saturated and layered soils under harmonic waves using the FE method and verified the results by corresponding analytical solutions. In addition, a 3D integrated numerical model—FSSI-CAS 3D—for fluid-structure-seabed-interaction was developed by Ye *et al.* (2013). The data exchange is implemented at the interface between the fluid domain and the seabed/marine structures domain adopting the coupling algorithm. The developed 3D numerical model is validated by an analytical solution and a laboratory wave flume test.

6.1.2 Load, extreme response due to nonlinearity of Morison's force

Since the 1950s, numerous studies have focused on the approximation and simplification of dynamic analysis to obtain extreme quasi-static responses of fixed offshore structures. One of these studies explores how to efficiently treat nonlinear terms of Morison's equation in strength and fatigue strength assessments. Reza *et al.* (2017) investigated response spectra of fixed offshore structures impacted by extreme waves based on the higher-order components of the nonlinear drag force. A steel jacket platform is simplified as a mass attached to a light cantilever cylinder; their corresponding deformation response spectra are estimated by utilising a generalised single degree of freedom system. The effect of the higher-order components of the drag force is compared to the linearised state for different sea surface levels. When the fundamental period of the offshore structure is approximately one-third of the main period of wave loading, the linearised drag term is not capable of achieving a reliable deformation response spectrum. Abu Husain *et al.* (2016) provide a method for predicting the extreme response for fixed offshore structures by the Monte Carlo time simulation technique. The method predicted the probability distribution of the extreme values of response during operation with the consideration of safety and efficiency. Considering the nonlinearity of the drag component of Morison's wave loading, the probabilistic analysis of the response is investigated with the effect of the sampling variability.

One of the methods employed in the derivation of the drag and inertia coefficients in Morison's equation is the conventional method of moments. However, the coefficients obtained from this method show considerable scatter due to the large sampling variability. Mohd Zaki *et al.* (2016) compared the sampling variability of the drag and inertia coefficients from the conventional method of moments with the sampling variability derived from two alternative forms of the method, i.e., method of linear moments and method of low-order moments. Simulated data have been applied to compare the efficiency of the three methods of moments.

6.1.3 Fatigue

In the fatigue assessment of jacket platforms, the small-scale leg diameter, which is often the drag-dominated and wave-induced force in these structures, can be addressed using either a linear form or a nonlinear form of the spectral Morison equation. However, incorporating a nonlinear form of the Morison equation to acquire the spectral density of the wave force, which is an important step in fatigue estimation, is complicated. Ding and Pang (2016) presented fatigue assessments that contain a nonlinear effect for a fixed offshore structure. The linear and nonlinear form of wave-induced force spectral densities are calculated in the frequency domain, and the fatigue life of the jacket platform is assessed in the time domain.

The results obtained from a computationally excessive full-scale time-domain analysis of an offshore jacket structure quantifies the errors from the assumptions and simplifications made in a spectral fatigue analysis. These findings also indicate that the simplifications involved cause not only well-known inaccuracy but also a lower fatigue resistance. Mohammadi *et al.* (2016) indicated the main causes of the inaccuracies of the spectral fatigue analysis and quantified these causes. In addition, the paper verified the efficiency of an approximation method developed in a previous study that drastically reduces the computational burden. Häfele *et al.* (2017) conducted interesting research on reducing the number of load cases for fatigue analysis on jacket structures. They performed a fatigue study with 2,048 design load cases and incrementally reduced the number of design load cases. The level of uncertainty in fatigue damage evaluation and the efficient selection of design load cases were addressed to reduce the computational effort for sophisticated jacket design procedures.

6.2 Floating offshore structures

6.2.1 Uncertainty and reliability analyses

Chatzi *et al.* (2016) provided an overview of 12 papers that address the subjects "uncertainty and reliability" in various fields. They discussed modelling, discretisation, and boundary conditions, as well as tools and methods. An increase in functional requirements for explosion protection and international design standards for offshore topside structures is observed. These standards require assessment of the structural robustness. Probabilistic models are necessary for deriving explosion properties, installation properties and environmental uncertainties. Czujko and Paik (2015) suggested reliability-based methods for accidental limit states to assess the robustness. The blast wall reliability requires two models: the first model is a probabilistic model for the explosion loads, and the second model is a deterministic nonlinear model of the blast walls. If both models are combined in a Monte Carlo simulation, then the exceedance curves can be derived from the results. The results of this new method show that the safety margins of blast wall structures are very small and indicate the need for new procedures for the assessment of safety against explosions.

6.2.2 Loads: nonlinear hydrodynamic loads and coupled loads

The significant variation of responses for floating offshore structures are wave, wind and current loading, especially of coupled loads and hydrodynamic loads. Recent studies have discussed the response of a mooring system and the effect on FPSO structures. Loukogeorgaki *et al.* (2015) presented a 3D experimental investigation of performance for a pontoon-type floating structure compared with the numerical simulation results. This study focused on the reaction of the structure under perpendicular and oblique regular waves, checked the tensions of a mooring system under pretension conditions, and attempted to determine the new equilibrium position for a mooring system under the effect from wave and current loading with three different incident wave angles. Sen (2015) analysed the motion response of a moored floating structure with large amplitudes and steep incident wave fields in a 3D numerical wave tank by a coupled time-domain solution scheme. The findings concluded that the motions of floating structures need to consider the nonlinearities not only in the hydrodynamics and hydrostatics but also in the modelling of the line stiffness. Roy *et al.* (2017) introduced nonlinear simulations to investigate the interaction between mooring lines and spar structures of an offshore spar platform. In this coupled time-domain analysis, the dynamic combination of drag, inertia, and bending coefficients of mooring systems were considered.

The large deformation under waves should be considered for computing the body motion of Very Large Floating Structures (VLFS); hydroelasticity theory has been developed to study the response of VLFS. To increase the computational efficiency, a multi-segment beam model is proposed by Sun *et al.* (2015a) to study a VLFS, which is a multi-module connected by hinge connectors. The results concluded that rigid body motion is dominant under long waves but elastic deformation dominates under short waves. The hydroelastic response is sensitive to the wave heading but the largest elastic deformation always occurred when the projection of the length of the VLFS on the wave heading direction is close to the wave length. Similarly, Zhang *et al.* (2015) utilised the multi-module models for calculating the dynamic characteristics of a floating airport.

The springing effect becomes another main issue not only for large-scale commercial ships but also for offshore structures. Kim and Kim (2015) provided a simple method for predicting the extreme loads for the tension force on a tension-leg platform considering the springing effect. The research presented a statistical observation of springing, including the second-order wave loads from sum-frequency wave forces.

6.2.3 Fatigue and fracture: coupled loads, safety margin

Repeated loads caused by waves, winds, and currents cause fatigue damage to offshore structures. Offshore structures include many members with complex geometries, such as stiffened plates and tubular joints under various loads. Therefore, substantial efforts have been made to propose a fatigue analysis procedure that is suitable for a structural member. Gam *et al.* (2017) proposed a fatigue analysis procedure for a vertical caisson on an FPSO unit subjected to a nonlinear wave loading. In the case of a sea water caisson, local stress due to the nonlinear Morison force and global stress due to hull girder loads simultaneously act. When performing fatigue analysis, the nonlinearity of the drag term in the Morison equation should be considered. The proposed method linearises the Morison force by introducing the linearisation coefficients and considers both loads in the frequency domain. Park *et al.* (2017) developed a procedure of stress analysis of the structural details near the rolling chock using the time-domain modal analysis technique, in which both the contact behaviour and friction behaviour can be accurately simulated. To perform the time-domain analysis focused on the contact and friction, the interaction between the hull and the tank was modelled via Coulomb friction.

The fatigue damage in the spectral method can be calculated from the standard deviation and the up-crossing rate of the stress amplitude spectrum. Cho *et al.* (2016b) introduced two practical approaches that can be applied when statistical data of the local loading are not available. In the first approach, the maximum stress range is assumed to always occur during the total cycles. Then, the local fatigue damage is very conservatively estimated, and the total fatigue damage is obtained by summation of the global and local fatigue damages. In the second approach, the local fatigue damage is estimated based on the assumption of the Weibull fitted local loading. The use of the cube root summation is proposed between the global fatigue damage and the local fatigue damage. Han *et al.* (2016) proposed two formulae to combine fatigue damage for offshore structures subjected to low-frequency and high-frequency Gaussian components. Extensive numerical simulations on bimodal spectra are performed to verify the accuracy of the two formulae; the results calculated by the two new formulae are satisfactory.

Fatigue assessment in the time domain is regarded as the most accurate method but is less adopted in practice as it is time-consuming. To improve the efficiency of the time-domain method, an innovative block partition and equivalence method of the wave scatter diagram is developed by Song *et al.* (2016b). After the wave scatter diagram is partitioned into several blocks, the equivalent wave height, wave period and occurrence probability of the representative sea states are determined based on a modified energy equivalent principle. The equivalent wave period of the representative sea state is calculated via the spectral moment formula. Combined with the determined wave period, the equivalent significant wave height can be determined by reversing the wave spectrum integral formula, in which the equivalent wave energy of a divided block of the wave scatter diagram is modified by introducing a factor to compensate for the effects of low- and high-amplitude cycles of fatigue damage.

A hybrid frequency-time domain method, which can be considered to be a hybrid of the spectral method and the time-domain analysis method, is proposed by Du *et al.* (2015). In the newly developed method, the spectral density function of structural stress is obtained in the frequency domain and then converted into a stress time history using an improved signal conversion approach. With this methodology, the fatigue damage of structures can be easily assessed with the rainflow counting method and the Palmgren-Miner rule. The newly developed damage assessment method can also avoid the complicated coupled dynamic analysis in the time-domain method, which significantly reduces the computation time.

For an FPSO unit converted from large oil tankers, predicting and extending their service life is critical. Yu *et al.* (2017) investigated the fatigue damage calculation procedure for an FPSO unit. The remaining fatigue life of the FPSO unit was evaluated by the method of spectral

analysis to determine the fatigue damage of the oil tanker during the operation period and the FPSO working period. Zhang *et al.* (2017a) highlighted the difficulties in evaluating the remaining fatigue life of offshore structures. The fatigue health monitoring system, which records the stress data of hot spots, was discussed in the paper. The location of monitoring was initially determined according to guidelines for the fatigue strength of a ship structure.

6.3 Other specific marine structures

6.3.1 RoRo vessels and car carriers

The vertical bending moments induced by abnormal waves on a bulk carrier and RoRo vessels are explored by Vásquez *et al.* (2016). The study focused on the influence of the hull geometry on the vertical bending moment in extreme sea conditions. The experimental data were used as benchmarks to validate the predictions by a partially nonlinear time-domain seakeeping numerical model. Clauss and Klein (2016) performed an experimental study to determine the vertical bending moment due to freak waves on three different types of ships, including a RoRo vessel. They revealed that critical loads and motions depend on combinations of wave height, wave group sequences, crest steepness, encountering speed and a ship's target position. The influence of the bow geometry was investigated in terms of block coefficient, bow flare angle and freeboard height. Stipčević *et al.* (2015) presented a feasibility study using lightweight, cost-effective sandwich panels in the upper decks of a car carrier. Sandwich panels are intended to carry vehicle loads and are supported with hull girder grillage. The study was performed in collaboration with a shipyard, and BV rules were considered.

6.3.2 Livestock carriers

Livestock carriers are ships that exclusively specialise in the transportation of large numbers of live animals (e.g., sheep, cattle). Two types of livestock carriers exist from a general/structural point of view:

- *Closed livestock carriers*, in which the majority all of animal pens are located within the closed holds and internal decks of a ship. From a structural point of view, closed type livestock carriers are similar to pure car carriers, car-truck carriers or similar closed box ship types, and their structural response is well documented and known.
- *Open livestock carriers*, in which the majority of animal pens are installed on superstructure open decks. This arrangement provides continuous natural ventilation of the pen areas while minimising the reliance on the supplementary mechanical ventilation system. These open-type livestock carriers can generate very complex structural responses, which are relatively poorly documented in the literature due to the small number of vessels.

The open livestock carrier can be classified as a ship with a strong hull-superstructure interaction due to an extensive superstructure that is characterised with large side shell openings and the absence of transverse/longitudinal bulkheads in the superstructure part (refer to Figure 4). The height of the superstructure is approximately equal to the height of the lower part of the hull, and its influence on the longitudinal strength of the ship is very important. The most suitable and accepted method for the final checking of the structural adequacy of ships with large superstructures is the 3D FE coarse mesh model of a complete ship (ISSC 1997). A direct strength calculation guideline for livestock carrier ships does not exist; thus, an existing guideline for a similar type of ships, such as RoRo or passenger ships, can be utilised (e.g., LR 2012, LR 2017b). The most important aspects and main challenges in the rational structural design of a large open-type livestock carrier for all structural design processes (concept, preliminary and detail) have been reported by Andrić *et al.* (2011, 2017a).

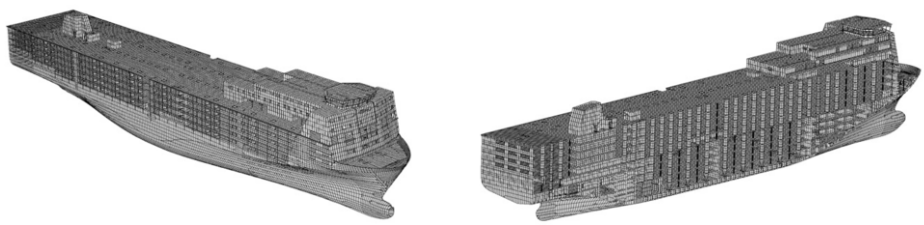

Figure 4: Full ship FE model of a livestock carrier (Andrić *et al.* 2017a).

A livestock carrier with a maximum length of 200 m that is constructed of mild steel is usually sufficient to satisfy the longitudinal strength requirements, and higher tensile steel is used to solve areas with stress concentration problems. Livestock carriers are loaded with relatively low deck loadings compared with multi-deck cargo ships (RoRo, car carriers) and are similar to cruise/passenger ships. Deck plating typically ranges between 5 to 8 mm and is covered with a special 2 to 3 mm lining for maintenance reasons, which reduce the need for corrosion addition. Some characteristics of livestock carriers are relatively fine hull lines and continuous distribution of lightweight loads, which implies that the ship is always in a hogging condition in still water, such as cruise ships. The combination of rule hogging waves and maximum still water bending moments produces maximal longitudinal and shear stresses, whereas the combination of rule sagging waves and minimum hogging still water bending moments can cause potential buckling problems in superstructure decks. The effective superstructure design is very important due to a regulation of weights and the vertical position of gravity due to stability requirements. Superstructure deck effectiveness according to the well-known Caldwell formulae (Caldwell 1957) can be expected to fall between 60 and 75% (Andrić *et al.* 2017). Large ventilation steel tubes and engine casings as large box-type structures have a significant influence on the primary stress distribution, and the higher bending stiffness of these structural parts cause an increase in the superstructure effectiveness. The transverse strength has been primarily carried by transverse bulkheads connected to large web frames. This type of ship has several watertight transverse bulkheads from double bottom to freeboard deck to satisfy the stability requirements in the damage condition. Several highly stressed areas can be identified on all examined transverse bulkheads, primarily in connection with ventilation tubes, partial casing bulkheads and strong web frames. Large ventilation tubes are other important load-carrying structural parts that can absorb part of a racking moment.

6.4 Concluding remarks

Research on offshore structures has been continuously driven towards the consideration of the load nonlinearity in the prediction of extreme loads and the fatigue analysis. The former has been addressed by the time-domain analysis for critical sea states in a wave scatter diagram; thus, the effort has been concentrated on the development of sophisticated hydrodynamic codes. Research on the latter has focused on obtaining an efficient and simplified method as performing an FE analysis for all sea states in a wave scatter diagram is not feasible. However, the fatigue analysis in time-domain analysis is gaining popularity due to the requirement of the estimation of the remaining fatigue life in life extension projects and structural health monitoring systems.

7. BENCHMARK STUDIES

The committee has performed two benchmark studies during the reporting period. The first study is an investigation of the discretisation of wave loads and its impact on the longitudinal structural behaviour in direct calculations using global ship models. The topic was selected due to the increased use of direct calculation procedures during the early stages in ship design, in particular concept and initial design, when the rules software cannot be employed due to the large amount of input data and detailed information that are required. In the design stage,

time is one of the main drivers; therefore, linear static analysis is common practice and considerable simplification in modelling is needed to maintain time efforts within the required targets. The objective of the study is to highlight the importance of identifying the lower limit in the simplification of physical phenomena to minimise mistakes in direct calculation analyses, design and procedures for verification of ship structures.

The second study is an analysis of FSI models performed on a stiffened plate with two different software. The objective is to evaluate the maximum impact pressure and maximum permanent deflection and calculate an equivalent uniform pressure for different rising velocities. The results are compared with the results of quasi-static models proposed by the Classification society.

7.1 Ship structural response from different wave load schematisation

This study investigates the longitudinal structural response of two ship structures using various wave load discretisation methods for wave load modelling. The study only focused on the structural behaviour due to vertical bending moment, and therefore, horizontal bending and torsion moments were neglected. The analysis was performed using linear static FE analysis on global ship models. Rules from the Classification society Lloyd's Register were selected as the reference for the calculation and evaluation of wave loads; however, the use of similar rules of another Classification society can achieve similar results. The following rules are employed in the study:

- Lloyd's Register Structural Design Assessment for Primary Structure of Passenger Ships (LR 2004), which is hereafter referred to as LR-SDA.
- Lloyd's Register Rules (LR 2014), which is hereafter referred to as LR-Rules.

Four wave load schemes referred to as load cases were compared for two ships with different mid-ship section structural geometries. Global displacements and stress responses were analysed and compared in two typical transverse sections to identify the differences between the load cases and the structures' responses. The study aims to provide guidance for designers, engineers, and analysts and highlight that different methods for representing the same wave load in an FE model can, in some cases, cause incorrect structural responses.

7.1.1 Description of the ship structures, models, loads and loading conditions

Two simplified ship structures were selected for the analysis, and FE global models were developed. The transverse sections of the ships are described in Figure 5, in which the main dimensions and scantlings are shown. The first model, which is shown in Figure 6a, has a typical transverse cross-section of a cargo ship box girder with a single bottom, single skin side shell, one strength deck and a transverse primary structure. The second model, which is shown in Figure 6b, has a typical structure for a passenger ship, a more complex topology than the topology of the cargo ship, a double bottom, a single skin side shell with openings, and a multiple deck superstructure with external bulkhead fitted with openings and one internal longitudinal bulkhead. The primary structure supporting the decks and double bottom consists of transverses/floors and girders, and pillar lines are fitted every two web frames according to the girders.

The ship data, loads and analysis results are presented with respect to the right-hand coordinate system defined in Figure 7:

- The origin is located at the intersection between the longitudinal plane of symmetry of the ship, the aft end of the ship's length (L) and the baseline.
- The x-axis is the longitudinal axis, positive forwards.
- The y-axis is the transverse axis, positive towards port.
- The z-axis is the vertical axis, positive upwards.

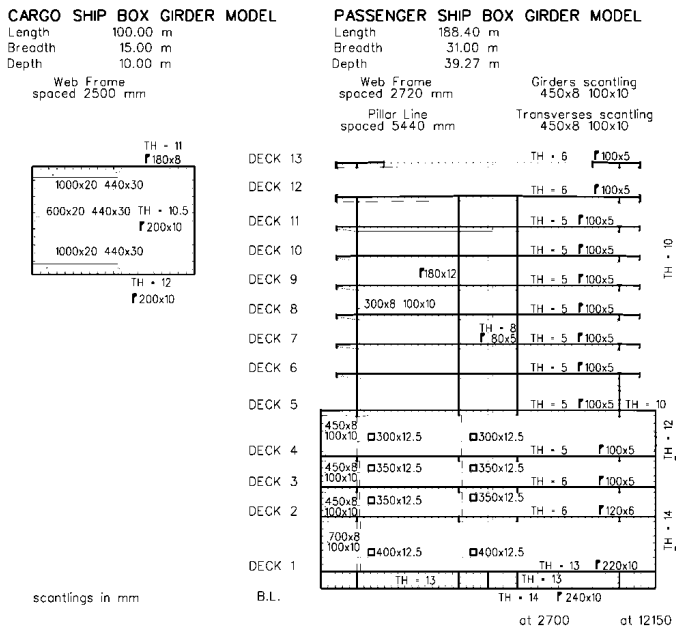

Figure 5: Cargo ship and passenger ship box girder: main dimensions and scantlings.

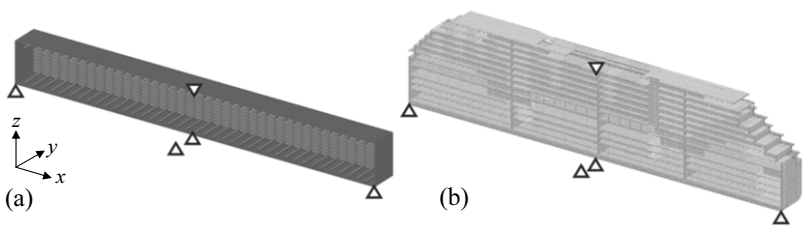

Figure 6: (a) Cargo ship box girder and (b) passenger ship box girder FE models with boundary conditions (only half-breadth model presented).

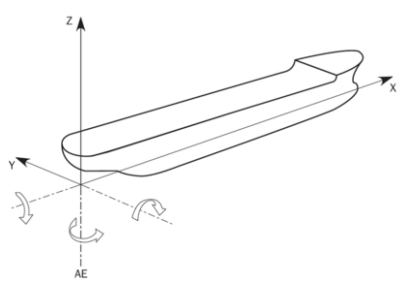

Figure 7: Reference coordinate system.

Two full-breadth box girder FE models of the two ships were developed with a coarse mesh size to represent the correct behaviour versus the longitudinal loads. Due to the different dimensions of the ships, the element size for the cargo ship model was approximately 150 mm, whereas the element size in the passenger ship model was approximately 1,400 mm. All primary structural elements were modelled with four-node 2D shell elements, whereas secondary elements such as stiffeners were represented by two-node 1D beam elements. The FE analyses were performed with the FE software MSC Patran as pre- and post-processor and MSC

Nastran as the solver. All presented stress results have been calculated in the elements' centroid and the mid-plane of the element thickness.

To prevent rigid body motions, as suggested in the LR-SDA, Pt. A, Ch. 1, Sec. 5.1, a set of six constraints was applied to both FE models (refer to the markers in Figure 6):

- $\delta_x = 0$: has been imposed to a point on the bottom, in the intersection between the transverse mid-ship section and the bottom.
- $\delta_y = 0$: has been imposed to a point on the bottom and the deck, in the intersection between the transverse mid-ship section and the longitudinal centre plane.
- $\delta_z = 0$: has been imposed to a point on the bottom, at the intersection between the stern and the bow transverse section with the longitudinal centre plane.

To assess the longitudinal strength of the ship FE models, the hogging design wave formulation for passenger ships, extracted from LR-Rules, Pt. 4, Ch. 2, Sec. 2, was selected for both of the ships. The longitudinal distribution of the vertical shear force and the vertical bending moment were calculated for the two ships. This distribution of loads represents an envelope of wave loading conditions. Thus, for the purpose of approximating these loads to a single loading condition, the formulation presented in LR-SDA, Pt. A, Ch. 1, Sec. 4.6 was applied; refer to Figure 8.

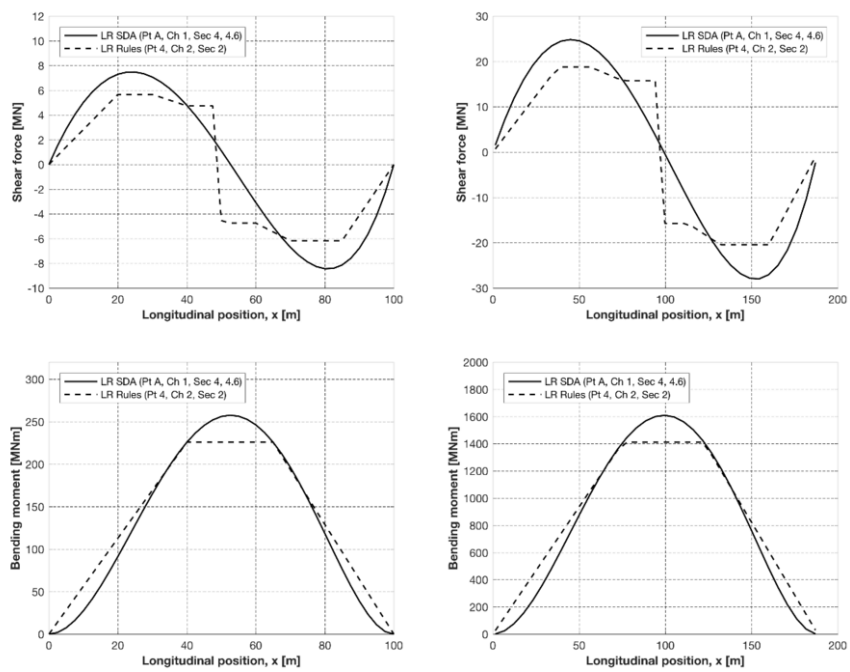

Figure 8: Shear force and bending moment longitudinal distributions for the cargo ship (left) and the passenger ship (right) box girders.

These approximate loads, which comprise a set of balanced loads, were applied to the FE models as nodal forces. To study the difference in the longitudinal strength response due to the load discretisation, four schemes referred to as load cases to apply these loading conditions were proposed, each with a different representation of nodal forces on the transverse sections. Figure 9 illustrates the four load cases for the cargo ship FE model:

- Load case (a): forces applied on the nodes at the centreline of all bottom transverses.
- Load case (b): forces applied on the side nodes of all bottom transverses.

- Load case (c): forces applied on all nodes of all bottom transverses.
- Load case (d): forces applied on all bottom nodes.

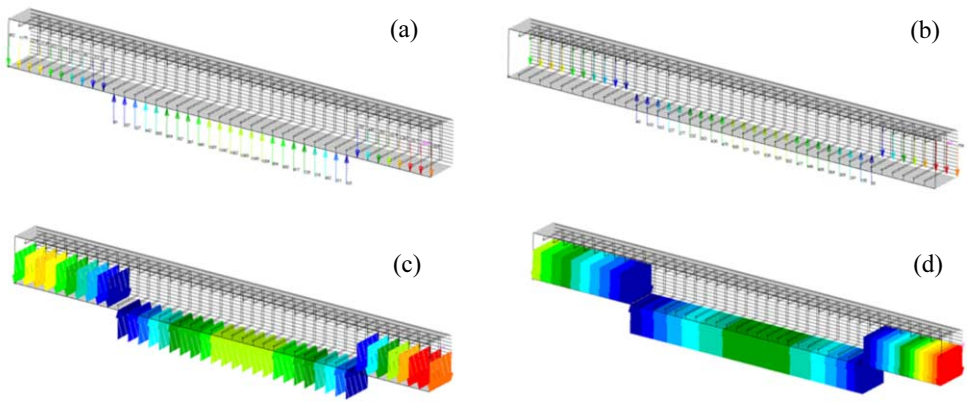

Figure 9: Example of distribution of nodal forces applied to the ship models, illustrated here for the cargo ship box girder FE model; (a) to (d) refer to the load cases.

7.1.2 Results

The first comparison of results was made on the deflection of the hull girder in two points, as shown in Figure 10. The two points were selected with the aim of monitoring the bending of the bottom structures due to the different applied local loads:

- Point 1: located at the intersection between the bottom, the transverse section at half-length and the longitudinal centre plane.
- Point 2: located at the intersection between the bottom, the transverse section at half-length and the side shell plane.

The stress responses of the models were compared in two reference sections, as shown in Figure 10, for the most significant stress tensor components:

- Section 1: located at $0.5\times L$, where σ_{xx} is presented at the bottom and the side shell.
- Section 2: located near $0.75\times L$, where τ_{xz} and σ_{zz} are presented at the side shell and the internal longitudinal bulkhead.

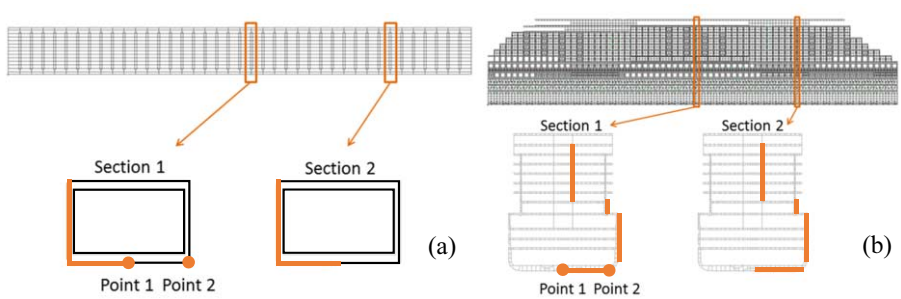

Figure 10: Location of the reference points and the sections for the (a) cargo ship and (b) the passenger ship.

The vertical displacements for the four load cases (a) to (d) are presented in Table 1. The results for the cargo ship in Point 2 show that the variation in the global vertical displacement due to the different load cases is approximately 1%, which can be considered negligible on

the global bending response. The load cases in Point 1 are slightly larger than the load cases in Point 2 but remain very low. The corresponding stress responses are presented in Figure 11. The responses confirm that no substantial differences in responses are observed between Point 1 and Point 2, with the exception of σ_{xx} at the bottom, where the secondary bending due to local loads has a larger influence. The global behaviour and responses of this simple but typical cargo ship box girder model is not very sensitive to the discretisation of the applied wave loads.

Table 1: Displacements in the *z*-direction.

	Cargo ship box girder, *z* [mm]		Passenger ship box girder, *z* [mm]	
Load case	Point 1	Point 2	Point 1	Point 2
(a)	132.1	108.2	110.6	103.3
(b)	105.4	107.7	98.8	102.8
(c)	119.9	106.9	104.4	102.3
(d)	119.1	106.3	104.8	102.1

For the passenger ship, the vertical displacements in Point 2, which are representative of global bending, reveal a small spread of approximately 1%. The difference in the values in Point 1 highlights the local bending on transverse structures, as shown in Table 1. The results for the longitudinal stress in Section 1 are presented in Figure 12. The results show a nonlinear distribution for the side shell and the internal bulkhead, which is typical for this type of transverse section. This distribution is caused by the presence of two longitudinal load-carrying structures connected by a deck. In this case, the stress values indicate a considerable difference in magnitude among the four load cases—approximately 5 to 10%. This difference is evident in the different slopes in the linear stress distribution on the side shell and the superstructure bulkhead.

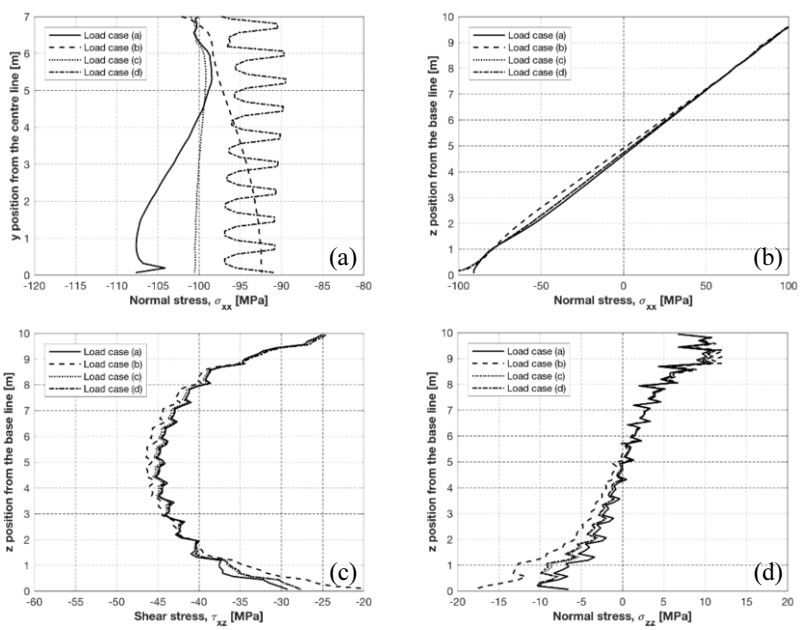

Figure 11: Cargo ship box girder model: stress components for Section 1 (a: bottom; b: shell) and Section 2 (c, d: shell).

If the passenger ship hull girder is considered as two connected beams—a beam that represents the hull and a beam that represents the superstructure—the two beams share the total load with a different percentage for each of the four load cases. This effect is visible in the shear stress in Section 2 in Figure 12. The stress values exhibit a spread of approximately 15% among the different load cases. Table 2 presents the calculated ratio of the section shear force performed by the hull and the superstructure girder. For this type of ship, the stress response and the load carrying ratio between two different longitudinal structural members depend on the method used in the wave load modelling by load (nodal force) discretisation.

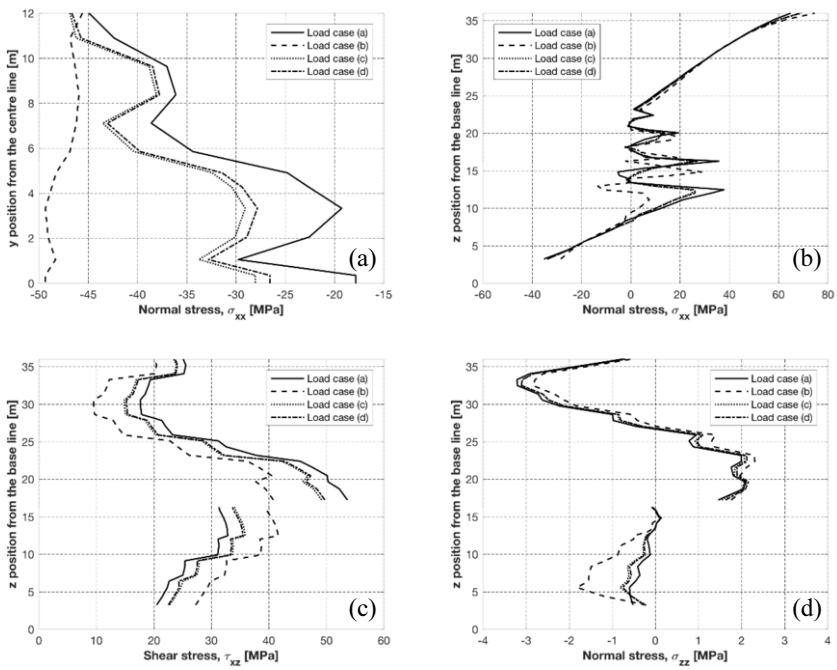

Figure 12: Passenger ship box girder model: stress components for Section 1 (a: bottom; b: shell and bulkhead) and Section 2 (c, d: shell and bulkhead).

Table 2: Shear load ratio between the hull and the superstructure girders.

Load case	Superstructure girder	Hull girder
(a)	0.45	0.55
(b)	0.32	0.68
(c)	0.40	0.60
(d)	0.41	0.59

7.1.3 Concluding remarks

In recent years, the use of the direct calculation method in the early stage of design of ships has become common practice. Due to short timelines, this phase of the structural design requires the use of quasi-static analysis and extensive simplification in modelling. The current benchmark study indicates the relevance of a proper representation of the loads in the direct analysis approach, especially in the study of the longitudinal behaviours of ship structures. Simplification in the schematisation of loads on a 3D model can cause an incorrect analysis of

ship structure global response and incorrect structural design, scantling or verification of structural elements.

The study reveals that general conclusions about the lower limit in the simplification of loads cannot be obtained, as it depends on the ship structure topology; thus, a dedicated study of ship types is needed to achieve this goal. The results of the study indicate that the force must be transversely distributed on the bottom shell nodes in the schematisation of wave loads. Regardless of the ship type, the lower limit in the simplification of loads is represented by load case (c). The force representation similar to load cases (a) and (b) will produce an incorrect structural response from the analysis for some ship types. To design novel or unusual ship structures and establish new direct calculation procedures and rules, designers and engineers must pay attention to the load discretisation method. In direct calculations, the closer the representation is to the physics of the phenomenon, the more realistic the behaviour of the ship FE model and more suitable the analysis.

7.2 FSI analysis of a stiffened plate subjected to slamming loads

Most slamming-related studies address the wedge impact and its water pile-up. In offshore structures, wave-induced slamming loads occur on flat structures, such as the upper deck box of semi-submersible drilling rigs or the topside platform of spar structures. Because the deadrise angle is zero, the effect of air trapped between the water and the flat structure should be considered. The effect from the FSI becomes more pronounced, and determining the slamming pressure acting on the structure becomes more complicated. The objective of this study is to compare two FSI analyses of a stiffened plate, in which two different commercial software packages have been employed: LS-Dyna and Star-CCM+/Abaqus multi-physics co-simulation (hereafter referred to as Star-CCM+/Abaqus). Both software packages are recognised software used for FSI simulation purposes in various fields.

The results of the two analyses are compared with respect to the maximum impact pressure and maximum permanent deflection. Equivalent uniform pressures that produce the same permanent deflections are presented. The results are also compared with the analytical models proposed by a Classification society for the calculation of the slamming pressure; this calculation is a function of the rising velocity. Generally, this velocity can be calculated from an air-gap analysis, which is part of the hydrodynamic analysis. The slamming pressure can be employed for strength assessment of the structure subjected to the slamming load.

7.2.1 Model description

The simulation model and its dimensions and boundary conditions are shown in Figure 13. Figure 13a shows the *x*-symmetric and the *y*-symmetric boundary conditions on the stiffened plate applied along the central vertical line and the central horizontal line, respectively. The upper and right sides are restrained in the *z*-direction. Thus, the model represents 1/4 of a stiffened plate surrounded by vertical deep girders or bulkheads.

The slamming load was represented by a moving block of water, as shown in Figure 13b. The dimensions of the slamming load in the *x*-*y* plane (length and width) were slightly smaller than the dimensions in the same plane of the stiffened plate because, if the water block would have had the same or larger dimensions as the stiffened plate, the water would pass through the stiffener and the plate would experience the impact force from the water and an additional drag force. The difference in sizes between the water block and the stiffened panel structure was adjusted to a sufficiently small size to have a negligible influence on the structural response of the stiffened plate. Other model details were defined as follows:

- Plate thickness: 15 mm.
- Stiffener size (web height×thickness + flange width×thickness): 300×10+120×10 mm.
- Stiffener spacing: 800 mm.
- Young's modulus: 210 GPa.

- Poisson's ratio: 0.3.
- Density of steel: 7,830 kg/m^3.
- Yield stress: 235 MPa.
- Material model: elastic-perfectly plastic (the strain-rate hardening effect is neglected).
- Vertical velocity of water at impact: 4, 5, 6, and 7 m/s.

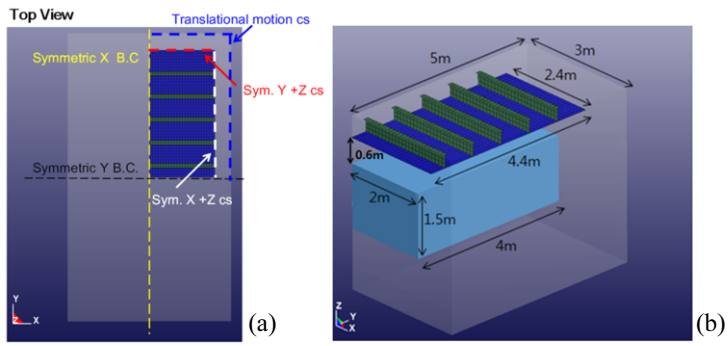

Figure 13: (a) Top view of the 1/4 model with boundary conditions (BC: boundary condition, sym: symmetric, and cs: constrained), and (b) 1/4 of the full simulation model.

7.2.2 Description of the simulation software packages and analyses

Two of the members in the committee had access to the FSI software packages LS-Dyna and Star-CCM+/Abaqus. This section gives a brief description of the specific modelling details required for each of the FSI analyses; see Table 3 for a brief summary.

Table 3: Brief summary of the two FSI software packages and models.

	LS-Dyna	Star-CCM+/Abaqus
Fluid model	Incompressible and inviscid	Compressible and viscous
Interaction effect	Penalty coupling method and multi-material method	Multi-physics co-simulation
Solver	Explicit	Implicit: both fluid and structure solvers
Model definition	One integrated model	Two separate models
Time step	1.0×10^{-5} s	1.0×10^{-3} s, 2nd order for fluid
Structural mesh size	100×100 mm	100×100 mm
Fluid mesh size close to structure	100×100×100 mm	100×100×5 mm
Gravity effect	Included	Included

LS-Dyna (Seoul National University)

LS-Dyna is a general-purpose FE software package that is often used to simulate FSI problems based on the assumption of incompressible and inviscid fluid. A Lagrangian mesh is used for the structure, and a Eulerian mesh is used for the fluid, such as water and air. In the Augmented Lagrangian Eulerian (ALE) method, the fluid calculation starts with the Lagrangian method. The material is deformed as in the Lagrangian formulation. The relative motion between the mesh and the material is computed, and an advection step is taken wherein element-state data are transferred back to the new configuration. In each time step, calculations are performed through two stages, resulting in a longer computational time. Through the ALE interface, the fluid and the structure interact with each other. The structure deforms under hydrodynamic pressure, and the fluid pressure is affected by the structural response. A multi-

material ALE formulation enables the modelling of a free water surface by allowing both air and water to be represented in the same element.

The simulation model in this study consists of four parts: air, water, plate and the stiffeners. The water and air components are modelled using 3D solid elements, and the stiffened plate is modelled using 2D shell elements, as depicted in Figures 14a and 14b. The 3D fluid elements are divided into three parts, where the mesh size in the z-direction of the 3D solid elements is different in each part while remaining uniform in the x- and y-directions. The fluid component close to the plate (the upper part), where the coupling between the fluid and the structure occurs, is modelled with fine high-density mesh with an element size of 100×100×100 mm. The shell element dimensions of the stiffened plate are the same as those for the fluid, i.e., 100×100×100 mm. The mesh size in the z-direction in the middle part of the fluid is doubled and is linearly increasing in the lower part, as shown in Figure 14c.

The plate and its stiffeners are modelled by shell Belytschko-Tsay formulation. The water and the air are modelled by the solid ALE multi-material formulation in LS-Dyna; see Table 4 for the properties of air and water. For water and air, a linear polynomial equation of state is used: $P = C_0 + C_1\mu + C_2\mu^2 + C_3\mu^3 + (C_4 + C_5\mu + C_6\mu^2)\times e$ where $\mu = (\rho/\rho_0) - 1$. For air, the gamma law is used by setting C_0=C_1=C_2=C_3=C_6=0, which is expressed as $P = (\gamma - 1)\times\rho\times e$, where γ is the ratio of specific heats, ρ is a defined reference air density and e is a specific internal energy. The gravitational effect is considered; however, to prevent initial deformation, it is not applied to the structure.

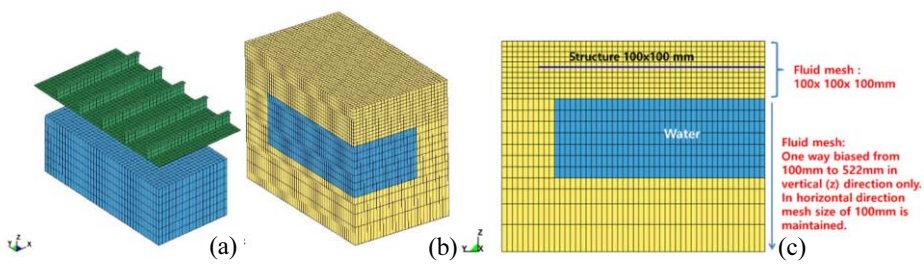

Figure 14: LS-Dyna models: (a) FE model of the stiffened plate and the water block, (b) geometry and mesh for the fluid domain, and (c) mesh configuration of the fluid domain.

Table 4: Water and air properties of EOS.

Parameter	Water	Air
ρ [kg/m³]	1,000	1.285
C_0; C_1	0.0; 2.06×10^9	0.0; 0.0
C_2; C_3	8.432×10^9; 8.014×10^9	0.0; 0.0
C_4; C_5; C_6	0.4394; 1.3937; 0.0	0.4; 0.4; 0.0
E_0; v_0	0.0; 0.0	0.0; 0.0

LS-Dyna uses a penalty coupling method that tracks the relative displacement between the fluid and the structure. Structural damping is not considered; hence, the coupling force can be considered proportional to the penetration depth and the penalty factor. The penalty factor is a multiplier of the contact stiffness between the materials in contact. A previous parametric study by Cheong *et al.* (2016) showed that the difference in calculated pressures for the penalty factors 0.01, 0.05, 0.1, 0.5 and 1.0 was minor. Thus, a penalty factor of 0.1 is considered reasonable and is used in this study. A time step of 1.0×10^{-5} s is automatically determined by the explicit solver in LS-Dyna.

Star-CCM+/Abaqus (Chalmers University of Technology)

A link between the two software packages Star-CCM+ and Abaqus is already available in the co-simulation tool. The FSI formulation in Star-CCM+/Abaqus is referred to as a multi-

physics co-simulation problem. Both air and water must be included in the fluid model, and the short time scales and high pressures included in the slamming event calls for a time-accurate analysis using compressible fluids. Viscous effects are also included to capture as much physics as possible. This forms an unsteady, compressible, two-phase and viscous problem.

The definition of the simulation model is quite similar to the model defined in LS-Dyna; however, some differences are found. The FE model for the plate and the stiffeners is shown in Figure 15a. The model is located between the upper and the lower plate surfaces in the fluid model of Figure 15b. Two volumes are created representing the main part of the domain and the plate. The 15-mm thick plate is subtracted from the main part to generate the internal boundaries of the plate, as depicted in Figure 15b. It is assumed that geometrical details of the upper (air) side of the fluid domain have a very small influence on the computed pressure on the lower (water) side. The geometry of the plate stiffeners is therefore not included in the fluid model. The mesh size in the main part of the fluid domain is 100×100×100 mm, and the shell element mesh size of the plate is taken as 100×100 mm. A local refinement (100×100×5 mm) is introduced close to the plate to resolve the fractions of water and air.

The RANS equations are solved using a k-ε turbulence model to represent the influence of viscosity. Both the upper and the lower sides of the plate in the fluid model are connected to the plate in the structural model. At each time step, the computed pressure distribution on the lower side of the plate of the fluid model is applied as a load on the structural model. The displacement distribution is then transferred to the fluid model and the deflection of the plate is updated. The volume mesh distribution is updated according to the deflection of the plate through a mesh morphing approach.

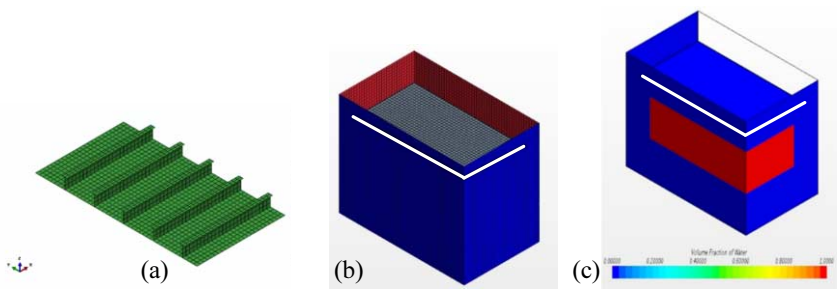

Figure 15: Model view: (a) FE model of the plate and the stiffeners, (b) geometry and mesh for the fluid domain, and (c) initial conditions of the volume fraction for water.

A second-order time stepping is used in the computations. The volume of fluid approach is used for the two-phase problem. The fraction of air and water is then computed for each finite volume. The compressibility for air is represented by the gas law in the computations. The compressibility for water is introduced via a user-defined field function of density through the Tait's equation as $\rho = \rho_0 \times ([p+B]/[p_0+B])^{1/A}$, where ρ_0 is a reference density, p is the computed total pressure, p_0 is a reference atmospheric pressure, $A = 7.15$ and $B = 3.047 \times 10^8$.

The initial conditions for the two-phase problem are introduced via user-defined field functions for the volume fractions of air and water. The volume fraction of water is shown in Figure 15c for the block of water. The effect of gravity is included, and the initial velocity is set to give the block of water the velocities 4, 5, 6 and 7 m/s when reaching the plate, taking gravity effects into account. At the inlet boundary (from below in Figure 15c) the volume fraction of air is 1.0, and the volume fraction for water is 0.0. The velocity for the incoming flow is set to a small positive value. A constant pressure condition is used at the outlet.

7.2.3 Results

The time histories from the two analyses of the total vertical force on the plate are plotted in Figure 16a, and those for the deflection at the centre of the plate are plotted in Figure 16b. The time history of total force for LS-Dyna is fluctuating, whereas that for Star-CCM+/Abaqus is smooth. The ALE method adopted by LS-Dyna uses the penalty coupling method, which uses a contact stiffness between fluid and structure. No use of damping in the coupling method results in the noisy pressure history. The method allows for a certain level of water penetration into the structure and a gap between the water and the structure. If the time history of the total vertical force for LS-Dyna is averaged over 0.01 s, it becomes more smooth and similar to that of Star-CCM+/Abaqus, as shown in Figure 16a. Even if the pressure levels of two simulations are similar, the pressure peak shapes are different. Star-CCM+/Abaqus shows two distinct peaks, whereas LS-Dyna shows two small peaks. This difference could be related to how to realise the complicated interactions among the fluid, structure and entrapped air between the two software packages. Further refinement of the fluid mesh along the vertical direction in the vicinity of the structure in Star-CCM+/Abaqus leads to more smooth and realistic interactions.

Another difference is that Star-CCM+/Abaqus shows negative pressure when the rising water rebounds from the stiffened plate, whereas LS-Dyna does not. In the case of LS-Dyna, negative pressure occurs in the vicinity of the plate centre, but the total force is positive when summed up over the plate. Moreover, the time history of deflection for LS-Dyna shows a smoother shape than that of the total vertical forces, as shown in Figure 16b, and the maximum values show a good agreement. The distribution of deflection over the plate at the moment of maximum deflection is presented in Figure 17.

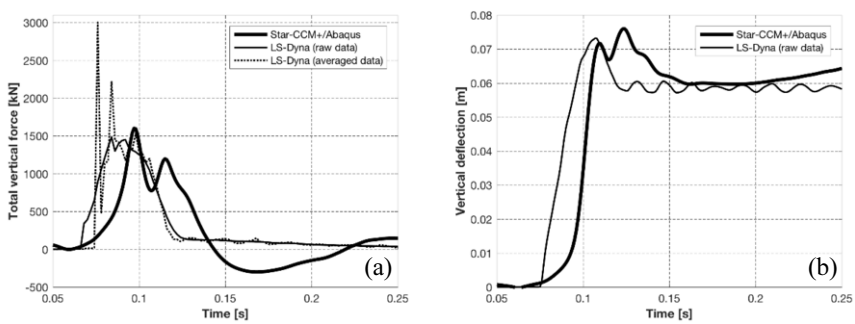

Figure 16: Results of two cases for 6 m/s of water speed: (a) time history of the total vertical force, and (b) time history of the deflection at the plate centre.

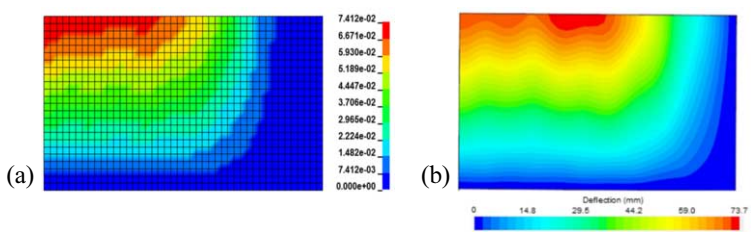

Figure 17: Distribution of deflections at the moment of maximum deflection, Δ_{max} (unit: mm): (a) LS-Dyna (Δ_{max} = 74 mm), and (b) Star-CCM+/Abaqus (Δ_{max} = 76 mm).

Table 5 summarises the maximum and permanent deflections from the FSI analyses at a node near the plate centre x = 0.1 m and y = 0.1. The results show good agreement between the LS-Dyna and Star-CCM+/Abaqus analyses.

Table 5: Comparison of maximum and permanent deflections.

	Maximum deflection, Δ_{max} [mm]		Permanent deflection, $\Delta_{residual}$ [mm]	
Velocity [m/s]	LS-Dyna	Star-CCM+/Abaqus	LS-Dyna	Star-CCM+/Abaqus
4	25	26	14	15
5	46	44	34	34
6	74	76	59	62
7	103	112	87	95

FSI analysis is quite time consuming, especially for complex structure configurations. Simplified formulations are used to be efficient in assessments in the early stages of a design, and they must also be reliable. One of the objectives of the study is to find the corresponding equivalent static and uniform pressure that results in the same permanent deformation as the FSI analysis. Table 6 presents the results from this study, listing the equivalent static slamming pressure coefficients that are comparable with those provided by DNV-RP-C205 (DNV 2010). The coefficients take into account the FSI effect, which becomes more pronounced as the deadrise angle decreases in the current case. According to DNV (2010), the space average slamming pressure can be calculated as $p_s = 0.5\rho C_P v^2$, where C_P should not be less than 2π (≈ 6.28) for flat bottom slamming with a deadrise angle of less than 4 degrees, considering air cushioning and 3D effects. As identified in Table 6, the obtained values of C_P depend on the water velocity and are much greater than 2π.

Table 6: Calculated equivalent static slamming pressure coefficients from the FSI analyses.

Velocity, v [m/s]	LS-Dyna		Star-CCM+/Abaqus	
	Pressure, p_s [kPa]	C_P	Pressure, p_s [kPa]	C_P
4	173.5	21.7	177.0	22.1
5	186.0	14.9	192.0	15.4
6	207.0	11.5	227.0	12.6
7	250.0	10.2	287.0	11.7
	Average:	14.6	Average:	15.5

7.2.4 Concluding remarks

LS-Dyna and Star-CCM+/Abaqus use different FSI techniques and different fluid models. Thus, the resultant time histories of impact pressure show some differences, i.e., LS-Dyna shows more fluctuations in the results than Star-CCM+/Abaqus. The difference in fluctuations is caused by the use of a more refined fluid mesh in the vicinity of the structure in Star-CCM+/Abaqus and the different interaction methods used among fluid, structure and the entrapped air. Nonetheless, the two software packages show good agreement in the maximum total vertical force and plate deflection for all water impact velocities. Because slamming is not accompanied with water breaking or turbulent flow at the moment of water impact, the ideal fluid model in LS-Dyna shows nearly the same results as the results of Star-CCM+/Abaqus. From the study on the equivalent static pressure, the pressure coefficient C_P is not constant over different water velocities; it tends to decrease when the velocity of water increases.

In the simulation with Star-CCM+/Abaqus, a further local grid refinement of the fluid domain around the structure was found to be necessary to resolve the volume distribution of water and air close to the surface of the plate. Although the refined fluid models require a high time resolution, it is expected to give a better prediction of the pressure peak and the effect of air cushion. The same local refinement would have a similar effect on the LS-Dyna results.

8. CONCLUSIONS AND RECOMMENDATIONS

The committee reviewed recent studies as defined by the committee mandate. The report presents a summary of current publications relevant to quasi-static analysis methods applied to ships and offshore structures. The summary consists of a general introduction to strength assessment approaches and a review of load modelling, structure modelling and response analysis, uncertainty and reliability analysis. Recent developments of rules and software systems are described. A review related to offshore and other specific marine structures is also included. Two benchmark studies—the first study investigates two ship structures and the second study explores an offshore structure—are described. The following paragraphs highlight conclusions and observations from the literature review and the benchmark studies.

Conclusions

The review of load modelling revealed that advancements in numerical simulations provide additional basic knowledge about complex events, such as sloshing, grounding, slamming, and extreme events. The research conducted during the reporting period indicates that a significant amount of research targets these areas. Collision and grounding are other areas of ongoing interest. Investigations of quasi-static approaches have been conducted to address these complex problems. The coupling of loads, in which fluid/air/structural models are being evaluated to address their impact, and the coupling of primary loads of structures, such as torsion and vertical bending, are additional areas of interest. This coupling manifests in several areas, such as the development of methodologies to evaluate the progressive collapse of structures and the development of analytical methods to understand this behaviour.

The chapter on structure modelling and response analyses highlighted the importance of structural assessment using quasi-static methods and its relevance to the modern structural design of ship and offshore structures. The committee considers the presented research to be similar to the ISSC Committee II.1 report in 2015. An area that has continued to develop during the reporting period comprises strength assessments of damaged structures. The implementation of quasi-static approaches in direct calculation software, particularly FE analyses, continues to receive significant attention from researchers. Local and global assessments focus on specific failure modes by application of a single load or multiple load combinations. FE analysis is continuing to replace experimental analysis primarily due to the increasing capability of commercially available software and hardware, which can run larger and more complex simulations than in the past, and due to the expense of undertaking physical experiments. However, the committee urges researchers to consider the use of appropriate experimental work to verify simulations. The boundaries of current understanding are always being pushed and may surpass the current verification of direct calculation tools. Therefore, verification is required to ensure that conclusions are drawn based on simulations that correctly reflect the physical world rather than an erroneous numerical phenomenon.

The topics of uncertainty and reliability analysis are important for the quasi-static response of ships and offshore structures because this type of analysis is related to uncertainties in quasi-static calculation models. Reliability analysis has become a practical and very powerful tool for decision making in ship design, design code calibration for ships and offshore structures, and maintenance planning during ship operation. The literature review discussed recent knowledge of uncertainties of various loads and structures, which affect the implementation of reasonable and practical reliability analyses. The most recent development in the use of a stochastic FE method for evaluating response uncertainty was reviewed, and it has the potential to become a powerful tool for future rational uncertainty analysis.

In the chapter on the development of rules and software systems, the development towards the use of direct calculation methods in ship design continues as reflected in the rules and calculation tools from the Classification societies, including increased use of 3D FE analyses, dynamic loading approaches and spectral fatigue analyses. The development of programs for the

fast generation of global strength models continues. However, a breakthrough development of an efficient and prevalent tool has not occurred. Small improvements, such as the use of macros, seem to be more efficient.

The literature review of offshore fixed platforms revealed many studies of the prediction of extreme quasi-static response considering the nonlinearity of Morison's force and the statistical characteristics of environmental loads. The use of reliability analysis for the uncertainty of soil properties is another unique feature of fixed platforms; some interesting studies have been presented during the reporting period. In the area of floating offshore structures, numerous efforts have been made to develop nonlinear and coupled hydrodynamic codes to predict extreme loads on not only the hull structure but also the mooring chains and risers by considering the nonlinear effects of second-order wave loads. Accidental loads, such as fire and explosion loads, which need to be determined in a probabilistic manner in the structural design of topside structures, have received considerable attention. Examples of specific marine structures that exhibit a unique structural design or arrangement specific to their functionality, e.g., livestock carrier vessels, were presented. Their strength assessment primarily depends on a direct FE analysis due to the lack of supporting classification rules.

In Chapter 7, the first benchmark study of ship structural response from different wave load schematisations included cargo ship and passenger ship box girder models. In recent years, the use of direct calculation methods in the early stage of the design of ships has become common practice. Due to short timelines, this phase of the structural design requires the use of quasi-static analysis and simplifications in modelling. The current benchmark study reveals the relevance of a proper representation of the loads in the direct analysis approach, especially in the study of the longitudinal behaviours of ship structures. Simplification in the schematisation of loads in a 3D model can cause an incorrect analysis of the global response of a ship structure and incorrect structural design, scantling design or verification of structural elements. The second benchmark study comprised an FSI analysis of a stiffened plate subjected to slamming loads. Despite differences between the simulation models and the underlying theory in the two software packages that were employed, the FSI results showed agreement. The resultant permanent deformation exhibits better agreement with actual values than the impact force, which is sensitive to the interaction mechanisms between the fluid and the structure. The software package LS-Dyna, which is developed based on the assumption of an ideal fluid, provides results similar to the CFD results. The spatially averaged slamming pressure according to DNV-RP-C205 (DNV 2010) was used to calculate the C_P value, which depends on the water velocity. The values of C_P varied among the applied software, and recommendations for future studies and model refinements were suggested for the case study of a stiffened panel structure and its loading conditions.

Recommendations

General recommendations for future research topics and specific recommendations that refer to Chapters 2 to 6 in this report are listed as follows:

- Advanced methods for mesh generation of FE models and new FE techniques.
- Improve methods to account for corrosion and fatigue in assessing structural strength.
- Uncertainties of internal loads and load effects on structural strength.
- Reliability-based lifecycle design.
- Risk-based inspection, maintenance and repair.
- Development of new rules and regulations by regulatory bodies.
- Structural aspects of specialised ships and offshore structures.

Chapter 2: Future efforts should focus on certain critical areas, such as a non-ice strengthened hulls that operate at high latitudes and the loading conditions that should be utilised to quasi-statically evaluate these vessels. Another area of interest is how the quasi-static response

methods begin to interact with other methodologies, such as structural health monitoring approaches, and special operations, in which a holistic view is being explored to provide the operator and designer with critical information while fusing data from various sources to make informed decisions. Quasi-static approaches for load modelling can be employed in algorithms to develop real-time feedback. With an increased use of numerical modelling via research efforts, numerical methods are addressing the analysis of alternatives and early-stage evaluations of ship designs, in which numerous alternatives can be optimised to achieve a higher relevance to quasi-static methods and ensure that numerical simulations provide reasonable solutions.

Chapter 3: To enable design iterations and rapidly implement a cost-effective design process in the detailed design phases, the committee recommends that researchers consider the development of design curves or equations that can be implemented to enable designers to assess the failure modes of structures under more complex loadings than current possible loadings. This assessment will ensure that structures are appropriately and efficiently designed and consider that individual load applications may be less efficient to ensure that a suitable reserve is provided between capacity and demand. As the applications of FE analysis, CFD and combined FSI approaches become more advanced, these methods can provide an understanding that is not possible or practical to achieve via experimentation, and the use of these methods to improve or develop existing formulations or provide new formulations should be considered. Detailed complex analysis is part of the design process, usually as the design detail increases. To avoid design constraints due to early decisions based on analytical methods that may not fully capture the structural arrangement or loading scenario in question, development of broader early-design tools should avoid unnecessary rework or conservative parameters in the design, which may increase key factors, such as cost and weight.

Chapter 4: The concepts of reliability and uncertainty analysis continue to be important research topics for the rational design of ships and offshore structures. Reliability analysis will continue to be applied to the practical decision-making procedure in ship design and the design code calibration procedure to enable the reliability method to become a standard. The evaluation of uncertainties that refer to wave loads considering elastic vibration and corresponding fatigue strength are important future research topics.

Chapter 5: The next committee should continue to focus on the development of new rules and regulations by regulatory bodies. The next committee should promote the advancement of "autonomous vessels" because research in this area may contribute to changes in rules and regulations, which may influence how ships are designed. A review of different methods for load application (e.g., simplified and equivalent design waves), applications in quasi-static response analysis and the associated impact on the structural design (benchmark study presented in Section 7.1) are also recommended.

Chapter 6: The impacts of nonlinear environmental loads are often determined based on short-term analysis, in which a time-domain nonlinear analysis is performed for some critical sea states selected from a wave scatter diagram using an environmental contour, i.e., H_s-T_p contour. This methodology may not be equivalent to a long-term extreme value that can occur once during the design lifetime of offshore structures. This issue has been recently identified as a potential future research topic. Regarding the fatigue of offshore and specific structures, nonlinear analysis is often required, but the computational effort is significant because a time-domain nonlinear analysis needs to be performed for all sea states in the wave scatter diagram. Although several simplified methods have been proposed, improvements are needed to facilitate the general and extensive use of these methods. Considering the practical use of a reliability analysis with many uncertain factors, its application to real projects remains unacceptable. The computational burden and lack of statistical information about many uncertain factors are the main reasons for these limitations. These issues must be improved, even if some deterioration in accuracy is inevitable.

REFERENCES

ABS. 2017. Guidance notes on springing assessment for container carriers and ore carriers. American Bureau of Shipping, Houston, TX, USA.

Abu Husain, M.K, Mohd Zaki, N.I., Johari, M.B. & Najafian, G. 2016. Extreme response prediction for fixed offshore structures by Monte Carlo time simulation technique. In Proceedings of the ASME 2016 35th International Conference on Ocean, Offshore and Arctic Engineering (OMAE2016), Busan, South Korea, 19-24 June 2016. (OMAE2016-54200).

AbuBakar, A. & Dow, R.S. 2016. The impact analysis characteristics of a ship's bow during collisions. In S.R. Rai, H.K. Shin, J. Choung & R.T. Jung (eds), Proceedings of the 7th International Conference on Collision and Grounding of Ship and Offshore Structures (ICCGS2016), Ulsan, Korea, 15-18 June 2016. Seoul: Hanrimwon Co. pp. 229-237.

Achtert, P., Brooks, I.M., Brooks, B.J., Moat, B.I., Prytherch, J., Persson, P.O.G. & Tjernström, M. 2015. Measurement of wind profiles by motion-stabilised ship-borne Doppler lidar. Atmospheric Measurement Techniques 8(11): 4993-5007.

Acin, M. & Kostson E. 2015. Tools and automation capabilities for modelling marine structures. In Proceedings of the 14th International Conference on Computer and Information Technology in the Maritime Industries (COMPIT2015), Ulrichshusen, Germany, 11-13 May 2015. pp. 428-432.

Aksu, S., Buannic, N., Hinrichsen, B., Kamsvag, F., Tanaka, Y., Tonelli, A., Vink, J.H., Ming Yang, J. & Yang, P. 2006. Technical Committee II.1 – Quasi-static response. In P.A. Frieze & R.A. Shenoi (eds), Proceedings of the 16th International Ship and Offshore Structures Congress (ISSC2006), Vol. 1, Southampton, UK, 20-25 August 2006. Dorchester: Henry Ling Ltd. pp. 175-261.

Aksu, S., Buannic, N., Chien, H.L., Daley, C., Highes, O., Kar, S., Lindemark, T., Netto, T.M., Bollero, A., Rim, C.W., Romanoff, J., Rörup, J., Tanaka, Y. & Zhuang, H. 2009. Technical Committee II.1 – Quasi-static response. In C.D. Jang & S.Y. Hong (eds), Proceedings of the 17th International Ship and Offshore Structures Congress (ISSC2009), Vol. 1, Seoul, Korea, 16-21 August 2009. Seoul: Seoul National University. pp. 211-287.

Aksu, S., Boyd, S., Cannon, S., Chirica, I., Hughes, O., Miyazaki, S., Romanoff, J., Rörup, J., Senjanovic, I. & Wan, Z. 2012. Technical Committee II.1 – Quasi-static response. In W. Fricke & R. Bronsart (eds), Proceedings of the 18th International Ship and Offshore Structures Congress (ISSC2012), Vol. 1, Rostock, Germany, 9-13 September 2012. Hamburg: Schiffbautechnische Gesellschaft. pp. 151-212.

Andrade, S.L., Gaspar, H.M. & Ehlers, S. 2017. Parametric structural analysis for a platform supply vessel at conceptual design phase - a sensitivity study via design of experiments. Ships and Offshore Structures 12(sup1): S209-S220.

Andrić, J., Grgić, M., Pirić, K. & Žanić, V. 2011. Structural assessment of innovative design of large livestock carrier. In Proceedings of the 14th International Congress of the International Maritime Association of the Mediterranean (IMAM2011), Genova, Italy, 13-16 September 2011. pp. 351-358.

Andrić, J., Prebeg, P., Pirić, K., Kitarović, S., Žanić, V., Čudina, P., Bezić, A. & Andrišić, J. 2016. FE based structural optimization according to IACS CRS-BC. In U.D. Nielsen & J.J. Jensen (eds), Proceedings of the 13th International Conference on Practical Design of Ships and Other Floating Structures (PRADS2016), Copenhagen, Denmark, 4-8 September 2016.

Andrić, J., Pirić, K., Prebeg, P., Andrišić, J. & Dmitrašinović, A. 2017a. Structural design and analysis of large "open type" livestock carrier. In S. Ehlers, J.K. Paik & Y. Bai (eds), Proceedings of the 2nd International Conference on Ships and Offshore Structures (ICSOS2017), Shenzhen, China, 11-13 September 2017. (ICSOS2017-006).

Andrić, J., Prebeg, P. & Pirić, K. 2017b. Influence of different topological variants on optimized structural scantlings of passenger ships. In C. Guedes Soares & Y. Garbatov (eds), Progress in the Analysis and Design of Marine Structures; Proceedings of the 6th International

Conference on Marine Structures (MARSTRUCT2017), Lisbon, Portugal, 8-10 May 2017. London: CRC Press. pp. 173-181.

Ao, L. & Wang, D. 2015. Ultimate strength of box girders with incline cracks. In Proceedings of the ASME 2015 34th International Conference on Ocean, Offshore and Arctic Engineering (OMAE2015), St. John's, Newfoundland, Canada, 31 May-5 June 2015. (OMAE2015-41608).

Arregui-Mena, J.D., Margetts, L. & Mummery, P.M. 2016. Practical application of the stochastic finite element method. Archives of Computational Methods in Engineering 23(1): 171-190.

Bai, Y., Yan, H.B., Cao, Y., Kim, Y., Yang, Y.Y. & Jiang, H. 2016. Time-dependent reliability assessment of offshore jacket platforms. Ships and Offshore Structures 11(6): 591-602.

Bandi, P., Detwiler, D., Schmiedeler, J.P. & Tovar, A. 2015. Design of progressively folding thin-walled tubular components using compliant mechanism synthesis. Thin-Walled Structures 95(1): 208-220.

Benhamou, A., Derbanne, Q. & de Lauzon, J. 2017. Structural reliability analysis applied on steel ships for rule partial safety factors calibration. In Proceedings of the ASME 2017 36th International Conference on Ocean, Offshore and Arctic Engineering (OMAE2017), Trondheim, Norway, 25-30 June 2017. (OMAE2017-61677).

Benson, S., Downes, J. & Dow, R.S. 2015. Overall buckling of lightweight stiffened panels using an adapted orthotropic plate method. Engineering Structures 85(1): 107-117.

Bentin, M., Zastrau, D., Schlaak, M., Freye, D., Elsner, R. & Kotzur, S. 2016. A new routing optimization tool-influence of wind and waves on fuel consumption of ships with and without wind assisted ship propulsion systems. Transportation Research Procedia 14(1): 153-162.

Bin, S., Zhiqiang, H., Jin, W. & Zhaolong, Y. 2016. An analytical method to assess the damage and predict the residual strength of a ship in a shoal grounding accident scenario. Journal of Ocean Engineering and Science 1(2): 167-179.

Burgan, B., Chen, A., Choi, J.W. & Ryu, Y. 2016. The use of coupled and uncoupled analysis techniques in the assessment of blast wall response to explosion. In Proceedings of the ASME 2016 35th International Conference on Ocean, Offshore and Arctic Engineering (OMAE2016), Busan, South Korea, 19-24 June 2016. (OMAE2016-55100).

Bužančić Primorac, B., Ćorak, M. & Parunov, J. 2015. Statistics of still water bending moment of damaged ships. In C. Guedes Soares & R.A. Shenoi (eds), Analysis and Design of Marine Structures; Proceedings of the 5th International Conference on Marine Structures (MARSTRUCT2015), Southampton, UK, 25-27 March 2015. London: CRC Press. pp. 491-497.

BV. 2014. Classification of offshore handling systems. Rule Note NR-595, August 2014. Bureau Veritas, Neuilly-sur-Seine, France.

BV. 2016. Certification of offshore access systems. Guidance Note NI-629, May 2016. Bureau Veritas, Neuilly-sur-Seine, France.

Caldwell, J.B. 1957. The effect of superstructures on the longitudinal strength of ships. Transactions of RINA 99(4): 664-681.

Calle, M.A.G. & Alves, M. 2015. A review-analysis on material failure modeling in ship collision. Ocean Engineering 106(1): 20-38.

Calle, M.A.G., Verleysen, P. & Alves, M. 2017. Benchmark study of failure criteria for ship collision modeling using purpose-designed tensile specimen geometries. Marine Structures 53(1): 68-85.

Campanile, A., Piscopo, V. & Scamardella, A. 2015. Statistical properties of bulk carrier residual strength. Ocean Engineering 106(1): 47-67.

Campanile, A., Piscopo, V. & Scamardella, A. 2016. Time-variant bulk carrier reliability analysis in pure bending intact and damage conditions. Marine Structures 46(1): 193-228.

Castegnaro, S., Gomiero, C., Battisti, C., Poli, M., Basile, M., Barucco, P., Pizzarello, U., Quaresimin, M. & Lazzaretto, A. 2017. A bio-composite racing sailboat: Materials selection, design, manufacturing and sailing. Ocean Engineering 133(1): 142-150.

Cerik, B.C. 2015. Ultimate strength of locally damaged steel stiffened cylinders under axial compression. Thin-Walled Structures 95(1): 138-151.

Chatzi, E.N., Papadimitriou, C. & Beck, J. 2016. Special issue on uncertainty quantification and propagation in structural systems. ASCE-ASME Journal of Risk and Uncertainty in Engineering Systems, Part A: Civil Engineering 2(3).

Chen, C.H., Zhu, Y.F., Yao, Y., Huang, Y. and Long, X. 2016a. An evaluation method to predict progressive collapse resistance of steel frame structures. Journal of Constructional Steel Research 122(1): 238-250.

Chen, N.Z. 2016. Hull girder reliability assessment for FPSOs. Engineering Structures 114(1): 135-147.

Chen, N.Z. 2017. Panel reliability assessment for FPSOs. Engineering Structures 130(1), pp. 41-51.

Chen, X., Kawamura, Y. & Okada, T. 2016b. Stochastic finite element method based on response surface methodology considering uncertainty in shape of structures. In U.D. Nielsen & J.J. Jensen (eds), Proceedings of the 13th International Conference on Practical Design of Ships and Other Floating Structures (PRADS2016), Copenhagen, Denmark, 4-8 September 2016.

Cheon, J.S., Jang, B.S., Yim, K.H., Lee, H.D., Koo, B.Y. & Ju, H. 2016. A study on slamming pressure on a flat stiffened plate considering fluid-structure interaction. Journal of Marine Science and Technology 21(2): 309-324.

Cho, S.R., Yoon, S.H., Park, S.H. & Song, S.U. 2016a. Collision damage and residual strength of box girder structures. In S.R. Rai, H.K. Shin, J. Choung & R.T. Jung (eds), Proceedings of the 7th International Conference on Collision and Grounding of Ship and Offshore Structures (ICCGS2016), Ulsan, Korea, 15-18 June 2016. Seoul: Hanrimwon Co. pp. 325-332.

Cho, T.M., Chun, M.S., Kim, H.J., Lee, D.Y. & Kim, B.K. 2016b. Practical review on fatigue damage estimation under combinations of global and local loadings. In Proceedings of the ASME 2016 35th International Conference on Ocean, Offshore and Arctic Engineering (OMAE2016), Busan, South Korea, 19-24 June 2016. (OMAE2016-54664).

Chojaczyk, A.A., Teixeira, A.P., Neves, L.C., Cardoso, J.B. & Guedes Soares, C. 2015. Review and application of artificial neural networks models in reliability analysis of steel structures. Structural Safety 52(Part A): 78-89.

Chu, B., Lee, S. & Chang, D. 2017. Determination of design accidental fire load for offshore installations based on quantitative risk assessment with treatment of parametric uncertainty. Journal of Loss Prevention in the Process Industries 45(1): 160-172.

Clauss, G.F. & Klein, M. 2016. Experimental investigation on the vertical bending moment in extreme sea states for different hulls. Ocean Engineering 119(1): 181-192.

Collette, M., Bronsart, R., Chen, Y., Erikstad, S.O., Georgiev, P., Giuglea, V., Jeong, H.K., Lazakis, I., Moro, L., Sekulski, Z., Sicchiero, M., Toyoda, M., Ventura, M. & Žanić, V. 2015. Technical Committee IV.2 – Design Methods. In C. Guedes Soares & Y. Garbatov (eds), Proceedings of the 19th International Ship and Offshore Structures Congress (ISSC2015), Vol. 1, Cascais, Portugal, 7-10 September 2015. London: CRC Press. pp. 459-518.

Ćorak, M., Parunov, J. & Guedes Soares, C. 2015a. Probabilistic load combination factors of wave and whipping bending moments. Journal of Ship Research 59(1): 11-30.

Ćorak, M., Parunov, J. & Guedes Soares, C. 2015b. Long-term prediction of combined wave and whipping bending moments of container ships. Ships and Offshore Structures 10(1): 4-19.

Ćorak, M., Parunov, J. & Guedes Soares, C. 2017. Structural reliability assessment of an oil tanker accidentally grounded in the Adriatic Sea. In Proceedings of the ASME 2017 36th International Conference on Ocean, Offshore and Arctic Engineering (OMAE2017), Trondheim, Norway, 25-30 June 2017. (OMAE2017-62278).

Cui, J., Wang, D. & Ma, N. 2017a. A study of container ship structures' ultimate strength under corrosion effects. Ocean Engineering 130(1): 454-470.

Cui, J., Wang, D. & Ma, N. 2017b. Elastic buckling of stiffened panels in ships under bi-axial compression. Ships and Offshore Structures 12(5): 599-609.

Czujko, J. & Paik, J.K. 2015. A new method for accidental limit states design of thin-walled structures subjected to hydrocarbon explosion loads. Ships and Offshore Structures 10(5): 460-469.

da Silva, G.A. & Cardoso, E.L. 2017. Stress-based topology optimization of continuum structures under uncertainties. Computer Methods in Applied Mechanics and Engineering 313(1): 647-672.

Darie, I. & Rörup, J. 2017. Hull girder ultimate strength of container ships in oblique sea. In C. Guedes Soares & Y. Garbatov (eds), Progress in the Analysis and Design of Marine Structures; Proceedings of the 6th International Conference on Marine Structures (MARSTRUCT2017), Lisbon, Portugal, 8-10 May 2017. London: CRC Press. pp. 225-233.

Decò, A. & Frangopol, D.M. 2015. Real-time risk of ship structures integrating structural health monitoring data: Application to multi-objective optimal ship routing. Ocean Engineering 96(1): 312-329.

Dekker, R. & Walters, C.L. 2017. A global FE-local analytical approach to modelling failure in localised buckles caused by crash. Ships and Offshore Structures 12(sup1): S1-S10.

Ding, W. & Pang, L. 2016. Structural fatigue assessment of offshore platform considering the effect of nonlinear drag force. In Proceedings of the ASME 2016 35th International Conference on Ocean, Offshore and Arctic Engineering (OMAE2016), Busan, South Korea, 19-24 June 2016. (OMAE2016-54870).

DNV. 2010. Environmental conditions and environmental loads. Recommended Practice DNV-RP-C205, October 2010. Det Norske Veritas, Høvik, Norway.

DNV. 2013. CSA - Direct analysis of ship structures. Classification Notes No.34.1, January 2013. Det Norske Veritas, Høvik, Norway.

DNV GL. 2015. Fatigue and ultimate strength assessment of container ships including whipping and springing. Class Guideline DNVGL-CG-0153, October 2015. DNV GL AS, Høvik, Norway.

DNV GL. 2016a. Rules for classification: Ships (RU-SHIPS) - https://www.dnvgl.com/rules-standards/. DNV GL AS, Høvik, Norway. [Accessed: 2017-12-01].

DNV GL. 2016b. Buckling. Class Guideline DNVGL-CG-0128, October 2015. DNV GL AS, Høvik, Norway.

DNV GL. 2016c. Container ship update - https://www.dnvgl.com/maritime/publications/. DNV GL AS, Høvik, Norway. [Accessed: 2017-12-01].

Do, D.M., Gao, W. & Song, C. 2016. Stochastic finite element analysis of structures in the presence of multiple imprecise random field parameters. Computer Methods in Applied Mechanics and Engineering 300(1): 657-688.

Dong, Y. & Frangopol, D.M. 2015. Risk-informed life-cycle optimum inspection and maintenance of ship structures considering corrosion and fatigue. Ocean Engineering 101(1): 161-171.

dos Santos Rizzo, N.A., Caire, M. & Bardanachvilli, C.A. 2015. Ultimate shear strength of FPSO stiffened panels after supply vessel collision. In Proceedings of the 25th International Ocean and Polar Engineering Conference (ISOPE2015), Kona, Big Island, Hawaii, USA, 21-26 June 2015. pp. 837-842.

Doshi, K., Roy, T. & Parihar, Y.S. 2017. Reliability based inspection planning using fracture mechanics based fatigue evaluations for ship structural details. Marine Structures 54(1): 1-22.

Dow, R.S., Hugill, R.C., Clark, J.D. & Smith, C.S. 1981. Evaluation of ultimate ship hull strength. In W. Maclean & J.B. O'Brian (eds), Proceedings of the Ship Structures Symposium '81: Extreme Loads Response, Arlington, VA, USA, 19-20 October 1982. pp. 133-148.

Du, J., Li, H., Zhang, M. & Wang, S. 2015. A novel hybrid frequency-time domain method for the fatigue damage assessment of offshore structures. Ocean Engineering 98(1): 57-65.

Ehlers, S., Guiard, M., Kubiczek, J., Höderath, A., Sander, F., Sopper, R., Charbonnier, P., Marhem, M., Darie, I., von Selle, H. & Peschmann, J. 2017. Experimental and numerical analysis of a membrane cargo containment system for liquefied natural gas. Ships and Offshore Structures 12(sup1): S257-S267.

Elhanafi, A. 2016. Prediction of regular wave loads on a fixed offshore oscillating water column-wave energy converter using CFD. Journal of Ocean Engineering and Science 1(4): 268-283.

Emami Azadi, R.M. 2017. Reliability study of a north-sea jack-up under ship impact. In Proceedings of the ASME 2017 36th International Conference on Ocean, Offshore and Arctic Engineering (OMAE2017), Trondheim, Norway, 25-30 June 2017. (OMAE2017-62501).

Estefen, S.F., Chujutalli, J.H. & Guedes Soares, C. 2016. Influence of geometric imperfections on the ultimate strength of the double bottom of a Suezmax tanker. Engineering Structures 127(1): 287-303.

Faisal, M., Noh, S.H., Kawsar, M.R.U., Youssef, S.A., Seo, J.K., Ha, Y.C. & Paik, J.K. 2017. Rapid hull collapse strength calculations of double hull oil tankers after collisions. Ships and Offshore Structures 12(5): 624-639.

Frangopol, D.M. & Soliman, M. 2016. Life-cycle of structural systems: recent achievements and future directions. Structure and Infrastructure Engineering 12(1): 1-20.

Fuglem, M., Stuckey, P. & Suwan, S. 2015. Estimating iceberg-wave companion loads using probabilistic methods. In Proceedings of the ASME 2015 34th International Conference on Ocean, Offshore and Arctic Engineering (OMAE2015), St. John's, Newfoundland, Canada, 31 May-5 June 2015. (OMAE2015-42172).

Fujikubo, M., Gaiotti, M., Grasso, N. & Rizzo, C.M. 2015. Effect of shear stresses onto the hull girder ultimate strength of a containership. In Proceedings of the 25th International Ocean and Polar Engineering Conference (ISOPE2015), Kona, Big Island, Hawaii, USA, 21-26 June 2015. pp. 1135-1143.

Fujikubo, M. & Tatsumi A. 2017. Progressive collapse analysis of a container ship under combined longitudinal bending moment and bottom local loads. In C. Guedes Soares & Y. Garbatov (eds), Progress in the Analysis and Design of Marine Structures; Proceedings of the 6th International Conference on Marine Structures (MARSTRUCT2017), Lisbon, Portugal, 8-10 May 2017. London: CRC Press. pp. 235-242.

Fukasawa, T. & Hiranuma, M. 2016. Considerations on the longitudinal strength of container ship from the viewpoint of extreme vertical wave bending moment. In U.D. Nielsen & J.J. Jensen (eds), Proceedings of the 13th International Conference on Practical Design of Ships and Other Floating Structures (PRADS2016), Copenhagen, Denmark, 4-8 September 2016.

Gam, M., Jang, B.S. & Park, J. 2017. A study on the fatigue analysis for a vertical caisson on FPSO subjected to the nonlinear wave loading. Ocean Engineering 137(1): 151-165.

Ganesan, S. & Sen, D. 2015. Direct time domain analysis of floating structures with linear and nonlinear mooring stiffness in a 3D numerical wave tank. Applied Ocean Research 51(1): 153-170.

Gannon, L., Liu, Y., Pegg, N. & Smith, M.J. 2016. Nonlinear collapse analysis of stiffened plates considering welding-induced residual stress and distortion. Ships and Offshore Structures 11(3): 228-244.

Gao, Y., Hu, Z., Ringsberg, J.W. & Wang, J. 2015. An elastic-plastic ice material model for ship-iceberg collision simulations. Ocean Engineering 102(1): 27-39.

Gaspar, B., Bucher, C. & Guedes Soares, C. 2015a. Reliability analysis of plate elements under uniaxial compression using an adaptive response surface approach. Ships and Offshore Structures 10(2): 145-161.

Gaspar, B. & Guedes Soares, C. 2015. System reliability analysis of a ship deck structure for buckling collapse and corrosion limit states. In C. Guedes Soares & R.A. Shenoi (eds), Analysis and Design of Marine Structures; Proceedings of the 5th International Conference on Marine Structures (MARSTRUCT2015), Southampton, UK, 25-27 March 2015. London: CRC Press. pp. 751-763.

Gaspar, B., Teixeira, A.P. & Guedes Soares, C. 2015b. Effect of the aspect ratio on the ultimate compressive strength of plate elements with non-uniform corrosion. In C. Guedes Soares & R.A. Shenoi (eds), Analysis and Design of Marine Structures; Proceedings of the 5th International Conference on Marine Structures (MARSTRUCT2015), Southampton, UK, 25-27 March 2015. London: CRC Press. pp. 765-774.

Gaspar, B., Teixeira, A.P. & Guedes Soares, C. 2016. Effect of the nonlinear vertical wave-induced bending moments on the ship hull girder reliability. Ocean Engineering 119(1): 193-207.

Gerlach, B. & Fricke, W. 2016. Experimental and numerical investigation of the behavior of ship windows subjected to quasi-static pressure loads. Marine Structures 46(1): 255-272.

Ghanbari Ghazijahani, T., Jiao, H. & Holloway, D. 2015. Experiments on locally dented conical shells under axial compression. Steel and Composite Structures 19(6): 1355-1367.

Ghanem, R.G. & Spanos, P.D. 2003. Stochastic finite elements: a spectral approach (Rev. Ed.). Courier Dover Publications, New York.

Glassman, J.D. & Garlock, M.E.M. 2016. A compression model for ultimate postbuckling shear strength. Thin-Walled Structures 102(1): 258-272.

Godani, M., Gaiotti, M. & Rizzo, C.M. 2015. Influence of air inclusions on marine composites inter-laminar shear strength. In Proceedings of the 25th International Ocean and Polar Engineering Conference (ISOPE2015), Kona, Big Island, Hawaii, USA, 21-26 June 2015. pp. 593-601.

Gordo, J.M. 2017. Compressive strength of double-bottom under alternate hold loading condition. In C. Guedes Soares & Y. Garbatov (eds), Progress in the Analysis and Design of Marine Structures; Proceedings of the 6th International Conference on Marine Structures (MARSTRUCT2017), Lisbon, Portugal, 8-10 May 2017. London: CRC Press. pp. 253-261.

Gordo, J.M. & Guedes Soares, C. 2015. Degradation of long plate's ultimate strength due to variation on the shape of initial imperfections. In C. Guedes Soares, R. Dejhalla & D. Pavleti (eds), Towards Green Marine Technology and Transport; Proceedings of the 16th International Congress of the International Maritime Association of the Mediterranean (IMAM2015), Pula, Croatia, 21-24 September 2015. London: CRC Press. pp. 345-354.

Gul, W. & Altaf, K. 2015. Evaluation of ultimate buckling strength of stiffened plate for marine structures. In M. Zafar-uz-Zaman (ed), Proceedings of the 12th International Bhurban Conference on Applied Sciences and Technology (IBCAST), Islamabad, Pakistan, 13-17 January 2015. New York: Curran Associates, Inc. pp. 527-536.

Guo, B., Bitner-Gregersen, E.M., Sun, H. & Helmers, J.B. 2016. Statistics analysis of ship response in extreme seas. Ocean Engineering 119(1): 154-164.

Han, C., Ma, Y., Qu, X., Yang, M. & Qin, P. 2016. A practical method for combination of fatigue damage subjected to low–frequency and high-frequency Gaussian random processes. Applied Ocean Research 60(1): 47-60.

Hansen, E.S., Eik, K.J. & Teigen S.H. 2015. Statistical methods for applying icing estimates in offshore design. In Proceedings of the 23rd International Conference on Port and Ocean Engineering under Arctic Conditions (POAC'15), Trondheim, Norway, 14-18 June 2015. 10 pages.

Hayward, R. & Lehmann, E. 2016. Application of a new proof of plate capacity under combined in-plane loads. In U.D. Nielsen & J.J. Jensen (eds), Proceedings of the 13th International Conference on Practical Design of Ships and Other Floating Structures (PRADS2016), Copenhagen, Denmark, 4-8 September 2016.

Hayward, R. & Lehmann, E. 2017. Development of a new proof of plate capacity under combined in-plane loads. Ships and Offshore Structures 12(sup1): S174-S188.

Heggelund, S.E., Storhaug, G., Gonçalves, A. & Austefjord, H. 2016. Equivalent design wave approach for fatigue assessment of ship shaped structures. In C. Guedes Soares & T.A. Santos (eds), Maritime Technology and Engineering III; Proceedings of the 3rd International Conference on Maritime Technology and Engineering (MARTECH2016), Lisbon, Portugal, 4-6 July 2016. London: CRC Press. pp. 489-495.

Heinonen, J. & Rissanen, S. 2017. Coupled-crushing analysis of a sea ice-wind turbine interaction-feasibility study of FAST simulation software. Ships and Offshore Structures 12(8): 1056-1063.

Heinvee, M. & Tabri, K. 2015. A simplified method to predict grounding damage of double bottom tankers. Marine Structures 43(1): 22-43.

Heo, Y. 2016. Challenges in structural engineering design and analysis of offshore plants under probabilistic vapor cloud explosion loads. In Proceedings of the ASME 2016 35th International Conference on Ocean, Offshore and Arctic Engineering (OMAE2016), Busan, South Korea, 19-24 June 2016. (OMAE2016-54096).

Hifi, N. & Barltrop, N. 2015. Correction of prediction model output for structural design and risk-based inspection and maintenance planning. Ocean Engineering 97(1): 114-125.

Holmberg, T. & Hunter, S.D. 2011. Increasing efficiency in the ship structural design process. In Proceedings of the 10th International Conference on Computer and IT Applications in the Maritime Industries (COMPIT2011), Berlin, Germany, 15-17 April 2011. pp. 536-550.

Horn, J.T.H. & Jensen, J.J. 2016. Reducing uncertainty of Monte Carlo estimated fatigue damage in offshore wind turbines using FORM. In U.D. Nielsen & J.J. Jensen (eds), Proceedings of the 13th International Conference on Practical Design of Ships and Other Floating Structures (PRADS2016), Copenhagen, Denmark, 4-8 September 2016.

Horn, J.T.H., Krokstad, J.R. & Amdahl, J. 2017. Joint probability distribution of environmental conditions for design of offshore wind turbines. In Proceedings of the ASME 2017 36th International Conference on Ocean, Offshore and Arctic Engineering (OMAE2017), Trondheim, Norway, 25-30 June 2017. (OMAE2017-61451).

Hosseini, S., Heidarpour, A., Collins, F. & Hutchinson, C.R. 2016. Strain ageing effect on the temperature dependent mechanical properties of partially damaged structural mild-steel induced by high strain rate loading. Construction and Building Materials 123(1): 454-463.

Huang, Z.Y., Wang, J.Y., Liew, J.R. & Marshall, P.W. 2015. Lightweight steel-concrete-steel sandwich composite shell subject to punching shear. Ocean Engineering 102(1): 146-161.

Hughes, O.F. & Paik, J.K. 2010. Ship structural analysis and design. Society of Naval Architects and Marine Engineers (SNAME), Jersey City.

Häfele, J., Hübler, C., Gebhardt, C.G. & Rolfes, R. 2017. Reconsidering fatigue limit state load sets for jacket substructures utilizing probability distributions of environmental states. In Proceedings of the 27th International Ocean and Polar Engineering Conference (ISOPE2017), San Francisco, CA, USA, 25-30 June 2017. pp. 266-273.

Hørte, T. & Sigurdsson, G. 2017. On the application of structural reliability analysis. In Proceedings of the ASME 2017 36th International Conference on Ocean, Offshore and Arctic Engineering (OMAE2017), Trondheim, Norway, 25-30 June 2017. (OMAE2017-62717).

IACS. 2015a. Longitudinal strength standard for container ships. IACS UR S11A, June 2015. International Association of Classification Societies, London, UK.

IACS. 2015b. Requirements for use of extremely thick steel plates in container ships. IACS UR S33 (Rev. 1), September 2015. International Association of Classification Societies, London, UK.

IACS. 2015c. Functional requirements on load cases for strength assessment of container ships by finite element analysis. IACS UR S34, May 2015. International Association of Classification Societies, London, UK.

IACS. 2015d. Application of YP47 steel plates. IACS UR W31 (Rev. 1), September 2015. International Association of Classification Societies, London, UK.

Ibrahim, R.A. 2016. Overview of structural life assessment and reliability, Part VI: crack arresters. Journal of Ship Production and Design 32(2): 71-98.

Iijima, K., Ueda, R. & Fujikubo, M. 2017. Numerical investigation into uncertainty of wave-induced vibration of large container ships due to ship operation. In Proceedings of the ASME 2017 36th International Conference on Ocean, Offshore and Arctic Engineering (OMAE2017), Trondheim, Norway, 25-30 June 2017. (OMAE2017-62336).

IMO. 2010. Adoption of the International Goal-Based Ship Construction Standards for Bulk Carriers and Oil Tankers. IMO Resolution MSC287(87). International Maritime Organisation, London, UK.

IMO. 2015. International Code for Ships Operating in Polar Waters (Polar Code). IMO Resolution MEPC 264(68). International Maritime Organisation, London, UK.

ISO. 2010. Petroleum and natural gas industries - Arctic offshore structures. ISO 19906. International Organization for Standardization, Geneva, Switzerland.

ISSC. 1997. Technical Committee II.1 – Quasi-Static Response. In T. Moan & S. Berge (eds), Proceedings of the 13th International Ship and Offshore Structures Congress (ISSC1997), Vol. 1, Trondheim, Norway, 18-22 August 1997. Oxford: Pergamon Press. pp. 123-186.

Iu, C.K. 2016. Nonlinear fire analysis of steel structure using equivalent thermal load procedure for thermal geometrical change. Fire Safety Journal 86(1): 106-119.

Jelovica, J. & Romanoff, J. 2015. Influence of shear-induced secondary bending on buckling of web-core sandwich panels. In C. Guedes Soares & R.A. Shenoi (eds), Analysis and Design of Marine Structures; Proceedings of the 5th International Conference on Marine Structures (MARSTRUCT2015), Southampton, UK, 25-27 March 2015. London: CRC Press. pp. 445-452.

Jelovica, J., Romanoff, J. & Klein, R. 2016. Eigenfrequency analyses of laser-welded web–core sandwich panels. Thin-Walled Structures 101(1): 120-128.

Jensen, J.J. 2015. Fatigue damage estimation in non-linear systems using a combination of Monte Carlo simulation and the First Order Reliability Method. Marine Structures 44(1): 203-210.

Jia, H. & Moan, T. 2015. Global responses of struck ships in collision with emphasis on hydrodynamic effects. Journal of Offshore Mechanics and Arctic Engineering 137(4): p. 041601-1 – 041601-14.

Jiang, L. & Zhang, S. 2015. Influence of lateral pressure on load-shortening behavior of stiffened panels under combined loads. In C. Guedes Soares & R.A. Shenoi (eds), Analysis and Design of Marine Structures; Proceedings of the 5th International Conference on Marine Structures (MARSTRUCT2015), Southampton, UK, 25-27 March 2015. London: CRC Press. pp. 453-462.

Jin, Y. & Jang, B.S. 2015. Probabilistic fire risk analysis and structural safety assessment of FPSO topside module. Ocean Engineering 104(1): 725-737.

Jin, Y., Kim, J.D. & Jang, B.S. 2015. Development of fire risk analysis procedure for semi-submergible drilling rig. In Proceedings of the 25th International Ocean and Polar Engineering Conference (ISOPE2015), Kona, Big Island, Hawaii, USA, 21-26 June 2015. pp. 787-792.

Jin, Y., Jang, B.S. & Kim, J. 2016. Fire risk analysis procedure based on temperature approximation for determination of failed area of offshore structure: Living quarters on semi-drilling rig. Ocean Engineering 126(1): 29-46.

John, A., Yang, Z., Riahi, R. & Wang, J. 2016. A risk assessment approach to improve the resilience of a seaport system using Bayesian networks. Ocean Engineering 111(1): 136-147.

Kamiński, M. & Świta, P. 2015. Structural stability and reliability of the underground steel tanks with the stochastic finite element method. Archives of Civil and Mechanical Engineering 15(2): 593-602.

Kang, H.J., Choi, J., Lee, D. & Park, B.J. 2017a. A framework for using computational fire simulations in the early phases of ship design. Ocean Engineering 129(1): 335-342.

Kang, K.Y., Choi, K.H., Choi, J., Ryu, Y. & Lee, J.M. 2016. Dynamic response of structural models according to characteristics of gas explosion on topside platform. Ocean Engineering 113(1): 174-190.

Kang, K.Y., Choi, K.H., Choi, J.W., Ryu, Y.H. & Lee, J.M. 2017b. Explosion induced dynamic responses of blast wall on FPSO topside: Blast loading application methods. International Journal of Naval Architecture and Ocean Engineering 9(2): 135-148.

Kawamura, Y., Kanou, Y., Osawa, N., Yamamoto, N., Shiotani, K., Kashima, K., Sakashita, S., Katoh, K. & Takano, S. 2015. Characterization and numerical simulation of corroded surface of coated steel plates in water ballast tank. In Proceedings of the 25th International Ocean and Polar Engineering Conference (ISOPE2015), Kona, Big Island, Hawaii, USA, 21-26 June 2015. pp. 514-520.

Khedmati, M.R., Memarian, H.R., Fadavie, M. & Zareei, M.R. 2016. Empirical formulations for estimation of ultimate strength of continuous aluminium stiffened plates under combined transverse compression and lateral pressure. Ships and Offshore Structures 11(3): 258-277.

Kim, D.H. & Paik, J.K. 2017. Ultimate limit state-based multi-objective optimum design technology for hull structural scantlings of merchant cargo ships. Ocean Engineering 129(1): 318-334.

Kim, D.K., Lim, H.L., Kim, M.S., Hwang, O.J. & Park, K.S. 2017a. An empirical formulation for predicting the ultimate strength of stiffened panels subjected to longitudinal compression. Ocean Engineering 140(1): 270-280.

Kim, H. & Quinton, B. 2016. Evaluation of moving ice loads on an elastic plate. Marine Structures 50(1): 127-142.

Kim, J.H., Park, J.S., Lee, K.H., Kim, J.H., Kim, M.H. & Lee, J.M. 2014. Computational analysis and design formula development for the design of curved plates for ships and offshore structures. Structural Engineering and Mechanics 49(6): 705-726.

Kim, J.H., Kim, Y., Yuck, R.H. & Lee, D.Y. 2015a. Comparison of slamming and whipping loads by fully coupled hydroelastic analysis and experimental measurement. Journal of Fluids and Structures 52(1): 145-165.

Kim, S.Y., Kim, Y. & Lee, J. 2017b. Comparison of sloshing-induced pressure in different scale tanks. Ships and Offshore Structures 12(2): 244-261.

Kim, T. & Kim, Y. 2015. Study on prediction method for the springing-induced tension responses of TLP. In Proceedings of the 25th International Ocean and Polar Engineering Conference (ISOPE2015), Kona, Big Island, Hawaii, USA, 21-26 June 2015. pp. 1386-1392.

Kim, Y.S., Youssef, S., Ince, S., Kim, S.J., Seo, J.K., Kim, B.J., Ha, Y.C. & Paik, J.K. 2015b. Environmental consequences associated with collisions involving double hull oil tanker. Ships and Offshore Structures 10(5): 479-487.

Kitarović, S., Andrić, J. & Pirić, K. 2015. Rational magnification of the plate elastic shear buckling strength. Thin-Walled Structures 94(1): 167-176.

Kitarović, S., Andrić, J. & Pirić, K. 2016. Hull girder progressive collapse analysis using IACS prescribed and NLFEM derived load-end shortening curves. Brodogradnja: Teorija i praksa brodogradnje i pomorske tehnike 67(2): 115-128.

Kotsidis, E.A., Yarza, P., Tsouvalis, N.G., de la Mano, R. & Rodriguez-Senín, E. 2015. Static and fatigue tests of hybrid composite-to-steel butt joints. In C. Guedes Soares & R.A. Shenoi (eds), Analysis and Design of Marine Structures; Proceedings of the 5th International Conference on Marine Structures (MARSTRUCT2015), Southampton, UK, 25-27 March 2015. London: CRC Press. pp. 617-625.

Kumar, J. & Wurm, F.H. 2015. Bi-directional fluid-structure interaction for large deformation of layered composite propeller blades. Journal of Fluids and Structures 57(1): 32-48.

Kumar, P., Zhang, H., Kim, K.I. & Yuen, D.A. 2016. Modeling wave and spectral characteristics of moored ship motion in Pohang new harbor under the resonance conditions. Ocean Engineering 119(1): 101-113.

Kvan, I. & Choung, J. 2017. Accuracy improvement of PCM using simple box girder-based LSE data. In C. Guedes Soares & Y. Garbatov (eds), Progress in the Analysis and Design of Marine Structures; Proceedings of the 6th International Conference on Marine Structures (MARSTRUCT2017), Lisbon, Portugal, 8-10 May 2017. London: CRC Press. pp. 277-288.

Lee, C.S., Kim, M.S., Choi, K.H., Kim, M.H. & Lee, J.M. 2015a. Numerical prediction method for elasto-viscoplastic behavior of glass fiber reinforced polyurethane foam under various compressive loads and cryogenic temperatures. In Proceedings of the ASME 2015 34th International Conference on Ocean, Offshore and Arctic Engineering (OMAE2015), St. John's, Newfoundland, Canada, 31 May-5 June 2015. (OMAE2015-42360).

Lee, D., Kim, K.H. & Choi, I. 2015b. Pressure-resisting capability of the knot area of the primary barrier for a LNG containment system. Ocean Engineering 95(1): 128-133.

Lee, J.M., Park, D.H., Kim, M.G., Kim, J.H., Seo, H.D. & Ahn, H.J. 2016a. Experimental study for estimating ultimate strength of curved plate under longitudinal compression. In U.D. Nielsen & J.J. Jensen (eds), Proceedings of the 13th International Conference on Practical Design of Ships and Other Floating Structures (PRADS2016), Copenhagen, Denmark, 4-8 September 2016.

Lee, S.J., Yeun, D.Y., Jun, S.H. & Oh, Y.T. 2016b. Ship collision analysis for FLNG hull structure. In S.R. Rai, H.K. Shin, J. Choung & R.T. Jung (eds), Proceedings of the 7th International Conference on Collision and Grounding of Ship and Offshore Structures (ICCGS2016), Ulsan, Korea, 15-18 June 2016. Seoul: Hanrimwon Co. pp. 225-228.

Leheta, H.W., Elhanafi, A.S. & Badran, S.F. 2017. Reliability analysis of novel stiffened panels using Monte Carlo simulation. Ships and Offshore Structures 12(5): 640-652.

Liao, P.K., Quéméner, Y., Lee, C.F. & Chen, K.C. 2015. Load uncertainties effects on the fatigue life evaluation by the common structural rules. In Proceedings of the ASME 2015 34th International Conference on Ocean, Offshore and Arctic Engineering (OMAE2015), St. John's, Newfoundland, Canada, 31 May-5 June 2015. (OMAE2015-41348).

Lim, H.U., Manuel, L., Low, Y.M. & Srinil, N. 2017. Uncertainty quantification of riser fatigue damage due to VIV using a distributed wake oscillator model. In Proceedings of the ASME 2017 36th International Conference on Ocean, Offshore and Arctic Engineering (OMAE2017), Trondheim, Norway, 25-30 June 2017. (OMAE2017-62413).

Lin, W., Zhu, G., Tang, Y., Zhao, C., Liu, X., Wang, C. & Qiu, A. 2015. Automatic recognition of hull transverse sections and rapid finite element modelling for cargo hold longitudinal structures. Proceedings of the Institution of Mechanical Engineers, Part M: Journal of Engineering for the Maritime Environment 229(2): 157-173.

Liu, B. & Guedes Soares, C. 2015. Simplified analytical method for evaluating web girder crushing during ship collision and grounding. Marine structures 42(1): 71-94.

Liu, B. & Guedes Soares, C. 2016. Assessment of the strength of double-hull tanker side structures in minor ship collisions. Engineering Structures 120(1): 1-12.

Liu, B., Villavicencio, R. & Guedes Soares C. 2015. Simplified method for quasi-static collision assessment of a damaged tanker side panel. Marine Structures 40(1): 267-288.

Lotsberg, I., Sigurdsson, G., Fjeldstad, A. & Moan, T. 2016. Probabilistic methods for planning of inspection for fatigue cracks in offshore structures. Marine Structures 46(1): 167-192.

Loukogeorgaki, E., Vasileiou, M. & Rapanta, E. 2015. 3D numerical and experimental investigation of the performance of a modular floating structure. In Proceedings of the 25th International Ocean and Polar Engineering Conference (ISOPE2015), Kona, Big Island, Hawaii, USA, 21-26 June 2015. pp. 1548-1555.

LR. 2004. Structural design assessment for primary structure of passenger ships. Lloyd's Register, London, United Kingdom.

LR. 2012. ShipRight design and construction, structural design assessment - Primary structure of Ro-Ro ships. March 2012. Lloyd Register, London, UK.

LR. 2014. Rules and regulations for the classification of ships. Lloyd's Register, London, United Kingdom.

LR. 2016a. Integrating integrity and class: applying RBI to hull structures - http://www.lr.org/en/news-and-insight/articles/applying-rbi-to-hull-structures.aspx. Lloyd's Register, London, UK. [Accessed: 2017-12-01].

LR. 2016b. New risk-based inspection (RBI) service combines hull integrity management with class to minimise cost - http://www.lr.org/en/news-and-insight/news/rbi-service-combines-hull-integrity-management-class-minimise-costs.aspx. Lloyd's Register, London, UK. [Accessed: 2017-12-01].

LR. 2017a. Rules and regulations for the classification of naval ships. January 2017. Lloyd's Register, London, UK.

LR. 2017b. ShipRight design and construction, structural design assessment - Procedure for primary structure of passenger ships. March 2017. Lloyd Register, London, UK.

Magoga, T., Aksi, S., Cannon, S., Ojeda, R. & Thomas, G. 2016. Comparison between fatigue life values calculated using standardised and measured stress spectra of a naval high speed light craft. In U.D. Nielsen & J.J. Jensen (eds), Proceedings of the 13th International Conference on Practical Design of Ships and Other Floating Structures (PRADS2016), Copenhagen, Denmark, 4-8 September 2016.

Mao, W., Li, Z., Ogeman, V. & Ringsberg, J.W. 2015. A regression and beam theory based approach for fatigue assessment of containership structures including bending and torsion contributions. Marine Structures 41(1): 244-266.

Marinatos, J.N. & Samuelides, M.S. 2015. Towards a unified methodology for the simulation of rupture in collision and grounding of ships. Marine Structures 42(1): 1-32.

Micone, N. & Waele, W.D. 2015. Comparison of fatigue design codes with focus on offshore structures. In Proceedings of the ASME 2015 34th International Conference on Ocean, Offshore and Arctic Engineering (OMAE2015), St. John's, Newfoundland, Canada, 31 May-5 June 2015. (OMAE2015-41931).

Milne, I.A., Delaux, S. & McComb, P. 2016. Validation of a predictive tool for the heading of turret-moored vessels. Ocean Engineering 128(1): 22-40.

Minorsky, V.U. 1959. An analysis of ship collision with reference to protection of nuclear powered plants. Journal of Ship Research 3(2): 1-4.

Mohammadi, S.F., Galgoul, N.S. & Starossek, U. 2016. Comparison of time domain and spectral fatigue analyses of an offshore jacket structure. In Proceedings of the 26th International Ocean and Polar Engineering Conference (ISOPE2016), Rhodes, Greece, 26 June-1 July 2016. pp. 978-985.

Mohammed, E.A., Benson, S.D., Hirdaris, S.E. & Dow, R.S. 2016. Design safety margin of a 10,000 TEU container ship through ultimate hull girder load combination analysis. Marine Structures 46(1): 78-101.

Mohd Zaki, N.I., Abu Husain, M.K. & Najafian, G. 2016. Derivation of Morison's force coefficients by three alternative forms of the method of moments. In Proceedings of the ASME 2016 35th International Conference on Ocean, Offshore and Arctic Engineering (OMAE2016), Busan, South Korea, 19-24 June 2016. (OMAE2016-54201).

Montes-Iturrizaga, R. & Heredia-Zavoni, E. 2016. Reliability analysis of mooring lines using copulas to model statistical dependence of environmental variables. Applied Ocean Research 59(1): 564-576.

Morikage, Y., Igi, S., Tagawa T. & Oi, K. 2016. Effect of compressive residual stress on fatigue crack propagation. In U.D. Nielsen & J.J. Jensen (eds), Proceedings of the 13th International Conference on Practical Design of Ships and Other Floating Structures (PRADS2016), Copenhagen, Denmark, 4-8 September 2016.

Morshedsoluk, F. & Khedmati, M.R. 2016. Ultimate strength of composite ships' hull girders in the presence of composite superstructures. Thin-Walled Structures 102(1): 122-138.

Nadim, F. 2015. Accounting for uncertainty and variability in geotechnical characterization of offshore sites. In T. Schweckendiek, A.F. van Tol, D. Pereboom, M.Th. van Staveren & P.M.C.B.M. Cools (eds), Geotechnical Safety and Risk V; Proceedings of the 5th International Symposium on Geotechnical Safety and Risk (ISGSR5), Rotterdam, The Netherlands, 13-16 October 2015. Open Access by IOS Press. pp. 23-34.

Niu, W.C., Li, G.L., Ju, Y.L. & Fu, Y.Z. 2017. Design and analysis of the thermal insulation system for a new independent type B LNG carrier. Ocean Engineering 142(1): 51-61.

Noh, S.H., Seo, J.K., Paik, J.K. & Youssef, S.A.M. 2016. Rapid assessment of hull girder collapse for corroded double hull oil tanker after collision. In Proceedings of the ASME 2016 35th International Conference on Ocean, Offshore and Arctic Engineering (OMAE2016), Busan, South Korea, 19-24 June 2016. (OMAE2016-54667).

Obisesan, A., Sriramula, S. & Harrigan, J. 2016. A framework for reliability assessment of ship hull damage under ship bow impact. Ships and Offshore Structures 11(7): 700-719.

Okada, T., Toyama, T. & Kawamura, Y. 2016. Theoretical study on structural arrangement to control strength of unstiffened bilge shell plating. In U.D. Nielsen & J.J. Jensen (eds), Proceedings of the 13th International Conference on Practical Design of Ships and Other Floating Structures (PRADS2016), Copenhagen, Denmark, 4-8 September 2016.

Okada, T., Toyama, T. & Kawamura, Y. 2017. Theoretical strength assessment of unstiffened bilge shell plating and some considerations on rule prescriptions. Journal of Marine Science and Technology 22(1): 85-100.

Osawa, N., Kanou, Y., Kawamura, Y., Takada, A., Shiotani, K., Takeno, S. & Katayama, S. 2016a. Fundamental study on underfilm corrosion simulation method based on cellular automaton. In U.D. Nielsen & J.J. Jensen (eds), Proceedings of the 13th International Conference on Practical Design of Ships and Other Floating Structures (PRADS2016), Copenhagen, Denmark, 4-8 September 2016.

Osawa, N., Kanou, Y., Kawamura, Y., Takada, A., Shiotani, K., Takeno, S., Katayama, S. & William, K.I. 2016b. Development of under-film corrosion simulation method based on cellular automaton. In Proceedings of the ASME 2016 35th International Conference on Ocean, Offshore and Arctic Engineering (OMAE2016), Busan, South Korea, 19-24 June 2016. (OMAE2016-54508).

Paik, J.K. & Thayamballi, A.K. 2003. Ultimate limit state design of steel-plated structures (1st edition). John Wiley & Sons Inc., Hoboken, NJ, USA.

Paris, L. & Dubois, A. 2017. Recent developments to evaluate global explosion loading on complex systems. Journal of Loss Prevention in the Process Industries 46(1): 163-176.

Park, D.K., Kim, D.K., Seo, J.K., Kim, B.J., Ha, Y.C. & Paik, J.K. 2015. Operability of non-ice class aged ships in the Arctic Ocean-part II: Accidental limit state approach. Ocean Engineering 102(1): 206-215.

Park, M.J., Choi, B.K. & Kim, Y. 2017. On the efficient time domain stress analysis for the rolling chock of an independent type LNG tank targeting fatigue damage evaluation. Marine Structures 53(1): 32-51.

Parunov, J., Smiljko, R., Gledić, I. & Bužančić Primorac, B. 2017. Finite element study of residual ultimate strength of a double hull oil tanker damaged in collision and subjected to bi-axial bending. In S. Ehlers, J.K. Paik & Y. Bai (eds), Proceedings of the 2nd International

Conference on Ships and Offshore Structures (ICSOS2017), Shenzhen, China, 11-13 September 2017. (ICSOS2017-007).

Paulauskas, V. 2016. Ship and quay wall mooring system capability evaluation. Transportation Research Procedia 14(1): 123-132.

Pedersen, P.T. & Zhang, S. 1998. On impact mechanics in ship collisions. Marine Structures 11(10): 429-449.

Pei, Z., Iijima, K., Fujikubo, M., Tanaka, S., Okazawa, S. & Yao, T. 2015. Simulation on progressive collapse behaviour of whole ship model under extreme waves using idealized structural unit method. Marine Structures 40(1): 104-133.

Pérez, R.F. 2015. A next-generation of 3D CAD tool for basic ship design. Ingeniería Naval No. 939(1): 85-91.

Petrolo, M. & Carrera, E. 2016. High-fidelity and computationally efficient component-wise structural models: an overview of applications and perspectives. Applied Mechanics and Materials 828(1): 175-196.

Rahm, M., Evegren, F., Ringsberg, J.W. & Johnson, E. 2017. Structural fire integrity testing of lightweight multiple core sandwich structures. In C. Guedes Soares & Y. Garbatov (eds), Progress in the Analysis and Design of Marine Structures; Proceedings of the 6th International Conference on Marine Structures (MARSTRUCT2017), Lisbon, Portugal, 8-10 May 2017. London: CRC Press. pp. 869-876.

Rahmdel, S., Kim, K., Kim, S. & Park, S. 2015. A novel stepwise method to predict ultimate strength reduction in offshore structures with pitting corrosion. Advances in Mechanical Engineering 7(8): p. 1-10.

Ranta, J., Polojärvi, A. & Tuhkuri, J. 2015. Ice load estimation through combined finite-discrete element simulations. In Proceedings of the 23rd International Conference on Port and Ocean Engineering under Arctic Conditions (POAC'15), Trondheim, Norway, 14-18 June 2015. 9 pages.

Redondo, L., Méndez, R. & Pérez-Rojas, L. 2016. An indirect method implementing effect of the wind on moored ship experimental tests. Ocean Engineering 121(1): 341-355.

Reed, H.M. & Earls, C.J. 2015. Stochastic identification of the structural damage condition of a ship bow section under model uncertainty. Ocean Engineering 103(1): 123-143.

Reis, A., Lopes, N., Real, E. & Real, P.V. 2016. Numerical modelling of steel plate girders at normal and elevated temperatures. Fire Safety Journal 86(1): 1-15.

Reza, T.M., Mani, F.D., Ali, D.D.M., Saied, M. & Saied, S.M. 2017. Response spectrum method for extreme wave loading with higher order components of drag force. Journal of Marine Science and Application 16(1): 27-32.

Ringsberg, J.W. 2015. Steel or composite car deck structure - a comparison analysis of weight, strength and cost. In C. Guedes Soares & R.A. Shenoi (eds), Analysis and Design of Marine Structures; Proceedings of the 5th International Conference on Marine Structures (MARSTRUCT2015), Southampton, UK, 25-27 March 2015. London: CRC Press. pp. 647-658.

Ringsberg, J.W., Bohlmann, B., Chien, H.L., Constantinescu, A., Heggelund, S.E., Hirdaris, S.E., Jang, B.S., Koko, T.S., Lara, P., Miyazaki, S., Sidari, M., van der Sluijs, B.R., Taczala, M., Wan, Z., Zamarin, A. & Økland, O. 2015. Technical Committee II.1 – Quasi-static response. In C. Guedes Soares and Y. Garbatov (eds), Proceedings of the 19th International Ship and Offshore Structures Congress (ISSC2015), Vol. 1, Cascais, Portugal, 7-10 September 2015. London: CRC Press. pp. 141-207.

Ringsberg, J.W., Heggelund, S.E., Lara, P., Jang, B.S. & Hirdaris, S.E. 2017. Structural response analysis of slamming impact on free fall lifeboats. Marine Structures 54(1): 112-126.

Rodrigues, J.M., Teixeira, A.P. & Guedes Soares, C. 2015. Probabilistic analysis of the hull-girder still water loads on a shuttle tanker in full load condition, for parametrically distributed collision damage spaces. Marine Structures 44(1): 101-124.

Roy, S., Ghosh, V., Dey, S., Vimmadi, S. & Banik, A.K. 2017. A coupled analysis of motion and structural responses for an offshore spar platform in irregular waves. Ships and Offshore Structures 12(sup1): S296-S304.

Ryu, M.C., Jung, J.H., Kim, Y.S. & Kim, Y. 2016. Sloshing design load prediction of a membrane type LNG cargo containment system with two-row tank arrangement in offshore applications. International Journal of Naval Architecture and Ocean Engineering 8(6): 537-553.

Saad-Eldeen, S., Garbatov, Y. & Guedes Soares, C. 2014. Compressive strength assessment of rectangular steel plates with a local dent or an opening. In C. Guedes Soares & T.A. Santos (eds), Maritime Technology and Engineering II; Proceedings of the 2nd International Conference on Maritime Technology and Engineering (MARTECH2014), Lisbon, Portugal, 15-17 October 2014. London: CRC Press. pp. 543-552.

Saad-Eldeen, S., Garbatov, Y. & Guedes Soares, C. 2015a. Residual strength of a severely damaged box-girder with non-uniform and inter-crystalline corrosion. In C. Guedes Soares & R.A. Shenoi (eds), Analysis and Design of Marine Structures; Proceedings of the 5th International Conference on Marine Structures (MARSTRUCT2015), Southampton, UK, 25-27 March 2015. London: CRC Press. pp. 521-531.

Saad-Eldeen, S., Garbatov, Y. & Guedes Soares, C. 2015b. Structural capacity of an aging box girder accounting for the presence of a dent. In C. Guedes Soares & R.A. Shenoi (eds), Analysis and Design of Marine Structures; Proceedings of the 5th International Conference on Marine Structures (MARSTRUCT2015), Southampton, UK, 25-27 March 2015. London: CRC Press. pp. 403-414.

Saad-Eldeen, S., Garbatov, Y. & Guedes Soares, C. 2016a. Strength assessment of steel plates subjected to compressive load and dent deformation. Structure and Infrastructure Engineering 12(8): 995-1011.

Saad-Eldeen, S., Garbatov, Y. & Guedes Soares, C. 2016b. Ultimate strength analysis of highly damaged plates. Marine Structures 45(1): 63-85.

Samuelides, M. 2015. Recent advances and future trends in structural crashworthiness of ship structures subjected to impact loads. Ships and Offshore Structures 10(5): 488-497.

Schiere, M., Bosman, T., Derbanne, Q., Stambaugh, K. & Drummen, I. 2017. Sectional load effects derived from strain measurements using the modal approach. Marine Structures 54(1): 188-209.

Schoefs, F., Chevreuil, M., Pasqualini, O. & Cazuguel, M. 2016. Partial safety factor calibration from stochastic finite element computation of welded joint with random geometries. Reliability Engineering & System Safety 155(1): 44-54

Seo, J.K., Cui, Y., Mohd, M.H., Ha, Y.C., Kim, B.J. & Paik, J.K. 2015. A risk-based inspection planning method for corroded subsea pipelines. Ocean Engineering 109(1): 539-552.

Sen, D. 2015. Direct time domain analysis of floating structures with linear and nonlinear mooring stiffness in a 3D numerical wave tank. Applied Ocean Research 51(1): 153-170.

Sepahvanda, K. 2016. Stochastic collocation-based finite element of structural nonlinear dynamics with application in composite structures. In MATEC Web of Conferences Vol. 83; The International Conference on Structural Nonlinear Dynamics and Diagnosis (CSNDD2016), 16 November 2016. Open Access by EDP Sciences. 5 pages (Paper No. 01009).

Shahbaztabar, A. & Ranji, A.R. 2016. Effects of in-plane loads on free vibration of symmetrically cross-ply laminated plates resting on Pasternak foundation and coupled with fluid. Ocean Engineering 115(1): 196-209.

Shi, X.H., Jiang, X., Zhang, J. & Guedes Soares, C. 2016. Residual ultimate strength of stiffened panels with pitting corrosion under compression. In C. Guedes Soares & T.A. Santos (eds), Maritime Technology and Engineering III; Proceedings of the 3rd International Conference on Maritime Technology and Engineering (MARTECH2016), Lisbon, Portugal, 4-6 July 2016. London: CRC Press. pp. 547-556.

Shin, K.H., Jo, J.W., Hirdaris, S.E., Jeong, S.G., Park, J.B., Lin, F., Wang, Z. & White, N. 2015. Two-and three-dimensional springing analysis of a 16,000 TEU container ship in regular waves. Ships and Offshore Structures 10(5): 498-509.

Singh, X. & Ahmad, S. 2015. Probabilistic analysis and risk assessment of deep water composite production riser against fatigue limit state. In Proceedings of the ASME 2015 34th International Conference on Ocean, Offshore and Arctic Engineering (OMAE2015), St. John's, Newfoundland, Canada, 31 May-5 June 2015. (OMAE2015-41576).

Soliman, M., Frangopol, D.M. & Mondoro, A. 2016. A probabilistic approach for optimizing inspection, monitoring, and maintenance actions against fatigue of critical ship details. Structural Safety 60(1): 91-101.

Son, M.J., Lee, J.Y., Park, H.G., Kim, J.O., Woo, J. & Lee, J. 2016. Development of 3D CAD/CAE interface in initial structural design phase of shipbuilding. Korean Journal of Computational Design and Engineering 21(2): 186-195.

Song, M., Kim, E., Amdahl, J., Ma, J. & Huang, Y. 2016a. A comparative analysis of the fluid-structure interaction method and the constant added mass method for ice-structure collisions. Marine Structures 49(1): 58-75.

Song, X., Du, J., Wang, S., Li, H. & Chang, A. 2016b. An innovative block partition and equivalence method of the wave scatter diagram for offshore structural fatigue assessment. Applied Ocean Research 60(1): 12-28.

Sormunen, O.V.E., Castrén, A., Romanoff, J. & Kujala, P. 2016. Estimating sea bottom shapes for grounding damage calculations. Marine Structures 45(1): 86-109.

Stagonas, D., Marzeddu, A., Cobos, F.X.G.I., Conejo, A.S.A. & Muller, G. 2016. Measuring wave impact induced pressures with a pressure mapping system. Coastal Engineering 112(1): 44-56.

Stefanou, G., 2009. The stochastic finite element method: past, present and future. Computer Methods in Applied Mechanics and Engineering 198(9): 1031-1051.

Stilhammer, J., Steenbock, C., & Bohm, M. 2015. A complete CAE process for structural design in shipbuilding. In Proceedings of the 14th International Conference on Computer and Information Technology in the Maritime Industries (COMPIT2015), Ulrichshusen, Germany, 11-13 May 2015. pp. 406-417.

Stipčević, M., Kitarović, S., Dundara, Đ. & Radolović, V. 2015 Evaluation of composite sandwich panel structural variants for fixed car decks in the upper cargo hold of the Ro-Ro car and truck carrier. In C. Guedes Soares, R. Dejhalla & D. Pavleti (eds), Towards Green Marine Technology and Transport; Proceedings of the 16th International Congress of the International Maritime Association of the Mediterranean (IMAM2015), Pula, Croatia, 21-24 September 2015. London: CRC Press. pp. 317-325.

Stone, K. & McNatt, T. 2017. Ship hull structural scantling optimization. In C. Guedes Soares & Y. Garbatov (eds), Progress in the Analysis and Design of Marine Structures; Proceedings of the 6th International Conference on Marine Structures (MARSTRUCT2017), Lisbon, Portugal, 8-10 May 2017. London: CRC Press. pp. 203-211.

Storhaug, G. & Aagaard, O. 2016. Calibration of hull monitoring strain sensors in deck including the effect of hydroelasticity. In Proceedings of the 26th International Ocean and Polar Engineering Conference (ISOPE2016), Rhodes, Greece, 26 June-1 July 2016. pp. 487-494.

Storhaug, G. & Andersen, I.M.V. 2015. Extrapolation of model tests measurements of whipping to identify the dimensioning sea states for container ships. In Proceedings of the 25th International Ocean and Polar Engineering Conference (ISOPE2015), Kona, Big Island, Hawaii, USA, 21-26 June 2015. pp. 114-122.

Storhaug, G., Laanemets, K., Edin, I. & Ringsberg, J.W. 2017. Estimation of damping from wave induced vibrations in ships. In C. Guedes Soares & Y. Garbatov (eds), Progress in the Analysis and Design of Marine Structures; Proceedings of the 6th International Conference

on Marine Structures (MARSTRUCT2017), Lisbon, Portugal, 8-10 May 2017. London: CRC Press. pp. 121-130.

Storheim, M. & Amdahl, J. 2014. Design of offshore structures against accidental ship collisions. Marine Structures 37(1): 135-172.

Storheim, M., Amdahl, J. & Alsos, H.S. 2017. Evaluation of nonlinear material behavior for offshore structures subjected to accidental actions. In Proceedings of the ASME 2017 36th International Conference on Ocean, Offshore and Arctic Engineering (OMAE2017), Trondheim, Norway, 25-30 June 2017. (OMAE2017-61861).

Storheim, M., Amdahl, J. & Martens, I. 2015. On the accuracy of fracture estimation in collision analysis of ship and offshore structures. Marine Structures 44(1): 254-287.

Sun, B., Hu, Z. & Wang, G. 2015a. An analytical method for predicting the ship side structure response in raked bow collisions. Marine Structures 41(1): 288-311.

Sun, J.Q., Wang, D.Y., Sun, Y.G. & Fu, S.X. 2015. Research on the characteristic of the multi-segment beam model of very large floating structure. In Proceedings of the 25th International Ocean and Polar Engineering Conference (ISOPE2015), Kona, Big Island, Hawaii, USA, 21-26 June 2015. pp. 1556-1563.

Sun, L., Niu, Z., Ma, G. & Li, Y. 2016. Risk evaluation of explosion in FPSO based on failure model and effect analysis. In Proceedings of the ASME 2016 35th International Conference on Ocean, Offshore and Arctic Engineering (OMAE2016), Busan, South Korea, 19-24 June 2016. (OMAE2016-54144).

Sun, L., Yan, H., Liu, S. & Bai, Y. 2017. Load characteristics in process modules of offshore platforms under jet fire: The numerical study. Journal of Loss Prevention in the Process Industries 47(1): 29-40.

Swidan, A., Thomas, G., Ranmuthugala, D., Amin, W., Penesis, I., Allen, T. & Battley, M. 2016. Experimental drop test investigation into wetdeck slamming loads on a generic catamaran hullform. Ocean Engineering 117(1): 143-153.

Syrigou, M.S., Benson, S.D. & Dow, R.S. 2015. Strength of aluminium alloy ship plating under combined shear and compression/tension. In C. Guedes Soares & R.A. Shenoi (eds), Analysis and Design of Marine Structures; Proceedings of the 5th International Conference on Marine Structures (MARSTRUCT2015), Southampton, UK, 25-27 March 2015. London: CRC Press. pp. 473-481.

Sørensen, J.D. 2017. Reliability analysis and risk-based methods for planning of operation and maintenance of offshore wind turbines. In Proceedings of the ASME 2017 36th International Conference on Ocean, Offshore and Arctic Engineering (OMAE2017), Trondheim, Norway, 25-30 June 2017. (OMAE2017-62713).

Takami, T., Ogawa, H., Miyata, T., Ando, T., Tatsumi, A., Hirakawa, S., Tanaka, Y. & Fujikubo, M. 2015. Study on buckling/ultimate strength of continuous stiffened panel under in-plane shear and thrust. In Proceedings of the 25th International Ocean and Polar Engineering Conference (ISOPE2015), Kona, Big Island, Hawaii, USA, 21-26 June 2015. pp. 1117-1122.

Tanaka, Y., Ogawa, H., Tatsumi, A. & Fujikubo, M. 2015. Analysis method of ultimate hull girder strength under combined loads. Ships and Offshore Structures 10(5): 587-598.

Tawfik, B.E., Leheta, H., Elhewy, A. & Elsayed, T. 2017. Weight reduction and strengthening of marine hatch covers by using composite materials. International Journal of Naval Architecture and Ocean Engineering 9(2): 185-198.

Temarel, P., Bai, W., Bruns, A., Derbanne, Q., Dessi, D., Dhavalikar, S., Fonseca, N., Fukasawa, T., Gu, X., Nestegård, A. & Papanikolaou, A. 2016. Prediction of wave-induced loads on ships: Progress and challenges. Ocean Engineering 119(1): 274-308.

Temple, D.W. & Collette, M.D. 2015. Minimizing lifetime structural costs: Optimizing for production and maintenance under service life uncertainty. Marine Structures 40(1): 60-72.

Tian, X., Liu, G., Gao, Z., Chen, P. & Mu, W. 2017. Crack detection in offshore platform structure based on structural intensity approach. Journal of Sound and Vibration 389(1): 236-249.

Travanca, J. & Hao H. 2015. Energy dissipation in high-energy ship-offshore jacket platform collisions. Marine Structures 40(1): 1-37.

Underwood, J.M., Sobey, A.J., Blake, J.I.R. & Shenoi, R.A. 2015. Ultimate collapse strength assessment of damaged steel plated grillages. Engineering Structures 99(1): 517-535.

Underwood, J.M., Sobey, A.J., Blake, J.I.R. & Shenoi, R.A. 2016. Compartment level progressive collapse strength as a method for analysing damaged steel box girders. Thin-Walled Structures 106(1): 346-357.

van Lieshout, P.S., den Besten, J.H. & Kaminski, M.L. 2017. Validation of the corrected Dang Van multiaxial fatigue criterion applied to turret bearings of FPSO offloading buoys. Ships and Offshore Structures 12(4): 521-529.

Varol, H. & Cashell, K.A. 2017. Numerical modelling of high strength steel beams at elevated temperature. Fire Safety Journal 89(1): 41-50.

Vásquez, G., Fonseca, N. & Guedes Soares, C. 2016. Experimental and numerical vertical bending moments of a bulk carrier and a roll-on/roll-off ship in extreme waves. Ocean Engineering 124(1): 404-418.

von Selle, H., Kahl, A., Storhaug, G. & Wolf, V. 2016. Latest research and rule development activities on fatigue strength of thick plates and higher tensile steels. In Proceedings of the 26th International Ocean and Polar Engineering Conference (ISOPE2016), Rhodes, Greece, 26 June-1 July 2016. pp. 1010-1016.

Wang, C., Cao, Y., Lin, W., Wang, L., Tang, Y. & Zhao, C. 2015a. An automated mesh generation algorithm for curved surfaces of ship longitudinal structures. Computer-Aided Design and Applications 12(1): 9-24.

Wang, R.H., Zou, X., Dou, P.L., Fang, Y.Y. & Luo, G. 2015b. Multi-scale investigation on residual strength of jacket platform with fatigue crack damage. In Proceedings of the ASME 2015 34th International Conference on Ocean, Offshore and Arctic Engineering (OMAE2015), St. John's, Newfoundland, Canada, 31 May-5 June 2015. (OMAE2015-41853).

Wang, Y., Wharton, J.A. & Shenoi, R.A. 2015c. Ultimate strength assessment of steel stiffened plate structures with grooving corrosion damage. Engineering Structures 94(1): 29-42.

Wnęk, A.D. & Guedes Soares, C. 2015. CFD assessment of the wind loads on an LNG carrier and floating platform models. Ocean Engineering 97(1): 30-36.

Woodward, M.D., van Rijsbergen, M., Hutchinson, K.W. & Scott, A. 2016. Uncertainty analysis procedure for the ship inclining experiment. Ocean Engineering 114(1): 79-86.

Wu, F., Gao, Q., Xu, X.M. & Zhong, W.X. 2015. A modified computational scheme for the stochastic perturbation finite element method. Latin American Journal of Solids and Structures 12(13): 2480-2505.

Xie, S., Yang, D., Liu, Y. & Shen, L. 2016. Simulation-based study of wind loads on semi-submersed object in ocean wave field. Physics of Fluids 28(1): p. 015106-1 – 015106-24.

Xu, N., Yue, Q., Bi, X., Tuomo, K. & Zhang, D. 2015a. Experimental study of dynamic conical ice force. Cold Regions Science and Technology 120(1): 21-29.

Xu, W., Duan, W. & Han, D. 2015b. Investigation into the dynamic collapse behaviour of a bulk carrier under extreme wave loads. Ocean Engineering 106(1): 115-127.

Xu, Y., Qian, Y. & Song, G. 2016. Stochastic finite element method for free vibration characteristics of random FGM beams. Applied Mathematical Modelling 40(23): 10238-10253.

Yamada, Y., Tozawa, S., Arima, T., Ichikawa, K. Oda, N., Kamita, K. & Suga, H. 2016. Effects of highly ductile steel on the crashworthiness of hull structure in oblique collision. In S.R. Rai, H.K. Shin, J. Choung & R.T. Jung (eds), Proceedings of the 7th International

Conference on Collision and Grounding of Ship and Offshore Structures (ICCGS2016), Ulsan, Korea, 15-18 June 2016. Seoul: Hanrimwon Co. pp. 217-223.

Yan, J.B., Wang, J.Y., Liew, J.R., Qian, X. & Zong, L. 2016a. Ultimate strength behaviour of steel–concrete–steel sandwich plate under concentrated loads. Ocean Engineering 118(1), pp. 41-57.

Yan, X., Huang, X., Huang, Y. and Cui, W., 2016b. Prediction of fatigue crack growth in a ship detail under wave-induced loading. Ocean Engineering 113(1): 246-254.

Ye, J., Jeng, D., Wang, R. & Zhu, C. 2013. A 3-D semi-coupled numerical model for fluid–structures–seabed-interaction (FSSI-CAS 3D): Model and verification. Journal of Fluids and Structures 40(1): 148-162.

Yeter, B., Garbatov Y. & Guedes Soares, C. 2015. Fatigue reliability of an offshore wind turbine supporting structure accounting for inspection and repair. In C. Guedes Soares & R.A. Shenoi (eds), Analysis and Design of Marine Structures; Proceedings of the 5th International Conference on Marine Structures (MARSTRUCT2015), Southampton, UK, 25-27 March 2015. London: CRC Press. pp. 737-747.

Ülker, M.B.C. 2014. Modeling of dynamic response of poroelastic soil layers under wave loading. Frontiers of Structural and Civil Engineering 8(1): 1-18.

Young, W.C. & Budynas, R.G. (2011). Roark's formulas for stress and strain (Eighth Edition). New York: McGraw-Hill.

Youssef, S.A., Faisal, M., Seo, J.K., Kim, B.J., Ha, Y.C., Kim, D.K., Paik, J.K., Cheng, F. & Kim, M.S. 2016. Assessing the risk of ship hull collapse due to collision. Ships and Offshore Structures 11(4): 335-350.

Yu, L., Ren, H., Liu, X., Sun, X. & Peng, Y. 2017. Study on the remaining fatigue life of FPSO based on spectral analysis. In Proceedings of the ASME 2017 36th International Conference on Ocean, Offshore and Arctic Engineering (OMAE2017), Trondheim, Norway, 25-30 June 2017. (OMAE2017-61428).

Yu, T., Yin, S., Bui, T.Q., Xia, S., Tanaka, S. & Hirose, S. 2016a. NURBS-based isogeometric analysis of buckling and free vibration problems for laminated composites plates with complicated cutouts using a new simple FSDT theory and level set method. Thin-Walled Structures 101(1): 141-156.

Yu, Z., Amdahl, J. & Storheim, M. 2016b. A new approach for coupling external dynamics and internal mechanics in ship collisions. Marine Structures 45(1): 110-132.

Yue, J., Dang, Z. & Guedes Soares, C. 2017. Prediction of fatigue crack propagation in bulb stiffeners by experimental and numerical methods. International Journal of Fatigue 99(1): 101-110.

Yulmetov, R. & Løset, S. 2017. Validation of a numerical model for iceberg towing in broken ice. Cold Regions Science and Technology 138(1): 36-45.

Zeitz, B., Harries S., Matthiesen A., Flehmke, A. & Bertram, V. 2014. Structural optimization of midship sections for container vessels coupling POSEIDON with CAESES/FRIENDSHIP framework. In Proceedings of the 13th International Conference on Computer and Information Technology in the Maritime Industries (COMPIT2014), Redworth, UK, 12-14 May 2014. pp. 60-71.

Zhang, H., Xu, D., Xia, S., Qi, E., Tian, C. & Wu, Y. 2015. Nonlinear network dynamic characteristics of multi-module floating airport with flexible connectors. In Proceedings of the 25th International Ocean and Polar Engineering Conference (ISOPE2015), Kona, Big Island, Hawaii, USA, 21-26 June 2015. pp. 1583-1590.

Zhang, H.H., Feng, G.Q., Ren, H.L. & Wang, Y.Z. 2017a. Research on the fatigue health monitoring system of the hull structure. In Proceedings of the 27th International Ocean and Polar Engineering Conference (ISOPE2017), San Francisco, CA, USA, 25-30 June 2017. pp. 973-980.

Zhang, J., Shi, X.H. & Guedes Soares, C. 2017b. Experimental analysis of residual ultimate strength of stiffened panels with pitting corrosion under compression. Engineering Structures 152(1): 70-86.

Zhang, J., Teixeira, A.P., Guedes Soares, C. & Yan, X. 2017c. Probabilistic modelling of the drifting trajectory of an object under the effect of wind and current for maritime search and rescue. Ocean Engineering 129(1): 253-264.

Zhang, S. 2016. A review and study on ultimate strength of steel plates and stiffened panels in axial compression. Ships and Offshore Structures 11(1): 81-91.

Zhang, S. & Pedersen, P.T. 2017. A method for ship collision damage and energy absorption analysis and its validation. Ships and Offshore Structures 12(sup1): S11-S20.

Zhang, S., Villavicencio, R., Zhu, L. & Pedersen, P.T. 2017d. Impact mechanics of ship collisions and validations with experimental results. Marine Structures 52(1): 69-81.

Zhang, X., Paik, J.K. & Jones, N. 2016. A new method for assessing the shakedown limit state associated with the breakage of a ship's hull girder. Ships and Offshore Structures 11(1): 92-104.

Zhang, X., Yang, H., Adaikalaraj, P.F.B., Low, Y.M. & Koh, C.G. 2017e. Structural reliability analysis for offshore drilling riser deployment operability. In Proceedings of the ASME 2017 36th International Conference on Ocean, Offshore and Arctic Engineering (OMAE2017), Trondheim, Norway, 25-30 June 2017. (OMAE2017-61575).

Zhang, Y., Huang, Y. & Meng, F. 2017f. Ultimate strength of hull structural stiffened plate with pitting corrosion damage under unaxial compression. Marine Structures 56(1): 117-136.

Zheng, C., Kong, X.S., Wu, W.G. & Liu, F. 2015. An analytical method on the elastic-plastic response of clamped stiffened plates subjected to blast loads. In Proceedings of the 25th International Ocean and Polar Engineering Conference (ISOPE2015), Kona, Big Island, Hawaii, USA, 21-26 June 2015. pp. 824-828.

This page intentionally left blank

Proceedings of the 20th International Ship and Offshore Structures Congress (ISSC 2018) Volume I – M.L. Kaminski and P. Rigo (Eds.)

doi:10.3233/978-1-61499-862-4-255

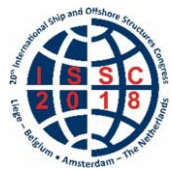

COMMITTEE II.2

DYNAMIC RESPONSE

COMMITTEE MANDATE

Concern for the dynamic structural response of ships and offshore structures as required for safety and serviceability assessments, including habitability. This should include steady state, transient and random response. Attention shall be given to dynamic responses resulting from environmental, machinery and propeller excitation. Uncertainties associated with modelling should be highlighted.

AUTHORS/COMMITTEE MEMBERS

Chairman: A. Ergin
E. Alley
A. Brandt
I. Drummen
O. Hermundstad
Y.C. Huh
A. Ivaldi
J. H. Liu
S. Malenica
O. el Moctar
R.J. Shyu
G. Storhaug
N. Vladimir
Y. Yamada
D. Zhan
G. Zhang

KEYWORDS

Dynamic response, slamming, whipping, springing, hydroelasticity, vibration, sloshing impact, noise, underwater noise, blast, explosion, shock, wind, wave, current, internal flow, propeller, machinery, vortex, model tests, full-scale measurement, monitoring, uncertainty, fatigue, damping, acceptance criteria, countermeasures.

CONTENTS

1. INTRODUCTION 258

2. SHIP STRUCTURES 258
2.1 Wave-induced vibrations 258
2.1.1 Full-scale measurements 259
2.1.2 Model tests 261
2.1.3 Analysis methods 264
2.2 Machinery- and propeller-induced vibrations 266
2.2.1 Propeller-induced vibration 266
2.2.2 Machinery-induced vibration 267
2.3 Sloshing impact 268
2.3.1 Experimental approaches 269
2.3.2 Numerical modelling 270
2.4 Shock response 271
2.4.1 Air blast 271
2.4.2 Underwater explosion 272
2.5 Noise 274
2.5.1 Interior noise 274
2.5.2 Air radiated noise 275
2.5.3 Underwater radiated noise 276
2.6 Damping and countermeasures 277
2.7 Monitoring 280
2.7.1 Definitions 280
2.7.2 Hull monitoring rules 280
2.7.3 Hull monitoring suppliers 282
2.7.4 Digitalization 282
2.8 Uncertainties 283
2.9 Standards and acceptance criteria 285
2.9.1 Wave-induced vibrations 285
2.9.2 Noise 287
2.9.3 Sloshing impacts 287

3. OFFSHORE STRUCTURES 287
3.1 Wave-induced vibration 287
3.2 Wind-induced vibration 288
3.3 Vortex-induced vibration 290
3.3.1 Experimental studies 290
3.3.2 Semi-empirical methods 292
3.3.3 Numerical methods 292
3.4 Internal flow-induced vibration 293
3.5 Equipment-induced vibration 294
3.6 Shock and explosion 295
3.7 Noise 295
3.7.1 Pile-driving-induced underwater noise 296
3.7.2 Mitigation of pile-driving-induced underwater noise 296
3.8 Damping and countermeasures 297
3.9 Monitoring 298
3.9.1 Goal and scope 299
3.9.2 Fatigue crack monitoring 299
3.9.3 Subsea monitoring 299
3.9.4 Monitoring of offshore wind turbines 300
3.10 Uncertainties 300

3.11 Standards and acceptance criteria 300
3.11.1 Wave-induced vibrations 300
3.11.2 Vortex-induced vibrations 301
3.11.3 Noise and vibration 301
3.11.4 Underwater noise 301

4. BENCHMARK STUDY 302
4.1 Introduction 302
4.2 Benchmark setup 302
4.3 Experimental results 303
4.4 Methods 303
4.5 Results 305
4.6 Conclusions 309

5. CONCLUSIONS 311

REFERENCES 314

1. INTRODUCTION

The content of this committee's report is dictated by its mandate and the expertise of its membership. Its structure and content follow along similar lines to that adopted in previous ISSC reports (ISSC 2015). This report examines state of the art methods and techniques in the field of dynamic responses of ships and offshore structures and assesses progress made in this subject area with a critical review of recently published material.

The subject areas undertaken by specialist task committees of ISSC 2018: Experimental Methods (V.2), Offshore Renewable Energy (V.4), Arctic Technology (V.6) and Subsea Technology (V.8), have an impact on the committee's mandate, which affects content of this report. Ice induced vibration have been entirely omitted because that is covered elsewhere (V.6 Arctic Technology). The subject areas of vortex induced vibrations, equipment induced vibrations, subsea and offshore wind turbine monitoring have been reviewed.

This report is subdivided, at the highest level, into two main sections (Sections 2 and 3) concerning the dynamic response of ships and offshore structures, respectively. Section 2 on ship structures is subdivided into sections that range from wave-induced vibration to standards and acceptance criteria. Particular attention is also paid to wave-induced vibration, machinery and propeller induced vibrations, sloshing impact, shock response, noise, damping and countermeasures, monitoring and uncertainties since they are considered as the main topics of this area. The section on offshore structures (Section 3) is further subdivided into eleven subsections. The section treats dynamic response to environmental excitations such as wave, wind, vortex, and operational excitations, such as internal flow and equipment. Specialist offshore topics of monitoring, noise, shock and explosion are also evaluated in Section 3.

Finally, this committee has undertaken a benchmark study regarding whipping responses, with a special focus on nonlinear strip theory and panel methods. The degree of variation in estimates produced by different methods and organizations is revealed, and comparisons with model test measured responses are provided.

2. SHIP STRUCTURES

2.1 Wave-induced vibrations

The influence of hydroelasticity on the global structural response of ships might become very important for some operating conditions. This is particularly true for very large ships for which the structural natural frequencies fall into the range of encounter frequencies, leading to a risk of hydroelastic resonance. This phenomenon is usually referred to as linear springing. Additionally, nonlinear or sum frequency springing may occur in a case where the wave excitation forces act with a higher order of the encounter frequency. On the other hand, the impulsive forces, arising from slamming, green water, underwater explosion, etc., can induce significant hydroelastic responses, regardless of the natural frequencies of hull structure. Indeed, the intensity of hydroelastic response depends mainly on the ratio between the duration of the impulsive force and natural period of hull structure. This phenomenon is usually referred to as whipping, and, contrary to springing, it is transient and usually occurs in heavy sea states. Therefore, its influence on the ship design is important with regard to the fatigue and extreme loading.

Full-scale measurements and model tests have been extensively conducted in recent years. These tests and measurements were mainly focused on unconventional large ships such as Very Large Container Ships (VLCS) and Ultra Large Container Ships (ULCS). These ships have pronounced bow flare and high speeds (over 20 knots). They also have relatively low natural frequencies. Much research has also focused on the effect of hydroelastic responses on fatigue performance of the ship structures.

2.1.1 Full-scale measurements

Results from several full-scale measurement campaigns have been reported. The focus has been on the effect of wave-induced vibrations on fatigue and extreme loading. Some campaigns are old and can be found in previous ISSC reports. However, some of the recent work present the analysis of these data with new and refreshing objectives. A list of recently reported measurements is given below:

- 2800 TEU container ship (Gaidai et al., 2016)
- 2800 and 4440 TEU container ships (Mao et al., 2015b)
- 4400, 8600, 9400 and 14000 TEU container ships (Andersen, 2014)
- 8400 and 8600 TEU container ships (Storhaug & Kahl, 2015)
- 8600 TEU container ship (Barhoumi & Storhaug, 2014)
- Several container ships (Storhaug, 2014a)
- 14000 TEU container ship (Ki et al., 2015)
- 4600 and 14000 TEU container ships (Kahl et al., 2015)
- 8600, 9400 and 14000 TEU container ships (Andersen & Jensen, 2015)
- 4600 and 14000 TEU container ships and a LNG carrier (Kahl et al., 2016)
- 56 m naval high speed light craft (Magoga et al., 2016)
- Several container ships and blunt ships (Storhaug et al., 2017b)
- 210 m Ro-Lo ship (Orlowitz & Brandt, 2014)

Reporting the contribution of wave-induced vibrations to fatigue damage in deck amidships has started to become a standard. Storhaug (2014a) summarized the results from seven container ships ranging from 2800 to 14000 TEU. The vibration damage contribution was in the range of 26 to 57% of the total fatigue damage, with a tendency of larger ships to vibrate more. Storhaug & Kahl (2015), on the other hand, reported a contribution of 36 to 42% on an 8400 TEU vessel on worldwide trade, and 56 and 61% on an 8600 TEU vessel on Asia to Europe and North Pacific trade, respectively. The latter ship had a high bow flare angle, but the results suggest that vibration damage is not sensitive to trade. Barhoumi & Storhaug (2014) studied the wind heading effect on the same 8600 TEU vessel, confirming that head and bow quartering seas dominated the fatigue and vibration damage contributions. They also observed that vibrations contribute significantly to fatigue damage in other headings including stern seas. This was also confirmed for a gas carrier by Storhaug & Kahl (2016). Ki et al. (2015) reported 50% contribution to the fatigue damage on a 14000 TEU vessel on Asia to Europe trade, for which Kahl et al. (2015) reported 57%. On a 4600 TEU vessel in worldwide trade, Kahl et al. (2015) reported 35% contribution to the fatigue damage (at 0.43L). Kahl et al. (2016), on the other hand, reported less vibration damage in the forward and aft regions of the same vessel (26% at 0.35L and 20% at 0.75L). This suggests that vibration damage is highest where the wave bending stress tends to be highest. Storhaug (2014a) also reported model test results of container ships in head seas, suggesting conservative estimates by head sea model tests compared to full scale.

In all cases above, Rainflow counting and Miner's sum have been used. Kahl et al. (2015) carried out fatigue tests based on measured whipping time series. It was confirmed that the contribution of vibrations was well reproduced with the combination of Rainflow counting and Miner's sum. The main contribution to vibration damage came from the low frequency loads, while the additional vibration cycles gave an insignificant contribution. This suggests that an equivalent low frequency wave load can be a useful approach in ship structural design. Kahl et al. (2015, 2016) also showed that most of the fatigue damage comes from the lower

frequency part of the stress spectra, despite the fact that the difference between spectra with and without vibration is relatively large at higher stress levels. Storhaug & Kahl (2016) showed that vibration damage and total fatigue damage on a gas carrier mostly came from head seas with 5 meters significant wave height.

Storhaug & Kahl (2015, 2016) and Kahl et al. (2016) refer to approved standard hull monitoring systems and recommend that fatigue rates be displayed onboard for easy understanding. The fatigue rate is defined as the ratio between the measured fatigue damage and the budget damage for a time interval, which is typically half an hour. For instance, if the fatigue rate is 90 over a day, it means that 3 months of fatigue budget is spent. Hull monitoring is used more frequently than full-scale measurements, and a mature bridge display can close the gap between design and operation, including the effect of wave-induced vibration.

Whipping contribution on extreme wave bending at amidships is another reported standard result. Storhaug & Kahl (2015) reported 48 to 59% increase in hogging for the 8600 TEU vessel and 25% for the 8400 TEU vessel with lower bow flare angle. Barhoumi & Storhaug (2014) illustrated that the IACS URS 11 dynamic hogging level was exceeded by 50% at the aft quarter length of the 8600 TEU container ship, due to whipping. That corresponds to a location where MSC Napoli broke in two. Ki et al. (2015) measured only a utilization of 45% in hogging and 76% in sagging on the 14000 TEU vessel during a short measurement period with a maximum significant wave height of 6.5 meters. Horizontal bending and torsion were however more utilized by 95% and 83%, respectively, suggesting that worst sea state was not head seas. Andersen (2014) studied several container vessels: 4400, 8600, 9200 and 14000 TEU container ships. The main conclusions are summarized as follows: Whipping can amplify the wave bending with up to 100% or more; the hogging moment may be as large as the sagging moment; and the governing vibration mode is 2-node vertical bending mode in bow quartering seas. Kahl et al. (2016) illustrated that, on a gas carrier with a hull monitoring system, the crew managed to keep the maximum wave bending moment with whipping below 80% of the rule level (first warning level), except in one half hour during 5 years where it reached 100% of the rule level (second warning level). This suggested that the hull monitoring system worked as intended and probably prevented the loading from exceeding the rule levels.

Torsional response on container ships is regarded as an important design issue. Storhaug & Kahl (2015) confirmed an increase of about 5% in the maximum torsional response due to torsional vibrations measured on a transverse deck strip on two container vessels, i.e. 8400 and 8600 TEU container ships. The vibration damage contribution was about 15-16% and 52-55% on the 8600 TEU and 8400 TEU vessels, respectively. This is the first time that torsional vibration was regarded as significant on a vessel. Ki et al. (2015) investigated the 14000 TEU vessel and estimated the torsional vibration damage as being 13% on the hull girder and up to 25% on the hatch corners. Kahl et al. (2015), however, claimed that, at the inner hatch corners on this 14000 TEU vessel, the torsional vibration was insignificant. Mao et al. (2015b) performed full-scale measurements on 2800 and 4400 TEU ships. Fatigue contributions from vertical bending, horizontal bending and torsion were studied utilizing a finite element model in one sea state, and linear regression analysis was used to obtain relations between wave loads and stresses. It was shown that high frequency warping and horizontal bending account for 10-15% of the vibration damage in the deck area. For structural details in the inner side areas, the vibration damage increases to 30% and 50%, respectively, due to the warping and warping combined with horizontal bending for the 4400 TEU vessel.

Damping affects the vibration levels for fatigue and extreme loading. By analyzing time series of the 8400 and 8600 TEU vessels, Storhaug & Kahl (2015) concluded that the effect of torsional vibration on fatigue was more significant on the 8400 TEU vessel having a structural damping (5% of critical damping) half that of the 8600 TEU vessel (10%). The reason for differences in damping on the similar vessels was not clear. Storhaug & Kahl (2016) estimated the damping for torsional vibration of an ultra-large container ship to be 5.3% of the criti-

cal damping at a frequency of 0.28 Hz. Storhaug et al. (2017b) compared six damping estimation methods with artificial data. The methods used time series mainly collected from approved hull monitoring systems of 21 ships, such as slender container ships, blunt oil tankers, ore carriers and gas carriers. For the 2-node vertical mode, the container ships had the highest damping, with an average level of 1.7 %. For the blunt ships, the average damping was estimated as 0.7 %. These values were proposed as target values for numerical analysis. It was also observed that there were no strong effects of vessel size, speed or amplitude dependence (nonlinear effects); however, uncertainties on these parameters were significant. Orlowitz & Brandt (2014) estimated the damping ratios for two node vertical mode of a 210 m long Ro-Lo ship to vary from 0.48 to 1.62% under three different operating conditions (cruising speeds of 0, 10 and 18 knots), showing significant increase in damping at the cruising speed of 18 knots. At the cruising speed of 18 knots, the frequency was also reduced by about 15%.

There are, unfortunately, examples where wave-induced vibration effects are either not estimated or excluded even though measured. Thompson (2016) used full-scale measurements to validate spectral fatigue analysis of a warship. A high sampling rate was used, but whipping was filtered away despite the recommendation of Sheinberg et al. (2011) that it be included. Magoga et al. (2016) compared measured and design stress spectra (load histogram) for fatigue analysis of a 56 m patrol boat. The 2-node vertical vibration mode at 5 Hz was included, and Rainflow counting was used for cycle counting. It was concluded that the stress spectra were well below acceptable levels, only up to about 45% of rule values during 4500 hours of measurements. The shape of the stress spectra was not represented by a Weibull shape parameter of 1.0, i.e. 2-parameter Weibull distribution with Weibull slope of 1.0, and design stress spectra was considered as conservative, possibly due to less severe trade than assumed in design.

Statistical considerations of the measured data are not frequently encountered. However, Gaidai et al. (2016) considered measurements on a 2800 TEU container ship operating in the North Atlantic. A bivariate Average Conditional Exceedance Rate (ACER) function was used to study the joint probability of deck stresses at amidships and aft quarter length. Jensen et al. (2014) carried out extreme value prediction using the Peak Over Threshold method (POT) and individual peak distribution in combination with Gumbel extreme value distribution. The POT method was regarded as the most useful and had the closest agreement with the measurements of a 9400 TEU vessel. Andersen & Jensen (2015) performed extreme value analysis on three container ships with load carrying capacities of 8600, 9400 and 14000 TEU, respectively, adopting the POT method and Gumbel extreme value distribution. The extreme value distributions, compared to URS11 rule values in hogging, suggested that there is a relatively high likelihood of exceeding the URS11 reference value. Clustering effects were also studied using the ACER function. The effect of clustering was confirmed for the 9400 TEU container vessel. Simple theoretical formulas were found suitable for moderate exceedance levels, but they cannot capture clustering effects. Andersen (2014) concluded that, for statistical extrapolation, there is no perfect method that fits all measurements, but the POT is regarded as a necessary starting point while the extreme value distribution needs to be confirmed useful.

2.1.2 Model tests

The effect of wave-induced vibrations in ship hull structures can be quantified by performing model tests, where the flexibility of the ship hull is also modeled. The most common way of doing this is to make a segmented, flexible backbone or hinged model. The main advantages of the former method are that the elastic backbone ensures a continuous stiffness distribution and that the strains are easily measured by strain gauges glued on to the beam. The hinged models consist of segments connected by rotational springs. With this method, it is reasonably straightforward to make a model with adjustable stiffness as, for instance, done by Drummen (2008). Data from Drummen (2008) were also used for the benchmark study that is presented in Chapter 4. A drawback of the segmented models with rotational springs is that the number of locations, where the forces can be measured, is limited.

Fully flexible models are basically a better representation of reality. There have, however, been a number of drawbacks with this modeling technique. The most important ones are cost and difficulties associated with building such models. A thorough review of the early use of fully flexible models was given by Wu et al. (2003). Since then, significant developments have been achieved in rapid prototyping. In order to see whether rapid prototyping could be a powerful tool for making a fully flexible model achievable, Bennett et al. (2015a), investigated the use of three-dimensional (3D) printing technologies for manufacturing structurally accurate flexible models. They discussed several 3D printing methods. All of these methods have constraints with regard to printer bed size. This results in the need to develop a modular approach for the construction of a ship model. For a typical example, the authors obtain a relation between model size and number of modules. For the same example, requirements for global and local scaling were discussed. From their work, the authors concluded that 3D printing is something that will enable fully flexible models to be realized in the future. Currently, however, the technique is not ready yet to be practically used. On the other hand, how fully flexible models perform in terms of modal damping has not been discussed yet.

Some tests with segmented models referenced in the open literature are as follows:

- 321 m long 10000 TEU container ship (Kim et al., 2015a, 2015c; Hong et al., 2015)
- 425 m long 500000 DWT ore carrier (Li et al., 2016b)
- 350 m long 450000 DWT ore carrier (Kim et al., 2015e)
- 112 m long catamaran (Lavroff et al., 2017; Davis et al., 2017).

The 321 m long container ship was tested as part of the WILS (Wave-Induced Loads on Ships) JIP (Joint Industry Project) at KRISO (Korea Research Institute of Ships and Offshore engineering). The model was made of six segments connected with a U-shaped steel backbone. The backbone was instrumented with more than 100 strain gauges to measure structural responses. The bow-flare and stern slamming loads were measured by distributing a number of load cells on the bow-flare and stern areas. The model was tested in regular and irregular waves with various speeds and relative wave headings. Kim et al. (2015c) used the data from the model tests to determine a correlation between slamming impact and whipping vibration. Their results, among others, confirmed that the impact force was proportional to the square of the water entry velocity. It was furthermore observed that, in regular waves and high speed conditions, the vertical bending moment due to the global flexural response was proportional to the slamming force. In irregular waves, it is more difficult to draw conclusions because of the difficulty in distinguishing between springing and whipping. Based on the same data, Kim et al. (2015a) performed an observational study and confirmed the presence of higher order harmonics in both vertical bending and torsional vibrations. Hong et al. (2015) also used the same data and studied the bow slamming loads. They found that it is not only the vertical relative motion but also the instantaneous longitudinal velocity that determines the impact force. This explains the high impact loads due to horizontal relative velocity induced by steep wave and ship forward velocity.

The 425 m long ore carrier was tested at the Harbin Engineering University towing tank. The model consisted of nine segments that were connected to a flexible backbone. The backbone was made up of four different beams. Three backbones with different stiffness values were investigated. The model was tested by Li et al. (2016b) in regular head waves. The periods of the regular waves were chosen such as to excite linear, second and third order springing. Their work confirmed that, as the stiffness and the natural frequency of the flexural vibration modes decrease, the importance of springing becomes more relevant.

Kim et al. (2015e) investigated an ore carrier of 350 m. The model consisted of six segments connected to a backbone. The backbone system is a tripod type truss structure, and a special connection structure was inserted at each connection so that the stiffness of the connection could be adjustable, allowing tuning of the natural frequency of the model. The model was tested in irregular head seas. The measured response was expressed in terms of a quadratic

Volterra series. From this study, it is found that the quadratic part of the global flexural response is comparable to the linear part and that the quadratic part tends to increase with increasing wave height.

Lavroff et al. (2017) tested a model of a 112 m long catamaran in regular head waves in the towing tank at Australian Maritime College, University of Tasmania. The model was made up of six segments; the midsection, two aft sections, two forward demi-hull segments and a separate bow segment. Hollow aluminum beams were rigidly mounted into the segments. Dedicated link elements were designed to connect the hollow beams and thus the natural frequency of the global vibration modes could be tuned. The damping of the model was recorded and turned out to be realistic when compared to full-scale results. During the model tests, a scale slam force equivalent to 2150 tons for the 112 m ship was measured. The contribution of the high frequency response was not mentioned. Davis et al. (2017) tested the same model in irregular head waves. From the tests slam loads, up to 132% of the hull weight were measured. The slam loads had a time scale similar to the period of the lowest global flexural vibration mode, indicating that a hydroelastic representation at model scale is also essential.

Storhaug (2014b) used data from model tests performed for 4400, 8600 and 13000 TEU container ships. The data was used for extrapolation to relevant durations for different sea states. The main question was what the dimensioning sea state is for a container vessel when whipping is included. From this study, it is concluded that it is not the highest sea states that lead to the highest bending moments. Due to the longer time spent in moderate sea states, maximum wave heights are dimensioning in these sea states. By comparing the extrapolations of the three vessels, it was found for whipping that vessel size is not a key factor, but bow flare angle is. There are, on the other hand, uncertainties associated with extrapolation methods. Therefore, Storhaug & Andersen (2015) studied four different extrapolation methods. The differences between the extrapolated values are observed as considerable. This suggests that it is necessary to be careful when selecting an extrapolation method. Due to its simplicity and reasonable accuracy, the method used by Storhaug (2014b) is regarded as useful. The ACER method developed by Naess & Gaidai (2009) is regarded as the most accurate one. The conclusions from Storhaug & Andersen (2015) still support those of Storhaug (2014b) that the moderate sea states from 7 to 9.5 m are dimensioning for the container ships. The model test results for the13000 TEU container ship were used by Zhu & Moan (2015) to investigate the effect of heading. For ships up to 200 m, the largest vertical bending moments typically occur in head waves. As the ship length increases to 300 m or above, vertical bending moments in oblique waves become significant.

Identifying slamming events in a robust manner is not a trivial task. In order to do this from vertical bending moments measured in model or full-scale tests, Dessi (2014) proposed two new approaches. The first approach uses wavelet analysis to derive the vertical bending moment time series at the frequency of 2-node vertical vibration mode. In the second approach, the time series of vertical bending moment is band-pass filtered. Subsequently, the envelope is calculated with a Hilbert transform. It is concluded that both methods can be used to assist determining the occurrence of slamming.

Panciroli & Porfiri (2015) used particle image velocimetry (PIV) during impact tests with a compliant wedge with varying water entry velocities. In this way, the pressure field is indirectly measured. Their investigation showed that the wedge flexibility strongly influences the hydrodynamic loading. The hydroelastic impact is found to be repeatable, both in terms of structural dynamics and hydrodynamic loading, confirming the feasibility of PIV-based pressure reconstruction in water entry problems.

An important recommendation for future model tests is that damping should be added for container vessels. In general, the damping ratio in model tests is found to be too low.

2.1.3 Analysis methods

The numerical modeling of springing and whipping is extremely complex since it requires full coupling of the hydrodynamic and structural solutions at each time step of the simulation. The most common hydroelastic models involve a structural model of the ship, a hydrodynamic model of the fluid and a coupling method ensuring that the interaction effects are properly accounted for. The structural model is usually a 3D Finite Element Model (FEM) or a beam model (Euler-Bernoulli, Timoshenko, Vlasov), and the fluid-structure coupling effects are commonly calculated by using the potential flow theory. Available modeling approaches are summarized in Table 1.

Fluid structure coupling effects are basically calculated by using two distinct approaches, namely strip theory and 3D Boundary Integral Equation (BIE) method. All these methods were established well before the year 2014, and no major improvements have been made since then. Most of the recent work concentrates on using those methods for practical applications. As far as the strip theory is concerned, there exist different variants which are in use for hydroelastic analysis (Bennet et al., 2015b; Cristea et al., 2015; Dhavalikar et al., 2015; Heo et al., 2016; Kawabe et al., 2016; Liu et al., 2017b; Matsui et al., 2016; Rajendran et al., 2016; Wang et al., 2016a; Wu, 2015). Strip theory formulations differ from each other according to the ways of accounting for nonlinear wave effects and forward speed.

Regarding 3D hydrodynamic seakeeping models, there are many variants which are proposed by, for instance, De Lauzon et al. (2015a), Im et al. (2016), Kashiwagi et al. (2015), Kim et al. (2015f), Kim & Kim (2014, 2016), Lee et al. (2015d), Malenica et al. (2015), Ren et al. (2016), Senjanovic et al. (2014), Shan et al. (2017), Southall et al. (2016), Yang et al. (2015b), Zhang et al. (2015, 2016a). These 3D seakeeping models differ in many aspects as indicated in Table 1. The degrees of accuracy and theoretical consistency vary from case to case but there is no clear candidate for the most efficient solution. For ships carrying liquid cargo such as LNG ships and tankers, it is also interesting to mention the work of Malenica et al. (2015), where, in addition to the global hydroelastic interactions, the local interactions within the tanks are also taken into account.

With regard to slamming, the situation is even worse because, within the potential flow theory, there is no consistent numerical model for 3D slamming. Therefore, 2D strip approach is mainly used in combination with strip theory models as well as with 3D seakeeping models. There are basically two 2D models, which are usually employed in analyses. The first one is the so called momentum theory approach, sometimes referred to as von Karman model. Due to its simplicity, this model is used in most of the numerical whipping codes either in combination with strip theory or 3D BIE based seakeeping codes. The second one is the Generalized Wagner Model (GWM). Within this model, the body boundary condition is imposed on the actual position of the entering surface. The GWM slamming model is used, for instance, by De Lauzon et al. (2015b), Kim et al. (2015b, 2015f) and Malenica et al. (2015). Some improvements were, however, proposed recently by De Lauzon et al. (2015b), Khabakhpasheva et al. (2014) and Helmers & Skeie (2015). It is also worth mentioning the method proposed by Lee et al. (2015d) and Southall et al. (2016), where 2D slamming simulations are performed by using CFD (OpenFoam) and coupled with the global hydroelastic model based on 3D potential flow theory. It is, however, not clear if this approach is fully consistent, because the interaction between the potential flow and CFD is not considered at each time step. With respect to slamming, it is also important to mention the determination of input parameters which should be given to slamming modules, i.e. the relative geometry before impact and the relative impact velocity. These modules, therefore, use only incident wave geometry and kinematics for predicting slamming induced forces, and thus, the effect of perturbation waves is ignored. It should also be noted that the relative impact velocity represents the mean velocity of the impacting section, and it does not include the changes in local flow. This is to say that the slamming impact is modeled as an impact on calm water. Finally, it is also important to mention that, most often, the water exit phase is either not modeled or modeled approximately (see, for instance, De Lauzon et al.,

2015b). All of these considerations point to the enormous difficulties related to the correct evaluation of slamming loads.

Table 1. Numerical whipping models based on potential flow hydrodynamics.

SEAKEEPING	Basic model	2D strip theory
		Full 3D
	Forward speed approximation	Encounter frequency
		Forward speed
	Linearization procedure	Uniform flow
		Double body flow
		Other
	Time integration	Direct
		Hybrid: Frequency + Time (Cummins approach)
	Numerical method	Rankine singularities
		Kelvin singularities
		Other
	Nonlinearities	Linear
		Weakly nonlinear FK - Incident
		Weakly nonlinear FK - Incident + perturbed
		Other
	Wave modelling	Regular waves
		Irregular waves
	Handling of horizontal motions	Lagrange multipliers
		Springs
		Other

SLAMMING	Theoretical model	Von Karman (or momentum theory)	
		GWM (Generalized Wagner Model)	
		Other (MLM, wedge…)	
	Sections orientation	Vertical	
		Inclined	
	Relative velocity	Wave	Incident wave
			Incident + perturbed wave
		Body	Rigid body
			Rigid + Elastic body

STRUCTURE AND COUPLING	Structural model	3DFEM
		Beam (Timoshenko …)
	Method of solution	Modal
		Direct
	Coupling principles	Weak (one way)
		Strong (two way)

In spite of all the developments on 3D seakeeping models using potential flow theory, it is fair to say that none of the proposed methods can fully and consistently model all the nonlinear aspects of the seakeeping in large waves. In principle, the 3D seakeeping models are more consistent and accurate, at least for springing analysis, but their use for whipping is conditioned by the limitations of 2D slamming models. Having said that, most of the studies report quite good comparisons with experimental results, especially in head waves, where the physical situation is simpler and the approximations, such as weakly nonlinear potential flow and 2D slamming conditions, are more likely to be valid.

Due to the limitations of the potential flow models, there are currently more developments on the seakeeping models that use CFD approaches. The CFD models are based on solving the Navier-Stokes or Euler equations using the so-called field methods (finite volumes, finite differences, particle methods), and they are in principle supposed to model any flow situation, provided that a sufficient number of cells is adopted. Due to the developments in numerical methods and computer power, it is now possible to run very complex seakeeping simulations in large waves in an efficient and theoretically consistent way. The price to pay (CPU time and engineering effort) is still large, but at least something more reasonable and more consistent can be done. This is particularly true for the predictions of slamming forces, which is one of the main drawbacks of the potential flow models. The CFD software, which is used most often for these applications, is the open source CFD code OpenFoam (see, for instance, Craig et al., 2015; el Moctar et al., 2017; Oberhagemann, 2016; Oberhagemann et al., 2015; Seng et al., 2014), but the use of the commercial CFD code StarCCM+ is also reported, for instance, by Kim (2015), Lakshmynarayanana et al. (2015) and Takami et al. (2017). In addition, the in-house code ICARE, which is based on the finite difference method, was used in Robert et al. (2015). The use of the CFD based numerical codes for seakeeping is relatively new, and there is considerable work ongoing in this area. These models will certainly play an increasingly important role in the future regardless of the expense because they seem to be the only possible way to include all the important aspects of whipping.

On structural side, the use of a beam model is reasonably justified due to a limited number of structural modes involved, especially when only bending is of concern. In case of more com-

plex situations, such as the torsional vibrations of ships with open cross sections (container ships), either a 3D FE model (Im et al., 2016) or an improved beam model (Senjanovic et al., 2014) should be adopted. 3D FE models are more robust, not only because the structural behavior is better represented but also because it allows for direct evaluation of the structural stresses at any particular point within the structure (see, for instance, Malenica & Derbanne, 2014; Im et al., 2016).

Finally, concerning the coupling procedures which are usually employed for modeling the hydroelastic interactions, the most common approach is the so-called modal approach because it is cheaper and simpler to put into practice. It seems that all of the numerical codes which are mentioned here use the modal approach either in combination with a beam or 3D FE model. This is true for all the seakeeping solvers that are based on potential flow theory or CFD (Seng et al., 2014). It is important to note that, within the modal approach, special care should be given to proper separation between the dynamic and quasi-static responses (Malenica & Derbanne, 2014). It also has to be said that some numerical codes, especially those based on commercial CFD software, use the so-called weak (or one way) coupling procedures, because the full coupling appears to be more difficult to realize.

2.2 Machinery- and propeller-induced vibrations

It is well-known that there are two major sources within a ship that induce vibrations under normal operating conditions on voyage: namely, main engine and propeller.

As for propeller-induced vibrations, accurate prediction of propeller forces is essential in the assessment of the design of ship structures. For the past three years, there have been several attempts for accurate prediction of propeller-induced hydrodynamic forces in actual operating conditions. Meanwhile, special devices have also been used to reduce the propeller-induced forces in a ship, and some of them have succeeded in validation of their effectiveness in full-scale tests. Furthermore, many researchers have paid attention to the dynamic interaction problem between the ship hull structure and propulsion shafting system.

As for engine-induced vibrations, in the period of this report, no major development has been reported in the open literature on numerical methods for vibration response analysis; most of the attention has been paid to vibration control and vibration reduction techniques. There is rather a small number of references to machinery-induced vibrations compared to other vibration sources as, for instance, wave-induced vibration. However, the topic is expected to come in focus again, primarily due to the introduction of so-called Comfort Class that was first introduced by DNV-GL in January 2011, and later by LR and BV, as other Classification Societies followed the DNV-GL breakthrough. The Comfort Class (requirements for the noise, vibration and indoor climate on board) is applicable to passenger and cargo ships, and it is more restrictive than Safety Class, forcing researchers to pay additional attention to machinery-induced vibrations.

2.2.1 Propeller-induced vibration

A group of studies has been reported on the numerical accuracy of propeller induced forces by using enhanced source models and considering actual ship motions in waves. Kim et al. (2014a) studied the hydrodynamic characteristics of non-cavitating propellers. In this study, an advanced source model is proposed based on the lifting surface theory, by considering source strength, its position and axial direction as unknown parameters. The matched-field inversion method is employed to find the unknown parameters. They calculated the pressure fluctuations on the hull based on the proposed model and showed that the results are in good agreement with measurements from model scale experiments. Finally, they concluded that the proposed source model is practically useful in predicting propeller induced forces at the early design stage. Abbas et al. (2015) presented a hybrid URANS (Unsteady Reynolds Averaged Navies Stokes) - LES (Large Eddy Simulations) model for prediction of unsteady forces on marine propellers, caused by the operation of propellers in non-uniform wake flows. From the

numerical simulations, strong thrust fluctuations up to 13% of the mean thrust is obtained. They concluded that a hybrid model is necessary to identify peak loading on marine propellers. Taskar et al. (2017) studied the propeller performance in terms of cavitation, pressure pulses and efficiency, not in calm water condition but in actual operating conditions. An 8000 DWT chemical tanker equipped with a twin-podded propulsion system is employed as a case vessel in this study. The effects of various factors affecting propeller performance in waves, such as wake variation, ship motions and speed fluctuation, are investigated using a propeller design software based on the vortex lattice theory. It is found that cavitation and pressure pulses due to wake variation increase substantially and that the effects of other factors are relatively small.

There have been several attempts to reduce pressure fluctuations on hulls or improve hydrodynamic performance of marine propellers by applying practical devices to the stern area of a ship, such as air-balloon or Rim Driven Thruster (RDT). Lee et al. (2015c) presented a design of rubber membrane filled with air near the propeller, which plays a role similar to a dynamic damper at the target frequency. The rubber membrane is fixed to the outer hull surface near the propeller, and its effectiveness is validated by pressure and acceleration measurements in a sea trial. They confirm that the amplitude of hull pressure is reduced and that the resultant vibration response decreases by more than 60%. Chen et al. (2017) calculated the hydrodynamic pressure acting on the blade surface of RDT, using the correlation method based on strip theory. Applying the calculated hydrodynamic pressure to each blade as excitation, the forced vibration response of the RDT is obtained and compared with that of the traditional Shaft Driven Propeller (SDP) with the same blade configuration. It is shown that the resonant amplification of the RDT in the unsteady thrust is still lower than that of the SDP by about 15 - 20 dB.

Conventionally, the shaft forces are mainly responsible from three different modes of shaft vibration in a marine propulsion system: namely, axial, whirling and torsional vibrations. Recently, it has been reported that the hull deformation may seriously change the mounting positions of shafting system, and the ship could not normally be operated under this condition (Leontopoulos, 2006). The shaft forces may also cause unwanted vibrations in the shaft system, owing to the coupled vibration with the hull structure. Zou et al. (2015b) investigated the nonlinear characteristics of a marine propulsion shaft, of which motion is coupled in longitudinal and transverse directions. The nonlinear equation of motion and its solution are obtained by Hamilton's principle and the Galerkin method, respectively. They showed that the bearing support stiffness, propeller mass and slenderness ratio have strong effects on the nonlinearity. Therefore, in whirling vibration analysis of such marine shafts, the nonlinear effects should be considered. Qu et al. (2017) developed a fully coupled vibro-acoustic model between a propeller shaft and a submarine pressure hull for predicting the coupled dynamic response induced by the propeller excitation. The entire structural system consisted of a rigid propeller, a main shaft, bearings and an orthogonally stiffened hull structure. The rings and stringers in the pressure hull are modeled as discrete structural elements. Through the numerical simulations, it is shown that both the axial and vertical stiffness of the bearings have significant effects on the dynamic response of the coupled system. Huang et al. (2017) developed coupled equations of torsional and longitudinal shaft vibrations. Based on this model, the natural frequencies and maximum accelerations in each direction were obtained. It is found that the natural frequencies are not affected significantly by the rotational shaft speed as well as the loading conditions. Meanwhile, the maximum acceleration increased with increasing rotational speed.

2.2.2 Machinery-induced vibration

As mentioned above, in the field of engine induced vibration, compared to other dynamic response issues inherent to ship, there is a relatively small number of publications. Han et al. (2015) estimated the fatigue life of a propulsion shaft from torsional vibration measurements, using the linear damage summation law. The torsional vibrations were measured using strain

gauges on the gear input shaft of the engine. The fatigue life of the reduction gear input shaft was estimated by using the Soderberg's safety evaluation method.

Most of other related references are devoted to dynamic response control, as also indicated in a special chapter dedicated to ship vibration and noise control in a book by Bai & Liang (2016). In this respect, Cinquemani & Braghin (2017) presented the design of an active standalone device to suppress vibrations on cruise ship funnels, generated by engines and exhaust stacks. The effectiveness of the device was confirmed by experiments. Guo et al. (2017) developed a model for coupling shaft torsional vibration with a speed control system for an engine, claiming that neglecting the coupling may lead to serious vibrations. The authors also state that, using their model, the speed control parameters can be tuned to predict a stable and safe-running condition for a diesel engine.

As part of recent efforts to reduce emissions and fuel consumption, ultra-long stroke engine (hereafter G-type engines) are now commonly used in eco-ships (Kim et al., 2017d). The best feature of G-type engines is their ability to generate greater power at lower engine speeds. In some recent cases, however, the operators of eco-ships have experienced problems of being unable to pass quickly enough through a critical engine speed. A hybrid (active-passive) isolator consisting of a maglev actuator and air spring is proposed and developed by Li et al. (2017). The dynamic characteristics of this hybrid isolator were analyzed and tested, and its stability and adaptability to shock and swing in the marine environment was improved by a compliant gap protection technique and a suspended structure. Kim et al. (2017d) reviewed the torsional vibration characteristics of a propulsion shafting system equipped with a fuel saving ultra-long stroke engine. The effects of waves on engine-propeller and propulsion performances were analyzed by Taskar et al. (2016).

2.3 Sloshing impact

The violent impact between liquid and structure is an important issue in the ship hydrodynamic community. There are several practical applications where liquid impact loading plays an important role: slamming, sloshing, green water, wave impact on the deck and many others. Extreme impact pressures can affect the integrity of the structure and should be considered with extreme care for the design of floating bodies. The physics of fluid impact phenomenon is extremely challenging both from the numerical and experimental points of view.

Many physical effects in sloshing have to be considered concurrently (gas cushion, liquid compressibility, boiling of liquid cargoes, aeration, thermal exchange, hydroelasticity, etc.). Meanwhile, in parallel with the correct characterization of the hydrodynamic loading, we must always keep the structural response in mind. This implies that the equations for fluid (liquid and gas) and structure must be solved simultaneously unless certain assumptions are made to uncouple them. Furthermore, the modeling of sloshing impact poses difficulties regarding the fact that the structure (Cargo Containment System–CCS) in contact with liquid (e.g. Liquefied Natural Gas - LNG) is extremely complex (combination of plywood, foam, perlite, special steel, triplex, invar, resin rope, etc.). An overview of the difficulties related to the modeling of violent impact situations is given in Malenica et al. (2017) and Dias & Ghidaglia (2018).

During the last three years, the investigation of sloshing impact has been pursued both by experimental and numerical means. Unfortunately, the opinion of this committee is that no significant progress has been made and there is still no efficient solution, neither experimental nor numerical. Most of the investigations concentrate on the evaluation of extreme pressures which occur during the impact, with the idea of simply applying these pressures to the structural model in a second step. However, due to the particular nature of the extreme impact pressures, which are highly localized both in space and time, capturing the pressure extremes correctly appears to be almost impossible both numerically and experimentally. It is thus regrettable that the coupled hydro-structure interaction has not been considered seriously yet. Indeed, even if the pressure distribution is evaluated correctly in time and space, the structural response could

not be evaluated by simply applying this pressure distribution on the structural model, because the important dynamic hydro-structure interaction effects will be still missing. This means that the highest pressures will not necessarily cause the highest structural responses.

2.3.1 Experimental approaches

Many model tests at different scales and with different objectives were proposed in the past. In particular, small-scale sloshing model tests became rather classical and many important facilities exist worldwide. The most typical sloshing model testing facilities use hexapods (e.g., see Kim et al., 2017a), which is very efficient in generating arbitrary time histories of the tank motions. The quantities measured are usually the local pressures and the overall forces on the tank. As far as the overall sloshing behaviour is concerned, the small-scale model tests are very useful and give a good qualitative impression of the violent fluid flow. Furthermore, the overall forces on the tank show good repeatability regardless of the model scale. This is because the overall sloshing behaviour is mainly driven by Froude scaling. However, when it comes to the measurements of the pressures, the situation is much more complicated both regarding the repeatability and accuracy of the measurements, especially for extreme events. Even if the impact pressures are measured accurately, it is still very difficult to scale them consistently to full-scale. For instance, the impact pressures generated by a breaking wave will be associated with an appreciable quantity of entrained and/or trapped air, and, as a result of this, Froude scaling leads to erroneous results. This is an extremely important drawback of the small-scale model tests and it is not likely that this problem will be solved in the near future. In the context of the small-scale model tests, it is also important to mention that generally flat surface tanks are used in the sloshing tests. However, two major CCS (MARKIII and NO96) have important geometrical discontinuities such as corrugations and raised edges which can significantly influence the local pressures.

Among the different experimental campaigns reported during the last three years, we can distinguish the classical small-scale model tests either in 2D or 3D and also the model tests dedicated to some specific aspects of the sloshing impact. The air pocket type impact was recently investigated by Firoozkoohi et al. (2017), Yang et al. (2016a), and Neugebauer et al. (2017), and it was shown that, for this particular type of impact, very similar and repeatable results can be obtained in terms of wave shapes and impact pressures. This is due to the facts that the air pockets are large enough and that the pressure measurements are known to be stable for this kind of situations. For other impact types, the pressure measurements differ significantly, and only the free surface geometry can be captured with fair accuracy.

The phase transition effects were investigated by Kim et al (2017c) by using hot water and bubbles, for air-pocket type impact. The conclusion is that the phase transition effects tend to damp both the peak and oscillations of the pressure in air pockets, confirming the numerical conclusions made by other authors (see, for instance, Ancellin et al., 2016; Behruzi et al., 2017). The effect of temperature was also investigated by Grotle et al. (2016) for LNG fuel tanks, and it was concluded that the lower liquid temperatures, relative to the saturation temperature, has a significant influence on the pressure. The scaling of pressures is a critical drawback of the sloshing model tests, and several investigations were carried out in order to quantify more precisely the effects of different scales (Kim et al., 2016, 2017b; Karimi et al., 2015, 2016a, 2016b; Wei et al., 2016; Frihat et al., 2017, 2016). In Karimi et al. (2015, 2016a, 2016b), and Frihat et al. (2017, 2016), the influence of the density ratio between the liquid and gas on impact pressure was also investigated. The conclusions from all these investigations confirm once again that the global flow is almost independent of both scaling and density ratio; however, the local flow and associated pressures are very much dependent on these parameters. Frihat et al. (2017, 2016) studied the influence of surface tension on sloshing impact pressures, through 2D sloshing tests with different density ratios. The preliminary conclusion is that the reduced surface tension leads to reduced pressures. The 3D effects of sloshing flow were investigated by Kim & Kim (2017), and it was shown that there exist significant differences between the 2D and 3D results for pressure measurements (pressure peak and

its position, affected area and pressure impulse). A comparative study on pressure sensors for sloshing experiments was performed by Kim et al. (2015d). It was reported that the pressure signals may be quite different, depending on the type of sensor installed on the tank wall. All these uncertainties in the pressure measurements have an important effect on the statistical properties of the measured pressure peaks. Some aspects of these difficulties are discussed in Cetin et al. (2017), where no definite conclusions were made regarding the most appropriate probability distribution to be used for the extrapolation of the measured pressure data.

Large-scale model tests were reported in Kimmoun et al. (2016). In those tests, wave impacts were generated on a horizontal plate, modelling a tank ceiling in a 2D wave flume. Wave impact tests were performed either with a flat ceiling or with a corrugated ceiling obtained by the addition of three solid corrugations representing the corrugations of MarkIII membrane at a scale of one half. The instrumentation consisted of high-speed video cameras synchronized with pressure sensors mounted both on the flat part of the ceiling and, for the first time, directly on the corrugations. Among other things, these experiments allowed for identifying the mechanism leading to high pressures on the corrugations. This may happen due to complex jet impact following the direct impact on ceiling. The authors claim that this phenomenon might be responsible from some deformations of the corrugations.

2.3.2 Numerical modelling

In Computational Fluid Dynamics (CFD), different numerical models proposed before for sloshing have been further investigated during the last three years. CFD tools (either commercial, open-source or user-developed) based on solving the Navier Stokes or Euler equations are most often applied with slightly different numerical strategies. A considerable amount of research work was reported on the use of OpenFoam software (Calderon-Sanchez et al., 2015; Diebold & Baudin, 2016; Firoozkoohi et al. 2017; Grotle & Aesoy, 2017; Lyu et al., 2017; Mai et al., 2015; Wang et al., 2016e). The OpenFoam is an open source software based on the finite volume method, and its capabilities seem to be similar to equivalent commercial codes. The numerical sloshing models using finite volume based commercial tools are reported in Behruzi et al. (2017) (Flow3D), Mokrani & Abadie (2016) (Thetis), Zou et al. (2015a) (Fluent), Yang et al. (2016a) (StarCCM+), Veldman et al. (2015) (Comflow). On the other hand, the numerical models based on the finite difference scheme were adopted by Arai et al. (2016), Liao et al. (2015) and Karuka et al. (2017). Furthermore, the use of meshless or particle methods was also reported in a number of study (Baetan, 2015 and 2017; Buruchenko & Canelas, 2017; Gong et al., 2016; Hwang et al., 2015a; Koh et al., 2015; Lind et al., 2015; Wang et al., 2016e; Zhang et al., 2017d). The main advantage of the particle methods is their ability to easily simulate complicated free surface flows, and their drawbacks are high CPU usage and difficulties related to the consistent treatment of the boundary conditions at the interface with rigid boundaries. Due to the difficulties of modelling the local details of 3D fluid structure interaction problems consistently by CFD methods, some less popular numerical methods were proposed for 2D impact problems. For instance, Scolan & Brosset (2017) proposed a potential flow method based on the desingularization technique, allowing for extremely fast and accurate modelling of the relative geometry between the fluid and structure just before the impact. This method also allows for coupling with more sophisticated purely numerical (Volume Of Fluid (VOF) or meshless) local impact methods, once the impact starts to occur. Hay et al. (2016) proposes a highly precise 2D numerical method based on the finite element technique with adaptive time and space refinements. Furthermore, Janssen et al. (2016) used the Lattice Boltzman model in combination with VOF approach for surface tracking, and they reported encouraging results for the generic 2D cases proposed by Scolan & Brosset (2017). Finally, in addition to the purely numerical methods, a limited number of analytical approaches for simple geometries was also proposed by Korobkin et al. (2017) and Zekri et al. (2015). The advantages of these methods are their extremely high precision and the possibility of taking into account the hydroelastic effects consistently. Therefore, the methods could be used for the validation of numerical methods.

With regard to structural responses (CCS and hull structure), a limited amount of work has been reported in the last three years. Cho et al. (2015) used ABAQUS to model the structure of a recently proposed new insulation system (KC1), with a special emphasis on the thermal behaviour. Hwang et al. (2015b) used the LS-Dyna software to investigate the nonlinear structural response of the CCS under impulsive loading deduced from dry drop tests. Jin et al. (2015) used ABAQUS to study the nonlinear structural response of the KC1 CCS under prescribed triangular impulsive loading. Kayal et al. (2016) employed ABAQUS to define a Triangular Impulse Response Function (TIRF) concept in order to efficiently model the linear structural response of the MARKIII CCS to an arbitrary time history of the prescribed external loading. Lee et al. (2015b) simulate the full-scale wet drop test experiments of the MARKIII CCS using the LS-Dyna, and they emphasize the nonlinear behaviour of polyurethane foam. Ringsberg et al. (2016) used ABAQUS to investigate the dynamic amplification of hull structural response by accounting for the influence of the CCS. The authors conclude that the dynamic amplification might be very important for some temporal load characteristics. In addition to the difficulties related to the modelling of pure structural behaviour, these methods still lack a consistent definition of pressure loading and fully consistent hydroelastic interaction model.

In conclusion, it may be said that, in spite of all the improvements reported on numerical tools and methods, there is still no fully consistent, reliable and efficient method, neither for fluid dynamic modelling nor for fluid structure interactions, which occur during sloshing impact.

2.4 Shock response

The shock and explosion-induced responses of ships are important to naval architects of both military and civilian vessels. The characteristics of the dynamic responses to shock and explosions are of a nonlinear nature on material and geometry, and different than caused by waves and machinery. The work of many researchers is devoted to shock and explosion loading, response and damage of ship structural elements, including composite hull structures.

2.4.1 Air blast

Air blast from both accidental and weapons explosions is an important form of ship structural loading. A key area of concern for blast response is explosion in an interior compartment, and potential damage due to internal explosion is a recent focus area of research. In the field of internal explosion loadings, quasi-static loading was a main concern. Duan et al. (2017) conducted a series of tests with aluminized explosives of different Al/O ratios, and the results showed that the quasi-static pressure gain was maximum at a ratio of Al/O = 0.99 that is almost half the value of the gain of the maximum bubble in an underwater explosion. Salvado et al. (2017) proposed a new method to estimate the peak pressure of an explosion in a compartment. Feldgun et al. (2016) have studied the internal energy of explosion and proposed a simplified approach based on the developed gas pressure, as well as on the Bernoulli equation, which is well-suited for simulation of partially confined explosions and properly describes the pressure relief and gas outflow from a vented compartment.

When a ship is attacked by a missile, the compartment of detonation is subject to shock loads that usually cause serious damage. Many researchers have worked to develop new methods for analysis and experimentation of response and damage of compartments subject to internal explosion. Yao et al. (2016, 2017a) suggested a new dimensionless number for the dynamic response of box-shaped structures subjected to internal blast loading that has clear physical meaning and leads to good correlation between the response of box-shaped structures and the blast energy. They designed three sets of steel box structures using a replica scaling law to investigate their responses under internal blast through experiments, and correction of the traditional scaling law was conducted. Yao et al. (2017b) conducted two series of experiments with different dimensions and different masses of explosive, and six damage modes were observed. Pickerd et al. (2016) conducted internal blast experiments on welded steel containers using digital image correlation to assess the deformation and strain. Weld defects such as

porosity and lack of fusion result in highly localized regions of strain that are difficult to account for in simulations. Karagiozova et al. (2015) investigated the response of partially confined hollow stainless steel cylinders to internal air blast loading. A theoretical model was developed for the deformation of a sandwich-walled cylinder configuration, and was used to analyse and interpret the process of the dynamic foam compaction and stress transmission to the outer wall.

2.4.2 Underwater explosion

Underwater explosions are a source of serious damage to ships due to potential loss of hull integrity. Shock loading is the basis for the response analysis and prediction. Recent research has focused on non-ideal explosives and near-field explosions. The underwater explosion loading properties of non-ideal explosives enriched with aluminium was investigated by Komissarov et al. (2015). The shock wave and bubble energy were measured, and it was found that the Al/O ratio is the key parameter that controls the energy output. The specific energy of an explosive charge highly enriched with aluminium can be more than twice that of TNT when the Al/O ratio is 1.85. Wang et al. (2016b) proposed a simple method to determine the mesh size for numerical simulations of near field underwater explosions. The ratio of the radius of the charge to the side length of the element equal to 3 was shown to be an adequate choice. Han et al. (2016) investigated the pressure load of double underwater explosions, including the effect of the detonation time difference and the distance between explosive sources on the resulting damage force. Wang et al. (2016f) combines the Level-Set Modified-Ghost-Fluid Discontinuous-Galerkin (LS/MGF/DG) method and the Boundary Element Method (BEM) to simulate bubble motion and associated pressures near a wall, and the numerical results were compared with experimental data. Zhang et al. (2015a, 2016c) used a Smoothed Particle Hydrodynamics (SPH) method with mesh-free and Lagrangian formulations to simulate the formation process of a shaped-charge jet. Zhang & Jiang (2015) proposed an improved shock factor based on the scattering effect caused by the diameter of smaller submerged cylindrical shells on different wavelength of the incident waves.

Responses of primary structural elements to shock are the basis of understanding and analysing the whole ship structural response. Beam and cylinder idealizations can be used to model the overall structure of surface ships and submarines, respectively. The panel is the typical primary structural member of a surface ship. Chen et al. (2016) investigated the theoretical response of a typical double-bottom structure subjected to underwater blast and established an approximate analytical model which is able to predict the response. Wang et al. (2016d) proposed a dynamic buckling criterion for stiffened plates subjected to an explosive shock wave and discussed the effects of various stiffening configurations on the dynamic and static buckling loads. Furey (2015) evaluated the stress-strain states and the hydrodynamic fields through analysis of stress in two submerged co-axial cylindrical shells and pressure fields in the inter-hull coupling fluid. Changes in behaviour were quantified by varying the relevant parameters of structures and fluid fields. Hsu et al. (2016) numerically investigated the response of three different beam cross-sections (circle, ellipse and streamline shapes) to an underwater explosion and concluded that a circular cross-section is stronger than others. Monteiro et al. (2016) conducted two sets of experiments to investigate the collapse of aluminium tubes to static and underwater explosion loadings, and some collapse phenomena were observed.

The dynamic response of ships to UNDerwater EXplosion (UNDEX) is very important for ship survivability due to the potential for serious damage. Recent research has concentrated on the damage and responses to near-field and contact explosions that are relevant to bubble dynamics and strong nonlinearity, respectively. In near-field UNDEX research, Nie et al. (2015) presented the regimes of underwater explosion for a submerged slender structure excited by pulsating bubble. Near-, middle- and far-fields are identified according to structural global responses. Equivalent dimensionless parameters are obtained by two different dimensional analysis methods, among which a dominant similarity parameter is found. Zhang et al. (2015b) conducted an experiment of a hull girder model subjected to near field underwater explosion at

mid-ship. The damage mechanism and mode were discovered by the experiment, and the coupling effect between the whole motion of hull girder and distortion of local structure was discussed. Wang et al. (2016c) developed a new analytical model to predict the damage of a simplified hull girder subjected to an UNDEX shock wave and its bubble pulsation load based on the rigid-plastic material model, the Vernon bubble model, and the modified hydro-plastic analysis method.

In the contact UNDEX research field, Zhang et al. (2015a, 2016c) investigated the damage of double-hulls to contact UNDEX with a simplified SPH method. It was found that either the polyurethane layer or water layer could have a protective effect for the second shell. Zhang et al. (2017b) performed experimental work on the response of multi-layered protective structures subjected to underwater contact explosions. Some important factors in plate damage are analysed, and the role of the compartments with different media on the damage and energy dissipation is discussed.

For stealth, light weight, and other advantages, composite structures are widely used in modern ships. Their response and damage to shock and explosion are areas of recent research. Primary areas of interest are Glass Reinforced Plastic (GRP), Styrene-Butadiene-Styrene (SBS), sandwich plates, and rubber-like material coating structures. Schiffer & Tagarielli (2015) presented a new experimental technique to allow laboratory-scale observation of underwater blast loading on circular quasi-isotropic glass/vinylester composite and woven carbon/epoxy plates. This included dynamic deformation and failure of the plates, as well as the sequence of cavitation events in water and the development of a theoretical model for the response of elastic orthotropic plates to underwater blast. Liu et al. (2017a) investigated the high velocity impact responses of newly designed sandwich panels with aluminum (AL) foam core and Fiber Metal Laminate (FML) skins by experimental methods. Gong & Khoo (2015) used the coupled BEM–FEM to handle the interaction of a composite structure and an underwater explosion bubble, and the mutual effects of relative location and the transient response of a composite submersible hull to an underwater explosive bubble for different charge weights and charge distances were investigated. Jin et al. (2016) investigated the effects of graded foam cores of a sandwich spherical shell subject to underwater explosion from the inner side. It was found that the core arrangement of low/medium/high is best for the case of a relatively strong core condition, and the configuration of high/medium/low has the best performance for the case of intermediate core strengths. Xiao et al. (2015) carried out a comparative study of honeycomb rubber coatings of the same material and total mass subjected to underwater explosion. Three types of cell topologies were considered. Three groups of live underwater explosion tests with different attack angles and stand-off distances were conducted on stiffened metal boxes covered with the coatings. The results show that the protective effects of different coatings are consistent under different attack angles and stand-off distances. Compression performance of the coatings plays a dominant role in underwater shock resistance.

The responses and damage of equipment and on-board systems to shock and explosion are of great concern to naval architects, as protection of their functionality is important to accomplish the ship's mission. Scavuzzo et al. (2015) presented a review of an experimental study and analytical demonstration to explain the effect of dynamic interaction on the shock or response spectrum. A practical example of interaction was studied, with four single mass dynamic systems mounted on a realistic deck and subjected to a high impact shock input. On-board equipment and systems are often comprised of many components, and the anti-shock capability of the components directly affects the anti-shock capability of the equipment. Guzas et al. (2015) used a variety of finite element modelling approaches to represent the behaviour of single solid bolts under static and dynamic tension loading, and simulation results were validated against experimental data from physical testing. Stenard et al. (2017) proposed a new approach for the Universal Adjustable Shock Mount (UASM) to reduce Total Ownership Cost (TOC), by making electronics upgrades on warships as easy as in the commercial sector. Hansen et al. (2016) set up a more precise method for load prediction on piping and small- to

medium-sized equipment than the current guidance, which may lead to underestimated explosion loads. Due to the complexity of responses of equipment to shock, reliable validation of anti-shock capability is usually by testing.

2.5 Noise

Noise emissions from shipping activities have been a great concern due to their negative impact on the environment. The ship onboard noise receives close attention due to the increasing awareness of health hazards caused by the long-term exposure of the crew to high noise and vibration levels, and due to the considerations of safety and comfort for crew and passengers. The latest regulatory document on noise levels onboard ship is issued by IMO (2014).

The underwater radiated noise also generates similar effects on the marine fauna, by causing an increase in the background noise of the oceans and modifying the ambient conditions of the fauna. The noise emissions may also interfere with acoustic sensors and underwater monitoring systems.

A proper noise assessment of a ship design is a very complex matter, due to several factors such as:

- The noise is generated by different entities located in different positions on board (machinery, propulsion, ventilation, auxiliaries, etc.);
- There are several mechanisms of transferring noise from one location to another (structural, airborne, waterborne, through ventilation ducts and pipes, etc.);
- There are different targets with different thresholds, or limits (internal, with regard to passenger and crew comfort – external, with regard to airborne noise pollution in coastal areas - underwater, with regard to disturbance to marine environment).

This committee report presents the results of the literature survey with regard to the "receiving environment". In this respect, it is noted that the general trend of the recent research is to provide a scientific baseline to the standardization of every aspect of the "noise onboard" issue.

Borelli et al. (2016a) presented a comprehensive review. They discuss that while in the field of interior noise there is a coherent set of rules constantly updated for both noise and vibration, in the new fields of application, namely external and underwater radiated noise, the situation is still far from settled. The work started with the concluded European project SILENV (Ship Innovative soLutions to rEduce Noise and Vibrations), for instance, is not complete yet and further investigations are still needed. Three new EU projects are following up the road mapped by the SILENV (2012):

- AQUO (Achieve QUieter Oceans by shipping noise footprint reduction),
- SONIC (Suppression Of underwater Noise Induced by Cavitation),
- MESP (Managing the Environmental Sustainability of Ports for a durable development).

2.5.1 Interior noise

Regarding interior noise, and referring to the above introduction on the adequacy of available norms to the state of the art technology, it is interesting to note that Beltran et al. (2014) commented on the new IMO code, MSC 337(91), as a lost opportunity for making a step ahead in protecting the seafarer's health and safety. According to the authors, the new code is not so different from the old one, IMO Resolution A.468 (XII), except for those vessels whose tonnage is above 10000 GT. The shipbuilding and noise control technologies are far ahead the new regulation.

Borelli et al. (2016b) also analysed these two regulations, but with regard to annoying tonal noise components in working spaces on board ships. They observed that the application of those norms is difficult in case of tonal components because of the imprecise definition of "tonal

component" (referred to as "obvious tonal component" in the MSC Resolution). A measurement campaign was carried out on three different Ro-Pax vessels for 79 different work spaces. The authors adopted another methodology, referred to as Italian Decree D.M. 16/3/98, to assess the presence of tonal components, and they observed significant occurrence of tonal components in different working spaces.

Blanchet & Caillet (2014) presented a methodology of combining different mathematical models into one for obtaining a full frequency coverage in the vibro-acoustic calculation of ship – a luxury yacht in the present case. The approach makes use of several methods and coupling schemes, such as Finite Element Method (FEM), Fast Multipole Method-Boundary Element Method (FMM-BEM), Statistical Energy Analysis (SEA) and FEM/SEA coupling, to represent structure, interior cabins, underwater fluid loading, insulation, etc. This approach may be adopted to describe the complete acoustical behaviour of ship, with regard to internal noise as well as air and underwater radiated noise.

Borelli & Schenone (2014) highlighted the need for an accurate preliminary assessment of internal noise levels on board ship in an early design stage. They developed a "source-patch-receiver" model to evaluate the acoustic performance of the HVAC system of an oceanographic research ship in its preliminary design stage. This simplified approach is proved to be effective in pointing out the weakness of the HVAC system, with respect to its acoustic performance, allowing for adequate countermeasures taken before starting construction.

2.5.2 Air radiated noise

The last committee report summarized the work carried out within the framework of the SILENV project. The ultimate scope of the project was to create an "acoustic green label", including noise targets and guidelines, for the purpose of quantifying the environmental sustainability of a ship in terms of acoustic emissions (internal, external and underwater). However, despite the conclusion of the project, there has been no serious attempt to adopt the outcomes of the project into a norm by classification societies or other normative bodies.

Regarding external airborne noise emissions from ships, Di Bella (2014) addressed the existing regulations. He points out that the assessment of external noise propagation requires more attention due to the fact that the measurement methods do not always fit to the type of vessel, and that the assessment of the noise is more difficult for larger vessels. For moored vessels, the effect of noise produced by the power supply and ventilation system can be significant on the surrounding environment. In case of cruise ships, the ship size does not allow for direct evaluation of the sound power emitted, and the ship therefore has to be considered as a sum of the individual sound sources, measured separately on board the ship. The measurements are then fed into a numerical model in order to calculate the impact on the surrounding environment. A review of available standards to perform this evaluation is provided. It is also noted by the author that there is currently no technical standard that can define unambiguously the methods for determining the sound power emitted from very large sources, such as cruise ships, in a complex environment like a harbour.

One important issue in assessing the level of noise emitted by a ship at berth is measuring the ship itself, without being affected by background noise or noise reflected by surrounding surfaces. An attempt to separate and investigate noise components individually is made by Kamali et al. (2014), by providing a 3D noise model of the port of Tripoli and identifying the different sources such as ship activities, port activities and passengers/visitors. The study emphasized that the noise emitted by a ship is not necessarily the strongest source and that a comprehensive acoustic characterization of the noise in a port area is extremely difficult due to its complex geometry, number of sources, etc. However, single characterization of the various sources is possible and can be inputted into a 3D acoustic model to allow for further scenarios.

A similar conclusion is also reached by Curcuruto et al. (2015) who performed a survey to characterize the noise emitted by ships moored in the Civitavecchia port area in Italy. They

measured the radiated noise by a cruise ship and a Ro-Ro vessel, respectively, using the methodology presented in the SILENV. They adopted a simplified methodology which was judged to be more suitable to describe complex areas like a port. The paper describes the difficulty encountered in switching off the external noise sources to characterize correctly the background noise. The authors suggest the characterization of noise sources to make a numerical model for noise mapping of the port area.

Fotini et al. (2016) mapped the noise emissions at the port area of Piraeus in Greece by taking into account the emissions from various sources such as moored vessels, passing vessels and other human activities. A digital model was created for the purpose of noise mapping, and each noise source was set as a point source (mooring places) or linear source (typical path of moving vessel). An interesting outcome of this study is that the noise disturbance from the vessel activities is almost insignificant. The noise from the road network adjacent to the port area or caused by mooring activities, etc. causes a bigger annoyance than the passage of a vessel.

Curletto et al. (2015) presents design solutions for the new FREMM frigates of the Italian Navy in order to reduce the external radiated noise emitted by the ships. A prediction study was performed to estimate the noise levels around the ships. It is noted that the measured noise levels confirm that the external noise levels generated by the ships are lower than the limits defined by the national rules and regulations.

Di Bella et al. (2016) presents a comparative study of methods for measuring large vessels during both navigation and mooring. Their conclusion, aligned with other studies, is that 3D acoustic mapping can be a useful tool to explore different noise scenarios, where the ship is not the only source contributing to the noise pollution in the surrounding area of a port. However, its characterization is difficult, and no unified and unambiguous method is available for the time being.

It may be argued that the characterization of the noise impact of a ship moored in a port environment is a very difficult task, because of a number of reasons:

- The ship is a “big” object and there has been no available standard or procedure yet to measure the emitted sound. Several efforts have been made, but those have not been transferred into a standard or a “class green label”;
- The measurements are generally affected by the background noise from the surrounding environment, which is not always easy to isolate. However, especially for the areas located in heavy trafficked commercial harbours, the ship is not always the strongest noise source, but other port activities such as loading/unloading, railways, etc. can be;
- The environmental background noise is also partially made by the ship itself, due to the reflections that are normally present in harbour, marina or shipyard areas.

The noise footprint of port activities may be evaluated using a digital model, in which the noise sources could be modelled individually. By using such a model tuned to real measurements, different scenarios could be explored, and, therefore, the expected “acoustic green label” or, more properly, the acoustic characterization of ships could be achieved. The development of a measurement procedure, free from reflection and other disturbances, is required, and, hence, newly built ships could be measured as part of normal sea trial or commissioning process.

2.5.3 Underwater radiated noise

Underwater radiated noise mainly comes from mechanical vibration (ship hull, engine, etc.) and marine propeller, either with or without the presence of cavitation. In the preceding committee report, the important issues such as noise mapping of seas and establishing limits on received underwater noise were discussed. In the present report, the focus of the research is still the same with small differences. More achievements have been made in the field of noise mapping of the oceans in this period of the committee report.

In this regard, Kaplan & Solomon (2016) examined the growth in emitted noise from three major segments in commercial shipping (container ships, oil tankers and bulk carriers) and argued that the maximum noise capacity of the global ship fleet could increase by 87%-102% on average by 2030 due to the combined effect of increased shipping, larger and noisier vessels, and longer cruising distances.

Audoly et al. (2016) summarized the results of the European research project AQUO. The project was created according to the Marine Strategy Framework Directive (MSFD), the European Union (EU), which requires from its member states to develop strategies that should lead to measures that achieve or maintain Good Environmental Status (GES) in European marine waters, by the year 2020. The AQUO Project demonstrated the feasibility of real time monitoring of the underwater noise footprint regarding shipping in a maritime area, using a predictive tool adopting Automatic Identification System (AIS) data and environmental information. Moreover, a number of recommendations was made for design, construction and management of ships and their routes in order to help yards and ship owners to improve the future fleet with respect to underwater noise emissions.

According to the requirements of the MSFD, some steps were also made in the direction of setting up a territorial noise monitoring plan, as indicated in Borsani et al. (2015). The authors describe how to establish an underwater noise monitoring system for the Italian seas. They used the shipping traffic data gathered by AIS applications to establish proper sensor positions and measuring methodology. The study is based on the adaptation of the MSFD, which considers the underwater noise as a descriptor for the environmental status of the European seas. The target is to provide a unified method to measure and quantify the underwater noise pollution in a way that enables comparisons among different countries.

A similar approach to comply with the requirements of the MSFD was also followed by Tegowski et al. (2016), who presented a methodology for correlating underwater ambient noise to shipping traffic by means of a noise prediction method. The project, called BIAS (Baltic Sea Information on the Acoustic Soundscape), has the main goal to monitor the shipping noise in the Baltic sea and to use it as input to a prediction model. The final goal of the project is to give the maritime authorities an effective tool to monitor the intensity of underwater noise caused by marine vessels without undertaking costly and difficult hydro-acoustic measurements.

In the framework of the European project AQUO, Dambra & Firenze (2015) performed an underwater acoustic assessment of a small vessel (less than 19 m) highlighting that the available standards are often calibrated on big ships and that they are not suitable for measuring small vessels. This requires further research and standards which consider vessel size.

As a noise abatement measure, Wochner et al. (2015) presented an underwater resonator system as a passive countermeasure for underwater radiated noise from different sources, including ships. The system uses Helmholtz resonators – already well known and widely used in airborne noise problems – in a completely new environment, namely in water. The system was tested at two offshore wind farm construction sites in the North Sea in 2014, and 20 to 40 dB sound level reduction was achieved in the frequency band of 20 Hz to 20 kHz.

Tiancheng et al. (2017) investigated the noise characteristics of a submerged exhaust by an experimental study. Through a series of experiments, the main sources of underwater exhaust noise were investigated. The results showed that the low frequency noise was dominant and mainly produced by the downstream two-phase flow. The intermediate frequency noise had a strong correlation with the gas velocity. The high frequency noise was mainly due to aerodynamic noise generated in the upstream pipeline.

2.6 Damping and countermeasures

Damping is an important factor in all dynamic response analyses, since resonance vibration levels are inversely proportional to the damping level, and the vibration cycles decay exponentially in time due to the damping after an impulsive loading. The level of damping there-

fore affects all forced responses, hence fatigue and extreme loading as well as vibration and acoustic levels. Modelling the damping is difficult due to the limited knowledge about the amount of damping in various materials, joints, etc. Therefore, accurate damping estimates, at least for the damping in structures, are usually found based on the measurement data.

Although the damping comes from several different sources, linear as well as nonlinear, it is usually modelled as equivalent viscous damping in structural response computations. There are several sources of damping affecting ship vibrations, and the most important ones are:

- material damping in the welded and un-welded structure;
- friction occurring in, e.g., joints, hatch covers and cargo;
- water friction;
- vortex shedding from sharp edges such as bilge keels, rudder, appendices;
- pressure wave generation;
- surface wave generation;
- artificially added damping.

Hydrodynamic damping is plausibly easier to compute numerically, compared with damping from material or friction, but it requires a very fine computational mesh. The models for hydrodynamic damping are, however, not well developed. el Moctar et al. (2016, 2017) reports a comprehensive study of numerical modelling methods for the hydrodynamic damping in extreme seas. They report that the hydrodynamic effects contribute significantly to the life cycle load spectra of wave-induced hull girder stresses. In the study, the model test measurements were used to validate the numerical simulations. The study also states that the damping has significant effects on both whipping and springing events, and it was also found that the hydrodynamic damping contributes substantially to the overall damping. Unfortunately, a direct comparison of the computed and measured hydrodynamic damping was not found possible.

Full-scale measurements are necessary to obtain data for actual operating conditions. Thus, Takahashi & Yasuzawa (2014) reports an Experimental Modal Analysis (EMA) test on a 310000 DWT VLCC (Very Large Crude Carrier), which was drifting without the engines on, in deep waters. The wind conditions, depth etc. are, however, not reported. The authors used stepped sine excitation in both vertical and lateral directions to obtain frequency response functions. The modal parameters, such as natural frequencies, damping factors and mode shapes, were then extracted using a commercial EMA software. The damping was found to be in the range of 0.1 – 1% of critical damping, which was reported to be significantly lower than those recommended by classification societies for container ships.

Orlowitz & Brandt (2014) applied Operational Modal Analysis (OMA) to a 19200 DWT and 210 m long RO-LO ship during sea trial (i.e. unloaded ship). The ship was equipped with 45 accelerometers, and the measurements were performed under three different operating conditions: anchored, and cruising with 10 knots and 18 knots, respectively. The cruising speed of 18 knots is the design speed of the ship. For the anchored and 10 knot cruising speed conditions, the damping ratios of the first three vertical bending modes were found to be between 0.2 and 0.6%. At the cruising speed of 18 knots, the damping ratios of the same modes increased significantly to 1.1 – 1.4%. The first two torsional modes had approximately stable damping ratios around 1%, and the first horizontal bending mode had 0.6 – 0.9% damping ratios at different speed conditions.

Particular attention has been paid to large container ships, as these ships are regarded as highly flexible with low natural frequencies, with high speed potential and significant bow flare. They are thus vulnerable to extreme and fatigue loadings from whipping and springing. Storhaug (2014a) used model and full-scale measurements to study whipping and springing and concluded that the damping needs to be studied in more detail. Andersen (2014) reported results on four container ships ranging from 4400 to 14000 TEU, equipped with strain gauges. Using the OMA analysis, the damping ratios of the 2- and 3-node vertical bending modes

were found to be between 1.3 – 2.5%, with container load. No correlation of damping with ship size was found.

Storhaug et al. (2017b) investigated 14 container ships between 1700 and 19000 TEU, two LNG ships of 85000 DWT, two ore carriers of 210000 DWT, one ore carrier of 220000 DWT and two oil tankers of 18000 and 268000 DWT, respectively. In the study, several techniques for damping estimates were compared. It was concluded that half power and log decrement techniques should not be used due to their inaccuracy. Instead, it was found that random decrements, spectral method, enhanced frequency domain decomposition and stochastic subspace identification were found reliable. The damping ratio of the 2-node vertical bending was found to be approximately 1.7%, on average, for the container ships, with no systematic differences between ships of various size or speed. Ore carriers, LNG, and oil tankers were found to have approximately 0.7% damping ratio on average, i.e. substantially lower than those for the container ships.

It is usually assumed that the 2-node vertical bending mode is more easily excited and gives the largest vibration bending moment amidships, dominating the vibration effect on fatigue. Shi et al. (2016) developed a model based on stochastic distribution of stresses caused by combined loads considering the slamming effects. They found that a 1% damping ratio yielded about 250 times greater up-crossing rate than a 10% damping ratio, and it is thus concluded that the damping has a greater effect on the fatigue reliability. Furthermore, Storhaug & Kahl (2015) investigated the effect of torsional vibration on fatigue for two container ships of 8400 TEU and 8600 TEU, respectively. On the 8600 TEU ship, the effect was found insignificant; however, it was expected to be significant for the 8400 TEU container ship. It is also interesting to note that the damping ratio of the first torsional mode was 9.7% and 5.2%, respectively, for the 8600 TEU and 8400 TEU container ships.

Recently, Pais et al. (2017) investigate vibration levels for a 60 m superyacht, both experimentally and numerically. The global damping ratio was calculated using a procedure based on dynamic finite element analysis. The propeller-induced pressures were applied to the finite element model of the ship structure, and the forced response spectrum was calculated. The spectrum was compared to the measured spectrum at the propeller blade frequency, and the damping was then iteratively altered until the computed forced response spectrum coincides with the measured one. It should be noted that this approach depends on the correctness of the applied pressure level. The damping was found to be 9-10% relative to critical damping.

Lavroff et al. (2017) reported the full-scale tests of two INCAT catamarans, one being 86 m long and other 96 m. They identified the damping ratios as 1.8% and 3.5% for the 96 m and 86 m ships, respectively. On the model tests of another ship, they found no frequency change with speed, but damping increased by 65% over the speed range 0 to 2.89 m/s, corresponding to full-scale speed of 20.6 m/s (40 knots). This increase in damping with increasing speed is in line with the full-scale measurements by Orlowitz and Brandt (2014) reported above.

Despite all the efforts made, the damping mechanisms and actual damping values, for ships in different operating conditions, are not fully understood. This is particularly true for modern large container ships as well as other ship types, for which whipping and springing responses are important. For the numerical investigation of springing and whipping in the design phase, according to guidelines produced by classification societies, a target damping is needed. There is thus a need for more full-scale data, together with the information on wind and wave conditions, ship speed as well as cargo condition and draft, which may affect the damping values. A step in the right direction is the revised hull monitoring rules by DNV-GL (2017a) which requires damping estimates to be automatically produced onboard when the hull vibrates.

As far as countermeasures are concerned, not much work seems to have been reported in the period of this report. On cruise ships and superyachts, where excessive vibrations cause discomfort for passengers, the damping materials such as rubber and elastomers are often added

for vibration mitigation and insulation purposes. Additionally, tuned dampers may be used for adding damping to the 2-node ship vertical bending mode.

2.7 Monitoring

The following topics are addressed here: definitions, hull monitoring rules, hull monitoring suppliers and digitalization. Monitoring with full-scale measurements of wave-induced vibrations is covered by Section 2.1.1.

2.7.1 Definitions

An attempt is made to standardize different terminology and technology in relation to monitoring. Condition Monitoring (CM) is often about collecting and observing data. The system used to collect data is referred to as a Condition Monitoring System (CMS), which is a system used for machinery, components and equipment within different industries. CMSs may be certified (DNV-GL, 2016f). On the other hand, Condition Based Maintenance (CBM) is more about using these data in maintenance strategies to define appropriate inspection intervals or CM program (DNV-GL, 2015). CMS is based on sensors, but manual readings may also be collected on board ships.

There is also a distinction between full-scale measurement and hull monitoring system. Both systems are based on sensor measurements, but the former is more for research and troubleshooting, while the latter represents more standard systems approved by the classification societies, according to their hull monitoring rules with associated class notations (Kahl et al., 2016). This means that the full-scale measurements may be done by non-approved equipment, which even may not be allowed to connect to other systems, and the systems are not necessarily intended to be permanent. For ships, hull monitoring is essentially related to the hull structure, but the hull monitoring rules from ABS, CCS and DNV-GL are more about sensor monitoring and not necessarily all about strain sensors (ABS, 2016a; CCS, 2015; DNV-GL, 2017a).

In the offshore industry, owners and operators generally have a larger group of technical staff, compared to those in the shipping industry. As a result, the operators are more involved with monitoring programs and rely less on the classification regulations. A hull monitoring system may be categorized as a Decision Support System (DSS) (Storhaug & Kahl, 2016), which is meant to provide input to onboard personnel to support their decision making activities. However, the DSSs normally contain more information about what-if scenarios, i.e. that the effects of changed conditions can be evaluated before they are executed. A hull monitoring system displays the consequences of a change after it has been done, so it is not fully a DSS.

The control and monitoring systems are also an important part of the rules (DNV-GL, 2017c) and they deal with machinery, systems and components, but not hull and structural response. In the changes to these rules, it was emphasized that the rules are also applicable to safety systems by using the terminology “control, monitoring and safety”.

2.7.2 Hull monitoring rules

Hull monitoring rules are covered here instead of in Section 2.9. There have been several revisions of the hull monitoring rules by the classification societies recently. This does not necessarily mean that significant changes have been made.

DNV-GL has a major revision of the rules associated with the class notation HMON (DNV-GL, 2017a). Time series from all sensors should be down-sampled and stored continuously. A 10 Hz sampling frequency is required for strain sensors. Statistics for all connected sensors should also be stored. The qualifier for vibration dose value has also been introduced and specified based on 3-axial accelerometers. Weighting is required separately for vertical and horizontal vibrations in the range from 0.4 to 10 Hz (ISO, 1997), basically covering the main global vibration modes. This is a subject for passenger ships. The qualifiers are also introduced for parametric roll and ice response monitoring, where the latter includes dynamic vi-

bratory response. The ice response requirements are more in functional nature rather than descriptive, compared to rules from other classification societies. That has been based on the experience collected from full-scale measurements of ice-going vessels in various research and joint industry projects (Nyseth, 2016). The HMON rules also have 18 different types of qualifiers referring to different types of sensors and features. It also gives clear requirements to reveal the effect of vibratory response, and the damping is required to be estimated for the governing vibration modes. Calibration of sensors is a topic which may be taken for granted. This is also emphasized more in the revised rules and includes the effect of static hydroelasticity. As stated by Storhaug et al. (2016), the strain based on the loading computer may be several percent off the target for calibration due to the hydroelastic effect. This uncertainty may increase significantly if cargo is on board during calibration, as stated by Storhaug et al. (2017a) who compared laser measurements with loading computer results.

The hull monitoring rules from NK (2017a) do not appear to have been revised significantly. They are associated with the class notation HMS*R when continuous recording is required. Fatigue or vibration are not even mentioned, but strain sensors are required to measure up to 5 Hz and accelerometers from 0 to 100 Hz so that at least the most important vibratory responses for the hull should be recorded.

BV's HULL-MON notation and associated rules (BV, 2017) do not appear to have been updated recently, with a frequency band up to 1 Hz on strain sensors and accelerometers. Whipping, springing and fatigue are not mentioned. A separate notation MON-Shaft is however included for shaft monitoring.

LR has a class notation SEA (HSS-n) added to their ShipRight notation, which involves the fitting of a hull stress monitoring system. VDR, N, M and L are additional notations related to voyage data recorder, navigation, motions and loading computer (LR, 2017a). The rules do not appear to have been revised recently, and they are very top level and do not contain detailed requirements. There is, however, a guide to these rules, describing more details (LR, 2008). It is stated in the rules that the fatigue should be estimated and that strain sensors and accelerometers should measure frequencies up to 5 Hz.

ABS have made a significant revision to their hull monitoring rules (ABS, 2016a). Some additional notations can be assigned following the main class notation HMn (n being 1 to 3); for instance, "Sea State", "LC" for loading computer connection, "Navigation", "Wind", "Shaft monitoring" and "SL" for shore link. Each sensor has an additional notation and number. It approaches to the flexibility in DNV-GL (2017a) rules, with the intention of supporting a digitized future. HM2+R is most relevant for the hull girder response, with R+ meaning that the data is recorded for later use. Whipping and springing are also mentioned in the context of both fatigue and extreme loading.

CCS (2015) hull monitoring rules support the class notation HMS for global strain sensors and HMS(), where the parenthesis contain a list of other sensors types. This is almost identical to the DNV-GL hull monitoring rules, with the class notation HMON (DNV-GL, 2017a), where the list also includes a number of sensors of different types. The CCS (2015) does not include a letter "N" requiring that the data should be stored by the class society. The CCS (2015) rules are almost identical to the DNV (2005) rules in content and includes the same requirements for the filtering and handling of the measured signals. The systems designed according to these rules will then involve fatigue and extreme loading and reveal the importance of whipping and springing.

Overall, the hull monitoring rules of several classification societies appear to lag behind the design requirements related to wave-induced vibrations (whipping), in particular for large container ships.

2.7.3 Hull monitoring suppliers

A list of suppliers of hull monitoring equipment for ships is given by Storhaug and Kahl (2016). About 19 suppliers are mentioned, but only four can be regarded as leading. Out of these four, only three are currently delivering new systems: Light Structures (Norway), Strainstall (UK) and SST (Korea). The fourth significant supplier, BMT Seatech (UK), is only maintaining old systems. Strainstall has delivered the most systems, but Light Structures is leading on a number of optical systems. Light Structures delivered many systems in recent years, e.g. on large container ships, naval/coast guard ships and offshore assets. These systems may contain more advanced instrumentations, while SST and Strainstall have more standardized systems with global strain sensors in the deck only. The smaller suppliers may also provide complicated instrumentation, which can be required in research projects.

Since 2006, the offshore industry has been developing their own standard for hull monitoring systems by joint industry projects like MONITAS. Hull monitoring software helps the operator with an approval of possible field lifetime extension and with an assessment of fatigue loading for relocation purposes. It explains reasons for potential deviation of the actual lifetime consumption from design predictions and translates the monitoring data into operational guidance and advice in an easily understandable format.

2.7.4 Digitalization

Digitalization is a global trend. There are several classification societies with hull monitoring rules which have optional requirements to store data, and they can potentially support this development. Another challenge, however, is to get this data to shore.

DNV-GL (2017a) and ABS (2016a) are supporting this, by having mandatory requirements to process and store data. The former has requirements to store statistical data for five years and time series for one year. The latter has a requirement of one year on statistical data. DNVGL (2017a) has a qualifier “D” for an online link to shore. ABS (2016a) has the notation “SL” for shore link, which can reduce the need for a one-year storage requirement on board. Further, DNV-GL (2017a) also has a qualifier “B” for backup to be annually sent to the class society. These two rule sets are also quite flexible on the content of data.

It is however not enough to have systems that measure, process, store and send data to shore. It is also necessary to have a system at shore to retrieve data, i.e. a database or platform. No significant information has been found on this, related to dynamic response, although it is a common practice in fields such as powering performance or machinery maintenance, where periodic transfer of data, storage and remote access have been addressed successfully. There is, however, a press release suggesting that NK (2015) decided to establish a data center and that the data center ShipDC was launched in May 2016 (NK, 2016). Another platform is Veracity (2016). This platform established a recommended practice (DNV-GL, 2017b) for a data quality assessment framework, which includes organizational maturity and data risk assessment. Knutsen et al. (2017) outlines the application of the recommended practice for the assessment of the data quality of sensor systems and time-series data. Many ISO references are utilized. Guan et al. (2016) defines a sensor system and gives an overview of sensor system reliability as a main challenge in daily use.

The aggregation of large amounts of monitoring data on a data platform can reveal new knowledge, for instance in relation to benchmarking of various dynamic responses. Articles related to these data platforms are yet to be seen. Manual comparison of smaller data sets has been done. A study into six years of full-scale measurement data, in combination with model tests and numerical tools, for a frigate type hull has been conducted by Hageman et al. (2014a, 2014b). This research showed a sensitivity between the performance of hydrodynamic tools and operating parameters, such as vessel speed and incoming wave direction. Storhaug (2014a) showed the importance of whipping and springing for a few ships from the model tests and full-scale measurements. From the model tests, the vibration damage contributions

for four container ship designs varied between 37 to 87% of the total damage in different trades for deck amidships. Similarly, the vibration damage contributions in the full-scale tests were estimated between 26 to 57% for seven container ship designs in deck amidships, suggesting a smaller contribution in full scale. However, the results from a frigate type hull (Drummen et al., 2014) suggest a contribution of only 7% in fatigue damage. This type of structure is much more rigid compared to a container vessel, which also operates in more severe sea states. The publications of similar findings on other ship types would be very welcome. Storhaug et al. (2017b) also collected and compared damping data for the governing vibration mode shapes of 21 ships, with an average damping of about 1.7% of the critical damping for container ships and about 0.7% for blunt ships like oil tankers, LNG vessels and ore carriers. Hageman & Drummen (2017) identified a damping ratio of around 0.7% for a frigate, but also showed large variability of this ratio and its sensitivity to vessel speed. The results from bigger data sets would be appreciated, and it is expected to be realized in the future through digitalization. A real starting point on digitalization was presented by Eisinger et al. (2016), who matched ship positions and wave data for many ships from huge databases, e.g. all the container ships in the North Atlantic over a period of three years, etc. The main result was that they encountered less severe conditions than expected due to their capabilities of avoiding storms. This information can be used in subsequent assessments of dynamic response.

2.8 Uncertainties

Uncertainty is in general an interval that contains exact solution with a certain degree of confidence. According to ISO (2008), it is a parameter, associated with the result of a measurement, which characterizes the dispersion of the values that could reasonably be attributed to the measurement. Uncertainty in measurement is used in almost all subject areas (ASME, 2014). It is an important index to estimate the quality of data from a measurement. The International Towing Tank Conference (ITTC) has recommended an alternative approach to experimental uncertainty (ITTC, 2014a; ITTC, 2014b).

There are different procedures for uncertainty assessment in Computational Fluid Dynamics (CFD) (Diez et al., 2017) as well as in Experimental Fluid Dynamics (EFD) (ITTC, 2014a; ITTC, 2014b).

In general, it is assumed that the uncertainties in the modeling of hydrodynamic loads are larger than those related to the structural responses. However, according to linear theory, the uncertainties in hydrodynamic loads are also valid for the structural responses.

Qiu et al. (2014) presented studies on uncertainties related to the prediction of loads and responses for ocean and offshore structures in accordance with the findings by the Ocean Engineering Committee of the International Towing Tank Conference (ITTC). The parameters that may cause uncertainties in ocean engineering model tests and full-scale tests were presented in terms of physical properties of the fluid, initial conditions, model definition, environment, scaling, instrumentation and human factors. A methodology for uncertainty analysis was described according to ISO (2008). This document reported about challenges related to the extrapolation of model test results to full scale.

Tenzer et al. (2015) presented the results of experimental investigations on impact loads. Uncertainties related to the measured impact loads and deformations of wedge-shaped structures were described. To investigate impact-induced hydroelastic effects on slamming pressures, four test bodies were examined. Two bodies were fitted with stiffened, rigid bottom plating and two bodies with thin elastic bottom plating, each case with 5° and 10° dead rise angles. The results were comprised of impact-induced pressures, accelerations, forces, and structural strains. Measurement repeatability, sampling rate effects and hydroelastic effects were investigated. The measured pressures and forces were compared with published experimental data. Additionally, this paper documents body geometries and test rig set-ups including instrumentation and experimental procedures.

Papanikolaou et al. (2014) highlights the importance of understanding and integrating uncertainties in the context of useful prediction tools for the assessment of ship wave-induced design loads. This is elaborated by presenting some recent advances in (a) modelling the combined hydrodynamic responses of ship structures using cross-spectral combination methods and in (b) implementing uncertainty models used for the development of modern decision support systems as guidance to ship master.

el Moctar et al. (2017) presented computational methods to assess slamming-induced hull whipping on sectional loads of ships in regular and irregular waves. The numerical methods solved the Reynolds-Averaged Navier-Stokes (RANS) equations coupled with the nonlinear rigid body motion equations of the elastic ship hull. Uncertainties related to discretization errors were investigated. The authors numerically investigated three container ships in regular waves, in random irregular long crested waves, and in deterministic wave sequences. Comparisons to experimental measurements agreed favorably. They relied on different wave models, including second order Stokes waves and nonlinear wave fields obtained from the solution of NonLinear Schrodinger (NLS) equations. Simulations in random irregular waves provided short-term ship response probability distributions under sea state conditions relevant for design loads.

Diez et al. (2017) presented a high fidelity Uncertainty Quantification (UQ) of a high-speed catamaran, with focus on (a) the validation methods for ship response in irregular waves and (b) the validation methods for a stochastic regular wave UQ method. The approach includes *a priori* CFD simulations by Unsteady Reynolds-Averaged Navier-Stokes (URANS), followed by *a posteriori* EFD campaign. The validation variables are the wave elevation, force, heave and pitch motions, vertical acceleration of the bridge and vertical velocity of the flight deck.

Earlier research by the researchers in UQ for ship hydrodynamics addressed URANS simulations of the Delft catamaran (100 m long with a displacement of 3225 t) in calm water with stochastic speed (Diez et al., 2014) and in stochastic regular and irregular waves (He et al., 2014). A rigorous statistical validation of ship response in irregular waves has been presented by Diez et al. (2015, 2016) and Sadat-Hosseini et al. (2015). The former presented a validation study of the Delft Catamaran in head waves free to heave and pitch (captive), comparing URANS CFD to EFD, and a regular wave UQ method was also formulated and validated against irregular wave benchmarks for both EFD and CFD. The latter presented a study of the fully-appended free-running model of a surface combatant for multiple headings, comparing URANS and potential flow CFD to EFD. The validation addressed time series values (referred to as primary variables) and mean-crossing wave amplitude, height and period (referred to as secondary variables) of wave elevation, forces/moments and motions/velocities/accelerations.

Eca & Hoekstra (2014) attempted to generalize the concept of Richardson extrapolation and propose uncertainty estimators based on truncated power series expansion formulations and least squares fitting to allow for large flexibility and data scatter in grid refinement studies.

2.9 Standards and acceptance criteria

Classification societies make rules for design of ships, and these rules specify requirements, scope, extent and acceptance criteria. The methods and procedures to be used may, however, be explained in class guidelines and recommended practices. Ships designed to these methods and procedures and satisfying the rule requirements may be assigned a class notation.

Classification societies take into consideration the requirements of IMO conventions and recommendations and set out or update their rules. International Association of Classification Societies (IACS), on the other hand, provide unified requirements and interpretations.

2.9.1 Wave-induced vibrations

A major milestone has been reached in the maritime industry within the topic of wave-induced vibrations. IACS issued unified requirements for longitudinal strength of container ships, URS11A (IACS, 2015). This reference document provides functional requirements to account for whipping in the ultimate capacity check (hull girder collapse) in the design of Post Panamax container ships with a breadth greater than 32.26 meters. Unless the classification societies make reservations against this document, it implies that all classification societies must adopt these requirements into their rules. IACS is thereby recognizing the contribution of whipping to the risk of breaking a vessel in two. It is, however, up to the class society to define how this should be accounted for. Derbanne et al. (2016) and Peschmann et al. (2016) explain the background leading up to this fundamental change. This development came as a result of the report from Marine Accident Investigation Branch (MAIB, 2008) based on the MSC Napoli accident, where the classification societies BV and DNV stated that whipping could have contributed to the accident. The report on the MOL Comfort accident (JAPAN, 2015) was also considered in this development.

There are, in principle, three types of changes in rules, related to whipping and springing:

- Rules for design of container ships have been changed to account for whipping and springing;
- Class notations associated with rule text have been developed;
- Class guidelines have been issued either as independent or supporting documents.

DNV (2010) had a high partial safety factor of 1.5 for the wave bending in the ultimate capacity check. Although it is not explicitly stated, this factor accounts for a significant amount of whipping contribution. Many of the classification societies have URS11A formulations included in their rules since 2016. DNV-GL (2016b) has a rule formula for whipping for container ships and for the ships with a breadth greater than 32.26 m. For long (length greater than 290 m), wide (beam greater than 47 m) or fast (maximum speed greater than 25 knots) ships, or for container ships with large bow flare (greater than 55 degrees), direct calculations are recommended. For fatigue strength assessment (DNV-GL, 2017d), vibration damage contributions from whipping and springing are also accounted for in the wave bending moment for all types of ships. This increases the wave bending moment between 10 and 20% depending on the ship beam. LR (2017b) has mandatory requirements in its rules through class notations WDA1 and WDA2 for container ships, with a beam above 32 m and a length above 350 m, respectively. The notations WDA1 and WDA2 both are based on direct calculation analysis. NK (2017b) uses a partial safety factor of 1.5 to account for whipping in the ultimate capacity check for Post Panamax container ships (beam gerater than 32.26 m) with a rule length exceeding 300 m. ABS (2016b) has an ultimate capacity formulation for container ships, where a whipping factor depending on the beam and ship length is included for ships above 130 m. For ships above 350 m, the guidance note (ABS, 2014a) must be followed.

BV, DNV-GL and LR have class notations for whipping and springing referred to as WhiSpn (n being a number from 1 to 3) (BV, 2017a; 2017b), WIV (DNV-GL, 2015a), ShipRight (WDAn, FDA SPR) (n being 1 or 2) (LR, 2017b), respectively. It should be noted that DNV-GL's WIV notation is not limited to container ships and includes both ultimate capacity and fatigue checks with whipping and springing. The rule requirements for container ships with formulas or factors are referred to as Level 1, while direct calculations are referred to as Level 2. Strictly speaking, BV's WhiSpn notation is not limited to a particular ship type, but it has been mainly applied to ultra large container ships. WhiSp1 notation covers the effect of linear springing in the fatigue damage assessment for ships between 300 m and 350 m. WhiSp2 corresponds to WhiSp1 notation with additional whipping computation for ultimate strength assessment, for ships above 350 m. WhiSp3 notation, on the other hand, corresponds to WhiSp2 notation with additional whipping computation for fatigue assessment. LR's WDA1 and WDA2 notations refer to Level 1 or Level 2 whipping design assessment procedures, while FDA SPR refers to springing fatigue analysis. The latter notation is for ships with a length above 350 m, but the length is reduced to 250 m in case of fast ships, based on an encounter frequency versus natural frequency criterion.

Several classification societies have issued guidelines for the calculation of whipping and springing effects. BV (2015) NR 583 is dedicated to whipping and springing assessment and it supports WhiSpn class notations. It also describes the methods and tools to be used for direct analysis of fatigue and extreme loading, including whipping and springing. DNV-GL (2015b) is totally revised to support the new class notation on Wave Induced Vibration (WIV), including whipping and springing. It also includes a semi-direct analysis for Level 1, where the wave bending moment for fatigue is directly calculated. It is also stated that model tests can be an alternative for Level 2, instead of a direct hydro-elastic analysis. However, the Level 2 analysis methodology is not described in detail, but presented by Oberhagemann et al. (2015). For blunt ships, ship specific Level 1 factors for fatigue are included in DNV-GL (2016c) class guideline. These can replace the beam dependent rule factors. ABS (2014a) has a guideline on whipping assessment for container ships, including a close-form method along with a numerical method. In the numerical method, the vessel speed is described as a function of significant wave height. Both extreme and fatigue loadings are included, but different North Atlantic wave scatter diagrams are employed for strength and fatigue assessments. ABS (2014b) also has a guideline for linear numerical springing analysis for fatigue assessments. KR (2017) has a guideline for whipping assessment of container ships by direct analysis methods associated with the class notation WHIP. This document refers to ultimate strength capacity and uses a design wave or sea state method. The wave environment is not clearly specified but the speed is defined to be 5 knots.

The methodologies from different classification societies used to calculate extreme whipping loads differ. Most of the classification societies ends up with a dimensioning sea state that is similar as in linear analysis at 5 knots or zero speed. However, for DNV-GL, the maximum achievable speed is calculated for each sea state, and the sea state with zero or negative speed is removed, where it is assumed that the ship is not able to maintain the heading. This results in much lower sea states becoming dimensioning with higher speeds (Oberhagemann et al. 2015). DNV-GL also uses CFD calculations with most likely extreme waves, while the other classification societies use boundary element methods in regular or irregular waves with 2D slamming. It, however, remains to be seen how the results compare when deriving adequate design values. The differences and consequences should be studied in more detail.

Regarding the rules or standards for wave-induced vibrations on fatigue and particularly for container ships, it is interesting to notice the criticism of Storhaug (2015). He combined the newly developed linear wave bending moment formulations from Derbanne et al. (2016) and pointed out that something should have been wrong with the wave loading level based on direct analysis from the IACS scatter diagram of North Atlantic (IACS, 2001). It was further commented that there should have been much more damage than the fleet experience suggest-

ed. Eisinger et al. (2016) matched ship positions from AIS with wave data from a wave model (ERA-Interim), and this suggested that the encountered wave conditions in the North Atlantic is less severe than IACS North Atlantic (IACS, 2001). This thereby basically supports the conclusions by Storhaug (2015). This overestimation of the wave loads was also recognized by Derbanne et al. (2016), who reduced the wave bending moment from direct calculations by 15% in URS11A (IACS, 2015). Achieving an improved wave environment for design of ships must be important for the industry, especially when wave-induced vibrations become explicitly accounted for.

2.9.2 Noise

IMO (2014) published a guideline for the noise levels on board ships for both passengers and crew members based on the A-weighted equivalent continuous sound level during time interval of at least 15 sec. Various noise levels were set for different spaces of ships with 1600 to 10000 GT and those greater than 10000 GT.

As for environmental noise resulting from traffic noise, WHO (2011) suggested that L_{night} (annual average night time road traffic noise level) of 40 dB should be implemented to avoid possible health risk; this is also true for shipping noise, as was discussed in Murphy (2014).

2.9.3 Sloshing impacts

Not much progress regarding the rules and guidelines for sloshing impact assessment has been introduced in the period of this report. This means that a direct calculation procedure for sloshing assessment is not yet possible, and the socalled comparative approach is still in use (ABS, 2014; BV, 2011; DNV-GL, 2016a). The philosophy of this approach is relatively simple and consists of comparing the loading and capacity of the new design with the reference ship which has never sustained damage due to sloshing impact. Small variants from one classification society to another exist, but they are not very significant.

3. OFFSHORE STRUCTURES

3.1 Wave-induced vibration

Wave-induced vibrations of offshore platforms, referred to as springing, ringing, or whipping, are challenging factors for offshore designers. In addition, ringing can not only cause a total breakdown even in moderate storms, but also can hamper daily operations and lead to fatigue failure. The variations in dynamic response with respect to water depth and tether tension are presented by showing their influence on springing and ringing response. Offshore platforms may be exposed to wave impacts and slamming in extreme wave conditions. Vertical wave loads on decks due to insufficient air-gap are a major concern for many in-service platforms. A numerical method, based on a fixed regular Cartesian grid system, for investigating wave impact loads on semi-submersible platforms in extreme sea states were described in Liao et al. (2017).

For preliminary design of risers and mooring lines, dynamic analyses of wave and floater-induced responses are frequently based on the application of regular waves with given amplitude and period. For a more comprehensive verification concept, a stochastic model of the ocean surface and wave kinematics is typically applied. The corresponding dynamic response will hence also be of a stochastic nature, which implies that suitable probability distributions of local maxima and extreme values need to be identified. As the response processes in general are of a non-Gaussian nature, this may frequently become a challenging task. Such response analyses, in general, need to be repeated for multiple sea states. This implies that considerable computational efforts are required, unless some kind of selection of important sea states is performed.

Ortega et al. (2017) identified and quantified the interaction of internal slug flow and wave loads on flexible riser dynamics by using two coupled in-house codes. One code carries out a global dynamic analysis of the slender structure using a finite element formulation. The other

program simulates the behaviour of the internal slug flow using a finite volume method. By means of distributed simulation, these two programs run synchronously and exchange information during the time integration process. A test case using hydrodynamic forces, according to the linear Airy wave theory coupled with an internal unstable slug flow, was analysed, and the results showed amplification of the dynamic responses due to the interaction between the two load types.

Grytøyr et al. (2017) studied four sets of measurement data for accurate assessment of the fatigue loads imposed on the subsea wellheads from Statoil, with the intention to quantify the degree of conservatism to be expected from drilling riser analysis. They found that the global drilling riser analyses accurately predict the cyclic loads on the subsea wellheads, provided that the input data are known with a high degree of detail, including riser tension setting, drill pipe tension variation over time and hydrodynamic loads. It is found that scatter in the results is due to the uncertainty inherent to several of the input parameters. It is also shown that the accumulated fatigue damage from a full drilling campaign can be established with a sufficient degree of accuracy. Directionality and spreading of the wave field can be handled by use of factors on the damage rate.

Vibration reduction can be achieved in many different ways, depending on the problem; the most common ones are stiffening, damping and insulation. Stiffening involves a sort of shifting the resonance frequency of the structure beyond the frequency band of excitation. Damping consists of reducing the resonance peaks by dissipating the vibration energy. Isolation is a method that can be used to prevent the propagation of disturbances to sensitive parts of the systems. Vibration control on marine offshore structures is challenging with self-excited nonlinear hydrodynamic forces, large deformations and highly nonlinear responses.

A study comparing the different schemes of controlling steel jacket offshore structures subjected to hydrodynamic wave forces is presented by Nourisola et al. (2015). The performances are evaluated in terms of control force and amplitude reduction.

Reducing the vertical motion is of practical importance when accounting for marine operations like drilling and oil production, making it desirable to minimize the heave motion to reduce its down time to weather. An increase in the hydrodynamic mass and damping, for instance, can be achieved by increasing the draft of the platforms. A good example of this is the turning point of the classical spar to a truss spar. Heave plates are also used for the purpose of generating huge added mass and reducing the steel weight and consequently the cost of the hull (truss spar). The resemblance with the Tuned Mass Damper (TMD) concept is discussed for a semi-submersible platform with heave plates by Liu et al. (2016b).

Kandasamy et al. (2016) gave a review of vibration control methods for marine offshore structures, which categories the general approaches as passive, active, semi-active and hybrid, respectively. This is then followed by a review of the specific marine offshore vibration control methods and a comparison of the approaches. The marine offshore structures considered in this review include jacket structures, Tension Leg Platforms (TLPs), spar structures, Floating Production Storage and Offloading vessels (FPSOs) and riser structures. It can be found that the general trend is progressing towards semi-active and hybrid vibration control from passive or active control, as they provide more practical approaches for implementation, possessing the advantages of passive and active control systems.

3.2 Wind-induced vibration

Wind-induced vibration is one of the important factors to the structural safety of offshore structures. In recent years, several papers have been published on wind-induced vibration, where the offshore structures as well as Offshore Wind Turbines (OWT) are investigated. These papers can be categorized into following two groups:

- Estimation of structural response due to wind loads,
- Control and reduction of wind-induced vibration using passive/active dampers.

Jia (2014) calculated the wind-induced fatigue damage of offshore structures using nonlinear time domain dynamic analysis. The author showed the effects of time step, time duration and flare boom connection stiffness on the response. The results for the static and dynamic analyses were compared, and it was concluded that it is important to consider the contribution of secondary structures such as flare and vent lines when assessing the wind-induced fatigue damage. In addition, the effects of gravity on the structure's fatigue damage were also studied, and non-Gaussian responses are discussed through the statistical investigation of the local responses. Finally, it is noted that the fatigue methodology presented can be extended to other offshore tubular structures exposed to wind excitation.

Liu et al. (2016a) investigated the wind-induced vibration of a large towering offshore oil platform using the results of a 1/100 scaled model test as well as finite element analysis. In order to obtain the lengthwise and crosswise fluctuating wind loads acting on the platform, a high frequency force balance experiment under various wind directions was carried out. Using the load distribution obtained by the experiment, a nonlinear finite element analysis, considering pile-soil interaction, was carried out. The acceleration and displacement of the large oil platform as response to wind load are estimated by using the finite element analysis. It is found that the RMS (Root Mean Square) of the fluctuating cross-wind load is about 10% of that lengthwise wind load. It is found that the wind-induced vibration mainly concentrates in the towering and hollowed-out structures and that RMS of the cross-wind acceleration is about 55-61% of the lenthwise-wind acceleration. It is therefore concluded that, for large towering platforms, special attention should be paid to the wind-induced response on the top and bottom of towering structures (derrick, crane, etc.) in wind-resistant designs.

Dezvareh et al. (2016) investigated the reduction of wind/wave-induced vibrations for JOWTs (Jacket-type Offshore Wind Turbines) using a passive vibration absorber called TLCGD (Tuned Liquid Column Gas Damper). Assuming various combinations of wind/wave loading conditions, a series of analysis were carried out for three different JOWTs using a nonlinear model in the time domain. The main parameters of the TLCGD are optimized to reach the minimum standard deviation of turbine nacelle displacements. The results indicate that, depending on the wind/wave combinations, the TLCGD can result in reductions up to 45% and 51% in turbine nacelle displacement standard deviation and maximum acceleration, respectively. It is pointed out that the TLCGD is well suited for fatigue critical JOWTs as it leads to more reduction in the standard deviation of the displacements compared with the maximum displacement.

Utsunomiya et al. (2015) presented a design methodology for a hybrid spar type floating wind-turbine installed in Japan. Moreover, the environmental design conditions such as Design Load Cases (DLCs), dynamic analysis and fatigue analysis are also presented briefly. A full-scale measurement and numerical analysis are carried out. Essentially, a design wind speed is obtained by a comparison between the annual maximum wind speed obtained by a Monte Carlo simulation of typhoons and the observation data at the site (estimated from the database of the past typhoons). From the load analysis results, it is concluded that, for the hybrid spar structure, a simple one-dimensional structural model can be used. Utsunomiya et al. (2017) presented an additional analysis and validation of the numerical analysis model. Application of wind loading to the tower structure is carried out based on the model of Utsunomiya et al. (2015). The modified simulation results are compared with the field data (experiment) in terms of natural periods of each Degree Of Freedom (DOF). The simulation results were in good agreement with the measured values, such as the power and mean value of the pitch response during power production.

Zuo et al. (2017) investigated a method using MTMDs (Multiple Tuned Mass Dampers) to control the tower vibration of OWTs. A finite elemental analysis of the offshore wind turbine tower vibrations induced by wind, sea wave and earthquake loading was presented. The tower responses of the original wind turbine (without control devices) are compared with those controlled by STMD (Single Tuned Mass Dampers) and MTMDs, and the robustness of the

proposed method is also discussed. The dynamic responses of the tower to the combined wind, sea wave and earthquake loads are calculated. It is observed that the fundamental vibration modes and higher vibration modes can be controlled effectively by the MTMDs. Furthermore, using smaller MTMDs can significantly improve the robustness of the control system.

Zhang et al. (2017a) presented different types of active control schemes, such as delayed feedback control, sliding model control, sampled-data control and network-based control, to suppress the vibration of offshore platforms. They also presented other control schemes, such as passive control schemes and semi-active control schemes.

3.3 Vortex-induced vibration

Vortex-Induced Vibration (VIV) is a phenomenon that cylindrical structures may experience due to interactions between the structure and ambient currents. These vibrations occur as a result of the oscillating forces caused by flow separation and vortex shedding. When VIV occurs, the structure is subjected to cyclic bending stresses, causing fatigue crack growth over time, which may eventually lead to fracture. In addition, the vibrations lead to an increase in the mean drag forces, referred to as drag amplification, causing enlarged static displacements and tensile forces. The vortex shedding triggers vibration, while the cylinder motion alters the flow, thus affecting the fluid forces. On the other hand, if the vortex shedding frequency is close to the natural frequency of the cylinder, large body motions are observed and this phenomenon is referred to as "lock-in".

3.3.1 Experimental studies

A survey of the published papers in recent years shows that the majority of the reported work is concerned with model tests. The typical scaling factors are within the range of 1:40-1:75. In the field of ocean engineering, simultaneously satisfying Reynolds and Froude scaling for the model and prototype conditions is impossible in practice. Full-scale testing is therefore necessary.

2D tests

In 2D tests, rigid cylinders with various geometric shapes are elastically mounted or forced to oscillate. The cylinder can either be towed in a towing tank (normally in calm water) or tested in a tank with current. This type of test can be used to study VIV characteristics of one short section of an elastic structure such as a riser.

Assi et al. (2014) investigated the effects of free-to-rotate splitter plates and a short-tail fairing on a rigid circular cylinder. The study shows that the rotational friction between the fairing and the cylinder reduces the VIV when the rotational friction is above a critical limit. The effect of the fairing is similar to that of a free-to-rotate splitter plate solution. A non-rotating fairing and splitter plates were found to develop severe galloping instabilities in 1-DOF experiments. The galloping phenomenon was the focus of a subsequent study by Assi & Bearman (2015), where the effect of a slotted splitter plate was examined. Hydrodynamic force decompositions and PIV measurements of the flow field around the plates confirmed that a transverse galloping mechanism drives the cylinder with splitter plates into high-amplitude vibrations.

Allen et al. (2015a) performed experiments on a cylinder with a combination of helical strakes and fairings at high Reynolds numbers. Tests were also conducted in a circulating water tunnel on an array of cylinders. The study shows that it is possible to mix helical strakes and fairings on one cylinder, but care must be taken as to the length and coverage. In the case of tandem cylinders, the responses are highly sensitive to the coverage on the upstream and downstream cylinders. Allen et al. (2015b) continued the studies by using the same experimental configuration where marine growth was simulated in the models. It was found that the presence of marine growth can affect the performance of the VIV suppression devices by reducing their effectiveness, and this may be amplified in the case of an array of cylinders. The paper also states that the study has not yet been complete, and there is still a substantial amount of research to be done to fully understand this phenomenon.

Cicolin & Assi (2015) presents a study investigating the influence of permeable meshes attached to a rigid cylinder on the VIV responses. Three different types of mesh geometries were investigated, and the results show that VIV responses are reduced by about 50-60% depending on the type of mesh used, but the effect on the drag varies.

3D tests

3D tests of long flexible pipes were carried out with varying geometries and boundary conditions. The test arrangements made it possible to create various flow conditions and current profiles. This type of test is typically used to study the VIV of risers, umbilical, free span pipelines and cables. It can also include realistic boundary conditions, for example, seabed for a Steel Catenary Riser (SCR).

Huera-Huarte (2014) studied VIV suppression by using splitter plates on a flexible circular cylinder. The coverage of elastically mounted splitter plates was varied along the length of the cylinder. The splitter plates were prohibited from rotation but allowed to hinge about the attachment point. The study shows that the VIV response can be reduced by up to 90% if splitter plates cover less than half length of the model. However, it was found that the performance of the splitter plate is dependent on the alignment of the incoming current. Thus, it is only applicable to known or easily controlled current headings.

The effect of surface roughness was studied by Gao et al. (2015) using a flexible circular cylinder. The roughness was altered by gluing sand to the surface of the cylinder, which in turn affected the flow over it. It was observed that in-line responses were increased with a rough cylinder, with lock-in occurring earlier compared to a smooth cylinder.

Wu et al. (2016a) presented a VIV model test study of a large aspect ratio flexible cylinder with staggered buoyancy elements. The test simulated a steel lazy wave riser, where the buoyancy section is a critical element of the design. The diameter ratio between the bare cylinder and buoyancy elements is a key factor in the response, where the response of the bare cylinder would lead to more fatigue damage even if the buoyancy element may have larger displacements.

More recently, Yin et al. (2017) carried out VIV tests on a full-scale riser model at prototype Reynolds numbers. This reduced the uncertainties that may be present when testing at Reynolds numbers smaller than full-scale or prototype Reynolds numbers. Forced oscillation tests were also performed along with tests on surface roughness, which is a critical parameter at prototype Reynolds numbers. The study concluded that the drag coefficient is dependent on the Reynolds number and surface roughness ratio. Also, at critical and supercritical flow regimes, the responses are not sensitive to Reynolds number. At subcritical flow regimes, however, the responses are distinctively larger.

Fan et al. (2015) and Yin et al. (2016) performed VIV tests on flexible cylinders, where both the top and bottom attachment points were examined, to model the full-scale effects and boundary conditions. In Fan et al. (2015), the bottom of the cylinder was connected to a setup modelling the seabed floor. Yin et al. (2016) investigated a drilling riser setup with different boundary conditions at the top and bottom for simulating the vessel, the well head or other aspects. In these studies, the characteristics of the top and/or bottom attachment points were found to influence the VIV responses.

The above studies have been mainly focused on VIV responses due to the presence of a current or an incoming flow field. Wang et al. (2014, 2015) and Fernandes et al. (2014) presented studies considering VIV of steel catenary risers induced by vessel motions. This is similar to oscillatory type flows. The results of these studies indicate that this type of vessel-induced vibrations plays a significant role in the fatigue damage to SCRs.

Full-scale tests

Extensive experimental research has been conducted to study VIV in the past several decades. However, most of the experimental work uses small-scale models and relatively low Reynolds

numbers (Re) - “subcritical” or even lower Reynolds number regime. There is a lack of understanding of the VIV in prototype Re flow regime. In addition, the surface roughness of the structure is also an important parameter, especially in the critical Re regime.

Yin et al. (2017) studied two full-scale rigid riser models with different surface roughness ratios in the towing tank of MARINTEK in 2014. Stationary tests, pure CrossFlow (CF) free oscillation tests, and forced/controlled motion tests were carried out. The conclusions were drawn that the drag coefficient depends on the Re number and surface roughness ratio. At critical and supercritical flow regimes, the displacement amplitude ratio is less sensitive to Re than to lower Re. The displacement amplitude ratio in the subcritical flow regime is significantly larger than in critical and supercritical flow regimes.

3.3.2 Semi-empirical methods

For the semi-empirical models, the work recently done is focused on the enhancement of existing codes to overcome some of the shortcomings of previous methods, on the benchmarking of different tools and on their validation with comparisons with model and full-scale experimental data.

A semi-empirical model for time domain simulation of cross-flow, vortex-induced vibrations of slender circular cylindrical structures is developed by Thorsen et al. (2014). A model for the synchronization between the lift force and structural motion is derived from already established data for the cross-flow excitation coefficient. The proposed model is tested by numerical simulations, and the results are compared to experimental observations. Comparison with experiments shows that the model is capable of reproducing important quantities, such as frequency, mode and amplitude, although some discrepancies were seen. In the studies by Thorsen et al. (2015, 2016), realistic estimates of the structural response through simulation of several experiments of flexible pipes in uniform, sheared and oscillatory flow were presented. The heave-induced VIV of an SCR with non-linear bottom contact was simulated. The response was in good agreement with measurements (Thorsen et al., 2017).

Ulveseter et al. (2017) modified the original semi-empirical, deterministic time-domain model, which was developed by Thorsen et al. (2014), into a new stochastic model. The stochastic feature is to make the mid-point of the synchronization range a slowly time-varying Gaussian process. The stochastic process introduces two new empirical coefficients, i.e. the standard deviation and the upper limit of spectral frequencies included in the process. Sheared flow experiments with a bare riser from the Norwegian Deepwater Programme (NDP) tests are used to verify the new stochastic approach against the measurements. Response sensitivity of the two new empirical coefficients is performed, trying to realistically capture both amplitude modulation and frequency variations in the riser experiments.

3.3.3 Numerical methods

Most of the work done in recent years concerning the VIV responses of isolated rigid and flexible cylinders was devoted mainly to improving the prediction capabilities of wake oscillator models rather than to the development of new CFD or semi-empirical models. In fact, a significant number of the published papers describe very sophisticated wake oscillator models able to capture the nonlinear multi-mode dynamics and interactions of flexible curved or straight structures undergoing VIV and to overcome the limitation of previous models in predicting the amplitude of oscillations. All of the traditional computational approaches have been adopted for the flow description including Direct Numerical Simulations (DNS), RANS methods, LES model and Detached Eddy Simulation (DES) using finite difference, finite volume and finite element scheme. In particular, several authors proposed space-time finite element as a valid tool to solve fluid-structure interaction problems with moving boundaries such as VIV of an elastic cylinder and to improve the convergence rate in iterative solution of the large scale non-linear equation system.

For instance, Postnikov et al. (2017) presented a new two degree-of-freedom wake oscillator model to describe vortex-induced vibrations of elastically supported cylinders capable of moving in cross-flow and in-line directions. The total hydrodynamic force acting on the cylinder is obtained here as a sum of lift and drag forces, which are defined as being proportional to the square of the magnitude of the relative flow velocity around the cylinder. Two van der Pol type oscillators are then used to model fluctuating drag and lift coefficients. As the relative velocity around the cylinder depends both on the fluid flow velocity and the velocity of the cylinder, the equations of motions of the cylinder in cross-flow and in-line directions become coupled through the fluid forces. Existing experimental data and CFD results are used to calibrate the proposed model and to verify the predictions of complex fluid-structure interactions for different mass ratios. The "super upper" branch phenomenon, exclusive for a two degree-of-freedom motion at low mass ratios, has been observed. The influences of the empirical parameters of the wake oscillators and fluid force coefficients on the dynamic responses are also discussed.

3.4 Internal flow-induced vibration

Despite the rapid development of offshore oil exploitation which involves a large number of pipelines to process oil and gas, a limited number of publications have been found on internal flow-induced vibration in the period of this report.

Eftekhari & Hosseini (2015) studied the thermomechanical stability of a cantilevered pipe spinning around its longitudinal axis and carrying an internal axial flow. The pipe is subjected to an axial force at the free end operating in a high temperature environment. The Extended Galerkin's Method (EGM), in conjunction with a proper representation of the displacements of the pipe, was used to solve the eigenvalue problem. The authors investigated the effects of spin rate and velocity of fluid flow on the stability, and they concluded that the system generally does not lose its stability by divergence, even with the existence of a compressive axial load.

Lu et al. (2016) proposed a multi-physics approach for characterizing Flow-Induced Vibrations (FIVs) in a subsea jumper (an M-shaped pipe providing a connection between manifold and tree) subject to internal fluid flow, downstream slug movemnt and ocean current. The authors successfully addressed the coupled vibration response problems of the subsea jumper; VIV due to the ocean current; FIV due to the internal flow and slug-induced vibration (SIV) due to the downstream slug. It is also mentioned that, compared to the VIV and FIV responses, the pressure fluctuation due to the downstream slug plays a dominant role in generating excessive vibrational response and potential fatigue failure in the subsea jumper.

Li et al. (2016a) investigated the fluid flow vibration of a subsea spanning pipeline conveying gas-water two-phase flow with two ends fixed. The dynamic behaviour of the pipeline was analysed at different flow velocities and volume fractions. The natural frequencies of the pipeline were compared with the structural system vibration frequencies, and the stress range was consequently obtained.

Alizadeh et al. (2016) used the Monte Carlo simulation method in conjunction with FEM for probabilistic self-excited vibration and stability analyses of pipes conveying fluid flow. For the fluid-structure interaction, the Euler-Bernoulli beam model was used for analysing pipe structure and plug flow model for representing internal fluid flow in the pipe. After comparing the randomness effects of fluid parameters on the system with those of structural parameters, it was concluded that the uncertainties in fluid parameters had much stronger effects, and the uncertainties in structural parameters could be ignored.

Meng et al. (2017) investigated the Internal Flow Effect (IFE) on the cross-flow VIV of a cantilever pipe discharging fluid. The study showed that when the internal flow velocity is small, the pipe loses energy to the inner flow and the VIVs can be depressed significantly. On the other hand, the pipe would lose its stability when the internal flow exceeds a critical value, which depends on the current velocity and dominant VIV mode.

3.5 Equipment-induced vibration

Many types of equipment are installed in offshore facilities for production, storage and unloading of oil and gas, and it is almost impossible to consider all of the equipment as excitation sources at a design stage. Therefore, it is necessary to determine the major equipment that degrade habitability in accommodation areas and structural integrity. According to a common practice of shipyards, the major equipment includes rotating machinery operated below 4800 rpm and reciprocating engines exceeding an output power of 30 kW. Some interesting papers related to this subject and published in the period of this report are reviewed.

Seawater hydraulic Axial Piston Motor (SAPM) is an important component in underwater tool systems of offshore facilities. The underwater tool system driven by seawater hydraulics has many advantages, including non-flammability, low operating cost, and low pollution potential to marine environment. One of the most important issues for the SAPMs is low vibration and noise behaviour. For instance, Yang et al. (2015a) proposed an integrated torque model of the hydraulic axial piston motor, which consists of a torque sub-model and a dynamic pressure sub-model, in order to design a seawater motor having a small torque fluctuation. They considered the effects of the dynamic pressure inside of the piston chamber, pre-compression angle and relief-groove obliquity in the integrated torque model. As a result, they showed that an adequate pre-compression could help diminish the pressure shock and that a large relief-groove obliquity decreases the output-torque fluctuation.

Gjinolli et al. (2016) presented analytical processes and design methods to develop a complex exhaust system for a reciprocating engine, which is a power source in offshore facilitipres. In their study, the acoustical and aerodynamic analyses were carried out for a muffler design considering the acoustic performance. Furthermore, the structural analysis was also conducted for evaluating the performance of the exhaust silencer and stack systems, in order to avoid a resonance with the main excitation of the engine.

Twin-screw multiphase pumps have been a good alternative to substitute the conventional pump used for fluid separation, liquid pumping and gas compression facilities, since they can pump mixtures of liquid and gas at very different gas volume fractions in a wide range of pressures. Ramos et al. (2016) proposed an analytical procedure to obtain the forced response of the rotors of twin-screw multiphase pumps. In a case study, only the self-weight of the rotor with a constant speed was considered in the forced vibration analysis in order to evaluate the maximum transverse displacements of the rotors.

Fluid flows downward inside the drill pipe and upward in the annulus between the riser and the drill pipe during the drilling operations. Therefore, significant riser oscillations are observed during deep water drilling operations. Blevins et al. (2016) investigated the riser drilling-induced vibrations. They proposed an analytical model for predicting riser vibrations during drilling operations. As a result, they showed that the fluid forces could cause riser vibrations with a rotating drill pipe and that the magnitude of the fluid force increases with increasing rotational speed of the drill pipe.

Decommissioning is quickly becoming an important field of activity and research for offshore structures for oil and gas production. The North Sea is one such area, with many installations approaching or exceeding their design life. Davidson et al. (2017) experimentally investigated the feasibility of a vibro-extraction method to extract a pile that was submerged in sand. In their study, the force required to extract the model pile was investigated under three different conditions for both loose and dense sand. A model-scale vibration source was designed to provide balanced, vertical sinusoidal vibration, and it was installed at the top of the pile. As a result, they showed that the pull-out load of the pile was reduced by 36% in dense sand and to the self-weight of the pile in loose sand.

3.6 Shock and explosion

An offshore structure may be subject to several types of shock loading, including internal explosion of oil, gas and other chemical matter, external explosion due to weapons attack, and seismic loading from foundation attachments to the sea floor. Many offshore structural engineers work to predict and control the risks caused by internal explosion of petrochemical products. Bang et al. (2016) proposed a method to predict the effect of hydrogen gas tank explosions on nearby pipelines and provided a conservative estimate of the worst-case accident scenario involving an instantaneous explosion of a large hydrogen mass leading to the formation of a shock wave. Darvishzadeh & Sari (2015) used CFD coupled with finite element methods (FEM) for analysis of the shock wave interaction with the structure and large pipe, including impact damage. CFD was also used for analysis of the air temperature increase in a modular structure subject to explosion. Salvado et al. (2017) proposed a thorough validation process of the numerical model and new methods to estimate the peak pressure in the compartment. Shi et al. (2017) presents a numerical procedure to derive analytical formulae to easily generate a Pressure-Impulse (P–I) diagram for corrugations with the Non-Linear Finite Element Analysis (NLFEA) method. Based on the numerical results, analytical formulae to predict the P–I diagram are derived. Gharib & Karkoub (2015) presented an experimental study on the effectiveness of the Linear Particle Chain Impact Damper (LPC ID) in reducing the vibrations of a single DOF frame structure under different shock excitations. Sohn et al. (2016) examined the effect of adding stiffeners to corrugated blast walls aboard offshore structures. Corrugated blast walls tend to buckle at the web-flange interface, and it was shown through FEA that adding flat plate stiffeners at this location improved blast resistance.

Reinforced material usage is a growing area for offshore structures. Recent research has focused on investigation of the blast resistance of reinforced concrete materials. Critical offshore infrastructure such as bridge abutments, petrochemical docking components, ports, and flood control devices often contain concrete structures, and their vulnerability to both accidental and intentional explosive loading makes the response of these structures to such loadings important to researchers. Li et al. (2016c) examined the effect of adding polyethylene, micro-steel, and hybrid steel-polyethylene fibre reinforcements to concrete slabs to improve blast response performance. Samples were cast and field blast-tested and, along with static material laboratory tests, show the performance improvements of using such fibres to reinforce concrete slab structures. Olmati et al. (2015) investigated the blast resistance of precast concrete panels not originally designed for such loads using a probabilistic numerical approach. The probability of a pre-cast concrete panel exceeding its limit state is generated, and fragility curves are computed using Monte Carlo simulations.

Response to seismic shock loading is also of interest to the offshore community. Wu et al. (2016b) validated the favourable response performance of a TMD under earthquake loading by numerical analysis and 1:200 scale model testing. The results indicated a reduction in the displacement and acceleration response of the structure with a TMD over one without, and that a properly tuned TMD would activate within the first 3 seconds of seismic excitation.

3.7 Noise

Exploration, construction, transport, drilling and production are important offshore activities. However, these activities may cause high levels of noise to be emitted into the surrounding environment. The activity of pile driving for the construction of foundations of wind turbines and other offshore structures may be the most important noise source, and therefore, much research has been published on this topic. These research activities may be divided into two major groups: those involving numerical and experimental methods for analysing the noise emitted due to pile driving and those involving noise mitigation measures.

3.7.1 Pile-driving-induced underwater noise

To predict the noise emission caused by pile-driving under offshore conditions, a numerical model was presented and validated by Göttsche et al. (2015). The model combines a finite element method with a Parabolic Equation (PE) technique to compute the pressure spectrum, sound exposure and peak level in a certain distance of the pile. The results are compared to measurements performed during two full-scale offshore tests. Furthermore, a procedure is presented to compute the acoustic properties of the sediment as a function of frequency, depth and density.

Fricke & Rolfes (2015) presented an approach for the prediction of underwater noise caused by pile driving, and it is validated based on *in situ* measurements. It can be concluded from their results that the overall approach and underlying assumptions are appropriate for the frequency range considered. The authors also concluded that it is a reasonable simplification to formulate the soil-structure interaction in terms of a perfect contact condition, without tangential slip between the pile and soil.

Schecklman et al. (2015) presented a hybrid modelling approach, that uses the PE technique with an empirical source model, to predict the underwater noise due to pile driving in shallow, inhomogeneous environments over long propagation ranges. The empirical source model uses a phased point source array to simulate the time-dependent pile source. The pile source is coupled with a broadband application of a PE wave propagation model that includes range-dependent geo-acoustic properties and bathymetry. The simulation results are in good agreement with acoustic observations of pile driving in the Columbia River. The authors found that the absolute depth of the bathymetry is the only factor that significantly affects long-range sound levels, while bathymetry variations create localized effects. The top sediment layer was shown to affect sound levels greatly.

Deng et al. (2016) developed a three-dimensional semi-analytical method, in which the pile is modelled as an elastic thin cylindrical shell governed by a variational equation, to predict vibration and underwater acoustic radiation caused by a hammer impact. The cylindrical shell is decomposed uniformly into shell segments whose motion is governed by the variational equation. The soil is modelled as uncoupled springs and dashpots distributed in three directions. The case study of a model subject to a non-axisymmetric force demonstrates that the radiated sound pressure has dependence on the circumferential angle. Furthermore, another case study including an anvil shows that the presence of the anvil tends to lower the frequencies and the peaks of sound pressure spectrum.

In many cases, the construction work takes place in shallow water environments, where the soil has a major impact on the resulting wave field. This is mainly due to the occurrence of multiple reflections, the excitation of head waves, and the possibility of energy tunnelling sound mitigation systems through the soil. Measuring these seismic arrivals enables further information to be gained about the local soil characteristics. Ruhnau et al. (2016) investigates the characteristics of direct as well as seismic arrivals within the frame of offshore pile driving based on measurement data collected at the wind farm Borkum Riffgrund located in the German Bight.

Farcas et al. (2016) reviewed the process of underwater noise modelling for environmental impact assessment and explored the factors affecting predictions of noise exposure. The consequences of errors and uncertainties in noise modelling can lead to significant pitfalls in the environmental impact assessment process. The authors therefore discussed the future research needs to reduce uncertainty in noise assessments.

3.7.2 Mitigation of pile-driving-induced underwater noise

Numerical studies considering a sound mitigation system was carried out by Heitmann et al. (2015) and Tsouvalas & Metrikine (2016). In the study of Heitmann et al. (2015), an accurate description of the impact hammer and the layered soil were used. The influences of several

mitigation systems on the underwater sound pressure level are evaluated with a numerical method. The construction guidelines were provided to define an optimal position for such a system. It was shown that the radius for the system should be as large as possible when only one system is used.

Tsouvalas and Metrikine (2016) performed a parametric study based on a semi-analytical model to analyse the principal mechanisms for the noise reduction due to the application of the air-bubble curtain placed around the pile. The results show that the noise reduction depends strongly on the frequency content of the radiated sound and on the characteristics of the bubbly medium. The distinction was made between the piles of large and small diameters due to the considerable difference in spectrum of noise generated. In the case of practical applications related to the installation of large foundation piles, only the lower end of the frequency spectrum is usually of interest.

Dardis et al. (2015) developed a new double-walled pile design with an air gap to decrease the noise transmitted into the sediment and water. The mechanisms of the noise generation in both single- and double-walled piles were described, and a full-scale field test was performed in the Puget Sound, Washington. The results showed that the use of double-walled piles reduced the peak sound pressure by more than 20 dB relative to single-walled piles, while only a 3 to 6 dB reduction was obtained using a bubble curtain.

3.8 Damping and countermeasures

Vibrations in offshore structures may be caused, for example, by

- engines and process equipment,
- wind excitation,
- wave excitation, or
- vortex induced excitation.

Excessive vibrations can cause problems of several kinds, such as

- safety issues, for example, fatigue,
- limited serviceability, for example, due to excessive noise levels,
- reduced platform productivity due to abrupt disasters.

Vibration mitigation is therefore an important area of study. Despite this, not much effort is devoted to research in this field. The main focus area in controlling vibrations in offshore structures is vibration absorbers. The vibration absorbers can be divided into three main categories: (i) passive devices, (ii) semi-active devices (mainly actively tuned passive devices), and (iii) active devices. Of these categories, the passive devices are the dominating category in operations today, due to their reliability and lack of requirement for an energy source. It can likely be expected, however, that the semi-active and active devices will be introduced more frequently in near future. There are therefore currently some research efforts spent on the development of such devices.

Kandasamy et al. (2016) contains an overview of techniques for vibration control in offshore structures. The most commonly used passive devices are TMDs and Tuned Liquid Dampers (TLDs), although the damping materials, such as rubber and synthetic elastomers, are also frequently used in the vibration control. Of these, the TMDs and TLDs are typically used to add damping to the first mode or first few modes of the structure to mitigate the total response to wave and wind loads, which cause fatigue. The damping materials are rather used for vibration isolation of machines and for reducing noise.

Lotfollahi-Yaghin et al. (2016) studied the efficiency of TLDs for the reduction of dynamic responses due to earthquakes on offshore jacket platforms. The results showed that the efficiency varies by earthquake, which is attributed to the frequency content of the earthquake energy. A new development of TMDs, the so-called Pounding TMD or PTMD, is reported by Li et al. (2015). The laboratory tests and numerical studies found the PTMD to be more robust

to off-tuning in comparison with the traditional TMDs. Xue et al. (2016) performs a robustness and control performance study of the PTMD. In this study, a model of an offshore platform is used, and the PTMD is found to suppress vibrations over a larger bandwidth than the traditional TMDs.

Damping is important for mitigating vibrations, and an accurate knowledge about damping is a necessity in forced response computations in order to obtain correct response levels, for example for fatigue estimations. Since analytical models for damping are missing, the damping levels normally need to be obtained by experiments. Gres et al. (2016) reports an assessment of damping for an offshore mono bucket foundation, using Operational Modal Analysis (OMA). They found the first mode of vibration to have approximately 1.1% relative damping. Yang et al. (2016b), on the other hand, present the OMA results of a jacket platform excited by ice loading. The first four modes of the jacket platform were found to have approximately 2 to 3.8% damping ratios. In an experimental study of a 1/10 model of an offshore jacket platform standing on soil in water, Mao et al. (2015a) found the damping ratio of the first mode of vibration to be between 3.6 and 4.4%. They also found that the contribution of the foundation degradation to the damping was small.

Zhang et al. (2017c) made a theoretical study of a Pall-type Frictional Damping (PFD), with shape memory alloy installed on the isolation layer of a jacket platform. They showed that the system is successful in reducing earthquake-induced vibrations. The damping ratios were obtained experimentally as approximately 4 to 5%.

Another area of interest is noise and comfort for personnel on board offshore platforms. Lee et al. (2015a) thus presents a design process for anti-vibration mounts for offshore structures accommodations. The design method allows mount type, allowable displacements and design loads to be selected. The method was verified on a scaled structure. Zhu et al. (2015) studied magnetorheological elastomers with alloys, adjusting stiffness and damping by varying a magnetic field around the material. The material was reported to be promising for adaptive vibration mitigation.

3.9 Monitoring

This section covers developments in the monitoring of offshore structures. In general, measurement campaigns cover a broad range of goals. Since structural dynamics are of lesser concern in the offshore industry, the monitoring campaigns, mainly focus on the assessments of maintenance needs, extreme responses and reliability of local structural details and components. Views on goals and scope of monitoring programs within offshore projects are discussed in Section 3.9.1. The monitoring programs aim to investigate the critical areas within the offshore structures. However, there are technical challenges associated with structural monitoring in such hostile environments.

Firstly, the development of fatigue cracks as a result of structural response is one of the major concerns in the offshore industry. This is often related to maintenance, but within the offshore industry, the fatigue can also be a safety issue, equivalent to structural overloading scenarios such as buckling, yielding and dents (collisions). Fatigue crack monitoring methods are discussed in Section 3.9.2.

Secondly, the dynamic response of subsea components is often challenging to monitor. Therefore, subsea monitoring systems may be enhanced with the analysis tools that enable derivation of system properties, which can otherwise not be obtained reliably. These are discussed in Section 3.9.3. Floating offshore wind applications feature different monitoring challenges compared to the oil and gas offshore industry. Monitoring solutions for the response of offshore wind plants are discussed in Section 3.9.4.

3.9.1 Goal and scope

Condition monitoring or integrity management is an important driver to perform offshore monitoring. Identification of physical damage remains a challenging item. An extensive review of damage identification methods, using the dynamic structural response, is provided by Sun et al. (2016). The authors discuss, among other things, sensor selection and placement, the performance of time domain and frequency domain identification methods and artificial intelligence, such as Genetic Algorithms. Next to the technical aspects of integrity management, organizational challenges also need to be addressed. Wisch & Spong (2016) discuss the playing field between operators, classification societies and authorities.

Monitoring programs can be used to achieve maintenance efficiency. May et al. (2015) show a cost-benefit analysis for two different monitoring approaches on an offshore wind turbine. They identify replacement costs, loss of production and logistics costs, resulting in an overall cost reduction of 6% when using a response monitoring system. The main challenge in cost-benefit analyses is to quantify the costs involved in a useful format.

Another goal of in-service monitoring is to gain an understanding of the real-life physics by setting up relationships between the measurements. This information can be used for the improvement of future projects. An example thereof, considering a 5 MW wind turbine using 2 years of in-service measurements, is discussed by Hu et al. (2015). An array of four bi-axial accelerometers was used for this purpose. This research shows the dependency between vibration characteristics and environmental conditions such as temperature, wind speed and operational conditions.

3.9.2 Fatigue crack monitoring

The development of fatigue cracks as a result of continuous wave loading and structural vibrations is receiving much attention from the offshore industry. Makaya et al. (2016) shows a theoretical study on fatigue crack detection using Guided Wave technology, wherein Lamb waves and Shear Horizontal waves are monitored during crack growth. The relations between different wave types can be used to locate the crack. Once the crack is discovered, monitoring of the crack may be necessary. Horst & Kaminski (2017) discussed the theoretical analysis and laboratory test of a fatigue crack monitoring device using magnetic flux leakage. The methodology does not require continuous monitoring, allowing for low power consumption. Bernasconi et al. (2015) showed in field testing that vibro-acoustic sensor systems can be used to monitor a 155 km long (subsea) gas pipeline over a prolonged period of time. One test described by the authors focussed on the detection of damage events and spilling, using a decommissioned pipeline. The authors detected impacts at a distance of 6 km and spilling events at 30 km.

3.9.3 Subsea monitoring

Subsea monitoring projects have been and still are challenging. Wang & Lu (2016) presents an overview of different technologies for monitoring the response of subsea lines and their maturity for ensuring integrity of mooring systems. The authors present solutions using load cells, inclinometers and GPS-based systems, discussing both technical and economic feasibility of these systems. An example of the latter system is presented and discussed by Minnebo et al. (2014). They discuss the setup and requirements for such a system. The observed motions of the floater can be used to identify failures of the mooring system.

Grytøyr et al. (2015) discuss the measurement of structural response of a wellhead using direct stain gauge and indirect accelerometer measurements. Their solution uses only subsea compatible equipment, all located on the drilling riser above the BlowOut Preventer (BOP). The estimates based on accelerometer measurements show good correspondence with the structural stresses measured on the BOP. Hørte et al. (2013) used a similar setup to examine the structural reliability of a wellhead. Their analysis shows that the uncertainty in the assessment is mainly related to the fatigue capacity, location measurements, Palmgren-Miner hypothesis and FE

analysis. Uncertainties in soil characteristics, cement level and stiffness of the BOP are of lesser importance. The analysis also shows a relation between the applied design fatigue factor and probability of failure.

Besides integrity management, the process control of subsea wells also offers considerable challenges. Letton et al. (2015) discusses the results of a joint industry effort to improve on various subsea well control topics, such as fluid sampling and flow meter verification.

3.9.4 Monitoring of offshore wind turbines

In the case of the monitoring of OWTs, direct monitoring may not be economically attractive or technically viable. OWTs are slender structures which can be monitored using a simple sensor setup in combination with powerful post-processing tools. Because of its different topology, the monitoring strategies in offshore wind differ from those in offshore oil and gas. Male & Lourens (2015) show a promising theoretical study into the development of a monitoring system which is able to identify load characteristics and, from there, determine the dynamic response consisting of accelerations and strains at various locations within the structure. Antoniadou et al. (2017) present an identification method to discover damage from response measurements. The method is successfully applied on wind turbine blades and gearboxes, which are the critical elements of an OWT.

3.10 Uncertainties

Floating offshore structures such as wind turbines often include many DOFs, variables, and excitation from both wind and waves, making the assessment of uncertainty in a test campaign challenging. In addition, it is important to consider many different conditions, requiring a large number of experiments to be run, including numerous repetitions. The variables can be strongly or weakly coupled, meaning that error sources can strongly influence each other. On the hydrodynamic side, offshore wind tests are similar to those done for seakeeping of offshore structures. Uncertainty quantification in the seakeeping field is also not well developed, and it is only recently getting attention (Kim & Hermansky, 2014; Hirdairs, 2014). Uncertainty quantification, however, is essential and needs to be pursued.

Qiu et al. (2014) identified parameters that may cause uncertainties in ocean engineering model tests, full-scale tests and numerical simulations, in terms of the physical properties of fluid, initial conditions, model environment, scaling, instrumentation and human factors. As an example, the uncertainty analysis method (ISO, 2008) was applied to the tests of a moored semi-submersible platform model. The combined and expanded uncertainties were quantified in experimental results including motion responses, air gap and mooring line tensions.

Junior et al. (2014) qualitatively addressed the consequences on uncertainty for the execution of an inclining test of a semi-submergible platform with a mooring system and risers at the production site and compared the results to the ones taken from typical inclining test procedures at sheltered waters, as defined by ASTM F1321. The authors applied uncertainty analysis by evaluating the propagation of uncertainties from the measurements to the final calculations.

Robertson (2017) examined the sources of uncertainty associated with the measured loads for a scaled, floating offshore wind test performed in a wave basin within the OC5 project (which is focused on validating offshore wind modelling tools by comparing simulated responses of selected offshore wind systems to physical test data). The research qualitatively examined the sources of uncertainty associated with the test to start a discussion of how to assess uncertainty for these types of experiments and to summarize what should be done during future testing to acquire the information needed for a proper uncertainty assessment.

3.11 Standards and acceptance criteria

3.11.1 Wave-induced vibrations

The offshore industry has not recognized wave-induced vibrations to the same extent as in maritime industry. However, offshore ships like FPSOs can utilize the same standards as in

maritime, for instance, rules for hull monitoring systems, e.g. HMON (DNVGL, 2017a) and voluntary class notations, e.g. WIV (DNV-GL, 2015a). NORSOK (2017) also includes local and global vibrations from slamming, dynamic analysis for fatigue, ultimate and accidental limit states. Hull monitoring systems have become more popular for such offshore ships, since a more flexible inspection regime, risk based inspection, is accepted. For some of these offshore ships, the classification society may also accept using maritime rules, which include the effect of wave-induced vibrations (DNV-GL, 2017d). It should, however, be emphasized that the offshore structures are related to low (current) to zero speed, which tend to reduce the effect of wave-induced vibrations, but on the other hand, such vessels operating in harsh environments may maintain head seas in more extreme weather conditions, which tends to increase the relative importance of whipping. The Monitas JIP is an example where this effect was briefly considered for fatigue (but not published).

For other offshore structures, class may lack rules and standards for wave-induced vibrations, but they may still request assessment of consequences and suggest that the resonance periods may be kept as low as possible. This could be related to innovative structures, such as ocean farms and other flexible offshore structures. For jack-ups, specific assessment of dynamic amplification is required for fatigue and ultimate limit state. For TLP, ringing and springing are well known phenomena that can contribute to fatigue damage of the tension loaded tethers.

3.11.2 Vortex-induced vibrations

VIV due to current and waves are well known within slender structures like free span pipelines and risers, but the vortex shedding can also cause low frequency dynamic response of mooring systems without any elastic response of the platform itself. These vibrations can then be dominated by low and high frequency responses, compared to wave frequency response, which makes Rainflow counting and time domain analysis a natural choice for fatigue assessment. For riser fatigue, this is covered by a recommended practice (DNV-GL, 2017e) which also includes a simplified method for this additional vibration effect. For free span pipelines, the VIV are both relevant in fatigue and in extreme loading, and even sensor monitoring is now included as an approach (DNV-GL, 2017f). For free spanning subsea power cables, VIV can also be part of the fatigue limit state requirements (DNV-GL, 2016d).

NORSOK (2017) includes VIV in general terms based on water flow and wind. NORSOK basically mentions vibration and dynamic response for all types of offshore structures and suggests that if the natural period is less than two seconds, a simplified method for estimating the dynamic amplification factor (DAF) can be used for a single DOF system, based on Baarholm et al. (2013).

Classification societies may also request the assessment of VIV caused by wind for slender topside equipment without having specific requirements in the rules. In certain cases, it is a question of reducing the natural periods to reduce the dynamic response levels.

3.11.3 Noise and vibration

While the comfort class notation COMF is mainly used within the maritime domain for passenger ships, the class guideline gives more general criteria, which can also be used within offshore accommodation units (DNV-GL, 2016e).

3.11.4 Underwater noise

Within the last couple of years, underwater noise generated by the installation of offshore windfarms has gained wide-spread concern. The guidelines for measuring underwater noise generated by windfarm constructions are given by ISO (2017), Dekeling et al. (2014a, 2014b and 2014c), BSH (2013) and Robinson et al. (2014) for ISO, EU, Germany and UK, respectively. According to BSH (2011), the sound exposure should not exceed 160 dB (re 1μPa) outside of a circle of 750 m radius.

4. BENCHMARK STUDY

4.1 Introduction

Throughout the maritime world, considerable effort is being spent on predicting loads associated with slamming (see, for instance, Kapsenberg & Thornhill, 2010). The ISSC 2012 Dynamic Response committee performed a benchmark study on the accuracy of the translation from these loads to the structural responses. Six participants entered the benchmark study. The goal of this benchmark was twofold. On the one hand, the degree of variation in estimates produced by different methods and organizations was revealed. On the other hand, the absolute error made in the analyses was investigated by reproducing model test responses. From the benchmark, it was concluded that the shapes and frequencies of the two and three node, dry and wet, horizontal and vertical flexural vibration modes determined by the participants were well in line with experimental results for four of the six participants. When participants applied different realistic but analytical pulses to their model, significant differences up to a factor of five were found. On the time series level, two of the six participants have results that correlate well. Details on the benchmark and the results were discussed by Drummen & Holtmann (2014). The benchmark considered a range of methods varying form empirical methods to determine the added mass to a coupled structural and RANS solver. Results for an intermediate one-way coupling were presented by Dhavalikar et al. (2015). The ISSC 2012 Dynamic Response committee benchmark study provided insight into the accuracy of the range of methods that is available for predicting the dynamic response of ships.

For performing long-term design calculations for ships, any kind of CFD calculation will generally be time consuming and thus may not be realistic, although it may be practical in future. Two- and three-dimensional panel methods will remain the primary approach for some years to come. In order to further investigate the accuracy of the predicted dynamic response, the ISSC 2018 Dynamic Response committee chose to also perform a whipping benchmark study. But this time, the focus was on nonlinear strip theory and panel methods.

4.2 Benchmark setup

Four participants entered the benchmark. Two research organizations (SINTEF Ocean and National Maritime Research Institute, NMRI) and two classification societies (BV and NK). The benchmark consisted of two parts. The first part is a comparison of the shape and natural frequencies of the first two global flexural modes. In the second part, a comparison is made between standard deviations of the total stresses and high frequency stresses at the three cross sections for 16 sea states. Participants were provided with the following data:

- Geometry consisting of points on a large number of cross sections,
- mass distribution along the length of the model,
- natural frequencies, shapes and damping ratios of the first three dry global vertical flexural vibration modes,
- time series (30min – 45min) of the wave at the Center of Gravity (COG) of the model for each of the 16 sea states.

Given this input data, participants were asked to provide the shapes and natural frequencies used in their method and to determine the vertical bending moments at the quarter lengths and amidships.

The experimental results that are used as a benchmark are presented in Section 4.3. Methods used by the participants are described in Section 4.4. Participants are referred to as A, B, C and D. Sections 4.5 and 4.6 respectively describe the results of the benchmark and its conclusions.

4.3 Experimental results

The model tests used as reference were performed in the towing tank at the Marine Technology Centre in Trondheim. The tank is 260 m long, 10.5 m wide and from 5.6 to 10 m deep. The double flap wave maker is able to produce both regular and irregular waves. The model tested was based on a container ship with a length between perpendiculars of 281 m. It has a large, flat, overhanging stern, a pronounced bow flare and a large bulb. The model was built to a scale of 1:45. More detailed information about the experimental setup was given by Drummen (2008). With reference to Section 2.1.2 a segmented hinged model was used. Figure 1 shows a picture of the model. As can be seen from the figure, the model consisted of four segments and three rotational springs. The stiffnesses of the springs were tuned to achieve the desired scale natural frequencies of the ship.

Figure 1. Picture of the segmented model

The model was tested in irregular head waves, as this condition is usually the most severe with respect to the vertical response. The chosen sea states are given in Table 2. The JONSWAP spectrum was used as the target wave spectrum. The peakedness parameter is also shown in Table 2. The forward speed was chosen to be constant in sea states with the same significant wave height and was based on full-scale measurements reported by Moe et al. (2005). The full-scale forward speeds of the model in the investigated sea states are also given in Table 2. For each sea state, three runs were conducted in waves that were realisations of the same spectrum. The realization periods were short enough to avoid repeating wave trains. The combination of the three runs resulted in a record length between 30 and 45 min full scale, depending on the chosen speed.

4.4 Methods

Table 3 summarizes the different approaches used by the participants. Participant A used a nonlinear strip theory approach where the radiation/diffraction forces were calculated with a BEM in frequency domain. The hydrodynamic radiation/diffraction force coefficients were represented in values of zero-cross wave frequency. The nonlinearities of the Froude-Krylov forces and hydrostatic restoring forces were taken into account. The nonlinearities of radiation and diffraction forces were also considered by using the "hydrodynamic coefficient table," which is prepared before time series calculations for various ship drafts and roll angles for each section, in frequency domain. All degrees of freedom except surge are considered in the computations. The slamming impact was calculated using the momentum theory. The structural model was an Euler-Bernoulli beam based on modal decomposition, and the first three global vertical flexural vibration modes were taken into consideration.

Table 2. Overview of irregular waves. H_s, T_p, γ and U denote significant wave height, peak period, peakedness parameter and vessel speed, respectively.

Run	H_s [m]	T_p [s]	γ [-]	U [kn]
1	3	10.6	1	22
2	3	13.4	1	22
3	3	16.3	1	22
4	3	19.1	1	22
5	5	10.4	1.5	20
6	5	13.4	1	20
7	5	16.3	1	20
8	5	19.1	1	20
9	7	9.5	5	16
10	7	13.4	1	16
11	7	16.3	1	16
12	7	19.2	1	16
13	9	9.5	5	12
14	9	12.8	2.3	12
15	9	16.3	1	12
16	9	19.1	1	12

Participant B used a strip theory approach in which the radiation forces were calculated with a boundary element method. Only heave and pitch were considered. Nonlinearities of the Froude-Krylov forces and hydrostatic restoring forces were considered, as well as slamming. The slamming impact was calculated using the momentum theory. Participant C used a hydro-elastic approach, based on a potential flow solver and a modal decomposition of the elastic motions on the first 2 natural vibration modes (vertical bending). The hydrodynamic radiation/diffraction is first solved in the frequency domain using a 3D BEM solver; in time-domain, the radiation forces are computed using a convolution integral and infinite frequency added mass values. The diffraction forces are recomposed from the frequency domain results, and the hydrostatic and incident wave loads are recomputed at each time step using the exact position of the ship and the incident wave profile. The slamming loads are computed using a

Table 3. Overview of methods used by participants in the study.

	Structural model	Added mass	Nonlinearities
A	Euler-Bernoulli beam	2D BEM	Froude-Krylov, hydrostatic restoring, radiation and diffraction (table), slamming (momentum theory)
B	Euler-Bernoulli beam	2D BEM	Froude-Krylov, hydrostatic restoring, slamming (momentum theory)
C	3D finite element model	3D BEM	Froude-Krylov, hydrostatic restoring, radiation and diffraction, slamming (Generalized Wagner Model)
D	Vlasov beam	2D BEM	Froude-Krylov, hydrostatic restoring, slamming (momentum theory)

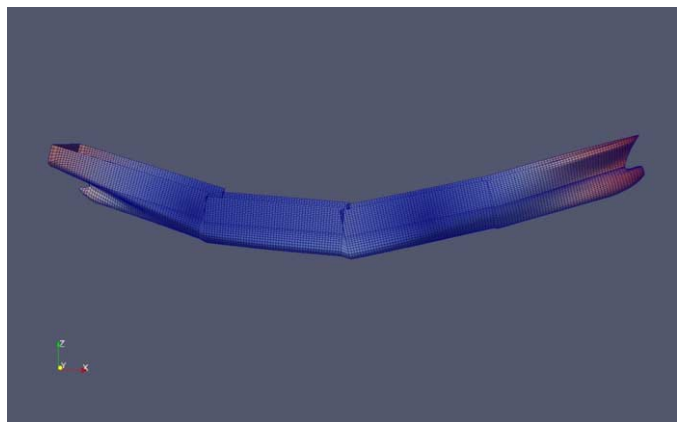

Figure 2. Illustration of two node vertical flexural vibration mode by Participant C.

2D-strip approach; on each 2D section, the GWM is adopted to compute the slamming pressures, which are then mapped onto the 3D mesh. For these particular head wave computations, the sway, roll and yaw motion are fixed to zero, and the surge motion is imposed to be equal to the re-composition of the frequency results. Figure 2 shows an illustration of the two-node vertical flexural vibration mode by Participant C.

Participant D used a nonlinear hydroelastic strip theory method for the predictions of wave-induced vertical motions, considering load effects in the ship with large amplitude motions and small hull deformations. The global hull deformation is approximated by an aggregate of flexible modes, and the wave-induced ship responses are obtained by modal superposition. The nonlinear effects in the vertical motions and cross-sectional load effects are introduced in the form of a nonlinear vertical excitation force. In this way, the relationship between the ship motions or the load effects and the excitation force can remain linear, while the excitation force is no longer linear with respect to the incident wave. The total nonlinear excitation force consists of a linear part as well as a nonlinear modification part. The nonlinear modification part is obtained as the convolution of the linear impulse response function and the nonlinear modification force. The considered nonlinearities are due to the slamming impact force, incident wave force and hydrostatic restoring force. The slamming impact force is determined from the momentum considerations and is neglected during water exit. Only the first global vertical flexural vibration mode was adopted.

4.5 Results

Figures 3 and 4 show the shapes of the first two global vertical flexural modes, respectively. In general, the calculated modes are well in line with the ones from the model tests. The model tests results are provided with a 95% confidence interval that is based on the results from several measurements. The mode shapes used by Participant C deviate most from the others. This is related to the fact that a 3D finite element model was used and that the mode shapes do not regard the neutral axis. The corresponding wet natural frequencies are presented in Table 4. Results from the participants are well in line with the experimental results.

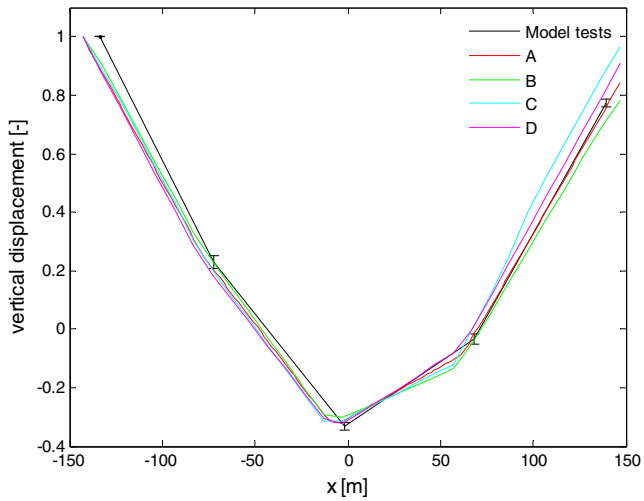

Figure 3. Shape of the first global vertical flexural vibration mode.

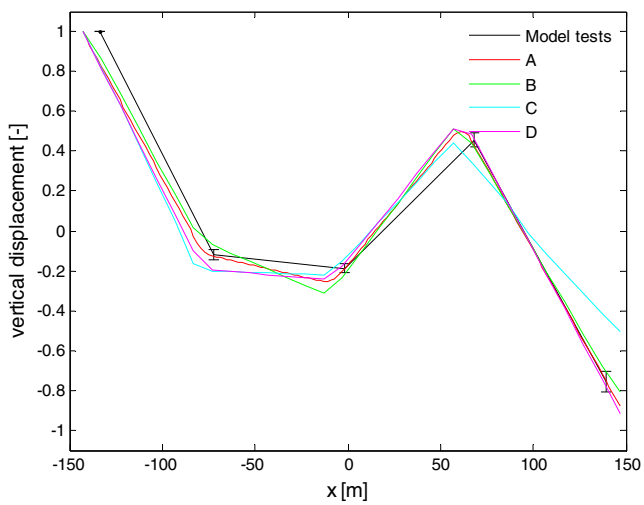

Figure 4. Shape of the second global vertical flexural vibration mode.

Table 4. Wet natural frequencies of the two- and three- node vertical flexural vibration modes.

	Two node mode [Hz]	Three node mode [Hz]
EXP	0.56	1.30
A	0.57	1.42
B	0.57	1.41
C	0.55	1.31
D	0.56	-

Figures 5, 6 and 7 show the unbiased standard deviations of the measured and predicted bending stresses at the three measurement sections. Participants were asked to provide vertical bending moments for these sections. These bending moments were transformed to stresses using 27.4 m^3, 30 m^3 and 30 m^3 as section modules for the forward, amidships and aft sections, respectively. This was combined with a stress concentration factor of two. The standard deviation of the stress was used as an important parameter in predicting the fatigue damage. The predicted number of cycles is also important. Due to page limitations, this was, however, omitted from the comparisons presented here. Each figure is built up of four subplots showing the stresses per wave height and speed, as a function of peak period. From Figure 5, it may be concluded that Participant A over-predicts the stresses on average by 30%, and Participant B slightly more than this, approximately 35%, on average. Participant C under-predicts by approximately 25%. Predictions in higher waves heights are better than in the lower wave heights. The stresses obtained by Participant D agree well with the experimental results and are within 5% on average. The stresses in the amidships section, shown in Figure 6, are predicted by Participant A and agree well with the experimental results. The predictions by Participant C under-predicts the experiments and are approximately 10% low, on average. Participant B under-predicts the stresses by approximately 20%. Participant C, on the other hand, over-predicts by 10%, on average. At the aft section, as seen in Figure 7, Participant C obtained very close agreement with the experimental measurements. On average, a difference of 4% is seen. Participants A and B slightly under-predict the stresses by about 10%. The predictions of Participant D show about 15% over-prediction, on average.

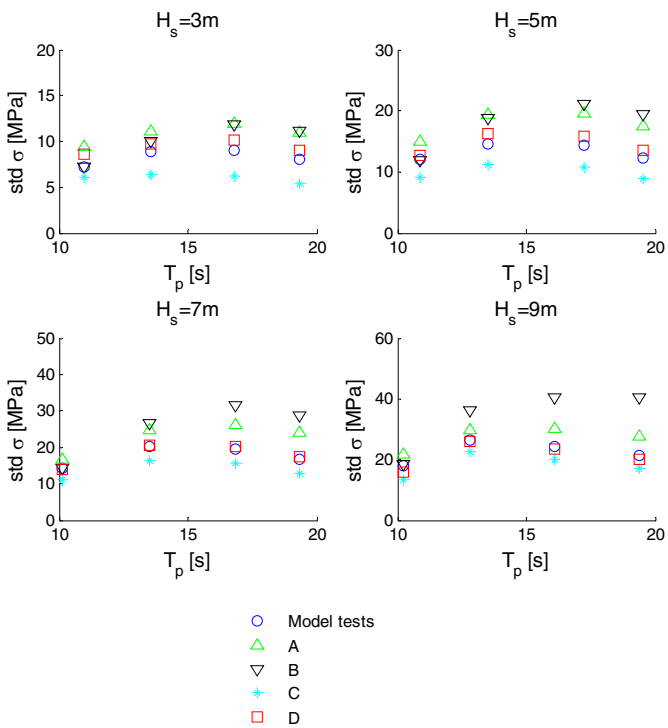

Figure 5. Standard deviation of the total stress at the forward section.

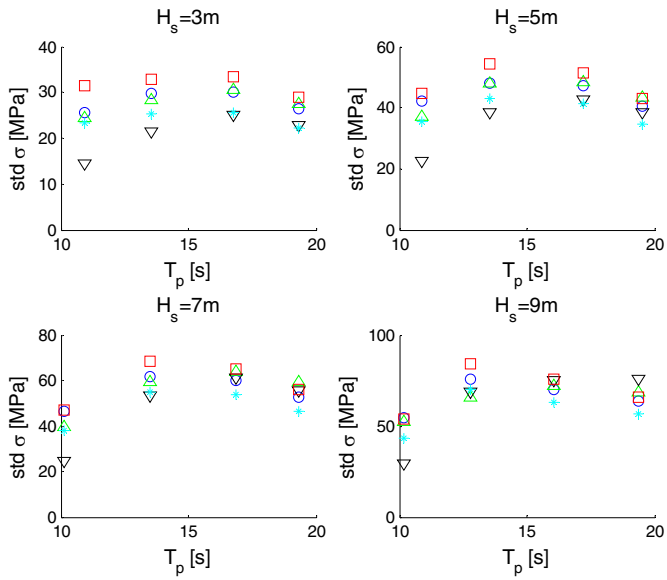

Figure 6. Standard deviation of the total stress at the amidships section.

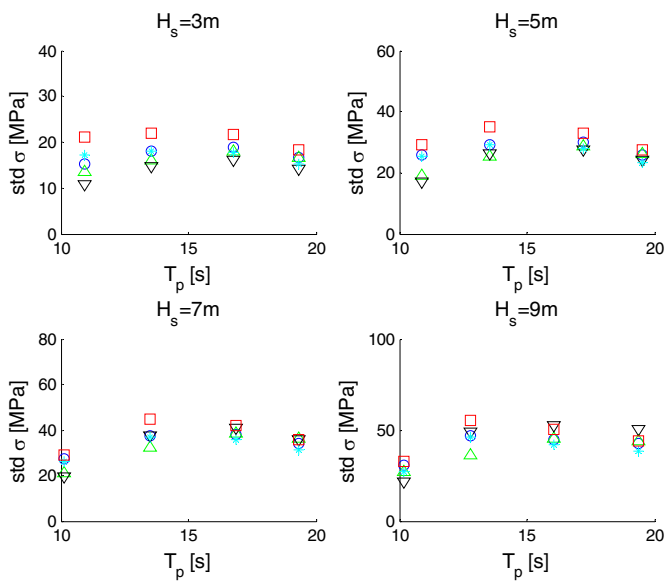

Figure 7. Standard deviation of the total stress at the aft section.

Figures 8, 9 and 10 present the unbiased standard deviations of the high frequency bending stresses at the three measurement sections. These were obtained by high-pass filtering the original stress signals using a cutoff frequency of 0.4 Hz. This excludes the stresses directly induced by the waves and only contains bending stresses as a result of vertical flexural vibrations of the global hull girder. The high frequency stresses are mainly induced by slamming. Participants A, B and D used the momentum theory to obtain the slamming force. Participant D adopted the GWM.

From Figure 8, it can be seen that stresses at the forward section predicted by Participants A, C and D agree quite well with experimental results except for the lowest wave height, where results are conservative. On average, the conservatism is about 20%, 15% and 50%, respectively. The results from Participant B are generally conservative by a factor 2.5. At the amidships, as shown in Figure 9, Participant C is well in line with the experimental results. On average, the results are 15% lower in comparison with the experimental measurements. On the other hand, Participant A estimated substantially high stresses for low wave heights and low stresses for high wave heights. The trend for Participant B is also similar, but it starts off with a reasonable estimate in the lower wave heights and a conservative prediction in the higher waves. The predictions by Participant D are on average about 60% conservative. At the aft section, as shown in Figure 10, Participant D over-predicts experimental results by 70%. Participant A is close to experiment results for low wave heights but under-predicts by about 20% for high wave heights. The trend for Participant B is again similar but starts off with a reasonable estimate in the lower wave heights and a conservative prediction in the higher waves. The results obtained by Participant C are close to experimental results, with a 2% difference on average.

4.6 Conclusions

In order to investigate the accuracy of the predicted dynamic responses, the ISSC 2018 Dynamic Response committee also chose to perform a whipping benchmark study. The focus of the study was on nonlinear strip theory and panel methods.

All of the computational codes involved in the benchmark calculations gave acceptable results. Higher and/or lower stresses are observed, depending on the stress location. The predicted high frequency stress components are scattered more than the total stresses. This may be caused by the differences in the methods for slamming impact computations. It should be noted that the differences between the methods using momentum theory are sometimes larger than those observed between the methods adopting momentum theory and GWM, respectively.

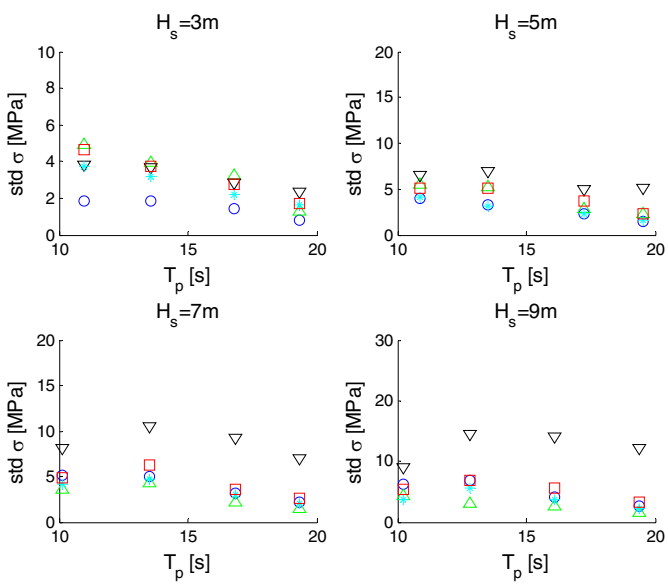

Figure 8. Standard deviation of the high frequency stress at the forward section.

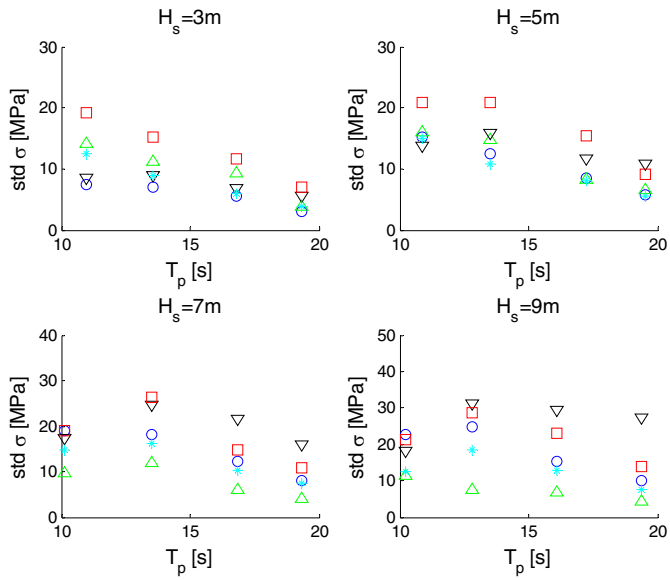

Figure 9. Standard deviation of the high frequency stress at the amidships section.

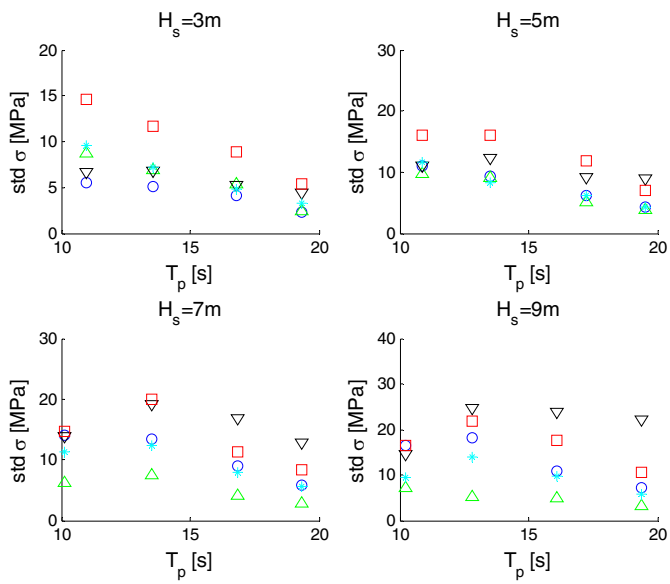

Figure 10. Standard deviation of the high frequency stress at the aft section.

In the present benchmark study, one participant used a 3D panel method, and the rest of participants 2D nonlinear strip theory methods. 3D methods need more computation time than 2D methods. However, according to the present results, 3D methods and 2D strip methods give comparable predictions, and clear differences between these two methods cannot be observed as far as the present benchmark study are concerned.

It is strongly pointed out that the present benchmark study is carried out for a specific experiment ship type for limited irregular sea states. Therefore, in order to derive generalized conclusions, more studies are needed.

5. CONCLUSIONS

Full-scale measurements and model tests in recent years have been focused on unconventional ships such as VLCS and ULCS. They also have relatively low natural frequencies. Most papers are related to only seven different container ships. Based on the attention around MSC Napoli and MOL Comfort, this is understandable, but wave-induced vibrations are not limited to container ships, and future studies should include other ship types as well. Also, the effects of sea state, heading, speed, size, loading condition, trade and structural location are well understood and addressed. There is also a rising trend that data is assessed based on standard hull monitoring systems rather than full-scale measurements from research projects. This trend should be supported and could accelerate the knowledge on a large number of ships and ship types. Only some papers have compared the measured or extrapolated values to design values, which is of particular interest for container ships in relation to IACS URS11A (IACS, 2015). It is recommended that statistical extrapolation of results for comparison with design values are used more frequently. Most studies are also related to vertical vibration, and it is recommended that more attention is given to torsional vibrations and other topics, such as vibration dose values and acceleration levels for cargo securing. Damping is a special challenge for numerical predictions, and better target values are needed. Mature hull monitoring systems can, however, close the gap between design and operational wave-induced vibrations.

Fully consistent modelling of whipping is still a challenge, and only approximate solutions exists. The future developments on the hydrodynamic side are likely to be based on CFD, because the potential flow models seem to reach their limits for the applications in large waves. Having said that, the potential flow models appear to be good enough for some operation conditions, such as head waves at low speed, and they can be used with confidence for the identification of the worst operating conditions from a whipping point of view. Since CFD cannot be practically used for long-duration simulations, the most efficient methodology for whipping assessment will combine the potential flow models (long-term simulations, identification of critical events) and CFD methods (short-term simulations for critical operating conditions).

Propeller-induced vibrations are still considered important in hull structure and shafting systems. In the period of this report, there have been some advances in numerical simulation of propeller excitation forces by considering dynamic interaction effects in shafting system under actual operation conditions. Many researchers have tried to make their numerical models to be practically useful in the prediction of propeller performance in terms of cavitation, pressure pulses and efficiency at early design stage. Also, application of CFD methods is reported. It is expected that there will be further attempts to improve the numerical accuracy of CFD methods for the prediction of propeller excitation forces. Meanwhile, practical devices are applied to ships for reducing the propeller forces, and some of them have succeeded in validation of their effectiveness through full-scale tests.

It is evident from the open literature that there has been no major development reported on the methods of analysis for engine-induced vibrations. Most attention has been paid to vibration control and vibration-reducing techniques. Also, there has been a rather small number of references on machinery-induced vibrations, compared to other sources. However, the topic is expected to come into focus again, due to the introduction of the so-called Comfort Class. Furthermore, some problems have been reported for ultra-long stroke engines with low engine speeds.

Sloshing-induced impacts are very important in the design of a ship tank and the CCS. In the reporting period, the investigation of sloshing impacts has been pursued by experimental and numerical means. Unfortunately, no significant progress has been made, and there is still no efficient solution, neither experimental nor numerical. It is also common practice in tank design to do model experiments for sloshing-induced impact effects. However, it is still very difficult to scale the measured pressures consistently to full-scale. On numerical side, it is

regrettable that the correct numerical modelling of coupled hydro-elastic interactions has not been considered seriously yet. CFD tools based on solving the Navier Stokes or Euler equations are most often applied with slightly different numerical strategies. A considerable amount of work has been reported on the use of OpenFoam software.

The shock- and explosion-induced responses of ships are important to military and civilian vessels. A key area of concern for blast response is explosion in an interior comportment. In the field of internal explosion loadings, quasi-static loading has been the main concern. In the reporting period, many researchers have proposed new methods for analysis and experimentation of response and damage of compartments subjected internal explosion. On the other hand, the dynamic response of ships to UNDerwater EXplosion (UNDEX) is very important for ship survivability due to the potential for serious damage. Recent research has concentrated on the damage and responses to near-field and contact explosions that are relevant to bubble dynamics and strong nonlinearity, respectively. Shock resistance performance of composite structures, such as GRP, SBS, sandwich plates and rubber-like material coating structures have been the area of recent research.

Regarding interior noise regulations, the new IMO code, MSC 337(91) is regarded as a lost opportunity for making a step ahead in protecting seafarer's health and safety. The new code is not so different from the previous one, IMO Resolution A.468 (XII), except for those vessels whose tonnage above 10000 GT. It has also been noted that the shipbuilding and noise control technologies are far ahead the new regulation. Furthermore, the application of these norms is found difficult in the case of tonal noise components because of their imprecise definition. Within the air radiated noise, the assessment of external noise propagation requires the measurement of sound power emitted from ship. However, there is no available technical standard for determining the sound power of very large sources, such as cruise ships in a complex environment like a harbor. 3D acoustic mapping can be a useful tool to explore different noise scenarios where the ship is not the only source contributing to the noise pollution of an area surrounding a harbor. With regard to underwater radiated noise, most research has focused on the fields of noise mapping of seas and establishing limits on received underwater noise, in this reporting period. Within the EU project AQUA, a number of recommendations are made for design, construction and management of ships and their routes to improve the future fleet on underwater noise emissions. A concluded project called BIAS had a main goal to monitor the intensity of underwater noise caused by shipping without undertaking costly and difficult hydro-acoustic measurements.

Despite all the efforts made, the damping mechanisms and actual damping values, for ships in different operating conditions, are not fully understood. In the forced vibration analysis of ship structures, damping is still accounted for in a simplified way, i.e. by lumping all of its components together through a constant damping coefficient specified as a percentage of critical damping. There is thus a need for more full-scale data, together with the information on wind, wave conditions and ship speed, as well as cargo condition and draft, which may affect the damping values. A step in the right direction is the revised hull monitoring rules by DNVGL (2017a) which requires damping estimates to be automatically produced onboard when the ship vibrates.

In this report, an attempt is made to standardize different terminology and technology in relation to monitoring, such as condition monitoring, condition monitoring system, condition based maintenance, etc. Also, a distinction is made between full-scale measurements and hull monitoring systems. The control and monitoring systems are also an important part of the rules, and they deal with machinery, systems and components. Recently, there have been several revisions of the hull monitoring rules by the classification societies. However, this does not necessarily mean that significant changes have been made. On the other hand, digitalization is a global trend, and some classification societies encourage storage and processing measurement data and sending it to shore. It is also necessary to have a system at shore to

retrieve data. Unfortunately, not much has been found on this, with regards to dynamic response.

IACS issued unified requirements for the longitudinal strength of container ships, URS11A (IACS, 2015), and classification societies changed their rules for container ships to account for whipping and springing. These changes arise because of the accidents of MSC Napoli and MOL Comfort. Criticism of the newly developed rules and standards has been made for wave-induced vibrations, especially for container ships, and overestimation of wave loads has been recognized. On the other hand, IMO (2014) published a guideline for the noise level on board ships for both passengers and crew members, and various noise levels were set for different spaces onboard ship. With regard to sloshing, not much progress has been made in the period of this report. This means that a direct calculation procedure for sloshing assessment is not yet possible, and the so-called comparative approach is still in useVibration in offshore structures due to environmental and operational loads continues to be a major concern for design. The dynamic analysis of wave-induced response is usually based on a stochastic model of the ocean surface and wave kinematics. The corresponding dynamic response is then obtained as a probability distribution of local maxima and extreme values. Vibration control is also an important topic for offshore structures. The methods employed are generally categorized as passive, active, semi-active and hybrid.

Wind-induced vibration is one of the important factors for the structural safety of offshore structures. Several investigations have been reported in the period of this report, targeting offshore platforms as well as offshore wind turbines. The recent literature generally involves the estimation of structural response due to wind loads and control and reduction of wind induced vibrations.

With regard to Vortex Induced Vibration (VIV), a survey of recent publications is mainly concern with model tests. The typical scaling factors are within the range of 1:40-1:75. It is impossible to simultaneously satisfy Reynolds and Froude scaling for model and prototype conditions, and this implies that full-scale testing is necessary. On the other side, most of the work done in recent years is devoted mainly to improving the prediction capabilities of wake oscillator models rather than to the development of new CFD or semi-empirical models. A significant number of papers describe very sophisticated wake oscillator models which are able to capture the nonlinear multi-mode dynamics and interactions of flexible curved or straight structures undergoing VIV.

Despite the rapid development of offshore oil exploitation which involves a large number of pipelines to process oil and gas, a limited number of publications have been found on internal flow-induced vibration in the period of this report.

Many types of equipment are installed in offshore facilities for production, storage and unloading of oil and gas. However, it is almost impossible to consider all the equipment as excitation sources at a design stage. According to the common practice of shipyards, the major equipment includes rotating machinery operated below 4800 rpm and reciprocating engines exceeding an output power of 30 kW. Some interesting papers have been published in the period of this report.

Offshore structures may be subjected to several types of shock loading, including internal explosion of oil, gas and other chemical matter, external explosions due to weapons attack, and seismic loading from foundation attachments to the sea floor. CFD has been generally employed coupled with finite element methods for analysis of the shock wave interaction with structures. On the other side, reinforced material usage is a growing area for offshore structures, and recent research has focused on the investigation of the blast resistance of reinforced concrete materials. Critical offshore infrastructure, such as bridge abutments, petrochemical docking components, ports, and flood control devices, often contain concrete structures, and their vulnerability to both accidental and intentional explosive loading makes the response of these structures to such loading important to researchers and designers.

The activity of pile driving for the foundation construction of wind turbines and other offshore structures may be the most important noise source, so much research work, therefore, has been published on this topic. These studies may be categorized as those involving numerical and experimental methods for analyzing the noise emitted due to pile driving, and those involving noise mitigation measures.

Regarding monitoring of offshore structures, the monitoring campaigns, mainly, focus on the assessments of maintenance needs, extreme responses and reliability of local structural details and components. Monitoring of fatigue cracks, subsea equipment and offshore wind turbines are important research topics in this field.

Floating offshore structures, such as wind turbines, include many degrees of freedom, variables, and excitation from both wind and waves, making the assessment of uncertainty in a test campaign challenging. In addition, it is important to consider many different conditions, requiring a large number of experiments to be run, including numerous repetitions. The variables can be strongly or weakly coupled, meaning that error sources can strongly influence each other.

The offshore industry has not recognized wave-induced vibrations to the same extent as in the shipbuilding industry. However, offshore ships like FPSOs can utilize the same rules and standards as in shipbuilding. For other offshore structures, class may lack rules and standards for wave-induced vibrations, but they may still request assessment of consequences and suggest that the resonance periods may be kept as low as possible. On the other side, for free-spanning subsea power cables, VIV can be part of the fatigue limit state requirements. NORSOK (2017) includes VIV in general terms based on water flow and wind. Furthermore, the comfort class notation COMF is mainly used for passenger ships, but the class guideline gives more general criteria which can also be used within offshore accommodation units.

Finally, this committee has undertaken a benchmark study regarding whipping responses, with a special focus on nonlinear strip theory and panel methods. The degree of variation in estimates produced by different methods and organizations is revealed, and comparisons with model test measured responses are provided.

REFERENCES

Abbas, N., Kornev, N., Shevchuk, I. & Anschau, P. 2015. CFD prediction of unsteady forces on marine propellers caused by the wake nonuniformity and nonstationarity. *Ocean Engineering* 104, 659-672.

ABS 2016a. *Guide for hull condition monitoring systems*. 15 December 2015 (updated March 2016). American Bureau of Shipping.

ABS 2016b. *Rules for building and classing steel vessels*. American Bureau Shipping.

ABS 2014. *Guidance notes on strength assessment of membrane-type LNG containment systems under sloshing*. American Bureau of Shipping.

ABS 2014a. *Guidance note on whipping assessment for container carriers*. American Bureau of shipping.

ABS 2014b. *Guidance note on springing assessment for container carriers*. American Bureau of Shipping.

Alizadeh, A.A., Mirdamadi, H.R. & Pishevar, A. 2016. Reliability analysis of pipe conveying fluid with stochastic structural and fluid parameters. *Engineering Structures* 122, 24-32.

Allen, D.W., Lee, L., Henning, D. & Liapis, S. 2015a. The effects of mixing helical strakes and fairings on marine tubulars and arrays. In *Proc. 34th International Conference on Ocean, Offshore and Arctic Engineering OMAE, St. John's, Newfoundland, Canada.*

Allen, D.W., Lee, L., Henning, D. & Liapis, S. 2015b. Practical design considerations for managing marine growth on VIV suppression devices. In *Proc. 34th International Conference on Ocean, Offshore and Arctic Engineering OMAE, St. John's, Newfoundland, Canada.*

Ancellin, M., Brosset, L. & Ghidaglia, J.-M. 2016. Preliminary numerical results on the influence of phase change on wave impact loads. In *Proc. 26th Int. Offshore and Polar Engineering Conference ISOPE, Rhodes, Greece.*

Andersen, I.M.V. 2014. *Full scale measurements of the hydro-elastic response of large container ships for decision support*. PhD thesis, Technical University of Denmark, Denmark.

Andersen, I.M.V. & Jensen, J.J. 2015. Extreme value prediction of the wave-induced vertical bending moment in large container ships. In *Proc. 7th Int. Conf. on Hydroelasticity in Marine Technology, Split, Croatia.*

Antoniadou, I., Dervilis, N., Papatheou, E., Maguire, A.E. & Worden, K. 2017. Aspects of structural health and condition monitoring of offshore wind turbines. *Philosophical Transactions A* 373.

Arai, M., Cheng, L.-Y., Wang, X., Okamoto, N., Hata, R. & Karuka, G. 2016. Sloshing and swirling behavior of liquid in a spherical LNG tank. In *Proc. 13th Int. Symp. on Practical Design of Ships and Other Floating Structures PRADS, Copenhagen, Denmark*.

ASME 2014. *Test uncertainty, performance test codes*. ASME PTC 19.1-2013.

Assi, G.R.S. & Bearman, P.W. 2015. Transverse galloping of circular cylinders fitted with solid and slotted splitter plates. *Journal of Fluids and Structures* 54, 263-280.

Assi, G.R.S, Bearman, P.W. & Tognarelli, M.A. 2014. On the stability of free-to-rotate short-tail fairing and a splitter plate as suppressors of vortex-induced vibration. *Ocean Engineering* 92, 234-244.

Audoly, C., Rousset, C., Baudin, E. & Folegot, T. 2016. AQUO Project - Research on solutions for mitigation of shipping noise and its impact on marine fauna - Synthesis of guidelines. In *Proc. 23rd International Congress on Sound and Vibration ICSV, Athens, Greece.*

Baarholm, G.S., Johansen, A., Birknes, J. & Haver, S. 2013. Estimation of equivalent dynamic amplification factor (EDAF) on a jacket structure. In *Proc. 32nd International Conference on Ocean, Offshore and Arctic Engineering OMAE, Nantes, France.*

Baeten, A. 2017. Fluid structure interaction analysis of composite structures exposed to sloshing. In *Proc. 27th Int. Offshore and Polar Engineering Conference ISOPE, San Francisco, USA.*

Baeten, A. 2015. Numerical analysis of liquid impact energy dissipation. In *Proc. 25th Int. Offshore and Polar Engineering Conference ISOPE, Hawaii, USA.*

Bai, Y. & Liang, J.W. 2016. *Marine structural design*, Second Edition, Butterworth-Heinemann.

Bang, B., Park, H.-S., Kim, J.-H., Al-Deyab, S.S., Yarin, A.L. & Yoon, S.S. 2016. Simplified method for estimating the effect of a hydrogen explosion on a nearby pipeline. *Journal of Loss Prevention in the Process Industries* 40, 112-116.

Barhoumi, B. & Storhaug, G. 2014. Assessment of whipping and springing on a large container vessel. *International Journal of Naval Architecture and Ocean Engineering* 6(2), 442-458.

Behruzi, P., Gaulke, D., Haacke, D. & Brosset, L. 2017. Modeling of impact waves in LNG ship tanks. *International Journal of Offshore and Polar Engineering* 27(1).

Beltrán, P., Salinas, R. & Moreno, A. 2014. The new IMO noise code: A lost technical opportunity. Irreversible and high cost consequences for fishermen and other seamen that will continue being deaf. In *Proc. 21st International Congress on Sound and Vibration ICSV, Beijing, China.*

Bennett, S.S., Downes, J., Dickson, T., Phillips, A.B. & Turnock, S.R. 2015a. Rapid prototyping of flexible models – a new method for model testing? In *Proc. 7th Int. Conf. on Hydroelasticity in Marine Technology, Split, Croatia.*

Bennett, S.S., Hudson, D.A. & Temarel, P. 2015b. The effect of abnormal wave sequences on 2D hydroelastic predictions of global loads. In *Proc. 7th Int. Conf. on Hydroelasticity in Marine Technology, Split, Croatia.*

Bernasconi, G., Giunta, G. & Chiappa, F. 2015. Gas filled pipelines monitoring using multipoint vibroacoustic sensing. In *Proc. 34th International Conference on Ocean, Offshore and Arctic Engineering OMAE, St. John's, Newfoundland, Canada.*

Blanchet, D. & Caillet, A. 2014. Full frequency noise and vibration control onboard ships. In *Proc. 21st International Congress on Sound and Vibration ICSV, Beijing, China.*

Blevins, R.D., Coughran, C.S., Utt., M.E. & Raghavan, K. 2016. Drilling-induced riser vibration. In *Proc. 26th Int. Offshore and Polar Engineering Conference ISOPE, Rhodes, Greece.*

Borelli, D., Gaggero, T., Rizzuto, E. & Schenone, C. 2016a. Holistic control of ship noise emissions. *Noise Mapping* 3, 107–119.

Borelli, D. & Schenone, C. 2014. Application of a simplified "source-path-receiver" model for HVAC noise to the preliminary design of a ship: A case study. In *Proc. 21st International Congress on Sound and Vibration ICSV, Beijing, China.*

Borelli, D., Schenone, C., Gaggero, M., Gaggero, T. & Rizzuto, E. 2016b. Seafarer's work exposure to tonal noise components. In *Proc. 23rd International Congress on Sound and Vibration ICSV, Athens, Greece.*

Borsani, J.F., Curcuruto, S. & Farchi, C. 2015. Setting up an underwater noise monitoring plan for Italian territorial waters. In *Proc. 22nd International Congress on Sound and Vibration ICSV, Florence, Italy.*

BSH 2013. *Standard: Investigation of the impacts of offshore wind turbines on the marine environment (StUK4)*. Bundesamt für Seeschifffahrt und Hydrographie, Federal Maritime and Hydrographic Agency.

BSH 2011. *Offshore wind farms: Measuring instruction for underwater sound monitoring, Current approach with annotations*. Bundesamt für Seeschifffahrt und Hydrographie, Federal Maritime and Hydrographic Agency.

Buruchenko, S.K. & Canelas, R.B. 2017. Validation of open-source SPH code DualSPHysics for numerical simulations of water entry and exit of a rigid body. In *Proc. International Conference on Ocean, Offshore and Arctic Engineering OMAE, Trondheim, Norway.*

BV 2017. *Rules for the classification of steel ships*. NR 467, July 2017, Part F, Chapter 5 Monitoring equipment. Bureau Veritas.

BV 2017a. *Rules for classification of steel ships*. Bureau Veritas.

BV 2017b. *Structural rules for container ships*. Rule note NR 625, Bureau Veritas.

BV 2015. *Whipping and springing assessment*. Rule note NR 583 DT R01 E. Bureau Veritas.

BV 2011. *BV guidance note NI 554, Design sloshing loads for LNG membrane tanks*. Bureau Veritas.

Calderon-Sanchez, J., Duque, D. & Gomez-Goni, J. 2015. Modeling the impact pressure of a free falling liquid block with OpenFoam. *Ocean Engineering* 103, 144-152.

CCS 2015. *Rules for classification of sea-going steel ships*. Part 8 Chapter 21 Hull monitoring systems. China Classification Society.

Cetin, E.C., Kim, S. & Kim, Y. 2017. Analysis of sloshing impact pressures using different extreme statistical theories. In *Proc. 27th Int. Offshore and Polar Engineering Conference ISOPE, San Francisco, USA.*

Chen, Y., Wang, L. & Hua, H.X. 2017. Longitudinal vibration and unsteady thrust transmission of the rim driven thruster induced by ingested turbulence. *Ocean Engineering* 131, 149-161.

Chen, Y., Yao, X. & Xiao, W. 2016. Analytical models for the response of the double-bottom structure to underwater explosion based on the wave motion theory. *Shock and Vibration* 2016.

Cho, Y.-B., Jin, K.-K., Yoon, I.-S., Yang, Y.-C. & Kim, Y.-G. 2015. A study of cryogenic-temperature structural behavior for KC-1 corner insulation system. In *Proc. 25th Int. Offshore and Polar Engineering Conference ISOPE, Hawaii, USA.*

Cicolin, M.M. & Assi, G.R.S. 2015. VIV response and drag measurements of circular cylinders fitted with permeable meshes. In *Proc. 34th International Conference on Ocean, Offshore and Arctic Engineering OMAE, St. John's, Newfoundland, Canada.*

Cinquemani, S. & Braghin, F. 2017. Decentralized active vibration control in cruise ships funnels. *Ocean Engineering* 140, 361-368.

Craig, M., Piro, D., Schambach, L., Mesa, J., Kring, D. & Maki, K. 2015. A comparison of fully-coupled hydroelastic simulation methods to predict slam-induced whipping. In *Proc. 7th Int. Conf. on Hydroelasticity in Marine Technology, Split, Croatia.*

Cristea, B., Mocanu, C.I. & Domnisoru, L. 2015. Non-linear hydroelastic and fatigue analyses for a very large bulk carrier. In: Soares, C.G. & Shenoi, R.S. (eds) *Advances in Marine Structures*. London, UK: Taylor & Francis Group.

Curcuruto, S., Marsico, G., Atzori, D., Mazzocchi, E. & Betti, R. 2015. Environmental impact of noise sources in port areas: A case study. In *Proc. 22nd International Congress on Sound and Vibration ICSV, Florence, Italy.*

Curletto, S., Pinto, O. & Dorsaneo, M. 2015. On the characterization of ship external noise. In *Proc. 22nd International Congress on Sound and Vibration ICSV, Florence, Italy.*

Dambra, R. & Firenze, E. 2015. Underwater radiated noise of a small vessel. In *Proc. 22nd International Congress on Sound and Vibration ICSV, Florence, Italy.*

Dardis, I.I., John, T., & Reinhall, Per G. 2015. New offshore pile for reduced acoustic emissions – results from full scale testing. In *Proc. 22nd International Congress on Sound and Vibration ICSV, Florence, Italy.*

Darvishzadeh, T. & Sari, A. 2015. CFD applications in offshore engineering. *Offshore Technology Conference, Houston OTC, Texas, USA.*

Davidson, C., Brown, M., Brennan, A. & Knappett, J. 2017. Decommissioning of offshore piles using vibration. In *Proc. 27th Int. Offshore and Polar Engineering Conference ISOPE, San Francisco, USA.*

Davis, M.R., French, B.J. & Thomas, B.J. 2017. Wave slam on wave piercing catamarans in random head seas. *Ocean Engineering* 135, 84-97.

De Lauzon, J., Benhamou, A. & Malenica, S. 2015a. Numerical simulations of WILS experiments. In *Proc. 25th Int. Offshore and Polar Engineering Conference ISOPE, Hawaii, USA.*

De Lauzon, J., Grgic, M., Derbanne, Q. & Malenica, S. 2015b. Improved generalized Wagner model for slamming. In *Proc. 7th Int. Conf. on Hydroelasticity in Marine Technology, Split, Croatia.*

Dekeling, R.P.A., Tasker, M.L., Van der Graaf, A.J., Ainslie, M.A, Andersson, M.H., André, M., Borsani, J.F., Brensing, K., Castellote, M., Cronin, D., Dalen, J., Folegot, T., Leaper, R., Pajala, J., Redman, P., Robinson, S.P., Sigray, P., Sutton, G.,Thomsen, F., Werner, S., Wittekind, D. & Young, J. 2014a. *Monitoring guidance for underwater noise in European seas, Part I: Executive summary*. JRC Scientific and Policy Report EUR 26557 EN, Publications Office of the European Union, Luxembourg, 2014, doi: 10.2788/29293.

Dekeling, R.P.A., Tasker, M.L., Van der Graaf, A.J., Ainslie, M.A, Andersson, M.H., André, M., Borsani, J.F., Brensing, K., Castellote, M., Cronin, D., Dalen, J., Folegot, T., Leaper, R., Pajala, J., Redman, P., Robinson, S.P., Sigray, P., Sutton, G.,Thomsen, F., Werner, S., Wittekind, D. & Young, J. 2014b. *Monitoring guidance for underwater noise in European seas, Part II: Monitoring guidance specifications*. JRC Scientific and Policy Report EUR 26555 EN, Publications Office of the European Union, Luxembourg, doi: 10.2788/27158.

Dekeling, R.P.A., Tasker, M.L., Van der Graaf, A.J., Ainslie, M.A, Andersson, M.H., André, M., Borsani, J.F., Brensing, K., Castellote, M., Cronin, D., Dalen, J., Folegot, T., Leaper, R., Pajala, J., Redman, P., Robinson, S.P., Sigray, P., Sutton, G.,Thomsen, F., Werner, S., Wittekind, D., Young, J. 2014c. *Monitoring guidance for underwater noise in European seas, Part III: Background information and annexes*. JRC Scientific and

Policy Report EUR 26556 EN, Publications Office of the European Union, Luxembourg, doi: 10.2788/2808.

Deng, Q., Jiang, W., Tan, M. & Xing, J.T. 2016. Modelling of offshore pile driving noise using a semi-analytical variational formulation. *Applied Acoustics* 104, 85-100.

Derbanne, Q., Storhaug, G., Shigunov, V., Xie, G. & Zheng, G. 2016. Rule formulation of vertical hull girder wave loads based on direct computations. In *Proc. 13th Int. Symp. on Practical Design of Ships and Other Floating Structures PRADS, Copenhagen, Denmark*.

Dessi, D. 2014. Whipping-based criterion for the identification of slamming. *International Journal of Naval Architecture and Ocean Engineering* 6, 1082-1095.

Dezvareh, R., Batgi, K., & Mousavi, S.A. 2016. Control of wind/wave-induced vibrations of jacket-type offshore wind turbines through tuned liquid column gas dampers. *Structure and Infrastructure Engineering* 12(3), 312-326.

Dhavalikar, S., Awasare, S., Joga, R. & Kar, A.R. 2015. Whipping response analysis by one way fluid structure interaction – A case study. *Ocean Engineering* 103, 10-20.

Di Bella, A. 2014. Evaluation methods of external airborne noise emissions of moored cruise ships: An overview. In *Proc. 21st International Congress on Sound and Vibration ICSV, Beijing, China.*

Di Bella, A., Remigi, F., Fausti, P. & Tombolato, A. 2016. Measurement method for the assessment of noise impact of large vessels. In *Proc. 23rd International Congress on Sound and Vibration ICSV, Athens, Greece.*

Dias, F. & Ghidaglia, J.-M. 2018. Slamming: Recent progress in the evaluation of impact pressures. *Annual Review of Fluid Mechanics* 50.

Diebold, L. & Baudin, E. 2016. Sloshing analysis of single impact wave & irregular motions in a 2D tank – Experiments & numerics. In *Proc. 26th Int. Offshore and Polar Engineering Conference ISOPE, Rhodes, Greece.*

Diez, M., Broglia, R., Durante, D., Olivieri, A., Campana, E.F. & Stern, F. 2017. Validation of uncertainty quantification methods for high-fidelity CFD of ship response in irregular waves. In *Proc. 55th AIAA Aerospace Sciences Meeting, Grapevine, Texas, USA.*

Diez, M., Broglia, R., Durante, D., Olivieri, D., Campana, E.F. & Stern, F. 2016. Statistical validation of a high-speed catamaran in irregular waves. In *Proc. 31st Symposium on Naval Hydrodynamics, September 11-16, 2016, Monterey CA, USA.*

Diez, M., Broglia, R., Durante, D., Campana, E.F. & Stern, F. 2015. Validation of high-fidelity uncertainty quantification of a high-speed catamaran in irregular waves. In *Proc. 13th International Conference on Fast Sea Transportation, Washington DC, USA.*

Diez, M., He, W., Campana, E.F. & Stern, F. 2014. Uncertainty quantification of Delft catamaran resistance, sinkage and trim for variable Froude number and geometry using meta models, quadrature and Karhunen–Loève expansion. *Journal of Marine Science and Technology* 19(2), 143-169.

DNV 2010. *Rules for classification of ships*. Det Norske Veritas.

DNV 2005. Rules for classification of ships/high speed, light craft and naval surface craft. Part 6 Chapter 11 Hull monitoring systems. Det Norske Veritas.

DNV-GL 2017a. *Rules for classification of ships*. Part 6 Chapter 9 Section 4. Hull monitoring systems – HMON. Det Norske Veritas - Germanischer Lloyd's.

DNV-GL 2017b. Recommended practise. Data quality assessment framework, edition January 2017. DNVGL-RP-0497.

DNV-GL 2017c. *Rules for classification of ships.* Part 4 Chapter 9. Control and monitoring systems, edition January 2017. Det Norske Veritas - Germanischer Lloyd's.

DNV-GL 2017d. *Rules for classification of ships: Hull girder loads*. Det Norske Veritas - Germanischer Lloyd's.

DNV-GL 2017e. *Riser fatigue. Recommended practise*. DNVGL-RP-F204, October 2017. Det Norske Veritas - Germanischer Lloyd's.

DNV-GL 2017f. *Free spanning pipelines. Recommended Practise*. DNVGL-RP-F105, June 2017. Det Norske Veritas - Germanischer Lloyd's.

DNV-GL 2016a. *Class Guideline: Sloshing analysis of LNG membrane tanks*. Det Norske Veritas - Germanischer Lloyd's.

DNV-GL 2016b. *Rules for classification of ships: Container ships - Hull girder strength*. Det Norske Veritas - Germanischer Lloyd's.

DNV-GL 2016c. *Fatigue assessment of ship structures*. DNVGL-CG-0129, Det Norske Veritas - Germanischer Lloyd's.

DNV-GL 2016d. *Subsea power cables in shallow water*. Recommended practise, DNVGL-RP-0360, March 2016. Det Norske Veritas - Germanischer Lloyd's.

DNV-GL 2016e. *Criteria for handling of excessive noise and vibration levels*. Class guideline, DNVGL-CG-0493, May 2016. Det Norske Veritas - Germanischer Lloyd's.

DNV-GL 2016f. *Certification of condition monitoring. Service specification*. DNVGL-SE-0439, edition June 2016. Det Norske Veritas - Germanischer Lloyd's.

DNV-GL 2015. *Survey arrangement for machinery condition monitoring*. Class guideline DNVGL-CG-0052, edition December 2015. Det Norske Veritas - Germanischer Lloyd's.

DNV-GL 2015a. *Rules for classification of ships*: *Wave induced hull girder vibration – WIV*. Det Norske Veritas - Germanischer Lloyd's.

DNV-GL 2015b. *Fatigue and ultimate strength assessment of container ships including whipping and springing*. DNVGL-CG-0153, Det Norske Veritas - Germanischer Lloyd's.

Drummen, I. 2008. *Experimental and numerical investigation of nonlinear wave induced load effects in containerships considering hydroelasticity*. PhD thesis, Norwegian University of Science and Technology, Trondheim, Norway.

Drummen, I. & Holtmann, M. 2014. Benchmark study of slamming and whipping. *Ocean Engineering* 86, 3-10.

Drummen, I., Schiere, M., Dallinga, R. & Stambaugh, K. 2014. *Full and model scale testing of a new class of US coast guard cutter.* Ship Structure Committee 2014, 18-20th May 2017, Linthicum Heights, USA.

Duan, X.-Y., Guo, X.-Y., Jiao, Q.-J., Zhang, J.-Y. & Zhang, Q.-M. 2017. Effects of Al/O on pressure properties of confined explosion from aluminized explosives. *Defense Technology* 13(6), 428-433.

Eca, L. & Hoekstra, M. 2014. A procedure for the estimation of the numerical uncertainty of CFD calculations based on grid refinement studies. *Journal of Computational Physics* 262, 104-130.

Eftekhari, M. & Hosseini, M. 2015. On the stability of spinning functionally graded cantilevered pipes subjected to fluid-thermomechanical loading. *International Journal of Structural Stability & Dynamics* 16(9).

Eisinger, E., Helmers, J.B. & Storhaug, G. 2016. A method for describing ocean environments for ship assessment. In *Proc. 6th International conference on Design for Safety, 28-30 November 2016, Hamburg, Germany*.

el Moctar, O., Ley, J., Oberhagemann, J. & Schellin, T.E. 2017. Nonlinear computational methods for hydroelastic effects of ships in extreme seas. *Ocean Engineering* 130, 659-673.

el Moctar, O., Ley, J., Oberhagemann, J. & Schellin, T.E. 2016. Advanced computational methods for hydroelastic effects of ships in extreme seas. *Ocean Engineering* 130, 659-673.

Fan, Y., Mao, H., Guo, H., Liu, Q. & Li, X. 2015. Experimental investigation on vortex-induced vibration of steel catenary riser. *China Ocean Engineering* 29(5), 691-704.

Farcas, A., Thompson, P.M. & Merchant, N.D. 2016. Underwater noise modelling for environmental impact assessment. *Environmental Impact Assessment Review* 57, 114-122.

Feldgun, V.R., Karinski, Y.S., Edri, I. & Yankelevsky, D.Z. 2016. Prediction of the quasi-static pressure in confined and partially confined explosions and its application to blast response simulation of flexible structures. *International Journal of Impact Engineering* 90, 46–60.

Fernandes, A.C., Mirzaeisefat, S. & Cascao, L.V. 2014. Fundamental behaviour of vortex self induced vibration (VSIV). *Applied Ocean Research* 47, 183-191.

Firoozkoohi, R., Abrahamsen, B.C. & Faltinsen, O.M. 2017. Study of an entrapped air pocket due to sloshing using experiments and numerical simulations. In *Proc. International Conference on Ocean, Offshore and Arctic Engineering OMAE, Trondheim, Norway.*

Fotini, C., Dalamagas, V., Dalamaga, D. & Sarantopoulos, G. 2016. Determination of ships as noise sources & noise mapping at passenger & cruise port of Piraeus. In *Proc. 23rd International Congress on Noise & Vibration ICSV, Athens, Greece.*

Fricke, M.B. & Rolfes, R. 2015. Towards a complete physically based forecast model for underwater noise related to impact pile driving. *Journal of the Acoustical Society of America* 137(3), 1564-1575.

Frihat, M., Brosset, L. & Ghidaglia, J.-M. 2017. Experimental study of surface tension effects on sloshing impact loads. *IWWWFB 32, Dalian, China.*

Frihat, M., Karimi, M.R., Brosset, L. & Ghidaglia, J.-M. 2016. Variability of impact pressures induced by sloshing investigated through the concept of 'singularization'. In *Proc. 26th Int. Offshore and Polar Engineering Conference ISOPE, Rhodes, Greece.*

Furey, C. 2015. *Parametric analysis of the shock response of a system of two submerged co-axial cylindrical shells coupled by the inter-shell fluid*. MSc. Thesis, Dalhousie University Halifax, Nova Scotia.

Gaidai, O., Storhaug, G. & Naess, A. 2016. Extreme large cargo ship panel stresses by bivariate ACER method. *Ocean Engineering* 123, 432-439.

Gao, Y., Fu, S., Wang, J., Song, L. & Chen, Y. 2015. Experimental study of the effects of surface roughness on the vortex-induced vibration response of a flexible cylinder. *Ocean Engineering* 103, 40-54.

Gharib, M. & Karkoub, M. 2015. Shock-based experimental investigation of the linear particle chain impact damper. *Journal of Vibration and Acoustics* 137 (6).

Gjinolli, A.E., Bremigan, C.D. & Morgan, J.S. 2016. Aero-acoustical and dynamic analysis of complex reciprocating engine exhaust systems. In *Proc. 26th Int. Offshore and Polar Engineering Conference ISOPE, Rhodes, Greece.*

Gong, K., Shao, S., Liu, H., Wang, B. & Tan, S.K. 2016. Two phase SPH simulations of fluid-structure interactions. *Journal of Fluid and Structures* 65, 155-179.

Gong, S.W. & Khoo, B.C. 2015. Transient response of stiffened composite submersible hull to underwater explosion bubble. *Composite Structures* 122, 229–238.

Göttsche, K.M., Steinhagen, U. & Juhl, P.M. 2015. Numerical evaluation of pile vibration and noise emission during offshore pile driving. *Applied Acoustics* 99, 51-59.

Gres, S., Fejerskov, M., Ibsen, L.B. & Damkilde, L. 2016. Experimental damping assessment of a full scale offshore Mono Bucket foundation. In *Proc. 27th International Conference on Noise and Vibration Engineering ISMA, Leuven, Belgium.*

Grotle, E. L. & Æsøy, V. 2017. Experimental and numerical investigation of sloshing in marine LNG fuel tanks. In *Proc. International Conference on Ocean, Offshore and Arctic Engineering OMAE, Trondheim, Norway.*

Grotle, E.L., Æsøy, V., Halse, K.H., Pedersen, E. & Li, Y. 2016. Non-isothermal sloshing in marine liquefied natural gas fuel tanks. In *Proc. 26th Int. Offshore and Polar Engineering Conference ISOPE, Rhodes, Greece.*

Grytøyr, G., Coral, F., Lindstad, H.B. & Russo, M. 2015. Wellhead fatigue damage based on indirect measurements. In *Proc. 34th International Conference on Ocean, Offshore and Arctic Engineering OMAE, St. John's, Newfoundland, Canada.*

Grytøyr, G., Hørte, T., Russo, M., Gregersen, K. & Aronsen, K.H. 2017. Comparison of global riser analysis to full scale measurements on the NCS. In *Proc. 36th Int. Conf. on Ocean, Offshore and Arctic Engineering OMAE, Trondheim, Norway.*

Guan, S., Taylor, C., Agarwal, A. & Sridhar, N. 2016. Understanding sensor system reliability. Position paper 2-2016. *DNVGL strategic research & innovation.*

Guo, Y., Li, W., Yu, S., Han, X., Yuan, Y., Wang, Z. & Ma, X. 2017. Diesel engine torsional vibration control coupling with speed control system. *Mechanical Systems and Signal Processing* 94, 1-13.

Guzas, E., Behan, K. & Davis, J. 2015. 3D finite element modeling of single bolt connections under static and dynamic tension loading. *Shock and Vibration* 2015.

Hageman, R., Aalberts, P., Shaik, M. & van den Boom, H. 2014a. Development of an advisory hull fatigue monitoring system. *The Transactions of Society of Naval Architects and Marine Engineers SNAME.*

Hageman, R. & Drummen, I. 2017. Modal analysis for the global flexural response of ships. *Marine Structures*, under review

Hageman, R., Drummen, I., Stambaugh, K., Dupeau, T., Herel, N., Derbanne, Q., Schiere, M., Shin, Y. & Kim, P. 2014b. *Structural fatigue loading predictions and comparisons with test data for a new class of US coast guard cutter*. Ship Structure Committee 2014, 18-20th May 2017, Linthicum Heights, USA.

Han, H.S., Lee, K.H. & Park, S.H. 2015. Estimate of the fatigue life of the propulsion shaft from torsional vibration measurements and the linear damage summation law in ships. *Ocean Engineering* 107, 212-221.

Han, R., Zhang, A. & Wang, S. 2016. Pressure load on rigid structure induced by double underwater explosions. In *Proc. 35th Int. Conf. on Ocean, Offshore and Arctic Engineering OMAE, Busan, Korea.*

Hansen, O.R., Kjellander, M., Martini, R. & Pappas, J.A. 2016. Estimation of explosion loading on small and medium sized equipment from CFD simulations. *Journal of Loss Prevention in the Process Industries* 41, 382-398.

Hay, A., Etienne, S., Pelletier, D. & Brosset, L. 2016. Accurate prediction of sloshing waves in tanks by an adaptive two-fluid incompressible front-tracking approach. In *Proc. 26th Int. Offshore and Polar Engineering Conference ISOPE, Rhodes, Greece.*

He, W., Diez, M., Zou, Z., Campana, E.F. & Stern, F. 2014. URANS study of Delft catamaran total/added resistance, motions and slamming loads in head sea including irregular wave and uncertainty quantification for variable regular wave and geometry. *Ocean Engineering* 74, 189-217.

Heitmann, K., Ruhnau, M., Lippert, T., Lippert, S. & von Estorff, O. 2015. Numerical investigation of the influence of different sound mitigation systems on the underwater sound pressure level due to offshore pile driving. In *Proc. 22nd International Congress on Sound and Vibration ICSV, Florence, Italy.*

Helmers, J.B. & Skeie, G. 2015. A Meshless boundary element method for simulating slamming in context of Generalized Wagner. *Journal of Offshore Mechanics and Arctic Engineering* 137.

Heo, K., Koo, W., Park, I.K. & Rye, J. 2016. Quadratic strip theory of higher order dynamic behavior of a large containership with 3D flow effects. *International Journal of Naval Architecture and Ocean Engineering* 8(2), 127-136.

Hirdaris, S. 2014. Special issue on uncertainty modelling for ships and offshore structures. *Ocean Engineering* 86(1) 1–2.

Hong, S.Y., Kim, K.W. & Kim, B.W. 2015. An experimental investigation on bow slamming loads on an ultra-large containership. In *Proc. 7th Int. Conf. on Hydroelasticity in Marine Technology, Split, Croatia.*

Horst, M.P. van der & Kaminski, M.L. 2017. Slit induced self magnetic flux leakage in a square steel plate. *To be published.*

Hørte, T., Russo, M., Macke, M. & Reinås, L. 2013. Benefit of measurements and structural reliability analysis for wellhead fatigue. In *Proc. 32nd International Conference on Ocean, Offshore and Arctic Engineering OMAE, Nantes, France.*

Hsu, C.-Y., Liang, C.-C., Teng, T.-L. & Nguyen, H.-A. 2016. The dynamic responses of the submersible vehicle mast with different cross-sectional shapes subjected to underwater explosion. *MATEC Web of Conferences* 54.

Hu, W.-H., Thöns, S., Rohrmann, R.G., Said, S. & Rücker, W. 2015. Vibration-based structural health monitoring of a wind turbine system Part II: Environmental/operational effects on dynamic properties. *Engineering Structures* 89, 260-272.

Huang, Q., Yan, X., Wang, Y., Zhang, C. & Wang, Z. 2017. Numerical modelling and experimental analysis on coupled torsional-longitudinal vibrations of a ship's propeller shaft. *Ocean Engineering* 136, 272-282.

Huera-Huarte, F.J. 2014. On splitter plate coverage for suppression of vortex-induced vibrations of flexible cylinders. *Applied Ocean Research* 48, 244-249.

Hwang, J.-O., Song, G.-D., Chun, S.-E., Bang, C.-S. & Joh, K.-H. 2015a. Direct assessment of LNG cargo containment system under sloshing loads. In *Proc. 25th Int. Offshore and Polar Engineering Conference ISOPE, Hawaii, USA.*

Hwang, S., Khayyer, A., Gotoh, H. & Park, J.-C. 2015b. Simulations of incompressible fluid flow-elastic structure interactions by a coupled fully Lagrangian solver. In *Proc. 25th Int. Offshore and Polar Engineering Conference ISOPE, Hawaii, USA.*

IACS 2015. *Unified requirements S11A (URS11A): Longitudinal strength standard for container ships.* International Association of Classification Societies.

IACS 2001. *Standard wave data*. International Association of Classification Societies.

Im, H.-I., Vladimir, N., Malenica, S. & Cho, D.-S. 2016. Hydroelastic response of 19,000 TEU class ultra large container ship with novel mobile deckhouse for maximizing cargo capacity. *International Journal of Naval Architecture and Ocean Engineering* 9(3), 339-349.

IMO 2014. I817E *Code on noise level on board ships*. International Maritime Organization.

ISO 2017. *ISO 18406:2017 - Underwater acoustics - Measurement of radiated underwater sound from percussive pile driving*. International Organization for Standardization.

ISO 2008. *ISO/IEC Guide 98-3:2008(E) Uncertainty of measurement – Part 3: Guide to the expression of uncertainty in measurement (GUM:1995).* International Organization for Standardization.

ISO 1997. *ISO 2631-1:1997-Mechanic vibration and shock - Evaluation of human exposure to whole-body vibration - Part 1: General requirements.* International Organization for Standardization.

ITTC 2014a. *General guidelines for uncertainty analysis in resistance test.* ITTC Procedure 7.5-02-02-02.

ITTC 2014b. *Example for uncertainty analysis of resistance tests in towing tank*. ITTC Procedure 7.5-02-02-02.1.

Janssen, C.F., Ueberrueck, M., Rung, T. & Behruzi, P. 2016. Real-time simulation of impact waves in LNG ship tanks with Lattice Boltzmann single-phase models. In *Proc. 26th Int. Offshore and Polar Engineering Conference ISOPE, Rhodes, Greece.*

JAPAN 2015. *Final report of committee on large container ship safety*. Committee on large container ship safety, The Maritime Bureau of Japan's Ministry of Land, Infrastructure, Transport and Tourism, Japan.

Jensen, J.J., Andersen, I.M.V. & Seng, S. 2014. Stochastic procedures for extreme wave induced responses in flexible ships. *International Journal of Naval Architecture and Ocean Engineering* 6, 1148-1159.

Jia, J. 2014. Investigations of a practical wind-induced fatigue calculation based on nonlinear time domain dynamic analysis and a full wind-directional scatter diagram. *Ships and Offshore Structures* 9(3), 272-296.

Jin, K.-K., Yoon, I.-S. & Yang, Y.-C. 2015. An effect of fluid-structure interaction for KC-1 cargo containment system under sloshing loads. In *Proc. 25th Int. Offshore and Polar Engineering Conference ISOPE, Hawaii, USA.*

Jin, Z., Yin, C., Chen, Y. & Hua, H. 2016. Graded effects of metallic foam cores for spherical sandwich shells subjected to close-in underwater explosion. *International Journal of Impact Engineering* 94, 23–35.

Junior, S.J., Esperanca, T.T.P., Sphaier, H.S. & Machado, C. 2014. Uncertainty analysis for inclining tests. In *Proc. 33rd International Conference on Ocean, Offshore and Arctic Engineering, San Francisco, California, USA.*

Kahl, A., von Selle, H. & Storhaug, G. 2016. *Full-scale measurement and hull monitoring on ships*. International Institute of Welding, Commission V, V-1675-15 (XV-1494-15).

Kahl, A., Fricke, W., Paetzold, H. & von Selle, H. 2015. Whipping investigations based on large-scale measurements and experimental fatigue testing. *International Journal of Offshore and Polar Engineering* 25(4), 247-254.

Kamali, W., Wahab, A.A., El Moghrabi, Y. & Kabbara, H. 2014. Survey on environmental noise in the port of Tripoli. In Proc. *21st International Congress on Sound and Vibration ICSV, Beijing, China.*

Kandasamy, R., Cui, F., Townsend, N., Foo, C.C., Guo, J., Shenoi, A. & Xiong, Y. 2016. A review of vibration control methods for marine offshore structures. *Ocean Engineering* 127, 279-297.

Kaplan, M.B. & Solomon, S. 2016. A coming boom in commercial shipping? The potential for rapid growth of noise from commercial ships by 2030. *Marine Policy* 73, 119-121.

Kapsenberg, G.K. & Thornhill, E.T. 2010. A practical approach to ship slamming in waves. In *Proc. 8th Symp. on Naval Hydrodynamics, Pasadena, California.*

Karagiozova, D., Langdon, G.S., Nurick, G.N. & Niven, T. 2015. The influence of a low density foam sandwich core on the response of a partially confined steel cylinder to internal air-blast. *International Journal of Impact Engineering* 92, 32-49.

Karimi, M.R., Brosset, L., Ghidaglia, J.-M. & Kaminski, M.L. 2016a. Effect of ullage gas on sloshing – Part II: Local effects of gas-liquid density ratio. *European Journal of Mechanics B/Fluids* 57, 82-100.

Karimi, M.R., Brosset, L., Ghidaglia, J.-M. & Kaminski, M.L. 2015. Effect of ullage gas on sloshing – Part I: Global effects of gas-liquid density ratio. *European Journal of Mechanics B/Fluids* 53, 213-228.

Karimi, M.R., Brosset, L., Kaminski, M.L. & Ghidaglia, J.-M. 2016b. Effects of ullage gas and scale on sloshing loads. *European Journal of Mechanics - B/Fluids* 62, 59-85.

Karuka, G.M., Arai, M. & Ando, H. 2017. Sloshing and swirling in partially loaded prismatic chamfered tanks. In *Proc. International Conference on Ocean, Offshore and Arctic Engineering OMAE, Trondheim, Norway.*

Kashiwagi, M., Kuga, S. & Chimoto, S. 2015. Time- and frequency-domain calculation methods for ship hydroelasticity with forward speed. In *Proc. 7th Int. Conf. on Hydroelasticity in Marine Technology, Split, Croatia.*

Kawabe, H., Shigemi, T., Matsumoto, I.K. & Toyoda, K. 2016. Estimation of quantitative influence of whipping on wave induced vertical bending moment for large containership. *NK Technical bulletin*.

Kayal, B., Benoit, A., Frihat, M. & Loysel, T. 2016. Introduction to a structural-based sloshing assessment for membrane containment system. In *Proc. 26th Int. Offshore and Polar Engineering Conference ISOPE, Rhodes, Greece.*

Khabakhpasheva, T.I., Kim, Y. & Korobkin, A.A. 2014. Generalised Wagner model of water impact by numerical conformal mapping. *Applied Ocean Research* 44, 29-38.

Ki, H.G., Park, S.G. & Jang, I.H. 2015. Full scale measurement of 14k TEU containership. In *Proc. 7th Int. Conf. on Hydroelasticity in Marine Technology, Split, Croatia.*

Kim, B.W., Hong, S.Y. & Kim, K.H. 2015a. Resonant and non-resonant whipping responses of a container model ship in regular and irregular waves. In *Proc. 7th Int. Conf. on Hydroelasticity in Marine Technology, Split, Croatia.*

Kim, D.H., Lee, K.H. & Seong, W.J. 2014a. Non-cavitating propeller noise modelling and inversion. *Journal of Sound and Vibration* 333, 424-437.

Kim, J., Kim, S.-Y., Kim, Y., Lee, K.-M. & Sung, Y.-J. 2017a. Experimental study of slosh-induced loads on LNG fuel tank of container ship. In *Proc. 27th Int. Offshore and Polar Engineering Conference ISOPE, San Francisco, USA.*

Kim, J.H. & Kim, Y. 2014. Numerical analysis on springing and whipping using fully-coupled FSI models. *Ocean Engineering* 91, 28–50.

Kim, J.H., Kim, Y., Yuck, R.H. & Lee, D.Y. 2015b. Comparison of slamming and whipping loads by fully coupled hydroelastic analysis and experimental measurement. *Journal of Fluids and Structures* 52, 145–165.

Kim, K.H., Kim, B.W. & Hong, S.Y. 2015c. Experimental study on correlation between slamming impact and whipping vibration for an ultra-large containership. In *Proc. 7th Int. Conf. on Hydroelasticity in Marine Technology, Split, Croatia.*

Kim, S.P. 2015. Nonlinear time domain simulations of slamming, whipping and springing loads on a containership. In *Proc. 7th Int. Conf. on Hydroelasticity in Marine Technology, Split, Croatia.*

Kim, S.-Y., Kim, K.-H. & Kim, Y. 2015d. Comparative study on pressure sensors for sloshing experiment. *Ocean Engineering* 94, 199-212.

Kim, S.-Y. & Kim, Y. 2017. Comparison of impact pressure on 2D and 3D tanks under harmonic excitation. In *Proc. 27th Int. Offshore and Polar Engineering Conference ISOPE, San Francisco, USA.*

Kim, S.-Y., Kim, Y. & Lee, J. 2017b. Comparison of sloshing-induced pressure in different scale tank. *Ships and Offshore Structures* 12(2), 244-261.

Kim, S.-Y., Lee, J. & Kim, Y. 2016. Study on scale effects on 3D sloshing flows. In *Proc. 26th Int. Offshore and Polar Engineering Conference ISOPE, Rhodes, Greece.*

Kim, Y. & Hermansky, G. 2014. Uncertainties in seakeeping analysis and related loads and response procedures. *Ocean Engineering* 86, 68-81.

Kim, Y., Lee, J.K. & Kim, J. 2017c. Experimental observation on the effects of liquid temperature and bubbles on impact pressure inside gas pocket. *International Journal of Offshore and Polar Engineering* 27(1).

Kim, Y., Ahn, I.G. & Park, S.G. 2015e. On the second order effect of the springing response of large blunt ship. In *Proc. 7th Int. Conf. on Hydroelasticity in Marine Technology, Split, Croatia.*

Kim, Y., Kim, J. & Kim, Y. 2015f. Development of a high-fidelity procedure for the numerical analysis of ship structural hydroelasticity. In *Proc. 7th Int. Conf. on Hydroelasticity in Marine Technology, Split, Croatia.*

Kim, Y. & Kim, J.H. 2016. Benchmark study on motions and loads of a 6750-TEU containership. *Ocean Engineering* 119, 262–273.

Kim, Y.G., Hwang, S.J., Cho, K.H. & Kim, U.K. 2017d. Characteristics of propulsion shafting system in ships with engine acceleration problems in the barred speed range. *Ocean Engineering* 145, 479-491.

Kimmoun, O., Brosset, L. & Dupont, G. 2016. Experimental study of wave impacts on a corrugated ceiling. In *Proc. 26th Int. Offshore and Polar Engineering Conference ISOPE, Rhodes, Greece.*

Knutsen, K.E., Lag, S., Brathhagen, S., Stang, J. & Myrseth, P. 2017. *Data quality assessment for sensor systems and time-series data*. DNVGL report no. 2017-0058, rev. 101, dated 9th February 2017.

Koh, C.-G., Luo, M., Bai, W. & Gao, M. 2015. Simulation of wave impact with compressible air entertainment based on consistent particle method. In *Proc. 34th International Conference on Ocean, Offshore and Arctic Engineering OMAE, St John's, Canada.*

Komissarov, P.V., Borisov, A.A., Sokolov, G.N. & Lavrov, V.V. 2015. Experimental comparison of shock and bubble heave energies from underwater explosion of ideal HE and explosive composite mixtures highly enriched with aluminum. *Physics Procedia* 72, 333 – 337.

Korobkin, A.A., Khabakhpasheva, T.I. & Malenica, S. 2017. Maximum stress of stiff elastic plate in uniform flow and due to jet impact (Jet impact onto a clamped elastic plate). *Physics of Fluids* 29(7).

KR 2017. *Guidance on strength assessment of containerships considering the whipping effect*. GC-19-E. 2017. Korean Register of Shipping.

Lakshmynarayanana, P., Temarel, P. & Chen, Z.-M. 2015. Coupled fluid structure interaction to model three-dimensional dynamic behaviour of ship in waves. In *Proc. 7th Int. Conf. on Hydroelasticity in Marine Technology, Split, Croatia.*

Lavroff, J., Davis, M.R., Holloway, D.S., Thomas, G.A. & McVicar, J.J. 2017. Wave impact loads on wave-piercing catamarans. *Ocean Engineering* 131, 263-271.

Lee, C.-H., Kim, S.-H. & Jeon, J.-H. 2015a. A study on structure-borne noise isolation by using AVM for offshore accommodation. In *Proc. 44th International Congress and Exposition on Noise Control Engineering INTER-NOISE, San Francisco, USA.*

Lee, D.-J., Shin, S.-B. & Suhr, J. 2015b. Effect of material behavior of PUF on dynamic response induced by fluid structure interaction in membrane type LNG cargo containment system. In *Proc. 25th Int. Offshore and Polar Engineering Conference ISOPE, Hawaii, USA.*

Lee, J.H., Lee, K.J., Kim, J.H. & Kim, B.K. 2015c. Sea-trial verification of air-filled rubber membrane for mitigation of propeller cavitation induced hull excitation. *Ocean Engineering* 110, 314-324.

Lee, Y., White, N., Southall, N. & Johnson, M.C. 2015d. Impact loads and whipping responses on a large container ship. In *Proc. 25th Int. Offshore and Polar Engineering Conference ISOPE, Hawaii, USA.*

Leontopoulos, C. 2006. *Shaft alignment and powertrain vibration*. American Bureau of Shipping.

Letton, W., Pappas, J.M. & Shen, J. 2015. More improvements to deepwater subsea measurement - Overview. In *Proc. Offshore Technology Conference OTC, Houston, USA.*

Li, F., Cao, J., Duan, M., An, C. & Su, J. 2016a. Two-phase flow induced vibration of subsea span pipeline. In *Proc. 26th International Ocean and Polar Engineering Conference, Rhodes, Greece.*

Li, H., Wang, D., Zhou, C.M., Zhang, K. & Ren, H. 2016b. Springing responses analysis and segmented model testing on a 500,000 DWT ore carrier. In *Proc. 35th Int. Conf. on Ocean, Offshore and Arctic Engineering OMAE, Busan, Korea.*

Li, H., Zhang, P., Song, G., Patil, D. & Mo, Y. 2015. Robustness study of the pounding tuned mass damper for vibration control of subsea jumpers. *Smart Materials and Structures* 24(9).

Li, J., Wu, C., Hao, H., Su, Y. & Liu, Z. 2016c. Blast resistance of concrete slab reinforced with high performance fiber material. *Journal of Structural Integrity and Maintenance* 1(2), 51-59.

Li, Y., He, L., Shuai, C.G. & Wang, C.Y. 2017. Improved hybrid isolator with maglev actuator integrated in air spring for active-passive isolation of ship machinery vibrations. *Journal of Sound and Vibration* 407, 226-239.

Liao, K., Duan, W., Ma, Q.-W., Ma, S., Zhao, B. & Hu, C. 2017. Numerical analysis of wave impact loads on semi-submersible platform. In *Proc. 36th Int. Conf. on Ocean, Offshore and Arctic Engineering OMAE, Trondheim, Norway.*

Liao, K., Hu, C. & Sueyoshi, M. 2015. Free surface flow impacting on an elastic structure: Experiment versus numerical simulation. *Applied Ocean Research* 50, 192-208.

Lind, S.J., Stansby, P.K., Rogers, B.D. & Lloyd, P.M. 2015. Numerical predictions of water air wave slam using incompressible-compressible smoothed particle hydrodynamics. *Applied Ocean research* 49, 57-71.

Liu, C., Zhang, Y.X. & Ye, L. 2017a. High velocity impact responses of sandwich panels with metal fibre laminate skins and aluminium foam core. *International Journal of Impact Engineering* 100, 139-153.

Liu, H., Chen, G., Lyu, T., Lin, H., Zhu, B. & Huang, A. 2016a. Wind-induced response of large offshore oil platform. *Petroleum Exploration and Development* 43(4), 708-716.

Liu, K., Liang, H. & Ou, J. 2016b. Numerical investigation of a tuned heave plate energy-harvesting system of a semi-submersible platform. *Energies* 9 (82), 1–22.

Liu, Y., Li, H., Zhang, K., Deng, B. & Peng, Y. 2017b. Analysis of the coupled horizontal and torsional loads of an ultra large containership. In *Proc. 27th Int. Offshore and Polar Engineering Conference ISOPE, San Francisco, USA.*

Lotfollahi-Yaghin, M.A., Ahmadi, H. & Tafakhor, H. 2016. Seismic responses of an offshore jacket-type platform incorporated with tuned liquid dampers. *Advances in Structural Engineering* 19(2), 227–38.

LR 2017a. *Rules and regulations for classification of ships*. Part 3 Chapter 16 Section 6 Ship event analysis. Lloyd's Register.

LR 2017b. *Rules and regulations for classification of ships: Container ships*. Lloyd's Register.

LR 2008. *Provisional rules, classification of ship event analysis systems*. *A guide to the rules and published requirements*. Lloyd's Register.

Lu, Y.J., Liang, C., Manzano-Ruiz, J.J., Janardhanan, K. & Perng, Y.-Y. 2016. Flow-induced vibration in subsea jumper subject to downstream slug and ocean current. *Journal of Offshore Mechanics and Arctic Engineering* 138, Article Number: 021302.

Lyu, W., el Moctar, O., Potthoff, R. & Neugebauer, J. 2017. Experimental and numerical investigation of sloshing using different free surface capturing methods. *Applied Ocean research* 68, 307-324.

MAIB 2008. *Report on the investigation of the structural failure of MSC Napoli English Channel on 18 January 2007*. Report No. 9/2008 A, Marine Accident Investigation Branch, Carlton House, Carlton Place, Southampton, UK.

Magoga, T., Aksu, S., Cannon, S., Ojeda, R. & Thomas, G. 2016. Comparison between fatigue life values calculated using standardised and measured stress spectra of a naval high speed light craft. In *Proc. 13th Int. Symp. on Practical Design of Ships and Other Floating Structures PRADS, Copenhagen, Denmark.*

Mai, T., Hu, Z.Z., Greaves, D.M. & Raby, A. 2015. Investigation of hydroelasticity: Wave impact on a truncated vertical wall. In *Proc. 25th Int. Offshore and Polar Engineering Conference ISOPE, Hawaii, USA.*

Makaya, K.R., Varelis, G.E. & Roff, A.G. 2016. Condition health monitoring of monopile and transition piece using guided wave testing. In *Proc. 26th Int. Offshore and Polar Engineering Conference ISOPE, Rhodes, Greece.*

Male, P. van der & Lourens, E. 2015. Operational vibration-based response estimation for offshore wind lattice structures. *Structural Health Monitoring and Damage Detection 7*.

Malenica, S. & Derbanne, Q. 2014. Hydro-structural issues in the design of ultra large container ships. *International Journal of Naval Architecture and Ocean Engineering* 6(4), 983-999.

Malenica, S., Diebold, L., Kwon, S.H. & Cho, D.-S. 2017. Sloshing assessment of the LNG floating units with membrane type containment system. Where we are? *Marine Structures* 56, 99-116.

Malenica, S., Vladimir, N., Choi, Y.M., Senjanovic, I. & Kwon, S.H. 2015. Global hydroelastic model for liquid cargo ships. In *Proc. 7th Int. Conf. on Hydroelasticity in Marine Technology, Split, Croatia.*

Mao, D., Zhong, C., Zhang, L. & Chu, G. 2015a. Dynamic response of offshore jacket platform including foundation degradation under cyclic loadings. *Ocean Engineering* 100, 35–45.

Mao, W., Li, Z., Ogeman, V. & Ringsberg, J.W. 2015b. A regression and beam theory based approach for fatigue assessment of containership structures including bending and torsion contributions. *Marine Structures* 41, 244-266.

Matsui, S., Murakami, C., Hanaoka, A. & Oka, M. 2016. Some considerations on the computational code for longitudinal strength design of a ship taking account of slamming and whipping loads. In *Proc. 31st Technical Exchange and Advisory Meeting on Marine Structures TEAM, Osaka, Japan.*

May, A., McMillan, D. & Thöns, S. 2015. Integrating structural health and condition monitoring: a cost benefit analysis for offshore wind energy. In *Proc. 34th International Conference on Ocean, Offshore and Arctic Engineering OMAE, St. John's, Newfoundland, Canada.*

Meng, S., Kajiwara, H. & Zhang, W. 2017. Internal flow effect on the cross-flow vortex-induced vibration of a cantilevered pipe discharging fluid. *Ocean Engineering*, 137, 120-128.

Minnebo, J., Aalberts, P.J. & Duggal, A. 2014. Deepwater mooring system monitoring with DGPS. In *Proc. 33rd Int. Conf. on Ocean, Offshore and Arctic Engineering OMAE, San Francisco, California, USA.*

Moe, E., Holtsmark, G. & Storhaug, G. 2005. Full scale measurements of the wave induced hull girder vibrations of an ore carrier trading in the North Atlantic. In: *Transactions of Royal Institution of Naval Architects, conference on design and operation of bulk carriers, London, UK.*

Mokrani, C. & Abadie, S. 2016. Conditions for peak pressure stability in VOF simulations of dam break flow impact. *Journal of Fluid and Structures* 62, 86-103.

Monteiro, L.L.S., Netto, T.A. & Monteiro, P.C.C. 2016. On the dynamic collapse of cylindrical shells under impulsive pressure loadings. *Journal of Offshore Mechanics and Arctic Engineering* 138(4).

Murphy, E. 2014. An assessment of residential exposure to environmental noise at a shipping port. *Environmental International* 63, 207-215.

Naess, A. & Gaidai, O. 2009. Estimation of extreme values from sampled time series. *Structural Safety* 31, 325-334.

Neugebauer, J., Liu, S., Potthoff, R. & el Moctar, O. 2017. Investigation of the motion accuracy influence on sloshing model test results. In *Proc. 27th Int. Offshore and Polar Engineering Conference ISOPE, San Francisco, USA.*

Nie, B.-C., Li, J.-C. & Zhang, H.-Q. 2015. On the regimes of underwater explosion for a submerged slender structure by pulsating bubble. *Marine Structures* 44, 85-100.

NK 2017a. *Rules for hull monitoring systems*. Nippon Kaiji Kyokai.

NK 2017b. *Rules for the survey and construction of steel ships*. Nippon Kaiji Kyokai.

NK 2016. Press release 6th May 2016. ShipDC launches with new leader at the helm. https://www.classnk.or.jp/hp/en/hp_news.aspx?id=1906&type=press_release&layout=3

NK 2015. Press release 7th December 2015. ClassNK establishes Ship Data Center to accelerate Big Date use in the maritime industry. https://www.classnk.or.jp/hp/en/hp_news.aspx?id=1759&type=press_release&layout=1.

NORSOK 2017. *Actions and action effects.* NORSOK standard N-003:2017, ICS 75.180.10, www.standard.no.

Nourisola, H., Ahmadi, B. & Tavakoli, S. 2015. Delayed adaptive output feedback sliding mode control for offshore platforms subject to nonlinear wave-induced force. *Ocean Engineering* 104, 1–9.

Nyseth, H. 2016. *Full scale measurements of ice-going vessels. Review of best practice for structural monitoring of ice-going vessels.* DNVGL report no. 2016-1197.

Oberhagemann, J. 2016. *On prediction of wave-induced loads and vibration of ship structures with finite volume fluid dynamic methods*. PhD Thesis, University of Duisburg-Essen, Germany.

Oberhagemann, J., Shigunov, V., Radon, M., Mumm, H. & Won, S.-I. 2015. Hydrodynamic load analysis and ultimate strength check of an 18000 TEU containership. In *Proc. 7th Int. Conf. on Hydroelasticity in Marine Technology, Split, Croatia.*

Olmati, P., Trasborg, P., Naito, C. & Bontempi, F. 2015. Blast resistant design of precast reinforced concrete walls for strategic infrastructures under uncertainty. *International Journal of Critical Infrastructures* 11(3), 197-212.

Orlowitz, E. & Brandt, A. 2014. Operational modal analysis for dynamic characterization of a Ro-Lo ship. *Journal of Ship Research* 58(4), 1-9.

Ortega, A., Rivera, A. & Larsen, C.M. 2017. Slug flow and waves induced motions in flexible riser. *J. Offshore Mech. Arct. Eng 140(1).*

Pais, T., Moro, L., Boote, D. & Biot, M. 2017. Vibration analysis for the comfort assessment of superyachts. *Journal of Marine Science and Application, 16, 323–333.*

Panciroli, R. & Porfiri, M. 2015. Analysis of hydroelastic slamming through particle image velocimetry. *Journal of Sound and Vibration* 347, 63-78.

Papanikolaou, A., Mohammed, E.A. & Hirdaris, S.E. 2014. Stochastic uncertainty modelling for ship design loads and operational guidance. *Ocean Engineering* 86, 47–57.

Peschmann, J., Storhaug, G., Derbanne, Q., Xie, G., Zheng, G., Ishibashi, K. & Kim, J. 2016. Impact study on the new IACS longitudinal strength standard for containerships (URS11A). In *Proc. 13th Int. Symp. on Practical Design of Ships and Other Floating Structures PRADS, Copenhagen, Denmark*.

Pickerd, V., Bornstein, H., McCarthy, P. & Buckland, M. 2016. Analysis of the structural response and failure of containers subjected to internal blast loading. *International Journal of Impact Engineering* 95, 40-53.

Postnikov, A., Pavlovskaia, E. & Wiercigroch, M. 2017. 2DOF CFD calibrated wake oscillator model to investigate vortex-induced vibrations. *International Journal of Mechanical Sciences*, 127, 176–190.

Qiu, W., Junior, J.S., Lee, D., Lie, H., Magarovskii, V., Mikami, T., Rousset, J.-M., Sphaier, S., Tao, L. & Wang, X. 2014. Uncertainties related to predictions of loads and responses for ocean and offshore structures. *Ocean Engineering* 86, 58-67.

Qu, Y., Su, J., Hua, H. & Meng, G. 2017. Structural vibration and acoustic radiation of coupled propeller-shafting and submarine hull system due to propeller forces. *Journal of Sound and Vibration* 401, 76-93.

Rajendran, S., Fonseca, N. & Soares, C.G. 2016. A numerical investigation of the flexible vertical response of an ultra large containership in high seas compared with experiments. *Ocean Engineering* 122, 293-310.

Ramos Jr., R., Oliveira Jr., S., Filho, E.C. & Silva, L.C.T. 2016. Evaluation of transversal displacement of the rotor of a twin-screw multiphase pump. In *Proc. 26th Int. Offshore and Polar Engineering Conference ISOPE, Rhodes, Greece.*

Ren, H., Zhang, K., Li, H. & Wang, D. 2016. Large containerships fatigue analysis due to springing and whipping. In *Proc. 35th Int. Conf. on Ocean, Offshore and Arctic Engineering OMAE, Busan,* Korea.

Ringsberg, J.W., Liljegren, A. & Lindhal, O. 2016. Sloshing impact response in LNG membrane carriers: a response analysis of the hull structure supporting the membrane tanks. In *Proc. 35th Int. Conf. on Ocean, Offshore and Arctic Engineering OMAE, Busan, Korea.*

Robert, M., Monroy, C., Reliquet, G., Ducoin, A., Guillerm, P. & Ferrant, P. 2015. Hydroelastic response of a flexible barge investigated with a viscous flow solver. In *Proc. 7th Int. Conf. on Hydroelasticity in Marine Technology, Split, Croatia.*

Robertson, A. 2017. Uncertainty analysis of OC5-DeepCwind floating semisubmersible offshore wind test campaign. In *Proc. 27th Int. Offshore and Polar Engineering Conference ISOPE, San Francisco, USA.*

Robinson, S., Lepper, P. & Hazelwood, R. 2014. *Good practice guide for underwater noise measurement*. National Measurement Office, Marine Scotland, The Crown Estate, Robinson, NPL Good Practice Guide No. 133, ISSN: 1368-6550.

Ruhnau, M., Heitmann, K., Lippert, T., Lippert, S. & von Estorff, O. 2016. Understanding soil transmission paths of offshore pile driving noise - Seismic waves and their implications. In *Proc. INTER-NOISE and NOISE-CON Congress and Conference, Hamburg, Germany.*

Sadat-Hosseini, H., Kim, D.H., Toxopeus, S., Diez, M. & Stern, F. 2015. CFD and potential flow simulations of fully appended free running 5415M in irregular waves, In *Proc. 15th World Maritime Technology Conference, Providence, Rhode Island, USA.*

Salvado, F.C., Tavares, A.J., Teixeira-Dias, F. & Cardoso, J.B. 2017. Confined explosions: The effect of compartment geometry. *Journal of Loss Prevention in the Process Industries* 48, 126-144.

Scavuzzo, R.J., Hill, G.D. & Saxe, P. 2015. The “spectrum dip”: Dynamic interaction of system components. *J. Pressure Vessel Technol.* 137(4).

Schecklman, S., Laws, N., Zurk, L.M. & Siderius, M. 2015. A computational method to predict and study underwater noise due to pile driving. *Journal of the Acoustical Society of America* 138(1), 258-266.

Schiffer, A. & Tagarielli, V.L. 2015. The response of circular composite plates to underwater blast: Experiments and modeling. *Journal of Fluids and Structures* 52, 130–144.

Scolan, Y.-M. & Brosset, L. 2017. Numerical simulation of highly nonlinear sloshing in a tank due to forced motion. *International Journal of Offshore and Polar Engineering* 27(1).

Scolan, Y.-M., Hay, A. & Brosset L. 2016. Some aspects of high kinematics in breaking waves due to sloshing. *IWWWFB, Plymouth, USA.*

Seng, S., Jensen, J.J. & Malenica, S. 2014. Global hydroelastic model for springing and whipping based on a free-surface CFD code (OpenFOAM). *International Journal of Naval Architecture and Ocean Engineering* 6(4), 1024-1040.

Senjanovic, I., Vladimir, N., Tomic, M., Hadzic, N. & Malenica, S. 2014. Global hydroelastic analysis of ultra large container ships by improved beam structural model. *International Journal of Naval Architecture and Ocean Engineering* 6(4), 1041-1063.

Shan, P., Wu, J. & Cai, S. 2017. Study of 18000 TEU container vessel's fatigue strength under influences of springing phenomenon. In *Proc. 27th Int. Offshore and Polar Engineering Conference ISOPE, San Francisco, USA.*

Sheinberg, R., Cleary, C., Stambaugh, K. & Storhaug, G. 2011. Investigation of wave impact and whipping response on the fatigue life and ultimate strength of a semi-displacement patrol boat. In *Proc. 11th Int. Conf. on Fast Sea Transportation FAST, Honolulu, Hawaii, USA*.

Shi, J., Zhu, Y., Chen, G., Zhang, R. & Guo, Z. 2017. Assessment on blast loading resistance capacity of corrugations on offshore cabins based on the P–I model. *Process Safety and Environmental Protection* 105, 237–249.

Shi, X.H., Teixeira, A.P., Zhang, J. & Soares, C.G. 2016. Reliability analysis of a ship hull structure under combined loads including slamming loading. *Ships and Offshore Structures, 11, 300–15.*

SILENV 2012. Deliverable 5.2 noise and vibration label proposal. *SILENV - Ships oriented Innovative soLutions to rEduce Noise and Vibrations (N&V), Collaborative project funded by the European Commission under the 7th Framework Program, Theme Transport - Grant Agreement N° 234182, available: http://www.silenv.eu/.*

Sohn, J., Kim, S., Seo, J., Kim, B. & Paik, J. 2016. Strength assessment of stiffened blast walls in offshore installations under explosions. *Ships and Offshore Structures* 11(5), 551-560.

Southall, N., Lee, Y., Johnson, M.C., Lin, F. & White, N. 2016. Coupling CFD with a time-domain ship motions method for prediction of slamming. In *Proc. 26th Int. Offshore and Polar Engineering Conference ISOPE, Rhodes, Greece.*

Stenard, J.K., Hlavaty, M. & Paulic, A. 2017. The case for a universal adjustable shock mount (UASM). *Naval Engineers Journal* 129(2), 123-126.

Storhaug, G. 2015. The consequence of whipping and springing in fatigue loading of container ships. In *Proc. 7th Int. Conf. on Hydroelasticity in Marine Technology, Split, Croatia.*

Storhaug, G. 2014a. The measured contribution of whipping and springing on the fatigue and extreme loading of container vessels. *International Journal of Naval Architecture and Ocean Engineering* 6(4), 1096-1110.

Storhaug, G. 2014b. Which sea states are dimensioning for container vessels when whipping is included? In *Proc. 33rd Int. Conf. on Ocean, Offshore and Arctic Engineering OMAE, San Francisco, California, USA.*

Storhaug, G., Aagaard, O. & Fredriksen, O. 2016. Calibration of hull monitoring strain sensors in deck including the effect of hydroelasticity. In *Proc. 26th Int. Offshore and Polar Engineering Conference ISOPE, Rhodes, Greece.*

Storhaug, G. & Andersen, I.M.V. 2015. Extrapolation of model tests measurements of whipping to identify the dimensioning sea states for container ships. In *Proc. 25th Int. Offshore and Polar Engineering Conference ISOPE, Hawaii, USA.*

Storhaug, G., Fredriksen, O., Greening, D. & Robinson, D. 2017a. Practical verification of loading computer by laser measurements. In *Proc. 6th International conference on marine structures MARSTRUCT, Lisbon, Portugal.*

Storhaug, G. & Kahl, A. 2016. Hull monitoring closing the gap between the design and operation. In *Proc. 6th Int. Maritime Conference on Design for Safety*, *Hamburg, Germany.*

Storhaug, G. & Kahl, A. 2015. Full scale measurements of torsional vibrations on Post-Panamax container ships. In *Proc. 7th Int. Conf. on Hydroelasticity in Marine Technology, Split, Croatia.*

Storhaug, G., Laanemets, K., Ringsberg, J. & Edin, I. 2017b. Estimation of damping from wave induced vibrations in ships. In *Proc. 6th Int. Conf. on Marine Structures MARSTRUCT, Lisbon, Portugal.*

Sun, L., Lu, Y. & Zhang, X. 2016. A review on damage identification and structural health monitoring for offshore platform. In *Proc. 35th International Conference on Ocean, Offshore and Arctic Engineering, OMAE, Busan, South Korea.*

Takahashi, H. & Yasuzawa, Y. 2014. Investigation on damping model for vibration response analysis using whole ship model. In *Proc. 24th International Ocean and Polar Engineering Conference ISOPE, Busan, Korea.*

Takami, T., Oka, M. & Iijima, K. 2017. Study on application of CFD and FEM coupling method to evaluate dynamic response of ship under severe wave condition. In *Proc. 36th Int. Conf. on Ocean, Offshore and Arctic Engineering OMAE, Trondheim, Norway.*

Taskar, B., Steen, S. & Eriksson, J. 2017. Effect of waves on cavitation and pressure pulses of a tanker with twin podded propulsion. *Applied Ocean Research* 65, 206-218.

Taskar, B., Yum, K.K., Steen, S. & Pedersen, E. 2016. The effect of waves on engine-propeller dynamics and propulsion performances of ships. *Ocean Engineering* 65, 262-277.

Tegowski, J., Koza, R., Pawliczka, I., Skóra, K., Trzcińska, K. & Zdroik, J. 2016. Statistical, spectral and wavelet features of the ambient noise detected in the southern Baltic sea. In *Proc. 23rd International Congress on Sound and Vibration ICSV, Athens, Greece.*

Tenzer, M., el Moctar, O. & Schellin, T.E. 2015. Experimental investigation of impact loads during water entry. *Ship Technology Research* 62, 47-59.

Thompson, I. 2016. Validation of naval vessel spectral fatigue analysis using full scale measurements. *Marine Structures* 49, 256-268.

Thorsen, M., Sævik, S. & Larsen, C. 2017. Non-linear time domain analysis of cross-flow vortex-induced vibrations. *Marine Structures* 51, 134–151.

Thorsen, M., Sævik, S. & Larsen, C. 2016. Time domain simulation of vortex-induced vibrations in stationary and oscillating flows. *Journal of Fluids and Structures* 61, 1–19.

Thorsen, M.J., Sævik, S. & Larsen, C.M. 2015. Fatigue damage from time domain simulation of combined in-line and cross-flow vortex-induced vibrations. *Marine Structures* 41, 200–222.

Thorsen, M., Sævik, S. & Larsen, C. 2014. A simplified method for time domain simulation of cross-flow vortex-induced vibrations. *Journal of Fluids and Structures* 49, 135–148.

Tiancheng, M., Wang, H., Zhou, J. & Wu, D. 2017. Noise analysis and control scheme of underwater exhaust process. In *Proc. 24th International Congress on Sound and Vibration ICSV, London, UK.*

Tsouvalas, A. & Metrikine, A.V. 2016. Parametric study of noise reduction by an air-bubble curtain in offshore pile driving. In *Proc. 23rd International Congress on Sound and Vibration ICSV, Athens, Greece.*

Ulveseter, J.V., Thorsen, M.J., Sævik, S. & Larsen, C.M. 2017. Stochastic modelling of cross-flow vortex-induced vibrations. *Marine Structures* 56, 260-280.

Utsunomiya, T., Sato, I., Kobayashi, O., Shiraishi, T. & Harada, T. 2017. Numerical modelling and analysis of a hybrid-spar floating wind turbine. In *Proc. 36th Conference on Ocean, Offshore and Arctic Engineering OMAE, Trondheim, Norway.*

Utsunomiya, T., Sato, I., Kobayashi, O., Shiraishi, T. & Harada, T. 2015. Design and installation of a hybrid-spar floating wind turbine platform. In *Proc. 34th Conference on Ocean, Offshore and Arctic Engineering OMAE,* Newfoundland, Canada.

Veldman, A.E.P., Luppes, R., van der Heiden, H.J.L., van der Plas, P., Helder, J. & Bunnik, T. 2015. Turbulence modeling for locally-refined free-surface flow simulations in offshore applications. In *Proc. 25th Int. Offshore and Polar Engineering Conference ISOPE, Hawaii, USA.*

Veracity 2016. https://www.dnvgl.com/data-platform.

Wang, X., Temarel, P., Hu, J. & Gu, X. 2016a. Hydroelastic analysis of an ULOC in waves. In *Proc. 13th Int. Symp. on Practical Design of Ships and Other Floating Structures PRADS, Copenhagen, Denmark.*

Wang, G., Wang, Y., Lu, W., Zhou, W., Chen, M. & Yan, P. 2016b. On the determination of the mesh size for numerical simulations of shock wave propagation in near field underwater explosion. *Applied Ocean Research* 59, 1–9.

Wang, H., Cheng, Y.S., Liu, J. & Gan, L. 2016c. Damage evaluation of a simplified hull girder subjected to underwater explosion load: A semi-analytical model. *Marine Structures* 45, 43-62.

Wang, J., Guo, J., Yao, X.L. & Zhang, A.M. 2016d. Dynamic buckling of stiffened plates subjected to explosion impact loads. *Shock Waves* 27(1), 37-52.

Wang, J., Fu, S., Baarholm, R., Wu, J. & Larsen, C.M. 2015. Out-of-plane vortex induced vibration of a steel catenary riser caused by vessel motions. *Ocean Engineering* 109, 389-400.

Wang, J., Fu, S., Baarholm, R., Wu, J. & Larsen, C.M. 2014. Fatigue damage of a steel catenary riser from vortex-induced vibration caused by vessel motions. *Marine Structures* 39, 131-156.

Wang, J., Wan, D., Chen, G. & Huang, W. 2016e. Comparative studies of 3-D LNG tank sloshing based on the VOF and IMPS methods. In *Proc. 26th Int. Offshore and Polar Engineering Conference ISOPE, Rhodes, Greece.*

Wang, L.-K., Zhang, Z.-F. & Wang, S.-P. 2016f. Pressure characteristics of bubble collapse near a rigid wall incompressible fluid. *Applied Ocean Research* 59, 183–192.

Wang, S. & Lu, P. 2016. On the monitoring of mooring system performance. In *Proc.* 21*st SNAME Offshore Symposium, Houston, USA.*

Wei, Z.-J., Wu, C.-J. & Guan, H. 2016. Experimental investigation of kinematic flow field in the geometric similar GTT tanks. In *Proc. 35th Int. Conf. on Ocean, Offshore and Arctic Engineering OMAE, Busan, Korea.*

WHO 2011. *Burden of disease from environmental noise*. World Health Organization.

Wisch, D. & Spong, R. 2016. Recommended practice for structural integrity management of floating offshore structures – A DeepStar 12401 product. In *Proc*. *Offshore Technology Conference, Houston OTC, Houston, USA.*

Wochner, M.S., Lee, K.M., McNeese, A.R. & Wilson, P.S. 2015. Underwater noise mitigation using a system of tuneable resonators. In *Proc. 22nd International Congress on Sound and Vibration ICSV, Florence, Italy.*

Wu, M.K. 2015. Fatigue analysis for a high-speed vessel with hydroelastic effects. In *Proc. 7th Int. Conf. on Hydroelasticity in Marine Technology, Split, Croatia.*

Wu, J., Lie, H., Constantinides, Y. & Baarholm, R.J. 2016a. NDP riser VIV model test with staggered buoyancy elements. In *Proc. 35th Int. Conf. on Ocean, Offshore and Arctic Engineering OMAE, Busan, Korea.*

Wu, Q., Zhao, X., Zheng, R. & Minagawa, K. 2016b. High response performance of a tuned-mass damper for vibration suppression of offshore platform under earthquake loads. *Shock and Vibration* 2016, Article ID 7383679.

Wu, Y.S., Chen, R.Z. & Lin, J.R. 2003. Experimental technique of hydroelastic ship model. In *Proc. 3rd Int. Conf. on Hydroelasticity in Marine Technology, Oxford, UK.*

Xiao, F., Chen, Y., Hua, H. & Zhu, D. 2015. Experimental and numerical investigation on the shock resistance of honeycomb rubber coatings subjected to underwater explosion. *Proceedings of the Institution of Mechanical Engineers, Part M: J. Engineering for the Maritime Environment* 229(1), 77–94.

Xue, Q., Zhang, J., He, J. & Zhang, C. 2016. Control performance and robustness of pounding tuned mass damper for vibration reduction in SDOF structure. *Shock and Vibration* 2016.

Yang, K.K., Kim, J., Kim, Y., Kim, S.Y. & Zhu, Z. 2016a. PIV measurement of violent sloshing flows and comparison with CFD computations. *International Journal of Offshore and Polar Engineering* 26(3).

Yang, L., Nie, S., Yin, S., Zhao, J. & Yin, F. 2015a. Numerical and experimental investigation on torque characteristics of seawater hydraulic axial piston motor for underwater tool system. *Ocean Engineering* 104, 168-184.

Yang, P., Gu, X., Tian, C., & Ding, J. 2015b. 3D hydroelastic response of a large bulk carrier in time domain. In *Proc. 7th Int. Conf. on Hydroelasticity in Marine Technology, Split, Croatia.*

Yang, W., Li, L., Fu, Q., Teng, Y., Wang, S. & Liu, F. 2016b. Identify modal parameters of a real offshore platform from the response excited by natural ice loading. In *Proc. 35th International Conference on Ocean, Offshore and Arctic Engineering OMAE, Busan, Korea.*

Yao, S., Zhang, D., Lu, F., Chen, X. & Zhao, P. 2017a. A combined experimental and numerical investigation on the scaling laws for steel box structures subjected to internal blast loading. *International Journal of Impact Engineering* 102, 36-46.

Yao, S., Zhang, D., Lu, F. & Li, X. 2017b. Experimental and numerical studies on the failure modes of steel cabin structure subjected to internal blast loading. *International Journal of Impact Engineering* 110, 279-287.

Yao, S., Zhang, D. & Lu, F. 2016. Dimensionless number for dynamic response analysis of box-shaped structures under internal blast loading. *International Journal of Impact Engineering* 98, 13-18.

Yin, D., Lie, H. & Baarholm, R.J. 2017. Prototype Reynolds number VIV tests on a full-scale rigid riser. In *Proc. 36th Int. Conf. on Ocean, Offshore and Arctic Engineering OMAE, Trondheim, Norway.*

Yin, D., Lie, H., Russo, M. & Grytøyr, G. 2016. Drilling riser model tests for software verification. In *Proc. 35th Int. Conf. on Ocean, Offshore and Arctic Engineering OMAE, Busan, Korea.*

Zekri, H.J., Korobkin, A.A. & Cooker, M.J. 2015. Liquid sloshing and impact in a closed container with high filling. *IWWWFB, Bristol, UK.*

Zhang, B.L., Han, Q.L. & Zhang, X.M. 2017a. Recent advances in vibration control of offshore platforms. *Nonlinear Dynamics* 89, 755-771.

Zhang, C., Yue, J., Liu, Z. & He, Z. 2015. A VBM research based on segmented model tests and numerical simulations for a river-to-sea ship. In *Proc. 25th Int. Offshore and Polar Engineering Conference ISOPE, Hawaii, USA.*

Zhang, J., Shi, X.H. & Soares, C.G. 2017b. Experimental study on the response of multi-layered protective structure subjected to underwater contact explosions. *International Journal of Impact Engineering* 100, 23-34.

Zhang, J., Zhehao, M., Liu, F., Zhang, C., Sharafi, P. & Rashidi, M. 2017c. Seismic performance and ice-induced vibration control of offshore platform structures based on the ISO-PFD-SMA brace system. *Advances in Materials Science and Engineering* 2017.

Zhang, K., Ren, H., Li, H. & Yan, L. 2016a. Nonlinear hydroelasticity of large container ship. In *Proc. 26th Int. Offshore and Polar Engineering Conference ISOPE, Rhodes, Greece.*

Zhang, W. & Jiang, W. 2015. An improved shock factor to evaluate the shock environment of small-sized structures subjected to underwater explosion. *Shock and Vibration* 2015.

Zhang, Y., Chen, X. & Wan, D. 2017d. Sloshing flows in an elastic tank with high filling liquid by MPS-FEM coupled method. In *Proc. 27th Int. Offshore and Polar Engineering Conference ISOPE, San Francisco, USA.*

Zhang, Z., Sun, L., Yao, X. & Cao, X. 2015a Smoothed particle hydrodynamics simulation of the submarine structure subjected to a contact underwater explosion. *Combustion, Explosion, and Shock Waves* 51(4), 502–510.

Zhang, Z., Wang, L., Silberschmidt, V.V. & Wang, S. 2016c. SPH-FEM simulation of shaped-charge jet penetration into double hull: A comparison study for steel and SPS. *Composite Structures* 155, 135–144.

Zhang, Z., Wang, Y., Zhao, H., Qian, H. & Mou, J. 2015b. An experimental study on the dynamic response of a hull girder subjected to near field underwater explosion. *Marine Structures* 44, 43-60.

Zhu, G., Xiong, Y.P., Daley, S. & Shenoi, R.A. 2015. Magnetorheological elastomer materials and structures with vibration energy control for marine application. In *Proc. 5th International Conference on Marine Structures MARSTRUCT, Southampton, UK.*

Zhu, S. & Moan, T. 2015. Effect of heading angle on wave-induced vibrations and extreme vertical bending moments in a ultra large container ship model. In *Proc. 7th Int. Conf. on Hydroelasticity in Marine Technology, Split, Croatia.*

Zou, C.-F., Wang, D.-Y. & Cai, Z.-H. 2015a. Effects of boundary layer and liquid viscosity and compressible air on sloshing characteristics. *International Journal of Naval Architecture and Ocean Engineering* 7(4), 670-690.

Zou, D., Rao, Z. & Ta, N. 2015b. Coupled longitudinal-transverse dynamics of a marine propulsion shafting under super harmonic resonances. *Journal of Sound and Vibration* 346, 248-264.

Zuo, H., Bi, K. & Hao, H. 2017. Using multiple tuned mass dampers to control offshore wind turbine vibrations under multiple hazards. *Engineering Structures* 141, 303-315.

This page intentionally left blank

Proceedings of the 20th International Ship and Offshore Structures Congress (ISSC 2018) Volume I – M.L. Kaminski and P. Rigo (Eds.)

doi:10.3233/978-1-61499-862-4-335

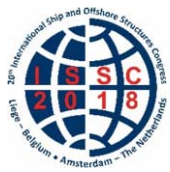

COMMITTEE III.1

ULTIMATE STRENGTH

COMMITTEE MANDATE

Concern for the ductile behaviour of ships and offshore structures and their structural components under ultimate conditions. Attention shall be given to the influence of fabrication imperfections and in-service damage and degradation on reserve strength. Uncertainties in strength models for design shall be highlighted. Consideration shall be given to the practical application of methods.

AUTHORS/COMMITTEE MEMBERS

Chairman: J. Czujko, *Norway*
A. Bayatfar, *Belgium*
M. Smith, *Canada*
M. C. Xu, *China*
D. Wang, *China*
M. Lützen, *Denmark*
S. Saad-Eldeen, *Egypt*
D. Yanagihara, *Japan*
G. Notaro, *Norway*
X. Qian, *Singapore*
J. S. Park, *South Korea*
J. Broekhuijsen, *The Netherlands*
S. Benson, *UK*
S. J. Pahos, *UK*
J. Boulares, *USA*

KEYWORDS

Ultimate strength; Load-carrying capacity; Ultimate limit states; Buckling collapse; Fabrication-Induced Initial Imperfections; In-service damage and degradation; Reliability

CONTENTS

1. INTRODUCTION 338

2. FUNDAMENTALS 339
   2.1 Introduction 339
   2.2 Understanding of ultimate strength 339
   2.3 Design for ultimate strength 339
      2.3.1 General 339
      2.3.2 International association of classification societies (IACS) 340
   2.4 Design for limit states 340
   2.5 Safety factors for ultimate strength 341

3. ASSESSMENT OF ULTIMATE STRENGTH 342
   3.1 Introduction 342
   3.2 Topside structures 342
   3.3 Analytical methods 343
      3.3.1 Closed form methods 343
      3.3.2 Progressive collapse methods 343
      3.3.3 Gaps 345
      3.3.4 Residual strength of damaged hulls 346
      3.3.5 Analytical assessment of damage 346
      3.3.6 Development of empirical formulas for residual strength 347
      3.3.7 Benchmark studies and gaps 347
   3.4 Numerical methods 348
      3.4.1 Idealised structural unit method (ISUM) 349
      3.4.2 Nonlinear FE method 350
   3.5 Experimental methods 352

4. PROBABILISTIC MODELS AND RELIABILITY ASSESSMENTS 353
   4.1 Introduction 353
   4.2 Reliability theory 354
   4.3 Reliability analyses 354
      4.3.1 Local structures 354
      4.3.2 Ship structures 354
      4.3.3 Corrosion wastage 355
      4.3.4 Grounding or collision 356
      4.3.5 Operational conditions and sea state 356
      4.3.6 Offshore structures 357

5. SHIP SHAPED STRUCTURES 357
   5.1 Introduction 357
   5.2 Review of state of the art 358
      5.2.1 Design for ultimate strength of ships 358
      5.2.2 Design for residual strength 363
   5.3 Developments in ultimate strength assessment 365
      5.3.1 Load combination and dynamic effects 365
      5.3.2 Composite and aluminium vessels; novel hull design 367
   5.4 Developments in the residual strength assessment of damaged vessels 368
   5.5 Areas for future development 370

6. MARINE STRUCTURES 372
   6.1 Introduction 372
      6.1.1 General 372
      6.1.2 Review of previous ISSC reports 373
   6.2 Standards and rules for the ultimate strength of marine structures 373

6.2.1 Offshore standards ... 373
6.2.2 Classification Societies rules and requirements ... 374
6.2.3 Design of offshore structures ... 375
6.2.4 Assessment of existing structures ... 376
6.2.5 Seismic design guidelines ... 376
6.2.6 Accidental damage and residual strength ... 377
6.2.7 Design of cold climate and arctic ... 378
6.3 Development in the assessment of the ultimate strength ... 378
6.3.1 Assessment of existing offshore structures ... 378
6.3.2 Seismic assessment ... 378
6.3.3 Arctic condition ... 379
6.3.4 Assessment of damage effect (collision, dropped objects and fire) ... 379
7. ULTIMATE STRENGTH OF STRUCTURAL COMPONENTS AND CONNECTIONS ... 381
7.1 Components and connections for ships and floating structures ... 381
7.1.1 Plates and stiffened panels ... 381
7.1.2 Plate connections ... 383
7.1.3 Beams and girders ... 383
7.1.4 Fabrication effects ... 384
7.2 Tubular members and components ... 385
7.2.1 Tubular members ... 385
7.2.2 Tubular joints ... 386
7.2.3 Other types of tubular components ... 387
7.2.4 Reinforced tubular components ... 387
7.3 Developments in other structural components ... 389
7.3.1 Aluminium components and connections ... 389
7.3.2 Composite components and connections ... 389
7.3.3 Windows and doors ... 389
8. MATERIALS ... 390
8.1 Introduction ... 390
8.2 Aluminium alloys ... 390
8.3 Composite structures ... 392
9. BENCHMARK STUDY ... 394
9.1 Ultimate strength of joints subjected to fire loads ... 394
9.1.1 Scope of benchmark ... 394
9.1.2 Strategy of benchmark study ... 395
9.1.3 Benchmark model ... 395
9.1.4 Results of benchmark study ... 400
9.1.5 Conclusions ... 412
9.2 Ultimate strength of box girders subjected to bending ... 412
9.2.1 Scope of benchmark ... 412
9.2.2 Strategy of benchmark ... 413
9.2.3 Benchmark models ... 413
9.2.4 Results of experiments ... 417
9.2.5 Results of benchmark study ... 417
9.2.6 Conclusions ... 420
10. CONCLUSIONS AND RECOMMENDATIONS ... 421
REFERENCES ... 424

1. INTRODUCTION

The work of this Committee III.1 is focused on the ultimate strength of ships and marine structures.

Ultimate strength is a point beyond which the loading exceeds structural capacity and the structure collapses. This point is a property defining the structure and used to measure its robustness and safety margins.

Existing industry design rules make only reference to the ultimate strength with relation to the local ultimate strength of structures and with relation to the ultimate strength of components. With respect to the global strength rules and standards do not refer to ultimate strength, as only after the design is completed, the question of ultimate strength is raised in an attempt to define the relation between loads and structural capacity.

As much as it is required to know the ultimate strength of the designed structure, calculating it poses a challenge. Ultimate strength is influenced by a number of mechanisms and cannot be defined by one value. Structures can fail in different ways depending on various types of acting loads. Ultimate strength, also called collapse mode, damage form, or damage mode in different sources, is associated with the form of damage resulting from the type of loading applied. Calculating ultimate strength gives multiple answers as different forms of damage mean different ultimate strength.

A number of factors challenge the calculation of the ultimate strength of a structure. These are the types of loads, the materials used, environmental factors or the fact that real-life structures are imperfect by definition as opposed to their design drawings.

The only way to find answers and reach reliable results while calculating ultimate strength is by application of sophisticated tools and through experiments. Good models of materials and structural elements, taking into account fabrication effects, as well as advanced software that represent material nonlinear behaviour, need to be utilized.

In the report, basic definitions, general description of design for ultimate strength and safety criteria for this type of design can be found in Section 2, Fundamentals.

In Section 3, Assessment of Ultimate Strength, empirical and analytical assessments of ships and marine structures are provided. Numerical and experimental methods are also discussed.

Probabilistic Models and Reliability Assessments are the subjects of Section 4.

Sections 5 and 6 focus on Ship Shaped Structures and Marine Structures respectively.

A detailed description of the methods applied to calculate ultimate strength can be found in Section 7, Ultimate Strength of Structural components and Connections.

Section 8, Materials, is focusing on the role of non-ferrous materials and their characteristics in resolving challenges associated with designing for ultimate strength.

Section 9 is a presentation of results of two benchmark studies performed by the Committee members. The objective of the first Benchmark was to predict the strength of structural joints of topside structures subjected to fires in order to compare different techniques (and solvers) in assessing the strength of these structures. The objective of the second Benchmark study was to validate the ultimate strength of the box girders under the pure bending moment using various finite elements solvers through comparison with the box girder buckling tests. This is a revisiting of Benchmark of ISSC2015, performed this time to identify possible sources of uncertainties and errors with reference to correct modelling and assessment of buckling tests.

The report is summarized in the last Section, Conclusions and Recommendations.

2. FUNDAMENTALS

2.1 Introduction

Ultimate strength is a property of a structure or structural component dependent on its topology, material properties and imperfections, assessed on local or global level, with distinct failure modes in tension and compression. Strength is the property of structures that resists the forces and moments that arise from tensile, compressive, shear, bending, or combined load effects exerted in service. The ultimate strength is normally assessed for a set of loads and boundary conditions at a time and dictates the maximum load that a structure can withstand prior to violating a safety criterion.

Since structural safety is a critical requirement, it is necessary that structures are provided with sufficient ultimate strength to ensure adequate safety margins. Safety margins are ensured with design methods and appropriate safety factors accounting for load types and associated uncertainties, through defined safety criteria.

2.2 Understanding of ultimate strength

There are a number of uncertainties related to the understanding of ultimate strength.

The ultimate strength of ships and offshore structures is affected by several factors resulting in non-linear structural behaviour. These factors include loads, temperatures, strain-rates, and time dependent material properties, as well as imperfections related to imperfect geometry and initial/residual stresses. In addition, complex nonlinear boundary conditions may be of great importance. The most prominent uncertainties affecting assessment results of ultimate strength are given in Table 1.

Table 1: Uncertainties in Ultimate Strength Assessment

Source of Uncertainty	
Geometric	**Material**
Model imperfections	Yield strength
Initial imperfection	Plasticity model
Boundary conditions	Stiffness (Young's Modulus)
Plate thickness	
Numerical/Software	
Mesh density	Element type
Solver	User's experience

There are currently three ways to assess the ultimate strength of ships and marine structures, namely experimental, numerical simulations and analytical modelling. The design of ships and marine structures can be performed by FEM. However, performing a nonlinear ultimate strength analysis considering material, geometric nonlinearities and initial imperfections is still expensive and time-consuming. Analytical methods are still being developed to make the structural analysis simplified and easier to use.

The adequacy of safety for structural components and overall structure are of obvious importance. Component failure is the starting point and the overall safety can be based on the reserve strength beyond the first nominal component failure. The ultimate strengths of components and connections are also important. These are discussed in Section 7.

2.3 Design for ultimate strength

2.3.1 General

Design for ultimate strength is concerned with the determination of safety levels when a loaded structure reaches a point beyond its capacity. For steel structures, the aspects often checked in

the ultimate limit state are resistance (yielding, buckling and/or the creation of plastic hinges) and stability (loss of equilibrium).

Variability of actions is only one aspect of the uncertainties surrounding design and it is addressed by applying appropriate partial safety factors. Variations in strength properties in the nonlinear region should be captured in the plasticity model with previous decisions on the finite element solver, mesh density, element type and boundary conditions.

Likewise, variations in initial geometric imperfections and deviations from nominal values are accounted for in the partial safety factors. Due consideration should be given in understanding structural behaviour beyond ultimate strength as the omission of structural elements in modelling can affect the collapse mechanism, return erroneous plastic hinges and shed loads unrealistically.

Determining safety in ultimate limit state design allows for decision-making in design by studying output such as load-carrying capacity often in the form of bending moment vs curvature.

2.3.2 International association of classification societies (IACS)

The Common Structural Rules (CSR) for Bulk Carriers and Oil Tankers entered into force on 1st July 2017 and superseded the 2015 CSR for Bulk Carriers and Oil Tankers (IACS, 2017). The IACS rules are applicable to hull structures of single side skin bulk carriers having a length L greater than 90 m or above, and to hull structures of double hull oil tankers having a length L greater than 150 m or above.

Structural strength is to be determined against buckling and yielding, while ultimate strength calculations are to include hull girder capacity and ultimate strength of plates and attached stiffeners. The requirements of the ultimate strength of the hull girder are based on the partial safety factor method.

The characteristic buckling strength is to be taken as the most unfavourable/critical buckling failure mode with distinct buckling criteria for stiffened panels, plates, stiffeners, vertically corrugated transverse and longitudinal bulkheads, horizontally corrugated longitudinal bulkheads, struts, pillars and cross ties. The allowable buckling utilisation factor for different structural members is given in CSR Chapter 8 Section 1, while specific geometric requirements of structural elements are to comply with the applicable slenderness and proportion requirements of CSR Chapter 8 Section 2.

The assessment of buckling capacity of plates and stiffened panels is carried out using analytical or FE methods taking into account different boundary conditions as discussed in CSR Chapter 8 Section 5. A more detailed description of assessing the hull girder ultimate capacity is given in CSR Appendix 2.

2.4 Design for limit states

In limit state design the structure is assessed against a predefined condition where a component, or the entire structure, fails to perform its intended function.

There are four types of limit states:

- Ultimate limit state (ULS); it is a limiting condition preventing a structure from attaining the maximum load carrying capacity with subsequent failure to support further load, excessive yielding, buckling, and loss of structural stability and/or excessive deformation.
- Fatigue limit state (FLS); it is a limiting condition where a structure undergoes cyclic loading with subsequent fracture.

- Serviceability limit state (SLS); it is a limiting condition affecting the ability of a structure to preserve its appearance, maintainability, durability or the comfort of its users under normal usage.
- Accidental limit state (ALS); it is a limiting condition that excessive structural damage takes place as a consequence of accidental loads (e.g. collision, grounding, explosion and fire).

Structures should be designed to avoid falling into the above limit states. Limit states are expressed by mathematical forms while the structural design is assessed for safety margins against a limit state.

Ships and offshore structures have been traditionally designed with the working stress design (WSD) method. Although the traditional safety factors in WSD have performed adequately, the actual safety levels of WSD-designed structures were never known. This led to the adoption of limit state design (LSD), or load resistance factor design (LRFD) method, which has now taken over as the primary design philosophy.

The main difference lies in the logic behind the two methods rather than the design process itself. The most apparent difference is that WSD uses a single safety factor without making a load distinction and accounting for load and strength variations at the same time. Designers compute the stresses in a member and need to ensure that the stress levels remain below a limiting value with a given safety factor. In WSD the stresses are nearly always computed with simplifications and assumptions, such as a linear elastic analysis. The WSD method neglects that a structure is seldom linear elastic and often yields.

The LRFD recognizes that there is load variation on a structural member, and in the behaviour of the member itself. The LRFD method deals with loads and structural capacity exclusively while utilising the concept of limit states, making a marked distinction between strength and serviceability. In addition, the LRFD attempts to deal with the variation in resistance due to material properties, geometry, member size and load variation. A set of partial safety factors is used for specific ultimate strength assessments, e.g. hull girder, bringing the LRFD method closer to a reliability-based design approach.

2.5 Safety factors for ultimate strength

Ultimate strength analysis is based on partial safety factors, addressing a limit state (See Section 2.4). It is important to note, that the partial safety factors can be different depending on refinement of calculation methodologies. This means that any safety factor specified by regulatory bodies are only valid as long as the recommended methodology within a design code or/rules is used.

As an example, the design condition for the ultimate or accidental limit state is expressed as

$$G = C_d - \sum D_{di} \geq 0 \tag{1}$$

where, G is the performance function, C_d and D_{di} are the design values of capacity (strength) and *i*-th load component, respectively.

In general terms, safety factors are applied to characteristic values of the structure's capacity and loading as follows:

$$\frac{C_k}{\gamma_C} - \sum \gamma_{Di} D_{ki} \geq 0 \tag{2}$$

where C_k and D_{ki} are the characteristic value of strength and *i*-th load component, respectively.

γ_C is a partial safety factor associated with uncertainties related to structural capacity, and takes into account uncertainties in the material properties; uncertainties in the structural

geometry, scantlings, and imperfections; uncertainties due to damage or age-related degradation of the structure; and uncertainties in the assessment method(s) used to determine C_k. Each type of uncertainty may be assessed separate partial safety factor, in which case γ_C is the product of two or more partial safety factors. γ_{Di} is the partial safety factor associated with the uncertainties in the loading, which for structures in a marine environment may be considerable.

The probabilistic approach is more rigorous when considering the effect of uncertainties. Based on this function and using the First-Order Reliability Method (FORM), a reliability index β can be defined. The reliability index is calculated as:

$$\beta = \frac{\mu_C - \mu_D}{\sqrt{\sigma_C^2 + \sigma_D^2}} \tag{3}$$

where, μ_C and μ_D are the mean value of strength and load, respectively, and σ_C and σ_D are the corresponding standard deviations. The reliability index β is a probabilistic attempt to assess the ultimate and accidental limit state instead of the partial safety factor approach. The reliability index must be greater than the target value to ensure safety. More details about the probabilistic approach are discussed in Section 4.

The partial safety factors values adopted in Classification recommended practices are determined by the probabilistic approach.

The IACS CSR Rules put forward use a partial safety factor to address modelling, geometrical and strength-prediction uncertainties in an ultimate strength assessment (Chapter 5 Section 2 in the CSR). Although it is recognized that the safety factors vary for different types of structures, the work of ISSC 2015 (ISSC, 2015) showed that the range of the ultimate strength of a box girder fell within the recommended IACS CSR partial safety factor.

Individual Classifications societies such ABS, BV, ClassNK, DNV GL, ISO and LR have also developed their own expressions of safety factors for the corresponding limit states. The partial safety factors are discussed in Section 5 and 6 for ship and marine structures, respectively.

3. ASSESSMENT OF ULTIMATE STRENGTH

3.1 Introduction

Assessment methods for ultimate strength aim to determine the maximum capacity that can be sustained by a structural component or system, taking into account the physical effects associated with its failure. This is a separate determination from the loading on a structure, which is mainly a function of the environment it operates in.

For marine structures, ultimate capacity assessment generally involves a realistic representation, with analytical, numerical or experimental models, of material constitutive relations and failure processes, and fabrication related effects; structural geometry, including imperfections; deflection and buckling phenomena; and boundary conditions. The methods to be used depend on the type of the structural component or system, its material, and its load regime.

The main focus of this section is on methods for determining ultimate strength of hull structures, with a discussion of topside structures of offshore platforms in Section 3.2.

3.2 Topside structures

The ultimate limit strength assessment of topside structures is studied separately from the global model of the facility for a series of load combinations corresponding to permanent, live (variable), environmental and deformation loads with the corresponding action factors following the LRFD methodology. It is usually two load combinations that need to be studied with earthquake acceleration being considered.

The topside model usually includes primary members with equipment loads and footprints accounted for. Structural members are being assessed for yield, stability and deflection against the relevant design requirements in the form of unity checks that help to size the members. As the numerical model at this stage does not include any structural details, usually in the form of specific joints, pedestals, conical transitions, stiffened panels, bulkheads and/or decks, any joints that happen to fail the code check are further studied in isolation with secondary and tertiary elements included in the model.

Detailed models are studied with advanced numerical codes taking into consideration elastic-plastic material properties to ensure ductility and hardening effects are accurately captured. Secondary structural elements and structural details known to affect the failure patterns and global model behaviour such as buckling and interaction with adjacent elements are also modelled. An example of the degree of the necessary structural detail is found in Section 9 of this work.

3.3 Analytical methods

With the development of numerical methods and the steady advances in model fidelity and realism, analytical methods are still of considerable value at the early design stage for rapid evaluation of trial designs; during an emergency response for rapid assessment of the damage effects; and for Monte Carlo simulation as in reliability analysis.

3.3.1 Closed form methods

Caldwell (Caldwell, 1965) first determined the longitudinal bending strength using a simplified geometry of the hull cross section and an assumed stress distribution at collapse taking into account plasticity and buckling.

Related closed form methods based on assumed stressed distributions were proposed by Mansour and Faulkner (1973), Faulkner and Sadden (1979), Frieze and Lin (1991), Paik and Mansour (1995), Paik et al. (2001), Qi and Ciu (2006) and Paik et al. (2013). These methods differ both in the assumed stress state and in the form used to express the ultimate strength.

The Common Structural Rules (CSR) for Double Hull Oil Tankers (IACS, 2006b) contained a "single step" method for determining the ultimate strength of a hull girder in sagging which expressed the ultimate bending strength M_U in the form

$$M_U = Z_{red}\sigma_{yd} \tag{4}$$

where σ_{yd} is the yield stress and Z_{red} is the reduced section modulus of the deck. The latter was to be determined using the "effective net area after buckling of the stiffened deck panel". However, this method was not included when the CSRs for oil tankers and bulk carriers were combined into the Harmonized Common Structural Rules (IACS 2014).

The main advantages of the closed-form methods are their relative simplicity and ease of calculation. Thus specialized software is generally not needed to use them, and any designer or analyst can directly implement these methods using a spreadsheet environment. The ALPS/US-HULL program includes the closed form methods developed by Paik et al (2001).

A significant limitation of these methods is that ultimate capacity of the hull is considered to occur when each structural element of the cross section reaches its peak capacity. This assumption neglects that ultimate failure is a progressive event, with some structural elements collapsing prematurely, and that in general the ultimate capacity occurs with some structural elements in a post-collapse state.

3.3.2 Progressive collapse methods

The next major development in ultimate strength assessment after Caldwell's work was due to Smith (1977), who proposed a method in which a hull section is subdivided into a number of

small, independently acting units, most of which are plate-beam combinations. Curvature is applied to the section, and the strain experienced by each individual unit is then determined by assuming that plane sections remain plane, i.e., that strain increases linearly with distance from the neutral axis. Based on this strain, the average stress in each unit is estimated taking into account whether it is in tension or compression, the yield strength of the material, and the buckling behaviour of the plating and stiffeners in compression. Summing the contributions over the section determines the bending moment. The curvature is incremented and calculations repeated, taking into account movement of the neutral axis as the response of individual units departs from linearity. The end result is a nonlinear moment-curvature relationship, the peak value of which defines the ultimate strength of the hull. For a recent review of the Smith method see Yao and Fujikubo (2016).

Smith originally developed the method for assessing the vertical bending strength, but the method was later extended to biaxial bending (Smith and Dow, 1986). In the original implementation in the Royal Navy's NS94 program, the average stress-strain response of structural elements was determined using nonlinear finite element analysis using equivalent beam models of structural units. Later versions of NS94 used libraries of pre-calculated load-shortening curves to rapidly determining the average stress-strain relationships of plates and stiffened plate units (Smith et al, 1992).

Adamchak (1982) developed a similar incremental method in which the average stress-strain relationship for longitudinally stiffened panels in compression is determined analytically, taking into consideration yielding, Euler-column buckling, stiffener tripping and lateral loading. This approach is implemented in the US Navy program ULTSTR.

Yao and Nikilov (1991) proposed an incremental approach similar to the Smith method in which an analytical method is used to determine the average stress-strain relationships of plates and stiffened panels, and developed the computer program HULLST based on this approach (Yao and Nikilov, 1992). Gordo and Guedes Soares (1993) proposed a similar approach, using analytical formulas for the average stress-strain relationships that considered yielding and the important buckling modes for stiffened plate columns. These were incorporated into a progressive collapse method for biaxial bending, and implemented in a computer code HULLCOLL (Gordo et al, 1996). A similar approach was adopted for the incremental-iterative method for hull girder ultimate strength in the CSR (IACS, 2006a, 2006b) and the HCSR (IACS, 2014). Choung et al (2014) describe an extension of the Smith method implemented in the program UMADS, and which takes into account the rotation of the neutral axis for asymmetric sections. Downes et al (2017) proposed improving the accuracy of the average stress-strain relationships of stiffened panels through nonlinear FEA of simple box girder models. They show that when the average stress-strain relationships are derived in this way progressive collapse predictions with the UMADS program compare well with nonlinear FEA. Computer codes for hull girder ultimate strength are summarized in Table 3.

The calculation of load-shortening curves using nonlinear FEA was reported by Smith (2010) and Choung et al (2012). Tayyar et al (2014) proposed calculating the average stress-strain relationships for stiffened panels in compression using a numerical method based on kinematic displacement theory, as an alternative to FEA.

The Smith incremental method has two principal limitations. One is that it considers pure longitudinal bending of a hull girder. When longitudinal bending moments occur in combination with shear and torsion loads, the plane sections remain plane assumption of Smith's method is not strictly valid. Container carriers may exhibit significant combined torsional and longitudinal bending response, and Tanaka et al (2015) developed an extension to the Smith method that first calculates the shear stress distribution in a cross section, and then uses this to modify the average stress-strain relationships of the plates and stiffeners for the longitudinal ultimate strength calculation. Kitarovic and Zanic (2014) proposed an alternative incremental

progressive-collapse method considering the hull girder as a thin-walled beam section subject to longitudinal bending and transverse shear. Their formulation considers warping of the deformed cross section due to a varying shear distribution is included in addition to longitudinal bending.

A second limitation of the Smith method is that it assumes interframe modes of collapse for structure in compression. This limits the application of the method to monohull ships constructed from mild and high-strength steel. Lightweight hulls constructed from very high-tensile steels or aluminium may not collapse in an interframe mode. Benson et al (2013a) developed a compartment level progressive collapse method in which grillage collapse modes of failure are included in a Smith method analysis framework.

Vessels can experience large local bottom deflections in empty cargo holds when situated between fully loaded holds. This bottom deflection associate with this alternate-hold loading condition can have a significant effect on the hogging strength of a vessel (Amlashi and Moan, 2008). Amlashi and Moan (2009) considered the extension of the Smith method to include double bottom bending through modification of the strains in the double bottom structure. This requires determining the curvature of the double bottom under inner and outer lateral pressure loads, a calculation that requires calibration with FEA. They also proposed a linear interaction relationship involving the ultimate strengths of hull girder and the double bottom which also has to be calibrated with FEA.

Fujikubo and Tatsumi (2016) also proposed an extension to the Smith method to account for deformation of a double bottom bending. In this approach, the structural elements making up the deck and sides are combined together in a single thin-walled beam finite element extending the length of a hold and incorporating the average stress-strain relationships used in Smith method. The double bottom of the hold is modelled as a grillage of beam elements comprising the longitudinal and transverse structure of the outer and inner bottom. The average stress-strain relationships for the beam elements in the double bottom are modified to account for the effect of transverse thrust due to the lateral pressure load.

The above limitations means the Smith method may not be suitable for unconventional hull forms such as multihulls, where transverse bending and torsional strength are important factors in the design (Pei et al, 2016).

3.3.3 Gaps

Analytical developments have primarily been focused on improving the accuracy of ultimate strength under longitudinal bending, in which the bending moment is applied by itself or in combination with other loads. This is understandable since it is a fundamental limit state required by the HCR and other classification society rules. Some Classification society rules also have requirements for shear strength assessment (DNV-GL, Lloyd's Naval Ship Rules, ref. Section 5.2). However, no comparable to the Smith method exists for progressive collapse assessment of shear strength. Numerical methods such as nonlinear FEM, ISUM or IFSEM need to be used.

Extension of progressive failure methods to more general purpose assessment of global hull girder strength (i.e., longitudinal bending, transverse shear strength, torsional strength) would seem to be within reach with the methods and tools now available. For example, the approach developed Tanaka et al (2015) for assessing the effect of torsion on longitudinal bending could be extended to predict ultimate torsional strength taking into account limit states of individual plate panels in shear. Progressive failure tools specialized for multihulls, aluminium and composite structures are also needed.

3.3.4 Residual strength of damaged hulls

Ship hull girders can experience damage ranging from normal in-service effects to large scale deformation and rupture. Typical damage events are those that occur under normal operational loads and include corrosion pitting, general corrosion, ductile fatigue cracking, and impact deformations. Atypical damage occurs as a result of exceptional or unexpected events and includes brittle cracking, deformations due to local buckling in extreme seas, deformation due to fire, gross deformation and rupture due to collision, grounding or explosion, and ballistic penetration.

Although design and maintenance improvements have greatly mitigated the risks posed by damage, the risk of a hull girder failure cannot be altogether eliminated and will increase with the accumulation of unrepaired damage, e.g. in aging vessels. A contributing factor in the hull girder failure of MOL COMFORT in 2013 is believed to have been the presence of pre-existing buckling damage in the outer bottom (ClassNK, 2014), although the true causes are still in dispute. Understanding the impact of damage on the strength margin of a vessel is essentially to avoiding catastrophes. With atypical damage event, it may not be possible to prevent loss of the ship, but residual strength design can help preserve the life of the crew long enough to permit safe evacuation and to limit loss of cargo and damage to the ocean and coastal environments.

Analytical approaches for assessing the residual ultimate strength of damaged hulls are generally of two types: (1) application of closed form and progressive collapse methods to damaged hull sections; and (2) application of numerical methods to damage cases to determine empirical relationships governing the residual strength. These are discussed in the following.

3.3.5 Analytical assessment of damage

Application of progressive collapse methods such as the Smith method to determine residual strength of damaged hulls was first reported by Smith and Dow (1981), who assessed the effect of interframe indentation damage on the bending strength of a naval vessel. In their approach, individual stiffened panels were statically deformed to represent the damaged structure. The average stress-strain relationships in tension and compression were then recalculated taking into account the deformation and residual stresses in the panels, and these were subsequently incorporated into the progressive collapse calculation.

In a similar manner, the effects of corrosion damage and fatigue cracks may be evaluated within the framework of existing progressive collapse tools. In general, these types of damage reduce the cross sectional area of the damaged structural elements, which reduces their load carrying capacity in tension and compression; and they affect the buckling behaviour of the structure either by increasing the slenderness or by introducing new sources of instability.

For application to gross damage due to collisions or grounding, the standard approach is removal of the damaged structure, neglecting the residual strength of deformed structure. This approach will be conservative in most cases; however, the removal of the damaged structure may leave long unsupported spans that can collapse in an overall mode that cannot be predicted by the simplified method.

Underwood et al (2016) predicted the ultimate strength of damaged steel box girders using a compartment-level assessment method in which intact structure is modelled with load-shortening curves, similar to Smith's method, and in which the load-shortening behaviour of damaged structure is modelled with a response surface method (kriging), derived from non-linear FEA of damaged grillage panels, as a means of introducing overall collapse modes in a simplified assessment framework.

The structural asymmetry introduced by large areas of gross damage may becomes important. Under vertical bending load the neutral axis rotates away from the horizontal. The biaxial

bending problem was previously considered by Smith and Dow (1986) and Smith and Pegg (2003) in terms of coupling of vertical and horizontal bending stiffness. More recently, Choung et al (2012) developed a version of the Smith method in which the position and rotation angle of the neutral axis plane is calculated and updated as bending moment loads are applied. Choung et al (2014) applied this method to crude carriers with collision and grounding damage modelled with element removal. Muis Alie et al (2012) derived a generalized expression for the incremental moment-curvature relation of an asymmetric cross section under biaxial bending. Fujikubo et al (2012) extended this work by deriving simplified formulae for the residual strength in terms of elastic properties of the section and the strength of a critical member. A similar concept has been pursued by Tekgoz et al (2015) in the context of asymmetric bending of an intact section to illustrate the effect of neglecting neutral axis rotation in asymmetric bending of an intact hull.

The closed form assessment method by Qi and Ciu (2006), which is based on analytical expressions for stiffened panels by Ciu et al (2000) was applied to the analysis of a bulk carrier with grounding damage. Recently, Parunov et al (2017) employed the modified Paik-Mansour analytical method within a reliability analysis of a double hull tanker with collision damage.

3.3.6 Development of empirical formulas for residual strength

Another approach to residual strength assessment of hulls has the application of nonlinear FEM or ISFEM to a wide range of damage assessments for ships of a similar design, and from the results to generate empirical relationships to describe the effect of the damage on the residual strength for use in emergency response scenarios. Paik et al (2012) developed empirical formulas for residual strength of double hull oil tankers with grounding damage to the double bottom. Their formula was a function of a grounding damage index (GDI), which is determined based on the effective cross sectional areas of the inner and outer bottom with and without damage. The empirical relationship is fit to numerical results on R-D diagram, plotting residual strength vs GDI. Kim et al (2013) used a similar approach to develop R-D diagrams and empirical relations for four container ship designs with grounding damage, and was the method was extended to include long term degradation due to corrosion by Kim et al (2014).

Youssef et al (2016) considered collision damage to oil tankers probabilistically, defining damage location and extent with random variables and probability distributions based on historical databases of collision events and finite element simulation of collision damage. Faisal et al (2017) used a similar methodology to performed rapid residual strength analyses of four oil tanker designs with collision damage, and compared the results with the IMO requirement for 90% remaining capacity after collision. Youssef et al (2017) used the same approach to develop empirical relations between the RSI and the collision damage index, defined as the ratio of the damaged and intact second moments of area, for four types of tanker.

3.3.7 Benchmark studies and gaps

Some significant benchmark studies have previously appeared that compared the performance of various simplified methods. ISSC (2000) presented benchmark analyses comparing the ultimate strengths in hogging and sagging of five different ship types. Several different implementations of the Smith method were compared, along with the Paik-Mansour simplified method and the ISUM method. The best agreement was obtained for a bulk carrier and a single hull tanker design with coefficients of variance (COV) of 5% or less in hogging and sagging. The worst agreements were for a container ship and a double hull tanker, with COVs of 12.3% and 13.8% in sagging.

Guedes Soares et al (2008) compared five different Smith method programs in the analysis of a fast ferry design. The maximum variations in the ultimate strength predictions of the intact vessel were about 8% for hogging and about 10% for sagging in comparison to the mean re-

sult. Four Smith method analyses were compared for the same structure with collision damage. In this case, the maximum variation among the methods was approximately 3% for the hogging strength and 10% for the sagging strength when residual stresses are taken into account. In comparison to nonlinear FE predictions, however, the average of the Smith method predictions was 0.6% larger in sagging, but 25% smaller in hogging.

Paik and Mansour (1995) compared the performance of 8 simplified methods for a series of box girder structures and tanker designs. In comparison to experimental results, the methods were usually within 10%, but errors up to 20% were common. Khedmati and Rashedi (2014) also compared 8 simplified methods for a series of box girder structures and a product carrier. For simple, single hull box girders most of the methods were within 10% of the experimental values, while for box girders with a double bottom, most greatly underpredicted the strength in hogging. For the product carrier, it was found that in comparison to nonlinear FE predictions all of the methods overestimated the ultimate strength in hogging and sagging. Predictions of the hogging strength were somewhat better than in sagging, but differences of 10 to 20% were normal. They concluded that Paik-Mansour, Faulkner-Sadden and the Frieze-Lin methods were more successful than the others tested.

3.4 Numerical methods

Marine and offshore structures are not only designed for long-term performance and reliability but also for safety levels aligned with industry standards. Powerful analysis tools are used for assessing ultimate strength, with the most popular methods employing the FE method, while others implement coupled solutions with CFD codes.

Despite the drawbacks that remain in these methods, designers can gain a better understanding of the operational safety margins and an increased confidence in operational decisions for contingency strategies.

Some of the most popular numerical codes employed for studying ultimate strength characteristics are presented in the following Tables. The benchmark study of this Committee employed a number of them as presented in Section 9.

Table 2 : Numerical Codes applicable to Ultimate Strength Analysis on Panel Level

Numerical Code	Organisation	Component Applicability
ALPS/ULSAP	Pusan National University	Stiffened/Unstiffened Panel
BV Adv. Buckling	Bureau Veritas	Stiffened Panel
DNV/PULS	DNV-GL	Stiffened/Unstiffened Panel
ANSYS	Ansys Inc.	Stiffened/Unstiffened Panel
ABAQUS	Abaqus Inc	Stiffened/Unstiffened Panel
MSC/MARC	MSC	Stiffened/Unstiffened Panel

Table 3: Numerical Codes applicable to Ultimate Strength Analysis on Hull Girder Level

Numerical Code	Organisation	Method
ALPS/ HULL	Pusan National University	ISFEM
ALPS/US-HULL	Pusan National University Paik et al. (2011)	Modified P-M Method
CSR	Common Structural Rules	
ANSYS	Ansys Inc.	FEM
ABAQUS	Abaqus Inc	FEM
LS-DYNA	Livermore Software Technology Corp.	FEM

NS94	UK Ministry of Defence (Smith and Dow, 1986)	Smith method
ULTSTR	US Navy (Adamchak, 1982)	Smith method
HULLST	Hiroshima University, Japan (Yao & Nikolov, 1992)	Smith method
HULLCOLL	Technical University of Lisbon (Gordo et al 1996)	Smith method
UMADS	Inha Univesity, Korea (Choung et al, 2014)	Smith method
ULTMAT	Canadian Dept of National Defence (Smith and Pegg, 2003)	Smith method
LRPASS/RESULT	Lloyd's Register (Rutherford and Caldwell, 1990)	Smith method
MARS2000	Bureau Veritas	Smith method
NAUTICUS/POSEIDEN	DNV-GL	Smith method
ProColl	Newcastle University (MAESTRO, 2017)	Compartment level analysis

Table 4: Numerical Codes applicable to Ultimate Strength Analysis on Beam/Column (Jacket & Topside Level)

Numerical Code	**Organisation**
NASTRAN	MSC Software
MSC Marc	MSC Software
LS-DYNA	LSTC
ANSYS	Ansys Inc.
ABAQUS	Abaqus Inc
USFOS	USFOS Reality Engineering

3.4.1 Idealised structural unit method (ISUM)

Although not a new method, ISUM models can yield reliable results for stiffened panels without expending enormous computational effort as in the FEM. The ISUM makes use of special purpose finite elements in which geometric and material nonlinearities within the element are represented by a limited number of degrees of freedom at the boundaries. Complex nonlinear deformations and ultimate limit states in plate and stiffened panels can therefore be modelled with large structural units that make up the structure. Despite that this method is inappropriate with regards to stiffener properties, ISUM has been used extensively for ultimate strength and accidental limit state design in the past with the necessary care. Its main advantage over other nonlinear FEM is that complex structures can be modelled with orders of magnitude fewer degrees of freedom.

A summary of pertinent ISUM theory, its application to nonlinear analysis and the concept for development of various ISUM units needed to analyse nonlinear behaviour of steel plated structures are described by Paik & Thayamballi (2003). For recent reviews of ISUM see Rashed (2016) and Oksina et al (2016).

Numerous ISUM element types have been developed over time; for the purposes of ultimate limit strength analysis the most popular ones are the deep girder unit (Ueda & Rashed, 1984), the tubular beam-column model (Ueda et al. 1983), the I section beam-column unit (Paik, 1995), the rectangular plate unit (Fujikubo et al., 2000) and the stiffened panel model (Paik, 1995). Other developments include plate elements that consider lateral pressure effects (Kaeding et al, 2005) and a shear plate element (Pei et al, 2010). Pei et al (2012) developed a hybrid ISUM/FEM modelling approach for hull structures in which ISUM is used for the

nonlinear failing part of the hull, and elastic FE is used for the rest of the structure. Pei et al (2015) used the same approach to simulate hull girder collapse under extreme wave loading.

3.4.2 Nonlinear FE method

The first application of the nonlinear FE method to hull girder ultimate strength was by Chen et al (1983). But in the years that followed, due to model size limitations imposed by software and hardware, the nonlinear FE method was mainly applied to limit state analysis of components. Hull girder strength developments were focused on simplified methods, and specialized numerical tools like ISUM and ISFEM.

Nonlinear FE studies of hull girder strength began regularly appearing in the literature ten years ago. Amlashi and Moan (2008) presented a nonlinear FE analysis of a bulk carrier in an alternate hold loading condition, taking into consideration the effect of lateral pressure on the double bottom in the assessment of ultimate vertical bending strength. This study identified many of the key modelling issues to be faced with nonlinear FE of hull girder strength in general. For a review of recent nonlinear FE studies of hull girder ultimate strength, see Section 5.3 and 5.4.

Based on a review of published studies, best practices for nonlinear FE modelling of steel mono-hulls are summarized below.

- The longitudinal extent of the model may range from one frame spacing to the entire length of the ship (Kim et al 2013). The longitudinal extent selected should be appropriate to the loading and response effects being modelled. For pure bending loads on an intact structure, a one frame-bay model may be sufficient; when considering combined lateral pressure and bending moment loading, a minimum model length of ½ + 1 + ½ holds or compartments is used (Amlashi and Moan, 2008); when considering torsional strength, at least one complete hold or compartment should be modelled so as to include the restraining effect of the transverse bulkheads. Full length models may be used for more realistic modelling of at-sea conditions or damage events (Yamada, 2014).
- For an intact structure under vertical bending, and with or without lateral pressure, a symmetrical model is generally adequate; where the structure is asymmetrically loaded or has asymmetric damage, then the full width must be modelled;
- Nonlinear plate/shell and beam element types should be used; first-order elements are normally the easiest to generate meshes for, but higher order elements may also be used;
- Element formulations must allow for geometric and material nonlinearity; large displacement and/or rotation formulations are necessary; large strain formulations are not strictly required, but may be used.
- An implicit solver is normally used, in which the loading and response are treated as quasi-static processes. However, explicit solvers, where the loading and response are treated as dynamic processes, have been used with some success for hull girder strength (ISSC 2015).
- The most commonly cited software tools are ANSYS, ABAQUS, MARC (implicit solvers) and LS-DYNA (implicit and explicit solver)
- A Newton-Raphson nonlinear solution algorithm is normally used with an implicit solver. The solution may be displacement-controlled, load-controlled, or use an arc-length method.

- With an implicit solver, it will be necessary to select an initial step size and convergence tolerance. Too large a tolerance will lead to inaccurate solutions; too small a step size may cause convergence difficulties.
- With an explicit solver, a time step size must be selected that is small enough to ensure convergence. Normally, this is a function of the size of smallest element in the model, and the material properties.
- Selective refinement of the model is recommended to keep the model size under control, with the smallest element size used in regions where buckling collapse is expected. Separate models for hogging and sagging are recommended so that refinement can be further limited to the compression failure zone.
- In refined regions, all longitudinals and transverses should be modelled with shell elements. Assuming first-order elements are used, at least 5 elements through the web depth, and 2 across the width of the flange, and at least 5 elements in the plating spanning the longitudinals (Amlashi and Moan, 2008). Fewer can be used with higher-order elements. It is advisable to conduct a mesh convergence study before finalizing element sizes.
- In the tension failure zone, and in other areas of the mesh outside of the compression failure zone, it is permissible to use beam elements for longitudinals;
- To speed the computations, it may be advantageous to activate nonlinearities only in elements where buckling collapse and/or yielding is expected to occur; linear elements can be used otherwise (Amlashi and Moan, 2008);
- A bilinear material formulation is normally acceptable for inelastic collapse calculations. For monotonic loading processes, either isotropic or kinematic hardening law may be used. If loading is reversing, then a kinematic hardening law should be used.
- Bending loads can be applied as a rotation or as a bending moment; which is best largely depends on the capabilities of the solver and the solution method to be employed. To efficiently distribute bending load across a section, it is advisable to tie all nodes in an end section of the model to a central located master node through rigid links or multipoint constraints, and apply, the bending load through the master node.
- Possible loading/constraint configurations are: one end fixed, the opposite end loaded; or both ends loaded and the midsection restrained. It is important not to over-restrain the model in the longitudinal direction as this could allow a non-zero net force to develop in the longitudinal direction.
- Hull girder strength is imperfection sensitive, so an efficient means of applying plating and stiffened shape imperfections is needed. Commons methods for doing this are (1) applying pressure loads to create deformations similar to imperfections; (2) compute linear buckling modes with appropriate plate and stiffener deformation and update the node locations; (3) use a computer program or macro to directly modify node locations.
- Weld-induced residual stresses may be important. Two methods for including these in a model are (1) directly specifying the initial stresses (using a separate computer routine or macro); or (2) modifying the stress-strain constitutive material properties to represent the net effect of the residual stresses under longitudinal bending.

Incorporating gross damage effects realistically in an ultimate strength calculation is still a developing field, and best practices are yet to be agreed upon. Benson et al (2013b) and Yamada (2014) used the LS-DYNA explicit solver in a two-step process: (1) high fidelity simulation of severe the impact event followed by (2) bending load applied to the damaged model until ultimate failure. Given the considerable progress in high-fidelity simulation of

damage events (Amdahl et al, 2013), this approach could be successful in capturing realistic extents of damage as well as residual stresses left by the damage process. At the other end of the spectrum is element removal, which has already been used extensively to represent the loss of structural capability (Petricic, 2015, Amante et al, 2016, and Muis Alie et al, 2016). A better means of representing the loss of capability that captures the effects of rupture, large deformations, and changes to material strength due to residual stresses would be beneficial.

A common pitfall with implicit solvers is their inability to find a converged solution as non-linearities develop due to singularities in the tangent stiffness matrix (ISSC 2015). Convergence difficulties are generally worse for hogging loads on hulls with double bottoms, due to the complexity of the structure arrangement and deformations. Possible solutions to the non-convergence problem are

- Reducing the load-step increment and restarting the computation at a previously converged solution
- Re-running the analysis with a larger or smaller convergence tolerance
- Re-running the analysis with different solution method: displacement control, force controlled or arc-length
- Reducing the longitudinal extent of the model or introducing symmetry
- Re-running the analysis using an explicit solver

A further issue to be faced is the partial safety factor to be used with nonlinear FE predictions of ultimate strength. The partial safety factors published in the HCSR and other classification society rules (see Section 5.2) are calibrated to the Smith method. Calibration of nonlinear FE predictions with carefully performed experiments is needed to establish an appropriate safety factor.

3.5 Experimental methods

The first ultimate strength assessments of ship hulls were done by experiment. The elastic bending test performed on HMS Wolf in 1903/04 and subsequent analysis work revealed the importance of plating effectiveness, shear lag and post-buckling effects when determining the bending rigidity of a hull (Lehmann, 2014).

Collapse of ship hulls under extreme loads was first investigated experimentally with the sagging and hogging tests performed on the US Navy destroyers Preston and Bruce in 1930/31 (Kell, 1931, Kell, 1940). A number of full-scale collapse tests were performed during World War II (Vasta, 1958); and the hogging collapse test on the Royal Navy destroyer Albuera in 1949/50 was the last full scale test of this kind to be performed (Lang and Warren, 1952).

Since then, experimental efforts have focused on reduced-scale testing of box girders and model ship hulls for the purposes of validating analytical and numerical methods. Notable early box girder tests were performed by Nishihara (1984) and Mansour et al (1990). Dow (1991) performed an ultimate bending strength test on a 1/3 scale model of a Leander class frigate.

More recently, Gordo and Guedes Soares (2009) experimentally test three longitudinally stiffened box girders fabricated from high tensile steel, while Saad-Eldeen et al (2011) tested a severely corroded steel box girder to failure. Gordo and Guedes Soares (2014) test three box girders fabricated from mild steel to determine the effect of varying transverse frame spacing. Lindemann et al (2016) tested two nominally identical longitudinally stiffened box girders to failure. In all of these experiments, a four point bending arrangement was used to load the specimens, and the quantities directly measured were the vertical applied load to the structure and the vertical deflection. These box girders are typically fabricated by welding, with either

external or internal longitudinal stiffeners and transverse frames. For ease of fabrication, flat bars are normally used for longitudinals.

Collapse behaviour in small-scale test specimens may not represent what occurs at full scale because the overall geometry, structural arrangement, scantlings and stiffener shapes are necessarily simplified in small scale models for cost and practicality reasons. Shi and Wang (2012) developed scaling relationships based on beam theory and from these designed a container ship model with a length scale factor of 1/20. Their model was tested to failure under four-point bending in a hogging condition. Garbatov et al (2015) performed dimensional analysis of the hull girder bending problem and determined that the requirements for first-order similarity can be met using box girder models subject to four-point bending, although complete similarity is not achievable. Calculations at model-scale and full-scale seem to confirm the scaling relationships.

Sun and Guedes Soares (2002) performed torsion tests on two identical box girder models with large deck openings in which pure torque was applied through two equal and opposite forces applied at diagonal corners of the models. Tanaka et al. (2015) experimentally tested three 1/13-scale models of three-hold sections of a 5250 TEU (post-Panamax) container carrier under combined vertical bending, vertical shear, and torsion. One end of each model was fixed to a rigid wall, and two point loads were applied to the other end. The ratios of the two point loads were varied to create different load combinations. Failure modes in torsion were identified as shear buckling of the side shell, buckling of the bilge corners, and rupture of the hatch corners.

Hull girder failure as a dynamic, multi-cycle event was modelled experimentally by Iijima et al. (2013), who used a 1/100 box section ship model comprised of two rigid sections joined by a sacrificial hinge mechanism to represent inelastic failure. The model was subject to whipping loads caused by impact from a dropped mass. Iijima et al (2015) used a similar apparatus subject to a “focused” wave train to represent extreme wave loading. They found that the development of plastic deformation in the hull resulted in a decrease in the still water bending moment, which reduces the rate of collapse under subsequent load cycles.

Dynamic hull girder failure was investigated by Zhang et al (2015) through an experiment that subjected a small-scale slender floating box girder structure to a close proximity underwater explosion directly below the midships position of the structure. The shock load from the explosion caused local damage to the bottom plating and subsequently plastic deformation and hinging of the hull girder.

4. PROBABILISTIC MODELS AND RELIABILITY ASSESSMENTS

4.1 Introduction

Whereas deterministic structural calculations use fixed geometrical and material parameters, probabilistic analysis is capable of assessing the effect of uncertainty on the ultimate strength. This is particularly relevant for buckling and collapse analysis which can be highly nonlinear and therefore sensitive to the structural parameters. Reliability assessment, which provides a framework for quantifying probabilistic analyses, is therefore particularly relevant to ultimate strength.

Reliability-based methods were first proposed by Mansour (Mansour, 1972) and Mansour and Faulkner (Mansour and Faulkner, 1972). Since then many studies have validated reliability-based ship structural design. It has been shown that reliability assessment is an efficient and practical method to evaluate uncertainty due to various parameters such as geometrical properties, material properties, operational conditions, corrosion wastage, fatigue cracking, wave loads and environment. Several studies on the reliability of the ultimate strength of the ship hull girder have been performed, aiming at developing and calibrating reliability-based design requirements or quantifying the reliability level between different designs.

Structural reliability assessment approaches have been used to develop partial safety factors in recent classification rules, including the Common Structural Rules. However, reliability-based methods are still not established in standard design practice.

This chapter provides a brief introduction to reliability theory, and then reviews recent literature related to reliability assessment of local structure, ship and offshore structures.

4.2 Reliability theory

Reliability is defined as the probability of a structure to perform a required function under stated conditions for a specified period of time. The parameters impacting the reliability of structures, like material property, have the characteristics of random variation. In general, mean value, standard deviation, coefficient of variation and distribution type is used to describe the numerical properties of random variation in the sense of probability. Through the analysis and calculation of probability problem, the level of reliability or safety of structure is often defined with reliability index or failure probability. The application of reliability assessment on ultimate strength of ship structure is carried out by methods of simulation methods like Monte Carlo simulation and probabilistic methods.

4.3 Reliability analyses

4.3.1 Local structures

Reliability analysis of local structures such as unstiffened plates, stiffened panels, shells, and tubular structures enables a deeper understanding of sensitivity to the localized geometrical and material uncertainties in a real structure. Of particular interest recently has been the effect of non-uniform corrosion and wastage. Silva et al. (Silva et al., 2013) proposed two new corroded plate surface models (hexahedron and hemisphere) to predict strength reduction with the effects of random non-uniform corrosion thickness distribution. Based on Monte Carlo simulation and regression analysis, empirical formulas accounting for different corrosion degradation surface shapes to predict ultimate strength reduction have been derived. These demonstrate a good accuracy and show that if the plate is exposed to a more aggressive environment, the random non-uniform hemisphere model becomes a more suitable modelling approach.

Further study by Silva et al. (Silva et al., 2014) proposed two possible formulations to define the ultimate strength failure events due to corrosion degradation. Based on the analysis of the ultimate strength of either the plate with distributed type of random non-uniform prismatic pits, or the plate with localized type of random non-uniform hemisphere pits, First Order Reliability Method, FORM, are applied to assess the structural reliability. Bounding techniques were also used to evaluate the joint failure modes for different correlations between the events.

Gaspar et al (2015a) established an adaptive response surface model is established as second-order polynomials by first-order reliability method. The thickness, material properties and amplitude of weld-induced initial distortions of plate elements are defined as basic random varieties produced by Latin hypercube sampling technique.

Although Monte Carlo simulation method is an effective approach to solve stochastic mechanics problems, the calculation is very large. In order to balance the relationship between computational cost and the accuracy of approximations, Kriging response surface method, based on the combination of first-order reliability method and Kriging interpolation models, a new method is proposed by Shi X T (2015). The advanced method can be applied in the structural reliability assessment with implicit limit state functions or nonlinear limit state functions.

4.3.2 Ship structures

With the increased operational time, age-related structural degradation such as corrosion wastage and fatigue cracks, if neglected, can lead to catastrophic failure. In an aggressive environment, a damaged hull suffering extreme waves, grounding or collision, may collapse if it

does not have adequate ultimate strength. At the time of construction, the uncertainties associated with material properties, geometrical properties and initial defect will also increase the failure probability of a structure. Hence, reliability assessment of ultimate strength of ships is necessary and it will provide useful and adequate information about the inspection planning, optimal operational routing or optimization design.

Gaspar et al (2016) investigate the reliability of a chemical tanker structure with a probabilistic representation of the wave-induced vertical bending moment. Based on direct calculation methods based on linear and nonlinear strip theory formulations and the most likely response wave method, model correction factors are used to account for the nonlinear effects on the vertical wave-induced bending moments. As a result, IACS-CSR formulation used to define the hull girder vertical wave induced bending moments underestimates the magnitude of the nonlinear effects. The hull girder reliability in sagging, predicted accurately by the direct calculations methods is significantly smaller.

As many extreme loads occur in short time periods under severe sea states, Shi et al (2016) assess the short-term ship structural reliability with an expression of stochastic process instead of extreme theory simplification. Still-water, wave- and slamming-induced loads are established by the random process theory. Up-crossing analysis and parallel system reliability method are used to evaluate the reliability. The influences of the damping ratio, slamming rate and correlation coefficient between wave and slamming loads, together with slamming rate have large influence on the failure probability. However, when the damping ratio is large, the correlation coefficient and the slamming rate could be neglected as they have little effect on the reliability.

Deng et al (2016) estimate the reliabilities of 33 ships navigating in Yangtze River by improved First Order and Second Moment method, FOSM, with consideration of the uncertainties of materials yield strength, still water bending moment and wave-induced bending moment. The partial safety factors for hull girder ultimate strength, still water bending moment and wave-induced bending moment are given as 1.35， 1.45 and 0.65. The function for probability assessment of ultimate strength is established.

4.3.3 Corrosion wastage

Campanile et al. (Campanile et al., 2014) investigated the influence of correlation among random variables in terms of time-dependent corrosion rate on the coefficient of variation of hull girder section modulus and ultimate bending moment capacity. As a result, with the uncorrelated variables leading to overestimate relevant lower bound values and the full correlation leading to underestimate them, it seems that full correlation among structural elements belonging to the same category of compartments is considered a suitable choice. Furthermore, the probability density distribution of hull girder section modulus and ultimate bending moment capacity de-fined as its lower bound values with 5% of exceedance are validated to follow normal distribution, not only under the uncorrelated variables derived by Lindeberg-Feller Central Limit Theorem, but also the full correlated variables derived by and Monte Carlo simulation method.

Xu (Xu, 2015) proposed a model correction factor method to assess the reliability, consider-ing the collapse of the midship cross section in sagging and hogging conditions as limit state. The MCFM as a special kind of response surface method requires less than 10 iterations and the application of the method relying on the adequacy of simplified structural model adopting the IACS-CSR incremental-iterative method.

Gaspar et al. (2015 b) analysed the ultimate strength of non-uniform corroded plate elements under uniaxial compression to evaluate the effects of the aspect ratio of plates. Based on the actual corrosion depth measurements in ship plate elements, the statistical properties of non-uniform reduction of thickness are described by a nonlinear time-dependent model. The random

field of corrosion is established by Monte Carlo simulation. The ultimate strength of plate elements is evaluated as a function of the aspect ratio, slenderness parameters and correlation length of the random field of corrosion. The ultimate compressive strength reduction due to the effect of the non-uniform corrosion patterns is particularly significant in the case of rectangular plate elements with aspect ratios typical of the longitudinal structures of the ship hull girder. The non-uniform corrosion patterns have shown to be particularly important in the case of rectangular plate elements with large aspect ratios, which is typically the case found in the longitudinal structures of the ship hull girder.

Garbatov, et al. (2016) studied the effect of sandblasting and sand paper cleaning on the mechanical properties of corroded steel specimens. An experimental assessment of tensile strength of small scale real steel corroded specimens is performed. Tension tests are performed to determine the mechanical properties of three groups of specimens, including non-maintained, sandblasted, and sandpaper cleaned, corroded specimen, allowing the estimation of the modulus of elasticity, yield stress, tensile strength, total uniform elongation and n and K strength parameters. Regression equations of the material properties are derived as a function of the degree of corrosion and maintenance actions. It is shown that these two methods of removing corrosion products from the surface of plate specimens have different effects on their mechanical properties and stress-strain relationships. Based on the achieved results a simplified stress-strain curve accounting for the corrosion degradation and maintenance actions is developed, which may be used for structural assessment of ageing marine structures.

4.3.4 Grounding or collision

Campanile et al. (Campanile et al., 2016) investigated time-variant bulk carrier structural reliability due to corrosion wastages in intact and damage conditions by FORM, SORM and Importance Sampling simulation, applying the corrosion wastage model and a modified incremental iterative method, to account for rotation of hull girder instantaneous neutral axis, in case of asymmetrical damage conditions. As a result, FORM underestimates time-variant annual failure probabilities up to 15%, compared to the SORM which is close to Importance Sampling simulation. Three different correlation models among corrosion wastages of structural members, no correlation, full correlation and full correlation among corrosion wastages of structural members belonging to the same category of compartments, are investigated in three different damage scenarios, as per CSR requirements, namely collision, asymmetrical and symmetrical groundings. In this aspect, maximum annual failure probabilities occur in intact condition under sagging and hogging, as annual failure probabilities in damage conditions are always lower than the intact ones, due to the low probability of occurrence of collision and grounding events, according to IACS casualty statistics.

Obisesan (Obisesan, 2016) proposes a novel stochastic framework by combining response surface methodologies, numerical simulations, simplified analytical computations and Advanced Structural Reliability Methods (ASRM) to assess the possibility of achieving the desired performance functions by ship structures. A plate resistance model is developed for hull damage assessment at the onset of failure. The reliability computations show that the probability of hull fracture increases as the hull deformation progresses, with maximum values occurring at the onset of outer hull fracture.

4.3.5 Operational conditions and sea state

Kwon and Frangopol (2012) proposed a system-based approach for estimating the time-variant reliability associated with the aging hull girder in the presence of potential failure modes under corrosion and fatigue. In this aspect, the time-variant random functions associated with corrosion and fatigue cracking can be formulated by using reduction factors in thickness and in length. In addition, effects of ship operational and sea environmental conditions on structural reliability in the intact hull condition were investigated. It was found that structural performance is more significantly affected by the sea states than the ship's operating speed. From a

comparison with previous research work addressing an intact VLCC, the presented estimates of the ultimate bending moments and reliability were found to be valid. Additionally, the safety margin of the VLCC was found to be insufficient for maintaining adequate safety levels for the required service life. Structural reliability analysis can be performed considering a single failure mode only. Under simultaneous presence of several failure modes, a series system model as well as a series-parallel system model can be used to estimate the system reliability.

4.3.6 Offshore structures

Chen, N. (Chen, N., 2016) studied four ship-shaped FPSOs to investigate the effects of the return period on the extreme value of vertical wave bending moment, environmental severity factor and corrosion effects on hull girder reliability. It is shown that the effects of the return period of extreme value of vertical wave bending moment on hull girder reliability decrease with the increase of the return period. FPSO hull girder reliability is very sensitive to the wave conditions of specific sites. It was also found that the corrosion effects on hull girder reliability are not as significant as the effects of the variation of the environmental severity factor. Further work is presented by Chen (Chen, 2017) where an assessment method for panel reliability of FPSOs is developed.

Horn and Jensen (2016) apply a combination of FORM and Monte Carlo simulation to a 10MW mono-pile offshore wind turbine. The innovation is the use of FORM within the extremes of the distribution to account for the outliers but without overly affecting the variance within the Monte Carlo simulations, as proposed by Jensen (2015). In order to complete the analyses in reasonable time, a simplified model is used within the iterations whilst a more detailed model is used to determine the final damage. This assumes that the design-point is the same for both models. However, there is only moderate difference between the simplified and detailed model, primarily because the aerodynamics are already greatly simplified in both models. The results demonstrate reduced uncertainty, but only if the FORM design-point is properly found.

5. SHIP SHAPED STRUCTURES

5.1 Introduction

The design of ships has seen considerable development in recent decades, with vessels of ever-increasing size and cargo carrying capacity entering service; with the widespread use of double hulls and double bottoms; and the proliferation of specialized vessel types (e.g., FPSOs, and LNG carriers).

The Harmonized Common Structural Rules (HCSR) for oil tankers and bulk carriers (IACS, 2017) (and its predecessor CSRs) require an ultimate hull girder strength check for all large vessels. The assessment methodology adopted in the HCSR for ultimate strength extends back several decades to the formative work of Caldwell (1965), Smith (1977) and others. It can be expected that similar requirements will be extended to all large vessels as design standards evolve and assessment methods mature. As this happens, ultimate strength requirements will likely need to be specialized according to the vessel type and construction material. An example of this is the recognition of the importance of load combination effects in certain large vessel types.

Accidents involving hull failure and their investigation play a major role in compelling changes to design rules, e.g., the inclusion of residual strength among the IMO's goal-based requirements, and recent changes to design rules for large container carriers. Further tailoring of ultimate and residual strength will be needed as experience is gained with operation of new types of vessels in extreme environments. Unconventional vessel designs and non-steel construction present challenges to the accurate assessment of ultimate strength in the absence of properly validated methods and tools.

5.2 Review of state of the art

5.2.1 Design for ultimate strength of ships

Common Structural Rules (CSR)

The Common Structural Rules for Bulk Carriers (CSR-BC) and for Double Hull Oil Tankers (CSR-OT) were two separate drafts established in 2005 and issued in 2006 by the International Association of Classification Societies (IACS, 2006a, b). The Common Structural Rules were of the first set of rules implemented for the safe design of these types of vessels.

The functional requirements in Chapter 3, Section 4 of the CSR-BC state that the strength criteria regarding hull girders, plating, and ordinary stiffeners of bulk carriers of 90 meters or more are to withstand maximum vertical longitudinal bending moment obtained by multiplying the partial safety factor and the vertical longitudinal bending moment at 10^{-8} probability level (IACS 2006 a). The multi-step outlined procedure for determining maximum bending moment capacity of bulk carriers follows the conventional Smith method that requires calculation of the vertical hull bending moment being considered, in maximum hogging and sagging conditions, which is to then be graphed against the transverse section curvature, χ. An incremental-iterative procedure, listed in Appendix 1 of CSR Chapter 5, is utilized for obtaining the M- χ curve. The maximum values of this curve are the ultimate bending moment capacities of a hull girder transverse section, in hogging and sagging condition. Checking criteria consists of confirming that at any hull transverse section, the bending moment being considered is less than or equal to the ratio of the ultimate bending moment capacity of the hull transverse section to the safety factor which is equal to 1.10 (IACS 2006 a).

For Oil Tankers, the CSR only enlists the ULS method with partial safety factors for hull girder strength. Otherwise it utilizes the more simplified Working Stress Design (WSD) method for strength requirements. For both CSR-BC and CSR-OT hull girder strength calculations, only vertical bending is considered. Effects of shearing force, torsion load, horizontal bending moment, and lateral pressure are neglected.

Harmonized Common Structural Rules (HCSR)

Over time, the IACS Council decided to refine and combine both CSR-OT and CSR-BC into a single set of rules that would resolve many issues not deemed in compliance with industry rules and regulations. In 2008, the IACS Counsel committed to the industry to combine the CSR-BC and CSR-OT into single set of rules known as the Harmonized Common Structural Rules. The harmonized rules, established in 2012, not only aided in eliminating problems with the Common Structural Rules, but also improved the technical background and managed to formulate new requirements for these types of vessels by combining the CSR-BC and CSR-OT rules for consistency as well as keeping specialized sections for each vessel type.

In the CSR-OT, the hull girder ultimate bending capacity is calculated using a single step WSD method, or the partial safety factor incremental-interactive method, whereas the CSR-BC only utilizes the incremental-interactive method. To comply with Goal Based Standards (GBS), IACS decided during the harmonization of the CSR to remove the single step method, enforcing the incremental-interactive method as the sole method for calculating the ultimate bending capacity for oil tanker vessel hull girders.

In the HCSR (IACS, 2017), the ultimate strength assessment is required for ships greater than 150 m, and is to be assessed at cross sections throughout the cargo hold region and machinery space. The Smith method approach defined in the HSCR gives load-shortening formulas for longitudinally and transversely stiffened panels and hard corner elements, allowing for failure in yielding, beam-column buckling, torsional buckling, web local buckling and plate buckling modes. The application of these load-shortening curves in the incremental-iterative method to

determine the bending moment and neutral axis location for each increment of curvature is defined in detail in Chapter 5, Appendix A-2 of the HCSR.

Once the ultimate bending strength, M_U, of a cross section is determined in hogging and sagging, the hull girder ultimate strength check requires that

$$M \leq \frac{M_u}{\gamma_M \gamma_{DB}} \tag{5}$$

where M is the vertical bending moment representing the extreme load on the vessel, γ_M is the "partial safety factor for the vertical hull girder ultimate bending capacity, covering material, geometric and strength prediction uncertainties" and is equal to 1.1, and γ_{DB} is the "partial safety factor for the vertical hull girder ultimate bending capacity, covering the effect of double bottom bending". The latter was introduced to account for the lateral loading effect on the ultimate strength of the hull girder due to external pressures acting on the outer plating and internal cargo pressures acting on inner bottom plating of the vessel (ISSC, 2015). For hogging, the HCSR requires γ_{DB} = 1.25 for bulk carriers in alternate empty hold condition, and γ_{DB} = 1.10 for oil tankers, and for bulk carriers not in alternate empty hold condition. For sagging, γ_{DB} = 1.0.

The hull girder ultimate strength check is to be applied throughout the cargo hold region and machinery space of a vessel. For bulk carriers it must be satisfied for seagoing, harbour/sheltered water and flooded loading conditions; for oil tankers it must be satisfied for seagoing, harbour/sheltered water conditions.

IACS Requirements for Container Ships

The Unified Requirement S11A "Longitudinal Strength Standard for Container Ships" (IACS, 2015) requires ultimate hull girder strength requirement in hogging and sagging for container carriers greater than 150 m. The Smith method to be used is the same as those specified in the HCSR, but nonlinear FEA is also sanctioned for determining the hull girder ultimate strength. The ultimate strength check is the same as in Eqn. (5) except the partial safety factor γ_M is 1.05, while γ_{DB}, is 1.15 in hogging, and 1.0 in sagging. Additional requirements for large container carriers include

- Yielding and buckling under additional hull girder loads (torsion and horizontal bending and static cargo torque) as well as local loads
- Strength assessment is to take account of the whipping contribution to the vertical bending moment.

The impact of the recent changes to UR S11A on container carrier design was investigated by Peschmann et al. (2016). It was found that loading requirements have changed significantly especially in sag condition. Of 70 different container carrier designs that were investigated it was found that about 10% would fail to meet the new ultimate strength requirement.

Goal Based Standards (GBS) and Gap Analysis

Regarding rules, regulations, and standards for ships, the Goal Based Standards (GBS) (IMO, 2010) are considered high level standards and procedures that do not dictate how a vessel will achieve compliance, but rather sets goals for allowing alternative ways for achieving compliance. The Goal Based Standards framework consists of five tiers. Tier I is the specified goal for design and construction of a new ship. Tier II is the functional requirements specified to achieve the outlined goal. Tier III involves the verification process of Tier IV, existing framework which consists of the class rules and prescriptive regulations. Tier V involves the applicable industry standards and codes of practices (Lei et al., 2015). The benefits of GBS are that the allowance it provides to industries to become more technically innovative for solving

design issues to reach the ultimate objective. Tier II of the GBS establishes 15 functional requirements for standards development which pertain to:

1. Design Life
2. Environmental Conditions
3. Structural Strength
4. Fatigue Life
5. Residual Strength
6. Protection against Corrosion
7. Structural Redundancy
8. Watertight & Weathertight Integrity
9. Human Element Consideration
10. Design Transparency
11. Construction Quality Procedures
12. Survey during Construction
13. Survey and Maintenance
14. Structural Accessibility
15. Recycling

CSR are most closely associated to the GBS through Tier IV but since the CSR were established before the GBS, some of the requirements of CSR do not fully comply with GBS. In anticipation of GBS functional requirements, new rules were added to HCSR to address the following functional requirements lacking in the original CSR: residual strength, structural redundancy, fatigue life, and design clarity (Lei et al, 2015).

According to Tier II-3, all ultimate strength calculations should include the ultimate hull girder capacity and the ultimate strength of plates and stiffeners. During operational conditions, no operational moments or stresses shall exceed 90% of the design (IMO 2015). It was determined that the HCSR would be 100% in compliance with this requirement, where the CSR failed. Overall, harmonizing the previous CSR regarding bulk carriers and double hull oil tankers allows for these rules to achieve full compliance with the GBS.

Non-CSR Covered Vessels

For a vessel type that is not addressed in the CSR, neither a bulk carrier nor an oil tanker, requirements for ultimate strength design come from classification societies. Rules covering ultimate hull girder strength of intact vessels are summarized below. For rules covering residual strength of damaged vessels, see Section 5.1.2.

American Bureau of Shipping (ABS)

ABS has published Rules for Building and Classing Steel Vessels which, in addition to CSR vessels, addresses ultimate strength criteria for: bulk carriers and tankers not covered HCSR, container carriers, and passenger vessels, liquefied gas carriers, chemical carriers, vessels intended to carry vehicles, water carriers, and membrane tank LNG carriers (ABS, 2016).

For container carriers, ABS utilizes the incremental-iterative method with partial safety factors as used in the CSR for ultimate hull girder strength (ABS, 2016). The Rules allow for alternative methods including FE analysis, given that the analysis methodology is reviewed and approved. The rules explain that the variables of a steel vessel, the still water bending moment, wave bending moment, and the ultimate capacity, are assigned a safety factor. These safety factors were determined from a structural reliability assessment approach and the long term load history distribution of the wave bending moment, which was derived from ship motion analysis for determining extreme wave bending moments (ISSC, 2012). This was done to demonstrate how critical failure modes of a ship are controlled.

Bureau Veritas (BV)

Bureau Veritas (BV)'s Rules for the Classification of Steel Ships (BV, 2016) require an ultimate strength check to be applied for ships greater than 170 m. With reference to Equation (5), BV defines the partial safety factor γ_M as the product of safety factors on resistance γ_R = 1.03 and material γ_m = 1.02, and γ_{DB} is not used. Ultimate strength assessment requirements include checking the structural strength under the worst, extreme quasi-static loading conditions. A Smith's method approach is used in which load-shortening curves can be determined taking into account elastic-plastic behaviour, beam-column buckling, torsional buckling, local web buckling, plate buckling, and buckling of transversely stiffened curved panels. The calculation method and load-shortening formulas used are very similar to the Smith's method approach defined in the HCSR, and can be calculated with BV's MARS software. Application or MARS software to BV ultimate strength check for an ultra large container carrier was demonstrated by Im et al (2016).

BV's Rules for Naval Ships, 2011, requires that the ultimate strength check be applied to ships greater than 90 m. The method specified for calculating the ultimate strength capacity is the same as in BV's Rules for the Classification of Steel Ships, except that the partial safety factor for resistance is γ_R = 1.15, instead of 1.03. Furthermore, the rules for wave bending load and the applicable partial safety factor also differ from the Steel Ships rules.

BV also publishes rules for Hull in Composite Materials and Plywood (BV, 2017), and Hull in Aluminium Alloys (BV, 2015) in which global hull strength is based on allowable stress criteria. Neither of these rules have hull girder ultimate strength requirements.

ClassNK

In ClassNK's Rules for the Survey and Construction of Steel Ships (ClassNK, 2016), hull girder ultimate strength assessment is required for container carriers greater than 150 m. The partial safety factors and load assessment method to be used are identical to the IACS S11A requirements. Ultimate strength assessments are to be carried out for sections between 0.2L and 0.75L, with "due consideration given to locations where there are significant changes in the hull cross section." The ultimate strength assessment method in this case is a Smith's method approach that is very similar to the method in the HCSR. ClassNK's rules have additional requirements for the hogging strength of container vessels greater than 300 m in length, or greater than 32.26 m in breadth. In this case, the ultimate strength check must also satisfy

$$M \leq M_{U\_DB} \tag{6}$$

where M is the extreme bending moment in hogging, and M_{U_DB} is the hull girder ultimate strength in hogging considering the effect of lateral pressure loading on the outer bottom. A direct calculation procedure is used for M_{U_DB} based on estimating ultimate stress of each structural element in a cross section, where the ultimate stress of outer bottom stiffened panels is reduced by the stresses due to local bending loads.

Germanischer Lloyd

In GL's Rules for Seagoing Ships (GL, 2012 a), (now superseded by DNV-GL rules) the ultimate vertical bending strength is to be determined and compared to loads in extreme conditions. Ultimate vertical bending strength is to be assessed using progressive collapse analysis based on a simplified incremental-iterative approach where the ultimate strength is defined as the peaks of a moment-curvature relationship in hogging and sagging. The method is applied to a ship cross section, which is subdivided into two types of elements (plate-stiffener combinations, and hard corners). Load-shortening curves include beam-column buckling, torsional buckling, web/flange local buckling and plate buckling modes of failure. Ultimate vertical shear force requirements are also defined, where the ultimate shear strength is

determined using a simplified determination of yield capacity of a cross section. In GL's Rules for Classification and Construction – Naval Ship Technology, (GL, 2012 b), the requirements for ultimate strength assessment are very similar to those of the Rules for Seagoing Ships.

Det Norske Veritas (DNV)

In DNV's Rules for Classification of Ships, (DNV, 2012 a), the CSA1, and CSA2 notations require that the ultimate sagging and hogging bending capacities be determined for the intact and damaged conditions. This check applies to tankers, gas carriers and bulk carriers. Ultimate strength is determined using DNV's HULS code, which computes the moment-curvature relationship of a hull section incrementally, using a separate code, PULS, to determine the strength of individual panels. For ultimate strength in hogging "all relevant local loads and double bottom effects shall be considered."

DNV's Rules for High Speed, Light Craft and Naval Surface Craft, (DNV, 2012 b), Part 3 Ch 2 contains hull girder strength check, which is required for all steel construction vessels of the type that fall under these rules. Strength in vertical bending is based on section modulus calculation, with deductions for openings. Part 3 Ch 3 of these rules applies to aluminium alloy hull structures, while Part 3 Ch 4 of the rules applies to composite hull structures. For both aluminum and composite construction, the hull girder strength requirements are similar to those for steel vessels (i.e. section modulus calculation).

DNV-GL

After the merger of DNV and GL in 2013, the newly formed DNV GL group released its first consolidated set of rules in 2015. The Rules for Classification – Ships, (DNV-GL, 2017) allow three different methods for determining the hull girder ultimate strength in vertical bending are permitted: (1) a multi-step method essentially the same as the Smith's method in the HCSR, and probably derived from the method in the old GL rules; (2) a single step method based on reduced effective area of compressed members, and which retains a link to DNV's PULS buckling code; and (3) a direct approach using nonlinear FEA. DNV-GL's Class Guideline document (DNVGL-CG-0128, 2016 b) provides guidance on nonlinear FEA for ultimate strength assessment. The hull girder ultimate strength check is to be applied to single-decked vessels with unrestricted service that are greater than 150 m in length, and is to be satisfied at specified cross sections in the vessel. The safety factors defined for the ultimate strength check are the same as for the HCSR; for container ships, the IACS UR S11A requirements must also be satisfied. DNV-GL's naval ship rules, 2015, have ultimate strength requirements based on a Smith's method calculation procedure.

Lloyd's Register (LR)

The Rules and Regulations for the Classification of Ships (LR, 2016), requires a hull girder ultimate strength assessment for container carriers greater than 150 m. The partial safety factors to be used in the ultimate strength check are the same as in the IACS S11A requirements. The method for determining the ultimate strength is specified in a guidance note. For other vessels, a longitudinal strength check is to be applied for all ships exceeding 65 m in length. Hull girder bending check is based on section modulus calculations for bending in the vertical direction. There is also a requirement for the maximum permissible shear stress in the presence of vertical hull girder shear forces.

In LR's Naval Ship Rules, 2017, the Extreme Strength Assessment (ESA2) notation contains requirements for vertical ultimate bending moment and vertical ultimate shear strength at critical cross sections. The ultimate bending strength calculation is to be "based on nonlinear stress strain curves which include the stress strain relationship in the post buckling phase." Extreme wave loads are determined by an empirical formula similar to that used for commercial vessels.

RINA

The Rules for the Classification of Ships (RINA, 2017) require an ultimate strength check for all ships greater than 150 m in length. For ships that are not container ships, the ultimate strength check, referring to Equation (5), defines the partial safety factor γ_M as the product of safety factors on resistance γ_R = 1.08 and material γ_m = 1.02, and γ_{DB} is not used. The ultimate strength calculation procedure is very similar to that of the HCSR, as are the formulas for the average stress-strain relationships of hard corners and stiffened panels. For container ships, RINA requirements match very closely the IACS UR S11A requirements.

The Rules for the Classification of Naval Ships (RINA, 2011) requires an ultimate strength check for all ships greater than 90 m in length. The ultimate strength check is similar to RINA's commercial rules except that the partial safety factor for resistance is γ_R = 1.15. The ultimate strength calculation procedure closely follows the methodology of the HCSR.

5.2.2 Design for residual strength

In general ships experience two types of structural damage. *In-service damage* comprises the normal processes of corrosion and fatigue cracking common in steel ships and are addressed in classification society rules through application of corrosion margins, fatigue design standards and a regular regime of inspections and maintenance. *Gross damage* comprises damage due to accidents, such as grounding, collisions and explosions, and in the case of naval vessels, damage due to military action. In the past, gross damage effects were not specifically addressed by ship design standards, and design for damage tolerance was implicit to traditional prescriptive design philosophies. With the advent of more rational design philosophies, such as IMO's GBS, there is recognition for the need to explicitly include tolerance to gross damage in structural designs to ensure a reasonable likelihood of survival in foreseeable accident scenarios.

Residual Strength is one of the fifteen Tier II Functional Requirements in the GBS for bulk carriers and oil tankers. Requirement II.5 states that

> *Ships shall be designed to have sufficient strength to withstand the wave and internal loads in specified damaged conditions such as collision, grounding or flooding. Residual strength calculations shall take into account the ultimate reserve capacity of the hull girder, including permanent deformation and post-buckling behaviour. Actual foreseeable scenarios shall be investigated in this regard as far as is reasonably practicable.*

The residual strength check in adopted in the HCSR (IACS, 2014) to comply with the residual strength required for ships greater than 150 m in length, at cross sections throughout the cargo hold region and machinery space,

$$M \leq \frac{M_{UD}}{\gamma_{RD}\, C_{NA}} \tag{7}$$

where M_D is the vertical bending moment in the damaged condition, $M_{UD}$is the vertical ultimate strength in the damaged condition, γ_{RD} is the partial safety factor for vertical hull girder bending capacity, to be taken as 1.0; and C_{NA} is a neutral axis coefficient, to be taken as 1.0 for grounding damage, and 1.1 for collision damage.

The HCSR defines the extent of damage to be applied to transverse cross sections in the residual strength assessments, as summarized in Table 5and Table 6.

Table 5: IACS-HCR damage extent for collision

Dimension in m	Single side	Double side
Height, h	0.75 *D*	0.6 *D*
Depth, d	*B*/16	*B*/16

Table 6: IACS-HCR damage extent for grounding

Dimension in m	Bulk carriers	Oil tankers
Height, h	min (B/20, 2)	min (B/15, 2)
Breadth, b	0.6 *B*	0.6 *B*

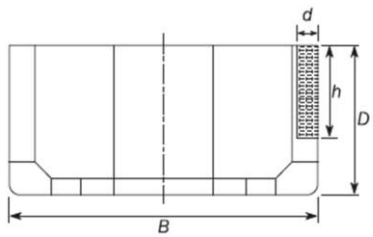

Figure 1 : IACS-HCR damage extent for collision

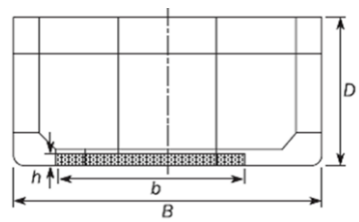

Figure 2: IACS-HCR damage extent for grounding

In the evaluation of the bending load M_D, the partial factor of safety for the vertical hull girder wave loading, γ_{WD}, is 0.67, compared to 1.2 in the intact case. This reflects that most collision and grounding incidents happen in coastal environments where wave heights are reduced, and that a vessel is not expected to operate in a damaged condition for a long duration.

The residual strength check is performed at damaged transverse cross sections using the Smith method approach specified for the ultimate strength assessment of the intact vessel, but with the effectiveness of structural elements reduced to zero in the damaged areas shown in Figure 1 and Figure 2. No attempt is made to estimate the residual strength of partially damaged members (e.g. deformed but not ruptured). The residual strength check is not limited to damaged cross sections only, but must be applied in undamaged cross sections, as the still water load distribution may have changed considerably from the intact condition as a result of flooding and/or loss or shifting of cargo. It is not mentioned in the HCSR, but when assessing cross sections fore and aft of the damaged region, it may be necessary to reduce the effectiveness of structure that falls in the stress shadows created by the removal of structure.

For vessels not applicable to HCSR, limited rules exist for residual strength assessment. A summary of residual strength requirements in other classification society rules is given below.

LR

Residual strength assessment notation (RSA) of the Naval Ship Rules (LR, 2017) may be awarded to designs if they meet requirements for residual strength. Three assessment levels are recognized: RSA1, RSA2, and RSA3. For the RSA1 notation, residual strength is assessed with a simplified method based on elastic theory (section modulus), and limits are defined for the longitudinal and shear stress in structural elements.

For the RSA2 notation, “residual strength after damage is to be verified using the ultimate strength analysis method which determines the ultimate strength of the hull after damage using direct calculation methods”. The ultimate strength in vertical bending and vertical shear are to be determined, but the evaluation method is not defined in detail. The requirement for residual strength is that (1) the maximum bending load applied to the hull must be less than 90% of the ultimate bending strength for both hogging and sagging; and (2) the maximum vertical shear load in the damaged hull must be no greater than 90% of the ultimate vertical shear strength.

For RSA3, "residual strength after damage is to be verified using a recognised FE code suitable for this type of analysis." The strength requirements to be met for RSA3 are not explicitly defined, but presumably are the same as for RSA2.

The extent of damage to be considered may be specified by the Ship Owner. Three damage levels are recommended for collision and grounding (length, breadth and height of damage region defined). Residual strength assessments are to be assessed at either three critical cross sections for each anticipated damage event, or at all critical cross sections for each anticipated damage event, depending on the damage level chosen.

DNV

For notations CSA1, CSA2 in DNV's Rules for Classification of Ships (DNV, 2012 a), ultimate sagging and hogging bending capacities are to be determined for the intact and damaged conditions. This check applies to tankers, gas carriers and bulk carriers. Damage cases to be evaluated are: (1) Collision with penetration of one side to a depth of B/16, with damage length of L/10 and two different damage heights; (2) Grounding with penetration of the single or double bottom to height of B/15 with two different damage sizes. Residual strength is determined using DNV's HULS code, similar to the way intact structures are analysed. The residual strength must be sufficient to withstand a load level determined using the damaged still water bending moment and two-thirds of the wave bending moment component used in the intact condition, the same as in the HCSR.

DNV-GL

DNV-GL's Naval Vessels rules (DNV-GL, 2015) have a class notation RSM for residual global strength capacity after damage due to military action. It differs from other residual strength rules as it requires that the vertical and horizontal bending capacity of the hull satisfy the residual strength check. Similarly the residual horizontal and vertical shear capacities of the damaged vessel are required to exceed shear forces in the damaged condition. The extent of damage to military action is an owner-defined requirement. Guidance provided for improving residual strength of a vessel includes the fitting of "longitudinal box girders immediately below the weather deck and at the bottom of the hull", and reinforces longitudinal stringers on the lower side shell and above the double bottom.

5.3 Developments in ultimate strength assessment

5.3.1 Load combination and dynamic effects

The hull girder failure of the 8100 TEU container carrier MOL COMFORT in 2013 (Figure 3), after only a few years of service, generated concern over the safety of this class of vessels and the adequacy of existing design rules for large container carriers in general. ClassNK (2014) and Sumi et al. (2015) published investigations of the MOL COMFORT and her sister ships. It was concluded that with this class of container carrier, hogging bending moments at 90% of ultimate strength could cause permanent plate buckling deformation in the outer bottom, resulting in damage observed in several of these vessels. The combination of the weakened hull plate, deviations in cargo weight, local pressure loads, plus regular wave loads and whipping effects could have resulted in a total load in the vessel a midships that was in excess of its ultimate strength. Recommendations from this work were that local loading must be taken into account when assessing hull girder strength of large container carriers in hogging, and that whipping must be taken into account in the assessment of maximum hull girder loads.

The influence of lateral loading on the ultimate strength has previously been investigated for bulk carriers (Amlashi and Moan (2008), Pei et al. (2012), Toh and Yoshikawa (2015)). Benchmark studies of a three-hold section of bulk carrier design were also performed for ISSC (2015). FE analyses for eight different loading cases (hogging and sagging, with and without imperfections, with and without lateral loads) were performed using 3-hold FE models in

alternate hold loading condition. Lateral loads (combined effect of cargo pressure on inner bottom and external pressure on hull exterior) were found to reduce the hogging ultimate strength up to 25%.

Figure 3: Hull girder failure of MOL COMFORT, 17 June 2013 (Photo: Mitsui O.S.K. Lines, Ltd).

As a result of the MOL COMFORT and MSC NAPOLI (MAIB 2008) accident investigations, combined load effects in container carriers are now receiving considerable attention. Tatsumi and Fuijkubo (2016) and Fujikubo and Tatsumi (2016) analysed the ultimate strength in hogging of an 8000 TEU container carrier considering the combined effect of the hull girder bending moment and lateral pressure loading. A 2-hold section in a ½ + 1 + ½ configuration was analysed with the nonlinear FEM (MSC/Marc) neglecting cargo weight. The lateral pressure load was predicted to reduce the ultimate collapse moment in hogging by 18.3%. The lateral pressure loading was also found to reduce the effectiveness of the inner bottom, thus contributing to the loss of strength. Matsumoto et al (2016) analysed the ultimate strength in hogging with lateral pressure loading on the outer hull for a series of container carrier designs ranging in size from 4000 to 10,000 TEU. Nonlinear FEM was used to determine ultimate strength with and without the lateral pressure load using a three hold model (½+ 1 + ½) in an unballasted condition and with the central cargo hold being empty. The reduction in hog strength resulting from the lateral pressure varies widely among the ship designs, from less than 5% to nearly 30%.

Due to the low torsional stiffness of container carriers relative to other large cargo vessels, the effect of torsional moment on ultimate strength is receiving increased attention. Alfred et al. (2016) analysed a 10,000 TEU container carrier with nonlinear FEA to determine an interaction curve for the extreme capacity of the vessel. They showed that the ultimate bending capacity is reduced by a pre-existing constant torsional moment on the hull girder; but even with the torsional moment close to the ultimate torsional strength, the reduction in bending strength is less than 20%. Under realistic torsional moments, the reduction in bending strength would be much less than this. A torsional moment produces high shear stress in the vertical side shell and longitudinal bulkhead, whereas the vertical bending produces high axial stresses in the hull bottom and the top of the shear strake. Thus the two loads do not interact strongly to reduce the bending strength.

Tanaka et al. (2015) performed a combined experimental and numerical study on 1/13-scale models of a 5250 TEU (post-Panamax) container carrier section. The models were subject to combined vertical bending, vertical shear, and torsion. Failure modes in torsion were identified as shear buckling of the side shell, buckling of the bilge corners, and rupture of the hatch corners. LS-Dyna models of the 3-hold section predicted similar failure modes as the experiments, but significantly overestimated the torsional strength of the model. A follow-up study by Tanaka et al. (2016) analysed the combined effect of vertical bending and torsion

using a whole-ship FEM for a similar vessel, and assessed the influence of different phasing of the torsional moment on the ultimate strength.

Gaiotti et al. (2016) studied the combined effects of shear and axial thrust on side shell panels in container ships using FEM. The ultimate strength under axial thrust was found to be significantly affected by shear stresses typical of those in the side shell of the container ship; but that the effect of shear can be exaggerated somewhat by higher than normal stresses induced at the boundaries of the panel.

Ciu et al. (2017) used nonlinear FEA to analyse the effects of corrosion on a 3100 TEU container carrier under combined vertical bending and torsion. After establishing the interaction curve for combined bending and torsion, an analytical surrogate model was used to study the effects of corrosion over the age of the vessel. They also considered the strength of the double bottom structure under combined longitudinal thrust and lateral pressure. Kim et al. (2014) investigated the effect of different corrosion addition guidelines on the midships ultimate strength of four bulk carrier designs. In comparison to designs with net scantlings, corrosion additions can increase the ultimate strength by as much as 50% for smaller vessels and over 30% for largest vessels.

Pei et al. (2015) considered progressive collapse using a whole ship model of a single-hull Kamsarmax bulk carrier acting under extreme wave loads using a combined standard-FEM/ISUM approach. The wave loading applied to the model resulting in hull girder vertical bending, vertical shear loads as well as lateral pressure applied to the hull exterior. The results showed a 20% reduction in hogging strength a midships resulting from the application of lateral loading when the bulk carrier is in the alternate heavy loading condition.

Investigations into the hull failures of MOL COMFORT and MSC NAPOLI both suggested the possible role of slamming-induced whipping in the failure of the hull, as well as highlighting the difficulty of predicting it accurately. Recent research on hull girder failure as a dynamic, multi-cycle event were performed by Iijima et al. (2013), who examined the collapse extent in a scale model under whipping loads and found that damage extent was reduced with shorter duration of bending moments in comparison to longer duration moments of the same magnitude. Iijima and Fujikubo (2015) performed an experimental study with a scaled model subjected to a succession of focussed waves in which a hull girder failure occurred progressively through the plastic deformation of a failure element in a hinged connection of the segmented model. Over the succession of wave encounters, the model exhibited a progressive reduction in the still water bending moment and an increase in the rotation angle at the failure section. Xu and Duan (2016) investigated the severity of the dynamic response near the ultimate capacity of a bulk carrier. They used a hinged model of the ship subject to a large amplitude focussed wave and a model of hull girder resistance based on the moment-curvature relationship determined by Smiths method. Derbanne et al. (2016) proposed a linear single degree of freedom model of a ship hull girder for investigating the dynamic response under combined still water, wave and slamming loads. The failure condition for the linear model is calibrated with a nonlinear assessment of the quasi-static ultimate strength of the hull girder. Zhang et al. (2016) determined the elastic shakedown limit by applying reversing bending moment loads to an oil tanker mid-section and considering local buckling and plasticity of the structure. They further propose the elastic shakedown limit as a safer measure of hull girder capacity than the ultimate strength determined under monotonic loading.

5.3.2 Composite and aluminium vessels; novel hull design

Composite and aluminium, although commonly used in small pleasure craft and fishing vessels, are only used in larger vessel hulls to meet specific performance design objectives (e.g., fast ferries, high-speed naval vessels, and special purpose vessels such as minesweepers). With the novel structural designs and exceptional operational requirements encountered with these

vessels, arises the possibility of extreme loads and failure modes not seen in conventional steel mono-hulls.

Welded aluminium possess unique material and fabrication-related properties that can severely impact structural performance (Collete and Sielski, 2013). However, standard ultimate strength analysis methods have limited applicability to welded aluminium structures due to the much lower strength and higher ductility of fusion welds and HAZ (Woelke et al., 2017) and the use of lightweight transverse stiffening. To account for the latter, Benson et al. (2013 a) applied a compartment-level analysis method, an extension of Smith's method which allows for overall (grillage) collapse modes to be included in additional to the standard interframe collapse modes to an aluminium catamaran design. Magoga and Flockhart (2014) evaluated the vertical and horizontal ultimate strength of an aluminium patrol boat midsection, taking into account weld-induced distortions, residual stresses, and material softening in heat affected zones (HAZ) using the ISFEM method.

Composites structures have a much higher strength to weight ratio in comparison to steel and can give outstanding performance and longevity. They are often ideal for weight-critical applications such as masts. They exhibit much less ductility than metals, and must be designed carefully to avoid premature cracking and delamination failures. The design of the attachment of composite topsides structure to steel hulls is especially important.

Morshedsoluk and Khedmati (2016) modelled the combined strength of the hull and superstructure of a composite passenger vessel using a coupled-beam method in which load-shortening behaviour of composite stiffened panels was determined with FEA and the Tsai-Wu failure criterion. The coupled beam analysis was used to predict the ultimate strength of a composite hull vessel and the effectiveness of superstructures of different lengths.

Pei et al. (2016) investigated the ultimate strength of a small waterplane area twin hull (SWATH) vessel and determined that the transverse bending moment and longitudinal torsion moment were the most important global loads to consider. They also considered combined action of these two bending load cases using nonlinear FEA and found the interaction effect to be small.

5.4 Developments in the residual strength assessment of damaged vessels

Traditionally, ships were designed for intact strength; residual strength in a damaged condition was accounted for implicitly through the conservatism in working stress design (WSD) philosophies. With the shift to limit-state and goal-based design approaches has come the recognition that residual strength should be addressed explicitly in design. On the one hand is a greater acceptance that ships will occasionally need to operate in a damaged condition; on the other hand is a greater emphasis placed on the preservation of human life at sea and on preventing environmental damage associated with shipping accidents. These considerations motivate the need to design for a limit-state approach to residual strength.

As outlined in the GBS Functional Requirement II.5, the design objective is to ensure that vessels have sufficient reserve structural capacity to survive foreseeable accidents. The HCSR requirements tend to assume the worst case for damage in collision and grounding; they idealize damage as simple removal of damaged structure from a cross section; and they consider only the vertical bending strength, and not the residual shear, torsional or horizontal bending capacity. Residual strength assessments arise for in-service vessels when damage is discovered during inspections, or immediately following a major damage incident. In the latter case, residual strength assessments are part of the emergency response, and rapid assessments using the most accurate information that can be obtained about the extent and severity of damage are essential.

Actual damage generally consists of regions of ruptured structure, surrounded by regions of plastic deformation. Both detract from the strength of the hull girder in different ways, and

neglecting the effects of plastic deformation damage will overestimate the residual strength (Yamada, 2014). Furthermore, a damaged vessel often develops a significant heel angle, such that a vertical bending moment is applied about a rotated neutral axis (Tekgoz et al., 2015); and that when the hull girder is damaged asymmetrically, a simple vertical bending moment will produce bending curvatures about two axes. Therefore a biaxial bending strength assessment is warranted (Muis and Alie, 2012). A number of studies have appeared that examine the effect of neutral axis rotation on the results predicted for asymmetrical damaged structure (Choung et al., 2012, Fujikubo et al, 2012). These studies point to the need for biaxial bending strength assessment, or combined bending and torsion strength assessment where hull girders have large openings, such as container ships, or gross damage.

Several researchers have developed rapid assessment tools based on empirical formulas for residual strength of hulls with grounding and collision damage. The methods were developed from the R-D diagram approach developed by Paik et al for tankers with grounding damage. A complete review of these developments is in 3.3.6.

More detailed studies of residual strength with gross damage are useful for gaining a better understanding mechanics of failure when damage is present. One issue is whether standard ultimate strength tools such as Smith's method are valid in the presence of gross damage, given their limitation to interframe modes of collapse. Petricic (2015) considered the effect of grounding and collision damage, modelled by element removal, in the residual bending strength of FPSO, tanker, bulk-carrier and container-carrier designs. The vertical bending ultimate strength with sixteen different cases of structural damage, differing in the transverse and longitudinal extent of the damage, was analysed for each vessel type with nonlinear FEA using ABAQUS. In the majority of cases, the failure mode was found to be interframe collapse, but in some cases overall collapse modes were observed when a deck or hull bottom was left with an extended unsupported edge as a result of element removal. Other nonlinear FEA assessments of ships with collision and grounding damage modelled by element removal were performed by Amante et al. (2016) and Muis Alie et al. (2016). The latter analysed a three-hold model of a bulk carrier under a vertical bending load and with the model constrained so as to allow rotation of the neutral axis to develop. Their results show that allowing neutral axis rotation results in a slightly lower ultimate strength, in comparison to models constrained to vertical bending only.

Underwood et al. (2016) predicted the ultimate strength of damaged steel box girders using a compartment-level assessment method and compared the results with those of nonlinear finite element analysis. Damage in the form of diamond-shaped openings was introduced in the box girder structure, and represented via element removal.

An issue with element removal as a simplified means of modelling damage is to what extent residual stresses introduced by the damage process affect the post-damage strength. This was investigated by Benson et al. (2013 b) who studied the ultimate strength of a severely damaged box girder structure, and determined that including residual stresses has the effect of increasing bending strength of the box girder by up to 10%. A few other studies incorporate the residual strength of damaged structural members into the hull girder residual strength assessment (Liu and Amdahl, 2012, Toh et al. 2015). Yamada (2014) used the LS-DYNA nonlinear code to simulate the extent of collision damage in a Capesize bulk carrier, and to subsequently calculate the residual ultimate strength in sagging, starting with the damaged FE model. The model with FEA-simulated damage shows a greater loss in sag strength in comparison to a model in which the damage is modelled by an element removal of the ruptured structure only.

Ehlers et al (2013) investigated the effect of low temperatures on the ultimate strength of a damaged LNG carrier. Damage extent was determined through collision simulations in an arctic environment using dynamic nonlinear FEA. The strength of the damaged hull was then determined using quasi-static nonlinear FEA and the Smith method. It was concluded that low

temperatures may actually improve the collision performance of the vessel, whereas temperatures as low as -60 C were found to affect hull girder strength very little.

5.5 Areas for future development

Classification society rules generally specify Smith's method incremental-iterative approach for ultimate strength assessment. This applies to the common types of vessel (tankers, bulk carriers). Ultimate strength assessment of container carriers under combined loading (bending and lateral pressure) is being addressed with special rules for these vessels mainly in response to the MOL COMFORT accident. Ultimate strength of other specialized types of vessels has not been addressed by rules specifically:

- LNG carriers and FLNG vessels, which are subject large thermal gradients resulting in pre-stressing of the primary structure. Thus far, no studies of the interaction of thermal loads and ultimate strength have been identified. A further risk with these vessels is accidental rupture of the containment system, due to excessive sloshing or impact, which could directly expose the primary structure to the very low temperature cargo (Sohn et al. 2017), although Ehlers et al (2013) found that arctic environment temperatures had little effect on strength.
- FPSOs, which are usually double hull tankers modified to receive risers and fitted with processing plants. They are subject to other special combinations of loads (ice impact loads in high latitudes combined with wave loads). Some studies have appeared on ultimate strength of FPSOs (Chen, 2016, and Petricic, 2015) but none have considered unique combinations of loading/damage for this type of vessel.
- Both FLNG and FPSOs are potentially subject to blast and fire loads due to accidental deflagration of gas cloud accumulations. No studies considering the ultimate strength in the with blast/fire damage have been identified.

The lack of rules for non-steel construction acts as a barrier to further development and more widespread use of aluminium and composite vessels. Ultimate strength requirements specific to aluminium and composite hull construction are generally lacking in the rules. This may be because aluminium vessels (e.g., fast ferries) are usually limited to low sea state conditions in coastal and inland waterways, and composite vessels tend to be small in size, and therefore global strength is secondary to other aspects of the design.

Existing methods for ultimate strength analysis are unsuitable for aluminium and composite. Databases of curves and formulas describing the load-shortening behaviour of steel stiffened panels are not applicable to aluminium or composite structure. For welded aluminium structure in particular there is a lack of data on alloy-specific imperfections and material softening in heat affect zones (HAZ), which have a major effect on structural performance (Magoga and Flockhart, 2014). Modelling methods and tools may also need to be adapted for aluminium and composite construction. For example, hull girder ultimate strength assessment using a single-frame bay model may not be suitable for aluminium construction because an interframe collapse mode is not ensured in lightweight designs (Benson et al, 2013a) and because of the softening from transverse frame fillet welds and seam welds (Rigo et al. 2004). Furthermore, extruded integral stiffened panels are seeing greater use in aluminium construction to reduce the number of fusion welds, and will need to be accounted for in future load-shortening curve developments (Magoga and Flockhart, 2014).

Incorporation of nonlinear FEA into design rules for hull girder ultimate strength is recognized by some class societies. However, there is a lack of guidance on how to use nonlinear FEA for hull girder ultimate strength. An exception is the DNV-GL class guidance document "Buckling" (DNV-GL, 2016) which contains some detailed guidance on nonlinear FEA analysis of ship components. Furthermore, partial safety factors specified for Smith's method may not be suitable for nonlinear FEA predictions.

The HCSR now includes requirements for residual strength assessment with grounding and collision damage for tankers and bulk carriers. Rules for residual strength are based on bending strength in the vertical direction only. Considerable research is being done to improve the modelling methods and increase fidelity of ultimate strength assessments with gross damage, aided in part by improvements in FEA software and increasing computing power. A number of studies consider damage in a probabilistic sense, and are developing simplified guidance for residual strength assessment intended for application in a damage incident.

Nonlinear FEA is used more and more for ultimate strength of both intact and damaged hull girders, but better tools are needed for

- Incorporating weld-induced imperfections (distortions and residual stresses) in complex FEA models of intact structures.
- Modelling damage due to accidental loads in a manner that is simplified but still more realistic than simple removal of damaged structure is needed. Incorporating damage directly from realistic simulations of damage events in ultimate strength assessments is challenging (Benson et al (2013b), Yamada (2014)).

Modelling of secondary damage effects (fire, flooding combined with structural damage) also requires more attention. Incorporating thermal effects in ultimate strength analysis is one way to tackle this. This applies to LNG carrier strength (low temperature effects) as well as to fire damage scenarios (high temperature effects). Temperature effects will also be important for aluminium vessels due to their low melting point.

Hull girder failure is normally treated as a single-cycle quasi-static process, but in fact it is a dynamic process in which collapse progresses over one or more load cycles. This is believed to have been a factor in the failure of MOL COMFORT (Sumi et al, 2015). Some initial studies by Iijima and Fujikubo (2015) focused on cumulative damage, and this is seen as an area of future development.

High-fidelity simulations of whole-ship finite element models subjected to extreme wave loads (Pei et al, 2015, Fujikubo et al, 2016) are becoming more common. Ultimate strength is assessed using distributions of pressure loads associated with extreme waves instead of the more idealized bending moments applied to single-frame bay to three-hold models now commonly used. The main drawback of the whole ship approach is the greater burden placed on the computer hardware and software, as well as on the modeller. The computational burden can be partially mitigated through refining models selectively, such that the maximum refinement is only applied to areas likely to undergo collapse. This can also help avoid computational difficulties arising from local collapse of secondary components well before ultimate failure of the hull. Standardized modelling guidelines covering the application of realistic loading, meshing and the modelling of imperfections would help reduce the uncertainty associated with such complex analysis methods and help increase their acceptance.

Improved methods for modelling real-world effects (e.g. weld-induced imperfections) are needed. One approach is direct simulation of fabrication processes, such as cold bending and welding of the plating and members, so as to replicate in a modelling and simulation environment the ship construction process. While progress in computational weld modelling has been reported (Fu et al. 2016 and Chen et al. 2015), but simulations are computationally intensive and tend to be limited to small components.

Nearly all assessments use hull geometry based on drawings, and consider assumed imperfections based on idealized sinusoidal shapes with amplitudes based on historical data. Laser scanning technology now exists to measure the actual shape of hull structure with sufficient accuracy for numerical model. This could be applied as the vessel is built (e.g. before launch and before outfit) to fully map the shape of the interior and exterior structure, above and below the waterline. The point-cloud data generated by scans could be used to create a “digital

twin" for life-cycle management of a vessel, including among other applications, the development of numerical models for ultimate strength assessment. This technology has great potential for determining the shape of a damaged vessel, as was shown by the laser scans performed on ROKS CHEONAN (Figure 4).

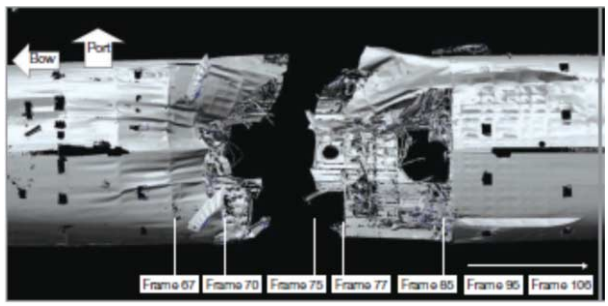

Figure 4: Laser scan image of damage to ROKS CHEONAN (Yoon et al, 2010).

Laser scanning, although efficient and portable, requires skilled personnel to perform the task and may take days to weeks for a complete vessel scan. Thus it is less well suited to emergency response scenarios where a very rapid assessment of damage extent is needed. Digital stereo photogrammetry shows more promise as a means for rapidly generating point clouds for damaged above-water structures. Photography could be carried out by crew members and the images sent to shored-based engineers for analysis. Measuring below water damage when the vessel is still afloat remains a considerable challenge. Hull-crawling or free swimming ROV-based technologies could also be used.

6. MARINE STRUCTURES

6.1 Introduction

6.1.1 General

Marine structures are engineering facilities constructed and installed in coastal zones, or open oceans for the exploitation of various marine resources, and support of marine operations. Generally, marine structures can be divided into two types: Fixed Platforms and Floating Production Systems as show in Figure 5. A detailed description of the type of structure is given in (API RP 2A WSD 2014), Section 4.6.

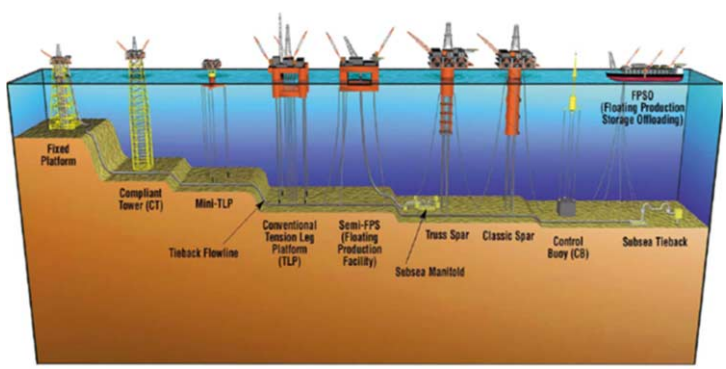

Figure 5: Illustration of different type of marine structure

6.1.2 Review of previous ISSC reports

ISSC (2012) provided a brief section on marine structures. The ultimate strength of a typical drilling semisubmersible was investigated in relation to the hydrodynamic loads. The residual strength of a semisubmersible platform column damaged by a ship collision was presented.

ISSC (2015) concluded that much effort was made at component level, but a systematic assessment of ultimate strength of offshore structures deserves further attention. Studies on ultimate strength of offshore structures were rather limited compared to the available documentation for ships and ship-shaped structures. In this report, the following aspects where presented:

- Effect of material properties on ultimate strength
- Aging factors (corrosion and fatigue)
- Evaluation of collision resistance
- Ultimate limit state based design

6.2 Standards and rules for the ultimate strength of marine structures

6.2.1 Offshore standards

Offshore structures are designed and assessed against international standards such as:

- Norsok N-series
- ISO 19900 (Series of standards for offshore structures)
- API

In addition, Classification Societies have developed their own requirements usually linked to the above standards. Design standards may differ with respect to items such as environmental loads, loading conditions, structural steel, and inspection, assessment of existing platform, accidental loading and seismic response.

Offshore installations have been traditionally designed following the Work Stress Design (WSD) approach. The standards developed through API based on WSD have been used for decades. In the 1980's API initiated to develop a LRFD (Load Resistance Factor Design) based design criteria for fixed offshore platform resulting in the first edition of API RP 2A (LRFD) published in 1993. Based on API 2A-LRFD, ISO 19902 was developed and has been updated to reflect the latest information. Over the last ten years the spreading of the new ISO 19900 series has altered the dependency on API. The Partial Safety factor method, generally known as LRFD, is now used as the primary design method in ISO.

As part of the collaboration efforts between ISO TC67/SC7 and API SC2 Offshore Structures committees, a standard harmonization scheme has been adopted, whereby the ISO standards have utilized existing API documents as starting point in developing the ISO standards. Abdel Ghobeim (2008) presented a rule development issues and discussed the need for harmonization and consistency between the various standards and regulations in the interest of meeting the target reliability and safety requirements of offshore exploration and production systems.

NORSOK

A new revision of NORSOK N-003, Actions and Actions Effects, 2017 was issued in March 2017. This standard is primarily written for the design of new facilities on the Norwegian continental shelf but in principle can also be applied to other areas. Main updates, relevant for the ultimate strength, are on the accidental actions due to ship collision, description of cold climate actions from sea ice, icebergs, icing and snow, wave impacts actions.

NORSOK N-004, Design of Steel Structures, 2004 only refers to ultimate strength in that it "should be evaluated by using a rational, justifiable engineering approach." However, this standard details how different forms of buckling should be accounted for in the design of

offshore structures. The structural analysis may be executed as linear elastic, simplified rigid-plastic, or elastic plastic; first order or second order may be used. All failure modes must be ductile, avoiding any brittle failure modes. As such, local and global buckling interaction effects must be avoided to satisfy adequate ductility.

Axial compression in tubular members must have a design axial force that is less than or equal to the design axial compressive resistance; the latter is calculated from the cross-sectional area, the characteristic axial compressive strength, and the material factor. The characteristic axial compressive strength for tubular members is either the in-plane, or out-of-plane buckling strength, whichever is smaller. This buckling strength considers the column slenderness parameter as well as the characteristic yield strength. The material factor depends on the shell slenderness parameter.

Tubular members subjected to external pressure may undergo hoop buckling; as such, the design hoop stress due to hydrostatic pressure must be less than or equal to the design hoop buckling strength. The design hoop stress due to hydrostatic pressure is calculated from the hydrostatic pressure, the hoop diameter, and the hoop thickness. The design hoop buckling strength considers the elastic hoop buckling strength, characteristic yield strength, and the material factor.

Tubular members subjected to a combination of compression, bending, and hydrostatic pressure must be proportioned to satisfy the requirements at all cross sections along their length. The requirements are based on two different methods: Method A assumes that the capped-end compressive forces due to the external hydrostatic pressure are not included in structural analysis. Method B assumes that such forces are included in the analysis as external nodal forces. Local buckling under a combination of axial compression and bending must have an equivalent design axial stress within the conical transition that is less than the local buckling strength of the conical transition divided by the material factor.

It should be noted that unstiffened thin-walled tubulars subjected to axial compression and bending are prone to sudden failures at loads well below the theoretical buckling loads predicted by classical small-deflection shell theory; therefore, the methods provided in this standard are more conservative for tubular elements than the methods historically used for other structures.

API

For calculating the Ultimate Strength of FPSO's, the API establishes values of design actions in both the PSF and WSD formats. The checks for Ultimate Strength mostly consider average stress levels over panels in possible buckling locations except in the cases for panels with large stress gradients in which the effect of the gradient shall be considered in the buckling evaluation. When evaluating buckling strength, membrane element stress data is to be used and pressure on such stresses shall be accounted for appropriately (API 2011). For fixed offshore platforms, API has also published a recommended practice including structural design. The recommended practice does not use US/PSF method, but the WSD method. However, the limit state and ultimate strength methods are included as alternative methods for Pile design.

6.2.2 Classification Societies rules and requirements

Offshore structures are not within the domain of the CSR as ships are, and there have been no major changes regarding the buckling and ultimate strength assessment. Guidance for Ultimate Strength standards and requirements are dictated by offshore standards and class societies which have developed own rules usually linked to the main standards of section 6 .2.1.

ABS

ABS (2017) has published multiple rules and guides which cover buckling and ultimate strength criteria for various offshore structures. These guides and rules include rules for Building and Classing Floating Production Installations, Guide for Building and Classing Floating Offshore

Liquefied Gas Terminals, Guide for Building and Classing Drilling ship, and Guide for the Buckling and Ultimate Strength Assessment of Offshore Structures. For Buckling and Ultimate Strength Assessment for Offshore Structures, an additional check was added to the buckling control concept. From section 3.7.5 of the guide, along with buckling and ultimate strength checks for plate and stiffened panels, a check is required for the overall strength of the stiffened panel to satisfy biaxial compression requirements.

Yu et al. (2016) present a comparison of the ABS WSD and the recently issued LRFD approach. The ABS LRFD-based structural design criteria are included in the mentioned guide for buckling and ultimate strength assessment for offshore structure (LRFD version) and Guide for load and resistance factor design criteria for offshore structure. The latter provides structural design criteria in a LFRD format for specific types of Mobile Offshore unit (MOUs), mobile offshore drilling unit and floating production installation. LFRD can be used as an alternative to the WSD. The main outcome of the study is that the two approaches can lead to the same results, with some difference related to the load combination. As described in the paper, the environmental loads are accounted with a higher partial safety factor as they are considered to be more uncertain and difficult to quantify compared to permanent and variable loads. Thus, the LRFD method tends to be more conservative than the WSD particularly when the environmental loads are dominant.

LR and BV

Lloyd's Register implemented similar buckling methods outlined in the HCSR regarding the Classification of Offshore Units. Alternatively, for offshore floating units, Bureau Veritas requires a check that a unit resist some of the impact conditions defined in the rules and includes the application safety factors to address uncertainties and inaccuracies from simplified allowable stress approaches.

DNVGL

DNV·GL also has several publications dedicated to offshore structure design requirements. For each type of offshore unit—ship-shaped, column-stabilized, and self-elevating—DNV·GL presents both the Ultimate Strength or LRFD approach as well as the WSD approach to ultimate strength calculations, allowing for flexibility in design strategy but including clearly stated objectives to adhere to GBS.

To support and provide guidelines to engineers working with the assessment of structural integrity using non-linear finite element analysis, DNV GL published a revised version of the DNV-GL-RP-C208 (20106). Guidelines on the requirements to finite element analysis, failure modes and example are given. A library of FE models suitable for collision analysis was also provided in Abaqus and LS-DYNA format. A possible analysis set-up to guarantee equivalent results in the two programs was investigated and presented by Storheim et al. (2016).

6.2.3 Design of offshore structures

The performance of a whole structure, or part of it, shall be described regarding a specified set of limit states beyond which the structure no longer satisfies the design requirements. The limit states are described in Section 2, Fundamentals.

As described in ISO, Ultimate Limit State for offshore structures covers:

- loss of static equilibrium of the structure, or of a part of the structure, considered as a rigid body (e.g. overturning or capsizing);
- failure of critical components of the structure caused by exceeding the ultimate strength (in some cases reduced by repetitive actions) or the ultimate deformation of the components;
- transformation of the structure into a mechanism (collapse or excessive deformation);

- loss of structural stability (buckling, etc.);
- loss of station keeping (free drifting).

ISO 19902 Petroleum and natural gas industries- Fixed Offshore Structure, 2007 defines the system reserve strength as the margin to withstand the environmental actions effect that exceed the design action effect and is evaluated as the Reserve Strength Ratio (RSR) as the ration between the ultimate capacity and design loading (usually 100-year loading).

> The structure ultimate strength may be determined by mend of suitable non-linear push over analysis from which the RSR can be calculated. The collapse analysis check can only be used for checking margins of safety against operational design loads (ULS) and accidental design loads (ALS). The indicators of the system strength for offshore jacket structure are based on nonlinear collapse analysis (push-over analysis).

6.2.4 Assessment of existing structures

Assessment of existing structures is performed to extend service life of the facility, as new methods of production and new discoveries may result in a request for life extension. From an economic point of view the continued use of an existing installation will in many cases be preferable, compared to a new installation. This will be preferable for several installations even with major modifications to the structure, Ersdal (2005). The requirements for assessment of an existing structure may differ from the design criteria for a new structure covering environmental criteria, loading conditions, foundation design, modelling, stress analysis, and acceptance criteria. For assessment of existing structures, actual platform data and experience is considered, thus eliminating some of the conservatism employed in design of new structures.

In general, an assessment will be needed in any of the possible changes to the initial design condition such as:

- Extension of service beyond the originally calculated design life
- Damage or deterioration of a primary structure
- Change of use
- Deviation from the original basis of design (increased load, inadequate deck height)
- Fatigue related issues

Due to the listed items, the RSR may decrease or increase, the assessment shall determine whether those aspects of the design that have been identified as no longer complying with original design criteria are fit-for-purpose and if the probability of failure associated to the life extension is acceptable. Prevention and mitigation measures for reducing the occurrence and the consequences of a structural failure should also be considered as part of the assessment process applying a risk based principle.

ISO 19902 (Clause 24) and API RP 2A WSD (reference to API RP 2SIM) gives procedures for the assessment of existing fixed structures. Assessment methods of different complexity are listed including ultimate strength analysis procedure which uses nonlinear calculation to demonstrate that the structure has adequate strength. The load condition may differ between the two standards as well as the target RSR. NORSOK N-006, Assessment of Structure Integrity for Existing Offshore Load-bearing Structures, 2009 includes some additional provisions compared to the other standards.

6.2.5 Seismic design guidelines

Seismic actions should be considered for platform in areas that are determined to be seismically active. ISO 19902 (Fixed steel offshore structures), ISO 19901-2 (Seismic design procedures and criteria) as well as Section 5.3.6 of API RP 2A give the guidelines regarding seismic design

and analyses of offshore platforms while NORSOK N-003, Action and Action Effects, 2007 gives brief description as the seismic activity is not a design issue in the North Sea.

The terms SLE (Strength Level Earthquake) and DLE (Ductility Level Earthquake) as used in API have been denoted ELE (Extreme Level Earthquake) and ALE (Abnormal Level Earthquake) in ISO.

API defines strength and ductility requirements for steel framed structure. The first are ensure that the strength and the stiffness are sufficient to withstand an event with a reasonable likelihood of being exceeded during the life of the platform.

Strength requirement are checked at the Extreme level earthquake (ELE). The ductility requirements ensure that the platform has sufficient reserve capacity to prevent its collapse during rare intense event, although structural damage may occur. The ductility requirements are checked for the abnormal level earthquake (ALE). Provisions on the evaluation of the seismic activity are given in 5.3.6.2.

Typically, nonlinear FE analyses (pushover or time history) are to be carried out to document the seismic behaviour. However, API does not provide detailed guidelines for failure and acceptance of individual elements, Nour El-Din (2014 a, b).

6.2.6 Accidental damage and residual strength

Offshore structures are designed against accidental loads to guarantee a level of safety where the main safety functions are not impaired by the accident or within a certain time following the accident. These loads are defined to prevent that the consequences of an accident are disproportional to the original cause. Accident events related to given probabilities of exceedance are also defined in the design standards.

Typical accidental actions are the impact from ship collision and dropped objects, fire and explosion, as given in API RP 2A, ISO 19902, and NORSOK N-004. Nonlinear FE analyses are typically used in this case to evaluate the ability of the system to withstand such actions.

NORSOK N-003, 2017 indicates that the accidental actions for offshore structure is specified with an annual probability of 10^{-4}. NORSOK N-001 illustrates a two-steps procedure to check the structure:

- Step 1: Resistance to accidental actions: The structure and related maritime systems should be checked to maintain the prescribed load carrying function for the defined accidental actions.
- Step 2: Resistance in damaged condition following local damage which may have been demonstrated under a), or following more specifically defined local damage, the facility shall continue to resist defined environmental conditions without suffering extensive failure, free drifting, capsizing, sinking or extensive damage to the external environment.

With respect to ship impact, in the last version of NORSOK N-003, 2017, the design collision energy is increased to 50 MJ (for head-on impact). This corresponds to a 10,000 tonnes OSV with a speed of 3 m/s. For side and stern impact, the speed remains 2 m/s. In addition, reference is made to bulbous bow and ice reinforces OSVs which typically have a different (stiffer) collision response compared to the raked bow vessel previously considered in the design collision event.

ISO 19902 differentiates between hazard groups when addressing accidental situations. A detailed description of the characterizations of such hazards and related probability if occurrence is also given in ISSC V.1 (2015). Hazard belonging to “group 2” with an annual probability of 10^{-3} to 10^{-4} are covered by the ALS scenarios.

A comprehensive Guidance Note standards was published by Lloyd's Register (2014). DNVGL-RP-C204 (2017) also provides guidelines on to the assessment of ship collision and other accidental scenarios.

When it comes to fire loads, the capacity of the structure to withstand the increase temperature induced by fire action shall be evaluated. Procedure to evaluate the structural resistance against fire load is given in Eurocode (EN 1991-1-2, EN 1993-1-2). Material degradation data as function of the temperature, formulae to calculate the temperature increase in members and design formulas to calculate the time that such members can withstand the given fire loads are given. Such calculations can also be performed by using nonlinear FE analysis.

6.2.7 Design of cold climate and arctic

The latest release of NORSOK N-003: 2017 includes a more comprehensive description of cold climate actions from sea ice, icebergs, icing and snow. When it comes to design against ice load, ISO 19906 suggests pressure area curves to be used in the local design of ship and offshore structure to resist ice impact. In ISO 19906, ice impact are defined by the extreme-level ice event (ELIE), which corresponds to an ULS case and an annual probability of exceedance of 10^{-2}. Loads from rare iceberg, are characterised by abnormal level ice event (ALIE) and corresponds to and ALS scenario with an annual probability of 10^{-4}.

NORSOK indicates that when designing against iceberg impact the same principle as ship impact can be used, distinguishing in ductility design, shared energy design and strength design. The latter implies that the structure can crush the ice suffering minor deformation. This approach typically leads to pressure area relationship and correspond to an ULS approach. For ALS scenario, this would lead to excessive structural dimensions and ductility design or shared energy may be used.

6.3 Development in the assessment of the ultimate strength

6.3.1 Assessment of existing offshore structures

Life extension requires re-assessment with incorporation of all changes and anomalies encountered since the day of the installation. Structural integrity is one of the major issues for ageing platform, especially if modification to the original design lead to higher loads which the structure was not designed for.

Global Ultimate Strength Assessment (GUSA) applied to the lifetime extension of ageing structure is a procedure to determine the probability of failure of the installation. The procedure, as described by Soom et al. (2015), includes nonlinear plastic collapse analyses, member importance analysis as simplified structural reliability analysis. Through push-over analyses, the ratio between the metocean design load (100 years) and the ultimate capacity is determined (this is the Reserve Strength Ration, RSR) identifying the first member failure and final collapse mechanism. These results are used as input to the simplified reliability analysis to determine an approximated figure for the platform reliability.

When a structure reaches their design service life, the fatigue life must be reassessed as part of the life extension. Yan Ji et at. (2016) carried out a series of experimental and numerical studies on the collapse of aged steel jacket structure affected by corrosion and cracks. The experimental tests, performed on a scaled model in intact, corroded and cracked conditions indicates a significant reduction in the capacity for the structure with 50 years' cracks (-30%) and corrosion without cracks (-27 %). The numerical studies have also indicated a knock-down even if the reduction is not as much as in the experimental tests.

6.3.2 Seismic assessment

For steel, offshore jacket structures, researches on the seismic performance evaluation and retrofit are relatively rare. Retrofitting of steel off-shore jacket structures is commonly carried out to extend the life of offshore platforms operating in seismic active regions.

Nour El-Din et al. (2014 a), investigated the performance of a jacket structure retrofitted with buckling restrained braces (BRBs) and conventional retrofitting (i.e. increase of brace areas, increase of thickness at the joints). BRB is a structural brace, designed to allow the system to withstand cyclical lateral loadings, such as earthquake-induced loading. In principle, these are characterised by a core element enclosed in a buckling restrained and therefore may reach yield both in tension as well as in compression.

An existing Jacket was used as case study and modelled with different conventional bracing configurations according to AP-2B2A, with a BRB solution applied to all the braces and BRB applied to the two upper stories.

Nonlinear static pushover analysis and incremental dynamic analysis were conducted to predict the seismic response of the jacket structure modelled with different bracing configurations, measuring strength and ductility. The results indicated that the use of BRB increase the ultimate strength of each structure with a better strength /weight increase ratio compared to conventional brace arrangement.

Nour El-Din et al. (2014 b) investigated the strength and ductility performances of a jacket platform designed with buckling restrained braces (BRB) and conventional braces. the structural configurations obtained by applying three different design methodologies are compared, including the pile-soil interaction performing a series of dynamic analysis to evaluate the progressive mechanisms. The study shown that the API requirements can be eased if conventional brace are replaced with BRB enhancing the seismic response in the ductility level earthquake but with minor advantages on strength response.

6.3.3 Arctic condition

A vast literature on material performance is artic condition is available, but it appears that less research was performed on systems and offshore structures

Ehlers and Ostby (2012) investigated the improved energy absorption capacity for artic materials. Kim et al. (2016) investigated the response of steel plates structure in artic environment. Both experimental test and numerical analyses were carried out. Material testing was performed at ambient at room temperature and -60 C including strain rate effects and the material models utilized in the numerical simulation were calibrated against such tests.

To efficiently increase the resistance against iceberg impact, Jia-Bao Yan et al. (2016) develop a nonlinear FE model for evaluating the performance of the sandwich steel-concrete-steel (SCS) with ultra-light cement composite and headed shear studs under patch load. In their study, a damaged plasticity failure criterion is used to evaluate the ultimate strength of the SCS. Two different approaches for modelling the interaction between the steel shear studs and the concrete were validated against a series of experimental tests. The applied damage criteria and the most detailed modelling technique show a satisfactory agreement with the experiment in terms of load defection curve and ultimate resistance for the SCS.

The validated model was then used to perform a parametric study on the curvature to identify the best ration of resistance and material used.

6.3.4 Assessment of damage effect (collision, dropped objects and fire)

DNV (2008) and NORSOK N-004 does not consider the residual strength of ship-shaped FPSOs after collision damages as a threat to the overall safety. However, according to NORSOK N-003, 2007, the damaged unit has to be capable to withstand the 100 years' load (without material and load factors).

Russo et al. (2009), investigated the residual hull girder strength of a damaged FPSO. The extent of the collision damages was defined by statistics (Harden series). The authors performed a comprehensive study of the loads hull girder loads acting in intact and damaged condition and

compared to the structural capacity. The damage extents were introduced by removing part of the structure from the model, while and the residual strength is calculated using simplified methods (Smith) and nonlinear FE analysis, indicating that the capacity is reduced to such level that the unit cannot withstand the environmental loads.

A continuation of this study was presented by Notaro et al. (2013). In this case the damage suffered by the FPSO was established by using nonlinear FE analysis considering 8000 tonnes bulbous bow OSV colliding with the FPSO. The damage was computed with different methods: first a simplified combination of the load deflection curves for the FSPO and OSV (as indicated in NORSOK N-004) was applied. Next, integrated nonlinear FE analyses were performed to obtain a more realistic estimate of the damage level. The residual strength was then investigated for selected damage extents but neglecting the effect of residual stresses induced by the collision load.

Notaro et al. (2015) presented a study on the collision resistance of jacket structure. The increased displacement of modern OSV and their different collision response may require additional consideration when evaluating the collision response of offshore structure. The study indicated that modern supply vessel can severely damage the installation; however, no post damage assessment was performed. The benefits of performing nonlinear FE analysis compared to the traditional approach given in NORSOK N-004 (with prescribed load deflection curves representative for the resistance of the ramming ship) are presented; when the response and energy dissipation is influenced by large changes in the contact surface and mutual deformation of the two objects the outcome of the FE analysis may differ significantly from the traditional methodology given in the standard. A similar procedure was applied by Levanger et al. (2016) to evaluate the collision response of a jack-up unit. The leg resistance to pushdown loads in damaged condition was evaluated for few selected damages indicating that large OSV vessel may lead to important reduction of the load bearing capacity.

The use of nonlinear FE analysis to assess the collision resistance of structures and other events dominated by large plastic deformations have been increasing over the last decades. In a design phase, only the material grade is known, hence engineers must adopt simplification with respect to the material properties and rely on minimum material strength data given in design standards. Storheim and Amdahl (2017) investigated the effect of various assumptions in the description of the material behaviour including stress-strain curves and strain rate effects with application to collision simulations. The localization of strains and therefore fracture are affected by the adopted stress-strain curves and the main parameters (such as yield ration, yield plateau and fracture strain) have significant statistical variation within a material grade

With respect to design against dropped objects, Kennedy et al. (2016) describe an application of the Sandwich Plate System (SPS) technology to the design of the impact protection deck for the well-bay deck area for a Tension Leg Platform (TLP) structure. Extensive nonlinear FE analysis (LS-DYNA and ABAQUS) were carried out to demonstrate the increase resistance against dropped object and the governing failure mechanism contributing to the energy dissipation.

Nonlinear finite element analyses are also applied to investigate the resistance to fire loads as an alternative to simplified methods as given in EUROCODE. A benchmark study on the structural resistance against fire loads was carried out by ISSC V.1 (2015). The ultimate strength of a deck structure in ambient temperature was first calculated trough pushdown analysis. Next, the fire load was estimated and applied to the structure to evaluate degradation as function of time due to the fire actions and the reduction in the ultimate strength. The benchmark highlighted how such analysis can be sensitive to different assumptions and analysis parameters resulting in possible large deviation in the obtained results.

Brubak (2016) focused on the comparison between simplified methods such as Eurocode EN 1991-1-2 and 1993-1-2 (2002, 2005) with the use of nonlinear FEA. The computed temperature in the time-domain were found in good agreement with the specification given in Eurocode,

while it was highlighted how the use of non-linear FE tools may estimate a longer time to collapse compared to explicit design formulas.

7. ULTIMATE STRENGTH OF STRUCTURAL COMPONENTS AND CONNECTIONS

This section presents the recent research and developments on the ultimate strength for structural components and connections in ship, floating and offshore structures.

7.1 Components and connections for ships and floating structures

7.1.1 Plates and stiffened panels

The past few years have observed substantial developments in the understanding of failure mechanism for stiffened plates and panels, as well as closed-form solutions to estimate the strength of these structural components. Zhang (2016) has performed a comprehensive review on the ultimate strength of steel plates and stiffened panels under axial compression. Zhang also presented a semi-empirical equation to predict the ultimate strength of stiffened panels under axial compression. He validated the accuracy of this formula by carrying out 110 numerical analyses and about 70 test results. The expressions takes the following form (Zhang, 2016).

$$\frac{\sigma_u}{\sigma_y} = \frac{1}{\beta^{0.28}} \frac{1}{\sqrt{1+\lambda^{3.2}}} \tag{8}$$

where λ denotes the stiffener slenderness ratio and β refers to the plate slenderness ratio.

In a recent effort to harmonize the proof of buckling strength for bulk carriers and oil tankers, Hayward and Lehmann (2017) have developed a new expression of plate capacities under combined in-plane loads with nonlinear buckling analyses. This new proof incorporates a more physically based approach towards tensile stress effects on plate capacity and better captures the influences of both plate slenderness and aspect ratio under compressive biaxial loads. Moreover, the new proof can be solved without the need for iterations and may be used directly with stresses obtained from FE analyses, thereby eliminating the need for a stress correction due to Poisson effects.

Seo et al. (2016) have examined the nonlinear structural behaviour and proposed design formulae to estimate the ultimate strength for stiffened curved plates under axial compression. Their work included elastic-plastic analyses on more than 400 cases considering different parameters such as slenderness ratio, curvature, and web height and stiffener shape. Their investigation reveals that the stiffener-induced failure mode can lead to a decrease in the ultimate strength of the curved plated structure coupled with an abrupt loss of in-plane rigidity.

Kim and Paik (2017) developed a multi-objective optimization procedure for the design of hull structural scantlings in VLCC. The optimization procedure includes both the minimum weight and the maximum safety as objective functions. Compared to the “as-built” reference ship, the new optimization reduces man-hours by 20%, decreases structural weight by 7% and improves the safety factors for the critical structural members.

Khedmati et al. (2017) developed empirical expressions for predicting ultimate compressive strength of welded aluminium stiffened plates used under combined transverse in-plane compression and different levels of lateral pressure. The collapse behaviour of stiffened panels under uniaxial/biaxial compression load and lateral pressure are investigated in the FE analysis by Xu et al. (2017 ab) It was found that the lateral pressure caused by water head might increase the load carrying capacity of the stiffened panels, which depends on the collapse mode that relates with the configurations of stiffener and plate.

Recent developments in innovative steel stiffeners arrangements to deck panels have emerged. Leheta et al. (2016) have proposed a Y-deck stiffener arrangement in contrast to the conventional T-shape stiffener, as illustrated in Figure 6. The Y-stiffeners lead to a substantial

increase in the overall panel safety margin to weight ratio by about 61%, compared to the conventional T-stiffeners.

Another stream of efforts on the ultimate strength of plates and panels focus on the assessment of plates with openings and damaged geometries. The influences of various geometrical characteristics of cracks on the residual ultimate strength of stiffened panels with locked cracks subjected to axial compressive loading have been analysed with the nonlinear FE method (Xu et al. 2015). It was found that the crack length affects slightly the ultimate strength where the crack lies in the longitudinal direction, while the disservice is significant when in the transverse direction. The ultimate strength of the cracked panel under uniaxial compressive load depends on the projected length of the crack which is perpendicular to the load direction.

Saad-Eldeen et al. (2016 a) have reported an experimental study on the strength of thin steel plates with a central elongated circular opening under uni-axial compression. Their study shows that the ultimate capacity of the plates decreases linearly with the increase in the opening size. For plates with small openings, the collapse mechanism remains very close to that of intact plates, while for plates with large openings, the plates behave like a column with predominantly column buckling mode.

Saad-Eldeen et al. (2016 b) investigated experimentally the residual structural capacity of steel plates with a large central ellipsoidal opening with and without locked cracks, subjected to uni-axial compressive load. A series of experimental tests have been carried out for plates with one large opening of different crack lengths. It was observed that with increasing the crack length, the dissipated energy up to the ultimate capacity is decreasing nonlinearly and affected by the combined action of the initial imperfections and the different crack responses to the applied load. The resilience of the plate with a combined action of an opening and cracks is decreasing linearly as the crack length increases. On the other hand, as the crack length increases, the toughness decreases in a nonlinear manner. For the tested plates with an opening and simultaneous cracks, a post-stress-strain model has been presented, in which the proportional and ultimate stress limits are defined, showing a decrease of the proportional limit and ultimate stress as the crack length increases.

Saad-Eldeen et al. (2016 c) studied the combined effect of both geometrical characteristics (opening and initial imperfections) and age-related damage (corrosion and cracks) on the local and global responses of thin rectangular steel plates. A series of experimental tests has been conducted for in-service steel plates with a circular opening, subjected to several damage actions and uniaxial compression. It was found that the direction of the imperfection amplitude in addition to the presence of cracks governs the collapse mode and increases the load carrying capacity of the plate rather than the increase of the plate thickness by 18% and the decrease of the initial imperfection amplitude by 20%. At the crack ends, with decreasing the breadth ratio, the ultimate stresses increase nonlinearly, taking into account the effect of corrosion degradation on the material mechanical properties.

A series of experiments for reinforced panels with a large circular and elongated lightening opening have been carried by Saad-Eldeen et al. (2017). The effect of different opening shapes, sizes as well as different initial imperfection shapes and amplitudes, on the loading carrying capacity are studied. It was observed that for the stiffened panels with a circular opening, the post-collapse shape is following the initial imperfection shape, regardless the imperfection amplitude. But for the stiffened panels, with an elongated circular opening, the final post-collapse shapes may be of any shape, except for the a height ratio of 0.37. For a large opening, introducing an elongated circular opening instead of a circular one, is more effective, as a solution in the case of a weight lightening opening, where the elongated one is reducing the weight by 37% more than in the case of a circular and provides the same strength capacity.

Zhao et al. (2016) have reported an experimental and numerical study on plate girders with openings in the web used in ship structures. Their study indicates that openings in the middle of

the web stiffener leads to a lower ultimate strength compared to openings located near the edge of the stiffener web. Kim et al. (2015) has recommended, through their extensive numerical investigation, the use of elasto-plastic analysis, which considers both the geometric and material nonlinearities to estimate the buckling or ultimate strength of plates with an opening. Their study also demonstrates that the doubling method around the opening appears to be a most effective stiffening method to enhance the resistance against compression loading.

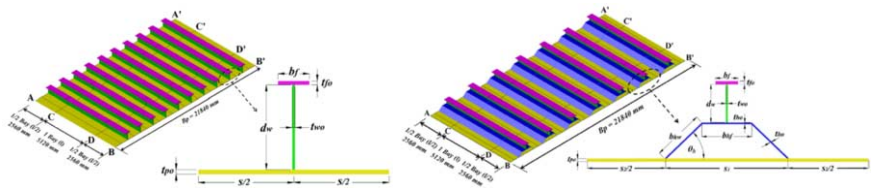

Figure 6: Configurations of the T- and Y-stiffeners [Leheta et al. (2016)].

Steel-concrete-steel plate structures have emerged to be a promising solution for arctic platforms under potential ice loading (Yan et al. 2016). Yan et al. (2016 a, b) have presented an investigation on the ultimate strength of steel-concrete-steel sandwich composite plates under patch loads and concentrated loads. Their experimental and numerical results reveal that the existing design equations in Eurocode 2 (2004) significantly over-estimates the strength of these sandwich plates. They have proposed modified equations to estimate the ultimate strength of steel-concrete-steel sandwich plates.

7.1.2 Plate connections

The recent research efforts on the welded plate connections focus on the ultimate strength of high-strength steel connections, for which the welding procedure causes adverse effect on their capacity. Khurshid et al. (2015) examine the influence of the weld metal yield strength on the load carrying capacity of S700 and S960 steels. Under-matched welds offset the beneficial effects of using high-strength steels. The decrease in the weld metal penetration also leads to a more significant reduction in the load-carrying capacity and ductility of the under-matched welds than that in the even-matched or over-matched welds. Zhao et al. (2016) have reported an experimental study on the post-weld heat treatment (PWHT) on the ductility and capacity of high-strength (S690) steel welded plate connections. They demonstrate that appropriate PWHT enhances the ductility of the welded connections at the expense of the connection strength. However, over heat-treated specimens show a significantly reduced strength.

7.1.3 Beams and girders

The deck structure of an offshore platform often employs beam or girder type structures, of which the ultimate strength remains critical in ensuring the safe operations of an offshore platform under an extreme loading event. El-Khoriby et al. (2016) have reported a numerical investigation on the strength of tubular flange plate girders with square web openings used in the deck of offshore platforms, as shown in Figure 7. Their study indicates that by locating the openings in the corners of the compression diagonals leads to effective reductions in the shear loss associated with the presence of the opening.

Daley et al. (2017) presents an investigation on the shear strength of unstiffened steel I girders. Their comparison of the experimental data with the classical shear buckling model presented by Balser (1961) demonstrates that the classical shear buckling model under-predicts significantly the shear strength of the I-girders when the web depth to thickness ratio exceeds 150.

Reis et al. (2017) presented a numerical investigation on the steel plate girders at normal and elevated temperatures. Their calibrated numerical analysis indicates that incorporation of the geometric imperfections in the numerical analysis remains essential for plate girders with an aspect ratio between 1.0 and 2.0.

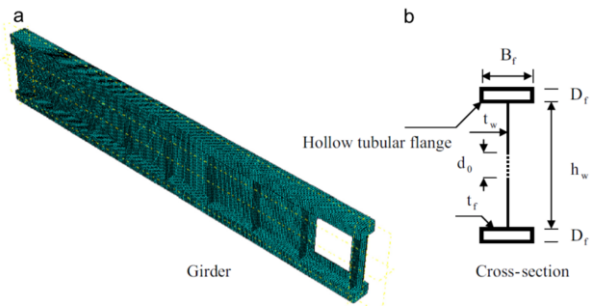

Figure 7: Configuration of the tubular flange plate girders with square web openings (El-Khoriby et al. 2016).

Some researchers have examined the ultimate strength of hull girders. Iijima et al. (2015) utilized a scale box-shape models to design a series of experiments in order to investigate the post collapse behaviour of hull girder under whipping loads. Tanaka et al. (2015) and Xu and Duan (2016) applied Incremental-iterative method (Smith method) to discuss the ultimate strength of hull girder under bending moment or combination of vertical moment and torsion. Zhang et al. (2016) utilized the intelligent supersize FE method (ISFEM) to assess the shakedown limit state of hull girder with breakage. The various assessment methods of ultimate strength for hull girder of ships or offshore structures might lead to different results and computation time. Several influential factors on the collapse behaviour of hull girder were discussed including boundary conditions, geometric ranges of finite element model, element types, loading methods and loading time by Xu et al. (2017 c). A proper numerical modelling configuration in explicit dynamic analysis is suggested to consider the balances between the accuracy and acceptable solution time.

7.1.4 Fabrication effects

The construction of ship structures may introduce significant weld-induced deformations and residual stresses, which can adversely influence the ultimate strength of the structures. Chen and Guedes Soares (2016) have examined the effects of the plate configurations on the weld-induced deformations for fillet-welded plates in ship structures, using three-dimensional thermo-elasto-plastic analyses. Their study concludes that the welding sequence induces asymmetric deformation pattern in plates with small stiffeners and the presence of residual stresses leads to 5-7% reductions in the ultimate strength of the plates. Estefen et al. (2016) have reported a combined experimental and numerical investigation on the effect of geometric imperfections on the ultimate strength of the double bottom of a Suezmax tanker. Their study focuses on the geometric imperfection caused during the construction of ships. They concluded that the shape of the initial imperfection closest to the elastic buckling mode has the most degrading effect on the ultimate strength of the hull structure. The presence of the geometric imperfection also accelerates the collapse of the bottom plates in a ship structure. Cubells et al. (2014) have adopted the photogrammetry approach to measure the initial imperfections for the ultimate strength assessment of plates, which provides an accurate input on the geometric imperfections for the subsequent ultimate strength analysis.

Tekgoz et al. (2015) investigated the effect of residual stress on the ultimate strength of a thin rectangular stiffened and single plate, through a moving heat source by changing heat input, heat speed, plate thickness and welding sequence. Modified material stress strain curves have been developed accounting for plate thickness that can be directly used in the non-linear finite element analyses of ultimate strength of thin plates. It has been found, for instance, that the plate thickness is the most influential parameter that affects the vertical displacement due to a moving heat source. The effect of the speed is more significant with respect to the heat distribution in

relation to the residual stress formation. The welding sequence is the most influential parameter that affects the lateral displacement of the stiffener due to a moving heat source, which leads to more load carrying capacity. The vertical displacement of the plate edges is quite influenced by the welding sequence and governs the buckling shape either oriented up or down depending on the welding sequence.

Fu et al. (2016) developed 3D thermo-mechanical finite element models to investigate the effects of welding sequence on welding induced residual stresses and distortions in T-joint welds. The validation of the numerical models was successfully done using some experimental tests. The obtained results show that the welding sequences have significant effects on the residual stresses and distortions, both in the magnitude and distribution mode.

Farajkhah and Liu (2016) conducted a 3D thermo-structural nonlinear finite element analyses to simulate metal inert gas (MIG) welding induced heat affected zone (HAZ), residual stress and distortion fields on the behaviour of tee-bar aluminium stiffened plates under compressive loading. It was found that MIG welding induced tensile and compressive residual stresses ranged from 72 to 77% and 18-36% of the base metal yield stress, respectively. The width of the HAZ around the weld line increases as the plate slenderness increases. The reduction in buckling strength of the tee-bar aluminium stiffened plates due to the presence of the HAZ and residual stress is as much as 10% and 16.5% respectively.

7.2 Tubular members and components

7.2.1 Tubular members

The recent research works on tubular members emphasize on the strength of high-strength steel tubular members, as well as tubular members under hazardous events. Ma et al. (2016) have reported an experimental study on the cold-formed steel tubular members, which consist of circular hollow sections (CHS) and rectangular hollow sections (RHS), with the material yield strength ranging from 700 MPa, 900 MPa and 1100 MPa. The current codes of practice provide a conservative estimation on the ultimate bending capacity of these tubular members. However, the lower material ductility decreases the rotational capacity of these high-strength tubular members compared to the normal-strength steel tubular members. Pournara et al. (2017) have reported a combined experimental and numerical study on the high-strength steel (grade 590) CHS members under axial compression and bending. The initial wrinkling imperfection affects the ultimate bending and axial capacity of tubular members. The existing design equations in EN-1993 and API RP 2A, based on mild steel members, provide reasonable but conservative assessments on the high-strength steel tubular members.

Wan and Zha (2016) have presented an experimental investigation on the concrete-filled circular hollow double steel tubular columns subjected to ISO 834-11 (2014) fire loading. The concrete-filled double steel tubular (CFDST) columns demonstrate better fire resistance with higher limiting temperatures than the normal concrete-filled steel tubes.

Buchanan et al. (2016) have proposed a continuous strength method (CSM), which allows the exploitation of strain hardening to unlock the overly conservative estimates of cross section capacity by existing design approaches based on elastic perfectly plastic material models. The comparison against 324 experimental data on circular hollow sections confirms that the CSM leads to more accurate and less scattered predictions on the axial and flexural capacities than do the existing design methods.

Van Es et al. (2016) have reported an experimental investigation on the bending strength of spiral welded steel tubes, followed by extensive numerical investigation by Vasilikis et al. (2016). The presence of girth welds and coil connection welds poses a negative influence on the tube resistance against local buckling. The numerical investigation on the spiral-welded cold-forming process indicates that the residual stresses are mainly in the hoop direction and equal about 80% of the yield strength. The residual stresses are independent of the cold forming angle

and steel grade, but there is a small effect of the *D*/*t* ratio. The numerical analysis demonstrates a beneficial effect of the residual stresses on the bending capacity of the tube in comparison to the stress free tubes.

Saad-Eldeen et al. (2018) investigated the effect of different geometrical parameters and imperfections on the ultimate bending moment capacity of multi-bay tubular reinforced structures, subjected to four-point bending, through conducting a series of nonlinear finite element analysis. It was observed that for a thickness bigger than 7 mm, the structure reaches its ultimate capacity without a post-collapse discharge, even with the presence of a combined initial imperfection. This gives an indication that the higher shell thickness is one of the most important controlling parameter in both local and global response of the cylindrical shell. With decreasing the R/t ratio, the ultimate bending moment increases nonlinearly. The number of half waves around the circumference has a significant effect on both flexural rigidity, ultimate load carrying capacity as well as the final deformation shape, which in some cases in the key parameter.

7.2.2 Tubular joints

A number of research efforts have attempted to address the ultimate strength of tubular joints under fire loadings. Shao et al. (2017) have presented a deformation rate criterion to estimate the strength of circular hollow section K-joints under elevated temperature, using results from calibrated finite element analyses. They have also proposed a reduction factor to be applied to K-joint strength at room temperature, so as to estimate the K-joint strength at an elevated temperature. Shao et al. (2017) have, in a separate study, examined the circular hollow section T-joint specimens under cyclic axial loading after they have been exposed to an elevated temperature 500 ^{o}C. The hysteretic performance of T-joints after exposed to an elevated temperature demonstrates minor deterioration in strength and ductility compared to the same T-joints under the same loading at the room temperature. Lan and Huang (2016) present a numerical study on the cold-formed stainless tubular X- and T-joints at different elevated temperatures ranging from 20 ^{o}C to 760 ^{o}C. Based on their numerical study, they have proposed a temperature reduction factor to estimate the joint strength, N_T, at temperature T,

$$N_T = \frac{k_{y,T}+k_{E,T}}{2} N_{20} \tag{9}$$

Where, $k_{y,T}$ and $k_{E,T}$ denote the reduction factor in the yield strength and elastic modulus at temperature T, while N_{20} refers to the joint strength at the room temperature. Fung et al. (2016) performed an experimental investigation on CHS T-joints under brace in-plane bending at an elevated temperature. The experimental results demonstrate a change in the failure mode caused the by the crack initiation at the weld toes under high temperature. The strength reduction at 700 ^{o}C is about 22% compared to the joint strength at the room temperature.

Some researchers have investigated the strength of tubular joints in the presence of a fatigue crack. Li et al. (2017) reported the experimental study on the strength of a fatigue-cracked circular hollow section TT-joint, and demonstrated that the load reduction factor in BS 7910 (2013) led to a conservative estimation on the strength of cracked multi-planar TT-joints. A number of research efforts (Gu et al. 2016, Aziz and Qian 2015, 2016) have proposed a non-dimensional deformation limit corresponding to the ultimate limit state for circular hollow section joints under axial tension and brace in-plane bending. To quantify the effect of fracture failure on the ultimate strength of tubular joints, Qian and Zhang (2015) have proposed an approach to integrate the material *J*-*R* curve in the limit load analysis of CHS joints dominated by fracture failure. Their approach predicts closely the ultimate capacity of the experimental CHS specimens with fracture failure.

A number of researchers have reported the ultimate strength of CHS joints with a curved chord (Chen et al. 2015, 2015 a, 2016). Figure 8 illustrates the configurations of the CHS joints with a curved chord. The ultimate strength for CHS joints with a curved chord generally exceeds that of the CHS joint with the same geometric parameters but a straight chord. However, the strength enhancement provided by filling the chord with concrete becomes less significant for joints with a curved chord than those with a straight chord in CHS X-joints and T-joints with a convex chord. For CHS T-joints with a concave chord, the strength enhancement by filling the chord with concrete is generally more significant in the joint with a straight chord than that with a concave chord, except for concave chords with a very small radius of curvature.

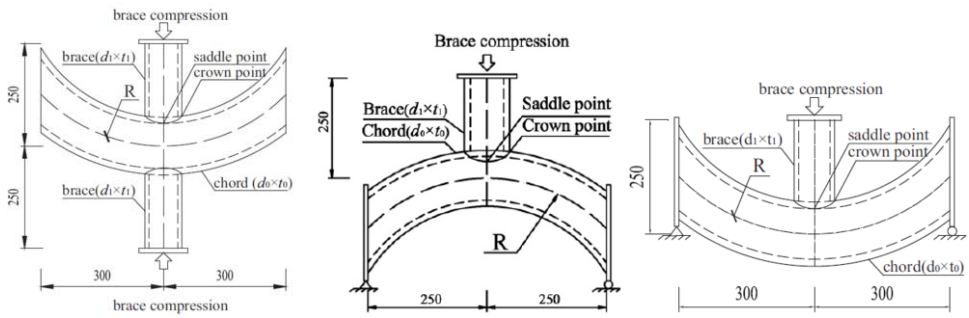

(a) (b) (c)

Figure 8: CHS joints with a curved chord: a) X-joints; b) T-joints with a convex chord; and c) T-joints with a concave chord.

7.2.3 Other types of tubular components

Elliptical hollow sections have recently emerged as an alternative structural solution to the conventional circular hollow sections. Qiu et al. (2017) have reported a numerical investigation on the slender concrete-filled elliptical hollow section members and concluded that the current design provisions in the European standard EN-1994-1-1 on circular hollow sections are applicable to the elliptical hollow sections. Liu et al. (2017) have presented a combined experimental and numerical study on the concrete-filled cold-formed elliptical hollow sections under axial compression. The ultimate strength of the concrete-filled elliptical hollow sections depends on four critical parameters, including the aspect ratio of the elliptical section, the steel-tube to concrete area ratio, the yield strength of the steel and the compressive strength of the concrete. Uenaka and Tsunokake (2016) have presented an experimental investigation on the concrete filled elliptical steel tubular members with large diameter-to-thickness ratio subjected to bending. Local buckling on the compressive side and fracture failure in the tensile side appear to the primary failure mechanisms observed in the experiment. Bending moment deformability increases as the diameter to thickness ratio of the specimen decreases, with the lowest deformability in the concrete-filled tube specimen with an outer diameter of 160 mm.

7.2.4 Reinforced tubular components

Different reinforcement schemes have emerged over the last few years to enhance the ultimate strength of tubular joints and components, e.g., by filling the circular hollow section with concrete, by wrapping fibre polymers on the external surface of the tubular members, by welding external plate stiffeners, etc.

Hou et al. (2017) have presented a numerical and theoretical study on the concrete-filled double-skin tubular (CFDST) K-joint with a circular hollow section brace subjected to axial loading. They have identified four failure mechanisms for the CFDST K-joints, namely the local buckling of the compression brace, chord plastification, chord punching shear and local bearing failure of the chord. Li et al. (2016, 2016 a) have investigated experimentally a number

of reinforced steel circular hollow section stub members under compression. Their study covers different types of reinforcement, including the seawater and seas-and concrete (SWSSC) filled stainless steel tube, carbon fibre reinforced polymer (CFRP) tube, basalt fibre reinforced polymer (BFRP) tube and glass fibre reinforced polymer tubes, a shown in Figure 9. The SWSSC filled tubes demonstrate significantly enhanced strength and ductility compared to the hollow tubes. The CFRP tubes indicate higher ultimate strength than the BFRP tubes. Fu et al. (2016) have proposed an efficient technique to install the carbon fibre-reinforced polymers (CFRP) on circular hollow section K-joints. The CFRP strengthened CHS K-joints delays, but not eliminate, the failure modes including chord plastification and punching shear, and lead to significant enhancement on the ultimate strength of CHS K-joints. Similarly, Lesani et al. (2015) have reported significant enhancement on the strength of CHS T- and Y-joints wrapped by glass fiber reinforced polymers.

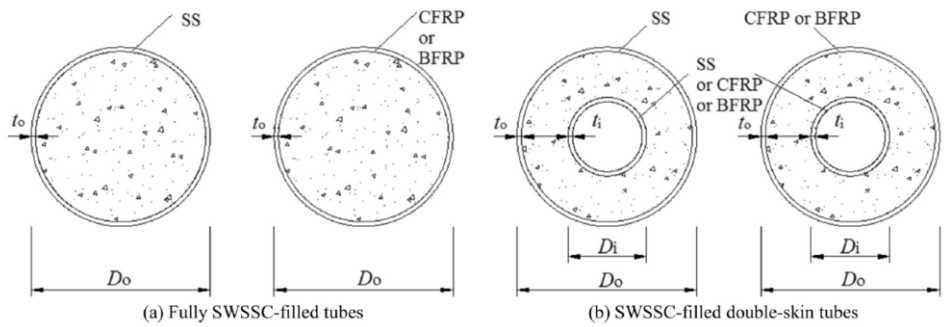

Figure 9: Different reinforcement schemes investigated by Li et al. (2016, 2016a).

Chen et al. (2016 a) have reported an experimental and numerical investigation on the double-skin CHS X-joints, for which PVC tubes are used as internal members. Their investigations demonstrate that double-skin X-joints with small chord hollow ratio (defined by the ratio of the hollow area inside the chord over the total area enclosed by the chord outer diameter) demonstrate similar ultimate strength as the fully grouted CHS X-joints, accompanied by poor ductility. In contrast, double-skin X-joints with large chord hollow ratio demonstrate similar ultimate strength levels as the hollow CHS X-joints with good ductility. Elchalakani et al. (2016) examined the plastic and yield slenderness limits for circular concrete filled tubes subjected to pure bending. They have derived new section slenderness limits for the compact and yield sections for concrete-filled tubes under pure bending. Dong et al. (2017) have presented an investigation on the effect of the external confinement in the form of FRP wraps or steel rings on reducing the delamination between the steel-concrete interfaces for concrete-filled steel tubes. They have proposed an equation to estimate the minimum confining stiffness required to prevent delamination between the concrete-steel interfaces.

Zhu et al. (2016) have presented a study on the circular hollow section T-joints with external plate stiffeners subjected to axial compression. Their study concludes that the strength enhancement by the stiffener is proportional to the length of the stiffener over the brace outer diameter ratio. For T-joints with the thickness of the stiffener exceeding the wall thickness of the chord, the strength enhancement becomes independent of the thickness of the stiffener. Nassiraei et al. (2016 a, b) have presented an investigation on the static strength of tubular T/Y-joints with collar and doubler plate reinforcement subjected to brace axial tension. Their calibrated numerical investigation indicates that the collar plate reinforced T and Y-joints demonstrate strength enhancement up to 200% and 180% respectively.

7.3 Developments in other structural components

7.3.1 Aluminium components and connections

The aluminium components and connections are widely used in offshore and ship structures. Recent research works on these structural components focus on challenging topics on the effect of impulsive loading, residual stresses, as well as aluminium panel optimization. Cerik (2017) investigated the response of fusion welded AA5083-H116 rectangular plates and orthogonally stiffened panels, often used in high-speed vessels and topsides of offshore platforms, under impulsive loading. His study indicates that the heat-affected zone (HAZ) imposes a strong influence on the ductility of the aluminium alloy structures under sudden lateral pressure loads. Van Hove and Soetens (2014) present the optimized cross-section design for aluminium shear panels in living areas on oil platforms. The optimized panels lead to a material reduction of 10% to 25% compared to the existing design for shear panels.

7.3.2 Composite components and connections

Composite materials, e.g., the carbon fibre reinforced polymer (CFRP), glass fibre reinforced polymer, polymer matric composites (PMC), etc., provide light-weight solutions which can lead to cost reductions in transport and installations. These materials become increasingly popular in the industry. However, further research works are necessary to advance the understanding on the ultimate strength of these structural components. Guz et al. (2017) present a review on the practical application of composite materials in the oil and gas industry, including GFRP, PMC and syntactic foams. They have also proposed an analytical model for thick-walled multi-layered filament-wound pipe under external pressure. De Barros et al. (2017) have presented an experimental study on the metal-composite repair for a component in FPSO. Their experimental results reveal that the steel plate reinforced by CFRP layer with a fillet (as shown in Figure 10) leads to a substantial increase (almost doubled) in the static strength.

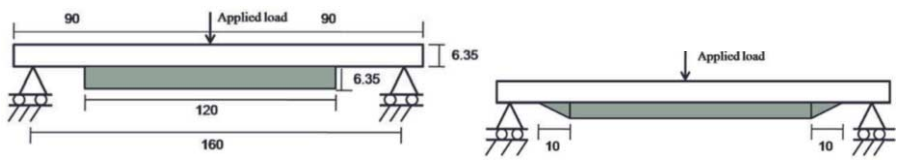

Figure 10: CFRP repair on a plate with and without a fillet (De Barros et al. 2017).

Yu et al. (2015) have presented a numerical investigation on reinforced thermplastic pipes (RTP) under combined external pressure and bending. Their analysis indicates that buckling has become a dominant failure mechanism for the RTP under this loading condition. The critical buckling load and buckling mechanism depends on the loading path. In the case of pressurization followed by rotation, buckling occurs in the kink mode, with a rapidly reduced buckling rotation with the increasing external pressure. In the case of rotation followed by pressurization, the RTP buckles immediately as the external pressure reaches the critical external pressure, which decreases as the applied rotation increases. Bai et al. (2015) have presented a theoretical model to analyze the collapse of RTP under pure external pressure, bending moment or combined external pressure and bending. Compared to a detailed 3-D finite element analysis, their theoretical model indicates a close agreement in the predicted collapse strength for pipes with $6 < D_0 / t < 12$.

7.3.3 Windows and doors

The use of very large glass windows in modern passenger vessels has posed additional challenges in the ultimate strength estimation of the side walls containing these windows. Ivaldi (2015) has summarized the growing trend in the yacht industry, highlighting the use of very large glass surfaces in modern pleasure crafts and passenger vessels. Frickie and Gerlach (2015) have presented some theoretical and numerical investigations on the effect of large openings

with and without windows on the shear stiffness of side walls in passenger ships. They have discussed the FE requirement for the wall structure with clamped or bonded glass pane. The clamped or bonded connection between the wall structure and glass pane requires a much finer mesh, whereas the glass pane can be modelled with large elements. The theoretical model based on the beam theory provides an alternative to compute the wall stiffness with an accuracy within 10%.

8. MATERIALS

8.1 Introduction

The specific influence of different materials to ultimate strength assessment continues to be of much interest. The use of higher tensile strength steels in critical structural areas is widely used, with particular attention given to its effects on ultimate strength when used in the upper decks of container ships and other large cargo vessels. Aspects related to high tensile steels are reviewed in preceding sections of this chapter, and are also investigated in the benchmark study summarised in Section 9. Use of non-ferrous metals is still mostly restricted to marine grade aluminium alloys, which continue to be used in high speed ships and other specialist craft. The ultimate strength behaviour of aluminium continues to be explored in relation to the adaptation of ultimate strength methods originally developed for steel structures. The potential use of composites for larger ships and offshore structures raises further challenges for ultimate strength assessment due to the highly bespoke stress-strain behaviour that can be produced with different materials and layup techniques.

8.2 Aluminium alloys

Marine grade aluminium alloy is a non-magnetic material with a relatively low specific weight (approximately 1/3 of steel) and an excellent formability. It can be forged, rolled in thin sheets and extruded in profiles with complex sections; such behaviours allow to the adoption of design solutions (type and geometry of structural elements, joint details) that are quite different from typical steel structures. Marine grade alloys are also particularly resistant to corrosion in marine environments. In recent years the use of aluminium alloy as the main structural material in large ship building programmes has been restricted to naval and high speed craft. Lamb et al (2011) provide a modern critical overview in the benefit and associated cost impacts of aluminium alloy for naval vessel construction, with an emphasis on the technologies used for the US Littoral Combat Ship (LCS). In the offshore sector aluminium alloy is more usually used in secondary structure, such as helidecks, where ultimate strength is an important assessment parameter.

In the structural engineering stage of an offshore helideck, Park et al. (2015) found that some design factors in Eurocode 9 are not clearly determined. Therefore, engineering decisions for some un-cleared design factors as well as methodology are newly developed. Figure 11 shows the engineering procedure with deformation based design for aluminium helideck proposed by Park et al. (2015).

Koo et al. (2014) evaluates the buckling/ultimate strength of an aluminium helideck pancake under helicopter landing impact. The evaluations with regard to the structural safety and stability of the developed aluminium pancake are carried out by BS EN 19999-1-1:2007 to comply with the design requirement. For verification with respect to evaluation by EUROCODE 9, a finite element analysis is performed.

Ha et al. (2015) developed the helideck structure with the large scaled aluminium pancake based on code check design through collaboration of experimental verification. In the structural engineering stage of the SAFE helideck, it is found that the design factors in Eurocode 9 are not clearly defined. Therefore, engineering decisions for some uncleared design factors as well as methodology are carried out. Furthermore, it is strongly recommended to ensure safety for the SAFE helideck structure in accordance with offshore regulations such as CAP437, NMA and NORSOK. Through the experimental tests such as coupon load test, fire test and friction test, the SAFE helideck structure is verified by certificate authority.

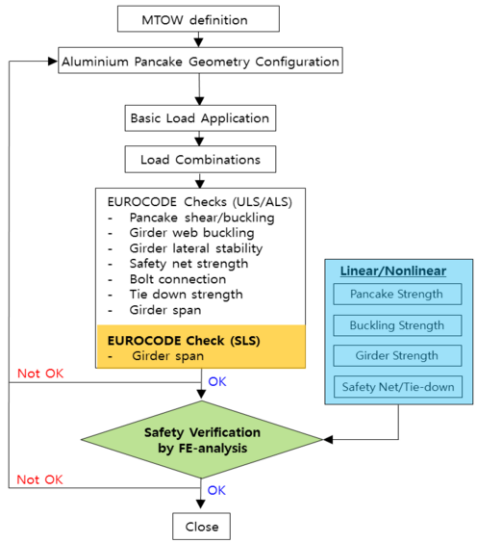

Figure 11: Design process for an offshore helideck including ultimate strength considerations (Park et al. 2015)

Seo et al. (2015) reported a numerical and experimental approach for optimal structural section design of offshore aluminium helidecks. The available literature on analyses and tests of the ultimate strength of stiffened aluminium plates is limited. Buckling tests on multi-span stiffened plates of aluminium AA5083 were carried out by Clarke (Clarke, 1987). The ultimate strength of stiffened aluminium plates under axial compression (Aalbeg et al., 1998) and bi-axial loading was studied using numerical and experimental methods. The results of the experimental and numerical analyses of torsional buckling were presented by Zha and Moan (Zha et al., 2000, 2001). Currently, there are limited published studies of new designs and/or profiles of aluminium helideck structures in offshore installations. In their study, a design procedure was developed based on section optimization techniques with experimental studies, industrial regulations and nonlinear finite element analyses. To validate and verify the procedure, a new aluminium section was developed and compared strength capacity with the existing helideck section profiles.

Seo et al. (2015) reported a numerical and experimental approach for optimal structural section design of offshore aluminium helidecks. Currently, there are limited published studies of new designs and/or profiles of aluminium helideck structures in offshore installations. In this study, a design procedure was developed based on section optimization techniques with experimental studies, industrial regulations and nonlinear finite element analyses. To validate and verify the procedure, a new aluminium section was developed and compared strength capacity with the existing helideck section profiles.

Maggiolini E et al. (2016) developed an optimised process to join 38 mm diameter tubes of 6082-T6 aluminium alloy using friction stir welding (FSW), and then to determine the fatigue performance under tension, torsion and tension–torsion loading conditions. The final outcome of the project is intended to be guidance for fatigue design of small diameter aluminium tubes joined by FSW, and his paper presents information on crack path and defects under the various loading conditions. Crack path analysis was performed using both low magnification stereo microscopy and scanning electron microscopy, in order to identify crack initiation sites, the direction of crack propagation and the interrelated influence of microstructure and weld geometry on the crack initiation path.

Khedmati et al. (2014) reported a numerical investigation into the effects of slamming impulsive loads on the elastic-plastic response of imperfect stiffened aluminium plates. In his study, the transient large deflection elastic–plastic responses of a number of stiffened aluminium panels subject to slamming impulsive loads are investigated. Several impact conditions are considered to study the influence of several structural factors such as heat affected zone (HAZ) arrangement, boundary conditions, thickness of plating, number of transverse frames and in-plane fixation. Based on these studies, several design-oriented conclusions are issued. Moreover, his paper outlines the various aspects of the influence of the HAZ presence on the strength of the slam-loaded panels with respect to loading time ratio.

Bardel et al. (2016) studied residual stresses induced by electron beam welding in a 6061 aluminium alloy. An instrumented fusion line has been performed together with macrographs in order to study the thermal field encountered during the process. These data were used to calibrate a thermal finite elements model of the process. Then, scanning electron microscopy characterizations were also performed to discuss the welding influence on grain size/shape as well as coarse precipitation state. Local deformations measured with a neutron diffraction experiment show a good agreement with the coupled modelling approach for all strain components and the "M" shaped residual strain curves, characteristic of age hardening alloys weld joints, is well reproduced.

8.3 Composite structures

Composite structures are increasingly being considered and used for lightweight material, advanced applications, in areas with high corrosion, and in areas requiring the integration of the structure with other ship systems. Uses include composites for naval vessels, patrol boats, counter measure vessels, and corvettes; composite sub-structures; composite masts; composite propulsion systems, propellers, propulsors and shafts; composite secondary structures and machinery-fittings; and composite submarine structures including pressure hulls, control surfaces, and telecom masts.

Composite and sandwich panels have some similar failure mechanisms compared to metallic panels. However, as composite and sandwich panels are usually layered structures, the interface between the layers poses a special challenge when determining the ultimate strength of these panels, and continues to be addressed in research papers.

Bai and Davidson (2016) addressed that concern by deriving a general form of governing equations for unsymmetrical the sandwich structures that includes both longitudinal and transverse interactions. A decoupled analysis procedure based on those governing equations that is applicable for design use is then developed. The model developed through the present research balances the complexity and accuracy by supplementing the transverse interaction as a decoupled subcase. Another important aspect of this study is that the governing equations are all solved with closed form solutions, which lends convenience to the future application in practical design and analysis. The upper and lower bounds of the solutions are derived and provided in the closed forms, and in that way the estimation of internal forces in composite structures is made possible. This study decouples the longitudinal land transverse interactions and investigates each of them theoretically.

Graczykowski et al. (2016) reported a preliminary research aimed at developing a comprehensive approach to modelling, manufacturing and optimal design of prestressed FRP composite structures. A simple and effective analytical model of prestressed composite is derived and further verified by two numerical models and the results of the experimental tests conducted on manufactured prestressed composite samples. Prestressing has a strong potential for improving mechanical properties of the composite structure including increase of strength, increase of stiffness and reduction of mass. The preliminary analysis of prestressed composites can be performed with the use of proposed analytical model, which gives results consistent with numerical simulations and measurements conducted on manufactured prestressed

composite elements. In addition, a process of preliminary design of prestressed composite can be performed by using described simple and efficient optimization-based method.

S.X. Wang et al. (2010) investigated low-velocity impact characteristics and residual tensile strength of carbon fibre composites laminates after impact through numerical and experimental methods. In that paper, impact force and residual strength of composite laminates were well predicted by FE model; it was created using a subroutine to enhance the damage simulation which included Hashin and Yeh failure criteria. Two different stacking sequences were investigated and the numerical degradation of residual tensile strength was compared with experimental results.

S.S. Saez et al. (2005) studied the residual compressive strength of different lay-up of laminated composites both numerically and experimentally. They obtained the trend of the average compression strength as a function of the impact energy, compared to nonimpacted specimens. All the tested laminated panels showed a similar trend: a fairly sharp reduction at low impact energy and less reduction when the impact energies increase. Failure of damaged laminates under uniaxial compression load was caused by local buckling of the sub-laminates originated in the impact. Among all the specimens, quasi-isotropic laminates showed better damage tolerance, since their normalized strength reduction was smaller at all the impact energies tested.

Cestino et al. (2016) reported a simplified procedure to identify the response at low velocity impact and evaluate, in a first approximation, the effect on the tensile and compressive structural behaviour. In this work, a simplified model to compute the initial damage characteristics in terms of maximum contact force, indentation depth and contact radius of panels subjected to low velocity impacts is proposed. Initially, the impact test results are presented in terms of maximum contact force as function of energy level and compared with experimental tests obtained by the Politecnico di Torino research group and by NASA. Afterwards, the developed delamination model and specific degradation factors are used to define the correct material for the initial damage zone of the 2D FEM simulations.

The Progressive Failure Analysis (PFA) permits attainment of the behaviour of the load as function of the global displacement, similarly to the experimental tensile test results in Figure 12

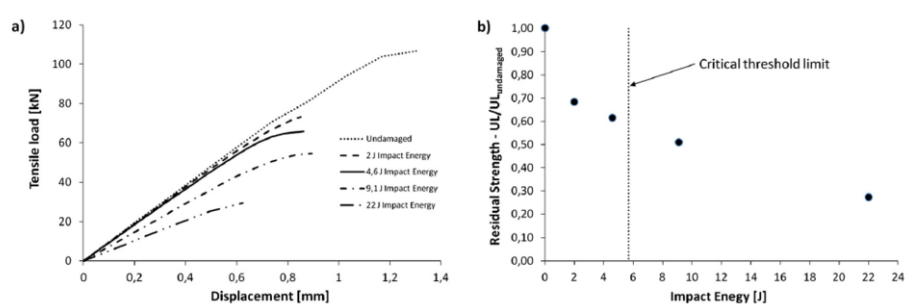

Figure 12 Comparison between the numerical behaviour under tensile load of the damaged specimens

The residual uniaxial and shear buckling capacity is studied by Cestino et al (2016). Nastran buckling analysis was carried out and compared with experimental tests. Figure 13 shows a good agreement between the experimental data and the numerical results, demonstrating the validity of the proposed model and a maximum reduction of the critical load of approximately 20% compared to the case without damage. Finally, an excellent agreement is obtained with a reduction of the shear buckling load that ranges of 10% to 30% according to the impact energy level. Figure 14 shows the comparable buckling behaviour captured in the experimental and numerical models.

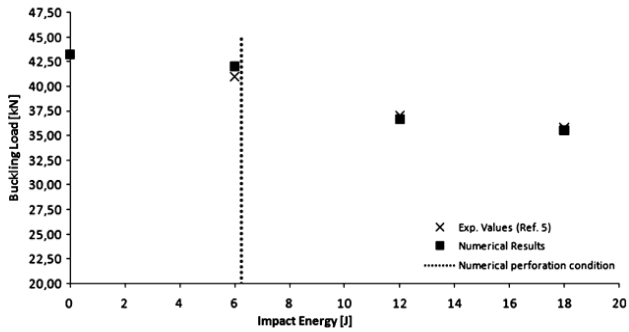

Figure 13 Comparison between the numerical and experimental results for uniaxial buckling behavior

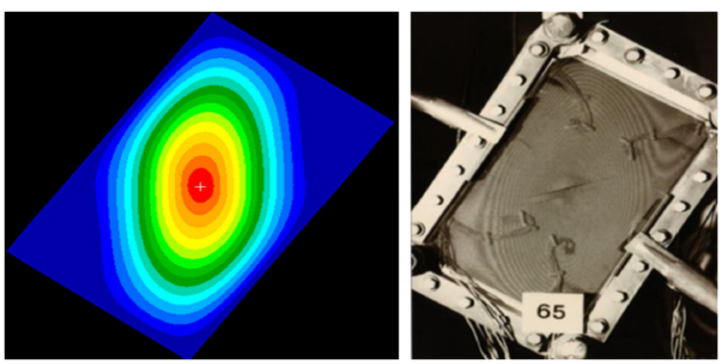

Figure 14 Buckling behaviour for positive shear load after impact at 22 J : (numerical and experimental)

9. BENCHMARK STUDY

9.1 Ultimate strength of joints subjected to fire loads

9.1.1 Scope of benchmark

Safety design of offshore topsides requires detailed assessment of the topside strength for accidental fires, explosions and other hazards. In order to document the safety of topside structure for fire loads, detailed evaluations and documentation is required regarding duration of fire action the structure can resist, amount of necessary Passive Fire Protection (PFP) or design changes when required.

Performing ultimate strength analysis of a structure under fire loads is not straightforward and involves many parameters that affect the results. The accuracy of an ultimate strength assessment can be reduced by the assumptions and limitations involved in modelling of structure, incorrect modelling of materials and selection of inappropriate types of nonlinear solvers for the analysis.

The objective of this benchmark study is to predict the strength of a typical topside joint structure subjected to fire and compare different techniques to assess the ultimate strength of these type of structures. The capabilities of modern software to simulate an incident which is possible to occur in the offshore installations are widely used to determine the strength during design of structures.

The following committee members have contributed to the benchmark:

Table 7 Committee members that have contributed to the fire load benchmark

Participation	Affiliation	Benchmark participant ID in figures	Analysis software
J. Czujko	Nowatec AS, Norway	P.1	USFOS, LS-DYNA
G. Notaro	DNV GL, Norway	P.2	USFOS, ABAQUS
D. Wang	Shanghai Jiaotong University, China	P.3	ABAQUS

9.1.2 Strategy of benchmark study

The purpose of the benchmark study is to assess the capability and accuracy of available techniques and software for the prediction of structural strength of topside structural joints under fire loads. Specific attention is given to the influence of:

1. Temperature development in the structure of joints.
2. Capacity prediction of joints for different values of temperature (duration of fire).

The strategy followed for the benchmark study is presented in Table 8.

Table 8 Strategy of the benchmark study

Title	Description
Primary study	1. Static analysis for all in-place loads 2. Push-down analysis, uniform pressure (or line load) until collapse 3. Fire analysis 4. Application of fire load defined by standard hydrocarbon fire curve
Parametric study	1. Effects of boundary conditions 2. Effects of modelling assumption, shell vs. beam element models

9.1.3 Benchmark model

9.1.3.1 Geometry

A common format CAD model of the selected topside structure was distributed to all participants, as shown in Figure 15. The CAD model is available both as 3D CAD and STEP files. The in-place loads acting on the structure were supplied to all participants, ref. Figure 15.

9.1.3.2 Material data

Strength properties of steel material

The structure is built from European grade structural steel S355. Nominal material properties are used as shown in Table 9. An isotropic bilinear elastic – perfect plastic strain model is assumed.

To perform the thermal and structural response analysis of structures under fire loads, the temperature dependency of the material properties need to be defined. Figure 16 presents the reduction factors for yield stress and elastic modulus at elevated temperature defined according to Eurocode 3 (EUROCODE, 2005).

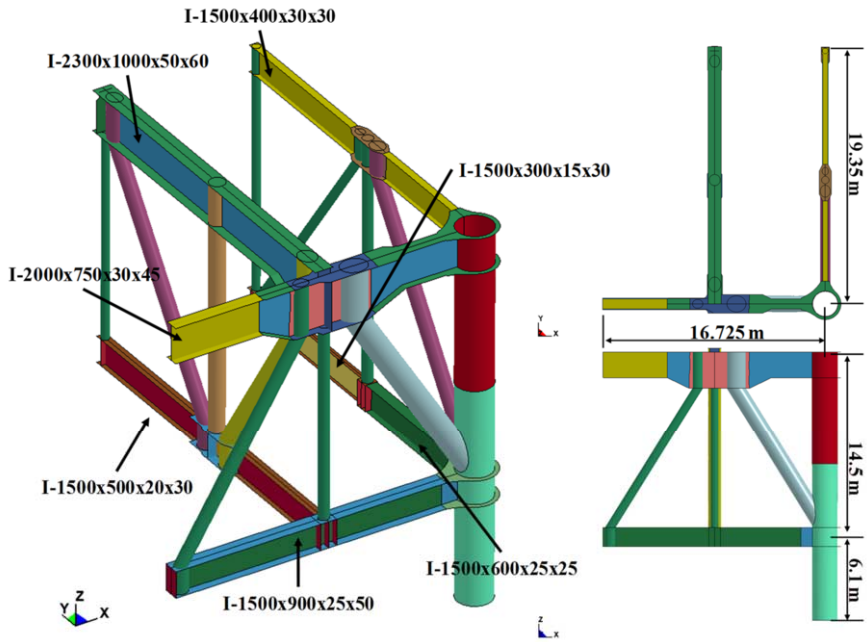

Figure 15 Main dimension and coordinate system.

Table 9 Material properties at room temperature

Young modulus [MPa]	210000
Poisson ratio [-]	0.3
Yield stress [MPa]	355
Ultimate tensile stress [MPa]	630
Density [Kg/m^3]	7850
Specific heat (J/Kg K)	439.8
Thermal conductivity (W/m K)	53.33

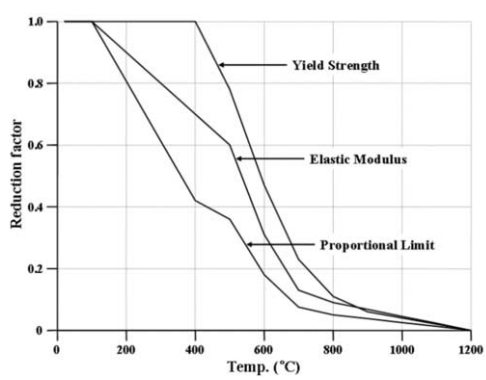

Figure 16 Reduction factors at elevated temperatures.

Thermal properties of steel material

The carbon steel material curves for elevated temperatures specified in Eurocode 3 were used in the thermal and structural analysis. Figure 17 shows the curves for specific heat capacity and thermal conductivity, respectively (EUROCODE, 2005).The surface emissivity of steel was set to 0.8 for all structural members exposed to fire.

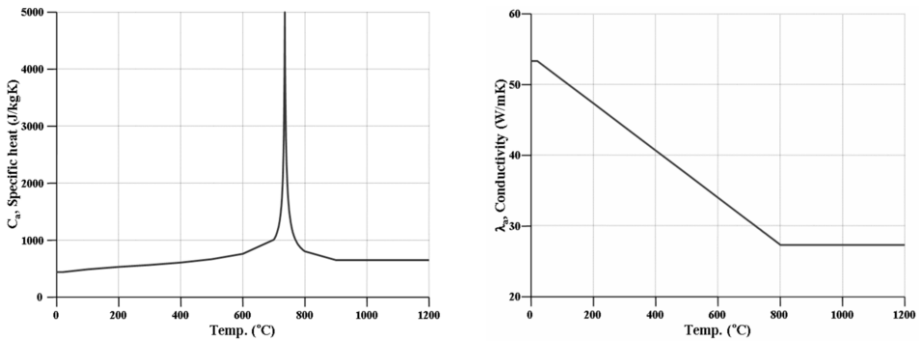

Figure 17 Properties of steel: specific heat capacity (left) and conductivity (right).

Table 10 presents the equations for thermal properties of carbon steel according to Eurocode (EUROCODE, 2005).

Table 10 Temperature dependent thermal properties

Thermal properties	*Equation*
Specific heat, C_a $(\mathrm{J/kgK})$	$\begin{cases} 425+7.73\times10^{-1}\theta_a-1.69\times10^{-3}\theta_a^{\,2}+2.22\times10^{-6}\theta_a^{\,3} & (20°C\le\theta_a<600°C) \\ 666+13002/(738-\theta_a) & (600°C\le\theta_a<735°C) \\ 545+17820/(\theta_a-731) & (735°C\le\theta_a<900°C) \\ 650 & (900°C\le\theta_a<1200°C) \end{cases}$
Thermal conductivity, λ_a $(\mathrm{W/mK})$	$\begin{cases} 54-3.33\times10^{-2}\theta_a & (20°C\le\theta_a<600°C) \\ 27.3 & (800°C\le\theta_a<1200°C) \end{cases}$
Thermal elongation, $\Delta l/l$	$\begin{cases} 1.2\times10^{-5}\theta_a+0.4\times10^{-8}\theta_a^{\,2}-2.416\times10^{-4} & (20°C\le\theta_a<750°C) \\ 1.1\times10^{-2} & 750°C\le\theta_a<860°C) \\ 2\times10^{-5}\theta_a-6.2\times10^{-3} & (860°C\le\theta_a<1200°C) \end{cases}$

Parameters for thermal analysis

The values of parameters needed to perform thermal analysis is given in Table 11.

9.1.3.3 Boundary conditions

The boundary conditions set for the target structure are as follows;

- The structure is fixed at the vertical column supporting point (position 1 in Figure 18)
- Other supporting points (positions 2-7 in Figure 18) are fixed except the vertical Z-directional translational motion which is free

Table 11 Parameter for thermal analysis

Parameter	*Value*
Configuration factor, Φ	1
Surface emissivity of the member, ϵ_m	0.8
Emissivity of fire, ϵ_f	1
Shadow effect, ksh	1
Convection heat transfer coefficient, α_c (W/m^2k)	50
Stefan–Boltzmann constant, σ (W/m^2k^4)	5.67E-08

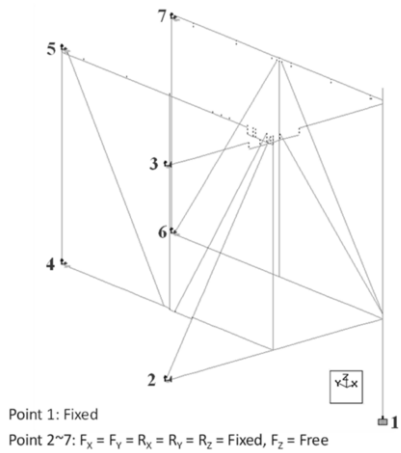

Figure 18 Boundary condition for the target topside structure.

Table 12 Summary of boundary conditions.

Boundary condition	Descriptions (fixed=1)
Point 1	The structure is fixed supported at the supporting point 1
Other points	2 (UX, UY, RX, RY, RZ =1, UZ =0) 3 (UX, UY, RX, RY, RZ =1, UZ =0) 4 (UX, UY, RX, RY, RZ =1, UZ =0) 5(UX, UY, RX, RY, RZ =1, UZ =0) 6 (UX, UY, RX, RY, RZ =1, UZ =0) 7 (UX, UY, RX, RY, RZ =1, UZ =0)

9.1.3.4 Loads

Mechanical actions

Three load cases are defined in Table 13. The target structure is initially loaded with self-weight gravity forces (LC1). A uniform line load is applied to the upper deck beams with a distribution shown in Figure 19. The design load case of 100kN/m / 250 KN/m is defined in LC2. This line load is progressively scaled until the structure collapses using a push-down type analysis (LC3).

Table 13 Mechanical load case summary.

Load case	*Loading condition*	*Based on*	*Remarks*
LC1	*Gravity*	=1.1*9.81 (m/s2)	Gravity loads are applied individually.
LC2	*Uniform line load*	=100 (kN/m), 250 kN/m	Uniform line loads are applied only on upper deck beams as showed in Figure 19.
*LC3**	*Uniform line load*	= LC2*scale factor	Uniform line load (LC2) with scale factor

*LC3 is used for push-down analysis

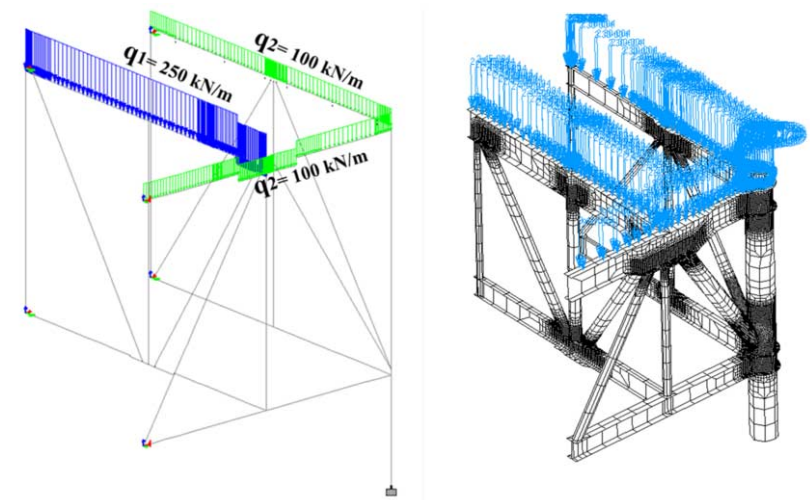

Figure 19 Uniform line load and pressure applied on the target structure

Fire actions

The target deck structure was subjected to fire actions defined by Standard Hydrocarbon fire curves.

In case of hydrocarbon fire, Eurocode provides the standard hydrocarbon fire equation as follows (EUROCODE, 2005);

$$\theta_g = 20 + 1080(1 - 0.325e^{-0.167t} - 0.675e^{-2.5t}) \quad (10)$$

Where, θ_g = gas temperature near the steel member in °C; and t = time in minutes.

Figure 20 shows the standard hydrocarbon fire curve applied in the benchmark.

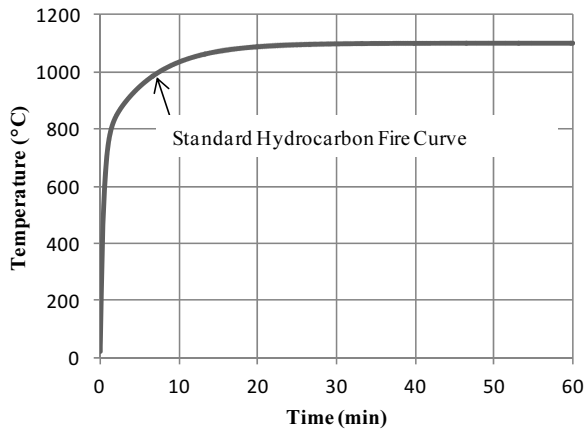

Figure 20 Standard hydrocarbon fire curve.

9.1.3.5 Monitoring of results

Figure 21 presents the location of monitoring points for reporting of deflections/damage during fire and residual deflections after fire over the target structure surface. The monitoring points considered were at the centre of the web of each I-beam. From a practical point of view the flange is more important, but it was decided to report the results on the centre of the web for simplicity reasons and to enable direct comparison to the beam element model. However, in case where the vertical column is extended up to the upper flange of main deck beam, the monitoring point was considered at the upper flange, otherwise at the centre of web.

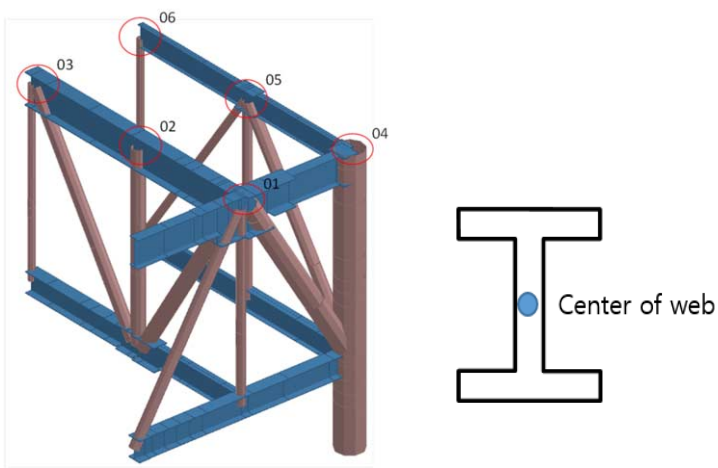

Figure 21 Location of monitoring points on the target structure, deformation and temperature.

9.1.4 Results of benchmark study

9.1.4.1 Static analysis

Static analysis considering in-place loads

Static analysis was performed by considering all in-place loads (self-weight and line load). Table 14 summarizes the modelling approach and reaction forces for in-place loads calculated by the participants of the benchmark study.

The static analysis shows close agreement between participants. This suggests that the modelling approach, mesh refinement and boundary conditions are consistent between participants.

Table 14 Modelling approach for benchmark study

Participant	*Software*	*Element type*	*Load (MN)*	
			LC1	*LC2*
Particip.1	*USFOS*	*Beam*	*3.117*	*8.448*
	LS-DYNA	*Shell*	*3.123*	*8.446*
Particip.2	*USFOS*	*Beam*	*3.042*	*8.448*
	ABAQUS	*Beam*	*3.042*	*8.448*
	ABAQUS	*Shell*	*3.186*	*8.454*

Table 15 Deflection at monitoring points due to in-place loads (*Unit: mm*); participant P.1

Load Case	*Model*	*M.P.1*	*M.P.2*	*M.P.3*	*M.P.4*	*M.P.5*	*M.P.6*
Gravity, LC1	*USFOS*	*1.31*	*2.68*	*3.2*	*0.23*	*0.91*	*1.46*
	LS-DYNA	*1.39*	*2.74*	*3.32*	*0.36*	*0.94*	*1.57*
Gravity (LC1) + Line Load (LC2)	*USFOS*	*6.12*	*14.54*	*17.49*	*0.89*	*4.38*	*7.53*
	LS-DYNA	*6.4*	*14.70*	*17.8*	*1.41*	*4.71*	*8.37*

9.1.4.2 Push-down analysis (with in-place loads)

Comparison of the collapse strength

In order to calculate the collapse strength of the target structure, push-down analysis was performed (LC3). Figure 22, Figure 23 and Figure 24 show the comparison of results for push-down analysis among all participants using shell and beam element models. The results indicate that the beam and shell element models have good agreement in the pre-collapse elastic region. The results show more substantial differences as the structure develops plasticity and approaches the collapse point. The collapse strength of structure reported by each participant differ by about ±7.5% with the mean value. On average beam element models show slightly higher predicted collapse strength, which may be due to a more restricted capability for modelling the spread of plasticity through the cross section. The ABAQUS beam model predicts a sharper transition from elastic to plastic region compared to all other results.

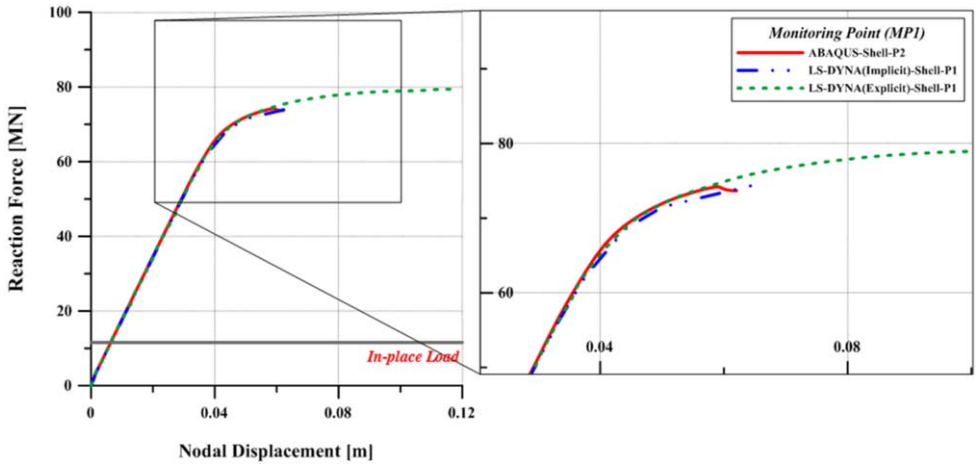

Participant	*Software*	*Element type/Time integration scheme*	*Load (MN)*	*Δ Collapse strength (%)*
Particip.1	*LS-DYNA*	*Shell/Implicit*	*74.43*	*-1.02*
	LS-DYNA	*Shell/Explicit*	*79.42*	*+5.62*
Particip.2	*ABAQUS*	*Shell*	*71.73*	*-4.61*
Average collapse strength			*75.19*	

Figure 22 Comparison of the collapse strength in shell element models

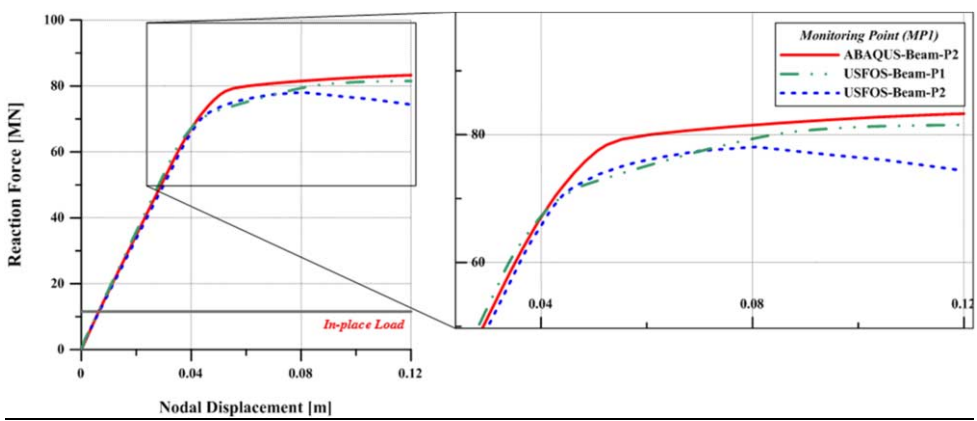

Participant	*Software*	*Element type/Time integration scheme*	*Load (MN)*	*Δ Collapse strength (%)*
Particip.1	*USFOS*	*Beam*	*81.49*	*+0.61*
Particip.2	*USFOS*	*Beam*	*78.08*	*-3.61*
	ABAQUS	*Beam*	*83.43*	*+3.00*
Average collapse strength			*81.00*	

Figure 23 Comparison of the collapse strength in beam element models

9.1.4.3 Heat transfer analysis

The objective of the benchmark study was to assess the capability and accuracy of available techniques for the prediction of structural response of topside structural joints subjected to a standard hydrocarbon fire curve.

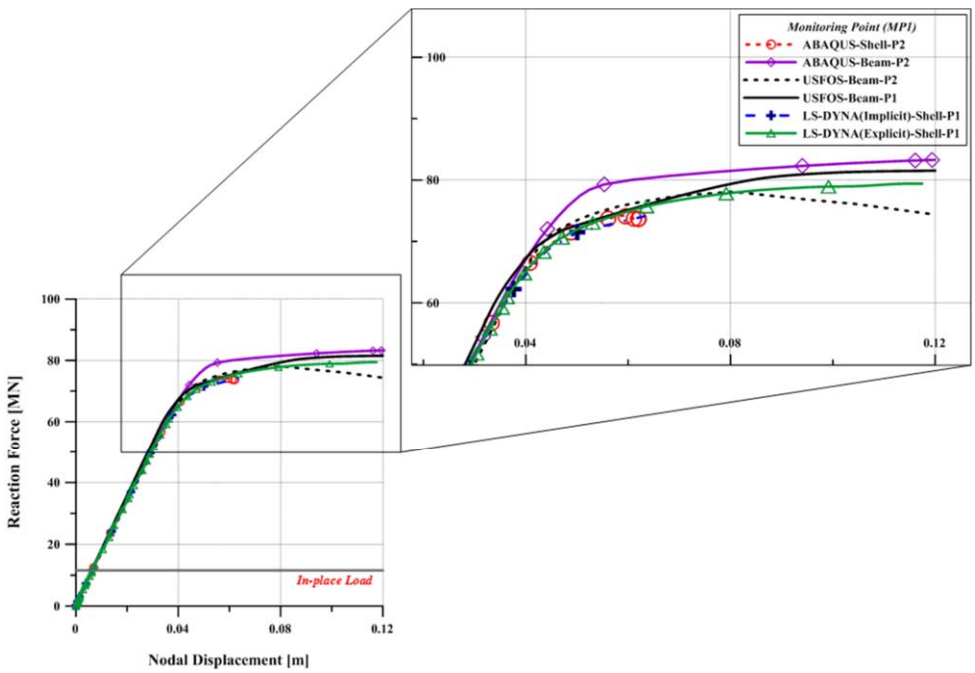

Participant	*Software*	*Element type/Time integration scheme*	*Load (MN)*	*Δ Collapse strength (%)*
Particip.1	*USFOS*	*Beam*	*81.49*	*+4.35*
	LS-DYNA	*Shell/Implicit*	*74.43*	*-4.70*
	LS-DYNA	*Shell/Explicit*	*79.42*	*+1.69*
Particip.2	*USFOS*	*Beam*	*78.08*	*-0.02*
	ABAQUS	*Beam*	*83.43*	*+6.83*
	ABAQUS	*Shell*	*71.73*	*-8.15*
Average collapse strength			*78.10*	

Figure 24 Comparison of the collapse strength with elements types

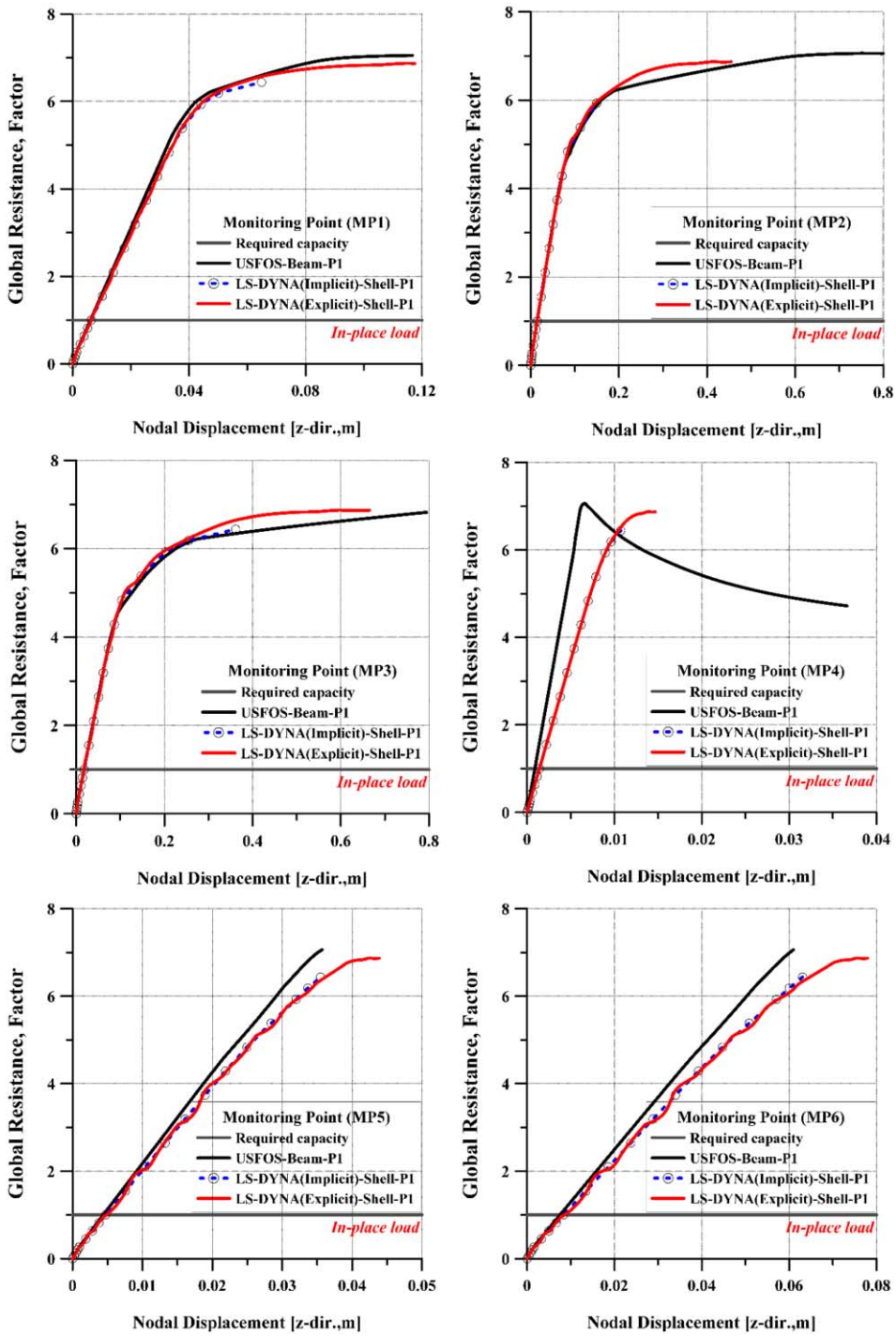

Figure 25 Comparison of results for push-down analysis between shell and beam element models at each monitoring point (from P.1)

Comparison of heat transfer analysis

Before presenting the results of the structural response once subjected to fire, the results of the heat transfer analysis are compared. Figure 26 shows location and thickness of the main beams and pipes. Figure 27, Figure 28 and Figure 29 show the results of heat transfer analysis for 60 minutes fires at three locations. These results show the development of high temperatures at all locations is similar in all FE models. This means the subsequent structural response analyses have a comparable starting point in terms of the heat transfer.

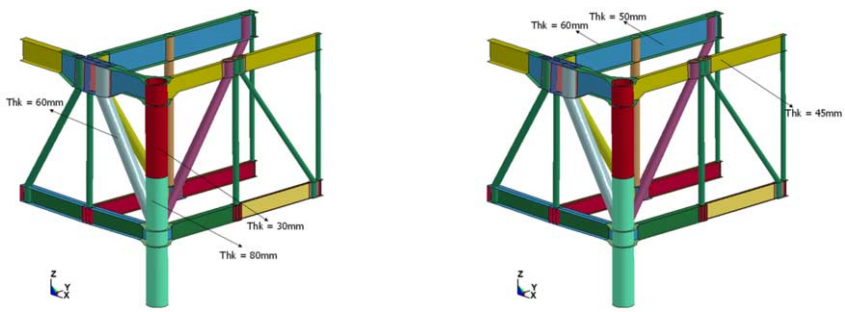

Figure 26 Location and thickness of pipes and beams

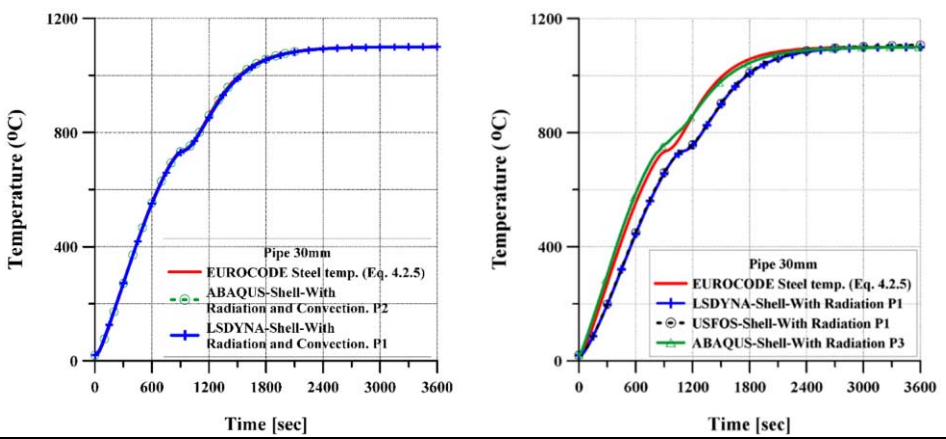

Software	*Element type/ Time integration scheme*	*Convection*	*Radiation*	*Temperature (°C) 1000s/2000s*	*ΔTemp. (%) at 1000s*	*ΔTemp. (%) at 2000s*
EUROCODE	-	-	-	*752/1077*	-	-
USFOS	*Beam*		✓	*710/1050*	*-5.58*	*-2.51*
LS-DYNA	*Shell/Explicit*		✓	*709/1045*	*-5.72*	*-2.97*
LS-DYNA	*Shell/Explicit*	✓	✓	*750/1075*	*-0.27*	*-0.19*
ABAQUS	*Shell*		✓	*787/1067*	*+4.65*	*-0.93*
ABAQUS	*Shell*	✓	✓	*753/1077*	*+0.13*	*0.00*

Figure 27 Comparison of results of the heat transfer analysis with different modelling approaches, pipe 30mm.

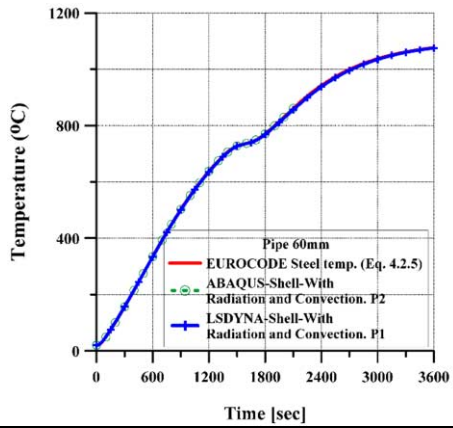

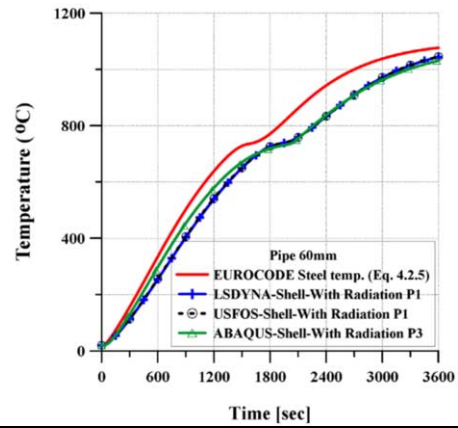

Software	*Element type /Time integration*	*Convection*	*Radiation*	*Temperature (°C) 1000s/2000s*	*Δ Temp. (%) at 1000s*	*Δ Temp. (%) at 2000s*
EUROCODE	-	-	-	*552/830*	-	-
USFOS	*Beam*		✓	*453/743*	*-17.93*	*-10.48*
LS-DYNA	*Shell/Explicit*		✓	*451/742*	*-18.29*	*-10.60*
LS-DYNA	*Shell/Explicit*	✓	✓	*550/825*	*-0.36*	*-0.60*
ABAQUS	*Shell*		✓	*500/734*	*-9.42*	*-11.57*
ABAQUS	*Shell*	✓	✓	*552/830*	*0.00*	*0.00*

Figure 28 Comparison of results of the heat transfer analysis with different modelling approaches, pipe 60mm.

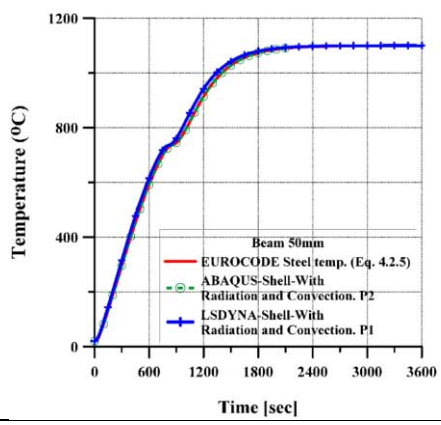

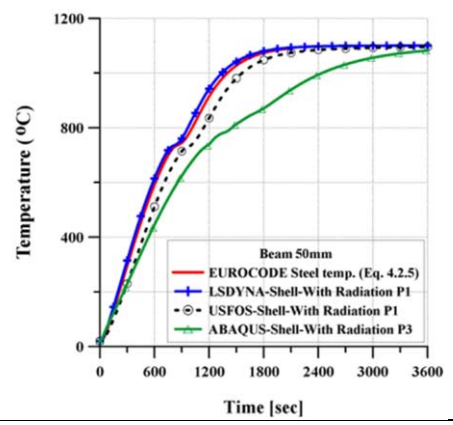

Software	*Element type /Time integration*	*Convection*	*Radiation*	*Temperature(°C) 1000s/2000s*	*ΔTemp. (%) at 1000s*	*ΔTemp. (%) at 2000s*
EUROCODE	-	-	-	*791/1087*	-	-
USFOS	*Beam*		✓	*735/1068*	*-7.08*	*-1.75*
LS-DYNA	*Shell/Explicit*		✓	*740/1077*	*-6.45*	*-0.92*
LS-DYNA	*Shell/Explicit*	✓	✓	*821/1090*	*+3.79*	*+0.28*
ABAQUS	*Shell*		✓	*620/734*	*-21.62*	*-32.47*
ABAQUS	*Shell*	✓	✓	*791/1087*	*0.00*	*0.00*

Figure 29 Comparison of results of the heat transfer analysis with different modelling approaches, beam 50mm.

9.1.4.4 Fire strength analysis

USFOS, Standard HC fire curve

The loading condition was the application of standard hydrocarbon fire curve on the whole structure. Figure 30 shows the temperature distributions and plastic utilization plot after 1580s of fire.

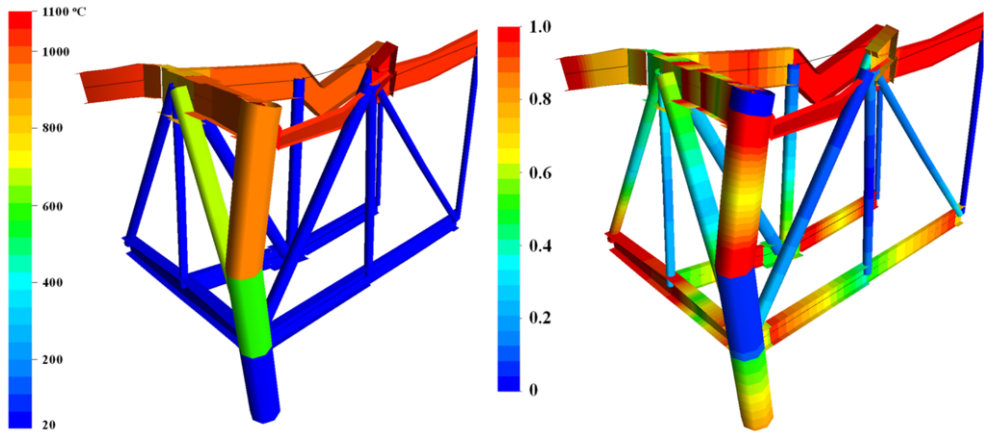

(a) Temperature distributions (b) Plastic utilization

Figure 30 Temperature distributions and plastic utilization plot at t =1580 s.

The deformed shape calculated by USFOS after 1580 s of fire in presented in Figure 31. Figure 32 shows the vertical deformation curve at monitoring points 1 and 2.

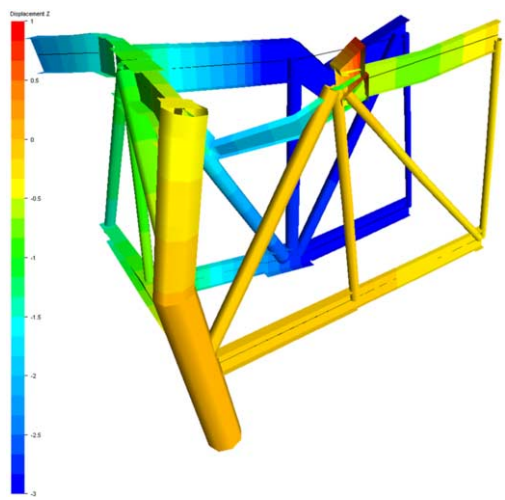

Figure 31 Deformed shape predicted by USFOS at collapse state.

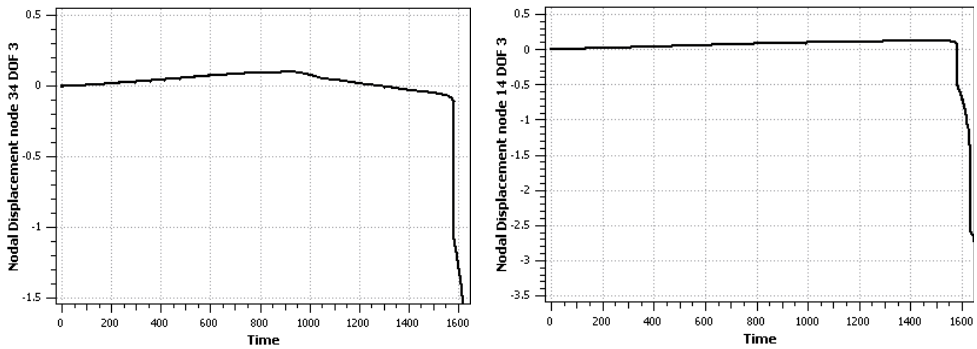

(a) Monitoring point 1 (b) Monitoring point 2

Figure 32 Vertical deformation curves at monitoring point 1 and 2.

USFOS, Standard HC fire curve. Push-down analysis

To check the global collapse time of target structure under defined fire loads, a push-down analysis was performed.

Push-down analysis is performed for different fire duration time (i.e. 5, 10, 15, 20 min etc.). The fire resistance versus global displacement is plotted for each case in Figure 33. The peak resistance of each case vs. fire time as presented in Figure 34. This single curve describes the performance of the structure during fire to demonstrate how the ultimate resistance degrades. The load resistance is presented as a global resistance factor compared to the design load (LC2). A value of under 1 means the capacity drops below the design demand. The analysis predicts that the collapse time is about 26 minutes from the start of the fire.

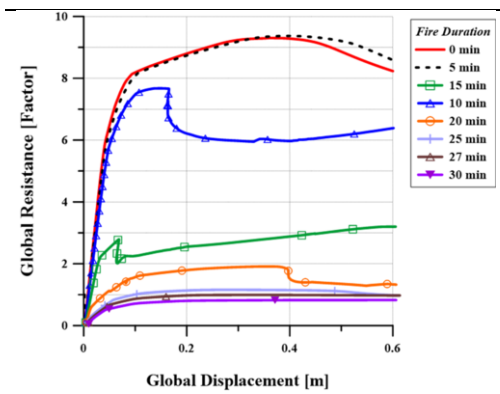

Figure 33 Ultimate resistance versus global displacement.

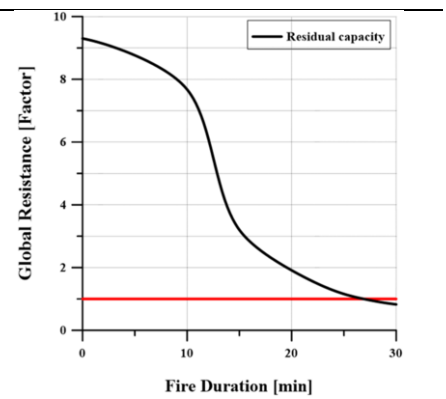

Figure 34 Ultimate resistance versus fire duration.

LS-Dyna, Standard HC fire curve

Fire structural consequence analysis has also been performed for the shell model. The analysis was performed both in explicit and implicit solvers. The implicit analysis stops at duration, t = 888 s and explicit analysis stops at t=986 s. Figure 35 to Figure 37 below illustrate the temperature distributions and displacements at this time calculated by LS-DYNA.

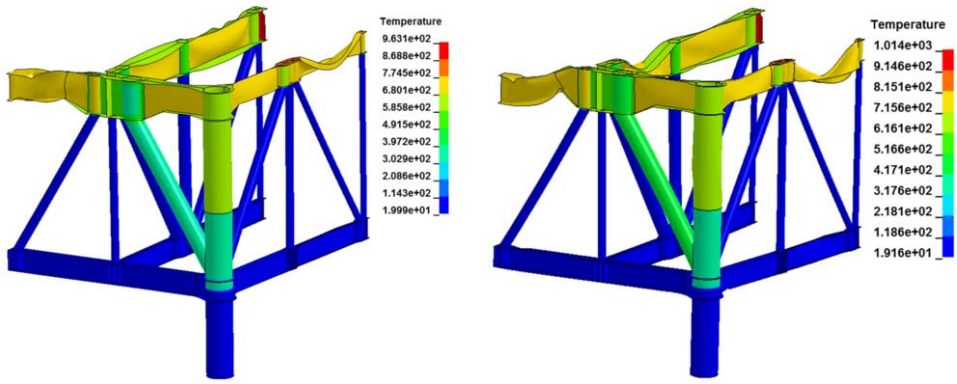

(a) Implicit, t = 888 s (b) Explicit, t =986 s

Figure 35 Temperature distributions predicted by LS-DYNA.

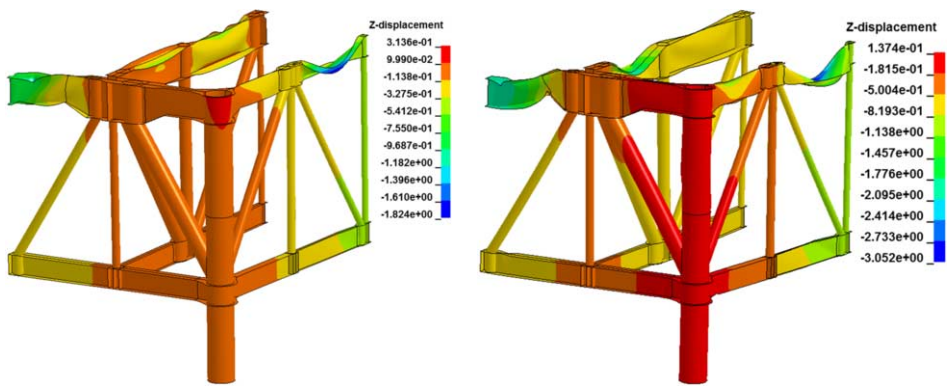

(a) Implicit, t = 888 s (b) Explicit, t =986 s

Figure 36 Deformed shapes at collapse state

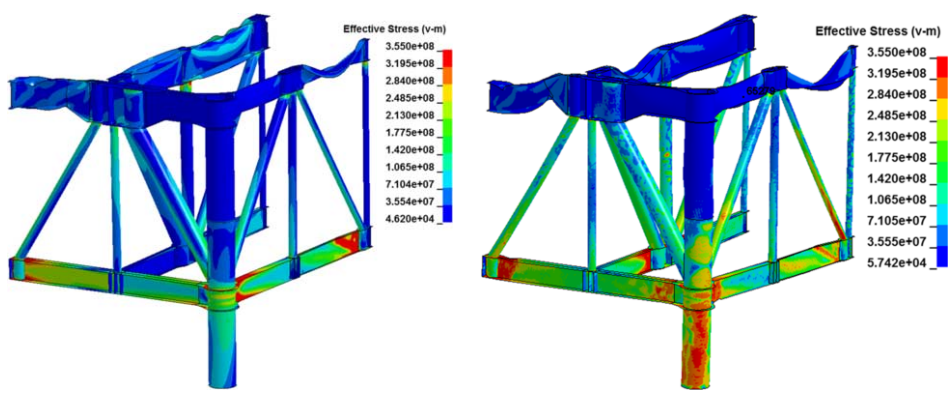

(a) Implicit, t = 888 s (b) Explicit, t =986 s

Figure 37 von-Mises stress distribution

9.1.4.5 Comparison of beam models vs. shell models results

Figure 38 shows the comparison of results for standard hydrocarbon fire between beam element model and shell element model. The results show that the shell model predicts the collapse time of the target structure earlier than the beam model.

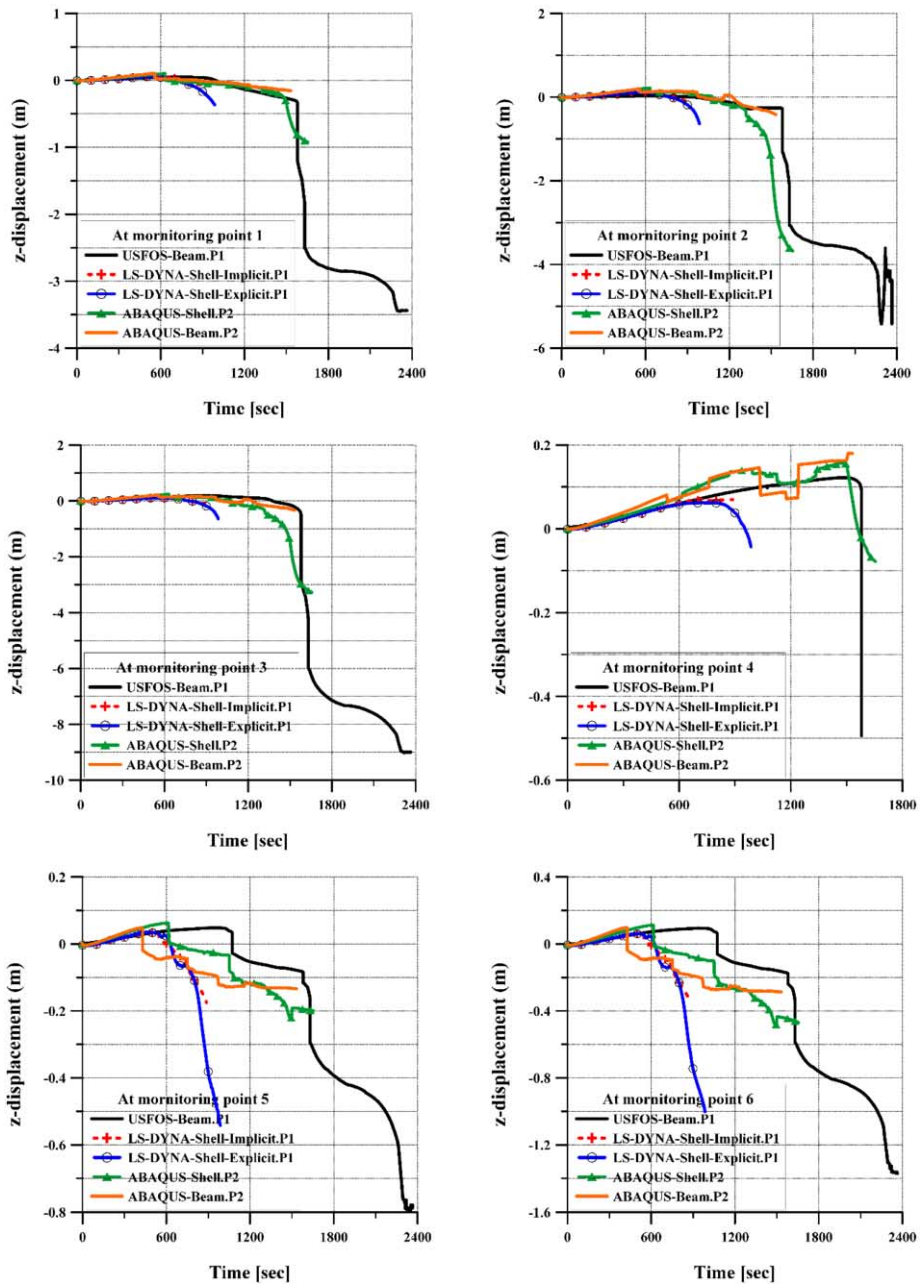

Figure 38 The comparison of results for standard hydrocarbon fire between beam and shell element model.

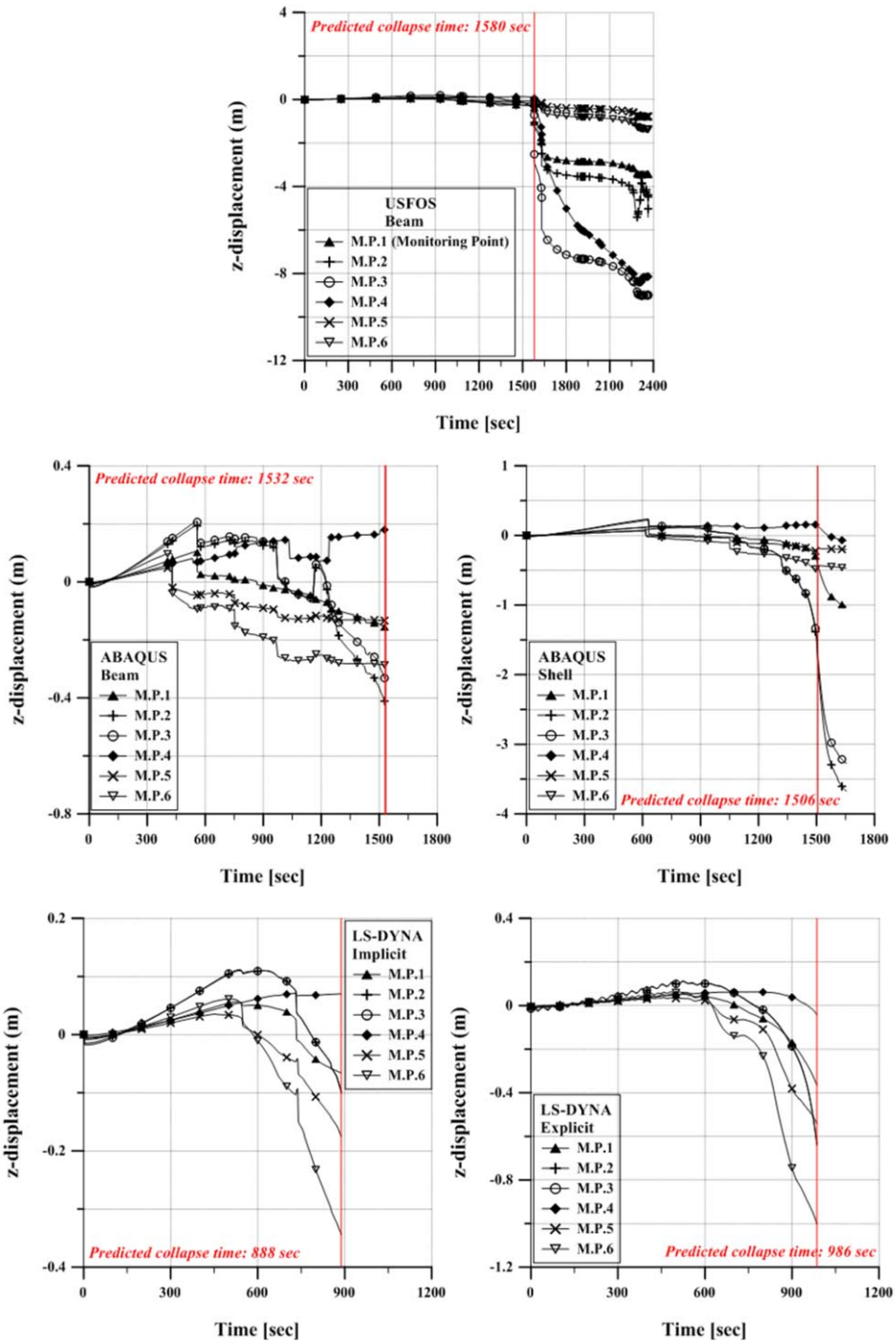

Figure 39 Comparison of predicted collapse time

Table 16 Comparison of collapse time predicted by participants

Participant	*Software*	*Element type/Time integration scheme*	*Predicted Collapse Time (sec)*
P.1	*USFOS*	*Beam*	*1580*
	LS-DYNA	*Shell/Implicit*	*888*
	LS-DYNA	*Shell/Explicit*	*986*
P.2	*ABAQUS*	*Beam*	*1532*
	ABAQUS	*Shell*	*1506*

9.1.5 Conclusions

The referenced benchmark study consisted of a relatively simple structural arrangement, i.e. a selected part of an offshore topside structure subjected to fire loads. Temperature of the structure due to fire loads calculated within the benchmark compared well with temperature calculated using EUROCODE when both the radiation and convection effects were included in the FE analysis. Predicted strength of joints under fire loads was significantly different for FE beam models and FE shell models. This benchmark proved to be complex enough to cause significant scatter in the results when analysed by a group of experts. This scatter was attributed to the underlying simulation assumptions made by the analysts. The results provide an invaluable insight into the variability of predictions when different factors are used for influential parameters, one of which being the analysts themselves.

9.2 Ultimate strength of box girders subjected to bending

9.2.1 Scope of benchmark

The objective of this benchmark study is to validate methods to predict the ultimate strength of box girders under pure bending moment using finite element analysis, specifically through comparison with three box girder buckling tests performed by the Technical University of Lisbon (IST), (Gordo, J. M., Guedes Soares, C., 2009). These box girders were previously analysed in ISSC 2015. Details of the experiments can be found in the ISSC report together with the original publications from IST. The analysis completed here differs from the previous ISSC report in the way the box girder is modelled using FEM.

In the previous ISSC all FEM analyses were modelled with the test section only. Bending moment was induced in these models using rigid body multi point constraints and incremental rotation. All results were presented as bending moment – curvature plots. The previous ISSC report shows good agreement between benchmark participants but significant differences between the FEM and experimental results. Conclusions drawn by the ISSC2015 committee included the difficulties to properly replicate the real boundary conditions from the experiment in a pure bending moment analysis applied to a prismatic section. The report also proposed that differences between the nominal and actual thickness of the plating could cause the large discrepancy between numerical and experimental results.

In this ISSC all FEM analyses were modelled with the entire test rig represented. This allowed the actual boundary conditions used in the experiment to be represented. All results are presented as load – displacement plots with displacement measured at the load application points. These analyses provide a more direct comparison to the experimental results, but do not necessarily induce the same load conditions on the boxes as previously completed in ISSC 2015.

A 3D geometry model of the three box girders was shared to facilitate this benchmark study. The models are available as STEP files.

The following committee members have contributed to the benchmark:

Table 17 Committee members contributed to the benchmark

Participant	Affiliation	Benchmark participant ID in figures	Solwers
J. Czujko	Norway	P.1	LS-DYNA
J. Broekhuijsen	The Netherlands	P.2	LS-DYNA
D. Wang	China	P.3	ABAQUS
D. Yanagihara	Japan	P.4	MSC Marc
M. C. Xu	China	P.5	ANSYS
J. Boulares	USA	P.6	ABAQUS
J.S. Park	Korea	P.7	NASTRAN

9.2.2 Strategy of benchmark

The objective of this benchmark study is to validate methods to predict the ultimate strength of box girders under pure bending moment using finite element analysis. The strategy followed for the benchmark study is presented in Table 18.

Table 18 Strategy of benchmark study

Title	Descriptions
Primary study	1. Accurate modelling of box girders geometry and representation of boundary conditions. 2. Application of static force/displacement to generate four point bending.

9.2.3 Benchmark models

9.2.3.1 Geometry

The target structures are 600x800mm box girders with different stiffener spacing and constructed from high tensile steel. The geometry of the target structures is shown in Figure 40 to Figure 43 and in Table 19. The total length of the box girders are 1000, 1100 and 1400 mm respectively with corresponding frame spacing of 200, 300 and 400 mm. In Table 19 the specimens are arranged in 3 groups: H4 for all of them means high tensile steel of 4 mm thickness; the second term indicates the spacing between longitudinal stiffeners; the last term is the frame spacing times the number of spans. The longitudinal stiffeners have flat bar shape of 20x4 mm (S690). The transverse frames have L profile of 50x28x6 and are made of mild carbon steel.

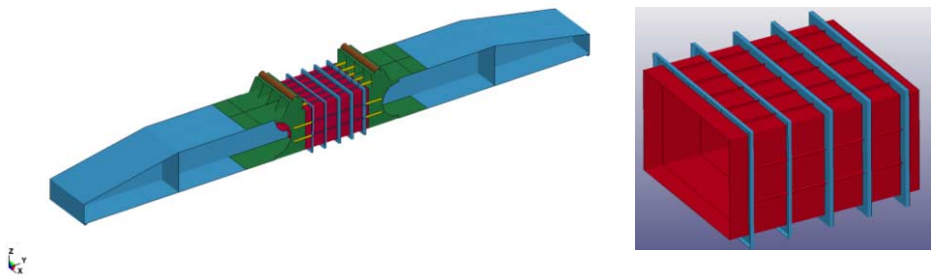

Box Girder – H200

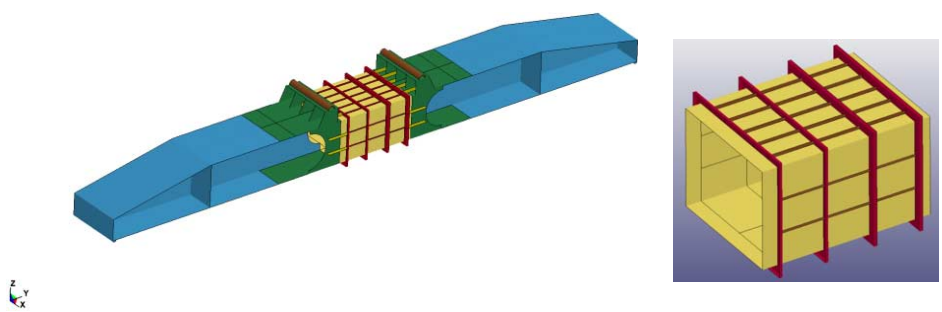

Box Girder – H300

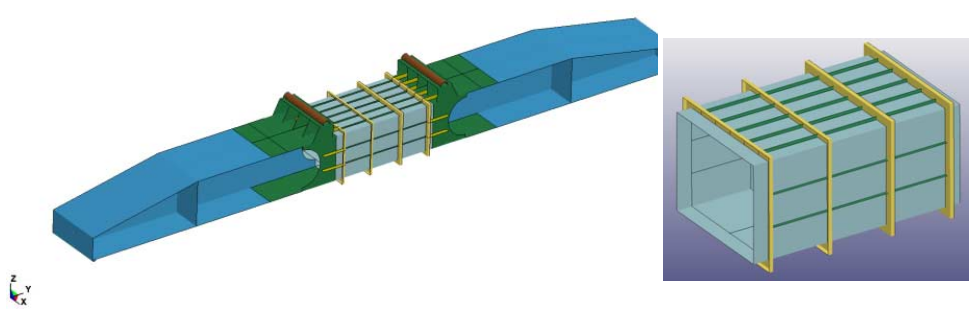

Box Girder – H400

Figure 40 Target box girders and supporting structure

Table 19 Characteristics of the box girders.

Box Girder	Length (mm)	Span (mm)	Breadth (mm)	Depth (mm)	Stiffeners
H200	100+4×200+100	200			B20×4mm,
H300	100+3×300+100	300	800	600	L50×28×6 mm
H400	100+3×400+100	400			(transverse frame)

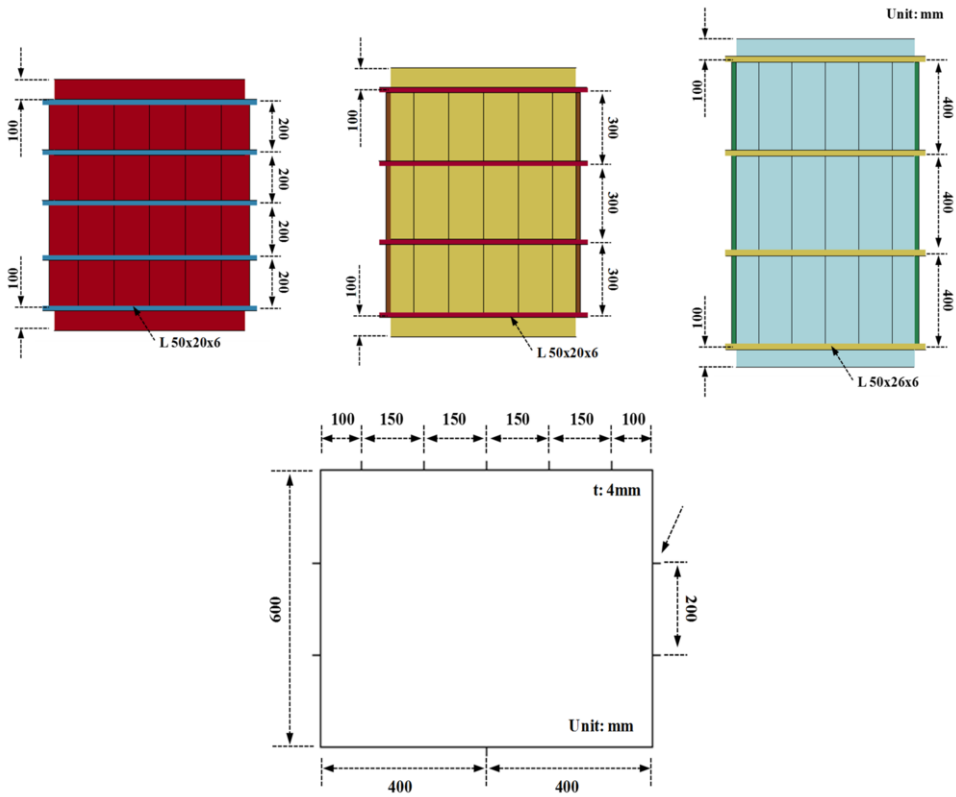

Figure 41 Main dimensions of box girder.

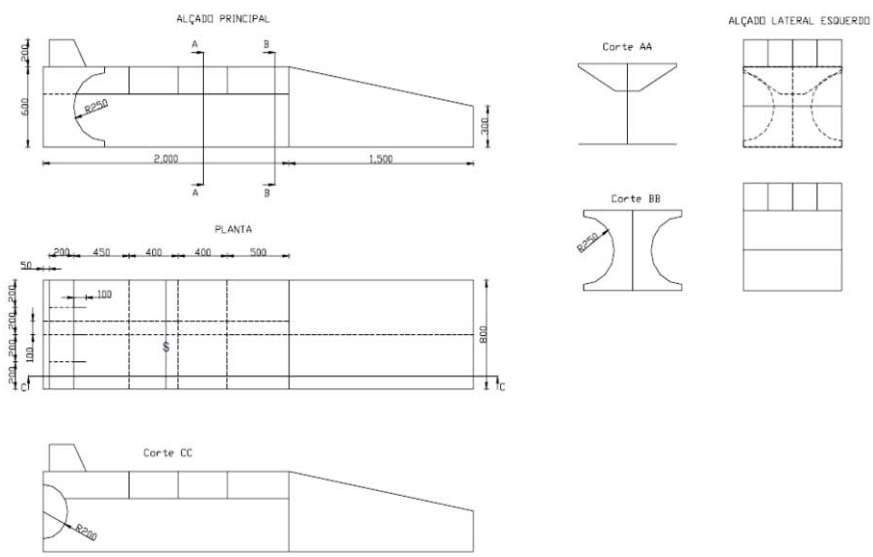

Figure 42 Geometry of the supporting structures

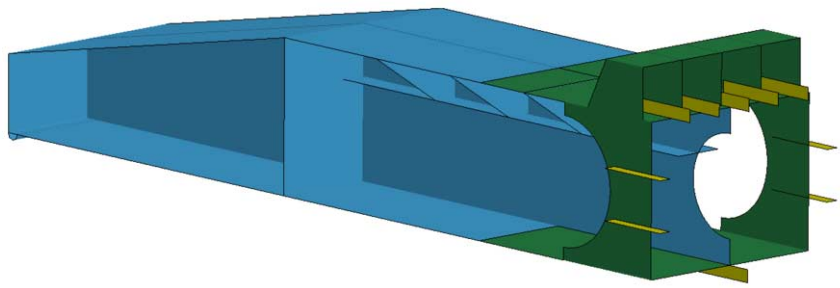

Figure 43 Supporting structure.

9.2.3.2 Material data

Material model for strength assessments are assumed to be bilinear elastic – plastic. For the present benchmark study, high tensile steel grade (S690) and mild steel are considered with nominal properties as given in Table 20.

Table 20 Nominal material properties of S690 and mild steel

	S690 steel (3 mm < Nominal thickness ≤ 50 mm)	**Mild carbon steel**
Items	Value	Value
Young modulus [MPa]	200000	200000
Poisson ratio [-]	0.3	0.3
Min. Yield stress [MPa]	732	235
Ultimate tensile stress [MPa]	808	400-520
Density [Kg/m^3]	7850	7850
Min. Elongation	15	22

9.2.3.3 Boundary conditions

The mechanical actions are applied by a four point bending rig. Load is applied through hydraulic jacks connected to a strong box. The box girders are welded between the outer supports while the outer edges of the supports are rested on the floor. Thus, the rig produces a four point bending load, with the central section under pure bending moment, including tension on the bottom and compression on the top of the box. Boundary conditions at the reaction points are simply supported. The load is applied from the strong box to tubular cross members welded onto the rig to represent a simply supported boundary condition, ref. Figure 44.

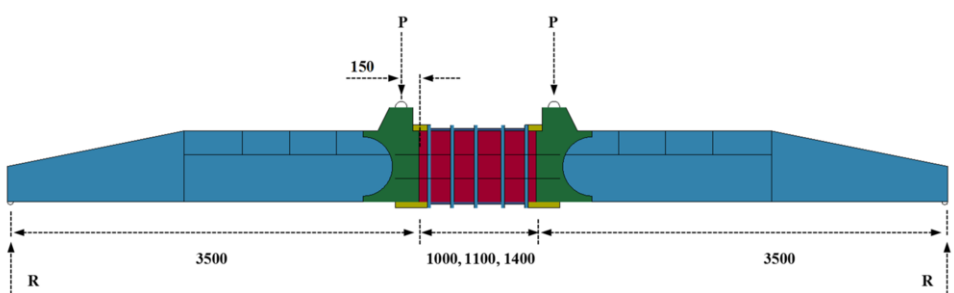

Figure 44 Boundary conditions

9.2.3.4 Loads

Loading of the box girders is performing by application of hydraulic jacks and increasing force as illustrated in Figure 44.

9.2.3.5 Monitoring of experiments

Monitoring of experiments was carried out by measuring deformation of the model at the location of application of loading and by measuring stresses at selected locations. Only the load-deformation behaviour of the models is the scope of the current benchmark.

9.2.4 Results of experiments

Figure 45 gives the capacity of box girders from experiments.

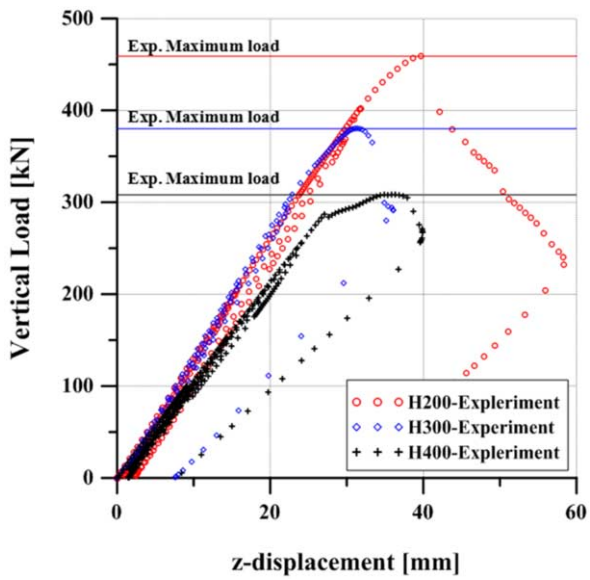

Figure 45 Experiment data of box giredrs

9.2.5 Results of benchmark study

The ultimate strength results from all analyses are plotted on the experimental load – displacement plots in Figure 46 to Figure 52. The complete load – displacement plots are omitted for clarity.

In the linear part of the test, most FEM analyses showed lower stiffness compared to the experiment. The transition to the nonlinear part of the test generally occurs at a lower load in the FEM analyses compared to the experiment. Some analyses, particularly by participants 3 and 4, show a sharp transition from the initial linear relationship to a lower stiffness well before the ultimate strength is attained suggesting a sudden transition of the buckling mode shape.

The ultimate strength of all boxes is generally predicted to be much lower in the FEM analyses compared to the experiments. This finding is consistent with the previous ISSC study. However the spread of results between participants is relatively wider, as highlighted by the normal distribution plots presented in Figure 49 to Figure 52.

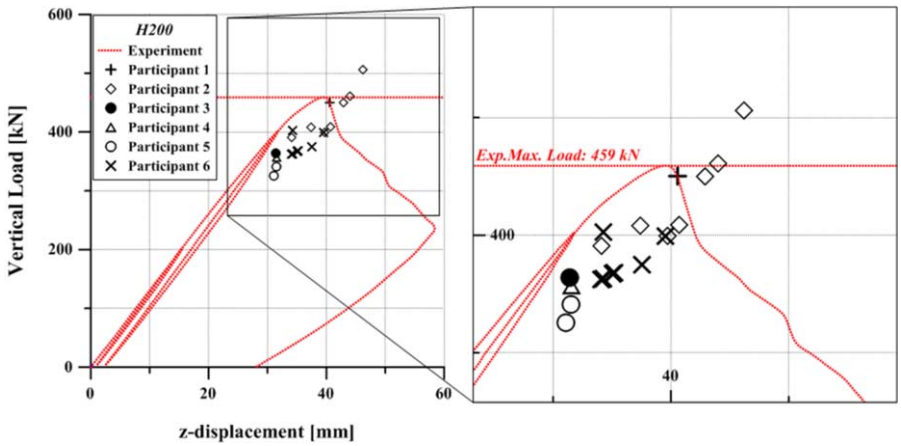

Figure 46 FEM ultimate strength compared to experiemntal results. H200

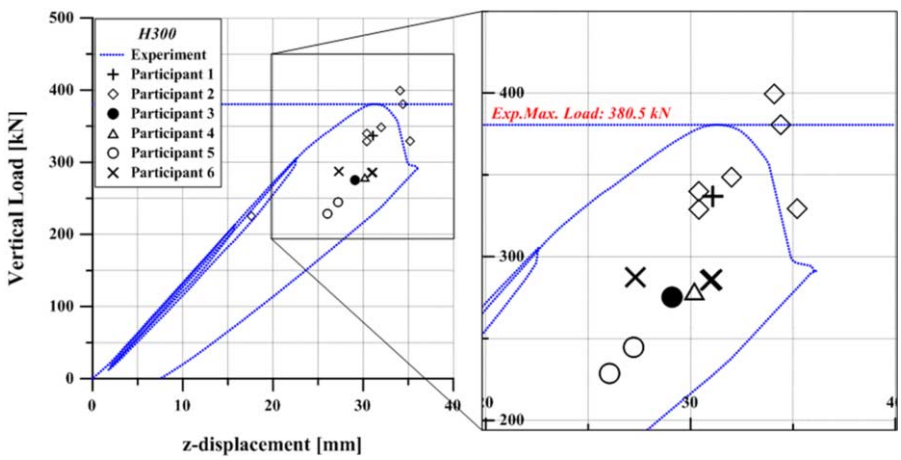

Figure 47 FEM ultimate strength compared to experiemntal results. H300

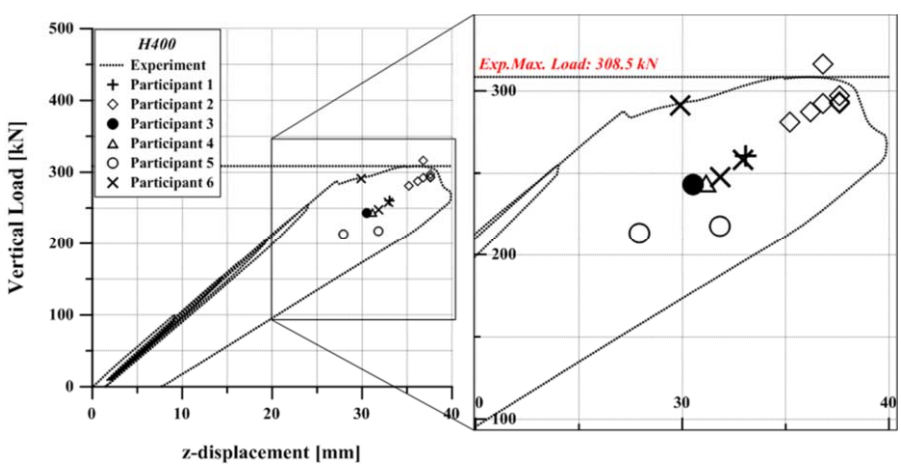

Figure 48 FEM ultimate strength compared to experiemntal results. H400

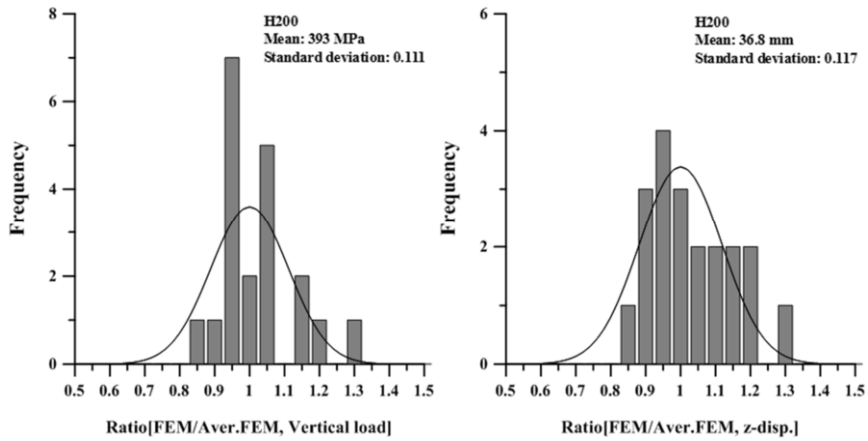

Figure 49 FEM predicted ultimate strength statistical distribution. H200

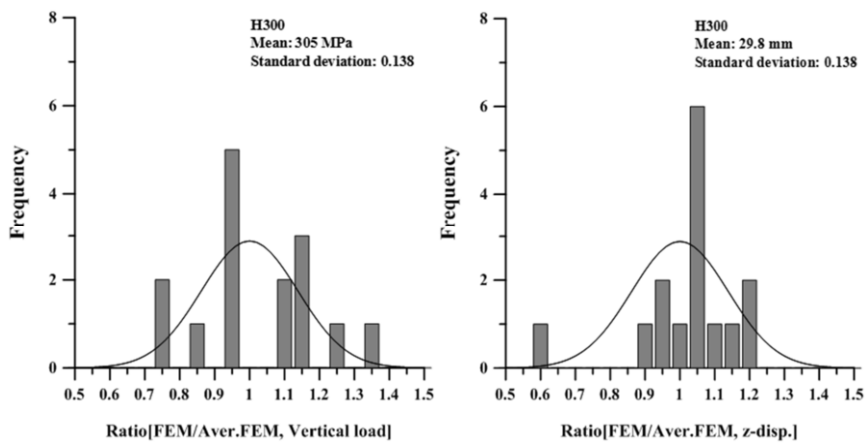

Figure 50 FEM predicted ultimate strength statistical distribution. H300

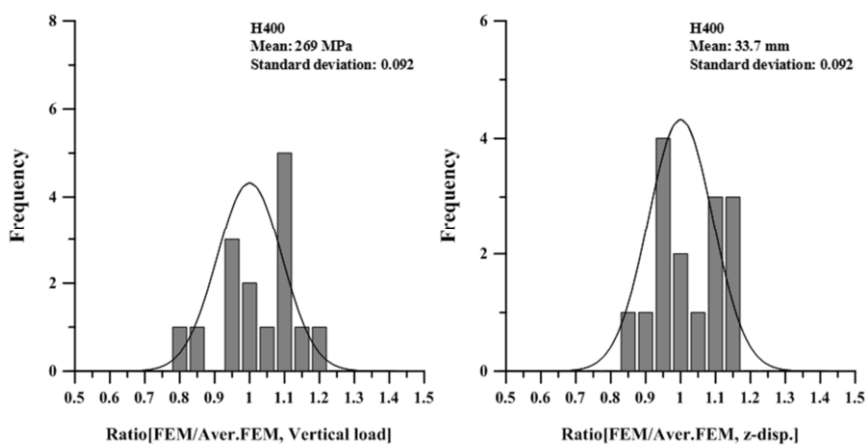

Figure 51 FEM predicted ultimate strength statistical distribution. H400

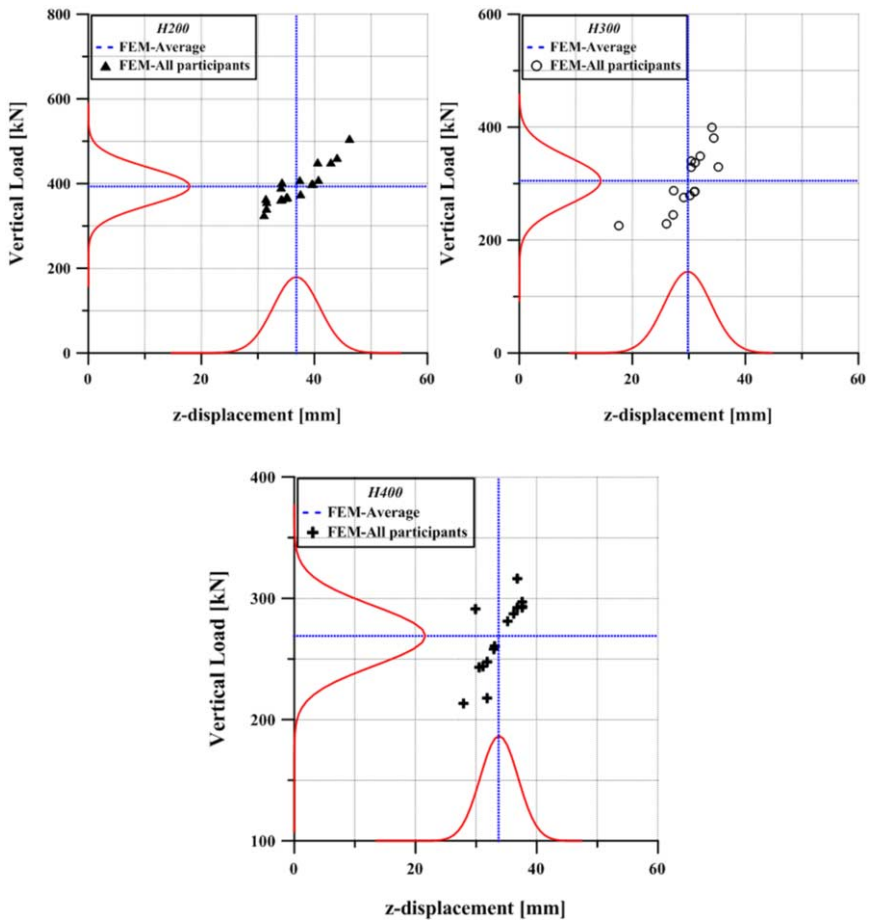

Figure 52 FEM predicted ultimate strength and displacement statistical distribution.

9.2.6 Conclusions

The benchmark results for the three box girders some similar findings to the previous ISSC report, but also give further insight into the uncertainty inherent in analyses of this type. The FEM analyses generally predict a lower ultimate strength compared to the equivalent experimental results. Poor equivalence of the geometrical dimensions and material models assumed for the FEM analyses may have a significant role in this discrepancy. The effect of the different boundary conditions used to load the FEM models is still difficult to ascertain. A previous FEM study, ISSC2015, compared both types of model using an otherwise identical model setup and found excellent correlation. Results from the previous ISSC report, where the setup of the FEM model was more tightly controlled between participants, also showed much better agreement. Taking this into account suggests that modelling parameters and options chosen by each participant, including exact degrees of freedom, mesh size, solver method, imperfections, residual stresses and material model, can significantly affect ultimate strength results using FEM. This study further demonstrates the difficulty in using FEM for reliable ultimate strength assessment.

10. CONCLUSIONS AND RECOMMENDATIONS

Conclusions

An ultimate strength assessment conveys a great amount of information about the structural response of a system beyond its capacity and helps to establish safety levels and criteria for ships and offshore structures. When applied in an appropriate and rigorous way, ultimate strength analysis leads to a better understanding of structural performance and realistic expectations of structural limits and safety margins. Ultimate strength methods such as nonlinear FEM and simplified progressive collapse method are now well established for ship and offshore structures as evidenced by their wide adoption in classification society rules. However, a continuing challenge for applying these methods successfully is the proper recognition and quantification of uncertainties in the geometrical and material properties of the target structure. This leads to sensitivity of results to the input data, and is compounded by uncertainties produced by the assumptions and approximations in the analysis methods. The outcome is that ultimate strength results should always be judged within a confidence interval, although this is often found to be difficult to properly define.

Reliability analysis and recommended indices as found in industry rules and practices provide a framework for incorporating ultimate strength assessments in design while taking into account these uncertainties. The reliability concept and its evaluation procedure are now fully accepted by structural engineers. However, reliability analysis still relies on comprehensive input data to define the uncertain properties of material and geometry, which often also depend on the manufacturing technology and subsequent in-service condition of the structure. These data sets are essential for reliability estimation yet still lacking for many ship and offshore structures. The literature review in this report shows relatively few research efforts focused on this over the ISSC period. It should also be noted that there is lack of practical structural design method based on the reliability and failure probability. Although the Monte Carlo method is widely used, efficient and accurate approximation is still required. Finally, failure analysis that accounts for the time parameter needs more attention. Most of the present literature is for static or quasi-static problems; but in many cases, the dynamic and time effects must be considered, such as wave slamming, impact and collision.

The ultimate strength in vertical bending at midships remains the dominant concern for intact ships. Simplified progressive collapse approaches have found their way into nearly all classification society rules for large vessels. Much progress has been recently reported in determining the bending strength under combined loading conditions (especially bending plus lateral pressure loading for bulk and container carriers; bending plus torsion for container carriers), where nonlinear FEA with multiple compartment models is maturing. For ship-shaped structure with damage, residual strength in vertical bending in the damaged region is the dominant concern. Simplified tools and methods for residual strength have seen extensive development for specific types of damage and hull types (e.g. grounding of double hull tankers), which are important for rapid assessment in event response scenarios. Requirements for hull residual strength are beginning to appear in classification society rules, and it is now accepted that assessments must take into account general (i.e. non-interframe) collapse mechanisms and the effects of structural asymmetry when gross damage is present.

With respect to marine structure, the committee has identified the governing standards and recommendations regarding several aspects of the design, lifetime and operation of marine facilities. Example of how these regulations are followed by engineering community have been reviewed. The main conclusion is that research in this field is not as extensive as it should be. While the focus is to the components and how their ultimate strength is affected by corrosion, cold climate and other agents, little attention is given to investigate how these agents can influence the global strength of a system. This finding can be considered in line with the conclusion given by ISSC III.I (2015) and ISSC III.I (2012).

On the other hand, the assessment of accidental limit states including ship impact, dropped objects, fire loads were found to be quite diffuse among the academic and engineering communities. This is believed to be driven by the increased accessibility and user's friendliness of today non-linear FE analysis tools and increased computational power which are making such calculation feasible in a manageable timeframe.

There is a significant future challenge to better address the ultimate strength of structural components and connection design. In contrast to the conventional research on a single ultimate failure mode, the future research effort should address the scenario-based failure event, which entails a series of triggers for ultimate failures. This includes impact followed by blast, and subsequently by fire. The research work must address the resistance and resilience of the structural component or connection under combined failure mechanisms or cascading mechanisms.

Another emerging challenge lies in the increasing use of the new materials, rendered possible by advanced manufacturing technology.

The statistical variation of material properties and its effect on the ultimate strength of a system can also be matter of research, involving reliability and knowledge of material behaviour to investigate how more accurate description of the material mechanical properties can (or not) have important effect on the capacity of a facility. Similarly, the effect of increase loads on existing structure and the consequences on such designs can be further investigated.

Additive manufacturing allows quick fabrication of complex structural components with sophisticated geometry, which are repeatedly used in floating and fixed structures. The 3-D printing technology is expected to advance and mature further, which means that 3-D printed structural components require comprehensive understanding and research from the material scale to the structural component scale.

Committee performed two Benchmark studies.

The objective of the first Benchmark was to predict the strength of structural joints of topside structures subjected to fires in order to compare different techniques (and solvers) in assessing the strength of these structures. The referenced benchmark study consisted of a relatively simple structural arrangement, i.e. a selected part of an offshore topside structure subjected to fire loads. Temperature of the structure due to fire loads calculated within the benchmark compared well with temperature calculated using EUROCODE when both the radiation and convection effects were included in the FE analysis. Predicted strength of joints under fire loads was significantly different for FE beam models and FE shell models. This benchmark proved to be complex enough to cause significant scatter in the results when analysed by a group of experts. This scatter was attributed to the underlying simulation assumptions made by the analysts. The results provide an invaluable insight into the variability of predictions when different factors are used for influential parameters, one of which being the analysts themselves.

The objective of the second Benchmark study was to validate the ultimate strength of the box girders under the pure bending moment using various finite elements solvers through comparison with the box girder buckling tests. This is a revisiting of Benchmark of ISSC2015, performed this time to identify possible sources of uncertainties and errors with reference to correct modelling and assessment of buckling tests. The FEM analyses generally predict a lower ultimate strength compared to the equivalent experimental results. Various assumptions regarding geometrical dimensions and material models used for the FEM analyses may have a significant role in this discrepancy. Taking this into account suggests that modelling parameters and options chosen by each participant, including exact degrees of freedom, mesh size, solver method, imperfections, residual stresses and material model, can significantly affect ultimate strength results using FEM. This study further demonstrates the challenges and difficulty in using FEM for reliable ultimate strength assessment.

Recommendations

Recommendations for future research work in ultimate strength are:

(1) Residual strength requirements in classification society rules should be further developed.

(2) First-principals based tools and methods with simplified representation of hull structure should be further developed for combined loading and damaged hulls.

(3) Greater efforts should be made to treat ultimate strength failures as a dynamic process.

(4) Whole-ship structural models should see greater use in assessing ultimate strength under increasingly realistic combinations of hull girder and local loads.

(5) More realistic assessment of damage should be further developed through the use of common models for both the simulation of the damage event and the post-damage residual strength assessment.

(6) New measurement technologies should be exploited to get accurate shape imperfection at build and throughout service life, and to determine damage extent and geometry following accidents.

(7) Structural response from other types of actions like blast or dropped objects should be addressed.

(8) Iceberg loads and impacts on offshore facility is a topic where more work should be carried out. This subject lays in between the scope of different committees (V.1: Accidental Limit state and V.6: Arctic Technology). More systematic studies of the different approaches to model the interaction between iceberg and a facility and the computed capacity against such loads should be carried out. Such research aims at identifying the possibilities, limitations and challenges related to current methods (ISO 19906 and the pressure area curve) and the use of more advanced methodologies such as carrying out impact analysis with a continuum model of the iceberg. This can highlight the differences between the given procedure, today state of the art and the needs for designers to rely on consolidated design approaches when addressing the structural capacity against iceberg load. The focus from this committee would be the effect of different models to the established capacity against such events, if that reliable ice loads are defined.

(9) Ultimate strength of specialized types of vessels has not been addressed by rules specifically:

i. LNG carriers and FLNG vessels, which are subject large thermal gradients resulting in pre-stressing of the primary structure. Thus far, no studies of the interaction of thermal loads and ultimate strength have been identified. A further risk with these vessels is accidental rupture of the containment system, due to excessive sloshing or impact, which could directly expose the primary structure to the very low temperature.
ii. FPSOs, which are usually double hull tankers modified to receive risers and fitted with processing plants. They are subject to other special combinations of loads (ice impact loads in high latitudes combined with wave loads). Some studies have appeared on ultimate strength of FPSOs but none have considered unique combinations of loading/damage for this type of vessel.
iii. Both FLNG and FPSOs are potentially subject to blast and fire loads due to accidental deflagration of gas cloud accumulations. No studies considering the ultimate strength in the with blast/fire damage have been identified.

Specific items that could be further investigated with respect to marine structures are:

(1) Development of benchmark models of different types of offshore platforms for the ultimate strength assessment;

(2) Verification of effects of modelling principles on the variation of ultimate strength assessment results;

(3) Effect of different material models applied when assessing the ultimate strength, including statistical variation of material properties;

(4) Effects of arctic conditions on the global ultimate strength, including but not limited to components.

REFERENCES

Abdel Ghoneim, G. (2008) Recent Developments in Offshore Codes, Rules and Regulations for Deepwater and Arctic E&P Systems, In Proceedings of the Eighteenth International Offshore and Polar Engineering Conference, Vancouver, BC, Canada, July 6-11, 2008.

ABS (2016) Rules of the Building and Classing of Steel Vessels, American Bureau of Shipping, Houston, TX.

ABS (2017) Guide for Building and Classing Drillships, 2017.

ABS (2017) Guide for Building and Classing Floating Offshore Liquefied Gas Terminals, 2017.

ABS (2017) Guide for the Buckling and Ultimate Strength Assessment of Offshore Structures, 2017.

ABS (2017) Rules for Building and Classing Floating Production Installations, 2017. Adamchak, J. (1982) ULTSTR: A Program for Estimating the Collapse Moment of a Ship's Hull Under Longitudinal Bending, DTNSRDC Report 82/076.

Alfred Mohammed, E., Benson, S., Hirdaris, S., Dow, R. (2016) Design safety margin of a 10,000 TEU container ship through ultimate hull girder load combination analysis, Marine Structures, 46, 78-101.

Amante, D., Chujutalli, J., Estefen, S. (2016) Hull girder ultimate strength of intact and damaged double hull tankers, In Proceedings of the ASME 2016 35th International Conference on Ocean, Offshore and Arctic Engineering (OMAE2016), 19-24 June 2016, Busan, South Korea.

Amdahl, J., Ehlers, S., Leira B. (2013) Collision and Grounding of Ships and Offshore Structures, London: CRC Press.

Amlashi, H., Moan, T. (2008) Ultimate strength analysis of a bulk carrier hull girder under alternatre hold loading condition – A case study Part 1: Nonlinear finite element modelling and ultimate hull girder capacity, Marine Structures, 21, 327-352.

Amlashi, H., Moan, T. (2009) Ultimate strength analysis of a bulk carrier hull girder under alternatre hold loading condition, Part 2: Stress distribution in the double bottom and simplified approaches, Marine Structures, 22, 522-544.

API (2011) Planning, Designing, and Constructing Floating Production Systems.

API RP 2A LRFD (2003) Recommended Practice for Planning, Designing and Constructing Fixed Offshore Platforms – Load and Resistance Factor Design, 1st edition reaffirmed, May 2003.

API RP 2SIM (2014) Structural Integrity Management of Fixed offshore Structure, 1st edition November 2014.

API RP 2A WSD (2014) Recommended Practice for Planning, Designing and Constructing Fixed Offshore Platforms – Working Stress Design, 22nd Edition, November 2014.

Arablouei, et al. (2016) Seismic Assessment of tension-leg platforms, In proceedings for Offshore Technology Conference (OTC 2016), Houston, Texas, USA, 2-5 May 2016.

Aziz, A., Qian, X. (2015) A toughness based deformation limit for fatigue-cracked X-joints under in-plane bending, Marine Structures, 52, 33-52.

Aziz, A., Qian, X. (2016) A deformation limit based on failure assessment diagram for fatigue-cracked X-joints under in-plane bending. Ship and Offshore Structures, 11, 182-197.

Bai, F., Davidson, J. S. (2016), Theory for composite sandwich structures with unsymmetrical wythes and transverse interaction, Engineering Structures 116, 178-191.

Bai, Y., Tang, J., Xu, W., Gao, Y., Wang, R. (2015) Collapse of reinforced thermoplastic pipe (RTP) under combined external pressure and bending moment. Ocean Engineering, 94, 10-18.

Balser, K. (1961) Strength of plate girders in shear, Fritz Engineering Laboratory Report No. 251-20, Lehigh University.

Bardel, D., Nelias, D., Robin, V., Pirling, T., Boulnat, X., Perez, M. (2016), Residual stresses induced by electron beam welding in a 6061 aluminium alloy, Journal of Materials Processing Technology 235, 1-12.

Benson, S., Downes, J., Dow, R. (2013 a) Compartment level progressive collapse analysis of lightweight ship structures, Marine Structures, 31, 44-62.

Benson, S., AbuBakar, A., Dow, R. (2013 b) A comparison of computational methods to predict the progressive collapse behaviour of a damaged box girder, Engineering Structures, 48, 266-280.

British Standard Institute (2013) BS7910:2013+A1:2015, Guide to methods for assessing the acceptability of flaws in metallic structures.

Brubak, L., Lofthaug, K., Steen, E. (2016) Strength analysis of deck structure subjected to fire, in the proceedings for the 13th PRADS2016, 4-8, September 2016, Copenhagen, Denmark.

Buchanan, C., Gardner, L., Liew, A. (2016) The continuous strength method for the design of circular hollow sections, Journal of Constructional Steel Research, 118, 207-216.

BV (2000) MARS2000 User Guide, Bureau Veritas. Neuilly sur Seine Cedex, France.

BV (2011), Rules for Classification of Naval Ships, Bureau Veritas, Neuilly sur Seine Cedex, France.BV (2016) Rules for Classification of Steel Ships, Bureau Veritas, Neuilly sur Seine Cedex, France.

BV (2015) Hull in Aluminium Alloys, NR 561. Bureau Veritas, Neuilly sur Seine Cedex, France.

BV (2016) Rules for Classification of Steel Ships, Bureau Veritas, Neuilly sur Seine Cedex, France.

BV (2017) Hull in Composite Materials and Plywood. NR 546, Bureau Veritas, Neuilly sur Seine Cedex, France.

Caldwell, J. B. (1965) Ultimate longitudinal strength, Transactions Royal Institution of Naval Architects (RINA), 107, pp. 411-430.Campanile, A., Piscopo, V., Scamardella, A. (2014) Statistical properties of bulk carrier longitudinal strength, Marine Structures, 39, 438-462.

Campanile, A., Piscopo, V., Scamardella, A. (2016) Time-variant bulk carrier reliability analysis in pure bending intact and damage conditions, Marine Structures, 46, 193-228.

Cestino, E., Romeo, G., Piana, P., Danzi, F., (2016) Numerical/experimental evaluation of buckling behaviour and residual tensile strength of composite aerospace structures after low velocity impact. Aerospace Science and Technology 54, 2016, pp.1-9

Cerik, B. C. (2017) Damage assessment of marine grade aluminium alloy-plated structures due to air blast and explosive loads, Thin-Walled Structures, 110, 123-132.

Cestino, E., Romeo, G., Piana, P., Danzi, F. (2016), Numerical/experimental evaluation of buckling behaviour and residual tensile strength of composite aerospace structures after low velocity impact, Aerospace Science and Technology 53, 1-9.

Chen, B. Q., Soares, C. G. (2016) Effects of plate configurations on the weld induced deformations and strength of fillet-welded plates, Marine Structures, 50, 243-259.

Chen, N. (2016) Hull girder reliability assessment for FPSOs, Engineering Structures, 14, 135-147.

Chen, N. Z. (2017) Panel reliability assessment for FPSOs, Engineering Structures. Vol 130, 41-51.

Chen, Y., Feng, R., Wang, C. (2015) Tests of steel and composite CHS X-joints with curved chord under axial compression, Engineering Structures, 99, 423-438.

Chen, Y., Feng, R., Wang, C. (2015 a) Tests of bare and concrete-filled CHS T-joints with concave chord under axial compression, Construction and Building Materials, 93, 144-156.

Chen, Y., Feng, R., Wang, C. (2016) Tests of CHS T-joints with convex chord under axial compression, Journal of Constructional Steel Research, 117, 139-151.

Chen, Y., Feng, R., Xiong, L. (2016 a) Experimental and numerical investigations on double-skin CHS tubular X-joints under axial compression, Journal of Constructional Steel Research, 106, 268-283.

Chen, Y., Kutt, L., Piaszczyk, C., Bienek, M. (1983) Ultimate Strength of Ship Structures. SNAME Transactions, 91, 149-168.

Chen, Z., Chen, Z., Shenoi, R. (2015) Influence of welding sequence on welding deformation and residual stress of a stiffened plate structure, Ocean Engineering, 106, 271-280.

Choung, J., Nam, J., Ha, T. (2012) Assessment of residual ultimate strength of an asymmetrically damaged tanker considering rotational and translational shifts of neutral axis plane, Marine Structures, 25, 71-84.

Choung, J., Nam, J., Ha, T. (2012) Slenderness ratio distribution and load-shortening behaviors of stiffened panels, Marine Structures, 26, 42-57.

Choung, J., Nam, J., Tayyar, G. (2014) Residual ultimate strength of a very large crude carrier considering probabilistic damage extents, International Journal of Naval Architecture and Ocean Engineering, 6, 14-26.Chun, Y. J. et al. (2016) Experimental and numerical study on collapse of aged jacket platforms caused by corrosion or fatigue cracking, Engineering Structures, 112 (2016) 14-22.

Ciu, J., Wang, D., Ma, N. (2017) A study of container ship structures' ultimate strength under corrosion effects, Ocean Engineering, 130, 454-470.

ClassNK (2014) Investigation Report on Structural Safety of Large Container Ships, Nippon Kaiji Kyokai, Japan.

ClassNK (2016) Rules for the Survey and Construction of Steel Ships, Nippon Kaiji Kyokai, Japan.

Collete, M., Sielski, R. (2013) Aluminum Ship Structures, In Proceedings of 2013 ASNE Day, American Society of Naval Engineers, Alexandria, VA.

Comité Européen de Normalisation (2004) EN 1992-1-1:2004 Eurocode 2 – Design of concrete structures, Part 1. 1: General rules and rules for buildings, CEN, 2004.

Comité Européen de Normalisation (2005) EN 1993-1-1:2005 Eurocode 3 – Design of steel structures, Part 1. 1: General rules and rules for buildings, CEN, 2005.

Cubells, A., Garbatov, Y., Soares, C. G. (2014) Photogrammetry measurements of initial imperfections for the ultimate strength assessment of plates, Transactions of RINA, International Journal of Maritime Engineering, 156, A291-A302.

Cui, W., Wang, Y., Pedersen, P. (2000) Strength of ship stiffened panels under combined loading, Journal of Ship Mechanics, 4(3), 58-86.

Daley, A., Davis, D. B., White, D. W. (2017) Shear Strength of unstiffened steel I-section members, Journal of Structural Engineering – ASCE, 143, 04016190.

De Barros, S., Banea, M. D., Budhe, S., De Siqueira, C. E. R., Lobão, B. S. P. (2017) Experimental analysis of metal-composite repair of floating offshore units (FPSO), The Journal of Adhesion, 93, 147-158.

Deng, L., Guo, J., Fang, C., Zou, L. Y. (2016) Reliability analysis of ultimate longitudinal strength for ships in Yangtze River, Presented at the Proceedings of the International Conference on Offshore Mechanics and Arctic Engineering (OMAE).

Derbanne, Q., de Lauzon, J., Bigot, F., Malenica, S. (2016) Investigations of the dynamic ultimate strength of a ship's hull girder during whipping, In Proceedings of PRADS2016, Copenhagen, Denmark, 4-8 Sep 2016.
DNV (2012 a) Rules for Classification of Ships, Det Norkse Veritas AS, Norway.
DNV (2012 b) Rules for Classification of High Speed, Light Craft and Naval Surface Craft, Det Norkse Veritas AS, Norway.
DNV-GL (2015) Rules for Classification – Naval Vessels. Part 3(Surface Ships), Ch1, Norway.
DNV-GL (2016) Buckling, Class Guideline DNVGL-CG-0128, Norway.
DNV-GL (2017 a) https://www.dnvgl.com/services/ship-design-and-verification-software-nauticus-2883, Date accessed: 23 Nov 2017.
DNV-GL (2017 b) Rules for Classification – Ships. Part 3(Hull), Chapter 5 (Hull girder strength), Norway.
DNV-GL-OS-C101 (2016) Design of Offshore Structures, General (LRFD Method), April 2016.
DNV-GL-RP-C204 (2017) Design against accidental loads, August 2017.
DNV-GL-RP-C208 (2016) Determination of structural capacity by non-linear finite element analysis methods, September 2016.
DNV-OS-C102 (2008) Structural Design of Offshore Ships, October 2008.
DNV-RP-C201 (2010) Buckling Strength of Plated Structures, October 2010.
Dong, C. X., Kwan, A.K.H., Ho, J. C. M. (2017) Effects of external confinement on structural performance of concrete-filled steel tubes, Journal of Constructional Steel Research, 132, 72-82.
Dow, R., (1991) Testing and analysis of a 1/3 scale frigate model, Advances in Marine Structures, 2, 749–773.
Downes, J., Tayyar, G., Kvan, I., Choung, J. (2017) A new procedure for load-shortening and elongation data for progressive collapse method, International Journal of Naval Architecture and Ocean Engineering, 9, 705-719.
Ehlers, S., Benson, S., Misirlis, K. (2013) Ultimate strength of an intact and damaged LNG vessel subjected to sub-zero temperature, In Collision and Grounding of Ships and Offshore Structures, Amdahl, Ehlers & Leira (Eds), London: CRC Press.
Ehlers, S., Østby, E. (2012) Increased crashworthiness due to arctic conditions – The influence of sub-zero temperature, Marine Structures, 28, 86-100.
Elchalakani, M., Karrech, A., Hassanein, M. F., Yang, B. (2016) Plastic and yield slenderness limits for circular concrete filled tubes subjected to static pure bending, Thin-Walled Structures, 109, 50-64.
El-Khoriby, S. R., Hassanein, M. F., Kharoob, O. F., Hadidy, A. M., Alnaggar, G. A. N. (2016) Tubular flange plate girders with corner square web openings in the panel of maximum shear: strength and behaviour, Thin-walled Structures, 99, 142-154.
Estefen, S. F., Chujutalli, J. H., Guedes Soares, C. (2016) Influence of geometric imperfections on the ultimate strength of the double bottom of a Suezmax tanker, Engineering Structures, 127, 287-303.
Eurocode (2002) EN 1991-1-2, Eurocode 1: Actions on structures - Part 1-2: General actions - Actions on structures exposed to fire.
Eurocode (2005) EN 1993-1-2, Design of steel structures - Part 1-2: General rules - Structural fire design.
Faisal, M., Noh, S., Kawsar, M., Youssef, S., Seo, J., Ha, Y., Paik, J. (2017) Rapid hull collapse strength calculations of double hull oil tankers after collisions, Ship and Offshore Structures, 12 (5), 624-639.
Farajkhah, V., Liu, Y. (2016) Effect of metal inert gas welding on the behaviour and strength of aluminium stiffened plates, Marine Structures, 50, 95-110.
Faulkner, D., Sadden, J. (1979) Toward a unified approach to ship structural safety, Transactions of RINA, 121, 1-28.

Frieze, P., Lin, Y. (1991) Ship longitudinal strength modelling for reliability analysis, In Proceedings of the Marine Structural Inspection, Maintenance and Monitoring Symposium, SSC/SNAME, III.C.1-20.

Frickie, W., Gerlach, B. (2015) Effect of large openings without and with windows on the shear stiffness of side walls in passenger ships, Ships and Offshore Structures, 10, 256-271.

Fu, G., Lourenco, M. I., Duan, M., Estefan, S. F. (2016) Influence of the welding sequence on residual stress and distortion of fillet welded structures, Marine Structures, 46, 30-55.

Fujikubo, M., Iijima, K., Pei, Z., Ko, H. (2016) Collapse analysis of ship hull girder in waves using idealized structural unit method, In Proceedings of the ASME 2016 35th International Conference on Ocean, Offshore and Arctic Engineering (OMAE 2016), 19-24 June 2016, Busan, South Korea.

Fujikubo, M., Kaeding, P., Yao, T. (2000) ISUM rectangular plate element with new lateral shape function, longitudinal and transverse thrust. J. Soc. Naval Architects Japan (187), 209-219.

Fujikubo, M., Muis Alie, M. Z., Takemura, K., Iijima, K., Oka, S. (2012) Residual Hull Girder Strength of Asymmetrically Damaged Ships − Influence of Rotation of Neutral Axis due to Damages Journal of the Japan Society of Naval Architects and Ocean Engineers 16: 131-140.

Fujikubo, M., Tatsumi, A. (2016) Ultimate strength of ship hull girder under combined longitudinal bending and local loads, In Proceedings of the 2nd International Conference on Safety & Reliability of Ships, Offshore & Subsea Structures (SAROSS 2016), 15-17 Aug 2016, Glasgow UK.

Fung, T. C., Tan, K. H., Nguyen, M. P. (2016) Structural behavior of CHS T-joints subjected to static in-plane bending in fire conditions, ASCE Journal of Structural Engineering, 04015155.

Fu, Y., Tong, L., He, L., Zhao, X. L. (2016) Experimental and numerical investigation on behavior of CFRP strengthened circular hollow section gap K-joints, Thin-Walled Structures, 102, 80-97.

Gaiotti, M., Fujikubo, M., Grasso, N.m Rizzo, C. (2016) Effect of Shear Stresses on the Ultimate Strength of the Hull Girder of a Containership, International Journal of Offshore and Polar Engineering, 26(2).

Garbatov, Y., Saad-Eldeen, S., Guedes Soares, C. (2015) Hull girder ultimate strength assessment based on experimental results and the dimensional theory, Engineering Structures. 100, 742-750.

Garbatov, Y., Parunov, J., Kodvanj, J., Saad-Eldeen, S., Guedes Soares, C. (2016) Experimental assessment of tensile strength of corroded steel specimens subjected to sandblast and sandpaper cleaning, Marine Structures, 49, 18-30.

Gaspar, B., Bucher, C., Soares, C.G. (2015 a) Reliability analysis of plate elements under uniaxial compression using an adaptive response surface approach, Ships and Offshore Structures, 10, 145–161.

Gaspar, B., Teixeira, A.P., Soares, C.G. (2015 b) Effect of the aspect ratio on the ultimate compressive strength of plate elements with non-uniform corrosion, in: Analysis and Design of Marine Structures.

Gaspar, B., Teixeira, A.P., Guedes, S. (2016) Effect of the nonlinear vertical wave-induced bending moments on the ship hull girder reliability, Ocean Engineering, 119, 193–207.

Gerhard Ersdal (2005) Assessment of Existing Offshore Structures for Life Extension, Doctoral Thesis, University of Stavanger.

GL (2012 a) Rules for Classification and Construction – I Ship Technology, 1 Seagoing Ships, Germanischer Lloyd, Hamburg, Germany.

GL (2012 b) Rules for Classification and Construction – III Naval Ship Technology, 1 Surface Ships, Germanischer Lloyd, Hamburg, Germany.

Gordo, J., Guedes Soares, C. (1993) Approximate load shortening curves for stiffened plates under uniaxial compression. In Integrity of Offshore Structures – 5 (Faulkner et al. Eds), UK: EMAS, 189-211.

Gordo, J. M., Guedes Soares, C. (2009) Tests on ultimate strength of hull box girders made of high tensile steel, Marine Structures 22(4): 770-790.

Gordo, J. M., Guedes Soares, C. (2014) Experimental analysis of the effect of frame spacing variation on the ultimate bending moment of box girders, Marine Structures 37: 111-134.

Gordo, J., Guedes Soares, C., Faulkner, D. (1996) Approximate Assessment of the Ultimate Longitudinal Strength of the Hull Girder, Journal of Ship Research, 40 (1) 60-69.

Graczykowski, C., Orlowska, A., Holnicki-Szulc J. (2016), Prestressed composite structures – Modeling, manufacturing, design, Composite Structures 151, 172-182.

Gu, B., Qian, X., Aziz, A. (2016) A toughness based deformation limit for X- and K-joints under brace axial tension, Frontiers of Structures and Civil Engineering, 10, 345-362.

Guedes Soares, C., Luis, R., Nikolov, P., Downes, J., Taczala, M., Modiga, M., Quesnel, T., Toderan, C., Samueltides, M. (2008) Benchmark study on the use of simplified structural codes to predict the ultimate strength of a damaged hull, International Shipbuilding Progress, 55, 87-107.

Guz, I. A., Menshykova, M., Paik, J. K. (2017) Thick-walled composite tubes for offshore applications: an example of stress and failure analysis for filament-wound multi-layered pipes, Ship and Offshore Structures, 12, 304-322.

Ha, YS., Park, JS., Koo, JB., Jang, KB., Seo, JK., Shin, WH., Seo, YK. (2015), Development of Large Scaled SAFE Helideck Structure, International Society of Offshore an Polar Engineers (ISOPE), ISBN : 978-1 880653 89-0.

Hayward, R., Lehmann, E. (2017) Development of a new proof of plate capacity under combined in-plane loads, Ship and Offshore Structures, 12, S174-188.

Horn, J. H., Jensen J. J. (2016) Reducing uncertainty of Monte Carlo estimated fatigue damage in offshore, Proceedings of PRADS 2016.

Hou, C., Han, L. H., Mu, T. M. (2017) Behavior of CFDST chord to CHS brace composite K-joints, Journal of Constructional Steel Research, 135, 97-109.

IACS (2006 a) Common Structural Rules for Bulk Carriers, International Association of Classification Societies.

IACS (2006 b) Common Structural Rules for Double Hull Oil Tankers, International Association of Classification Societies.

IACS (2014) Common Structural Rules for Bulk Carriers and Oil Tankers, International Association of Classification Societies.

IACS (2017) Common Structural Rules for Bulk Carriers and Oil Tankers, International Association of Classification Societies.

IACS (2015) Longitudinal Strength Standard for Container Ships (UR S11A), In Requirements concerning Strength of Ships.

Iijima, K., Susaki, Y., Fujikubo, M. (2013) Scaled model tests for the post-ultimate strength collapse behaviour of a ship's hull girder under whipping loads, Ships and Offshore Structures, 10(1), 31-38.

Iijima, K., Fujikubo, M. (2015) Cumulative collapse of a ship hull girder under a series of extreme wave loads, Journal of Marine Science and Technology, 20 (3). 530-541.

Im, H., Vladimir, N., Malenica, S., Cho, D., Ryu, H. De Lauzon, J., (2016) Ultimate strength check of HHI SkyBench ultra large container ship considering slamming and whipping effects, In Proceedings of PRADS2016, Copenhagen Denmark, 4-8 Sep 2016.

IMO (2010) Adoption of the International Goal-Based Ship Construction Standards for Bulk Carriers and Oil Tankers, Resolution MSC.287(87), 20 May 2010.

IMO (2015) International Goal-Based Ship Construction Standards for Bulk Carriers and Oil Tankers.

ISO (2014) ISO 834-11:2014, Fire resistance tests – elements of building construction – part 1.1: specific requirements for the assessment of fire protection to structural steel elements.
ISO 19900 (2002) Petroleum and natural gas industries - General Requirements for Offshore Structures, 1st edition, December 2002.
ISO 19901-1 (2005) Petroleum and natural gas industries - Specific requirements for offshore structures - Part 1: MetOcean Design and Operating Conditions, 1st edition, November 2005.
ISO 19901-2 (2004) Petroleum and natural gas industries - Specific requirements for offshore structures – Part 2: Seismic Design Procedures and Criteria, 1st edition, November 2004.
ISO 19902 (2007) Petroleum and natural gas industries - Fixed Steel Offshore Structures, 1st edition, December 2007.
ISO 19906 (2010) Petroleum and natural gas industries – Arctic Offshore Structure, 1st edition, December 2010.
ISSC (2000) ISSC Committee III.1: Ultimate Strength, In Proceedings of the 13th International Ship and Offshore Structures Congress, (Ed. Ohtsubo & Sumi).
ISSC (2012) Ultimate Strength. ISSC Committee III.1.
ISSC (2015) Accidental Limit State, ISSC Committee V.1
ISSC (2015) Ultimate Strength. ISSC Committee III.1.
Ivaldi, A. (2015) Growing length in the megayacht industry and structure-related design topics, Ships and Offshore Structures, 10, 221-231.
Jensen, J. J., (2015) Fatigue damage estimation in nonlinear systems using a combination of Monte Carlo simulation and the First Order Reliability Method, Marine Structures, 44:203–210.
Jia-Bao Yan (2016) Damage plasticity based numerical analysis on steel–concrete–steel sandwich shells used in the Arctic offshore structure, Engineering Structures 117, 542–559
Kaeding, P., Olaru, V., Fujikubo, M. (2004) Development of ISUM Plate Element with Consideration of Lateral Pressure Effects and its Application to Stiffened Plates of Ships, In Proceedings of the 9th International Symposium on the Practical Design of Ships and Other Floating Structures, 1, 148-155.
Kell, C. (1931) Investigation of Structural Characteristics of Destroyers “Preston” and “Bruce” Part I – Description, SNAME Transactions, 39, 35-64.
Kell, C. (1940) Investigation of Structural Characteristics of Destroyers “Preston” and “Bruce” Part II – Analysis of Data and Results, SNAME Transactions, 48, 125-172.
Kennedy, S., Kong, J., Notaro, G., Brinchmann, K., Kaur, J., Hwang, O., Lim, J., Khoo, C., Chow, W., H. (2016) Dropped Object SPS Impact Protection Deck For Well Bay Area, in the proceedings for the 13th PRADS2016, 4-8 September 2016, Copenhagen, Denmark .
Khedmati, M., Rashedi, A. (2014) Nonlinear finite element modelling and progressive collapse analysis of a product carrier under longitudinal bending, Applied Ocean Research, 48, 80-102.
Khedmati, MR., Pedram, M. (2014), A numerical investigation into the effects of slamming impulsive loads on the elastic–plastic response of imperfect stiffened aluminium plates, Thin-walled Structures 76, 118–144.
Khedmati, M. R., Memarianv, H. R., Fadavie, M., Zareei, M. R. (2017) Empirical formulations for estimation of ultimate strength of continuous aluminium stiffened plates under combined transverse compression and lateral pressure, Ships and Offshore Structures, 11(3), pp. 258-277.
Khurshid, M., Barsou, Z., Barsoum, I. (2015) Load carrying capacities of Butt Welded Joints in High Strength Steels, ASME Journal of Engineering Materials and Technology, 041003.
Kim, D. H., Paik, J. K. (2017) Ultimate limit state-based multi-objective optimum design technology for hull structural scantlings of merchant cargo ships, Ocean Engineering, 129, 318-334.

Kim, D., Kim, B., Seo, J., Kim, H., Zhang, X., Paik, J. (2014) Time-dependent residual ultimate longitudinal strength - grounding damage index (R-D) diagram, Ocean Engineering, Vol., 76, 163-171.

Kim, D., Kim, S., Kim, H., Zhang, X., Li, C., Paik, J. (2014) Ultimate strength performance of bulk carriers with various corrosion additions, Ships and Offshore Structures, 10 (1), 59-78.

Kim, D., Pedersen P., Paik, J., Kim, H., Zhang, X., Kim, M. (2013) Safety guidelines of ultimate hull girder strength for grounded container ships, Safety Science, Vol. 59, pp. 46-54.

Kim, D., Park, D., Kim, H., Kim, B., Seo, J., Paik, J. (2013) Lateral pressure effects on the progressive hull collapse behaviour of a Suezmax-class tanker under vertical bending moments, Ocean Engineering, 63, 112-121.

Kim, J. H., Jeon, J. H., Park, J. S., Seo, H. D., Ahn, H. J. (2015) Effect of reinforcement on buckling and ultimate strength of perforated plates, International Journal of Mechanical Sciences, 92, 194-205.

Kim, K. J., Lee, J. H., Park D. K., Jung, B. G., Paik, J. K. (2016) An Experimental and numerical study on nonlinear impact responses of steel-plated structures in artic environment, International Journal of Impact Engineering, 93, 99-115.

Kitarovic, S., Zanic, V. (2014) Approximate approach to progressive collapse analysis of the monotonous thin-walled structures in vertical bending, Marine Structures, 39, 255-286.

Koo, JB., Park, JS., Ha, YS., Jang KB., Suh YS. (2014), International Society of Offshore an Polar Engineers (ISOPE), ISBN : 978-1 880653 91-3.

Kwon, K., Frangopol, D. M. (2012) System Reliability of Ship Hull Structures Under Corrosion and Fatigue, Journal of Ship Research, 56, 234-251.

Lamb, T., Beavers N., T Ingram, T., Schmieman T. S. (2011) The Benefits and Cost Impact of Aluminum Naval Ship Structure. Journal of Ship Production and Design. Vol 27(1) pp. 35-49(15).

Lang, D., Warren, W. (1952) Structural Strength Investigation of Destroyer Albuera, Transactions of the Institute of Naval Architecture, 94, 243-286.

Lan, X., Huang, Y. (2016) Structural design of cold-formed stainless steel tubular X- and T-joints at elevated temperatures, Thin-Walled Structures, 108, 270-279.

Leheta, H. W., Elhanafi, A. S., Badran, S. F. (2016) A numerical study of the ultimate strength of Y-deck panels under longitudinal in-plane compression, Thin-Walled Structures, 100, 134-146.

Lehmann, E. (2014) The Historical development of the Strength of Ships, In The History of Theoretical, Material and Computational Mechanics, 1 (E. Stein, Ed.) Berlin: Springer-Verlag, 267-295.

Lei, W., Quan, W. Z., H. J. Hao (2015) Comparative analysis of HCSR based on ultimate strength of intact ships and residual strength in damaged condition, Analysis and Design of Marine Structures, V, 513-519.

Lesani, M., Bahaari, M. R., Shokrieh, M. M. (2015) FRP wrapping for the rehabilitation of Circular Hollow Section (CHS) tubular steel connections, Thin-Walled Structures, 90, 216-234.

Levanger, H., Notaro, G., Hareide, O. J. (2016) Collision response and residual strength of Jack-up structure, In the proceedings for the 13th PRADS2016, 4-8 September 2016, Copenhagen, Denmark.

Li, C., Zhu, A., Ren, H., Zhou, X. (2016) Application of the incorporated meshing technique to non-linear FE analysis of hull girder ultimate strength, In Proceedings of the ASME 2016 35th International Conference on Ocean, Offshore and Arctic Engineering (OMAE2016), OMAE2016-55094.

Li, T., Lie, S. T., Shao, Y. B. (2017) Fatigue and fracture strength of a multi-planar circular hollow section TT-joint, Journal of Constructional Steel Research, 129, 101-110.

Li, Y. L., Zhao, X. L., Raman Singh, R. K., Al-Saadi, S. (2016) Experimental study on seawater and sea sand concrete filled GFRP and stainless steel stub columns, Thin-Walled Structures, 106, 390-406.

Li, Y. L., Zhao, X. L., Raman Singh, R. K., Al-Saadi, S. (2016 a) Tests on sea water and sea sand concrete-filled CFRP, BFRP and stainless steel tubular stub columns, Thin-Walled Structures, 108, 163-184.

Lindemann, T., Kaeding, P., Backhaus, E. (2016) Experimental determination of the ultimate strength of box girder specimens, In Proceedings of the ASME 2016 35th International Conference on Ocean, Offshore and Arctic Engineering (OMAE2016), OMAE2016-54140.

Nishihara S. (1984) Ultimate longitudinal strength of mid-ship cross section, Naval Architecture and Ocean Engineering, 22, 200-214.

Liu, F., Wang, Y., Chan, T. M. (2017) Behavior of concrete-filled cold-formed elliptical hollow sections with varying aspect ratios, Thin-Walled Structures, 110, 47-61.

Liu, Z., Amdahl, J. (2012). Numerical and simplified analytical methods for analysis of the residual strength of ship double bottom, Ocean Engineering Vol. 52, pp. 22-34.

LR (2014) Guidance Notes for Collision Analysis, November 2014.

LR (2016) Rules and Regulations for the Classification of Ships, Lloyd's Register, London, UK.

LR (2017) Rules and Regulations for the Classification of Naval Ships, Lloyd's Register, London, UK.

Maggiolini, E., Tovo, R., Susmel, L., James, M.N., Hattingh, D.G. (2016), Crack path and fracture analysis in FSW of small diameter 6082-T6 aluminium tubes under tension-torsion loading, International Journal of Fatigue.

Nassiraei, H., Lotfollahi-Yaghin, M. A., Ahmadi, H. (2016 a) Static strength of offshore tubular T/Y-joints reinforced with collar plate subjected to tensile brace loading, Thin-Walled Structures, 103, 141-156.

Nassiraei, H., Lotfollahi-Yaghin, M. A., Ahmadi, H. (2016 b) Static performance of doubler plate reinforced tubular T/Y-joints subjected to brace tension, Thin-Walled Structures, 108, 138-152.

NORSOK Standard (2010) N-001 - Integrity of Offshore Structures, 7th edition, June 2010.

NORSOK Standard (2007) N-003 - Action and Action Effects, 2nd edition, September 2007.

NORSOK Standard (2017) N-003 - Action and Action Effects, 3rd edition, March 2017.

NORSOK Standard (2004) N-004 - Design of Steel Structures, 2nd edition, October 2004.

NORSOK Standard (2009) N-006 - Assessment of Structure Integrity for Existing Offshore Load-bearing Structures, 1st edition, March 2009. Notaro, G., Østvold, T., Steen, E., Oma, N. (2013) Collision Damages and Residual Hull Girder Strength of a Ship Shaped FPSO, In the proceedings for the 12th PRADS2013, pp. 1011~1019, 20-25 October, 2013, CECO, Changwon City, Korea.

Notaro, G., Johansen, A., Selåas, S., Nybø, T. (2015) Estimation of High Energy Collision Response for Jacket Structure, In the proceedings of the ASME 2015 34th International Conference on Ocean, Offshore and Arctic Engineering (OMAE2015), May 31-June 5, 2015, St. John's, Newfoundland, Canada.

Nour El-Din et al. (2014 a) Seismic Performance Evaluation and Retrofit of Fixed Jacket Offshore Platform Structures, Journal of Performance of Constructed Facilities, October 2014.

Nour El-Din et al. (2014 b) Seismic performance of pile-founded fixed jacket platforms with chevron braces, Structure and Infrastructure Engineering, 2015, Vol. 11, No. 6, 776–795, Maintenance, Management, Life-Cycle Design and Performance, Published on line May 2014.

Maestro (2017) https://maestromarine.com/maestro-base-module/procoll-hull/, Date accessed: 21 Nov 2017.

Magoga, T., Flockhart, C. (2014) Effect of weld-induced imperfections on the ultimate strength of an aluminium patrol boat determined by the ISFEM rapid assessment method, Ships And Offshore Structures, 9(2), 218-235.

MAIB (2008) Report on the investigation of the structural failure of MSC Napoli English Channel on 18 January 2007, Marine Accident Investigation Branch, Southampton UK, April 2008.

Ma, J. L., Chan, T. M., Young, B. (2016) Experimental investigation of cold-formed high strength steel tubular beams. Engineering Structures, 126, 200-209.

Mansour, A. E. (1972) Probabilistic design concepts in ship structural safety and reliability, SNAME Trans., 80, 64-97.

Mansour, A. E., Faulkner, D. (1972) On applying the statistical approach to extreme sea loads and ship hull strength, RINA Trans., 114, 273-314.

Mansour, A., Faulkner, D. (1973) On applying the statistical approach to extreme sea loads and ship hull strength. Transactions of RINA, 115, 227-313.

Mansour, A., Yang, J. and Thayamballi, A. (1990) An Experimental Investigation of Ship Hull Ultimate Strength, SNAME Transactions, 98, 411-439.

Mat Soom E. et al. (2015) Global Ultimate Strength Assessment (GUSA) for Lifetime Extension of Ageing Offshore Structures, Proceedings of the Twenty-fifth (2015) International Ocean and Polar Engineering Conference, Kona, Big Island, Hawaii, USA, June 21-26, 2015.

Matsumoto, T., Shigemi, T., Kidogawa, M., Ishibashi, K., Sugimoto, K. (2016) Examination of effect of lateral loads on the hull girder ultimate strength of large container ships, In Proceedings of the ASME 2016 35th International Conference on Ocean, Offshore and Arctic Engineering (OMAE2016), 19-24 June 2016, Busan, South Korea.

Morshedsoluk, F., Khedmati, M. (2016) Ultimate strength of composite ships' hull girders in the presence of composite superstructures, Thin-Walled Structures, 102, 122-138.

Murray, J. (1947) Longitudinal bending moments, London: Lloyd's Register of Shipping.

Muis Alie, M., Fuijikubo, M., Iijima, K., Oka, S., Takemura, K. (2012) Residual Longitudinal Strength Analysis of Ship's Hull Girder with Damages, Proceedings of the Twenty-second International Offshore and Polar Engineering Conference, 831-838.

Muis Alie, M., Sitepu, G., Sade, J., Mustafa, W, Nugraha, A., Saleh, A. (2016) Finite Element analysis on the hull girder ultimate strength of asymmetrically damaged ships, In Proceedings of the ASME 2016 35th International Conference on Ocean, Offshore and Arctic Engineering, OMAE2016-54041.

Obisesan, A., Sriramula, S., Harrigan, J. (2016) A framework for reliability assessment of ship hull damage under ship bow impact, Ships and Offshore Structures 11, 700–719.

Qi, E., Cui, W. (2006) Analytical method for ultimate strength calculations of intact and damaged ship hulls, Ships and Offshore Structures, 1 (2), 153-163.

Oksina, A., Lindemann, T., Kaeding, P., Fujikubo, M. (2016) Idealized Structural Unit Method – A review of the current formulation, In Proceedings of the ASME 2016 35th International Conference on Ocean, Offshore and Arctic Engineering (OMAE2016), OMAE2016-54186.

Paik, J., Hughes, O., Mansour, A. (2001) Advanced Closed-Form Ultimate Strength Formulation for Ships, Journal of Ship Research, 45 (2), 111-132.

Paik, J.K. (1995) Advanced idealised structural units considering the excessive tension deformation effects, J. Hydrospace Technology, 1 (1), 125-145.

Paik, J. K., Freize, P. A. (2001) Ship structural safety and reliability, Progress in Structural Engineering and Materials, Vol. 3(2), 198-210.

Paik, J., Kim, D., Park, D., Kim, H. (2012) A new method for assessing the safety of ships damaged by grounding, Trans RINA, 154 (A1) International Journal of Maritime Engineering.

Paik, J., Kim, D., Park, D., Kim, H., Mansour, A., Caldwell, J. (2013) Modified Paik-Mansour formula for ultimate strength calculations of ship hulls, Ships and Offshore Structures, 8, (3-4), 245-260.

Paik, J.K., Thayamballi, A.K. (2003) A concise introduction to the idealized structural unit method for nonlinear analysis of large plated structures and its application, Thin-Walled Structures, 41 (4), 329-355.

Paik, J., Mansour, A. (1995) A simple formulation for predicting the ultimate strength of ships, Journal of Marine Science and Technology, 1, 52-62.

Park, JS., Ha YS., Jang KR. (2015), Aluminium helideck design for Eurocode9 with deformation based design, ICSOT Korea: Safety of Offshore and Subsea Structures in Extreme and Accidental Conditions, 15-16 September 2015, Busan, Korea.

Parunov, J., Rudan, S., Corak, M. (2017) Ultimate hull-girder strength-based reliability of a double-hull oil tanker after collision in the Adriatic Sea, Ships and Offshore Structures, 12, 555-567.

Pei, Z., Chen, J., Ciu, C., Zhu, Z., Yang, P., Zhu, L. (2016) Research on Ultimate Strength of SWATH under Combined Loads, In Proceedings of the 26th International Ocean and Polar Engineering Conference, Rhodes, Greece, ISOPE 1005-1009.

Pei, Z., Iijima, K., Fujikubo, M., Tanaka, S., Okazawa, S., Yao, T. (2015) Simulation on progressive collapse behaviour of whole ship model under extreme waves using idealized structural unit method, Marine Structures, 40, 104-133.

Pei, Z., Iijima, K., Fujikubo, M., Tanaka, Y., Tanaka, S., Okazawa, S., Yao, T. (2012) Collapse Behaviour of a Ship Hull Girder of Bulk Carries under Alternative Heavy Loading Condition, Proceedings of the 22nd International Offshore and Polar Engineering Conference, 839- 846.

Pei, Z., Takami, T., Gao, C., Fu, J., Tanaka, Y., Iijima, K., Fujikubo, M., Yao, T. (2010) Development of ISUM Shear Plate Elements and Its Application to Progressive Collapse Analysis of Plates under Combined Loading, In Proceedings of the 20th International Offshore and Polar Engineering Conference, 4, 773-780.

Peschmann, J., Storhaug, G. Derbanne, Q., Xie, G., Zheng, G., Ishibashi, K., Kim, J., (2016) Impact Study on the new IACS Longitudinal Strength Standard for Containerships (UR S11A), Proceedings of PRADS2016, Copenhagen, Denmark, 4-8 Sep 2016.

Petricic, M. (2015) Survivability of hull girder in damaged condition, SSC report SSC-442, Ship Structures Committee.

Pournara, A. E., Karamanos, S. A., Mecozzi, E., Lucci, A. (2017) Structural resistance of high-strength steel CHS members, Journal of Constructional Steel Research, 128, 152-165.

Qian, X., Zhang, Y. (2015) Translating the material fracture resistance into representations in welded tubular structures, Engineering Fracture Mechanics, 147, 278-292.

Qiu, W., McCann, F., Espinos, A., Romero, M. L., Gardner, L. (2017) Numerical analysis and design of slender concrete-filled elliptical hollow section columns and beam-columns, Engineering Structures, 131, 90-100.

Rashed, S. (2016) ISUM – Its birth, growth and future, In Proceedings of the ASME 2016 35th International Conference on Ocean, Offshore and Arctic Engineering (OMAE2016), OMAE2016-54479.

Reis, A., Lopes, N., Real, E., Real, O. V. (2017) Numerical modelling of steel plate girders at normal and elevated temperatures, Fire Safety Journal. 86, 1-15.

Rigo, P., Sarghiuta, R., Otelea, SC., Pasqualino, I., Wan, Z., Yao, T., Toderan, C., Richir, T. (2004) Ultimate strength of aluminium stiffened panels: sensitivity analysis, In the 9th International Symposium on Practical Design of Ships and other Floating Structures, Luebeck Travemuende, Germany, 2004 Sep 12–17.

RINA (2011) Rules for the Classification of Naval Ships, 1 July 2011, RINA S. p. A., Genova, Italy.

RINA (2017) Rules for the Classification of Ships, 1 January 2017, RINA S. p. A., Genova, Italy.

Roeder, C. W. (1990) Comparison of LRFD and Allowable Stress Design Methods for Steel Structures, 5th Seminario de Ingenieria Estructural, San Jose, Costa Rica, Nov. 1990.

Russo, M., Renaud, F., Steen, E., Kippenes, J., Oma, N. (2009) Residual Strength of a FPSO Vessel After Collision Damages, In proceedings for the 28th international conference on Ocean, Offshore and Artic Engineering (OMAE 2009) , Honolulu, Hawaii 31st May-5 June 2009.

Rutherford, S., Caldwell J. (1990) Ultimate Strength of Ships: A Case Study, SNAME Transactions, 98, 441-471.

Saad-Eldeen, S., Garbatov, Y., Soares, C. G. (2011) Experimental assessment of the ultimate strength of a box girder subjected to severe corrosion, Marine Structures 24(4): 338-357.

Saad-Eldeen, S., Garbatov, Y., Soares, C. G. (2016 a) Experimental strength assessment of thin steel plates with a central elongated circular opening, Journal of Constructional Steel Research, 118, 135-144.

Saad-Eldeen, S., Garbatov, Y., Soares, C. G. (2016 b) Experimental investigation on the residual strength of thin steel plate with a central elliptic opening and locked cracks, Ocean Engineering, 115, 19-29.

Saad-Eldeen, S., Garbatov, Y., Soares, C. G. (2016 b, c) Experimental strength analysis of steel plates with a large circular opening accounting for corrosion degradation and cracks subjected to compressive load along the short edges, Marine Structures, 48, 52-67.

Saad-Eldeen, S., Garbatov, Y., Soares, C. G.. (2016) Fast approach for ultimate strength assessment of steel box girders subjected to non-uniform corrosion degradation, Corrosion Engineering, Science and Technology, 51, 60-76.

Saad-Eldeen, S., Garbatov, Y., Soares, C. G. (2017) Experimental compressive strength analyses of high tensile steel thin-walled stiffened panels with a large lightening opening, Thin-Walled Structures, 113, 61-68.

Saad-Eldeen, S., Garbatov, Y., Soares, C. G. (2018) Ultimate bending capacity of multi-bay tubular reinforced structures, in: C. Guedes Soares, A.P. Teixeira (Eds.) Maritime Transportation and Harvesting of Sea Resources, Taylor & Francis Group, London, UK, 2018, pp. 671-678.

Saez, S.S., Barbero, E., Zaera, R., Navarro, C. (2005), Compression after impact on thin composite laminates, Compos. Sci. Technol. 65 (13), 1911–1919.

Seo, JK., Park, DK., Jo, SW., Park, JS., Koo, JB., Ha, YS., Jang, KB. (2016), A numerical and experimental approach for optimal structural section design of offshore aluminium helidecks, Thin-walled Structures.

Seo, J. W., Song, C. H., Park, J. S., Paik, J. K. (2016) Nonlinear structural behavior and design formulae for calculating the ultimate strength of stiffened curved plates under axial compression, Thin-Walled Structures, 107, 1-17.

Shao, Y. B., He, S., Yang, D. (2017) Prediction of static strength for CHS tubular K-joints at elevated temperature, KSCE Journal of Civil Engineering, 21, 900-911.

Shao, Y. B., He, S., Zang, H., Wang, Q. (2017) Hysteretic behavior of tubular T-joints after exposure to elevated temperature, Ocean Engineering, 129, 57-67.

Shi, G., Wang, D. (2012) Ultimate strength model experiment regarding a container ship's hull structures, Ships and Offshore Structures 7(2), 165-184.

Shi, X., Teixeira, Â. P., Zhang, J., Soares, C. G., (2015) Kriging response surface reliability analysis of a ship-stiffened plate with initial imperfections, Structure and Infrastructure Engineering 11, 1450–1465.

Shi, X. H., Teixeira, A. P., Zhang, J., Soares, C. G. (2016) Reliability analysis of a ship hull structure under combined loads including slamming loading, Ships and Offshore Structures 11, 300–315.

Silva, J. E., Garbatov, Y., Soares, C. G. (2013) Ultimate strength assessment of rectangular steel plates subjected to a random localized corrosion degradation, Engineering Structures, 52, 295-305.

Silva, J. E., Garbatov, Y., Soares, C. G., (2014) Reliability assessment of a steel plate subjected to distributed and localized corrosion wastage, Engineering Structures, 59, 13-20.

Smith, C. (1977) Influence of local compressive failure on ultimate longitudinal strength of a Ship's hull, In: Proceedings of 3th international symposium on practical design in shipbuilding, p. 73–9.

Smith, C., Dow, R. (1981) Residual Strength of Damaged Steel Ships and Offshore Structures, Journal of Constructional Steel Research, 1 (4), 2-15.

Smith, C., Dow, R. (1986) Ultimate strength of a ship's hull under biaxial bending, ARE TR 86204, Admiralty Research Establishment, Dunfermline UK.

Smith, C., Anderson, N., Chapman, J., Davidson, P., Dowling, P. (1992) Strength of stiffener plating under combined compression and lateral pressure. Transactions of RINA, 134, 131-147.

Smith, M., Pegg, N. (2003) Automated Assessment of Ultimate Hull Girder Strength, Journal of Offshore Mechanics and Arctic Engineering, 125(3), 211-218.

Smith, M. (2010) A load shortening curve library for longitudinally stiffened panels. DRDC Atlantic TM 2010-140, Defence R&D Canada – Atlantic, Dartmouth, Canada.

Sohn, J., Bae, D., Bae, S., Paik, J. (2017) Nonlinear structural behaviour of membrane-type LNG carrier cargo containment systems under impact pressure loads at -163 °C, Ships and Offshore Structures, 12 (5) 722-733.

Storheim, M., Amdahl, J. (2017) On the sensitivity to work hardening and strain-rate effects in nonlinear FEM analysis of ship collisions, Journal of Ships and Offshore Structure, Volume 12, 2017.

Storheim, M., Notaro, G., Johansen, A., Amdahl, J. (2016) Comparison of ABAQUS and LS-DYNA in Simulations of Ship Collisions, in the proceedings of the 2016 ICCGS conference, 15-18 June, 2016, University of Ulsan, Ulsan, Korea.

Sun, H., Guedes Soares, C. (2003) An experimental study of ultimate torsional strength of a ship-type hull girder with a large deck opening, Marine Structures, 16, 51–67.

Sumi, Y., Fujikubo, M., Fujita, H., Kawagoe, Y., Kidogawa, M., Kobayashi, K., Nakano, T., Iwano, J., Takahira, T., Tamura, K., Ueda, N. (2015) Final Report of Committee on Large Container Ship Safety, Japan.

Tanaka, Y., Hashizume, Y., Ogawa, H., Tatsumi, A., Fujikubo, M. (2016) Analysis method of ultimate strength of ship hull girder under combined loads – application to an existing container ship, In Proceedings of the ASME 2016 35th International Conference on Ocean, Offshore and Arctic Engineering (OMAE2016), Busan, South Korea, 19-24 June 2016.

Tanaka, Y., Ogawa, H., Tatsumi, A., Fujikubo, M. (2015) Analysis method of ultimate hull girder strength under combined loads, Ships and Offshore Structures, 10(5), 587-598.

Tayyar, G., Nam, J., Choung, J. (2014) Prediction of hull girder moment-carrying capacity using kinematic displacement theory, Marine Structures, 39, 157-173.

Toh, K., Yoshikawa, T. (2015) A study on the effect of lateral loads on the hull girder ultimate strength of bulk carriers, In Proceedings of the 5th International conference on Marine Structures (MARSTRUCT 2015), 425-434.

Tatsumi, A., Fujikubo, M. (2016) Finite element analysis of longitudinal bending collapse of container ship considering bottom local loads, In Proceedings of the ASME 2016 35th International Conference on Ocean, Offshore and Arctic Engineering (OMAE2016), Busan, South Korea, 19-24 June 2016.

Tekgoz, M., Garbatov, Y., Guedes Soares, C. (2015) Ultimate strength assessment of a container ship accounting for the effect of neutral axis movement, In Proceedings of 2nd International Conference on Maritime technology and Engineering, 417-424.

Tekgoz, M., Garbatov, Y., Guedes Soares, C. (2015) Ultimate strength assessment of welded stiffened plates, Engineering Structures, 84, 325–339.

Toh, K., Maeda, S., Yoshikawa, T. (2015) A Study on the Simplified Calculation Method for the Hull Girder Ultimate Strength of Damaged Hull Structures, ISOPE-I-15-764, International Society of Offshore and Polar Engineers.

Ueda, Y., Rashed, S. M. H. (1984) The idealised structural unit method and its application to deep girder structures. Computers & Structures, 18 (2), 277-293.

Ueda, Y., Rashed, S. M. H., Nakacho, K., Sasaki, H. (1983) Ultimate strength analysis of offshore structures – application of idealised structural unit method. J. Kansai Society Naval Architects Japan. 190, 131-142 (in Japanese)

Uenaka, K., Tsunokake, H. (2016) Behavior of Concrete Filled Elliptical Steel Tubular Deep Beam under Bending-Shear, Structures, 10, 89-95.

Underwood, J., Sobey, A., Blake, J., Shenoi, R. (2016) Compartment level progressive collapse strength as a method for analysing damaged steel box girders, Thin Walled Structures, 106, 346-357.

Vasilikis, D., Karamanos, S. A., Van Es, S. H. J., Gresnigt, A. M. (2016) Ultimate bending capacity of spiral-welded steel tubes – PartII: Predictions, Thin-Walled Structures, 102, 305-319.

Vasta, J. (1958) Lessons Learnt from Full-Scale Ship Structural Tests, SNAME Transactions, 66, 165-243.

Van Es, S. H. J., Gresnigt, A. M., Vasilikis, D., Karamanos, S. A. (2016) Ultimate bending capacity of spiral-welded steel tubes – Part I: Experiments, Thin-Walled Structures, 102, 286-304.

Van Hove, D., Soetens, F. (2014) Optimization of aluminium stressed skin panels in offshore applications. Materials, 7, 6811-6831.

Wan, C. Y., Zha, X. X. (2016) Nonlinear analysis and design of concrete-filled dual steel tubular columns under axial loading, Steel and Composite Structures, 20, 571-597.

Wang, H.D., Liang, X.F., Yi, H., Li, D. (2016) A Bayesian Networks Based Method for Ship Reliability Assessment, Presented at the Proceedings - 46th Annual IEEE/IFIP International Conference on Dependable Systems and Networks, DSN-W 2016, pp. 25–30.

Wang, S.X., Wu, L.Z., Ma, L. (2010), Low-velocity impact and residual tensile strength analysis to carbon fibre composite laminates, Mater. Des. 31 (1), 118–125.

Woelke, P., Hiriyur, B., Nahshon, K., Hutchinson, J. (2017) A practical approach to modeling aluminium weld fracture for structural applications, Engineering Fracture Mechanics, 175, 72-85.

Xu, M. C., Song Z. J., Pan J. (2017 c) Study on influence of nonlinear finite element method models on ultimate bending moment for hull girder, Thin-Walled Structures, 234 (Accepted).

Xu, M. C., Song Z. J., Pan J., Guedes Soares, C. (2017 a) Ultimate strength assessment of continuous stiffened panels under combined longitudinal compressive load and lateral pressure, Ocean Engineering, 139 , 39-53.

Xu, M. C., Song Z. J., Pan J., Guedes Soares, C. (2017 b) Study on the influence of the initial deflection and load combination on the collapse behaviour of continuous stiffened panels, International Journal of Steel Structures, SSIJ-D-17-00009R2 (Accepted).

Xu, M. C., Teixeira, A. P., Soares, C. G. (2015) Reliability assessment of a tanker using the model correction factor method based on the IACS-CSR requirement for hull girder ultimate strength, Probabilistic Engineering Mechanics, 42, 42-53.

Xu, M. C., Guedes Soares, C. (2015) Effect of a central dent on the ultimate strength of narrow stiffened panels under axial compression, International Journal of Mechanical Sciences, 100, 68-79.

Xu, W., Duan, W. (2016) Prediction and parametric study on the severity of collapse of a Capesize bulk carrier under extreme wave loads, Ships and Offshore Structures, 11(6):655-666.

Yao, T. (2016) Evaluation of ultimate hull girder strength in longitudinal bending – historical review and Smith's method, In Proceedings of the ASME 2016 35th International Conference on Ocean, Offshore and Arctic Engineering (OMAE2016), Busan, South Korea, 19-24, June 2016.

Yao, T., Fujikubo, M. (2016) Buckling and Ultimate Strength of Ship and Ship-like Floating Structures, Oxford, UK: Butterworth-Heinemann.

Yao, T., Nikolov, P. (1991) Progressive Collapse Analysis of a Ship's Hull under Longitudinal Bending, Journal of the Society Naval Architects of Japan, 170, 449-461.

Yao, T., Nikolov, P. (1992) Progressive Collapse Analysis of a Ship's Hull under Longitudinal Bending (2nd Report), Journal of the Society Naval Architects of Japan, 172, 437-446.

Yan, J. B., Liu, X., Liew, J. Y. R., Qian, X., Zhang, M. H. (2016) Steel-concrete-steel sandwish system in Arctic offshore structures, materials, experiments and design. Materials and Design, 91, 111-121.

Yan, J. B., Wang, J. Y., Liew, J. Y. R., Qian, X., Liang, Z. (2016 a) Ultimate strength behavior of steel-concrete-steel sandwich plate under concentrated loads. Ocean Engineering, 118, 41-57.

Yan, J. B., Wang, J. Y., Liew, J. Y. R., Qian, X., Li, Z. (2016 b) Punching shear behavior of steel-concrete-steel composite plate under patch loads. Journal of Constructional Steel Research, 121, 50-64.

Yamada, Y. (2014) Numerical study on the residual ultimate strength of hull girder of a bulk carrier after ship-ship collision, in Proceedings of the ASME 2104 33rd International conference on Ocean, Offshore and Arctic Engineering (OMAE 2014), San Francisco, CA, 8-13 June 2014.

Yoon, D., Park, J., Eccles, T., Powell, A., Manley D., Widholm, A. (2010) Joint Investigation Report On the Attack Against ROK Ship Cheonan, Ministry of National Defence, Republic of Korea.

Youssef, S., Noh, S., Paik, J. (2017) A new method for assessing the safety of ships damaged by collisions, Ships and Offshore Structures, 12, 862-872.

Youssef, S., Faisal, M., Seo, J., Kim, B., Ha, Y., Kim, D. Paik, J., Cheng, F., Kim, M. (2016) Assessing the risk of ship hull collapse due to collision, Ships and Offshore Structures, 11(4) 335-350.

Yu. et al. (2016) New LFRD-Based design criteria for mobile offshore units and floating production Installations, In proceedings for Offshore Technology Conference (OTC 2016), Houston, Texas, USA, 2-5 May 2016.

Yu, K., Morozov, E.V., Ashraf, M.A., Shankar, K. (2015) Numerical analysis of the mechanical behavior of reinforced thermoplastic pipes under combined external pressure and bending, Composite Structures, 131, 452-461.

Zhang, S. M. (2016) A review and study on ultimate strength of steel plates and stiffened panels in axial compression. Ship and Offshore Structures, 11:1, 81-91.

Zhang, X., Paik, J. K., Jones, N. (2016) A new method for assessing the shakedown limit state associated with the breakage of a ship's hull girder, Ships and Offshore Structures, 11(1),92-104.

Zhang, Z., Wang, Y. Zhao, H., Qian, H., Mou, J. (2015) An experimental study on the dynamic response of a hull girder subjected to near field underwater explosion, Marine Structures, 44, 43-60.

Zhao, M. S., Chiew, S. P. and Lee, C. K. (2016) Post weld heat treatment for high strength steel welded connections, Journal of Constructional Steel Research, 122, 167-177.

Zhao, Y., Yan, R., Wang, H. (2016) Experimental and numerical investigations on plate girders with perforated web under axial compression and bending moment. Thin-Walled Structures, 97, 199-206.

Zhu, L., Han, S., Song, Q. M. Ma, L. M., Wei, Y., Li, S. W. (2016) Experimental study of the axial compressive strength of CHS T-joints reinforced with external stiffening rings, Thin-Walled Structures, 98, 245-251.

This page intentionally left blank

Proceedings of the 20th International Ship and Offshore Structures Congress (ISSC 2018) Volume I – M.L. Kaminski and P. Rigo (Eds.)

doi:10.3233/978-1-61499-862-4-441

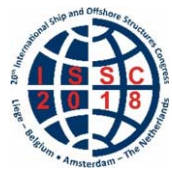

COMMITTEE III.2

FATIGUE AND FRACTURE

COMMITTEE MANDATE

Concern for crack initiation and growth under cyclic loading as well as unstable crack propagation and tearing in the ship and offshore structures. Due attention shall be paid to the suitability and uncertainty of physical models and testing. Consideration is to be given to practical application, statistical description and fracture control methods in design, fabrication and service.

COMMITTEE MEMBERS

Chairman: Y. Garbatov, *Portugal*
S.K. Ås, *Norway*
K. Branner, *Denmark*
B.K. Choi, *South Korea*
J. H. Den Besten, *The Netherlands*
P. Dong, *USA*
I. Lillemäe, *Finland*
P. Lindstrom, *Sweden*
M. Lourenço de Souza, *Brazil*
G. Parmentier, *France*
Y. Quéméner, *China* (*Taiwan*)
C.M. Rizzo, *Italy*
J. Rörup, *Germany*
S. Vhanmane, *India*
R. Villavicencio, *UK*
F. Wang, *China*
J. Yue, *China*

EXTERNAL CONTRIBUTORS

Andoniu, A., *France*, Chen, K-C., *China* (*Taiwan*), Dong, Y., *Portugal*, Eggert, L., *Germany,* Negi, A., *India*, Parihar, Y., *India,* Parsoya, V., *UK*, Uzunoglu, E., *Portugal,* Qin, Y., *The Netherlands*

KEYWORDS

Fatigue, fracture, steel, aluminium, polymer composites, damage accumulation, crack growth, fabrication, inspection, maintenance, reliability, design, verification, fitness for service, rules, standards.

CONTENTS

1. FATIGUE AND FRACTURE LOADING 445
1.1 Fatigue loading 445
1.1.1 Metocean description 445
1.1.2 Waves 446
1.1.3 Current 448
1.1.4 Wind 449
1.1.5 Temperature and ice 449
1.1.6 Earthquakes and soil interaction 450
1.1.7 Operations 450
1.1.8 Loading interaction 451
1.2 Fatigue loading calculation 451
1.2.1 Rules, standards, codes and guideline-based assessment 451
1.2.2 Direct assessment 452
1.3 Fracture loading 454

2. MATERIAL PROPERTIES AND TESTING 454
2.1 Material properties 454
2.1.1 Monotonic material behaviour 454
2.1.2 Cyclic material behaviour 455
2.1.3 Fracture properties 455
2.1.4 Fatigue properties 456
2.1.5 Materials 456
2.1.6 Arc-welded and laser welded joints 457
2.1.7 Friction stir welded joints 457
2.1.8 Corrosive environment 458
2.1.9 Similarity 459
2.2 Polymer composites testing 459
2.2.1 Sub-components 460
2.2.2 Full-scale components 460
2.3 Testing methods and measurement techniques 461

3. FATIGUE DAMAGE ACCUMULATION APPROACHES 462
3.1 Overview 463
3.2 Damage criterion advances 463
3.2.1 Hotspot structural stress 464
3.2.2 Effective notch stress 464
3.2.3 Effective notch strain 466
3.2.4 Notch stress intensity 466
3.2.5 Strain energy density (SED) 466
3.2.6 Peak stress 467
3.2.7 Battelle structural stress 467
3.2.8 Total stress 467
3.2.9 Crack tip stress or strain intensity 468
3.2.10 Crack tip energy release rate 470
3.3 Damage mechanics criterion advances 470
3.4 Complete strength criteria 470
3.4.1 Multiaxiality and amplitude variability 470
3.4.2 Mean- and residual stress 474
3.4.3 Time and frequency domain 475
3.4.4 Environment 476
3.5 Total life criteria 477

3.6 Multi-scale criteria 478
3.7 Damage criterion statistics 480

4. CRACK GROWTH APPROACHES 480
4.1 Defects and initial cracks 480
4.2 Crack sizing during in-service inspection 481
4.3 Modelling 481
4.3.1 Paris relations 481
4.3.2 Modified relations 482
4.4 Parameter estimates 484
4.5 Experimental data 484
4.6 Numerical simulations 484
4.6.1 Loading sequence 484
4.6.2 Residual stress 485
4.6.3 Simulation on different crack forms and positions 485
4.6.4 Damage mechanics models 486
4.6.5 Polymer composites 487
4.7 Crack growth assessment statistics 487
4.8 Service life extension 488

5. FABRICATION, DEGRADATION, IMPROVEMENTS AND REPAIR 489
5.1 Fabrication imperfections 489
5.1.1 Misalignments and distortions 489
5.1.2 Welding induced defects 490
5.1.3 Initial crack size 492
5.2 In-service degradation 493
5.3 Strength improvement 493
5.4 Polymer composite patch repairs 496

6. FATIGUE RELIABILITY 497
6.1 Statistical descriptors 498
6.1.1 Fatigue loading 498
6.1.2 Fatigue damage accumulation 499
6.1.3 Crack growth 500
6.2 Limit state functions 500
6.2.1 Fatigue damage accumulation 500
6.2.2 Crack growth 501
6.3 Calibration factors for design 502
6.4 Fatigue service lifetime estimate 504
6.4.1 Fatigue damage accumulation 504
6.4.2 Crack growth 505

7. FATIGUE DESIGN AND VERIFICATION BASED ON RULES, STANDARDS, CODES AND GUIDELINES 506
7.1 Common Structural Rules (CSR) 506
7.1.1 Fatigue capacity 507
7.1.2 Fatigue Loads 507
7.1.3 Fatigue assessment 508
7.2 DNV·GL regulations 508
7.3 Lloyd's Register (LR) regulations 509
7.4 Bureau Veritas (BV) regulations 510
7.5 Indian Register of Shipping (IRS) regulations 511
7.6 Comparison of simplified fatigue approaches 512

7.6.1 Loading 513
7.6.2 Response 514
7.6.3 Assessment 517
7.7 International Gas Carrier (IGC) code 517

8. CONCLUSIONS AND RECOMMENDATIONS 518
8.1 Fatigue and fracture loading 518
8.2 Material properties and testing 519
8.3 Fatigue damage accumulation approaches 519
8.4 Crack growth approaches 520
8.5 Fabrication, degradation, improvements and repair 520
8.6 Fatigue reliability 521
8.7 Fatigue design and verification based on rules, standards, codes and guidelines 521

REFERENCES 522

1. FATIGUE AND FRACTURE LOADING

Fatigue loading may act either sequentially or simultaneously at different periods of the ship and offshore structures lifetime. The Chapter focus is on environmental loading, e.g. associated with waves, wind, current and temperature as well as operational loadings like the successive loading and unloading of the cargo and motion-induced contributions. For offshore structures, it also includes loading encountered during transit/transportation (e.g. from the yard to the operating location), as well as during installation (e.g. piling of fixed foundation).

Fracture is related to unstable crack propagation, depending on strain rate and temperature effects.

1.1 Fatigue loading

The time-varying fatigue loadings are typically environment and operations induced.

1.1.1 Metocean description

The metocean description aims to determine the environmental conditions in which a ship or offshore structure may experience during its service life based on past observations. Data may be obtained from meteorological records combined with hind-casting for locations where data is not available or insufficient. In the last decades, satellite data has been used as a source for defining the sea states. Such data is obtained as a sequence of historical sea states, wind, current, temperatures, etc. The basic assumption is that climate change may be neglected in view of the time scale of typical design lives, and thus that the statistical distribution of the environmental parameters (sea states, wind, current and temperature) are assumed to stay unchanged. Then, the information is organized according to the need of the designer to estimate the fatigue damage. A common procedure consists of defining a table of long-term distributions of sea states, referred to as a Scatter Diagram. Scatter Diagrams provide information regarding statistical distributions of sea states without consideration regarding the sequence of those sea states, e.g. evolution of sea states before and after a storm event. When the linear Palmgren-Miner rule for damage assessment is employed the Scatter Diagrams are sufficient to provide a reasonably accurate lifetime estimate. On the contrary, when the damage accumulation is nonlinear as for the crack growth model that involves the threshold effect, the sequence of sea state occurrences may significantly influence the fatigue damage and crack growth estimates. Therefore, the statistical description of sea states can be improved using a storm model. For ships, the environmental conditions experienced by the structure depend not only on the metocean description of each region along the shipping route but also on the time spent in each area, which implies its forward speed. The forward speed also significantly influences the ship motions and thus the load amplitudes, as well as the number of waves encountered during the design life and thus the number of load cycles. Finally, when needed by the designer, the Scatter Diagram can be reorganized per seasons, wave directions, and, especially for offshore units, according to current and wind speeds and directions. As such, all relevant environmental parameters, with respect to fatigue, can be statistically correlated.

For ships, the design metocean description depends on the trading pattern of the ship. Ships designed for deep sea operations are supposed to be able to navigate worldwide. It is generally admitted that the worst navigating condition corresponds to the North Atlantic environment and that a Scatter Diagram is accordingly provided by IACS (2001) in association with an assumed averaged ship speed set to ¾ of the ship service speed for any relative wave headings. Although this approach may be considered too conservative given the negligible part of the world fleet of bulk carriers and oil tankers continuously operating in North Atlantic environment, IACS (2014b) justifies this assumption by the appropriate margin it provides for the rules fatigue assessment methodology that omits the dynamic response contribution, e.g. springing and whipping, to the total fatigue damage. Therefore, for ships not verified accordingly to the CSR, the utilization of a milder environment for the fatigue assessment of ships should be conditional

on the assessment of the fatigue considering the quasi-static and dynamic wave loads. An alternative metocean description, the so-called "Worldwide Environment", results in a significant wave height 20% smaller than the one produced by the IACS North Atlantic scatter diagram. So far, no standard metocean description has been commonly accepted by Classification Societies for ships with restricted navigation conditions. Upon Class agreement, a specific metocean description may be employed for ships operating in a dedicated area.

For offshore structures, an accurate metocean description for the dedicated site can be carried out from meteorological data when long-term measurements are available. Contrary to ships fatigue assessment that only considers waves, the good statistical reproduction of the correlation between all involved environmental parameters, e.g. wave, winds and current, can have a significant effect on the accuracy of the fatigue assessment. Additionally, in contrast to ships, an offshore structure cannot avoid the worst meteorological conditions by changing their route. Those extreme events may have a significant impact on the fatigue life of the unit, especially when considering the underload and overload effects on the fatigue retardation. The metocean description of waves is generally available far from the shore. To determine the fatigue load history, a first step in the analysis involves rebuilding the local metocean description at the actual location of the offshore structure, commonly in shallow water. Different approaches have been proposed to transfer spectrum energy from deep sea to nearshore (Wang et al., 2016a), but simplified approaches are not easily validated and fully nonlinear approaches such as the Enhanced Spectral Boundary Integral (ESBI) remain more reliable despite the calculation cost. This local metocean description is generally checked by in situ measurements, but the measurements duration is generally not sufficient to provide an exhaustive description of the local metocean description.

1.1.2 Waves

Amongst all the loads and environmental effects considered in this Chapter, the wave-induced loads are generally the most influential. Especially for ships, fatigue analysis is usually based on wave-induced loads only. The wave-induced loads are estimated based on the ships patterns in navigation or operation, i.e. the metocean description, and the response of ship and offshore structures in terms of motions. For the metocean description, the Scatter Diagram is a simplified way to provide a statistical representation of the sea state for each area. The drawback of such wave scatter diagrams is that information regarding the evolution of the sea states at a specific event, such as before and after a storm, is lost. The storm model aims to organize sets of sea states to simulate the sequence of sea states during a depression. The current sources of sea states for design such as those in (Hogben et al., 1986) are not suitable for identifying the correlation among the sea-states. A model based on a Fourier series expansion is proposed in (Minoura, 2016) involving both seasonal and non-seasonal parameters. The parameters involved in the model are the significant wave height, wave period, wind velocity, and their correlations. This approach allows the consideration of retardation of crack propagation as a result of overloads observed in the previous storm, as presented in (Yan et al., Hodapp et al., 2015), that may lead to more optimistic predictions compared to assessments employing the usual assumption of linear fatigue damage accumulation.

Actual ship routes are driven by trade request, time of delivery and fuel consumption, but they can also occasionally be modified due to meteorological considerations. At the design stage, for ships with unrestricted notation, the most conservative environment is generally considered, and it supposes continuous operations in the North Atlantic Ocean. This conservative assumption can be mitigated by the fact that the crew may modify the route according to the meteorological forecast condition.

Additionally, forward speed is a function of sea conditions. In the head sea, cargo ships experience involuntary speed reduction due to added hydrodynamic resistance and power limitation of the propulsion engine. Besides, the crew may voluntarily reduce the speed or slightly change

the heading to reduce motion which will modify the load distribution in terms of intensity and period.

Ships navigating in coastal conditions may avoid the worst sea conditions due to the proximity to a harbour. Their mission profile involves the area of operation that implies the maximum distance between a port and the operational limitations including the speed. This speed limitation is, so far, only dependent on sea state conditions in terms of wave height as observed by organizations appointed by national authorities, although wave steepness and relative heading are equally important for determining the severity of wave loads.

In addition to the Class Notation, an unrestricted and other navigation notation may be assigned to ships such as summer zone, the tropical zone of the coastal area or sheltered area. The actual area of navigation of a merchant ship has not been exhaustively analysed. Some analyses are available on the actual routes versus the seasons. Data obtained using an Automatic Identification System, AIS, completed with the Geo-maritime-economy for a deep-sea navigation between the Gibraltar and North America coast is provided in (Vettor & Guedes Soares, 2015). On another hand, decreasing fatigue loads in a coastal navigation are the results of not only a lower level of wave heights but also the proximity to a port or safe sheltered anchorage which allows access before a storm.

Ships may be subjected to operational limitations. High-Speed Crafts are not allowed to navigate beyond a certain wave height and their ship-master/crew must observe the speed limitations that depend on the sea states. Some operations for offshore structures are not allowed beyond certain sea conditions, considered as not permissible.

Sea States Wave Spectra

Generally speaking, sea-state description involves significant wave height, wave period (e.g. mean zero up-crossing period), and wave direction. In addition, parameters related to the bandwidth and the corresponding wave spread (Li et al., 2015c) lead to lower fatigue load predictions.

Some more sophisticated models involve multi-directional spectra with different height and period according to direction. These multi-directional spectra may be important for moored offshore structures where heading in addition to wave direction depends on wind and the current. With multi-directional spectra, wave spectrum can be combined with wind spectrum inducing transverse responses that cannot be reproduced by unidirectional load considerations.

In near-shore conditions, the metocean description is generally not known a priori and designers use a dedicated methodology to obtain near-shore sea states from the known deep-water metocean description (Jaouën et al., 2016). It involves translating deep water sea states to shallow water sea states with combined effects of wind and current, with respect to the bathymetry and the boundary conditions. This involves a large number of combined sea states, winds and currents, in the order of thousands. These methodologies should be more detailed by Committee I.1.

Slamming, Whipping, and Springing

With the increasing size of the ship and offshore structures, e.g. container ships, floating airports or large fixed platforms, wave effects can induce resonant responses to natural frequencies of the hull girder. The resulting vibration due to the resonance phenomenon, namely springing, may increase the fatigue damage even in moderate sea states. For large ships in moderate sea states, the forward speed may favour the springing phenomenon, especially in head seas where the forward speed increases the wave encounter frequency to the level of the hull girder Eigenfrequency. For more severe sea states, the slamming of the ship's fore end and, occasionally, of the aft end can induce transient hull girder vibrations, also named whipping, with higher amplitude than those occurring during springing events (Liao et al., 2015). However, it can be anticipated that the crew will appropriately modify the course and speed of the ship to mitigate

the slamming load's intensity and consequently will reduce the whipping contribution to total fatigue.

Very large floating structures, e.g. offshore structures, are sensitive to springing, and its contribution to total fatigue damage is thus significant. Therefore, the evaluation of springing contribution to fatigue life is essential for the demonstration of the feasibility of a project. So far, there is no common approach to calculate the springing response of large container ships and its effect on the fatigue life of the ship structural details. The critical wave frequencies method is used in (Lee et al., 2014) to predict the springing response and fatigue life of a 10,000 TEU container ship, where fluid-structure interaction models were used to investigate the springing response and effects on design bending moments. A boundary element method and a finite element method were employed for coupling the fluid and structure domain problems, while the ship vibration modes and natural frequencies were calculated by idealizing the ship structure with the Timoshenko beam. The numerical analyses were validated by comparison with small-scale and full-scale measurements. The case of the study showed that the fatigue life of a large container ship can be reduced by 20% when considering the springing effect. Following the study in (Lee et al., 2014), the springing contribution to the total fatigue of a 20,000 TEU container ship at hotspot locations dominated by wave-induced vertical bending and torsional moments was investigated in (Im et al., 2015). A hydro-elastic numerical approach was employed that took into account the springing effect in the frequency-domain, for which the ship motions and associated bending and torsion moments were evaluated using a hydrodynamic software. Such load responses were compared between rigid and flexible bodies to investigate the effect of springing response on fatigue damage.

Furthermore, slamming may induce a high level of resonant response and, when repeated, the resulting damage can significantly contribute to the total fatigue damage. Tests on plating subjected to slamming loads show that the pressure history was not significantly affected by structural distortions due to repeated impacts as investigated in (Shin et al., 2016). Additionally, FE analyses were carried out, which produced progressive damage results for comparisons with those observed on test specimens. Alternatively, a computational fluid dynamic (CFD) method based on RANS formulation were used in (Zhu et al., 2016) to evaluate slamming pressure history on the wet deck of a SWATH. The numerical model's prediction compared well with the model tests' measurements. In order to extrapolate those test results to ships, the authors proposed a pressure coefficient to relate the slamming pressure to the velocity of water entry. A complete procedure to assess the whipping loads and their effect on fatigue is provided in (BV, 2015) that involves slamming load evaluation based on CFD formulations or Boundary Element Methods, seakeeping analysis and hydro-structure computations in the time-domain. Full-scale measurements have been carried out on container ships and are presented in (Kahl et al., 2015, Storhaug & Kahl, 2015) to evaluate the effect of whipping on the fatigue damage. Those large ships are prone to respond to slamming either with vertical or torsional modes of vibration. For the analysed ship in (Storhaug & Kahl, 2015), the observed damping corresponding to the torsional mode of vibrations is higher than that of the vertical mode when whipping occurs. Consequently, the torsional whipping contributes less to the total fatigue compared to the vertical bending mode from which the contribution was found to be significant. The combination of the quasi-static and whipping response is addressed in (Kahl et al., 2015), and a simplified approach is proposed that considers only the quasi-static wave induced loads magnified by the whipping effect, while the remaining whipping load cycles are disregarded, being deemed as having a negligible effect on fatigue.

1.1.3 Current

Current induces both constant and variable loads. Generally, current effects are disregarded for ships as being negligible compared to the forward speed effect. For bottom-fixed offshore structures, the current effect can significantly contribute to the total load and is considered as a constant load with slow variations, e.g. a few cycles per day for tidal current, a few cycles per week

or even per year for wind-induced currents. For moored floating offshore units, the current can induce indirect quasi-statically varying loads by changing mooring conditions. For pipes and risers, current may produce vortices with relatively high frequencies that generate the Vortex Induced Vibration (VIV) phenomena, whereas, for offshore moored floating units (e.g. Spars, semi-submersibles, TLPs and buoys) the current can generate vortices with a low frequency that can induce Vortex Induced Motions (VIM) phenomena.

For pipes and risers, VIV occurs when the vortex frequency that mainly relates to the structure diameter and current velocity is close to an eigenfrequency of the structure. For the case of a Steel Catenary Riser (SRC), numerical simulations were conducted in (Yin et al., 2015), which show that the predicted VIV-induced fatigue damage is very sensitive to the Reynolds number and the surface roughness according to flow regime (e.g. subcritical, critical or supercritical). Especially, higher fatigue damage is produced in a supercritical condition.

The boundary conditions of pipes and risers lying on the seabed are difficult to reproduce as they relate to soil behaviour, contact conditions, etc... As a result, fatigue assessment in the frequency-domain that assumes the linearity of the loads may become inaccurate with the variation of the stiffness and damping induced by the contact with the soil. Time-domain simulations were conducted in (Kahl et al., 2015) using Thorsen's hydrodynamic forces where the vortex shedding frequency corresponds to the pipe Eigen-frequency and which the lock-in is modelled through an empirical relationship. For a given current velocity, the results show a high sensitivity of the structure response to the various boundary condition settings in terms of stiffness and damping.

The VIM phenomena, encountered by moored floating offshore units subjected to current can degrade fatigue lives of the mooring lines' connections and risers. VIM occurs when the current-induced vortex shedding frequency meets the natural period of the floating unit, and it is usually predicted based on model tests or CFD simulations (Ye et al., 2016), although, especially for design purpose, simplified approaches are available.

With respect to fatigue assessment, the difference between VIM leading to large efforts i.e. large fluctuating forces and moment, generally leading to large displacements, with a low number of cycles and VIV leading to lower efforts, but often exciting vibration modes, with a higher number of cycles, is not critical in the sense that only the result in terms of effort and number of cycles is important. However, for the analysis of the phenomena, the existence of a resonant response is always challenging to simulate numerically, especially regarding the setting of the damping at the design stage to which the resonant response is highly sensitive.

1.1.4 Wind

For ships, wind loads are considered negligible compared to wave loads and are omitted in the fatigue assessment.

For bottom-fixed offshore wind turbines, the loads due to wind fluctuations in terms of speed and direction are important to fatigue damage evaluation. A methodology that consists of reproducing the stress range distribution using a rain flow method and organizing the resulting signals in a set of "events" corresponding to typical patterns, and reducing each event in a set of equivalent constant amplitudes was proposed in (Dragt et al., 2016).

1.1.5 Temperature and ice

Temperature loads may contribute to the total fatigue damage following environmental and operational conditions in terms of low cycle fatigue. Temperature loads are considered for gas carriers and particularly LNG carriers due to temperature variations during loading/unloading operations as indicated in the International Code for the Construction and Equipment of Ships Carrying Liquefied Gases in Bulk (IGC code). But other sources of temperature loads exist, such as the daily variation of air temperature combined with the solar radiation on the steel

plates combined with sea temperature or ballast temperature. Based on information available to date, the contribution of temperature loads to total fatigue damage seems limited and is generally disregarded except for gas carriers during loading/unloading operations. The main reason is that the accurate evaluation of the thermal expansion of structural components requires a fine description of the temperature field in the structure, and those data are generally missing. Besides, for the LNG tanks of gas carriers, the thermal expansion is included in the scope of the design scenarios for fatigue assessment, particularly during loading and unloading operations. As the stress range due to thermal loads during loading and unloading is, for some details, considerably higher than the stress range due to waves, the resulting fatigue damage can be significant not only due to the thermal stress range itself but also due to its interaction with wave-induced stress ranges. The thermal load cycle is combined with loads due to loading and unloading and with loads at sea to form the largest cycle of a given voyage within the Rain flow cycles counting process.

Ice loads are difficult to assess for fatigue damage using a standard approach as there is no consensus on loading scenarios. For this reason, loads recorded from voyages are essential to deduce design loads from actual load sequences experienced by ships. An estimation of the fatigue damage of a Korean Icebreaker based on two recording sequences of 55 days and 99 days was conducted in (Hwang et al., 2016). The fatigue assessment was based on strain measurements conducted in the bow thruster room on the side-shell. Further research is needed in that domain as it seems difficult to extrapolate from such a low set of voyages to define patterns of ice fatigue loads. Additionally, it may be expected that the ice fatigue loads would strongly depend on the ice environment, and on the shape and the power of the ship. Moreover, it can be anticipated that ships designed for regularly navigating in ice conditions are significantly reinforced and that the wave loads contribution to the fatigue should decrease accordingly.

1.1.6 Earthquakes and soil interaction

Soil interaction effects are to be considered. Frequent earthquakes may contribute to the fatigue of bottom-fixed offshore units. But so far, few events have been experienced and no publication is available. However, soil reactions to loads applied on the foundation of a fixed offshore unit are largely considered during design. The soil stiffness depends on the level of loads applied and the soil response is not linear (Dubois et al., 2016). This implies that dynamic response calculation should involve a determination of the stiffness of the foundations.

1.1.7 Operations

Operational loads, such as the cargo loading conditions for ships, are considered as constant during each phase of its service life. However, these constant loads have an effect on the structural fatigue behaviours since the resulting mean stresses act in combination with residual stresses from fabrication processes as well as from previous load histories, as presented in Chapters 3 and 4. Additionally, the interactions between constant and time-varying loads should be considered consistently with meteorological conditions. For example, heavy ballast conditions occur in the case of a storm, while normal ballast conditions are encountered in mild sea states. Therefore, the combination of constant and time-varying loads need to be carefully addressed at the design stage.

For ships, Classification Societies provide a set of typical loading conditions, associated with a constant load and a fraction of life. The light ballast is disregarded as being exceptional. A partial loading is not accounted for in tankers since navigations in partial loading are highly dependent on the oil market. For bulk carriers, four loading conditions are typically considered for the fatigue assessment: homogenous, alternate, heavy, and normal ballast. For LNG carriers in navigation, the tanks are either full or empty. For container ships, barges and passengers-ships, a single representative loading condition may be considered. For dredgers, LNG carriers, and FPSOs, frequent loading and offloading may imply the possibility of low cycle fatigue damage which should be combined with wave-induced fatigue damage.

For submersibles and submarines, compressive loading due to deep diving may be a source of fatigue because local yielding at hot spot areas under maximum compression may change residual stress states, resulting in a local tensile residual stress field which may cause crack growths. For those units, the contribution of such low cycle fatigue damage induced by repeated deep diving can be significant comparing with wave-induced fatigue damage. Although this phenomenon is frequently observed on naval submarines, it is not often reported in the literature for the sake of confidentiality.

Loading/unloading caused damage is generally negligible for deep-sea ships. Nevertheless, for ships navigating in protected areas with short trips, loading/unloading-induced fatigue damage can become significant due to the large stress range resulting from loading/unloading allowed by rules, e.g. for large dredgers. Therefore, loading/unloading should be combined with the other loads. The same can be said for offshore structures, e.g. FPSOs, FSO tanks during operation. Moreover, for all types of cargo ships, loading and unloading caused fatigue damage cannot be ignored.

1.1.8 Loading interaction

As mentioned above, ship and offshore structures are subjected to different types of loads and the fatigue damage accumulation resulting from the superposition of different environmental loads e.g. wind, wave, current, is not a simple sum of the damages produced for each load calculated separately. However, it is extremely time-consuming to simulate numerically the integrated loads related to the considered unit in its design environment, as well as the associated structural response, especially for a long duration such as design life. Therefore, most of the researchers tend to address that question by proposing simplified approaches, defining a kind of equivalent cycles allowing calculating stress cycles giving the damage experienced by the structure. For example, a study presented in (Ormberg & Bachynski, 2015) simulated the contribution of waves to the fatigue of a spar wind tower and then super-imposed the wind contribution. Various simulations have been carried out to consider the individual effect of wind and associated turbulence with an increasing level of complexity of the wind models, and then by combining the different wind models with the wave loads. This work discusses the validity of the long-term data needed for the fatigue assessment that is often limited to the sea states distribution, whereas the good correlation between the distribution of wind spectra and waves can have a significant effect on the fatigue assessment.

1.2 Fatigue loading calculation

1.2.1 Rules, standards, codes and guideline-based assessment

For ships, Classification Societies mostly stipulate a simplified approach for the fatigue load determination by providing a set of simplified load cases defined in the “Rules” which provides expressions related to the principal and the subdivision arrangement of the ship navigating in various loading conditions for a given design wave environment. To define the set of simplified rules on loads, Classification Societies mostly adopted the Equivalent Design Wave method (EDW), which is based on the principle that a few design waves maximizing the load components will maximize the stress range response at given structural hot spots for a target probability level. The long-term stress range distribution is then usually represented by a two-parameter Weibull distribution scaled on that reference probability load response. More details are provided in Chapter 7 that compares four Class rules' fatigue assessment methodologies. The study presented in (Hauteclocque et al., 2016) employed the EDW method to define the rules loads to be applied for the fatigue assessment of container ships. IACS (2014a) described also the technical background of the determination of the CSR fatigue rules loads using the EDW methods.

For offshore units, Classification Societies mostly provide direct approaches for the fatigue loads determination. The fatigue loads assessment by direct approaches implies, firstly, an improved knowledge of environmental conditions which are usually applicable for offshore units that are designed for a given location, and then the direct evaluation of the loads through computational fluid dynamic (CFD) methods. The hydrodynamic loads exerted on slender structural members are usually evaluated using the Morison equation, while seakeeping analyses are often conducted through boundary element methods (BEM) using either a wave Green's function or Rankine source in frequency or time-domain to assess the loads and motions of floating units, as well as the associated mooring system's internal loads. Direct approaches are thus employed for ship-shaped offshore units such as FPSOs for which a set of simplified fatigue load cases are provided by the Class as for ships, but correction factors are applied to account for the specific wave environment. For offshore units made of slender structural members (e.g. jacket) or floating units with atypical floater design (e.g. semi-submersible) the loads directly evaluated using CFD methods for the design metocean description are to be applied on the structural model because the diversity of their arrangement makes the formulation of a set of simplified loads impractical. It is worth noting that, alternatively, the fatigue load assessment by direct approaches can be used for ships by the Classification Societies granted that the calculation method provides at least the same level of safety than that implicitly taken in the rules.

In general, although direct approaches may lead to more realistic long-term load predictions compared with the rule-based simplified approach, the design requirements of the Classification Societies include more or less explicit margins to ensure a safety level of the fatigue predictions, so that the fatigue life evaluations cannot be directly compared to that corresponding to actual structural conditions once in operation. Eventually, for the structural design, the level of safety of the fatigue predictions produced by direct approaches must be at least as high as the one implicitly taken by the rules' simplified approach.

1.2.2 Direct assessment

Ship and offshore structures are subjected to numerous environmental parameters, e.g. wind, wave current, which can induce various responses in terms of internal loads and also motions in the case of floating structures. Existing software packages used for ship and offshore structural design are generally able to calculate directly the stresses from environmental information and structural descriptions. Nevertheless, applied forces remain the criteria allowing for validating the calculations and helping for design improvement. This has been summarized in (Strach-Sonsalla & Muskulus, 2016) for Floating Offshore Wind Turbines considering the type of floating platform in terms of floating stability, accounting for wave effects, wind fluctuations effects, current combined with motion effects, inertial efforts and mooring effects.

The calculation methods employed to evaluate the applied forces can involve various levels of complexity. The most advanced methods involve time-domain calculations that give accurate results but are very time-consuming. Time-domain calculations (Lee et al., 2014) may be particularly relevant when the employed strength model considers the overload or underload effects on fatigue retardation. As at the design stage, an exact sequence of loads experienced by the structure is not known, methods are thus developed to create an equivalent load signal, that is consistent with the statistical characteristics of a design environment, enabling the reproduction of the sequence effect on fatigue. However, mostly, the fatigue assessment methodologies ignore such effects and assume the linearity of the fatigue process over the life of the unit, e.g. Palmgren-Miner's Sum. Indeed, the high computational cost required to reproduce accurately in the time-domain the design metocean description and to evaluate its effect on the entire design life of the unit motivates the researcher to propose methodologies that represent a good trade-off between accuracy and time-efficiency of the computations. Those methodologies lie thus on numerous assumptions that simplify the problem and which the validity with respect to the accuracy of the fatigue assessment is confirmed by comparison with time-domain simulations.

A wide-spread direct approach for the fatigue assessment of ships or offshore structures, is the spectral fatigue analysis that consists in deriving the load spectrum response to a wave spectrum by the determination of the Response Amplitude Operators (RAO) of the considered loads to a unit wave amplitude in a condition of period bandwidth (Li et al., 2015c). For ships, the loads exerted on the hull by the waves and the associated motions and motion-induced loads are generally assumed linear, while the wind and current effects are neglected. Therefore, the RAO of the loads can be evaluated in the frequency domain. When the applied efforts are not too dependent on wave frequency, fatigue calculation can be carried out on the base of a simplified distribution of loads which reduces the number of regular wave conditions to be analysed compare to long-term time-domain simulations, and the long-term fatigue assessment can be conducted through a spectral analysis. However, the assumption of the linearity of the loads may become questionable for broadband phenomena, e.g. slamming loads and slamming-induced whipping response, for which time-domain simulations are recommended for a more accurate consideration of their contribution to the fatigue. Besides, adjustments are also studied to overcome the linearity limitation of the spectral analysis. Although the intermittent wetting loading of ships' side shell is a non-linear phenomenon, a study (Bigot et al., 2016) analysed the fatigue of side longitudinal stiffeners using spectral analysis with a specific processing on the area of intermittent wetting responding to a fixed arbitrary probability of relative wave elevation set to 10^{-4}, called "footprint". The accuracy of the footprint method with irregular waves was validated, especially for stiffeners located above the mean free surface, by comparison with time-domain analyses. For bottom-fixed offshore units, the obvious non-linearity of the internal loads to the environmental parameters (e.g. wave, wind and current) makes the spectral approach not directly applicable. However, a possible approach for the fatigue assessment consists in mixing time-domain calculations and spectral approach. To limit the number of time-domain analyses, (Peng et al., 2015) carried out a condensation of sea states having the same zero-crossing period. An "equivalent" significant wave height was assumed to generate the same damage with all the sea states involved. Obviously, the structural internal loads were assumed proportional to the significant wave height, which is questionable in case of important non-linearity.

Yet, for some applications, the spectral analysis approach is deemed too time-consuming as it implies the load evaluations for numerous wavelengths and headings. The equivalent design wave (EDW) and equivalent design sea state (EDS) methods are thus developed to limit the amount of ship response calculations to regular waves and irregular waves, respectively. The sea states may thus be summarized by a single equivalent design wave which the frequency corresponds generally to the maximum response. A coefficient that considers the variation of the response according to the frequency is then applied to the equivalent wave's response. This equivalent sea state approach is not always accurate enough as the shape of the waves varies with the frequency. A multi equivalent wave that enables, in principle, a better distribution in space of the efforts was proposed in (Brandão et al., 2015). The Equivalent Design Waves approach depends on the assumed metocean description and the target return period. A generalization of design wave depending on the metocean description and the probability of the sea state selected for the design condition was proposed in (Hauteclocque et al., 2016). An example is provided with a probability of 10^{-2} accordingly to the CSR reference loads for fatigue assessment.

Finally, for some load cases, the conventional CFD methods, e.g. Morison equation, BEM, may not be accurate enough to provide reliable fatigue load assessment. Advanced CFD methods including viscous effect based on the RANS formulation can improve the precision of the load evaluation granted that the models are calibrated on measurements. In situ observations are too complex to be employed as reference data, whereas model testing in a basin with controlled conditions are more adapted to verify the accuracy of the considered numerical models. Such advanced CFD methods can be employed to assess the containerships' slamming loads that contribute to the fatigue, (BV, 2015) as well as to evaluate VIM-induced loads on risers or

semi-sub (DNV, 2010a, Hyunchul et al., 2017) for the floating offshore units. CFD VIM or VIV results are validated versus experimental tests (Maximiano et al., 2017) that do not always predict accurately in situ observations (Koop et al., 2016). For risers, the VIV phenomena are mostly determined based on the empirical model (Ulveseter & Sævik, 2017, Voie et al., 2017, Wu et al., 2017, Yin et al., 2017) using the Morison equation, but the hydrodynamic parameters are directly calibrated based on tests measurements in a basin (Yin et al., 2015). The results from testing on regular waves with the results of a simulation of a Multi-Body System representing a floating wind turbine, loaded using Computational Fluid Dynamic software were compared in (Beyer et al., 2015).

1.3 Fracture loading

Fracture is related to unstable crack propagation in one of three modes, i.e. opening Mode-I, sliding mode-II or tearing mode-III. Especially in the material toughness transition area, the fracture strength is highly dependent on the temperature and on the strain rate. Regarding the temperature, the concern goes for operations in low-temperature regions where higher steel grades are required to ensure a sufficient toughness of the material. Besides, the level of strain rate that influences the fracture is associated with the considered extreme load scenario that is commonly assumed to occur once in the life of the unit. On one hand, the static and quasi-static loads will induce a negligible strain rate at the crack tip and are described in the ultimate limit state (see Technical Committee III.1) which includes typically the maximum wave-induced bending moment for ships and overturning moment for bottom-fixed offshore units. On the other hand, the dynamic loads may generate significant strain rate response at the crack tip and are described in the accidental limit state (see Specialist Committee V.1) which typically includes the dropped object scenario, but also ice or slamming impact and earthquake for the case of bottom-fixed units. For example, the drop on a Sandwich Plate System of an object of 3 tons was considered in (Kennedy et al., 2016) to investigate the shock-absorption capacity of a ductile material. The settings of this accidental condition could also be considered to evaluate the fracture strength of a brittle material when associated with a pre-existing crack and low-temperature environment.

Temperature degrades material resistance to brittle fracture in the context of fracture mechanics. Service temperature can be inferred from meteorological records of minimum temperature established for air. Material requirements in terms of transition temperature are established according to the area where ships or offshore structure are operating.

Finally, despite the critical importance for the safety of the identification and the quantification of events that can lead to a sudden rupture related to fracture mechanics, it is worth noting that, observed fractures almost never occur for marine structure in as-built condition. When such events occur, they are generally analysed as the result of an abnormal extensive fatigue crack propagation that already strongly degrades the fracture strength.

2. MATERIAL PROPERTIES AND TESTING

2.1 Material properties

Current research on material properties is important for fatigue design of the ship and offshore structures. However, cyclic data is typically expensive to obtain, explaining why correlations to cheaper monotonic material properties are also the subject of studies (Zonfrillo, 2017).

2.1.1 Monotonic material behaviour

The current research is focused on failure strain and its dependency on stress triaxiality, strain path and strain rate. The traditional way of obtaining failure strain from tensile tests is questionable as upon necking both the stress state and strain path are changing. To obtain failure strain under various stress triaxiality conditions, e.g. pure shear, uniaxial tension, equi-biaxial tension and plane strain tension, different specimen geometries have been proposed (Choung et

al., 2014, Roth & Mohr, 2016, Erice et al., 2017, Gruben et al., 2017). Common failure criteria for uniaxial- (Calle et al., 2017), as well as proportional and non-proportional multiaxial loading conditions, have been investigated using dedicated tensile test specimen geometries for different strain rates. To improve the performance of phenomenological failure criteria, the strain hardening exponent has been involved as an independent parameter for better approximations of the fracture locus and envelope (Šebek et al., 2016).

Simulation of fracture behaviour in large stiffened panel type of structures often involves shell finite element models for computational efficiency reasons. The failure strain for shell elements is a mesh-size dependent and is usually calibrated using data from tensile tests involving a uniaxial stress state. However, a full-scale punch test of a clamped stiffened panel revealed a stress state dependency as well, varying between equi-biaxial and plane strain tension (Kõrgesaar et al., 2017).

2.1.2 Cyclic material behaviour

During cyclic loading, the material can exhibit cyclic strain hardening or softening. To model the elastic-plastic behaviour correctly, cyclic hardening or softening behaviour needs to be accounted for because of residual stress relaxation and is one of the consequences of cyclic material behaviour. High-Frequency Mechanical Impact (HFMI) of weld toe notches provides acyclic behaviour that needs to be sufficiently understood.

Fatigue strength improvement due to HFMI-treatment is attributed to beneficial compressive residual stress state and introducing strain hardening of the material if cyclic loading is applied. Investigation of a high-strength base material, heat affected zone and the HFMI-treated material shows continuous cyclic softening for all material zones (Mikkola et al., 2016). Using numerical simulations, including cooling-rate dependent phase transformations, and experimental results, an analytical relaxation model has been utilized to show that a reasonable residual stress state estimate for applications in the high-cycle fatigue region can be obtained. In particular, for carbon steels, the volume change due to austenitic-martensitic phase transformation is essential (Leitner et al., 2017). In addition to temperature dependent quasi-static material properties such as Young's modulus, ultimate strength, Poisson's ratio and density, the cooling-rate dependent phase transformation has also been considered in the simulation. It is highlighted that especially for carbon steels, volume change due to austenitic-martensitic phase transformation is essential in order to compute the local residual stress states properly. During HFMI-process the cyclic hardening needs to be considered.

2.1.3 Fracture properties

Fracture toughness is a general term referring to the resistance of a material to unstable crack growth and propagation. In case a small-scale yielding criterion is satisfied, i.e. the crack tip plastic zone is relatively small in comparison to the crack length, it can be characterized by means of the elastic crack-tip stress intensity factor, K or equivalently the elastic energy release rate, G. When a small-scale yielding criterion is not met, the non-linear elastic J-integral, crack-tip opening displacement, CTOD, crack-tip opening angle, CTOA or plasticity-corrected stress intensity factor should be used. While the fracture toughness of brittle material can be expressed as a single-valued property, fracture toughness is a general term referring to a material's resistance to crack extension, which may be more properly expressed as a function of temperature and crack tip constraint.

A thorough overview of fracture toughness testing including recent advances and ASTM standardization is available (Zhu & Joyce, 2012). Attention has been paid to guidelines on how to choose and measure the appropriate fracture parameter. Effects of loading rate, temperature, crack tip constraint as well as fracture instability have been reviewed as well.

The crack tip constraint significantly influences the measured fracture toughness and focus is typically on high constraint (plane strain) values. In case the crack tip constraint is low, dedicated specimens and procedures exist; subject of a comprehensive review (Zhu, 2015, 2016, Ruggieri, 2017). Comparative studies of available test methods using single edge notch tension specimens together with crack tip opening displacement- and J-integral values have been presented (Park et al., 2017, Zhu, 2017, Zhu et al., 2017).

For ultra-high-strength steel, the temperature dependent fracture properties have been investigated with respect to the transition between brittle and ductile fracture. An improved transition criterion has been proposed Wallin et al. (2015).

A new cohesive zone model has been introduced in order to provide a uniform description of both stable crack growth and elastoplastic fracture. Damage accumulation includes both monotonic as well as cyclic contributions. Computational results have been found in agreement with mixed-mode fracture and fatigue test data for austenitic stainless steel (Li et al., 2015a).

2.1.4 Fatigue properties

In order to obtain a better statistical description of material fatigue properties, probabilistic S-N curves have been proposed for constant and variable amplitude loading involving the spectral loading shape (Baptista et al., 2017, D'Angelo & Nussbaumer, 2017).

A Brinell hardness based definition of S-N curves has been proposed, covering fatigue resistance from the first cycle up to the giga-cycle region in a single function. Test results obtained using specimens of various steel grades are in agreement with lifetime estimates (Bandara et al., 2016).

The fatigue strength of welded structures hardly depends on static strength. High-frequency impact treatment can be used for improvement. Tests have been conducted to quantify the influence of HFMI-treatment induced compressive residual stress and modified strain hardening behaviour on the fatigue strength. HFMI-treated materials show increased fatigue strength at smaller strain amplitudes and decreased fatigue strength at larger strain amplitudes in comparison to the base material (Mikkola et al., 2016).

2.1.5 Materials

Very high cycle fatigue tests for three kinds of high strength low-alloy steels have been investigated (Li et al., 2015b). The steels included two high-carbon-chromium bearing steel and a chromium-nickel-tungsten gear steel subjected to axial loading and rotating bending. The subsurface inclusion-induced crack nucleation and propagation process could be divided into four stages: (i) crack nucleation around the inclusion within the Fine Granular Area (FGA); (ii) micro crack growth within the FGA; (iii) stable macro crack growth outside the FGA and within the fisheye; (iv) unstable macro crack growth outside the fisheye. A crack nucleation life prediction method for the stage (i) and a crack growth life prediction method for stages (ii) and (iii) were modelled respectively. The crack growth lives observed in tests by stage (ii) and (iii) occupied a tiny fraction of the whole fatigue life, while the predicted crack nucleation life was nearly equal to the total fatigue life.

High-cycle fatigue tests to determine the influence of mean stress on the initiation mechanism in a 2.5%Cr-1%Mo steel used in riser tube connectors for offshore oil drilling was conducted in (Gaur et al., 2016). Tests were run at 7 different R ratios: -1, -0.5, 0, 0.25, 0.5 (runout at $3 \cdot 10^6$ cycles), and 0.6 and 0.7 (runout at 10^7 cycles). Surfaces were polished (R_a<0.4μm), and fracture surfaces were investigated in Scanning Electron Microscopy (SEM), X-ray Powder Diffraction (XRD) and Energy Dispersive X-Ray Spectroscopy (EDS). For R=-1, -0.5 and 0, surface initiation was observed without any defect present. For R=0.25, cracks initiated predominately from internal flaws, which evolved to “fish-eye” patterns for a relatively low number of cycles. No crack growth was observed for R≥0.6 for N<10^7 cycles. The slope of specimen S-N curves

tended to decrease for higher mean stress, and the endurance limits were found to follow the Gerber parabola.

Uniaxial creep tensile tests using Cr-Mo-V steel round bar specimens with diameter 10 mm at different stress levels at 566℃ was carried out in (Zhang et al., 2015). The measurements showed that the creep behaviour of the steel complied with Norton's law and exhibited different Norton model parameters in low and high-stress regimes, which could be written as the stress-regime dependent creep model (2RN model). The transition stress was approximately 250 MPa.

High cycle dwell fatigue (HCD) tests on blunt compact tension specimens to understand and quantify the effect of creep-induced tensile residual stresses on crack growth was performed in (Chen et al., 2016). The creep/relaxation occurred in compression. The tests at 250ºC indicated that in two-minute HCD cycles tests the total life reduced fourfold relative to a baseline 0.5 Hz cycle, and that crack growth rate increased locally by a mean factor of 6 in the notch. In the baseline specimen, the creep-induced tensile residual stress was found to accelerate the local crack growth rate 4 times compared to not considering creep correction.

2.1.6 Arc-welded and laser welded joints

Welded steel structures are widely used in ship and offshore industries, where operational loading is typically stochastic, and the sequence may lead to either acceleration or retardation of the crack growth rate. Fatigue tests on welded thick-walled C-Mn steel specimens in as-welded and stress relieved conditions were conducted (Maljaars et al., 2015). Some of the specimens were subjected to constant amplitude (CA) loading, with and without overload (OL), while others were subjected to two types of variable amplitude (VA) loading, namely, random loads and wave loads. It has been observed that crack growth retardation in the as-welded and stress relieved specimens was similar in CA loading with OLs. The loading & response ratio ($R \geq 0.3$) showed little influence on the crack growth rate and random loading caused a crack growth rate of the same magnitude as that of the CA tests. Wave loading resulted in a crack growth rate that was substantially lower than for CA. The stress ranges were nearly equal for the two types of VA loads.

Welded X65 offshore pipes with an outer diameter of 32" and 1" wall thickness were cut into fatigue coupons and tested in four-point bending (Pang et al., 2017). Tensile stresses occur at pipe outer surface of the weld cap. The objective of the study was to observe the coalescence and shape evolution of multiple cracks in welded structures. During the tests, 12 to 22 cracks were observed by identifying the ratchet marks, and the locations of each crack initiation site are recorded to support the development of a new proposed model. The predicted crack propagation lifetime for the crack distributions observed using the BS 7910 (BS7910, 2005) design curve is about 10% of the experimental life, suggesting that the predicted life is overly conservative.

2.1.7 Friction stir welded joints

Friction stir welding (FSW) provides a lower cost alternative for steel pipelines construction, replacing the conventional arc welding processes (Sowards et al., 2015). FSW was not yet used in pipelines, but advances in the research suggest that this technique should become feasible soon. FSW does not involve melting of metal and does not require consumables or shielding gas. A solid-state weld is fabricated by inserting a non-consumable welding tool into the steel at the mating surfaces and mechanically mixing the metal to form a permanent joint. The heat input is lower than in conventional consumable welding, which prevents solidification cracking, reduces the size of the heat affected zone, and reduces the magnitude of the residual stresses (Aydin & Nelson, 2013).

The influence of FSW in the fatigue crack propagation of API X80 pipeline steel was analysed in (Sowards et al., 2015). Compact tension specimens were machined from two orientations in the base metal and the weld metal. Fatigue crack propagation in the stir zone and across the

welds was observed to be dependent on residual stresses interacting with the propagating cracks. Residual stresses reduce the rate of fatigue crack growth at all levels of applied stress intensity amplitude, but as the crack grows, the residual stresses are relieved, gradually reducing its effect. The fatigue crack growth rate in FSW welds of X52 pipeline steel was analysed in (Ronevich et al., 2017). Tests were performed for the base metal (BM), the centre of the weld and 15mm away from the weld. High-pressure hydrogen gas (21 MPa) was used to assess the effects of hydrogen accelerated fatigue crack growth. Results pointed out that accelerated fatigue crack growth of the FSW was marginally greater than in the base metal and off-centre regions. Also, similar hydrogen accelerated fatigue crack growth was observed for FSW and conventional arc welds from similar grade pipes.

An extensive experimental study on the fatigue performance of friction stir welded 6-mm thick DH35 marine grade steel was presented in (Polezhayeva et al., 2015b). The study included fatigue and tensile tests, geometry and hardness measurements, microstructure and fracture surface examinations. The effect of process speed was also investigated. The results showed higher fatigue strength compared to International Institute of Welding, IIW (Hobbacher, 2013, Jonson et al., 2016b) design curve for conventional welds and a newly developed S-N curve for friction stir welded joints was proposed.

2.1.8 Corrosive environment

Steel jackets are widely utilized in the offshore oil industry. The jackets are designed for a service life ranging from 15 to 20 years, however, it is estimated that over two-thirds of the world's jackets will be used for 5-10 years beyond their intended design life. Life extension is possible by managing the overall safety and uncertainties in terms of structural degradation and repair decisions (Tan et al., 2016). Fatigue and corrosion play major roles in structural degradation; thus much attention has been paid to assess the residual strength of ageing jackets, and to an extent, the jackets' life. An experimental study on the collapse of ageing steel jackets due to corrosion or fatigue cracks was conducted in (Ji et al., 2016). They prepared three jacket models (1:40-scale); one cracked, one corroded, and one intact as a reference. The damage and the corrosion degradation were imposed on the corresponding models according to the Paris' relation and unique corrosion (with different thickness-corrosion rates in submerged areas and atmospheric ones) to model 15-year ageing. Both the crack-damaged and corroded jacket models failed by local tearing, likely due to elevated localized stresses in the joints of the legs and braces. The intact model failed by global failure.

Experiments have shown that the fatigue life in a corrosive environment is remarkably decreased compared to air. The effect of general corrosion and pitting can be assessed by testing corroded and non-corroded specimens in the air (Garbatov et al., 2014a), whereas corrosion fatigue tests to assess the complex interacting effects of mechanical and environmental factors on fatigue are complex, especially when considering the time-dependent nature of corrosion. Engineering methods accounting for corrosion have been introduced in some design guidelines, defining levels of corrosion damage to reduce the ship structural strength.

The coupling effect of stress and the time-dependent corrosion deterioration in Q235 steel was studied in (Yang et al., 2016). The relation between mechanics and corrosion during elastic deformation was investigated by performing uniaxial tensile tests in 3.5 wt.% NaCl solution and 5 to 7 ppm dissolved oxygen. Time-dependent corrosion acceleration due to stress was analysed using FEA. They found that (i) the corrosion of welded joints was accelerated because of the combined effect of corrosion and stress concentration, (ii) the fatigue coupled with non-uniform corrosion was more detrimental than fatigue coupled with uniform corrosion.

Offshore wind farm monopile structures experience dominant cyclic frequencies in the range of 0.3-0.4Hz. To evaluate the fatigue crack propagation behaviour fatigue tests on six compact tension specimens made of S355J2+N steel in the air and in laboratory simulated seawater under free corrosion was carried out in (Adedipe et al., 2015). In the air tests, R=0.1 loading at 2

Hz was applied, and fatigue crack lengths were monitored by Alternating Current Potential Difference, direct current potential difference, and back face strain. For the tests in simulated seawater, a load ratio of R=0.1 was used with loading frequencies 0.3, 0.35 and 0.4 Hz, and BFS was adopted to monitor the crack growth. The tests showed that (i) similar crack growth rates were observed using the three test frequencies. (ii) The fatigue growth behaviour of S355J2+N steel both in the air and in seawater was consistent with BS7910 (2005).

2.1.9 Similarity

To translate test results into fatigue design, the link between the small-scale specimens and the actual structure needs to be understood. Similarity and transferability of small-scale fatigue test results have recently been studied using full-scale fatigue testing of structures. Fatigue tests of full-scale 4-mm thick laser-hybrid welded passenger ship deck panels and the small-scale specimens cut from the same structures were performed in (Lillemae et al., 2017). The results were in good agreement given that the initial distortion shape and geometrical nonlinearity are considered in the analysis. The fatigue strength of full-scale railway axels was compared to one of the scaled specimens in (Yamamoto et al., 2017) and the difference was found to be within the error margin. The fatigue strength of full-scale U-rib bridge steel deck specimens under the vehicle loads was investigated in (Kainuma et al., 2016). The fatigue crack propagation in bulb stiffeners was studied using numerical analysis and full-scale experiments in (Yue et al., 2017).

Full-scale structure testing and in-service measurements are also carried out to validate calculation models. Full-scale fatigue tests of ship propellers in order to validate the proposed fatigue model was carried out in (Ezanno et al., 2015). The results of a spectral fatigue analysis were compared to the strain gauge measurements carried out on the board of a naval vessel during the sea trial in (Thompson, 2016).

2.2 Polymer composites testing

This section focuses on how polymer composite materials and structures are tested with wind turbine blades as the application in focus. In the design process of wind turbine blades, tests at several scales can be performed to estimate the material properties and to verify the computational design models used to estimate the load-bearing capacity, illustrated in Figure 1. Currently, only coupon and full-scale tests are required to certify wind turbine blades according to the IEC 61400 standard for wind turbines.

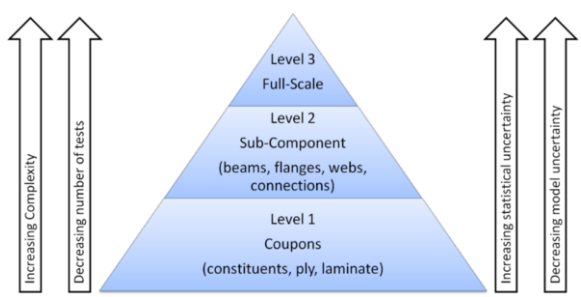

Figure 1: Level of tests assessing of load bearing capacity of wind turbine blades.

At the coupon level, small test specimens with the basic material are tested to determine the material properties and their statistical characteristics in both ultimate and fatigue limit states. The test specimens at the coupon level are normally relatively inexpensive to produce and several different tests with many repetitions can be performed.

At the subcomponent level, parts of a wind turbine blade are tested to determine the load-bearing capacity of selected parts and to verify computational models for potential critical details.

Subcomponents are in general more expensive and complicated to test than coupons, which lead to fewer tests for each subcomponent.

At the full-scale level, prototypes of the blade are tested both in static and dynamic conditions following the requirements of the IEC 61400-23 (IEC-61400-23, 2014) standard for full-scale testing. Full-scale blade tests are typically performed on one or two blades to verify that the blade type has the load carrying capability and service life provided for in the design. Since the cost of a blade itself is high and the time needed for the dynamic test can be several months for large blades, then also the cost due to the waiting time for market introduction is significant.

2.2.1 Sub-components

Initial work on how to plan and apply subcomponent tests; i.e. a simplified component test, in the design process of wind turbine blades was done in the project: "Experimental Blade Research – Phase 2 (EBR2)" (Sørensen et al., 2013, Eder et al., 2015). Parts of this work were then used for making the new DNV GL rotor blade standard (DNV-GL, 2015), which for the first time makes it possible to use subcomponent testing as part of the wind turbine blade certification (Pansart, 2015). A subcomponent test method designed to check the compressive strength of the trailing edge region in wind turbine blades under simplified loading was first proposed in (Eder et al., 2015, Branner et al., 2016) and then later further developed under the EU-funded project IRPWind in cooperation with Knowledge Centre WMC (Lahuerta et al., 2017) and Fraunhofer IWES Rosemeier (Rosemeier et al., 2017). Finite element simulations showing that the proposed static subcomponent test method is promising in obtaining the compressive strength of the trailing edge region under simplified loading were performed in (Branner et al., 2016). It was found that the failure load and the failure mode are very similar to that found in full-blade tests for the analysed test specimen.

2.2.2 Full-scale components

Currently the IEC61400-23 and DNVGL-ST-0376 standards require that blade fatigue testing is carried out by testing blades in two directions – flap wise and edgewise – one direction at a time. During their lifetime, wind turbine rotor blades are exposed to high dynamic loads, resulting from cyclic changes in gravity direction, centrifugal forces, and changing wind conditions such as average wind speed, turbulence intensity, rapidly changing wind direction, wind shear, extreme wind gusts and site-specific loads such as wake effects from neighbouring wind turbines. The broad and complex load spectrum results in the accumulation of a significant amount of fatigue damage over the turbine lifetime. Fatigue is, therefore, a major failure mechanism in wind turbine blades. The currently required fatigue testing methods are not representing the real service loads very well and there are therefore attempts to develop more realistic test methods. One method is dual-axis fatigue testing where the flap-wise and the edgewise directions are tested simultaneously (Hughes et al., 1999). This approach is shown to be more representative of the loading in service and can thus contribute to a potentially more realistic testing of wind turbine blades (Greaves et al., 2011).

A biaxial fatigue test performed in (Snowberg et al., 2014) is demonstrating how resonant fatigue test methods can be used to simultaneously apply flap-wise and lead-lag loads to a full-scale wind turbine blade. This biaxial resonant fatigue testing method will complete the test faster than single-axial testing because of this simultaneous application.

Several potential biaxial fatigue test scenarios for a fictional 60 m blade are examined in (Post, 2014). Three alternative approaches for configuring a biaxial fatigue test were considered: (i) a quantum biaxial fatigue test where the flap and lead-lag directions are excited at separate resonance frequencies resulting in a variable and nominally random phase angle between the two test directions; (ii) a phase-locked test with frequency ratio of 1:1 where the lead-lag frequency is reduced to the flapping frequency by adding virtual mass at multiple stations; and finally (iii) a phase-locked test with a frequency ratio of 1:2 where the flapping frequency is reduced

slightly using virtual masses to run at exactly one-half of the lead-lag frequency. It was found that the ability to achieve moment distributions relatively close to the target with relatively small virtual masses gives the 1:2 phase-locked test approach a good chance of success in a commercial test program including a possible reduction in test time.

A method for calibrating strain gauges was developed in (Greaves et al., 2016). It accounts for the misalignment of the applied loads by including the effects of winch cable angle during calibration pulls, which are only partially accounted for with the crosstalk method. This has shown to be a significant cause of errors with the current best practice technique proposed in the standards. The method also has the advantage that it allows strain readings from an arbitrary number of gauges to be included in any given blade section, which would reduce errors arising due to noise.

For wind turbine blade testing, there are two research needs – more realistic loading and faster testing. The standard certification tests used today are not representing the real world very well. Blades are exposed to torsion and bending in different directions at the same time. There is consequently a need for fatigue test methods that better match the loads to which the blades are exposed to in real operational conditions. As blades become larger the time needed to perform the necessary certification tests become longer as blades are tested at resonance. This is a challenge for the industry as 100 m blades are expected to take more than a year to test. There is, therefore, a need to shorten the test time. Multi-axis test methods seem to answer to both these needs.

2.3 Testing methods and measurement techniques

For material model calibration and simulation verification purposes, material testing is virtually indispensable, although often costly and time-consuming. Research efforts have been put into the characterization of the very high cycle fatigue resistance (lifetimes exceeding 10^7 cycles) using different techniques. In contrast to high cycle fatigue showing crack development predominantly at the surface, very high cycle fatigue cracks typically start to develop subsurface at fine granular regions introducing fisheyes at the fracture surface (Stanzl-Tschegg, 2014).

Ultrasonic testing permits frequencies up to 20-30 kHz. It is energy efficient and makes a low noise, but the specimen design is limited. Other challenges include strain rate- and thermal effects. The frequency effects on quenched and tempered steel and aluminium alloy were recently investigated in (Schneider et al., 2016), showing that fatigue resistance of aluminium is more dependent on the environment (laboratory air versus vacuum) and steel on the strain rate.

Ultrasonic fatigue testing under multiaxial and variable amplitude loading conditions has recently also received an increasing research attention. Biaxial ultrasonic fatigue tests with axial and torsional load components were carried out and compared to the strain gauge data obtained with the equivalent specimen tested in the biaxial servo-hydraulic machine with the frequency of 0.5 Hz in (Vieira et al., 2016). The results showed good agreement. A new ultrasonic testing device for biaxial testing of flat smooth disc specimens was presented in (Brugger et al., 2017). Ultrasonic variable amplitude fatigue tests on aluminium alloy with stress ratios R=-1.0, 0.1 and 0.5 was performed in (Mayer et al., 2014). The results were compared to ultrasonic constant amplitude tests as well as to results obtained from a servo-hydraulic testing machine in (Fitzka & Mayer, 2016). Similar tests for high strength steel were performed in (Sander et al., 2016).

One alternative testing methodology of servo-hydraulic and ultrasonic testing includes electrodynamic shakers, with testing frequencies up to approximately 1 kHz. Their advantage is the response amplification in the resonant area, which means that the excitation can be small. As for ultrasonic testing, the method is limited by specimen design. Example of research carried out using such equipment is given by e.g. (Khalij et al., 2015).

The use of digital image correlation (DIC) in fatigue and fracture testing as an alternative measuring technique has increased in recent years. Examples can be found in (Lopez-Crespo et al.,

2015a, Hos et al., 2016, O'Connor et al., 2016, Vasco-Olmo & Diaz, 2016, Gonzales et al., 2017, Hosdez et al., 2017, Jandejsek et al., 2017, Mokhtarishirazabad et al., 2017). Also, the calibration of the potential drop technique to determine the crack size has recently been presented by e.g. (Doremus et al., 2015, Tumanov et al., 2015, Berg et al., 2017). DIC and thermographic measurements to define the fatigue strength from static tests and validation with the fatigue tests was presented in (Corigliano et al., 2017).

Fatigue crack sizing method in a larger structure using ultrasonic guided waves was presented in (Pahlavan & Blacquiere, 2016). A thermographic method to detect the exact crack initiation location and the crack growth time is presented in (Krewerth et al., 2015).

The fatigue cracks growth in stainless steel by comparing simultaneously measured acoustic emissions and infrared thermography data was studied in (Barile et al., 2016). An experimental technique to assess the fatigue damage accumulation rate by evaluating the heat energy around the crack tip with an infrared camera was presented in (Meneghetti & Ricotta, 2016). Crack length measurements under non-continuous thermal conditions are carried out and discussed in (Ewest et al., 2016).

3. FATIGUE DAMAGE ACCUMULATION APPROACHES

Fatigue involves physics across several interactive resistance dimensions, distinct contributions in different stages of the (accumulative) damage process and a range of scales. Joints connecting ship and offshore structural members are typically fatigue sensitive and require particular attention in this respect. For arc-welded joints in metallic structures, assessment concepts developed over time are classified with respect to the type of information, geometry, parameter and process zone, including plane and life regime annotations, providing an overview (Section 3.1). Recent advances are highlighted (Section 3.2).

Continuum and discrete damage mechanics models can be adopted as well to estimate crack initiation and growth lifetime using respectively damage evolution functions which describe the deterioration of the material mechanical properties and cohesive zone or damage mechanism formulations (Section 3.3).

The fatigue damage criterion defines the fatigue strength and lifetime estimate accuracy from a modelling perspective and controls the reliability level that can be achieved, while confidence is a matter of sufficient test data. Developments aim to improve the still incomplete similarity (equal strength value should provide the same lifetime) and trends can be observed towards complete strength, total life and multi-scale modelling. Fatigue damage criteria tend to become more generalized formulations and the number of corresponding fatigue resistance curves reduce accordingly, satisfying small-scale specimen, large-scale specimen and full-scale structure welded joint fatigue resistance similarity at the same time.

Incorporating all four interacting fatigue resistance dimensions explicitly in the model description eliminates influence factors (e.g. for multiaxiality, residual stress, variable amplitude loading & response and corrosion) and provides a complete fatigue damage criterion (Section 3.4). Correlation of medium and high cycle fatigue; involving respectively a crack growth and initiation governing lifetime, requires matching of crack damaged and intact geometry parameters to provide a total life fatigue damage criterion (Section 3.5). Additional macro, meso and micro fatigue damage mechanism information – physics at a smaller scale – can be used to enhance an engineering based model, providing a multi-scale fatigue damage criterion (Section 3.6).

Because the fatigue damage sources in materials are randomly distributed, the critical (i.e. largest) one defines the fatigue resistance. The probability of fatigue induced failure can conceptually be estimated using a series system description: a geometry (i.e. structural member assembly) is as weak as its weakest material link, introducing the statistics of extremes to the fatigue damage criteria formulations (Section 3.7).

3.1 Overview

Fatigue involves physics across four interacting dimensions: material, geometry, loading & response and environment. Material and geometry typically define the reference resistance; loading & response and environment are involved as influence factors.

Different assessment concepts; fatigue damage criteria and corresponding resistance curves, accounting for endurance and mechanism contributions, have been developed over time and reviewed, including recent contributions (Fricke, 2003, Radaj et al., 2006, Hobbacher, 2009, Radaj et al., 2009a, Radaj et al., 2009b, Rizzo, 2011, Fricke, 2015, Radaj, 2015, Vormwald, 2015, Hobbacher, 2016, Lotsberg, 2016), proposed to be classified (Den Besten, 2019) according to (Figure 2):

- global or local information criteria,
- intact or crack damaged geometry criteria,
- stress (intensity), strain (intensity) or energy (density) parameter criteria,
- point, line or area/volume- and defect size or crack increment process zone criteria
- with annotations:
- critical, integral or invariant plane criteria,
- infinite or finite life region criteria.

The scale relative to the hotspot defines if the fatigue damage criterion is a global one at structural detail level or a local one taking (weld) notch information into account.

Fatigue damage criteria involving the structural response of the intact geometry type: stress, strain or energy, depending on work hardening, elastoplasticity and multiaxiality considerations, are related to the stress or strain concentration factor as governing crack initiation parameter. Crack damaged geometry criteria: crack tip stress intensity, strain intensity or energy density, are linked to the growth controlling stress or strain intensity factor. Alternatively, continuum and discrete damage mechanics models can be adapted to estimate the initiation and growth lifetime contribution using respectively damage evolution functions which describe the deterioration of the material mechanical properties and cohesive zone or damage mechanism formulations.

Following the critical distance theory (Taylor, 2007) the considered process zone relates the response mode-I, -II and -III specific, plane geometry characteristic and (elastoplastic) microstructural material properties for a particular environment at the different stages of the fatigue damage process to the weld notch geometry effective fatigue damage criterion: a fatigue limit- or threshold parameter in the infinite life region and initiation- or growth resistance criterion in the finite life region. For intact geometry parameters the process zone can be defined in terms of distance, length, area or volume; for crack damaged ones in terms of defect size or crack increment. The process zone values are either constant in the infinite life region or response level dependent on the finite life region since the relative initiation and growth contributions to the total fatigue lifetime are response level dependent.

Fatigue damage criteria are typically developed for a certain plane and lifetime region as reflected in the annotations. Shifting application from one plane or region to another, however, has modelling consequences, particularly important for multiaxial loading & response conditions.

3.2 Damage criterion advances

Following the fatigue assessment concept overview, damage criteria advances and highlights will be discussed and evaluated regarding modelling capabilities and assessment results.

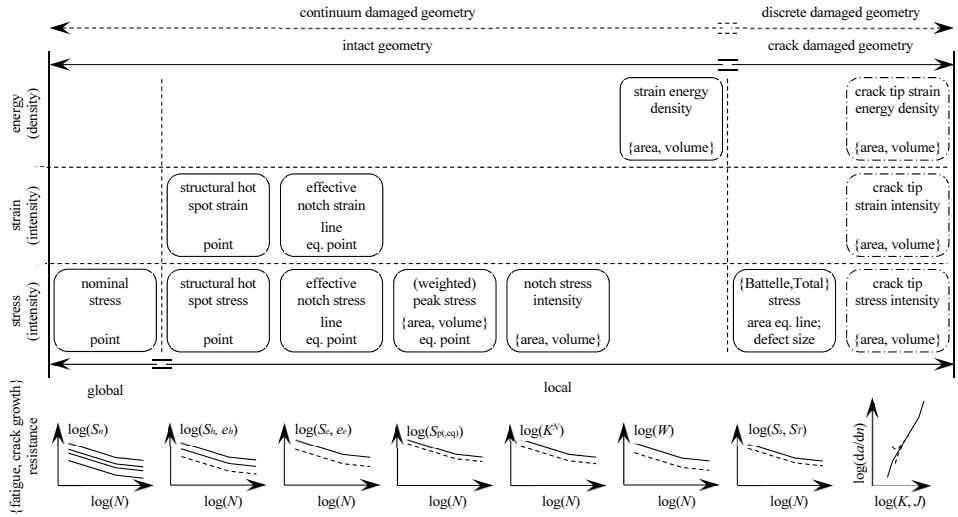

Figure 2: Fatigue assessment concept overview (Den Besten, 2019).

3.2.1 Hotspot structural stress

Based on a 3D solid finite element formulation, a less mesh-sensitive calculation procedure has been proposed and verified satisfying the original definition. The traction based structural stress has been calculated using either a force- or work equivalent approach involving the internal nodal forces on the imaginary cut planes (Lotsberg, 2016), in a similar manner as has been proposed before (Dong, 2005, Taylor, 2007, Kim et al., 2015).

Following the '1 [mm]' and 'equivalent zero' stress location proposals in through-thickness direction, the weld toe hotspot location value itself has been adopted in order to obtain a structural hot spot stress estimate eliminating thickness (i.e. stress gradient) effects (Dong, 2010).

Fatigue test results for arc-, laser- and hybrid welded steel thin plate specimens have been analysed using the structural hot spot stress concept. Angular misalignment induced secondary bending requires (non-linear) plate straightening to be explicitly incorporated because of significant structural response effects (Fricke et al., 2015, Remes et al., 2015). A resistance curve slope value of 5 shows a better fit in comparison to the commonly adopted value of 3.

For box-stiffened panels in watertight (hot spot type C) and non-watertight (hot spot type A) configuration fatigue resistance information has been obtained and compared to data available in the literature using the structural hot spot stress concept. Particular attention has been paid to the local weld geometry induced structural stiffness for shell finite element models (Yokozeki & Miki, 2016).

A comparison of tubular joint structural hot spot stress concentration factors obtained using DNV·GL guidelines and FE analyses showed that for simple uni-planar joints the guideline-based values provide realistic estimates. However, the influence of local (weld) geometry can be significant (Maheswaran & Siriwardane, 2016).

3.2.2 Effective notch stress

An effective notch stress estimate can be obtained by averaging the notch stress distribution over a microstructural material characteristic length (Neuber) or by adopting a value at a critical distance from the notch (Peterson). Average characteristic length values have been proposed analysing fatigue resistance data of steel welded joints: 0.40 [mm] and 0.10 [mm] respectively (Baumgartner et al., 2015), although principally response level dependent ones are required in

the finite lifetime region because the initiation and growth contributions are response level dependent. An averaged stress or a critical distance value can be adopted to prevent for structural strengthening or weakening in case of thin plate joint applications like typically introduced for the IIW based fixed reference radius of 1 [mm] using the peak stress as effective notch stress estimate.

Examining the fatigue lifetime consequences of small notches, the classical results of Neuber and Peterson can be interpreted as average/critical stress or strain over a small volume that depends on the solution of a continuum mechanics elasticity problem. Using examples, this interpretation permits generalization of results to cases outside the range of parameters considered in conventional design (Szabo et al., 2016).

Using notched bar specimen fatigue test results, the microstructural material characteristic length has been shown to be loading & response level dependent indeed. A linear relationship has been proposed (Krzyzak et al., 2015).

The fatigue strength data scatter observed for laser-hybrid welded 3 [mm] steel plate butt joints have been related to the actual weld profile using high-resolution measurements (Liinalampi et al., 2016). Adopting the effective notch stress as damage criterion, captured using stress averaging rather than a fictitious notch radius, shows that the most likely – material characteristic – stress averaging length is significantly smaller than the commonly assumed value of 0.4 [mm] for joints with larger plate thickness – a geometry parameter.

The fatigue strength of Invar (Fe-Ni) alloy welded joints, typically used in LNG containment systems, has been established using raised edge- and overlap joint specimens adopting the effective notch stress concept. The IIW prescribed reference radius of 0.05 [mm], a blunt crack tip value, has been applied because the plate thickness is less than 1.5 [mm]. For a resistance curve slope of 5, the FAT class is established at 434 [MPa] for a principal stress based response; a value below 630 [MPa] corresponding to the IIW steel FAT class (Oh et al., 2014).

Using ordinary- and total least squares regression (the latter does not distinguish an independent- and a dependent parameter), fatigue resistance data of as-welded butt joints has been investigated using the effective notch stress concept. The strength value obtained using ordinary least squares and a fixed slope of 3, FAT198, is below the IIW defined value: FAT225. For a total least squares regression the fatigue strength value increases significantly. The local mean (residual) stress may explain some inconsistencies between data series as reported in the literature (Nykanen & Bjork, 2015).

Crack initiation locations in lap joints and cover plates for weld toe- and weld root notches have been identified by using Neuber´s stress averaging rather than the IIW procedure involving the peak stress related to a reference radius of 1 [mm]. The reference radius induced key-hole for weld root notches typically provides an overestimated effective notch stress. Results are in agreement with experimental observations (Dong & Guedes Soares, 2015b).

For mixed mode-I and -II response conditions at V-shaped notches with a root hole, the loading & response and geometry dependent support factor have been investigated analytically and numerically adopting a maximum tangential stress based crack angle in order to enable Neuber's stress averaging along the crack path (Berto, 2015b).

In case the weld notch stress concentration is relatively low, like for weld toe notches of butt joints containing a non-negligible real notch radius, the typically adopted IIW reference radius of 1 [mm] may require a modification. Depending on the response level the plane geometry reference resistance may become important since fatigue damage could develop in the base material rather than in the heat affected zone; the base material curve is governing in the medium cycle fatigue range (Rother & Rudolph, 2011).

3.2.3 Effective notch strain

The far-field structural response is typically elastic, whereas cyclic (notch) plasticity is a requirement to develop fatigue damage, illustrating the importance of elastoplasticity relations. Neuber's rule has been widely adopted.

Analytical elastoplastic stress and strain estimates at the root of V-shaped sharp and blunt notches have been obtained for a mode-III response condition, relating the elastic and plastic control volume averaged strain energy density contour lines. For blunt notches the point-wise relation is in agreement with Neuber's rule; for sharp notches, a strain hardening correction becomes involved (Zappalorto & Lazzarin, 2014, Zappalorto, 2015).

Introducing an advanced mean (residual) stress model, the effective notch strain formulation has been modified (Savaidis & Malikoutsakis, 2016). Fatigue test data of motor truck axle casings containing intermittent welds including the governing starts and stops, obtained for different types of loading at different load ratios, has been used for verification purposes and good agreement has been observed.

Paying particular attention to the fatigue assessment of weld ends (starts and stops) in thin-plated structures, effective notch strain concept improvements concerning mean (residual) stress effects including relaxation have been proposed and verified (Malikoutsakis & Savaidis, 2014).

An effective notch strain estimate has been obtained for a welded joint in a web-frame corner of a ship (Dong & Guedes Soares, 2015a). Uncertainties with respect to material and geometry properties have been taken into account (Dong & Guedes Soares).

Abnormal (freak) wave loading induced low cycle fatigue consequences have been investigated for an offshore wind turbine. Adopting Neuber's rule the linear elastic stress has been translated to a local strain criterion (Yeter et al., 2014b, 2015e, 2016a).

3.2.4 Notch stress intensity

A benchmark study regarding the numerical computation of the weld notch stress intensity shows that an extensive effort in terms of a very fine mesh or a high polynomial degree in case of *p* refinement is required in order to obtain accurate estimates (Fischer et al., 2016a).

The available resistance design curves for the notch stress intensity concept have been questioned with respect to misalignment effects, which should be included for local fatigue damage criteria (Fischer et al., 2016c).

3.2.5 Strain energy density (SED)

A state-of-the-art concept review (Radaj, 2015) shows the modelling developments for the fatigue strength assessment of sharp and blunt V-notches subjected to uniaxial loading, systematically extended to (mixed) multiaxial conditions. Applications to welded joints are provided and numerical computations using coarse finite element meshes are proven to be acceptable for accurate local strain energy density evaluations.

Taking advantage of coarse mesh finite element models sufficient to obtain the peak stress (Section 3.2.6) based notch stress intensity factor estimates, closed-form expressions for the strain energy density as a function of the notch stress intensity have been related to the peak stress and have been verified to be a rapid procedure to evaluate the strain energy density in a systematic comparison to direct (fine mesh) finite element results (Meneghetti, 2015, Meneghetti et al., 2015). Using nodal stresses, modelling of the control volume is even not required anymore, and still accurate averaged strain energy density values can be obtained. Extending the application for long cracks to short cracks (at notches) require that except the first order stress intensity higher order terms need to be considered as well, the second order

term; the T-stress. The first order term is obtained using the crack tip node, the second order term using selected nodes along the crack edge (Campagnolo et al., 2016).

Re-analysis of welded joint fatigue test data provided a slightly different strain energy density control volume radius; a material property. The notch stress intensity based fatigue strength values changed accordingly (Fischer et al., 2016c).

Fatigue tests have been conducted using specimens containing artificial notches with different notch radius, opening angle, material structure and material strength to validate the strain energy density fatigue design curve for different types of welded joints and failure locations. Differences in endurance (intercept logC) and mechanism (slope m) show that care should be taken when assessing welded joints with geometry and loading and response conditions different from the data used to establish the design curve (Fischer et al., 2016b).

A benchmark study regarding the numerical computation of the strain energy density shows that accurate estimates can be obtained, even for a relatively coarse mesh. However, if the involved control area increases more than the local stress concentration, the strain energy density can be underestimated, like that shown for a butt joint geometry (Fischer et al., 2016a). Using the weld notch stress intensity based strain energy density fatigue damage criterion, fatigue test data involving joints connecting bulb profiles has been re-analysed and shows in relation to the available design curve similar or even better accuracy if compared to other criteria (Fischer et al., 2015).

3.2.6 Peak stress

The (elastic) peak stress is a simplified finite element based fatigue damage criterion approximating the weld notch stress intensities and weld notch strain energy densities at V-shaped notches. A state-of-the-art review shows a link to the effective notch stress as well, allowing for knowledge transfer from one concept to the other (Radaj, 2015).

Using the weld notch stress intensity based peak stress fatigue damage criterion, fatigue test data involving joints connecting bulb profiles have been re-analysed and shows in relation to the available design curve similar or even better accuracy if compared to the nominal-, structural hot spot- and effective notch stress concept (Fischer et al., 2015).

The weld toe and weld root failure induced fatigue strength of butt joints has been investigated using the weld notch stress intensity based peak stress as damage criterion. Since the loading and local geometry effects like notch angle and plate thickness are considered, a single design curve has been established for steel and aluminium as typical construction materials. The peak stress calculation has been verified for specific element types in the commercial software Ansys library (ANSYS, 2009, Meneghetti, 2015, Meneghetti et al., 2015).

3.2.7 Battelle structural stress

Fatigue-induced failure of welded joints is either weld toe or weld root-induced. Following previous developments, an analytical effective stress formulation involving the normal and shear traction structural stress components has been established to determine the failure mode transition and can be used as well to obtain the minimum required weld dimensions to ensure weld toe induced failure. The closed form solution defines, for weld root-induced failures, the critical weld throat plane and provides a weld toe failure induced equivalent stress, meaning the master S-N curve formulation can be adopted to estimate fatigue lifetime (Xing & Dong, 2016). Low cycle fatigue applications have developed as well involving the structural strain (Dong et al., 2014, Xing et al., 2016, Xing et al., 2017).

3.2.8 Total stress

Aiming to improve similarity, another crack damaged geometry baseline (equivalent point) criterion has been proposed (Besten, 2015). The Mode-I far-field stress distribution in each cross-section along the weld seam has been related to semi-analytical through-thickness weld notch

stress distribution formulations along the expected crack path, involving a self-equilibrating weld geometry stress – consisting of a local V-shaped notch- and weld load carrying part – and equilibrium equivalent global structural field stress contribution; a refinement of a well-known definition. Exploiting (non-)symmetry conditions, a generalized formulation demonstrating stress field similarity has been observed and extends to the welding induced thermal residual stress distribution. A linear superposition of the two distributions provides the total one. Fatigue scaling requires the complete distribution to be considered and the stress intensity factor has been adopted to translate the intact geometry related notch stress distributions into a crack damaged equivalent, turning the stress field similarity into a stress intensity similarity. Cyclic mechanical- and quasi-constant thermal residual loading introduce a crack growth driving force and defects may develop into cracks. Modifying Paris' equation, a two-stage micro- and macro-crack growth relation is developed to include both the weld notch and far-field characteristic contributions. The crack growth model integration yields a medium cycle fatigue single slope resistance relation, a joint resistance curve correlating arc-welded joint lifetime and the (finite life) total stress criterion. A random fatigue limit formulation has been adopted to incorporate high cycle fatigue taking the transition in fatigue damage mechanism from growth dominant to initiation controlled into account. As-welded small-scale specimen complete and censored data has been used to establish one (family of damage tolerant engineering) joint fatigue resistance curve(s). Full-scale structure representative large-scale specimen data has been examined to verify a small-scale specimen data scatter band fit.

3.2.9 Crack tip stress or strain intensity

An improved crack growth rate model involving the crack tip stress intensity has been proposed and validated using titanium alloy test data to estimate and unify a wide range of (creep) crack growth rates, including loading & response ratio-, overload- and dwell time effects. A simplified model has been derived and can be easily used to obtain lifetime estimates based on two series of basic mechanical properties of material (Wang et al., 2014, Wang et al., 2015a, Wang et al., 2015b).

Taking advantage of a new normalized fatigue crack growth model, an extension has been proposed and validated by adopting the cyclic J-integral or crack tip strain intensity rather than the stress intensity in order to incorporate the generalized elastoplastic crack tip conditions (Correia et al., 2016).

A previously proposed crack growth rate model for prediction of the S-N characteristics of metallic components with large microstructural defects has been extended to materials that do not show large defects on the fracture surfaces (Zerbst & Madia, 2015). An approach based on a cyclic R-curve analysis is proposed to establish the initial defect size. The principle is explained and demonstrated by a first application to welded joints.

A theoretical model for the fatigue crack growth rate has been established based on the effective crack tip cyclic plastic zone involving an empirical crack closure expression and the low cycle fatigue properties. A good fit with experimental data has been obtained (Shi et al., 2016).

Recognizing the difference between the analysis tools needed for design and maintenance to estimate crack growth, modelling of small defects developing into cracks and ways to determine the short crack growth rate characteristics from long crack growth data have been discussed (Jones, 2014). It is shown how existing models can be used and how variations in crack growth histories can be accounted for.

Adopting the strategy to model crack growth as shape perturbation of a domain with existing cracks, a numerical approach has been proposed to simplify the crack growth computation and yet yield accurate results. Results prove the accuracy in comparison to numerical and experimental results available in the literature (Formica & Milicchio, 2016).

Williams' crack tip stress field power series expansion has been used to estimate the extent of the nonlinear zone, important for the fatigue assessment of non-brittle materials (Vesely et al., 2016). The characteristics could be potentially incorporated into methods to determine the fatigue behaviour descriptors of materials exhibiting nonlinear failure. The developed procedures simplify the analysis of the description of mechanical fields at a greater distance from the crack tip considerably.

A modification of the Gauss–Chebyshev method for stress intensity factor computation has been proposed, incorporating the Richardson extrapolation method (Dubey & Kumar, 2016). The more accurate solution has been obtained after a few numbers of iterations in comparison to the method in its original form.

A procedure for fatigue life assessment of welded joints based on a plasticity-corrected stress intensity factor range is developed using monotonic fracture mechanics techniques and has been modified for cyclic loading. A so-called cyclic resistance R-curve for short cracks has been introduced (Madia et al., 2017). The procedure has been validated with a large number of test results for different materials and welding methods. The stress intensity factor solutions of semi-elliptical cracks with high aspect ratios in plates and thick walled cylinders have been parametrically investigated under various stress distributions adopting a virtual crack closure-integral method (Okada et al., 2016). For the cracks in thick-walled cylinders, the stress intensity can be approximated using flat plate solutions.

Different (extended) finite element method based mode-I stress intensity factor calculation methods have been compared (Fischer & Fricke, 2015) for compact tension specimens. The J- and interaction-integral provide relatively accurate results. Although extended finite element methods show crack modelling advantages, oscillations in 3D have been observed due to extraction domains. The best results are obtained with domain integrals using the finite element method with a refined mesh.

Finite element- as well as analytical solutions are employed to obtain the stress intensity factor for similar and dissimilar welds in lap-shear joints underpinned and clamped boundary conditions (Sung & Pan, 2016). Solutions indicate that clamped boundary conditions reduce the stress intensity factor for a given geometry about 7% for similar welds and about 20% for dissimilar welds, providing a higher welded joint fatigue lifetime.

The limitations associated with implicit and explicit representations of cracks in the extended finite element method are investigated for non-planar 3D cracks in a numerical study and a novel hybrid approach has been developed. Effectiveness has been demonstrated using examples (Sadeghirad et al., 2016).

An overview of adaptive re-meshing techniques to evaluate the crack front shape evolution and fatigue life has been provided, including a systematic identification of the main numerical (and physical) variables affecting the accuracy (Branco et al., 2015). Several issues are still unsolved. Future challenges include the development of more efficient procedures to estimate (3D) crack paths and fatigue lives in complex geometries subjected to non-proportional mixed-mode loading. Computational algorithms being able to perform automatic transitions from the surface or corner cracks through cracks for both in-plane and out-of-plane propagation are required as well. Other challenges include non-symmetrical crack growth, propagation in non-isotropic materials, defect-crack interactions and crack interaction in case of mixed-mode loading.

To estimate the residual fatigue life once cracks are identified, a semi-analytical approach has been proposed involving analytical stress intensity factor formulations as well as finite element method solutions. Its potential is demonstrated by studying the crack propagation effects on the fatigue lifetime of typical joints (Lou et al., 2015).

Numerical crack propagation simulations have been performed for different welded joint geometries to investigate the influence of geometry complexity (Fischer et al., 2015, Fischer et

al., 2016c, Fischer et al., 2016b). The stress gradient over the plate thickness, the apparent plate thickness and the notch effect slows down the crack propagation rate if the same stress value being effective for fatigue appears at the weld toe. The weld load-carrying level, the weld flank angle and the geometrical configuration affect both the notch effect and the local stress concentration. Accordingly, the fatigue assessment using a single-point fatigue parameter might be problematic because the crack propagation phase is strongly affected by the stress distribution along the crack path.

An equivalent initial defect size has been determined to estimate the fatigue strength of welded joints. One experimental data point is involved, reflecting the stress concentration effect at the fatigue critical location which is assumed to be approximately equivalent to a crack in an unwelded plate. The fatigue lifetime is calculated using the Paris relation accordingly. Application using constant amplitude fatigue data shows good agreement between the calculated and experimental fatigue lifetimes (Mikkola et al., 2015).

3.2.10 Crack tip energy release rate

Linear elastic fracture mechanics have provided a basis to describe damage growth using stress intensity factors or strain energy release rates. Discussing the fatigue crack growth equations presented in the literature, it is demonstrated that the principles of similarity in current methodologies have not yet been well established. As a consequence, corrections for the loading & response ratio effect are misunderstood and an alternative principle of similitude using cyclic work and strain energy release is proposed (Alderliesten, 2016).

The complex-valued finite element method is proposed as a new virtual crack extension method to compute the energy release rate (Millwater et al., 2016). Using a complex Taylor series expansion, the energy release rate is obtained as a numerical derivative of the strain energy with respect to a crack extension. This method retains the conceptual simplicity of numerical differentiation but eliminates numerical issues regarding perturbation of the crack size. The obtained energy release rate shows the same accuracy as the J-integral based results.

3.3 Damage mechanics criterion advances

Continuum or discrete damage mechanics criteria can be adopted to estimate the initiation and growth lifetime contribution using respectively damage evolution functions to describe the deterioration of the material mechanical properties (e.g. based on effective stress or Young's modulus as intact geometry parameters) and crack cohesive zone or -damage mechanism formulations (Den Besten, 2019).

To address plasticity – particularly useful for notched geometries, a damage-coupled elasto-plastic constitutive model has been employed enhancing the typically linear elastic continuum damage mechanics criteria. Both uniaxial and multiaxial non-proportional loading & response conditions can be dealt with. Damage estimates are compared to experimental data and agree well (Shen et al., 2015).

3.4 Complete strength criteria

The fatigue damage criterion defines in terms of resistance the fatigue strength scatter; i.e. structural integrity, and can be improved towards complete strength (Den Besten, 2019) by taking the resistance dimensions: material, geometry, loading & response (e.g. multiaxiality, mean- and residual stress) and environment (e.g. corrosion) dimensions explicitly into account.

3.4.1 Multiaxiality and amplitude variability

Although the ship and offshore structural stiffness distribution is predominantly orthotropic (stiffened panels) or member orientation defined (trusses, frames), both loading and geometry induced multiaxial welded joint far field response locations can be observed, consisting of Mode-I and mode-III contributions in the typically thin-walled structural members; a 3rd fatigue

resistance dimension aspect. At the weld notch locations, the response is multiaxial by definition because of cross-sectional (stiffness) changes, introducing the (geometry induced) mode-II component. The considered plane, i.e. of the critical, integral or invariant type can principally be adopted for all fatigue damage criteria and is typically correlated to another loading & response component: (random) variable amplitude behaviour, paying attention to non-proportionality coming along with principal stress directional changes.

For critical plane based multiaxial fatigue damage criteria, plane selection is very important. In order to understand crack development, calculated stress-strain fields have been represented in polar diagrams to show the loci of maximum stresses or strains with respect to the plane orientation. Measured crack paths can be superimposed. Cracks in plane geometries were found to develop at both planes of maximum normal or shear strains and there might be equal chances for a crack to initiate and grow along different paths. Regions showing at which planes cracks could possibly initiate and grow have been obtained (Albinmousa, 2016).

The ratio of the Mode-I normal- and mode-III shear resistance is lifetime-dependent, meaning that in case the fatigue damage criterion is an equivalent stress the involved coefficients are principally lifetime dependent as well. For several critical planes based on equivalent stress fatigue damage criteria, the lifetime estimate consequences have been investigated using experimental data for several materials. In comparison to the conventional approach involving constant coefficients, improved results have been obtained (Karolczuk et al., 2016).

The accuracy of the Modified Manson Coffin Curve concept in estimating fatigue lifetime of metallic materials subjected to complex constant and variable amplitude multiaxial loading & response has been investigated (Wang & Susmel, 2016). The adopted critical plane is based on the maximum shear strain variance of the deviatoric strain time series. Resolving shear strain cycles using rain-flow counting and incorporating mean stress effects using the hydrostatic strain component, the sound agreement between lifetime estimates and experimental data has been obtained.

Taking damage contributions from the normal- and shear strain amplitude, the hydrostatic mean strain as well as path-dependency into account a critical plane approach has been proposed for plane geometry low cycle fatigue applications. Validation using experimental data for different materials demonstrates the effectiveness (Li et al., 2014a, Jiang et al., 2016, Tao et al., 2016). Elastoplastic response calculations are an important element of low cycle fatigue assessment. In case of non-proportional multiaxiality 6D, incremental plasticity calculations are required to correlate all stress and strain components. However, a large number of multiaxial fatigue problems involve tension/compression, bending and torsion loads, which are associated with only one normal and one shear stress component. A new 2D incremental elastoplasticity formulation has been introduced integrating non-linear kinematic hardening models and non-proportional hardening effects in a very efficient way. Tension-torsion calculations from more general 6D models are exactly reproduced, but with less than one-fifth of the computational cost. Validation provided good agreement (Wu et al., 2016).

A critical plane based model utilizing the theory of critical distances has been proposed for multiaxial high-cycle fatigue lifetime evaluation (Liu, 2015). The maximum shear stress range plane is defined as the critical one. The maximum effective shear stress amplitude and the maximum effective normal stress, obtained by averaging the stress in the hemisphere volume around the maximum stress point, are the involved damage parameters. Lifetime estimates are in good agreement with aluminium plane- and notched geometry test data.

An elastoplastic generalized strain parameter involving normal- and shear contributions, representing respectively growth and initiation contributions, has been proposed as fatigue damage criterion. The plane showing maximum damage is adopted as the critical one. Analysis results and notched geometry experimental data are in agreement (Ince & Glinkab, 2016).

The effective notch stress has been obtained for V-shaped notches with root hole subjected to mixed-mode I and II response conditions (Berto, 2015a). The involved fictitious notch radius is determined as a function of the real notch radius, the microstructural support length and the notch opening angle. Adopting Neuber's original procedure an analytical formulation has been established to provide the microstructural support factor as a function of the mixed-mode ratio and the notch opening angle. Values have been verified using finite element models.

Relating the structural hot spot stress fatigue damage criterion and a critical plane approach, the welded joint multiaxial fatigue resistance has been investigated for different loading & response conditions, showing its effectiveness through substantive test data (Li et al., 2014a, Jiang et al., 2016, Tao et al., 2016).

Although not much mixed-mode crack growth rate test data under non-proportional loading conditions are available in the literature, some presented data (Feng et al., 2006) continues to be a subject of intense investigations (Mei & Dong, 2016, 2017b, a). The 90 [deg] out-of-phase mixed-mode I and III loading & response case seems the most puzzling one and available models hardly offer a reasonable explanation of the data trends. Adopting the moment-load-path based fatigue damage criterion definition (Dong et al., 2010), coupled with a geometric mean based maximum effective stress intensity factor, a two-parameter non-proportional mixed-mode crack growth model seems to provide a rather satisfactory data correlation (Mei & Dong, 2017b). In addition to its ability to consistently capturing proportional and non-proportional loading & response fatigue damage effects, the path-dependent-maximum-range and moment-load-path based approach has been adapted for fatigue design and lifetime evaluation of welded structures (Dong, 2001) by developing an equivalent structural stress range parameter, which includes the mean stress- and far-field stress gradient induced size effects (Dong et al., 2010). A comparison of lifetime estimates for welded joint test data available in the literature to IIW (Hobbacher, 2013) as well as Eurocode 3 (CEN, 2005) results demonstrates its effectiveness.

Experimental studies show that a non-proportional multiaxial constant amplitude loading & response is more damaging than a proportional one and depends on the involved loading & response path as well as material. Under non-proportional multiaxial variable amplitude loading & response conditions, any fatigue assessment concept must also provide an effective method to establish the number of cycles, either by counting or a stochastic approach.

One important development towards developing an integrated definition of a multiaxial fatigue damage criterion and a multiaxial (half) cycle counting procedure is the path-dependent-maximum-range / moment-load-path based approach (Mei & Dong, 2016, 2017b, a). One deficiency in the original path-dependent-maximum-range approach (Dong et al., 2010, Wei & Dong, 2014) addressed is that non-proportionality induced fatigue damage is calculated based on path length traversed in either stress or strain space. Both simple and rather complex forms of non-proportional multiaxial loading & response paths were examined for demonstrating the method's effectiveness in test data correlation (including structural steel and aluminium welded joints) as well as its applications for fatigue design of welded structures (Wei & Dong, 2014). Based on Wang and Brown's reversal counting method, a new critical plane approach has been proposed for plane geometries based on a weight-averaged maximum shear strain range. For low- and medium cycle fatigue test data the approach shows satisfactory lifetime estimates (Li et al., 2014a, Jiang et al., 2016, Tao et al., 2016).

For random amplitude multiaxiality, a stochastic damage estimate can be obtained by adopting Laplace distributions (Karlsson et al., 2016). Explicit formulae for the expected value of the rain flow damage index as a function of excess kurtosis are provided for correlated loads. Measurement results have been used for illustration and demonstration purposes showing the accuracy of the damage estimate.

The effectiveness of common equivalent stress- and strain-based fatigue damage criteria have been evaluated and areas of improvement have been discussed. Mixed-mode hypotheses, sequence- and size effects are considered to be most important and require further investigation, as well as the development of simplified procedures in order to reduce computation time (Vormwald, 2015).

Bi-axial fatigue tests have been conducted using plane geometry specimens in order to validate critical plane based fatigue damage criteria with respect to crack orientation and lifetime estimate. Conservative, as well as non-conservative results, have been obtained (Lopez-Crespo et al., 2015b).

Common equivalent stress- and strain based multiaxial fatigue damage criteria have been evaluated using experimental data (Gates & Fatemi, 2016). Mean stress effects were considered as well using different models. Variable amplitude lifetime estimates are compared to constant amplitude values to highlight similarities and differences in lifetime trends. Overall, mixed results were obtained. Both constant and variable amplitude fatigue lifetimes are predicted well for notched geometries. The importance of stress gradient effects has been demonstrated as well. However, for plane geometries, a consistent trend of non-conservative lifetime estimates for variable amplitude loading conditions has been observed.

Observing fatigue test results for the plane- and notched geometries, cracks initiate at the maximum shear plane. Lifetime estimates obtained using different multiaxial fatigue damage criteria show mixed results, typically lacking consistency for different loading & response paths (Gates & Fatemi, 2014).

Laser-stake welding can be used to produce steel sandwich panels, joining plates of 10 [mm] thickness with web plates. Fatigue tests were performed applying axial, shear and in-phase multiaxial loading to the panels. A nominal- and effective notch stress fatigue damage assessment shows that Eurocode 3 and IIW interaction equations can provide safe designs (Fricke et al., 2016).

To evaluate the performance of different multiaxial fatigue damage criteria for welded joints, the probability of achieving a non-conservative fatigue lifetime estimate has been calculated using experimental data collected from the literature. A large variety in safety has been observed, especially for non-proportional loading & response (Pedersen, 2016).

For the assessment of multiaxial fatigue in welded joints, a wide variety of methods have been suggested. For comparison purposes, several load cases were defined. Considering codes as well as models available in the literature, it has been concluded that non-proportional variable amplitude loading has a significant negative impact on the fatigue lifetime estimates (Van Lieshout et al., 2016).

A preliminary study has shown up to what extent multi-axiality can affect fatigue damage for welded joints in a container ship (Bufalari et al., 2017).

The weld root-induced fatigue strength of inclined butt joints in a proportional multiaxial far field response condition has been investigated using the nominal- and effective notch stress as fatigue damage criterion (Khurshid et al., 2016). To account for multi-axiality, the former has been used in combination with the modified Gough–Pollard interaction equation, the Eurocode 3 guideline and the DNV standard; the latter criterion involved a principal stress- and Von Mises stress hypothesis as well as the modified Wöhler curve approach. Results are evaluated along with data published in the relevant literature. The modified Wöhler curve approach seems to be the most suitable tool for multiaxial fatigue evaluation in case of a far-field multiaxiality.

Adopting a single edge notch specimen subjected to eccentric non-symmetric four-point bending, crack growth has been investigated incorporating the mixed-mode I and II contributions. The crack growth direction is estimated using different criteria including the maximum tangential stress, the strain energy density and the crack tip displacement. Multi-parameter fracture

mechanics involving several terms of Williams' power series solution has been employed. Whereas for the tangential stress and strain energy density criteria the first order term is accurate enough, the crack tip displacement criterion requires higher order terms to be involved (Malikova et al., 2015, 2016).

To improve understanding of proportional and non-proportional mixed-mode I and III loading & response conditions the crack growth behaviour at notches have been investigated experimentally using digital image correlation, providing a crack path, crack growth lifetime, crack tip deformations and crack closure information (Hos et al., 2016).

Fatigue crack propagation in case of biaxial tensile loading has been investigated (Gotoh et al., 2015). Tests are performed by investigating phase effects. An advanced fracture mechanics approach has been developed based on the re-tensile plastic zone generating a stress criterion for crack propagation and simulation results are compared to measurement data.

Mixed-mode I, II and III propagation of a pressurized circular crack subjected to various loading conditions has been investigated numerically (Schwartzkopff et al., 2016). The proposed crack front propagation algorithm based on the maximum tangential stress criterion aligns well with published results. The algorithm consumes only a fraction of the time needed for a numerical simulation and could be useful for design.

3.4.2 Mean- and residual stress

A mechanical loading & response cycle is defined by two parameters, for example, amplitude or range and mean stress; another 3rd fatigue resistance dimension aspect. Both parameters contribute to fatigue damage up to some extent, depending on (base) material properties; either metals or polymer composites. For welded joints, the quasi-constant welding-induced residual stress acts as mean stress as well.

A phenomenological fatigue resistance relation for single crystal metals, including lower and upper bound asymptotic behaviour corresponding to respectively ultimate strength and endurance limit, has been established. The stress amplitude- and mechanical mean stress contribution have been superimposed. Validation using experimental data with mechanical loading & response ratios in a large range varying from negative up to high positive values provided good results. Application to polycrystalline metals is suggested (Chandran, 2016).

Low- and medium cycle displacement controlled fatigue resistance information for base metal has been obtained at different mean strain values. Mean strain has been found to be more important in the medium cycle fatigue range. In terms of modelling, different existing models have been validated and in particular, Morrow's model provides good results (Carrion et al., 2017).

More displacement controlled fatigue resistance information for base metal has been obtained at several mean strain values. In general, the fatigue life decreases with increasing loading & response ratio and becomes more important for decreasing amplitude. An empirical model has been modified in order to obtain more accurate lifetime estimates (Hao et al., 2015).

For a super elastic metal, the mean stress and -strain effects on low- and medium cycle fatigue resistance have been investigated. Adopting a stress or strain based fatigue damage criterion including respectively a mean stress or strain correction, no satisfactory results have been obtained. An energy-based fatigue damage criterion incorporating both stress and strain has been selected, involving the dissipated energy density as well as the tensile elastic energy density to incorporate tensile mean stress effects (assuming that compressive mean stress does not affect fatigue damage), in order to obtain accurate lifetime estimates (Mahtabi & Shamsaei, 2016).

Knowing that for increasing loading & response level, the material temperature increases as well, a two-parameter heat energy fatigue damage criterion has been proposed. The criterion includes the specific heat loss and thermos-elastic temperature corresponding to the maximum cycle level, respectively incorporating the stress range and mean stress contributions. The

model correlates base metal medium cycle fatigue test data for a wide range of loading & response ratios (Meneghetti et al., 2016).

In case of high-temperature applications, both mechanical and thermal loading & response cycles can be important, and creep-fatigue may become an important failure mode. A modified strain energy density exhaustion model has been proposed, including mean stress effects. Accurate lifetime estimates have been obtained in comparison to base metal test data at different temperatures and loading & response conditions (Wang et al., 2016b). Based on a strip-yield methodology a new creep-fatigue crack extension model has been presented. Comparison to experimental data for a range of materials, temperatures and stresses shows its capabilities and limitations (Andrews & Potirniche, 2015).

The quasi-constant welding-induced residual stress distribution close to the weld notch is typically tensile like the mechanical loading induced response. To quantify the residual stress effects on fatigue strength, the residual stress distribution in terms of the weld notch stress intensity has been translated into a strain energy density formulation. Numerical analysis has shown that for high far-field stress levels the residual stress is redistributed and even converted into a compressive distribution. The residual stress redistribution has been found to be negligible for lower far field response levels. A tensile residual stress reduces the fatigue strength (Ferro, 2014).

The fatigue crack growth behaviour of high strength steel welds has been investigated, paying attention to the influence of microstructure and welding-induced residual stress. An effective stress intensity factor range has been proposed as a crack growth driving force (Wang et al., 2017b).

Using thermo-mechanical finite element calculations, the welding-induced residual stress redistribution has been investigated for cyclic loading & response conditions. The first few cycles show a significant residual stress release. An analytical model validated using measurements, has been proposed to estimate the relaxation (Xie et al., 2017). Redistribution is cyclic loading & response magnitude and -ratio dependent (Wang et al., 2017a). Adopting non-linear continuum damage mechanics, the high-cycle fatigue consequences has been investigated for a welded T-joint. A comparison to test results demonstrates its effectiveness (Lee et al., 2016).

The influence of mean stress on the fatigue resistance of polymer composite materials has been investigated and a phenomenological model has been proposed; a sum of two power terms. Six calibration parameters are involved, reflecting from loading and response point of view the tension and compression contributions from the amplitude and mean; two parameters defining a cycle, as well as material dependency. Accurate lifetime estimates have been obtained for different materials and loading & response ratios using a one parameter set, even for material data not involved in the calibration process, meaning material dependency is limited and the loading & response and geometry effects are generally applicable (Flore & Wegener, 2016).

The modified Chaboche continuum damage model has been proposed introducing non-linear mean stress dependence for fatigue assessment of polymer composites based on orthotropic damage evolution. Haigh diagrams and fatigue resistance curves have been constructed to illustrate the model capabilities (Desmorat et al., 2015).

3.4.3 Time and frequency domain

The loading & response characteristics allow for analysis in the time and frequency domain; another 3rd fatigue resistance dimension aspect. Generally speaking, frequency (i.e. spectral) domain approaches are considered less reliable but more efficient, as concluded when addressing the recent developments in the multiaxial frequency domain (Benasciutti et al., 2016). Time domain approaches, on the other hand, are more accurate but computationally expensive.

A new frequency domain approach for fatigue damage calculation in case of random multiaxial loading has been developed adopting an equivalent critical plane criterion, combining the power

spectral density functions of the involved stress components. A comparison of lifetime estimates and test results shows satisfactory agreement (Carpinteri et al., 2016).

A frequency-domain fatigue life estimation algorithm based on statistical energy analysis for structures subjected to high-frequency loading has been proposed as well. It has been observed that when evaluated at 1/3-octave bands, the root mean square value of the power spectral density function was sufficiently refined to provide meaningful life estimates (Wang et al., 2016c).

To take mean stress corrections into account, a frequency domain approach has been presented based on a direct transformation of the zero-mean stress power spectral density, which is applicable for both narrow and broadband signals. Four different probability density functions have been adopted and the Derik's formula provides a good description in comparison to test results (Niesłony & Böhm, 2016).

Based on machine learning a frequency domain method has been developed for fatigue analysis in the case of random loading (Durodola et al., 2017). The network is trained on readily identifiable parameters, such as resistance curve parameters and spectral moments. Obtained lifetime estimates are similar to time domain simulation results and improve the classical frequency domain values.

For critical hot spots in offshore wind turbines, typically a time domain analysis is performed to account for the simultaneous wind and wave induced loading as well as structure-soil interaction. For the less critical ones, a frequency domain approach can be adopted. Lifetime estimates have been obtained for different long-term response distributions, including Rayleigh and Dirlik. Akaike's information criterion has been adopted to judge the results and Dirlik's formula provides results closest to time domain simulation results (Yeter et al., 2014b, 2015e, 2016a).

Frequency domain results can consistently provide lower fatigue lifetime estimates. Two sources have been identified: an overestimated response spectrum and the Rayleigh distribution assumption. Opting for time domain calculations, the damage surface in the scatter diagram has been approximated meaning only a few sea states have to be simulated. The computational efforts are significantly reduced while maintaining high accuracy (Mohammadi et al., 2016b).

To combine the advantages of time and frequency domain approaches, the structural response spectral density function is obtained in the frequency domain and consequently converted into a response time history by using an improved signal conversion approach. The fatigue damage can be assessed using rain flow counting – important for non-proportional multiaxiality as well – and a damage accumulation model, like the one from Palmgren-Miner. The advantage is that a Rayleigh distribution assumption associated with a narrow band random process is not required. Calculations show that the hybrid approach results are more accurate in comparison to the frequency domain results and takes less computation time in comparison to a time domain approach (Du et al., 2015).

3.4.4 Environment

Ship and offshore structures, including oil and gas transport systems, operate in an aqueous and often sulphide containing sour-brine environment, meaning corrosion may appear in the material (geometry) surface. Corrosion, a 4th resistance dimension element, accelerates the fatigue damage process by deteriorating the material and geometry defined reference resistance (Den Besten, 2019). A considerable interest in improving empirical models has been observed by accounting for some of the mechanisms involved in corrosion and corrosion fatigue. The aim is to reduce conservatism and improve assessment concepts to estimate remaining lifetimes. The latter is particularly relevant since improvements have resulted in structures being operational beyond their intended lifespan. Alternative energy sources point to hydrogen storage and transportation, meaning hydrogen assisted cracking investigations are needed as well.

Using 3D surface measurements, the pitting distribution and morphology of pre-corroded steel plates have been established. Deep-narrow and wide-shallow pits have been identified, as well as a superposition of the two. For different exposure times, fatigue tests provided resistance information. Sharp and interacting pits significantly reduce the fatigue lifetime. An FE model has been used to establish the critical pit dimensions, providing the defect size for fracture mechanics based calculations to estimate the fatigue lifetime. Measurements and calculation results provided comparable results (Xu & Wang, 2015).

Single pit corrosion fatigue strength information at 10^9 cycles for steel at three different mean stress levels has been used to validate a modified El Haddad crack growth threshold model. Safe estimates are generally obtained, in contrast to the Murakami's empirical model (Harkegard, 2015).

Murakami's empirical fatigue damage criterion is difficult to apply in case the local stress state is multiaxial, like for irregular corrosion induced pitting geometries. A non-local Crossland equivalent stress criterion has been proposed; an averaged circular volume based criterion involving a critical distance, i.e. diameter. Corrosion affected fatigue strength information obtained at 10^7 cycles has been used to estimate the most likely critical diameter. FE analysis shows that for identical defects there is no interaction if the distance exceeds three times the critical diameter (May et al., 2015).

The corrosion rate in the heat affected zone, at the weld toe location, is typically higher in comparison to base material values because of the welding-induced residual stress level close to yield and the mechanical loading and geometry induced stress concentration, introducing non-uniform corrosion. The probability of fatigue induced failure increases and taking the time-dependent response into account, mechanochemical fatigue damage estimates have been obtained adopting the structural hot spot stress concept (Yang et al., 2016).

To incorporate mean stress effects affecting crack growth in a corrosive environment, a modified linear elastic crack growth model has been proposed, considering the relative crack opening period; i.e. area rather than amplitude only, as a damaging portion of a cycle. Both the strength and mechanism parameters, intersect logC and slope m, are affected. Model estimates and sinusoidal constant amplitude experimental data correlate fairly well (Adepipe et al., 2016).

To model crack growth in gaseous hydrogen conditions, a corrosion-crack correlation model has been proposed, based on Foreman's modification of the Paris relation incorporating the mechanical loading & response ratio and fracture toughness. Adopting a hydrogen-enhanced de-cohesion theory, the crack tip plastic zone size has been used to include frequency effects as well. Experiments demonstrated the model effectiveness (Cheng & Chen, 2017b).

3.5 Total life criteria

Correlation of medium and high cycle fatigue; involving respectively a crack growth and initiation governing lifetime, requires matching of crack damaged and intact geometry parameters to provide a total life fatigue damage criterion (Den Besten, 2019).

During the time, the arc-welding induced defect size has become smaller because of technological and modelling developments (Lassen, 1990, Verreman & Nie, 1996, Darcis et al., 2006, Zhang & Maddox, 2009, Hobbacher, 2010, Chattopadhyay et al., 2011, Zerbst & Madia, 2015). Values decreased from 1.00 [mm] down to 0.05 [mm], meaning even for welded joints, although the lifetime is often assumed to be growth dominated, the crack initiation contribution to the total lifetime increases in the high-cycle fatigue region.

Correlation of the initiation and growth lifetime quantifies the individual contributions and requires matching crack damaged and intact geometry parameters (e.g. notch stress intensity factor and crack tip stress intensity factor) to provide a total life fatigue damage criterion improving the strength and lifetime estimates.

Several 2-stage 2-parameter models have been proposed involving an assumed transition crack size based on different arguments: theoretical (e.g. fracture mechanics modelling restrictions), practical (e.g. detectability) as well as phenomenological (e.g. critical distance), affecting the (initiation/growth) ratio up to a large extent. A slightly different 2-stage 2-parameter model is based on a transition rate: the intact geometry stress distribution rate is equal to the crack growth rate, meaning the transition is not defined a priori. The adopted initiation and growth contributions have been incorporated adopting respectively a critical plane criterion and the crack tip stress intensity factor. Lifetime estimates are in good agreement with experimental results (Socie et al., 1979, Chakherlou et al., 2012, Mohammadi et al., 2016b).

Question is whether a 2-parameter concept is the best solution to include 2-stage behaviour. Except for the transition size, the actual as-welded joint fatigue test data is only used for calibration purposes of some crack initiation model parameters or not involved at all, assuming a series of initiation and growth similarity conditions of (standard) specimen and as-welded joints rather than a one-to-one correspondence between model lifetime estimate and *S-N* test data; a welded joint fatigue resistance similarity. As an alternative to a 1-stage 1-parameter model (e.g. the stress intensity factor as crack damaged geometry parameter and the Paris relation using a defect size equal to the intact geometry material characteristic micro and meso structural length; (Mikheevskiy et al., 2015)) or a 2-stage 2-parameter model, a 2-stage 1-parameter model like the Battelle equivalent- or Total stress can be adopted. A natural transition from a growth governing to an initiation dominated lifetime is, for example, possible by introducing a loading & response level dependent elastoplasticity coefficient (Besten, 2015), changing the crack growth characteristic from non-monotonic to monotonically increasing.

For fretting fatigue damage applications, distinct crack initiation and growth contributions have been established both numerically and experimentally, involving respectively Crossland's criterion and Paris' relation. The nucleation – growth transition has been determined to calibrate a critical distance, used as nucleation criterion location and initial crack size in order to establish the nucleation and growth lifetime (Gandiolle et al., 2016).

The multiple mechanisms in high- and very high cycle fatigue require strategies bridging multi-scale experiments and higher fidelity models. Approaches have been discussed paying particular attention to modelling of microstructure sensitive driving forces and thresholds, including challenges to predict the transition of failure mechanisms at different response levels (Castelluccio et al., 2016). Applying full-field calorimetric measurements, cyclic slip-induced microplasticity – the primary damage mechanism in the very high cycle fatigue region – has been evaluated based on an experimental energy balance. A relation to fatigue life has been established using the Manson-Coffin relation (Wang et al., 2017b).

An elastoplastic strain energy based fatigue damage model has been proposed, involving the atom dislocation movement induced crack initiation- as well as crack growth energy terms. Loading & response ratio effects are incorporated, adopting Walker's model. Using a variety of different metals with initiation and growth data available in literature the model has been validated. Damage estimates are in agreement with experimental results, although at very low strain levels some inaccuracies have been observed (Huffman, 2016).

Over the past decades, strain energy (density) has been used as fatigue damage criterion for both crack initiation- and crack growth dominated lifetimes separately. A generalized energy relationship has been developed and can be used to estimate initiation as well as growth dominated fatigue (Mohammadi et al., 2016a).

3.6 Multi-scale criteria

Additional macro-, meso- and micro-fatigue damage mechanism information – physics at a smaller scale – can be used to enhance an engineering based model, providing a multi-scale fatigue damage criterion. Following the macro-scale developments from global to local fatigue

damage criteria during the time the continuum mechanics lower bound is approaching and a correlation to the 'netherworld' (i.e. to meso- or even micro-scale physics) is a next step (Den Besten, 2019), for both base and polymer composite materials.

Numerical multi-scale models have been introduced in a new class of finite element methods, involving nodal or element enrichment, respectively X-FEM and E-FEM, meant to alleviate some of the continuum damage mechanics model limitations. To describe both short and long crack growth behaviour, a cohesive zone model and a 2D elemental enriched finite element model have been coupled. Element enrichment allows for the displacement jump over the crack front, meaning no special interface elements are required in contrast to traditional finite element modelling. Following calibration of the model parameters using the long crack mode-I Paris relation properties, a comparison of the mixed-mode short crack path simulation results and experimental data obtained using electronic backscatter diffraction shows a good correlation (Panwar et al., 2016).

Adopting the Chaboche non-linear continuum damage mechanics model, an intrinsic crack size; a process zone criterion reflecting short crack growth considerations has been derived correcting the linear elastic stress intensity factor expression. The proposed model is applicable for short and long cracks and incorporates loading & response ratio-, amplitude variability- and loading sequence effects including single and multiple overloads. Good correlation with test results has been obtained (Zhang et al., 2016a).

Using the crack density (i.e. effective stress) as a key parameter, a continuum fatigue damage mechanics criterion has been derived, modelling the trans-scale process from nucleation of many short cracks to the growth of a few long cracks, eventually up to fracture. Calibrating the five model parameters using damage evolution curves, good correlation with experimental results have been obtained (Sun et al., 2016).

The fatigue damage process from micro-defect to macro-fracture can be characterized using an energy density zone model involving scale transition functions. Parameter estimates require fatigue resistance information of plane- and notched geometries. The fatigue resistance scatter terms have been shown to be predominantly a consequence of microscopic effects (Zhang et al., 2016b).

Due to the multi-scale architecture of polymer composite materials, a wide variety of failure mechanisms can be observed. Multi-scale modelling approaches have been proposed to estimate high-cycle fatigue, based on weak spots showing visco-elastoplastic material behaviour. Scale transition has been achieved using non-linear mean-field homogenization (Krairi et al., 2016).

Since uncertainties exist in both micro- and macro-scale parameters, the fatigue performance of six commonly used failure criteria has been compared using a multi-scale reliability analysis. Homogenization methods; i.e. rule of mixtures, Mori-Tanaka and computational homogenization are adopted to link the scales and to translate uncertainties from micro- to macro-scale. In a comparison to a single-scale analysis, more accurate reliability estimates can be obtained (Zhou et al., 2016).

A new stress-based multi-scale criterion has been proposed, involving fiber as well as matrix induced failure at a microscopic level. For engineering purposes, interface-related failure has been ignored meaning the fiber size should be carefully determined. As soon as the finite (shell) element based macroscopic stress distribution has been obtained, the microscopic stresses are calculated using representative volume elements at a set of reference points; i.e. maximum stress points for different elementary loading conditions, to establish the damage evolution. Validation using open-hole off-axis tension tests show good agreement between experimental results numerical estimates (Li et al., 2014b).

A cohesive zone- and two-scale continuum damage model are coupled to estimate delamination induced fatigue of polymer composites. At macro-scale, the response is considered to be elastic; at micro-scale elastoplasticity is involved and obtained using representative volume elements (Amiri-Rad et al., 2015).

Decomposition of several signals, such as mechanical vibration and acoustic signals, into multi-scale intrinsic mode functions by the empirical mode decomposition technique has been conducted and a new adaptive multi-scale spectral features selection approach has been proposed, based on a sphere criterion which was applied to the intrinsic mode function frequency spectra (Tang et al., 2016).

3.7 Damage criterion statistics

At a materials level, crack initiation is typically related to plasticity at the micro- and mesoscale w.r.t. grain boundaries, dislocations, corrosion pits, manufacturing induced defects as well as inclusions, voids and pores. However, their character is random in terms of size, orientation, number and location. Concerning growth, the governing material bulk properties of Young's modulus are random as well. At a structures level, (weld) geometry parameters are random variables, meaning that the character of fatigue resistance information is essentially stochastic. Because of the random nature of the wind and wave induced loading, the response as well as the fatigue damage assessment involves reliability and confidence.

The weakest link theory has been related to the effective notch stress criterion to include both the (weld) volume induced- and response gradient induced size effects for different welded joint geometries. Using fatigue test data the most likely model parameter values are obtained and lifetime estimates are obtained in the data scatter band (Blacha & Karolczuk, 2016).

By integrating rough set theory; a tool to deal with uncertain knowledge, and neural network technology with particle swarm optimization to establish the fatigue resistance relation, hybrid intelligent technology has been established to obtain lifetime estimates. Simulation results show that estimates are more accurate than conventional neural network technology based ones (Yang et al., 2015).

4. CRACK GROWTH APPROACHES

Fatigue damage development includes initiation and growth contributions. Fatigue crack growth assessment has become increasingly used as an important part of Engineering Critical Assessment (ECA) for demonstrating fitness for service of the ship and offshore structures like FPSO's, maintenance or any need for repair (Song & Dong, 2016). Furthermore, manufacturing and construction quality acceptance are increasingly relying on ECA-based quantitative assessment methodologies as well to establish acceptance manufacturing defects or discontinuities below which fatigue crack propagation lives are deemed adequate to meet lifetime requirements. In contrast to fatigue damage accumulation approaches, crack growth approaches are based on the theory of fracture mechanics assuming that structures and materials inevitably contain defects that may develop during manufacturing and construction or during a certain period of service. Therefore, crack growth approaches have become an important tool for preventing fatigue failure of engineering structures, as has been discussed by numerous researchers over the last two decades for applications in the ship and offshore structures.

4.1 Defects and initial cracks

Welded structures contain various forms of defects such as porosities, inclusions, micro-cracks resulted from welding processes, often serving as the origin for fatigue crack development under service loading and environment. The effects of such initial crack-like defects or quantifiable initial cracks caused by service loading on remaining structural lives require fracture mechanics based crack propagation approaches to ensure safe operation of the ship and offshore structures. However, fracture mechanics applications in the ship and offshore structures are

complicated for complex structural details which are typically exposed to complex stress concentration behaviours at hot spot positions with sudden geometrical changes as holes or corners where fatigue cracks are typically found during regular inspection intervals. This means that crack-like defects much larger than those implicit in fatigue design curves, once found during inspections must be quantitatively evaluated to demonstrate a structural detail that contains such crack-like defects is fit for continued service. For fracture mechanics treatment, these crack-like defects can be characterized by surface cracks, through-thickness cracks and embedded cracks (Yeter et al., 2015b). Further discussions on applications in the various ship and offshore structures are given in (Yan et al., 2016), for pressure vessels in (Ding et al., 2015), pipelines in (Zhang et al., 2016c), some offshore structure details in (Lotsberg et al., 2016) among others.

4.2 Crack sizing during in-service inspection

Fatigue crack growth analysis can be carried out to demonstrate that a structure containing a flaw fits for a continued operation to a required lifespan, which must be accompanied by in-service inspection measures to mitigate any uncertainties in fracture mechanics based crack growth assessment. In-service inspection to detect fatigue cracks and determine their sizes is normally performed to ensure that potential cracks in the structure, which may have been present from the initial delivery or have arisen at a later stage during service, do not exceed a critical size determined from a fracture instability evaluation such as those given in BS 7910 in terms of failure assessment diagrams. A well-established reliability of a non-destructive testing (NDT) is typically applied, which characterizes the method's ability to detect an existing crack as a function of the crack size and uncertainty associated with the sizing of a crack of interest. Often, further calibration of a given NDT method may be required to improve the probability of detection and minimize uncertainty. An analysis methodology with calibrated initial defects was presented to make inspection planning less time consuming and less complex to perform (Lotsberg et al., 2016).

4.3 Modelling

Crack growth approaches based on fracture mechanics is then adopted as a basis to determine the detection curves. When planning inspection, it is important to assess the consequence of a potential fatigue crack at a considered hot spot.

Approaches based on fracture mechanics principles are implemented in the form of a Paris type of empirically observed power relationship between the stress intensity factor range and crack growth rate, which allows an estimation of crack propagation life from an initial crack size to a final crack size. The final crack size is often determined through fracture instability or global structural collapse analysis, based on the FAD (failure assessment diagrams) approach in well-established FFS (fitness-for-service) or ECA (engineering critical assessment) procedures, e.g., BS 7910 or API 579 RP-1/ASME FFS-1. There exist various crack growth models as reported in the literature, most of which represent somewhat extended or modified versions of the original Paris relation. Over the last three years, some models are further assessed and some extended to accommodate important parameters identified. These parameters include those related to material, structure, environment, loading etc. In this section, the current applications of crack growth rate models in fatigue and fracture analysis of ship and offshore structures as reported in the recent literature are reviewed and discussed.

4.3.1 Paris relations

The Paris relation is still a widely-accepted formula (Ilman et al., 2016, Ji et al., 2016, Soliman et al., 2016, Zhang et al., 2016c). Although this model includes only region-II of the crack growth rate curve, it is widely used because region-II represents the majority of the fatigue life for many structural components (Branco et al., 2015). A multi-objective optimization problem and solved it to simultaneously provide an effective and reliable decision-making approach, in

which the Paris relation is used to describe the crack growth rate was formulated in (Soliman et al., 2016).

The Paris relation with the stress intensity factor range replaced with a normalized strain energy release rate range, i.e., $da/dN=C(\triangle G/G_C)^m$. was adopted in (Harper & Hallett, 2015). The same reference also proposed a method for determining the constants C and m through a linear variation in the form of $C=(G_1/G_T)C_I+(G_2/G_T)C_{II}$ and $m=(G_1/G_T)m_I+(G_2/G_T)m_{II}$ for applications in composite tidal turbine blades. Here, G_I and G_{II} are the model I and mode II components of the total strain energy release rate, G_T, which is extracted from the numerical model and m_I, C_I, m_{II}, C_{II} are the pure model I and the mode II Paris relation constants extracted from experimental data. Further improvement to the current Paris relation fatigue model may be possible if mixed mode fatigue data becomes available.

A similar fatigue crack growth relation, $da/dN=C\Delta G^m$, is adopted in (Zhang et al., 2016c) when conducting fatigue analysis on offshore pipelines with embedded cracks. From the point of view of energy consumption, the mixed mode theory is adopted to calculate the equivalent fracture energy release rate G_{eqivC}. One of the mixed-mode models is expressed as $G_{eqivC}= G_{IC}+(G_{IIC}-G_{IC})[(G_{II}+G_{III})/(G_I+ G_{II}+ G_{III})]^{\eta}$.

Under non-proportional mixed mode loading conditions, most recent developments in introducing a moment of load path or MLP method seem to show great promise, as discussed in (Wei & Dong, 2014), which is further proven by evaluating a large amount of crack growth rate test data under non-proportional loading conditions (Mei & Dong, 2017b). The validity of such an approach has been validated using non-proportional multiaxial loading test data as given in (Mei & Dong, 2016, 2017a). The MLP method can be used for arbitrary variable amplitude multiaxial loading conditions through a multiaxial cycle counting procedure given in (Wei & Dong, 2014).

It is pointed out in (Lotsberg et al., 2016) in demonstrating probabilistic methods for the planning of inspection for fatigue cracks in offshore structures that small changes in basic assumptions for fatigue analysis can have a significant influence on the predicted crack propagation lives. Analysis results from fracture mechanics are dependent on factors such as crack growth parameters, initial crack size, and stress intensity factors. The Paris and Erdogan equation at any point along the crack front is used to calculate the fatigue crack growth per stress cycle.

4.3.2 Modified relations

Some new formulae are proposed. However, most of the new formulae added more parameters, or changed the original parameters of the Paris relation, with the result that a large amount of experimental C and m data cannot be directly used. To remedy this, the unique curve model, $da/dN=C[(\Delta K_{eq0})^m-(\Delta K_{th0})^m]$ and $\Delta K_{eq0}=M_R M_P \Delta K$ was proposed in (Huang et al., 2016), which is used in recent years for prediction of fatigue crack growth in a ship detail under wave-induced loading (Yan et al., 2016), taking advantage of the existing C and m database and at the same time taking the stress ratio and loading sequence into consideration. The determination of all parameters in the model is explained sufficiently. This model combines simplicity and practicability and has the potential for future use. To consider the effect of residual stress, the nominal stress intensity factor and the stress ratio are changed to $\Delta K_{eff}=(K_{max}+K_{res})-(K_{min}+K_{res})$ and $R_{eff}=(K_{min}+K_{res})/(K_{max}+K_{res})$ respectively, as adopted in (Ilman et al., 2016). The fatigue life of cruciform welded joints by considering both the effect of residual stresses and the influence of the weld toe geometry was estimated in (Tchoffo Ngoula et al., 2017). Fatigue crack growth analyses are performed by using the node release technique, together with the finite element program ABAQUS. The effective cyclic J-integral is used as crack tip parameter in a relation like the Paris equation for the calculation of the fatigue life. An analytical model to determine CTOD for a cracked component subjected to cyclic axial in-plane loading was proposed in (Dong et al., 2016). A simple fracture mechanism-based model for fatigue crack

growth assumes a linear correlation between the CTOD and the crack growth rate da/dN. The effects of stress ratio and crack closure were investigated by elastic-plastic finite element stress-strain analysis of a cracked component. The crack opening displacement can characterize the crack tip state at large scale yielding constant amplitude fatigue crack growth.

Variable amplitude loading history should be considered for fatigue analysis of ship and offshore structures. To explain variable amplitude loading effects, the Space-state model and the generalized Willenborg model were applied in (Maljaars et al.) by comparing them with the fatigue tests on welded, thick-walled C-Mn steel specimens subjected to CA (constant amplitude) loads with and without OL (overload) and of two types of VA (variable amplitude) loads. The Space-state model is found to be a relatively simple and useful tool for simulation of VA fatigue loads and VA sequences, but in the case of 'wave' load, the model was unable to predict the fatigue life. It shows that the Willenborg model provides good predictions of retardation effects in case of single overloads but when underloads exist, the model is not able to predict the fatigue life accurately. The modified Paris relation, $da/dN=C(\Delta Keff)^m$, was adopted in (Hodapp et al., 2015) when performing nonlinear fatigue crack growth of ship structures under variable amplitude stress by making the value of the stress intensity factor in crack opening level a time-dependent value. When discussing an improved procedure for generating standardized load-time histories for ship and offshore structures, applied the model $da/dN=(AM^m)/[1-(K_{max}/K_C)^n]$ combining the definitions of M and K'_{op}, $M=K_{max}-K'_{op}-\Delta K_{effth}$ and $K'_{op}=øK_{op}=øf_{op}K_{max}$, to consider the load sequence effect by introducing a parameter ø (Li, 2015).

The crack growth approaches accounting for the retardation effect have been applied for the fixed offshore wind turbine support under both constant and variable amplitude loading history (Yeter et al., 2015b, a).

Various approaches have been employed for the fatigue assessment of multiple surface cracks. Fitness-for-service codes, e.g., BS 7910 or API 579 RP-1, usually assume crack propagation of adjacent cracks without interaction and a re-characterization of multiple or complex flaws into a single crack of maximum dimensions after certain proximity conditions are observed. Another accepted concept is the fatigue crack closure (Elber, 1971), which explains how stresses lower than a crack opening stress can be insufficient to propagate the crack (Elber, 1971). However, the predicted life is usually conservative. An improved fatigue life analyses for multiple cracks were developed in (Pang et al., 2017) considering crack coalescence stage and fatigue crack closure. The predicted remaining fatigue life shows similarity with the experimental results.

A corrosion-crack correlation model for fatigue crack growth influenced by the hydrogen embrittlement to be used in pipeline carbon steels under gaseous hydrogen conditions was proposed in (Cheng & Chen, 2017a, b). The model is developed based on the correlation of the environment-affected zone and the plastic zone. In the model, the fatigue crack growth rate considers the influence of fracture toughness by the Forman equation and the stress-driven hydrogen diffusion and the hydrogen-enhanced de-cohesion hypothesis are used to describe the critical frequency and the "transition" stress intensity factor. In addition, the phenomenon of the cracking growth rate plateau is described by an approximation involving the stress ratio and the threshold stress intensity factor range.

A phenomenological fatigue crack propagation model for API-5L X100 pipeline steel exposed to high-pressure gaseous hydrogen was proposed in (Amaro et al., 2014). The material response in hydrogen at $da/dN<3\times10^{-4}$ mm/cycle was observed to be primarily affected by the hydrogen concentration, resulting in a hydrogen-dominated mechanism. The response in hydrogen at $da/dN>3\times10^{-4}$ mm/cycle results from fatigue-dominated mechanisms. The proposed model predicts fatigue crack propagation as a function of applied ΔK and hydrogen pressure.

4.4 Parameter estimates

Fatigue crack growth is dependent on various parameters from structural geometries, stress state, material properties, loading history and environmental conditions. Those parameters are typically incorporated into an appropriate crack growth model for assessing propagation behaviour of a fatigue crack. Stress intensity factor or its range is the most important parameter in commonly-used crack growth models. The stress intensity factor as a function of crack size depends significantly on the local stress field and crack size. The complexity increases when a change in stress distribution during crack growth is to be accounted for. With the aid of advanced computation techniques, the application of crack growth approaches in the ship and offshore structures have become more common in recent years (Yeter et al., 2014a, b, Matic et al., 2015, Yeter et al., 2015b, a, e).

4.5 Experimental data

The crack growth rate model used for fatigue and fracture analysis is derived and supported by basic crack growth data of the material. The crack growth rate database of different materials is enriched gradually by published articles and reports. For example, recently, the experimental crack growth data of pre-cracked 7050, 7075, 5083 and 6061 aluminum plates under fatigue conditions in a corrosive environment as the basis of investigating the effect of composite repair patch was given in (Schubbe et al., 2016). The fatigue crack growth data of AA 5083 metal inert gas (MIG) welded joints under static thermal tensioning by experiments was provided in (Ilman et al., 2016).

4.6 Numerical simulations

With the aid of high-performance computers, the numerical simulation is an alternative way for extensive parametric studies, replacing a large amount of costs on the experimental set up to conduct fatigue crack experimental tests. Progress in the computational modelling of fracture and fatigue with the advent of cohesive zone theory and more recently with the extended finite-element techniques will improve the basic understanding of fracture processes (Matic et al., 2015). The progress of computation techniques such as finite method and meshless methods makes the calculation of stress intensity factors (SIF) and crack shape development easier for ship details and offshore structures. During the last three years, the application of crack growth approaches on fatigue analysis of ship details and offshore structures has mainly been concentrated in the study by the aid of finite element method. Crack growth modelling is concentrated on structural details as tidal turbine blades, cruciform welded joints, pressure vessel steel, multi-planar DX-joint welds, offshore pipelines, aged jacket platforms etc. (Ding et al., 2015, Harper & Hallett, 2015, Ji et al., 2016, Tchoffo Ngoula et al., 2017). For example, a series of numerical analyses on the fatigue properties of multi-planar DX-joint welds were carried out in (Liu et al., 2015). The study mainly covered FE modelling of DX-joints, HSS analysis of DX-joint welds, and SIF study of weld cracks. The SIF of a crack in a ship detail was investigated in (Yan & Huang, 2015).

4.6.1 Loading sequence

One of the most important advantages of numerical simulation is to help to understand the load sequence effect by simulating the load history of the cracked body as real as possible. Stochastic nonlinear fatigue crack growth predictions for simple specimens were made, subject to representative ship structural loading sequences through a time-dependent stress intensity factor, which is based on the evolution of a rate-independent, incremental plasticity model simulating combined nonlinear kinematic and isotropic hardening (Hodapp et al., 2015). The result is a mechanistic rather than phenomenological numerical model requiring only experimentally measured fatigue crack growth rates under constant amplitude cyclic loading and a full material constitutive model defined through experimental push-pull tests for the same material. This

approach permits a consideration of material behaviours which are physically relevant to structural steels, yet necessarily omitted in the similar application of a strip-yield model. Both experimental and numerical studies to follow cracking damage in steel cylinder/plane fretting fatigue contact subjected to variable loading conditions were performed in (Gandiolle et al., 2016). To formalize crack nucleation prediction, the Crossland multiaxial fatigue behaviour was applied at a critical distance to consider the severe fretting fatigue gradients. The crack propagation rate was formalized using the Kujawski's fatigue crack driving force parameter and coupling the Paris relation of the material. Constant fretting fatigue conditions and variable fretting fatigue sequences were investigated. The influence of different plastic laws was investigated. An iterative method to simulate 3D fatigue crack propagation in crystalline materials is proposed based on the computation of a damage indicator based on plastic activity around the crack tip (Proudhon et al., 2015). By post-processing, this quantity after a given loading sequence, local crack direction and growth rate are estimated along the crack path. A Multi-Scale FEM Crack Growth model successfully extends the finite element analysis of plasticity-induced crack closure to variable amplitude, high-cycle fatigue by considering a physically accurate, time-dependent loading sequence (and hence stress intensity factor) applicable to ship structures in the marine environment, capable of considering material constitutive models which are suited to cyclic plasticity in structural steels was proposed in (Li, 2015). A numerical simulation of the fatigue crack propagation under superimposed stress histories containing different frequency components with several mean stress conditions was conducted in (Matsuda & Gotoh, 2015). The numerical simulation of fatigue crack propagation based on an advanced fracture mechanics approach using the RPG (Re-tensile Plastic Zone Generating) stress criterion was improved to enable the extraction of the effective stress history for fatigue crack propagation under superimposed stress histories.

An approach to assess the probabilistic life of mixed-mode FCG by coupling of finite element analysis and Kriging-based reliability methods was used in (He et al., 2015). A simulation program (FCG-System) is developed to simulate the fatigue crack path and to compute the corresponding fatigue life. Numerical applications dealing with FCG are presented to illustrate the numerical efficiency and accuracy of the proposed approach.

4.6.2 Residual stress

The plasticity effects on fatigue growth for a physically short crack was simulated in (Alfredsson et al., 2016). The material description comprised the Drucker-Prager yield surface, non-associated flow rule and non-linear combined hardening. The material's strength differential effect was the key difference explaining why compressive residual stresses instead of crack face closure were responsible for the short crack effect in this material. (Zhou & Jia, 2015) investigated the crack propagation behaviour in cast quenched and tempered steel after one overload cycle in tension as well as in compression on short cracks in deeply notched specimens. The crack propagation after overload cycles is investigated by inspection of the fatigue threshold R-curve and fatigue crack propagation rate. A fatigue crack growth (FCG) model for specimens with well-characterized residual stress fields using experimental analysis and finite element (FE) modelling was studied in (Garcia et al., 2016). The FE FCG models were developed using a linear elastic model, a linear elastic model with crack closure and an elastic-plastic model with crack closure. The results demonstrate that the negative part of the stress cycle with a fully closed crack contributes to the driving force for the FCG and thus should be accounted for in the fatigue life estimates.

4.6.3 Simulation on different crack forms and positions

The residual strength of a pin-loaded lug and a finite plate with semi-elliptical crack emanating from a hole are examined by a new analytical methodology which analyses the crack propagation process in terms of the life estimation and crack front evolution (Boljanovic et al., 2016). The stress field and the stress intensity factor were computed by applying both analytical and

numerical approaches, and the two-parameter driving force model was implemented for the fatigue life estimation and the crack front evolution. A 2D Finite Element model of an edge crack, in which the combined effects of the travelling Hertzian load (the contact pressure which conforms to the Hertzian contact theory) and the lubricant are accounted for, was developed in (Dallago et al., 2016). A pressurization is implemented by applying the external contact pressure acting on the crack mouth to the crack faces and the new fluid pressure inside the crack is found by an iterative procedure based on the condition of constant volume. The contribution of fluid entrapment to the stress intensity factors is investigated through an extensive parametric analysis.

A numerical simulation of crack propagation due to thermal cycling on a circular disc was performed in (Qayyum et al., 2016). The effect of the length of cracks and interaction between adjacent cracks has been investigated. The variation in Stress Intensity Factor (SIF), hoop stress and Crack Mouth Opening Displacement (CMOD) has been plotted as a function of primary/secondary crack lengths and a number of cracks. Results show a significant drop in hoop stress, SIF and CMOD with an increase in the number of cracks, thus limiting the number of cracks possible in a thermal fatigue crack network.

A systematic investigation has been carried out on the fracture resistance behaviour of offshore pipelines containing an elliptical embedded crack under cyclic tension loadings (Zhang et al., 2016c). The extended finite element method (XFEM) is adopted for numerical simulations. The influences of different initial crack lengths and stress ratios on fatigue crack growth are investigated in detail. Furthermore, the comparison between the values obtained from the theoretical analysis, (BS7910, 2005) and current investigation is made on the fatigue crack growth rate, from which it is obvious that the results obtained by XFEM are reasonable and reliable.

4.6.4 Damage mechanics models

Advanced simulation techniques should integrate a proper damage model to judge crack growth. The fish-eye fatigue crack growth after crack nucleation for very high cycle fatigue was investigated in (Nguyen et al., 2015). An iterative procedure based on three-dimensional finite element analyses is developed to conduct crack growth simulations. The stress intensity factors are used to estimate the fatigue crack growth by integrating the fatigue crack relation between the initial and final crack lengths. The formation of short cracks at notched members of super alloy single crystals under high-temperature low cycle fatigue was analysed in (Bourbita & Rémy, 2015). A damage model based on a visco-plastic strain energy density and dilation energy density is used to describe short crack growth and fatigue life of smooth specimens.

The seismic performance of welded joints with different weld access hole geometries and the effect of crack initiation and growth on the load carrying capacity of welded joints was discussed in (Tong et al., 2016). A continuum damage mechanics model used previously for monotonic loading was reformulated to account for the extremely low cycle loading condition.

Crack propagation under mixed-mode loading by means of the finite element method was simulated in (Al-Mukhtar, 2016). The numerical integration of the Paris' equation was carried out. The effect of normal and transverse applied load on crack propagation was presented. The results confirm the use of a fracture mechanics approach in the biaxial fracture.

A fracture mechanics approach to the phenomenon of the fatigue crack propagation in geometries such as plates and sheets was presented in (Toribio et al., 2016). A numerical procedure was designed and implemented starting from a discretization of the crack front and considering a sort of crack advance on the basis of the Paris relation, governed by the stress intensity factor obtained in (Newman & Raju, 1981).

The effect of shapes of circular hole defects on the rolling contact fatigue (RCF) crack initiation and propagation in high strength steel by RCF test and synchrotron radiation micro-computed

tomography (SR micro CT) imaging was clarified in (Makino et al., 2016). The mechanism of RCF crack propagation was discussed by finite element analysis.

Two important aspects of fatigue crack growth at negative stress ratios have been investigated. First, the controlling crack tip loading parameters are discussed (Benz & Sander, 2015) and an alternative stress based parameter has been correlated with the crack tip loading for negative loads. Second, the deformation mechanisms at negative stress ratios are discussed, and a new method is proposed in order to visualize the plastic deformations even at the negative loading part.

The crack growth behaviour of a pressure vessel steel was predicted in (Ding et al., 2015). The approach consists of elastic-plastic finite element stress-strain analysis of a cracked component and application of a multiaxial fatigue damage criterion to access the crack growth. Discussions are made to relate the characteristics of the crack growth behaviour of the material to the cyclic deformation of the material and to the contact of cracked surfaces.

Three-dimensional finite element analyses studied both crack initiation and propagation in a gear tooth. A damage mechanics approach was used to model crack initiation on the surface of a gear tooth due to the Rolling Contact Fatigue (RCF) (Ghaffari et al., 2015). A finite element model was developed to study the effects of friction on the fatigue crack initiation life.

4.6.5 Polymer composites

With the wide application of polymer composite materials in the ship and offshore structures, the study on the failure is ongoing. The advanced numerical modelling techniques of composite tidal turbine blades demonstrate the development of numerical techniques for modelling the growth of interfacial cracks (Harper & Hallett, 2015). The effect of moisture ingress on the bending fatigue of laminated composites was investigated in (Meng et al., 2016). A 2D Finite Element model (FEA) was developed to simulate the fatigue crack propagation based on virtual crack closure technique, while a 3D FEA model was developed to investigate the edge effect on fatigue crack propagation. A 4-step fatigue failure theory was proposed to explain the moisture effects on the crack propagation under bending fatigue.

The traditional phantom node method for crack propagation modelling of composite materials under fatigue loading was extended in (Wang & Xu, 2016). A fatigue damage variable related to experimental crack propagation rate was combined with the static one for interface property degradation, and a bilinear cohesive law considering damage initiation was used for quasi-static cracking modelling.

4.7 Crack growth assessment statistics

Fatigue cracks can appear at various locations along the ship structure and may occur at early stages in the service life of a ship or offshore structure. Due to the presence of significant uncertainties associated with crack initiation and propagation, the planning of inspection, monitoring and/or repair actions should be performed probabilistically.

A probabilistic framework for incorporation of risk and updating in the inspection of fatigue-sensitive details of ship structures, considering that fatigue cracks as a structural deterioration mechanism may lead to unanticipated out of service for naval ships, was developed in (Dong & Frangopol, 2015, 2016). The computation associated with fatigue damage is performed using fracture mechanics and uncertainties are considered within this process. As indicated, the fatigue crack size increases significantly with time and uncertainties are incorporated into the process. The uncertainties are also associated with inspection events. The outcomes of an inspection event are affected by many factors, such as the type of inspection method, human factors, and inspection quality. Consequently, uncertainties should be incorporated into the risk-informed decision making and updating. A useful flowchart for risk-informed inspection planning of fatigue-sensitive details is proposed which is illustrated on fatigue-sensitive details of

an existing tanker. Random variables associated with the fatigue crack limit state are analysed. It is pointed out that future research is needed to include nonlinear fracture mechanics in the damage assessment of fatigue-sensitive details and the effects of multiple fatigue cracks on the structural capacity should be considered in future studies for the risk assessment of fatigue-sensitive structures.

At the same time, a probabilistic approach for inspection, monitoring, and maintenance optimization for ship details under fatigue effects on the basis of the crack growth approach was proposed in (Soliman et al., 2016). Based on the stress profile and the crack geometry at the damaged location, intervention times and types are determined by solving an optimization problem which simultaneously minimizes the life-cycle cost, maximizes the expected service life, and minimizes the expected maintenance delay over the life-cycle.

4.8 Service life extension

Service life extension measures can be taken when cracks are observed. A composite patch repair is gaining popularity as it counters most of the problems faced by conventional renewal repairs. Extensive studies can be found in the literature addressing the efficiency of this novel repair method using techniques which meet higher performance and monitoring standards than these commonly found in naval applications. The efficiency of practices widely used in the ship repair industry for the implementation of composite patch repairing was addressed in (Karatzas et al., 2015). To this end, steel plates repaired with composite patches were tested under fatigue loading. The composite patches consisted of carbon fibers in an epoxy matrix and were directly laminated to the steel surface using the vacuum infusion method. Two different surface preparation methods, namely grit-blasting and mechanical treatment with the use of a needle gun were studied. In addition, to account for the harsh environmental conditions during the operating life of the structure and to study its effect on the repair, two different ageing scenarios were considered. The non-destructive evaluation of the patches was performed so as to assess the quality of the repair, and the evolution of debonding during testing.

An investigation of the performance for a composite repair patch to prolong the service life of pre-cracked 7050, 7075, 5083 and 6061 aluminum plates under fatigue conditions in a corrosive environment was performed in (Schubbe et al., 2016). Both insulated graphite–epoxy and boron–epoxy composite patches were evaluated for the effects of corrosion fatigue. The repair patches consisted of unidirectional plies (laminae) oriented in the loading direction. The improvement of service life and the effect that a corrosive environment had on crack propagation rates for the repaired aluminum plates were examined. The bond durability between the aluminum plates and the boron patch were also assessed. As expected, the introduction of salt water during testing greatly increased crack growth rates and has been quantified for comparison. The graphite patch consistently showed positive results compared to the boron patch for 6061 aluminum samples. The same system on 5083 aluminum had mixed results. Examination of potential 5083 sensitizations due to elevated cure cycles are discussed. The boron–epoxy repairs showed a positive life improvement in both lab air and salt water-exposed environments for 7050 and 7085 aluminums while the graphite–epoxy repair accelerated crack growth rates in the saltwater environment.

A rational method for determining the appropriate size of a stop hole, in which both high-cycle and low-cycle fatigue analyses are carried out according to the long-term and short-term wave-induced loading was proposed in (Chen, 2016). The time to initiate a new crack at a stop hole subjected to the long-term wave induced loading is predicted by the use of characteristic S–N curves and the Palmgren–Miner's rule. The time to initiate a new crack of a stop hole within severe sea conditions is calculated by strain-life methods in terms of the short-term wave loading induced in severe sea conditions. The effects of the return period of the potential severest sea condition, the crack length, and the environmental severity factor on the remaining service life of a stop hole are investigated.

5. FABRICATION, DEGRADATION, IMPROVEMENTS AND REPAIR

Fatigue strength of ship and offshore structures is largely affected by inherent defects and imperfections. More than often, such effects are included in safety (ignorance) factors rather than explicitly assessed. However, the trend is towards a more and more explicit and rational consideration of them in the design practice allowed by modern design procedures.

Two categories of imperfections may be distinguished: fabrication imperfections, existing at different levels in a structure just after construction, and in-service degradations, occurring during the lifetime of the structure.

Fabrication imperfections may be further categorized into misalignments and distortions, weld induced defects and initial crack size. Other imperfections include variations in material properties. In-service degradations also affect fatigue behaviour of structures: while corrosion and other degradation phenomena variously influence fatigue strength and introduce very large uncertainties in the fatigue assessment process, inspection and maintenance techniques are advancing as well. The reader is referred to the reports of Technical Committee V.2 - Experimental Methods and of Technical Committee V.7 - Structural Longevity for further and specific information on the matter. Thus, inspection and monitoring strategies, as well as maintenance issues, are only partially covered in this section and with particular emphasis on fatigue and fracture of the ship and offshore structures. The subject following a risk-based approach to the optimum inspection and maintenance planning for ship structures was recently addressed in (Dong & Frangopol, 2015, 2016).

Fabrication imperfection and in-service degradation countermeasures have been introduced and are continuously developed in construction to minimize detrimental effects on fatigue behaviour. Moreover, besides current recommendations on fabrication tolerances and post-weld improvement techniques (IACS, 2012), steel materials with enhanced fatigue resistance are now available for the shipbuilding industry.

A very comprehensive review paper has been recently published in six parts (Ibrahim, 2015a, b, c, d, 2016a, b), rationally presenting several aspects of structural life assessment of ship structures.

5.1 Fabrication imperfections

5.1.1 Misalignments and distortions

To improve the energy efficiency of the ship and offshore structures, new lightweight solutions are required. This is possible by utilizing thinner plates together with modern laser and laser-hybrid welding technologies. In thin plates ($t<5$mm), the main challenge is their proneness to larger distortions during production because of their lower bending stiffness. As distortions cause secondary bending, which increases the structural stress, the large distortions can lead to significant reduction in fatigue strength. In this regard, the traction structural stress method (Dong, 2005, 2010, Dong et al., 2014) coupled with analytically derived stress concentration factors for two typical distortion modes (Dong et al., 2017a, Dong et al., 2017b) showed rather promising results. Based on the experimental results from small-scale specimens (Lillemae et al., 2017) and numerical welding simulations (Tekgoz et al., 2013a, b, 2014, Garbatov et al., 2016a), the distortions can be larger and also with a different shape in comparison to the thick plate. In addition, the straightening of the thin plate under axial tension loading can result in the non-linear relation between structural stress and nominal stress (Fricke et al., 2015, Remes et al., 2017). The recent full-scale tests prove these findings. Initial distortions in full-scale 4-mm thick laser-hybrid welded ship structures were measured and reported in (Lillemäe et al., 2016, Lillemae et al., 2017). The fatigue test results showed that when initial distortion shape and geometrical nonlinearity are properly considered, the small- and full-scale specimens have equal fatigue strength with small scatter. The geometrical nonlinearity means in practice that the commonly used stress magnification factor given in classification rules is not suitable for

thin-plate structures. Thus, further studies are required to develop new design methods as well as quality limits for the distortions. For thicker plates (t>5 mm), the structural behaviour is linear, and plates are not curved close to welds. Then analytical formulations for stress magnification factors are possible.

However, the consideration of surrounding structures and boundary conditions can cause challenges. New analytical formulations for stress magnification factors were introduced in (Xing & Dong, 2016) for different geometrical configurations and boundary conditions of cruciform joints and discussed the validity of the stress magnification factor equations given in current rules (BS7910, 2005, DNV, 2010b). The authors show that some of the existing solutions are valid under a narrower set of conditions than documented and some seem to be an insignificant error.

The distortion is always related to the residual stress. The tensile residual stress increases the mean stress for fatigue loading and thus, decreases the fatigue strength. Therefore, it is important to develop the welding and manufacturing methods, which at the same time result in small residual stress and distortion. Welding simulations to predict distortions and residual stress are developed by several researchers.

The influence of thermo-mechanical material properties of T-joints made of different steel grades was studied with the conclusion that for the prediction of residual stresses, only the yield stress needs to be temperature-dependent (Bhatti et al., 2015). For the assessment of angular distortions with acceptable accuracy, the heat capacity, yield stress and thermal expansion should be employed as temperature dependent in the welding simulations. Several studies analysed the welding distortions by a nonlinear thermo-elasto-plastic approach and compared them with the experiments, which showed the same trend, but up to 20% higher values (Chen et al., 2014a, Chen et al., 2014b, Hashemzadeh et al., 2014, Hashemzadeh et al., 2015b, a, 2016, Chen et al., 2017, Hashemzadeh et al., 2017a). The development of reliable methods to predict distortions and residual stress in large ship structures still requires a significant amount of further work. At this stage, the simulation methods can provide new ideas for further development of manufacturing. For instance, in (Ilman et al., 2016) a method to mitigate distortions and residual stress by static thermal tensioning was developed and demonstrated the resulting increase in fatigue strength. The weld area was cooled and areas further from the weld were heated to 100, 200 and 300ºC. Out of plane distortion was reduced using a stretching effect generated by static thermal tensioning treatment, which counterbalanced the distortion induced by welding. Also, harmful tensile residual stresses were reduced and to some extent, also beneficial compressive residual stresses could be formed.

A broad research project involving both academia and industry and dealing with naval vessels has been recently reported in (Huang et al., 2014a, Huang et al., 2016): actual measurements were comprehensively analysed and their effect on structure strength estimated.

5.1.2 Welding induced defects

Welded high strength steel and thin plates are more sensitive to dimensional accuracy than thicker plates (Remes & Fricke, 2014, Dong et al., 2017a, Dong et al., 2017b). The fatigue strength of thin laser-hybrid welded butt joints using the notch stress approach and micro-scale measurements of the weld geometry were studied in (Liinalampi et al., 2016). The notch stress was defined using the Neuber's stress averaging approach, where no fictitious rounding of the notch is needed. A significantly smaller averaging length than commonly assumed for welded joints was required to capture the increased notch stress due to sharp notches caused by e.g. axial misalignment. As a result, the scatter in the test results was significantly reduced. In addition to that, the variation in the material properties causes the asymmetrical distribution of welding-induced residual stresses and distortions (Hashemzadeh et al., 2017b).

Plate butt joints made of normal and high strength steels of 4-mm in thickness produced by different welding methods were investigated in (Lillemäe et al., 2016), with the most important factors influencing fatigue strength being the weld height and the flank angle. Also, visible non-continuous undercuts had an important effect, even though the mean values from the weld geometry analysis showed a very small undercut. The correlation between the weld toe radii and fatigue strength was weak, unlike often suggested (Jonson et al., 2011, Jonson et al., 2016a).

Similarly, investigations showed that weld flank angle has a significant influence on the fatigue strength of 10-mm thick high strength steel cruciform joints, while weld toe radius effect seems insignificant, possibly because pre-cracks was found (Tchoffo Ngoula et al., 2017).

The effect of the undercuts on the fatigue strength of 6-mm thick ultra-high-strength steel butt joints was studied in (Ottersbock et al., 2016). They concluded that the fatigue strength of defective specimens is within the scatter band of the non-defective ones if the support effects are considered. Fatigue strength assessment of butt welded specimens whose defect level was found non-conforming to the acceptance criteria was also carried out in (Cosso et al., 2016). After appropriate numerical and experimental analyses by properly considering the fabrication imperfection effects, the specific structures were demonstrated to be safe enough for the intended service.

A dedicated fatigue test on butt welded specimens notched in way of the weld to validate Strain Energy Density SED-N curves was carried out in (Fischer et al., 2016b). Noticeably, the Notch Stress Intensity Factor (N-SIF) based fatigue assessment approaches inherently consider the very local weld notch geometry, hence potentially including notch geometry effects. While stress relieving of residual stress was generally carried out in all tested series, various notch geometries, microstructure (i.e. notch in HAZ, weld or parent material) and steel types were fatigue tested. Namely, the advantages of these tests are that both the exact notch geometry and the local stress range at the notch, including misalignment effects, were carefully identified and considered in experimental data analysis. However, the fabrication imperfections may change the post weld distortions and residual stress leading to a significant impact on fatigue strength (Hashemzadeh et al., 2017c).

When discussing the weld geometry, the question arises how to measure and define the variables of weld geometry such as the toe radii. Three different non-destructive methods to assess the weld geometry were compared in (Harati et al., 2014). All three methods are applicable, but the radius highly depends on the evaluation procedure. Weld Impression analysis is an economic and sufficient option when only the weld toe radius in a single point is needed. If the whole 3D image of the weld profile is needed, the Structured Light Projection is a good choice.

The fact that different operators ended up with different results for the common weld surface evaluation methods was studied in (Stenberg et al., 2015). Therefore, an algorithm was developed which assesses weld bead surface geometry and automatically defines the toe radius and the toe angle along the weld.

Another question is how to include the weld quality in the fatigue assessment. The suitability of the effective notch stress and Battelle's structural stress method for evaluating the fatigue strength of thin and thick normal and thick high quality cruciform and T-joints was studied in (Stenberg et al., 2015). The actual weld geometry was not included, the notches were rounded with fictitious radius: $R = 0.05$ mm for $t = 2$ mm, $R = 0.3$ mm for $t = 4$ mm and $R = 1$ mm for $t > 5$ mm. The authors concluded that both methods work, but the notch stress resulted in smaller scatter. Effective notch stress method was able to consider the increased weld quality by increasing the design curve by 25% for each step in the quality class (STD181-0004). Also, stochastic methods have been recently proposed to evaluate the fatigue strength based on random (Schoefs et al., 2016) or real weld geometries (Lang & Lener, 2016). Finally, high weld quality leads to longer short crack growth periods and this might be the reason for the observed shallower slope of the S-N curve (Remes et al., 2017).

It is well known that the weld quality influences the fatigue strength significantly, but it is not always easy to define what is required for high quality and which parameter has the decisive effect. Existing ISO quality standards (ISO13919-1, 1996, ISO12932, 2013, ISO5817, 2014) define the limiting values for weld size, shape and defects, and divide welds into 3 different categories accordingly. However, these quality levels do not have a straightforward link to the fatigue strength. Efforts have been made to link quality categories with certain fatigue strength (STD181-0004, Barsoum & Jonson, 2011, Jonson et al., 2011, Hobbacher & Kassner, 2012) and based on this the IIW has recently published a guideline (Jonson et al., 2016a). The guideline can be considered as a first draft of the applicability of e.g. thin plates ($t < 5$ mm) has not been validated.

In addition to welded joints, also the cut plate edges are fatigue critical details in the ship and offshore structures. Fatigue critical cut edges are in e.g. window corners of a large passenger ship. The increased fatigue strength for high strength steels with improved surface quality has been demonstrated and the need to update the rule highlighted in (Stenberg et al., 2016).

5.1.3 Initial crack size

One of the main influencing factors on the fatigue performance of materials is the initial crack size, and there have been a large number of research efforts devoted to investigating the impact (Matic et al., 2015, Liu et al., 2016, Reddy et al., 2016). Although there is a need for a unified definition of the fatigue crack initiation and propagation, there is no agreement in which the phases of the fatigue crack growth could be divided with an exact definition: microscopic, small and macroscopic. Generally, cracks with lengths lower than 10^{-1} mm are regarded as microscopic ones, whose growth is dominated by the microstructure texture. The size of the microscopic crack is marked as an initiation size, which is consistent with the first stage of the fatigue process. When the crack length is within the interval of 10^{-1} mm and 1mm, which is the so-called early growth stage, the crack is considered as a small crack. The initiation stage of the fatigue crack is determined by the shortest uni-oriented detectable microscopic crack.

Fatigue tests on six compact tension specimens made of S355J2+N steel (ISO EN 10025 standard, IACS-AH36) in the air and in laboratory-simulated seawater under free corrosion conditions were carried out in (Adedipe et al., 2015). All specimens were pre-cracked in the air at a loading ratio of 0.1 and loading frequency of 5 Hz. Crack lengths in these tests were monitored by four methods in all: Alternating Current Potential Difference (ACPD), the direct current potential difference (DCPD), optical measurements through the StreamPix5 digital camera and travelling microscope, and back face strain (BFS). The BFS method was found particularly effective in the simulated seawater environment, while both DCPD and BFS methods were reliable and cost-effective for the crack growth measurement in the corrosion environment.

A general fatigue life prediction procedure was presented in (Correia et al., 2016), which was based on the CCS crack growth rate model (Blasón et al., 2015) and the proposed approach was used to obtain the fatigue data of a notched plate made of P355NL1 steel, in which the Equivalent Initial Flaw Size (EIFS) concept had been employed. As the EIFS concept assumes that materials had defects acting like initial cracks, this EIFS was usually smaller than the crack initiation concept of the local/Fracture Mechanics integrated approaches.

Fatigue crack growth data of P335NL1 steel using CT specimens under several stress R-ratios, applying the EIFS approach and employing a back-extrapolation calculation was analysed in (Alves et al., 2015). The EIFS concept assumed the material includes intrinsic defects acting like initial flaws, and the equivalent initial size a_i calculation is based on cyclic J-integral, which is used to consider the elastic-plastic deformations in the crack-tip area as $da/dN=f(\Delta J)$, where da/dN is the fatigue crack growth rate, and ΔJ is the range of the cyclic J-integral and the fatigue life N can be estimated by integrating from the final crack size, a_i to the final one a_f.

Generally, the EIFS might be calculated through an inverse analysis, and some endeavour had been made to estimate the EIFS directly adopting the Kitagawa Takahashi diagram (Kitagawa & Takahashi, 1976).

5.2 In-service degradation

Various degradation effects influence fatigue behaviour like surface roughness, crater, groove, linear, spot and common wearing, general and pitting corrosion. However, relatively few papers were found in the surveyed literature on this specific aspect. It should be admitted that it is extremely difficult to obtain data, from both dedicated tests and in situ measurements, about fatigue behaviour of welded structures. On top of this, numerical simulations appear to be extremely difficult to be carried out and examples of research work ongoing in this very challenging field are presented in (Brennan, 2013, Garbatov et al., 2014a, Garbatov et al., 2014b, Garbatov, 2016, Garbatov et al., 2016b).

5.3 Strength improvement

Different strategies have been followed to improve fatigue strength of ship and offshore structures in the past years ranging from new materials to post-welding treatments and other fabrication processes. The IIW has recently updated a booklet on the matter (Haagensen & Maddox, 2013). It provides guidance for the practical use of each method, including equipment, weld preparation and operation and allows a more predictable implementation of the most widely applied improvement methods.

Mostly, improvement methods are intended to improve the fatigue strength of welds. However, parent material too may undergo fatigue failures. Fatigue tests of different strength steel specimens treated by grinding or by grinding followed by sandblasting, i.e. using post-cutting treatments that are suitable for shipyard conditions, were carried out in (Korhonen et al., 2013, Remes et al., 2013). The resulting surface roughness, hardness profile, and residual stress were measured. The investigation shows that post-cutting treatments suitable for shipyard conditions can considerably increase the fatigue strength of the high-strength steel used in opening corners of a large-scale structure. Sandblasting after grinding increases the surface roughness, but reduces the fatigue strength only slightly.

High strength steels have huge potential in enabling new lightweight designs. However, welding introduces stress concentration and initial defects into the material. As higher strength steel is more sensitive to initial defects (de Jesus et al., 2012), a phenomenon called notch sensitivity, the increased fatigue strength is lost. In addition, harmful tensile residual stresses are introduced by welding. By appropriate post-weld treatment of fatigue-critical details, the initial defects, as well as harmful tensile residual stresses, can be removed.

Post-weld treatment methods can be divided into two groups, the ones that improve the weld shape, such as toe grinding and tungsten inert gas (TIG)-dressing, and the ones, which alternate the residual stress state such as the High-Frequency Mechanical Impact (HFMI) treatment. In fact, the local plastic deformation of the impacted material causes changes in microstructure, geometry and the residual stress state. Therefore, the increase of the fatigue strength is a combination of weld geometry improvement as well as the residual stress modification.

The High-Frequency Mechanical Impact (HFMI) has significantly developed as a reliable, effective and user-friendly method for post-weld fatigue strength improvement technique for welded steel structures. One possible approach to fatigue assessment for HFMI-improved joints by analysing several IIW documents reporting HFMI technology results was presented in (Marquis et al., 2013). A companion paper has also been prepared concerning HFMI equipment, proper procedures, safety, training, quality control measures, and documentation in (Marquis & Barsoum, 2014). Lack of standards and guidelines prevent the wide application of improvement methods since their effect is not accurately predicted for the time being.

Tests of 68 available HFMI-improved welds subjected to overloads or pre-fatigue loads at various loading conditions representative of the ship and offshore structures prior to fatigue testing were presented in (Yildirim & Marquis, 2015). A review of current IIW guidelines is also reported. Indeed, class rules are seldom considering the beneficial effect of improvement methods because of uncertainties in quantifying their effect on real structures and in-service conditions. An overview of the recent results on fatigue strength improvement by HFMI-treated high-strength steel welded joints is presented in (Yıldırım, 2016).

The effect of HFMI treatment on the weld toe geometry and the fatigue strength of fillet welded extra high strength steel, σ_y = 1,300 MPa was studied in (Harati et al., 2016b). The weld toe radius did not change noticeably after the treatment, but the profile was more uniform. The fatigue strength increase was not as significant as expected because the quality of the as-welded joints was already quite high. A deeper analysis of the same results, including the effect of residual stress, was presented in (Harati et al., 2016a).

The fatigue strength of hammer peened S690 butt joints was studied in (Lefebre, 1993). The increase in fatigue strength was in accordance with the proposed guideline (Marquis et al., 2013), even though the hammer peening did not improve the local toe geometry as often assumed, but introduced crack-like folds instead. Based on this it seems that compressive residual stresses played the key role.

Various High-Frequency Hammer Peened (HFHP) ultra-high-strength steel (S960, S110 and S1300) joint types with different plate thicknesses were studied in (Berg & Stranghoner, 2016). They show the conservatism of existing design proposals. However, the study included only the constant amplitude loading with the stress ratio of R=0.1.

The high strength steel grades S690 and S960 in as-welded and HFMI-treated condition, both before and after stress-relief annealing was investigated in (Leitner et al., 2015b). Fatigue tests at a stress ratio of R=0.1 showed a significant increase of the fatigue strength due to the HFMI-treatment compared to an as-welded condition. The superimposed post-heat treatment, however, lowers the fatigue strength, but not back to the level of an initial as-welded state. They also discuss the change in mean stress due to clamping of the specimens with considerable angular misalignment. The effect of post-heat treatment on as-welded and HFMI-treated mild steel joints (S355) is discussed in (Leitner et al., 2015a). They show that additional post-weld heat treatment is not beneficial. As no changes in distortions and microstructure were observed, the decrease in fatigue strength can mainly be attributed to the relief of manufacturing induced (as-welded/HFMI-treated) prior compressive residual stresses to an almost zero stress value.

(Deng et al., 2016) studied numerically the effect of HFMI treatment on the stress state close to weld toe of the butt joint made of different material grades. Structural stress approaches with through-thickness and linear surface extrapolation was applied and characteristic fatigue strength values were proposed and compared with the values from literature and available experimental data.

Numerical investigations on the improvement of non-load-carrying welded cruciform joints by ultrasonic impact treatment (UIT) including thermo-mechanical welding simulation and dynamic elastic-plastic FE analysis was performed in (Yuan & Sumi, 2016). A 3D simulation method is based on thermo-mechanical welding simulation, the dynamic elastic-plastic FE analysis and fracture mechanics-based fatigue life assessment. The predicted plastic deformation and residual stress resulting from UIT as well as the fatigue strength under various R-ratios agree relatively well with the experiments. It is found that UIT is beneficial up to R<0.5. The results not only clearly distinguish the fatigue strengths of as-welded and UIT-processed welded joints, but also show the effects of preloads and stress ratios, so that the proposed solution method may provide an effective tool to simulate improvement methods in engineering structures.

Also in (Leitner et al., 2016) a setup of a closed simulation loop including a thermo-mechanical coupled weld simulation, numerical computation of the HFMI-process and fatigue assessment by the local stress/strain and crack propagation approaches were presented. Comparison with experimental residual stresses and fatigue strength show generally reasonable agreement. Linear elastic fracture mechanics-based approach works well for as-welded joints but needs further development to consider the enhanced crack initiation period of HFMI-treated welds properly.

Even though the fatigue improvement methods considered in these papers are available to the industry for quite some years, their simulation testifies the interest in reliably estimating the enhancing effect in the design process.

In case of post-weld treatment methods, where fatigue strength increase is mainly due to beneficial compressive residual stress, the influence of variable amplitude loading, and high-stress ratios becomes extremely important as these might relax the compressive residual stresses.

The effect of loading history on non-load carrying specimens improved by ultrasonic impact treatment was studied in (Polezhayeva et al., 2015a). The investigation aimed to determine whether loading histories specific to marine and offshore structures cause shakedown of compressive residual stress produced by HFMI treatment and therefore affect fatigue resistance of welded joints improved by these methods. A significant relaxation of compressive residual stresses is achieved by application of compressive cycles in fatigue testing, depending on both stress level and number of applied cycles. The beneficial effect of the HFMI is therefore reduced. The influence of the load history on the improvement effects on fatigue strength by the Ultrasonic Peening was confirmed experimentally in (Deguchi et al., 2012) testing several joint type specimens. In addition, they identified some cases that have the possibility of decreasing or increasing the improvement effects on fatigue strength by Ultrasonic Peening and suggested some efficient methods of the Ultrasonic Peening for ship structures.

The influence of spectrum loading including pre- and overloads on the fatigue strength of HFHP-treated S1100 stiffener and butt joint specimens were studied in (Berg et al., 2016). The stress ratio was R=0.1 in both constant and variable amplitude loading, and they observed similar fatigue strength under both loadings, i.e. fatigue strength improvement was not lost under VAL.

The fatigue behaviour of the impact treated mild steel (yield strength 356 MPa) cruciform and lap joints under variable amplitude loading, including effects of high R-ratios and overloads was studied in (Ghahremani et al., 2015). Two types of variable amplitude loading histories and nominal, structural and effective notch stress approaches were used. The results showed fatigue strength improvement under VAL also with stress ratios R>0.4.

A methodology for variable amplitude fatigue analysis of as-welded and HFMI-treated structural steel based on effective strain-life and a strain-based fracture mechanics model was proposed in (Ghahremani et al., 2016). With the proposed method, accurate or in some cases conservative predictions were obtained compared to experiments.

The combined effect of microstructure, geometry and residual stress were systematically studied in (Mikkola & Remes, 2016, Mikkola et al., 2017). They concluded that even if compressive residual stress is completely relaxed at R=0.5 and $S_{min} \leq -0.6\sigma_y$, the post-weld treatment still results in fatigue strength increase due to weld toe geometry improvement and strain hardening. A new recommendation for fatigue design was proposed in (Mikkola et al., 2016). The fatigue strength of HFMI-treated high strength steel joints under constant and variable amplitude block loading with the stress ratio of R=0.1 was studied in (Leitner et al., 2015b). The results showed good accordance with the constant amplitude tests when the equivalent stress range was calculated assuming a damage sum of D=0.5 in finite-life regions and D=0.3 in high-cycle regions.

The lightweight potential of high strength steels treated by HFMI under constant and variable amplitude loading was discussed in (Yıldırım, 2015, 2016). They considered longitudinal attachments made of S700 steel and tested with the stress ratio of R=-1. The fatigue strength was increased under both constant and variable amplitude loading, although the improvement under VAL was smaller. They also discuss the Gassner versus Wöhler lines. The Gassner line involves plotting $\Delta\sigma$max vs. N to failure and allows designers to easily compare fatigue strength with other potential failure modes like global yielding or buckling.

A review of the fatigue data of welds improved by TIG-dressing was presented in (Yildirim & Marquis, 2015, Yıldırım, 2016). The influence of high-stress ratios on the fatigue strength of TIG-dressed ultra-high strength steel fillet welds is studied in (Skriko et al.). They showed a 30% reduction in characteristic fatigue strength when stress ratio was increased from R=0.1 to R≥0.5. They also presented weld toe radius and residual stress measurement results before and after TIG-dressing.

Low transformation temperature filler material is an alternative method to reduce detrimental tensile residual stresses or even induce beneficial compressive residual stresses (Ooi et al., 2014). However, as the weld toe profile is not improved by this technique, the fatigue strength increase is not obtained at high-stress ratios (Bhatti et al., 2013). They reported increased fatigue strength compared to traditional filler material under constant amplitude loading with R=0.1 and variable amplitude loading with R=-1, but no increase under R=0.5. The relative effects of residual stress and weld toe geometry on the fatigue strength of 8-mm thick high strength steel cruciform joints welded with the Low Transformation Temperature filler material were studied in (Harati et al., 2015). Based on the results, the residual stress had higher influence.

Also, the alternative welding methods could be applied to achieve favourable weld shape. (Holmstrand et al., 2014) showed that the extended weld leg and weaved toe line increase the fatigue strength as the flank angle is decreased. The analysis showed that the crack initiated from the undercut. Weaved weld toe is however not suitable for longitudinal loading.

Increased fatigue strength of σ_y = 355 MPa steel obtained with a welding procedure that produces smooth undercut like the one achieved with weld toe grinding or HFMI treatment was presented in (Astrand et al., 2016). When aiming for large weld toe radius, the penetration depth is getting close to the base plate and thus there is an increased chance of harmful cold laps. Therefore, a smooth undercut would be even better than large radius without the undercut. Also, the position of welding with respect to a load carrying fatigue critical notch of the fillet weld influences the fatigue strength (Barsoum & Jonson, 2011). For example, the horizontal welding position creates a sharp transition for the load carrying weld toe because of the gravity, while the vertical position creates a sharper transition for a non-load carrying weld notch and a smooth transition for the load-carrying one.

T-welded joints connecting the web and panel plates made of Q345D steel via CO2 gas shielded arc welding before and after shot peening (SP) was chosen in (Gan et al., 2016). The static loading test and fatigue tests were carried out on peened and unpeened specimens, and the fatigue tested specimens were prepared with different peening intensities (PI). The tests showed: (i) all SP treatments could change the surface residual stresses 1 mm from the weld toe, (ii) the depth of the compressive residual stress field and the maximum compressive residual stresses tended to increase with higher PI, while the fatigue life of the T-weld was not always increased with the PI increasing, (iii) a PI of 0.3 mmA could result in twice the fatigue life.

5.4 Polymer composite patch repairs

Worth mentioning are EU projects like Co-patch (www.co-patch.com), whose objective is to identify design procedures to accept polymer composite patches as permanent repairs and/or reinforcements of steel structures and Mosaic (https://trimis.ec.europa.eu/project/materials-

onboard-steel-advancements-and-integrated-composites#tab-outline), partly devoted to replacement of specific structural parts of the ship with composite materials also in view of better fatigue behaviour.

Among the others, studies were carried out to assess the improvement on fatigue strength at corner openings by adding suitable composite patches to the steel plates. Their effect is not only to locally stiffen the structure but also to obtain a faired and less notched geometry.

Comprehensive strength and fatigue testing of composite patches for ship plating fracture repair were carried out in the frame of a joint research project in the USA and reported in (Karr et al., 2015, Karr et al., 2016).

Experimental investigation of the behaviour of an adhesively bonded, hybrid, composite-to-steel butt joint was carried out in (Karatzas et al., 2015). Two types of joints were tested, e.g. one involving only the adhesive and one involving a combination of the adhesive and bolts. The goal was to obtain lighter and more fatigue resistant structural details compared to metallic ones.

Borrie et al. (2015) studied the combined effect of marine environment and fatigue loading on the bond behaviour between CFRP and steel. The results show that even in short-term exposures, the protection and maintenance of such rehabilitated structures are paramount in ensuring their strength and resilience over time.

Several numerical simulation strategies of the composite to steel bonding were presented in (Tomaso et al., 2014). The aim of the work was to simulate the delamination of interfaces. Theoretical fundamentals of each method were considered identifying the main geometrical, i.e. the overlap length. Numerical results were compared to experimental tests thus benchmarking the simulation quality against the elastic stiffness of the joint and its failure load. Similar simulation strategies were also presented in (Godani et al., 2014, Godani et al., 2015) the numerical and experimental analysis of the interlaminar shear strength of composites and in (Nebbia et al., 2015a, Nebbia et al., 2015b) the numerical and experimental characterization of yacht steel plates coated by fillers.

6. FATIGUE RELIABILITY

The new information that can be derived from fatigue tests and uncertainties related to the previous chapters could be analysed, revealing the overall integral picture including different limit state functions, sensitivity analysis (what factors are more important than others, etc.) to be included here.

Structural reliability is not a new phenomenon now in ship design procedures. Reliability assessment is being used to support engineering, operational and maintenance scheduling decisions using the techniques of the risk assessment in ship structures. Traditionally, the reliability of a structural component is defined as the probability of maintaining its ability to fulfil its design purpose for some time under specified environmental and operational conditions. Time-dependent conditions will have the greatest influence on the reliability outcome. Therefore, it is expected that the ship structure reliability needs to account for the following influencing parameters (i) time-dependent corrosion and fatigue damage accumulation, (ii) uncertainties in strength (fatigue damage accumulation and crack growth), (iii), uncertainties in operational loads, (iii) maintenance periods, (iv) safety and consequences of failure.

In the context of fatigue reliability, in general, two approaches are often considered to describe the fatigue limit state: S-N and fracture mechanics based crack growth approaches. The fatigue reliability assessment considers the uncertainties induced by all parameters involved in the fatigue assessment treating them as basic stochastic variables. Yet, obtaining the correct and reliable statistical information of the stochastic variables is one of the main challenges.

In this chapter, the following sections describe the attention paid towards statistical descriptors involved in the fatigue reliability assessment, limit state functions, reliability index, partial safety factors and their calibration and the fatigue reliability based life prediction assessment.

6.1 Statistical descriptors

The fundamental basis of the fatigue reliability assessment of ship and offshore structures is the probabilistic description of fatigue failure influencing parameters, which account for the uncertainties in strength (fatigue damage accumulation, crack growth) and fatigue load. These uncertainties are to be considered by treating them as basic random variables and are represented in terms of statistical distributions (distribution type, mean and standard deviation, etc.).

There could be various uncertainties in the fatigue failure, such as:

- Current condition of the ship structure
- Time-dependent degradation of strength due to corrosion
- Crack initiation and growth with time
- Quality of construction and maintenance practices
- Weld distortion and residual stresses
- Weld details
- Stress concentration factors
- Material property variability
- S-N curve parameters, etc.

Methodologies developed to account for the uncertainties related to strength and load are described in the following sections.

6.1.1 Fatigue loading

The loads acting on the ship and offshore structures are uncertain due to many factors, including wave height, period and distribution. The uncertainties in the fatigue load are as important as strength uncertainties. Determination of reliable fatigue load considering various influencing factors is still a challenging task. The sources of load uncertainties are:

- Modelling of fatigue loads
- Wave-induced global bending moment
- Slamming loads
- Exposure to a variety of loads
- Operational variations and different operating areas

The uncertainties in the wind and wave-induced loading on an offshore wind turbine supporting structure to evaluate the probability of failure and the dynamic behaviour of the structure was determined based on the finite element method were studied in (Yeter et al., 2015c, d, 2016b, 2017c). The results of the fatigue damage assessment were obtained by employing the S-N, fracture mechanics, and the strain-based approaches. The results of the reliability analysis were presented as a function of the offshore wind turbine operational scenarios in a way to allow determining what operating conditions should be avoided. It was proposed that the narrow-band load may be improved by a proper correction factor accounting for the existence of a wideband loading to achieve close outcomes compared to the rain flow solution in the time domain. The performed sensitivity analysis showed that the uncertainty with respect to the wind loading is substantially important.

The First Order Reliability Method (FORM) and Monte Carlo Simulation (MCS) methods of reliability analysis to compute the fatigue damage in offshore wind turbine to demonstrate that the uncertainties related to fatigue damage estimation of non-linear systems are highly dependent on the tail behaviour and extreme values of the stress range distribution was compared in

(Horn & Jensen, 2016). It has been shown that the standard deviation is reduced up to 30% for load cases where the fatigue damage distribution deviates from the normal distribution.

A fatigue damage estimation procedure for non-linear systems subjected to stochastic load excitations uses a combination of Monte Carlo simulations (MCS) and the FORM was proposed in (Jensen, 2015), where FORM is used to get a more accurate description of the upper tail behaviour of the probability distribution of the rain flow counting damage estimation. The study undertook a specific example dealing with the stresses in a tendon in a tension leg platform subjected to second order wave forces and observed that the coefficient of variation (COV) is reduced by a factor larger than three. Also, the total computational effort for the present example was reduced by one order of magnitude for the same prediction accuracy in the fatigue damage estimation. Stationary conditions are assumed and therefore for a long-term analysis, the proposed calculations have to be done for all pertinent stationary sea states. The FORM analysis does not need to be recalculated if only the significant wave height is changing as the FORM reliability index is strictly inversely proportional to the significant wave and thus the calculation time gets reduced.

In case of stochastic loading & response and non-linear system behaviour, the spectral calculation of fatigue damage estimates can be rather time-consuming. Usually, the Monte Carlo (Hammersley & Handscomb, 1975) simulation is applied, but if the number of simulations is relatively small the coefficient-of-variation can be large because of the sensitivity w.r.t. large simulation values. If the safety index is linearly related to damage, the first order reliability method can be used in addition to obtain a better estimation of the damage distribution tail, reducing the coefficient-of-variation. An example shows that a reduction by a factor 3 is possible (Jensen, 2015).

For the fatigue assessment of containerships, a time efficient response calculation procedure has been proposed. The hull girder finite shell element model could be replaced by a beam model, but the torsion induced response estimates would introduce quite large errors. Using a shell element model, the relation between the loading and the structural response has been established for an arbitrary sea state in a few time steps. The result has been used to estimate the generalized relationship for an arbitrary sea state using linear regression analysis. The procedure is almost as time efficient as for a finite beam element model. General capabilities of the regression method still need to be checked (Mao et al., 2015).

Assessing fatigue of catenary risers, the touchdown point requires attention. One of the challenges is related to riser – seabed interaction. Adopting a non-linear model, the geotechnical parameter sensitivity has been investigated because of the considerable uncertainty. Fatigue reliability is not extensively investigated for riser design and a first-order reliability method has been adopted to estimate the fatigue safety index (Elosta et al., 2014).

6.1.2 Fatigue damage accumulation

The uncertainties in the load determination are transferred to the uncertainties in computed stresses. The uncertainties associated with the fatigue capacity through empirical S-N curves are accounted for by modelling K as a Log-Normal distributed stochastic variable. The experimentally developed S-N curves are the basis of the fatigue damage accumulation methodology. However, S-N curves are developed based on relatively small structures and their failure does not necessarily reflect the actual failure scenario of the ship structure, which is a very large and highly redundant structure.

In the S-N curve based approach to a fatigue reliability assessment, the role of the stress concentration factor (SCF) is very important. Uncertainties in SCF computation was studied in (Ogeman et al., 2014.). They reviewed the different direct calculation procedures for how to obtain the SCF based on fatigue assessment guidelines. The effect of different element types (shell and solid) and local stress extrapolation methods to the fatigue damage estimation was

studied for both longitudinal and bending (vertical and horizontal) load conditions in a container ship of 4,400TEU. It was shown that the use of the solid element or 8 node shell element approach would give conservative results. However, no attempt to verify experimental data has been performed. The authors also pointed out the effect of the bracket thickness and stiffener flange on SCF.

6.1.3 Crack growth

Fatigue crack propagation is also affected by many parameters such as initial crack size, history of local nominal stresses, and load sequence (Dong & Frangopol, 2015). In addition, there are uncertainties related to the crack growth parameters in the Paris Erdogan equation, in geometry functions for the plate solution and the weld notch and in the initial defect distribution. Other uncertainties are the effect of residual stresses and mean stress and threshold value for crack growth. The crack size at fracture is another uncertainty which can be important for the structural reliability as the probability of detecting a crack is increasing with the crack size (Lotsberg et al., 2016).

It is of a significance to evaluate the risk associated with marine vessels to manage the ship routing. A series of factors ranging from weather, sea states, uncertainties in structural capacity and load effects to the decision maker's attitude towards the expected consequences of the ship routing will affect the risk encountered in the travel, and thus play roles in ship routing decisions. A structural reliability approach is suggested in (Dong & Frangopol, 2016), where the support system deals with the uncertainties in the structural capacity and loading to investigate the fatigue damage. In the procedure, four important aspects, related to the repair cost, cumulative fatigue damage, total travel time, and carbon dioxide emissions are treated as the consequences of the decision, and the Multi-Attribute Utility Theory (MAUT) is adopted to reach a balanced combination of various attributes.

A probabilistic approach is proposed for the failure risk assessment of a welded ship structure with respect to the fatigue damage caused by multiple site cracks (Feng et al., 2012b, a, 2014, Huang & Sridhar, 2016). The initiation and propagation of fatigue cracks often occur at weld toes while the welded structure is subjected to alternating loading and to account for the interaction of multiple fatigue cracks and inherent uncertainties in the fatigue crack growth process, a probabilistic model for fatigue crack growth is developed based on the Paris relation. The probabilities of fatigue failure of multiple cracks in the welded structure are estimated by using the reliability analysis. Then, the failure risk assessment for the welded structure with multiple site cracks is performed based on the fatigue reliability estimation. As the service life of ship structures is usually very long, in-service maintenance activities for the locations of critical fatigue damage in ship structures are necessary to ensure the integrity of structures. The failure risk associated with the fatigue crack growth can be updated through inspections and repairs based on the probabilistic model of the damage detection. The effects of the in-service inspection quality and frequency are investigated with respect to the risk assessment of structural fatigue failure.

6.2 Limit state functions

The instantaneous reliability may be obtained by defining the limit state function, which defines the failure domain; safe or unsafe. Failure can be defined considering several criteria depending upon many considered influencing parameters or uncertainties.

6.2.1 Fatigue damage accumulation

Exceeding a certain damage level or fatigue safety ratio (generally equal to one), the fatigue safety levels are some examples of the damage accumulation limit state function. The Palmgren-Miner rule forms the basis of the damage accumulation limit state function. A limit state function to determine the accumulated failure probability was proposed in (Lotsberg et al., 2016) as $M(t) = \Delta - D(t)$, where Δ is a function describing the uncertainty in the Palmgren-

Miner damage accumulation and D(t) is accumulated fatigue damage at time t based on S-N data.

A methodology of the reliability assessment based on a direct finite element analysis of the ship hull structures based on the distribution of structural strains was developed in (Feng et al., 2015). The distributions of ship structural strains in the short and long-term sea states were defined first by using the FE method and further derived the extreme strain accounting for the stochastic origin of the still water and wave-induced loads. The limit state function based on the von Mises stress failure criterion is used. The ship structural response in still water was calculated based on the FE method identifying the structural strain, which was normally distributed. Both the global and local load effects were considered and only the full loading condition of a bulk carrier was analysed.

The fatigue reliability of the fixed offshore wind turbine support structures based on the spectral fatigue damage assessment was studied in (Yeter et al., 2015c, 2017c). The adequate limit state functions are developed accounting for the physical, statistical, measurement, and modelling uncertainties. The developed limit state functions also addressed the narrow-banded approximation. The system reliability was estimated accounting for the correlation between the welded tubular joints of the modular jacket offshore wind turbine structures (Yeter et al., 2016c).

6.2.2 Crack growth

Fatigue cracks can appear at various locations in the ship structure and may occur at early stages in the service life. Due to the presence of significant uncertainties, associated with the crack initiation and propagation, the planning of inspection, monitoring and/or repair actions should be performed probabilistically. The fracture mechanics crack growth based limit state function may include the exceedance of a critical crack size, critical number of cycles or critical stress intensity factor (Ibrahim, 2015a).

A stochastic Gamma process was modelled in (Guida & Penta, 2015), mainly to derive the distribution of the time to reach any crack size. In the model, the proposed time to reach a given crack size is considered a random process over the crack size domain, giving rise to three main advantages: the time to reach any crack size is completely defined by its first-order distribution, the process exactly coincides with the postulated deterministic crack growth rate model, and it can account for the presence of both heterogeneity and load conditions, and it is capable of predicting the main stochastic features of the time to first reach a given crack length as a function of the load conditions.

A probabilistic framework for incorporation of risk and updating in the inspection of fatigue-sensitive details of ship structures, considering that fatigue cracks as a structural deterioration mechanism may lead to unanticipated out of service of naval ships was developed in (Dong & Frangopol, 2015). The computation associated with fatigue damage is performed using the fracture mechanics and uncertainties considered within this process. As indicated, the fatigue crack size increases significantly with time and uncertainties are incorporated into the process. The uncertainties are also associated with inspection events. The outcomes of an inspection event are affected by many factors, such as the type of the inspection method, human factors, and inspection quality. Consequently, uncertainties should be incorporated into the risk-informed decision making and updating. The random variables associated with the fatigue crack limit state are analysed. It is pointed out that future research is needed to include the nonlinear fracture mechanics in the damage assessment of fatigue-sensitive details and the effects of multiple fatigue cracks on the structural capacity have to be taken into account in future studies for the risk assessment of fatigue-sensitive structures.

A probabilistic approach for inspection, monitoring, and maintenance optimization for ship details under fatigue effects on the basis of the crack growth approach was proposed in (Soliman

et al., 2016). Based on the stress profile and the crack geometry at the damaged location, intervention times and types are determined by solving an optimization problem, which simultaneously minimizes the life-cycle cost, maximizes the expected service life, and minimizes the expected maintenance delay over the life-cycle.

An approach to assess the probabilistic life of mixed-mode FCG by coupling of the finite element analysis and the Kriging-based reliability methods was proposed and studied in (He et al., 2015). A simulation program (FCG-System) is developed to simulate the fatigue crack path and to compute the corresponding fatigue life. Numerical applications dealing with FCG are presented to illustrate the numerical efficiency and accuracy of the proposed approach.

The probability of the existence of defects, fatigue damage and crack growths in the offshore wind turbine support structures subjected to abnormal wave and wind-induced loads is very high and may occur at a faster rate in a low cycle fatigue regime and crack growth, leading to a dramatic reduction in the service life of structures. It is therefore vital to assess the safety and reliability of offshore wind turbine support structures in the sea. To this regard, the reliability analysis incorporating low cycle fatigue and crack growth of an offshore wind turbine support structure during the service life was performed in (Yeter et al., 2016b). The analysis includes different loading scenarios and accounts for the uncertainties related to the structural geometrical characteristics, the size of the manufacturing and service life defects, crack growth, material properties, and the model assumed in the numerical analyses. The probability of failure is defined as a serial system of two probabilistic events described by two limit state functions. The first one is related to a crack initiation based on the local strain approach and the second one on the crack growth applying the fracture mechanics approach. The limit state function introduced in (Yeter et al., 2015d) is developed in such way that the critical crack size is estimated based on the failure assessment diagram, which takes into account yielding and fracture failure conditions.

6.3 Calibration factors for design

The purpose of the code calibration based on the reliability assessment is to arrive at codes that give a uniform and acceptable design for the entire scope and the code is intended to cover and avoid unnecessary costly designs.

A reliability-based partial safety factor code will, to a large extent, reflect the variabilities and uncertainties of the governing quantities. It is therefore essential that these variabilities are properly documented. Such information can be used in other contexts than the ones they originally were collected for. The design codes and their partial safety factors cannot be used in other contexts than the ones they originally were intended for, i.e. their validity is generally restricted to the original scope of the code.

In the reliability analysis, design variables are regarded as random variables with certain levels of uncertainties. A basic method of reliability analyses is the partial safety factor method, referred to as a Level I method, where only the characteristic mean value of each uncertain parameter is used. In Level II methods, the mean values and standard deviations for the uncertain parameters are used, assuming normal distributions. Methods based on the first-order reliability index are used in Level II and can be used to calibrate Level I methods. In Level III, uncertain parameters are modelled by their joint distribution functions, and reliability is assessed based on the probability of failure. Level III methods can be used to calibrate Level II methods. In Level IV, the consequence of failure is also accounted for, considering costs and benefits of construction, maintenance and repair.

Fatigue reliability of structures not subject to inspection is typically based on the SN approach and the linear damage summation. When inspections are planned, the fracture mechanics approach is applied, which allows for updating the reliability based on the presence of cracks. This allows accounting for the condition of the structure, and the reliability can be quantified

from the code by a calibration. For a Level I method, this calibration entails analysing the structure for trial design parameters, each resulting in a reliability index and a set of important factors. For each stochastic variable is assigned a safety factor, and these are found when the calculated reliability index matches the target reliability index. The partial safety factor method is based on both engineering judgement and statistical estimates of the characteristic values (when standard deviations can be calculated analytically). The characteristic values are adjusted by division with partial safety factors that take values between 1.0 to 1.5.

A method for calibrating fatigue design factors for a wave energy converter fixed to the seabed was presented in (Ambuhl et al., 2015). Designs based on inspection and without inspection were considered, relying on a crack growth model for the former and SN curves for the latter. Fatigue design factors, ranging from 1.0 to 6.5, were found for a range of inspection intervals and inspection methods.

In Level II methods, each uncertain variable is described by a mean and a variance, in addition to the covariance between the variables. In the reliability index method, the limit state function is transformed into standard space. The transformed variables have a mean value of 0 and a standard deviation of 1. The reliability index, denoted β, is the distance between the design point to the origin in standard space. The probability of failure Pf is found from the reliability index by evaluating the standard normal cumulative distribution function Φ as $Pf=\Phi(-\beta)$.

Level III requires numerical integration or approximate analytical methods. First-order reliability method (FORM) and second-order reliability method (SORM) are widely used to calculate the failure probability by approximating the limit state function by a first-order or second-order function at the design point. These methods give good results for the small probabilities typically applied in the structural reliability analysis. Alternatively, numerical simulations can be used, such as the Monte Carlo, Latin hypercube, and importance sampling, which give the failure probability as the failure ratio of the simulations.

A new methodology to calibrate structural reliability models (prediction models for anodes, coating, corrosion, crack, etc.) output was presented in (Hifi & Barltrop, 2015). The methodology combines data from experience and prediction models to correct the structural reliability models.

The S-N test data represent a total number of stress cycles to failure (defined as through thickness crack) for a known constant stress range. When performing crack growth analysis, it is required that the initial crack size is known. Two different methodologies for calibration of the fracture mechanics to the S-N test data to obtain comparable results were presented in (Lotsberg et al., 2016) as: (i) the S-N fatigue life is a sum of crack initiation and crack growth. This implies a definition of a suitable critical deterministic crack size a_0, and calibration of a suitable distribution of the crack initiation time, N_i, until such a crack size is developed; and further fatigue life can be described by crack growth; (ii) the S-N fatigue life is assumed to be equal to the crack growth life. This implies an assumption that the crack growth starts from the first stress cycle and a suitable distribution of the initial fictitious crack size a_0 is calibrated.

Several authors have proposed methods for reliability updates following inspection (Lassen & Recho, 2015, Luque & Straub, 2016, Soliman et al., 2016, Schneider et al., 2017). Reliability indices can be derived for different inspection outcomes using the Bayesian inference, while the Paris' constants are typically derived from the SN curves. This can also be used for inspection planning, and DNV-GL has recently published a recommended practice on probabilistic methods for inspection planning of offshore structures, as reported in (Lotsberg et al., 2016).

A reliability-based inspection framework for very large crude carriers was proposed in (Doshi et al., 2017). The crack length as found by the visual inspection was treated as both deterministic and normally distributed with two levels of standard deviations. The inspection intervals were

similar for both deterministic and stochastic crack length evaluations, and significantly shorter compared to NDT. Few studies have been published on Level IV methods.

A framework for establishing system reliability of multiple fatigue locations, considering the correlation between these and consequences of failure was presented in (Dong & Frangopol, 2016). Several authors report on improved numerical procedures and generalized approaches that can account for sequence effects or multiple site damage in a system reliability framework. Several methodologies were presented in (Feng et al., 2012b, a, Huang et al., 2012, 2013, Feng et al., 2014, Huang et al., 2014b, c, Feng et al., 2015, Huang & Sridhar, 2016) based on hot-spot calculations from the finite element analyses, where the reliability of the system is modelled as a series of critical hot-spot details.

A method to improve the accuracy of reliability estimates found by Monte Carlo simulations was proposed in (Jensen, 2015). By deriving the fatigue damage from the failure probability, he was able to demonstrate better accuracy in the tail end of the rain flow damage probability distribution.

Computational methods for assessing the fatigue reliability under variable amplitude loading were presented in (Altamura & Straub, 2014). They show that not assuming constant amplitude loading may yield non-conservative results compared to the variable amplitude model where the sequence effects are accounted for.

The fatigue reliability analysis was incorporated in (Yeter et al., 2017b) as a risk-based multi-objective design optimization. The Pareto frontier is adopted to identify the optimal design solutions within the feasible design space the probabilistic evaluation is performed for these optimal design solutions using FORM, and the second-order Ditlevsen bounds are used to solve the multi-dimensional system reliability problem accounting economic criteria. The levelised cost of energy (LCOE) is considered as the top-level objective function. Also, a time-variant probabilistic assessment of the life-cycle of offshore wind turbine support structures accounting for the uncertainties and their propagation in time is studied in (Yeter et al., 2017a). Several scenarios involving different uncertainties were investigated. Under these scenarios, the life-cycle of the OWT support structure is analysed considering a threshold for an offshore wind turbine to be a viable investment. The results aimed to aid to develop a multi-dimensional framework for decision-makers to attain cost-effective and profitable (long-term) offshore wind energy projects.

A method for estimating the fatigue reliability of butt welds in a submarine pressure hull was presented in (Liu et al., 2014). The initial crack size is treated as a random variable, using the probability density evolution method to simplify the problem. This allowed probability distributions to be calculated and the fatigue reliability could be estimated for random loading and uncertain material parameters without the need for numerical simulations. The Monte Carlo simulation and a probabilistic crack propagation approach, accounting for the uncertainty of the residual stresses in stiffened panels were used in (Mahmoud & Riveros, 2014).

6.4 Fatigue service lifetime estimate

Depending on the information available, the ship and offshore structure stage and the aim of the reliability analysis, a fatigue service lifetime estimate can be obtained using either a fatigue damage accumulation or crack growth approach.

6.4.1 Fatigue damage accumulation

At the design stage, the actual state of the structure is not known in general. The material has not been ordered and only information with respect to the fabrication and inspection process may be available. The type of information expected is the probability of economic loss by failure during the expected service lifetime. For this kind of analysis, a model based on the damage

accumulation is generally preferred. The defined probability of failure depends on the kind of risk assessed.

A time-dependent structural reliability methodology involving fatigue and fracture failure modes at component and system level has been developed for marine vessel applications (Ayyub et al., 2015). Corrosion has been accounted for, although corrosion-fatigue interaction is not considered.

Considering the dent size and applied loading, the fatigue reliability as a function of the number of load cycles has been established for pipelines (Garbatov & Guedes Soares, 2017). The model consists of a series of segments, characterized by the fatigue strength properties and reliability descriptors derived from a Weibull model analysis. The developed approach may be used to identify practical scenarios for inspections and repair.

The fatigue damage accumulation consequences for random corrosion characteristics have been investigated (Cui et al., 2016). Assuming the corrosion depth can be modelled using a lognormal distribution, the corrosion induced fatigue damage is lognormal distributed as well. When cracks are discovered, but no reasonable renewal of the cracked part is possible immediately a provisional repair; a crack stopping hole is commonly carried out allowing the structure to continue its operational service. This repair does not belong to the recognized designs and its efficiency has to be demonstrated, in particular, the time lag before a new initiation in the crack stopping hole. Based on the material properties and a mean stress or a maximum stress, it has been shown that the reliability index increases when the radius of the crack stopping hole increases (Chen, 2015).

Offshore wind turbine supporting structures are subjected to both wind and wave induced loads. A fatigue analysis for the installation of a wind turbine in the Aegean Sea was presented (Bilionis et al., 2015). A full wind and wave correlation has been adopted, as it considered the most extreme situation.

6.4.2 Crack growth

During the inspection, the structural state is better known and particularly, possible flaws are carefully investigated at least at the hot spot area. The aim of the probabilistic analysis is to assess the likelihood of a sudden structural collapse by brittle fracture within the period to the next inspection. Considering the consequences of such a kind of collapse, which may involve human fatalities, the crack growth approach combined with brittle fracture criteria may be preferred. The acceptable probability of failure may be different from any previous case as the consequences may be different.

Among the factors affecting the fatigue damage accumulation, the effect of corrosion randomness on the fatigue damage accumulation was analysed in (Cui et al., 2016). If the corrosion depth can be modelled by a lognormal law they analysed the result of the damage accumulation in terms of an additional fatigue damage which can be modelled by a lognormal law. When the cracks are discovered, but no reasonable renewal of the cracked part is possible immediately, a provisional repair is commonly carried out allowing the structure to continue its operational service. This repair does not belong to the recognized designs and its efficiency is to be demonstrated and particularly the time lag before a new initiation in the crack stopping hole.

Chen (2015) carried out an analysis based on the material properties and a mean stress or a maximum stress. Obviously, the model shows that the reliability index increases when the radius of the crack stopping hole increases. Wind turbine supporting structures are also subjected to fatigue due to both wind and waves. An analysis of fatigue in the Aegean Sea on the installation of a wind turbine was presented in (Bilionis et al., 2015). One challenging question is the correlation between the sea states and the wind. As no correct answer is available, the most extreme situation has been considered a full correlation.

Based on the S-N curve approach, a methodology for the time-dependent structural reliability of marine vessels based on fatigue and fracture failure modes for life predictions at the component and system levels was developed in (Ayyub et al., 2015). The proposed method also accounts for the effect of corrosion on the fatigue reliability while predicting the fatigue reliability and life. However, it does not account for corrosion-fatigue interaction.

An interesting approach was presented in (Garbatov & Guedes Soares, 2017) where different failure criteria considering a dent size and applied load are analysed and fatigue reliability as a function of a number of load cycles is defined. The analysed pipeline is modelled as a series of segments, where any of them is characterized by the fatigue strength properties and reliability descriptors derived from the Weibull model analysis. The developed approach may be used to identify practical scenarios for inspections and repair, accounting for the fatigue and corrosion damage tolerance and load subjected to the pipeline.

7. FATIGUE DESIGN AND VERIFICATION BASED ON RULES, STANDARDS, CODES AND GUIDELINES

The primary objective of various Class rules, regulations and codes applicable to ship and offshore structures is to ensure that the design and analysis process results in the construction of the ship and offshore structures that can resist both extreme loads and cyclic operating loads. This section focuses mainly on the design methodologies for fatigue assessments provided by the Classification Societies. Characteristics of the IACS Common Structural Rules for Bulk Carriers and Oil Tankers (CSR) are summarized and compared to the rules of four Classification Societies that are applicable to non-CSR ships. Changes and updates in the class rules of DNV-GL, LR, BV and IRS in the years 2015-2017 are presented here. Furthermore, the main differences to CSR-rules are highlighted.

A comparison of the fatigue life assessment of a deck longitudinal stiffener end connection for a BC-A bulk carrier was carried out accordingly to the five class rules presented in this Chapter. Additionally, a benchmark study was also conducted to compare the fatigue predictions by spectral analysis of a bulk carrier's deck transverse butt-weld joint that involved direct load evaluation by various CFD methods and different rules processing the fatigue damage.

Furthermore, the latest updates in the IGC-Code addressing fatigue are presented.

7.1 Common Structural Rules (CSR)

The Common Structural Rules for Bulk Carriers and Oil Tankers (CSR) recently issued by IACS consolidated the fatigue assessment methodologies already introduced since some years in previous rules of classification societies (Horn et al., 2013, Shijian et al., 2013, IACS, 2015, 2016). Referring to the categorization of fatigue assessment approaches (see Ch.3), the structural stress approach is basically applied, denoted as “hot spot stress” in the rules. The evaluation of the hot spot stress can be carried out according to different procedures; the possible calculation approaches for ship structures are described in full detail in the rules.

It is worth noting that only fatigue cracks initiating from the toe of the weld and propagating into the plate and fatigue cracks initiating from a free edge of non-welded details are assessed while e.g. root cracks are not explicitly checked but covered by a standard design of structural details. However, the scope of fatigue analysis has been expanded with respect to former CSR and other individual class rules.

Fatigue induced by low cycle loads such as cargo variations or impact loads such as sloshing in partially filled tanks which may induce fatigue damage is not explicitly considered. Beside IACS documentation, a summary external paper about CSR was authored by Jiameng et al. (2016) providing some hints of possible impact and consequences on ship scantlings. The margins taken during the rules development regarding the fatigue assessment based on numerous

classification societies' experience by a comparison with direct spectral fatigue assessment for an oil tanker and a bulk carrier was estimated in (Quemener et al., 2015).

In the following, the main items of the CSR assessment procedure are briefly outlined.

7.1.1 Fatigue capacity

In the rule application of the structural stress approach, the hot spot stress value may be calculated by SCF or directly by the FE analysis. Structural details to be checked are listed and hot spot stress range evaluated either by:

- simplified stress analysis, i.e. nominal stress (beam theory) x Tabulated “SCF”
- finite element stress analysis, i.e. very fine mesh FE model
- screening fatigue assessment (50mm x 50mm mesh), i.e. nominal stress (fine mesh FE model) x tabulated "η".

The latter evaluates the hot spot stress using an FE model already available for other limit state verifications and a magnification factor defined on purpose to obtain a screening and to avoid the very fine mesh analysis. Fatigue assessment by very fine mesh analysis can be omitted for standard details listed in rules for which SCFs are available or other details assessed using the screening procedure; as a result, very fine mesh modelling is necessary for critical and non-standard details failing the screening procedure.

Readout points in FE models are carefully defined in the rules either for very fine or fine mesh models.

CSR applies the DEn S-N curves “B”, “C” (free edge) and “D” (welded joints), with modification on slope value for B and C curve, in-air environment. Specific S-N curves in the corrosive environment are also provided with a single slope. The time in the corrosive environment was initially set to 2 and 5 years depending on the structural member location, but that duration was recently doubled by urgent rule amendments (IACS, 2016).

For steel with specified minimum yield stress value higher than 390 N/mm^2 and for steels with improved fatigue performance, the S-N curves to be used are considered on a case-by-case basis. Mean stress effect and thickness effect correction are included following the IIW guidelines format. In particular, the mean stress effect is revised with a lower bound in compression mean stress set to 0.3 and 0.9 at zero mean stress. Additionally, the thickness effect exponent relates to the type of structural detail and is comprised between 0.0 and 0.25 according to IIW recommendations. Finally, surface finishing factors for the base material are also provided.

Noticeably, weld improvement methods are considered as supplementary means of achieving the required fatigue life only and are applicable to corrosion free conditions, albeit with the limitation of the benefit of post-weld treatment by T/1.47 (i.e. 17 years is the minimum required the life of an improved detail). Only weld geometry control and defect removal by burr grinding are considered as the basic methods at the fabrication stage. The application of post-weld fatigue improvement is subject to limitations and adequate workmanship control for construction.

7.1.2 Fatigue Loads

According to IMO-GBS (IMO, 2015), 25 years life is required for ships, which is the target considered in CSR-H rules also for fatigue assessment. Rule quasi-static wave induced loads are based on the North Atlantic wave environment. A Weibull distribution function is used to obtain the stress time history, calibrated at 10^{-2} probability level with shape parameter equal to 1.0 as this is the less sensitive point for calibration of the statistical distribution (Derbanne et al., 2011).

The fatigue stress range for each load case of each loading condition is defined by selecting 5 EDW and obtaining the corresponding load cases but differently, from other limit state checks,

the wave maximizing the heave and pitch accelerations in a head sea and oblique sea respectively are not considered to limit the computational burden. Loading conditions have been defined according to ship commercial practice and recently updated as far as bulk carrier types BC-B and BC-C is concerned (IACS, 2016). Damage is evaluated based on the stress range obtained from the predominant load case in each loading condition (e.g. full load, ballast, …), including all mentioned correction factors.

While a conventional ship speed of 5knots is assumed for extreme loads, for fatigue assessment the speed is ¾ V_{design}.

7.1.3 Fatigue assessment

Apart from detail design standards that provide welding requirements at critical structural details to prevent specific types of fatigue failure, the Palmgren-Miner linear summation of damage is implemented in the rules, duly considering the contribution of ship loading conditions as well as load cases. The hot spot stress range is evaluated by applying different methods and checked against S-N curves based on the structural stress approach. The worst-case principal stress components acting within or outside ±45° of the perpendicular to the weld toe are considered.

Instead of correction factors to account for corrosion effects, S-N curves for the corrosive environment are introduced and the fatigue damage is calculated for in air and corrosive environments, implicitly stating the time period during which the corrosion protection is effective.

It is worth noting that the corrosion is also accounted for when evaluating the acting stress by deducting half of the design corrosion margin from the gross thickness. This net scantling approach enables simply to reproduce the average thickness diminution through the ship's design life.

7.2 DNV·GL regulations

As a consequence of the merger, it became necessary to merge the former DNV (DNV, 2015) and former GL rules (GL, 2015) into one common set of rules. The rules came into force in January 2016, but for a transition time until July 2017 the DNV and GL rules were to be kept valid. The opportunity was used, and many small improvements were introduced. The load concept from Common Structural Rules for Bulk Carriers and Oil Tankers (CSR), which has been developed by the International Association of Classification Societies, (IACS, 2015), has been used as a basis. It has been improved to be applicable also for other ship types, e.g. also for small and slender ships. The fatigue capacity part is also aligned with CSR, but very much based on what has already been used by DNV and GL. Well proven parts from former rules have been kept. The topological structure has been taken from former DNV with a relatively short rule part with fundamental requirements and acceptance criteria and with a supporting class guideline with a detailed description of the fatigue strength assessment methods and approaches. The rules can be found in DNV GL rules for Classification, Ships, Part 3 Hull, Chapter 9 Fatigue (DNV-GL, 2017c) and the class guideline in DNVGL-CG-0129 Fatigue assessment of ship structures (DNV-GL, 2017a).

While in the past 20 years' lifetime was assumed, the design life has now been increased to 25. This is due to nowadays improved coating systems and inspection schemes. However, the corresponding number of load cycles for the calculation of fatigue damage depends on ship length. It is 8.6 10^7 for a ship of about 90 m in length and reduces to, e.g., 6.4 10^7 for 400 m length. This reflects the increase of encounter periods for larger ships in the same wave environment, leading to fewer load cycles at the same time.

Same Weibull distribution function as in CSR is used to obtain the stress time history, calibrated at 10^{-2} probability level with shape parameter equal to 1.0. The background is that the damage contribution of high-stress ranges is rather small due to the associated low number of cycles.

Depending on the S-N curve used, for a straight-line spectrum, the highest damage density fits with or is close to the quarter of the maximum stress range.

As DNV was using the hot-spot stress approach and GL the nominal stress approach, now both can be used, i.e., either the stress concentration factor K for serving the hot-spot concept or the FAT classes serving the nominal stress concept.

A revised thickness and size effect has been introduced where not only the base plate thickness is considered but also the length of transverse attachments, cruciform joints, and butt welds.

For consideration of corrosion a simplification has been done, the effect of which is however small. Other rules and standards use separate SN-curves for corrosive environments. But as measured corrosion progress scatters very much in practice, the related damage contribution is taken as based on the S-N curve in the air and then multiplied by 2.0. The amount of time to be considered in a corrosive environment is defined based on compartment type and content and ranges between 0 and 5 years. For target lifetimes above 25 years, the formulation for the predicted lifetime is made independent of the target lifetime, assuming a regular maintenance regime.

The mean stress effect, which can be important when details are exposed to compression, is handled similarly to how it has been in DNV and in GL. The pronounced effect of residual stresses and its shakedown on the mean stress effect, as it is considered in CSR for bulk carrier and tanker, is not relevant for typical loading conditions of other ship types and accordingly not applied in DNV-GL rules.

All full-scale measurements have confirmed that wave-induced hull girder vibrations, referred to as whipping (transient, e.g., from bow flare impact) and springing (resonant), contribute to the fatigue accumulation. The contribution is represented by applying a minimum equivalent increase to the wave bending moment, which is well correlated with the governing vibration mode of the hull girder. The increase is dependent on the beam of the vessel for both slender and blunt vessels, and in practice has a significant contribution for details in the deck, less in the bottom and close to insignificant in the side shell. For container ships, more ship specific and more sophisticated considerations are possible according to DNV GL class guideline for fatigue and ultimate strength assessment of container ships including whipping and springing (DNV-GL, 2017b).

7.3 Lloyd's Register (LR) regulations

The Lloyd's Register Rules and Regulations for the Classification of Ships (LR, 2016a) indicate that the fatigue performance of the hull structure is to be assessed in accordance with the applicable ShipRight Fatigue Design Assessment (FDA) procedures (LR, 2016c). The ShipRight FDA notation is assigned when the appraisal satisfies the requirement of 20 years' fatigue life based on the LR Fatigue Wave Environment (Worldwide) trading pattern. This assessment is mandatory for new oil tanker and bulk carrier configurations over 190 meters in length which are not constructed in accordance with the IACS Common Structural Rules (CSR), but it is not applicable to ships approved using the CSR.

The ShipRight FDA SPR notation is assigned as a supplement to the FDA notations when the fatigue performance of the hull structure considers the effects of the continuous vibrational response of the hull girder in waves (springing). Details for assessment of fatigue including hull girder springing loads can be found in (LR, 2014).

The ShipRight Fatigue Design Assessment (FDA) procedure (LR, 2016c) applies to oil tankers, LNG and LPG carriers, bulk and ore carriers and container ships and requires three possible levels of assessments:

- FDA Level 1 (LR, 2009): the proposed joint configurations at critical areas are compared with the structural design configurations specified in the Structural Detail Design Guide, which can offer an improved fatigue life performance.
- FDA Level 2 (LR, 2015, 2016b): this is a spectral direct calculation procedure based on parametric databases to compute the wave-induced loads and motions and simplified structural models which utilize LR's PC-Windows based software. This procedure is intended for the analysis of secondary stiffener connections.
- FDA Level 3 (LR, 2016d): this is a full spectral direct calculation procedure based on first principles computational methods, such as hydrodynamic load and ship motion analysis to determine the wave-induced loads and motions, and finite element analysis (global 3D FE model and local zoom FE model) to determine the structural response. It is intended mainly for the analysis of primary structural details.

For the FDA Level 2 and FDA Level 3, the Fatigue Wave Environment trading patterns have been derived for specific ship types using worldwide trading statistics. For all these trading patterns the probability of encountering a particular sea condition and wave heading is obtained from a voyage simulation program which makes use of global wave statistical data and applies seakeeping criteria to modify the ship speed and heading (LR, 2016c). The North Atlantic Wave Environment is based on the route from Norway to USA (East Coast) where the voyage simulator program is also used to obtain the operation probability profile. The simulation of the voyages using anticipated ship's operational profiles together with the hydrodynamic and structural mathematical models determine the stress range and associated number of cycles.

The FDA procedures adopt a unit load approach to estimate the total stress response by combining the results of discrete unit load cases and the applied loads. The unit cases include hull girder global loadings, external hydrodynamic wave pressure loads, and internal cargo/water ballast inertia pressure loads. All these loads are further computed for any loading condition and sea state resulting from the hydrodynamic analysis and voyage simulation. The distribution and magnitude of internal inertia pressure loads are determined by simplified expressions for each ship motion.

Both FDA Level 2 and FDA Level 3 adopt a hot spot stress approach in conjunction with the Palmgren-Miner cumulative damage rule. The LR hot spot reference design S-N curve represents the fatigue strength of the welded material in air, including the stress concentration due to the local notch at the weld toe. It consists of two slopes modified as per the Haibach correction at the 10^7-stress cycle and a reduction factor for corrosive operational environments. Additional stress concentration factors to account for construction tolerances and plate thickness effects may be applied (LR, 2016d). The mean stress correction is included to reduce the overall stress range when the stress cycle is in compression.

7.4 Bureau Veritas (BV) regulations

Bureau Veritas Rules concerning fatigue for steel ships are involved in NR 467 (BV, 2016b). Specific rules have been developed for containerships NR 625 (BV, 2016a). These rules involve a part dedicated to loads including fatigue loads defined in the framework of design load scenarios. In each scenario, Hot Spot Stress ranges are calculated according to a specified spectral approach. In addition, a class notation Whisp NR 583 considers whipping and springing.

NR 445 (BV, 2016c) deals with offshore structure. As dedicated to a structure where the operator specifications are generally very detailed this Classification rule is more focused on the objectives of the assessment including for fatigue than aiming to provide a comprehensive procedure to assess the structure. Within the objectives, different loads are involved due to waves, inertia, vortex shedding, and slamming. Fatigue life is addressed involving linear cumulating

of damage or alternatively fracture mechanics. The rules for each type of ship, ship-shaped offshore structure or tubular structure, fixed or floating, refer to NI 611 for fatigue assessment.

An assessment based on a fracture mechanics approach has been introduced, to assess the validity of inspection planning. Fracture mechanics is applicable from flaw detection up to fracture criterion in terms of a Failure Assessment Diagram. When no crack is detected e.g. at design stage the initial crack assumed is defined by the capacity of NDE implemented during the inspection.

The failure modes considered are detailed, including initiation at the weld toe, initiation at the weld root, initiation on shared surfaces and initiation in bolted assemblies. The stress calculations, particularly in the case of Finite Element Models, are clarified.

The load model involves different levels of refinement; from a simplified rule-based approach to different direct calculation approaches, spectral or time domain. Different methodologies are proposed for long-term simulation such as design sea states, equivalent design waves, spectral approaches, up to direct simulation. Nonlinear effects such as intermittent wetting and whipping are addressed.

In alignment with CSR, the reference stress has been changed from notch stress to hotspot structural stress as well as S-N curves accordingly. The reference fatigue stress incorporates the mean stress effect and plate thickness effect as given in (IACS, 2015). When relevant methods to model weld beads effects are provided. Nevertheless, for some classes of details an alternative definition of stresses is retained, such as structural stress in the weld bead for root initiation or a dedicated stress definition for bolted assemblies.

Fatigue strength corresponding to a cathodic protection condition for welded assemblies is involved. The effect of weld improvement is considered by using S-N curves with a lower slope and higher fatigue limit. For free edges, the applicable S-N curve depends on the treatment of shared surfaces and particularly the treatment of edge corners. The capacity of remaining fatigue life evaluation is addressed with crack propagation analysis. Concerning offshore units, the case of unit conversion is addressed. The fatigue damage of the unit before conversion is to be included in the total damage. The issues related to the impossibility of inspection or impossibility of repair are also addressed in term of increasing the design fatigue life.

7.5 Indian Register of Shipping (IRS) regulations

IRS rule approach for simplified fatigue assessment of ship structures is aligned with the IACS recommendation 56 (IACS, 1999). Based on above approach internal guidance notes are to be utilized for simplified fatigue assessment of ships except CSR ships. For CSR oil tanker and bulk carrier, fatigue analysis is to be performed using the IACS Common Structural Rules (IACS, 2015).

The computation of loads in simplified approach is to be referred to the IRS Rules and Regulations for the Construction and Classification of Steel Ships (IRS, 2016a, b). All the design loads used for fatigue assessment which include local loads (external and internal pressure) and hull girder loads in still water and in waves are based on Equivalent Design Approach (EDW).

The nominal or hot-spot stress based approach can be considered as per the guidance notes. Details mandated for evaluation of the hotspot stress are provided in IRS Rules for Bulk Carriers and Oil Tankers (IRS, 2016a, b). Stresses induced due to applicable loads are to be evaluated using beam theory. The long-term distribution of stress ranges is assumed to be defined by the two-parameter Weibull distribution. These two parameters are scaling factor which is defined by reference stress range and shape parameter which depends on location and probability level of loads. In simplified fatigue assessment, the shape parameter is assumed to equal to one, same as CSR at a given probability level of loads of 10^{-2}. The reference fatigue

stress incorporates the mean stress effect, plate thickness effect and warping effect as given in the rules (IRS, 2016a, b). The total number of cycles for design life is computed by considering the 25 years of ship's life. All the structural properties are computed based on a net thickness approach. Net thickness of local support members is to be obtained by deducting 0.5tc from the gross thickness.

The fatigue damage is computed using the Palmgren-Miner summation rules. The characteristic fatigue strength of structural details is referred from the design S-N curves (UK-HSE, 1990, IACS, 1999). For fatigue damage estimation, both air and corrosive environment are considered in the analysis.

7.6 Comparison of simplified fatigue approaches

Besides the common fatigue approach for oil tankers and bulk carriers in CSR, each Classification Society uses its own simplified procedure for fatigue checks of other ship types. These individual fatigue procedures differ more or less from the CSR approach, although the principal method is similar and in alignment with the Unified Recommendation No. 56 of the International Association of Classification Societies (IACS, 1999).

Most procedures are based on the identification of two critical dynamic load cases for each of the relevant loading conditions. Therefore, in each load case, an evaluation is performed of the stresses induced by global loads of the hull girder and stresses due to local loads (external wave pressure and internal inertial pressure) to identify the cases with the maximum and minimum total stress. On the resulting maximum nominal stress range stress concentration factors are applied to account for the geometry of the investigated structural detail. From the reference stress range and its associated probability, a stress range distribution is derived. This distribution, coupled with the Miner's hypothesis of linear accumulated damage and to S-N curves describing the fatigue strength, provides the background for all verifications, even if the way such verification is formulated, and the type of final output can differ. The various steps of this general framework are analysed in more detail in the following.

The detail selected for comparison of simplified checks in the present chapter is the end connection of the deck stiffener at the same location (y=21.4m, z=24.54m) as considered in the spectral benchmark. The midspan of the stiffener is located at Fr. 154 (x=127.76m, x/L=0.4481) and the investigated end connection cross at Fr. 157 (x=130.34m, x/L=0.4547). The stiffener type is a symmetrical bulb profile corresponding to a T-profile of the size 263*12.0*89*27.0. Connected to the deck plate of t=36mm with a stiffener distance of 700mm. Every 5.16m the deck stiffener is supported by a web frame and connected with a web stiffener FB 110*14. All material properties have a yield strength of 355 N/mm².

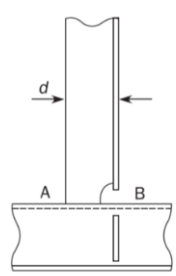

Figure 3: End connection type

Regarding this sample case, formulations of considered class rules in respect of fatigue capacity and fatigue loads have been compared. The LR rules are not considered in this comparison, as the LR procedures FDA Level 2 and FDA Level 3 (see Section 7.3) are based on spectral direct calculations and not a simplified procedure for fatigue checks.

However, the fatigue damage determined by applying the LR FDA Level 2 approach is also given for reference (see Table 7). The LR assessment considers the four loading conditions and it is based on the LR North Atlantic wave environment (LR, 2015, 2016c, b). This operational profile together with the hydrodynamic load motions, obtained from parametric databases, and the structural mathematical models determine the stress range and associated number of cycles (see Section 7.3). Therefore, intermediate calculations of the loads and motions, as well as the associated stress range, cannot be provided here as they will vary for each individual sea state.

7.6.1 Loading

For a sample case in the upper hull, the vertical hull girder bending is the dominating load component. For quantification of the vertical wave bending moment, all class societies refer to the unified requirement S11 (IACS, 1989). Load combinations effected by horizontal bending and torsional moment are not of relevance for the investigated location in the upper hull and accordingly not explicitly considered here.

In IACS unified requirement S11, the wave vertical bending moment (MWV) refers to an exceedance probability of 10-8. For fatigue, it is useful to scale this extreme value, which may occur only once in ship's lifetime, down to a value more representative for fatigue behaviour. In newly developed CSR (IACS, 2015) an exceedance probability of 10-2 was introduced for the fatigue loads and some of the class societies apply this load level for fatigue in their own rules, too. The probability factor in Table 1 describes the ratio between the 10-8 hogging wave bending moment and the considered fatigue amplitude.

Table 1: Hull girder loads at 0.45 x/L

Permissible still water moment						
M_{SW} hog [MNm]		4,300				
M_{SW} sag [MNm]		-4,000				
Vertical wave bending moment		acc. IACS UR S11				
10^{-8} M_{WV} hog [MNm]		6,245				
10^{-8} M_{WV} sag [MNm]		-6,563				
		CSR	DNV GL	LR	BV	IRS
Probability for fatigue		10^{-2}	10^{-2}	Sec 7.6	10^{-8}	10^{-2}
Homogen	Factor probability	0.218	0.218	-	-	0.218
	Factor hull girder vibration	1.0	1.2	-	1.0	1.0
	M_{WV} fatigue amplitude [MNm]	1,362	1,634	Sec 7.6	6,938	1,389
	M_{SW} applied [MNm]	-1,600	-4,000	-1,316	n/a	-1,600
Alternate	Factor probability	0.218	-	-	-	0.218
	Factor hull girder vibration	1.0	-	-	-	1.0
	M_{WV} fatigue amplitude [MNm]	1362	-	Sec 7.6	-	1389
	M_{SW} applied [MNm]	3,225	-	3,272	-	3,225
Normal Bal.	Factor probability	0.223	0.223	-	-	0.223
	Factor hull girder vibration	1.0	1.2	-	1.0	1.0
	M_{WV} fatigue amplitude [MNm]	1,393	1,671	Sec 7.6	6,938	1,420
	M_{SW} applied [MNm]	3,440	4,300	2,969	n/a	3,440
Heavy Ballast	Factor probability	0.221	-	-	-	0.221
	Factor hull girder vibration	1.0	-	-	-	1.0
	M_{WV} fatigue amplitude [MNm]	1,385	-	Sec 7.6	-	1,412
	M_{SW} applied [MNm]	-3,000	-	-1,660	-	-3,000

For the investigated detail, the mean stress is dominated by the assumed still water moment M_{SW}. According to some class rules permissible still water moments are applied. CSR consider reduced still water moments for the different loading conditions.

Local loads are generated on the outer hull by external hydrodynamic pressures and on tank and cargo hold boundaries by inertial pressures exerted in the liquid or bulk cargo by ship's local accelerations. Formulations are provided for combined accelerations at the investigated stiffener location as the sum of ship's translational and rotational accelerations. Listed reference values correspond to the fatigue exceedance probability for the relevant load case of the different loading conditions.

7.6.2 Response

Stresses from global and local loads are summarized in Table 3 to 6 for the considered loading conditions. In all rules, local external loads are not relevant to fatigue strength of deck stiffeners. As per CSR, local internal loads are neglected for fatigue strength of deck stiffeners.

Nominal stress components are multiplied by stress concentration factors (SCF) to get hotspot stresses or notch stresses. These corrections are applied during the evaluation of single components to allow different SCFs for global and local stresses.

Table 2: Combined accelerations at deck stiffener location

Loading Conditions with CSR default values		CSR	DNV GL	LR	BV	IRS
	Probability for fatigue	10^{-2}	10^{-2}	Sec.7.6	10^{-5}	10^{-2}
Homogen T=17.5 m GM =5.59 m k_r = 16.31 m	Relevant EDW	HSM	HSM	Sec.7.6	n/a *	HSM
	Long. acceleration amplitude [m/s²]	-0.245	-0.205		a, b: 0.868 c, d: 0.0	-0.245
	Trans. acceleration amplitude [m/s²]	0.0	0.0		a, b: 0.0 c, d: 5.341	0.0
	Vert. acceleration amplitude [m/s²]	0.421	0.431		a, b: 2.097 c, d: 7.160	0.422
Alternate T=17.5 m GM =9.32 m k_r = 18.64 m	Relevant EDW	HSM	-	Sec.7.6	-	HSM
	Long. acceleration amplitude [m/s²]	-0.245	-		-	-0.245
	Trans. acceleration amplitude [m/s²]	0.0	-		-	0.0
	Vert. acceleration amplitude [m/s²]	0.421	-		-	0.422
Normal Bal. T=9.07 m GM =15.38 m k_r = 20.97 m	Relevant EDW	HSM	HSM	Sec.7.6	n/a *	HSM
	Long. acceleration amplitude [m/s²]	-0.219	-0.143		a, b: 1.056 c, d: 0.0	-0.219
	Trans. acceleration amplitude [m/s²]	0.0	0.0		a, b :0.0 c, d: 5.074	0.0
	Vert. acceleration amplitude [m/s²]	0.162	0.165		a, b: 2.097 c, d :2.493	0.162
Heavy Ballast T=11.51 m GM =11.65 m k_r = 18.64 m	Relevant EDW	HSM	-	Sec.7.6	-	HSM
	Long. acceleration amplitude [m/s²]	-0.220	-		-	-0.220
	Trans. acceleration amplitude [m/s²]	0.0	-		-	0.0
	Vert. acceleration amplitude [m/s²]	0.235	-		-	0.235

* Accelerations acc. BV-rules are provided for four load cases individually

Table 3: Stresses in Homogen Condition

		CSR	DNV GL	LR	BV	IRS
	Relevant EDW	HSM	HSM	Sec 7.6	n/a	HSM
Local stress	Internal pressure range [kPa]	-	-	-		-
	Bending stress per unit pressure	1.799	1.715	Sec 7.6		-
	Nominal bending stress range [MPa]	-	-	-		-
	Stress concentration factor, SCF	1.60	1.60	1.43	1.65	1.40
Global stress	Load combination factor for M_{WV}	1.0	1.0	-	a,b: 0.625 c, d: 0.4	1.0
	Global stress per 10^3 unit M_{WV}	21.01	21.31	Sec 7.6	n/a	21.42
	Nominal global stress range [MPa]	57.24	69.65	-	n/a	58.19
	Stress concentration factor, SCF	1.28	1.28	1.43	1.30	1.28
Total stress incl. SCF						
	Fatigue stress range [MPa]	74.26	89.14	-	a: 290.0 b: 0.0 c: 134.5 d: 97.7	74.49
	Mean stress [MPa]	-43.04	-109.10	Sec 7.6	n/a	-43.87
	Factor mean stress	0.665	0.700	0.700	1.0	0.664

Table 4: Stresses in Alternate Condition

		CSR	DNV GL	LR	BV	IRS
	Relevant EDW	HSM	-	Sec 7.6	-	HSM
Local stress	Internal pressure range [kPa]	-	-	-	-	-
	Bending stress per unit pressure	1.799	-	Sec 7.6	-	-
	Nominal bending stress range [MPa]	-	-	-	-	-
	Stress concentration factor	1.60	-	1.43	-	1.40
Global stress	Load combination factor for M_{WV}	1.0	-	-	-	1.0
	Global stress per 10^3 unit M_{WV}	21.01	-	Sec 7.6	-	21.42
	Nominal global stress range [MPa]	57.24	-	-	-	58.19
	Stress concentration factor	1.28	-	1.43	-	1.28
Total stress incl. SCF						
	Fatigue stress range [MPa]	74.26	-	-	-	74.49
	Mean stress [MPa]	86.76	-	Sec 7.6	-	82.25
	Factor mean stress	1.00	-	1.00	-	1.00

Table 5: Stresses in Normal Ballast

		CSR	DNV GL	LR	BV	IRS
	Relevant EDW	HSM	HSM	Sec 7.6	n/a	HSM
Local stress	Internal pressure range [kPa]	-	0.549	-		1.947
	Bending stress per unit pressure	1.799	1.715	Sec 7.6		1.488
	Nominal bending stress range [MPa]	-	-0.941	-		4.803
	Stress concentration factor	1.60	1.60	1.43	1.65	1.40
Global stress	Load combination factor for M_{WV}	1.0	1.0	-	a, b: 0.625 c, d: 0.4	1.0
	Global stress per 10^3 unit M_{WV}	21.01	21.31	Sec 7.6		21.42
	Nominal global stress range [MPa]	58.50	71.19	-		59.48
	Stress concentration factor	1.28	1.28	1.43	1.30	1.28
Total stress incl. SCF						
	Fatigue stress range [MPa]	74.88	89.84	-	a:291.2 b19.6 c:19.0 d:14.7	78.22
	Mean stress [MPa]	92.54	127.07	Sec 7.6		99.81
	Factor mean stress	1.00	1.00	1.00	1.0	1.00

Table 6: Stresses in Heavy Ballast

		CSR	DNV GL	LR	BV	IRS
	Relevant EDW	HSM	-	Sec 7.6	-	HSM
Local stress	Internal pressure range [kPa]	-	-	-	-	1.956
	Bending stress per unit pressure	1.799	-	Sec 7.6	-	1.488
	Nominal bending stress range [MPa]	-	-	-	-	4.824
	Stress concentration factor	1.60	-	1.43	-	1.40
Global stress	Load combination factor for M_{WV}	1.0	-	-	-	1.0
	Global stress per 10^3 unit M_{WV}	21.01	-	Sec 7.6	-	21.42
	Nominal global stress range [MPa]	58.14	-	-	-	59.11
	Stress concentration factor	1.28	-	1.43	-	1.28
Total stress incl. SCF						
	Fatigue stress range [MPa]	74.40	-	-	-	77.77
	Mean stress [MPa]	-80.71	-	Sec 7.6	-	-76.73
	Factor mean stress	0.466	-	0.700	-	0.505

Table 7: Fatigue assessment

		CSR	DNV GL	LR	BV	IRS
Long term	Probability for fatigue	10^{-2}	10^{-2}	Sec.7.6	10^{-5}	10^{-2}
	Factor environment (NA=1.0 or WW=0.8)	1.0	0.8	1.0	1.0	1.0
	Weibull shape factor for long-term distribution.	1.0	1.0	Sec 7.3		1.0
Capacity	S-N curve in air FAT class [MPa]	90	90	Sec 7.3	90	D
	Factor thickness effect	1.013	1.000	1.030		1.000
Homogen	Fraction of time	0.25	0.50	0.20		0.25
	Number of cycles in 10^6	17.156	34.313	Sec 7.3	a, b: 5.489 c, d: 10.978	17.118
	Reference stress range [MPa]	49.34	49.92	-	a: 290.0 b: 0.0 c: 134.5 d: 97.7	49.49
	Partial damage in air	0.0383	0.0850	-	0.24*	0.0387
	Partial damage (corrosive)	0.0333	0.0425	-	-	0.0336
Alternate	Fraction of time	0.25	-	0.30	-	0.25
	Number of cycles in 10^6	17.156	-	Sec 7.3	-	17.118
	Reference stress range [MPa]	74.20	-	-	-	74.48
	Partial damage in air	0.1799	-	-	-	0.1823
	Partial damage (corrosive)	0.1133	-	-	-	0.1146
Normal Ballast	Fraction of time	0.20	0.50	0.20		0.2
	Number of cycles in 10^6	13.725	34.313	Sec 7.3	a,b,c: 7.318 d: 0.0	13.694
	Reference stress range [MPa]	75.84	71.69	-	a:291.2 b:19.6 c:19.0 d:14.7	78.22
	Partial damage in air	0.1554	0.3344	-	0.25*	0.1732
	Partial damage (corrosive)	0.0968	0.1672	-	-	0.1062
Heavy Ballast	Fraction of time	0.30	-	0.30	-	0.3
	Number of cycles in 10^6	20.588	-	Sec 7.3	-	20.542
	Reference stress range [MPa]	35.132	-	-	-	39.30
	Partial damage in air	0.0106	-	-	-	0.0175
	Partial damage (corrosive)	0.0144	-	-	-	0.0202
Final Result	Total damage	0.642	0.629	0.595	0.49	0.687
	Damage limit	< 1.0	< 1.0	< 1.0	<0.98	<1.0
	Fatigue life [years]	32	40	42	40	31
	Fatigue life limit [years]	>25	>25	> 25	>20	>25

* Corrosion effect is provided by a factor of 1.1 on the damage in the air

7.6.3 Assessment

All fatigue checks presented here are based on a long-term stress range distribution which is used in combination with an S-N curve to compute the damage accumulated according to the Palmgren-Miner's Rule. In most cases, a long-term Weibull distribution is applied. This is identified by a shape parameter and by a reference stress range at the used probability level.

The S-N curves characterize the fatigue strength capacity and are represented by two straight lines in a semi-logarithmic plot with a slope of 3 and 5 for welded details. The change of slope is usually at 10^7 cycles and the reference FAT class at $2 \cdot 10^6$ cycles. The fatigue strength is to assess with S-N curve in the air and in corrosive environments. Design life is divided into two intervals corresponding to unprotected (corrosive) and protected (dry air) environment.

Finally, a check is performed on the detail to assess if it satisfies a minimum fatigue strength requirement. While the general background of checks is the same, the way they are formulated can be a comparison against limit values of the predicted damage and/or respectively fatigue life or a comparison of the reference stress range with an allowable value.

7.7 International Gas Carrier (IGC) code

The resolution of the Maritime Safety Committee MSC.370(93) 'Amendments to the international code for the construction and equipment of ships carrying liquefied gases in bulk, IGC code (IGC, 2014), adopted on 22 May 2014, replaces the resolution MSC.5(48), referred here as 'old IGC code'. While the amendments affected all chapters of the IGC code, the interest here is on Chapter 4 'Cargo Containment' which goal is 'to ensure the safe containment of cargo under all design and operating conditions having regard to the nature of the cargo carried'. Chapter 4 has been completely reorganized, covering general requirements for all types of containment systems and for individual tanks. The main changes related to fatigue design assessment are summarized next.

Part A 'Cargo Containment' initially provides details of the functional requirements. Of interest is that the design life of the containment system shall not be less than the design life of the ship and that it shall be designed for North Atlantic environmental conditions and relevant long-term sea state scatter diagrams for unrestricted navigation.

Part A also covers new requirements for the inspection/survey plan for the cargo containment system, and how it shall be designed and built to ensure safety during operation, inspection and maintenance. This relates closely to the section 'Fatigue design conditions' which contains requirements for tank members where leakage monitoring systems do not work until cracks reach a critical state, and in-service inspection plans do not show visual detection of cracks.

In this case, the fatigue design criterion Cw (maximum allowable cumulative fatigue damage) is reduced to 0.1 or the crack propagation period is increased to three times the lifetime of the tank. However, for tank members where the in-service inspection plan can demonstrate cracks are visually detectable in service, Cw can be increased to 0.5, and the crack propagation period can be decreased to three times the inspection interval.

Regarding the design of the secondary barrier, the acceptance in-service will require the critical defect sizes of the secondary barrier to be defined.

In Part C 'Structural Integrity', under section 4.18.2 'Fatigue design conditions', it is indicated that the S-N curves shall be based on a 97.6 % probability of survival corresponding to the mean-minus-two-standard-deviation curves of relevant experimental data up to final failure (paragraph 4.18.2.4.2). This introduces clear design S-N curves for initial crack calculation.

Also, it is introduced clear design criteria for crack propagation analysis to determine (1) crack propagation paths in the structure, (2) crack growth rate, (3) the time required for a crack to cause a leakage from the tank, (4) the size and shape of through-thickness cracks, and (5) the time required for detectable cracks to reach a critical state.

For locations of the tank where the effective defect or crack development detection cannot be assured, an enhanced Cw of 0.1 or less is required for some areas of the containment system, particularly the attachment of the pump tower base support to the inner bottom (Cw was before 0.5). This requirement covers the primary members of prismatic Type B containment systems.

Part E 'Tank Types' introduces a clear design philosophy for Type C independent tanks, where the fatigue stress range is less than the fatigue limit. Here, the tanks' design is based on pressure vessel criteria modified to include fracture mechanics and crack propagation criteria.

For membrane tanks, it is also indicated that structural elements not accessible for in-service inspection, and where a fatigue crack can develop without warning, shall satisfy fatigue and fracture mechanics requirements. This means it may be necessary to assess crack propagation for the weld junction of the pump tower base support and the inner hull.

8. CONCLUSIONS AND RECOMMENDATIONS

The recent developments in fatigue and fracture of ships and offshore structures have been revised here. The major concern was the fatigue crack initiation and growth under cyclic loading as well as the unstable crack propagation in the ship and offshore structures.

Special attention was paid to load-induced fatigue, material properties and testing related to fatigue and fracture. Revision of the advances in the fatigue damage accumulation and crack growth approaches was also made.

Due attention was dedicated to the fabrication, improvements and in-service maintenance with respect to the suitability and uncertainty of physical models and testing. Consideration was given to fatigue design and verification based on Rules, standard and guidelines and reliability assessment performed in three benchmark studies (Garbatov et al., 2017, Lillemäe-Avi et al., 2017, Rörup et al., 2017) that will be presented and discussed in the third volume of the Proceedings of the 20th International Ship and Offshore Structures Congress.

462 references, covering the last four years, were reviewed and discussed in the report. The references discussed in the report originate from 2017 - 11%, 2016 - 37%, 2015 - 31%, 2014 - 10% and 2013 - 6%.

The reference list includes publications from 46 international journals, many book chapters, conference proceedings, rules, guidelines and standards. The first most cited journals are International Journal of Fatigue - 32%, Marine Structures - 11%, Engineering Fracture Mechanics, 10%, Fatigue and Fracture of Engineering Materials and Structures, 7%, Welding in the World, 4%, Ocean Engineering, 3%, Engineering Failure Analysis, 3%, Journal of Ship Production and Design, 3%, Theoretical and Applied Fracture Mechanics, 2%, Materials and Design, 2%, Composite Structures, 2%, Engineering Structures, 2%, Journal of Constructional Steel Research, 2%, Structural Safety, 2% and Ships and Offshore Structures, 2%.

The most discussed topics translated into key-words are: fatigue, 36%, strength, 15%, weld, 11%, crack, 10%, fracture, 8%, steel, 7%, ship, 6%, experiment, 6%, load, 6%, mechanics, 5%, offshore, 4%, reliability, 3%, damage, 2%, numerical, 2%, energy, 2%, residual, 2%, rules, 2%, corrosion, 2%, failure, 2%.

Several discussions and conclusions were derived and presented here, according to the already revised topics in different report chapters.

8.1 Fatigue and fracture loading

Fatigue loads are very complex and case dependent. They depend on either the environmental actions or the ability to obtain correct efforts from environmental conditions. Design metocean description is in principle solved for the loads in situ as the location is well known and metocean description analyses are generally undertaken before the operation. Design metocean description is more questionable for ships or offshore structure during transportation. Recommendation

34 of IACS propose a scatter diagram close to the North Atlantic condition to be associated with a speed equal to ¾ of maximum speed for calculation of fatigue loads. Especially for common cargo ships, it is likely to be a conservative approach. As fatigue damage is more sensitive to frequent sea states encountered by a ship than to the extreme sea states, fatigue analyses based on the actual trading pattern rather than on the worst conditions may provide better information on the predicted fatigue experienced by a fleet and knowledge on the scatter of fatigue loads on common ships, allowing a rational judgment on the suitability of the present approach for fatigue load determination and then allowing estimating/setting a reasonable safety margin. Fatigue loading due to navigation in ice conditioned e.g. navigation in the Arctic Ocean should be addressed as not currently considered in the ship design.

8.2 Material properties and testing

For fatigue and fracture assessment of materials, components and structures, material testing is virtually indispensable for calibrating material models and verifying simulations. More accurate consideration of material properties is an important topic for the future since numerical tools are developing rapidly, enabling more accurate modelling of manufacturing, e.g. welding, and strength properties under more complex loading paths. It is realized that both the fracture resistance and criteria depend on the stress state, which may be different in the standard test specimens and in actual structures. Failure strain also depends on the strain path and strain rate. Cyclic material properties of various zones of the welded joints are also a topic for research, recently especially for HFMI-treated weld toes. In fatigue testing, the friction stir welded steel joints have received increasing attention with the hope of application to marine, offshore and pipeline structures soon. New results have also been published for very high cycle fatigue of base material, fatigue in a corrosive environment or under temperature loads and for full-scale testing of structures. Digital image correlation during fatigue and fracture testing is not anymore, an alternative method but has become a new norm. Future research probably brings more experimental evidence for the fatigue crack initiation and short crack growth at microstructural levels as such test methods become more available.

8.3 Fatigue damage accumulation approaches

Joints connecting ship and offshore structural members are typically fatigue sensitive. In this respect welded joint fatigue assessment concepts developed over time have been classified and evaluated regarding the type of information, geometry, parameter and process zone as well as plane and life region annotations (Section 3.1). Fatigue involves several resistance dimensions, distinct contributions in different stages of the damage process as well as physics over a range of scales and the concept overview, as well as the concept criteria advances (Section 3.2), show that from modelling perspective, not all (governing) physics are incorporated explicitly.

Continuum or discrete damage mechanics criteria can be adopted to estimate the initiation and growth of lifetime contributions. Without being complete, it should be mentioned that damage mechanics criteria can be adopted as well to model fatigue phenomena. The same physics can be incorporated and may even provide better opportunities to obtain more accurate lifetime estimates (Section 3.3).

The fatigue damage criterion defines in terms of resistance the fatigue strength scatter and can be improved. Modelling developments and trends of fatigue damage criteria towards complete strength, total life and multi-scale criteria are identified (Section 3.4). The interacting material, geometry, loading & response (multiaxiality and amplitude variability, mean- and residual stress, time or frequency domain formulation) and environment resistance dimensions become explicitly incorporated, specifying the fatigue strength as well as initiation, growth and propagation induced damage process contributions and physics at different scales.

Material and geometry typically define the reference resistance; loading & response and environment are involved as influence factors. Most modelling and assessment publications paying

attention to fatigue damage criteria advances are (still) related to uniaxial response conditions, since the ship and the offshore structural response is predominantly Mode-I defined, even if the loading is multiaxial. Fatigue damage criteria developments are ongoing in this respect – focus seems to be on critical plane approaches – and comparisons to the available guidelines have been made (Section 3.4.1). Consistency with experimental results for different loading & response conditions is typically lacking. A rather broad range of mean and residual mean stress models are available and developments in this respect involve mainly the application of existing ones rather than introducing modelling advances (Section 3.4.2). Frequency domain approaches are considered less reliable but more efficient. Time domain approaches, on the other hand, are more accurate but computationally expensive. To combine the advantages of time and frequency domain approaches, hybrid approaches are under development (Section 3.4.3). Corrosion and gaseous hydrogen induced environmental fatigue damage consequences are under investigation and modelling start to allow for quantification (Section 3.4.4).

To quantify the relative initiation, growth and propagation contributions to fatigue lifetime, correlation of intact and crack damaged geometry parameters are required. Typically, either an intact or crack damaged geometry parameter is adopted and if both are incorporated separately, the transition is predefined. An important challenge seems to be the development of a loading & geometry dependent correlation of intact and crack damaged geometry parameters without predefined transition (Section 3.5).

Additional macro-, meso- and micro-fatigue damage mechanism information – physics at a smaller scale – can be used to enhance fatigue damage criteria, providing a multi-scale fatigue damage criterion (Section 3.6). Following the macro-scale developments from global to local fatigue damage criteria over time, the continuum mechanics lower bound is approaching and a correlation to the 'netherworld' (i.e. to meso- or even micro-scale physics) is the next step. Developments involve typically numerical modelling.

Fatigue damage accumulation is typically a random process. Reliability and confidence with respect to fitting parameters and lifetime can be established, but some contributors (e.g. size effects) can be explicitly incorporated in the fatigue damage criterion in order to provide more accurate lifetime estimates (Section 3.7).

8.4 Crack growth approaches

Fatigue crack growth approaches based on the theory of Fracture Mechanics have become an important tool for preventing fatigue failure of the ship and offshore structures during certain periods of service. The application of fatigue crack growth approaches on evaluation of the failure of ship and offshore structural details such as tidal turbine blades, cruciform welded joints, pressure vessel steel, multi-planar DX-joint welds, offshore pipelines, and aged jacket platforms have been discussed by many researchers in the last few years by using some extended crack growth models considering variable influential factors, which is typically realized by combining the theories with new simulation techniques.

However, some newly developed methods and theories in the field of fatigue and fracture have not been applied to ship and offshore structures, and fatigue crack growth approaches are still not well documented in the specifications for the ship and offshore structures.

8.5 Fabrication, degradation, improvements and repair

There is a clear gap between structural modelling and reality due to several assumptions and approximations introduced to make practically feasible and cost-efficient the design process. As far as fatigue strength is concerned, fabrication induced imperfections, as well as in-service degradation effects, are far to be considered in structural analyses explicitly, duly considering their actual quantification. Rather, safety/correction factors are generally adopted.

Nevertheless, it is already time to fully consider them in the design process and the trend outlined by the literature presented in this chapter and in the benchmark studies carried out by the Committee is clear: suitable technologies are available to adequately collect necessary data and, if properly applied, they largely improve the final design.

Two main categories of fabrication-induced imperfections have been identified: geometrical and welding induced. In both cases, applications leading to improved design have been found. It can be underlined that fatigue assessment approaches need to be improved to be able to consider these more accurate input data. The most recent developments of fatigue assessment approach as described in previous chapters of this report are probably driven also by the above trends.

Certainly, corrosion degradation is an issue. However, it is considered only marginally in this chapter if it can only be settled with the availability of sound experimental data. This remains an open issue and a significant gap to be filled in the next years.

It is noted that fatigue improvement and repair methods are nowadays emerging fast and more and more widely applied. It is, however, necessary to develop rules and regulations to create a common playground for their adequate development.

8.6 Fatigue reliability

It has been noticed from the recent publications in the field of fatigue reliability that the research investigations are favouring the fracture mechanics based approaches rather than the SN based approaches. Therefore, the reliability analysis and service life prediction based on the fracture mechanics approach is more frequently used. While doing so, there are relatively fewer investigations in the review period of this report pertaining to the corrosion-fatigue interaction. Future studies need to focus on the understanding of the interaction mechanism between the fatigue damage and corrosion degradation and their effect on the reliability and risk-based structural assessments. Certainly, the reliability techniques are becoming mature and well understood and software are being made available.

8.7 Fatigue design and verification based on rules, standards, codes and guidelines

With the introduction of CSR for bulk carrier and oil tanker in 2015, the classification societies are aligning their own fatigue regulations more with CSR. Although a complete harmonization is not expected and some regulations were already aligned before, a progress for the examined class rules in this report is identified by following observations:

- 25-year fatigue life is the minimum design lifetime for all societies.
- A minimum time in corrosive environments is considered by all rules.
- In principle for all rules, the thickness effect is adopted from CSR with an exponent, which relates to the type of structural detail.
- Three of the four considered class societies (DNVGL, BV and IRS) analyse stiffener end connections on the basis of the S-N curve “D” respectively FAT90 in conjunction with a simplified stress analysis, i.e. Nominal stress x Tabulated “SCF”.
- Two class societies (DNVGL and IRS) adopt the fatigue load concept with 10^{-2} probability level and equivalent design waves (EDW). A third (BV) introduced it too, but at this time for container ships only.

The pronounced effect of residual stresses and its shakedown on the mean stress effect, as it is considered in CSR for bulk carriers and tankers, is not relevant for typical loading conditions of other ship types and consequently not adopted by any other class rules in general.

The two benchmark studies carried out for this report, demonstrate for the simplified assessment as well as for the stochastic spectral approach, comparable results for the combined fatigue

damage. Nevertheless, in case of the spectral approach single loading conditions exhibit obvious differences in the fatigue damage mainly due to different hydrodynamic loads and mean stress effects and give an identification for further harmonization efforts.

REFERENCES

Adedipe, O., Brennan, F. & Kolios, A. 2015. Corrosion fatigue load frequency sensitivity analysis. *Marine Structures,* 42**,** 115-136.

Adepipe, O., Brennan, F. & Kolios, A. 2016. A relative crack opening time correlation for corrosion fatigue crack growth in offshore structures. *Fatigue & Fracture of Engineering Materials & Structures,* 39**,** 395-411.

Al-Mukhtar, A. M. 2016. Mixed-Mode Crack Propagation in Cruciform Joint using Franc2D. *Journal of Failure Analysis and Prevention,* 16**,** 326-332.

Albinmousa, J. 2016. Investigation on multiaxial fatigue crack path using polar stress-strain representation. *International Journal of Fatigue,* 92**,** 406-414.

Alderliesten, R. C. 2016. How proper similitude can improve our understanding of crack closure and plasticity in fatigue. *International Journal of Fatigue,* 82**,** 263-273.

Alfredsson, B., Arregui, I. L. & Hazar, S. 2016. Numerical analysis of plasticity effects on fatigue growth of a short crack in a bainitic high strength bearing steel. *International Journal of Fatigue,* 92**,** 36-51.

Altamura, A. & Straub, D. 2014. Reliability assessment of high cycle fatigue under variable amplitude loading: Review and solutions. *Engineering Fracture Mechanics,* 121**,** 40-66.

Alves, A. S. F., Sampayo, L. M. C. M. V., Correia, J. A. F. O., De Jesus, A. M. P., Moreira, P. M. G. P. & Tavares, P. J. S. 2015. Fatigue life prediction based on crack growth analysis using an equivalent initial flaw size model: Application to a notched geometry. *ICSI 2015, the 1st International Conference on Structural Integrity Funchal,* 114**,** 730-737.

Amaro, R. L., Rustagi, N., Findley, K. O., Drexler, E. S. & Slifka, A. J. 2014. Modelling the fatigue crack growth of X100 pipeline steel in gaseous hydrogen. *International Journal of Fatigue,* 59**,** 262-271.

Ambuhl, S., Ferri, F., Kofoed, J. P. & Sorensen, J. D. 2015. Fatigue reliability and calibration of fatigue design factors of wave energy converters. *International Journal of Marine Energy,* 10**,** 17-38.

Amiri-Rad, A., Mashayekhi, M., van der Meer, F. P. & Hadavinia, H. 2015. A two-scale damage model for high cycle fatigue delamination in laminated composites. *Composites Science and Technology,* 120**,** 32-38.

Andrews, B. J. & Potirniche, G. P. 2015. Constitutive creep-fatigue crack growth methodology in two steels using a strip yield model. *Engineering Fracture Mechanics,* 140**,** 72-91.

ANSYS 2009. Online Manuals, Release 12.

Astrand, E., Stenberg, T., Jonson, B. & Barsoum, Z. 2016. Welding procedures for fatigue life improvement of the weld toe. *Welding in the World,* 60**,** 573-580.

Aydin, H. & Nelson, T. W. 2013. Microstructure and mechanical properties of hard zone in friction stir welded X80 pipeline steel relative to different heat input. *Materials Science and Engineering a-Structural Materials Properties Microstructure and Processing,* 586**,** 313-322.

Ayyub, B. M., Stambaugh, K. A., McAllister, T. A., de Souza, G. F. & Webb, D. 2015. Structural Life Expectancy of Marine Vessels: Ultimate Strength, Corrosion, Fatigue, Fracture, and Systems. *ASME Journal of Risk and Uncertainty in Engineering Systems Part B-Mechanical Engineering,* 1**,** 1-13.

Bandara, C. S., Siriwardane, S. C., Dissanayake, U. I. & Dissanayake, R. 2016. Full range S-N curves for fatigue life evaluation of steels using hardness measurements. *International Journal of Fatigue,* 82**,** 325-331.

Baptista, C., Reis, A. & Nussbaumer, A. 2017. Probabilistic S-N curves for constant and variable amplitude. *International Journal of Fatigue,* 101**,** 312-327.

Barile, C., Casavola, C., Pappalettera, G. & Pappalettere, C. 2016. Analysis of crack propagation in stainless steel by comparing acoustic emissions and infrared thermography data. *Engineering Failure Analysis,* 69**,** 35-42.

Barsoum, Z. & Jonson, B. 2011. Influence of weld quality on the fatigue strength in seam welds. *Engineering Failure Analysis,* 18**,** 971-979.

Baumgartner, J., Schmidt, H., Ince, E., Melz, T. & Dilger, K. 2015. Fatigue assessment of welded joints using stress averaging and critical distance approaches. *Welding in the World,* 59**,** 731-742.

Benasciutti, D., Sherratt, F. & Cristofori, A. 2016. Recent developments in frequency domain multi-axial fatigue analysis. *International Journal of Fatigue,* 91**,** 397-413.

Benz, C. & Sander, M. 2015. Reconsiderations of fatigue crack growth at negative stress ratios: Finite element analyses. *Engineering Fracture Mechanics,* 145**,** 98-114.

Berg, J., Stranghoener, N., Kern, A. & Hoevel, M. 2016. Variable amplitude fatigue tests at high-frequency hammer peened welded ultra-high strength steel S1100. *21st European Conference on Fracture, (Ecf21),* 2**,** 3554-3561.

Berg, J. & Stranghoner, N. 2016. Fatigue behaviour of high-frequency hammer peened ultra-high strength steels. *International Journal of Fatigue,* 82**,** 35-48.

Berg, T., von Ende, S. & Lammering, R. 2017. Calibration of potential drop measuring and damage extent prediction by Bayesian filtering and smoothing. *International Journal of Fatigue,* 100**,** 337-346.

Berto 2015a. A criterion based on the local SED for the fracture assessment of cracked and V-notched components. *Theoretical and Applied Fracture Mechanics,* 76.

Berto, F. 2015b. Crack initiation at V-notch tip subjected to in-plane mixed mode loading: An application of the fictitious notch rounding concept. *Frattura Ed Integrita Strutturale,* 34**,** 169-179.

Besten, J. H. d. 2015. *Fatigue resistance of welded joints in aluminium high-speed craft: a total stress concept.* PhD.

Beyer, F., Choisnet, T., Kretschmer, M. & Cheng, P.-W., 2015, Coupled MBS-CFD Simulation of the IDEOL Floating Offshore Wind Turbine Foundation Compared to Wave Tank Model Test Data, Proceedings of the 25th International Ocean and Polar Engineering Conference, Hawaii, USA, Paper ISOPE-I-15-272.

Bhatti, A. A., Barsoum, Z., Murakawa, H. & Barsoum, I. 2015. Influence of thermo-mechanical material properties of different steel grades on welding residual stresses and angular distortion. *Materials & Design,* 65**,** 878-889.

Bhatti, A. A., Barsoum, Z., van der Mee, V., Kromm, A. & Kannengiesser, T. 2013. Fatigue strength improvement of welded structures using new low transformation temperature filler materials. *Fatigue Design.* 192-201.

Bigot, F., Mahérault-Mougin, S. & Derbanne, Q., 2016, Comparison of different models for the fatigue analysis of details subject to side shell intermittent wetting effect, Proceedings of the 13th International Symposium on Practical design of ships and other floating structures, Copenhagen, Denmark.

Bilionis, D., V., B. & Vamvatsikos, D., 2015, Probabilistic Fatigue Life Assessment of an Offshore Wind Turbine in Greece, Proceedings of the 25th International Ocean and Polar Engineering Conference, Kona, Hawaii, USA, 684-691.

Blacha, L. & Karolczuk, A. 2016. Validation of the weakest link approach and the proposed Weibull based probability distribution of failure for fatigue design of steel welded joints. *Engineering Failure Analysis,* 67**,** 46-62.

Blasón, S., Rodríguez, C. & Fernández-Canteli, A., 2015, Fatigue characterization of a crankshaft steel: use and interaction of new models, Proceedings of the 5th International Conference on Crack Paths, Ferrara, Italy.

Boljanovic, S., Maksimovic, S. & Djuric, M. 2016. Fatigue strength assessment of initial semi-elliptical cracks located at a hole. *International Journal of Fatigue,* 92**,** 548-556.

Borrie, D., Liu, H. B., Zhao, X. L., Raman, R. K. S. & Bai, Y. 2015. Bond durability of fatigued CFRP-steel double-lap joints pre-exposed to marine environment. *Composite Structures,* 131**,** 799-809.

Bourbita, F. & Rémy, L. 2015. A combined critical distance and energy density model to predict high-temperature fatigue life in notched single crystal super alloy members. *International Journal of Fatigue,* 84**,** 17-27.

Branco, R., Antunes, F. V. & Costa, J. D. 2015. A review on 3D-FE adaptive remeshing techniques for crack growth modelling. *Engineering Fracture Mechanics,* 141**,** 170-195.

Brandão, C. S., Correa, F. N. & Jacob, B. P., 2015, Generation of Multiple Equivalent Regular Waves for Preliminary Analyses of Floating Production Systems, Proceedings of the 25th International Ocean and Polar Engineering Conference, Hawaii, USA, Paper ISOPE-I-15-073.

Branner, K., Berring, P. & Haselbach, P. U., 2016, Subcomponent testing of trailing edge panels in wind turbine blades, Proceedings of the 17th European Conference on Composite Materials.

Brennan, F. P., 2013, The need for variable amplitude corrosion fatigue materials data for Offshore Wind & Marine Renewable energy steel support structures, Proceedings of the 3rd International Conference of Engineering Against Failure, 745-751.

Brugger, C., Palin-Luc, T., Osmond, P. & Blanc, M. 2017. A new ultrasonic fatigue testing device for biaxial bending in the gigacycle regime. *International Journal of Fatigue,* 100**,** 619-626.

BS7910 2005. *British Standard BS7910, Guide to methods for assessing the acceptability of flaws in metallic structures,* London, BSI.

Bufalari, G., Kaminski, M. L., Van Lieshout, P. S. & Den Besten, J. H., 2017, Numerical comparative study of multiaxial fatigue methods applied to welded joints in a container vessel, Proceedings of the Symposium on Structural Durability in Darmstadt, Germany.

BV 2015. Rules Notes NR 583 Whipping and Springing Assessment. Paris: Bureau Veritas.

BV 2016a. Rules Note NR 625 Structural Rules for Container Ships. Paris: Bureau Veritas.

BV 2016b. Rules Notes 467 Rules for the Classification of Steel Ships. Paris: Bureau Veritas.

BV 2016c. Rules Notes NR 445 Rules for the Classification of Offshore Units. Paris: Bureau Veritas.

Calle, M. A. G., Verleysen, P. & Alves, M. 2017. Benchmark study of failure criteria for ship collision modelling using purpose-designed tensile specimen geometries. *Marine Structures,* 53**,** 68-85.

Campagnolo, A., Meneghetti, G. & Berto, F. 2016. Rapid finite element evaluation of the averaged strain energy density of mixed-mode (I plus II) crack tip fields including the T-stress contribution. *Fatigue & Fracture of Engineering Materials & Structures,* 39**,** 982-998.

Carpinteri, A., Fortese, G., Ronchei, C., Scorza, D. & Vantadori, S. 2016. Spectral fatigue life estimation for non-proportional multiaxial random loading. *Theoretical and Applied Fracture Mechanics,* 83**,** 67-72.

Carrion, P. E., Shamsaei, N. & Daniewicz, S. R. 2017. Fatigue Behaviour of Ti-6Al-4V ELI Including Mean Stress Effects. *International Journal of Fatigue,* 99**,** 87-100.

Castelluccio, G. M., Musinski, W. D. & Mcdowell, D. L., 2016, 93:387-396. 2016. Computational micromechanics of fatigue of microstructures in the HCF-VHCF regimes[J]. *International Journal of Fatigue,* 93**,** 387-396.

CEN 2005. Eurocode 3: design of steel structures. European Committee for Standardisation.

Chakherlou, T. N., Taghizadeh, H., Mirzajanzadeh, M. & Aghdam, A. B. 2012. On the prediction of fatigue life in double shear lap joints including interference fitted pin. *Engineering Fracture Mechanics,* 96**,** 340-354.

Chandran, K. S. R. 2016. A constitutive equation for the S-N fatigue behaviour of metal single crystals and validation by the physical definition of fatigue endurance limit. *International Journal of Fatigue,* 91**,** 21-28.

Chattopadhyay, A., Glinka, G., El-Zein, M., Qian, J. & Formas, R. 2011. Stress analysis and fatigue of welded structures. *Welding in the World,* 35**,** 2-21.

Chen, B. Q., Hashemzadeh, M., Garbatov, Y. & Guedes Soares, C. 2014a. Numerical and parametric modelling and analysis of weld-induced residual stresses. *International Journal of Mechanics and Materials in Design,* 11**,** 439-453.

Chen, B. Q., Hashemzadeh, M. & Guedes Soares, C. 2014b. Numerical and experimental studies on temperature and distortion patterns in butt-welded plates. *International Journal of Advanced Manufacturing Technology,* 72**,** 1121-1131.

Chen, B. Q., Hashemzadeh, M. & Guedes Soares, C. 2017. Validation of numerical simulations with X-ray diffraction measurements of residual stress in butt-welded steel plates. *Ships and Offshore Structures***,** 1-10.

Chen, N.-Z., 2015, Reliability-Based Low-Cycle Fatigue Assessment for Crack-Stopping Hole., Proceedings of the 25th International Ocean and Polar Engineering Conference, Kona, Hawaii, USA, 503-507.

Chen, N. Z. 2016. A stop-hole method for marine and offshore structures. *International Journal of Fatigue,* 88**,** 49-57.

Chen, X., Lados, D. A., Pettit, R. G. & Dudzinski, D. 2016. A physics-based model for evaluating hot compressive dwell effects on fatigue crack growth in 319 cast aluminium alloys. *International Journal of Fatigue,* 90**,** 222-234.

Cheng, A. K. & Chen, N. Z. 2017a. Corrosion fatigue crack growth modelling for subsea pipeline steels. *Ocean Engineering,* 142**,** 10-19.

Cheng, A. K. & Chen, N. Z. 2017b. Fatigue crack growth modelling for pipeline carbon steels under gaseous hydrogen conditions. *International Journal of Fatigue,* 96**,** 152-161.

Choung, J., Nam, W., Lee, D. & Song, C. Y. 2014. Failure strain formulation via average stress triaxiality of an EH36 high strength steel. *Ocean Engineering,* 91**,** 218-226.

Corigliano, P., Epasto, G., Guglielmino, E. & Risitano, G. 2017. Fatigue analysis of marine welded joints by means of DIC and IR images during static and fatigue tests. *Engineering Fracture Mechanics,* 183**,** 26-38.

Correia, J. A. F. O., Blason, S., De Jesus, A. M. P., Canteli, A. F., Moreira, P. M. G. P. & Tavares, P. J. 2016. Fatigue life prediction based on an equivalent initial flaw size approach and a new normalized fatigue crack growth model. *Engineering Failure Analysis,* 69**,** 15-28.

Cosso, G. L., Rizzo, C. M. & Servetto, C. 2016. Fitness-for-service assessment of defected welded structural details by experimental evaluation of the fatigue resistance S-N curve. *Welding in the World,* 60**,** 847-858.

Cui, J., Wang, D. & Ma, N., 2016, Spectral Fatigue Analysis Considering Probabilistic Corrosion Effects: A Case Study of Container Ship's Hatch Coaming Detail, Proceedings of the 35th International Conference on Ocean, Offshore and Arctic Engineering, Busan, South Korea.

D'Angelo, L. & Nussbaumer, A. 2017. Estimation of fatigue S-N curves of welded joints using advanced probabilistic approach. *International Journal of Fatigue,* 97**,** 98-113.

Dallago, M., Benedetti, M., Ancellotti, S. & Fontanari, V. 2016. The role of lubricating fluid pressurization and entrapment on the path of inclined edge cracks originated under rolling-sliding contact fatigue: Numerical analyses vs. experimental evidences. *International Journal of Fatigue,* 92**,** 517-530.

Darcis, P., Lassen, T. & Recho, N. 2006. Fatigue behaviour of welded joints part 2: Physical modelling of the fatigue process. *Welding Journal,* 85**,** 19s-26s.

de Jesus, A., Matos, R., Fontoura, B., Rebelo, C., Simões da Silva, L. & Veljkovic, M. 2012. A comparison of the fatigue behaviour between S355 and S690 steel grades. *Journal of Constructional Steel Research,* 79**,** 140-150.

Deguchi, T., Mouri, M., Hara, J., Kano, D., Shimoda, T., Inamura, F., Fukuoka, T. & Koshio, K. 2012. Fatigue strength improvement for ship structures by Ultrasonic Peening. *Journal of Marine Science and Technology,* 17**,** 360-369.

Den Besten, J. H. 2018. Fatigue damage criteria classification, modelling developments and trends for welded joints in marine structures. *Ships and Offshore Structures*, https://doi.org/10.1080/17445302.2018.1463609.

Deng, C. Y., Liu, Y., Gong, B. M. & Wang, D. P. 2016. Numerical implementation for fatigue assessment of butt joint improved by high-frequency mechanical impact treatment: A structural hot spot stress approach. *International Journal of Fatigue,* 92**,** 211-219.

Derbanne, Q., Rezende, F., de Hauteclocque, G. & Chen, X. B., 2011, Evaluation of Rule-Based Fatigue Design Loads Associated at a New Probability Level, Proceedings of the 21st International Ocean and Polar Engineering Conference, Maui, Hawaii, USA.

Desmorat, R., Angrand, L., Gaborit, P., Kaminski, M. & Rakotoarisoa, C. 2015. On the introduction of a mean stress in kinetic damage evolution laws for fatigue. *International Journal of Fatigue,* 77**,** 141-153.

Ding, Z. Y., Gao, Z. L., Wang, X. G. & Jiang, Y. Y. 2015. Modelling of fatigue crack growth in a pressure vessel steel Q345R. *Engineering Fracture Mechanics,* 135**,** 245-258.

DNV-GL 2015. Rotor blades for wind turbines. DNV-GL.

DNV-GL 2017a. Class Guideline DNVGL-CG-0129: Fatigue Assessment of Ship Structures. Oslo: DNV GL.

DNV-GL 2017b. Class Guideline DNVGL-CG-0153: Fatigue and Ultimate Strength Assessment of Container Ships including Whipping and Springing. Oslo: DNV GL.

DNV-GL 2017c. DNVGL-RU-9111:2015-7, Rules for Classification. Oslo: DNV GL.

DNV 2010a. Dynamic Risers. *DNV-OS-F201.* Det Norske Veritas.

DNV 2010b. *Recommended Practice, Fatigue Design of Offshore Steel Structures*.

DNV 2015. Rules for Classification of Ships, Part 3 Hull and Equipment -Main Class, Chapter 1, Hull structural design -Ships with length 100 metres and above, Section 16 Fatigue Control. Oslo: Det Norske Veritas.

Dong, P. 2001. A Practical Stress Definition and Numerical Implementation for Fatigue Analyses. *International Journal of Fatigue,* 23**,** 865-876.

Dong, P. 2005. A robust structural stress method for fatigue analysis of offshore/marine structures. *Journal of Offshore Mechanics and Arctic Engineering-Transactions of the ASME,* 127**,** 68-74.

Dong, P. 2010. The Master SN Curve Method an Implementation for Fatigue Evaluation of Welded Components in the ASME B&PV Code. *Section VIII, Division 2 and API 579-1/ASME FFS-1.*

Dong, P., Pei, X., Xing, S. & Kim, M. H. 2014. A structural strain method for low-cycle fatigue evaluation of welded components. *International Journal of Pressure Vessels and Piping,* 119**,** 39-51.

Dong, P., Xing, S. & Zhou, W. 2017a. Analytical treatment of welding distortion effects on fatigue in thin panels: Part I – closed-form solutions and implications. *In:* Guedes Soares, C. & Teixeira, A. (eds.) *Maritime Transportation and Harvesting of Sea Resources.*

Dong, P., Zhou, W. & Xing, S. 2017b. Analytical treatment of welding distortion effects on fatigue in thin panels: Part II – applications in test data analysis. *In:* Guedes Soares, C. & Teixeira, A. (eds.) *Maritime Transportation and Harvesting of Sea Resources.*

Dong, P. S., Wei, Z. G. & Hong, J. K. 2010. A path-dependent cycle counting method for variable-amplitude multi-axial loading. *International Journal of Fatigue,* 32**,** 720-734.

Dong, Q., Yang, P., Xu, G. & Deng, J. L. 2016. Mechanisms and modelling of low cycle fatigue crack propagation in a pressure vessel steel Q345. *International Journal of Fatigue,* 89**,** 2-10.

Dong, Y. & Frangopol, D. M. 2015. Risk-informed life-cycle optimum inspection and maintenance of ship structures considering corrosion and fatigue. *Ocean Engineering,* 101**,** 161-171.

Dong, Y. & Frangopol, D. M. 2016. Incorporation of risk and updating in inspection of fatigue-sensitive details of ship structures. *International Journal of Fatigue,* 82**,** 676-688.

Dong, Y. & Guedes Soares, C., 2015a, Estimation of effective notch strain for fatigue strength assessment of welded structures under multiaxial stress state, *In:* Guedes Soares, C., Dejhalla, R. & Pavletic, D., eds., Towards Green Marine Technology and Transport, Taylor & Francis Group, London, UK, 397-406.

Dong, Y. & Guedes Soares, C., 2015b, On the fatigue crack initiation point of load-carrying fillet welded joints, *In:* Guedes Soares, C., Dejhalla, R. & Pavletic, D., eds., Towards Green Marine Technology and Transport, Taylor & Francis Group, London, UK, 407-406.

Dong, Y. & Guedes Soares, C. 2017. Uncertainty analysis of local strain and fatigue crack initiation life of welded joints under plane strain condition. *In:* Guedes Soares, C. & Garbatov, Y. (eds.) *Progress in the Analysis and Design of Marine Structures.* Taylor & Francis Group, London, UK.

Doremus, L., Nadot, Y., Henaff, G., Mary, C. & Pierret, S. 2015. Calibration of the potential drop method for monitoring small crack growth from surface anomalies - Crack front marking technique and finite element simulations. *International Journal of Fatigue,* 70**,** 178-185.

Doshi, K., Roy, T. & Parihar, Y. S. 2017. Reliability-based inspection planning using fracture mechanics based fatigue evaluations for ship structural details. *Marine Structures,* 54**,** 1-22.

Dragt, R. C., Maljaars, J. & Tuitman, J. T., 2016, Including Load Sequence Effects in the Fatigue Damage Estimation of an Offshore Wind Turbine Substructure, Proceedings of the 26th International Ocean and Polar Engineering Conference Rhodes, Greece, Paper ISOPE-I-16-653.

Du, J. F., Li, H. J., Zhang, M. & Wang, S. Q. 2015. A novel hybrid frequency-time domain method for the fatigue damage assessment of offshore structures. *Ocean Engineering,* 98**,** 57-65.

Dubey, G. & Kumar, S. 2016. Improvement in the numerical method for integrating weight function of pre-cracked specimen. *Engineering Fracture Mechanics,* 154**,** 83-91.

Dubois, J., Thieken, K., Terceros, M., Schaumann, P. & Achmus, M., 2016, Advanced Incorporation of Soil-Structure Interaction into Integrated Load Simulation, Proceedings of the 26th International Ocean and Polar Engineering Conference, Rhodes, Greece, Paper ISOPE-I-16-570.

Durodola, J. F., Li, N., Ramachandra, S. & Thite, A. N. 2017. A pattern recognition artificial neural network method for random fatigue loading life prediction. *International Journal of Fatigue,* 99**,** 55-67.

Eder, M. A., Branner, K., Berring, P., Belloni, F., Toft, H. S., Sørensen, J. D., Corre, A., Lindby, T., Quispitup, A. & Petersen, T. K. 2015. Experimental Blade Research - phase 2. DTU Wind Energy.

Elber, W. 1971. The Significance of Fatigue Crack Closure. *Damage and Tolerance in Aircraft Structure,* 485**,** 230-242.

Elosta, H., Huang, S. & Incecik, A. 2014. Wave loading fatigue reliability and uncertainty analyses for geotechnical pipeline models. *Ships and Offshore Structures,* 9**,** 450-463.

Erice, B., Roth, C. C. & Mohr, D. 2017. Stress-state and strain-rate dependent ductile fracture of dual and complex phase steel. *Mechanics of Materials,* Article in press.

Ewest, D., Almroth, P., Sjodin, B., Simonsson, K., Leidermark, D. & Moverare, J. 2016. A modified compliance method for fatigue crack propagation applied on a single edge notch specimen. *International Journal of Fatigue,* 92**,** 61-70.

Ezanno, A., Doudard, C., Moyne, S., Calloch, S., Millot, T. & Bellevre, D. 2015. Validation of a high-cycle fatigue model via calculation/test comparisons at structural scale: Application to copper alloy sand-cast ship propellers. *International Journal of Fatigue,* 74**,** 38-45.

Feng, G., Wang, D., Garbatov, Y. & Guedes Soares, C. 2015. Reliability analysis based on a direct ship hull strength assessment. *Journal of Marine Science and Application,* 14**,** 389-398.

Feng, G. Q., Garbatov, Y. & Guedes Soares, C. 2012a. Fatigue reliability of a stiffened panel subjected to correlated crack growth. *Structural Safety,* 36-37**,** 39-46.

Feng, G. Q., Garbatov, Y. & Guedes Soares, C. 2012b. Probabilistic model of the growth of correlated cracks in a stiffened panel. *Engineering Fracture Mechanics,* 84**,** 83-95.

Feng, G. Q., Garbatov, Y. & Guedes Soares, C. 2014. Fatigue reliability of deck structures subjected to correlated crack growth. *Journal of Marine Science and Application,* 12**,** 413-421.

Feng, M. L., Ding, F. & Jiang, Y. Y. 2006. A study of loading path influence on fatigue crack growth under combined loading. *International Journal of Fatigue,* 28**,** 19-27.

Ferro, P. 2014. The local strain energy density approach applied to pre-stressed components subjected to cyclic load. *Fatigue & Fracture of Engineering Materials & Structures,* 37**,** 1268-1280.

Fischer, C. & Fricke, W. 2015. Influence of local stress concentrations on the crack propagation in complex welded components. *Frattura Ed Integrita Strutturale,* 38**,** 99-108.

Fischer, C., Fricke, W. & Rizzo, C. M. 2015. Fatigue assessment of joints at bulb profiles by local approaches. *In:* Guedes Soares, C. & Shenoi, A. (eds.) *Analysis and Design of Marine Structures.* London, UK: Taylor & Francis Group.

Fischer, C., Fricke, W. & Rizzo, C. M. 2016a. Experiences and recommendations for numerical analyses of notch stress intensity factor and averaged strain energy density. *Engineering Fracture Mechanics,* 165**,** 98-113.

Fischer, C., Fricke, W. & Rizzo, C. M. 2016b. Fatigue tests of notched specimens made from butt joints at steel. *Fatigue & Fracture of Engineering Materials & Structures,* 39**,** 1526-1541.

Fischer, C., Fricke, W. & Rizzo, C. M. 2016c. Review of the fatigue strength of welded joints based on the notch stress intensity factor and SED approaches. *International Journal of Fatigue,* 84**,** 59-66.

Fitzka, M. & Mayer, H. 2016. Constant and variable amplitude fatigue testing of aluminum alloy 2024-T351 with ultrasonic and servo-hydraulic equipment. *International Journal of Fatigue,* 91**,** 363-372.

Flore, D. & Wegener, K. 2016. Modelling the mean stress effect on fatigue life of fibre reinforced plastics. *International Journal of Fatigue,* 82**,** 689-699.

Formica, G. & Milicchio, F. 2016. Crack growth propagation using standard FEM. *Engineering Fracture Mechanics,* 165**,** 1-18.

Fricke, W. 2003. Fatigue analysis of welded joints: state of development. *Marine Structures,* 16**,** 185-200.

Fricke, W. 2015. Recent developments and future challenges in fatigue strength assessment of welded joints. *Proceedings of the Institution of Mechanical Engineers Part C-Journal of Mechanical Engineering Science,* 229**,** 1224-1239.

Fricke, W., Remes, H., Feltz, O., Lillemae, I., Tchuindjang, D., Reinert, T., Nevierov, A., Sichermann, W., Brinkmann, M., Kontkanen, T., Bohlmann, B. & Molter, L. 2015. Fatigue strength of laser-welded thin-plate ship structures based on nominal and structural hot-spot stress approach. *Ships and Offshore Structures,* 10**,** 39-44.

Fricke, W., Robert, C., Peters, R. & Sumpf, A. 2016. Fatigue strength of laser-stake welded T-joints subjected to combined axial and shear loads. *Welding in the World,* 60**,** 593-604.

Gan, J., Sun, D., Wang, Z., Luo, P. & Wu, W. G. 2016. The effect of shot peening on fatigue life of Q345D T-welded joint. *Journal of Constructional Steel Research,* 126**,** 74-82.

Gandiolle, C., Fouvry, S. & Charkaluk, E. 2016. Lifetime prediction methodology for variable fretting fatigue loading: Plasticity effect. *International Journal of Fatigue,* 92**,** 531-547.

Garbatov, Y. 2016. Fatigue strength assessment of ship structures accounting for a coating life and corrosion degradation. *International Journal of Structural Integrity,* 7**,** 305-322.

Garbatov, Y., Dong, Y., Rörup, J., Vhanmane, S. & Villavicencio, R. 2017. Fatigue reliability of butt-welded joints based on spectral fatigue damage assessment. *In:* Guedes Soares, C. & Teixeira, A. (eds.) *Maritime Transportation and Harvesting of Sea Resources.* London: Taylor & Francis, 611-617.

Garbatov, Y. & Guedes Soares, C. 2017. Fatigue reliability of dented pipeline based on limited experimental data. *International Journal of Pressure Vessels and Piping,* 155**,** 15-26.

Garbatov, Y., Guedes Soares, C. & Masubuchi, K. 2016a. Residual Stresses and Distortion in Welds. *Reference Module in Materials Science and Materials Engineering.* Elsevier, 1-30.

Garbatov, Y., Guedes Soares, C. & Parunov, J. 2014a. Fatigue strength experiments of corroded small-scale steel specimens. *International Journal of Fatigue,* 59**,** 137-144.

Garbatov, Y., Guedes Soares, C., Parunov, J. & Kodvanj, J. 2014b. Tensile strength assessment of corroded small-scale specimens. *Corrosion Science,* 85**,** 296-303.

Garbatov, Y., Parunov, J., Kodvanj, J., Saad-Eldeen, S. & Guedes Soares, C. 2016b. Experimental assessment of tensile strength of corroded steel specimens subjected to sandblast and sandpaper cleaning. *Marine Structures,* 49**,** 18-30.

Garcia, C., Lotz, T., Martinez, M., Artemev, A., Alderliesten, R. & Benedictus, R. 2016. Fatigue crack growth in residual stress fields. *International Journal of Fatigue,* 87**,** 326-338.

Gates, N. & Fatemi, A. 2014. Notched fatigue behaviour and stress analysis under multiaxial states of stress. *International Journal of Fatigue,* 67**,** 2-14.

Gates, N. & Fatemi, A. 2016. Multiaxial variable amplitude fatigue life analysis including notch effects. *International Journal of Fatigue,* 91**,** 337-351.

Gaur, V., Doquet, V., Persent, E., Mareau, C., Roguet, E. & Kittel, J. 2016. Surface versus internal fatigue crack initiation in steel: Influence of mean stress. *International Journal of Fatigue,* 82**,** 437-448.

Ghaffari, M. A., Pahl, E. & Xiao, S. P. 2015. Three-dimensional fatigue crack initiation and propagation analysis of a gear tooth under various load conditions and fatigue life extension with boron/epoxy patches. *Engineering Fracture Mechanics,* 135**,** 126-146.

Ghahremani, K., Walbridge, S. & Topper, T. 2015. High cycle fatigue behaviour of impact treated welds under variable amplitude loading conditions. *International Journal of Fatigue,* 81**,** 128-142.

Ghahremani, K., Walbridge, S. & Topper, T. 2016. A methodology for variable amplitude fatigue analysis of HFMI treated welds based on fracture mechanics and small-scale experiments. *Engineering Fracture Mechanics,* 163**,** 348-365.

GL 2015. Rules for Classification and Construction, I - Ship Technology, Part 1: Seagoing Ships, Chapter 1 - Hull Structures. Hamburg: Germanischer Lloyd.

Godani, M., Gaiotti, M. & Rizzo, C. M. 2014. Interlaminar shear strength of marine composite laminates: Tests and numerical simulations. *Composite Structures,* 112**,** 122-133.

Godani, M., Gaiotti, M. & Rizzo, C. M., 2015, Influence of air inclusions on the marine composites inter-laminar shear strength, Proceedings of the 25th International Ocean and Polar Engineering Conference, Kona, Hawaii Big Island.

Gonzales, G. L. G., Gonzalez, J. A. O., Castro, J. T. P. & Freire, J. L. F. 2017. A J-integral approach using digital image correlation for evaluating stress intensity factors in fatigue cracks with closure effects. *Theoretical and Applied Fracture Mechanics,* 90**,** 14-21.

Gotoh, K., Niwa, T. & Anai, Y. 2015. Numerical simulation of fatigue crack propagation under biaxial tensile loadings with phase differences. *Marine Structures,* 42**,** 53-70.

Greaves, P. R., Dominy, R. G., Ingram, G. L., Long, H. & Court, R. 2011. Evaluation of dual-axis fatigue testing of large wind turbine blades. *Journal of Mechanical Engineering Science,* 226**,** 1693-1704.

Greaves, P. R., Prieto, R., Gaffing, J., van Beveren, C., Dominy, R. & Ingram, G. 2016. A novel method of strain - bending moment calibration for blade testing. *Journal of Physics: Conference Series 753*.

Gruben, G., Morin, D., Langseth, M. & Hopperstad, O. S. 2017. Strain localization and ductile fracture in advanced high-strength steel sheets. *European Journal of Mechanics a-Solids,* 61**,** 315-329.

Guida, M. & Penta, F. 2015. A gamma process model for the analysis of fatigue crack growth data. *Engineering Fracture Mechanics,* 142**,** 21-49.

Haagensen, P. J. & Maddox, S. J. 2013. *IIW Recommendations on methods for improving the fatigue strength of welded joints: doc. IIW-2142-110,* Paris (France), International Institute of Welding, Woodhead Publishing.

Hammersley, J. & Handscomb, D. 1975. *Monte Carlo Methods,* London, Methuen.

Hao, H., Ye, D. Y., Chen, Y. Z., Mi, F. & Liu, J. Z. 2015. A study on the mean stress relaxation behaviour of 2124-T851 aluminum alloy during low-cycle fatigue at different strain ratios. *Materials & Design,* 67**,** 272-279.

Harati, E., Karlsson, L., Svensson, L. E. & Dalaei, K. 2015. The relative effects of residual stresses and weld toe geometry on fatigue life of weldments. *International Journal of Fatigue,* 77**,** 160-165.

Harati, E., Ottosson, M., Karlsson, L. & Svensson, L. E., 2014, Non-destructive measurement of weld toe radius using Weld Impression Analysis, Laser Scanning Profiling and Structures Light Projection methods, Proceedings of the First International Conference of Welding Non-destructive Testing, Teheran, Iran.

Harati, E., Svensson, L., Karlsson, L. & Widmark, M. 2016a. Effect of high-frequency mechanical impact treatment on fatigue strength of welded 1300MPa yield strength steel. *International Journal of Fatigue***,** 96-106.

Harati, E., Svensson, L. E., Karlsson, L. & Hurtig, K. 2016b. Effect of HFMI treatment procedure on weld toe geometry and fatigue properties of high strength steel welds. *21st European Conference on Fracture, (Ecf21),* 2**,** 3483-3490.

Harkegard, G. 2015. Short-crack modelling of the effect of corrosion pits on the fatigue limit of 12% Cr steel. *Fatigue & Fracture of Engineering Materials & Structures,* 38**,** 1009-1016.

Harper, P. W. & Hallett, S. R. 2015. Advanced numerical modelling techniques for the structural design of composite tidal turbine blades. *Ocean Engineering,* 96**,** 272-283.

Hashemzadeh, M., Chen, B. Q. & Guedes Soares, C. 2014. Numerical and experimental study on butt weld with dissimilar thickness of thin stainless steel plate. *The International Journal of Advanced Manufacturing Technology,* 78**,** 319-330.

Hashemzadeh, M., Garbatov, Y. & Guedes Soares, C. 2015a. Numerical Investigation of the Thermal Fields due to the Welding Sequences of Butt-welds. *In:* Guedes Soares, C. & Santos, T. A. (eds.) *Maritime Technology and Engineering.* London, UK: Taylor & Francis Group, 533-543.

Hashemzadeh, M., Garbatov, Y. & Guedes Soares, C. 2015b. Reduction in weld induced distortions of butt welded plates subjected to preventive measures. *In:* Guedes Soares, C. & Shenoi, A. (eds.) *Analysis and Design of Marine Structures V.* London, UK: Taylor & Francis Group, 581-588.

Hashemzadeh, M., Garbatov, Y. & Guedes Soares, C. 2016. Reduction in welding induced residual stresses and distortions of butt welded plates subjected to heat treatments. *In:* Guedes Soares, C. & Santos, T. (eds.) *Maritime Technology and Engineering.* London: Taylor & Francis Group, 481-488.

Hashemzadeh, M., Garbatov, Y. & Guedes Soares, C. 2017a. Analytically based equations for distortion and residual stress estimations of thin butt-welded plates. *Engineering Structures,* 137**,** 115-124.

Hashemzadeh, M., Garbatov, Y. & Guedes Soares, C. 2017b. Assessment of distortion and residual stresses in butt-welded plates made of different steels. *In:* Guedes Soares, C. & Teixeira, A. (eds.) *Maritime Transportation and Harvesting of Sea Resources.* 617-625.

Hashemzadeh, M., Garbatov, Y. & Guedes Soares, C. 2017c. Distortions and residual stress analysis of thin butt welded plates accounting for manufacturing imperfections. *In:* Guedes Soares, C. & Garbatov, Y. (eds.) *Progress in the Analysis and Design of Marine Structures.* London: Taylor & Francis Group, 623-630.

Hauteclocque, G., Monroy, C. & Bigot, F., 2016, New rules for container-ships Formulae for wave Loads, Proceedings of the 13th International Symposium on Practical design of ships and other floating structures, Copenhagen, Denmark.

He, W. T., Liu, J. X. & Xie, D. 2015. Probabilistic life assessment on fatigue crack growth in mixed-mode by coupling of Kriging model and finite element analysis. *Engineering Fracture Mechanics,* 139**,** 56-77.

Hifi, N. & Barltrop, N. 2015. Correction of prediction model output for structural design and risk-based inspection and maintenance planning. *Ocean Engineering,* 97**,** 114-125.

Hobbacher, A. 2009. *Recommendations for Fatigue Design of Welded Joints and Components, IIW doc.1823-07, Welding Research Council Bulletin 520,* New York, International Institute of Welding.

Hobbacher, A. 2010. New developments at the recent update of the IIW recommendations for fatigue of welded joints and components. *Steel Construction,* 4**,** 231-242.

Hobbacher, A. 2013. IIW recommendations for fatigue design of welded joints and components, IIW-doc. XIII-2460-13.

Hobbacher, A. 2016. *Recommendations for fatigue design of welded joints and components,* Switzerland, Springer International.

Hobbacher, A. & Kassner, M. 2012. On Relation between Fatigue Properties of Welded Joints, Quality Criteria and Groups in ISO 5817. *Welding in the World,* 56**,** 153-169.

Hodapp, D. P., Collette, M. D. & Troesch, A. W. 2015. Stochastic nonlinear fatigue crack growth predictions for simple specimens subject to representative ship structural loading sequences. *International Journal of Fatigue,* 70**,** 38-50.

Hogben, N., Da Cunha, L. F. & Ollivier, H. N. 1986. *Global Wave Statistics*, Urwin Brothers Limited.

Holmstrand, T., Mrdjanov, N., Barsoum, Z. & Astrand, E. 2014. Fatigue life assessment of improved joints welded with alternative welding techniques. *Engineering Failure Analysis,* 42**,** 10-21.

Horn, G. E., Arima, T., Baumans, P., Bøe, A. & Ocakli, H., 2013, IACS Summary of the IMO GBS and the Harmonised Common Structural Rules, TSCF 2013 Shipbuilders Meeting.

Horn, H. & Jensen, J., 2016, Reducing uncertainty of Monte Carlo estimated fatigue damage in offshore wind turbines using FORM, Proceedings of the 13th International Symposium on Practical design of ships and other floating structures, Copenhagen, Denmark.

Hos, Y., Freire, J. L. F. & Vormwald, M. 2016. Measurements of strain fields around crack tips under proportional and non-proportional mixed-mode fatigue loading. *International Journal of Fatigue,* 89**,** 87-98.

Hosdez, J., Witz, J. F., Martel, C., Limodin, N., Najjar, D., Charkaluk, E., Osmond, P. & Szmytka, F. 2017. Fatigue crack growth law identification by Digital Image Correlation and electrical potential method for ductile cast iron. *Engineering Fracture Mechanics,* 182**,** 577-594.

Huang, T. D., Harbison, M., Kvidahl, L., Niolet, D., Walks, J., Christein, J. P., Smitherman, M., Phillippi, M., Dong, P. S., DeCan, L., Caccese, V., Blomquist, P., Kihl, D., Wong, R., Sinfield, M., Nappi, N., Gardner, J., Wong, C., Bjornson, M. & Manuel, A. 2016. Reduction of Overwelding and Distortion for Naval Surface Combatants. Part 2: Weld Sizing Effects on Shear and Fatigue Performance. *Journal of Ship Production and Design,* 32**,** 21-36.

Huang, T. D., Harbison, M., Kvidahl, L., Niolet, D., Walks, J., Stefanick, K., Phillippi, M., Dong, P., DeCan, L., Caccese, V., Blomquist, P., Kihl, D., Wong, R., Nappi, N., Gardner, J., Wong, C., Bjornson, M. & Manuel, A. 2014a. Reduction of Overwelding and Distortion for Naval Surface Combatants, Part 1: Optimized Weld Sizing for Lightweight Ship Structures. *Journal of Ship Production and Design,* 30**,** 184-193.

Huang, W., Garbatov, Y. & Guedes Soares, C. 2012. Fatigue damage assessment of stiffener-frame structures. *In:* Guedes Soares, C., Garbatov, Y., Sutulo, S. & Santos, T. (eds.) *Maritime Technology and Engineering.* London, UK: Taylor & Francis Group.

Huang, W., Garbatov, Y. & Guedes Soares, C. 2013. Fatigue reliability assessment of a complex welded structure subjected to multiple cracks. *Engineering Structures,* 56**,** 868-879.

Huang, W., Garbatov, Y. & Guedes Soares, C. 2014b. Fatigue reliability assessment of correlated welded web-frame joints. *Journal of Marine Science and Application,* 13**,** 23-31.

Huang, W., Garbatov, Y. & Guedes Soares, C. 2014c. Fatigue reliability of a web frame subjected to random non-uniform corrosion wastage. *Structural Safety,* 48**,** 51-62.

Huang, W. & Sridhar, N. 2016. Fatigue Failure Risk Assessment for a Maintained Stiffener-Frame Welded Structure with Multiple Site Cracks. *International Journal of Applied Mechanics,* 8.

Huffman, P. J. 2016. A strain energy based damage model for fatigue crack initiation and growth. *International Journal of Fatigue,* 88**,** 197-204.

Hughes, S., Musial, W. & Stensland, T., 1999, Implementation of two axes servo-hydraulic system for full-scale testing of wind turbine blades., Proceedings in Windpower, 67–76.

Hwang, M.-R., Lee, T.-K., Kang, D.-H. & Suh, Y. S., 2016, A Study on Ice-induced Fatigue Life Estimation Based on Measured Data of the AR-AON, Proceedings of the 26th International Ocean and Polar Engineering Conference, Rhodes, Greece, Paper ISOPE-I-16-486.

Hyunchul, J., Kyoung, J., Kim, J. W., Yan, H. & Wu, G., 2017, CFD of fully coupled mooring and riser effects on vortex-induced motion of semi-submersible Proceedings of the 36th International Conference on Ocean, Offshore and Arctic Engineering, Trondheim, Norway, Paper OMAE2017-62433.

IACS 1989. Longitudinal Strength Standard, IACS Unified Requirement S11. London: International Association of Classification Societies.

IACS 1999. Fatigue assessment of ship structures IACS Recommendation No. 56. London: International Association of Classification Societies.

IACS 2001. Standard Wave Data. *Recommendation 34.*

IACS 2012. Common Structure Rules for Double Hull Oil Tankers, Consolidated version, July 2012.

IACS 2014a. Equivalent Design Wave (EDW) for Fatigue Loads, *Technical Background report for the Harmonized Common Structural Rules.*

IACS 2014b. Hull girder vibration. *Technical Background report for the development of the CSR.*

IACS 2015. Common Structural Rules for Bulk Carriers and Oil Tankers. London: International Association of Classification Societies.

IACS. 2016. *Technical Background Documents for CSR* [Online]. http://www.iacs.org.uk/publications/. [Accessed 1 October 2016.

Ibrahim, R. A. 2015a. Overview of Structural Life Assessment and Reliability, Part I: Basic Ingredients of Fracture Mechanics. *Journal of Ship Production and Design,* 31**,** 1-42.

Ibrahim, R. A. 2015b. Overview of Structural Life Assessment and Reliability, Part II: Fatigue Life and Reliability Assessment of Naval Ship Structures. *Journal of Ship Production and Design,* 31**,** 100-128.

Ibrahim, R. A. 2015c. Overview of Structural Life Assessment and Reliability, Part III: Impact, Grounding, and Reliability of Ships under Extreme Loading. *Journal of Ship Production and Design,* 31**,** 137-169.

Ibrahim, R. A. 2015d. Overview of Structural Life Assessment and Reliability, Part IV: Corrosion and Hydrogen Embrittlement of Naval Ship Structures. *Journal of Ship Production and Design,* 31**,** 241-263.

Ibrahim, R. A. 2016a. Overview of Structural Life Assessment and Reliability, Part V: Joints and Weldments. *Journal of Ship Production and Design,* 32**,** 1-20.

Ibrahim, R. A. 2016b. Overview of Structural Life Assessment and Reliability, Part VI: Crack Arresters. *Journal of Ship Production and Design,* 32**,** 71-98.

IEC-61400-23 2014. Wind turbines - Part 23: Full-scale structural testing of rotor blades. Geneva, Switzerland.

IGC 2014. Annex 6 Resolution MSC.370(93): Amendments to the International code for the construction and equipment of ships carrying liquefied gases in bulk IGC Code.

Ilman, M. N., Kusmono, Muslih, M. R., Subeki, N. & Wibowo, H. 2016. Mitigating distortion and residual stress by static thermal tensioning to improve fatigue crack growth performance of MIG AA5083 welds. *Materials & Design,* 99**,** 273-283.

Im, H.-I., Vladimir, N., Malenica, S., Ryu, H. R. & Cho, D. S., 2015, Fatigue Analysis of HHI Sky Bench 19000 TEU ultra-large container ship with springing effect included, Proceedings of the 7th International Conference on Hydroelasticity in Marine Technology, Split, Croatia.

IMO. 2015. *Focus on IMO - International goal-based ship construction standards for bulk carriers and oil tankers* [Online]. http://www.imo.org/en/OurWork/Safety/SafetyTopics/Pages/Goal-BasedStandards.aspx. [Accessed 1 October 2016.

Ince, A. & Glinka, G. 2016. Innovative computational modelling of multiaxial fatigue analysis for notched components. *International Journal of Fatigue,* 82**,** 134-145.

IRS 2016a. Rules and Regulation for the construction and classification of steel ships. Mumbai: IRS.

IRS 2016b. Rules for Bulk carriers and Oil tankers. Mumbai: IRS.

ISO5817 2014. Welding - Fusion-welded joints in steel, nickel, titanium and their alloys (beam welding excluded) - Quality levels for imperfections.

ISO12932 2013. Welding. Laser-arc hybrid welding of steels, nickel and nickel alloys. Quality levels for imperfections.

ISO13919-1 1996. Welding - Electron and laser-beam welded joints - Guidance on quality levels for imperfections - Part 1: Steel.

Jandejsek, I., Gajdos, L., Sperl, M. & Vavrik, D. 2017. Analysis of standard fracture toughness test based on digital image correlation data. *Engineering Fracture Mechanics,* 182**,** 607-620.

Jaouën, F., Waals, O., Jong, M. d., Hout, A. v. d. & Christou, M., 2016, Methodology for the Design on LNG Terminals in Nearshore Environment, Proceedings of the 35th International Conference on Ocean, Offshore and Arctic Engineering, Busan, Korea, Paper OMAE2016-54724.

Jensen, J. J. 2015. Fatigue damage estimation in nonlinear systems using a combination of Monte Carlo simulation and the First Order Reliability Method. *Marine Structures,* 44**,** 203-210.

Ji, C. Y., Xue, H. Z., Shi, X. H. & Gaidai, O. 2016. Experimental and numerical study on collapse of aged jacket platforms caused by corrosion or fatigue cracking. *Engineering Structures,* 112**,** 14-22.

Jiameng, W., Gang, W. & Shijian, C., 2016, Ramification Study on IACS Harmonized Common Structural Rules: Impact on Structural Design and Scantlings, SNAME Maritime Convention, Houston Texas (USA), SNAME, 124-143.

Jiang, C., Liu, Z. C., Wang, X. G., Zhang, Z. & Long, X. Y. 2016. A structural stress-based critical plane method for multiaxial fatigue life estimation in welded joints. *Fatigue & Fracture of Engineering Materials & Structures,* 39**,** 372-383.

Jones, R. 2014. Fatigue crack growth and damage tolerance. *Fatigue & Fracture of Engineering Materials & Structures,* 37**,** 463-483.

Jonson, B., Dobmann, G., Hobbacher, A., Kassner, M. & Marquis, G. 2016a. *IIW guidelines on weld quality in relationship to fatigue strength,* IIW Paris, IIW Collection.

Jonson, B., Dobmann, G., Hobbacher, A., Kassner, M. & Marquis, G. 2016b. *IW Guidelines on Weld Quality in Relationship to Fatigue Strength*, Springer.

Jonson, B., Samuelsson, J. & Marquis, G. B. 2011. Development of Weld Quality Criteria Based on Fatigue Performance. *Welding in the World,* 55**,** 79-88.

Kahl, A., Fricke, W., Paetzold, H. & von Selle, H. 2015. Whipping Investigations Based on Large-Scale Measurements and Experimental Fatigue Testing. *International Journal of Offshore and Polar Engineering,* 25**,** 247-254.

Kainuma, S., Yang, M. Y., Jeong, Y. S., Inokuchi, S., Kawabata, A. & Uchida, D. 2016. Experiment on fatigue behaviour of rib-to-deck weld root in orthotropic steel decks. *Journal of Constructional Steel Research,* 119**,** 113-122.

Karatzas, V. A., Kotsidis, E. A. & Tsouvalis, N. G. 2015. Experimental Fatigue Study of Composite Patch Repaired Steel Plates with Cracks. *Applied Composite Materials,* 22**,** 507-523.

Karlsson, J., Podgorski, K. & Rychlik, I. 2016. The Laplace multi-axial response model for fatigue analysis. *International Journal of Fatigue,* 85**,** 11-17.

Karolczuk, A., Kluger, K. & Lagoda, T. 2016. A correction in the algorithm of fatigue life calculation based on the critical plane approach. *International Journal of Fatigue,* 83**,** 174-183.

Karr, D., Baloglu, P., Cao, T., Douglas, A., K., N., Ong, K. T., Rohrback, B. & N., S. 2015. *Strength and fatigue testing of composite patches for ship plating fracture repair,* www.shipstructures.org.

Karr, D., Douglas, A., Ferrari, C., Cao, T., Ong, K., Si, N., He, J., Baloglu, C., White, P. & Parra-Montesinos, G. 2016. Fatigue testing of composite patches for ship plating fracture repair. *Ships and Offshore Structures*.

Kennedy, S., Kong, J. S. K., Notaro, G., Brinchmann, K., Kaur, J., Hwang, O., Lim, J., Khoo, C. & Chow, W. H., 2016, Dropped Object SPS Impact Protection Deck for Well Bay Area, Proceedings of the 13th International Symposium on Practical design of ships and other floating structures, Copenhagen, Denmark.

Khalij, L., Gautrelet, C. & Guillet, A. 2015. Fatigue curves of a low carbon steel obtained from vibration experiments with an electrodynamic shaker. *Materials & Design,* 86**,** 640-648.

Khurshid, M., Barsoum, Z., Barsoum, I. & Dauwel, T. 2016. The multiaxial weld root fatigue of butt welded joints subjected to uniaxial loading. *Fatigue & Fracture of Engineering Materials & Structures,* 39**,** 1281-1298.

Kim, Y., Oh, J. S. & Jeon, S. H. 2015. Novel hot spot stress calculations for welded joints using 3D solid finite elements. *Marine Structures,* 44**,** 1-18.

Kitagawa, H. & Takahashi, S., 1976, Applicability of fracture mechanics to very small cracks or cracks in the early stage, Proceedings of the 2nd International Conference on Mechanical Behaviour of Materials, ASM, 627-631.

Koop, A., de Wilde, J., Condino Fujarra, A. L., Rijken, O., Linder, S., Lennblad, J., Haug, N. & Phadke, A., 2016, Investigation on the reasons for possible difference between VIM response in the field and in model tests, Proceedings of the 35th International Conference on Ocean, Offshore and Arctic Engineering, Busan, Korea, Paper OMAE2016-54746.

Kõrgesaar, M., Romanoff, J. & Remes, H. 2017. Influence of material non-linearity on load carrying mechanism and strain path in stiffened panel. *Procedia Structural Integrity,* 5**,** 713-720.

Korhonen, E., Remes, H., Romanoff, J., Niemela, A., Hiltunen, P. & Kontkanen, T. 2013. Influence of surface integrity on the fatigue strength of high strength steel in balcony openings of cruise ship structures. *In:* Guedes Soares, C. & Shenoi, A. (eds.) *Analysis and Design of Marine Structures* London, UK: Taylor & Francis Group, 255-261.

Krairi, A., Doghri, I. & Robert, G. 2016. Multiscale high cycle fatigue models for neat and short fiber reinforced thermoplastic polymers. *International Journal of Fatigue,* 92**,** 179-192.

Krewerth, D., Lippmann, T., Weidner, A. & Biermann, H. 2015. Application of full-surface view in situ thermography measurements during ultrasonic fatigue of cast steel G42CrMo4. *International Journal of Fatigue,* 80**,** 459-467.

Krzyzak, D., Robak, G. & Lagoda, T. 2015. Determining fatigue life of bent and tensioned elements with a notch, with use of fictitious radius. *Fatigue & Fracture of Engineering Materials & Structures,* 38**,** 693-699.

Lahuerta, F., de Ruiter, M. J., Espinosa, L., Koorn, N. & Smissaert, D., 2017, Assessment of wind turbine blade trailing edge failure with sub-component tests, Proceedings of the 21st International Conference on Composite Materials.

Lang, R. & Lener, G. 2016. Application and comparison of deterministic and stochastic methods for the evaluation of welded components' fatigue lifetime based on real notch stresses. *International Journal of Fatigue,* 93**,** 184-193.

Lassen, T. 1990. The Effect of the Welding Process on the Fatigue Crack-Growth. *Welding Journal,* 69**,** S75-S81.

Lassen, T. & Recho, N., 2015, Risk-Based Inspection Planning for Fatigue Damage in Offshore Steel Structures, Proceedings of the International Conference on Offshore Mechanics and Arctic Engineering.

Lee, C. H., Chang, K. H. & Do, V. N. V. 2016. Modelling the high cycle fatigue behaviour of T-joint fillet welds considering weld-induced residual stresses based on continuum damage mechanics. *Engineering Structures,* 125**,** 205-216.

Lee, Y., White, N., Wang, Z., Tong, J., Xiao, Y. & Qihua, L., 2014, Springing Loads and Fatigue Assessment on Large Container Ships, Proceedings of the 24th International Ocean and Polar Engineering Conference Busan Korea, Paper ISOPE-I-14-339.

Lefebre, G., 1993 1993, Extra-High-Strength Grades: The Steel for Tomorrow Offshore Application?, Proceedings of the 12th International Conference on Offshore Mechanics and Arctic Engineering, ASME, New York, USA, 199-205.

Leitner, M., Gerstbrein, S., Ottersbock, M. & Stoschka, M. 2015a. Fatigue strength of HFMI-treated and stress-relief annealed high-strength steel weld joints. *Fatigue Design.* 477-484.

Leitner, M., Gerstbrein, S., Ottersbock, M. J. & Stoschka, M. 2015b. Fatigue strength of HFMI-treated high-strength steel joints under constant and variable amplitude block loading. *3rd International Conference on Material and Component Performance under Variable Amplitude Loading, Val 2015,* 101**,** 251-258.

Leitner, M., Khurshid, M. & Barsoum, Z. 2017. Stability of high-frequency mechanical impact (HFMI) post-treatment induced residual stress states under cyclic loading of welded steel joints. *Engineering Structures,* 143**,** 589-602.

Leitner, M., Simunek, D., Shah, S. & Stoschka, M. 2016. Numerical fatigue assessment of welded and HFMI-treated joints by notch stress/strain and fracture mechanical approaches. *Advances in Engineering Software*.

Li, B. 2015. A new approach of fatigue life prediction for metallic materials under multiaxial loading. *International Journal of Fatigue,* 78.

Li, B. C., Jiang, C., Han, X. & Li, Y. 2014a. A new path-dependent multiaxial fatigue model for metals under different paths. *Fatigue & Fracture of Engineering Materials & Structures,* 37**,** 206-218.

Li, H., Yuan, H. & Li, X. 2015a. Assessment of low cycle fatigue crack growth under mixed-mode loading conditions by using a cohesive zone model. *International Journal of Fatigue,* 75**,** 39-50.

Li, W., Deng, H. L., Sun, Z. D., Zhang, Z. Y., Lu, L. T. & Sakai, T. S. 2015b. Subsurface inclusion-induced crack nucleation and growth behaviours of high strength steels under very high cycle fatigue: Characterization and microstructure-based modelling. *Materials Science and Engineering a-Structural Materials Properties Microstructure and Processing,* 641**,** 10-20.

Li, X., Guan, Z. D., Li, Z. S. & Liu, L. 2014b. A new stress-based multi-scale failure criterion of composites and its validation in open hole tension tests. *Chinese Journal of Aeronautics,* 27**,** 1430-1441.

Li, Y., Chen, Y., Shi, Z., Xie, W. & Ni, K., 2015c, Study on Global Fatigue Analysis for Deep-water Tension-Leg Platform Based on Simplified Spectral Method, Proceedings of the 25th International Ocean and Polar Engineering Conference Hawaii, USA, Paper ISOPE-I-15-229.

Liao, P. K., Lee, Y. J., Lin, H. J., Tsai, S. C., Chien, H. L., Chang, B. C. & Luo, G. M. 2015. Springing effect on the fatigue life of an 8000 TEU container ship. *In:* Shenoi, G. S. (ed.) *Analysis and Design of Marine Structures.* UK.

Liinalampi, S., Remes, H., Lehto, P., Lillemae, I., Romanoff, J. & Porter, D. 2016. Fatigue strength analysis of laser-hybrid welds in thin plate considering weld geometry in microscale. *International Journal of Fatigue,* 87**,** 143-152.

Lillemäe-Avi, I., Remes, H., Dong, Y., Garbatov, Y., Quéméner, Y., Eggert, L., Sheng, Q. & Yue, J. 2017. Benchmark study on considering welding-induced distortion in structural stress analysis of thin-plate structures. *In:* Guedes Soares, C. & Garbatov, Y. (eds.) *Progress in the Analysis and Design of Marine Structures.* London: Taylor & Francis Group, 387-394.

Lillemäe, I., Liinalampi, S., Remes, H., Avi, E. & Romanoff, J., 2016, Influence of welding distortion on the structural stress in thin deck panels, Proceedings of the 13th International Symposium on Practical design of ships and other floating structures, Copenhagen, Denmark.

Lillemae, I., Liinalampi, S., Remes, H., Itavuo, A. & Niemela, A. 2017. Fatigue strength of thin laser-hybrid welded full-scale deck structure. *International Journal of Fatigue,* 95**,** 282-292.

Liu 2015. A multiaxial HCF life evaluation model for notched structural components. *International Journal of Fatigue,* 80.

Liu, B., Garbatov, Y. & Guedes Soares, C. 2015. Non-linear finite element analysis of crashworthy shields of offshore wind turbine supporting structures. *In:* Guedes Soares, C. & Shenoi, A. (eds.) *Analysis and Design of Marine Structures.* London, UK: Taylor & Francis Group, 693-702.

Liu, G. J., Zhong, B. L., Tian, X. J., Chen, P. F. & Mu, W. L. 2016. Numerical analysis on the HSS and SIF of multi-planar DX-joint welds for offshore platforms. *Ocean Engineering,* 127**,** 258-268.

Liu, Y., Yi, H. & Chen, L. Y. 2014. Submarine pressure hull butt weld fatigue life reliability prediction method. *Marine Structures,* 36**,** 51-64.

Lopez-Crespo, P., Moreno, B., Lopez-Moreno, A. & Zapatero, J. 2015a. Characterisation of crack-tip fields in biaxial fatigue based on high-magnification image correlation and electro-spray technique. *International Journal of Fatigue,* 71**,** 17-25.

Lopez-Crespo, P., Moreno, B., Lopez-Moreno, A. & Zapatero, J. 2015b. Study of crack orientation and fatigue life prediction in biaxial fatigue with critical plane models. *Engineering Fracture Mechanics,* 136**,** 115-130.

Lotsberg, I. 2016. *Fatigue design of marine structures,* New York, United States, Cambridge University Press.

Lotsberg, I., Sigurdsson, G., Fjeldstad, A. & Moan, T. 2016. Probabilistic methods for planning of inspection for fatigue cracks in offshore structures. *Marine Structures,* 46**,** 167-192.

Lou, B., Zhang, S., Tong, J., Wong, S., Cheng, F. & Hirdaris, S. 2015. A fracture mechanics-based approach for the analysis of crack growth at weld joints of ship structures. *In:* Guedes Soares, C. & Shenoi, A. (eds.) *Analysis and Design of Marine Structures.* London, UK: Taylor & Francis Group.

LR 2009. ShipRight Design and Construction: Fatigue Design Assessment - Level 1 Procedure Structural Detail Design Guide. London, UK: Lloyd's Register Group Limited.

LR 2014. ShipRight Design and Construction: Structural Design Assessment - Guidance Notes on the Assessment of Global Design Loads of Large Container Ships and Other Ships Prone to Whipping and Springing. *DRAFT version.* London, UK: Lloyd's Register Group Limited.

LR 2015. ShipRight 2014.2 User Guide FDA Level 2 Spreadsheet. London, UK: Lloyd's Register Group Limited.

LR 2016a. Rules and Regulations for the Classification of Ships. Part 3 Ship Structures (General), Chapter 16 ShipRight Procedures for the Design, Construction and Lifetime Care of Ships. London, UK: Lloyd's Register Group Limited.

LR 2016b. ShipRight 2014.2 User Guide FDA Level 2 Assessment. London, UK: Lloyd's Register Group Limited.

LR 2016c. ShipRight Design and Construction: Fatigue Design Assessment - Application and Notations (Notice 1 and Notice 2). London, UK: Lloyd's Register Group Limited.

LR 2016d. ShipRight Design and Construction: Fatigue Design Assessment - Level 3 Procedure Guidance on Direct Calculations (Notice 1). London, UK: Lloyd's Register Group Limited.

Luque, J. & Straub, D. 2016. Reliability analysis and updating of deteriorating systems with dynamic Bayesian networks. *Structural Safety,* 62**,** 34-46.

Madia, M., Zerbst, U., Beier, H. T. & Schork, B. 2017. The IBESS model - Elements, realisation and validation. *Engineering Fracture Mechanics,* Article in press.

Maheswaran, J. & Siriwardane, S. C. 2016. Fatigue life estimation of tubular joints - a comparative study. *Fatigue & Fracture of Engineering Materials & Structures,* 39**,** 30-46.

Mahmoud, H. & Riveros, G. 2014. Fatigue reliability of a single stiffened ship hull panel. *Engineering Structures,* 66**,** 89-99.

Mahtabi, M. J. & Shamsaei, N. 2016. A modified energy-based approach for fatigue life prediction of super elastic NiTi in presence of tensile mean strain and stress. *International Journal of Mechanical Sciences,* 117**,** 321-333.

Makino, T., Neishi, Y., Shiozawa, D., Kikuchi, S., Okada, S., Kajiwara, K. & Nakai, Y. 2016. Effect of defect shape on rolling contact fatigue crack initiation and propagation in high strength steel. *International Journal of Fatigue,* 92**,** 507-516.

Malikoutsakis, M. & Savaidis, G. 2014. Fatigue assessment of thin-welded joints with pronounced terminations. *Fatigue & Fracture of Engineering Materials & Structures,* 37**,** 782-799.

Malikova, L., Vesely, V. & Seitl, S. 2015. Estimation of the crack propagation direction in a mixed-mode geometry via multi-parameter fracture criteria. *Frattura Ed Integrita Strutturale,* 33**,** 25-32.

Malikova, L., Vesely, V. & Seitl, S. 2016. Crack propagation direction in a mixed mode geometry estimated via multi-parameter fracture criteria. *International Journal of Fatigue,* 89**,** 99-107.

Maljaars, J., Pijpers, R. & Slot, H. 2015. Load sequence effects in fatigue crack growth of thick-walled welded C-Mn steel members. *International Journal of Fatigue,* 79**,** 10-24.

Mao, W. G., Li, Z. Y., Ogeman, V. & Ringsberg, J. W. 2015. A regression and beam theory-based approach for fatigue assessment of containership structures including bending and torsion contributions. *Marine Structures,* 41**,** 244-266.

Marquis, G. & Barsoum, Z. 2014. Fatigue strength improvement of steel structures by high-frequency mechanical impact: proposed procedures and quality assurance guidelines. *Welding in the World,* 58**,** 19-28.

Marquis, G. B., Mikkola, E., Yildirim, H. C. & Barsoum, Z. 2013. Fatigue strength improvement of steel structures by high-frequency mechanical impact: proposed fatigue assessment guidelines. *Welding in the World,* 57**,** 803-822.

Matic, P., Geltmacher, A. & Rath, B. 2015. Computational aspects of steel fracturing pertinent to naval requirements. *Philos Trans A Math Phys Eng Sci,* 373**,** 321-325.

Matsuda, K. & Gotoh, K. 2015. Numerical simulation of fatigue crack propagation under superimposed stress histories containing different frequency components with several mean stress conditions. *Marine Structures,* 41**,** 77-95.

Maximiano, A., Koop, A., de Wilde, J. & Gonçalves, R. T., 2017, Experimental study on the vortex-induced motions (VIM) of a semi-submersible floater in waves, Proceedings of the 36th International Conference on Ocean, Offshore and Arctic Engineering, Trondheim, Norway, Paper OMAE2017-61543.

May, M., Saintier, N., Palin-Luc, T. & Devos, O. 2015. Non-local high cycle fatigue strength criterion for metallic materials with corrosion defects. *Fatigue & Fracture of Engineering Materials & Structures,* 38**,** 1017-1025.

Mayer, H., Fitzka, M. & Schuller, R. 2014. Variable amplitude loading of Al 2024-T351 at different load ratios using ultrasonic equipment. *International Journal of Fatigue,* 60**,** 34-42.

Mei, J. F. & Dong, P. S. 2016. A new path-dependent fatigue damage model for non-proportional multi-axial loading. *International Journal of Fatigue,* 90**,** 210-221.

Mei, J. F. & Dong, P. S. 2017a. An equivalent stress parameter for multi-axial fatigue evaluation of welded components including non-proportional loading effects. *International Journal of Fatigue,* 101**,** 297-311.

Mei, J. F. & Dong, P. S. 2017b. Modelling of path-dependent multi-axial fatigue damage in aluminum alloys. *International Journal of Fatigue,* 95**,** 252-263.

Meneghetti 2015. Averaged SED evaluated rapidly from the singular peak stresses by FEM - cracked components under mixed mode loading. *Theoretical and Applied Fracture Mechanics,* 79.

Meneghetti, G., Campagnolo, A. & Berto, F. 2015. Fatigue strength assessment of partial and full-penetration steel and aluminium butt-welded joints according to the peak stress method. *Fatigue & Fracture of Engineering Materials & Structures,* 38**,** 1419-1431.

Meneghetti, G. & Ricotta, M. 2016. Evaluating the heat energy dissipated in a small volume surrounding the tip of a fatigue crack. *International Journal of Fatigue,* 92**,** 605-615.

Meneghetti, G., Ricotta, M. & Atzori, B. 2016. A two-parameter, heat energy-based approach to analyse the mean stress influence on axial fatigue behaviour of plain steel specimens. *International Journal of Fatigue,* 82**,** 60-70.

Meng, M. Z., Le, H. R., Grove, S. & Rizvi, M. J. 2016. Moisture effects on the bending fatigue of laminated composites. *Composite Structures,* 154**,** 49-60.

Mikheevskiy, S., Glinka, G. & Cordes, T., 2015, Total life approach for fatigue life estimation of welded structures, Proceedings of the 3rd International Conference on Material and Component Performance under Variable Amplitude Loading, Prague, Czech Republic.

Mikkola, E., Marquis, G., Lehto, P., Remes, H. & Hanninen, H. 2016. Material characterization of high-frequency mechanical impact (HFMI)-treated high-strength steel. *Materials & Design,* 89**,** 205-214.

Mikkola, E., Murakami, Y. & Marquis, G. 2015. Equivalent crack approach for fatigue life assessment of welded joints. *Engineering Fracture Mechanics,* 149**,** 144-155.

Mikkola, E. & Remes, H. 2016. Allowable stresses in high-frequency mechanical impact (HFMI)-treated joints subjected to variable amplitude loading. *Welding in the World*.

Mikkola, E., Remes, H. & Marquis, G. 2017. A finite element study on residual stress stability and fatigue damage in high-frequency mechanical impact (HFMI)-treated welded joint. *International Journal of Fatigue,* 94**,** 16-29.

Millwater, H., Wagner, D., Baines, A. & Montoya, A. 2016. A virtual crack extension method to compute energy release rates using a complex variable finite element method. *Engineering Fracture Mechanics,* 162**,** 95-111.

Minoura, M., 2016, Stochastic Sea State Model based on Fourier Series Expansion, Proceedings of the 26th International Ocean and Polar Engineering Conference Rhodes, Greece, Paper ISOPE-I-16-325.

Mohammadi, M., Zehsaz, M., Hassanifard, S. & Rahmatfam, A. 2016a. An evaluation of total fatigue life prediction of a notched shaft subjected to cyclic bending load. *Engineering Fracture Mechanics,* 166**,** 128-138.

Mohammadi, S. F., Galgoul, N. S., Starossek, U. & Videiro, P. M. 2016b. An efficient time-domain fatigue analysis and its comparison to spectral fatigue assessment for an offshore jacket structure. *Marine Structures,* 49**,** 97-115.

Mokhtarishirazabad, M., Lopez-Crespo, P., Moreno, B., Lopez-Moreno, A. & Zanganeh, M. 2017. Optical and analytical investigation of overloads in biaxial fatigue cracks. *International Journal of Fatigue,* 100**,** 583-590.

Nebbia, G., Gaiotti, M., Rizzo, C. M. & Caleo, A. 2015a. Mechanical characterization of yachts and pleasure crafts fillers. *In:* Guedes Soares, C. & Shenoi, A. (eds.) *Analysis and Design of Marine Structures.* London, UK: Taylor & Francis Group, 627-635.

Nebbia, G., Gaiotti, M., Rizzo, C. M., Caleo, A. & Ivaldi, A., 2015b, Mechanical behaviour of fillers: tests and comparisons, Proceedings of Design & Construction of Super & Mega Yachts, Genoa, Italy, Royal Institution of Naval Architects.

Newman, J. C. & Raju, I. S. 1981. An Empirical Stress-Intensity Factor Equation for the Surface Crack. *Engineering Fracture Mechanics,* 15**,** 185-192.

Nguyen, H. Q., Gallimard, L. & Bathias, C. 2015. Numerical simulation of fish-eye fatigue crack growth in very high cycle fatigue. *Engineering Fracture Mechanics,* 135**,** 81-93.

Niesłony, A. & Böhm, M. 2016. Frequency-domain fatigue life estimation with mean stress correction. *International Journal of Fatigue,* 91**,** 373-381.

Nykanen, T. & Bjork, T. 2015. Assessment of fatigue strength of steel butt-welded joints in as-welded condition - Alternative approaches for curve fitting and mean stress effect analysis. *Marine Structures,* 44**,** 288-310.

O'Connor, S. J., Nowell, D. & Dragnevski, K. I. 2016. Measurement of fatigue crack deformation on the macro- and micro-scale: Uniform and non-uniform loading. *International Journal of Fatigue,* 89**,** 66-76.

Ogeman, V., Mao, W. & Ringsberg, J., 2014., Uncertainty in Stress Concentration Factor Computation for Ship Fatigue Design, Proceedings of the 33rd International Conference on Ocean, Offshore and Arctic Engineering, San Francisco, California, USA.

Oh, D. J., Lee, J. M. & Kim, M. H. 2014. Fatigue strength assessment of Invar alloy weld joints using the notch stress approach. *Engineering Failure Analysis,* 42**,** 87-99.

Okada, H., Koya, H., Kawai, H., Li, Y. S. & Osakabe, K. 2016. Computations of stress intensity factors for semi-elliptical cracks with high aspect ratios by using the tetrahedral finite element (fully automated parametric study). *Engineering Fracture Mechanics,* 158**,** 144-166.

Ooi, S. W., Garnham, J. E. & Ramjaun, T. I. 2014. Review: Low transformation temperature weld filler for tensile residual stress reduction. *Materials & Design,* 56**,** 773-781.

Ormberg, H. & Bachynski, E. E., 2015, Sensitivity of Estimated Tower Fatigue to Wind Modeling for a Spar Floating Wind Turbine, Proceedings of the 25th International Ocean and Polar Engineering Conference, Hawaii, USA, Paper ISOPE-I-15-385.

Ottersbock, M. J., Leitner, M., Stoschka, M. & Maurer, W. 2016. Effect of weld defects on the fatigue strength of ultra-high-strength steels. *Xviii International Colloquium on Mechanical Fatigue of Metals (Icmfm Xviii),* 160**,** 214-222.

Pahlavan, L. & Blacquiere, G. 2016. Fatigue crack sizing in steel bridge decks using ultrasonic guided waves. *NDT & E International,* 77**,** 49-62.

Pang, J. H. L., Hoh, H. J., Tsang, K. S., Low, J., Kong, S. C. & Yuan, W. G. 2017. Fatigue crack propagation analysis for multiple weld toe cracks in cut-out fatigue test specimens from a girth welded pipe. *International Journal of Fatigue,* 94**,** 158-165.

Pansart, S., 2015, A new rotor blade standard for high product quality and flexible certification, European Wind Energy Association, Paris, France.

Panwar, S., Sun, S. & Sundararaghavan, V. 2016. Modelling fatigue failure using the variational multiscale method. *Engineering Fracture Mechanics,* 162**,** 290-308.

Park, D.-Y., Tyson, W. & Gravel, J.-F. 2017. CANMET SENT test method, updates and applications. *International Jornal of Pressure Vessels and Piping,* Article in press.

Pedersen, M. M. 2016. Multiaxial fatigue assessment of welded joints using the notch stress approach. *International Journal of Fatigue,* 83**,** 269-279.

Peng, B.-F., Chen, C.-Y. & Llorente, C., 2015, Time History and Spectral Fatigue Analyses of Deepwater Offshore Truss-Spar Platform under In-service and Trans-ocean Tow Conditions, Proceedings of the 25th International Ocean and Polar Engineering Conference, Hawaii, USA, Paper ISOPE-I-15-741.

Polezhayeva, H., Howarth, D., Kumar, M., Ahmad, B. & Fitzpatrick, M. E. 2015a. The effect of compressive fatigue loads on fatigue strength of non-load carrying specimens subjected to ultrasonic impact treatment. *Welding in the World,* 59**,** 713-721.

Polezhayeva, H., Toumpis, A. I., Galloway, A. M., Molter, L., Ahmad, B. & Fitzpatrick, M. E. 2015b. Fatigue performance of friction stir welded marine grade steel. *International Journal of Fatigue,* 81**,** 162-170.

Post, N. 2014. Fatigue Test Design: Scenarios for Biaxial Fatigue Testing of a 60-Meter Wind Turbine Blade. National Renewable Energy Laboratory, NREL/TP-5000-65227.

Proudhon, H., Li, J., Wang, F., Roos, A., Chiaruttini, V. & Forest, S. 2015. 3d simulation of short fatigue crack propagation by finite element crystal plasticity and remeshing. *International Journal of Fatigue,* 82.

Qayyum, F., Shah, M., Shakeel, O., Mukhtar, F., Salem, M. & Rezai-Aria, F. 2016. Numerical simulation of thermal fatigue behaviour in a cracked disc of AISI H-11 tool steel. *Engineering Failure Analysis,* 62**,** 242-253.

Quemener, Y., Liao, P.-K., Lee, C.-F. & Chen, K.-C., 2015, Load uncertainties effects on the fatigue life evaluation by the Common Structural Rules, Proceedings of the 34th International Conference on Ocean, Offshore and Arctic Engineering, Newfoundland, Canada.

Radaj, D. 2015. State-of-the-art review on the local strain energy density concept and its relation to the J-integral and peak stress method. *Fatigue & Fracture of Engineering Materials & Structures,* 38**,** 2-28.

Radaj, D., Lazzarin, P. & Berto, F. 2009a. *Fatigue assessment of welded joints under slit-parallel loading based on strain energy density or notch rounding.*

Radaj, D., Sonsino, C. M. & Fricke, W. 2006. *Fatigue assessment of welded joints by local approaches*, Woodhead publishing.

Radaj, D., Sonsino, C. M. & Fricke, W. 2009b. Recent developments in local concepts of fatigue assessment of welded joints. *International Journal of Fatigue,* 31**,** 2-11.

Reddy, S., Jaswanthsai, V., Madhavan, M. & Kumar, V. 2016. Notch stress intensity factor for center cracked plates with crack stop hole strengthened using CFRP: A numerical study. *Thin-Walled Structures,* 98**,** 252-262.

Remes, H. & Fricke, W. 2014. Influencing factors on fatigue strength of welded thin plates based on structural stress assessment. *Welding in the World,* 58**,** 915-923.

Remes, H., Korhonen, E., Lehto, P., Romanoff, J., Niemelä, A., Hiltunen, P. & Kontkanen, T. 2013. Influence of surface integrity on the fatigue strength of high-strength steels. *Journal of Constructional Steel Research,* 89**,** 21-29.

Remes, H., Peltonen, M., Seppänen, T., Kukkonen, A., Liinalampi, S., Lillemäe, I., Lehto, P., Hänninen, H. & Romanoff, J. 2015. Fatigue strength of welded extra high-strength and thin steel plates. *In:* Guedes Soares, C. & Shenoi, A. (eds.) *Analysis and Design of Marine Structures.* London, UK: Taylor & Francis Group.

Remes, H., Romanoff, J., Lillemae, I., Frank, D., Liinalampi, S., Lehto, P. & Varsta, P. 2017. Factors affecting the fatigue strength of thin-plates in large structures. *International Journal of Fatigue,* 101**,** 397-407.

Rizzo, C. M. 2011. Application of advanced notch stress approaches to assess fatigue strength of ship structural details: literature review. *Report 655, Schriftenreihe Schiffbau.* Hamburg, Germany.: Technische Universität Hamburg-Harburg.

Ronevich, J. A., Somerday, B. P. & Feng, Z. 2017. Hydrogen accelerated fatigue crack growth of friction stir welded X52 steel pipe. *International Journal of Hydrogen Energy,* 42**,** 4259-4268.

Rörup, J., Garbatov, Y., Dong, Y., Uzunoglu, E., Parmentier, G., Andoniu, A., Quéméner, Y., Chen, K.-C., Vhanmane, S., Negi, A., Parihar, Y., Villavicencio, R. & Yue, J. 2017. Round robin study on spectral fatigue assessment of butt-welded joints. *In:* Guedes Soares, C. &

Teixeira, A. (eds.) *Maritime Transportation and Harvesting of Sea Resources.* London: Taylor & Francis, 663-671.

Rosemeier, M., Basters, G. & Antoniou, A., 2017, Benefits of sub-component over full-scale blade testing elaborated on a trailing edge bond line design validation, Proceedings of Wind Energy Science Conference.

Roth, C. C. & Mohr, D. 2016. Ductile fracture experiments with locally proportional loading histories. *International Journal of Plasticity,* 79**,** 328-354.

Rother, K. & Rudolph, J. 2011. Fatigue assessment of welded structures: practical aspects for stress analysis and fatigue assessment. *Fatigue & Fracture of Engineering Materials & Structures,* 34**,** 177-204.

Ruggieri, C. 2017. Low constraint fracture toughness testing using SE(T) and SE(B) specimens. *International Journal of Pressure Vessels and Piping,* Article in press.

Sadeghirad, A., Chopp, D. L., Ren, X., Fang, E. & Lua, J. 2016. A novel hybrid approach for level set characterization and tracking of non-planar 3D cracks in the extended finite element method. *Engineering Fracture Mechanics,* 160**,** 1-14.

Sander, M., Muller, T. & Stacker, C. 2016. Very high cycle fatigue behaviour under constant and variable amplitude loading. *21st European Conference on Fracture, (Ecf21),* 2**,** 34-41.

Savaidis, G. & Malikoutsakis, M. 2016. Advanced notch strain based calculation of S-N curves for welded components. *International Journal of Fatigue,* 83**,** 84-92.

Schneider, N., Bodecker, J., Berger, C. & Oechsner, M. 2016. Frequency effect and influence of testing technique on the fatigue behaviour of quenched and tempered steel and aluminium alloy. *International Journal of Fatigue,* 93**,** 224-231.

Schneider, R., Thons, S. & Straub, D. 2017. Reliability analysis and updating of deteriorating systems with subset simulation. *Structural Safety,* 64**,** 20-36.

Schoefs, F., Chevreuil, M., Pasqualini, O. & Cazuguel, M. 2016. Partial safety factor calibration from stochastic finite element computation of welded joint with random geometries. *Reliability Engineering & System Safety,* 155**,** 44-54.

Schubbe, J. J., Bolstad, S. H. & Reyes, S. 2016. Fatigue crack growth behaviour of aerospace and ship-grade aluminum repaired with composite patches in a corrosive environment. *Composite Structures,* 144**,** 44-56.

Schwartzkopff, A. K., Xu, C. S. & Melkoumian, N. S. 2016. Approximation of mixed mode propagation for an internally pressurized circular crack. *Engineering Fracture Mechanics,* 166**,** 218-233.

Šebek, F., Kubík, P., Hůlka, J. & Petruška, J. 2016. Strain hardening exponent role in phenomenological ductile fracture criteria. *European Journal of Mechanics-A/Solids,* 57**,** 149-164.

Shen, F., Voyiadjis, G. Z., Hu, W. & Meng, Q. 2015. Analysis on the fatigue damage evolution of notched specimens with consideration of cyclic plasticity. *Fatigue & Fracture of Engineering Materials & Structures,* 38**,** 1194-1208.

Shi, K. K., Cai, L. X., Qi, S. & Bao, C. 2016. A prediction model for fatigue crack growth using effective cyclic plastic zone and low cycle fatigue properties. *Engineering Fracture Mechanics,* 158**,** 209-219.

Shijian, C., Yiqian, L. & Weiqiang, Q., 2013, Comparison Analysis between CSR-OT and CSR-H for Corrugated Bulkhead of Large Product Tanker, TSCF 2013 Shipbuilders Meeting.

Shin, H. K., Lee, D. W., Park, J. & Cho, S.-R., 2016, Damage of plates due to repeated impulsive pressure loadings, Proceedings of the 13th International Symposium on Practical design of ships and other floating structures, Copenhagen, Danmark.

Skriko, T., Ghafouri, M. & Bjork, T. 2017. Fatigue strength of TIG-dressed ultra-high-strength steel fillet weld joints at high-stress ratio. *International Journal of Fatigue,* 94**,** 110-120.

Snowberg, D., Dana, S., Hughes, S. & Berling, P. 2014. Implementation of a Biaxial Resonant Fatigue Test Method on a Large Wind Turbine Blade.: National Renewable Energy Laboratory, NREL/TP-5000- 61127.

Socie, D. F., Morrow, J. & Chen, W. 1979. A procedure for estimating the total fatigue life of notched and cracked members. *Engineering Fracture Mechanics,* 11**,** 851-859.

Soliman, M., Frangopol, D. M. & Mondoro, A. 2016. A probabilistic approach for optimizing inspection, monitoring, and maintenance actions against fatigue of critical ship details. *Structural Safety,* 60**,** 91-101.

Song, S. & Dong, P. 2016. Residual stresses at weld repairs and effects of repair geometry. *Science and Technology of Welding and Joining,* 22.

Sørensen, J. D., Branner, K. & Toft, H. S. 2013. Milestone 6: Recommendations for future sub component tests. *EUDP: Experimental Blade Research - Phase 2.* Aalborg University & DTU.

Sowards, J. W., Gnaupel-Herold, T., McColskey, J. D., Pereira, V. F. & Ramirez, A. J. 2015. Characterization of mechanical properties, fatigue-crack propagation, and residual stresses in a microalloyed pipeline-steel friction-stir weld. *Materials & Design,* 88**,** 632-642.

Stanzl-Tschegg, S. 2014. Very high cycle fatigue measuring techniques. *International Journal of Fatigue,* 60**,** 2-17.

STD181-0004 Volvo Group Weld Quality Standard.

Stenberg, T., Barsoum, Z. & Balawi, S. O. M. 2015. Comparison of local stress based concepts-Effects of low-and high cycle fatigue and weld quality. *Engineering Failure Analysis,* 57**,** 323-333.

Stenberg, T., Lindgren, E., Barsoum, Z. & Barmicho, I. 2016. Fatigue assessment of cut edges in high strength steel - Influence of surface quality. *Engineering Failure Analysis*.

Storhaug, G. & Kahl, A., 2015, Full-Scale Measurements of Torsional Vibration on Post-Panamax container ships Proceedings of the 7th International Conference on Hydroelasticity in Marine Technology, Split, Croatia.

Strach-Sonsalla, M. & Muskulus, M., 2016, Dynamics and Design of Floating Wind Turbines Proceedings of the 26th International Ocean and Polar Engineering Conference, Rhodes, Greece, ISOPE -I-16-702.

Sun, B., Xu, Y. L. & Li, Z. X. 2016. Multi-scale model for linking collective behaviour of short and long cracks to continuous average fatigue damage. *Engineering Fracture Mechanics,* 157**,** 141-153.

Sung, S. J. & Pan, J. 2016. Further investigation of stress intensity factor solutions for similar and dissimilar welds in lap-shear specimens under clamped loading conditions. *Engineering Fracture Mechanics,* 166**,** 60-81.

Szabo, B., Actis, R. & Rusk, D. 2016. Predictors of fatigue damage accumulation in the neighbourhood of small notches. *International Journal of Fatigue,* 92**,** 52-60.

Tan, C., Lu, Y. S. & Zhang, X. T. 2016. Life extension and repair decision-making of ageing offshore platforms based on DHGF method. *Ocean Engineering,* 117**,** 238-245.

Tang, J., Yu, W., Chai, T. Y., Liu, Z. & Zhou, X. J. 2016. Selective ensemble modelling load parameters of ball mill based on multi-scale frequency spectral features and sphere criterion. *Mechanical Systems and Signal Processing,* 66-67**,** 485-504.

Tao, Z. Q., Shang, D. G., Liu, H. & Chen, H. 2016. Life prediction based on weight-averaged maximum shear strain range plane under multiaxial variable amplitude loading. *Fatigue & Fracture of Engineering Materials & Structures,* 39**,** 907-920.

Taylor, D. 2007. *The Theory of Critical Distances; A New Perspective in Fracture Mechanics,* Linacre House, Jordan Hill, Oxford, United Kingdom, Elsevier.

Tchoffo Ngoula, D., Beier, H. T. & Vormwald, M. 2017. Fatigue crack growth in cruciform welded joints: Influence of residual stresses and of the weld toe geometry. *International Journal of Fatigue,* 101**,** 253-262.

Tekgoz, M., Garbatov, Y. & Guedes Soares, C. 2013a. Finite element modelling of the ultimate strength of stiffened plates with residual stresses. *In:* Guedes Soares, C. & Romanoff, J. (eds.) *Analysis and Design of Marine Structures.* London, UK: Taylor & Francis Group, 309-317.

Tekgoz, M., Garbatov, Y. & Guedes Soares, C., 2013b, Ultimate strength assessment of a stiffened plate accounting for welding sequences, *In:* Chang-Sup Lee, S.-H. V., ed., Proceedings of the 11th International Symposium on Practical Design of Ships and other Floating Structures, Changwon City, Korea, CECO, 1089-1095.

Tekgoz, M., Garbatov, Y. & Guedes Soares, C. 2014. Strength assessment of a stiffened panel based on the modified stress curve approach. *In:* Guedes Soares, C. & Santos, T. A. (eds.) *Maritime Technology and Engineering.* London, UK: Taylor & Francis Group, 503-510.

Thompson, I. 2016. Validation of naval vessel spectral fatigue analysis using full-scale measurements. *Marine Structures,* 49 256-268.

Tomaso, E., Risso, G., Gaiotti, M. & Rizzo, C. M., 2014, Numerical Simulation Strategies of Single Lap Joints, Proceedings of the 24th International Ocean and Polar Engineering Conference, Busan, Korea.

Tong, L. W., Huang, X. W., Zhou, F. & Chen, Y. Y. 2016. Experimental and numerical investigations on extremely-low-cycle fatigue fracture behaviour of steel welded joints. *Journal of Constructional Steel Research,* 119**,** 98-112.

Toribio, J., Matos, J. C. & Gonzalez, B. 2016. Aspect ratio evolution associated with surface cracks in sheets subjected to fatigue. *International Journal of Fatigue,* 92**,** 588-595.

Tumanov, A. V., Shlyannikov, V. N. & Kishen, J. M. C. 2015. An automatic algorithm for mixed-mode crack growth rate based on drop potential method. *International Journal of Fatigue,* 81**,** 227-237.

UK-HSE 1990. Offshore installations: guidance on design and construction. London.

Ulveseter, J. V. & Sævik, S., 2017, In-Line vibrations of flexible pipes, Proceedings of the 36th International Conference on Ocean, Offshore and Arctic Engineering, Trondheim, Norway, Paper OMAE2017-61325.

Van Lieshout, P. S., Den Besten, J. H. & Kaminski, M. L. 2016. Comparative study of multiaxial fatigue methods applied to welded joints in marine structures. *Frattura Ed Integrita Strutturale,* 37**,** 173 – 192.

Vasco-Olmo, J. M. & Diaz, F. A. 2016. Experimental evaluation of the effect of overloads on fatigue crack growth by analysing crack tip displacement fields. *Engineering Fracture Mechanics,* 166**,** 82-96.

Verreman, Y. & Nie, B. 1996. Early development of fatigue cracking at manual fillet welds. *Fatigue & Fracture of Engineering Materials & Structures,* 19**,** 669-681.

Vesely, V., Sobek, J., Frantik, P. & Seitl, S. 2016. Multi-parameter approximation of the stress field in a cracked body in the more distant surroundings of the crack tip. *International Journal of Fatigue,* 89**,** 20-35.

Vettor, R. & Guedes Soares, C. 2015. Detection and Analysis of the Main Routes of Voluntary Observing Ships in the North Atlantic. *Journal of Navigation,* 68**,** 397-410.

Vieira, M., Reis, L., Freitas, M. & Ribeiro, A. 2016. Strain measurements on specimens subjected to biaxial ultrasonic fatigue testing. *Theoretical and Applied Fracture Mechanics,* 85**,** 2-8.

Voie, P., Wu, J., Resvanis, T. L., Larsen, C. M., Vandiver, J. K., Triantafyllou, M. & Baarholm, R., 2017, Consolidation of empirics for calculation of VIV responses, Proceedings of the 36th International Conference on Ocean, Offshore and Arctic Engineering, Trondheim, Norway, Paper OMAE2017-61362.

Vormwald, M. 2015. Multi-challenge aspects in fatigue due to the combined occurrence of multiaxiality, variable amplitude loading, and size effects. *Frattura Ed Integrita Strutturale,* 33**,** 253-261.

Wallin, K., Pallaspuro, S., Valkonen, I., Karjalainen-Roikonen, P. & Suikkanen, P. 2015. Fracture properties of high-performance steels and their welds. *Engineering Fracture Mechanics,* 135**,** 219-231.

Wang, C. & Xu, X. W. 2016. An extended phantom node method study of crack propagation of composites under fatigue loading. *Composite Structures,* 154**,** 410-418.

Wang, F., Cui, W. C., Pan, B. B., Shen, Y. S. & Huang, X. P. 2014. Normalised fatigue and fracture properties of candidate titanium alloys used in the pressure hull of deep manned submersibles. *Ships and Offshore Structures,* 9**,** 297-310.

Wang, F., Cui, W. C., Wang, Y. Y. & Shen, Y. S. 2015a. Overload and dwell time effects on crack growth property of high strength titanium alloy TC4 ELI used in submersibles. *In:* Guedes Soares, C. & Shenoi, A. (eds.) *Analysis and Design of Marine Structures.* London, UK: Taylor & Francis Group.

Wang, F., Wang, K. & Cui, W. C. 2015b. A simplified life estimation method for the spherical hull of deep manned submersibles. *Marine Structures,* 44**,** 159-170.

Wang, J., Ma, Q. W. & Yan, S., 2016a, Numerical Investigation on Spectrum Evolution of Narrow-Banded Random Waves in Shallow Water Based on KdV and Fully Nonlinear Model Proceedings of the 35th International Conference on Ocean, Offshore and Arctic Engineering, Busan, Korea, Paper OMAE2016-54169.

Wang, Q., Liu, X. S., Yan, Z. J., Dong, Z. B. & Yan, D. J. 2017a. On the mechanism of residual stresses relaxation in welded joints under cyclic loading. *International Journal of Fatigue,* 105**,** 43-59.

Wang, R. Z., Zhang, X. C., Tu, S. T., Zhu, S. P. & Zhang, C. C. 2016b. A modified strain energy density exhaustion model for creep-fatigue life prediction. *International Journal of Fatigue,* 90**,** 12-22.

Wang, X. G., Feng, E. S. & Jiang, C. 2017b. A microplasticity evaluation method in very high cycle fatigue[J]. *International Journal of Fatigue,* 94**,** 6-15.

Wang, Y. & Susmel, L. 2016. he Modified Manson-Coffin Curve Method to estimate fatigue life under complex constant and variable amplitude multiaxial fatigue loading. *International Journal of Fatigue,* 83**,** 135 - 149.

Wang, Y. Y., Chen, H. B. & Zhou, H. W. 2016c. A fatigue life estimation algorithm based on Statistical Energy Analysis in high-frequency random processes. *International Journal of Fatigue,* 83**,** 221-229.

Wei, Z. G. & Dong, P. S. 2014. A generalized cycle counting criterion for arbitrary multi-axial fatigue loading conditions. *Journal of Strain Analysis for Engineering Design,* 49**,** 325-341.

Wu, H., Meggiolaro, M. A. & de Castro, J. T. P. 2016. Computational implementation of a non-linear kinematic hardening formulation for tension-torsion multiaxial fatigue calculations. *International Journal of Fatigue,* 91**,** 304-312.

Wu, J., Lekkala, B. R., Ong, M. C., Passano, E. & Voie, P. E., 2017, Prediction of combined IL and CF VIV of deep-water risers, Proceedings of the 36th International Conference on Ocean, Offshore and Arctic Engineering, Trondheim, Norway, Paper OMAE2017-61766.

Xie, X. F., Jiang, W. C., Luo, Y., Xu, S. G., Gong, J. M. & Tu, S. T. 2017. A model to predict the relaxation of weld residual stress by cyclic load: Experimental and finite element modelling. *International Journal of Fatigue,* 95**,** 293-301.

Xing, S. Z. & Dong, P. S. 2016. An analytical SCF solution method for joint misalignments and application in fatigue test data interpretation. *Marine Structures,* 50**,** 143-161.

Xing, S. Z., Dong, P. S. & Threstha, A. 2016. Analysis of fatigue failure mode transition in load-carrying fillet-welded connections. *Marine Structures,* 46**,** 102-126.

Xing, S. Z., Dong, P. S. & Wang, P. 2017. A quantitative weld sizing criterion for fatigue design of load-carrying fillet-welded connections. *International Journal of Fatigue,* 101**,** 448-458.

Xu, S. H. & Wang, Y. D. 2015. Estimating the effects of corrosion pits on the fatigue life of steel plate based on the 3D profile. *International Journal of Fatigue,* 72**,** 27-41.

Yamamoto, M., Makino, K. & Ishiduka, H. 2017. Comparison of crack growth behaviour between full-scale railway axle and scaled specimen. *International Journal of Fatigue,* 92**,** 159-165.

Yan, X., Huang, X. & Liu, F., 2014, Research on the application of storm model in fatigue life prediction for offshore platform, *In:* Zheng, I., ed., Proceedings of the 2014 International

Conference on Industrial, Mechanical and Manufacturing Science, Taylor & Francis Group, 49-52.

Yan, X. S. & Huang, X. P. 2015. Prediction of fatigue life reliability for ship details based on crack growth. *Shanghai Jiaotong Daxue Xuebao/Journal of Shanghai Jiaotong University,* 49**,** 214-219.

Yan, X. S., Huang, X. P., Huang, Y. C. & Cui, W. C. 2016. Prediction of fatigue crack growth in a ship detail under wave-induced loading. *Ocean Engineering,* 113**,** 246-254.

Yang, S. O., Yang, H. Q., Liu, G., Huang, Y. & Wang, L. D. 2016. Approach for fatigue damage assessment of welded structure considering coupling effect between stress and corrosion. *International Journal of Fatigue,* 88**,** 88-95.

Yang, X. H., Zou, L. & Deng, W. 2015. Fatigue life prediction for welding components based on hybrid intelligent technique. *Materials Science and Engineering a-Structural Materials Properties Microstructure and Processing,* 642**,** 253-261.

Ye, W., Ran, A., Li, J., Li, G., Tang, X., Wang, Z. & Hongwu, W., 2016, Tapered Column Deep Draft Semi-submersible (TCDD-Semi) Platform for Dry-tree Application, Proceedings of the 26th International Ocean and Polar Engineering Conference Rhodes, Greece, Paper ISOPE-I-16-703.

Yeter, B., Garbatov, Y. & Guedes Soares, C. 2014a. Fatigue damage analysis of a fixed offshore wind turbine supporting structure. *In:* Guedes Soares, C. & Pena, F. (eds.) *Developments in Maritime Transportation and Exploitation of Sea Resources.* London, UK: Taylor & Francis Group, 415-424.

Yeter, B., Garbatov, Y. & Guedes Soares, C. 2014b. Spectral fatigue assessment of an offshore wind turbine structure under wave and wind loading. *In:* Guedes Soares, C. & Pena, F. (eds.) *Developments in Maritime Transportation and Exploitation of Sea Resources.* London, UK: Taylor & Francis Group, 425-433.

Yeter, B., Garbatov, Y. & Guedes Soares, C. 2015a. Assessment of the retardation of in-service cracks in offshore welded structures subjected to variable amplitude load. *In:* Guedes Soares, C. (ed.) *Renewable Energies Offshore.* London, UK: Taylor & Francis group, 855-863.

Yeter, B., Garbatov, Y. & Guedes Soares, C. 2015b. Fatigue crack growth analysis of a plate accounting for retardation effect. *In:* Guedes Soares, C. & Santos, T. A. (eds.) *Marine Technology and Engineering.* London, UK: Taylor & Francis Group, 585-595.

Yeter, B., Garbatov, Y. & Guedes Soares, C. 2015c. Fatigue reliability assessment of an offshore supporting structure. *In:* Guedes Soares, C. & Santos, T. A. (eds.) *Marine Technology and Engineering.* London, UK: Taylor & Francis Group, 671-681.

Yeter, B., Garbatov, Y. & Guedes Soares, C. 2015d. Fatigue reliability of an offshore wind turbine supporting structure accounting for inspection and repair. *In:* Guedes Soares, C. & Shenoi, A. (eds.) *Analysis and Design of Marine Structures.* London, UK: Taylor & Francis Group, 737-747.

Yeter, B., Garbatov, Y. & Guedes Soares, C. 2015e. Low cycle fatigue assessment of offshore wind turbine monopile supporting structure subjected to wave-induced loads. *In:* Guedes Soares, C., Dejhalla, R. & Pavletic, D. (eds.) *Towards Green Marine Technology and Transport.* London: Taylor & Francis Group, 287-294.

Yeter, B., Garbatov, Y. & Guedes Soares, C. 2016a. Evaluation of fatigue damage model predictions for fixed offshore wind turbine support structures. *International Journal of Fatigue,* 87**,** 71-80.

Yeter, B., Garbatov, Y. & Guedes Soares, C., 2016b, Reliability of offshore wind turbine support structures subjected to extreme wave-induced loads, Proceedings of the 35th International Conference on Ocean, Offshore and Arctic Engineering, Busan, South Korea, ASME, paper OMAE2016-54240.

Yeter, B., Garbatov, Y. & Guedes Soares, C. 2016c. Structural design of an adaptable jacket offshore wind turbine support structure for deeper waters. *In:* Guedes Soares, C. & Santos,

T. (eds.) *Maritime Technology and Engineering.* London: Taylor & Francis Group, 583-594.

Yeter, B., Garbatov, Y. & Guedes Soares, C. 2017a. Probabilistic life-cycle assessment for offshore wind turbines. *In:* Guedes Soares, C. & Teixeira, A. (eds.) *Maritime Transportation and Harvesting of Sea Resources.* 1229-1241.

Yeter, B., Garbatov, Y. & Guedes Soares, C. 2017b. Risk-based multi-objective optimisation of a monopile offshore wind turbine support structure. *Proceedings of the 36th International Conference on Ocean, Offshore and Arctic Engineering.* Trondheim, Norway, paper OMAE2017-61756.

Yeter, B., Garbatov, Y. & Guedes Soares, C. 2017c. System reliability of a jacket offshore wind turbine subjected to fatigue. *In:* Guedes Soares, C. & Garbatov, Y. (eds.) *Progress in the Analysis and Design of Marine Structures.* London: Taylor & Francis Group, 939-950.

Yıldırım, H. 2015. Review of fatigue data for welds improved by tungsten inert gas dressing. *International Journal of Fatigue,* 79**,** 36-45.

Yıldırım, H. 2016. Recent results on fatigue strength improvement of high-strength steel welded joints. *International Journal of Fatigue*.

Yildirim, H. & Marquis, G. 2015. Fatigue data of High-Frequency Mechanical Impact (HFMI) improved welded joints subjected to overloads. *In:* Guedes Soares, C. & Shenoi, A. (eds.) *Analysis and Design of Marine Structures.* London, UK: Taylor & Francis Group, 317-322.

Yin, D., Passano, E. & Larsen, C. M., 2017, Improved In-Line VIV prediction for combined In-Line and Cross-Flow VIV responses, Proceedings of the 36th International Conference on Ocean, Offshore and Arctic Engineering, Trondheim, Norway, Paper OMAE2017-61715.

Yin, D., Wu, J. & Lie, H., 2015, VIV Prediction of Steel Catenary Riser - A Reynolds Number Sensitivity Study, Proceedings of the 25th International Ocean and Polar Engineering Conference, Hawaii, USA, Paper ISOPE-I-15-125.

Yokozeki, K. & Miki, C. 2016. Fatigue evaluation for longitudinal-to-transverse rib connection of orthotropic steel deck by using structural hot spot stress. *Welding in the World,* 60**,** 83-92.

Yuan, K. L. & Sumi, Y. 2016. Simulation of residual stress and fatigue strength of welded joints under the effects of ultrasonic impact treatment (UIT). *International Journal of Fatigue,* 92**,** 321-332.

Yue, J., Dang, Z. & Guedes Soares, C. 2017. Prediction of fatigue crack propagation in bulb stiffeners by experimental and numerical methods. *International Journal of Fatigue* 99**,** 101-110.

Zappalorto 2015. Neubers rules and other solutions - theoretical differences and formal analogies and energy interpretations. *Theoretical and Applied Fracture Mechanics,* 79.

Zappalorto, M. & Lazzarin, P. 2014. Some remarks on the Neuber rule applied to a control volume surrounding sharp and blunt notch tips. *Fatigue & Fracture of Engineering Materials & Structures,* 37**,** 349-358.

Zerbst, U. & Madia, M. 2015. Fracture mechanics based assessment of the fatigue strength: approach for the determination of the initial crack size. *Fatigue & Fracture of Engineering Materials & Structures,* 38**,** 1066-1075.

Zhang, D., Huang, X. P. & Cui, W. C. 2015. A procedure to predict fatigue crack growth of ship structures under complex loading condition. *Chuan Bo LI Xue/Journal of Ship Mechanics,* 19**,** 541-552.

Zhang, J., Yang, S. & Lin, J. 2016a. A nonlinear continuous damage model based on short-crack concept under variable amplitude loading. *Fatigue & Fracture of Engineering Materials & Structures,* 39**,** 79-94.

Zhang, J. R., Fan, L. & Tang, X. S. 2016b. Energy density zone model and fatigue life prediction considering microscopic effects. *Fatigue & Fracture of Engineering Materials & Structures,* 39**,** 1542-1556.

Zhang, Y. H. & Maddox, S. J. 2009. Fatigue life prediction for toe ground welded joints. *International Journal of Fatigue,* 31**,** 1124-1136.

Zhang, Y. M., Fan, M., Xiao, Z. M. & Zhang, W. G. 2016c. Fatigue analysis on offshore pipelines with embedded cracks. *Ocean Engineering,* 117**,** 45-56.

Zhou, X. Y., Gosling, P. D., Ullah, Z., Kaczmarczyk, L. & Pearce, C. J. 2016. Exploiting the benefits of multi-scale analysis in reliability analysis for composite structures. *Composite Structures,* 155**,** 197-212.

Zhou, Z. G. & Jia, L. J. 2015. Damage index for crack initiation of structural steel under cyclic loading. *Journal of Constructional Steel Research,* 114**,** 1-7.

Zhu, L., Guo, K., Duan, L., Liu, J., Wang, H. & Wang, X., 2016, Wet-deck slamming pressure on SWATH-consideration for practical design, Proceedings of the 13th International Symposium on Practical design of ships and other floating structures, Copenhagen, Denmark.

Zhu, X.-K. 2017. Progress in development of fracture toughness test methods for SENT specimens. *International Journal of Pressure Vessels and Piping,* Article in press.

Zhu, X. K. 2015. Advances in Fracture Toughness Test Methods for Ductile Materials in Low-Constraint Conditions. *Pressure Vessel Technology: Preparing for the Future,* 130**,** 784-802.

Zhu, X. K. 2016. Review of fracture toughness test methods for ductile materials in low-constraint conditions. *International Journal of Pressure Vessels and Piping,* 139**,** 173-183.

Zhu, X. K. & Joyce, J. A. 2012. Review of fracture toughness (G, K, J, CTOD, CTOA) testing and standardization. *Engineering Fracture Mechanics,* 85**,** 1-46.

Zhu, X. K., Zelenak, P. & McGaughy, T. 2017. Comparative study of CTOD-resistance curve test methods for SENT specimens. *Engineering Fracture Mechanics,* 172**,** 17-38.

Zonfrillo, G. 2017. New Correlations Between Monotonic and Cyclic Properties of Metallic Materials. *Journal of Materials Engineering and Performance,* 26**,** 1569-1580.

This page intentionally left blank

Proceedings of the 20th International Ship and Offshore Structures Congress (ISSC 2018) Volume I – M.L. Kaminski and P. Rigo (Eds.)

doi:10.3233/978-1-61499-862-4-549

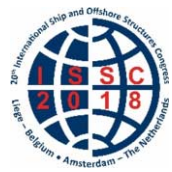

COMMITTEE IV.1

DESIGN PRINCIPLES AND CRITERIA

COMMITTEE MANDATE

Concern for the quantification of general sustainability criteria in economic, societal and environmental terms for marine structures and for the development of appropriate principles for rational life-cycle design using these criteria. Special attention should be given to the issue of Goal-Based Standards as concerns their objectives and requirements and plans for implementation. Possible differences with the safety requirements in existing standards developed for the offshore, maritime and other relevant industries and of the current regulatory framework for ship structures shall be considered. Role of reliability-based design codes and requirements as well as their calibration to established safety levels

AUTHORS/COMMITTEE MEMBERS

Chairman: Matthew Collette, *USA*
Zhihu Zhan, *China*
Ling Zhu, *China*
Vedran Zanic, *Croatia*
Tetsuo Okada, *Japan*
Toshiro Arima, *Japan*
Rolf Skjong, *Norway*
Han Koo Jeong, *South Korea*
Gennadiy Egorov, *Ukraine*

KEYWORDS

Design principles; design criteria; goal-based design; sustainability; accidental loading; on-boarding monitoring; decision support; polar design criteria; inland vessels; human performance; human error

CONTENTS

1. INTRODUCTION 551

2. CONCEPTS AND DEVELOPMENTS IN PRINCIPLES AND CRITERIA 551
2.1 Sustainability and Lifecycle Principles 551
2.2 Goal-Based Approaches 554
2.3 In-Service Reassessment for Life Extensions 555
2.4 Human Performance in Engineering and Criteria Evaluation 558
2.4.1 The Challenge of Human Performance in Engineering 558
2.4.2 Past Work 558
2.4.3 Scope of the Current Review 560
2.4.4 Review of Ongoing Research 560
2.4.5 Assessment of the State of the Art of Engineering Human Performance Criteria 563
2.5 Inland and Coastal Vessels 564

3. PRINCIPLES AND CRITERIA FOR USING ON-BOARD MONITORING DATA 566
3.1 Code and Safety Updating Offline 566
3.2 Full-Scale Measurement Campaigns 567
3.3 Decision Support Systems 568
3.4 Onsite Estimation of Ocean Waves 568

4. PRINCIPLES AND CRITERIA FOR ACCIDENTAL LOADS 570
4.1 Collision and Grounding 570
4.1.1 Collision 571
4.1.2 Grounding 575
4.1.3 Failure criteria 578
4.2 Slamming 579
4.3 Explosion and Fire 581
4.3.1 Principles and criteria for structures under blast loading 581
4.3.2 Principles and criteria for fire induced hazards 583

5. PRINCIPLES AND CRITERIA FOR ARCTIC OPERATION 584
5.1 Arctic Operational Environment 584
5.2 Ice Load Prediction 585
5.3 Design Approaches for Ice Loaded Hull Structures with Application to Structural Design 587
5.4 Assessment of Ice Class Rules 590

6. CONCLUSIONS 591

REFERENCES 592

1. INTRODUCTION

Design principles and criteria form the overall framework for assessing marine structures against societal sustainability goals for economic, social, and environmental performance. Recent ISSC Committee IV.1 reports have focused their coverage on the extensive developments in the areas of both sustainable design approaches and the emergence of goal-based standards at the IMO. Over the last two decades, developments in these areas have been rapid. However, as seen in the shorter ISSC IV.1 report of 2015, fundamental developments for addressing such goals appears to be tapering off. During this mandate period, the committee found the focus switching to implementing and verifying goal-based standards and regulations.

Thus, the structure of the current committee report reflects these developments. First, this report reviews the developments in the framework for both sustainability and goal-based standards during our mandate period. Then, following the shift into implementation in these areas, the committee's work focuses on recent developments in several areas relating to design principles and criteria. A special chapter on using on-board monitoring data for both decision support and rule development is presented. As the cost of gathering weather and structural response data for vessels at sea falls dramatically, the best ways to use such data in support of structural integrity requires careful exploration. In-service updating from such monitoring systems could allow improved lifecycle performance, including longer asset lives, enhanced safety, and reduced environmental and property risks from in-service failures. As the marine structures themselves change, such as the recent explosion in containership sizing, the ability to weave in-service measurements back into design criteria has become essential.

Two additional focus chapters provide further insight into the development of rules and criteria in related areas. Accidental load estimation is covered, as the direct simulation of marine structures in accidental conditions is becoming increasingly common. Such analysis can further reduce the negative impact of marine structures by directly minimizing adverse outcomes in accidental conditions. Then, a review of Polar criteria, including a brief summary of ice load prediction methods and a review of the comparisons between different rule sets is presented. Complementing the longer chapters, shorter sections review developments supporting sustainability design. A short section on in-service reassessment for life extension covers recent criteria and procedures for both offshore oil structures and the emerging challenge of aging offshore wind turbine structures. A review of inland navigation developments and reliability-based design approaches are included. Finally, a review of the role of human error in engineering analysis, and methods to control and prevent such errors when establishing design methods and criteria are also included in the report. This report should be read in conjunction with several additional ISSC reports which cover fundamental developments in related fields. The work on in-service re-assessment and on-board monitoring is complemented by the work of specialist committee V.7 on Structural Longevity, especially their Chapter 3. The work in both Polar and accidental loading is complemented by specialist committees V.6 and V.1 respectively. Finally, owing to the tight coupling between design principles and design tools, the report of committee IV.2 also complements the work here.

2. CONCEPTS AND DEVELOPMENTS IN PRINCIPLES AND CRITERIA

2.1 Sustainability and Lifecycle Principles

The foundation on Sustainability and lifecycle principles remain the same from the 2015 Committee's work in this area, and the introduction to that report is reproduced here to provide a consistent background definition:

> The present report, as the previous ISSC reports of Committee IV.1, follows the same general definition of sustainability that was given by the Brundtland Commission of the United Nations: "economic development which meets the needs

of the present generation without compromising the ability of future generations to meet their own needs"(UN-WECD, 1987).

A sustainable development of the maritime transport involves therefore a detailed consideration of all the negative implications such transport mode has for the human society (social costs) and a proper assessment of compliance to the general sustainability target, based on a cost/benefit analysis.

As stated by Korzhenevych et al. (2014), transportation contributes significantly to economic growth and enables a global market. Transport modes, however, also produce negative effects. Shipping traffic, in particular, contributes to air and water pollution and shipping accidents to losses in terms of human lives, economical losses and ecological damages. These effects give rise to costs that can be expressed in monetary terms and affect in various ways the Society: health costs caused by air pollution (due to NOx, SOx, PM, …), lives lost and loss of biodiversity in traffic accidents, costs related to the world scale climate impact of shipping, etc.

These societal costs are referred to as external costs, that sum up to those directly borne by the transport first and second parties (private or internal costs, such as: wear, tear and energy cost due to the ship operation, own time costs, transport fares and transport taxes and charges (port fees, pilot, insurance, etc.)). The same kind of classification applies to benefits: first and second parties take advantage of most of them, even though society also experiences a gain.

The external costs of transportation are generally not paid by transport actors and hence not taken into account when they take a decision about a transport activity. Internalization of external costs means making such effects part of the decision-making process of transport first actors. This can be done directly through regulation, i.e. issuing specific requirements in terms of operational and/or design control measures, or indirectly, providing suitable incentives to transporters with market-based instruments (e.g. taxes, charges, emission trading, etc.). Combinations of these basic types are also possible.

In other terms, the role of the Regulator is to assess if and under which conditions a transport activity is acceptable from a Societal viewpoint and to establish a Regulatory Framework able to control the societal losses and redistribute their costs in a balanced way, in particular on the first actors of the transportation process (internalization of the external costs). In a technical analysis of sustainability, it is important that all external costs are included. All kinds of costs incurred during the lifetime of the product must be assessed. Additionally, some social costs are incurred also long after the product lifetime has expired, as is the case for the CO_2 emitted during the lifetime of the product. It is also important to include external costs of all raw materials that goes into the product, like e.g. the steel used to construct a ship. In a comparison of sustainability of e.g. different transport mode, it is also important to properly account for the differences in tax regimes. The key point of this concept is a proper evaluation of the external costs, (also called social or implied costs) that are now not directly perceived as such by the actors. This means, in a first place, the identification of all implications (negative and, in case, positive) of the transportation process and a quantification on a monetary scale.

The design principles described in ISSC IV.1 committee from 2015 have been applied in a recent study on damage stability for passenger ships (Hamann, 2015). Prior to this study, which is based on the EU Impact Assessment (IA) Guidelines (EU, 2009), a Formal Safety Assessment (FSA) per IMO (2013) had been carried out by Vassalos et al. (2016). Both the IA and

the FSA used the same risk acceptance criteria as recommended in Spouge and Skjong (2014), also published in Spouge et al. (2015). The difference between the two approaches, FSA and IA, is described in Skjong (2015).

The main technical difference between the approaches is that the IA include all external costs in the analysis. This is not normally done in an FSA, although there is nothing in the IMO FSA Guidelines that indicates that this shall not be done. For this specific case of damage stability, the Risk Control Options (RCOs) that were considered involved design changes that would change the fuel consumption and the steel weight of the ships. Per the FSA Guidelines the increased cost of fuel and steel had been included. However, per the IA Guidelines the external costs of the fuel had to be included also (Mainly CO_2, SO_x, NO_x, NMVOC, and PM) as well as the external costs of steel (from steel production). Since the issue mainly related to investing in increased safety, the key question was therefore: Would the inclusion of external costs (largely from environmental impacts) change the recommendation?

The basis for the recommendations are in both cases the Net Cost of Averting a Fatality (NCAF).

$$NCAF = (\Delta Cost - \Delta Economic\ Benefits)/\Delta PLL$$

ΔCost is the life cycle cost of the RCO, ΔEconomic Benefits are the life cycle economic benefits (e.g. the reduced risk of loss of ship) and ΔPLL is the reduction in Potential Loss of Life. The difference between the two are due to the external costs. Table 1 contains the results for small cruise ships. In Hamann (2015), there are results for large cruise ships and for small and large Ro-Pax ships. There are also sensitivity studies, and the RCOs are described in detail.

Table 1: NCAF (€ million) per the FSA and IA Guidelines respectively (Small Cruise Ship)

	RCO 1	RCO 2	RCO 3	RCO 4	RCO 5	
NCAF (FSA)	-0.11	6.6	8.9	7.7	9.9	
NCAF (IA)	-0.11	6.6	9.9	8.4	13	
	RCO 6	RCO 7	RCO 8	RCO 9	RCO 6 (C+G)	RCO 9(C+G)
NCAF (FSA)	14	31	28	7.8	2.8	1.5
NCAF (IA)	20	42	39	9.4	3.7	1.8
C+G implies that the effect of the RCO for both Collision and Grounding are included						
RCO 1	Sill increased on external weathertight aft doors					
RCO 2	Vs.01 + Deck 3 made watertight for comp n.2 and n.3					
RCO 3	Vs.02 + Cross flooding section within DB void spaces improved adding pipes					
RCO 4	Vs.03 + Two weathertight door added and a watertight door added on BK deck					
RCO 5	Vs.04 + Increased Beam by 0.2m (new B=20.2m)					
RCO 6	Vs.04 + Increased Beam by 0.5m (new B=20.5m)					
RCO 7	Vs.06 + Increased freeboard by 0.25m					
RCO 8	Vs.07 + Increased Beam by 0.5m (new B=21m)					
RCO 9	Vs.04 + Increased Beam by 0.1m (new B=20.1m)					

Assuming a criterion of €7million per life saved, the recommendation from the IA and FSA would be identical (green). Assuming a criterion of €8million, RCO4 and RCO9 would change from being recommended per FSA, but not per IA (yellow). It should be noted that the NCAF for RCO1 is negative. This is because the RCO can be recommended for commercial reasons (the economic benefits are larger than the costs), in addition to the resulting life saving.

The damage stability case is unique in respect to the formulation of the regulatory requirements. Since SOLAS (IMO, 2009) damage stability requirements have been probabilistic. The implication is that the requirement is a so-called Required Index, R. The attained index, A, is a

reflection of the conditional probability that a ship survives (not sinking or capsizing) a collision with water ingress. The requirement is thus simply A>R. The RCOs mentioned in Table 1 are therefore only used as examples of how to demonstrate that the damage stability can be improved, and make it possible to calculate the improvement and the costs. A designer is free to choose any other RCOs or design options as long as the requirement is fulfilled. At the Maritime Safety Committee of the International Maritime Organization the recommendations were adopted in June 2017 and will enter into force in 2020. The required index R, is a function of the number of people on board.

The IA carried out in EMSA III had a reduced scope, as only the RCOs identified by FSA was subject to a reanalysis based on the IA Guidelines. In a complete IA, there might have been other RCOs that could be recommended.

There are currently many cases of regulations where there is a conflict of interest between ship safety and environmental protection. To extend the IMO approach in the FSA Guidelines to including all external costs in the assessment of regulatory options would therefore have clear advantages and constitutes a consistent and transparent regulatory philosophy.

2.2 Goal-Based Approaches

The work at the International Maritime Organization (IMO) relating to Goal Based Standard (GBS) was initiated in 2002 with a submission by Greece (Greece, 2002) 'Building Robust Ships'. The paper argued that "competition for newbuilding orders between classification societies makes it imperative to have unified standards on all fundamental aspects of ship design and construction". The paper referred to the fact that by SOLAS II-1/3-1 IMO delegated the task of monitoring, verification and certification of the design and construction of ships to classification societies, but that this was not enough. In the view of Greece, IMO should invite the International Association of Classification societies (IACS) to complete without delay the development of Unified Standards and to submit them for consideration and endorsement by way of an MSC Resolution, with a view to amending SOLAS regulation II-1/3-1 and making their application mandatory through reference to the Resolution.

The later development of Goal Based Standards for Bulk Carriers and Tankers are described in in Section 5.1 of the 2015 report of this committee. The audit process of the Rules of the Classification Societies was carried out per plan. Twelve IACS member societies submitted their rules, and the IMO Maritime Safety Committee (MSC) spring meeting in 2016 marked a critical milestone. Unexpectedly, the audit resulted in five non-conformities in the common IACS structural rules etc., whose main component is "Common Structural Rules for Bulk Carriers and Oil Tankers" (IACS, 2015a), and one in the Lloyd's Register submission. However, having fully considered the GBS audit reports (IMO, 2016a) as well as IACS' plans to rectify non-conformities (IMO, 2016b) etc., the MSC "overwhelmingly confirmed that the information provided by the Submitters (12 IACS member ROs) demonstrates that their rules conform to the GBS Standards." (IMO, 2016c) It was agreed that "the identified non-conformities are to be rectified" and "requested the ROs to address the identified observations in the future, taking into account the recommendations made by the audit teams and the Corrective Action Plans" (IMO, 2016d).

Upon receipt of the document MSC 98/6/1 submitted by IMO Secretary-General, containing the GBS non-conformities verification audit report, the IMO Maritime Safety Committee confirmed that the request of MSC 96 that the identified non-conformities be rectified and that the whole process of the initial verification audit was successfully completed in accordance with the GBS Verification Guidelines (IMO, 2017a).

Peschmann et al. (2017) summarized the above and highlighted some of the challenges noted during the implementation and verification of the GBS Standards based on the latest investigations carried out by IACS with respect to safety margins within the rules and the principles of

rule validation and benchmarking. The current work at IMO relates to amending the audit process based on the experience gained. Specifically, this relates to amending "Guidelines for Verification of Conformity with Goal Based Ship Construction standards for Bulk Carriers and Oil Tankers" (IMO, 2010). This work is scheduled to be completed in the spring meeting of MSC in 2018.

The MSC is also discussing how to conduct GBS maintenance verification audits and agreed that IACS and its member societies should submit rule change information by 31 March 2018 and then the outcome of the first maintenance audit will be considered in the autumn meeting of MSC in 2018 (IMO, 2017b).

IMO also developed the 'Generic Guidelines for Developing IMO Goal Based Standards'(IMO, 2015a), and there is a clear tendency at IMO to develop new Codes in a goal based format. For example, the recent 'IGF Code' (IMO, 2015b) and 'Polar Code' (IMO, 2015c, 2014) are both goal based and entered into force on January 1st 2017. It seems that the trend of developing goal-based codes is firmly established. The codes are mandated by anchoring them into the conventions.

The work at IMO, has also inspired the 'Naval Ship Code' to be developed in the Goal Based format, see http://www.navalshipcode.org/.

The development of the Goal Based Standard/Safety Level Approach (GBS/SLA) as an alternative to the Generic GBS is also described in the 2015 version of this committee's work, Section 5.1. This approach, which is formally risk based and linked to Formal Safety Assessment (IMO, 2015d) is still debated at IMO MSC. Draft guidelines are available.

It is to be noted that the current probabilistic damage stability regulations described in Chapter 2.3 is already based on GBS/SLA principles. The requirement to damage stability (the Goal) is simply to comply with the required index (R). There is full freedom of the designer how to achieve this. There are verified software tools available. The method is probabilistic, and as explained in Chapter 2.3 the required index for passenger ships has been justified by FSA (and EU Impact Assessment).

2.3 In-Service Reassessment for Life Extensions

While most work on structural design principles and criteria addresses newbuildings, there is growing interest in extending the service lives of existing ships and offshore structures beyond their original design life. Such extensions typically require reassessment of the structural adequacy, while making allowances for both the service life of the structure to date, and changes to structural design codes since the structure entered service.

Extending the life of offshore oil and gas platforms remains one of the most active areas of research into structural criteria. Chapter 4 of the report of specialist committee V.7, Structural Longevity, covers analysis framework and sensor development in this area, this section focuses primarily on the development in assessment criteria and regulations for these structures. By 2005, the majority of the fixed offshore platforms worldwide were already operating beyond their design life (Moan, 2005). Initial work before the current mandate period on North Sea oil platforms provided criteria for life extensions. This includes an Aging and Life Extension (ALE) project conducted by the United Kingdom Health and Safety Executive from 2011-2013 under the name KP4, and Norwegian standards N-006 and U-009 dealing with platforms and subsea components respectively. Within the mandate period, mainly periodic updating of these approaches was observed, such as a new edition of N-006 in 2015. Nezamian and Nicolson (2016) provided a recent overview of strategies for FPSO life extension, including an example for a FPSO operating off of Africa. Notably, they highlight the need to manage platform integrity beyond classification-society based criteria to maximize the profitability of the platform for the owner.

During the period of the committee's mandate, oil platforms in the Gulf of Mexico were the focus of progress in life-extension criteria. Compared to the North Sea platforms, the Gulf of Mexico platforms have several unique challenges. In U.S. waters, the floating infrastructure is only now beginning to approach their design life, with many platforms still less than 20 years old (Phillips and Martyn, 2016). Life extension regulations did not exist for this sector at the beginning of the current mandate period, and the committee has been able to trace the development of criteria over the last three years. Additional challenges in U.S. waters include a fractured regulatory approach, where both the U.S. Coast Guard and the Bureau of Safety and Environmental Enforcement (BSEE) are responsible for oversight, with the Coast Guard focused on the hull system and BSEE focused on mooring and production systems. Neither agency is equipped to directly approve life-extension plans but wish to approve a review of the plans conducted by a third-party certified verification agent (CVA). Classification societies have been proposed as CVAs, but CVAs are not formally limited to such organizations. Finally, and perhaps most significantly, the ocean environment in the Gulf of Mexico is now more severe than assumed during the initial design of many platforms in the 1990s. This change is partly a result the frequent significant hurricanes observed in the 2000-2010 period. This results in higher environmental loading on the platforms, which must be assessed during the service life extension (Hua et al., 2017; Rosen et al., 2016).

Phillips and Martin (2016) provide an initial overview of the criteria for life extension, and historical failure data underpinning the U.S. Coast Guard's efforts in this area. This was followed by official guidance and criteria for re-assessment of platforms within the United States jurisdiction in the Gulf of Mexico presented in the form of a letter from CAPT JD Reynolds, dated 19 January 2016 (Reynolds, 2016). The letter outlines a three-step approval process consisting of: an initial plan for the life extension, a baseline survey to establish the current condition of the platform, and an engineering and risk assessment. These three steps will be reviewed by both the United States Coast Guard and BSEE. The letter further recommends review by a third-party CVA such as a classification society. The flowchart is shown below in Figure 1. Of note, production process equipment and subsea equipment is not typically assessed in this process (Hua et al., 2017). Two published accounts of moving a platform through this process have also recently appeared. Hua et al. (2017) present an overview of the life extension process for the *Neptune* spar, the world's first production spar, installed in Viosca Knoll in the Gulf of Mexico. This 215m classic spar was installed in 1996 with a 20-year design life, and Noble Energy wished to extend the life at least three years. While the inspection and condition of the spar was generally satisfactory, the site-specific design storm condition had increased significantly. The 100-year storm calculated in 1995 had 12.1m significant wave height with a 39 m/sec wind speed. By 2014, these values had increase to 14.8m and 43.8m/sec respectively. For this spar, the higher values were not problematic as the effective weight of the platform had been reduced as many risers had been removed from the platform, but it does highlight the potential role of new design storms in complicating service life extensions.

Gallagher et al. (2017) provide a similar overview for the *Genesis* spar, another classic spar installed in 1998 with a 20-year design life. In this case, a 10-year life extension was proposed based on remaining field conditions. Given the spar's location, the design storm conditions did not change to the extent of the *Neptune* spar. A proprietary risk matrix develop by Chevron was used in this analysis, and an important finding of the assessment was that there are significant financial risks to the owner during the life extension that should also be assessed along with the safety risks. The authors note that this is caused in part by the standard operating procedure of shutting down production and evacuating the platform for an approaching hurricane. This significantly reduced the life safety and environmental risks associated with the platform, but the financial risks of remain. The authors noted that their philosophy was to track both risks, and while only the safety risk required regulatory approval, before investing in the life extension, the financial risk also needed to be controlled. The American Bureau of Shipping has served as the CVA on several life extension projects in the Gulf of Mexico. In support of

this role, during the mandate period, they released a first guidance note on the life extension process, which was then updated in May of 2017 (American Bureau of Shipping, 2017). During the mandate period, little research into new principles to apply for life extension appeared. There were many publications extending and refining existing assessment methods for life extension such as spectral fatigue (e.g. (Aeran and Gudmestad, 2017)), but the review of such calculation-specific methods primarily belongs to other ISSC committees. Tan et al. (2016) was one of the few exceptions, proposing to apply a novel DHGF-based theory to life extension decision making. This paper includes an example of the life-extension of a shallow water platform with a 15-year design life in the Bohai Bay.

Interest in life extension plans for offshore renewables is also growing, especially as the age of the oldest major offshore wind turbine farms begins to approach their design life. Ziegler and Muskulus (2016) note that in the early 2020s the first major windfarms such as "Anholt" and "London Array" will begin to reach their second decade of service. In general, maintenance modeling and optimization of such farms during operation as received extensive attention, as well as determining when the end of useful life is likely to occur (see Shafiee and Sørensen (2017) for a recent review paper on these topics). However, there appears to be a gap in methodology at the present for the structural system. Most such work in the past has focused more on the mechanical system of gearboxes, generators, and auxiliary equipment on the turbine and less on the turbine structure itself. Onshore wind farms are ahead of offshore wind farms in developing solutions, with expectations of strong market demand for life extension strategies in the next five years (Ziegler et al., 2018).

During the current mandate period the first research and criteria for structural life extension have begun to appear, starting the process of filling this gap. Work at NTNU has begun to look and offshore wind turbine crack growth for life extension (Ziegler et al., 2016; Ziegler and Muskulus, 2016), including the impact of load sequence and seasonality on interpreting inspection results. DNV-GL has issued guidance notes on life extension for both onshore and offshore wind turbines (DNVGL, 2016a), while Bureau Veritas has issued a white paper on life extension (Bureau Veritas, 2017). Bureau Veritas divides the life extension approach into three categories depending on how much in-service and site-specific data is available. The Danish strategic industry-government-industrial partnership Megavind has also issued a white paper on life extension (Megavind, 2016), including location-specific failure modes and areas of concern. Megavind divides life extension strategies into four categories depending on the type of monitoring data available, ranging from no measurements through complete multi-year load, wind speed, and turbulence measurements. The similarity between this approach and the Bureau Veritas approach further highlights the growing need for through-life data collection to support cost-effective life extension. Life extension considerations for other offshore renewable energy systems seems largely unexplored at the moment, reflecting perhaps that these systems have lagged wind turbines in large-scale adoption. However, a PhD thesis exploring the component reliability drivers for tidal stream devices has recently appeared (Delorm, 2014). Such initial work may lay the foundation for future efforts to address wave and tidal devices as well.

Commercial and naval ship life extensions criteria development have not been as active as the offshore criteria, perhaps a reflection of the challenging economic conditions for commercial shipping during this mandate period. The papers that appeared mainly dealt with calculation methodologies, not principles and criteria, and thus the primary review of this information can be found in Committee V.7. Looking at the higher-level trends from these papers, there is some similarity to the developments in the offshore world that are worth commenting on. A spectral fatigue re-analysis of a Moss-type LNG carrier to support service life extension was presented in a Korean-language paper by Park (2016). Similar to the offshore oil and wind turbine life extension approaches proposed, this method relied heavily on customizing the wave exposure to the known routes of the ships. Soliman et al. (2016) provide a probabilistic framework to plan inspection, monitoring and repair against the three objectives of service life, life-cycle

cost, and the delay in detecting potentially critical defects. This approach is partly adapted from the bridge maintenance approaches. As the approach focuses more on operational decisions, the principles explored are possible to apply for mid-life updates as well as design-stage studies. Naval vessel publications that focus on service life extensions also appear rare. Most of what has been proposed has focused on building optional service life extension in at the beginning of the design life. Temple and Collette (2017) provided a framework to trade between different cost aspects during design assuming probabilistic service life extension profiles, while Knight et al. (2015) proposed a variant of real-option theory to evaluated include extra structural capacity in a naval vessel at the design phase for a potential life extension later.

2.4 Human Performance in Engineering and Criteria Evaluation

2.4.1 The Challenge of Human Performance in Engineering

Despite significant progress in including allowance for operational human error into marine design procedures and standards, the marine community has not extensively explored the role of human error in engineering analysis, decision making, and approval assessment itself. Such engineering errors have been shown to contribute to many in-service failures in both marine and other structural systems. Additionally, as engineering analysis methods and performance criteria become more complex the role of human factors in successfully assessing compliance with the required criteria is growing. Thus, in assessing structural design criteria, the questions emerge how should the human engineer's limitation be considered in criteria development? And are there any recommended standards or procedures for accounting for such error?

Other industries have examined the role of analysis errors on business performance, including notable work in the financial industry. The ability of humans to manage complex software systems has also been studied extensively in both aviation and medicine. However, little recent work has appeared on these issues in the marine industry. By contrast, the civil engineering structural community has actively pursued the study of engineering error. Given the similarities between civil and marine steel structures, many of their findings appear applicable and enlightening for the marine community. This section will review both marine and civil studies on human error in engineering.

2.4.2 Past Work

Modern investigations of the human performance of engineers during structural design date to the 1970s and 1980s (Melchers, 1984; Melchers and Harrington, 1983), during the transition to reliability-based LRFD design codes. As various sources of uncertainty in structural loading and resistance were quantified, the performance of human engineers was also examined. Both historical failures and engineer's performance on simple tasks were examined. Overall, it was estimated that roughly 40% of failures stem from errors during the design phase (Melchers, 1984), a figure which appears to have remained remarkably stable with current civil engineering data from Europe (Terwel et al., 2014). Additionally, error rates for individual engineering tasks were shown to be roughly 1% for simple engineering steps such as table lookup, 2% for two-step calculations, 5% for not understanding written documentation. When combined into overall design processes, error rates were shown to be as high as 14% for the design of 2-D portal frames, which are not complex structures (Melchers, 1989, 1984). More recent work has confirmed similar error rates on simple 2-D structures some 30 years later, at least in the civil engineering community (Fröderberg, 2014).

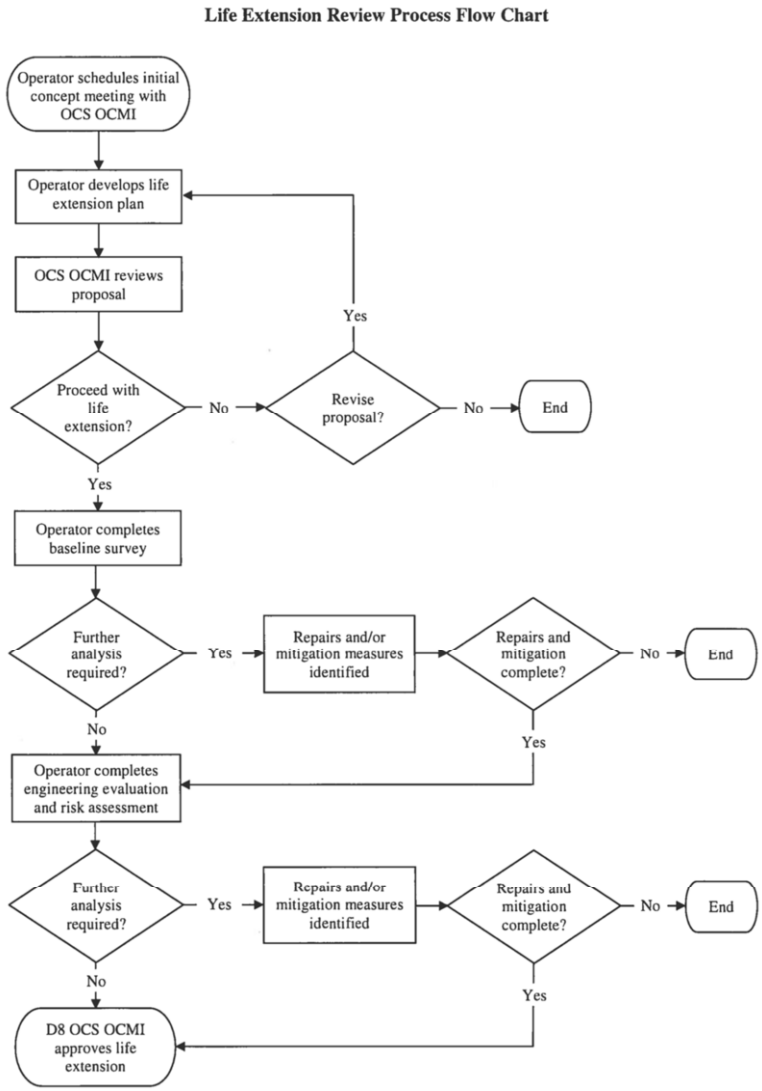

Figure 1: Approval Flowchart for Life Extension on U.S.-Regulated Gulf of Mexico Floating Platforms (Reynolds, 2016)

Shortly after this initial work, a major study of human error in the marine field was published by Bea (1994). For a mix of marine structures for vessel and offshore application, Bea built upon and largely confirmed the work of Melchers and others in the proceeding decade. Engineering human error during design and construction, including both knowledge and communication lapses appears be significant in the marine world. Given the potential magnitude of human engineering errors, and the difficulty in mathematically modeling such errors, the first generation of reliability-based LRFD codes did not include provisions for human error in the partial safety factors used to cover other uncertainties. Instead, the literature at the time (Bea,

1994) focused on quality control and review as the most beneficial approach to minimizing the impact of human error. The late 1980s and early 1990s saw the emergence of Total Quality Management, ISO 9001, and other similar quality-focused approaches which supported the idea that engineering management would be the best method to reduce human error. However, recent post-TQM/ISO 9001 studies in the civil engineering field continue to show roughly the same error rates and error types as these initial studies. Therefore, it is reasonable to ask how successful the quality management principle has been. Such a review will also shed light on the work around human error to further understand how it may impact the design principles and criteria used for marine structures.

2.4.3 Scope of the Current Review

In investigating the issues around the performance of human engineers, recent work in two areas was sought out:

- The occurrence of errors originating from a mismatch between the design codes and numerical models used in marine structural engineering and the engineer's understanding of these codes and models. Since the late 1980s, both the number and complexity of design codes has increased, and the same type of increase occurred for numerical modeling. Thus, the types of errors experienced today may be different or more concerning.
- Errors in communication of model assumptions and meaning between team members, or between the team and approval bodies. As design and approval work continues to rely on large, often globally-dispersed teams, and the design tasks and models used become more complex, the role of communication and team dynamics is expected to grow.

Specifically excluded from this taxonomy is the broader issue of validation and verification of specialized numerical codes. Such V&V approaches have been extensively discussed in the literature. V&V is a distinct problem from that addressed here: that of models created by the engineers in the act of design and approval of a particular vessel or offshore structure. The analysis of human performance of the engineering team appears in its infancy in the marine world. Other domains, such as aviation and medical surgery have performed extensive analysis of both the factors impacting team performance, as well as the development of errors between numerical systems assisting the team and the team members. The remainder of this section will explore ongoing research in different areas relating to human engineering performance. First, the limited work done on the impact of ISO 9001 quality certification will be reviewed, followed by a discussion of mental model discrepancies as a framework for exploring error. Then, the impact of design codes, spreadsheet tools, finite element analysis, and group settings will be reviewed in turn. Finally, conclusions and commentary on the current state-of-the-art will be provided.

2.4.4 Review of Ongoing Research

The ability to formalize quality management to improve company performance and reduce human error continues to be a topic of research. The ISO 9001 certification, built from the quality management ideas explored in the late 1980s and early 1990s has received significant attention. As engineering errors are rarely publically discussed or reported in a central location to allow statistical examination, direct studies of the impact of ISO 9001 on engineering performance are limited. However, recent studies on overall corporate financial performance, presumably positively impacted by reducing human error has been mixed. A recent review of 397 publically-traded firms in the United States, but not exclusively engineering firms, noted a significant positive impact on corporate financial performance following ISO 9001 certification (Aba et al., 2015). However, work in Italy has not confirmed these findings for manufacturing firms in that country (Franceschini et al., 2016; Galetto et al., 2017). Concerns around interpretations of ISO standards include the idea the compliance only certifies that a company has a checking

system in place, not auditing that actual checks are carried out correctly (Fröderberg, 2014). Additionally, ISO-required checking systems are internal checks, but recent research on major land-based structural designs in Hong Kong has shown the benefit to using an external audit approach in place of internal checks (Palaneeswaran et al., 2014). In certain sectors of the marine industry, classification societies provide exactly this external review role. Thus, class-approved and non-class approved structures may have significantly different human engineering concerns.

Much of the recent work on human performance in engineering has stepped away from categorizing human errors on small piecemeal tasks of engineering calculations to look at broader issues of how humans work with engineering problems. This tracks with increasing evidence that errors in the overall conception of the problem are significant, perhaps more so, than individual errors in calculation steps. Additionally, such conceptual errors are difficult to catch with self-checking compared to purely mathematical or table-lookup errors. This line of thinking points to the concept of the engineering mental model – the engineers vision of the structure and its environment – as key to understanding the process of engineering analysis.

The growing complexity of structural design codes has emerged as a potential cause of human error during engineering. In many cases, structural mass can be reduced by using more in-depth analysis or requiring consideration of additional potential failure modes. Such improvements are highly worthwhile overall, owing to the improved efficiency of lighter structures, and improved safety from more rigorous checks. With modern computational support, the added calculations in such procedures are not expected to cause additional errors. However, more complex codes may lead to more severe problems in understanding and correctly using the code (Bulleit, 2008) owing to its complexity. Such complexity can also cause the engineer to focus on each component in isolation, and miss the overall system view of the structure leading to incorrect analysis (Björnsson, 2016). Others have suggested that design codes be progressive – starting with simple basic analysis that clearly links the code provisions to underlying structural dynamics, and then allowing more refined analysis as an option when it will lead to reduced structural material or cost (Muttoni and Ruiz, 2012). Such an approach also has the advantage of following the overall design process, where the final design emerges from rough initial concepts. In doing so, the engineer will be forced to start with a strong overall view of the system, and then refine local structural assessments as needed later in the design process.

A range of computer models are also used in the development and assessment of marine structural designs. While perhaps the most pedestrian, the basic spreadsheet is still in widespread use today. At the 2012 ISSC, Committee IV.2 reported on the engineering software in use in marine structural design, and spreadsheets were highlighted as an important and commonly used tool in the structural design and approval process (Pradillon et al., 2012). Spreadsheets allow any engineer or other user to automate and program calculations as they see fit. Unfortunately, this end-user programming has been shown to be difficult to quality control. An entire organization, the European Spreadsheet Risks Interest Group (www.eusprig.org) is now dedicated to tracking such errors. Recent surveys of business software spreadsheets have indicated that almost one out of four spreadsheets with formulas in them contain basic Excel errors, and that emails passing spreadsheets around were ripe for confusion about versioning and control of the documents (Hermans and Murphy-Hill, 2015). Previous work had indicated even higher overall error rates, though not all errors impacted the final results of the spreadsheet as currently used (Powell et al., 2009). Recent work continues to focus on the ideas of the problem of understanding spreadsheets by users who did not develop the spreadsheet, with lack of context for exploring the spreadsheet's formulas and structure cited as a key concern (Kohlhase et al., 2015). The difficulty in understanding context ties into the concept of mental model developed above. Spreadsheets feature normally-hidden formulas that are often written in cell notation instead of problem variables, making them difficult to understand for engineers who did not build them. Procedures and standards for improving spreadsheet and detecting errors are now

emerging (Mireault, 2015; *The FAST Standard 02b*, 2016), however, much of this work currently focuses on financial spreadsheets, not engineering calculations.

Beyond spreadsheets, informal discussions have also highlighted the role in which engineer's mental models may diverge from more complex numerical models of structures. For example, users who are not the developers of an in-house analysis code may be confronted with a large number of tunable settings whose impact and role are not clearly captured in the limited code documentation. In this situation, analysts of differing levels of experience with the code may produce very different results (Dr. Paul Hess, Personal Communication October 2017). Lack of transparency in the underlying model is not limited to in-house codes however. Research indicates that complex design codes, commercial software, and group settings can all lead to mismatches between engineer's mental models, often leading to human engineering errors. Recent work in both aviation, marine operations, and medicine has explored this type of problem. In aviation, the term used is "mode error" or "mode confusion" where the crew's mental model of what the automated system on the aircraft are doing departs from the reality (Sarter and Woods, 1995). Similar issues in developing mental models have been reported in marine dynamic positioning operations (Øvergård et al., 2015; Sætrevik et al., 2018). While engineers operate under lower time pressure than aviation or marine operations, there is still reason to believe the mental model – computer model divide is reason for concern. However, there is no evidence yet of researchers using these error frameworks to explore human errors in engineering design.

Finite element analysis is perhaps the most commonly used advanced calculation tool in structural design. Thus, work on the engineer's experience of finite element analysis is a logical place to look for the impact of human errors. Similar to spreadsheets, most FEA codes contain GUIs where mesh, element, and simulation options are buried under complex tree structures, menus, and dialog boxes. Similar to mode errors in automated systems, one wonders if the analyst is always fully aware of what model options are currently active. Indeed, human error in using finite element codes was one of the major reasons for disagreements mentioned in a round-robin study of determining crack trip stress intensity factors in piping systems (Han et al., 2016). This conclusion has been echoed by other authors previously in larger structures (Sgambi, 2005).

Beyond the difficulties in correctly using complex finite element codes, the impact of the complex analysis method on the engineer's focus has also been investigated. The demands of building and completing an FEA model can cause the engineer's focus to immediately be drawn to the lowest levels of structural detail, thus missing larger system effects. This effect was captured in a study by Fröderberg (2015), where the results of 14 Swedish engineers independently designing identical truss systems ended up with solutions whose weights had a coefficient of variation of 28%. These engineers had at least a MSc level of education and averaged 12 years of experience. Particularly, the difficulty in quickly iterating through geometry concepts in finite element software was noted, as the finite element software modeling requirements tended to lock them into their initial concept. Similar concerns of complex software reducing the system-level understanding have been voiced previously (Luth, 2011). The similarity between losing system-level understanding with advanced analysis tools explored here and of losing system-level understanding with complex design codes discussed earlier is notable. Such similarity implies that it is not so much the software's layout or GUI that matters, but how the calculations and modeling required impacts the part of the problem that the engineer focuses on.

Studying interactions with structural codes, spreadsheets, and analysis tools only captures human error originating from a single human engineer operating in isolation. However, most marine structural design is now done in a team setting, with a variety of engineers working on the same project. For more complex projects, it is also likely that these engineers would be geographically dispersed. Such team settings mean that communication of engineering results, and indeed the development of a shared mental model of the structure are also important. While

general team dynamics has been widely studied for the past 30 years, structural engineering teams have also recently received research attention. Communication lapses between team members has long been highlighted in civil and marine engineering as a contributor to human mistakes (Atkinson, 1999; Bea, 1994). More recent work on this concept in civil engineering structures has determined that the fragmentation of most design-build engineering sequences contributes to these communication lapses (Love et al., 2012). When a sequential, over-the-wall approach is used with designers, approval bodies, and final builders, even when potential errors are identified it is difficult to "move upstream against the natural flow of the process" (Love et al., 2012) to rectify the problem.

The growing acceptance that the information flow through design teams is central to understanding errors has led to several recent studies to focus on how teams process information, using analogies to social graph models (such as Facebook). A formal model of information flow in engineering teams has recently been proposed (Schneider and Liskin, 2015). This model has been extended to include the influence of social mood on the success of design communication in 34 software engineer teams (Klünder et al., 2016) and to more formally link to social network analysis (Kiesling et al., 2016). Similar efforts to use social network theory to describe the ability to identify and manage design errors in different organizational structures has been explored by At Hattab and Hamzeh (2015). Finally, drawing inspiration from stream-of-variation modeling, Strickland (2015) proposed the Process Failure Estimation Technique to study the composition of marine design teams and the likelihood of errors propagating through design processes. All of these works are at early stages, and the research does not appear to be immediately ready to transition into real-world decision guidance, criteria, or standards. There has been a rapid growth in wider social network analysis techniques recently, and a number of publications that have appeared in this area in the last two years focusing on engineering teams. This situation indicates that studying design team social dynamics is an area of growing interest in the quest to reduce human errors.

In large civil-engineering structural design studies, the design team has also been shown to be a potential source of error correction. Mentoring, supervision, work culture, and thoughtful review of the work of others have all been claimed to reduce error rates in large structural engineering projects in recent studies (Fröderberg, 2014; Love Peter E. D. et al., 2015; Love Peter E. D. and Smith Jim, 2016; Palaneeswaran et al., 2014). Many of these studies are qualitative in nature, based on experience or interviews, however their conclusions are notably consistent. The success of such approaches points to a potential path forward, less structured and formal than ISO 9001, that would allow complex design code and analysis tools to be used while minimizing the types errors discussed above.

2.4.5 Assessment of the State of the Art of Engineering Human Performance Criteria

The role of human error during the engineering design and approval stage of marine structures remains unclear. The last significant marine-focused work is now 25 years old. Recent work, primarily in the land-based civil engineering community, has highlighted several reasons to be concerned about such errors: they represent a significant portion of total errors and in-service failures, there is reason to suspect that more complex regulatory codes and numerical models are impacting how engineers view structural systems, and complex social dynamics in team settings have also been shown to impact information flow and the ability to detect and correct human errors. Related work, primarily in the business community, is showing that ISO 9001 certification alone may not be the best way to reduce human design error, and that even spreadsheet models suffer from many of the same problems noted about design codes and advanced numerical models. Additionally, social network approaches to studying engineering design teams are growing rapidly and may provide a new set of tools to investigate engineering error. Given this situation, it appears that more research into how human engineers interact with complex codes and models in the marine domain, and how human engineers work together in teams in the marine domain, is clearly needed.

2.5 Inland and Coastal Vessels

Vessels which transport cargoes and passengers on rivers and coastal routes play noticeable role in economy of many countries. Usually such vessels do not make international voyages. That is why design of their hulls is defined by Rules of classification societies and national requirements. As practice shows, river and river-sea vessels are classified in classification society which represents the country of planned operation.

For numbers related to Russia, reference is made to Egorov and Egorov (2017), mentioning for dry cargo about 857 motor vessels and 4190 barges, for tankers 652 motor vessels and 692 barges and, finally, 2730 pusher and tug boats and 1336 passenger vessels.

In Ukraine as to Egorov (2012) there are 299 dry-cargo self-propelled vessels and 596 dry-cargo barges, 52 self-propelled tankers and 32 oil barges, 286 tug-pushers and 190 passenger vessels.

The actual age of river-sea vessels at decommissioning is about 45-50 years. Additionally, about 10% of vessels are lost in accidents before this age. Average age of existing vessels is about 40 years. Therefore, in next 5-10 years more than 50% of fleet operated now will be quite objectively decommissioned and volumes of transportations on water transport will reduce.

An overall picture of the dimension of inland water transport (IWT) in Europe can be derived by the recent survey by the Central Commission for the Navigation of the Rhine (CCRN, 2016). There, about 8000 dry-cargo vessels and 1,650 tankers are mentioned, with various sizes. An analysis of the state and age of this fleet is reported in the same paper. In the United States, 2016 statistics include both coastwise and inland vessels, with an overall fleet size of 32,353 barges, 3,215 push-type towboats which are primarily used on river systems (USACE, 2017).

Of course, new river and river-sea vessels are under construction (Egorov et al., 2016a). In accordance with (Egorov et al., 2016a), such vessels include more effective solutions:

- maximal usage of actual way conditions;

- extremely full hull contours which earlier were not applied in world practice (Egorov et al., 2016a);

- expanding of transported cargoes – project cargoes, chemicals, combination of dry cargoes and oil products on one vessel (for example, in one side – oil products, in another – road metal), so called combined vessel, f.e. Seven 5745t DWT vessels of Marine Engineering Bureau RST54 project were built in 2014-2016 in Russia;

- decrease of air draught to pass bridges without requiring bridges to open;

- effect of "rotator" operation scheme when 2-3 barges are working with one pusher;

- usage of pushed barge in combination with a self-propelled vessel.

For example, in 2000-2016 317 new cargo self-propelled vessels have been built in the former Soviet Union. Among them 301 are of coast and river-sea class, 16 are of river class.

It is also necessary to draw attention to the passenger segment. In August 2016 the keel of river-sea high-comfort passenger vessel was laid down in Astrakhan (Egorov et al., 2016b). Delivery is planned in 2019. It is a diesel-electric vessel where three quarters of the cabins have individual balconies, and area of cabins – 19-21 sq.m – conforms to all standards of modern cruise and hotel industry. There are all types of necessary passenger amenities (restaurants, SPA-centers, fitness, bars, etc.). All native leading cruise companies took part in development of project. The vessel completely meets their requirements. The vessel will work at classical river lines, and also make voyages from river ports to marine ports, including the Caspian-sea round voyage and a routing Moscow - Rostov-on-Don - Sevastopol - Sochi.

As for Rules and Regulations, for more than six decades, UNECE Inland Transport Committee (ITC) has promoted the development of international inland water transport at European level. A recent document exploiting the characteristics and advantages of this transport mode is the White Paper on Efficient and Sustainable Inland Water Transport in Europe (UNECE, 2011).

UNECE provides a platform for intergovernmental cooperation to facilitate IWT. An important target of UNECE is the development of a unified normative framework at the European level. This is particularly needed as the IWT suffers, even at a European level, from a historical infrastructural, institutional, legal and also technical fragmentation, due to the presence of local institutions (River Commissions: Danube – DC, Rhine – CCNR, Mosel – MC, Sava – SC) providing requirements for their specific river basins on various overlapping subjects.

For the design stage from technical and safety requirements side main instruments: Resolution №24 – CEVNI: European Code for Inland Waterways; Resolution №61 – Recommendations on Harmonized Europe-Wide Technical Requirements for Inland Navigation Vessels; European Agreement concerning the International Carriage of Dangerous Goods by Inland Waterways (ADN); Resolution №57 – Guidelines and Recommendations for River Information Services; Guidelines for passenger vessels also suited for carrying persons with reduced mobility.

Resolution №61 of UNECE includes 20B chapter which contains special provisions applicable to river-sea navigation vessels. The chapters' rules were based on Russian River Register rules. On this moment Chapter requires updates in positions of coupling devices, sailing areas and some others.

In the February 2017 Fiftieth session of Working Party on the Standardization of Technical and Safe-ty Requirements in Inland Navigation (SC.3/WP.3) of UNECE took place in Geneva (UNECE, 2017). The Marine Engineering Bureau presented information about new built fleet and about conversion experience (main developments are in UNECE document ECE/TRANS/SC.3/WP.3/2017/6). Representatives of European river commissions showed great interest to conversions because of the large number of older vessels in the fleet in Europe. In Russia, such conversions were performed in 2003-2012. A number of regulations and guidance documents have been produced to establish criteria for such reconstruction and re-use: Construction of Inland Navigation Vessels and Combined (River-Sea) Vessels with the Use of Components of Used Vessels (P.003-2003) and Renovation of Inland Navigation Vessels and Combined (River-Sea) Vessels with the Use of Components of Used Vessels (P.041-2014).

Between 2003 and 2012, 89 vessels were built in compliance with P.003-2003, "Construction of Inland Navigation Vessels and Combined (River-Sea) Vessels with the Use of Components of Used Vessels". However, construction re-using existing vessel components ceased in 2012. At this time, the Technical Regulations on the Safety of Inland Waterway Transport Facilities in the Russian Federation entered force. These requirements require the presence of double bottom and double sides for tankers and vessels transporting dangerous cargoes, eliminating the ability to re-use existing vessel components.

CCNR offered in 2015 a European Standard laying down Technical Requirements for Inland Navigation vessels (ES-TRIN, 2015) which is mandatory for EU and CCNR Member States. In future CCNR plans to unite the Rules of Resolution 61 of ENECE, Rhine vessel inspection regulations (RVIR) of CCNR and Directive 2016/1629 of EU on the base of ES-TRIN. In 2017 ES-TRIN will include new provisions for fire-fighting systems, cranes, traditional crafts, navigation and information equipment, elevating wheelhouses, reference updates to EN/ISO Standards and so on.

In the United States, a new regulatory scheme, 46 CFR Subchapter M, was published on 20 June 2016 for inland and coastal towing vessels. This scheme moves the inland and river fleet into a formally inspected status. While much of the discussion during the development and implementation of this rule has focused on the operational impacts and regulations contained

in the subchapter, for structural systems is does now formally specify that vessel designs must comply with an approved classification society standard, though class need not be maintained during the operation of the vessel.

3. PRINCIPLES AND CRITERIA FOR USING ON-BOARD MONITORING DATA

3.1 Code and Safety Updating Offline

On 18 January 2007, the 4,419TEU container ship MSC Napoli suffered a catastrophic failure at the engine room bottom and partial hull girder failure at this location, while navigating the English Channel in heavy seas. The investigation made by Marine Accident Investigation Branch (MAIB), UK has identified factors which contributed to the failure. One of the recommendations made by MAIB was to initiate research into the development and use of technological aids for measuring hull stresses on container ships (MAIB, 2008). Six years after that on 17 June 2013, the 8,110TEU container ship MOL COMFORT suffered a collapse in way of her midship bottom and broke in two, while crossing the Indian Ocean. Following this accident, thorough investigation was conducted by Ministry of Land, Infrastructure, Transport and Tourism (MILT), Japan, and ClassNK (ClassNK, 2014; MILT, 2015, 2013). In the investigation report, ClassNK mentioned to consider the utilization of hull monitoring systems to provide useful information for ships referring to the data obtained from the on-board full scale measurement.

Apart from these events during this decade, hull monitoring systems emerged and attracted attention around two decades ago, and several classification societies introduced rules and requirements for the hull monitoring system, including ClassNK, DNVGL, and CCS i-Ship. One of such rules is DNVGL's HMON notation (DNVGL, 2016b). In case of large container ships, HMON requires monitoring of 4 global longitudinal stresses (midship port and starboard, L/4 from midship port or starboard), global transverse stress at transverse deck strip amidships, loading computer systems, ship position, speed/course, speed log, power output and revolutions of propulsor and the wind condition, while recommending monitoring of vertical acceleration at fore part, transverse acceleration in the 0.4L midship area, ship motion in six degrees of freedom, longitudinal stress close to the bottom amidships (port and starboard), double bottom bending, bending/shear stress in pillar bulkheads, lateral loads at bottom near the forward perpendicular and side for slamming impact, gyro compass heading and wave condition. In response to the recent large container ship casualties as mentioned above, IACS (2015b) published new longitudinal strength standards for container ships (UR S11A). UR S11A stipulates that hull girder ultimate strength assessment consider whipping response when assessing the vertical bending moment in all Classification Society procedures. Accordingly, IACS member societies amended their rules, as deemed necessary. For examples, ClassNK (2017) developed an evaluation procedure to assess the hull girder ultimate strength with taking into account of local pressure loads acting on the bottom plating in addition to the whipping contribution. DNVGL (2016c) covers this requirement by introducing a closed-form formula of the partial safety factor for the additional whipping contribution. With respect to hull monitoring, it is stipulated that this contribution of whipping can be mitigated by 30% for ships with the class notation HMON(G). This kind of rational combination of monitoring system and design conditions may open up a new horizon, where the ship master's judgement on safe navigation in rough seas depends on quantitative failure risk or fatigue damage accumulation displayed by the monitoring system, rather than the master's five physical senses and intuition. However, effectiveness of such systems or the relationship between navigational decision making and structural design conditions are not yet clear, and significant research activities are necessary in this area.

Another important benefit expected to be obtained from in-service measurements is improvement of design accuracy by updating design load assumptions using the measured data. Zhu et al. (2017) proposed a new framework to update the load model used in design stage from measured wave load data in service. They proposed a two-level offline lifetime load updating scheme,

where corrections to hydrodynamic predictions are established first, and a hierarchical Bayesian models were utilized as learning approaches. This kind of approach is becoming increasingly important, allowing updating under varying operational profiles and wave climates in the future.

3.2 Full-Scale Measurement Campaigns

Full scale measurements of ship hull structures have long been carried out for various kinds of ships in order to confirm structural behavior of ships in actual service at sea. Especially in response to the rapid enlargement of container ships due to the worldwide economic growth and increased seaborne trade, many hull condition monitoring projects on large container ships were conducted during the recent decade.

An early example of such measurements can be seen in Okada et al. (2006), where they carried out measurements of longitudinal bending stresses and deflections of hatch openings for three years on a 6,690TEU Post-Panamax container ship, and showed that in general the measured results were in good agreement with the design assumptions, except that the measured deflections of the cross decks were much smaller than the design assumptions. They also revealed that significant whipping responses were observed, which may increase the fatigue damage twice. Toyoda et al. (2008) made similar full scale measurements on another Post-Panamax container ship. Storhaug et al. (2007) measured stresses onboard a large 294m container ship operating in the North Atlantic, and concluded that the wave induced vibration affects fatigue strength and hull girder ultimate strength and that design considerations of such responses are necessary. Heggelund et al. (2010) assessed measure data on an LNG carrier during a period of about twelve months, and showed that the contribution from vibration to the fatigue damage was as large as 30 – 50% of the total damage, while Koo et al. (2011) showed that the contribution from vibration on an 8,000TEU container ship was about 30%. Heggelund et al. (2011) reported measurement results on an 8,600TEU container ship operating between East Asia and Europe, and confirmed that the fatigue loading of critical details are dominated by the vibrations. Based on measurement campaigns onboard a Panamax and a Post-Panamax container ship, Rathje et al. (2013) obtained damage increase of the factor 2.36 caused by high-frequency vibrational response. However, they also pointed out that the vessels of the fatigue lives of 13~16 years including vibrational fatigue damage have experienced no significant damage, even for ships operating world-wide for more than 20 years, and that the contribution of high-frequency loads in assessing the overall strength of large container ships does not seem to be fully resolved yet. Ki et al. (2015) examined measurement results on a 14,000TEU container ship, and concluded that considerable fatigue damage increase by hydro-elastic behavior could be identified.

In general, all these full-scale measurement campaigns were conducted using one selected ship during several months or years for research purposes. Therefore, due to the limited number of target ships and limited number of measurement locations and sensors, analysis and evaluation of the measured data are as a result confined to, for example, statistical characteristics of longitudinal bending moment, whipping occurrence and so on. To further expand the analysis scope to statistical analysis of the encountered sea state, determination of statistical characteristics of both dynamic and static loadings, and analysis of actual navigational decisions, it is necessary to carry out a systematic and consistent full-scale measurement campaign, obtaining "Big Data" with regard to ship responses, navigational parameters and encountered sea states. To this end, Okada et al. (2017) started a large scale measurement project using ten (10) 14,000 TEU class large container ships, where a hull stress monitoring system and ship information management system are installed onboard all the 10 ships as standard facilities, aiming at effective feedback to rationalize design and maintenance, and also effective support for safe and efficient navigation.

3.3 Decision Support Systems

One of the important measures to support officers onboard to make proper decisions on ship operation in rough seas and increase the operational safety of ships may be a real time onboard measurement system. Nielsen et al. (2009) suggested a procedure to incorporate random variables and associated uncertainties in the calculations of the outcrossing rates that are the basis for risk-based decision support system. They pointed out that for the purpose of decision support, it is necessary to estimate future ship responses within a time scale of the order of 1~3 hours taking into account speed and course changes. Nielsen et al. (2011) further carried out stress monitoring, and proposed a decision support methodology based on extreme structural responses and fatigue damage accumulation.

Deco et al. (2015) used structural health monitoring data to update the prediction of structural performance, proposing a simulation-based technique for Bayesian updating. They solved multi-objective optimization problems and obtained Pareto-optimal sets of navigation route and ship speed, in which the objective functions are the estimated time of arrival, mean total risk, and fuel cost. It is expected that this kind of studies can provide decision makers a strong support to navigate efficiently avoiding the risk exceeding the required target. Dong et al. (2016) further studied multi-criteria based decision making approach, including repair loss associated with flexural failure, fatigue damage accumulation, total travel time and carbon dioxide emissions as the criteria, employing multi-attribute utility theory. They showed that this approach can determine the optimum ship route and ship performance, simultaneously taking into account the decision maker's preferences with regard to the risk-taking and risk-averse attitude for each criterion.

3.4 Onsite Estimation of Ocean Waves

Onsite estimation of the waves which each individual ship is actually encountering is important for various purposes such as proper decision for the ship operation, rationalization of structural design through comparison of assumed loads and actual loads, estimation of hull damage all over the ship under the sea state which the specific ship has encountered, and its application to rationalized maintenance of hull structure. There are many measures to identify encountering waves including visual observation, wave radar, wave forecast and hindcast. Each of them has advantages and disadvantages over other measures, but the method to precisely measure the actual sea state which the ship is encountering is not established yet.

As a promising technique to fulfill this target, usage of measured ship responses as wave sensors (wave buoy analogy) has been studied over several decades. Pros and cons of each estimation method are summarized in Table 2 based on the interpretation of the current literature, where we can recognize that the estimation using ship response is promising once the accurate estimation methodologies are established.

Nielsen (2016) made a comprehensive review and pointed out that the concept of the wavy buoy analogy is not yet widely used in practice, but it has matured to a level that would be applicable for shipboard decision support system. Nielsen (2006) applied various methods to identify on-site wave spectrum from ship responses, and compared a parametric method which assumes the wave spectrum to be composed by parameterized wave spectra and a non-parametric method where the directional wave spectrum is found directly as the values in a completely discretized frequency-directional domain without a priori assumptions on the spectrum. As a result, he concluded that "it is difficult to propose one of the ship response-based methods in favor of the other, since they perform equally well". This was later confirmed through a larger study by Nielsen et al. (2013) on actual sea state estimation using more than 100 hours of response data collected from a 9,400 TEU large container ship in service.

Table 2: Pros and cons of various wave estimation methods

Method	**Accuracy**	**Represent the encountering sea state?**	**Simultaneous post processing and usage of the data**	**Cost**
Visual observation	Not good (Medium for significant wave height and wave period, but impossible to obtain wave spectrum)	Good	Impossible	Good
Wave radar system	Medium	Good	Good	Expensive
Wave hindcast	Good	No good (Estimation grid distance: 50~100km)	Impossible	Good
Estimation using ship responses to waves	Under development (Good results reported in literature, but wave frequencies for which the ship does not respond will be filtered out)	Good	Good	Good

Nielsen et al. (2012) made another comprehensive study on parametric modelling of the directional wave spectra based on sea trial data of a Canadian Navy research ship, and showed that the wave buoy analogy provided slightly better sea state estimates than a wave radar system on average, for the studied data. In this study, the sensitivity of sea state estimates was investigated by using sets of different vessel responses as input for the wave buoy analogy. It was shown that different combinations of motion components significantly influenced sea state estimates of the wave buoy analogy. Therefore, it is very important to select appropriate sets of ship responses, which are most suitable for each specific case. The methodologies of this suitable selection of appropriate combination of ship responses are far from being established, developing such as selection methodology is a challenge for future research in this area.

Pascoal et al. (2008) presented a numerical procedure using a non-parametric formulation which allows for a low constraint on spectral shape estimation. They discussed appropriate smoothing methodology of the spectral shape, which is important because the problem is underdetermined and there are many alternative solutions of the spectra giving a minimum objective function value.

Montazeri et al. (2016) further studied wave estimation by optimizing parameters of directional wave spectra to minimize the difference between the energies of a set of measured ship responses and the corresponding theoretical spectral moments. A partitioning procedure to separate swell and wind seas was applied. In this study, they pointed out that the responses of a large ship with a high inertia filter out the high frequency part of the wave spectrum, leading to poor estimation of higher frequency components, and suggested that it may be beneficial to use wave bending moment, which is more sensitive to the higher frequencies than ship motions. In this regard, Yoshihira et al. (2017) estimated wave spectrum in a numerical tank from the calculated

ship responses in artificially generated long-crested head sea irregular waves. As the ship responses, pitch, heave and longitudinal bending stress were used, and as a result, they concluded that the wave estimation based on longitudinal bending stress was the closest to the artificially generated wave spectrum, thus demonstrating the possibility of the effectiveness of longitudinal bending stress as the input for the wave estimation.

Iseki et al. (2015) investigated the short-term variability of ship responses by cross-spectrum analysis. Using long stationary time series during 20 minutes, the transition of amplitudes and relative phase angles of the cross-spectra during 1~6 minutes duration has been investigated by iterative analyses with a few seconds of time shifting, and as a result, they showed that the short-term variability of the relative phase angle was observed and the variability may compromise the accuracy of the wave buoy analogy in effect. In fact, stationary operational conditions with duration of at least 10~15 minutes are considered to be necessary to perform the spectral analysis (Nielsen, 2016), and this direct disadvantage of the frequency domain approaches to be applied to real time sea state estimation on board have recently initiated studies where the direct time domain sea state estimation is sought (Nielsen et al., 2015; Pascoal and Guedes Soares, 2009)

Wave estimation using offshore structures without forward speed is also in progress. Da Silva Bispo et al. (2016) reported wave estimation results from a monitoring campaign on a turret FPSO off the Brazilian coast in comparison with data supplied by a radar system. Mas-Soler et al. (2017) used a semi-submersible platform as a motion-based wave sensor to improve accuracy of the estimation in extreme wave conditions, and showed good agreement with experimental results in a wave basin.

4. PRINCIPLES AND CRITERIA FOR ACCIDENTAL LOADS

Well-validated design principles and criteria for ships and offshore structures are crucial to increasing the safety level of those structures subjected to accidental loads from various causes. The assessment of different types of accidental loads that may cause damage to ship and offshore structures, are reviewed here, such as the loads induced by collision and grounding, slamming, explosion and fire. Details of analytic developments in this area have been covered by several ISSC committees. In the current congress, specialist committee V.1 is examining accidental limit state formulations. In previous work, advances were reported in the recent reports of ISSC committees/specialists committees such as ISSC 2012: I.2, II.2, V.1 and V.7 and ISSC 2015: I.2, II.2, V.1, V.2 and V.5.

4.1 Collision and Grounding

Eleftheria et al. (2016) provided a historical overview of the development of regulations around collision and grounding . They noted that responses to accidents, particularly those with large loss of life, have driven the introduction of new regulations and the strengthening of existing regulations, particularly at the International Maritime Organization (IMO). This has largely been a successful effort, as the rate of accidents has reduced significantly. They state that at the present time, more than 80% of the accidents are related to human factors. Such a high contribution from human factors has led to a focus on active safety measures, targeting the ship's operation. Focusing on active measures can reduce the frequency of accidents. Passive safety measures, which will be the focus of this section, are those related to the ship's design and technology (Eleftheria et al., 2016). These approaches primarily contribute to reducing the consequence of an accident when it does occur. In the structural domain, actions such as simulating collision and grounding to improve the crashworthiness of structures can reduce damage and flooding extents, reducing the consequence of the accident in terms of the ship or platform's stability or residual structural strength.

4.1.1 Collision

Ship and platform collisions can lead to serious vessel safety, environmental pollution, and economic consequences (B. Sun et al., 2015). The current approaches to analyze ship collisions can be generally grouped into five categories: empirical formula method, simplified analytical method, numerical method and experimental method, as well as the recent risk assessment method. Amongst these methods, simplified analytical method and numerical method have been the most widely used methods, while the empirical formula method has a limit on its accuracy due to data limitation. Because of its uncertainty of the scaling factor, the experimental method mainly focuses on the structural dynamics of components or parts of the ship, and this method is very pricy. The risk assessment method combines the probabilistic theory with the structural mechanics, considering the frequency and the consequence of ship collision accident together.

(1) Risk assessment of ship collision

Eleftheria et al. (2016) presented a recent review of the historical record of ship incidents. This work was designed to both support Formal Safety Assessment (FSA) activities, and to look for patterns with ship age and regulations. Their work was in part motivated by reports in the mid-2000s that the safety level in the marine industry was worsening and examined both the frequency of accidents and the corresponding consequences. Eleftheria et al.'s findings indicated that the overall safety level seems relatively constant. They also included a deeper investigation about possible relationships between accident rates and ship's age, but no simple findings could be made, the relationship was more complex than initially thought. This work is notable for the breadth and detail sub-type investigation of the fleet which can inform structural collision and grounding scenarios.

Ship collision risk may be obtained from the historical data, expert opinions and mathematical calculations. However, the past data may be improper and inadequate to predict the likelihood of future occurrences. Meanwhile, the expert opinions may introduce a high degree of subjectivity. For these reasons, mathematical calculations have been widely used to predict the risk of ship collision. Huang et al. (2016) introduced a collision risk assessment method based on Velocity Obstacle (VO). They applied VO to distinguish the dangerous velocities and to judge the collision probability. The ship maneuverability was also considered to find the reachable velocities (RV) in a given time window. With the percentage of dangerous velocities in all RV being defined as the collision risk, the assessment model by Huang et al. (2016) can identify the collision dangers as well as measure the probability of surviving in the encounter situation, regarding to its maneuverability.

The quantitative risk assessment (QRA) technique is a formal and systematic approach to estimate the likelihood and consequences of hazardous events, and to present the results quantitatively as the risk to people or environment. Chai et al. (2017) proposed a QRA model to evaluate the risk of a ship being involved in ship collisions, by taking into account the frequency and consequence of all possible accident scenarios. The proposed QRA model "consists of a collision frequency estimation model, an event tree and consequence estimation models. While the event tree comprises five intermediate events including ship type, ship size, loading condition, hull damage and survivability, two ''generic" mathematic models are developed to estimate the human life loss and oil pollution caused by ship collisions, respectively" (Chai et al., 2017) .

In addition, Spent Nuclear Fuel (SNF) transportation is considered to be a very urgent problem for those plants situated offshore with a shortage of SNF storage space. Christian and Kang (2017) followed the methodology as required by SOLAS 2009 (IMO, 2009) to assess the risks of maritime spent nuclear fuel transportation with a probabilistic approach. In their study, event trees detailing the progression of collisions leading to the damage of the transport casks were constructed. Parallel and crossing collision probabilities were formulated based on the Poisson

distribution. The Automatic Identification System (AIS) data were processed with the Hough Transform algorithm to estimate the possible intersections between the shipment route and the marine traffic. Monte Carlo simulations were done to compute collision probabilities and impact energies at each intersection. Possible safety improvement measures through a proper selection of operational transport parameters, including shipment routes, ship's cruise velocity, number of transport casks carried in a shipment, the casks' stowage configuration and loading order on board the ship, are investigated. The proposed methodology is successful in quantifying ship collision and cask damage frequency, and it will be effective in assisting decision making processes to minimize risks in maritime spent nuclear fuel transportation.

The uncertainty analysis is required to be carried out in the Formal Safety Assessment (FSA) as required by IMO. Sun et al. (2018) combined the Monte Carlo random sampling of probability distribution functions with the a-cuts for fuzzy calculus to propagate the uncertainties. In addition, they proposed a method for time window selection to estimate the magnitude of uncertainties. . Sun et al. also present a FSA case-study on cruise ships. The results of this study show that the uncertainty analysis generates a two-dimensional area on the FN diagram for a given degree of confidence, rather than a single FN curve which would result without uncertainty. Sun et al. claim that the area result provides more information to authorities when considering which risk control measure would be effective.

As there are many marine accidents including collisions worldwide, it is necessary but quite difficult to establish all the causes contributing to the accidents. Common classification systems need to be considered to examine all those accidents. Yıldırım et al. (2017) reviewed large amount of marine accidents using the Human Factors Analysis and Classification System (HFACS). It suggested that risk assessment of the effective accident type must be conducted according to the different voyage situation or local conditions. Endrina et al. (2018) conducted a risk analysis study for RoPax ships using the FSA method by IMO and established the collision risk model through an Event Tree.

(2) The mechanism of ship collision

Experimental tests of real-size ships demand heavy financial investment, complicated logistic, intensive labor, and heavy-duty equipment. Hence, most of the collision experiments only deal with large-scale sections of ship structures subjected to impact loads, rather than complete ship structures. Oshiro et al. (2017) described collision tests of scaled ship structures, giving special attention to some similarity complications that are frequent in real tests. For instance, the yielding stress and material strain rate of the model are different from those of the prototype. Since the standard similarity laws are unable to deal with those issues, it is shown how to modify the scaling factors to generate a replica similar to the corresponding prototype. The methodology depicted in this paper can be used as guidance for scaled impact tests of vessels and other types of large structures.

Numerical analysis of ship collision is extremely complex undertaking, which involves developing mathematic models for at least three complicated tasks including deriving procedures for calculation of the probability of ship collisions in a given area, analysis of external dynamics and investigation of internal mechanics. For external dynamics of ship collision, Pedersen and Zhang (1998) developed simplified analytical, closed-form expressions for the energy released for crushing and the impact impulse during ship collisions, by only considering the motions of the ships in the horizontal plane. Their analyses are validated with numerical simulations and good agreement has been achieved. This analytical model is well suited for inclusion in a probabilistic calculation model for analyzing the damage of ship structures due to collisions. Furthermore, Zhang et al. (2017) further validated this analytical model with a large number of experimental results that can be found in literature and reasonable agreement is achieved. In their paper, a simple concept to account for the effective mass of liquids with free surface carried on board of a ship is adopted. In addition, the new modified model could be expanded to take into account the effect

of ship roll on the energy released for crushing. The well-known empirical method between the absorbed energy and the damaged volume was proposed by Minorsky (1958) and developed by Pedersen and Zhang (2000). The calculation accuracy was improved by taking the structural arrangement, material properties and damage mode into account. The method was re-examined in Zhang and Pedersen (2017). Good agreement between the simple expression results and experimental results from published papers was obtained. The improved method can be used for the assessment of ship collision damage. However, using the energy based method for the calculation of the structure damage did not provide sufficient details of damage. When predicting the absorbed longitudinal energy, the uncoupled method did not consider the factors like the damage extent. Numerical simulation of a ship collision is an appropriate alternative choice but extremely complex.

It is noted that for most collision analysis, a static approach is used as most incident involved low speed collision. When such methods are applied to relatively high-speed collision, the dynamic effects should be assessed and appropriate design criteria are to be specified.

To reduce the risk of structural impact damage, much attention has been paid to enhancing the understanding of the mechanisms of ship collision and grounding accidents (Luís et al., 2009; Prestileo et al., 2013). For the collision of double hull ships, the rupture of the inner hull should be avoided until all the impact energy is dissipated, to prevent severe economic loss and casualty. Thus, it is crucial to accurately assess the impact resistance of ship double hulls in the preliminary structural design. Liu and Soares (2015) presented a simplified analytical method to examine the crushing resistance of web girders subjected to local static or dynamic in-plane loads, providing preliminary design tools to assess the internal mechanics of ship collisions and thus developing crashworthiness designs of the double-hull structural components.

Prabowo et al. (2017) studied the rebounding phenomenon of a striking ship. They studied the rebound effect on the structural crashworthiness performance of the struck ship. A series of impact scenarios are defined to estimate the behaviour of the struck ship during and after impact by the striking ship. Prabowo et al. summarized these results as crashworthiness criteria.

The study of repeated impacts is of practical significance in many engineering applications. Zhu and Faulkner (1996) firstly conducted study on plates subjected to repeated lateral wedge impacts and applied the method to the design of a semi-submersible hit by supply vessels. Experimental investigation and theoretical work based on the rigid-perfectly plastic method were performed. Both the theoretical solutions and experimental observations demonstrated that no pseudo-shakedown occurs in the studied cases. Simple formulae were first presented to evaluate the dynamic response of repeatedly impacted plates, which can provide engineers and designers with information for the preliminary design of plating against repeated impact loads.

Huang et al. (2000) performed repeated mass impact tests on fully clamped circular plates made from aluminum alloy and square plates made from mild steel. It was observed that the elastic strain energy increases with increase of the transverse displacements for an axially restrained plate. It was pointed out that, the elastic behavior plays an important role and cannot be ignored in the analysis of the pseudo-shakedown of structures. Thus, the maximum elastic energy that structures can absorb can be of great significance for the preliminary design of plating of ships under repeated impact loadings.

Jones (2014) reviewed the research results reported in Zhu and Faulkner (1996), Huang et al. (2000) and Cho et al. (2014). It was pointed out that a plate subjected to repeated identical mass impact loadings does not achieve a pseudo-shakedown state after some inelastic behavior, except in the special state when small enough loadings can be absorbed due to an increase of the elastic range with an increase in the plate deflection.

Thus, through a comparative study between the research results of Zhu and Faulkner (1996), Huang et al. (2000) and Jones (2014), it can be suggested that, different with the structural

design under single impact where the rigid-perfectly plastic assumptions can achieve relatively accurate predictions for the structural behaviour, the material elasticity cannot be neglected in the preliminary design of marine structures against repeated impact loads.

For offshore structures installed in cold regions and ice-classed ships, the influence of the repetition of the impact loadings has been investigated in recent years. Cho et al. (2014) performed both experimental and numerical investigations into the effect of repeated impacts on the response of steel beams at room and sub-zero temperatures, for applications to the structural design of polar class vessels subjected to repeated mass impacts from ice floes or similar impact scenarios. Zhu et al. (2015) presented a new ice load-response model to study the structural response of ice-classed ship plates under repeated impacts from drifting ice. It was demonstrated that the repeated ice-load nature shall be considered in the ice-classed ship design. Based on two commonly used design requirements for the specified permanent plastic deformation, the design plate thickness was given based on a plastic design principle. In the plate design example, the design curves and design formulae were both given and the latter one is straightforward and easy to use in Ice Rules for repeated ice impact problems.

(3) Fluid-structure interaction problem in ship collision

To ensure an accurate and reasonable investigation of the causes of marine accidents, full-scale ship collision, grounding, flooding, capsizing, and sinking simulations would be the best approach, which is based on the highly advanced Modeling & Simulation (M&S) system of Fluid-Structure Interaction (FSI) analysis technique, using advanced FSI codes such as LS-DYNA. Lee et al. (2017) presented the findings from full-scale ship collision, grounding, flooding, capsizing, and sinking simulations of marine accidents, and demonstrated the feasibility of this approach for investigating the causes of marine accident.

Yu et al. (2016a) summarized the challenges of solving the full FSI problem during a ship collision. There is a need to keep both complex and non-linear internal structural dynamics and external hydrodynamics together in one simulation. However, Yu et al. make the point that most numerical structural methods are poorly suited to effectively model the surrounding water in a collision. Thus, some sort of interfacing approach is necessary. The Arbitrary Lagrangian Eulerian (ALE) fluid-structure interaction (FSI) method appears to be popular for both ship-ship/ship-ice collisions. This allows coupling of different solver types in the different domains, and hydrodynamics can be incorporated into the collision response, see, for instance, Song et al. (2017).

Although the ALE method is capable of coupling both the external and internal mechanics, such simulation is too time-consuming. Yu et al. (2016a) presented a coupled procedure in ship collisions to predict the detailed structural damage together with reasonable accuracy and little additional computational cost. Yu et al. stated that for the preliminary design stage, “this method is especially useful since the detailed ship hull profile is not needed. The method is capable of efficiently coupling the global ship motions and structural responses with reasonable accuracy and little additional computational cost”.

Yu et al. (2016b) firstly established a coupled ship collision analysis model in which the hydrodynamic loads are calculated based on linear potential-flow theory and then are integrated into the nonlinear finite element code LS-DYNA. By this model, a fully coupled six degrees of freedom (6DOF) dynamic simulation of ship collision and grounding accidents can be achieved. The proposed method is capable of predicting both the 6DOF ship motions and structural damage simultaneously with good efficiency and accuracy.

Liang et al. (2017) proposed a new method to simulate the structural dynamic response of ship structure, considering its coupling with water motion in the ship’s internal tanks using the structural acceleration as a connection. This study provides a numerical calculation model applicable for the safety assessment of ships carrying liquid in the design stage, which may also have a

potential application in the structural design for ships carrying fluids such as the LNG carrier, oil tanker or other vessels in ballast condition.

4.1.2 Grounding

Grounding is one of the most common and destructive maritime accidents. Recently the European Maritime Safety Agency (European Maritime Safety Agency, 2015) has carried out a review of past accidents to passenger ships. The results showed that in the period from 1990 to 2013, there are 126 grounding accidents and 44% of them (56 ships) suffering major damages. The review also indicated that there is an increasing risk from grounding to ship safety. For designing safe ship structures and preventing the unfavorable consequences of ship grounding, much research has been done by using experimental method, non-linear finite element method, simplified analytical method and statistical method and probabilistic method. As a rational design procedure, Amdahl et al. (1995) suggested that the following four items are considered elementary for safe design: scenario definition, global and local structural performance calculation, post-accident evaluation and acceptance criteria. Careful definition of grounding scenarios is crucial to assessing the responses of ship hulls in accident and post-accident. Meanwhile, proper criteria are needed to predict the failure of structures. Using such a design procedure, especially in the preliminary design stage, it is essential that the structural performance of various designs can be quickly checked and compared for a large number of potential accident scenarios.

Seabed obstructions play an important role in determining the extent of grounding damage on ships. According to the seabed topology with reference to bottom size, the seabed obstacles can be grouped into three types: rock, reef and shoal (Alsos and Amdahl, 2007). In addition, the grounding scenarios can be defined according to the damage mechanisms of ship bottom structures, such as stranding and raking and shoal grounding.

(1) Stranding

Stranding is a scenario similar to ship collision, in which, the ship structures are laterally penetrated by indenters. Normally, a stranding grounding does not include forward ship speed, instead the ship settles on the obstacle. Wang et al. (2000) conducted a series of tests to study the behaviour of double hull ships under stranding scenarios, with varying load locations and indenter radius. The results showed that the indenter radius and the load location have very strong influences on the behaviour of a double hull structure. Alsos and Amdahl (2009) carried out quasi-static penetration tests of the stiffened plates to investigate the resistance to penetration of stiffened plates. The results showed that the stiffener has an influence on the fracture strain, residual strength and toughness of the plate.

(2) Raking

Raking is a grounding scenario where a ship strikes a rock-type obstruction while underway with forward speed. It may also be referred to as a powered grounding, as the ship's machinery pushes the vessel onto and along the obstruction. Given the ability to puncture several compartments owing to the forward speed during raking, it can be a severe type of grounding for both vessel flooding and pollution. Therefore, understanding the structures' resistance to raking is an important design task, including during preliminary design.

Thomas and Wierzbicki (1992) proposed a grounding damage prediction model including plate cutting, plate tearing and girder tearing for double hull tankers. Wang et al. (1997) proposed a simple method for damage prediction of ship raking over a rock by assembling four primary failure modes: stretching failure for transverse members, denting, tearing and concertina tearing for bottom plates. Zhang (2002) proposed a semi-empirical formula to estimate the average horizontal grounding force. The formula is based on a parametric study and the longitudinal and transverse members are smeared to the shell plating with an equivalent thickness method. Hong and Amdahl (2008) developed a theoretical model for ship bottom longitudinal girders

crushed during a raking scenario. The mean horizontal resistance of ship longitudinal girders was derived by considering the crushing distance and wave angle. Simonsen et al. (2009) proposed a simplified grounding damage prediction method based on full-scale test and the finite element analysis. Abubakar and Dow (2013) also studied the grounding damage with the finite element method. Based on these grounding simulations, it can be concluded that the transverse bulkheads help to increase the average horizontal grounding force level by approximately 15% (Heinvee and Tabri, 2015). By incorporating four load-resisting mechanisms including friction, stretching, bending and fracture, Zeng et al. (2016) proposed an analytical method for the steady state response of plate torn by a rigid cone indenter to assess the crashworthiness of a ship during raking. Sun et al. (2017) presented an analytical mechanical method to predict the bottom structural response. In their study, the bottom plating and transverse floor were assumed to be the major independent structures contributing to the grounding resistance. The aforementioned prediction models and analytical methods are used to elaborate the internal mechanics of ship grounding, with those prediction methods, it is possible to quickly assess the crashworthiness of ships during the structural design phase.

In addition to the simplified analytical method, numerical simulations and empirical formula have also been widely used to analyze the behaviour of ship bottom structures in real ship grounding accidents. Kuroiwa (1996) used the non-linear FEM to simulate a practical accident case in which a single hull oil tanker was torn by a single rock. The grounding force and resulted damage were reported. Pedersen and Zhang (2000) proposed a revised Minorsky method to calculate the absorbed energy of the grounded ships, by taking into account the different damage modes and structural arrangements. Zhu et al. (2002) examined a grounding scenario of multiple rocks based on a cargo ship grounding incident. The results showed that 51% of the initial kinetic energy was absorbed by the four major damages involving continuous rupture and 42% was absorbed by the five major damages involving continuous indentation without rupture.

Based on a set of numerical simulations of tankers and regression analysis, Heinvee and Tabri (2015) presented analytical expressions for a rapid prediction of grounding damage of double hull tankers by omitting the influence of the longitudinal and transverse bulkheads. Later, Heinvee et al. (2016) took into account the influence of the longitudinal and transverse bulkheads in the grounding damage analysis of double hull tankers. The results showed that the longitudinal bulkhead substantially increases the average grounding force and the transverse bulkhead has little influence on the average grounding force. Moreover, to improve the prediction of the onset of the inner bottom failure, a failure criterion for inner bottom was also proposed (Heinvee et al., 2016):

$$\delta = (0.75\frac{a}{B} + 1.17)h_d \tag{1}$$

where, δ is critical penetration depth; h_d denotes the double bottom height; a is the rock size and B is the ship breadth.

(3) Shoal grounding and residual strength

Different from the raking scenario which involve a rocky bottom obstacle tearing a vessel, ships may ground over more blunt obstructions with large contact surfaces such as smooth shoal. In this case, indentation and denting damage rather than tearing damage is likely to occur for the ship bottom structures. Although the bottom may not rupture when the ship moves over a blunt-type sea floor, it may threaten the global hull girder resistance and give rise to even worse consequences such as the hull collapse (L. Hong and J. Amdahl, 2008; Pedersen, 1994). Therefore, in the preliminary design stage or after a grounding accident, it is necessary to predict the residual ultimate strength of the damaged ship.

The requirements of the ultimate longitudinal hull girder strength are usually determined by considering the still-water and wave-induced loads. But the soft grounding accidents resulting

in overall failure of the ship hull indicate that the requirements of the ultimate longitudinal hull girder strength should take into account the arising loads during grounding incidents. Pedersen (1994) and Pedersen and Simonsen (1995) discussed this failure mode of ships and developed mathematical models to analyze the responses of a ship grounded on relatively plane sand. The grounding event was divided into two phases, i.e. the initial ideal plastic impact phase and sliding phase, to gain insight into the mechanics of soft grounding scenario. The results showed that the extreme values of grounding-induced sagging shear force aft of amid ship and sagging bending moment were mostly higher than the IACS requirement for the wave-induced shear force and bending moment. The studies are useful for structural strength design and reducing the catastrophic consequence of soft grounding event.

Pedersen (1994) developed a mathematical model and conducted scaled model tests to analyze the responses of a ship grounded on relatively plane sand. The grounding force, sectional shear forces and bending moments were determined. Besides, the results showed that severe shoal grounding may collapse the hull girder.

Hussein and Soares (2009) provided on of the first studies of residual strength under the IACS Common Structural Rules (CSR. They studied the residual strength of three double hull tankers designed according to these rules. They considered different damage scenarios for both side and bottom grounding, while examining different damage sizes to define a lower bound limit of strength which might be used for design. They calculated the residual strength using the Progressive Collapse Method (PCM) and based on the failure modes defined in the new rules.

Luís et al. (2009) used first-order reliability methods (FORM) to conduct a reliability analysis of a damaged double hull tanker. They assumed an accidental grounding centered on the keel, which they state is the worst possible scenario from a strength degradation point of view. The ultimate strength of the damaged tanker in the reliability analysis is calculated by means of a specific structural code. They simulated damage by removing the damaged elements from the model.

Hong and Amdahl (2012) studied the primary deformation modes of the longitudinal girder, the transverse floor and the bottom plating in a shoal grounding accident. Later Yu et al. (2015) investigated the characteristic deformation mechanism of stiffeners on double-bottom longitudinal girders in a shoal grounding accident. Based on the improved Smith's method considering the residual contributions of the damaged structures mentioned above. Sun et al. (2016) proposed a simplified analytical method to predict the ultimate strength of a damaged ship hull girder subjected to shoal grounding.

(4) Regulations on the grounding damages

Comparing to the regulations on the collision damages, less attention has been paid to the risk from grounding. Most regulations just assume that a double bottom with ample height would be enough to provide protection and to ensure safety. For example, the SOLAS 2009 (IMO, 2009) sets a minimum double bottom height of B/20. MARPOL (IMO, 2006) set a minimum double bottom height of B/20 for fuel tanks and of B/15 for cargo tanks. However, the required double bottom may be penetrated in some grounding scenarios. According to the GOALDS statistics (Bulian and Francescutto, 2010), the probability of exceedance of the SOLAS 2009 standard double bottom height is equal to 27.3% (95% confidence interval:[16.1%,41.0%]), while the probability of exceedance of the increased double bottom height, in case of passenger ships with large lower holds, is 14.5% (95% confidence interval:[6.5%,26.7%]). Besides, some grounding accidents show that grounding damage may occur at the side rather than at the bottom of the ship, such as the most recent grounding accident to Costa Concordia in 2012. The High Speed Craft Code (HSC Code) (IMO, 2008) considered this kind of side damage scenario and set stability requirements for this side racking damage. The European Maritime Safety Agency (2015) also studied the side damage due to grounding by reviewing the past grounding accidents. Based on the grounding accidents databases, probabilistic models for bottom damage

characteristics and side damage characteristics due to grounding were described. In addition, the distribution functions for the variables describing the location and extent of corresponding damage were reported. Furthermore, with the probabilistic approach, the European Maritime Safety Agency (2015) presented a proposal to assess survivability of passenger ships in damaged condition due to the grounding or contact accident. The probabilistic framework was studied to determine an attained subdivision index for survivability to grounding and contact accidents leading to hull breach and water ingress. In this framework, two factors, named "s-factor" (the probability of survival) and "p-factor" (the probability of flooding some compartments), were adopted.

4.1.3 Failure criteria

In the metal forming industry, the Forming Limit Diagram (FLD) was studied extensively since the early 50's. Zhu and Atkins (1998) proposed failure criteria using two types of diagram, 'necking' Forming Limit Diagram (FLD) and 'fracture' Forming Limit Diagram (FFLD), to predict the necking and fracture of ship structures under the impact of collision and grounding. There is extensive work on the grounding and failure prediction as a result of Joint Industry Project on Tanker Safety let by MIT between 1993 and 1999. Using the concept of FLD, real grounding incidents were assessed by Zhu et al. (2002). However, there are many factors affecting the forming limit of metal materials, such as strength level, strain-hardening exponent, strain-rate sensitivity factor, material imperfection, plastic anisotropy and pre-strain. For these reasons, Alsos et al. (2008) proposed the BWH instability criterion by combining the Hill's local necking analysis (Hill, 1952) with the Bressan and Williams (1983) shear stress criterion to analyze sheet metal instability. The BWH instability criterion describes the FLD in the stress space and determines the onset of local necking of structures. Jie et al. (2009) studied FLD by taking into account the strain rate sensitivity of the material and proposed a formulation for ε_{1f}. Based on the work of Jie et al. (2009), Abubakar and Dow (2013) used the FLD to predict the maximum deformation of the ship structures before necking. By considering the limitation of the strain-based FLD which is only useful on the case of proportional loading, Stoughton and Yoon (2012) derived a stress-based forming limit criterion from the strain-based FLD. The results showed that the stress-based FLD was independent of loading history. For this reason, it could be more accurate to predict the damage of ship structures under grounding accidents which suffer complex loading history. Hoogeland and Vredeveldt (2017) carried out a series of full thickness material failure tests with maritime plates to study the full thickness effect on the FLD. The results showed that the FLD based on Swift-Hill theory (Hill, 1952; Swift, 1952) had a conservative value and the effect of the multi-axiality needed to be considered in the failure criteria. This was also addressed by Bao and Wierzbicki (2004). Liu et al. (2017) proposed an expression to estimate the critical failure strain of coarse meshed ship structures struck by an indenter with hemispherical shape.

During collision events of marine structures, more complex variables such as loading or deformation histories, strain gradients, out-of-plane loading and stress concentrators at plate intersections would have strong influences on the plate failure. Calle et al. (2017) conducted experimental tests on purpose-designed samples, which particularly explained the performance of the failure criteria under different triaxiality ranges induced by the stress concentrators and high strain gradients.

Storheim et al. (2015) assessed "some of the current state-of-the-art fracture criteria that are applicable to coarsely meshed shell structures through comparison with various indentation experiments and a full-scale collision event". Storheim et al. investigated the robustness of each criterion applied in a design situation. The work particularly focused on the extent each criterion would give reasonable results when applied over wide range of problem. This assessment was made while restricting calibration to only data from a uniaxial tensile test.

In addition, some other failure criteria were proposed. Germanischer Lloyd (Scharrer et al., 2002) suggested a through thickness strain criterion called GLF. Peschmann (2001) proposed a maximum plastic strain criterion called PES. In addition, Törnqvist (2003) developed the RTCL damage criterion by combining the modified Cockcroft–Latham–Oh damage criterion (Cockcroft and Latham, 1968) with the Rice–Tracey damage criterion (Rice and Tracey, 1969). Ehlers et al. (2008) used the three failure criteria to model the ship collision. The results showed that the force penetration curves were influenced by mesh size. Alsos et al. (2009) adopted the finite element method with the RTCL damage criterion and the BWH instability criterion respectively to simulate the penetration tests of the stiffened plates (Alsos and Amdahl, 2009). The numerical results showed good performance of the two failure criteria.

4.2 Slamming

Von Karman (1929) started the research into slamming by studying the maximum pressure acting on a seaplane float during landing by the application of momentum theorem. Based on the kinematic description of the impact dynamics, Ochi and Motter (1973) established a method to predict the necessary information on slamming characteristics and hull responses of a ship at an early design stage, which is known as the Ochi Oriented Criterion. However, this criterion does not take the slamming cluster, stern slamming and bow-flare slamming into account, which may lead to wrong conclusions (Dessi, 2014). Hence, probabilistic models for the prediction of extreme stress and fatigue damage are needed for ships in slamming conditions. A common model assumes that the wave-induced stress is considered to be a stationary Gaussian process, while both the shipping and combined stress processes are non-stationary (Jiao, 1996). Kapsenberg and Thornhill (2010) proposed an approximation method based on momentum theory by which the statistical properties of the impact loads from slamming could be derived. Based on the partial safety-factor-based design criterion, Paik et al. (2004) developed strength criteria of ship structures against impact pressure loads. Realistic characteristics of slamming pressure actions were addressed in terms of the pressure-time history involving the rise time, peak pressure, duration time and type of pressure decay. Considering bow flare slamming, Zhu (2007) presented the common structural damage patterns and damage statistics and typical cases caused by slamming. A flow-chart of slamming impact pressure and strength assessment was presented and a typical example of containership is illustrated to perform the bow-flare slamming impact pressure calculation. In design against bow flare slamming, the local details should not be overlooked, especially at the connection. In addition, some suggestions for design criteria of local details were proposed. The reduction factor of effective plastic Section Modulus for tilted web plate was given. The ISSC 2012 Dynamic Response committee performed a benchmark study of slamming and whipping (Parunov, 2012). The goal of this benchmark study was twofold. On the one hand, the degree of variation in estimation by different methods and organizations was revealed. On the other hand, the absolute error made in the analyses was investigated by comparison with the measured responses from model tests. Drummen et al. (2009) used the model test results of a flexible segmented backbone model of a ferry to investigate the absolute error. Yang (2017) proposed a semi-empirical formula to calculate the slamming pressure due to plunging wave breaking on a sloping sea dike. Sun and Wu (2013) and Sun et al. (2015) have done symmetrical studies into the hydrodynamic problem of oblique water entry by the three-dimensional incompressible velocity potential theory with the fully nonlinear boundary conditions on the moving free surface and body surface boundary. This work gave information on the pressure distribution on the wetted solid surface.

In both slamming research and ship design pressure for slamming, the drop test has been widely used, and design curves are obtained based on the pressure coefficients and associated motion predictions (Chuang, 1970; Hagiwara and Yuhara, 1975; Hayman et al., 1991; Zhao et al., 1996; Zhu and Faulkner, 1995). A series of drop-test experiments was performed by Swidan et al. (2016) to "investigate the hydrodynamic loads experienced by a generic wave-piercer catamaran hull form during water impacts. The experiments, which focus on the characterization

of the unsteady slamming loads on an arched wet deck, were conducted using a servo-hydraulic slam testing system that allows the model to enter the water at a range of constant speeds up to 10 m/s. A strong relationship between water-entry velocity and slamming force was found and an empirical relationship is proposed to estimate the magnitude of the slamming force as a function of the impact velocity". This relationship is of great importance for the catamaran design to provide an estimation of the slamming force for a broader range of relative impact velocities. Sruthi and Sriram (2017) studied the slamming forces on a jacket using the improved methodology and experiment method. In their study, a slamming coefficient was proposed for the jacket structures. The method can also be used for estimating the impact loads on complex structures. Ringsberg et al. (2017) demonstrated the practical use of "quasi-response" prediction methods for the assessment of slamming loads on modern free fall lifeboats. Drop test experiment of lifeboats were conducted and presented.

Faltinsen (2000) and Faltinsen et al. (2004) pointed out that slamming should be considered in the framework of structural dynamics response and integrated with the global flow analysis around a ship or ocean structure or with violent fluid motion inside a tank. Thomas et al. (2003) investigated the whipping response of the structure, with the principal structural response frequencies being identified through spectral analysis. Thomas et al. (2006) studied the influence of slamming and whipping on the fatigue life of a large high-speed catamaran. Dessi and Ciappi (2013) investigated the dependence of the whipping response on the impact velocity. However, the accident with the container ship MSC Napoli showed that slamming and slamming-induced whipping were not yet soundly incorporated in the rules of Classification Societies. For this reason, a whipping oriented criterion based on the analysis of the peak of the induced high-frequency VBM response occurring closely after a water-impact was proposed (Dessi, 2014). Magoga et al. (2017) presented an investigation into various methods for identifying slams for structural response analysis. The stress criterion, stress rate criterion and a slam criterion based on the fatigue damage incurred in a structural item were studied in the paper. Hassoon et al. (2017) simulated the behaviour of composite wedges under slamming impact with the presence of damage by employing the finite element method. To investigate the situation, the hydro-elastic influence was analyzed as both a kinematic effect due to deflection of the composite panel and a dynamic effect caused by the interaction between the water and the structure.

As to the slamming impact calculation, Das and Batra (2011) simulated the slamming impact of rigid and deformable hull bottom panels by using the coupled Lagrangian and Eulerian formulation in the commercial software LS-DYNA. Veen and Gourlay (2012) applied the Smoothed Particle Hydrodynamics (SPH) algorithm to two-dimensional hull impact problems in order to simulate the ship slamming. Simulations are made for cones (or other shaped solid objects) of various deadrise angles and different oblique entries, and detailed results have been presented in terms of the free surface shape, pressure distribution on the wetted solid surface, and so on. Sun and Wu (2014) investigated the hydrodynamic problem of a three-dimensional (3D) water column impacting on a solid wall through the boundary element method (BEM). Lv and Grenestedt (2015) modelled the slamming pressure as a high-intensity peak followed by a lower constant pressure traveling at constant speed along the beam. Kim et al. (2015) proposed a numerical method utilizing a 3-D Rankin panel method, 1-D/3-D finite element methods, and a 2-D generalized Wagner model. Wang and Soares (2016) calculated the slamming occurrence probability and slamming loads on a ship hull in irregular waves by using the Arbitrary-Lagrangian Eulerian(ALE) algorithm. Datta and Siddiqui (2016) presented a theoretical hydro-elastic analysis of an axially loaded uniform Timoshenko beam, with intermediate end fixities, undergoing hydrodynamic impact-induced bottom slamming. Marrone et al. (2017) studied slamming loads on LNG tank insulation panels by using an enhanced Smoothed Particle Hydrodynamics (SPH) model. Experimental data involving wet drop tests of both flat and corrugated panels have been performed and the pressures during the impact have been measured at several points along the panel surface.

4.3 Explosion and Fire

4.3.1 Principles and criteria for structures under blast loading

The design for ships and offshore structures subjected to explosion loading has been concerned by each Classification Society since World War II. Many relevant principles and criteria have been formulated, among which the Quantitative Risk Analysis (QRA), Probabilistic risk assessment and P-I diagram method are widely used. With the development of the offshore oil and gas exploitation and transportation industries, designs method for special categories of ships such as LNG, FPSO and FPDSO, considering explosion loading, has been studied by many researchers. The principles and criteria for these ships under explosion loading are more stringent than other ships due to their higher risk.

(1) Explosion load

Generally, the explosion load can be divided into two scenarios: net reaction force and surface load. For ships and offshore structures, each kind of explosion load might be further divided into static pressure, dynamic pressure, reflected pressure and overpressure (Lloyd's Register, 2015). At present, the explosion loading is usually assumed to be a uniform pressure pulse with rectangular shape, triangle shape, or exponent shape. The impulsive loading is employed when the loading duration is ultra-short. The most famous assumed pressure is the triangle pulse loading. Over the past decades, many studies have been devoted to investigating the effect of pulse shape. The earliest study on the effect of pulse shape can be traced back to Symonds (1953), who found that the final deflection of a free beam subjected to a concentrated force pulse only depends on the total impulse and peak load of the pulse. Hodge (1956) remarked that this conclusion was valid only for loading intensities far beyond the yield load; otherwise this simplification may result in large errors.

Based on a large number of experimental research and theoretical analysis work, many scholars summarized empirical formulas for the calculation of the parameters of the blast wave in the ideal air and gave their reasonable scope of application. In the calculation of the peak value of the explosion pressure, Brode (1959) used the finite difference method to solve the Lagrange equation of motion, and obtained the empirical formula for the peak overpressure of the blast wave in an ideal gas. Through a large number of experiments, the expression of the peak value of shock wave overpressure was obtained by Henrych and Abrahamson (1979). Wu and Hao (2005) proposed an empirical formula for calculating the overpressure peak for structural response analysis of surface explosions. The results from early empirical formulae were generally in the middle or lower value, thus there was a risk of underestimating the shock wave. Compared with the empirical formula, the numerical simulation results tended to be low. Wu and Gao (2014) proposed a method to correct the results of numerical simulation by empirical formulae. Those empirical formulae have a small gap in the far field, but the difference between the results in the near field is large. Therefore, the calculation of near field explosion is best based on experimental results.

Youngdahl (1971, 1970) proposed two correlation parameters to eliminate pulse shape effects. In his studies, the dynamic response of a structure under a general loading pulse can be approximated by using a rectangular pulse impulse with an effective load and pulse duration. In addition, an empirical estimation of the structural response duration was suggested. A triangular shaped pressure loading pulse was studied by Jones (1973) and the results implied that a rectangular plate remained rigid for certain loading. The applicability of Youngdahl's approximation to various structures under pulse loading was verified by Zhu et al. (1986).

Zhao et al. (1995, 1994) firstly discovered the "saturated impulses" in the large plastic dynamic response of the structure under moderate-intensity pulsed loading, and made a reasonable explanation of this phenomenon from the perspective of rigid plasticity theory. Zhu and Yu (1997) proposed the elastic-plastic "saturated impulses" of the square plates and the "saturation time" of the structure subjected to the pulsed loading. Besides, based on the elasto-plastic analysis

method, the authors proposed the "maximum deformation" and "permanent deformation" of the two “saturated impulse". A theoretical model for rigid-plastic responses of common structural members was established by using the bound theorems, as exhibited by Li and Jones (2016). In addition, it also reveals that Youngdahl’s empirical estimation for the structural response duration generally gives a lower bound of the actual response duration. More recently, Ren et al. (2014) examined the applicability of the foundation equivalent method proposed by Youngdahl for a tensor skin and found that this method is applicable not only to stable structures, but also to geometrically unstable structure such as tensor skin. The scaling effect of using a fixed square plate under a rectangular pressure pulse as a typical example of saturation has been studied (Zhu et al., 2017b). Zhu et al. (2017a) studied the effect of the pulse shape of linearly decaying pressure pulse, and proposed an equivalent method based on saturation impulse. The comparison with non-linear FE results showed the proposed method made a major improvement on Youngdahl's by considering the saturation of structures. In the design of structural components involving plastic deformation, the pressure Linear Decaying and Exponentially Decaying pulses can be treated as an equivalent Rectangular Pulse. This will significantly simplify the plate design calculation involving plastic deformations when design acceptance criteria are given. More recently, Bai et al. (2017a) studied the boundary condition effect for the saturated impulse using both rigid-plastic model and elastic-plastic model. In his study, the elastic-plastic numerical predictions showed good agreement with the experimental results in terms of both the permanent deflection and transient deformation profiles given by Zhu (1996). In 2017, Bai et al. (2017b) further studied the saturated impulse for square plate under Linearly Rising Exponentially Decaying (LRED) considering transient plastic hinge lines.

(2) Structure response analysis

Each classification society formulates the accidental limit state (ALS) for structures under accidental loading. For explosion loading, the following ALS should be considered where relevant, which is taken from NORSOK Standard Z-013, Edition 3:

a. Global structural collapse;
b. Rupture or unacceptable deflection of an explosion barrier, including unacceptable damage to passive fire protection of the barrier and cable or pipe penetrations;
c. Damage to equipment or piping resulting in unacceptable escalation of events, including damage due to deflection or damage of supporting structure;
d. Unacceptable damage to safety critical equipment or systems which need to function after the explosion.

Generally, the response of structural components can conveniently be classified into three categories according to the duration t_d of the explosion pressure pulse relative to the fundamental period of vibration T of the component: Impulsive domain ($t_d/T < 1/3$); Dynamic domain, ($1/3 < t_d/T < 10$); and Quasi-static domain, ($t_d/T > 10$).

In principle, the probabilistic explosion load distribution obtained based on the QRA or probabilistic risk assessment should be presented as a frequency distribution of overpressure and impulse, i.e., Pressure-Impulse diagram (P-I diagram). P-I diagram uses have been widely documented, see for example Abrahamson and Lindberg (1976), Morton (1966), Smith and Hetherington (1994), Li and Meng for a hitorical overview of their use on structural and injury critiera (2002).

(3) Leakage and ignition

The loss of containment of LNG or LPG can result in a range of scenarios which could cause serious explosion damage. However, it is basically limited to liquid jet, two phase jet and an evaporating pool, depending on the storage conditions of the liquid and the ambient conditions. Therefore, jets, liquid, pool formation, pool spread and evaporation are the non-negligible

scenarios. Lloyd's Register noted that the research for these aspects of LNG spills is thinner than for vapor dispersion models (Lloyd's Register, 2015). Lloyd's notes that the UK HSE has issued a state-of-the-art review of LNG source term modeling (Webber et al., 2010). At the current time, this reference appears to be the most up-to-date source model evaluation. .

Immediate spontaneous ignition is considered to occur so quickly after the leak has started that the scenario results in a fire (since no gas cloud has been accumulated). It should be documented that ignition within a few seconds after the leak has started will not result in significant explosion loads unless such early scenarios are included in the explosion analysis.

(4) Numerical simulation method

Along with the development of computer technology and numerical analysis theory, the Direct Load Measurement (DLM) based on the Finite Element Modeling (FEM) is applied by many Classification Societies.

The probabilistic procedure requires a large set of different release and explosions scenarios to be analyzed. NORSOK Z-013 and Lloyd's Register note that symmetry considerations, reasoning and simplifications based on sound physics may be used to reduce the number of scenarios for consideration. Simplified relations between input parameters and results from the CFD simulations can be used for extrapolating results from both gas dispersion and explosion simulations, provided that their validity and limitations are documented. As a general principle, any uncertainty in such simplifications should be compensated by added conservatism (Lloyd's Register, 2015).

The accuracy of the DLM method will accordingly be dependent on the size of the control volume of the grid used in the CFD simulations relative to the object size. Many efforts have been made to investigate the validation of numerical simulation method, and the topic for numerical simulation of explosion has been well discussed in many international conferences such as ISOPE and OMAE.

However, for load receptors far away from the gas clouds where CFD simulations may be too time-consuming or expensive, more simplified methods for calculating far field blasts can be applied. In this case, the accuracy and/or conservatism of the results should be addressed.

4.3.2 Principles and criteria for fire induced hazards

The fire response of structures is traditionally studied by assuming that the heat-flow problem is separable from the structural analysis. However, when changes in geometric characteristics associated with structural distress change the heat-flow problem, the interaction between heat flow and structural response can be handled by iterative process.

To fill the gap between the simple calculation method and the finite element method, an approach based on the elastic and plastic methods for fire resistance analysis is developed (Wong, 2001). FDS, which is a CFD model for fire-driven fluid flow, can numerically solve a set of Navier-Stokes equations appropriate for low-speed, thermally-driven flow with an emphasis on smoke and heat transport from fires (Mcgrattan et al., 2010).

Large offshore topsides are often steel beam and truss structures, and some work has been done in similar areas. Sun et al. (2012a, 2012b) examined two-dimensional steel framed structures under fire loading with different fire locations. The analysis used both static and dynamic models depending on the stability of the structure. Naser and Kodur (2016) presented critical factors that influence the onset of local buckling in steel beams when exposed to fire conditions. A three-dimensional nonlinear finite element model capable of accounting for critical factors that influence local instability in fire-exposed steel beams is developed. Luongo and Contento (2015) resolved the nonlinear elastic problem for planar frames made of rectilinear beams subjected to thermal loadings.

Research on the properties of steel structures under the combined action of fire and explosion loads is relatively less. However, the response analysis of steel structures under the combined action of fire and explosion loads have become more important after the "9/11"event in the United States (Tan et al., 2017).

With regard to the nonlinear response of steel frame under fire and explosion loads, Song et al. (2000) and Izzuddin et al. (2000) proposed an adaptive numerical analysis method to evaluate the influence of blast loading on the fire resistance capability of steel structures. Mirmomeni et al. (2015) implemented a comprehensive test program to investigate the post-impact fire properties of Grade 350 steel under well-defined conditions. The test results indicate that the effects of these combined actions are profoundly different from those in which the structure is individually subjected to either high strain rate or thermal loading. Xi et al. (2014) adopted the governing equations in the form of finite difference to describe the response of steel beams under the combined effects of fire and impulsive loads.

Liew and Chen (2004) and Liew (2008) adopted the mixed element method to analyze the steel frame that was locally impacted by blast loading and caused the fire. The response behavior of steel structures under blast and fire loadings were investigated, and the influence of blast loading on the fire resistance capability of multistory steel frames was elaborated.

The sequence of fire and explosion loads applied on the steel structures was rarely considered in previous studies. Two scenarios that apply fire and explosion loads in different orders all have strong engineering backgrounds. A substantial amount of research results has recently emerged for the scenario in which the explosion load is applied followed by a fire. However, related research results for the scenario in which explosion load is applied during a fire are currently rare (Tan et al., 2017). As indicated in the study of Xi et al. (2014), the strain rate constitutive model related to the temperature should be considered in this situation. However, relevant experimental data are currently generally lacking. Two scenarios are discussed in this study. In this study, the blast resistance capability of steel structures during a fire is represented by the peak amplitude of the pulse load–impulse (P–I) diagram, while the fire resistance performance of steel structures after the action of an explosion load is represented by the Tcr–I diagram.

Tan et al. (2017) has studied the pulse shape effects on the fire and blast resistance capabilities of steel beams. The peak amplitude of the pulse load–impulse curve and the critical temperature–impulse curve is proposed to distinguish safe and unsafe areas. Two scenarios that apply fire and explosion loads in different orders are considered. Numerical analysis results show that the blast resistance capability of steel beams sequentially decreases under the action of exponential, triangular, and rectangular pulse loads; the effects of rectangular, triangular, and exponential explosion pulse loads on the fire resistance performance of steel beams consecutively decrease; and the pulse shape effects on the fire resistance capability of steel beam decreases with the increase in dynamic load ratio.

5. PRINCIPLES AND CRITERIA FOR ARCTIC OPERATION

5.1 Arctic Operational Environment

With melting ice caps covering the Arctic areas, the Northern Sea route connecting the Far East and Europe becomes available for the navigation of commercial ships during the summer time. Ensuring an appropriate level of reliability and acceptable performance for such marine structures in the Arctic requires the consideration of risk and reliability in their structural design. Harsh environmental features such as geographic remoteness, ice-covered areas, ice loading, icing, floating ice, winterization, and hydrodynamic interactions is part of important design aspects for those structures. For instance, floating ice such as icebergs can damage offshore and sub-sea structures and sometimes this yields serious consequences to the Arctic environment. Meanwhile, field data collected from Arctic voyages can be served as fundamental information

to further increase the design capabilities of marine structures in the Arctic. As an example, the icebreaking research vessel ARAON voyaged to the Chukchi and Beaufort seas during the summer season, and performed ice field trials (Lee et al., 2014), see Figure 2.

Figure 2: ARAON in the Arctic Sea (Lee et al., 2014)

In total four ice field trials are conducted to understand the ship performance under the Arctic operational environment. Various ice properties like ice load and thickness, and navigational information for the ship such as speed, engine power and hull strength data from strain gauges are gathered as well as air temperature, wind speed and the heading of the ship. This section reviews recent work for load prediction and criteria development in the Arctic, ISSC specialist committee V.6 report on the Arctic Technology provides a wider overview of Arctic development.

5.2 Ice Load Prediction

Prediction of the ice load is an important design factor to secure the reliable structures of polar ships that navigate in ice-covered waters because the ice load is the most dominant load acting on the ships. In general, the magnitude of ice-induced load is greater than that of wave-induced load including slamming loads. Ice load components can be categorized as global ice load and local ice load. The former is usually results hull girder bending moments and the latter is often the pressure acting on local hull structure. Ice type, ice thickness, ice failure modes, ice-hull structure interaction, and ship speed are parameters that influence design pressure from the ice. In understanding the responses between the ice load and hull structure, the time history of the ice load on hull structure needs to be identified. Therefore, determination of the accurate ice load acting on the ships requires a good understanding on the mechanism of interaction between the ice load and the ships to enhance the safety level of the ships in the Arctic. Research on the mechanical properties of the ice has become increasingly important. It is understood that the ice has stochastic material properties because various natural parameters affect its mechanical and physical properties. Furthermore, the brittle feature of the ice adds complexity to the ice-hull structure interaction. At present, there are discrepancies in dealing with the ice load between rule-based design approaches and ice field test measurement approaches, and existing numerical programs cannot satisfactorily simulate the mechanical properties of the ice yet.

Research efforts made so far to improve the ice load prediction capabilities generally fall into numerical, experimental and ice field test categories, and some representative work of in each category is introduced in the following.

For the modelling of the ice behaviour, a constitutive relation of ice with high strain rates was proposed, and this approach develops a numerical integration algorithm based on a plasticity

failure criterion (Pernas-Sánchez et al., 2012). For the ice subjected to a multiaxial state of stress, a continuum damage model for its temperature dependent creep response is proposed. In this model, a thermo-viscoelastic constitutive law for the ice creep, and a local orthotropic damage accumulation law for tension, compression and shear stresses are considered (Duddu and Waisman, 2012). In the ice impact load case, a strain rate sensitive ice material model is developed by considering physics and phenomena governing spherical ice impact. Predicted ice failure progression from this model shows a good agreement with the ice crack propagation observed from the ice impact test (Tippmann et al., 2013). Structural response of a stiffened panel under the ice load is obtained from finite element method (FEM) and rule-based method, and they are compared for the estimation of design load (Erceg et al., 2015). FEM alone or combined finite element and discrete element methods (FEM-DEM) based simulation approaches are also used to predict the ice load. Two-dimensional FEM-DEM simulation approach is demonstrated for predicting the maximum ice load from the ice-hull structure interaction. Based on 110 simulations with two different plastic limit values, the statistics of the ice load from the simulation is studied, and this approach is suggested for the improvement of the ice load prediction (Ranta et al., 2015). Discrete element-based models have some advantages over continuum-based models, because the ice fracture propagation is discrete in nature. Thus, DEM is applied to simulate the global resistance acting on the hull structure in level ice under different ice thickness and ship speed. In this approach, the breaking process of ice cover and the size distribution of broken ice floes can be obtained, and the ice load in each contact pair is determined through the contact detection between ice particle element and hull element in the simulation. Field data are employed to check the accuracy of the DEM numerical approach. The ice force acting on the icebreaker by a repetitive ice-ship contact depends on the size of ice floe and ice concentration that affect ice failure mode. Numerical models for the simulation of ice floes' distribution when icebreaker is advancing into ice-covered water with pack ice have been developed to calculate the ice load. In these models the motion of ice floes due to collisions with a vessel is expressed by rigid body equations (Sawamura and Kioka, 2016).

Full scale experiments involving the ice-hull structure interaction are conducted in which significant deformation is observed. Stiffened panels are considered to represent the hull structure and laboratory made ice blocks are loaded on the panels to observe large scale plastic deformation (Manuel et al., 2015). Non-linear FE analysis of the panels is performed, and a comparison between the experiment and simulation is carried out. This approach demonstrates a practical way of estimating the local ice load on the hull structure. High velocity impact of ice spheres is also experimented to estimate the ice load in dynamic nature, and experimental procedures are developed (Pernas-Sánchez et al., 2015).

Ice field test programs are conducted to predict the actual ice load acting on the ships operating in the Arctic. Ships navigating in ice-covered water should comply with route specific ice-induced load. Full scale pressure distributions are obtained from the ice field test by Japanese Ocean Industries Association (JOIA) to investigate the effect of spatially localised load on the local hull structure such as a grillage. Similarly, the characteristics of the local ice load and ice load signal acting on the side shell in the bow section of ARAON is investigated through the ice field test (Lee et al., 2016, 2014). The local ice load signal refers to fluid impact pressure and it is different from the ice load in terms of physical aspects. The shape characteristics of the load signal shows similar trend in the signal characteristics, such as peak and decaying shape. The local ice load is obtained from 6 degrees of freedom (DOF) internal measurement system and FE analysis. The measurement system treats ARAON as a rigid body and measures whole ship motion and the global ice load from the full-scale ice sea trial data. As a part of results, the pressure-area curves are developed as shown in Figure 3.

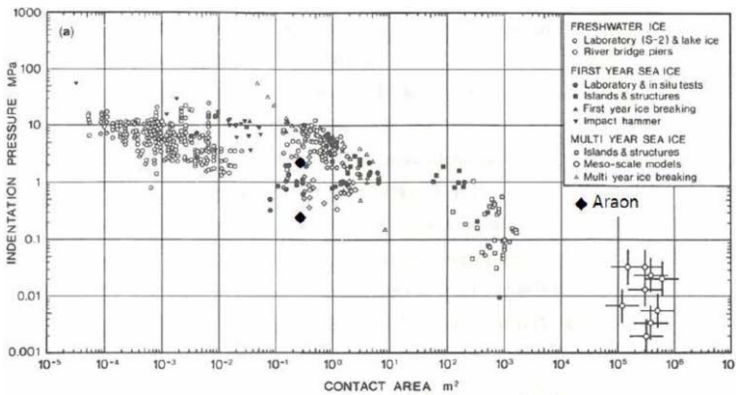

Figure 3: Pressure levels measured on ARAON in comparison with existing pressure-area curve (Lee et al., 2014).

5.3 Design Approaches for Ice Loaded Hull Structures with Application to Structural Design

Erceg et al. investigated structural responses of a stiffened plated structure subjected to full-scale ice pressure distributions obtained from field measurements. Within rule-based design method, Finnish-Swedish Ice Class Rules (FSICR), and probabilistic design method approaches for the ships in the Arctic, the plate responses are analysed using LS-Dyna and ANSYS finite element model solutions. From the two different design method approaches for the plated structure, the higher von Mises stress values are obtained from the full-scale ice pressure distributions than both FSICR and the probabilistic approaches (Erceg et al., 2015). Ice ridge, iceberg and ice islands are examples of floating ices in the Arctic. Among them, an iceberg has the highest impact and chance of interaction with the ships and subsea facilities in the Arctic. Kim et al. (2017) focus on iceberg, and investigate the factors related to the interaction between iceberg and the subsea structure such as areal density, iceberg drift arising from wind, wave, current, uncertain iceberg shape and subsea structure types.

Based on the dynamic response of the hull structure under impact in which the deformation of the impacting object is not considered, the structural analysis of plated structure subjected to repeated ice load has been investigated by Zhu et al and others. From this ice-plated structure interaction analysis, design curves and formulae are derived for the structural design of the ice classed ships using the design criterion based on allowable permanent deformation (Zhu et al., 2015). Damage resistance of laminated composite structures due to hail ice impact is experimented by Rhymer et al. (2012). This impact case may create internal damage to the laminate that is not visually detectable and is therefore a damage tolerance concern. A laminate manufactured from carbon and epoxy materials are considered and it is subjected to high velocity ice sphere, i.e., simulated hail ice. Gagnon and Wang (2012) conduct the numerical simulation of collision between a loaded tanker and an iceberg using LS-Dyna. In the simulation, hydrodynamics and validated crushable foam ice model are taken into account. Using the same simulation program, LS-Dyna, the structural analysis of an arctic LNG carrier is performed by Gagnon et al. (2017). Different iceberg masses, iceberg shapes and water condition are considered in the modelling and it is validated using the data from growler impact test in National Research Council Canada's ice tank facility and full-scale measurements. Wet and dry case simulations are developed to calculate the hull deflections, and it is noted that wet case simulation provides more realistic results, see Figure 4.

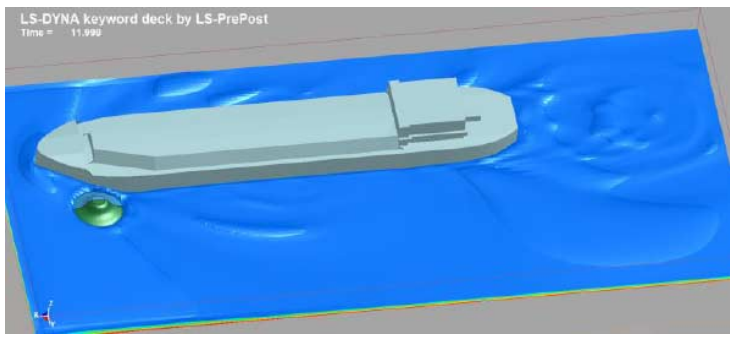

Figure 4: Ship-ice collision modelling using LS-Dyna (Gagnon et al., 2017)

Flow of ice around both fixed and floating offshore structures of different shapes can be predicted by using a multi-model approach. Through this simulation-based approach in the design of the arctic offshore structures, ensuring of no excessive pile-up and encroachment on the topside facilities, and prediction of the load on the structures consistent with the relevant design codes and standards can be investigated. The simulator program based on a multi-model approach is developed by Dudal et al. (2015). This simulator is capable of simulating ice flow and calculating the load on conical or sloping walled structures where ice sheet fracture is dominated by bending (see, Figure 5). Thus, it predicts the ice behaviour and load applied on offshore structures accounting for water current and interaction among the structures, ice sheet, ice floe, ice blocks and the seabed.

Figure 5: Modelling of underwater ice flow (Dudal et al., 2015)

Pang et al. (2015) presents a comprehensive survey of the literature on the cohesive element method (CEM) applied to the ice-hull structure interaction. CEM is a kind of blending between FEM and DEM that improves the drawbacks on both FEM and DEM solutions. CEM can model the full-scale ice sheets undergoing continuous crushing without violating the conservative laws. It is noted that the structure becomes softened with increasing cohesive element density, and for this case, a scaling law needs to be considered for cohesive element properties such as different mesh sizes. A three-dimensional DEM bonded particle model is used to simulate the ice. In such an approach, blocks of the ice are not modelled by a single particle instead the blocks are modelled by a collection of bonded particles that can break into smaller blocks as bonds fail (Morgan, 2016). It enables the simulation to have a better understanding on the fracture process and rubble behaviour of the ice.

It is critical to understand the salient failure modes of ice features for the structural design of icebreakers. Lu et al. (2015) defined that “The dominant failure modes are influenced by the structural properties, interaction process, and characteristics of the ice features. For an ice feature of finite size with relatively small lateral confinement, splitting failure has been frequently observed during ice-structure interactions”. Lu et al. (2015) proposed a conservative

classification of ice floes out-of-plane failures under an edge load. Besides, the ice fracture processes are highly influenced by variability associated with flaw structure and contact conditions, Taylor and Jordaan (2015) develops a probabilistic fracture mechanics model to model the localized fracture events for ice specimens with ice edge taper angles ranging from 0 to 45 degrees. The crack instability criteria are formulated for compressive and tensile stresses. Hendrikse and Metrikine (2015) propose a new mechanism to explain ice-induced vibrations. They propose a model where the variations in ice-contact area impact the ice load magnitude, and that these variations drive the ice induced vibrations. They propose a numerical model built around the dominate aspects of this mechanism. This model is claimed to predict all regimes of ice induced vibrations of compliant structures as well as being able to reproduce the aperiodic characteristics of ice loading on rigid structures.

Risk and reliability aspects need to be incorporated in the design of arctic offshore structures to secure acceptable performance. Thomas (2015) develops the ultimate and accidental limit states with respect to the risk and reliability of the offshore structures. It is demonstrated that all risk events, including those from very rare environmental events beyond abnormal level, need to be characterized in order to assess risks and ensure appropriate planning, documentation and management. Ayele and Barabady (2017) propose a simplified risk-based offshore structure design methodology with respect to the Arctic environment. They consider risk factors like choice of material, equipment, support strategies, physical environment, human factors and HSE (Health, Safety, and Environment), which are additional risk factors beyond the traditional risk factors. All these risk factors are taken into account because of the stringent requirements in terms of emissions to the atmosphere and discharge to the sea as well as design procedures with respect to risk reduction measures such as prevention of risk incidents, control of risk incidents, and mitigation measures. A proposed risk-based arctic offshore structure design methodology from the literature is shown in Figure 6.

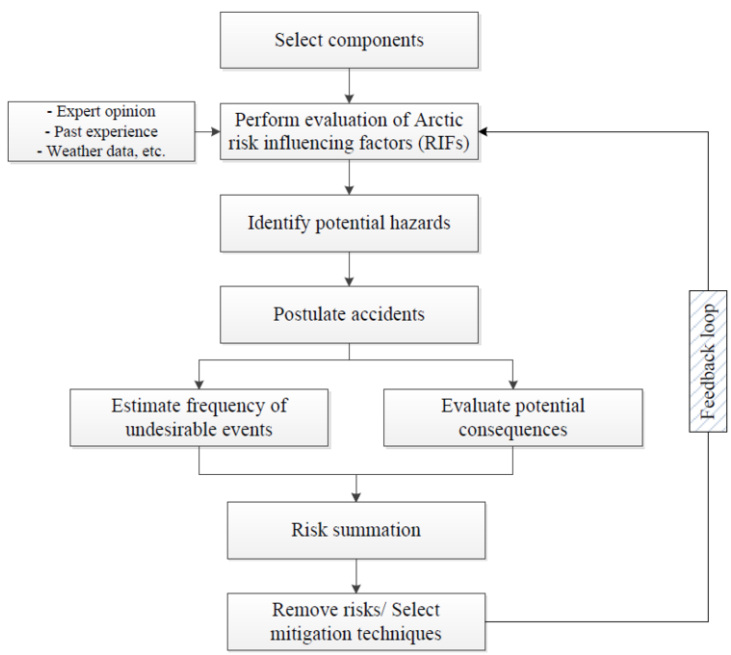

Figure 6: A simplified risk-based offshore structures design methodology for Arctic operating conditions (Ayele and Barababy, 2017)

Ki et al. report on full-scale impact test of a newly built arctic LNG carrier according to ARC 7 class of the Russian Maritime Register of Shipping (RMRS). This has performed to check

the acceptance of hull structures and weld strength with respect to impact load. 7 tons of steel with controlled dropping height is used to experimentally simulate the impact load equivalent to encountered ice load. Iterative drop object analysis result is used to determine the drop height, and the ice load for ARC 7 requirement is calculated using direct ice load calculation method. The nonlinear analysis is performed to check the hull and Cargo Containment System (CCS) strength with respect to the calculated ice load (Ki et al., 2017).

5.4 Assessment of Ice Class Rules

Development of the harmonized ice class rules for the ships in the Arctic by International Association of Classification Societies (IACS) reduces the large variety of different ice class rules resulting in an easier selection process for an adequate ice class rules meeting the functional requirements assigned for the ships. Riska (2013) analyzed the design point that is the limit state together with the frequency the limit state is reached at different ice class rules. The analysis is based mostly on the ice load from first year ice but also ice regimes where the multi-year ice occurs. The comparison is done by using two example ships (8,000 DWT chemical carrier and 20,000 DWT bulk carrier) and scantling is obtained from different ice class rules. Both FSICR and IACS polar rules are used (Riska and Kaṁäṙainen, 2012). The design equations for ice loads from IACS rules are examined through the relation among ice load, iceberg's buttock angle and velocity (Choi et al., 2012). Also several ice class rules such as American Bureau of Shipping (ABS), DNV- GL, RMRS and FSICR are referenced, and new design formula is proposed based on the intensive investigation of referenced various rule-based formulae and experimental results. Based on laboratory impact test and modification of DNV-GL ice class rules and IACS Polar class rules, the authors suggest design equations for impact ice load.

The objective of International Organisation for Standardisation (ISO) 19906 is to ensure that complete structures including substructures, topside structures, floating production vessel hulls, foundations and mooring systems in arctic and cold regions are provided with an appropriate level of reliability with respect to personnel safety, environmental protection and asset value. ISO 19906 demonstrates an improvement from the traditional approach to the design of offshore structures which are largely derived from steel jackets and lattice tower structures. Nowadays ISO 19906 is used in all countries with arctic interests for assessment of ice scenarios and ice actions, for design of structures in ice environments and for the ice-structure interaction (Muggeridge et al., 2017). In ISO 19906, the limit state design covers design situations arising from extreme operation, abnormal, and accidental events so that the desired structural reliability is verified for the relevant limit states (Thomas, 2017). If the ultimate limit state (ULS) is considered on the extreme and abnormal design situations, ISO 19906 provides requirements, recommendations and guidance for the design of offshore structures in the Arctic and cold regions.

FSICR have their origin in the rules first put forth in 1890. Since that time, the rules have evolved and, at present, FSICR can be considered as an industrial standard for designing ships for first-year ice environment. Decades of experience including numerous damage surveys and full-scale measurements make FSICR as the rules being incorporated in most major classification societies, though new research findings have also influenced the rule development (Riska, 2013; Riska and Kämärainen, 2011).

Kim et al. (2015) investigate differences in the ice load and plate thickness requirement between IACS and RMRS rules. To understand the background and limitations of those rules, assumptions made for design formulations and ice class factors are reviewed. It is noted that the ice load from IACS is based on an oblique collision with a large ice floe having a 150 degree front angle. This ice load acting on the hull structures is acquired from an average pressure that is uniformly distributed over a rectangular load patch area which depends on ice category, hull angles and ship displacement. In case of RMRS, the ice load is obtained from maximum pressure in the ice-hull structure contact area. The main difference between two approaches is that IACS utilizes Sanderson's pressure-area relationship, in which the average pressure decreases

with increasing nominal contact area whereas the RMRS approach assumes an intermediate crushed layer and uses the Navier-Stokes equations to determine ice-pressure distributions over the nominal contact area. Both IACS and RMRS have almost the same rule principles, and they provide very close results: IACS and RMRS rules assume the ice pressure and the load height as a function of ice geometry, ice mechanical characteristics and parameters of the vessel. The design of plates and stiffeners in Arctic vessels is performed considering a combination of experience, empirical data and structural analysis. Especially design factors driving the shell plating for the ships are based on two assumptions, namely the ice load calculation and structural resistance calculation.

6. CONCLUSIONS

During the current mandate period the committee found encouraging developments in structural design philosophy and criteria. Based on the extensive prior coverage of goal-based standards and sustainability in design from this committee, it is gratifying to see the implementation of these approaches at IMO and other national regulators now appearing. The review of IACS CSR to GBS marks a major milestone in the adaption of this philosophy, and the continued use of formal safety assessments and other design approaches discussed in prior IV.1 reports is also encouraging. It is possible that the next ISSC IV.1 committee will be able to start to summarize lessons learned from these large-scale applications of the goal and sustainability-based design principles.

It is also clear that in-service monitoring data is becoming a major factor in both structural design and life extension. The ability, or perhaps in future, need, to revisit structural adequacy based on in-service monitoring results represents a potential shift in design philosophy. To date, such philosophy focuses more on improving design-stage rules and regulations without considering reassessment. As reviewed in this report, life extension approaches are often categorized depending on the type of through-life data available. With the rapid growth of aging wind farms and the continue aging of oil platforms, in-service monitoring for fixed structures is likely to continue to increase. The detailed review of ship-based in-service monitoring shows that this problem is hard, and not yet fully resolved despite a clear demand signal from recent containership mishaps. While much development is clearly apparent from the literature reviewed, and the notable instrumentation campaigns underway, a clear tie to updating goal or sustainability criteria is not yet present. How the results of such studies will influence both design and operational-phase criteria must still be explored.

A more wide-ranging study of accidental loads and polar criteria was also presented. The direct analysis of accidental loads during design is a precursor to effective regulation of the performance of marine structures in accidental limit states. Collision, grounding, fire, and explosion load estimating approaches were all reviewed. Polar operations continue to grow, and our review of polar loading and design codes highlights similar needs, if not technology, to more conventional operations. Risk-based approaches are favored given the unique nature of the polar regions and the relative lack of operational experience compared to more temperate climates. Likewise, rule comparison and harmonization appear to be growing concern for researchers, with several publications exploring such aspects during the mandate period.

Inland and coastal vessel developments were also reviewed, with numerous criteria updates noted. The unique challenges of the inland waterways provide a contrast to ocean service criteria. However, it is not yet clear to what extent sustainability and goal-based implementations are being attempted in this industry. Here, the lack of a venue such as IMO leads to an even more fragmented and hard-to-track regulatory approach. Our shorter review of human error in assessing criteria found the marine industry little changed since the last major work in this space 20 years ago. However, related human-structural engineering problems in the civil engineering domain have been more recently explored, highlighting potential dangers of increasingly-

computerized engineering approaches. More investigation into the role of the human engineer in implementing ever-more-complex design criteria assessments seems warranted at this point.

REFERENCES

Aba, E.K., Badar, M.A., Hayden, M.A., 2015. Impact of ISO 9001 certification on firms financial operating performance. Int J Qual & Reliability Mgmt 33, 78–89. https://doi.org/10.1108/IJQRM-02-2014-0021

Abrahamson, G.R., Lindberg, H.E., 1976. Peak load-impulse characterization of critical pulse loads in structural dynamics. Nuclear Engineering and Design 37, 35–46.

Abubakar, A., Dow, R.S., 2013. Simulation of ship grounding damage using the finite element method. International Journal of Solids & Structures 50, 623–636.

Aeran, A., Gudmestad, O.T., 2017. Guidelines for Estimating Remaining Fatigue Life of Ageing Offshore Jacket Structures V03AT02A039. https://doi.org/10.1115/OMAE2017-62059

Al Hattab, M., Hamzeh, F., 2015. Using social network theory and simulation to compare traditional versus BIM–lean practice for design error management. Automation in Construction 52, 59–69. https://doi.org/10.1016/j.autcon.2015.02.014

Alsos, H.S., Amdahl, J., 2009. On the resistance to penetration of stiffened plates, Part I – Experiments. International Journal of Impact Engineering 36, 799–807.

Alsos, H.S., Amdahl, J., 2007. On the resistance of tanker bottom structures during stranding. Marine Structures 20, 218–237.

Alsos, H.S., Amdahl, J., Hopperstad, O.S., 2009. On the resistance to penetration of stiffened plates, Part II: Numerical analysis. International Journal of Impact Engineering 36, 875–887.

Alsos, H.S., Hopperstad, O.S., Törnqvist, R., J. Amdahl, 2008. Analytical and numerical analysis of sheet metal instability using a stress based criterion. International Journal of Solids & Structures 45, 2042–2055.

Amdahl, J., Kavlie, D., Johansen, A., 1995. Tanker grounding resistance, in: PRADS 1995. Presented at the Proceedings of the 6th PRADS Conf., Seoul, Korea.

American Bureau of Shipping, 2017. Guidance Notes on Life Extension Methodology for Floating Production Installations. ABS, Houston, Texas.

Atkinson, A.R., 1999. The role of human error in construction defects. Structural Survey 17, 231–236. https://doi.org/10.1108/02630809910303006

Ayele, Y.Z., Barababy, J., 2017. Risk-based offshore facility design (RB-OFD) under arctic operational conditions, in: Proceedings of the 24th International Conference on Port and Ocean Engineering under Arctic Conditions. Presented at the POAC 2017, Busan, Korea.

Bai, X., Zhu, L., Yu, T.X., 2017a. Saturated impulse for pulse-loaded rectangular plates with various boundary conditions. Thin-Walled Structures 119, 166–177.

Bai, X., Zhu, L., Yu, T.X., 2017b. Saturated impulse for fully clamped square plates under blast loading. International Journal of Mechanical Sciences In Press. https://doi.org/10.1016/j.ijmecsci.2017.08.047

Bao, Y., Wierzbicki, T., 2004. On fracture locus in the equivalent strain and stress triaxiality space. International Journal of Mechanical Sciences 46, 81–98.

Bea, R., 1994. The Role of Human Error in Design, Construction, and Reliability of Marine Structures (No. SSC-378). Ship Structure Committee, Washington D.C.

Björnsson, I., 2016. From Code Compliance to Holistic Approaches in Structural Design of Bridges. Journal of Professional Issues in Engineering Education and Practice 142, 02515003. https://doi.org/10.1061/(ASCE)EI.1943-5541.0000255

Bressan, J.D., Williams, J.A., 1983. The use of a shear instability criterion to predict local necking in sheet metal deformation. International Journal of Mechanical Sciences 25, 155–168.

Brode, H.L., 1959. Blast Wave from a Spherical Charge. The Physics of Fluids 2, 217–229.

Bulian, G., Francescutto, A., 2010. Exploratory data analysis of grounding data from the updated GOALDS database and assessment of requirements and assumptions in SOLAS Ch. II-1 Part B-2 Regulation 9. GOALDS Project.

Bulleit, W., 2008. Uncertainty in Structural Engineering. Practice Periodical on Structural Design and Construction 13, 24–30. https://doi.org/10.1061/(ASCE)1084-0680(2008)13:1(24)

Bureau Veritas, 2017. Guidelines for Wind Turbines Lifetime Extension - Version 0. Bureau Veritas, Paris, France.

Calle, M.A.G., Verleysen, P., Alves, M., 2017. Benchmark study of failure criteria for ship collision modeling using purpose-designed tensile specimen geometries. Marine Structures 53, 68–85.

CCRN, 2016. Market insight inland navigation in Europe. Central Commission for the Navigation of the Rhine, Strasbourg, France.

Chai, T., Weng, J., De-qi, X., 2017. Development of a quantitative risk assessment model for ship collisions in fairways. Safety Science 91, 71–83.

Cho, S.-R., Truong, D.D., Shin, H.K., 2014. Repeated lateral impacts on steel beams at room and sub-zero temperatures. International Journal of Impact Engineering 72, 75–84.

Choi, Y.-H., Choi, H.-Y., Lee, C.-S., Kim, M.-H., Lee, J.-M., 2012. Suggestion of a design load equation for ice-ship impacts. International Journal of Naval Architecture and Ocean Engineering 4, 386–402. https://doi.org/10.2478/IJNAOE-2013-0105

Christian, R., Kang, H.G., 2017. Probabilistic risk assessment on maritime spent nuclear fuel transportation (Part II: Ship collision probability). Reliability Engineering & System Safety 164, 136–149.

Chuang, S.-L., 1970. Investigation of impact of rigid and elastic bodies with water (No. 3248). David W Taylor Naval Ship Researh and Development Center, Bethesda MD.

ClassNK, 2014. Investigation Report on Structural Safety of Large Container Ships. The Investigative Panel on Large Container Ship Safety, ClassNK, Japan.

Cockcroft, M.G., Latham, D.J., 1968. Ductility and the workability of metals. Journal Institute of Metals 33–39.

da Silva Bispo, I.B., Queiroz Filho, A.N., Tannuri, E.A., Simos, A.N., 2016. Motion-Based Wave Inference: Monitoring Campaign on a Turret FPSO, in: Proceedings of the 35th International Conference on Ocean, Offshore and Arctic Engineering. Presented at the OMAE 2016, ASME, Busan, Korea, p. V007T06A040. https://doi.org/10.1115/OMAE2016-54956

Das, K., Batra, R.C., 2011. Local water slamming impact on sandwich composite hulls. Journal of Fluids & Structures 27, 523–551.

Datta, N., Siddiqui, M.A., 2016. Hydroelastic analysis of axially loaded Timoshenko beams with intermediate end fixities under hydrodynamic slamming loads. Ocean Engineering 127, 124–134.

Decò, A., Frangopol, D.M., 2015. Real-time risk of ship structures integrating structural health monitoring data: Application to multi-objective optimal ship routing. Ocean Engineering 96, 312–329. https://doi.org/10.1016/j.oceaneng.2014.12.020

Delorm, T., 2014. Tidal stream devices: Reliability preidciton models during their conceptual and development phases. (PhD Thesis). Durham University.

Dessi, D., 2014. Whipping-based criterion for the identification of slamming events. International Journal of Naval Architecture & Ocean Engineering 6, 1082–1095.

Dessi, D., Ciappi, E., 2013. Slamming clustering on fast ships: From impact dynamics to global response analysis. Ocean Engineering 62, 110–122.

DNVGL, 2016a. DNVGL-ST-0262: Lifetime extension of wind turbines.

DNVGL, 2016b. Rules for Classification, Ships, Part 6 Additional class notations, Chapter 9 Survey arrangements, Section 4 Hull monitoring systems - HMON.

DNVGL, 2016c. Rules for Classification, Ships, Part 5 Ship types, Chapter 2 Container ships, Section 4 Hull girder strength.

Dong, Y., Frangopol, D.M., Sabatino, S., 2016. A decision support system for mission-based ship routing considering multiple performance criteria. Reliability Engineering & System Safety 150, 190–201. https://doi.org/10.1016/j.ress.2016.02.002

Drummen, I., Wu, M.K., Moan, T., 2009. Experimental investigation of the application of response conditioned waves for long-term nonlinear analyses. Marine Structures 22, 576–593.

Dudal, A., Septseault, C., Béal, P.-A., Le Yaouanq, S., Roberts, B., 2015. A new arctic platform design tool for simulating ice-structure interaction, in: Proceedings of the 23rd International Conference on Port and Ocean Engineering under Arctic Conditions. Presented at the POAC 15, Trondheim, Norway.

Duddu, R., Waisman, H., 2012. A temperature dependent creep damage model for polycrystalline ice. Mechanics of Materials 46, 23–41. https://doi.org/10.1016/j.mechmat.2011.11.007

Egorov, A.G., 2012. Concepts of river-sea dry-cargo vessels for Dnipro and Danube rivers. Ports of Ukraine 9, 14–18.

Egorov, G.V., Efremov, N.A., Shablikov, N.V., 2016a. XXI century river civil shipbuilding: analysis and tasks. Maritime Market 1, 18–29.

Egorov, G.V., Egorov, A.G., 2017. River and river-sea vessels: Role of "old" series of vessels and their perspectives. Maritime Market St. Petersburg 1.

Egorov, G.V., Ilnitskiy, I.A., Kalugin, Y.V., 2016b. Grounding of concept of cruise river-sea passenger vessel for work as well in Caspian and Black sea. Reporter of ONMU 2, 98–126.

Ehlers, S., Broekhuijsen, J., Alsos, H.S., Biehl, F., Tabri, K., 2008. Simulating the collision response of ship side structures: A failure criteria benchmark study. International Shipbuilding Progress 55, 127–144.

Eleftheria, E., Apostolos, P., Markos, V., 2016. Statistical analysis of ship accidents and review of safety level. Safety Science 85, 282–292.

Endrina, N., Rasero, J.C., Konovessis, D., 2018. Risk analysis for RoPax vessels: A case of study for the Strait of Gibraltar. Ocean Engineering 151, 141–151.

Erceg, B., Taylor, R., Ehlers, S., 2015. Structural response comparison using different approaches to account for ice loading, in: Proceedings of the 23rd International Conference on Port and Ocean Engineering under Arctic Conditions. Presented at the POAC 15, Trondheim, Norway.

ES-TRIN, 2015. European Standard laying down Technical Requirements for Inland Navigation vessels - Edition 2015/1. Adopted by European Committee for drawing up Standards in the field of Inland Navigation (CESNI), Strasbourg, France.

EU, 2009. Impact Assessment Guidelines.

European Maritime Safety Agency, 2015. Evaluation of risk from raking damages due to grounding, Final report. European Maritime Safety Agency, Brussels, Belgium.

Faltinsen, O.M., 2000. Hydroelastic slamming. Journal of Marine Science & Technology 5, 49–65.

Faltinsen, O.M., Landrini, M., Greco, M., 2004. Slamming in marine applications. Journal of Engineering Mathematics 48, 187–217.

Franceschini, F., Galetto, M., Mastrogiacomo, L., 2016. ISO 9001 certification and failure risk: any relationship? Total Quality Management & Business Excellence In Press, 1–15. https://doi.org/10.1080/14783363.2016.1253466

Fröderberg, M., 2015. Conceptual Design Strategy: Appraisal of Practitioner Approaches. Structural Engineering International 25, 151–158. https://doi.org/10.2749/101686614X14043795570615

Fröderberg, M., 2014. The human factor in structural engineering: A source of uncertainty and reduced structural safety (PhD Thesis). Lund University, Lund, Sweden.

Gagnon, R.E., Wang, J., 2012. Numerical simulations of a tanker collision with a bergy bit incorporating hydrodynamics, a validated ice model and damage to the vessel. Cold Regions Science and Technology 81, 26–35. https://doi.org/10.1016/j.coldregions.2012.04.006

Gagnon, R.E., Wang, J., Seo, D., Ki, H., Choi, J., Park, S., 2017. Arctic LNG carrier structural risk analysis for iceberg collisions, in: Proceedings of the 24th International Conference on Port and Ocean Engineering under Arctic Conditions. Presented at the POAC 17, Busan, Korea.

Galetto, M., Franceschini, F., Mastrogiacomo, L., 2017. ISO 9001 certification and corporate performance of Italian companies. Int J Qual & Reliability Mgmt 34, 231–250. https://doi.org/10.1108/IJQRM-04-2015-0064

Gallagher, D.J., Abadin, J.A., Madden, D.J., 2017. Genesis Spar Continued Service - A Case Study. Presented at the Offshore Technology Conference, Offshore Technology Conference. https://doi.org/10.4043/27937-MS

Greece, 2002. Building Robust Ships, MSC 76/5/10. IMO MSC 76th Session, London, UK.

Hagiwara, K., Yuhara, T., 1975. Study on wave impact load on ship bow. Mitsubishi Heavy Industries Technical Review 12, 113–121.

Hamann, R., 2015. Impact assessment compilation part 1; Impact assessment in accordance with the EC IA (No. 2015–1194, Rev. 3). European Maritime Safety Agency, Lisboa, Portugal.

Han, C.-G., Chang, Y.-S., Kim, J.-S., Kim, M.-W., 2016. Round Robin Analyses on Stress Intensity Factors of Inner Surface Cracks in Welded Stainless Steel Pipes. Nuclear Engineering and Technology 48, 1412–1422. https://doi.org/10.1016/j.net.2016.05.006

Hassoon, O.H., Tarfaoui, M., Moumen, A.E., 2017. Progressive damage modeling in laminate composites under slamming impact water for naval applications. Composite Structures 167, 178–190.

Hayman, B., Haug, T., Valsgard, S., 1991. Response of fast craft hull structures to slamming loads, in: Proceeedings of 1st International Conf on Fast Sea Transportation. Presented at the FAST 91, Trondheim, Norway, pp. 381–399.

Heggelund, S.E., Storhaug, G., Choi, B.-K., 2011. Full Scale Measurements of Fatigue and Extreme Loading Including Whipping on an 8600TEU Post Panamax Container Vessel in the Asia to Europe Trade, in: 30th International Conference on Ocean, Offshore and Arctic Engineering. Presented at the OMAE 2011, American Society of Mechanical Engineers, Rotterdam, The Netherlands, pp. 273–282. https://doi.org/10.1115/OMAE2011-49378

Heggelund, S.E., Storhaug, G., Oma, N., 2010. Consequence of whipping and springing on fatigue and extreme for a LNG vessel based on onboard measurements, in: 11th International Symposium on Practical Design of Ships and Other Floating Structures. Presented at the PRADS 2010, Rio de Janeiro, Brazil, pp. 1173–1179.

Heinvee, M., Tabri, K., 2015. A simplified method to predict grounding damage of double bottom tankers. Marine Structures 43, 22–43.

Heinvee, M., Tabri, K., Kõrgesaar, M., Urbel, A., 2016. Influence of longitudinal and transverse bulkheads on ship grounding resistance and damage size. Presented at the International Conference of Collision and Grounding of Ships and Offshore Structures, 15-18 Jun.

Hendrikse, H., Metrikine, A., 2015. Interpretation and prediction of ice induced vibrations based on contact area variation. International Journal of Solids and Structures 75–76, 336–348. https://doi.org/10.1016/j.ijsolstr.2015.08.023

Henrych, J., Abrahamson, G.R., 1979. The Dynamics of Explosion and Its Use. Elsevier Scientific Pub. Co. ;, Amsterdam.

Hermans, F., Murphy-Hill, E., 2015. Enron's Spreadsheets and Related Emails: A Dataset and Analysis, in: Proceedings of the 37th International Conference on Software Engineering. Presented at the ICSE 2015, IEEE, Florence, Italy, pp. 7–16.

Hill, R., 1952. On discontinuous plastic states, with special reference to localized necking in thin sheets. Journal of Mechanics Physics of Solids 1, 19–30.

Hodge, P.G.J., 1956. The influence of blast characteristics on the final deformation of circular cylindrical shells. Journal of Applied Mechanics 23, 617–624.

Hoogeland, M., Vredeveldt, A.W., 2017. Full thickness material tests for impact analysis verification, in: Progress in the Analysis and Design of Marine Structures. Presented at the MARSTRUCT 2017, Lisbon, pp. 449–458.

Hua, D., Paradkar, M., Garcia, S., Young, S., Hogelin, P., Webb, T., Farmakakis, K., 2017. Neptune Spar Life Extension Assessments. Presented at the Offshore Technology Conference, Offshore Technology Conference. https://doi.org/10.4043/27857-MS

Huang, Y., van Gelder, P., Mendel, M., 2016. Imminent ships collision risk assessment based on velocity obstacle, in: Walls, L., Revie, M., Bedford, T. (Eds.), Risk, Reliability and Safety: Innovating Theory and Practice. CRC Press, Taylor & Francis Group, 6000 Broken Sound Parkway NW, Suite 300, Boca Raton, FL 33487-2742, pp. 693–700. https://doi.org/10.1201/9781315374987-105

Huang, Z.Q., Chen, Q.S., Zhang, W.T., 2000. Pseudo-shakedown in the collision mechanics of ships. International Journal of Impact Engineering 24, 19–31.

Hussein, A.W., Guedes Soares, C., 2009. Reliability and residual strength of double hull tankers designed according to the new IACS common structural rules. Ocean Engineering 36, 1446–1459. https://doi.org/10.1016/j.oceaneng.2009.04.006

IACS, 2015a. Common Structural Rules for Bulk Carriers and Oil Tankers, Version 1st Jan 2015. International Association of Classification Societies (IACS).

IACS, 2015b. UR S11A Longitudinal Strength Standard for Container Ships -. International Association of Classification Societies (IACS).

IMO, 2017a. Report of the Maritime Safety Committee on its ninety-eighth session - MSC 98/23.

IMO, 2017b. Report of the GBS Working Group - MSC 98.7/WP.7.

IMO, 2016a. GBS verification audit reports submitted by audit teams - MSC 96/5.

IMO, 2016b. Corrective Action Plans submitted by IACS and its member recognized organizations (Part 1, in response to the non-conformities identified during GBS verification audit) - MSC 96/5/1 and Addendum 1 and 2.

IMO, 2016c. Promulgation of rules for the design and construction of bulk carriers and oil tankers of an or-ganization, which is recognized by Administrations in accordance with the provisions of SO-LAS regulation XI-1/1, confirmed by the Maritime Safety Committee to be in conformity with the goals and functional requirements of the Goal-based Ship Construction Standards for Bulk Carriers and Oil Tankers - MSC.1/Circ. 1518.

IMO, 2016d. Report of the Maritime Safety Committee on its ninety-sixth session - MSC 96/25.

IMO, 2015a. Generic Guidelines for Developing IMO Goal Based Standards - MSC.1./Circ.1394/Rev. 1.

IMO, 2015b. International Code of safety for Ships using Gases or Other Low-Flashpoint Fuels (IGF CODE) -MSC.391(95).

IMO, 2015c. International Code for Ships Operating in Polar waters - MEPC.264(68).

IMO, 2015d. Revised Guidelines for Formal Safety assessment (FSA) for use in the IMO Rule Making Process - MSC-MEPC.2/Circ.12/Rev.1.

IMO, 2014. International Code for Ships Operating in Polar waters - MSC.385(94).

IMO, 2013. Revised Guidelines for Formal Safety Assessment (FSA) for Use in The IMO Rule-Making Process - MSC-MPEC.2/Circ.12.

IMO, 2010. Adoption of the Guidelines for Verification of Conformity with Goal-Based Ship Construction Standards for Bulk Carriers and Oil Tankers - Resolution MSC.296(87).

IMO, 2009. International Convention for the Safety of Life at Sea (SOLAS). International Maritime Organization, London, UK.

IMO, 2008. “International Code of Safety for High-Speed Craft, 2000 (2000 HSC Code)”, as amended.

IMO, 2006. “International Convention for the Prevention of Pollution from Ships, 1973, as modified by the Protocol of 1978-MARPOL 73/78”, as amended.

Iseki, T., Nielsen, U.D., 2015. Study on Short-term Variability of Ship Responses in Waves. The Journal of Japan Institute of Navigation 132, 51–57. https://doi.org/10.9749/jin.132.51

Izzuddin, B.A., Song, L., Elnashai, A.S., Dowling, P.J., 2000. An integrated adaptive environment for fire and explosion analysis of steel frames—Part II:: verification and application. Journal of Constructional Steel Research 53, 87–111.

Jiao, G., 1996. Probabilistic prediction of extreme stress and fatigue damage for ships in slamming conditions. Marine Structures 9, 759–785.

Jie, M., Cheng, C.H., Chan, L.C., Chow, C.L., 2009. Forming limit diagrams of strain-rate-dependent sheet metals. International Journal of Mechanical Sciences 51, 269–275.

Jones, N., 2014. Pseudo-shakedown phenomenon for the mass impact loading of plating. International Journal of Impact Engineering 65, 33–39.

Jones, N., 1973. Slamming damage. Journal of Ship Research 17, 80–86.

Kapsenberg, G.K., Thornhill, E.T., 2010. A practical approach to ship slamming in waves. Presented at the Proceedings of 28th Symposium on Naval Hydrodynamics, California, pp. 12–17.

Ki, H.G., Choi, J., Park, S.G., Han, S.K., 2017. Ice collision analysis and alternative full scale impact test for ARC 7 LNG carrier, in: Proceedings of the 24th International Conference on Port and Ocean Engineering under Arctic Conditions. Presented at the POAC 17, Busan, Korea.

Ki, H.G., Park, S.G., Jang, I.H., 2015. Full scale measurement of 14k TEU containership, in: Hydroelasticity in Marine Technology. pp. 311–328.

Kiesling, S., Klünder, J., Fischer, D., Schneider, K., Fischbach, K., 2016. Applying Social Network Analysis and Centrality Measures to Improve Information Flow Analysis, in: Product-Focused Software Process Improvement, Lecture Notes in Computer Science. Presented at the International Conference on Product-Focused Software Process Improvement, Springer, Cham, pp. 379–386. https://doi.org/10.1007/978-3-319-49094-6_25

Kim, B., Kim, H., Ha, S., Liu, Y., Choi, K., 2017. A study for the state-of-the-art on arctic issues for floating ices and subsea operations, in: Proceedings of the 24th International Conference on Port and Ocean Engineering under Arctic Conditions. Presented at the POAC 17, Busan, Korea.

Kim, E., Amdahl, J., Stroheim, M., Løset, S., 2015. Understanding the effect of assumptions on shell plate thickness for arctic ships, in: Proceedings of the 23rd International Conference on Port and Ocean Engineering under Arctic Conditions. Presented at the POAC 15, Trondheim, Norway.

Kim, J.H., Kim, Y., Yuck, R.H., Lee, D.Y., 2015. Comparison of slamming and whipping loads by fully coupled hydroelastic analysis and experimental measurement. Journal of Fluids & Structures 52, 145–165.

Klünder, J., Schneider, K., Kortum, F., Straube, J., Handke, L., Kauffeld, S., 2016. Communication in Teams - An Expression of Social Conflicts, in: Human-Centered and Error-Resilient Systems Development, Lecture Notes in Computer Science. Springer, Cham, pp. 111–129. https://doi.org/10.1007/978-3-319-44902-9_8

Knight, J.T., Collette, M.D., Singer, D.J., 2015. Design for flexibility: Evaluating the option to extend service life in preliminary structural design. Ocean Engineering 96, 68–78. https://doi.org/10.1016/j.oceaneng.2014.12.035

Kohlhase, A., Kohlhase, M., Guseva, A., 2015. Context in spreadsheet comprehension. Presented at the CEUR Workshop Proceedings, pp. 21–27.

Koo, J.B., Jang, K.B., Suh, Y.S., Kim, Y.S., Kim, M.K.S., Yu, H., Tai, J.S.C., 2011. Fatigue Damage Assessment Based On Full Scale Measurement Data For a Large Container Carrier, in: Proceedings of the Twenty-First International Offshore and Polar Engineering Conference. Presented at the ISOPE 2011, International Society of Offshore and Polar Engineers, Maui, Hawaii, USA.

Korzhenevych, A., Dehnen, N., Bröcker, J., Holtkamp, M., Meier, H., Gibson, G., Varma, A., Cox, V., 2014. Update of the Handbook on External Costs of Transport (No. Ricardo-AEA/R/ ED57769). Ricardo-AEA, London.

Kuroiwa, T., 1996. Numerical simulation of actual collision and grounding accidents. Presented at the Proceedings of Int. Conference on Design and Methodologies for Collision and Grounding Protection of Ships, San Francisco, California.

L Hong, J Amdahl, 2012. Rapid assessment of ship grounding over large contact surfaces. Ships & Offshore Structures 7, 5–19.

L. Hong, J. Amdahl, 2008. Plastic mechanism analysis of the resistance of ship longitudinal girders in grounding and collision. Ships & Offshore Structures 3, 159–171.

Lee, J.-H., Kwon, Y.-H., Rim, C.-W., Lee, T.-K., 2016. Characteristics analysis of local ice load signals in ice-covered waters. International Journal of Naval Architecture and Ocean Engineering 8, 66–72. https://doi.org/10.1016/j.ijnaoe.2016.01.001

Lee, S.G., Lee, J.S., Lee, H.S., Park, J.H., Jung, T.Y., 2017. Full-scale Ship Collision, Grounding and Sinking Simulation Using Highly Advanced M&S System of FSI Analysis Technique. Procedia Engineering 173, 1507–1514.

Lee, T.-K., Lee, J.-H., Kim, H., Rim, C.W., 2014. Field measurement of local ice pressures on the ARAON in the Beaufort Sea. International Journal of Naval Architecture and Ocean Engineering 6, 788–799. https://doi.org/10.2478/IJNAOE-2013-0213

Li, Q.M., Jones, N., 2016. Foundation of Correlation Parameters for Eliminating Pulse Shape Effects on Dynamic Plastic Response of Structures. Journal of Applied Mechanics 72, págs. 172-176.

Li, Q.M., Meng, H., 2002. Pulse loading shape effects on pressure–impulse diagram of an elastic–plastic, single-degree-of-freedom structural model. International Journal of Mechanical Sciences 44, 1985–1998.

Liang, Q., Zhu, L., Zhang, S., Chen, M., 2017. Numerical Modeling of Dynamic Response of Water Tank in Collision. Presented at the ASME 2017 International Conference on Ocean, Offshore and Arctic Engineering.

Liew, J.R., 2008. Survivability of steel frame structures subject to blast and fire. Journal of Constructional Steel Research 64, 854–866.

Liew, J.R., Chen, H., 2004. Explosion and fire analysis of steel frames using fiber element approach. Journal of Structural Engineering 130, 991–1000.

Liu, B., Soares, C.G., 2015. Simplified analytical method for evaluating web girder crushing during ship collision and grounding. Marine Structures 42, 71–94.

Liu, B., Villavicencio, R., Zhang, S., Soares, C.G., 2017. A simple criterion to evaluate the rupture of materials in ship collision simulations. Marine Structures 54, 92–111.

Lloyd's Register, 2015. Guidance Notes for the Calculation of Probabilistic Explosion Loads.

Love, P.E.D., Lopez, R., Edwards, D.J., Goh, Y.M., 2012. Error begat error: Design error analysis and prevention in social infrastructure projects. Accident Analysis & Prevention, Intelligent Speed Adaptation + Construction Projects 48, 100–110. https://doi.org/10.1016/j.aap.2011.02.027

Love Peter E. D., Ackermann Fran, Teo Pauline, Morrison John, 2015. From Individual to Collective Learning: A Conceptual Learning Framework for Enacting Rework Prevention. Journal of Construction Engineering and Management 141, 05015009. https://doi.org/10.1061/(ASCE)CO.1943-7862.0001013

Love Peter E. D., Smith Jim, 2016. Toward Error Management in Construction: Moving beyond a Zero Vision. Journal of Construction Engineering and Management 142, 04016058. https://doi.org/10.1061/(ASCE)CO.1943-7862.0001170

Lu, W., Lubbad, R., Løset, S., 2015. Out-of-plane failure of an ice floe: Radial-crack-initiation-controlled fracture. Cold Regions Science and Technology 119, 183–203. https://doi.org/10.1016/j.coldregions.2015.08.009

Luís, R.M., Teixeira, A.P., Soares, C.G., 2009. Longitudinal strength reliability of a tanker hull accidentally grounded. Structural Safety 31, 224–233.

Luongo, A., Contento, A., 2015. Nonlinear elastic analysis of steel planar frames under fire loads. Computers & Structures 150, 23–33.

Luth, G.P., 2011. VDC and the Engineering Continuum. Journal of Construction Engineering and Management 137, 906–915. https://doi.org/10.1061/(ASCE)CO.1943-7862.0000359

Lv, J., Grenestedt, J.L., 2015. Analytical study of the responses of bottom panels to slamming loads. Ocean Engineering 94, 116–125.

Magoga, T., Aksus, S., Cannon, S., Ojeda, R., Thomas, G., 2017. Identification of slam events experienced by a high-speed craft. Ocean Engineering 140, 309–321.

MAIB, 2008. Report on the investigation of the structural failure of MSC Napoli English Channel on 18 January 2007 (No. 9/2008). Marine Accident Investigation Branch, Southampton, UK.

Manuel, M., Colbourne, B., Daley, C., 2015. Ship structure subjected to extreme ice loading: Full scale laboratory experiments used to validate numerical analysis, in: Proceedings of the 23rd International Conference on Port and Ocean Engineering under Arctic Conditions. Presented at the POAC 15, Trondheim, Norway.

Marrone, S., Colagrossi, A., Park, J.S., Campana, E.F., 2017. Challenges on the numerical prediction of slamming loads on LNG tank insulation panels. Ocean Engineering 141, 512–530.

Mas-Soler, J., Simos, A.N., de Mello, P.C., Tannuri, E.A., Souza, F.L., 2017. A Preliminary Assessment of the Use of a Large Semi-Submersible Platform As a Motion-Based Wave Sensor, in: 36th International Conference on Ocean, Offshore and Arctic Engineering. Presented at the OMAE 2017, ASME, Trondheim, Norway, p. V001T01A061. https://doi.org/10.1115/OMAE2017-61454

Mcgrattan, K.B., Baum, H.R., Rehm, R.G., Hamins, A., Forney, G.P., Floyd, J.E., Hostikka, S., Prasad, K., 2010. Fire Dynamics Simulator (Version 5) Technical Reference Guide. NIST Special Publication 4, 206–207.

Megavind, 2016. Strategy for Extending the Useful Lifetime of a Wind Turbine. Megavind.

Melchers, R.E., 1989. Human Error in Structural Design Tasks. Journal of Structural Engineering 115, 1795–1807. https://doi.org/10.1061/(ASCE)0733-9445(1989)115:7(1795)

Melchers, R.E., 1984. Human error in structural reliability assessments. Reliability Engineering 7, 61–75. https://doi.org/10.1016/0143-8174(84)90017-9

Melchers, R.E., Harrington, M.V., 1983. Structural reliability as affected by human error. Presented at the Proc, 4th Int. Conf. Applications Statistics Probability Soil Struct. Eng., Florence, Italy, pp. 683–694.

MILT, 2015. Final report of Committee on Large Container Ship Safety. Committee on Large Container Ship Safety, Ministry of Land, Infrastructure, Transport and Tourism, Japan.

MILT, 2013. Interim report of Committee on Large Container Ship Safety. Committee on Large Container Ship Safety, Ministry of Land, Infrastructure, Transport and Tourism, Japan.

Minorsky, V.U., 1958. An analysis of ship collisions with reference to protection of nuclear power plants (No. NP-7475). Sharp (George G.) Inc., New York.

Mireault, P., 2015. Structured spreadsheet modeling and implementation. Presented at the CEUR Workshop Proceedings, pp. 32–38.

Mirmomeni, M., Heidarpour, A., Zhao, X.-L., Hutchinson, C.R., Packer, J.A., Wu, C., 2015. Mechanical properties of partially damaged structural steel induced by high strain rate loading at elevated temperatures–an experimental investigation. International Journal of Impact Engineering 76, 178–188.

Moan, T., 2005. Reliability-based management of inspection, maintenance and repair of offshore structures. Structure and Infrastructure Engineering, Struct. Infrastruct. Eng. (UK) 1, 33–62.

Montazeri, N., Nielsen, U.D., Juncher Jensen, J., 2016. Estimation of wind sea and swell using shipboard measurements – A refined parametric modelling approach. Applied Ocean Research 54, 73–86. https://doi.org/10.1016/j.apor.2015.11.004

Morgan, D., 2016. An improved three-dimensional discrete element model for ice-structure interaction, in: Proceedings of the 23rd IAHR International Symposium on Ice. Ann Arbor, MI.

Morton, H.S., 1966. Scaling the effects of air blast on typical targets (No. TG-733). The Johns Hopkins University Applied Physics Laboratory, Silver Springs, MD.

Muggeridge, K.J., McKenna, R.F., Spring, W., Thomas, G., 2017. ISO 19906 update - An international standard for arctic offshore structures, in: Proceedings of the 24th International Conference on Port and Ocean Engineering under Arctic Conditions. Presented at the POAC 17, Busan, Korea.

Muttoni, A., Ruiz, M.F., 2012. Levels-of-Approximation Approach in Codes of Practice. Structural Engineering International 22, 190–194. https://doi.org/10.2749/101686612X13291382990688

Naser, M.Z., Kodur, V.K.R., 2016. Factors governing onset of local instabilities in fire exposed steel beams. Thin-Walled Structures 98, 48–57.

Nezamian, A., Nicolson, R.J., 2016. Asset integrity assessment and management program for life preservation of a purpose built FPSO and associated subsea system facilities. Presented at the Proceedings of the International Conference on Offshore Mechanics and Arctic Engineering - OMAE. https://doi.org/10.1115/OMAE2016-54257

Nielsen, U.D., 2016. A Review of Sea State Estimation Procedures Based on Measured Vessel Responses. Journal of the Japan Society of Naval Architects and Ocean Engineers 23.

Nielsen, U.D., 2006. Estimations of on-site directional wave spectra from measured ship responses. Marine Structures 19, 33–69. https://doi.org/10.1016/j.marstruc.2006.06.001

Nielsen, U.D., Andersen, I.M.V., Koning, J., 2013. Comparisons of means for estimating seas states from an advancing large container ship, in: 12th International Symposium Practical Design of Ships and Other Floating Structures. Presented at the PRADS 2013, Changwon City, Korea, pp. 250–258.

Nielsen, U.D., Bjerregard, M., Galeazzi, R., Fossen, T.I., 2015. New concepts for shipboard sea state estimation. IEEE, pp. 1–10. https://doi.org/10.23919/OCEANS.2015.7404386

Nielsen, U.D., Friis-Hansen, P., Jensen, J.J., 2009. A step towards risk-based decision support for ships – Evaluation of limit states using parallel system analysis. Marine Structures 22, 209–224. https://doi.org/10.1016/j.marstruc.2008.08.002

Nielsen, U.D., Jensen, J.J., Pedersen, P.T., Ito, Y., 2011. Onboard monitoring of fatigue damage rates in the hull girder. Marine Structures 24, 182–206. https://doi.org/10.1016/j.marstruc.2011.03.003

Nielsen, U.D., Stredulinsky, D.C., 2012. Sea state estimation from an advancing ship – A comparative study using sea trial data. Applied Ocean Research 34, 33–44. https://doi.org/10.1016/j.apor.2011.11.001

Ochi, M.K., Motter, L.E., 1973. Prediction of slamming characteristics and hull response for ship design. Transactions - Society of Naval Architects and Marine Engineers 81, 144–176.

Okada, T., Kawamura, Y., Kato, J., Ando, H., Yonezawa, T., Kimura, F., Toyoda, M., Yamanouchi, A., Arima, T., Oka, M., Matsumoto, T., Kakizaki, H., 2017. Outline of the research project on hull structure health monitoring of 14,000TEU large container ships (in Japanese). Conference Proceedings of Japan Society of Naval Architects and Ocean Engineers 24, 31–35.

Okada, T., Takeda, Y., Maeda, T., 2006. On board measurement of stresses and deflections of a Post-Panamax containership and its feedback to rational design. Marine Structures 19, 141–172. https://doi.org/10.1016/j.marstruc.2006.09.001

Oshiro, R.E., Calle, M.A.G., Mazzariol, L.M., Alves, M., 2017. Experimental study of collision in scaled naval structures. International Journal of Impact Engineering 110, 149–161.

Øvergård, K.I., Sorensen, L.J., Nazir, S., Martinsen, T.J., 2015. Critical incidents during dynamic positioning: operators' situation awareness and decision-making in maritime operations. Theoretical Issues in Ergonomics Science 16, 366–387. https://doi.org/10.1080/1463922X.2014.1001007

Paik, J.K., Lee, J.M., Shin, Y.S., Wang, G., 2004. Design principles and criteria for ship structures under impact pressure loads arising from sloshing, slamming and green seas. Transactions - Society of Naval Architects and Marine Engineers 112, 292–313.

Palaneeswaran, E., Love, P., Kim, J.T., 2014. Role of Design Audits in Reducing Errors and Rework: Lessons from Hong Kong. Journal of Performance of Constructed Facilities 28, 511–517. https://doi.org/10.1061/(ASCE)CF.1943-5509.0000450

Pang, S.D., Zhang, J., Poh, L.H., Law, E., Yap, K.T., 2015. The modelling of ice-structure interaction with cohesive element method: Limitations and challenges, in: Proceedings of the 23rd International Conference on Port and Ocean Engineering under Arctic Conditions. Presented at the POAC 15, Trondheim, Norway.

Park, J.-B., 2016. Life extension of moss LNG carriers using full spectral fatigue analysis. Journal of the Korean Society of Marine Engineering 40, 10–16. https://doi.org/10.5916/jkosme.2016.40.1.10

Parunov, J., 2012. ISSC 2012 - The 18th international ship and offshore structures congress. Brodogradnja 63, 372–374.

Pascoal, R., Guedes Soares, C., 2009. Kalman filtering of vessel motions for ocean wave directional spectrum estimation. Ocean Engineering 36, 477–488. https://doi.org/10.1016/j.oceaneng.2009.01.013

Pascoal, R., Guedes Soares, C., 2008. Non-parametric wave spectral estimation using vessel motions. Applied Ocean Research 30, 46–53. https://doi.org/10.1016/j.apor.2008.03.003

Pedersen, P.T., 1994. Ship grounding and hull-girder strength. Marine Structures 7, 1–29.

Pedersen, P.T., Simonsen, B.C., 1995. Dynamics of ships running aground. Journal of Marine Science & Technology 1, 37–45.

Pedersen, P.T., Zhang, S., 1998. On impact mechanics in ship collisions. Marine Structures 11, 429–449.

Pedersen, P.T., Zhang, S.M., 2000. Absorbed energy in ship collisions and grounding - Revising Minarsky's empirical method. Journal of Ship Research 44, 140–154.

Pernas-Sánchez, J., Artero-Guerrero, J.A., Varas, D., López-Puente, J., 2015. Analysis of Ice Impact Process at High Velocity. Exp Mech 55, 1669–1679. https://doi.org/10.1007/s11340-015-0067-4

Pernas-Sánchez, J., Pedroche, D.A., Varas, D., López-Puente, J., Zaera, R., 2012. Numerical modeling of ice behavior under high velocity impacts. International Journal of Solids and Structures 49, 1919–1927. https://doi.org/10.1016/j.ijsolstr.2012.03.038

Peschmann, J., 2001. Energy absorption computations of ship steel structures under collision and grounding (translated from German language) (PhD Thesis). Technical University of Hamburg.

Peschmann, J., Selle, H., Jankowski, J., Horn, G., Arima, T., 2017. IACS common structural rules as an element of IMO goal based standards for bulk carriers and oil tankers, in: Proceedings of the 6th International Conference On Marine Structures. Presented at the MARSTRUCT 2017, CRC Press/Balkema, Lisbon, Portugal, pp. 297–304. https://doi.org/10.1201/9781315157368-35

Phillips, T., Martyn, D., 2016. A Coast Guard Perspective: Evaluation of Continued Service Proposals for Floating Offshore Facilities. Presented at the Offshore Technology Conference, Offshore Technology Conference. https://doi.org/10.4043/27264-MS

Powell, S.G., Baker, K.R., Lawson, B., 2009. Impact of errors in operational spreadsheets. Decision Support Systems 47, 126–132. https://doi.org/10.1016/j.dss.2009.02.002

Prabowo, A.R., Bae, D.M., Sohn, J.M., Zakki, A.F., Cao, B., Cho, J.H., 2017. Effects of the rebounding of a striking ship on structural crashworthiness during ship-ship collision. Thin-Walled Structures 115, 225–239.

Pradillon, J.Y., Chen, C.P., Collette, M., Czaban, Z., Erikstad, S., Giuglea, V., Jiang, X., Rigo, P., Roland, F., Takaoka, Y., Zanic, V., 2012. Committee IV.2 Design Methods, in: Proceedings of the 18th International Ship and Offshore Structures Congress. Schiffbautechnische Gesellschaft e.V., Hamburg, Germany, pp. 507–577.

Prestileo, A., Rizzuto, E., Teixeira, A.P., Soares, C.G., 2013. Bottom damage scenarios for the hull girder structural assessment. Marine Structures 33, 33–55.

Ranta, J., Polojärvi, A., Tuhkuri, J., 2015. Ice load estimation through combined finite-discrete element simulations, in: Proceedings of the 23rd International Conference on Port and Ocean Engineering under Arctic Conditions. Presented at the POAC 15, Trondheim, Norway.

Rathje, H., Kahl, A., Schellin, T.E., 2013. Semi-Empirical Assessment of Long-Term High-Frequency Hull Girder Response of Containerships. International Journal of Offshore and Polar Engineering 23, 292–297.

Ren, Y.T., Qiu, X.M., Yu, T.X., 2014. The sensitivity analysis of a geometrically unstable structure under various pulse loading. International Journal of Impact Engineering 70, 62–72.

Reynolds, J.D., 2016. United States Coast Guard 16711/OCS D8(ocs) Policy Letter 01-2016.

Rhymer, J., Kim, H., Roach, D., 2012. The damage resistance of quasi-isotropic carbon/epoxy composite tape laminates impacted by high velocity ice. Composites Part A: Applied Science and Manufacturing 43, 1134–1144. https://doi.org/10.1016/j.compositesa.2012.02.017

Rice, J.R., Tracey, D.M., 1969. On the ductile enlargement of voids in triaxial stress fields. Journal of the Mechanics & Physics of Solids 17, 201–217.

Ringsberg, J.W., Heggelund, S.E., Lara, P., Jang, B.S., Hirdaris, S.E., 2017. Structural response analysis of slamming impact on free fall lifeboats. Marine Structures 54, 112–126.

Riska, K., 2013. Development of the Finnish-Swedish Ice Class Rules using recent research results, Invited Lecture.

Riska, K., Kaṁäṙainen, J., 2012. Comparison of Finnish-Swedish and IACS ice class rules, in: RINA International Conference on the Ice Class Ships. Royal Institute of Naval Architects, pp. 43–62.

Riska, K., Kämärainen, J., 2011. A review of ice loading and the evolution of the finnish-swedish ice class rules. Transactions - Society of Naval Architects and Marine Engineers 119, 265–298.

Rosen, J., Johnstone, D., Sincock, P., Potts, A.E., Hourigan, D., 2016. Application of reliability analysis to re-qualification and life extension of floating production unit moorings. Presented at the Proceedings of the International Conference on Offshore Mechanics and Arctic Engineering - OMAE. https://doi.org/10.1115/OMAE2016-54677

Sætrevik, B., Ghanonisaber, S., Lunde, G.E., 2018. Power imbalance between supply vessels and offshore installations may impede the communication of safety issues. Safety Science 101, 268–281. https://doi.org/10.1016/j.ssci.2017.09.010

Sarter, N.B., Woods, D.D., 1995. How in the World Did We Ever Get into That Mode? Mode Error and Awareness in Supervisory Control. Human Factors: The Journal of the Human Factors and Ergonomics Society 37, 5–19. https://doi.org/10.1518/001872095779049516

Sawamura, J., Kioka, S., 2016. Numerical modelling of icebreaking and ice-clearing for an icebreaker advancing in sea ice, in: Proceedings of the 23rd IAHR International Symposium on Ice. Ann Arbor, MI.

Scharrer, M., Zhang, L., Egge, E.D., 2002. Final report MTK0614 - Collision calculations in naval design systems (No. ESS 2002.183 Version 1). Germanischer Lloyd, Hamburg, Germany.

Schneider, K., Liskin, O., 2015. Exploring FLOW Distance in Project Communication, in: Proceedings of the Eighth International Workshop on Cooperative and Human Aspects of Software Engineering, CHASE '15. IEEE Press, Piscataway, NJ, USA, pp. 117–118.

Sgambi, L., 2005. Handling model approximations and human factors in complex structure analyses. Presented at the Proceedings of the 10th International Conference on Civil, Structural and Environmental Engineering Computing, Civil-Comp 2005.

Shafiee, M., Sørensen, J.D., 2017. Maintenance Optimization and Inspection Planning of Wind Energy Assets: Models, Methods and Strategies. Reliability Engineering & System Safety In Press. https://doi.org/10.1016/j.ress.2017.10.025

Simonsen, B.C., Törnqvist, R., Lützen, M., 2009. A simplified grounding damage prediction method and its application in modern damage stability requirements. Marine Structures 22, 62–83.

Skjong, R., 2015. Impact assessment compilation part 2; Comparison between IMO FSA and the EC IA (No. 2015–1024, Rev. 1). European Maritime Safety Agency, Lisboa, Portugal.

Smith, P.D., Hetherington, J.G., 1994. Blast and ballistic loading of structures. Butterworth-Heinemann, Oxford, UK.

Soliman, M., Frangopol, D.M., Mondoro, A., 2016. A probabilistic approach for optimizing inspection, monitoring, and maintenance actions against fatigue of critical ship details. Structural Safety 60, 91–101. https://doi.org/10.1016/j.strusafe.2015.12.004

Song, L., Izzuddin, B.A., Elnashai, A.S., Dowling, P.J., 2000. An integrated adaptive environment for fire and explosion analysis of steel frames—Part I:: analytical models. Journal of Constructional Steel Research 53, 63–85.

Song, M., Ma, J., Huang, Y., 2017. Fluid-structure interaction analysis of ship-ship collisions. Marine Structures 55, 121–136.

Spouge, J., Skjong, R., 2014. Risk Level and Acceptance Criteria for Passenger Ships. First interim report, part 2: Risk Acceptance Criteria (No. PP092663/1-1/2, Rev. 2). European Maritime Safety Agency, Lisboa, Portugal.

Spouge, J., Skjong, R., Olufsen, O., 2015. Risk Acceptance and Cost Benefit Criteria Applied in the Maritime Industry in Comparison with Other Transport Modes and Industries, in: Proceedings of the 12th International Conference on the Stability of Ships and Ocean Vehicles. Presented at the STAB 2015, Glasgow, Scotland, pp. 283–292.

Sruthi, C., Sriram, V., 2017. Wave impact load on jacket structure in intermediate water depth. Ocean Engineering 140, 183–194.

Storhaug, G., Moe, E., 2007. Measurements of wave induced vibrations onboard a large container vessel operating in harsh environment, in: 10th International Symposium on Practical Design of Ships and Other Floating Structures. Presented at the PRADS 2007, American Bureau of Shipping, Houston, TX, United states, pp. 64–72.

Storheim, M., Amdahl, J., Martens, I., 2015. On the accuracy of fracture estimation in collision analysis of ship and offshore structures. Marine Structures 44, 254–287.

Stoughton, T.B., Yoon, J.W., 2012. Path independent forming limits in strain and stress spaces. International Journal of Solids & Structures 49, 3616–3625.

Strickland, J., 2015. A Design Process Centric Application of State Space Modeling as a Function of Communication and Cognitive Skills Assessments (PhD Thesis). University of Michigan, Ann Arbor.

Sun, B., Hu, Z., Wang, G., 2015. An analytical method for predicting the ship side structure response in raked bow collisions. Marine Structures 41, 288–311. https://doi.org/10.1016/j.marstruc.2015.02.007

Sun, B., Hu, Z., Wang, J., 2017. Bottom structural response prediction for ship-powered grounding over rock-type seabed obstructions. Marine Structures 54, 127–143.

Sun, B., Hu, Z., Wang, J., Yu, Z., 2016. An analytical method to assess the damage and predict the residual strength of a ship in a shoal grounding accident scenario. Journal of Ocean Engineering & Science 1, 167–179.

Sun, M., Zheng, Z., Gang, L., 2018. Uncertainty Analysis of the Estimated Risk in Formal Safety Assessment. Sustainability 10, 321. https://doi.org/doi:10.3390/su10020321

Sun, R., Huang, Z., Burgess, I.W., 2012a. The collapse behaviour of braced steel frames exposed to fire. Journal of Constructional Steel Research 72, 130–142.

Sun, R., Huang, Z., Burgess, I.W., 2012b. Progressive collapse analysis of steel structures under fire conditions. Engineering Structures 34, 400–413.

Sun, S.L., Wu, G.X., 2014. Self-similar solution for oblique impact of a water column with sharp front on a wall and its zero inner angle steady limit. Physics of Fluids 26, 072108. https://doi.org/doi.org/10.1063/1.4892617

Sun, S.L., Wu, G.X., 2013. Oblique water entry of a cone by a fully three-dimensional nonlinear method. Journal of Fluids & Structures 42, 313–332.

Sun, S.Y., Sun, S.L., Wu, G.X., 2015. Oblique water entry of a wedge into waves with gravity effect. Journal of Fluids & Structures 52, 49–64.

Swidan, A., Thomas, G., Ranmuthugala, D., Amin, W., Penesis, I., Allen, T., Battley, M., 2016. Experimental drop test investigation into wetdeck slamming loads on a generic catamaran hullform. Ocean Engineering 117, 143–153.

Swift, H.W., 1952. Plastic instability under plane stress. Journal of the Mechanics & Physics of Solids 1, 1–18.

Symonds, P.S., 1953. Dynamic load characteristics in plastic bending of beams. Journal of Applied Mechanics 20, 475–481.

Tan, C., Lu, Y., Zhang, X., 2016. Life extension and repair decision-making of ageing offshore platforms based on DHGF method. Ocean Engineering 117, 238–245. https://doi.org/10.1016/j.oceaneng.2016.03.048

Tan, Y., Xi, F., Li, S., Zhou, Z., 2017. Pulse shape effects on the dynamic response of a steel beam under combined action of fire and explosion loads. Journal of Constructional Steel Research 139, 484–492.

Taylor, R.S., Jordaan, I.J., 2015. Probabilistic fracture mechanics analysis of spalling during edge indentation in ice. Engineering Fracture Mechanics 134, 242–266. https://doi.org/10.1016/j.engfracmech.2014.10.021

Temple, D., Collette, M., 2017. Understanding lifecycle cost trade-offs for naval vessels: minimising production, maintenance, and resistance. Ships and Offshore Structures 12, 756–766. https://doi.org/10.1080/17445302.2016.1230039

Terwel, K., Boot, W., Nelisse, M., 2014. Structural unsafety revealed by failure databases. Proceedings of the Institution of Civil Engineers - Forensic Engineering 167, 16–26. https://doi.org/10.1680/feng.13.00019

The FAST Standard 02b, 2016. . FAST Standard Organization.

Thomas, G., 2017. Design situations and limit states in the design of arctic offshore structures, in: Proceedings of the 24th International Conference on Port and Ocean Engineering under Arctic Conditions. Presented at the POAC 17, Busan, Korea.

Thomas, G., 2015. Risk and reliability in the design of arctic offshore structures, in: Proceedings of the 23rd International Conference on Port and Ocean Engineering under Arctic Conditions. Presented at the POAC 15, Trondheim, Norway.

Thomas, G., Davis, M.R., Holloway, D.S., Roberts, T., 2006. The effect of slamming and whipping on the fatigue life of a high-speed catamaran. Australian Journal of Mechanical Engineering 3, 165–174.

Thomas, G.A., Davis, M.R., Holloway, D.S., Watson, N.L., Roberts, T.J., 2003. Slamming Response of a Large High-Speed Wave-Piercer Catamaran. Marine Technology 40, 126–140.

Thomas, P.F., Wierzbicki, T., 1992. Grounding Damage To Double Hull Tank Vessels, in: Proc of 2nd Int Offshore and Polar Eng Conf. Presented at the ISOPE 1992, ISOPE, San Francisco, USA, pp. 108–116.

Tippmann, J.D., Kim, H., Rhymer, J.D., 2013. Experimentally validated strain rate dependent material model for spherical ice impact simulation. International Journal of Impact Engineering 57, 43–54. https://doi.org/10.1016/j.ijimpeng.2013.01.013

Törnqvist, R., 2003. Design of Crashworthy Ship Structures (PhD Thesis). DTU, Lyngby, Denmark.

Toyoda, M., Okada, T., Maeda, T., Matsumoto, T., 2008. Full scale measurement of stress and deflections of Post-Panamax container ship, in: Design & Operation of Containerships. RINA, London.

UNECE, 2017. Renovation of inland and river-sea vessels in the Russian Federation - ECE/TRANS/SC.3/WP.3/2017/6.

UNECE, 2011. White paper on Efficient and Sustainable Inland Water Transport in Europe-ECE/TRANS/SC.3/189.

UN-WECD, 1987. Our Common Future. United Nation World Commission on Environment and Development - the Brundtland Commission.

USACE, 2017. The U.S. Waterway System 2016 Transportation Facts & Information. Navigation and Civil Works Decision Support Center U.S. Army Corps of Engineers, Alexandria, Virginia.

Vassalos, D., Hamann, R., Zaraphonitis, G., Luhmann, H., Kuusisto, T., 2016. Combined assessment of cost- effectiveness of previous parts, FSA compilation and recommendations for decision making (No. 2015–0404, Rev. 3). European Maritime Safety Agency, Lisboa, Portugal.

Veen, D., Gourlay, T., 2012. A combined strip theory and Smoothed Particle Hydrodynamics approach for estimating slamming loads on a ship in head seas. Ocean Engineering 43, 64–71.

Von Karman, T., 1929. The impact on seaplane floats during landing (321). National Advisory Committee for Aeronautics (NACA), Washington D.C.

Wang, G., Arita, K., Liu, D., 2000. Behavior of a double hull in a variety of stranding or collision scenarios. Marine Structures 13, 147–187.

Wang, G., Ohtsubo, H., Liu, D., 1997. A simple method for predicting the grounding strength of ships. Journal of Ship Research 41, 241–247.

Wang, S., Soares, C.G., 2016. Stern slamming of a chemical tanker in irregular head waves. Ocean Engineering 122, 322–332.

Webber, D.D.M., Gant, S.E., Ivings, D.M.J., Jagger, S.F., 2010. LNG Source Term Models for Hazard Analysis: a Review of the State-of-the-Art and an Approach to Model Assessment (Research Report No. RR789). Health and Safety Executive, London, UK.

Wong, M.B., 2001. Elastic and plastic methods for numerical modelling of steel structures subject to fire. Journal of Constructional Steel Research 57, 1–14.

Wu, C., Hao, H., 2005. Modeling of simultaneous ground shock and airblast pressure on nearby structures from surface explosions. International Journal of Impact Engineering 31, 699–717.

Wu, Y., Gao, X., 2014. Numerical simulation for the explosion shock waves and correction of calculation formula of Overpressure [J]. Journal of Huaqiao University (Natural Science) 35, 321–326.

Xi, F., Li, Q.M., Tan, Y.H., 2014. Dynamic response and critical temperature of a steel beam subjected to fire and subsequent impulsive loading. Computers & Structures 135, 100–108.

Yang, X., 2017. Study on slamming pressure calculation formula of plunging breaking wave on sloping sea dike. International Journal of Naval Architecture & Ocean Engineering 9, 439–445.

Yıldırım, U., Başar, E., Uğurlu, Ö., 2017. Assessment of collisions and grounding accidents with human factors analysis and classification system (HFACS) and statistical methods. Safety Science In Press. https://doi.org/10.1016/j.ssci.2017.09.022

Yoshihira, Y., Okada, T., Kawamura, Y., Terada, Y., 2017. A study on the estimation method of an ocean wave spectrum using measured hull responses on 14,000TEU large container ships. Conference Proceedings of Japan Society of Naval Architects and Ocean Engineers 24, 37–42.

Youngdahl, C.K., 1971. Influence of pulse shape on the final plastic deformation of a circular plate. International Journal of Solids & Structures 7, 1127–1142.

Youngdahl, C.K., 1970. Correlation Parameters for Eliminating the Effect of Pulse Shape on Dynamic Plastic Deformation. Journal of Applied Mechanics 37, 744–752.

Yu, Z., Amdahl, J., Storheim, M., 2016a. A new approach for coupling external dynamics and internal mechanics in ship collisions. Marine Structures 45, 110–132.

Yu, Z., Hu, Z., Wang, G., 2015. Plastic mechanism analysis of structural performances for stiffeners on bottom longitudinal web girders during a shoal grounding accident. Marine Structures 40, 134–158.

Yu, Z., Shen, Y., Amdahl, J., Greco, M., 2016b. Implementation of Linear Potential-Flow Theory in the 6DOF Coupled Simulation of Ship Collision and Grounding Accidents. Journal of Ship Research 60, 119–144.

Zeng, J., Hu, Z., Chen, G., 2016. A steady-state plate tearing model for ship grounding over a cone-shaped rock. Ships & Offshore Structures 11, 245–257.

Zhang, S., 2002. Plate tearing and bottom damage in ship grounding. Marine Structures 15, 101–117.

Zhang, S., Pedersen, P.T., 2017. A method for ship collision damage and energy absorption analysis and its validation. Ships and Offshore Structures 12, S11–S20.

Zhang, S., Villavicencio, R., Zhu, L., Pedersen, P.T., 2017. Impact mechanics of ship collisions and validations with experimental results. Marine Structures 52, 69–81.

Zhao, R., Faltinsen, O., Aarsnes, J., 1996. Water entry of arbitrary two-dimensional sections with and without flow separation. Presented at the Proceedings of the 21st symposium on naval hydrodynamics, Trondheim, Norway, National Academy Press, Washington, DC, USA, pp. 408–423.

Zhao, Y.P., Yu, T.X., Fang, J., 1995. Saturation impulses for dynamically loaded structures with finite-deflections. Structural Engineering & Mechanics 3, 583–592.

Zhao, Y.P., Yu, T.X., Fang, J., 1994. Large dynamic plastic deflection of a simply supported beam subjected to rectangular pressure pulse. Archive of Applied Mechanics 64, 223–232.

Zhu, G., Huang, Y.G., Yu, T.X., Wang, R., 1986. Estimation of the plastic structural response under impact. International Journal of Impact Engineering 4, 271–282.

Zhu, J., Collette, M., 2017. A Bayesian approach for shipboard lifetime wave load spectrum updating. Structure and Infrastructure Engineering 13, 298–312. https://doi.org/10.1080/15732479.2016.1165709

Zhu, L., 2007. Development of requirements to safeguard large container ships from the effects of bow flare slamming. Lloyd's Register Technical Association.

Zhu, L., 1996. Transient deformation modes of square plates subjected to explosive loadings. International Journal of Solids and Structures 33, 301–314.

Zhu, L., Atkins, A.G., 1998. Failure criteria for ship collision and grounding. Proceedings of Practical Design of Ships and Mobile Units. Amsterdam: Elsevier.

Zhu, L., Bai, X.Y., Yu, T.X., 2017a. The saturated impulse of fully clamped square plates subjected to linearly decaying pressure pulse. International Journal of Impact Engineering 110, 198–207.

Zhu, L., Faulkner, D., 1996. Damage estimate for plating of ships and platforms under repeated impacts. Marine Structures 9, 697–720.

Zhu, L., Faulkner, D., 1995. Design pressure for the wet-deck structure of twin-hull ships, in: Third International Conference on Fast Sea Transportation. Presented at the FAST 95, Schiffbautechnische Gesellschaft, Lubeck, Germany, pp. 257–269.

Zhu, L., He, X., Chen, F., Bai, X., 2017b. Effects of the Strain Rate Sensitivity and Strain Hardening on the Saturated Impulse of Plates. Latin American Journal of Solids and Structures 13.

Zhu, L., James, P., Zhang, S., 2002. Statistics and damage assessment of ship grounding. Marine Structures 15, 515–530.

Zhu, L., Shi, S., Yu, T., 2015. A new ice load-response model for structural design of ice classed ships, in: Proceedings of the 25th International Ocean and Polar Engineering Conference. Presented at the ISOPE 2015, Kona, Hawaii.

Zhu, L., Yu, T.X., 1997. Saturated impulse for pulse-loaded elastic-plastic square plates. International Journal of Solids & Structures 34, 1709–1718.

Ziegler, L., Gonzalez, E., Rubert, T., Smolka, U., Melero, J., 2018. Lifetime extension of onshore wind turbines: A review covering Germany, Spain, Denmark, and the UK. Renewable and Sustainable Energy Reviews 82, 1261–1271. https://doi.org/10.1016/j.rser.2017.09.100

Ziegler, L., Muskulus, M., 2016. Lifetime extension of offshore wind monopiles: Assessment process and relevance of fatigue crack inspection, in: 12th EAWE PhD Seminar on Wind Energy in Europe. Presented at the 2016 EAWE PhD Seminar, DTU Lyngby, Denmark.

Ziegler, L., Schafhirt, S., Scheu, M., Muskulus, M., 2016. Effect of Load Sequence and Weather Seasonality on Fatigue Crack Growth for Monopile-based Offshore Wind Turbines. Energy Procedia, 13th Deep Sea Offshore Wind R&D Conference, EERA DeepWind'2016 94, 115–123. https://doi.org/10.1016/j.egypro.2016.09.204

This page intentionally left blank

Proceedings of the 20th International Ship and Offshore Structures Congress (ISSC 2018) Volume I – M.L. Kaminski and P. Rigo (Eds.)

doi:10.3233/978-1-61499-862-4-609

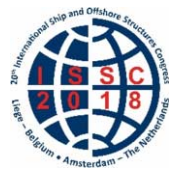

COMMITTEE IV.2

DESIGN METHODS

COMMITTEE MANDATE

Concern for the synthesis of the overall design process for marine structures, and its integration with production, maintenance and repair. Particular attention shall be given to the roles and requirements of computer-based design and production, and to the utilization of information technology.

AUTHORS/COMMITTEE MEMBERS

Chairman: I. Lazakis, *UK*
R. Bronsart, *Germany*
J-D Caprace, *Brazil*
Y. Chen, *China*
P. Georgiev, *Bulgaria*
I. Ilnitskiy, *Ukraine*
L. Moro, *Canada*
P. Prebeg, *Croatia*
J. Mendonça Santos, *Netherlands*
Z. Sekulski, *Poland*
M. Sicchiero, *Italy*
R. Sielski, *USA*
W. Tang, *China*
M. Toyoda, *Japan*
J. Varela, *Portugal*

KEYWORDS

Design Methodology, Product Lifecycle Model, Optimization, Offshore structures, Classification Society software, Lifecycle Structural Management, CAD, Design Software

CONTENTS

1. INTRODUCTION 612

2. DESIGN METHODS 613
2.1 Design methods 613
2.1.1 Optimization methods 613
2.1.2 Surrogate modelling and variable fidelity approaches 615
2.1.3 Other relevant structural design approaches 617
2.2 Review of ship structural design for X 619
2.2.1 Design for life-cycle performance 620
2.2.2 Design for maintenance & repair 621
2.2.3 Design for safety 623

3. DESIGN TOOL DEVELOPMENT 625
3.1 CAD Systems for Naval Architecture 625
3.2 Virtual Reality and Augmented Reality 626
3.3 Specialized structural simulation packages 627
3.4 Risk-based design software tools 629
3.4.1 Software Platform 630
3.4.2 Hazard Identification Tools and Risk Assessment Tools 630
3.5 Optimization Tools 631

4. OFFSHORE STRUCTURES 632
4.1 Introduction 632
4.2 Design Methodology in Offshore Structures Design 634
4.3 Design Challenges, Progress & Trends 634
4.3.1 Standardization 635
4.3.2 Oil & Gas E&P Counter Cycle 636
4.3.3 Asset Integrity & Maintenance 637
4.3.4 Design & Methodology Developments 639
4.4 Survey on Offshore Structures Design Software 642
4.4.1 Overview and characterization of respondents 642
4.4.2 Naval Architecture Tools 644
4.4.3 Structural Design Tools 648
4.4.4 Software Integration & New Technology 650
4.5 Foresight in Offshore Structures Design 651

5. STATE-OF-ART VS. STATE-OF PRACTICE 653
5.1 Motivation, background, and aim 653
5.2 State-of-the-art 654
5.2.1 Bibliometrics 654
5.2.2 Main research topics and their bibliometrics 655
5.2.3 Design methodology 657
5.2.4 Design tools 659
5.2.5 Optimization developments 660
5.2.6 Life cycle management 661
5.3 State-of-practice 661
5.3.1 Technology Readiness Level - TRL 662
5.3.2 ISSC IV.2 Committee point of view 664

6. COMPARISON OF CLASSIFICATION SOCIETY SOFTWARE 665
6.1 Introduction 665

6.2 The IACS Common Structural Rules 665
6.2.1 H-CSR rules requirements 666
6.3 Comparison of classification society tools for H-CSR 668
6.3.1 H-CSR software packages 669
6.3.2 Aframax tanker modelling for prescriptive rule calculation 673
6.4 Industry point of view 675
6.5 Conclusions 676

7. LIFECYCLE DATA MANAGEMENT 676
7.1 Tool development 677
7.2 Data interchange and standards 679
7.3 Structural and system health monitoring tools 681

8. OBSTACLES, CHALLENGES AND FUTURE DEVELOPMENTS 684
8.1 Common Structural Rules for Bulk Carriers and Oil Tankers 684
8.2 Energy Efficiency Design Index (EEDI) 686
8.3 The new design paradigm 687
8.4 Formulation of accurate optimization models including FEA 687
8.5 Analytical methods for impact analysis 687
8.6 Development a complete risk assessment frame-work for ship accident 688
8.7 Mega container ship 688
8.8 Unmanned ships 688

9. CONCLUSIONS 689

ACKNOWLEDGMENTS 691

REFERENCES 691

1. INTRODUCTION

Design methods for ships and offshore structures and their integration with production, maintenance and repair continued to be an area of great interest and further development in the 20th ISSC Committee work. Together with updating the themes covered in the previous Committee work, the current Committee also expanded its remit with additional aspects of key interest. In this respect, Chapter 2 presents the work performed on design methods following the work of the preceding ISSC IV.2 Committee presenting either large activity or (arguably) great potential for improvement. This is related to the various strategies for handling the two-way mapping between the form space and the function space related to design; that is, identifying basic decision support methods that bring a designer from a set of needs and requirements all the way to a final design description. In particular, this aspect is oriented to the discovery/selection of the best match between the available synthesis methods and available/required structural analysis methods/tools.

Over the last few years, the development of the design tools for marine structures has been characterized by the extension of the software packages functionalities in order to create tools, which can be used from the early design phases of a new ship, throughout its entire life. These design tools address several aspects of the design of a ship, such as safety, hazard scenarios and risk assessment, life-cycle maintenance, accident scenarios, and optimization. The analysis of the state-of-the-art scientific literature has shown that integration of these functionalities in the design tools have led to two different approaches in the development of the tools: monolithic software and modular systems. The above is addressed in Chapter 3 together with the recent progress of Computer-Aided Design (CAD) packages for ship design, focusing on the new 3D capabilities of this software and on the impact that 3D design is having on the maritime industry.

Following the previous Committee's official discusser suggestion, the current Committee also included a chapter particularly related to offshore structures. In this respect, Chapter 4 addresses the developments within the offshore structures design methodology and the related design challenges, latest progress and trends. In addition to the above, a survey on offshore structures design software was conducted identifying the tools and software being used for the design of offshore structures and related activities (e.g. engineering, construction, etc.). The survey also depicted the usage of various tools employed by offshore vs. ship designers as well as trying to identify existing differences related to the main activity of the stakeholders and tool usage nuances associated with different offshore units/structure types.

Chapter 5 follows another aspect suggested by the previous Committee's official discusser; that is the presentation of the state-of-the-art vs. state-of-practice. This is a new theme into the ISSC IV.2 Committee's work in order to bridge the gap in between the research work presented within the Committee's remit and the practical applications that stem out of it. The above address one of the key ISSC Committees' tasks to identify knowledge resulting from research, which is novel, validated and is relevant to use by industry and regulatory bodies. In this respect, the adoption of a Theory to Practice Ready Papers (TPRP) approach is suggested by the current Committee for high quality and impact research work.

Chapter 6 presents the results of a benchmark study on the comparison of classification societies' software employing the most up-to-date IACS Common Structural Rules for double hull oil tankers. In this respect, an Aframax double hull tanker is analyzed using six specific classification societies' software tools.

Lifecycle management is a key feature from the initial stages of design up to the end of a ship's operating life and becomes an increasingly important issue in industry due to various reasons. Chapter seven addresses these issues and further developments both at operating and environmental point of view. Moreover, this chapter presents the data integration from early design to dismantling of the ship while the use of smart sensors as part of digitalization is also explored.

Finally, key obstacles, challenges and future developments, which will have an impact on the Committee's work, are also presented at the end of this report.

2. DESIGN METHODS

Following the work of the preceding ISSC IV.2 Committee that defines ship structural design methodology, the work of the current Committee focuses on both pf them. Each one presents either large activity or (arguably) great potential for improvement. The first aspect relates to the various strategies for handling the two-way mapping between the form space and the function space related to design that is, identifying basic decision support methods that bring a designer from a set of needs and requirements all the way to a final design description. In other words, this aspect is oriented to the discovery/selection of the best match between the available synthesis methods and available/required structural analysis methods/tools. This aspect will be covered in subsection 2.1, titled Review of Design methods. The second aspect is related to Design for X, where "X" represents a specific goal such as operability, environment, safety, or production. It will be covered in subsection 2.2, titled Review of ship structural design for X. Several others "X" are also listed in the Chapter 6.

2.1 Design methods

Any methodology for the ship structural design needs to be part of the ship design methodology and as such it is under the time constraints relevant to the ship design process, which can range from several weeks to several months. At the same time, the used methodology needs to satisfy all the demands prescribed by the applicable rules e.g. new IACS Harmonized Common Structural Rules (HCSR) for bulkers and oil tankers. In such environment, it is evident that it is necessary to find the right balance between the characteristics of the design problem and available/applicable analysis and synthesis methods.

2.1.1 Optimization methods

According to Coello et al. (2007), general search and optimization techniques can be classified into three categories: deterministic, stochastic (random) and mathematical programming methods (Figure 1).

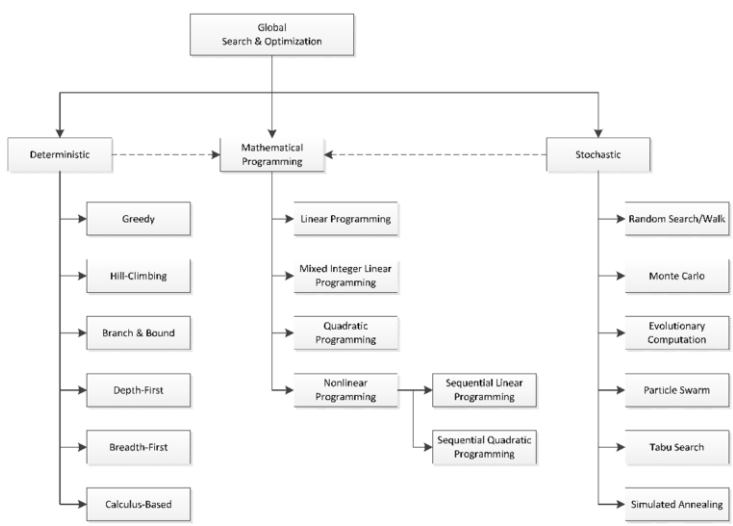

Figure 1: Classification of global search and optimization methods

In general, two types of optimization algorithms are of a special interest to ship structural design. The first ones are the generally applicable multi-objective optimization algorithms capable of obtaining the Pareto frontier that can provide the designers with the valuable insight into the trade-off between the improvement of one objective and deterioration of other objectives. The

second ones comprise computationally efficient single objective optimization algorithms capable of exploiting the structural analysis tools characteristics. However, in order to enable ship structural optimization of a realistic global ship structure (full ship models or three hold models), it is still necessary to employ two separate options. One can use the tools based either on prescribed classification society rules, or to simplify the structural problem inside the optimization loops in order to reduce the number of degrees of freedom of the original/standard FEM model. Optimization approaches with FEM models are also used for dimensioning of realistic local structures such as for the hatch covers.

Romanoff et al. (2016) presents review of the development of an effective direct strength analysis approach utilizing homogenization, the finite element method, and optimization. Homogenization is used to transform the originally periodic, stiffened plate or web-frame structure to an equivalent single layer (ESL) plate or beam structure, respectively. This makes the finite element analysis (FEA) very fast and allows modeling of the stiffness and mass of the complex structure accurately. In most of the cases, classical first-order shear deformation theory (FSDT) is adequate, but new structural solutions require enhancement of the theory to account for the influence of strain gradients. The averaged response produced by FEA is transformed to periodic response to enable the prediction of spatially fluctuating stresses and first fiber estimate of the strength. The paper summarizes recent developments on the approach with respect to quasi-static and vibratory response, but also non-linear response such as post-buckling and tensile failure under multi-axial loading. It is emphasized that one of the main benefits of using ESL in ship structural design is that is allows meshing of the structures with different (optimal) mesh densities needed for different types of analyses. Using this approach Raikunen (2016) performed optimization of a passenger ferry using the ship global 3D FE-model and ESL approach. This structural analysis approach was coupled with particle swarm optimization (PSO) code capable of searching effectively global optimums. The ship was meshed for primary ($\sigma 1$) level structural analysis using a coarser mesh, while the tertiary responses were analyzed by using sub-models at certain regions.

Um and Roh (2015) applied Sequential Quadratic Programming (SQP) and genetic algorithms to determine optimal principal dimensions of the hatch covers of a 180,000-ton bulk carrier. Some dimensions representing the shape of the hatch cover were selected as design variables and some design considerations related to the maximum stress, maximum deflection, and geometry of the hatch cover were selected as constraints. Minimization of the weight of the hatch cover was selected as an objective function. FEM model of hatch cover was made in ANSYS using only shell elements for modelling of plates, strong beams and stiffening. Single objective multi-start approach based on the combination of GA and SQP in the final phases of optimization was used to find global, not just local optimum.

Na and Karr (2016) proposed a Pareto Strategy (PS) multi-objective function method developed by considering the search direction based on Pareto optimal points, the step size, the convergence limit and random number generation. The success points between just before and current Pareto optimal points are considered. PS method can also apply to single objective function problems, and can consider discrete design variables, such as plate thickness, longitudinal space, web height and web space. The optimum design results are compared with existing Random Search (RS) multi-objective function method and Evolutionary Strategy (ES) multi-objective function method by performing the optimum designs of double bottom structure and double hull tanker which have discrete design values and using minimal dimension rules-based approach. Its effectiveness is shown by comparing the optimum results with those of RS method and ES method.

Vaucorbeil and Patron (2017) used genetic algorithms to optimize the design of the gun foundation of an Offshore Patrol Vessel. The methodology considers the main properties of materials and the loads acting on foundation, such as gun blast pressures, recoil force and dynamic inertial forces. Design constraints are related to the maximum allowable stresses, fatigue failure,

and natural frequencies of the structure. The objective variable is to minimize the weight of the foundation by altering the thicknesses of metallic elements, while satisfying the design criteria of the classification societies. FEMs are used to determine the state of stress through static structural analysis, and the natural frequencies of the structure through modal analysis. The method is therefore based on a two-way coupling between the genetic algorithm-based optimizer and the finite element solver. The authors claim that its implementation provides potential to efficiently search for optimized designs, and that the optimization tool can be used to automate the structural design of any portion of the ship.

Garbatov and Georgiev (2017) also applied a multi-objective nonlinear optimization method to a stiffened plate, in this case subjected to combined stochastic compressive loads. A genetic algorithm with a termination criterion is employed, which considers the minimization of the weight and structural displacement, as a dual objective structural response. Instead of performing complex structural analysis, as the previous methods, this method resorts to a reliability analysis based on design constraints, which is incorporated into the optimization procedure. The reliability index is employed to identify the topology of the stiffened plate as a part of the Pareto frontier solution obtained as a result of the optimization algorithm.

2.1.2 Surrogate modelling and variable fidelity approaches

Surrogate / approximation / metamodeling process, is the key to surrogate assisted optimization. It can be stated that surrogate modeling actually evolves from classical Design of Experiments (DoE) theory, in which polynomial functions are used as response surfaces, or surrogate models. Steps necessary for the generation of surrogate models include planning of experiments or sampling, execution of simulations with original analysis methods, generation or creation of selected surrogate model and validation of surrogate model adequacy. However, there are a number of research studies, including some in the ship structural design field, which generate surrogate models suffering from accuracy.

Although often neglected or not taken with enough care, it is necessary to have a metric that will enable reliable selection of surrogate modelling technique to be used. In Jin et al. (2001) the authors have compared different techniques and suggested the next performance metrics for use:

- Accuracy – the capability of predicting the system response over the design space of interest.
- Robustness – the capability of achieving good accuracy for the different problem types and sample sizes.
- Efficiency – the computational effort required for constructing the surrogate model and for predicting the response for a set of new points by surrogate models.
- Transparency – the capability of illustrating explicit relationships between input variables and responses.
- Conceptual Simplicity – the ease of implementation.

Andrade et al. (2017) speculate that direct optimization routine on every single part of the hull is not feasible with today's numerical methods and probably, according to the Bremermann's limit, will never be possible. They propose parametric structural design as a promising alternative for hull design, capable of combining weight reduction, material efficiency and safety. The objective of the paper was to demonstrate the application of a design of experiments sensitivity study for a parametrically modelled global structure of a platform. The concept of the procedure was shown, through a simplistic design optimization of a mid-ship section subjected to bending moment, that it is possible to determine valid regressions for ships structural models at a conceptual level using DoE in combination with FEA.

Andric et al. (2017a), emphasize that for multi-deck ships with extensive superstructures (such as passenger ships, RoPax, etc.) the global structural response can be particularly complex.

Main global topological parameters (e.g. size of side openings, stiffness of longitudinal bulkheads, etc.) have dominant influence on the shape of hull girder stress distributions over the ship height. The paper also proposes uses of DoE techniques to systematically study the influence of multiple topological parameters on the global structural response obtained by FEM analysis. The paper demonstrates that use of simplified FEM on passenger ship and how different topological variants can lead to different optimal structural scantlings with regards to chosen design objectives (mass, VCG, etc.). As a second step, after selection of the preferred geometry/topology variant, the authors propose and demonstrate use of both multi objective (MOPSO) and single objective scantling optimization (SLP) using the same FEM model of selected topo/geo variant.

Ma et al. (2016), presented an approach, newly implemented in software MAESTRO, capable of optimizing realistic structures. It combines multi-objective GA local optimization of a part of structure with the same scantlings, called design cluster, with the optimization on the global level where global measures like vertical center of gravity can be used as objective. At global level, design variables are designs that are to be selected from a set of Pareto solutions of each design cluster. The approach has successfully been applied for midship and full ship FEA based optimization of a naval frigate.

The same optimization approach and tool (MAESTRO) is used in Kim and Paik (2017) where it was applied for a design of a VLCC-class double hull oil tanker. The paper is more focused on using the Paik's ultimate limit state library ALPS/ULSAP for evaluation of stiffened panels adequacy and ALPS/HULL for evaluation of hull girder ultimate strength. Neither loads nor adequacy are done according to current IACS CSR BC&OT, however the use of partial safety factors that could be used to accommodate results to some extent is mentioned. Kim and Paik (2017) also propose an optimization approach for the design of preliminary hull structural scantlings (see Figure 2) as an improvement to the current industry standard based on the manual scantlings remodeling/feasibility checks. However, the proposed procedure, does not include automatic implementation of loads defined by IACS CSR BC&OT Rules, nor check of feasibility by IACS CSR BC&OT adequacy criteria, which could present a problem for the use of the proposed procedure in industry for the design of merchant ships that need to satisfy IACS CSR BC&OT.

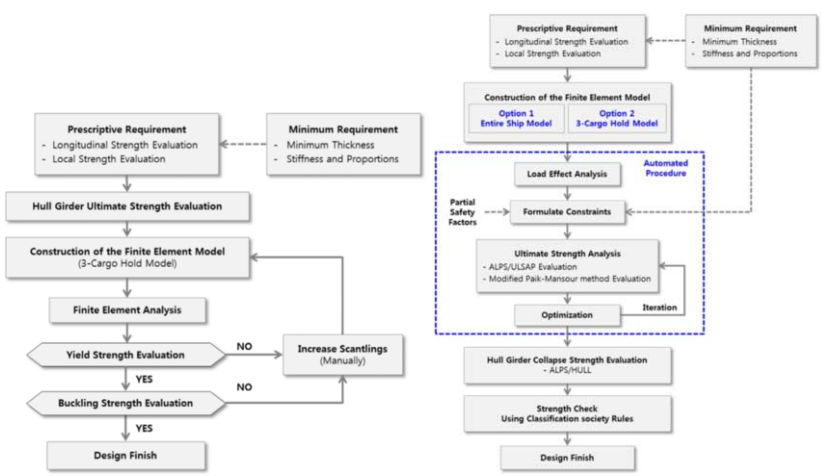

Figure 2: Approaches for the design of preliminary hull structural scantlings; a) Industry standard (IACS 2012) b) Optimization approach proposed by Kim & Paik (2017)

An optimization-based approach for the design of preliminary hull structural scantlings of ships classified by IACS CSR BC rules is further elaborated in Andric et al. (2016). The authors also specify the need for topology/geometry variants investigation using the same or simplified FE models. The proposed approach includes automatic FE model loading and feasibility checks using criteria prescribed by IACS Rules. The proposed design approach is applied on the industrial structural design of Handymax bulk carrier, made in close cooperation between ship owner team, shipyard team and university, using the in-house software OCTOPUS CSR coupled with MAESTRO. Optimization approach is very similar to the one given Ma et al. (2016), although single objective SLP algorithm was used on the optimization sub-problem/design cluster level.

Lee et al. (2015) proposed a design process composed of three parts: definition of geometry, generation of response surface, and optimization process. To reduce the time for performance analysis and minimize the prediction errors, the approximation model is generated using the Backpropagation Artificial Neural Network (BPANN) which is considered as a Neuro-Response Surface Method (NRSM). The optimization is done for the generated response surface by the non-dominated sorting genetic algorithm-II (NSGA-II). Through case studies of marine system and ship structure (substructure of floating offshore wind turbine considering hydrodynamic performance and bulk carrier bottom stiffened panels considering structure performance using NLFEA), the applicability of the proposed method for multi-objective side constraint optimization problems have been confirmed.

Knight (2017) presents a so called medium-fidelity approach which is in between the two main approaches normally taken for the early-stage structural design of multi-hulls: the high fidelity FEM of the ship from the very beginning, and the use of rules, class society guidelines and engineering safety factors. The approach consists in modelling the ship hull with complete subdivision using non-uniform rational basis splines (NURBS) surfaces and assumes that sectional loads are provided by hydrodynamics tools. The design of the structure is handled in two steps: (1) the convergence of the structural design, subjected to longitudinal load information, to maximize the objective functions; (2) the verification of the structural design subjected to longitudinal and transversal load information. In this case, physics-based solutions are applied for structural strength calculations.

2.1.3 Other relevant structural design approaches

Currently, the design methodology applied to ship structures is heavily supported and even based on digital simulations of common conditions and scenarios which occur during the ship's life-cycle. This trend becomes even wider with the continuous increasing of the computational power available, even for small to medium design offices and shipyards. New solutions for specific structural arrangements are digitally modelled and intensively tested and optimized in specialized simulation and optimization tools. Although the computational simulation and analysis of structures is already a common practice, the Classification Societies' (CS) rules are still fundamental on the design of marine structures. Since 2012 the IMO Goal Based Standards (GBS) were adopted and implemented by the SOLAS convention. Based on the GBS standards, IACS and their associated CS members developed the common structural rules, which dictate now the main guidelines for the structural design of bulk carriers and oil tankers, (Peschmann et al. (2017).

The Finite Element Method (FEM) has become one of the most common methods to analyse the effects of loads on ship structures and suggest corrections and/or improvements to the structure in early design phases. The large amount of research work during the latest years on ship structural design, which uses this methodology, reveals that the FEM will continue as one of the preferred methods to design and check ship structures in the next years. Among the most relevant and recent research works, demonstrating the importance of this method, are the ones published by Andric et al. (2017b), Joung et al. (2017a), and Cherian et al. (2017).

Andric et al. (2017b) presents an example of modern procedure in structural design of an "Open Type" livestock carrier. This type of ship represents a structural challenge due to the partial but effective participation of the superstructure both in the longitudinal and transverse/racking strength due to the absence of transverse bulkheads in the superstructure. The work highlights the required cooperation between construction yards, Classification Societies and faculty design teams as an example of modern procedure in rational structural design. They define three different design stages, in which FEMs become more complex and mature: (1) the Concept Design Phase (CDP) in which the Rule based tool is combined with generic FE model to ensure realistic calculation of primary stress distribution; (2) the Preliminary Design Phase (PDP) where only the full ship FEM model is capable of simulating realistic 3D effect of Hull/superstructure interaction without restricting assumptions; and (3) the Detailed Design Phase (DDP) where a very fine FE mesh is used to analyze and solve stress concentration problems identified in PDP phase.

FEM analysis is also used by Joung et al. (2017a) in aluminum pressure vessels for deep sea systems, concerning the global buckling phenomena and the effectiveness of connection parts of the pressure vessel. Cherian et al. (2017) describe the design development of an offshore barge suitable for the transportation of heavy modules. In order to define the final dimensions of the barge, main focus was given on local and global strength considering various operations the barge was intended for. The structural design was based on the structural requirements and scantling calculations as well as on the ABS rules to define transverse and watertight bulkheads, web frames, longitudinal bulkheads, aft pump room construction, bollards, and sponsons. The structural design was then submitted to Finite Element (FE) analysis using ANSYS Mechanical. The philosophy behind the development of the FE model was to produce a relatively simple global model and then add detail to the critical zones where high tensions were expected due to the complexity of the geometry or due to the high stresses applied to the structure. The replacement of structural members such as stiffeners by equivalent plate thickness was also used as a simplification method. Local FEMs were produced and analyzed including the models of the aft pump room and the stern subjected to rocker arm loads. The purpose of these local models was to analyze or check specific structural characteristics that required more attention. For the specific case analyzed, the use of global and local FEMs with different levels of detail, proved to be a successful method to obtain the final construction on time with the required reliability and effectiveness.

Physical tests using scale models of ship structures are still very useful to evaluate the efficiency of the structural design of a ship. However, both experimental and numerical analysis require a detailed design and structural assessment of the physical model to be used in the towing tank. With this in mind, Dessi et al. (2017) documented their design approach and testing effort devoted to providing a reliable and well identified physical model before towing tests are carried out. Their main target phenomenon is the wet deck slamming, which is a challenging Fluid-Structure Interaction (FSI) problem for both experimental and numerical analysis. The study concludes that a systematic set of tests for identifying the structural properties of the elastic bodies interacting with the fluid, gives the chance to validate or even update the structural models included in the FSI solver.

Digital simulations of casualty scenarios are also being used to assess the reliability of the ship structures during the design phase. Ko et al. (2017) is one example of this approach, where specific ship-to-ship collision simulations in which a striking ship bow collides with the side of a struck ship, are studied. Their added value was to consider the structure of the striking ship also deformable, and therefore, capable of observing energy when the collision occurs. Nonlinear finite element method (NFEM) computations provided by LS-DYNA were applied for different collision scenarios, namely regarding the speeds and collision angles between ships. The results showed that the structural damages caused by a deformable striking ship bow are significantly different from the ones caused by a rigid structure. The maximum penetrations and

structural crashworthiness between deformable and rigid bow models are different, which has impact on ship survivability or on the amount of oils spills. Rodrigues and Guedes Soares (2017) study the vertical loads progression caused by a flooding process for a shuttle tanker in full load condition, damaged amidships. Maximum values of the vertical bending moments are obtained and compared with the intact values. Parunov et al. (2017) use a NFEM to assess the residual ultimate strength of an Aframax-class double hull oil tanker damaged in collision and subjected to both horizontal and vertical bending moments. Two different types of damage are considered: damage of the outer shell only, and damage of both the outer and inner shell. Results for quick estimation of the damage ship's residual strength are printed as residual strength versus damage height diagrams. The procedure for rapid assessment of the residual strength is based on regression equations obtained from the FEM simulations, and according to the authors, may be useful for classification societies when developing rules regarding accidental limit states.

Vibrations affecting the ship structures have been taken into consideration by Dominguez et al. (2017) when designing the structural arrangement of ships. They consider the hydro-vibration analysis of the hull girder as a very important part in the design stages of the ship. Within the scope of their study, vibrations are mainly caused by encountering wave loads, or by the interaction between the ship's driveline and rudder. The methodology used to analyze the hull-girder vibrations induced by the propeller-rudder interaction of a coastal patrol vessel in the design phase is presented. The methodology considers the excitation of the propeller, the natural frequencies of the drive line, rudder, and structure of equipment foundations, the added mass and dumping of both the propeller and hull girder. Once more, FEM allowed to carry out structural modifications to comply with recommended limits of vibration effects. If applied during the design phase, the methodology may be used to detect possible failures, especially when there is resonance risk in the propulsion line.

Marinic-Kragic et al. (2016) proposed the Reduced Parameter Set (RPS) shape parameterization methods, which were compared to classical B-spline parameterization. It has been shown that the proposed shape parameterization methods are able to keep the shape generality while lowering the number of shape parameters on three mutually different test ship hull shapes. The developed multidisciplinary workflow integrating the proposed shape parameterization, hydrodynamic prediction tool and structural scantling rules proves that it is possible to have a numerical procedure that autonomously synthesizes the 3D shapes. The complex workflow was realized in modeFRONTIER using ANSYS Geometry Modeler, ANSYS Fluent and implementation of ISO 12 215 rules for composite monohull scantlings of small craft under 24 m.

Drimer et al. (2017) introduces a method for the structural design of planing hulls, which combines rules, theoretical solutions, and numerical analysis into a practical design procedure. The presented method provides an efficient tool for the determination of load effects when dynamics, hydro-elasticity, and nonlinear geometry are important, where existing design rules apply static linear assessment. The paper presents a database of simulation results in a wide range of parameters, practical for design. The direct calculations are valid for high strains, above yield, and the presented results may be used for limit state design as well. A limit state design needs to assess fatigue limit state as well, which is a scope for a future work. A design example demonstrates the application of the suggested method and shows a saving of about 20% of the bottom plates thicknesses, relative to design by rules.

2.2 Review of ship structural design for X

A summary of the most recent developments related to the design for specific performance aspects, also known as "Design-for-X" (DfX), is given in this subsection. From a structural design point-of-view, the most relevant DfX aspects are design-for-production and design-for-safety. Both of these will be handled separately later in this chapter. In general, DfX's concept puts the emphasis on the performance achievement, and, at least in principle, has no specific

requirements towards the specific design solution or the design process to be followed. Following the trends indicated by the work of the previous Committee, DfX is closely related to the current trend towards goal-based design methodologies in general and risk-based design in, endorsed by recent International Maritime Organization (IMO) regulations.

2.2.1 Design for life-cycle performance

Ventura and Soares (2015) presented development of voyage scenarios as a valuable tool in ship design for the estimate of the sailing and port times and operational costs. In the scope of the ongoing development of a software tool for the ship concept design, the voyage model was further detailed in order to support a more complete description of the ports and routes resulting in a more precise estimate of the port and sailing times, the fuel consumptions and the operational costs. The concept of voyage leg was expanded to allow the description of regions with specific environmental conditions or ship operation parameters. These enhancements are particularly relevant for liner ships, which have a higher number of port calls (by comparison with bulk carriers and tankers) and sail often with partial loads. The ship synthesis model was extended to include hull form generation, hydrostatics calculations, compartment modeling, EEDI and ship emissions estimates. A design procedure considering the ship synthesis model, the voyage model and the ship service conditions to be used in optimization procedures was presented. Some of the advantages of this implementation based on a spreadsheet is the possibility to use any design parameters as design variable and to have all the results exposed and available to specify constraints and to be used directly or indirectly (through utility functions) in objective functions, without the need to change the model. A simple numeric example was produced as a validation test of the functionality of the global procedure.

Lindstat et al. (2015) presented an interesting study that challenges the traditional environmental regulations approach for shipping activities. The study investigates the possibility of fulfilling the requirements for low levels of harmful emissions in ports and coastal areas without sacrificing the benefits at high seas of low cost bunker oil and its overall climate cooling effect. Continued use of HFO 2.7% Sulphur outside of the ECA in combination with clean fuels within the ECA is indicated to both retain the global cooling effect of shipping and reduce harmful emissions close to land. This indicates that IMO and other authorities should reconsider decisions to globally reduce allowable Sulphur content in fuels from 3.5% to 0.5% by 2020. Burning dirty fuels at high seas in an engine optimized for fuel economy (hence also raising the NOs), gives climate cooling benefits, and this more than compensates for the warming effect of reducing harmful SO_x and NO_x emissions close to land and human populations.

According to the authors, another problem with the IMO approach is that engines tuned to comply with ECA emission restrictions risk increasing greenhouse gas emissions, perhaps an irony of placing a ‘local first’ focus on environmental regulations. In addition, the study indicates that hybrid power setups give lower environmental impact than the standard engine solutions and a lower annual fuel bill. However, for fuel prices, which are 50% of the 2012–2014 average, the economic argument for investing in more advanced engine solutions weakens. One potential incentive to be considered forward is that vessels burning fuels with high Sulphur content beyond 2020 have to install either hybrid engine systems or advanced engine control systems linked to verifiable automatic reporting systems to ensure that the dirty fuel is burned only at high seas, and that the vessel complies with SO_x and NO_x obligations in the current and future ECAs. Implementation of such systems currently is entirely feasible technically.

Marques et al. (2017a) developed a simple and fast model to be applied in optimization problems about selection of marine dual-fuel low-speed diesel engines. Following that, Marques et al. (2017b) presented a new approach to perform the optimized selection of liquefied natural gas carriers’ propulsion system including the mainly financial aspects. It is an important study because with the new environmental restrictions the use of boil-off gas (BOG) is an alternative as cleanest than conventional fuels through dual-fuel diesel engines. A model to optimize the

selection of LNG carriers' propulsion system towards synthesis, design and operation, as well as the needed models, has been presented. The work is based on a particular study of a ship that has to accomplish three different service speeds. The objective function maximizes the net present value of the project. Finally, this study can assist marine engineers and ship-owners to design and outline the operation of liquefied natural gas carriers.

Knight et al. (2015) presented a new type of real options analysis used to evaluate the worth of an option to Extend the Service Life (ESL options) of an aluminum structure from twenty to twenty-five years. It is an early application of Prospect theory-Based Real Options Analysis (PB-ROA) in naval design. PB-ROA abstracts the principles of real options analysis to suit naval design applications where the assets do not generate cash flows, and there for one cannot define value in monetary terms. Instead, the example in this paper defines the utility of a structural design based on three components: structural availability, cargo capacity, and producibility. The utility is contingent on risk factors like the time to crack initiation of a welding detail which is included using stochastic fatigue analysis. From an entire Pareto front of optimal structural designs, the options analysis exposes a partition in the design space which could be valuable in a design setting. The partitioning reveals the conditions in which certain candidate designs maximize the present value of future flexibility. Ultimately, this paper demonstrates a new approach to valuing flexibility in preliminary structural design that may generate useful insight for early stage decision makers.

2.2.2 Design for maintenance & repair

Raptodimos et al. (2016a) presented a framework for the acquisition of measurements pertinent to condition monitoring, maintenance and repairs of ships. Several types of raw signals are acquired. Acquisition at different frequencies was considered as well as the use of sensors, periodic measurements, or both. The suggested framework was evaluated in a case study performed on board a Panamax-class containership. Key data collection sources were identified through this case study and the data collection process was demonstrated. Raptodimos et al. (2015) also presented the data acquisition performed as part of EU FP7 Inspection Capabilities for Enhanced Ship Safety (INCASS) project. Both machinery and structural measurements were acquired. In the case of structural data acquisition, tiltmeters and Inertial Measurement Units (IMUs) were installed. This framework was validated on board a tanker vessel as part of an INCASS measurement campaign and further elaborated in a study by Raptodimos et al. (2016b).

Furthermore, data requirements of various maritime stakeholders including ship operators, Classification Societies, consultancy companies and maritime regulators and policy makers were described in INCASS project report (2014a). These requirements covered a diverse range of vessels (i.e. tanker, bulk carrier and container ship). This report additionally considered main machinery and equipment systems, sub-systems and components in order to derive a final selection of systems to be monitored and evaluated. Through this iterative process, the following components were identified: main engine, turbocharger, pump systems including fuel oil supply, lube oil as well as main and cargo pumps (tanker ship only). Dikis and Lazakis (2016) suggested a Machinery Risk/Reliability Analysis (MRA) tool that considers components' failure and degradation utilizing raw recorded data. The presented methodology involves the generation of a Markov Chain arrangement integrated with Bayesian Belief Networks (BBNs).

The latter framework is further detailed in (INCASS, 2014b). A case study was presented using simulated data of Main Engine (M/E) measurements culminating in a prognostic tool thus predicting physical (i.e. temperatures, pressure) and reliability values over time for the mentioned ship system. Complementing the above, Lazakis et al. (2016) suggested a Decision Support System (DSS) framework that utilizes the output of the MRA tool developing a user-friendly graphical interface (Dikis and Lazakis, 2016). Current performance is presented alongside

warnings, failures, and in-depth analysis demonstrating the development of predicted information throughout the ship system and component lifecycle. Case studies of the DSS output using simulated faulty data as input is presented. Once raw data are acquired, the MRA and MRA DSS tools provide a complete solution for Condition Based Maintenance (CBM) of ship systems.

Additional work related to the design for maintenance and repairs of ship systems was performed by Taheri et al. (2016). The authors utilized a combination of BBN and Markov chains tor the reliability analysis and maintenance decision making for the lubricating oil system of a Suezmax vessel. Raptodimos and Lazakis (2016) presented a methodology utilizing Artificial Neural Networks (ANNs) in order to monitor and predict physical parameters of selected physical parameters in order to predict future values and subsequently propose correct maintenance actions and decisions. The suggested framework was validated through the prediction of exhaust gas temperature of a cylinder of a two-stroke marine diesel engine. Accordingly, Raptodimos and Lazakis (2017) combined the above with Fault Tree Analysis (FTA) in order to identify most critical ship systems and components.

Gkerekos et al. (2016) also suggested a database for the storage of machinery measurements and developed a self-learning model for the condition monitoring of ship machinery based on vibration measurements. This model was based on a two-class Support Vector Machine (SVM) classifier, able to discern between healthy and faulty observations. A case study based on data obtained through a measuring campaign showcase the soundness of the suggested database design. Furthermore, the vibration monitoring model was validated using a wind turbine dataset. In addition to the above, Gkerekos et al. (2017) also developed a self-learning model for condition monitoring of machinery components using raw physical data collected through measuring campaigns on board vessels. A one-class SVM classifier was developed. In this case model training was based only on observations that were deemed healthy. In the included case study, new data points were considered by the model and the model returned the similarity of new data points to the ones used for training purposes. Given a big-enough and diverse dataset, the suggested methodology can be utilized for machinery condition monitoring.

Li et al. (2016a) also developed an analysis tool that can provide long-term prediction of vertical wave bending moment which impact the ship structural loading and can thus provide information and early warnings for suggested inspection, maintenance and repairs of ships structural components. Accordingly, Li et al. (2016b) suggested a methodology where wave-induced vertical bending moment are estimated based on raw data obtained from onboard tiltmeter units. Both studies provided results which were shown in the developed ship structural DSS tool described in a study by (INCASS, 2014c).

Moreover, following the work performed by Dhillon (2006) who suggests an alternative perspective to design for maintenance and repair under the scope of maintainability, diligent inspection of systems in order to feed observations back to design stage and thus optimize design through this cycle. In this respect, Koch et al. (2016) provide an overview of methods that can be used for automated inspection of ship structures. First, robotic systems, including aerial platforms and magnetic crawlers are described in depth. The data that each platform can collect are discussed along with the relevant data analysis. Finally, data transfer options and data management are discussed. A thorough market survey of tools and strategies available for marine inspections is included in INCASS (2015a). There, the importance of robotic means for access and monitoring for inspection solutions is highlighted. Accordingly, Kolyvas et al. (2015) propose a photogrammetry-based methodology for remote visual inspection of vessels' cargo holds through 3-dimensional models. The suggested methodology aims to reduce the time required for in-situ surveying and lead to more targeted surveys. Photogrammetry applications on board cargo vessels are further discussed by Stentoumis et al. (2016). There, image data are combined

with the data collected from a terrestrial scanner in order to increase the fidelity of 3-dimensional models. In this sense, data collection becomes semi-automatic and can be used as part of several hull-monitoring applications.

Ortiz et al. (2014) present a methodology for the inspection of internal and external vessel spaces through the use of Micro Aerial Vehicles (MAVs). Specifically, this paper focuses on the self-localization algorithm used. Positive results obtained from this application are also included. INCASS (2015b) discusses the processing and analysis of inspection data acquired through robotic means. Specifically, this includes the design of a mosaicking tool that stitches together multiple images captured by robots in order to supply the surveyor with image composites, allowing defects to be displayed in their full extension. Accordingly, environment reconstruction tools based on photogrammetry are included in order to build a 3D model of the inspected area. Additionally, novel defect detection tools that can work with both individual images and image composites are discussed. As the detection tools are based on image saliency, prior defect characterization is not required. Bonnin-Pascual and Ortiz (2014) describe the methodology followed for corrosion detection using automated visual inspection as a data source. In this case, two algorithms based on the combination of weak classifiers are proposed, Weak-classifier Colour-based Corrosion Detector (WCCD) and AdaBoost based Corrosion Detector (ABCD). These are trained to detect areas that present signs of corrosion. While misclassification tests showed comparable results from both algorithms, WCCD presented shorter execution times and better results when qualitatively evaluated.

2.2.3 Design for safety

Almost all existing conventions, rules and guidelines use descriptive language to satisfy the specific requirements of ship design. These requirements are called prescriptive requirements. According to the traditional ship design method, the safety performance of the ship is specified by the prescribed requirements. However, with the development of technology and the emergence of new design concepts, innovative designs that break through the existing prescribed requirements are emerging.

Currently, there are provisions in many IMO conventions for acceptance of alternatives and/or equivalents to prescriptive requirements in many areas of ship design and construction, providing convenience for the implementation of innovative designs. The International Maritime Organization (IMO) Maritime Safety Committee, at its ninety-second session (12 to 21 June 2013), approved the “Guidelines for the Approval of Alternatives and Equivalents as Provided for in Various IMO Instruments” (MSC.1/Circ.1455) (IMO, 2013). One approach to the approval of an alternative and/or equivalent design is to carry out a risk analysis for the alternative and/or equivalent design and compare it to overall risk evaluation criteria, which is called risk-based ship design method.

Risk-based ship design method is to integrate the risk analysis method and reliability analysis method into the design process of ships, which can provide guidance for the novel design. The risk assessment is carried out in the design stage of the ship. Then, the safety level of the alternative and/or equivalent design is compared with the traditional design based on the safety equivalence principle. Safety requirements are no long constraints, but optimization goals in this method.

Since 2014, the study of ship risk has been carried out mainly focusing on the comprehensive risk assessment of collision, grounding, fire, oil spill and other accidents. Research on risk-based ship design is relatively few. Konovessis et al. (2013) detailed a solution by developing a formalized methodology for risk assessment through effective storing and processing of historical data combined with data generated through first-principle approaches. The method should help to generate appropriate risk models in the selected platform (Bayesian networks) which can be employed for decision making at design stage.

Ehlers et al. (2014) suggested that ships transiting ice-covered waters are not designed according to physical measures but according to economic and empirical design measures. They introduced a holistic treatment of the design relevant features and their identification to improve safe Arctic operations and transport, mainly focusing on design relevant Arctic aspects related to extreme and accidental ice events. Noh et al. (2014) proposed a new methodology that combines dynamic process simulation (DPS) and Monte Carlo simulation (MCS) to determine the design pressure of fuel storage tanks on LNG-fueled ships. The combination of MCS with long-term DPS reveals the frequency of the exceedance pressure. The exceedance curve of the pressure provides risk-based information for determining the design pressure based on risk acceptance criteria.

Youssef et al. (2014) presents a Quantitative Risk Assessment (QRA) for double hull oil tankers that have collided with different types of ships. And exceedance curves are established that can be used to define the collision design loads in association with various designs. Zaman et al. (2015) conducted a complete Formal Safety Assessment (FSA) research in the Malacca Strait using AIS as a data resource. Yang et al. (2015) proposed a generic framework of risk-based winterization to facilitate the application of formal method and eliminate some limitations of the formal approach. Results from their article validated the effectiveness and feasibility of using risk-based winterization on vessel designs. Praetorius et al. (2017) presented the findings of a pilot study with the objective to introduce the Functional Resonance Analysis Method (FRAM) as a method to enrich FSA studies through structured expert input. The results of the study show that FRAM has the potential to enrich hazard identification as a complementary tool.

Risk-based design also has a wide range of applications in other areas, such as the civil engineering field. Maes et al. (2015) suggested that various civil engineering fields suffer from a perception that people fail to consider "beyond extreme" scenarios. They distinguished between three broad classes of events: far-out extremes for heavy-tailed hazards, scenarios marked by very unlikely combinations of events (perfect storms), and so-called unknowable unknowns and identified which objectives, which tools, and which risk measures can be used, and which lessons can be learned.

Reliability analysis is capturing the attention of ship designers regarding the structural arrangement, and Joung et al. (2017b) presents a study on the structural reliability and availability analysis, taking into account the uncertainties of material properties, environmental loads, and tolerance in construction, and the economic efficiency. A method to calculate the structure availability was developed based on the estimation of the failure probability for the structure design life. The target failure probability is then obtained by altering the CoV of the involved random variables, and the lifetime span and costs are computed based on the target probability of failure. The obtained CoV can be used as a guideline for the manufacturer.

In conclusion, the risk-based design concept has been gradually accepted in recent years. However, it is still in the development stage and its progress is relatively slow. the current progress and existing problems are as below. Risk-based design methods have attracted the attention of ship designers, and have been applied to the initial design (conceptual design) stage of risk-based design. The quantitative assessment methods and methods to deal with uncertain problems have had a certain development, such as the introduction of Bayesian network method, fuzzy set method and so on. Risk-based ship design methods are used in the design of new ships (e.g. polar ships), but the application is still few in a wider range of vessels' designation. Consideration can be given to the design of vessels such as container ships and LNG ships. The current research is mostly focused on the analysis of individual ship or individual accident scenarios.

3. DESIGN TOOL DEVELOPMENT

Over the last few years, the development of the design tools for marine structures has been characterized by the extension of the software packages functionalities in order to create tools which can be used since the early design phases of a new ship, throughout its entire life. These design tools further integrate several aspects of the design of a ship, such as safety, hazard scenarios and risk assessment, life-cycle maintenance, accident scenarios, and optimization. The analysis of the state-of-the-art scientific literature has shown that integration of these functionalities in the design tools have led to two different approaches in the development of these tools: monolithic software, where the software house develops a single software package which integrates functionalities of other software packages, and modular systems, where the tool developers focus their activity on the improvement of the capabilities of a software package to interact and exchange data with other design tools. Furthermore, this section presents the recent progress on Computer-Aided Design (CAD) packages for ship design, focusing on the new 3D capabilities of this software and on the impact that 3D design is having on the maritime industry. Particular attention is paid to the development of Virtual Reality and its use in ship design. Later, the progress in new simulation packages for ship structural design is presented; in particular, the progress in the risk-based design software tools and in the structural optimization tools is discussed.

3.1 CAD Systems for Naval Architecture

Since the last ISSC Congress, the Computer-Aided Design (CAD) packages for the maritime industry have been reviewed and developed by many authors. The proceedings of ISSC 2012 (Pradillon et al., 2012) presents an overview of the main CAD systems which are widely used in ship design and ship building, and the capabilities of these packages to interface and exchange data with other specialized software packages that are used throughout the design-cycle of new ships. The updates of these packages were presented in the proceedings of ISSC 2015 (Collette et al., 2015), where the authors highlighted the efforts and the advances done by researchers and software developers in the triennium 2012-2015 in high-fidelity simulations and smooth data exchanges between CAD software packages and specialized design tools.

Since the last ISSC, this trend in the development of the CAD software packages has been continued and reinforced. We can divide CAD tools in two main categories: 2D drawing and 3D modeling programs. Several authors focused their research activities on the development of the 3D modeling of CAD software packages for the maritime industry. Larkins et al. (2015) highlighted that the use of a single 3D product model throughout the subsequent design phases of a ship can reduce design errors and production cost. The authors show the advantages that several companies have gained using 3D models not only for subsequent design phases, but also for interdepartmental communication and workflow organization using the Marine Information Model from ShipConstructor Software Inc. (SSI). The advantages of using 3D models are also highlighted by Morais et al. (2015) who use 3D modeling to support the management of welding processes on ships. According to the authors, 3D models provide intuitive visualizations and can be used to improve communication in a process that account for approximately 10% of total cost.

The advantages introduced by 3D modeling in ship design are partially reduced as 3D modeling is a time-consuming activity that requires to build-up a 3D model in the early design phase. In order to overcome this disadvantage, some authors have focused their research activity on the development of interface between different software packages in order to speed-up the creation of 3D models and allow the re-use of the same model in different analysis during the entire design of a ship.

Cabos et al. (2015) developed an interface between NAPA Steel and DNV GL's POSEIDON for model re-use. In particular, the proposed interface allows the designer to interface a CAS system (NAPA Steel) with class rule calculation software (POSEIDON). The authors tested the

new procedure and interfaces in the design of a 14400 TEU and the results of these tests showed a significant increasing in the efficiency of the hull design process decreasing dramatically the efforts for building a global POSEIDON structural model (The Naval Architect, 2015). Lindner et al. (2015) presented a modular system which combines a CAD system with a Product Data Management System (PDM) and allows the designers to create a 3D model used for the concept design of a new ship since the early design phases.

Koelman et al. (2015) developed a design system which interfaces a general purpose CAD system with specific ship design software packages. The system was tested in a pilot case where the internal layout of a ship, and in particular those structural components which are frequently modified during the design process (e.g. bulkheads and deck panels), was designed using the proposed design system. The results showed a reduction in the ship design time and a consistency of the system over the entire process. Moreover, the smooth exchange of data during the entire application implied that no performance degradation was experienced. Even if the authors recognize that this system should be developed more in order to be extensively applied to ship design, they emphasize that coupling dedicated software packages rather than developing monolithic software is a good strategy to improve data exchange among designers.

Building on the concept that big data exchange and efficient creation of 3D models are essential aspect to optimize design quality and reduce design time, several authors have recently developed interfaces and efficient data exchange systems in order to allow different dedicated software packages to collaborate with each other (The Naval Architect, 2016a). Morais et al. (2016) show that open architecture of software packages is the key to making a best-of-breed approach work. Indeed, open architecture of software packages allows the development of interfaces among specialized tools and allow the designers to use best-of-breed applications in each design task. In order to improve the 3D modeling potential of the software 3DEXPERIENCE, Dassault Systemes, class society Bureau Veritas (BV), the Shanghay Merchant Ship Design & Research Institute (SDARI) developed a pilot project where a single 3D model has been created for all the calculation and analysis performed using BV's VeriSTAR calculation tools (The Naval Architect, 2016b). Zagkas and Spanos (2015) present a unified designer-centered workflow between modeling and analysis which allows the designers to create a single 3D CAD model that can be used for structural and hydrodynamic analysis. This workflow simplifies the design phases and allow the designers to effectively use the CFD-based loads in the linear static FE analysis. The integration between CAD modeling and structural FE analysis has been also developed by Stilhammer et al. (2015) presents an integrated user environment for modeling and visualization called HyperWorks and developed by Altair Engineering. Acín and Kostson (2015) present a FEA system (Strand7) which can be used to analyze marine structures. The main innovation presented by this FEA system is the use of a programming interface (API) for the automation of repetitive tasks.

3.2 Virtual Reality and Augmented Reality

Concerning the trends observed during the latest decade, the future of ship industry will inevitably go through the use of Virtual Reality (VR) and Augmented Reality (AR) as key technologies for the design, production and operation of ships (Bertram 2017). Smarter design processes will consider the long-term economic and ecological pressure for energy efficiency. CAD (Computer Aided Design) systems towards 3D PDMs (Product Data Models) allow to perform a large variety of analyses and simulations, and the ship design is nowadays a simulation-based process. As result, simulation, Naval Architecture, and CAD/CAE packages are getting more sophisticated with more accurate geometry representation and more advance physical models.

According to Morais et al. (2017), currently there are two major players using VR in Maritime Industry: the Virtalis and the Techviz. Their main clients in this field are the DSNS (French Navy projects), the Keppel FELS (Offshore builder), the Hyundai Mipo Dockyard (one of the

world's largest shipbuilders), BAE (British Navy projects), the Dalian (Big Chinese shipbuilder), and the Irving and Fleetway (Canadian Navy Project). Immersive VR systems such as big caves or head mounted displays, are only used by companies typically involved in defense or in very large-scale shipbuilding. Smaller companies building workboats, ferries, or yachts use CAD software's associated viewing applications. Although VR is accepted as a future key technology in ship design and shipbuilding, the fact that it has not been more widely adopted demonstrates that there are still serious concerns, particularly in shipbuilding industry. Morais et al. (2017) denote that the main challenges that are still being solved, are related to the lack of perceived benefit vs cost on using this technology, and the need for an up to date 3D model of the ship and ship structures. The solution for the first challenge consists in identifying in which areas does the VR brings real added value to shipbuilding, while for the second, is to make VR a natural extension of CAD and current workflows. This will lead to an increased adoption of VR in Maritime Industry.

A good example of the using these technologies is described by Cabos et al. (2017), where the use VR techniques for remote inspection of the hull and for structural condition assessment, is discussed. Currently, the survey of the hull structure requires the physical presence of a surveyor, however, with the use of upcoming inspection techniques such as drones and self-localizing cameras, opens window for the remote inspections, with lower costs, risks and time spent. In fact, a large portion of the surveyor's activity during the inspection, is related to physically accessing the structure for assessing hull condition. This, generally, is not an easy task due to narrow manholes in double bottom ballast tanks, or quite high elevations in cargo holds, and the accurate reporting of findings on the exact location, requires good orientation skills, for example, when examining a double bottom tank. Furthermore, the physical presence of the surveyor inside cargo or ballast tanks, requires a much more extensive, costly and time-consuming preparation of the structure and inner space, than an inspection performed by a drone or a robot.

Cabos et al. (2017) describe a scenario for remote hull survey performed by an autonomous or remote-controlled drone. The survey planning and preparation is done in office, which includes the identification in a 3D model of the ship, the target structures for the inspection. This will serve as a guide for the scanning task performed on-board by the drone. The spatial inspection data, which includes, geo-referenced photos and eventually measurements of thicknesses, deformations or cracks, is collected and mapped into the 3D model of the ship, which can then be explored by the class surveyor in virtual space using VR capabilities for navigating, orientating and interacting with the data on the virtual model reflecting the actual hull condition. The IRIS system described by Wilken et al. (2015) is mentioned as one of such system which captures (visual) inspection data inside hull compartments.

3.3 Specialized structural simulation packages

Over the last three years, we have noticed an increase interest in the development of specialized software packages for the design of ship structures using specific structural tools. The trend in ship transportation in building larger ships and the development of more advanced rules for class approval increased the request of specialized tools that allow ship designers to an accurate evaluation of loads acting on ship structures and on their response to these loads (Jörg et al. 2016). For these reasons, researchers paid particular attention in the development of new FEA software tools which include multi-physics analysis. Im et al. (2016) and Vladimir et al. (2016) developed a mathematical model, called WhiSp2, which can be used to perform an ultimate strength analysis of the ship structures taking into account slamming induced whipping. They applied the developed method to evaluate the design of a HHI SkyBench TM 19,000TEU ultra large container vessel. The hydro-structural analysis is performed using the code HOMER, while the ultimate bending capacity of the hull girder is evaluated using MARS, both these codes are developed by Bureau Veritas.

Multi-physics simulations for the evaluation of structural elastic response of ships and offshore structures have been also investigated by Ma et al. (2017). They proposed a new numerical coupling model between Smoothed Particle Hydrodynamics (SPH) and Structural Finite Element Method (FEM) in order to evaluate the Fluid Structure Interaction (FSI) behavior. This work complements the outcomes of a previous study developed by the authors on the coupling of SPH with a structure model with nonlinear beam developed to predict the occurrence of structural ringing under green water. The new numerical FSI numerical model allows fast simulations when both GPU acceleration and CPU parallel calculation technique are used. The results of the simulations presented by the authors and validated against experimental data in the case of a 2D beam elastic beam impact problem and this analysis shows the accuracy of the obtained results. Darie and Rörup (2017) developed a tool for the ultimate strength analysis of hull girders. The tool evaluates the load scenario using a hydrodynamic approach based on 3D Rankine method, the calculated loads are then transferred to a global structural FE model which is used to evaluate the ultimate strength ships by nonlinear analysis.

With regards to the Finite Element Analysis, we have noticed an increased interested in the development of automatic procedure for the generation of FE models and in particular in the improvement of the efficiency of the pre-process phase of the FE modeling, i.e. the development of the model geometry and mesh. The primary aim of these research activities is the development of procedure and software tools which speed up the pre-processing phase of FEA, decreasing the overall design cost. Korbetis et al. (2015) developed a method using ANSA preprocessor which allows designers to define multiple models which can serve different simulation analyses. The main advantage of this new tool is the automatic definition of different representations of the ship model according to the FE analysis that will be performed.

Korbetis et al. (2017) presented the new solver EPILYSIS for Finite Element Analysis (FEA), as the new product of the BETA CAE Systems software suite. In the paper, the authors describe two representative applications of the solver: the determination of maximum stresses and critical areas of a typical VLCC vessel subjected to three different loading conditions, and the analysis of a nonlinear-contact strength for a ship's rudder. Models' setup is conducted with the aid of the ANSA pre-processor, which generates detailed Finite Element models of the hull structures, complying with the meshing requirements of the Classification Societies. The results produced by the EPILYSIS are compared with a commercial FEA software using the META post-processor. Conclusions highlight the absolute coincidence between solvers regarding the deformation of the structure and the similar stress results for quadratic mesh elements. However, for triangular elements there is a much higher divergence. The authors also highlight the high performance of EPILYSIS, namely when the computation is parallelized.

Acín and Kostson (2015) presented some of the tools of FE analysis system (Strand 7) that can be used to automate repetitive tasks in FE structural analysis. The system presents a programming interface (API) that be used through most of the traditional programming language or development environment. Auto-modeling tools and procedures are also required by shipyards and ship designers of bulk carriers and tankers. The Harmonized Common Structural Rules (CSR-H) have been effective since July 1, 2015. The new rules have increased the required FE modeling of tankers and bulk carriers, since the FE model has to simulate the Fore and Aft parts of a ship, in addition to the midship part. Moreover, the mandatory areas for fine mesh analysis are also increased. This has affected the ship design, increasing the man-hours needed to perform the structural design and increasing the design cost of shipbuilders (Shibasaki, 2016). Myeong-jo et al. (2016) presented an auto-modeling tool which generates longitudinal FE models automatically using cross-section models for prescriptive rules analysis. They also introduced Auto-FE-Modeling which automatically generates FE models of ship structures, based on 3D CAD models. These tools are included in SeaTrust-HullScan, software tool developed by the Korean Register (KR).

The design of ship and offshore structures is characterized by a high level of uncertainty related to the shape of the structures, e.g. welding deformation, effect of misalignments, corrosion wastage). In order to evaluate the effect of the randomness of input parameters on the response of ship and offshore structures, designers and researchers usually use Monte Carlo Methods (MCM) combined with FE analysis. This method, called Stochastic Finite Element Method (SFEM), is often computational costly. In order to overcome this issue, Chen at al. (2016) developed an SFEM based on the Stochastic Response Surface Methods (SRSM) developed by Ghanem and Spanos (1991) that use Polynomial Chaos Expansions (PCE) instead of MCM. Chen et al. (2016) validated the new SFEM tool benchmarking the results of the methodology formulated for a 2D problem with the results obtained using MCM.

Some specialized software package may improve the structural design and the construction process. The developments in numerical methods have enabled simulations to reach the stage where it can solve an increasing number of problems that interest the shipbuilding and offshore industry. Caprace et. al (2017) proposed a benchmark study to understand the influence of the modeler's practice and FEM codes on the welding simulation outcomes. Results of various thermo- mechanical simulation models are confronted to the experimental results developed in ANSYS, SYSWELD, VIRFAC, and ABACUS. Although computational efficiency is a critical limitation of the application of computation welding mechanics (CWM) simulation to large structures, it is evident that welding simulation is quite successful in predicting welding distortion and residual stresses.

Several authors have recently developed procedures and tool to evaluate the structural response of ships and offshore structures subject to impacts. These analyses are usually performed using FE explicit non-linear general purpose software, such as LS-DYNA, ABAQUS, DYTRAN, NASTRAN, ANSYS. The high computational cost of these simulations trigged research activities aimed at the development of tools based on analytical methods that allow the estimation of forces and energy developed in ship collisions and allow the designers to select the worst crash scenario in a preliminary analysis. In this context, Principia and ICAM (Institut Catholique d'Arts et Métiers) developed the SHARP tool (Paboeuf et al., 2015). This tool is based on super-element method and allows the evaluation of crushing resistance of the impacted substructures, with respect to the penetration of the striking ship. The main advantage of SHARP is that it allows a fast evaluation of different collision scenarios. This allows the designer to identify the worst collision scenarios and to perform explicit FE nonlinear analysis on the selected case. More recently, Pire et al. (2017) developed an analytical simplified algorithm which allows the estimation of crushing forces and impact energy in an impact between ships and offshore structures. Yuan et al. (2017) also focused their activity on the development of a simplified method that take into account fluid inertia forces and fluid damping forces for the analysis of ship collisions.

3.4 Risk-based design software tools

In the European research field, ship safety research focused on the EU SAFEDOR project. Kaneko proposed for the ship risk assessment of the overall approach in 2002 and outlined the risk modeling methods in 2007. After years of development, the risk analysis method and reliability analysis methods has played a role in the design of ships, the alternative and/or equivalent design, and the development of regulations and specifications. The Safety Level Approach (SLA) is a risk-based approach, aimed at establishing a uniform risk level for ships and determining the risk level of existing rules. The safety objectives of ships are expressed in a risk-level way. In the case of risk-based ship design method, SLA can be used to develop safety objectives expressed in the form of risk.

Formal Safety Assessment (FSA) is an important tool for risk analysis and is of great importance for SLA and risk-based ship design. FSA method can evaluate the safety level of the existing rules and the cost-benefit ratio of the risk control measures required by the existing

rules. One of the most important contributions of the FSA is to determine the risk acceptance criteria using the ALARP principle and conduct a comprehensive evaluation of the cost-benefit ratio to achieve the goal of adjusting the safety level. It is necessary to establish a complete risk assessment framework for ship accident to support risk-based ship design. Moreover, the risk-based ship design process has not yet formed a mature process framework.

3.4.1 Software Platform

Considering risk indicators as a standard of structural safety, it is necessary to carry out a risk assessment of the structure and to define a safety objective and a functional objective. According to the "Guidelines for the Approval of Alternatives and Equivalents as Provided for in Various IMO Instruments" (IMO, 2013), the main process of alternative and/or equivalent designs is as following:

- Preliminary design,
- Preliminary design analysis,
- Preliminary design approval,
- Final design,
- Final design analysis,
- Final design approval.

SLA can be used to develop safety objectives which are expressed in form of risk and FSA can play the role of a risk decision tool in the alternative and/or equivalent designs framework, the alternative and/or equivalent designs processes are shown in Figure 3.

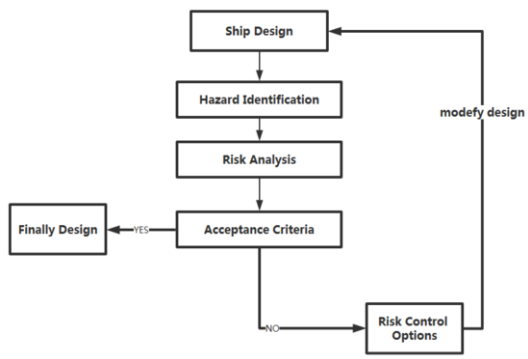

Figure 3: Risk - based ship design flow chart

The components of the software platform can be built based on formal safety assessment (FSA) software, including hazard identification tools and risk assessment tools. The function of the software platform can be mainly designed to provide assistance for the "Preliminary design analysis" process and "Final design analysis" process. The main function is to conduct safety assessments and verify whether the design ship will meet the risk acceptance criteria. In addition, the platform will put forward risk control options (i.e., improvements to preliminary design) to provide assistance in order to revise the preliminary design.

3.4.2 Hazard Identification Tools and Risk Assessment Tools

Regarding risk identification, lots of commercial software is available in the field of marine engineering, including PHA-Pro, Kyrass, Sabaton. These safety management software packages can be directly transferred from marine engineering to ship design and perform the same role in safety assessment. Hazard identification tools are designed to identify dangerous scenarios for the designed ships. For example, Sabaton is a software tool that supports Failure Mode and Effects Analysis (FMEA) and failure mode and hazard analysis. The results of the

analysis are generally applied to design improvements to eliminate system failures or to mitigate component failure.

With regards to risk assessment, the software is divided into two categories: the first one is related to generic modeling tools, such as CARA-FaultTree for fault tree construction and analysis, and PDAT-Plus and Hugin for bayesian network construction and quantification. The second one is dedicated to a specific type of accident. This kind of software is more widely used in the field of marine engineering, such as ASAP, COLLIDE and son on. In the field of ship engineering, such software tools are much less, among which the CARCAT tool is the most perfect one.

The risk assessment tools are designed for the second step of a FSA process, determining the possibility and severity of the risk for the preliminary design, and comparing it with the risk acceptance criteria. The software CARCAT is a comprehensive tool with a full range of functions to assess risk and analyze the frequency and consequences of ship collision and grounding accidents.

3.5 Optimization Tools

The reports presented by the ISSC IV.2 – Design Methods committee at ISSC 2012 and ISSC 2015 Congresses presented a thorough analysis of the development of optimization methods and tools for the design, production, and life cycle management of ships. Both the reports emphasized the key role of these methods and tools in the design phases of a ship, as well as during ship operations where they are used as decision support tools to find out best alternative for ship repair tasks. Indeed, given the complexity of ships' structures and engineering systems installed on-board, the application of optimization methods to ship design and life cycle management can sensibly reduce costs without affecting vessels' safety and functionality.

Over the last three years, we have observed that these methods and tools have been developed further. This section presents the last developments of the optimization tools. Lee et al. (2015) presented a framework for optimal design of sub-structures of floating-type offshore wind turbine to be used in the early design phases. This framework is based on the neuro-response surface method (NRSM) and is composed of three parts: the definition of the geometry, the generation of the design space, and an optimization process. The authors tested the effectiveness of this method in the design of a 5MW TLP-type wind turbine. Yang et al. (2015) developed a robust design optimization (RDO) framework for the design of the supporting structures of offshore wind turbines. They applied the developed methodology to the case of a 5MW offshore wind turbine including in the analysis the metamodel technology with Kriging model in order to replace the time consuming finite element models for dynamic response analysis. The outcomes obtained applying this methodology where compared with the results of a Deterministic Optimization (DO) showing that the reliability of constraints in RDO was much higher than in DO and this implies that RDO is reliable even under the influence of uncertainties.

Pillai et al. (2016) also focused their research activity on the development of optimization tools for the optimization of offshore wind farms. In their study, they implemented a modular framework which uses a discrete genetic algorithm. The methodology takes a holistic approach to optimize turbine placement and intra-array cable network while minimizing the cost of energy. Kolios et al. (2016) extended the widely used Techniques for Order of Preference by Similarity to Ideal Solution (TOPSIS) method in order to take into account stochastic inputs. They implemented the proposed methodology in a numerical tool and they used the tool in the decision analysis of an offshore wind turbine support structures.

With regards to the development of optimization tools for the design of ship structures, over the last three years we have noticed that researchers have focused their activity on the implementation of tools which perform the optimization of structures in order to reduce the amount

of FE analysis, tools for multidisciplinary optimization, and tools for ship shape and size optimization. Romanoff et al. (2016) presented a review of the development of a direct analysis approach which uses homogenization, finite element method and optimization. The homogenization is used to transform an originally periodic, stiffened plate or web-frame structure to an equivalent single layer (ESL) plate or beam structure, respectively. This speeded up the FE analysis and allowed the modeling of the stiffness and mass of complex structures accurately. Koroglu et al. (2016) implemented a procedure for the optimization of large ship structures using surrogate models. The procedure uses surrogate models which overcome the curse of dimensionality by a special decomposition method. The effectiveness of this procedure has been tested in three test structures and the outcomes showed the benefits of this procedure, including automatic design creation and optimization, effective usage of stream processors and model reuse.

The impact of the IACS H-CSR on the design of oil tankers and bulk carriers is discussed more in detail in Chapter 6. In this section, we want to highlight the fact that the entrance into force of these harmonized rules has drastically increased the amount of direct analysis of ship structures. Moreover, the structural design according to these new rules require the utilization of an integrated design system. Andric et al. (2016) developed a formal optimization procedure for the structural design of ships according to H-CSR rules. The procedure was implemented in a structural design system, called OCTOPUS-CSR which can be used in the concept and preliminary design phase. The authors tested the new tool in the design of new bulk carriers to be built in ULIANIK group shipyards, and they showed the efficiency of this tool in controlling structural scantling while reducing ship production cost. Kim et al. (2017) developed a multi-objective full optimization technique for the optimum design of hull structural scantling for merchant cargo ships that are modelled by plate-shell FE. The technique developed by the authors is applied to the structural scantling of a very large crude oil carrier (VLCC). They presented that using this procedure they are able to satisfy the strength requirements of the H-CSR.

With regards to multidisciplinary optimization, Stone and McNatt (2017) show how the integrated hydrodynamic and 3D finite element code MAESTRO can be used for the evaluation of the design loads, the structural response, working stresses, limit state evaluation, hull girder ultimate strength evaluation and structural optimization. In the paper, they optimized the cross section of a frigate minimizing the structural weight and maximizing the structural safety.

Optimization of hull size and shape has been investigated by Sugita and Suzuki (2016) who developed an algorithm for the optimization of hull sizing. In their study, the authors modeled this problem including a range of design criteria and an objective function which had to be minimized. The outcomes of their calculations were compared with the results obtained using the commercial software (DNV Sesam). Kragic et al. (2016) implemented a reduced parameter set parameterization method based on integral B-spline surface capable of both shape and topology variations. The authors applied this method in a multidisciplinary ship hull optimization workflow which integrated shape parameterization with hydrodynamic, structural and geometry analysis tools.

4. OFFSHORE STRUCTURES

4.1 Introduction

Exploration and exploitation of ocean-based resources such as oil, gas, renewable energies, seabed minerals or offshore food farming (fish or algae) has historically been the major driver for the development of offshore structures. A crude definition of an offshore structure is that of a structure or unit without permanent access to dry land, often required to stay in position performing its mission at an offshore location. Many diverse types of offshore structures exist and its classification is, to some extent, in the eye of the beholder. A reasonable first distinction may be made between fixed and floating offshore structures, from which one may intuitively derive that the latter structures are used floating either moored to the seabed or dynamically positioned,

and the former structures are fixed to the seabed. Bottom founded offshore structures are steel jackets (with which the development of the offshore industry commenced), steel compliant towers or concrete gravity based structures (GBS). Spar platforms, tension leg platforms (TLP), semi-submersibles or ship-shaped (e.g. floating, production, storage and offloading (FPSO) units) units are examples of floating offshore structures.

Several aspects drive the option to employ one or another type of offshore structure. Water depth is certainly the main driver to depart from a fixed to a floating structure solution. Size and form are, in addition to water depth, determined by a variety of factors such as mission/function and associated requirements and environmental conditions. For instance, the same type of floating offshore unit will differ significantly when designed for oil and gas exploration (e.g. drillship or drilling semi-submersible) or for oil and gas production (e.g. FPSO, production semi-submersible); differences are even more pronounced for a certain type of offshore structure designed for different market segments, as for instance an oil and gas drilling jack-up vs. an offshore windmill installation jack-up. Function also allows distinguishing mobile offshore structures, units that are able to move from one location to the other to perform its task. These also come in different shapes and sizes and can work in a floating condition or supported at the seabed (e.g. jack-ups).

Despite sharing common ground in terms of design methodology, the particulars of each different design together with a strong dependency on previous specific experience lead to addressing design and associated methods separately for different types of offshore structures. Given the numerous types of offshore structures and its different purposes, book or textbook references addressing its design, and its structural design in particular, are equally spread as it is difficult and impractical to cover all in a single reference. This is shown in the paragraphs below where the Committee reviews books published on the subject of offshore structures design during the period covered by the current Committee's work.

The second edition of Bai and Jin (2016) aims to cover the latest developments in design codes, engineering practices and research in the field of marine structures. Several chapters are dedicated to offshore structures and despite the main focus being offshore ship-shaped structures, other types are also addressed. This new edition includes a noteworthy new chapter entirely dedicated to offshore fixed platforms and FPSOs, dealing with risk and reliability and asset integrity management considerations.

El-Reedy (2015) is a recent book publication allocating the focus wholly on fixed offshore structures and setting out to stand as a guide on structural design calculations pertaining to fixed offshore platforms, achieving this by systematically going through case studies and worked examples. Useful information on theory, principles, practices and design codes is also included supporting main goal of a more practical design guide. The book contains a whole chapter where a step by step guide covering the procedure for using software for the structural design and calculations of an offshore structure, which albeit being written for a specific software (SACS) may support the same procedure using other software tools. Another recently published book devoted to fixed offshore structures is Chandrasekaran and Jain (2017), which addresses the concepts of material selection, environmental loads, choice of structural form, construction and repair methodologies, structural health monitoring and rehabilitation of ocean structures.

Following the theoretical background provided in Part 1 of the Handbook of Bottom Founded Offshore Structures, the work of Vugts and Zandwijk (2016) presents various aspects of the fixed offshore steel structures during their full life cycle. All aspects from conceptual design, construction, installation, operation and structural integrity management to their eventual decommissioning and removal are covered in this handbook. Their study contains two chapters devoted to specific structure types – jack-ups and compliant bottom founded structures – where

their particulars are treated from an introductory/overview level to detail structural design challenges. Overall this handbook stands as a solid, comprehensive reference for both students as well as practicing offshore engineers.

Chandrasekaran (2015) and Chandrasekaran (2016) are references targeting mainly offshore oil and gas structures. Both explain the fundamentals and advanced concepts concerning the design of the various types of offshore platforms and outline the different stages of marine structure analysis and design. The former focuses and elaborates on the integration of the concepts of structural dynamics with the FORM-evolved design of offshore structures. A structural engineering perspective drives the material of the latter reference, at the price of some neglect for other design aspects. However, the structural focus is the deliberate goal of the book, and in this sense, it serves is purpose as a useful complementary reference, for students or practitioners.

The encyclopedia of maritime and offshore engineering is a reference work covering the design, construction and operation of ships, offshore installations and other marine structures used for transportation, exploration and exploitation of ocean-based resources including oil, gas and renewable energy. It contains a volume devoted to offshore technology and structures, in which are included chapters dedicated to specific offshore structures, such as fixed, floating or jack-ups. For all topics covered this reference elaborates on all disciplines and aspects of the design of the structures, also including operational and regulatory considerations. Carlton et al. (2017) is a wide-ranging, up to date asset for anyone partaking in the life cycle of an offshore structure, a valuable addition to the library of any student or professional.

4.2 Design Methodology in Offshore Structures Design

Offshore structures design is, as in the case of ship design, an ad-hoc process, in the sense that all design considerations and the multiple engineering disciplines convene to a solution focused on the intended mission or function for the structure/unit. For this purpose, the design methodology used for offshore structures is intrinsically a holistic approach where the successful coordination of multiple technical and non-technical factors is the key to effectively arrive at the envisioned solution. All elements partaking in design are intimately interconnected, affect one another and ultimately the overall goal (mission performance). An illustrative example of this is given in Mendonça Santos and Alves (2016), where the authors describe the impact of stability considerations for a drillship on load carrying capacity and motions, then affecting structural design and its output, possibly influencing other aspects such as installed power and fuel consumption and following performance items like speed and station-keeping; all ultimately affecting cost and the overall design goal.

In essence, the design of an offshore structure/unit is hence always Design for X (DfX) multi-objective problem in which specific important performance indicators and properties are dealt with concurrently. In the context of offshore structures some of these design objectives stand out: design for operations and efficiency (mission), design for safety, design for environment, design for cost, design for maintenance and design for production. Irrefutably market and economic conditions dictate, at a certain point in time, the weight allocated to the different X's in the design process, though under no circumstances will any of these main factors be left unattended. For instance, as design for cost gains more weight due to economic reasons, design for operations and efficiency will remain as the primal goal, more attention will be paid to the design for production and maintenance but it is likely no compromises are allowed considering design for safety and environment. This fact has the positive effect of always pushing development and challenging the design of offshore structures.

4.3 Design Challenges, Progress & Trends

During the period covered by the 20th ISSC the offshore industry continued experiencing a downturn driven by low oil prices, market uncertainty and as a result severe cutbacks in capital

expenditure by oil and gas companies. This has had a profound impact in the oil & gas and related segments (e.g. construction, support, etc.) and imposed new challenges and a rethinking of priorities as far as design is concerned. As mentioned by Anderson and Pickup (2017), this downturn has forced leaner cost structures, flatter organizations and is pushing for more efficient designs that will structurally lower the cost of development.

The shift of focus to cost adjusting to the new low oil price environment lead to significant changes to the paradigm of offshore structures/units design. None has been more impacted than the deepwater sector, as the challenges of water depth, remoteness from existing infrastructure and exposure to extreme environmental conditions render deepwater facilities "one-of-a-kind" designs, representing high complexity and high cost developments. Khurana et al. (2017) present the transcript of an industry panel discussion on the "lower for longer" oil price scenario highlighting design optimization and standardization as key innovations and design approaches for successfully achieving cost reduction for offshore project developments.

4.3.1 Standardization

A strategy of standardization and repetition is viewed as a promising opportunity for improving cost efficiency going forward, a point made by Hodapp et al. (2017) before discussing a design standardization for a floating production semi-submersible and pointing out some key elements believed necessary in achieving cost effectiveness through standardization: repetition of proven design vs. complex one-off design, scalability of the design for different demands, use of common design standards and specifications, use of standardized materials, equipment, fabrication and installation plans.

Standardization, including that of design, is a very noticeable trend and a subject of many publications by various authors, with a perceivable emphasis on the offshore floating production sector. Jung et al. (2017) describe the standardization of a FPSO hull going through design procedures dealing with establishing design basis, hull configuration, tank arrangement and structural scantlings for the midship section. A standardized and simplified production semi-submersible for marginal offshore field production is presented by Pallanich (2017), highlighting the effect of employing a proven hull design, an open truss deck forgiving with late equipment deliveries from fabrication and the importance of embracing a "going back to basics" in terms of design specification.

Tanaka and Takano (2017) address the challenges of applying a standard design for a FPSO solution and the authors propose a modular design and construction concept coping with those issues. Particular attention is given to modularizing structural design, methods and calculations employed to customize the FPSO hull and topside modules are described comprehensively. Other design considerations, such as hull form design, and used tools and methods are also covered therein. Example of success of implementation of standardization and related cost reduction on FPSO projects are addressed in Portella and de Souza Lima (2016), underlining design standardization as fundamental to improve construction productivity and cost reduction, and providing in depth considerations regarding the related structural design and analyses. Origins of these standard FPSOs can be found in de Andrade et al. (2015). Based on this experience, Nunes et al. (2016) discuss a study on its application on larger capacity FPSOs.

Tippee (2017) reports on a standardization JIP involving shipyard and classification societies aiming at improving design and construction efficiencies of offshore oil and gas installations. Details of this offshore standardization JIP are given in Lee et al. (2017), where insights into material, design, procedures and equipment standardization are presented and a methodology to pursue it is proposed. Wyllie, Newport and Mastrangelo (2017) give an owner and operator perspective on the benefits and limits of FPSO standardization, by reviewing different standardization approaches, looking back at previous examples and based on the design and operational experience suggest guidance on the achievable extent of standardization.

Classification societies have joined offshore industry efforts in reducing development costs, Benyessaad, Barras and Rocha (2017a, 2017b) propose solutions, such as the involvement of class from early stages of design and projects or embracing new technologies for maintenance, to the effect of cost reduction without compromising safety. The standardization trend is not exclusive to the deepwater sector, this focus on repeatability and optimization towards cost efficient designs is also being applied to fixed offshore structures. An example of the application of the "design once, build many" approach to the design of offshore platforms was presented by Gill and Henzell (2017), where the authors discuss the scalability, modularity and time and cost efficiency gains of such design approach.

4.3.2 Oil & Gas E&P Counter Cycle

Despite the fact that standardization has also been a recurring theme in the oil and gas exploration sector, here focus appears to be directed at specifications, requirements and procedures rather than standard designs. For instance, after a buildup of the drilling fleet with many units resembling one another, owners have recently pushed introducing unique designs and features for existing and future units so to differentiate themselves from the competition. Some design developments have been published following this set challenge of innovating and differentiating while keeping a tight leash on cost.

An example of this is the innovative drillship moonpool designed by Hendriks, Claassen and Chalkias (2015), targeting to reduce moonpool sloshing, increase safety onboard and reduced resistance and fuel consumption. Developed by extensive CFD analysis and later model testing, the new shape presents introduce new structural challenges overcome by also extensive finite element analysis and a design optimization in view of constructability. Hendriks et al. (2017) have proposed a transverse moonpool design which results in a reduction of hull cross section and structural integrity was verified by finite element analysis. Both the aforementioned references are also examples of a trend to incorporate CFD in early design stages with the purpose of shape optimization and as new unconventional shapes arise, so do the associated structural challenges. Other studies supporting this trend can be found in Darvishzadeh and Sari (2015) and Kim et al. (2015) both discussing the applications of CFD in offshore engineering. Scherl and Sodomaco (2016) is yet another example of a proposal for drillship with a double moonpool arrangement where the authors showcase the interaction between CFD and structural analysis in the design process. Relevant work on the derivation of hydrodynamic pressures acting on moonpool structures has been done by Rezende and Barcarolo (2017), who drew a methodology employing CFD analysis for that purpose. These results have a direct impact on the structural design and analysis of moonpool structures as this work has certainly been input to related Bureau Veritas rules and guidelines on the subject. Kim et al. (2016) presented a study on the strength and fatigue assessment of extended bilge keels for FPSO or FLNG units also using CFD in early stages of design.

It is recognized that the oil and gas exploration (drilling) and production markets are somewhat counter-cyclical, having its up and downturns out of phase. In the current low oil price status, exploration is on a downturn and operators are focusing on production and as a result attention has been more directed at production assets and consequently much research and design work has been dedicated to production units, such as the description of the design and fabrication process of the world's deepest production FPSO given by Moore et al. (2017).

A new shaped TLP to meet current cost reduction pressure was proposed and described by Zou (2016). The authors go about the several design tasks and compare the results for this new design with those of a conventional shape one and claim, amongst other things, it has more efficient structural design based on gains of reduced hull split forces and shear forces the structure is subject to. Kim and Jang (2016) document a global optimization method used for the preliminary design of a TLP using a simulated annealing algorithm that automatically controls

the overall processes of modelling and assessment. More details on the application of this optimization algorithms to the design of TLP can be found in Kim and Jang (2016).

Antony et al. (2015) discuss the key drivers, constraints and criteria considered in the design of a spar platform. The authors document many aspects of the design process from early stages to final installation of the unit. Taylor et al. (2015) describe the design of a production semisubmersible based on a "one size fits most" philosophy which allegedly allows faster and less costly delivery schedules. Tian et al. (2017) discuss the hull sizing process of a proprietary semisubmersible production unit design by employing a methodology that allows generating a very large number of hull configurations then subject to a optimization routine to derive a final solution. The authors present quite some detail on the input used in the method including that of weight estimation.

The design philosophy behind a new light weight semisubmersible concept was presented by Wang et al. (2017), extensively documenting the hull structural design and analyses performed up to a FEED level on this 3 column production unit up. A tapered column deep draft production semisubmersible concept was proposed by Ye et al. (2017), featuring variable cross section columns in view of optimizing the wave force cancelation effects of conventional semisubmersible units. Covering many aspects of the novel design the authors present results from the global strength analysis confirming the feasibility of the concept. In line with the production assets focus Moe and Laranjinha (2017) take a different perspective and rather than considering a new solution the authors look into the converting distressed semi-submersible drilling units to floating production units. The authors outline a design methodology for this purpose, covering, amongst other things, technical requirement for the necessary structural modifications and upgrades.

Already on a growth path, liquefied natural gas (LNG) solutions have gained a boost in interest from the pressure of cost reduction throughout the industry as a cheaper alternative to common fuels with benefits of lower emissions. As a result several publications on LNG applications have been noted, such as, for example, the cylindrical FLNG unit proposed by Odeskaug (2015), the holistic approach to design and operate FLNGs by, Kheireddine et al. (2016) of DNV-GL, the article by Talib and Germinder (2016) covering the development of innovative FLNG solutions with considerations on the entire offshore-nearshore chain or the concept FLNG semi-submersible presented by Zou (2017). Vieira et al. (2016) present a comprehensive approach to the design of FLNG structures referred to as a synthesis approach which is based on considering many design aspects at an early stage, generating a large number of candidate solutions then used to make design choices towards an optimal solution.

4.3.3 Asset Integrity & Maintenance

The current low oil price environment has led to less exploration expenditure and oil and gas operators weigh their interest on production. A direct consequence of this is an increased focus on the existing installations, and the vast majority of the world's oil and gas facilities are mature assets, as mentioned by Haïdar (2016), who reports results from an industry survey showing that over 50% of the platforms are reaching or exceeding their design life. Asset integrity, life extension and maintenance have thus come to the center stage and much publications related to these subjects have been noticed. As noted by Rosen et al. (2016) the most cost-effective solution for producing assets in a low oil price environment is extending the life of the ageing structures past their original design life.

Boutrot et al. (2017a), (2017b) describes a methodology developed by Bureau Veritas for engineering reassessment of aging offshore units focusing on the two main degradation mechanisms: corrosion and fatigue. The use of a digital twin, its interface with conventional hydrodynamic and structural analysis and condition assessment calculations to build up a risk-based inspection program are some of the topics addressed. This work follows that of Boutrot and Legregeois (2016). Liu et al. (2016) presents the ABS class approach life extensions of floating

production units, covering procedures and requirements for the related structural analyses of different types of units. Lloyds Register has developed a new cloud-based software with a target of 40% reduction in maintenance as well as operational expenditures for offshore assets, as reported by Leon (2017), another example of the growing employment of digitalization in this field. Moir (2016) presents an example of how an online monitoring system helped assessing the integrity of a North Sea platform. Lessons learned from a case study of an online asset integrity system is described by Wallace and Champlin (2016), highlighting the benefits of having accurate real-time data in place for managing the integrity of offshore assets.

A joint industry project was created on hull inspection techniques and strategy responding to the increased interest by owners of floating offshore assets designed to keep station for extended periods of time, e.g. FPSOs or drilling rigs. The goals and several pilot projects of this JIP are described by Constantinis (2017).

Gallagher and Rush (2016a), (2016b) describes a methodology and considerations for performing an early stage life extension assessment for offshore floating facilities and stressing that such assessment should be holistic, considering all aspects of the facility, not just an analytical assessment of hull strength/fatigue and moorings, Then followed by a general overview of design and construction decisions helping the planning and execution of a structural integrity management program while improving the long term structural integrity performance of offshore floating structures. Wisch and Spong (2016) present a recommended practice for structural integrity management of floating offshore structured, a draft of what may become a common use API document in the future.

Kemp (2016) describes the development and implementation of a risk based integrity management system applied to ageing production facilities and how this facilitated the process of life extension of the structures. Mat Soom et al. (2016) established a methodology for reliability-base design and assessment for ageing fixed offshore structures, applied to structural safety and integrity management, and having looking into the uncertainties of determining the probability of failure of the structures for its remaining service life. Agusta et al. (2017) formulated a decision theoretical basis for inspection planning of offshore structures based on Bayesian decision theory and Value of Information analysis. To illustrate the Value of Information based inspection planning approach the authors looked into an asset integrity management example concerning one fatigue hot spot for which optimal inspection and repair times were determined. Brief notes on further research and extension of the approach are also referenced therein.

Albright Jr (2017) notes the advances in drone technology and the increased interest by operators to include them as tools for inspection and maintenance of their offshore assets. The author discusses the particular problem of handling the process of data transfer, ingestion, storage and access, named “drone data dilemma”, in that scenario. On a similar topic Boman (2017) reports on ongoing progress in exploiting big data to create digital twins of oil and gas facilities and showcase on example pilot project of such technology driving costs down and increasing productivity on a drilling unit. Moir (2017) discusses the advantages of employing unmanned aerial vehicles (UAV) or drones for the inspection of offshore units. The ability to provide high definition imagery, video and thermal data for both general visual and close visual inspections with minimal interference with the unit’s operation and keeping humans out of the harm’s way make drones and effective, efficient and safe alternative to current inspection methods.

Applicable to asset integrity and maintenance of offshore structures is the study of Kefal and Oterkus (2017) that investigates the applicability of a new state-of-the-art methodology, called inverse Finite Element serving a structural health monitoring system providing real-time structural feedback on displacement and stress monitoring of offshore structures. Requirements on the design life of offshore structures are being pressed beyond the 20-25 years as existing installations are pushed to produce for longer than originally designed for. Acknowledging this fact Hernæs and Aas (2015) discuss an alternative approach to a longer design life, therein a 50

year span is considered, proposing a maintenance based design in which the structure and equipment would be continuously condition monitored allowing uninterrupted assessment of the remaining life of the assets. Canny (2016) presents an innovative approach to conduct well intervention and workover operations on platforms with limited structural capacity, the latter not being exclusive to aged facilities operating past their design life but rather a common challenge faced with smaller offshore platforms with wells drilled by jack-ups.

Current low oil price economics adversely affect the construction market as new build ventures are considered less favorable by operators. Still some relevant work related to construction is of noteworthy mentioned, such as the methodology development of modeling and simulation techniques for erection of modular construction of offshore platforms by Seo and Kim (2015). This methodology makes use of 3D laser scanning measurement data, a technology and technique also referred by Greeson and Waller (2016) as key to achieve accurate dimensional control in construction but also in a variety of offshore projects including setting of equipment, damage assessments, modification, refurbishment, and integration of structure, piping, and other components. Dai et al. (2015) proposed utilizing a heuristic genetic algorithm approach for offshore structures construction spatial scheduling taking into account uncertainties. Beckman (2016) reports on how the use of an integrated data system assisted and eased the construction process of offshore fixed platforms.

4.3.4 Design & Methodology Developments

The offshore industry is ever evolving and new structure types and shapes are being developed to either optimize existing solutions or to serve novel purposes (e.g. offshore renewables, food farming or seabed mining) and thus always pushing the development of offshore structural design. This report intentionally does not account for developments in offshore renewables which are covered by the work of Committee V.4. The offshore industry has seen a renovated interest in deep sea mining translating into publications of recent projects such as Chopra (2016) discussing the methodology and challenges faced during the design of the claimed first seabed mining vessel project. Starting with an overview of major milestones on deep sea mining projects of the 70's and 80's, Knodt et al. (2016) discuss the technology transfer between deepwater drilling and deep sea mining and present the state of the art engineering and technology developments applied therein. The authors also touch upon ongoing and upcoming deep sea mining research projects.

Aquaculture is another sector that has gained significant interest over the last years and a lot of research and development efforts are being made to move fish farming offshore. Following this new design solutions are being proposed, such as the ship-shaped and semi-submersible concepts presented by Lin et al. (2017) and Lin and Ong (2017) respectively. Both articles note structural design as a major challenge as a result of the departure from regular shapes and stress the need for further work and research to address it. Buck and Langan (2017) collect several publications on the subject of offshore aquaculture in which developments and projects are presented and considerations are made on structures for open sea aquaculture. Jack-up structures continue to stand as a significant and relevant work horse of the offshore oil & gas industry and its use in offshore wind turbine installation and maintenance has contributed to a continued interest and associated research and development on this type of structures.

Recurring topics are those associated with the design of spudcans and foundation analysis, as with installation and relocation operations. Zhang et al. (2015) propose a novel design aiming at improving foundation performance looking at global bearing capacity, spudcan fixity and resistance against punch-through. Lee et al. (2015) also look into novel spudcan shapes though the focus herein is on punch-through issues. Zhang et al. (2015) review the semi-analytical and numerical methods used in spudcan penetration analysis, by using large deformation finite element analyses and comparing it to experimental results the authors examine the existing guideline methods for penetration analysis. Fallah et al. (2015) used a probabilistic Eulerian finite

element analysis to estimate spudcan penetration then compared with measured data and claiming the introduced method can produce reasonable prediction of spudcan penetration considering the uncertainties involved in the problem. A 3D large deformation analysis is also used by Zhang et al. (2015) concerning structural analysis required in jack-up reinstallation processes. Tho et al. (2015) present a case study of spudcan re-penetration analysis also using a large deformation finite element approach. Tho et al. (2015) compare coupled and decoupled approaches to interaction problems between jack-ups spudcans and the adjacent platform piles.

Tian et al. (2016) proposed an alternative numerical method to investigate the combined loading failure envelopes of jack-up foundations in soil. Skau et al. (2015) present a numerical study showing how non-linear hysteretic foundation behavior may significantly affect the overall dynamic behavior of jack-ups in extreme conditions when compared to that with a linearized foundation model currently standing as industry practice. The authors make aware that generalization of the presented analysis procedure to all jack-ups and conditions may not be applicable, suggesting the need to extend the study to broader set of units and conditions.

A procedure for establishing non-linear stress-strain relationships to be used as input to finite element analyses of jack-up footings was presented by Jostad et al. (2015), calculating non-linear load-displacement relationships (foundation stiffness', which play an important role on dynamic behavior and structural utilization of jack-up platforms) of the individual footings are then divided into cyclic and total (average plus cyclic) components to be used as input to the dynamic and quasi-static structural analyses of the jack-up. The authors compare the obtained bearing capacity envelope and rotational stiffness' with industry standard practices concluding the latter fail to guarantee conservative results in some cases.

For drilling jack-ups which tend to stay on location for longer periods and hence are subject to less relocation operations, boulders are generally removed from the location where the rig is to be installed. In the case of windfarm development, the frequency of jack-up relocation is such that renders such operation uneconomical. Following on this Curtis and Allan (2015) conducted a finite element study on the interaction between boulders and jack-up spudcans with the intent to provide some guidance on deciding on boulder removal for jack-up installation. Another possible issue encountered during jack-up installation is the interaction with existing subsea templates, which is dealt with by Engin et al. (2015) by using two finite element modeling approaches for spudcan penetration analysis and trying to overcome difficulties encountered by using conventional large deformation finite element in such studies.

Carre et al. (2017) showcase how using an advanced simulation model has helped in optimizing jack-up relocation operations, encompassing extraction and installation analyses. The described methodology accounts for soil stiffness, spudcan shape, jacking speed, and compares the calculated loads with the structural capacity of the legs and jacking system to obtain permissible wave height curves. A simplified spudcan-soil interaction analysis for touchdown during jack-up installation was investigated by Chang and Liu (2016), using CFD and finite element simulations for the purpose of establishing touch-down operational limits.

Koole and van der Kraan (2015) review dynamic behavior phenomena pertaining to the design of modern jack-ups, looking into the methodology described in the readily available guidelines and covering important topics of wind loading and the push of using jack-ups in deeper waters. Janssen et al. (2016) show the effectiveness of the proposed add-on spudcans in extending the operating capabilities of jack-ups in view of operations in deeper waters and associated higher environmental loads.

Ha et al. (2016) discuss recent damages to living quarters (LQ) structures of jack-ups reported during tow due to slamming and green water phenomena and subsequently propose an engineering procedure for the structural design of jack-up LQ structures considering global and local loads in the finite element model in a departure from commonly used simplified models.

Ji et al. (2015) describe the different finite element analyses and models required for the structural assessment in the design of jack-ups. McLaren (2017) looks into effective leg buckling length factors used in the calculation of leg axial strength of single member leg jack-ups, focusing on the leg-hull interface the author considers how accounting for the stiffness of the global system and the load distribution between legs can lead to more appropriate values for buckling length factors. Mobbs and Stiff (2017) discuss the development of an approach to assess effective shear areas of jack-up chords. On the subject of jack-up under vessel impact, Raithatha and Stonor (2015) investigated the ability of the jack-up to survive the vessel impact by means of an effective non-linear dynamic analysis. Levanger et al. (2016) describe the use of non-linear finite element analysis accounting for progressive change in the contact surface and stiffness of impacted jack-up leg and impacting vessel in the assessment of the collision response of a jack-up.

Rules and regulations often become a design driver by triggering the reconsideration of previous design assumptions due to newly introduced requirements or the questioning of the validity of long standing requirements in view of market developments. Ebrahimi et al. (2015) discuss how rule changes influence the design and performance of offshore vessels and criticize the lack of balancing perspective methodology leading to possibly unnecessary cost overruns in future designs and call for a reality check advocating for a criticality review of new regulations by the industry. On a similar note Carra et al. (2017) outline the methodology for establishing robustness criteria for FPSO design in view of handling low probability extreme events. Kitchen (2015) deliberates on how rules and regulations can impede design innovation of spar structures and discusses how risk-based design could replace traditional prescriptive rules and stand as a better solution to allow design innovation meeting actual market drivers without compromising safety. After recent incidents of wave impacts on semisubmersibles structures, the regulatory regime pertaining to air gap considerations and related structural requirements has been review and updated. Pessoa and Moe (2017) look into this subject and investigate the impact of the new rules on the design of drilling semisubmersibles, namely by comparing it to current industry practices.

Yu et al. (2016) have proposed a novel load and resistance factor design (LRFD) based design criteria for the design of mobile offshore units and floating production units, claiming a better compatibility with the working stress design (WSD) criteria which is quite popular in the offshore design community. As a verification exercise the authors present study cases of a column stabilized production unit and a jack-up unit.

Design methodologies and new tools used in the design of offshore structures continue to progress driven by the everlasting pursuit of development and effort to ease the execution of complex tasks. Such an example is the dynamic sub-structuring approach to improve the current practice global structural dynamic analysis of topside/hull systems proposed by Majed et al. (2016) claiming the higher fidelity of the presented method will render local models and analyses obsolete thus with direct time and cost savings in the structural design process. Oh et al. (2017) propose a novel finite element approach related to the analysis of load-carrying structures with nonlinear contact and frictional behavior, e.g. LNG independent tanks and hull structures, based on static load and stiffness condensation. Kim et al. (2017) introduced a method to design the arrangement of offshore platform topsides by means of an expert system and multistage optimization. Presenting a benchmark study based on a FPSO the authors suggest such method can yield optimal arrangements.

Maslin (2017) reports on the application of artificial neural networks to aid in the design of floating production units during the concept and early stages of design. By input of previous FPSO design data, the neural network system will learn from it and being linked and able to perform several engineering calculations makes the design iterations and the evaluation of different solutions a much easier task. Engebretsen, Shu and Borgen (2017) have used artificial neural networks to estimate hydrodynamic sectional loads for FPSOs.

4.4 Survey on Offshore Structures Design Software

The Committee conducted a survey on software usage in offshore structures design and its results are presented and reviewed herein. A web-based survey was distributed amongst stakeholders in the offshore industry with the objective of identifying the tools and software being used in and for the design of offshore structures and related activities (e.g. engineering, construction, etc.). Other goals of this survey comprised trying to note different tools used by offshore vs. ship designers as well as trying to identify existing differences related to the main activity of the stakeholders and tool usage nuances associated with different offshore units/structure types. The survey also examined the subjects of software and tool integration in the design of offshore structures and the use of new technology in the design process.

4.4.1 Overview and characterization of respondents

Despite the survey being sent to a large number of industry players, being easily accessible and having a limited number of questions, the Committee only received fully completed survey answers from 23 respondents. It is acknowledged that the sample size may be small and hence insufficient for statistical inference at a desirable confidence level. The gathered answers are however deemed to be representative enough to show trends and draw indicative conclusions.

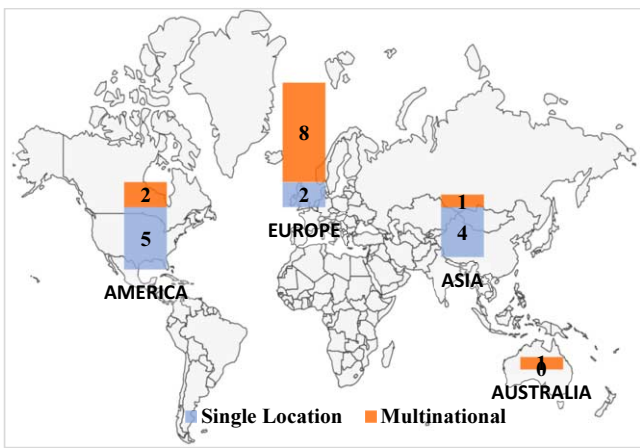

Figure 4: Survey respondents – regional distribution & international presence

Figure 4 provides the total number of respondents and their regional distribution, where the respondents were grouped per continent (America encompassing North and South Americas). The offshore industry is worldwide spread, however the numbers give an indication of where the major hubs/clusters are located, America and Europe being where the industry is more mature. It should be noted that Africa is very important and established offshore market, though the expression of local companies involved in the design, engineering and construction of offshore structures is small.

A distinction with respect to international presence was made by splitting the companies into multinationals and single location. The reason for this lies in the fact that the vast majority of players in the offshore industry (alike commercial shipbuilding a true global market) act on a worldwide scale irrespective of having presence in multiples locations (herein called multinational) or at a single location, i.e. single location does not translate into local business. The latter is the case for 100% of the companies that participated in the survey. There is no correlation between this differentiation regarding international presence and company size, i.e. several companies have presence in multiple regions but still are small or medium enterprises (less than

500 employees) and typically shipyards are enterprises with a large number of employees at a single location.

Company profiles are portrayed in Figure 5 showing the companies' distribution by primary activity and per region. Results corroborate the known fact that Asia is the epicenter of construction, all respondent shipyards being from this region. Only one of these shipyards works exclusively for the offshore industry, the other four working in the merchant shipbuilding industry as well. One company indicated its primary activity as design, construction and operation of FPSO units, thus being an owner.

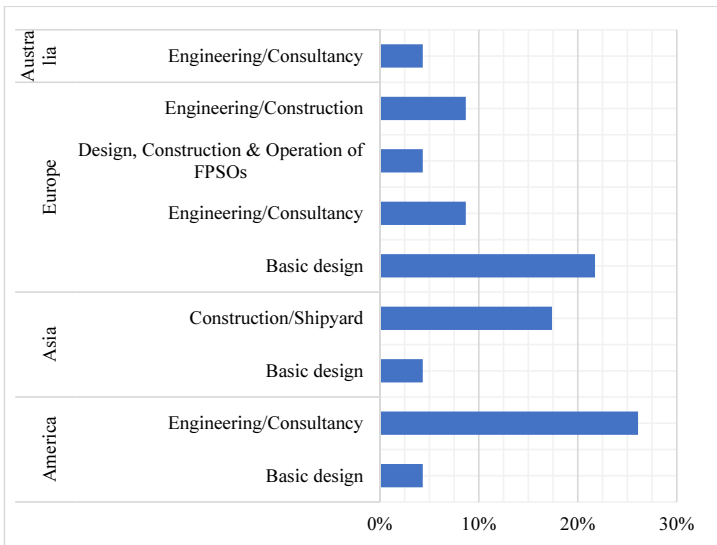

Figure 5: Company primary activity

It can be noted that there is a significant number of companies having basic design as primary activity suggesting a larger number of independent design houses when compared to the shipbuilding industry. This is further evidenced by the fact that out of the 43.5% companies that indicated being involved in a single activity, half are dedicated to basic design of offshore structures/units. The remainder of the companies have indicated be involved in multiple activities related to offshore structures/units, the distribution per activity is shown in Figure 6.

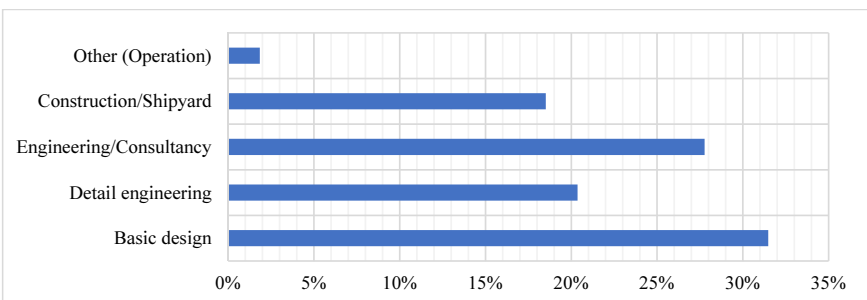

Figure 6: All activities related to offshore strucutures/units design

The vast majority of companies (91.3%) are involved in the design of different types of offshore structures/units, only a few are dedicated to a single type. Circa 71% of all the companies work

in the mobile offshore structures/units market, 61% being involved with floating offshore structures/units. The share of companies participating in the survey that are involved with fixed offshore structures is smaller. The distribution of type of structures/units in the companies' work portfolio is pictured below, at a glimpse these results do not really mirror the population of existing offshore structures/units when considering fixed vs. mobile structures or even considering the different types of mobile structures/units. Yet these results give an indication of size of the market in terms of parties involved in the design of the different type of structures.

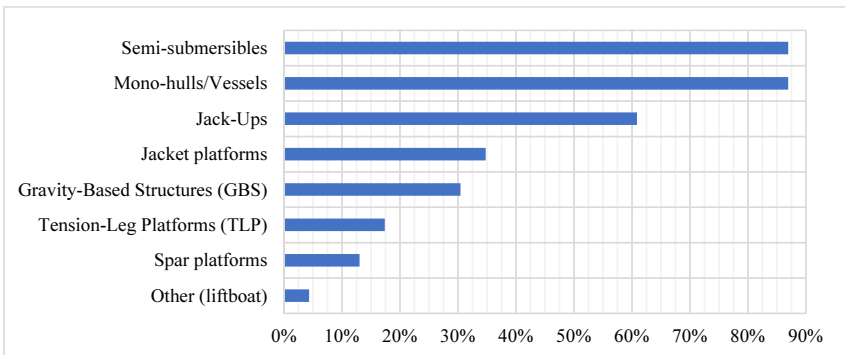

Figure 7: Type of offshore structures/units

No correlation was found between structure/unit type and region, confirming the earlier statement with regards to the global nature of the offshore industry but also that the different types of structures/units are employed offshore worldwide. With respect to the mission/function of the offshore structures/units most companies indicated to be involved in a multiple sector, only two companies indicating to be dedicated to a single purpose structure/unit. The results (Figure 8) show, as expected, that the largest share is taken by offshore units for the oil & gas market.

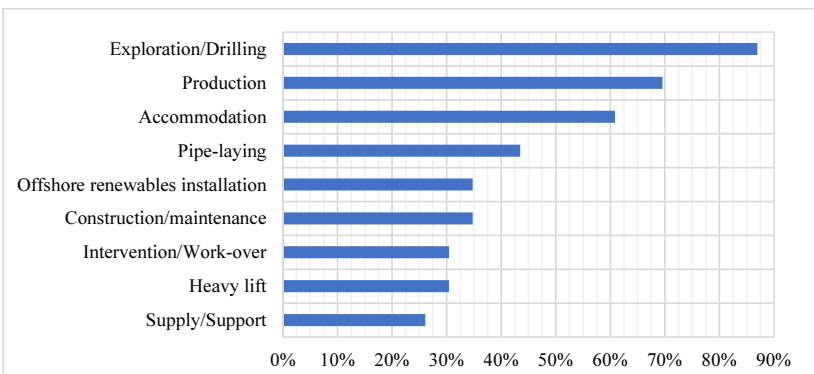

Figure 8: Mission/function of offshore units

4.4.2 Naval Architecture Tools

A large number of different software suites was indicated to be used regarding the design of hull and/or shape of offshore structures (Figure 9). Most companies employ multiple tools, only 2 companies having indicated the use of a single software tool for this purpose. Noteworthy is the usage of 2D tools (91.3% of all respondents) for this purpose, and still 13% have noted to

use 2D tools only. Another interesting point is the high percentage (43.5%) of use of engineering calculation software for designing hull/shape though this result is likely to be biased by the large number of respondents involved in engineering and consultancy work that are likely less involved in early stages of design when hull/shape is developed.

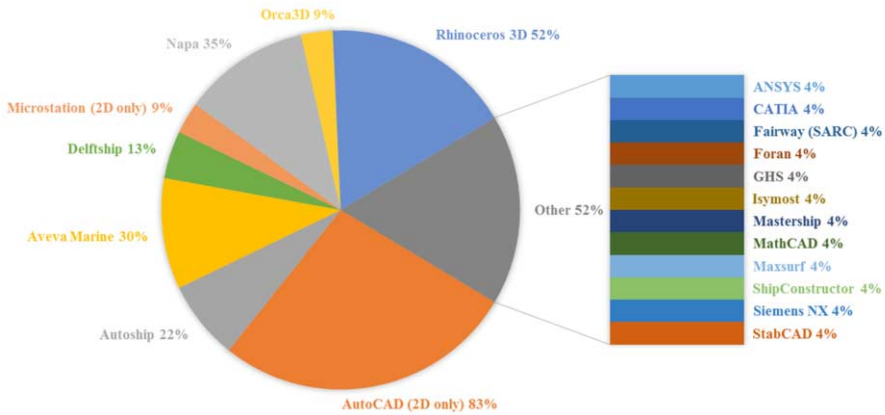

Figure 9: Hull/shape design software usage

AutoCAD is the predominant tool used in 2D drafting tasks, as can be seen from the replies outlined in

Table 1. In fact, only 3 out of the 23 respondents have indicated to use another tool in addition to AutoCAD. Irrespective of the size of or primary activity of the company, all use it, making AutoCAD the standard in 2D drafting.

Table 1: 2D drafting software usage

Software	**Usage**
AutoCAD	100%
Microstation	13%
Draftsight	9%

Shipyards & engineering/consulting companies are the users of integrated naval architecture suites, both shipyards and larger engineering/consulting firms using multiple packages. Overall 71% of respondents have indicated that they used a naval architecture package as a tool in the design of offshore structures/units. The usage of such integrated packages amounts to 29% for companies primarily involved in basic design which is considerable. It is noted that the larger, more complete (in terms of integrating more design aspects and tools) suites, such as Aveva Marine or Napa, take the larger share of usage (Figure 9).

Regarding the tasks performed with integrated naval architecture packages, results suggest these suites are utilized equally at different design stages (Figure 10) and those using these tools do so covering all design activities they are involved with. Usage for fabrication and assembly management scored lower as this matches the number of respondents involved in actual construction activities. It is interesting to note that one company has opted to develop an in-house integrated naval architecture tool; in-house development of tools of such magnitude is somewhat unexpected.

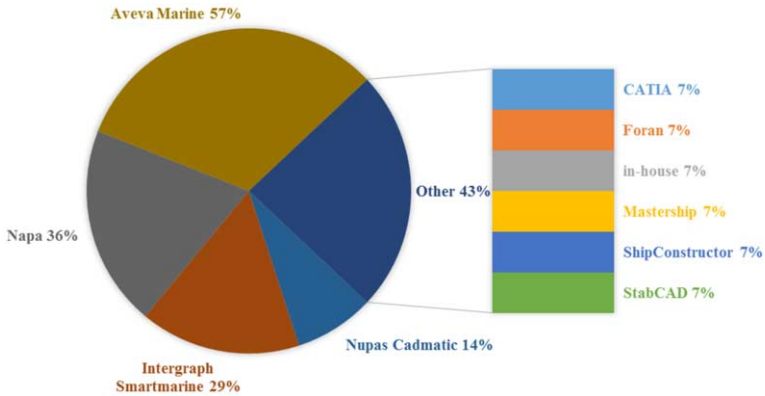

Figure 10:Use of integrated naval architecture packages

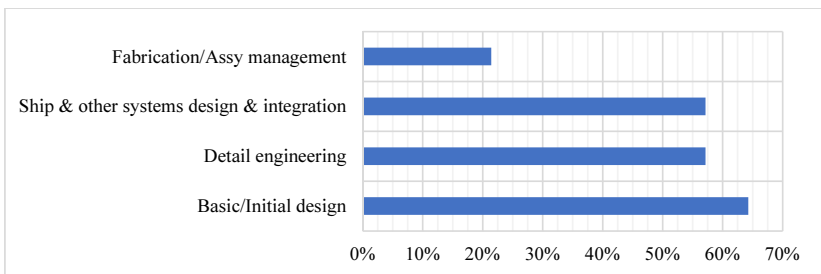

Figure 11: Tasks performed with naval architecture packages

Only 2 out 23 noted not to perform stability calculations in the offshore structures/units design loop. Most companies opt for a single tool for such calculations (circa 71% of those performing stability analysis). The distribution of the different tools used is pictured in Figure 12.

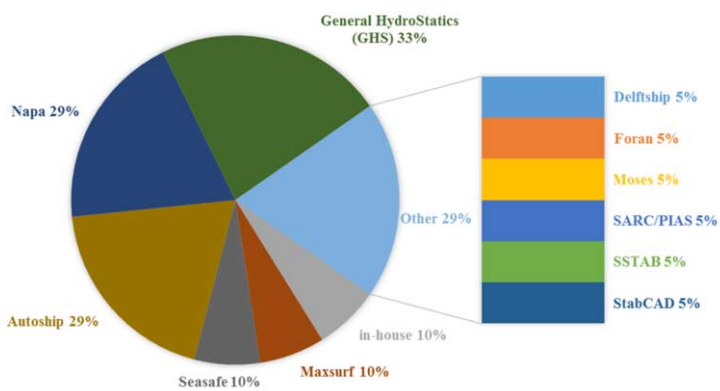

Figure 12: Software used for stability analysis

The number of respondents performing hydrodynamic calculations is similar to that reported for the case of stability analysis; only 3 out of 23 do not include hydrodynamic calculations in

their offshore structures/units design efforts. With respect to usage of multiple tools, the scenario is the opposite as in this case only 20% of those performing such tasks employ a single hydrodynamic calculation tool.

The results for usage of software hydrodynamic analysis have been grouped in high level bins: commercial, classification society and other (accounting for in-house developments) tools. The main reason for this is to identify the usage of software developed by classification societies despite the fact that these are also commercial in the sense of being available in the market and competing with the other existing packages (note in addition that in the field of hydrodynamics the weight of rule and regulatory items is less significant when compared to other disciplines, e.g. structural design). It is interesting to note the very significant portion of usage (55% of those using hydrodynamic software) taken by software packages developed by the classification societies. The results show (Figure 13) that Wamit and Ansys Aqwa are the hydrodynamic calculation tools preferred in the offshore industry. Noteworthy to mention that only one integrated naval architecture package was indicated as a hydrodynamics analysis tool.

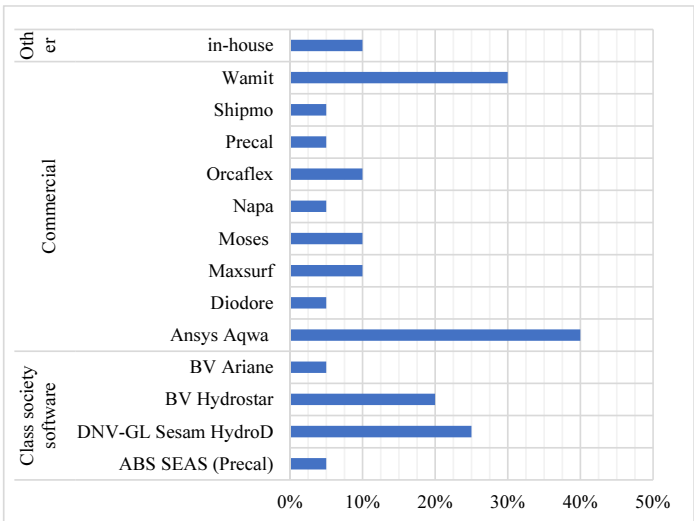

Figure 13: Software used for hydrodynamic analysis

In reply to the question of whether computational fluid dynamics (CFD) was being used in the design process of offshore structures/units, 35% of respondents indicated to perform CFD analysis as part of the design process, and considering those employing CFD analysis in the design, all have as primary activity basic design, with one noteworthy exception of a shipyard. The distribution of tools employed in CFD analysis (percentages amongst those performing it) is presented in Table 2.

Table 2: CFD analysis integration in the design process

Software	**Usage**
CD-adapco Star-CCM+	62.5%
OpenFOAM	25.0%
ANA (LEMMA)	12.5%

4.4.3 Structural Design Tools

Most parties use multiple tools in the initial design stage, in particular regarding scantling design, only 36% of respondents indicated to solely use classification society software. Results suggest a common practice of a balanced mix of hand calculations, in-house tools (e.g. spreadsheets) and classification society software specific for that purpose for establishing main scantlings in early stages of structural design (refer to pie chart in Figure 14).

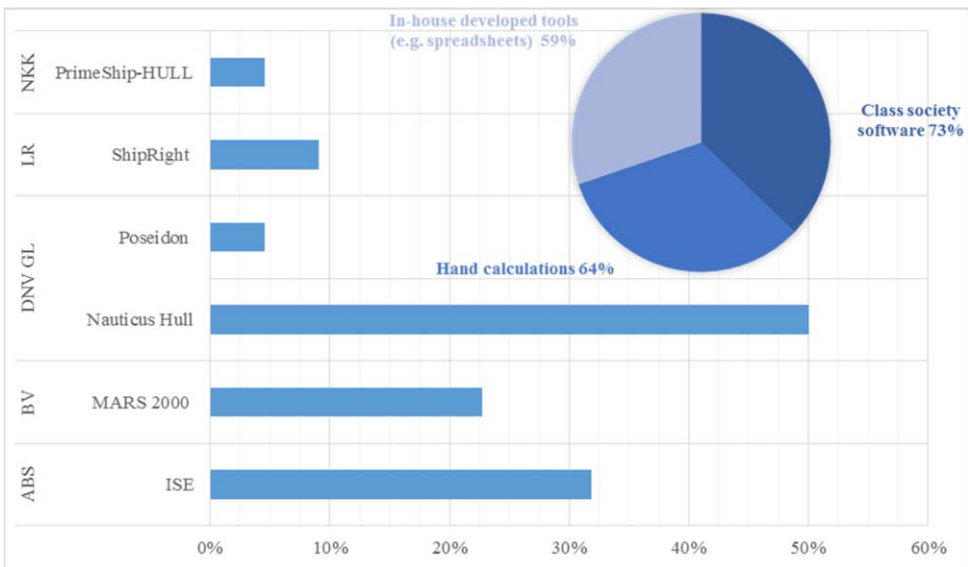

Figure 14: Tools used in structural early design stage

Drilling down into the Classification Society software used for scantling design one can notice the largest share is taken by DNV-GL, ABS and BV. These results confirm expectations noting that these Classification Societies (especially DNV-GL and ABS) lead the market in terms of offshore structures/units in class. All companies incorporate finite element analysis (FEA) in the structural design process and the primary tool of choice for this purpose is a commercial software (75%) vs. classification software (15%). The differentiation between commercial and Classification Society software is more significant in the context of structural design since the Classification Society tools tend to be specifically developed for the marine and/or offshore industry albeit having the possibility of being used as generic FEA packages as are their commercial counterparts.

There is an almost equal split between companies using a single FEA tool and those using multiple, there is, however, no correlation between company primary activity and the use of multiple FEA tools. It looks as though that the use of multiple FEA tools is correlated to companies being involved in the design of multiple offshore structures/unit types. The distribution of use of different FEA suites is shown in Figure 15. The Classification Society software has not been scrutinized as the large number of different tools was deemed too detailed for the purpose. A review of classification software may be found in this Committee's ISSC 2015 report, many tools overlapping ship and offshore structures design.

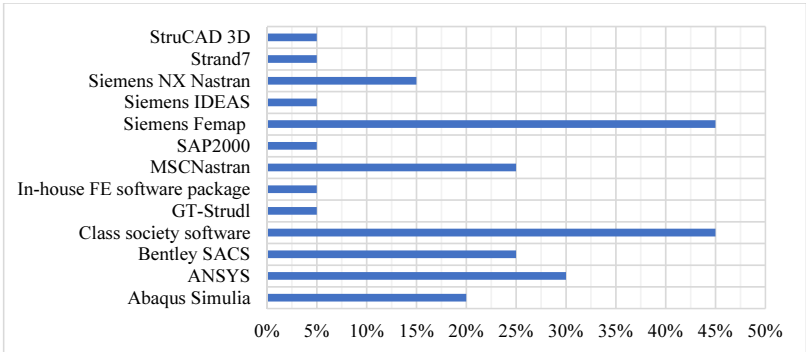

Figure 15: Software used for finite element analysis

The task of checking rule and regulatory compliance for FEA is primarily handled by the use of in-house post-processing tools integrated and interfacing with FEA packages, this being the case for 90% of the respondents (Table 3), circa 48% using only such tools for the task. Second in line are classification society software suites, with a share of 55%, and a quarter (25%) of the respondents indicated to perform rule and regulation compliance checks exclusively with such software. No correlation was found between company primary activity and tool choice.

Table 3: Rule & regulation compliance check for FEA

Tool	**Usage**
Class society software	55%
In-house FE software package	5%
In-house post-processing tools integrated/interface with FE packages	90%
SACS	5%

As for rule compliance checks, in-house developed tools are the preferred choice (Table 4) for managing the hydrodynamic load transfer to FE in direct calculations and 52% of companies performing direct calculations (73% of total respondents) resort only to these tools for this purpose. Again, the second tools of choice are classification society software. Also in this case no correlation was found between company primary activity and tool choice.

Table 4: Tools for hydrodynamic – FEA interface

Tool	**Usage**
ANSYS AQWA	10%
Class society software	30%
In-house package	10%
In-house post-processing tools interface with hydro-FE packages	80%

The greater part of respondents includes structural optimization as part of the design process (refer to Table 5). The tasks and/or goals of structural optimization vary, though a trend for weight optimization is patent in the responses. With respect to tools employed, the choice seems

to lay with commercial software tools, in particular with generic FEA packages having structural optimization capabilities.

Table 5: Structural optimization in the design process

Is structural optimization part of the design process?	Yes: 71%	No: 29%
In which cases is it used?	**Tools used:**	
• To facilitate construction and decrease the weight; • Principal dimensions of hull, structural arrangement, shape of main supporting members, etc.; • Initial scantling evaluation together with FE verification; • Determination of scantlings in relation to span-spacing for weight optimization; • Location and amount of bulkheads in relation to structural efficiency; • Elevated Conditions (jack-ups); • Follow minimum basic scantling rules, and then reinforce critical areas only as needed minimizing weight	• Nastran • Ansys • StruCAD • Abaqus • In-house tools	

4.4.4 Software Integration & New Technology

The design process of offshore structures/units involves direct calculations to a great extent, the departure design solely on the basis of prescriptive rules being the norm. This fact makes the issue of software integration and interface between different design tools very significant. In order to understand and paint a picture of the trend of development regarding this matter, the survey included a set of questions where the respondents could scale their degree of agreement. These questions are transcribed in Table 6 and the answers are shown below (Figure 16).

Results suggest a trend towards agreeing with the need to put effort into having the existing tools and software develop into fully integrated packages with smooth interface between different disciplines and/or design tasks. This is further reinforced the portrayed disagreement with respect to development being focused on the separate packages and the agreement with the need to have commercial tools strengthen the capabilities regarding integration of different packages/tasks rather than this being done via in-house developments.

Table 6: Offshore structures/units design software integration development trends

Question:	**Do you agree with the following statement?**
Q1	Offshore structures/units design tools and software should develop into fully integrated packages with smooth interface between different disciplines/design tasks (e.g. structural, hydrodynamics, stability, shape development, etc.)
Q2	The focus of offshore structures/units design tools and software development should remain in the separate packages (e.g. structural, hydrodynamics, stability, shape development, etc.).
Q3	More commercial tools/software should be developed regarding integration of different packages (e.g. structural, hydrodynamics, stability, shape development, etc.) vs. in-house developed solutions.

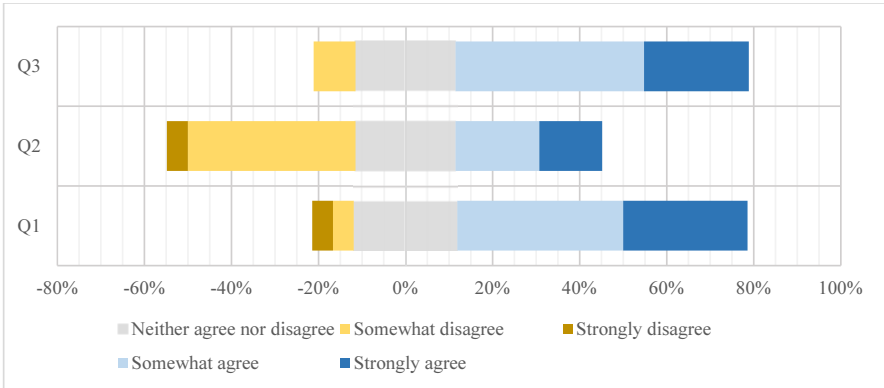

Figure 16: Offshore structures/units design software integration development trends

It is quite interesting when one compares the opinions about where tool development should focus with respect integration and interfacing to the somewhat low usage of integrated naval architecture packages reported earlier (refer to 0). It looks as though that more than advocating for the development of one-stop-shop type of tools, like integrated naval architecture suites, companies involved in the design of offshore structures/units tend to see the need to place effort in developing smooth integration between the different packages/tools. This is somewhat expected as integration and interface between different disciplines and related tools is known fact and a reported as a recurring issue. This also explains the agreement with having commercial tools developing smooth integration features rather than having companies engaging in such time consuming tasks and in turn removing focus from their main task of actually designing offshore structures/units.

A small percentage of respondents have indicated to use virtual reality tools aiding the design process (Table 7), and in fact it appears this technology is predominantly used for marketing purposes. It is however noted that virtual reality tools have been reported to be used for design review and interference check purposes. It is difficult to draw conclusions on the trend usage of virtual reality tools in or as an aid to the design process given the small sample size of survey respondents and also due to the very limited number of respondents employing such techniques.

Table 7: Virtual reality tools usage

Are Virtual Reality (VR) tools used in the design process or as a marketing tool?	Yes: 14%	No: 86%
If yes, for which purpose?	**Tools used:**	
• Marketing; • Design review & interference checking.	• Autodesk 3DS Max • Intergraph	

4.5 Foresight in Offshore Structures Design

The “lower for longer” oil price environment is expected to remain as one the most significant design drivers concerning oil & gas offshore structures in the coming years. It is expected that the trend of design standardization, optimization and ensuing design for cost effectiveness will continue in the coming years and actually endure beyond the current downturn. In a short term oil & gas production and related structures design will get more attention than other areas of

the oil & gas value chain. Interest in LNG structures and infrastructure solutions will continue to grow pushed by both economic and environmental reasons.

Notwithstanding oil & gas operators are starting to reconsider exploration efforts as the need to replenish hydrocarbon reserves starts to become more and more relevant. The restart of exploration activities is expected to initially take place in the North Sea and thus focused on harsh environment structures/units. Overall, the focus on cost effectiveness while considering innovative designs pursuing competitive differentiation will remain instrumental for designing exploration offshore structures/units in the future.

The growth of other offshore sectors is deemed to continue and with it the need for research, development and new designs and methods. Offshore renewables, mainly driven by wind energy, will continue to mature with floating wind solutions likely to take the driving seat in terms of research and development. Deep sea mining and offshore food farming (both fish and algae) will be the subject of attention over the coming years and research and development efforts are needed to effectively mature these industries to the next level. Energy and associated environmental considerations will also contribute to open sea farming gaining momentum noting, for instance, recent stated intent of kelp farming potential to replace up to 20% of fuel production in the US.

On the subject of production structures/units it is noteworthy to mention several points raised by de Beer (2017) such as the fact that corrosion and fatigue are still the number one problem in FPSOs needing as much attention as ever and hence making design for corrosion imperative. New inspection techniques using drones and other unmanned vehicles and design for such features were also indicated as a trend. The survey conducted by Haïdar (2016) also points towards this, results showing a growth in the use of new technologies for inspection and maintenance. As risk-based inspection gains solid ground there is a need for reliable damage development models; a need to study and establish criteria to judge current state of damage as well as criteria to judge criticality.

Another interesting design issue discussed by de Beer (2017) was the 10,000 year case that currently is being required by regulatory bodies as design case (commonly employed in air gap of semisubmersibles or TLP tendon compression assessment) for FPSOs structures though it should perhaps be treated as a survivability and robustness check. Similar cases of rules, regulations or specifications going beyond practical parameters and driving design and end cost past actual requirements are found for exploration units, e.g. recent classification rules for drillships have imposed 100-year design wave considerations for what are inherently mobile units that in reality avoid such harsh conditions. Another example are requirements set for the design of dynamically positioned units which historically and systematically result in over powered designs having power plants operated far from optimal with adverse effects fuel consumption and emissions. Solutions to these issues require collaboration to reach a common ground between all stakeholders in the industry and research and development is needed from owners, designers, regulatory bodies and academia alike.

The subject of treatment of abnormal (low probability) events in offshore structures design was also addressed by Morandi (2017) and adding the challenge of how to deal with these in the advent of digitalization and big data. The author mentioned stochastic finite element analysis is not being used to the expected extent in offshore structures design, especially compared with other industries; and the need to effectively consider area statistics versus single point statistics in the design of offshore structures.

In both aforementioned keynote lectures a call of attention was made by presenting examples that highlighted the lack of attention to engineering first principles by young engineers. In fact, this opinion is shared by a large extent of the veteran community in the offshore industry. While

it is generally acknowledged that the use of computer tools is essential in the design of structures/units, solid knowledge and understanding of the basics is fundamental to properly make use of the available technology. Academia should, in its educational tasks, thus make an effort to generate graduates with well-balanced knowledge of first principles and computer tools and methods.

Digitalization, big data and automation issues are expected to gain much interest in the near future. Already with many ongoing pilot projects and successful applications to asset integrity and maintenance management as well as operational optimization, it is believed that this technology will leap into design as noted by Wiley (2015) discussing a single software solution for design, operations and optimization. It is foreseeable that the industry will make use of the enormous potential of utilizing data from existing and operating units to reconsider design assumptions and ultimately leading to technically and commercially optimized solutions.

Computer aided design and tools are key to the offshore structures design process which relies heavily on direct calculations, more so than in the case of commercial ship design. From the survey conducted by the Committee one can identify that software integration is still an important issue as communication and translation of data between different packages is still consuming a considerable amount of time in the design process. More than having one tool fitting all trades, the industry would benefit from development towards seamless integration and communication between the existing tools.

5. STATE-OF-ART VS. STATE-OF PRACTICE

5.1 Motivation, background, and aim

State-of-the-art vs. state-of-practice is a new theme into the ISSC IV.2 committee's work in order to initiate the discussion and bridge the gap in between the research work presented within the committee's remit and the practical applications that may stem of it. The above was initially highlighted by Prof. Moan acting as official discusser of the ISSC 2015 Committee IV.2 Design methods report (Moan, 2015). The above distinction in between state-of-the-art vs. state-of-practice research refers to design methodology that will improve the practical design approach, optimization tools implemented in practice and new knowledge provided through research papers related to current practices in monitoring and inspections especially of hull structures. Prof. Moan referred to one of the key ISSC Committees' tasks *"…to identify knowledge resulting from research which is novel, validated and relevant for use by the industry and regulatory bodies. It is important that the Committee highlight the papers of greatest potential value for the users*". In particular, he addressed the status of reliability–based design in practice as well as the most significant R&D results in terms of industrial application.

A quick look through Oxford dictionary suggests that the term "state-of-practice" unlike the term "state-of-the-art" is not fully defined. Taking into account that "practice" is the actual application or use of an idea, belief, or method, as opposed to theory related to it, the "state-of-practice" definition will provide an indication of the best design process which will be also integrated with production, maintenance and repair available in everyday engineering systems.

In this respect, a common approach that is often used to access information related to state-of-practice related engineering applications is the use of questionnaires distributed to industrial stakeholders. This approach was employed by Committees IV.1 and IV.2 within their ISSC2003 report (ISSC2003, 2003). The questionnaire of Committee IV.1 addressed the use of systems engineering methods and general trends stemming from it resulting in twelve responses being received from different organizations and countries of origin. On the other hand, Committee IV.2 used a questionnaire-based survey to collect information related to the actual use of IT systems within shipyards and also examine the expected improvements based on practical IT applications. In this case a higher response rate was observed including 17 questionnaires

returned by a large range of shipyards located in Asia and Europe (ranging from SMEs to big shipyards, employing from 60 up to 11,000 employees).

In its ISSC2012 report, Committee IV.2 decided to distribute a web-based survey among shipbuilding stakeholders concerning IT tools and data exchange applications (ISSC2012, 2012). Target audience of this survey included shipyards, design offices, research centres, software vendors as well as universities. In this case, the Committee report included feedback from 23 stakeholders which were deemed insufficient to draw specific conclusions; however provided a representative body of information good enough to analyze and suggest the application trends within the shipbuilding industry. One of the main conclusions reached was that more effort is required with regards to better integration of data originating from the initial design stages to the final disposal phase of ship life cycle. Having in mind all the knowledge and results stemming from the previous Committee efforts and reports, Committee IV.2 applied a quantitative analysis[1] approach in order to provide a thorough and as complete as possible picture of the trends in the design methods industrial applications.

5.2 State-of-the-art

5.2.1 Bibliometrics

According to Pendlebury (2008), bibliometrics (sometimes called scientometrics) turns the main tool of science, quantitative analysis, on itself. This approach is widely used by universities, policymakers, information specialists and librarians, and researchers themselves for quantitative evaluation of publication and citation data to analyze the level of R&D.

The Organization for Economic Co-operation and Development (OECD) Report (OECD, 2015) presents the actual level of technology and innovation for growth. One of the conclusions in the report is that an increasing gap between basic research and the development of new products and processes exists (Figure 17). Although the applied research and experimental development efforts have more than doubled since 1985, they remain well below the amount of basic research. Another significant indication is the continuous growth of the amount of basic research over the years. The latter is also supported by a study performed by the University of Ottawa stating that approximately 2.5 million new scientific papers are published each year (University of Ottawa, 2017).

In this respect, in the bibliometrics numbers provide the following information: papers in indexed journals; papers per year on average; papers in top journals (various definitions); number of total citations and number of relative ones i.e. citations per paper compared with citations per paper in the field over the same period; citations vs. expected citations; percentage of papers cited vs. uncited compared to field average; rank within field or among peer group by papers, number of citations, or number of citations per paper (Pendlebury, 2008)

The implementation of bibliometrics in the following sections is based on the following assumptions:

- The number of reviewed papers is a testimony to the interest of researchers and practitioners in a relevant engineering field;
- The ISSC Committee includes experts from all over the world and thus provides a broad basis for reviewing the publications;
- The Committee members have extensive experience that helps them to highlight significant publications and provide further insight into the subject matter.

[1] "If you can measure that of which you speak, and can express it by a number, you know something of your subject; but if you cannot measure it, your knowledge is meager and unsatisfactory." William Thomson, Lord Kelvin

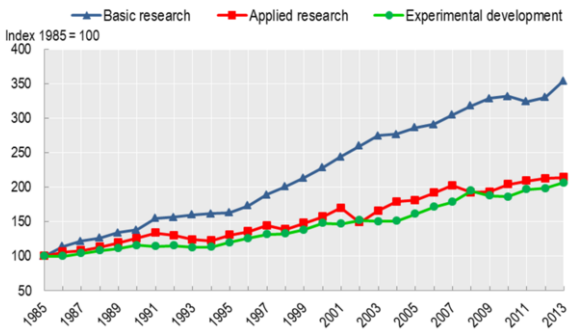

Figure 17: Trends in basic and applied research and experimental development in the OECD area, 1985-2013 (OECD, 2015). Note: *Constant price index (USD PPPs 1985 = 100). The index has been estimated by chain-linking year-on-year growth rates that are calculated on a variable pool of countries for which balanced data are available in consecutive years and no breaks in series apply*.

5.2.2 Main research topics and their bibliometrics

In order to have a structured approach into identifying the main research topics of interest and their bibliometrics, the current Committee IV.2 members analyzed the main committee topics addressed during the last three Congresses (period 2006-2015) also including the ones suggested for inclusion in the 2018 report. This resulted in identifying the most common topics and areas of interest including sub-sections mentioned in at least of three of the reports (Fig. 18). As can be observed, the most frequently mentioned sub-sections are related to: Design methodology (DM); Design tools (DT): Optimization developments (OPT); and Life Cycle Management (LCM). In some cases, there is no clear distinction in between some of the formulated topics addressed within the papers, e.g. there are papers discussing on the design tools particularly developed for LCM while some other papers consider the optimization of lifecycle costing.

Sub Chapter	ISSC2009 Seoul KOREA	ISSC2012 Rostock GERMANY	ISSC2015 Lisbon PORTUGAL	ISSC2018 Liege – BELGIUM & Delft – The NETHERLANDS
1	Design and production processes	Design for Life Cycle	Design methodology	Design methods
2	Information technology	Available Design Methods	Design tools	Design tool development
3	Maintenance and repair	Available Modelling and Analysis Tools	Optimization developments	Offshore Structures
4	Multi-criteria and multi-stakeholder optimization	Optimization and Decision Support Tools	Classification society software review	State-of-art vs. State-of-practice
5	Recent design tool developments	Product Lifecycle Data Management	Structural lifecycle management	Comparison of Classification Society software
6				Lifecycle data management
Period	2005-2008	2008-2011	2011-2014	2014-2017

Figure 18: Main research topics in the Committee IV.2 reports during the last four ISSC Congresses

Moreover, the sub-section on "Maintenance and repair" addressed within the ISSC 2009 report (ISSC2009, 2009) was incorporated in "Product Lifecycle Data Management" at the next Congress. In more recent developments, there is no specific sub-section on IT implementation mentioned after the ISSC 2009 report as this is nowadays used in a number of different applications and is covered within other sub-sections. The focus on Class software mentioned at the ISSC2015 report was appreciated as a good step forward and was deemed necessary to further incorporate it in the following Committee report as well. The new chapter of ISSC2018 Congress "Offshore structures" includes a review of papers in design methodology in offshore structures design and the number of them is included in topic DM (DMoff). Similarly, the number of papers in subchapter "Asset Integrity & Maintenance" is taken into account in LCM (LCMoff).

Summarizing the above, the number of reviewed papers in the four thematic areas of the last four ISSC is presented in Figure 18. Furthermore, Figures 19-20 present the number of papers by year of publication for the mentioned topics.

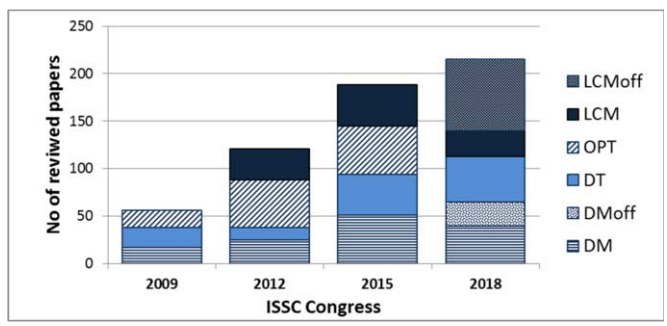

Figure 19: Number of reviewed papers in Committee IV.2 pre topic over the years

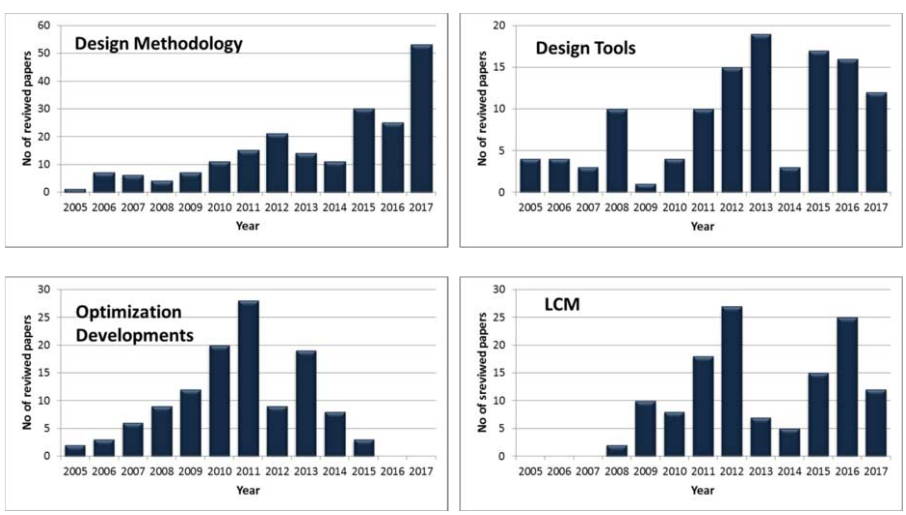

Figure 20: Number of reviewed papers of the selected research topics in relation to the year of publication

From the graphs shown above, the following conclusions can be derived:

- There is a steady increase in the total number of papers reviewed within ISSC IV.2 Committee "Design methods", which coincides with the general tendency of increasing scientific publications over the years. This number has been almost 4 times larger for the past 10 years;
- The number of considered papers over the years for the topics is cyclical. The maximum is followed by a reduced number of papers in all of the topics.
- The information shown above validates the Committee suggestions to re-organise the structure of some of the report sections. For example, one of the Committee's first suggestions was to have no dedicated sub-section on optimization developments in ISSC 2018 report. Instead it was suggested to include the implementation of optimization techniques as a sub-section within the "Design tools" main section;
- The number of papers published at the year before or after the Congress is smaller according to the presented statistics (it is clear for 2014 for DT). One reason for this could be the closure of the report almost a year before the congress, and not the consideration of the last year publications by the next committee. This should be taken into account in the work of all ISSC Committees.

The next sections give a brief description of the main topics highlighted during the past congresses in the above specified scientific fields. In this respect, the information provided below is a summary of the information presented in other sections of this Chapter and will rather provide general information about the research focus over the years and main conclusions drawn; therefore, there will be no specific reference to material already presented elsewhere. Such review and the conclusions from the present report will provide the reader with valuable information on topics that researchers have been focusing on over more than the past 10 years.

5.2.3 Design methodology

The main focus of the papers concerning design methodology during the ISSC 2009 report is related to the development of 3D CAD applications based on NURBS methodology (that is the standard approach today) and implementation in production process. Key advantages of the development of 3D CAD models are related to the improvement of production by generating production material information, simulating preconstruction, speeding up data modification time, and erection planning. The developed methodology and supporting tools allows users to easily generate the hull structural model at the initial design stage. Such 3D model permits the generation of a finite element representation of ship's structure. The studies focus on the application of a single NURBS surface representing a sea-going ship hull, to create developable surfaces and describing a hull fairing process based on the use of a NURBS ruled surface method (Cross-Fix Method).

In order to prevent distortion and to improve the quality during construction of the ship a methodology for the use of Transient Thermal Tensioning (TTT) is suggested. The first tests showed eliminating of the buckling at 5 mm plate after the implementation of TTT. The main themes of research in design methodology in the period 2008-2011 were better described as *Design for X* approach and rationality and probabilistic modelling. It was acknowledged that the systems approach made a deep impact on ship design methodology and can be used as a common platform for new developments and innovative design techniques.

Today ship design is also highly integrated with other design development activities, such as production, costing, quality control, among others. At the same time essential parts of the modern shipbuilding industry are environmental concerns, safety, passenger comfort, and life-cycle issues. Within this paradigm shift, the new designs should facilitate the productivity sequence, be cost-effective, incorporate aspects related to safety and environmental considerations while also being functionally efficient.

The review of ISSC 2012 report concluded that many "Design for X" (DfX) processes have been developed in order to correct the inadequacies of the designs during the ship initial design stages. Shortly DfX is defined as "… *process of pro-actively designing products to optimize all the functions throughout the life of the product*…" (ISSC2012, 2012). So "Design for X" can incorporate various aspects including among others Design for Production, Design for Manufacturing, Design for Assembly, Design to Cost, Design for Simplicity, Design for Maintenance, Design for environment, Design for Safety, Design for Life Cycle Cost, Design for Robustness, and Design for Six Sigma.

Economy together with safety and environmental protection remains the most essential goal of commercial ship design. Ship safety is essential as economic objectives too. This concerns the following aspects: safety of human lives, the risks of damage to or loss of ship and cargo, and the hazards to the environment. Some of the most important results of this research effort are also related to the quantification of risks at the early design stage.

Moreover, several Formal Safety Assessment (FSA) studies have been developed in the framework of EU funded SAFEDOR project that supported the IMO MSC associated work. The FSA methodology helps also the Classification Societies to develop risk-based acceptance criteria for their own rules. During the same period pioneering work has made random processes amenable to probabilistic modelling such as the irregular seaway and ship collisions and groundings. An example of the above is the compartmentation of double hull tankers, optimization, design optimization and structural reliability. In the implementation of CAD external and in-house interfaces remain heterogeneous. The conclusion is that larger scale integration is not yet fully realized. The ISSC 2015 report also highlighted the development of the "Design for X" approach. In this case the most relevant DfX aspects from structural design point-of-view are the design-for-production and design-for-safety. In general, DfX's concept places emphasis on the performance achievement, and is closely related to the goal-based design methodologies in general and risk-based design in particular. In this regard, IMO and the International Association of Classification Societies (IACS) decided to move from prescriptive concepts to probabilistic assessment methods and Goal-Based Standards (GBS). The ISSC 2015 report (ISSC2015, 2015) emphasised on the challenge to transfer from rules-based to risk-based design. The concluding by suggesting that the implementation of the risk-based design in ship design requires considerable time and effort.

One third of the reviewed papers in the ship design methodology section are related to the developments in ship form-function mapping and corresponding search in the defined design space. In this case, the design is considered as a mapping process from the function space that defines needs and requirements, to a form space containing the description of the final design. To support the mapping process there are several competing strategies i.e. set-based search strategies or using knowledge-based systems in the design process.

The main tool employed in this form-to-function mapping is the analysis methods tool that allows for a fast and efficient evaluation of specific design alternatives as part of an overall design process. The wide adoption of CFD and FEA tools has contributed to a tendency towards implementation of high fidelity models in the early ship design stages. To alleviate this, two approaches are considered. The first one is a more efficient, seamless integration of high fidelity tools into CAD software; the second one is related to a more efficient search through the design space by updating key empirical methods or by applying surrogate modelling. A slightly different approach to using simulation for analyzing system performance is performed by using discrete event models such as metocean, fleet logistics, and ice ones that capture the complex operation of a ship. Such an approach provides a more detailed and realistic representation of the operational profile of the vessel as opposed to idealized design cases.

5.2.4 Design tools

In most cases design tools are related to solving optimization tasks, thus it is challenging to separately consider them. The ISSC 2009 committee report highlighted the use of the Hybrid Co-evolution based multi-objective Particle Swarm Optimization (HCPSO) tool. The tool combines co-evolution, game theory and extremum analysis to develop an effective optimization approach. In this respect, three topics are reviewed: CAD/CAE systems; design tools for production and cost and design considerations for fire and smoke.

As a typical feature in CAD/CAE implementation, the use of graphic tools (AutoCAD, Microstation, etc.) to finalize the classifications drawings and other software codes is performed. This approach provides the opportunity to easily write-out customized macros and generate a topological and parametric structural model (NAPA, NAPASteel). The main conclusion is that the design tool together with producing a structural model should be able to extract the classification drawing and to generate an FEM model to be processed by the most common dedicated codes.

In order to withstand the competition, the shipyards must be able to accurately assess costs. In this case, the methods for estimating production costs are classified into two groups: top-down and bottom-up approaches. The top-down approach determines the production cost from global ship parameters i.e. ship type, main dimensions, weight of the hull, the block coefficient, ship area etc. The bottom-up, approach is based on automatic extraction and identification of structural features, such as cut-outs, weld lines, and bevels, from CAD/CAM data. Fire is also a hazard that can be highly complex, thus the ISSC 2015 report highlights research related to fire simulation. The final conclusion is that the coupling of design, evacuation and structural software could provide a substantial area of research for the next decade.

The state of development of tools for the design of marine structures of the ISSC 2012 report is characterized by increased scope, integration and transfer of advanced analysis tools into the early stages of ship design. Three groups of tools are reviewed i.e., naval architecture packages; specialized and general purposes CAD systems and tools to manage inventory of hazardous material data. The report provided information on naval architecture software packages for relatively simple calculations of hydrostatics to advanced packages employed for the analysis of ship performance aspects. The following general purpose CAD systems were considered: CATIA; CADDS5; AVEVA; ShipConstructor; FORAN; Paramarine; Inteliship; Nupas-Cadmatic.

A good example of a software package that follows the requirements of international convention for the “Safe and Environmentally Sound Recycling of Ships” concerning the hazardous material data is the PrimeShip-Inventory provided by ClassNK. The ISSC 2012 report also included a survey of the current practice that was mentioned above. The survey included a questionnaire on the implementation of CAD tools, Class Society tools, general purpose structural analysis tools and CFD tools.

The review of the research in the area of design tools of the ISSC 2015 report was focused on the following topics: further development of the tools; tools for lifecycle cost modelling; links between design tools and production and operational phases. A review of software developed by Classification Societies was provided. Software provided by ten Classification Societies was compared and capabilities of approximately eighty types of software tools and applications were described. The tools were divided in two main categories: tools for the assessment process of the ship structure and tools for the Project Lifecycle Management (PLM). No benchmark study was performed but the evaluation was carried out answering a number of key questions. Common for all software tools was the increased use of 3D FEA, on-line collaboration and extension of data/model usage throughout the ship lifecycle.

Extensive development in linking multiple tools in order to conduct a more comprehensive structural evaluation of new ships and offshore structures were reported. A particularly active area was the one linking the output of either 3D potential flow codes or CFD codes to FEA. Much work was also focused on code linking and automation and the development of stand-alone structural design tools. Concerning the lifecycle assessment (LCA) the conclusion was that much work remains to be done to move LCA into a practical method for vessels under construction.

5.2.5 Optimization developments

The contribution and considerable progress to the optimization developments during the ISSC 2009 committee work and considerable progress in the field is are related to the EU funded project IMPROVE (2006-2009). The project objective was to deliver an integrated decision support system for a methodological assessment of ship design so as to provide a rational basis for making decisions pertaining to the design, production and operation of three new ship generations (LNG, ROPAX and Chemical Tanker) by applying the novel Multi-Stakeholder Design (MSD) approach. As a result, the generated design alternatives demonstrated the following potential improvements: increased carrying capacity; decreased steel and production cost; increased safety measures via the rational distribution of material and improved operational performance and efficiency, including a benefit on maintenance costs for structure and machinery, and reduced fuel consumption.

The project did not develop new mathematical optimization methods but integrated existing Design Support Systems (DSS) in the design process. Four optimization packages were considered as follows: LBR5 - for optimization of ship structures at the conceptual design stage in terms of cost, weight and stiffness; MAESTRO – the software combines rapid ship-oriented structural modelling, large scale global and fine mesh FE analysis structural failure evaluation; scantlings and topology optimization; OCTOPUS – for simplified FEM response calculations at concept design phase, ultimate strength and system reliability evaluations combined with a set of optimization solvers; CONSTRUCT – for structural assessment and optimization of ship structures in the early design stage of ships. The software applies the Coupled Beams method for evaluation of the structural response and the fundamental failure criteria.

The Multi-disciplinary Design and Optimization (MDO) system consists of the synthesis design method for several ship subsystems i.e. hull form definition and optimization; seakeeping; structural design optimization; general and cargo arrangement design and optimization; propulsion machinery sub-systems design; local sub-systems such as- outfit, electrics and handling systems. Due to the high computational expense of such analyses, approximation methods such as design of experiments combined with response surface models are used. Since the approximation model acts as a surrogate for the original code, it is often referred to be a surrogate model or metamodel (i.e. a “model of a model”). A variety of approximation models exist including polynomial response surfaces, kriging models, radial basis functions, neural networks and multivariate adaptive regression splines.

The focus in the overview of the tools which led to the ISSC 2012 committee report is related to large scale optimization techniques, i.e. surrogate modelling, decomposition and coordination. The selection of appropriate surrogate method depends mostly on the characteristic of physical phenomenon that is approximated. Multi-disciplinary optimization methods require decomposition of the problem into individual optimization problems that are coupled. Some of the existing coordination methods include: Optimization by Linear Decomposition (OLD), Concurrent Subspace Optimization (CSSO), Collaborative Optimization (CO), Bi-level Integrated Systems Synthesis (BLISS) etc.

The optimization developments are broadly discussed in the ISSC 2015 committee report by referring to the Design Support Systems (DeSS). The overall design procedure, including the optimization utility is composed of three main steps: design problem identification, design

problem formulation, and design problem solution. Although, there is no new approach proposed since 2011 the report presented summary of research and application of optimization for ships and offshore structures. Important subsets of the overall optimization problem are optimization for production and optimization for lifecycle costing. The application of optimization methods has been examined in the light of achievements in parallel processing and hardware developments and implementation of surrogate modelling and variable fidelity approaches.

5.2.6 Life cycle management

The challenges related to ship life cycle are initially considered in the ISSC 2012 Committee IV.2 report. An extensive review was presented in two subchapters: Design for life cycle and Product lifecycle data management. In the first subchapter the Committee report presented the achievements in the following topics: integrated life cycle management; design loop and lifecycle data management; and drivers for integrated life cycle management. The second subchapter highlighted the state-of the art and current practice in Product Lifecycle Management (PLM). The final conclusion of the ISSC 2012 report was that the maritime industry has not yet routinely applied robust PLM solutions for design and operation of vessels.

In addition to the above, the chapter of the ISSC 2015 report on "Structural lifecycle management" contained four sections: Tool Development, Data Interchange and Standards, Integration with Repair, and Integration with Structural Health Monitoring Systems. The report summarized the outcomes of this section suggesting the vital role of an integrated lifecycle system that connects the overall design process with other operational parameters such as repairs and maintenance. Further to the latter, challenges related to the above is the application of such methodology on a full ship/marine environment. An accurate assessment of the increased performance and benefits to the vessel's structure was not possible at that time due to the lack of full-scale testing of such a system.

5.3 State-of-practice

Connecting research and practice has always been a challenging task. The continuous updated research literature needs to include practical applications. Mohram and Lawler III (2011) define three rationales for closing the gap between research and practice. These are related to instrumental and pragmatic arguments; values- based positions, and methodological and epistemological arguments.

Instrumental and pragmatic arguments postulate that it is a common interest to researchers and practitioners to close the relevance gap. Values-based arguments are connected to the views of researchers about: how they spend their time; responsibility to ensure that knowledge reaches practitioners; their criteria for good research and the topics they research. The last rationale involves the view that valuable knowledge can only be created when there is a close connection between research and practice.

The most important methodologies for connecting research to practice according to Mohram and Lawler III (2011) are:

- *Participation and collaboration*; including four approaches: basic research (that is informed by knowledge from other stakeholders); collaborative research; design/evaluation research (that entails eliciting and studying new designs and practices) and action/intervention research (that is generating knowledge in the process of solving the problem of a particular client);
- *Knowledge combination*; Combining theoretical knowledge from different disciplines with knowledge from practice when trying to understand a complex problem;
- *Studying problems in context*; Whereas researchers tend to ignore or to control the information that is relevant to an understanding of the text the practitioners look for contextual similarity to determine whether knowledge from research can be applied in their setting;

- *More prediction, less retrospection*; Researchers often employ methodologies to find out what patterns of relationships currently exist, rather than what would happen if the organization changed the way it operated.

Beyond this theoretical insight into the link between research and practice, the following sections shortly describe practical approaches that can assist with the work of the ISSC Committees to close the loop between research and practice, particularly referring to the Technology Readiness Levels.

5.3.1 Technology Readiness Level - TRL

The development and introduction of Technology Readiness Levels (TRL) is a method of estimating technology maturity of a research program during the acquisition process. TRL were originally suggested by NASA in 1974 and formally defined in 1989 and eventually adopted in 1990 introducing a 9 scale level (Banke, 2010). There are different definitions available but these are conceptually similar. Some differences though exist in terms of maturity at a given technology readiness level. Table 8 compares the NASA and European Commission (EC) suggested definitions (EC 2017). The aim in this case is to use the TRL distinction to provide suggestions on which type of research project proposals should be funded aiming at a minimum TRL threshold and also used in evaluation of the mentioned research proposals.

Table 8: Comparison of the NASA and EC TRL definitions

TRL	NASA Definition	EC (HORIZON 2020) definition
1	Basic principles observed and reported	Basic principles observed
2	Technology concept and/or application formulated	Technology concept formulated
3	Analytical and experimental critical function and/or characteristic proof of concept	Experimental proof of concept
4	Component and/or breadboard validation in laboratory environment	Technology validated in lab
5	Component and/or breadboard validation in relevant environment	Technology validated in relevant environment (industrially relevant environment in the case of key enabling technologies)
6	System/subsystem model or prototype demonstration in a relevant environment (ground or space)	Technology demonstrated in relevant environment (industrially relevant environment in the case of key enabling technologies)
7	System prototype demonstration in a space environment	System prototype demonstration in operational environment
8	Actual system completed and 'flight qualified' through test and demonstration (ground or space)	System complete and qualified
9	Actual system 'flight proven' through successful mission operations	Actual system proven in operational environment (competitive manufacturing in the case of key enabling technologies; or in space)

The European Association of Research and Technology Organizations (EARTO) also suggests a thorough and structured TRL scale as a research & innovation policy tool (EARTO, 2014). In their report, EARTO indicates some limitations of the use of TRL scale as follows:

- Lack of attention to setbacks in technology maturity – the higher TRL levels also requires additional research;
- Single technology maturity approach – the limitation is connected with the focus on a single technology;
- Focus on product development rather than manufacturability, commercialization and organizational changes – non-technological aspects like readiness of an innovation to go to market or the readiness of an organization to implement the innovation, are not taken into account;
- Context specificity of TRL scales – i.e. the scale needs to be adapted to the specific purposes of the organization.

In this respect, EARTO provides a further description of the TRL scale included in Annex 1 (EARTO, 2014), a summary of which is presented in Figure 21

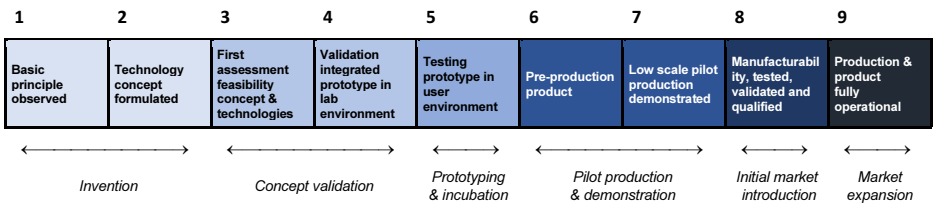

Figure 21: EARTO description of TRL scale (adopted from (EARTO, 2014)

Following the above, the US Transportation Research Board (TRB) also suggested the notion of practice-ready papers. TRB is one of six major divisions of the US National Research Council, which serves as an independent adviser to the federal government and others on scientific and technical questions of national importance, and which is jointly administered by the National Academy of Sciences, the National Academy of Engineering, and the Institute of Medicine. The standing committees in the TRB Design and Construction Group have been identifying and cataloguing practice-ready papers since 1998.

A practice-ready paper is a paper in which the research results presented and discussed make a contribution to the solution of current or future transportation problems or issues for practitioners. To nominate a practice-ready paper there are several guidelines:

- The paper must be recommended for presentation at the Annual TRB Meeting. (Publication in the Transportation Research Record is not a requirement.);
- The research results presented and discussed in the paper should be ready for immediate implementation or with minimal additional research or implementation effort;
- The paper should contain guidance on additional effort required for implementation;
- The research should make a major contribution to the solution of current or future problems or issues;
- Benefits that can be derived from implementation of the research should be evident - for example, cost savings, increased safety, or improved environmental impact.

In 2010, TRB automated the process of finding practice-ready papers by launching its Practice-Ready Papers (PRP) database (US TRB 2017).

5.3.2 ISSC IV.2 Committee point of view

Driven by an understanding of the extremely important link between research and practice while also considering all the previous approaches and work performed by previous Committees, the current ISSC "Design methods" Committee moves forward to reduce the gap between research and practice. The main purpose of the suggested proposal is to identify in a reliable and structured way research papers and relevant literature, which can lead to potential high impact applications of mentioned research, particularly applicable within the context of the ISSC Committees' work. In this respect, the suggestion for Theory to Practice Ready Papers (TPRP) approach can be formalized as follows:

- Development of a roadmap for proper organizing and conducting research quickly reaching practical applicability and corresponding presentation in the field of interest e.g. ship and offshore structures and associated systems;
- Formulation of guidelines for nomination and evaluation of TPRP.

Table 9 briefly presents the Committee suggestion for the levels of preparation for a TPRP by analogy to the Technology Readiness Levels described above.

Table 9: ISSC IV.2 suggested levels of Theory-to-Practice-Ready Papers (TPRP)

TPRP	Level title	Level description
1	Critical review of existing literature	Initial level of readiness, state-of-the-art publication
2	Methodology outline	Knowledge acquired from existing literature is transformed into novel research and development
3	Feasibility study	Feasibility of the methodology suggested at TRL 2 is evaluated
4	Methodology elaborated	Methodology outlined at TRL 2 is now fully elaborated
5	Lab/simulated case study validation	TRL 4 methodology tested through a simulated case study or at lab conditions
6	Small scale case study validation	TRL 5 methodology tested through a real-data small scale case study
7	Full-scale deployment	Practice-ready research deployed at full-scale

The levels correspond to organizing and conducting independent research by a separate author/s or scientific institution, according to a topic that will have direct/indirect relevance to an industrial assignment and will eventually lead to high industrial impact. Although this is a first effort in such a direction, which also needs to be followed by a more analytical investigation to provide further details, it can provide a draft guide streamlined to fir the ISSC Committees work.

Further to the above TPRP scale, more details on the above can be provided as part of the following ISSC Committee work. The results and agreed TPRP papers and relevant literature can be presented during the next Congress. A further suggestion would be for each ISSC Committee to elaborate and evaluate potential papers, which can be appropriate for using within the suggested TPRP approach.

6. COMPARISON OF CLASSIFICATION SOCIETY SOFTWARE

6.1 Introduction

Over the last few years, Classification-Societies (CS) have provided ship designers and surveyors with software tools to evaluate the scantlings of ship's structures. The report of the IV.2 – Design Methods Technical Committee (TC) presented at ISSC2000 provides a first overview of the CS tools and defines a set of criteria for the analysis and categorization of these software packages. The growth on the supply of CS software tools and their development over the previous 15 years, were the driver of a study conducted by the IV.2 – Design Methods TC of ISSC 2015 IV.2. The study built on the previous TC's report and extended the survey to 10 major CS, including tools and functionalities which support ship designers and surveyors from the early design stage, towards the entire ship life.

Since the software packages reviewed in ISSC 2015 were strictly related to the specific rules of the classification societies who developed them, direct comparison was not immediate. In this scenario the issue of IACS Common Structural Rules introducing a set of regulation recognized by all IACS's CS, presents an interesting updating also from this point of view.

6.2 The IACS Common Structural Rules

The IACS Common Structural Rules (IACS 2006a, 2006b), issued in April 2006, were developed as separate rule sets:

- IACS Common Structural Rules for Double Hull Oil Tankers (CSR-OT)
- IACS Common Structural Rules for Bulk Carriers (CSR-BC)

While maintaining prescriptive requirements based on experience, these rules extended the use of the Direct Strength Analysis (DSA) in ship's structural design, introducing complex scantling evaluation formulae, and increasing the load cases to be verified for the local scantling, often explicitly requiring Finite Element Analysis (FEA). Aided design CS tools immediately became necessary, with the growing demand by surveyors and designers of specific tools which are able to ensure the robustness of the required analysis and the correctness of the analysis outcomes, reducing at the same time the engineering time and cost.

The two rule sets of the IACS-CSR prescribed two different methodologies to be applied to oil tankers and bulk carriers, even in some fundamental technical matters which should be commonly treated for all types of ships. This was an important issue from the perspective of shipyards and designers involved in ship structural designs (Shibasaki, 2016). The harmonization of these two rule sets was IACS' resulting activity, and CSR-OT and CSR-BC were superseded by the new unified Common Structural Rules for Bulk Carrier and Oil Tankers (CSR BC & OT), referred as Harmonized CSR, H-CSR or CSR-H, issued on 1st January 2014 and entered into force on 1st July 2015.

As for the evaluation and assessment of the structural analysis results, it is a matter of course that the issue of the new H-CSR has increased ship designers work load regarding, for example, the number of loading conditions, numerical models, and parts and details to be analyzed. In this regard, each CS has developed its own software tool for the structural assessment according to the H-CSR and offers it to the shipbuilding industry and in particular to ship designers who are expected to use it to verify the compliance of the design with the rules. In other words, it is practically impossible to design oil tankers without the software tool provided by the CS. Therefore, today the cost of the structural design for shipyards is directly affected by the quality, convenience, functionality, efficiency, and accuracy of the software provided by CS (Shibasaki, 2016).

The new H-CSR not only replaced the separate rules for bulk carriers and oil tankers with harmonized rules but also introduced some new requirements. There are two major changes in H-CSR compared to the old CSR. The first is the prescriptive rule changes including load cases,

minimum thickness, tank pressure and so on. The second is the extended scope of FEA including coarse mesh, fine mesh and fatigue analysis. A study on the design changes and weight increases due to the issue of the new prescriptive rules and the FEA of the whole cargo hold was conducted by Un-Chul Choi (2016). The report shows that the introduction of the H-CSR has resulted in the hull structure being strengthened due to yielding and fatigue in cargo hold region and that approximately two months more are required for the structural design of a new vessel when compared with the old CSR.

The experience gained with the application of the CSR moved most of the CS to develop dedicated tools before the entrance into force of the new rules. Since these tools apply common requirements, they have definitely become independent from the specific classification societies in charge of the classification of a new construction, and may be chosen by the designer considering the offered functionalities.

6.2.1 H-CSR rules requirements

The evaluation criteria defined in previous ISCC IV.2-Design Methods reports are generally applicable to all CS tools. On the other hand, being the requirements of H-CSR very specific, an efficient way to evaluate related software tools should start from a rule analysis, especially considering that these rules emphasize the work flow to be use by the designers for their correct applications.

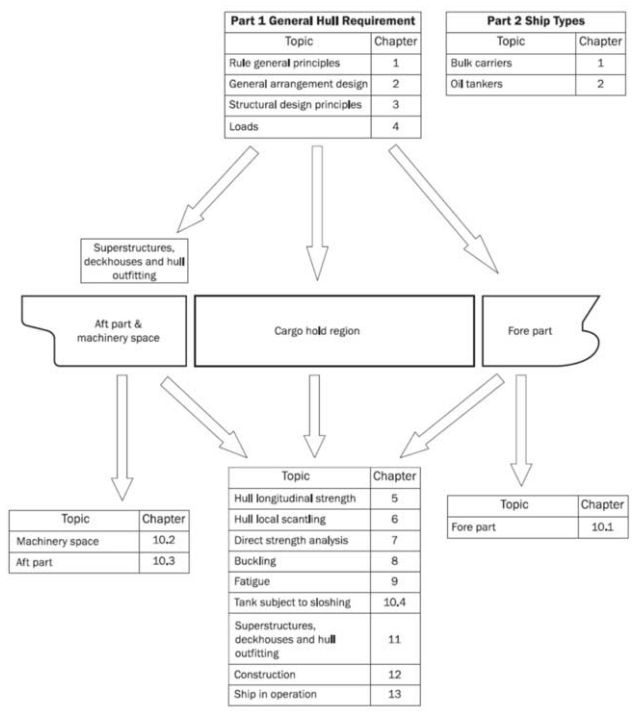

Figure 22: Application of the Rules CSR BC & OT (IACS 2017)

H-CSR are divided into two parts: Part 1 provides requirements common to all types of ships and Part 2 which adds specific regulations for each ship type (Oil tankers and Bulk Carriers). Each part's chapter refers to specific topics that can be also mapped considering the applicability region as described in Pt 1, Ch 1, Sec 1. [2.2.3]. Mapping of rules requirements are shown in Figure 22 (IACS CSR BC & OT).

It is also interesting to emphasize that, as per requirement Pt 1, Ch 1, Sec 1. [4.1.1] the designer should take care that the parts of the structure not covered by H-CSR rules are in compliance with the relevant requirements of CS's Rules. Requirements are divided as follows:

- Minimum requirements to be applied irrespective of all other requirements prescribing minimum thickness, independent to the specific minimum yield stress, and minimum stiffness and proportion, based on buckling failure modes;
- Load-capacity based requirements to assess structural members controlling one particular failure modes. In general Working Stress Design (WSD) method is applied in the requirements, except for the hull girder ultimate strength where Partial Safety Factor (PSF) method is applied. Summary of loading scenarios and corresponding rule requirements are presented in Pt 1, Ch 1, Sec 2. Table 1.

Structural response analysis is to be approached using Beam theory or FE analysis verifying acceptance criteria summarized in Pt 1, Ch 1, Sec 2 Table 2 and 3. Indication for the verification of compliance is given for both, new buildings, and ships in service.

H-CSR include also detailed requirements about structural arrangements, guiding the designer to a sort of standard project. In section Pt 1, Ch1, Sec 4 [3.7.1] an extended part is dedicated to structure nomenclature that could also be used to identify structural members and details subject to verification of compliance. Figure 22, abstracted from this section has been provided as an example. Table 11 in section 6.3.1 of this report, refers to a generic item "Prescriptive", introduced to give the evidence of software capabilities to support the assessments of these parts.

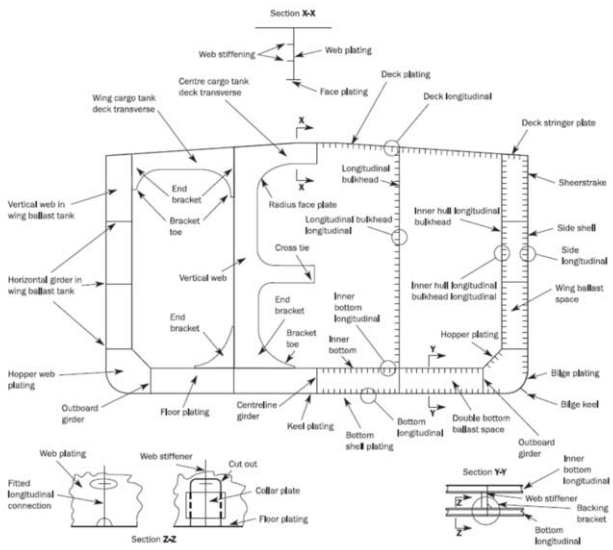

Figure 23: Mid cargo hold transverse section of double hull tanker (CSR BC & OT, IACS(2017))

Pt 1, Ch 4 relevant to loads is the most demanding part of rules in terms of computation time in particular when applied to direct analysis. Dynamic load cases, ship motion and acceleration, hull girder loads (wave and still water in intact and flooded condition), external and internal loads, are taken into account and combined as per requirements of Sec 2 of the same chapter.

Pt 1, Ch 7 is dedicated to Direct Strength analysis. Details are provided about meshing, properties input, loads applications, screening and results analysis for global, local fine and local very fine mesh models. Figure 24, abstracted from this chapter clearly show the flow chart of required assessments.

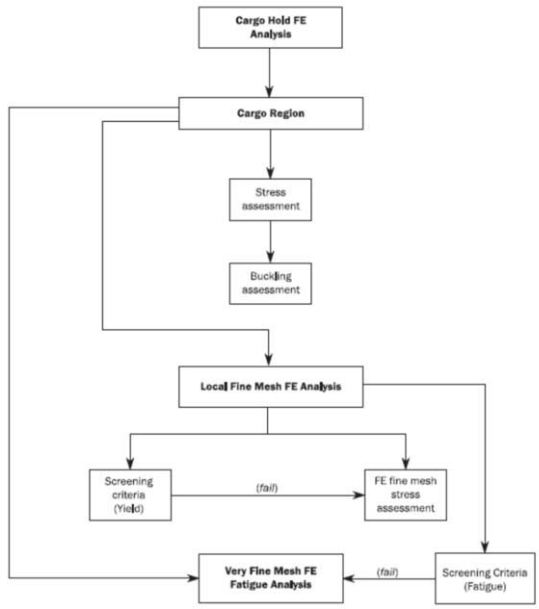

Figure 24: Flow diagram of finite element analysis (CSR BC & OT, IACS (2017))

The shipbuilding industry has recently started applying the H-CSR to the design of new tankers and bulk carriers. However, the substantial increased amount of FEA required by these rules created a big burden which impacted the structural design phase, mainly in terms of man hours and design cost for shipbuilders (Shibasaki, 2016).

Although H-CSR have been reviewed by the Industry, there are still some issues to be discussed for real ship design, especially for some new designs. Cai et al. (2016) presented the design of a new Aframax tanker designed to meet the requirements of new CSR. The authors performed the prescriptive calculation, and the direct strength analysis for the whole cargo holds, including yielding, buckling and fatigue. The impact of New CSR will be discussed as well as some technical issues, such as the shear force adjustment outside the cargo region, modeling and buckling evaluation of manhole region.

So et al. (2016) discussed the effect of H-CSR. The 50K class product carriers have been investigated and evaluated with H-CSR which was newly issued. From the investigation, there is not a great change in FE analysis. Certain methods have been introduced for FE analysis targeting outside midship region. Consequently, invisible areas for designer became much clearer than before. The main cause of the increased hull weight comes from the local scantling requirements such as minimum requirement, corrosion addition and change of loading sets, etc.

Study on Fatigue Strength for Tank Structures subject to H-CSR was report by Seo et al (2016), this report shows that detailed FE fatigue analysis for H-CSR and IACS Urgent Rule Change Proposal (URCP), and pointed out that there were locations the standard design recommended by H-CSR which should have sufficient fatigue strength did not comply with H-CSR fatigue requirement when FE fatigue analysis applied. And FE fatigue analysis based on URCP shows that fatigue life decreases up to 20%.

6.3 Comparison of classification society tools for H-CSR

As previously mentioned, a specialized software tool for structural assessment according to H-CSR is now essential in order to perform oil tankers and bulk carriers structural design and comply with the complex and extinguishable H-CSR requirement. Especially, not only ship

designers but also CS surveyors are eager to use proper, usable and confident software tools. There are available a few H-CSR software tools which Classification Societies has recently developed and structural designers and surveyors has started to use. Hereinafter, the available H-CSR software tools are summarized and software functions of beginning design stage are briefly compared.

Bureau Veritas (BV), China Classification Society (CCS), American Bureau of Shipping (ABS) and Lloyds Register (LR), DNV-GL, Korean Register of Shipping (KR), and Nippon Kaiji Kyokai (ClassNK) have already released their own H-CSR software tools and are updating them in order to add new functionalities and fix bugs. This means that there are available 6 and more software packages.

Malcolm Latache (2017) reported that Common Structural Rule Software LLC (CSRS), which has been jointly developed by ABS and LR, and ClassNK have recently updated their own software tools to incorporate the new version of IACS H-CSR, which entered into force in July 2017. CSRS released version 2.5 of the CSR Prescriptive Analysis (PA) and CSR Finite Element Analysis (FEA) software. ClassNK released a new version of its software, PrimeShip-HULL (HCSR) Ver.4.0.0 incorporates the 2017 rule amendment. Latache also showed not only that these new versions of the software tools improved their user-friendly functions in order to support surveyors and designers. As reported in Table 10, also the other CS have updated and released new versions of the software tools that comply with the new version of H-CSR.

Table 10: CSR BC & OT Software updating according rule changes

CSR BC & OT Rule versions	BV	CCS	CSRS (ABS/LR)	DNVGL	KR	ClassNK
January 2015	✓	✓	✓	✓	✓	✓
Rule change 2017/07/01	✓	✓	✓	✓	✓	✓

Figure 25 shows the distribution of the present fleet of oil tankers with length equal to or greater than 150m and bulk carriers with length equal to or greater than 90m under survey of major IACS classification societies, and shows the number of ships (N) and gross register tonnage (GRT). Data have been provided by http://maritime.ihs.com/ and are updated to October 2017. Since H-CSR entered into force, there are not enough available data on the fleet under construction designed according new requirements. The presented charts consider the actual on-going ships and include in fact vessels non classified according CSR or H-CSR. The verification of data is out the scope of present work and the has been used only to suggest the actual trend which is expected to be also meaningful for the influence of IACS classification societies developed software in the near future.

6.3.1 H-CSR software packages

H-CSR software functionalities are summarized in Table 11 and Table 12. All the packages are suited to perform prescriptive rule calculation and direct strength analysis (DSA). All of them are already updated to the new H-CSR updated in July 2017. Data exchanges from/to CAD software packages are also considered.

As previously mentioned, H-CSR tools are able to perform two calculation phases, prescriptive rule calculation and direct stress analysis. The first phase is the calculation of structural scantlings according to rules requirement and 2-D analysis of the hull cross section. The second phase is 3-D Finite Element and DSA.

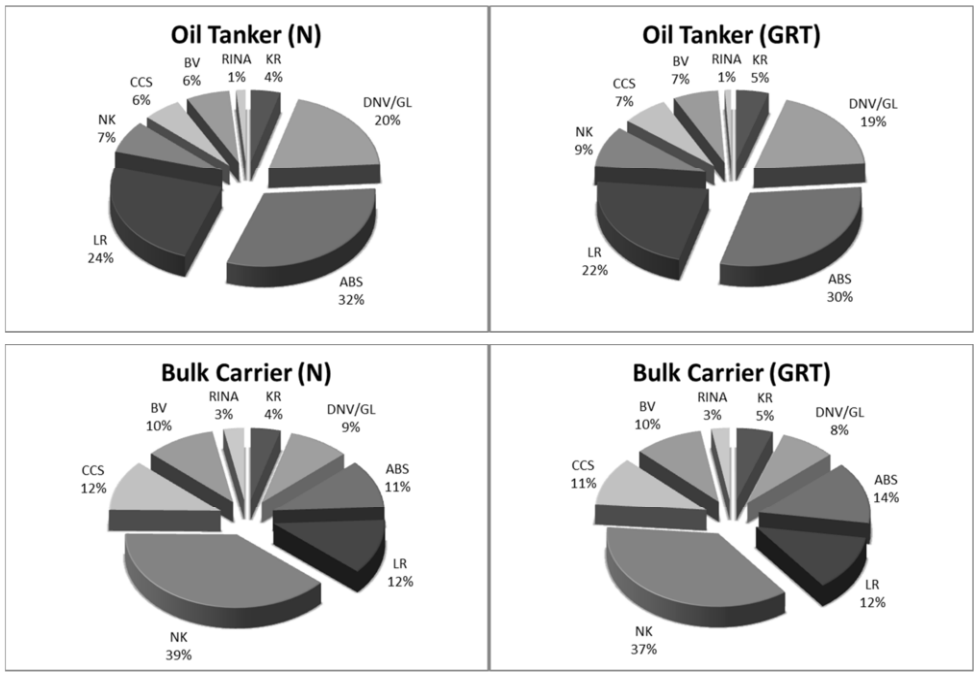

Figure 25: BC & OT under major classification societies survey

Table 11: Application and function matrix of classification software for H-CSR - Prescriptive

Prescriptive Rule Calculation Software		BV	CCS	CSRS (ABS/LR)	DNVGL	KR	ClassNK
		MARS	COMPASS CSR-SDP	CSR Prescriptive Analysis	Nauticus Hull	SeaTrust-HullScan	PrimeShip-HULL (HCSR) /Rules
Componets covered	Mid hold	✓	✓	✓	✓	✓	✓
	Fore/aft hold	✓	✓	✓	✓	✓	✓
	Bow/engine room/stern	✓	✓	✓	✓	✓	✓
	Primary supporting members	✓	✓	✓	✓	✓	✓
Assesments Supported	Minimum thickness	✓	✓		✓		✓
	Section properties	✓	✓	✓	✓		✓
	Presciptive ..	✓	✓	✓	✓		✓
	Ultimate stregth	✓	✓	✓	✓		✓
	Sloshing	✓	✓	✓	✓	✓	✓
	Bottom slamming	✓	✓	✓	✓	✓	✓
Input Mode	2D or 3D based	2D	2D	2D	2D	Both	Both
	Manual modeling	✓	✓	✓	✓	✓	✓
	Import from CAD	NAPA Steel	✓(semi-auto)		✓	NAPA/CAD	✓
	Export to CAD		NA				✓
	Inter Face	✓	✓		DXF		XML
	CSRH loading	✓	✓	✓	✓	✓	✓
Report Generation	Auto report generation	✓	✓	✓	✓	✓	✓
	MS EXCEL	✓				✓	✓
	MS WORD / PDF	✓	✓	✓	✓		✓

All H-CSR software tools provide the users with manuals that may be read thorough when use H-CSR software. Different format are used, such as standalone documents (e.g. BV, CCS, ClassNK) or online interactive manual (e.g. DNV-GL).

When creating a model for the structural scantling of a ship, the user should input the main characteristics of the ship, such as ship dimensions, compartment dimensions and positioning, frame intervals, location of water tight bulkheads, draft at several loading conditions, still water bending moment etc. Figure 26 shows a snap shot of data input to longitudinal strength members.

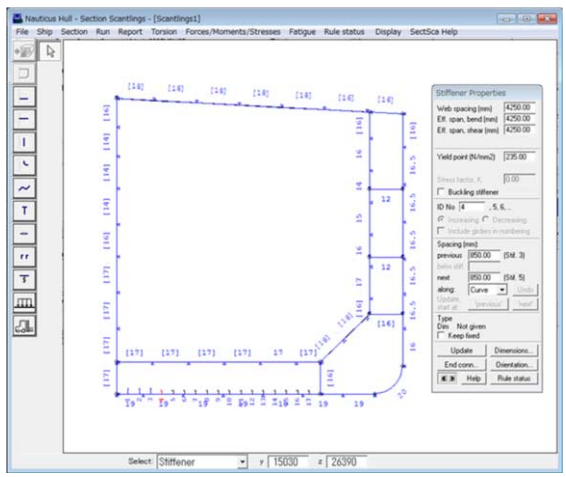

Figure 26: Inputting longitudinal strength members on H-CSR Software tool

Hereinafter, we introduce the modelling procedure to be followed in the very early stage of H-CSR prescriptive rule. First, the software makes hold compartments based on user input dimensions and compartment data. The designer input the main supporting members, arrangement and scantling of longitudinal strength members, typical transverse web section, detail shape of transverse web attached to longitudinal etc. Beside this, corrosion reductions are automatically calculated with user input compartment and tank data. Once the user has defined the main input data for the ship, the H-CSR loads are generated. At this point, the section modulus and the other relevant geometric characteristics of the midship sections can be calculated. In order to simplify and speed up this initial phase, some software tools provide the designers with wizards and/or parametric input methods.

A user friendly graphical user interface simplifies the assessment of the results. The results showed by the software tool highlight each member which needs to be modified after calculation because it doesn't satisfy the rules requirements. Reports are automatically generated by the software and WORD and/or EXCEL format file are obtained. Usually EXCEL format files have detailed information such as each calculation steps, dominant load, corrosion values adopted to members etc.

Information shown in Tables 11 and 12 were obtained from each of classification societies by October 2017 and some functions of prescriptive rule calculation in Table 11 were confirmed in this report.

As stated before, the H-CSR Rules gave extinguish number of FE load cases, and FEA function to support design is one key of the packages. Some packages work with commercial FEA software such as FEMAP, HyperWorks, MSC-Patran and MSC-Nastran and Siemens NX. DSA supporting functions are available in the packages. The functions of auto-meshing and auto-buckling panel should be assessed in detail, because the size and shape of finite elements is very important for the structural analysis (Shibasaki, 2016).

Table 12: Application and function matrix of classification software for H-CSR - DSA

Direct Strength Analysis Software		BV	CCS	CSRS (ABS/LR)	DNVGL	KR	ClassNK
		VeriSTAR Hull	COMPASS CSR-SDP	CSR FE Analysis	Nauticus Hull+GeniE	SeaTrust -HullScan	PrimeShip-HULL (HCSR)/DSA
Base FEA software	Pre and Post processing	FEMAP	Patran	Patran	GeniE	SeaTrust -HullScan	HyperWorks Patran
	Solver	NX/MSC Nastran	MSC Nastran	NX/MSC Nastran	Sestra	MSC Nastran	Nastran / OptiStruct
Componets covered	One lump analysis (every hold at once)						✓
	Global strength (3 hold)	✓	✓	✓	✓	✓	✓
Assesments Supported	Yield check (global model)	✓	✓	✓	✓	✓	✓
	Buckling check (global)	✓	✓	✓	✓	✓	✓
	Structual Optimization*	✓	✓				✓
	Auto screening (fine mesh)	✓	✓	user input and program calculation	✓	✓	✓
	Yield check (fine mesh)	✓	✓	✓	✓	✓	✓
	Auto screening (very fine)	✓	✓	user input and program calculation		✓	✓
	Fatigue life calculation	✓	✓	✓	✓	✓	✓
	Bottom slamming Impact(quasi-static analysis)		✓	Rule calculator + FEA	Rule calculator + 3D-Beam		✓
Input Mode	Import from CAD	✓			✓	✓	✓
	Import compartment	✓ (NAPA Steel)	✓ (NAPA)	✓			✓ (NAPA)
	Corrosion deduction	✓	✓	✓	✓	✓	✓
	Auto meshing coarse		✓		✓	✓	✓
	Auto meshing fine	✓	semi-auto		✓	✓	✓
	Detail shape database (fine)		✓			✓	✓
	Auto meshing very fine	✓	semi-auto		✓	✓	✓
	Detail shape database (very fine)		✓	✓		✓	✓
	Auto buckling panel	✓	✓	✓	✓	✓	✓
	CSRH boundary condition	✓	✓	✓	✓	✓	✓
Report	Auto report generation	✓	✓	✓	✓	✓	✓
	MS EXCEL	✓		✓	✓		✓
	MS WORD	✓	✓	✓	✓	✓	

Once the analysis is completed, auto screening functions are able to identify highly stressed areas in the fine mesh and very fine mesh models. Yield and fatigue life are evaluated according to the H-CSR. Moreover, the tools are equipped with an automatic Report generator which is available on each package for WORD and/or EXCEL format. The relevant input data of the analyzed ship structures, and the outcomes from the analysis are organized and reported in the output document.

Because of the time consuming analysis required to perform the structural design according to H-CSR, CS have developed and are developing flexible functions which are expected to save man-hours in the overall structural design process. SeaTrust-HullScan, which is the structural design assessment software of KR, can automatically generate 2D cross section models for H-CSR Prescriptive calculations and FE models for H-CSR DSA, using 3D CAD models. If a 3D CAD model is not provided, it can generate FE models by connecting two or more cross sections previously modelled in the software for the prescriptive calculation. In the case that a 3D CAD model is provided, it can import the 3D CAD geometry by IGES and hierarchical model data by XML or THS, 2D cross sections can be generated by intersecting with YZ plane, and FE models can be generated surface meshing with the constraint of stiffener. The properties of plate and stiffener can be inherited automatically. Auto-modeling for fine mesh and very fine mesh (t by t) with properties inherited from coarse meshes based on parametric method is also provided in SeaTrust-HullScan software. These functionalities provided by SeaTrust-HullScan will enhance productivities in generating both FE model and Cross section model for H-CSR software (Myeong-jo Son, 2016)

In Shiptec China 2016 (2016), it was reported that CCS is developing a new generation H-CSR software tool, called Compass3D. This software package integrates rapid 3D CAD modeling of ship structures, auto FE modeling, ship stability calculation, H-CSR prescriptive rule calculation and DSA. The CAD/FEM system is developed on the top of Siemens NX platform. 3D ship structure model could be rapidly built by merely inputting key parameters. Any interested cross section and idealization model specified by H-CSR can be generated automatically from the 3D CAD model and be used for prescriptive rule calculation directly. A function of transforming CAD model into FE model which satisfies the requirements of H-CSR is also be provided. It can handle plate seam, bracket toe, hole and stiffener end connection, such as stiffener of transverse web connected longitudinals. It can automatically generate the material, plate thickness, and stiffener profiles, and can automatically import the relationship between structures and compartment, which will be defined in H-CSR DSA.

6.3.2 Aframax tanker modelling for prescriptive rule calculation

The data related to principal dimensions and midship sections of the ship used in this benchmark study were provided by DNV-GL. Figure 27 shows the midship section of this ship. Thanks to the data, the committee members generated structural models by means of CS tools and calculated midship section modulus and ultimate strength capacity of the subject ship. These calculation steps are performed at the beginning of the design stage, and a huge amount of calculations, such as local scantling calculation, direct stress analyses with finite element model, fatigue strength calculations with very fine mesh finite elements etc., normally follow this initial steps in order to have the design project approved by the CS. BV, CCS, CSRS(ABS/LR), DNV-GL and ClassNK provided H-CSR prescriptive rule calculation software tool in order to perform this study.

Starting from the data provided by DNV-GL, the committee members created the midship section of this tanker using the different CS tools provided by the aforementioned CS. It is worth pointing out that the committee members didn't attended any course or received any specific training in order to use these software tools. Nevertheless, the user-friendliness of the tools interface, the well-organized manuals of the software tools, and the support of the CS allowed the members to obtain the results presented in Table 13. It is advised that well experienced designers, surveyor, expert software developers in CS may obtain different results.

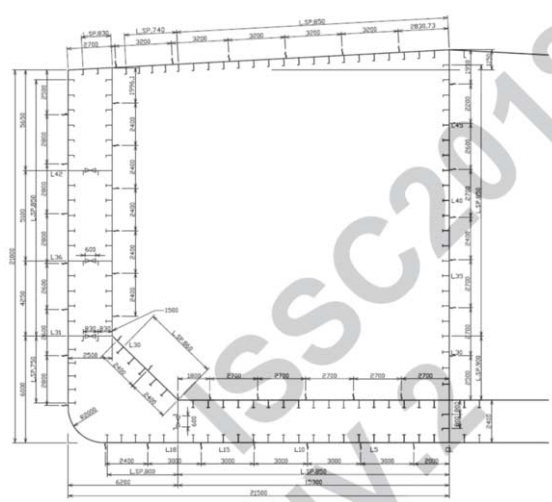

Figure 27: Midship section of template aframax tanker drawn by the committee members

Table 13: Comparison of first output from H-CSR software

Software Name	Template Ship	Mars2000	COMPASS-SDP	Prescriptive Analysis		NAUTICUS	PrimeShip Hull	MAX	MIN	MAX-MIN
Classification Society	(Template)	BV	CCS	ABS LR (*)	ABS LR (*)	DNVGL	NK			
Section Modulus										
Cross Sectional Area, Total	1.00	1.00	1.01	0.99	1.00	1.00	1.00	1.01	0.99	0.02
Actual Hull Iy	1.00	1.00	1.00	0.99	1.00	1.00	1.00	1.00	0.99	0.01
Neutral Axis	1.00	1.00	1.00	1.01	1.01	1.00	1.00	1.01	1.00	0.01
Actual Hull Iy/z at Bottom	1.00	1.00	1.00	0.99	0.99	1.00	1.00	1.00	0.99	0.02
Actual Hull Iy/z at Deck	1.00	1.00	1.00	1.00	1.00	1.00	1.00	1.00	1.00	0.00
Ultimate Bending Capacity										
Hogging (Mu)	1.00	1.00	1.00	0.99	1.01	1.00	1.02	1.02	0.99	0.03
Sagging (Mu)	1.00	1.00	0.99	1.01	1.02	1.00	1.02	1.02	0.99	0.03

*: Data input and calculation were carried out by separate two parties

Hereinafter, the results obtained by the committee members are summarized and discussed. Even if a detailed cross-checking of the input data should be performed to verify in detail their accuracy, cross checking the outcomes of the analysis, reported in Table 13, we notice that there are very little differences among the CS software tools. For instance, the difference in section modulus ranges between -1.5% and 1%. Nevertheless, this small difference may affect the results obtained in the following steps of the structural analysis and we recognize that it may not be satisfactory for structural designers, shipyards and surveyors. Indeed, the reproduction of calculation is not guaranteed if the ship's data are re-input to perform the structural assessment, or an existing ship needs to be classified under a different CS.

Moreover, the compliance of the structural assessment to the H-CSR is based on the outcomes of the calculations performed with these tools. Different input data can lead to different final structural scantling of the ship under design. We think that the difference in the obtained outcomes may be arisen from uncertainty of data input, such as detailed location of longitudinal, start end point of knuckle or curve of outer end of inner bottom plate etc. Some software packages support user friendly input and semi-automatically definition of the coordinates of the longitudinals, but these supporting functions made it difficult to adjust input data and brought small differences between the software. We found different input methods of size for T profiles or longitudinal stiffeners, face plate thickness is neglected in the T profile web height or included. For cut-out modeling on section modulus calculation, in some software tool environments, the user is able to directly model cut-outs while other software packages need one plate to divide the strakes. Specific know-how for each software is necessary and this may reduce the willingness of the users in the tool selection or change. From the trying out the software packages and the result comparison, and a common user interface of input data should be suggested for all designers belonging to shipyards, and know-how of using and input software shall be shared among all users.

The calculation method of hull girder ultimate capacity is described in Part 1 Chapter 5 Appendix 2 Hull Girder Ultimate Capacity of the H-CSR Rules. Because input data was longitudinal members on midship section and not 3D FE model, incremental-iterative method was carried out as described in the Rules. The section areas calculated using each software tool varied within 1% (see Table 13), but the results of ultimate bending capacities varied up to 2%. The differences in the outcomes might be generated by the detailed calculations included in the software, such as step calculation division, peak findings and so on. And detailed programming technics are not shown in the H-CSR. Therefore, as H-CSR software providers, CS are suggested to open the methodologies implemented in the tools and cross check these among the different CS.

Even if these calculations are performed in the first steps of the structural design, main dimensions, characteristics, compartment data, and all longitudinal members are required to be input. Once these data have been input, loads and local strength calculations are simultaneously calculate based on the H-CSR Rules. Then, three-dimensional models are created in the software

environment and direct strength analysis can be performed in the following steps. This means that the committee members input almost all data for local strength calculation by themselves and found that there are still small differences on the outcomes from the black-box. From the experience acquired in this study, opening detailed calculation procedures implemented in the software packages and not shown in the H-CSR booklet will be very helpful for all designers and surveyors. A thorough discussion and enhancement of calculation procedures on an open platform for all structural designers will bring superior design bases on the H-CSR.

6.4 Industry point of view

Due to the implementation of H-CSR, the shipbuilding industry faces new challenges requiring higher demand on resources and standards in order to design ships that comply with the new rules. This can lead to the increase of hull structure weight. Rather than increasing the man-hours at the construction site, the extent of coverage in structural analysis at the designing stage has mostly increased. Furthermore, the come-into-force of the new rules has dramatically increased the overall amount of structural details which need to be assessed. Consequently, the amount of structural analysis that should be made at the designing stage has significantly increased, and this has extended the design process. As a result, it has been more difficult than before to supply new ships to the ship owners in a timely manner. With regards to the increased design cost due to the increased designing work, it may be unavoidable that part of this cost growth is reflected in ship price, generating new problems for the industry as a whole.

The purpose of the H-CSR software tools provided by Classification Societies is on one hand to check the conformity of the shipyard's design results with the H-CSR. On the other hand, Classification Societies should recognize that it is also a tool for shipyards and designing companies for designing H-CSR compliant ships. Therefore, the software should satisfy the following conditions (Shibasaki, 2016):

- Ease of inputting design information, visibility of the information, and ease of modification of inputs;
- In respect of structural analysis, full functions for creating the analysis models satisfying the rule requirement;
- Calculation time without causing tediousness;
- In respect of output, ease of visual checking of results;
- Particularly for the display of the dominant loading case;
- Display functions for deformation plots and principal stress;
- Comprehensible reporting capabilities.

This report shows the first stage of the use of H-CSR software. Six different committee members input dimensions and local scantling data, created a 2-D structural model for longitudinal strength calculation and compared the outcomes of the simulations. Each H-CSR software tool offered by the Classification Societies has different input methodologies, different operational ways and different output formats. This implies that there are difficulties to directly compare input data and results from the software tools. This may explain the little discrepancies in the result of this study, discrepancies that have been obtained even if the committee members input the data from the same template of an Aframax tanker design. The H-CSR software with common methodology for data input, modeling, interface and output evaluation might be more expected to decrease slight disharmony of result and furthermore work hours.

Moreover, industries highlight the need of support, not only in checking the compliance to the rules, but also in the optimization of the ship design, in order to mitigate the impact of the rules in particular on new ships weights and costs. Andric et Al. (2016) investigated the possibility of optimization of design introducing as variables not only the scantling but also compartments geometry considering its influence in strength and in loads distribution. Since classification

societies software are mainly closed, the proposed approach, based on in-house developed modules, takes few advantages from dedicated tools capabilities. In this scenario, even not considering optimization functionalities directly implemented in classification societies software, a future further development of input – output functionalities, may become an important goal to be pursued.

6.5 Conclusions

Over the last few decades, Classification Societies have provided shipbuilding industry, surveyors, and consultants with software tools, and most of these have had a significant and positive impact on the shipbuilding industry. CSR-OT and CSR-BC were implemented as separate rule sets in April 2006, these rule sets already had many load cases and complex evaluation formulae which required specialized CSR software. In January 2015, H-CSR brought an enormous amount of load cases and complex formulae for the design of new tankers and bulk carriers. This implies that nowadays there is no way to design these types of ships without specialized H-CSR software tools.

There are some H-CSR software packages already offered by Classification Societies which are used in actual ship design. In this study, the committee members used five different H-CSR software tools, thanks to the cooperation from Classification Societies, and the fundamental function of input structural model and results obtained from several software tools were compared. An Aframax tanker was used as template ship. Six different committee members input these data in the software tools in order to model the midship section of the ship and perform some first analysis according to the H-CSR rules. The results obtained from software were almost same, but differences in the input methodologies and modeling techniques of structural details, viewings, result outputs generated some difficulties in obtaining close numerical results and comparing these outcomes. This might also occur in the actual ship design and the H-CSR has forced huge efforts and challenges for the users, increasing the design time and cost of the new ships. Therefore, an improvement of the software tools with a cooperation of Classification Societies should be expected right away.

Since the assessment criteria stated in the H-CSR are recognized by all the IACS Classification Societies, it is expected that, in the future, they will be extended to a larger range of ship types. Moreover, working on H-CSR tools, Classifications Societies developed interesting functionalities for assessment of prescriptive requirements, data exchange, modeling, meshing, load case management and results analysis whose applicability may be already easily adapted on other kind of vessels.

The almost parallel developments of harmonized rules and software tools for their application has to be considered as a good example of integrations between research, regulations and practice. The advantages are not only for the final users, designers and surveyors, but also for the rulers who, thanks to well-timed feedback, expect to bring a stronger rationally based rules sets evaluating also the effects of requirements on the design with their continuous efforts.

7. LIFECYCLE DATA MANAGEMENT

Current trends in the maritime industry, in particular increasing digitalization and automation, mean that there is a need to take a more holistic approach to include the entire lifecycle of a vessel, embracing shipbuilding and shipping. The industry is increasingly demanding more environmentally friendly solutions, combined with greater efficiency and easier diagnostics and maintenance of equipment and systems. Data exchange and the availability of data both onboard ships and ashore will be of increasing importance.

Lifecycle management is key from design to the end of a ship's operating life and becomes an increasingly important issue in industry due to various reasons. Operating costs determine a big part in the financing of a ship and thus need to be minimized as far as practicable. On the other hand, from an environmental point of view, the use of resources during production of the

ship and of the production for the fuels required during operation is becoming key interest as soon as alternative fuels (other than conventional liquid fossil fuels) are used. Moreover, data integration from early design to dismantling of the ship is expected to save time and costs in the future. A second big issue in Lifecycle management is the data integration from early design to dismantling.

As a result, data integration became more and more a yard specific issue. Finally, there is also a trend towards smart sensors as part of digitalization. This chapter is divided in three sections entitled Tool development, Data interchange and standards and finally Structural and system health monitoring tools.

7.1 Tool development

It has been shown that leading shipyards carry out their own designs with a huge variety of design tools. The integration of such design tools in the design process (including planning and production) is not an easy task and different handicaps must be tackled today. Two main philosophies can be observed: an "all in one provider" for a number of tools integrated in to one big package (e. g. AVEVA Marine, CATIA, SENER Marine) or the use of specialized tools (Best in Class) with higher integration efforts to be covered by shipyard IT-experts. Both philosophies have advantages and drawbacks and each shipyard has to decide on their optimum approach. In contrast, smaller shipyards often outsource the design and/or work with specific design offices.

The scope of integration is a bigger challenge and not realized in many cases. Indeed, many independent challenges (hydrodynamic optimization, intact and damage stability, strength and vibration assessment, hull fairing, etc.) solved by CAE software's in early design stage and requirements for subsequent detailed design and planning purposes as supported by ERP software's do not actually always allow for a fully integrated design process and data handling. However, first steps have been taken by the industry to tackle these challenges.

Wagner, et al. (2015) present a IT solution that might work in the short-run, they give an overview on Enterprise Architecture Management (EAM) and discuss the application of the methodology in the context of shipbuilding (Product Lifecycle Management) PLM illustrating the advantages but also the main challenges. EAM shows a large potential based on the integrated management of the different architectural layers and helps to manage the change. The analysis provides the best support for the business processes but also to react to customer initiated changes to these processes.

Similarly, Thakker, et al. (2015) illustrate the implementation of 'One Portal' as a single source for all information that is relevant for an employee working in a shipbuilding organization. It should facilitate an employee entering or working in an organization to exactly navigate or search for their processes and go through the work instructions and training material relevant to their process tasks. Such information, which is spread across different applications is becoming available within few steps (or clicks). This work announces a potential increase of 18% in efficiency of finding the information.

Roth (2016) presented a sub-project of Siemens PLM Software to support shop floor workers with a tool that provides the backflow of information into the PLM system in an open and lightweight way. The demonstrator aims at the individual manufacturing industry, such as shipbuilding. One of the prerequisites was to enable partners to update their heterogeneous software systems with as-built shop floor information. Also, a benchmark of different ways to assess the possible methods was demanded. The concept of the software is presented as well as the valuation model for the comparison of PLM-supported process landscapes - especially regarding the data formats being used and the reduction of iteration cycles between shop floor level and construction department. Production Planning and the simulation of production processes are well under way in the maritime industry. However, a serious gap can be identified between

those data needed for simulation and those provided by the various design tools. The industry is currently not able to provide a proper flow of information without such gaps in the processes.

Addressing this issue, a potential solution has been presented by Bruun Ludvigsen et al. (2016). This paper proposes a digital twin simulation platform, "Nauticus Twinity", with the vision of providing a more efficient verification scheme for the maritime industry. A digital twin of a vessel consists of a number of simulation models that are continuously updated to mirror its real-life twin. Combining existing technology through implementation of Functional Mock-up Interface (FMI) enables a platform for collaborative simulation and integration of complex systems. A key feature of the simulation platform is the open architecture allowing integration and co-simulation of models developed by DNV-GL and partners. The developed platform facilitates new tools for design, classification, verification, commissioning, condition monitoring, and decision-making throughout a vessel's life cycle. This development focuses on co-simulation and use of digital twins for the new build phase and includes an example of how Nauticus Twinity can improve the commissioning and the verification process for complex integrated systems.

Life cycle management can be approached from three different perspectives: Financial, environmental and customer care including data handling during operation. For decision-making purposes, CAPEX (capital expenditure) as well as OPEX (operational expenditure) must be considered during the design phase of a new vessel. Increasing attention on operating costs has led the builders of complex ship types to assess the operating costs in early design stage (beside typical challenge of offering best price in just designing and building the vessel).

From an environmental point of view, reduction of energy and related GHG-emissions is on the top of the agenda. Other emissions like SOX, NOX are under discussion since many years through the introduction of Emission Controlled Areas. The release of particular matter is getting in focus in ports. For an assessment of the environmental impact, existing methodologies need to be adapted for needs of the maritime industry. Simulation tools for life cycle performance are partly used in large yards and with a focus on structural performance. Systematic life cycle performance assessment is carried out only by leading yards for individual components as well.

Cepeda, et. al (2017) presented a tool development to improve the operating life of a ship' fleet through the use of slow steaming strategies to reduce the operational cost and the emissions. The study proposes a simulation model considering historical data of a bulk carrier's fleet composed by 13 ships from a unique ship owner where the actual navigation condition is compared with a slow steaming and an ultra-slow steaming strategy of navigation. This model considers the speed, fuel consumption cargo transported, and particularly the CO_2 and SO_X emissions. The paper shows that SS has reduced emissions by around 22% over 1 year fulfilling the target of IMO, and savings in operational costs, considering fuel consumption and emissions (CO_2 and SO_X). The use of this tool can help to simulate scenarios with historical data, assisting ship owners in making decisions about the number of ships in their fleet and establishing best operating strategies.

European projects like InterSHIP, BESST, JOULES and THROUGHLIFE have led to significant improvements in larger industry, however smaller companies are lagging behind. There has been encouragement in the industry to integrate the "Life Cylce Analysis in 7 days" along with the "Design in 7 days", so that a complete analytical overview of the ship would be obtained even during the design phase of the ship. However, integration of design tools based on a life cycle management approach is not available yet. Challenges arising from the introduction of new maritime products and small series (complex prototypes) are to be overcome by the industry. Design Tool Integration has been on the agenda continuously, whereas additional life cycle thinking has attracted interest more recently.

7.2 Data interchange and standards

The capabilities of a Ship Design (SD) or CAD (Computer Aided Design) system to import and export data from or to other systems, is nowadays a decisive factor for the penetration and success of such tools in a highly competitive software market. The design of a ship may include several gigabytes of data regarding the ship geometry, structures, equipment, hydrostatics, hydrodynamics and maneuverability, which is processed and represented by different SD or CAD systems, with different data input/output formats, protocols and standards. Despite the differences between systems, the need to communicate between them, has motivated an intensive research on ship data interchange and standards in general, and particularly on ship structural data. The current section describes the latest research on this topic during the last three years.

Lukas, et al. (2015) discuss the potential of 3D data in the ship lifecycle. They study the use of 3D data in various phases of the ship lifecycle, by compiling information among 17 shipyards and maritime suppliers in Germany. The following interesting results are highlighted:

- During the design phase, the 17 companies use 18 different 3D tools with possible different data format.
- AutoCAD™ is still the most used CAD application among these companies
- 75% of the participating companies see an increasing demand for exchanging 3D data between different systems, internally or with external partners

These results highlight the importance of 3D data exchange between CAD systems, and the authors of the study give special importance to open formats and interfaces. The open formats, IGES, STEP, VRML97, X3D, JT and 3DPDF, currently available in the market, were compared using twenty performance criteria. The results have shown that if only a visual representation is necessary, VRML and X3D can be recommended as well as JT. If additional product data such as Product Manufacturing Information is necessary, JT is the clear winner of the benchmark. The success of the X3D format resides on its web version, the X3DOM, which allows visualizing X3D models in common web browsers without any plugin. However, for the case of the JT format, domain-specific specifications are still required.

One of the subjects considered very important for the data exchange between systems, is the simplification of the data to an adequate level of detail depending on the purpose of its use. (Kwon, et al., 2015) present and discuss in detail the simplification of feature-based 3D CAD assembly data of ship and offshore equipment. They also highlight the importance of 3D CAD systems in the process of design, production and delivery in shipbuilding industry. Shipyards and equipment suppliers have different needs with regards to the complexity of 3D CAD data. In general, equipment suppliers create 3D CAD data with a high level of detail (LOD) in order to manufacture the equipment.

On the other hand, shipyards focus mainly in installing the equipment provided by the suppliers, and therefore need to make simplified 3D CAD data to reduce the amount of data to be stored and manipulated in large 3D CAD models. In the study, the authors propose a new evaluation metrics considering geometric and non-geometric information, such as feature volume, ports and outer-boundaries (the modelling requirements of the shipyards), and the characteristics of assembly data. They implemented a simplification system based on the evaluation metrics, and the data to be stored was reduced to at least 25% of the original 3D CAD assembly data, while ports, outer boundaries, and connectivity between CAD parts were maintained. Although the results were good, the authors recognize that there is still work to be done on the evaluation of the quality of the simplified model and on the different connectivity types that are considered in assembly models.

One of the most popular data format in Maritime Industry is the ISO 10303 (STEP) – AP218 product data exchange files. In this case, the standard defines an agreed-upon syntax and struc-

ture of 3D modelling constructs and annotations for tolerances and dimensions so that all participants in the manufacturing supply chain can understand each other's models. The STEP AP specifies its information model in EXPRESS modelling language, defining entity-attribute relationships. Lipman and Lubell (2015) discuss the conformance of software applications to the STEP standard, which presents two main challenges: (1) the gap between product design concepts, as presented to software developers, and the concepts in the data model defined in the standard; (2) the correct implementation of the semantics as defined in the standard into the software application.

In order to overcome these challenges, the use of the PMI (Product Manufacturing Information), whose representation is specified in ISO 10303 Standard, is recommended. The PMI consists of a set of annotations and attributes, such as geometric dimensioning and tolerancing, surface texture specifications, finish requirements, process notes, material specifications, and welding symbols, associated with CAD model edges and faces in order to define product geometry and specifications. Lipman and Lubell (2015) show that correct implementation of PMI representation and presentation in STEP files will facilitate the automated-downstream consumption of PMI. Currently the PMI is only implemented in AP203 and AP214, but it is expected and desirable to be expanded to AP218 in a near future.

In the last three years, research of data exchange and standardization as focused also on database systems for data management and visualization. The AVEVA's Asset Visualization is one of such tools, described by Thomson and Gordon (2016), which provides a view of the entire digital asset from the 'as design' to the 'as-operated' phases throughout the life cycle of the ship. The philosophy behind the system is that asset visualization is more than the realistic representation of physical objects. It must concern also the visualization of abstract data associated with the engineering asset. With this in mind, the system captures all data and documents regardless of their source format or authoring systems, classifying and organizing them according to business processes that will consume it. This is achieved by the so called AVEVA NET Gateways, which provide interfaces to these information sources, validate data against defined project data standards and produce web-viewable renditions of documents and drawings.

Another tool developed by the SHIPDEXTM Protocol Maintenance Group, is the Shipdex Viewer. The SHIPDEXTM, described by (Vatteroni, 2016), is an electronic and standardized data format based on XML schemas. It results from a customization for shipping community of the S1000D international specification for the production of technical publications. The SHIPDEX stores ship data in modular units produced in XML format, according to specific XML schemas that are provided together with the specification. It supports links to external documents with illustrations, drawings, multimedia objects in different formats, and it is composed by the following "information sets" regarding the ship lifecycle: (1) Description and operation; (2) Maintenance procedures; (3) Troubleshooting; (4) Illustrated parts data (IPD); (5) Service bulletin; and (6) Maintenance planning. All the data is stored and managed by the so called Common Source Database (CSDB), which is accessed by a proprietary developed user-interface.

A slightly different approach is presented by Morais et al. (2016). They claim that the issue of the data exchange between systems, depends on the ease with which programs can be integrated. The way a software is designed plays a key role in determining that ease of integration as well as future flexibility, and the use of an underlying open architecture is the only way to achieve this goal. This requires an open architecture base platform over which dedicated software is developed. An example of this is given by the Autodesk/SSI shipbuilding software solution which builds on top of the SQL and AutoCAD platforms, on top of which sits SSI's ShipConstructor Marine Information Model (MIM) plus other tools, on top of which sits ShipConstructor and other applications, on top of which sit other applications connected via what SSI calls the SSI Enterprise-Platform.

7.3 Structural and system health monitoring tools

The process of implementing systems able to detect damages on engineering infrastructure is referring to structural health monitoring (SHM). A damage is defined as changes of the material and/or its geometric properties. Several novel methodologies and SHM technologies has been developed recently and latest research on this topic are presented below. Both, cost reduction and prolongation of life cycle of structure are the two main objectives focused by this technology.

An overview of lifecycle management processes for machinery and equipment is provided in Koch, et al. (2015). In this paper, a methodology for building a full ship risk model and decision support system is suggested. Specifically, the collection and storage of measurements such as pressure, flow, temperature, combustion performance, and vibration are elaborated. These are combined with data obtained from robotic platforms and voyage recordings. Accordingly, an innovative data management system for ship machinery using a catalogue data model has been suggested by Taheri, et al. (2015). There, different types of databases are compared, with similarities and differences explained. A ship case study where raw measurements are stored in a suitable database are included. There, inputs from multiple sources are stored and combined before being fed to data analysis tools. Through the presented case study, graph type databases proved to be the most effective choice for marine condition monitoring applications, using both static and dynamic input sources.

The study by Ravina, (2017) analyses a concept design of an autonomous mechatronic unit for inspection of holds, is oriented to inspection of the interior walls of vessels, in particular tanks and holds, difficult or dangerous to reach and requiring a large number of measurements. A concept design of a self-moving unit for inspection of holds and tanks of cargo ships is proposed: feasibility and applicability are shown in this study. This system is not designed for a complete replacement of skilled technicians, but as support of inspections in spaces dangerous or difficult to reach. The study is based on tanker ships, however in many ship type is fundamental to perform periodic inspections to monitor the thickness of the hull, of welding and of metallic walls in general. The different design phases are described in the paper, showing the feasibility of the proposal. The structural parts of the unit are analyzed designing two different geometries, and the support plate is analyzed from the structural point of view with finite elements techniques: it is composed of two parts which are mutually connected in the assembling phase of the robot.

Decò, et al. (2015) develop a risk-informed approach for ship structures that integrates structural health monitoring (SHM) information. Through an application, real-time optimal short-range routing of ships is presented. Decò, et al. (2015) present an approach for the integration of SHM data, through Bayesian updating, into risk real-time assessment of ship hulls. A novel closed-form solution for short term statistics based on Raleigh prior distribution is developed and compared with a simulation-based technique. Then, an approach for real-time optimal routing of ships has been presented. Two-and three-objective optimization problems are solved by minimizing the estimated time of arrival (ETA), total risk, and fuel costs. The results are shown in the form of Pareto-optimal sets. Mission profiles including total risk, reliability index, fuel cost, ship path, ship speed, and cumulative time from departure are obtained for a Joint High-Speed Sea lift. The information obtained from SHM and different sea weather maps are integrated with in the developed optimization framework.

Other studies use finite element method with improvement algorithms to evaluate specific structural elements. An algorithm named as inverse Finite Element Method (iFEM) was developed at NASA Langley Research Centre and used by Kefal et al. to evaluate specifics elements, ships and systems in some of their works. The first study in this area is about the perform displacement and stress monitoring of a typical chemical tanker mid-ship based on iFEM methodology (Kefal, et al., 2016). The iFEM formulation is based upon the minimization of weighted-least-

squares functional and requires discrete strain data obtained from on-board sensors in order to reconstruct the displacement, strain, and stress fields. In-house hydrodynamic and finite element software are utilized for simulating the on-board strain-sensor data in order to represent a floating structure in real sea environment. The results obtained from FEM analysis is utilized as a source to simulate in-situ strain data used in iFEM analysis as input. Finally, iFEM and FEM displacements are compared and the effects of locations and number of sensors on iFEM solution accuracy are discussed. This iFEM algorithm is a very promising system for health monitoring, performing a precise shape- and stress-sensing of marine structures.

An additional (Kefal, et al., 2016) study of displacement and stress monitoring of a Panamax containership is performed based on the iFEM methodology. Several direct FEM analyses of the parallel mid-body are performed using the hydrodynamic wave bending and torsion moments. Then, experimentally measured strains are simulated by strains obtained from high-fidelity finite element solutions. (Kefal, et al., 2016) present three different iFEM case studies of the parallel mid-body are performed utilizing the simulated sensor strains, pure vertical bending case, pure horizontal bending case and pure torsion case. Then, the deformed shape and von Mises stresses of the containership are reconstructed using in-situ strain data obtained from each proposed network of strain-sensors. According to the accuracy of the displacement and stress results, the optimum strain-sensor locations are identified and clearly demonstrated for each iFEM case study. Finally, the numerical results confirmed the robustness of the iFEM methodology for monitoring multi-axial deformations and stresses of a Panamax containership floating in beam sea waves.

The use of finite element methods is deepened by other authors and combined with other methods to get better results. The use of finite element methods is deepened by other authors and combined with other methods to get better results. Yan et al. (2015) combine the Bayesian framework with extended finite element method (XFEM) to provide a statistical approach for nondestructive multi-flaw identification considering uncertainties from modeling errors and measurement noise. Specially, a trans-dimensional reversible jump Markov chain Monte Carlo (RJMCMC) method is employed to draw the posterior distributions of the flaw parameters due to the missing knowledge of the number of flaws. This analysis is in order to monitor structures to detect flaws at an early stage to prevent catastrophic failure.

The Bayesian methods are also used to estimate the fatigue damage present in offshore platforms by Green, et al. (2016). This first involves running a series of Finite Element simulations, thus establishing how the modal characteristics of an offshore structure model vary as a function of its material properties. Data based modelling techniques are then used to emulate the Finite Element model, as well as estimates of model error. The uncertainties associated with estimating the hyper parameters of the data-based modelling techniques are then analyzed utilizing Markov chain Monte Carlo (MCMC) methods. The resulting analysis takes account of the uncertainties which arise from measurement noise, model error, model emulation and parameter estimation. The use of use finite element methods in oil and gas industry is also present as structural and system health monitoring tools. The study of Kefal et al. (2017) investigates the applicability of iFEM, for displacement and stress monitoring of offshore structures for the first time in the literature. Displacement and stress solutions obtained from iFEM analysis are compared to those of reference solutions.

Shen et al. (2015) propose a new damage assessment method for aging offshore platforms based on dynamic tests, it provides information on whether damages occurred between the times of two adjacent measurements. A numerical offshore platform will be used to demonstrate the proposed method, including noisy modal parameters, low damage severity, and spatial incompleteness. The model uses one theoretical improvement is that the requirement for using the stiffness matrix of the finite element model (FEM) to replace the one of the measured models can be ignored in the calculation of the modal strain energy (MSE) of the measured model. The

other improvement is that the influences of the damages accumulated before the first measurement on the damage detection that occurs between the two measurements can be reduced greatly. The numerical studies also demonstrate that the proposed method can localize the damages that occur between the times of two adjacent measurements and evaluate these damages properly, even in spatially incomplete situations.

Moreover, in the oil and gas industry the fatigue-life prediction of offshore pipelines becomes a major issue to ensure the integrity and reliability of offshore pipelines since many catastrophic failures of piping components were caused by fatigue crack growth. Fatigue crack growth of pipelines has been studied extensively by experimental tests. It is well recognized that scale factors and the large amount of costs on the experimental set up are major challenges to conduct a full-scale fatigue test. The adequate confidence to design offshore oil and gas system productions should be built upon a series of preliminary fatigue tests using full-scale numerical simulations. Zhang et al. (2016) make a systematic investigation about the fracture resistance behavior of offshore pipelines containing an elliptical embedded crack under cyclic tension loadings. Extended finite element method (XFEM) is adopted for numerical simulations. The influences of different initial crack length and stress ratio on fatigue crack growth are investigated in detail. In addition, the thorough interpretation and discussion on fatigue response of the flawed pipe lines with the elliptical could be helpful in designing offshore oil and gas system productions.

The structural and system health monitoring tools have not only been designed to prevent failures and to systematize inspections, but in the future for maintaining and increasing oil and gas production. Related to this are studies for exploring the potential for extending the lifetime of offshore platforms by implementation of Structural Monitoring Systems (SMS). The paper by Skafte et al. (2014) use an expansion technique as a first step in the sequence of assessing the actual lifetime of a platform. Mode shapes and natural frequencies are estimated using operational modal analysis. The mode shapes are then expanded by expressing each experimental mode shape as an optimal linear combination of selected modes from a finite element model. The offshore platform of the case study, Valdemar, which is fully instrumented with accelerometers, GPS, strain gauges and wave radars, is chosen as a case study. Results show that the measured response can be expanded with high precision, which provides valuable information when assessing the actual lifetime of the platform. It is also shown that the expansion technique can be used for assessment of measurement uncertainties.

Skafte et al. (2017) study the offshore structures by the continuously dynamic loading from wind and waves to which it is subjected. The monitoring the vibrations of the structure using real time operating data enables an assessment of the general health state of the structure. Skafte et al. (2017) propose a method for full-field strain estimation by combining experimental measurements with a well correlated Finite Element (FE) model. This study presents how the response of an offshore structure can be divided into two parts: The low frequency response from the quasi-static effect of the wave load, and the high frequency response from the dynamic properties of the structure. It is further demonstrated how strain histories below the waterline can be estimated using accelerations measured on the topside of the structure. The low frequency response is expanded using the quasi-static Ritz-vectors, and the high frequency response is expanded using modal decomposition. This work should be seen as a first step towards a general framework for fatigue monitoring of offshore structures. The work shows promising results regarding estimation of the strain history in unknown points.

The INCASS (Inspection Capabilities for Enhanced Ship Safety) EU FP7 project dedicated a work package to the development of a database system product for lifecycle data management. (INCASS, 2014b) report provided an overview of system architecture and general workflow supported by the developed database system, including descriptions of main applications and components. Specific applications focusing on the handling of machinery and equipment were additionally developed. An additional (INCASS, 2014c) project report elaborated on the data

exchange capabilities of the developed software along with details on the implementation of the OpenHCM format for the exchange of structural condition monitoring data and the derivation of the respective MCM format for machinery condition monitoring data. Accordingly, (INCASS, 2016a) presented the functions that have been implemented to allow for ship-to-shore data transfer. Finally, in (INCASS, 2016b) the design of the Central Stochastic Database (CSD) is presented, following the description of individual tools provided in previous deliverables. The latter report illustrated the data flow between other INCASS tools and the CSD.

8. OBSTACLES, CHALLENGES AND FUTURE DEVELOPMENTS

The Committee see the following important trends in ship and offshore structural design based on what we have seen in the recent years: (1) IACS Common Structural Rules for Bulk Carriers and Oil Tankers, (2) IMO Energy Efficiency Design Index (EEDI), (3) new design paradigm, (4) accurate optimization models including FEA, (5) analytical methods for impact analysis, (6) complete risk assessment frame-work for ship accident, (7) mega container ship, (8) unmanned ships. These concepcts can also identify areas of future industrial and / or research developments. Based on these trends, we see the challenges and obstacles described in more detail below.

8.1 Common Structural Rules for Bulk Carriers and Oil Tankers

In July 2015 the Harmonised Common Structural Rules for Bulk Carriers and Oil Tankers (CSR BC&OT, HCSR) suggested by the International Association of Classification Societies (IACS) entered into force (IACS 2014). The HCSR replaced the separate rules set of the Common Structural Rules for Bulk Carriers (CSR-BC) introduced by IACS (2012a) and the Common Structural Rules for Double Hull Oil Tankers (CSR-OT) IACS (2012b) and harmonized the two rule sets into one. Furthermore, the HCSR introduced some new requirements. In the previous rule set initially implemented in April 2006, the rules were developed by separate teams working on either the ones for bulk carriers or the ones for double hull oil tankers. Such an approach necessitated the harmonization of different rule sets, which should be based on the same fundamental structural strength theory and natural phenomena. To be more precise, HCSR are applicable only for double hull oil tankers that have a length of more than 150 meters. For HCSR, though applicable for bulk carriers, it is important to note that these are suggested for bulk carriers exceeding a length of 90 meters and can be either single or double skin. The following ships, though are classified as bulk carriers by designers, need not be designed in compliance to HCSR: Ore-Bulk-Oil Carriers or OBO Carriers, Combination Carriers, Bulk carriers carrying woodchips or similar cargo, Bulk carriers with self-unloading facilities. In the above cases, HCSR compliance is not required, as these are to be designed following the rules of the authorizing Classification Society. All IACS member Classification Societies are required to enforce the HCSR requirements after they are officially in effect on 1 July 2015.

Referring to the challenges that the HSCR application will need to address, Shibasaki (2016) suggested that “Due to the implementation of HCSR, the shipbuilding industry faces new challenges requiring higher demand on resources and in standards in order to comply with the new rules compared to the former CSR, which can lead to the increase of hull structure weight. Rather than increasing the man-hours at the construction site, the extent of coverage in structural analysis at the designing stage mostly increased, and the parts and regions subject to detailed structural analysis have dramatically increased. Consequently, the amount of structural analysis that should be made at the designing stage has significantly increased, which prolonged the design period. As a result, it has been more difficult than before to supply new ships to the ship owners in a timely manner. As for the cost increase due to the increased designing work, it may be unavoidable some of that increase is reflected in ship price, thus becoming a problem for the industry as a whole.”

Since the HCSR has focused on oil tankers and bulk carriers, it has allowed for the time and scope to define permissible limits of loading, and formulas to establish the appropriate scantling

criteria, depending on all loading patterns that can be considered in bulk carriers and oil tankers of all configurations of tanks and holds. This also includes all possible combinations for alternate hold loading in case of bulk carriers.

Considering the above, HCSR are more demanding that the replaced rule set. The scope of the FEM, ultimate, buckling and fatigue strength analyses required increased considerably resulting in increased ship safety. The analyses are to be directly performed for the whole cargo holds/tanks region of the ship while in the previous two rule sets such analyses was required mainly for the midship region. Moreover, the previous rules only provided for snippets of instructions for modelling the ship hull for finite element analysis. Moreover, HCSR has included detailed instructions of the procedures to be followed to model each part of the hull also following industry standards on checking the adequacy of calculated scantlings by finite element analysis. Modelling and correct meshing of end connections is very important in obtaining correct results, hence the new rules have defined methods and boundary conditions to be maintained while modelling the hull girder and local strengthening structures.

Moreover, the calculation workload necessary under HCSR requirements will be at least threefold in comparison to (former) CSR requirements. HCSR assures comprehensive assessment of the entire ship hull structure. The replacement of CSR by HCSR requirements will no doubt improve bulk carriers and tankers hull safety in terms of structural strength, but also generate immense workload in the design process. Consequence assessments studies performed indicated that CSR requirements are slightly more demanding compared to the previous rule sets while also increasing the scantlings will not be greater than 3%, in general (PRS 2017). In this respect, unifying and harmonizing the technical requirements of the CSR for tankers and bulk carriers, HCSR incorporate new requirements for more comprehensive structural analysis at the design stage, including FEM analyses covering the entire range of cargo hold structures, as well as new formulae for buckling, fatigue, and residual strength criteria to enhance safety and reliability.

HCSR requirements also entail the development of sophisticated IT tools. Classification Societies have developed software platforms for calculating hull strength of bulk carriers and tankers in line with the projected IACS HCSR. Computer programs are used to calculate thickness plating and plating stiffeners cross section, to perform zone strength FEM analysis, calculate fatigue life, and resistance to buckling and hull design load during hull bending. The majority of Classification Societies have started developing own computer systems which will allow to effectively carry out analysis required by HCSR in order to assist ship designers with the design of hull structures. The developed software can be used to prepare technical reports and to verify the compliance of designed vessels with international standards. The methods of finite element model analysis have also been incorporated into the procedures followed by the FEA modules used by Classification Societies. Software packages facilitating efficient generation of FEM meshes, the input of local and global loads to FEM models, “automatic” assessment of resistance to buckling of the hull structure and the calculation of geometric stress for fatigue life are becoming indispensable.

Following the above, HCSR currently receive continuous feedback from industry practical working conditions. The new goal-based HCSR mark the beginning of changes that should improve ship structural safety and the need for designers, Classification Societies, shipyards and the industry to expedite efforts and catch up with scientific progress and public expectations. Classification Societies need to endeavor and be ready to share knowledge and experience with other stakeholders of the maritime market. Following the first version of the HCSR issued in 2015, the HCSR was updated to include a corrigenda and an urgent rule change notice, which were published and became effective on 1st July 2017.

Further to the above, updating of the HCSR is ongoing. Issues to be discussed are related to the interpretation of thickness effects in the simplified fatigue strength calculation, the minimum

still water bending moment for yield strength evaluation and the fatigue strength evaluation. Following a private communication with an IACS member (IACS, 2016) "Since the adoption of the Common Structural Rules (CSR), IACS has been committed to transparency and consistency in the implementation and application of the Rules. The IACS CSR Knowledge Centre (KC) was established to facilitate this." The KC had been quite useful across the industry including shipbuilders and Classification Societies, since it allowed for access to common interpretation and feedback from all relevant industry stakeholders. Eventually, the IACS CSR Knowledge Center (the KC) was not available since August 2016 (IACS, 2016):

"*Since the adoption of the Common Structural Rules (CSR), IACS has been committed to transparency and consistency in the implementation and application of the Rules. The IACS CSR Knowledge Centre (KC) was established to facilitate this. After a careful review of the input from the industry, IACS has decided to make the KC an internal database available to IACS members only. This decision was taken to avoid misunderstandings and early application of proposed Rule Changes"*.

The industry will be able to raise questions and provide input to any IACS member, and IACS members will document questions and answers to the KC to continue to support uniformity and consistency. Proposed Rule Changes will follow the formal Rule Change Proposal Process. As you are aware, this process provides industry with two opportunities to comment, one directly in response to IACS consultations and the other by way of input to the technical committees of IACS' Member societies."

While at the moment the IACS CSR KC website is not available to non-IACS Members, the new rules apply to all bulk carriers over 90 meters long and all oil tankers over 150 meters long contracted on and after July 1, 2015. In this respect, a future challenge remains with regards to the ship structural design and optimization of the Common Structural Rules for Bulk Carriers and Oil Tankers.

8.2 Energy Efficiency Design Index (EEDI)

The methodology of ship structural design to optimize the Energy Efficiency Design Index (EEDI) was developed since the reduction of CO2 emissions has been the key target since IMO's Marine Environment Protection Committee (MEPC) published its findings in 2009 (IMO 2009a). At the same time, IMO published a report IMO (2009b) containing: (i) present and future emissions from international shipping; (ii) the possibilities for reduction of these emissions through technology and policy; and (iii) impacts on climate from these emissions. A number of measures resulting in technical and operational reductions were made mandatory in 2011. In this respect, IMO working group suggested that all new ships above 400 GT would have to implement the new EEDI in the near future.

The adoption by IMO of mandatory reduction measures for all ships from 2013 onwards will lead to significant emission reductions. Among these and nearly all new built ships have to conform is Energy Efficiency Design Index (EEDI). The international maritime community expect that the EEDI will result in more energy efficient ships, in reduced emissions of Green House Gas (GHG) emissions, in environmental effectiveness and in significant contribution by shipping industry to the global efforts to stem climate change. This provides a method of establishing the minimum efficiency of new ships depending on their type and size. With increasing competition, the key to companies' survival will be to design and operate the ships efficiently. The following year, IMO published a report IMO (2014) which provides an update of the estimated GHG emissions for international shipping in the period 2007 to 2012.

IMO accepted that such an index should reflect only the technical aspects such as the optimization of engines, hull and propeller or the use of non-fossil fuels, and not the operational or commercial aspects. According to IMO (2017), the EEDI formula is not applicable to all ships. Indeed, it is explicitly recognized that it is not suitable for all ship types (particularly those not

designed to transport cargo) or for all types of propulsion systems, (e.g. ships with diesel-electric, turbine or hybrid propulsion systems will need additional correction factors). Indeed, the first iteration of the EEDI methodology has been purposefully developed for the largest and most energy-intensive segments of the world merchant fleet and cover the following ship types: oil and gas tankers, bulk carriers, general cargo ships, refrigerated cargo carriers and container ships. For ship types not covered by the current formula, suitable formulae will be developed in due course to address the largest emitters first.

In the current phase designers relied on retrofit solutions in order to achieve slight gains related to ship structural efficiency. In later phases tougher restrictions will be imposed which will necessitate additional changes in the structural design. The potential technologies suggested which may improve the EEDI can be related to: (1) hulls with less resistance and improved steering configurations, (2) more efficient aft-ship, propeller and rudder arrangements, (3) lower energy consumption in main and auxiliary engines, (4) switch from oil to natural gas as main fuel, (5) miscellaneous technologies to reduce minor energy consumers (deck paint, pipe insulation, lighting, air conditioning, etc.), (6) zero or minimum ballast configurations (e.g. by alternative design or ship type), (7) marine fuel cells; and hybrid ships (e.g. wind power, solar panels, and use of light materials, etc.). Following the above suggested options, it would be beneficial to investigate whether the EEDI methodology will influence the ship structural design and related methodologies developed to address such a challenge. That is: ship structural design and optimization for Energy Efficiency Design Index (EEDI).

8.3 The new design paradigm

Today's ship structural design is highly integrated with other design development activities, such as production, costing, quality control, among others. At the same time essential elements of the modern shipbuilding industry are related to environmental concerns, safety, passenger comfort, and life-cycle issues. Within this paradigm shift, the new designs should facilitate the productivity sequence, be cost-effective, incorporate aspects related to safety and environmental considerations while also being functionally efficient. The challenge: provide a new design paradigm that will take into account of the entire life cycle of ship structure.

8.4 Formulation of accurate optimization models including FEA

In order to enable ship global structural optimization in a realistic way, it is still necessary to either use simple tools, like the tools based on prescribed classification society rules, or use a method of problem simplification within the optimization loops in order to reduce the number of degrees of freedom of the original/standard FEM model. The challenge: identify the methods needed to build accurate global structural models in order to solve ship and offshore structural optimization tasks that take into account the FEA; however, without excessive simplification of structural modelling.

8.5 Analytical methods for impact analysis

Several authors have recently developed procedures and tools to evaluate the structural response of ships and offshore structures subject to impacts. These analyses are usually performed using a FE explicit non-linear general purpose software. The high computational cost of these simulations triggered research activities aimed at the development of tools based on analytical methods that allow the estimation of forces and energy developed in ship collisions in a preliminary analysis. Such methods should be able to carry out a fast evaluation of different collision scenarios. This allows the designer to identify the worst collision scenarios and to perform explicit FE nonlinear analysis on the selected case. The challenge: employ analytical methods that allow the estimation of forces and energy developed in ship collisions in a preliminary analysis.

8.6 Development a complete risk assessment frame-work for ship accident

The risk-based design concept has been gradually accepted in recent years. However, it is still at a development stage and its progress is relatively slow. The current research in this subject is mostly focused on the analysis of individual ship or individual accident scenarios. It is necessary to establish a complete risk assessment framework for ship accident scenarios to support risk-based ship design. The challenge: a complete risk assessment framework investigating ship accident scenarios to support risk-based ship design.

8.7 Mega container ship

Mega container ships with cargo capacity in the range of 12,500-22,000TEU provided shipowners with increased earnings due to economies of scale. The latest figures show that the container vessels capacity is set to increase to unprecedented heights (The Maritime Executive, 2017. However, the above expansion is also prone to associated challenges. Among them, structural design and optimization of ever larger container ships is of key importance. De Haas and Burnay (2017) discuss the issues and challenges associated with mega container ships and the actions that can be taken to mitigate the risks associated with designing, building and operating this new class of vessel:

"*The exceptional size of the hull and its inherent flexibility could ultimately prove to be limiting factors for the mega container ship. Issues such as 'springing' or 'whipping' are still to be fully understood and more research and full-scale measurements are required to ensure adequate structural capacity over the ship's lifetime. Relocating the accommodation structure from the stern, to amidships can help reduce the longitudinal bending moments but the naval architect must still resolve related issues such as shaft alignment and manage the deflections that will occur during operation - the larger the ship, the longer the shaft and the greater challenge to ensuring satisfactory shaft alignment. The ultimate hull girder strength could still be limited by the thickness of the steel used as practically, it is very difficult to manufacture mild steel plate much thicker than around 100mm. Areas such as hatch coaming tables, can be very sensitive to excessive forces, especially in bending and hence the natural tendency would be to look at utilizing high tensile steel, but the significant increase in material costs could have a negative impact on the profitability of operating the vessel.*".

According to the OECD International Transport Forum report (OECD/ITF, 2015), efficiency gains from larger ships have been steadily declining – and further increase in maximum container ship size could increase the overall cost of transporting goods. However, with the latest 'mega-ships', economies of scale may have reached their peak. Bigger ships deliver economies of scale at sea, but they also involve greater costs associated with cargo handling, additional investment in ports, and greater concentration of risk. As reported by The Economist (2013) and The Financial Times (2015), global trade growth will be much slower than decades ago. The construction of vessels with cargo capacity of or beyond 25,000 TEUs may be a challenging task in the near future. Research and design work related to the construction of such units may therefore be slowed down or even suspended. The challenge: structural design and optimization of 25,000TEU container vessels. The obstacle: slow down or stop further work in this area (Bonney 2015).

8.8 Unmanned ships

In recent years, a rapid development of technology has been observed related to the emergence of the first unmanned ships or such vessels for which the human intervention during the voyage will be minimal. According to analysts, this may already be the case as soon as 2025. Towards that direction, industry consortia have set a number of key milestones for the development of unmanned ships (Fig. 28): 2020 – reduced number of crews through the introduction of remote support; 2025 – remote-controlled unmanned vessels in offshore shipping, 2030 – remote-controlled unmanned ocean-going vessels; 2035 – Autonomous unmanned ocean vessels (Rolls-

Royce, 2017), explicitly by definition no one is onboard. It is expected that the use of an autonomous vessel would minimize the operating costs of such ships and maximize its capacity (better use of hull shape). Other industry sources suggest that the first autonomous zero emissions ship will be ready for 2010 (Green4Sea, 2017).

Maritime administrations, class societies and designers should already be prepared for the coming challenge. Discussions have been initiated on how today's international rules can be applied to modern technologies and ships that will change the face of shipping. One of the paramount challenges however remains on how to adapt legislation especially related to security issues. It will be necessary, in addition to technological development, to prepare appropriate standards and requirements for maritime safety management. With extensive experience in maritime safety and the knowledge of other areas of the economy, we can prepare for the arrival of a new stage in shipping history. It needs to be investigated whether the existing methods of structural design of manned ships can be used without the substantial changes for autonomous vessels. If not, then it will be necessary to undertake all the necessary work to update and develop such standards. The challenge: ship structural design and optimization for autonomous shipping.

Figure 28: The next steps in autonomous ship development (Rolls-Royce, 2017).

9. CONCLUSIONS

The Committee performed an extensive and thorough analysis of the ships and offshore industry review on design methods over the last three years, which revealed a number of interesting features. In this case, Chapter 2 continues the work on optimization methods, surrogate modelling and variable fidelity approaches. “Design-for-X” (DfX) including Design for life-cycle performance, Design for maintenance & repair and Design for safety remain a strong topic and a summary of the most recent developments related to the design for specific performance aspects has been provided. Following the trends indicated by the work of the previous Committee, DfX is closely related to the current tendency towards goal-based design methodologies in general and risk-based design in more details, also recently endorsed by International Maritime Organization (IMO) regulations.

Related to the most recent updates with regards to the development of the design tools for marine structures, Chapter 3 provides the progress of Computer-Aided Design (CAD) packages for ship design while particular focus is placed on the development of Virtual Reality and Augmented Reality tools and their use in ship design. Additional work performed on new simulation packages for ship structural design and risk-based design software tools is also presented in this Chapter.

Moreover, despite sharing common ground in terms of design methodology principles, the specific particulars of each different offshore structural design together with a strong dependency

on previous specific experience, have led to addressing structural design and associated methods separately for different types of offshore structures. These are addressed in Chapter 4 discussing the topics of design methodology used in offshore structures design, the design challenges and trends, the standardization and asset integrity and maintenance, as well as the design and methodology developments. Moreover, a survey on the use and application of design software used for offshore structures modelling was performed covering an area of major interest.

State-of-the-art vs. state-of-practice was a new theme into the ISSC IV.2 committee's work in order initiate the discussion and bridge the gap in between the research work presented within the committee's remit and the practical applications that may stem out of it. Taking into account that "practice" is the actual application or use of an idea, belief, or method, as opposed to theory related to it, the "state-of-practice" definition provided the best design process which will be also integrated with production, maintenance and repair available in everyday engineering systems. Initially examining the areas of most interest within the last four Committees' work, chapter 5 introduced a way to bridge the gap in between research and applications by suggesting the Theory-to-Practice-Ready Papers (TPRP).

In Chapter 6, the examination of various Classifications Societies software continued to take place following the preceding Committee's work. This time the Committee decided to expand its scope to provide a benchmark study comparing the application of the latest version of the Harmonized CSR of various classification societies in the case of a double hull tanker. While there are difficulties to directly compare input data and results from the software tools due to different input methodologies, operational ways and output formats, this may explain the small discrepancies in the result of this study, even if the Committee members used input data from the same template of an Aframax tanker design. Moreover, industry highlight the need of support, not only in checking the compliance to the rules, but also in the optimization of the ship design, in order to mitigate the impact of the rules in particular on new ships weights and costs. Moreover, working on H-CSR tools, Classifications Societies developed interesting functionalities for assessment of prescriptive requirements, data exchange; modeling, meshing, load case management and results analysis whose applicability may be already easily adapted on other kind of vessels.

Chapter 7 presented the latest developments and trends in the lifecycle management of ships including the updates on tool development, data interchange and standards and structural and system health monitoring tools. Current trends in the maritime industry, in particular increasing digitalization and automation, mean that there is a need to take a more holistic approach to include the entire lifecycle of a vessel, embracing shipbuilding and shipping. The industry is increasingly demanding more environmentally friendly solutions, combined with greater efficiency and easier diagnostics and maintenance of equipment and systems. Data exchange and the availability of data both on-board ships and ashore will be of increasing importance. Moreover, data integration from early design to dismantling of the ship is expected to save time and costs in the future. A second big issue in lifecycle management is the data integration from early design to dismantling.

Finally, the last chapter introduced areas, which will be of particular importance and interest in the coming years. This reflects the continuing efforts on common structural rules for bulk carriers and oil tankers, the Energy Efficiency Design Index (EEDI), the unmanned ships and the mega container ship and the formulation of accurate optimization models including FEA. Additional areas of future scope can be the analytical methods for impact analysis, the development a complete risk assessment framework for ship accident and the development of a new design paradigm considering the entire ship production sequence.

ACKNOWLEDGMENTS

The Committee would like to acknowledge the work provided by Mr. Christos Gkerekos and Mr. Yiannis Raptodimos, research students at the University of Strathclyde, in coordinating references and providing grammatical editing of the report. The Committee members would also like to acknowledge the support of the American Bureau of Shipping, Bureau Veritas, China Classification Society, Lloyds Register, DNV-GL, Korean Register of Shipping, and Nippon Kaiji Kyokai (ClassNK) who provided the software tools for the structural assessment of ship structures according to the Harmonized Common Structural Rules. The Committee would also like to extend its appreciation to the Registro Italiano Navale for providing the data reported in Figure 4.

REFERENCES

Acín, M. and Kostson, E. (2015) Tools and Automation Capabilities for Modeling Marine Structures. In: Proceedings of the 14th International Conference on Computer Applications and Information Technology in the Maritime Industries (COMPIT'15), Ulrichshusen, pp 418-432.

Agusta, A., Thöns, S. and Leira, B. J. (2017) Value of Information-Based Inspection Planning for Offshore Structures, in. 36th International Conference on Ocean, Offshore and Arctic Engineering, Trondheim, Norway: ASME, p. V03BT02A035.

Albright Jr, R. A. (2017) Solving the Drone Data Dilemma, in Redefining Offshore Development: Technologies and Solutions: 22nd Offshore Symposium 2017: Houston, Texas, USA, 02 February 2017. Red Hook, NY: SNAME/Curran Associates, Inc.

Anderson, J. D. and Pickup, M. (2017) Evolving Business Models, Concepts will drive Offshore Recovery, Offshore Magazine. Available at: http://www.offshore-mag.com/articles/print/volume-77/issue-5/upstream-investment/evolving-business-models-concepts-will-drive-offshore-recovery.html.

Andrade Sthéfano L., Gaspar Henrique M. & Ehlers Sören (2017) Parametric structural analysis for a platform supply vessel at conceptual design phase – a sensitivity study via design of experiments. Ships and Offshore Structures. Vol. 12, N. sup. 1. Pp S209-S220.

Andric, J, Piric, K, Prebeg, P, Andrisic, J, Dmitrasinovic, A. (2017b) Structural design and analysis of large "open type" livestock carrier, ICSOS 2017: Proceedings of the International Conference on Ships and Offshore Structures, Sören Ehlers & Jeom Paik & Young Bai (Eds.), Shenzhen, China, 11-13 September, 2017.

Andric, J., Prebeg, P. and Piric, K., (2017a) Influence of different topological variants on optimized structural scantlings of passenger ships, Progress in the Analysis and Design of Marine Structures, MARSTRUCT 2017, Lisbon.

Andric, J., Pero, P., Piric,P., Kitarovic, S., Zanic, V., Cudina, P., Bezic, A. and Andrisic, J. (2016) FE based structural optimization according to IACS CSR-BC. In: Proceedings of the 13th International Symposium on PRActical Design of Ships and Other Floating Structures (PRADS 2016), Copenhagen.

Andric, J., Prebeg, P., Piric, K., Kitarovic, S., Zanic, V., Cudina, P., Bezic, A. and Andrisic, J. (2016) FE based structural optimization according to IACS CSR-BC, In: Proceedings of the 13th International Symposium on PRActical Design of Ships and Other Floating Structures (PRADS 2016), Copenhagen.

Andric, J., Prebeg, P., Piric, K., Kitarovic, S., Zanic, V., Cudma, P., Bezic, A. and Andrisic, J. (2016) 'FE based structural optimization according to IACS CSR-BC', in PRADS 2016 - Proceedings of the 13th International Symposium on PRActical Design of Ships and Other Floating Structures.

Antony, A., Park, Y.-C., Zou, J. and Jamnongpipatkul, A. (2015) Gulfstar - Naval Architecture From Design to Hull Installation, in. Offshore Technology Conference, Houston, Texas, USA: Society of Petroleum Engineers.

Bai, Y. and Jin, W. (2016) Marine Structural Design. 2nd Ed. Oxford: Butterworth-Heinemann.

Banke, J. (2010, August 20) Technology Readiness Levels Demystified. Retrieved from https://www.nasa.gov/topics/aeronautics/features/trl_demystified.html, accessed on: 01/11/2017

Beckman, J. (2016) Information Management System assists V. Filanovsky Construction Process, Offshore Magazine. Available at: http://www.offshore-mag.com/articles/print/volume-76/issue-12/engineering-construction-installation/information-management-system-assists-v-filanovsky-construction-process.html.

Benyessaad, O., Barras, S. and Rocha, G. (2017a) How Classification Societies can be Efficiently Involved in the Current Offshore Industry Cost Reduction Era, in. Offshore Technology Conference, Houston, Texas, USA: Society of Petroleum Engineers.

Benyessaad, O., Barras, S. and Rocha, G. (2017b) How Classification Societies can be Efficiently Involved in the Current Offshore Industry Cost Reduction Era, in Redefining Offshore Development: Technologies and Solutions: 22nd Offshore Symposium 2017: Houston, Texas, USA, 02 February 2017. Red Hook, NY: SNAME/Curran Associates, Inc.

Bertram, V. (2017) Future of Shipbuilding and Shipping – A Technology Vision. In: Proceedings of the 16th International Conference on Computer Applications and Information Technology in the Maritime Industries (COMPIT'17), Cardiff, pp. 17-30.

Boman, K. (2017) Drilling Deeper into Data, Offshore Engineer. Available at: http://www.oedigital.com/component/k2/item/16287-drilling-deeper-into-data (Accessed: October 3, 2017).

Bonney, J. (2015) Maersk CEO: 25,000-TEU ships possible but not practical, Mar 02, 2015, https://www.joc.com/maritime-news/container-lines/maersk-ceo-25000-teu-ships-possible-not-practical_20150302.html, accessed on 13 November 2017.

Bonnin-Pascual, F. and Ortiz, A. (2014) Corrosion Detection for Automated Visual Inspection. In: ALIOFKHAZRAEI, D. M. (ed.) Developments in Corrosion Protection.

Boutrot, J. and Legregeois, N. (2016) Integrity Management Services for Floating Units from Design to Decommissioning, in Emerging offshore technology and deepwater trends: 21st Offshore Symposium 2016: Houston, Texas, USA, 16 February 2016. Red Hook, NY: SNAME/Curran Associates, Inc.

Boutrot, J., Giorgiutti, Y., Rezende, F. and Barras, S. (2017a) Reliable and Accurate Determination of Life Extension for Offshore Units, in: Offshore Technology Conference, Houston, Texas, USA: Society of Petroleum Engineers.

Boutrot, J., Giorgiutti, Y., Rezende, F. and Barras, S. (2017b) Reliable and Accurate Determination of Life Extension for Offshore Units, in Redefining Offshore Development: Technologies and Solutions: 22nd Offshore Symposium 2017: Houston, Texas, USA, 02 February 2017. Red Hook, NY: SNAME/Curran Associates, Inc.

Bruun Ludvigsen, K., Kristian Jamt, L., Husteli, N. and Smogeli, Ø. (2016) Digital Twins for Design, Testing and Verification throughout a Vessel's Life Cycle. In: COMPIT '16 - 15th International Conference on Computer and IT Applications in the Maritime Industries.

Buck, B. H. and Langan, R. (eds) (2017) Aquaculture Perspective of Multi-use Sites in the Open Ocean: the Untapped Potential for Marine Resources in the Anthropocene. Cham: Springer International Publishing (Environment).

Cabos, C., Tietgen, B., Kang, B.S., Ha S. and Hulkkonen, T. (2015) 3D Ship Design from the Start - An Industry Case Study. In: Proceedings of the 14th International Conference on Computer Applications and Information Technology in the Maritime Industries (COMPIT'15), Ulrichshusen, pp 257-268.

Cabos, C., Wolf, V. and Feiner, P. (2017) Remote Hull Surveys with Virtual Reality. In: Proceedings of the 16th International Conference on Computer Applications and Information Technology in the Maritime Industries (COMPIT'17), Cardiff, pp. 444-453.

Cai, S., Sheng, L., Shan, P., Sun, Y., Liu, Y., and Liu, K., (2017) Application of New Common Structural Rules on Aframax Tankers, Tanker Structure Cooperative Forum 2016, Shipbuilders Meeting (http://www.tscforum.org/news/2016_list.aspx)

Canny, S. A. (2016) An Innovative Approach to Well Intervention and Workover Operations on Platforms With Limited Structural Capacity, in: Offshore Technology Conference, Houston, Texas, USA: Society of Petroleum Engineers.

Caprace. J. - D., Fu, G., Carrara, J. F., Remes, H. and Shin, S. B. (2017). A benchmark study of uncertainness in welding simulation, Marine Structures, Volume 56, pp 69-84.

Carlton, J., Jukes, P. and Choo, Y. S. (eds.) (2017) Encyclopedia of Maritime and Offshore Engineering. Chichester, UK: John Wiley & Sons, Ltd.

Carra, C., Potts, A. E., Johnstone, D. and Kilner, A. A. (2017) Determination of Rational Robustness Criteria for FPSO Design, in. Offshore Technology Conference, Houston, Texas, USA: Society of Petroleum Engineers.

Carre, D., Mcarthur, L., Simpson, A., Zhang, P. and Vazquez, J. H. (2017) GSF Galaxy I Jackup Case Study for Optimizing Rig Move Performance in North Sea Using an Advanced Simulation Model, in Redefining Offshore Development: Technologies and Solutions: 22nd Offshore Symposium 2017: Houston, Texas, USA, 02 February 2017. Red Hook, NY: SNAME/Curran Associates, Inc.

Cepeda, M. A. F., Assis, L. F., Marujo, L. G. and Caprace, J. - D. (2017). Effects of slow steaming strategies on a ship fleet, Marine Systems & Ocean Technology, Volume 12 (3), September 2017, pp 178-186.

Chandrasekaran, S. (2015) Dynamic Analysis and Design of Offshore Structures. New York, NY: Springer Berlin Heidelberg (Ocean Engineering & Oceanography).

Chandrasekaran, S. (2016) Advanced Marine Structures. Boca Raton: CRC Press/Taylor & Francis Group.

Chandrasekaran, S. and Jain, A. K. (2017) Ocean Structures: Construction, Materials, and Operations. 1st Ed. Boca Raton, FL: CRC Press/Taylor & Francis Group.

Chang, G.-A. and Liu, M.-L. (2016) Simplified Spudcan and Soil Interaction Analysis for Jackup Touch-Down, in Future offshore technology and sustained reliability: 20th Offshore Symposium 2015: Houston, Texas, 17 February 2015. Red Hook, NY: SNAME/Curran Associates, Inc.

Chen, X., Kawamura, Y. and Okada, T. (2016). The Stochastic Finite Element Method based on Response Surface Methodology Considering Uncertainty in Shape of Structures. In: Proceedings of the 13th International Symposium on PRActical Design of Ships and Other Floating Structures (PRADS 2016), Copenhagen.

Cherian L, Mathew T, Land J, Evans J. (2017) The design and analysis of a heavy transportation and jacket launch barge, Progress in the Analysis and Design of Marine Structures, Guedes Soares & Garbatov (Eds.), Taylor & Francis Group, 2017, pp. 213 221.

Choi, U., (2016). Impact of Harmonized CSR for oil tanker, Tanker Structure Cooperative Forum 2016, Shipbuilders Meeting (http://www.tscforum.org/news/2016_list.aspx)

Chopra, G. S. (2016) World's First Seabed Mining Vessel – Design Challenges, in. Offshore Technology Conference, Houston, Texas, USA: Society of Petroleum Engineers.

Coello Coello, C. A., Lamont, G. B., and Van Veldhuizen, D. A., 2007, Evolutionary algorithms for solving multi-objective problems, Springer, New York.

Collette, M., Bronsart, R., Chen, Y., Erikstad, S.O., Georgiev, P., Giuglea, V., Jeong, H.K., Lazakis, I., Moro, L., Sekulski, Z., Sicchiero, M., Toyoda, M., Ventura, M. and Zanic, V. (2015). Design Methods, In: Proceedings of the 19th International Ship and Offshore Structures Congress (ISSC 2015), Cascais: CRC Press, pp. 459-518.

Constantinis, D. (2017) Operators, Class Societies targeting Safer, more Informative Hull Inspections, Offshore Magazine. Available at: http://www.offshore-mag.com/articles/print/volume-77/issue-8/productions-operations/operators-class-societies-targeting-safer-more-informative-hull-inspections.html, accessed on 03/11/2017..

Curtis, H. and Allan, P. (2015) A Finite Element Study of Boulder Interaction with Spudcans, in Meyer, V. (ed.) Frontiers in offshore geotechnics III: proceedings of the Third International Symposium on Frontiers in Offshore Geotechnics (ISFOG 2015), Oslo, Norway, 10-12 June 2015. Boca Raton London New York Leiden: CRC Press/Balkema.

Dae, H.K. and Paik, J.K. (2017). Ultimate limit state-based multi-objective optimum design technology for hull structural scantlings of merchant cargo ships. Ocean Engineering, Volume 129, pp. 318-334

Dai, L., Hu, H. and Chen, F. (2015) A GA-based heuristic approach for offshore structure construction spatial scheduling under uncertainty, Ships and Offshore Structures, 10(6), pp. 660–668.

Darie, I. and Rörup, J. (2017). Hull girder ultimate strength of container ships in oblique sea. In: Progress in the Analysis and Design of Marine Structures - Proceedings of the 5th International Conference on Marine Structures (MARSTRUCT 2017). Lisbon: Taylor & Francis Group, pp. 225-233.

Darvishzadeh, T. and Sari, A. (2015) CFD Applications in Offshore Engineering, in. Offshore Technology Conference, Houston, Texas, USA: Society of Petroleum Engineers.

de Andrade, A. M. T., Vaz, C. E. M., Ribeiro, J., Lopreato, L. G. R. and do Nascimento, R. F. S. (2015) Offshore Production Units for Pre-Salt Projects, in. Offshore Technology Conference, Houston, Texas, USA: Society of Petroleum Engineers.

de Beer, T. (2017) Practical Aspects of Structural Integrity of FPSOs (keynote lecture), in. The 6th International Conference on Marine Structures (Marstruct 2017), Lisbon, Portugal.

de Haas, J. (2017) Ship Surveys: The Challenges Associated with Mega Container Ships, https://www.bmt.org/industry-insights/market-insights/ship-surveys-the-challenges-associated-with-mega-container-ships/, accessed on 10 November 2017.

Decò, A. and Frangopol, D. (2015). Real-time risk of ship structures integrating structural health monitoring data: Application to multi-objective optimal ship routing. Ocean Engineering, 96, pp.312-329.

Dessi D, Faiella E, Geiser J, Alley E, Dukes J. (2017) Design and structural testing of a physical model for wetdeck slamming analysis, Progress in the Analysis and Design of Marine Structures, Guedes Soares & Garbatov (Eds.), Taylor & Francis Group, 2017, pp. 3-12.

Dhillon, B. S. 2006 Maintainability, Maintenance, and Reliability for Engineers.

Dikis, K. and Lazakis, I. 2016. Dynamic Risk and Reliability Assessment of Ship Machinery and Equipment. Proceedings of the Twenty-sixth (2016) International Ocean and Polar Engineering Conference. 26 June-2 July 2016, Rhodes, Greece.

Dominguez R, Cali Y, García J. (2017) Forced vibration analysis of the hull girder by propeller excitation and rudder interaction, Progress in the Analysis and Design of Marine Structures, Guedes Soares & Garbatov (Eds.), Taylor & Francis Group, 2017, pp. 77-86.

Drimer, N., Moshkovich, Y. and Neuberg, O. (2017) 'A design method for planing hulls, considering hydro-elasticity and nonlinear dynamic structural response', Ships and Offshore Structures. Taylor & Francis (Ships and Offshore Structures), 12(7), pp. 971–979. doi: 10.1080/17445302.2016.1187362.

EARTO. (2014, April 30). Retrieved from The TRL Scale as a Research & Innovation Policy Tool, EARTO Recommendations: http://www.earto.eu/publications1.html, accessed on: 01/11/2017

Ebrahimi, A., Brett, P. O., Agis, J. J. G., Brandt, U. and Gaspar, H. M. (2015) The Influence of Rule Changes on Design and Performance of Offshore Vessels – Myths Meet Reality, in. World Maritime Technology Conference, Providence, Rhode Island, USA: SNAME.

EC (2017). European Commission Technology Readiness Levels (TRL), http://ec.europa.eu/research/participants/data/ref/h2020/other/wp/2016_2017/annexes/h2020-wp1617-annex-g-trl_en.pdf, accessed on: 02/11/2017

Ehlers S, Kujala P, Veitch B, et al. Scenario based risk management for Arctic shipping and operations[C]// ASME 2014 33rd International Conference on Ocean, Offshore and Arctic Engineering. American Society of Mechanical Engineers, 2014: V010T07A006.

Ehlers, S., Kujala, P., Veitch, B., Khan, F. and Vanhatalo, J. (2014). Scenario based risk management for Arctic shipping and operations. In: Proceedings of ASME 2014 33rd International Conference on Ocean, Offshore and Arctic Engineering. San Francisco: American Society of Mechanical Engineers, Volume 10.

El-Reedy, M. A. (2015) Marine Structural Design Calculations. 1st Ed. Oxford: Butterworth-Heinemann.

Engebretsen, E., Shu, Z. and Borgen, J. E. (2017) Estimating Hydrodynamic Sectional Loads for FPSOs Using Artificial Neural Networks, in. 36th International Conference on Ocean, Offshore and Arctic Engineering, Trondheim, Norway: ASME, p. V001T01A048.

Engin, H. K., Khoa, H. D. V. and Jostad, H. P. (2015) Finite Element Analyses of Spudcan – Subsea Template Interaction during Jack-up Rig Installation, in Meyer, V. (ed.) Frontiers in offshore geotechnics III: proceedings of the Third International Symposium on Frontiers in Offshore Geotechnics (ISFOG 2015), Oslo, Norway, 10-12 June 2015. Boca Raton London New York Leiden: CRC Press/Balkema.

Fallah, S., Gavin, K. and Moradabadi, E. (2015) Estimation of Spudcan Penetration using a Probabilistic Eulerian Finite Element Analysis, in Meyer, V. (ed.) Frontiers in offshore geotechnics III: proceedings of the Third International Symposium on Frontiers in Offshore Geotechnics (ISFOG 2015), Oslo, Norway, 10-12 June 2015. Boca Raton London New York Leiden: CRC Press/Balkema.

Gallagher, D. and Rush, N. (2016a) Continued Service of Offshore Floating Structures, in Future offshore technology and sustained reliability: 20th Offshore Symposium 2015: Houston, Texas, 17 February 2015. Red Hook, NY: SNAME/Curran Associates, Inc.

Gallagher, D. and Rush, N. (2016b) Optimized Structural Integrity Management based in Design, in Future offshore technology and sustained reliability: 20th Offshore Symposium 2015: Houston, Texas, 17 February 2015. Red Hook, NY: SNAME/Curran Associates, Inc.

Garbatov Y, Georgiev P. (2017) Optimal design of stiffened plate subjected to combined stochastic loads, Progress in the Analysis and Design of Marine Structures, Guedes Soares & Garbatov (Eds.), Taylor & Francis Group, 2017, pp. 243 252.

Ghanem, R., Spanos, P. (1991). Stochastic Finite Elements: A Spectral Approach, New York: Springer-Verlag.

Gill, R. and Henzell, S. (2017) Design Once, Build Many, Offshore Engineer. Available at: http://www.oedigital.com/production/item/15885-design-once-build-many (Accessed: October 5, 2017).

Gkerekos, C., Lazakis, I. and Theotokatos, G. (2016) Ship Machinery Condition Monitoring using Vibration Data through Supervised Learning. International conference on Maritime Safety and Operations. 13-14 October 2016, Glasgow, U.K.

Gkerekos, C., Lazakis, I. and Theotokatos, G. (2017) Ship Machinery Condition Monitoring Using Performance Data Through Supervised Learning. RINA Smart Ships Technology. 24-25th January 2017, London, U.K.

Green P.L., Tygesen U.T. and Stevanovic N. (2016) Bayesian Modelling of Offshore Platforms. In: Atamturktur S., Schoenherr T., Moaveni B., Papadimitriou C. (eds) Model Validation and Uncertainty Quantification, Volume 3. Conference Proceedings of the Society for Experimental Mechanics Series. Springer, Cham

Green4Sea (2017) World's first autonomous zero emissions ship planned for 2020, https://www.green4sea.com/worlds-first-autonomous-zero-emissions-ship-planned-for-2020/, accessed on 06/11/2017.

Greeson, T. D. and Waller, M. G. (2016) A Solution to Accurate Offshore Dimensional Control, in Emerging offshore technology and deepwater trends: 21st Offshore Symposium 2016: Houston, Texas, USA, 16 February 2016. Red Hook, NY: SNAME/Curran Associates, Inc.

Ha, Y. S., Park, J. S., Koo, J. B., Cho, B. J., Ma, K. Y. and Jang, K. B. (2016) Engineering Establishment of Living Quarters for Jack-Up Rig Structures, in. 35th International Conference on Ocean, Offshore & Arctic Engineering, Busan, South Korea: ASME, p. V003T02A079.

Haïdar, T. (2016) Time and Tide Wait for No Man: The Importance of Structural Integrity. Bentley.

Hendriks, S., Claassen, L. and Chalkias, D. (2015) Magellan Class Drillship: Designing the Rig of the Future, in. Offshore Technology Conference, Brazil: Society of Petroleum Engineers.

Hendriks, S., Man, P. de, Zijderveld, G. and Diemen, C. van (2017) Euryale Moonpool - Innovative Naval Architecture Design Enables Full Dual Drilling Accessibility on a Drillship, in. Offshore Technology Conference, Houston, Texas, USA: Society of Petroleum Engineers.

Hernæs, S. and Aas, T. (2015) An Alternative Approach to 50 Years Design Life, in. Offshore Technology Conference, Houston, Texas, USA: Society of Petroleum Engineers.

Hodapp, D., Ma, W., Wisch, D. and Lee, M.-Y. (2017) Improving Cost Efficiency in Floating Production Facilities: Semi-Submersible Design Standardization, in. Offshore Technology Conference, Houston, Texas, USA: Society of Petroleum Engineers.

IACS (2006a) Common Structural Rules for Double Hull Oil Tankers, January 2006.

IACS (2006b) Common Structural Rules for Bulk Carriers, January 2006.

IACS (2012a) Common Structural Rules for Bulk Carriers, July 2012.

IACS (2012b) Common Structural Rules for Double Hull Oil Tankers, July 2012.

IACS (2014). Common Structure Rules for Bulk Carriers and Oil Tankers 1 JAN 2014, International Association of Classification Societies

IACS (2016). Private communication, IACS, August 2016.

IACS (2006a) Common Structure Rules for Bulk Carriers, International Association of Classification Societies

IACS (2006b) Common Structure Rules for Oil Tankers, International Association of Classification Societies

IACS (2017). Common Structure Rules for Bulk Carriers and Oil Tankers 01 JAN 2017 version, International Association of Classification Societies

Im, H.I., Vladimir, N., Malenica, Š., Cho, D.S., Ryu, H.R. and De Lauzon, J. (2016) Ultimate strength check of HHI SkyBenchTM ultra large container ship considering slamming and whipping effects, In: Proceedings of the 13th International Symposium on PRActical Design of Ships and Other Floating Structures (PRADS 2016), Copenhagen.

IMO (2009a) Prevention of Air Pollution From Ships, Marine Environment Protection Committee, MEPC 59/4/47, 22 May 2009.

IMO (2009b) Second IMO GHG Study 2009, International Maritime Organization (IMO), London, UK, April 2009; Buhaug, Ø., Corbett, J.J., Endresen, Ø., Eyring, V., Faber, J., Hanayama, S., Lee, D.S., Lee, D., Lindstad, H., Markowska, A.Z., Mjelde, A., Nelissen, D., Nilsen, J., Pålsson, C., Winebrake, J.J., Wu, W., Yoshida, K.

IMO (2013) MSC.1/Circ.1455, Guidelines for the Approval of Alternatives and Equivalents as Provided for in Various IMO Instruments. London: IMO, p. 51.

IMO (2014) Reduction of GHG Emissions From Ships, Third IMO GHG Study 2014 – Final Report, Marine Environment Protection, Committee, MEPC 67/Inf.3, 25 July 2014.

IMO (2017) EEDI - rational, safe and effective. International Maritime Organisation (IMO), http://www.imo.org/en/MediaCentre/HotTopics/GHG/Pages/EEDI.aspx, accessed on 30 August 2017.

IMO MSC.1/Circ.1455 , Guidelines for the Approval of Alternatives and Equivalents as Provided for in Various IMO Instruments [Z].2013.

INCASS (2014a) Deliverable D4.2 Stakeholders' data requirements. WP4 - Machinery & Equipment Modelling & Analysis. Inspection Capabilities for Enhanced Ship Safety EC FP7 Project.

INCASS (2014b) Deliverable D5.3 Database: Structural and Machinery Interface. WP5 - Database Development & Implementation. Inspection Capabilities for Enhanced Ship Safety EC FP7 Project.

INCASS (2014c) Deliverable D5.4 Data Exchange. WP5 - Database Development & Implementation. Inspection Capabilities for Enhanced Ship Safety EC FP7 Project.

INCASS (2015a) Deliverable D2.1 Technological tools and components for the conduction of automated or supported survey activities. WP2 - Intelligent Monitoring Systems. Inspection Capabilities for Enhanced Ship Safety EC FP7 Project.

INCASS (2015b) Deliverable D2.2 Integrated tool for visual data analysis. WP2 - Intelligent Monitoring Systems. Inspection Capabilities for Enhanced Ship Safety EC FP7 Project.

INCASS (2016a) Deliverable D5.5 Ship shore communications. WP5 - Database Development & Implementation. Inspection Capabilities for Enhanced Ship Safety EC FP7 Project.

INCASS (2016b) Deliverable D5.6 Central database delivery. WP5 - Database Development & Implementation. Inspection Capabilities for Enhanced Ship Safety EC FP7 Project.

ISSC2003 (2003) In 15th International Ship and Offshore Structures Congress (ISSC) 2003 Report, Commettee IV.2.

ISSC2009 (2009) In 15th International Ship and Offshore Structures Congress (ISSC) 2003 Report, Commettee IV.2.

ISSC2012 (2012) In 18th International Ship and Offshore Structures Congress (ISSC) 2012 Report, Commettee IV.2.

ISSC2015. (2015). In 19th International Ship and Offshore Structures Congress (ISSC) 2015 Report, Commettee IV.2.

Janssen, J., Hofstede, H., Hoogeveen, M. and Wu, J.-F. (2016) Improvement of Jack-Up Operating Capability using add-on Spudcans, in Emerging offshore technology and deepwater trends: 21st Offshore Symposium 2016: Houston, Texas, USA, 16 February 2016. Red Hook, NY: SNAME/Curran Associates, Inc.

Ji, Z., Gang, C., Jian, M., Yuhan, W. and Wei, Z. (2015) The Study on Hull Structure Strength Analysis and Opening Calculation of CJ46 Jack-Up Drilling Unit, in. 34th International Conference on Ocean, Offshore and Arctic Engineering, St. John's, Newfoundland, Canada: ASME, p. V007T06A066.

Jin, R., Chen, W., and Simpson, T. W. (2001) "Comparative studies of metamodelling techniques under multiple modelling criteria," Structural and Multidisciplinary Optimization, 23(1), pp. 1-13.

Jostad, H. P., Torgersrud, Ø., Engin, H. K. and Hofstede, H. (2015) A FE procedure for calculation of fixity of jack-up foundations with skirts using cyclic strain contour diagrams, in. 16th International Conference: The Jack-Up Platform, London.

Joung, T., Choi, H., Lee, S., Kim, J., Lee J., Oh T. (2017) A Study on the Global Buckling Analysis and Structural Effectiveness of Connection Parts of Pressure vessel, ICSOS 2017: Proceedings of the International Conference on Ships and Offshore Structures, Sören Ehlers & Jeom Paik & Young Bai (Eds.), Shenzhen, China, 11-13 September, 2017.

Joung T., Park B., Choung C. (2017) Performance Test Analysis and Structural Safety Assessment by using Reliability Analysis, ICSOS 2017: Proceedings of the International Conference on Ships and Offshore Structures, Sören Ehlers & Jeom Paik & Young Bai (Eds.), Shenzhen, China, 11-13 September, 2017.

Jung, J. J., Lee, I. H., Chung, B. Y., Kim, S. E. and Kim, S. H. (2017) Standardization of FPSO Hull with 2MMbbls Storage Capacity for West Africa, in. Offshore Technology Conference, Houston, Texas, USA: Society of Petroleum Engineers.

Kefal, A. and Oterkus, E. (2017) Shape and Stress Sensing of Offshore Structures by using Inverse Finite Element Method, in. The 6th International Conference on Marine Structures (Marstruct 2017), Lisbon, Portugal: CRC Press/Taylor & Francis Group.

Kefal, A. and Oterkus, E. (2017). Shape and stress sensing of offshore structures by using inverse finite element method. In: MARSTRUCT 2017, the 6th International Conference on Marine Structures. Taylor & Francis Group.

Kefal, A. and Oterkus, E. (2016) Displacement and stress monitoring of a chemical tanker based on inverse finite element method. Ocean Engineering, 112, pp.33-46.

Kefal, A. and Oterkus, E. (2016) Displacement and stress monitoring of a Panamax containership using inverse finite element method. Ocean Engineering, 119, pp.16-29.

Kemp, D. (2016) A Risk Based Approach to Managing the Integrity of Aging Production Facilities in the Gulf of Mexico, in. Offshore Technology Conference, Houston, Texas, USA: Society of Petroleum Engineers.

Kheireddine, H., Chen, D. and Timms, J. (2016) Introducing Holistic Approach for the Design and Operation of FLNG Development, in. Offshore Technology Conference, Houston, Texas, USA: Society of Petroleum Engineers.

Khurana, S., D'Souza, R., Yanosek, K., Christ, F. and Meeks, P. (2017) Bringing Upstream Projects to Final Investment Decision, in. Offshore Technology Conference.

Kim, D. H. and Paik, J. K. (2017) 'Ultimate limit state-based multi-objective optimum design technology for hull structural scantlings of merchant cargo ships', Ocean Engineering. (Ocean Engineering), 129(Supplement C), pp. 318–334. doi: https://doi.org/10.1016/j.oceaneng.2016.11.033.

Kim, J. D. and Jang, B.-S. (2016) Application of Multi-Objective Optimization for TLP Considering Hull-Form and Tendon System, Ocean Engineering, 116, pp. 142–156.

Kim, J. W., Jang, H., Kyoung, J., Baquet, A. and O'Sullivan, J. (2015) CFD-Based Numerical Wave Basin for Offshore Floater Design, in. Offshore Technology Conference, Houston, Texas, USA: Society of Petroleum Engineers.

Kim, J.-D. and Jang, B.-S. (2016) Application of the Global Optimization Method to the Preliminary Design of Tension Leg Platforms, in. 35th International Conference on Ocean, Offshore & Arctic Engineering, Busan, South Korea: ASME, p. V003T02A077.

Kim, S. P., Petricic, M., Xie, G., Wu, G. and Seah, R. (2016) Strength and Fatigue Assessment of Extended Bilge Keels for FPSO/FLNG, in. Houston, Texas, USA: Offshore Technology Conference.

Kim, S.-K., Roh, M.-I. and Kim, K.-S. (2017) Arrangement Method of Offshore Topside Based on an Expert System and Optimization Technique, Journal of Offshore Mechanics and Arctic Engineering, 139(2), p. 021302.

Kitchen, P. (2015) Process Support and Marine Systems in the Hull - Innovation Meets Regulation, in. Offshore Technology Conference, Houston, Texas, USA: Society of Petroleum Engineers.

Knight J. (2017) Rapid, early-stage ultimate limit state structural design for multihulls, Progress in the Analysis and Design of Marine Structures, Guedes Soares & Garbatov (Eds.), Taylor & Francis Group, 2017, pp. 269 275.

Knight, J. T., Collette, M. D. and Singer, D. J. (2015) 'Design for flexibility: Evaluating the option to extend service life in preliminary structural design', Ocean Engineering. (Ocean Engineering), 96 (Supplement C), pp. 68–78. doi: https://doi.org/10.1016/j.oceaneng.2014.12.035 .

Knodt, S., Kleinen, T., Dornieden, C., Lorscheidt, J., Bjørneklett, B. and Mitzlaff, A. (2016) Development and Engineering of Offshore Mining Systems - State of the Art and Future Perspectives, in. Offshore Technology Conference, Houston, Texas, USA: Society of Petroleum Engineers.

Ko, Y., Kmi, S. and Paik, J. (2017) Contribution of a deformable striking-ship structure to the structural crashworthiness of ship-ship collisions, ICSOS 2017: Proceedings of the International Conference on Ships and Offshore Structures, Sören Ehlers & Jeom Paik & Young Bai (Eds.), Shenzhen, China, 11-13 September, 2017.

Koch, T., Smith, M. and Tanneberger, K. (2015) Improving Machinery & Equipment Life Cycle Management Processes. In: COMPIT '15 - 14th International Conference on Computer and IT Applications in the Maritime Industries. Volker Bertram.

Koelman, H., van der Zee, J. and de Jonge, T. (2015) A Virtual Single Ship-Design System Composed of Multiple Independent Components, In: Proceedings of the 14th International Conference on Computer Applications and Information Technology in the Maritime Industries (COMPIT'15), Ulrichshusen, pp 126-134.

Kolios A.J., Rodriguez-Tsouroukdissian, A. and Salonitis K. (2016) Multi-criteria decision analysis of offshore wind turbines support structures under stochastic inputs. Ships and Offshore Structures. Volume 11 (1), pp 38-49.

Konovessis, D., Cai, W. and Vassalos, D. (2013) Development of Bayesian Network Models for Risk-Based Ship Design[J]. Journal of Marine Science and Application, 2013, 12(2):140-151.

Konovessis, D., Cai, W. and Vassalos, D. (2013) Development of Bayesian Network Models for Risk-Based Ship Design. Journal of Marine Science and Application, Volume 12 (2), pp. 140-151.

Koole, T. and van der Kraan, M. (2015) Modern Jack-Ups and their Dynamic Behaviour, in. 15th International Conference: The Jack-Up Platform, London.

Korbetis, G., Chatzimoisiadis, S. and Drougkas, D. (2015) Automated Interoperability from Concept Design to Multidisciplinary FE Analysis. In: Proceedings of the 14th International Conference on Computer Applications and Information Technology in the Maritime Industries (COMPIT'15), Ulrichshusen, pp 116-125

Korbetis, K., Chatzimoisiadis, S. and Drougkas, D. (2017) EPLYSIS, a New Solver for Finite Element Analisys. In: Proceedings of the 16th International Conference on Computer Applications and Information Technology in the Maritime Industries (COMPIT'17), Cardiff, pp. 190-200.

Koroglu, S.A. and Ergin, A. (2016) A decomposition method for surrogate models of large scale structures, Journal of Marine Science and Technology, Volume 21 (2), pp 325–333

Kwon, S., Kim, B.C., Mun, D. and Han, S. (2015) Simplification of feature-based 3D CAD assembly data of ship and offshore equipment using quantitative evaluation metrics. Computer-Aided Design, 59, pp.140-154.

Larkins, D. Waldie, M. and Morais, D. (2015) Utilizing a Single 3D Product Model throughout the Design Process. In: Proceedings of the 14th International Conference on Computer Applications and Information Technology in the Maritime Industries (COMPIT'15), Ulrichshusen, pp: 465-472.

Latarche, M. (2017). Class Societies update CSR software suites. The Naval Architect. March 2017 pp. 36-37

Lee, J.-C., Shin, S.-C. and Kim, S.-Y. (2015) "An optimal design of wind turbine and ship structure based on neuro-response surface method" Int. J. Nav. Archit. Ocean Eng. 7:750~769

Lee, H. D., Son, J.-S., Kim, I.-H. and Jeong, H.-N. (2017) Offshore Standardization Process and Criteria Development for EPC Project, in. Offshore Technology Conference, Houston, Texas, USA: Society of Petroleum Engineers.

Lee, J. M., Kim, Y. H., Hossain, M. S., Hu, Y., Won, J. H., Park, J. S. and Jun, M. J. (2015) Use of Novel Spudcan Shapes for Mitigating Punch-Through Hazards, in. 15th International Conference: The Jack-Up Platform, London.

Lee, J., Sung, S., Kim, S., Kraus, A. and Lee, J. (2015) An optimal sub-structure for a TLP-type wind turbine based on neuro-response surface method, Journal of Marine Science and Technology, Volume 20 (4), pp 604–616.

Leon, A. (2017) Managing Maintenance, Offshore Engineer. Available at: http://www.oedigital.com/technology/software/item/14355-managing-maintenance.

Levanger, H., Notaro, G. and Hareide, O. J. (2016) Collision Response and Residual Strength of Jack-up Structure, in. 13th International Symposium on Practical Design of Ships and Other Floating Structures (PRADS'2016), Copenhagen, Denmark.

Lin, L. and Ong, M. C. (2017) A Preliminary Study of a Rigid Semi-Submersible Fish Farm for Open Seas, in. 36th International Conference on Ocean, Offshore and Arctic Engineering, Trondheim, Norway: ASME, p. V009T12A044.

Lin, L., Jiang, Z. and Ong, M. C. (2017) A Preliminary Study of a Vessel-Shaped Offshore Fish Farm Concept, in. 36th International Conference on Ocean, Offshore and Arctic Engineering, Trondheim, Norway: ASME, p. V006T05A006.

Lindner, H., Schenk, S., Bronsart, R., Ebeling, B., Frömming, K. and Kluwe, F. (2015) A Modular System Architecture for the Early Ship Design by Combining a 3D-CAD System with a Product Data Management System, In: Proceedings of the 14th International Conference on Computer Applications and Information Technology in the Maritime Industries (COMPIT'15), Ulrichshusen, pp. 135-146.

Lindstad, H., Eskeland, G. S., Psaraftis, H., Sandaas, I. and Strømman, A. H. (2015) 'Maritime shipping and emissions: A three-layered, damage-based approach', Ocean Engineering. (Ocean Engineering), 110(Part B), pp. 94–101. doi: https://doi.org/10.1016/j.oceaneng.2015.09.029.

Lipman, R. and Lubell, J. (2015) Conformance checking of PMI representation in CAD model STEP data exchange files. Computer-Aided Design, 66, pp. 14-23.

Liu, S., Hua, D., Machado, C. and Wu, J.-F. (2016) Class Approach for Life Extension Process of Floating Production Installations, in Emerging offshore technology and deepwater trends: 21st Offshore Symposium 2016: Houston, Texas, USA, 16 February 2016. Red Hook, NY: SNAME/Curran Associates, Inc.

Ma Ming, Brown, A., McNatt, T. and Freimuth, J., (2016) Naval ship hull structural scantling optimization by reducing weight, increasing safety and lowering verticalcenter of gravity, Marine Technology Conference, SNAME, Seattle, USA.

Ma, C., Oka, M., and Iijima, K. (2017) A numerical simulation for coupling behavior between smoothed particle hydrodynamics and structural finite element method. In: Progress in the Analysis and Design of Marine Structures - Proceedings of the 5th International Conference on Marine Structures (MARSTRUCT 2017). Lisbon: Taylor & Francis Group, pp. 21-28.

Maes, M. A. and Dann, M. R. (2017) Freak Events, Black Swans, and Unknowable Unknowns: Impact on Risk-Based Design[C]// International Probabilistic Workshop. 2017.

Maes, M.A. and Dann, M.R. (2017) Freak Events, Black Swans, and Unknowable Unknowns: Impact on Risk-Based Design. In: Proceedings of the 14th International Probabilistic Workshop, Ghent: Springer, pp. 15-32.

Majed, A., Mansour, A., Chinello, L. and Wan, Y. (2016) A Dynamic Substructuring Approach to Improved Global Structural Dynamic And Stress Analysis of Topside/Hull Systems, in Emerging offshore technology and deepwater trends: 21st Offshore Symposium 2016: Houston, Texas, USA, 16 February 2016. Red Hook, NY: SNAME/Curran Associates, Inc.

Marinic-Kragic, I., Vucina, D. and Curkovic, M. (2016) 'Efficient shape parameterization method for multidisciplinary global optimization and application to integrated ship hull shape optimization workflow', Computer-Aided Design. (Computer-Aided Design), 80(Supplement C), pp. 61–75. doi: https://doi.org/10.1016/j.cad.2016.08.001.

Marinić-Kragić, I., Vučina, D. and Ćurković, M. (2016) Efficient shape parameterization method for multidisciplinary global optimization and application to integrated ship hull shape optimization workflow, Computer-Aided Design, Volume 80, pp 61-75.

Marques, C. H., Belchior, C. R. P., Caprace, J. - D. (2017a). A model to optimise the selection of marine dual-fuel low-speed diesel engines, Marine Systems & Ocean Technology, Volume 12 (3), September 2017, pp 138-149.

Marques, C. H., Belchior, C. R. P., Caprace, J. - D. (2017b). An approach to optimise the selection of Lng carriers' propulsion system, Engenharia Térmica (Thermal Engineering), Volume 16 (1), June 2017, pp 37-45.

Maslin, E. (2017) Neural Networking by Design, Offshore Engineer. Available at: http://www.oedigital.com/component/k2/item/14810-neural-networking-by-design.

Mat Soom, E., Abu Husain, M. K., Mohd Zaki, N. I., Azman, N. U. and Najafian, G. (2016) Reliability-Based Design and Assessment for Lifetime Extension of Ageing Offshore Structures, in. 35th International Conference on Ocean, Offshore & Arctic Engineering, Busan, South Korea: ASME, p. V003T02A044.

McLaren, A. R. (2017) An Investigation into the Global Sway Buckling Failure mode of Jack-up Units and its Impact on the Calculation of Effective Length Factors for Individual Legs, in. 16th International Conference: The Jack-Up Platform, London.

Mendonça Santos, J. and Alves, C. (2016) A Wind Heeling Moment Curve for Ship-shaped MODU early Design Stability Considerations, in Maritime Technology and Engineering III: Proceedings of the 3rd International Conference on Maritime Technology and Engineering (MARTECH 2016, Lisbon, Portugal, 4-6 July 2016). Guedes Soares & Santos (Eds). Taylor & Francis Group.

Moan, T. (2015) Official discussion, Committee IV.2, Design Methods ISSC 2015. In 19th International Ship and Offshore Structures Congress (pp. 995-1008). Cascais, Portugal.

Mobbs, B. and Stiff, J. J. (2017) Effective Shear Areas of Jack-up Chords – Development of a Logical Approach to Assessment, in. 16th International Conference: The Jack-Up Platform, London.

Moe, A. M. and Laranjinha, M. (2017) Design Methodology for Converting a MODU into a FPU, in. Offshore Technology Conference, Houston, Texas, USA: Society of Petroleum Engineers.

Mohrman, E.S.A. and Lawler III, E.E. (2011) Research for Theory and Practice: Framing the Chalenge. In E. S.A. Mohram and E.E.Lawler III, Useful Research: Advancing Theory and Practice (pp. 9 -35). San Francisco: Berrett-Koehler.

Moir, C. (2016) Online Monitoring System Helps Assess Integrity of North Sea Platform, Offshore Magazine. Available at: http://www.offshore-mag.com/articles/print/volume-76/issue-11/european-supplement/online-monitoring-system-helps-assess-integrity-of-north-sea-platform.html.

Moir, S. (2017) Improving Offshore Inspection Efficiency through UAV Inspections, in Redefining Offshore Development: Technologies and Solutions: 22nd Offshore Symposium 2017: Houston, Texas, USA, 02 February 2017. Red Hook, NY: SNAME/Curran Associates, Inc.

Moon, S.C., Jeong, S., Song, H.C. and Na, S.S. (2016) Development of automated algorithm of integrated structural design system based on CSR-H for bulk carrier. In: Proceedings of the 29th Asian-Pacific Technical Exchange and Advisory Meeting on Marine Structures (TEAM2015), Vladivostock.

Moore, B., Easton, A., Cabrera, J., Webb, C. and George, B. (2017) Stones Development: Turritella FPSO - Design and Fabrication of the World's Deepest Producing Unit, in. Offshore Technology Conference, Houston, Texas, USA: Society of Petroleum Engineers.

Morais, D., Waldie, M. and Danese, N. (2016) Open Architecture Applications: The Key to Best-of-Breed Solutions. In: Proceedings of the 15th International Conference on Computer Applications and Information Technology in the Maritime Industries (COMPIT'16), Lecce, pp 223-233.

Morais, D., Waldie, M. and Danese, N. (2016) Open Architecture Applications: The Key to Best-of-Breed Solutions. In: COMPIT '16 - 15th International Conference on Computer and IT Applications in the Maritime Industries. Volker Bertram.

Morais, D., Waldie, M. and Darren, L. (2017) The evolution of Virtual Reality in Shipbuilding. In: Proceedings of the 16th International Conference on Computer Applications and Information Technology in the Maritime Industries (COMPIT'17), Cardiff, pp. 128-138.

Morais, D., Waldie, M. and Larkins, D. (2015) Completely Rethinking Weld Management: Leveraging 3D Models and Visualization. In: Proceedings of the 14th International Conference on Computer Applications and Information Technology in the Maritime Industries (COMPIT'15), Ulrichshusen, pp 382-393

Morandi, A. (2017) Challenges in the Structural Design of Jack-up and Semi-submersible Rigs (keynote lecture), in. The 6th International Conference on Marine Structures (Marstruct 2017), Lisbon, Portugal.

Na Seung-Soo, Karr Dale G. (2016) Development of Pareto strategy multi-objective function method for the optimum design of ship structures, International Journal of Naval Architecture and Ocean Engineering, Available online 24 October 2016, ISSN 2092-6782, http://dx.doi.org/10.1016/j.ijnaoe.2016.06.001

Naruse, Y., and Kawamura, Y. (2015) A comparison of structural reliability of ultimate strength of bulk carriers before and after the effectuation of CSR. In: Proceedings of the 29th Asian-Pacific Technical Exchange and Advisory Meeting on Marine Structures (TEAM2015), Vladivostock.

Noh Y, Chang K, Seo Y, et al. Risk-based determination of design pressure of LNG fuel storage tanks based on dynamic process simulation combined with Monte Carlo method [J]. Reliability Engineering & System Safety, 2014, 129:76-82.

Noh, Y., Chang, K., Seo, Y. and Chang D. (2014) Risk-based determination of design pressure of LNG fuel storage tanks based on dynamic process simulation combined with Monte Carlo method. Reliability Engineering & System Safety, Volume 129, pp. 76-82.

Nunes, G. C., Lopreato, L. G. R., Da Silva Ferreira, M. D. A., Vilamea, E. M. and De Oliveira, G. P. H. A. (2016) Petrobras Approach to FPSO Cost Reduction, in. Offshore Technology Conference, Houston, Texas, USA: Society of Petroleum Engineers.

Odeskaug, L. (2015) The Cylindrical Hull Concept for FLNG Application, in. Offshore Technology Conference, Houston, Texas, USA: Society of Petroleum Engineers.

OECD (2015) OECD Science. Technology and Industry Scoreboard 2015. OECD.

OECD/ITF (OECD International Transport Forum) (2015) The Impact of Mega-ships, May 2015.

Oh, M.-H., Boo, S.-H., Lee, P.-S., Kim, J.-M., Moon, J.-S. and Sim, W.-S. (2017) Applications of the Static Condensation Technique to Nonlinear Structural Analysis of Floating Offshore Structures, in. 36th International Conference on Ocean, Offshore and Arctic Engineering, Trondheim, Norway: ASME, p. V03BT02A031.

Paboeuf, S., Le Sourne, H., Brochard, K. and Besnard, N. (2015) A damage assessment tool in ship collisions. In: Proceedings of RINA, Royal Institution of Naval Architects - Damaged Ship III, International Conference on Damaged Ship III. London, pp. 21-31

Pallanich, J. (2017) Flexible Floater, Upstream Online, 3 April. Available at: http://www.upstreamonline.com/upstreamtechnology/1236053/flexible-floater.

Parunov J, Rudan S, Gledić I, Primorac B. (2017) Finite element study of residual ultimate strength of a double hull oil tanker damaged in collision and subjected to bi-axial bending, ICSOS 2017: Proceedings of the International Conference on Ships and Offshore Structures, Sören Ehlers & Jeom Paik & Young Bai (Eds.), Shenzhen, China, 11-13 September, 2017.

Pendlebury, D. A. (2008) WHITE PAPER Using Bibliometrics in Evaluating Research. Thomson Reuters.

Peschmann, J., von Selle, H., Jankowski, J., Horn, G. and Arima, T. (2017) IACS common structural rules as an element of IMO goal based standards for bulk carriers and oil tankers, Progress in the Analysis and Design of Marine Structures, Guedes Soares & Garbatov (Eds.), Taylor & Francis Group, 2017, pp. 297-304.

Pessoa, J. M. and Moe, A. M. (2017) Air Gap on Semisubmersible MODUs Under DNVGL Class - Current & Future Design Practice, in. Offshore Technology Conference, Houston, Texas, USA: Society of Petroleum Engineers.

Pillai, A.C., Chick, J., Johanning, L., Khorasanchi, M. and Pelissier, S. (2016) Optimization of Offshore Wind Farms Using a Genetic Algorithm. International Journal of Offshore and Polar Engineering, Volume 26 (3), pp. 225–234.

Pire, T., Echeverry, S., Rigo, P., Buldgen, L. and Le Sourne, H. (2017) Validation of a simplified method for the crashworthiness of offshore wind turbine jackets using finite elements simulations. In: Progress in the Analysis and Design of Marine Structures - Proceedings of the 5th International Conference on Marine Structures (MARSTRUCT 2017). Lisbon: Taylor & Francis Group, pp. 497-505.

Poll, P., Park, Y. C., Converse, R., Godfrey, D. and Gian, M. (2015) Gulfstar - Structural Design of the Classic Spar Hull for Improved Constructability, in. Offshore Technology Conference, Houston, Texas, USA: Society of Petroleum Engineers.

Portella, R. B. and de Souza Lima, H. A. (2016) Cessão Onerosa FPSOs - Challenges and Achievements Conducting Four Simultaneous Hull Conversion Designs, in. Offshore Technology Conference, Houston, Texas, USA: Society of Petroleum Engineers.

Pradillon, J., Chen, C., Collette, M., Czaban, Z.J., Erikstad, S.O., Giuglea, V., Jiang, X., Rigo, P., Roland, F., Takaoka, Y. and Zanic, V. (2012) Design Methods, In: Proceedings of the 18th International Ship and Offshore Structures Congress (ISSC 2012), Rostock, pp: 507-576.

Pradillon, J.Y., Chen, C.P., Collette, M., Czaban, J.Z., Erikstad, S.O., Giuglea, V., Jiang, X., Rigo, P., Roland, F., Takaoka, Y., and Zanic, V. (2012). Design Methods. In: Proceedings of the 18th International Ship and Offshore Structures Congress (ISSC 2012). Vol. 1 pp. 507-576. Rostock.

Praetorius, G., Graziano, A., Schröder-Hinrichs. J. U. and Baldauf, M. (2017) FRAM in FSA—Introducing a Function-Based Approach to the Formal Safety Assessment Framework[M]// Advances in Human Aspects of Transportation. Springer International Publishing, 2017.

Praetorius, G., Graziano, A., Schröder-Hinrichs, J.U. and Baldauf, M. (2017). FRAM in FSA—Introducing a Function-Based Approach to the Formal Safety Assessment Framework. In: N. Stanton, S. Landry, G. Di Bucchianico G. and A. Vallicelli, eds, Advances in Human Aspects of Transportation. Advances in Intelligent Systems and Computing, Volume 484. Springer, Cham

Proceedings of the 2003 ISSC (2003), 14th International Ship and Offshore Structures Congress

PRS (2017) Private communication, Polish Register of Shipping, (PRS), September 2017.

Raikunen J, (2015) "Optimization approach for passenger ship structures using Finite Element Method", M.Sc. thesis, Aalto University, School of Engineering, 2015.

Raithatha, A. and Stonor, R. W. P. (2015) Efficient Non-linear Dynamic Analysis of Elevated Jack-Ups under Vessel Impact, in. 15th International Conference: The Jack-Up Platform, London.

Ravina, E. (2017). Concept design of an autonomous mechatronic unit for inspection of holds. In: Proceedings of the 6th International Conference On Marine Structures (Marstruct 2017). London: Taylor & Francis Group.

Rezende, F. C. and Barcarolo, D. (2017) Moonpool Effects on the Structural Assessment of Drillships, in Redefining Offshore Development: Technologies and Solutions: 22nd Offshore Symposium 2017: Houston, Texas, USA, 02 February 2017. Red Hook, NY: SNAME/Curran Associates, Inc.

Rodrigues J, Guedes Soares C. (2017) Still water vertical bending moment in a flooding damaged ship, Progress in the Analysis and Design of Marine Structures, Guedes Soares & Garbatov (Eds.), Taylor & Francis Group, 2017, pp. 35-42.

Rolls-Royce (2017) Autonomous Ships. The next step, http://www.rolls-royce.com/~/media/Files/R/Rolls-Royce/documents/customers/marine/ship-intel/rr-ship-intel-aawa-8pg.pdf, accessed on 6 November 2017.

Romanoff Jani, Jasmin Jelovica, Eero Avi, Bruno Reinaldo Goncalves, Mihkel Körgesaar, Joni Raikunen, Heikki Remes, Ari Niemelä, JN Reddy and Petri Varsta, (2016), Use of an Equivalent Single Layer Plate Theory in Ship Structural Design, PRADS 2016, Copenhagen, September 2016

Romanoff, J., Jelovica, J., Avi, E., Goncalves, B.R., Körgesaar, M., Raikunen, J., Remes, H., Niemelä, A., Reddy, J.N. and Varsta P. (2016). Use of an Equivalent Single Layer Plate Theory in Ship Structural Design. In: Proceedings of the 13th International Symposium on PRActical Design of Ships and Other Floating Structures (PRADS 2016), Copenhagen.

Rörup, J., Maciolowski, B. and Darie, I. (2016). FE-based strength analysis of ship structures for a more advanced class approval. In: Proceedings of the 13th International Symposium on PRActical Design of Ships and Other Floating Structures (PRADS 2016), Copenhagen.

Rosen, J., Potts, A., Sincock, P., Carra, C., Kilner, A., Kriznic, P. and Gumley, J. (2016) Novel Methods for Asset Integrity Management in a Low Oil-Price Environment, in. Offshore Technology Conference, Houston, Texas, USA: Society of Petroleum Engineers.

Roth, M. (2016). Recording As-Built via an Open and Lightweight Solution Supplemented by a Process Evaluation Model. In: COMPIT ’16 - 15th International Conference on Computer and IT Applications in the Maritime Industries. Volker Bertram.

Scherl, G. and Sodomaco, P. (2016) Two are Better than one a Hydrodynamic-Structural Case Study, in Future offshore technology and sustained reliability: 20th Offshore Symposium 2015: Houston, Texas, 17 February 2015. Red Hook, NY: SNAME/Curran Associates, Inc.

Seo, H., Park, S., and Jung, J. (2017). Study on Fatigue Strength for Tank Structures subject to Harmonized CSR, Tanker Structure Cooperative Forum 2016, Shipbuilders Meeting

Seo, J. K. and Kim, D. E. (2015) An Efficient Erection Simulation Methodology for the Modular Construction of Offshore Platform Based on Points Cloud Data, in. 34th International Conference on Ocean, Offshore and Arctic Engineering, St. John’s, Newfoundland, Canada: ASME, p. V001T01A002.

Shen, J., Liu, F., Li, H., Xu, L. and Liang, B., (2015). Assessment of the damages occurring between two adjacent measurements for an aging offshore platform. Ocean Engineering, 109, pp.372-380.

Shibasaki K. (2016) Shipbuilding industry’s perspective on the new IACS Common Structural Rules. In: Tanker Structure Cooperative Forum 2016, Shipbuilders Meeting. Busan. Available at: http://www.tscforum.org/news/2016_list.aspx

Shibasaki, K. (2015) Shipbuilding Industry's perspective on the new IACS Common Structural Rules. In: Proceedings of the 7th meeting of the Tanker Structure Co-operative Forum (TSCF2016). Busan. (http://www.tscforum.org/news/2016_list.aspx)

Shibasaki, K. (2016) Shipbuilding industry’s perspective on the new IACS Common Structural Rules, TSCF (Tanker Structure Co-operative Forum) 2016 SBM (Shipbuilders Meeting), 26 - 27 October 2016, Korea.

Shiptec China (2016). 12th International Shipbuilding, Marine Equipment and Offshore Engineering Exhibition for China, http://www.chinaexhibition.com/trade_events/7071-Shiptec_China_2016_12th_International_Shipbuilding,_Marine_Equipment_and_Offshore_Engineering_Exhibition_for_China.html, accessed on 03/11/2017.

Skafte, A., Kristoffersen, J., Vestermark, J., Tygesen, U.T. and Brincker, R., 2017. Experimental study of strain prediction on wave induced structures using modal decomposition and quasi static Ritz vectors. Engineering Structures, 136, pp.261-276.

Skafte, A., Tygesen, U.T. and Brincker, R., 2014. Expansion of mode shapes and responses on the offshore platform Valdemar. In Dynamics of Civil Structures, Volume 4 (pp. 35-41). Springer, Cham.

Skau, K. S., Torgersrud, Ø., Jostad, H. P., Hofstede, H. and Hermans, S. (2015) Linear and Nonlinear Foundation Response in Dynamic Analyses of Jack-up Structures, in Meyer, V. (ed.) Frontiers in offshore geotechnics III: proceedings of the Third International

Symposium on Frontiers in Offshore Geotechnics (ISFOG 2015), Oslo, Norway, 10-12 June 2015. Boca Raton London New York Leiden: CRC Press/Balkema.

So, H.Y., Bae, M.N., and Min, D.K. (2017). MR. Tanker with Harmonized CSR, Tanker Structure Cooperative Forum 2016, Shipbuilders Meeting (http://www.tscforum.org/news/2016_list.aspx)

Son, M., Gyun Park, H., Lee, J.Y., Lee, J. Jong-oh Kim, J. and Woo, J. (2016). Development of Auto FE Modeling for enhancement of the productivity in modeling based on CSR-H. In: Proceedings of the 13th International Symposium on PRActical Design of Ships and Other Floating Structures (PRADS 2016), Copenhagen.

Son, M., Park, H.G., Lee, J.Y., Lee, J., Kim, J., and Woo, J. (2016) Development of Auto FE Modeling for enhancement of the productivity in modeling based on CSR-H. Proceedings of the 13th PRADS2016, Copenhagen.

Stilhammer, J., Steenbock, C. and Bohm, M. (2015). A Complete CAE Process for Structural Design in Shipbuilding, In: Proceedings of the 14th International Conference on Computer Applications and Information Technology in the Maritime Industries (COMPIT'15), Ulrichshusen, pp 406-417.

Stone, K. and McNatt, T. (2017). Ship hull scantling optimization. In: Progress in the Analysis and Design of Marine Structures - Proceedings of the 5th International Conference on Marine Structures (MARSTRUCT 2017). Lisbon: Taylor & Francis Group, pp. 203-211.

Sugita, S. and Suzuki H. (2016). A study on TLP hull sizing by utilizing optimization algorithm. Journal of Marine Science and Technology, Volume 21 (4), pp. 611–623

Taheri, A., Lazakis, I. and Koch, T., 2015, September. An innovative machinery data management system for ships using a catalogue data model. In 16th International Congress of the International Maritime Association of the Mediterranean, IMAM 2015.

Talib, J. H. and Germinder, B. (2016) Game-Changing Floating LNG Solutions, in. Houston, Texas, USA: Offshore Technology Conference.

Tanaka, S. and Takano, K. (2017) Next Generation Hull-Platform "Noah-FPSO Hull" Based On Modular Design And Construction Concept, in. 36th International Conference on Ocean, Offshore and Arctic Engineering, Trondheim, Norway: ASME, p. V001T01A063.

Taylor, J. D., Foret, R. and Buchert, S. (2015) SS Delta House - Topsides Design Philosophy, in. Offshore Technology Conference, Houston, Texas, USA: Society of Petroleum Engineers.

Thakker, B. (2015). Portals in Shipbuilding. In: COMPIT '15 - 14th International Conference on Computer and IT Applications in the Maritime. Volker Bertram.

The Economist (2013) When giants slow down, Jul 27th 2013, https://www.economist.com/news/briefing/21582257-most-dramatic-and-disruptive-period-emerging-market-growth-world-has-ever-seen, accessed on 10 November 2017.

The Financial Times (2015) OECD cuts world growth forecast, https://www.ft.com/content/4ac6334e-86cd-11e5-90de-f44762bf9896, accessed on 10 November 2017.

The Maritime Executive (2017) CMA CGM Confirms Order for 22,000 TEU Mega-Ships, https://maritime-executive.com/article/cma-cgm-confirms-order-for-22000-teu-mega-ships, accessed on 6 November 2017.

The Naval Architect (2015). 3D design approach saves time and money, Volume February, pp. 50-51

The Naval Architect (2016) Collaboration not competition is the new 3D reality, Volume April, pp. 32-34

The Naval Architect (2016) Smart connected & Bigger – IT for Ships, Volume April, pp. 24-26

Tho, K. K., Chan, N. and Paisley, J. (2015) Comparison of Coupled and Decoupled Approaches to Spudcan-Pile Interaction, in Meyer, V. (ed.) Frontiers in offshore geotechnics III: proceedings of the Third International Symposium on Frontiers in Offshore Geotechnics (ISFOG 2015), Oslo, Norway, 10-12 June 2015. Boca Raton London New York Leiden: CRC Press/Balkema.

Tho, K. K., Chan, N., Zhou, Y., Liu, J. and Zhou, S. (2015) Case Study of Spudcan Re-penetration Analysis using Large Defirmation Finite Element Approach, in. 15th International Conference: The Jack-Up Platform, London.

Thomson, D. and Gordon, A. (2016). Maritime Asset Visualisation. In: COMPIT '16 - 15th International Conference on Computer and IT Applications in the Maritime Industries. Volker Bertram.

Tian, Y., Zheng, T., Zhou, T. and Cassidy, M. J. (2016) A New Method to Investigate the Failure Envelopes of Offshore Foundations, in. 35th International Conference on Ocean, Offshore & Arctic Engineering, Busan, South Korea: ASME, p. V001T10A002.

Tian, Z. K., Kirkland, B., Radanovic, B. and Dasilva, O. (2017) Opti® Series Production Semi-Submersible Hull Sizing Process, in Redefining Offshore Development: Technologies and Solutions: 22nd Offshore Symposium 2017: Houston, Texas, USA, 02 February 2017. Red Hook, NY: SNAME/Curran Associates, Inc.

Tippee, J. (2017) Standardization JIP Aims to Improve Design and Construction Efficiencies, Offshore Magazine. Available at: http://www.offshore-mag.com/articles/print/volume-77/issue-3/asia-pacific/standardization-jip-aims-to-improve-design-and-construction-efficiencies.html, accessed on 03/11/2017.

Um T.-S. and Roh M.-I. (2015) "Optimal dimension design of a hatch cover for lightening a bulk carrier" Int. J. Nav. Archit. Ocean Eng. (2015) 7:270~287

Un-Chul Choi. (2016) Impact of Harmonized CSR for oil tanker, Tanker Structure Cooperative Forum 2016, Shipbuilders Meeting,26-27 October 2016, Busan, South Korea

University of Ottawa. (2017). 21st century science overload, http://www.cdnsciencepub.com/blog/21st-century-science-overload.aspx, accessed on 03/11/2017.

US TRB. (2017). US Transportation Research Board, http://prp.trb.org, accessed on 3/11/2017

van Lukas, U., Ruth, T., Deistung, E. and Huber, L. (2015). Leveraging the Potential of 3D Data in the Ship Lifecycle with Open Formats and Interfaces. In: COMPIT '15 - 14th International Conference on Computer and IT Applications in the Maritime. Volker Bertram.

Vatteroni, M. (2016). A Standard Protocol for Exchanging Technical Data in the Maritime Industries. In: COMPIT '16 - 15th International Conference on Computer and IT Applications in the Maritime Industries. Volker Bertram.

Vaucorbeil A, Patron K. (2017) Optimization of the gun foundation structure of an offshore patrol vessel using a modern genetic algorithm, Progress in the Analysis and Design of Marine Structures, Guedes Soares & Garbatov (Eds.), Taylor & Francis Group, 2017, pp. 131-137.

Ventura M. and Soares C. Guedes. (2015) "Integration of a voyage model concept into a ship design optimization procedure". Towards Green Marine Technology and Transport (2015): 539-548

Vieira, D. P., Lavieri, R. S., Rocha, T. P., Dotta, R., Rampazzo, F. and Nishimoto, K. (2016) A Synthesis Model for FLNG Design, in. 35th International Conference on Ocean, Offshore & Arctic Engineering, Busan, South Korea: ASME, p. V001T01A015.

Vladimir, N., Senjanović, I., Malenica, Š., De Lauzon, J., Im, H., Choi, B.K. and Seung Cho, D. (2016). Structural Design Of Ultra Large Ships Based On Direct Calculation Approach. Journal of Maritime & Transportation Sciences, Volume 1, pp. 63-79

Vugts, J. H. and Zandwijk, K. van (2016) Handbook of Bottom Founded Offshore Structures. Part 2: Fixed Steel Structures. 1st Ed. Delft: Eburon.

Wagner, L., Grau, M. and Enders, O. (2015). Enterprise Architecture Management in Shipbuilding PLM. In: COMPIT '15 - 14th International Conference on Computer and IT Applications in the Maritime Industries. Volker Bertram.

Wallace, G. and Champlin, T. (2016) Online Asset Integrity Management and Operational Optimisation through Online Integrity Monitoring, in. Offshore Technology Conference, Houston, Texas, USA: Society of Petroleum Engineers.

Wang, M., Wang, J., Cheng, Z., Bai, Y., Fu, D. and Luo, Y. (2017) A New Light-weight Semi-Submersible FPS for Offshore Marginal Oil and Gas Field Development, in Redefining Offshore Development: Technologies and Solutions: 22nd Offshore Symposium 2017: Houston, Texas, USA, 02 February 2017. Red Hook, NY: SNAME/Curran Associates, Inc.

Wiley, L. (2015) Deriving Value from Integrating Engineering Design and Automation with Offshore Operations, in. Offshore Technology Conference, Houston, Texas, USA: Society of Petroleum Engineers.

Wilken, M., Cabos, C., Baumbach, D., Buder, M., Choinowski, A., Griessbach, D. and Zuev, S. (2015). IRIS – an innovative system for maritime hull structures. In: Proceedings of RINA, Royal Institution of Naval Architects - International Conference on Computer Applications in Shipbuilding 2015, ICCAS 2015. Bremen, pp. 219-226.

Wisch, D. and Spong, R. (2016) Recommended Practice for Structural Integrity Management of Floating Offshore Structures - A DeepStar 12401 Product, in. Offshore Technology Conference, Houston, Texas, USA: Society of Petroleum Engineers.

Wyllie, M., Newport, A. and Mastrangelo, C. (2017) The Benefits and Limits of FPSO Standardisation, in. Offshore Technology Conference, Houston, Texas, USA: Society of Petroleum Engineers.

Yan, G., Sun, H. and Waisman, H., 2015. A guided bayesian inference approach for detection of multiple flaws in structures using the extended finite element method. Computers & Structures, 152, pp.27-44.

Yang M, Khan F, Oldford D, et al. Risk-based Winterization on a North Atlantic-based Ferry Design[J]. Journal of Ship Production & Design, 2015, 31(2):1-11.

Yang, H. and Zhu, Y. (2015). Robust design optimization of supporting structure of offshore wind turbine, Journal of Marine Science and Technology, December 2015, Volume 20 (4), pp 689–702

Yang, M., Khan, F., Oldford, D. and Sulistiyono, H. (2015). Risk-based Winterization on a North Atlantic-based Ferry Design. Journal of Ship Production & Design, Volume 31 (2), pp. 1-11.

Ye, W., Ran, A., Li, J., Li, G., Tan, X., Wang, Z. and Wu, H. (2017) A Viable Dry Tree Semi-Submersible Concept with Tapered Columns, in Redefining Offshore Development: Technologies and Solutions: 22nd Offshore Symposium 2017: Houston, Texas, USA, 02 February 2017. Red Hook, NY: SNAME/Curran Associates, Inc.

Youssef, S., Kim, Y.S., Paik, J.K. and Turgut Ince, S. (2014). Quantitative risk assessment for collisions involving double hull oil tankers. Transactions of the Royal Institution of Naval Architects Part A: International Journal of Maritime Engineering. Volume 156, pp. A157-A174

Yu, Q., Tan, P.-L., Lo, T.-W. and Chow, W.-Y. (2016) New LRFD-Based Design Criteria for Mobile Offshore Units and Floating Production Installations, in. Offshore Technology Conference, Houston, Texas, USA: Society of Petroleum Engineers.

Yuan, Q., Zhang, Y. and Li X.B. (2017). A new simplified method to investigate the side-by-side collision of two ships, In: Progress in the Analysis and Design of Marine Structures - Proceedings of the 5th International Conference on Marine Structures (MARSTRUCT 2017). Lisbon: Taylor & Francis Group, pp. 541-547

Zagkas, V. and Spanos, G.T. (2015). An Integrated Workflow for Rapid Structural and Hydrodynamic Analysis of Ships and Offshore Structures. In: Proceedings of the 14th International Conference on Computer Applications and Information Technology in the Maritime Industries (COMPIT'15), Ulrichshusen, pp 563-571

Zaman, M.B., Kobayashi, E., Wakabayashi, N., Maimun, A. (2015). Development of Risk Based Collision (RBC) Model for Tanker Ship Using AIS Data in the Malacca Straits, Procedia Earth and Planetary Science. Volume 14, pp. 128-135.

Zhang, W., Cassidy, M. J. and Tian, Y. (2015) 3D Large Deformation Finite Element Analyses of Jack-up Reinstallations near Idealised Footprints, in. 15th International Conference: The Jack-Up Platform, London.

Zhang, X. Y., Li, Y. P., Yi, J. T., Lee, F. H., Tan, P. L., Wu, J. F. and Wang, S. Q. (2015) A Novel Spudcan Design for Improving Foundation Performance, in Meyer, V. (ed.) Frontiers in offshore geotechnics III: proceedings of the Third International Symposium on Frontiers in Offshore Geotechnics (ISFOG 2015), Oslo, Norway, 10-12 June 2015. Boca Raton London New York Leiden: CRC Press/Balkema.

Zhang, Y., Khoa, H. D. V., Meyer, V. and Cassidy, M. J. (2015) Jack-up Spudcan Penetration Analysis: Review of Semi-analytical and Numerical Methods, in Meyer, V. (ed.) Frontiers in offshore geotechnics III: proceedings of the Third International Symposium on Frontiers in Offshore Geotechnics (ISFOG 2015), Oslo, Norway, 10-12 June 2015. Boca Raton London New York Leiden: CRC Press/Balkema.

Zhang, Y.M., Fan, M., Xiao, Z.M. and Zhang, W.G., 2016. Fatigue analysis on offshore pipelines with embedded cracks. Ocean Engineering, 117, pp.45-56.

Zou, J. (2016) Development Of Secondary Column Enhanced TLP Concept for Central Gulf Of Mexico, in Emerging offshore technology and deepwater trends: 21st Offshore Symposium 2016: Houston, Texas, USA, 16 February 2016. Red Hook, NY: SNAME/Curran Associates, Inc.

Zou, J. (2017) Conceptual Study of a Paired-Column Semi-Submersible Platform for A 1.5 MTPA FLNG, in Redefining Offshore Development: Technologies and Solutions: 22nd Offshore Symposium 2017: Houston, Texas, USA, 02 February 2017. Red Hook, NY: SNAME/Curran Associates, Inc.

Subject Index

acceptance criteria 255
accidental loading 549
aluminium 441
benchmark study 171
blast 255
buckling collapse 335
cables/risers 101
CAD 609
class rule-related software 171
classification society software 609
climate change 1
corrosion 171
countermeasures 255
crack growth 441
current 1, 255
damage accumulation 441
damping 255
data source 1
decision support 549
deep water 1
design 441
design condition 1
design criteria 549
design methodology 609
design principles 549
design software 609
design waves 101
direct calculations 171
dynamic response 255
environment 1
experiments and testing 171
explosion 255
extreme load 171
fabrication 441
fabrication-induced initial imperfections 335
fatigue 101, 255, 441
fatigue assessment 171
finite element analysis 171
fitness for service 441
floating offshore wind turbines 101
fracture 441
full-scale measurement 255
goal-based design 549
green water 101
human error 549
human performance 549
hydroelasticity 101, 255
IACS common structural rules 171
ice 1
IMO goal-based standards 171
impact loads 171
in-service damage and degradation 335
inland vessels 549
inspection 441
internal flow 255
lifecycle structural management 609
lifting operation 101
load modelling 171
load-carrying capacity 335
loads due to collision and grounding 101
machinery 255
maintenance 441
model tests 255
modelling 1
monitoring 255
mooring system 101
noise 255
ocean 1
offshore structures 171, 609
on-boarding monitoring 549
operational condition 1
optimisation 171
optimization 609
polar design criteria 549
polymer composites 441
probabilistic approach 171
probabilistic method 101
product lifecycle model 609
propeller 255
quasi-static response 171
reliability 335, 441
reliability analysis 171
residual strength 171

rogue waves 1
rules 441
sea level 1
shallow water 1
ship structures 171
shock 255
slamming 101, 255
sloshing 101
sloshing impact 255
springing 255
standards 441
steel 441
strength assessment 171
stress response calculation 171
structural integrity 171
sustainability 549
ultimate limit states 335
ultimate strength 335
uncertainty 1, 255
uncertainty analysis 101, 171
underwater noise 255
verification 441
vibration 255
vortex 255
vortex induced motions 101
vortex induced vibrations 101
wave 1, 255
wave induced loads 101
whipping 101, 255
wind 1, 255

Author Index

Alley, E. 255
Andrić, J. 171
Arima, T. 549
Ås, S.K. 441
Babanin, A. 1
Bai, W. 101
Bayatfar, A. 335
Benson, S. 335
Bentamy, A. 1
Boulares, J. 335
Brandt, A. 255
Branner, K. 441
Broekhuijsen, J. 335
Bronsart, R. 609
Campos, R. 1
Caprace, J.-D. 609
Chen, Y. 609
Choi, B.K. 441
Collette, M. 549
Czujko, J. 335
de Hauteclocque, G. 101
Den Besten, J.H. 441
Dhavalikar, S. 101
Dong, P. 441
Dong, S. 1
Drummen, I. 255
Egorov, G. 549
el Moctar, O. 255
Ergin, A. 255
Fang, C.-C. 101
Fonseca, N. 101
Fu, T. 1
Garbatov, Y. 441
Georgiev, P. 609
Gramstad, O. 1
Hänninen, S. 101
Heggelund, S.E. 171
Hermundstad, O. 255
Homma, N. 171
Huang, Y.T. 171
Huh, Y.C. 255
Ilnitskiy, I. 609
Ivaldi, A. 255
Jang, B.S. 171
Jelovica, J. 171
Jeong, H.K. 549
Johannessen, T.B. 101
Kaminski, M. v
Kapsenberg, G. 1
Kawamura, Y. 171
Lara, P. 171
Lazakis, I. 609
Lien, V. 101
Lillemäe, I. 441
Lindstrom, P. 441
Liu, J.H. 255
Lourenço de Souza, M. 441
Lützen, M. 335
Malenica, S. 255
Mao, W. 1
Mendonça Santos, J. 609
Miyake, R. 1
Moro, L. 609
Morooka, C. 101
Mumm, H. 101
Murphy, A.J. 1
Notaro, G. 335
Ogawa, Y. 101
Okada, T. 549
Pahos, S.J. 335
Park, J.S. 335
Parmentier, G. 441
Prasetyo, F. 1
Prebeg, P. 609
Prpic-Orsic, J. 101
Qian, X. 335
Qiu, W. 1
Quéméner, Y. 441
Rigo, P. v
Ringsberg, J.W. 171
Rizzo, C.M. 441
Rörup, J. 441
Saad-Eldeen, S. 335
Sagrillo, L. 1
Sekulski, Z. 609
Shyu, R.J. 255

Sicchiero, M. 609
Sidari, M. 171
Sielski, R. 609
Skjong, R. 549
Smith, M. 335
Song, K.H. 101
Storhaug, G. 255
Tang, W. 609
Tian, C. 101
Toyoda, M. 609
Uğurlu, B. 101
Underwood, J.M. 171
Varela, J. 609
Vhanmane, S. 441
Villavicencio, R. 441
Vladimir, N. 255
Wang, D. 335
Wang, F. 441
Wang, J. 171
Wang, S. 101
Xu, M.C. 335
Yamada, Y. 255
Yanagihara, D. 335
Yang, D. 171
Yue, J. 441
Zanic, V. 549
Zhan, D. 255
Zhan, Z. 549
Zhang, G. 255
Zhu, L. 549

This page intentionally left blank

This page intentionally left blank

The International Ship and Offshore Structures Congress (ISSC) is a forum for the exchange of information by experts undertaking and applying marine structural research. The aim of the ISSC is to facilitate the evaluation and dissemination of results from recent investigations, to make recommendations for standard design procedures and criteria, to discuss research in progress and planned, to identify areas requiring future research and to encourage international collaboration in furthering these aims. Ships and other marine structures used for transportation, exploration and exploitation of resources in and under the oceans are in the scope of the ISSC.

This publication contains the 8 Technical Committee reports presented and discussed at the 20th International Ship and Offshore Structures Congress (ISSC 2018) held in Liège (Belgium) and Amsterdam (The Netherlands), 9–14 September 2018.

The reports of the 8 Specialist Committees are published in volume 2 of the Progress in Maritime Science and Technology book series. The Official discusser's reports, all floor discussions together with the replies by the committees, will be published after the congress in electronic form.

ISBN 978-1-61499-861-7

ISBN 978-1-61499-861-7 (print)
ISBN 978-1-61499-862-4 (online)
ISSN 2543-0955 (print)
ISSN 2543-0963 (online)

IOS Press